United States
Environmental Protection
Agency

Office of Research and
Development
Washington DC 20460

EPA/600/P-95/001aF
April 1996

EPA

Air Quality Criteria for Particulate Matter

Volume I of III

EPA/600/P-95/001aF
April 1996

Air Quality Criteria for Particulate Matter

Volume I of III

U.S. Environmental Protection Agency
Region 5, Library (PL-12J)
77 West Jackson Boulevard, 12th Floor
Chicago, IL 60604-3590

National Center for Environmental Assessment
Office of Research and Development
U.S. Environmental Protection Agency
Research Triangle Park, NC 27711

Printed on Recycled Paper

DISCLAIMER

This document has been reviewed in accordance with U.S. Environmental Protection Agency policy and approved for publication. Mention of trade names or commercial products does not constitute endorsement or recommendation for use.

PREFACE

On April 30, 1971 (Federal Register, 1971), in accordance with the Clean Air Act (CAA) Amendments of 1970, the U.S. Environmental Protection Agency (EPA) promulgated the original primary and secondary National Ambient Air Quality Standard (NAAQS) for particulate matter (PM). The reference method for measuring attainment of these standards was the "high-volume" sampler (Code of Federal Regulations, 1977), which collected PM up to a nominal size of 25 to 45 μm (so-called "total suspended particulate," or "TSP"). Thus, TSP was the original indicator for the PM standards. The primary standards for PM, measured as TSP, were 260 $\mu g/m^3$, 24-h average not to be exceeded more than once per year, and 75 $\mu g/m^3$, annual geometric mean. The secondary standard was 150 $\mu g/m^3$, 24-h average not to be exceeded more than once per year.

In accordance with the CAA Amendments of 1977, the U.S. EPA conducted a re-evaluation of the scientific data for PM, resulting in publication of a revised air quality criteria document (AQCD) for PM in December 1982 and a later Addendum to that document in 1986. On July 1, 1987, the U.S. EPA published final revisions to the NAAQS for PM. The principle revisions to the 1971 NAAQS included (1) replacing TSP as the indicator for the ambient standards with a new indicator that includes particles with an aerodynamic diameter less than or equal to a nominal 10 μm ("PM_{10}"), (2) replacing the 24-h primary TSP standard with a 24-h PM_{10} standard of 150 $\mu g/m^3$, (3) replacing the annual primary TSP standard with an annual PM_{10} standard of 50 $\mu g/m^3$, and (4) replacing the secondary TSP standard with 24-h and annual PM_{10} standards identical in all respects to the primary standards.

The present PM AQCD has been prepared in accordance with the CAA, requiring the EPA Administrator periodically to review and revise, as appropriate, the criteria and NAAQS for listed criteria pollutants. Emphasis has been place on the presentation and evaluation of the latest available dosimetric and health effects data; however, other scientific data are also presented to provide information on the nature, sources, size distribution, measurement, and concentrations of PM in the environment and contributions of ambient PM to total human exposure. This document is comprised of three volumes, with the present one (Volume I) containing Chapters 1 through 7.

This document was prepared by U.S. EPA's National Center for Environmental Assessment-RTP, with assistance by scientists from other EPA Office of Research and Development laboratories (NERL; NHEERL) and non-EPA expert consultants. Several earlier drafts of the document were reviewed by experts from academia, various U.S. Federal and State government units, non-governmental health and environmental organizations, and private industry. Several versions of this AQCD have also been reviewed in public meetings by the Agency's Clean Air Scientific Advisory Committee (CASAC). The National Center for Environmental Assessment (formerly the Environmental Criteria and Assessment Office) of the U.S. EPA's Office of Research and Development acknowledges with appreciation the valuable contributions made by the many authors, contributors, and reviewers, as well as the diligence of its staff and contractors in the preparation of this document.

Air Quality Criteria for Particulate Matter

TABLE OF CONTENTS

Volume I

1. EXECUTIVE SUMMARY 1-1

2. INTRODUCTION 2-1

3. PHYSICS AND CHEMISTRY OF PARTICULATE MATTER 3-1

4. SAMPLING AND ANALYSIS METHODS FOR PARTICULATE MATTER AND ACID DEPOSITION 4-1

5. SOURCES AND EMISSIONS OF ATMOSPHERIC PARTICLES 5-1

6. ENVIRONMENTAL CONCENTRATIONS 6-1
Appendix 6A: Tables of Chemical Composition of Particulate Matter 6A-1

7. HUMAN EXPOSURE TO PARTICULATE MATTER: RELATIONS TO AMBIENT AND INDOOR CONCENTRATIONS 7-1

Volume II

8. EFFECTS ON VISIBILITY AND CLIMATE 8-1

9. EFFECTS ON MATERIALS 9-1

10. DOSIMETRY OF INHALED PARTICLES IN THE RESPIRATORY TRACT 10-1
Appendix 10A: Prediction of Regional Deposition in the Human Respiratory Tract Using the International Commission on Radiological Protection Publication 66 Model 10A-1
Appendix 10B: Selected Model Parameters 10B-1
Appendix 10C: Selected Ambient Aerosol Particle Distributions 10C-1

11. TOXICOLOGICAL STUDIES OF PARTICULATE MATTER 11-1

TABLE OF CONTENTS (cont'd)

Volume III

12. EPIDEMIOLOGY STUDIES OF HEALTH EFFECTS ASSOCIATED WITH EXPOSURE TO AIRBORNE PARTICLES/ACID AEROSOLS 12-1

13. INTEGRATIVE SYNTHESIS OF KEY POINTS: PARTICULATE MATTER EXPOSURE, DOSIMETRY, AND HEALTH RISKS 13-1

Appendix 13A: References Used To Derive Cell Ratings in the Text Tables 13-6 and 13-7 for Assessing Qualitative Strength of Evidence for Particulate Matter-Related Health Effects 13A-1

TABLE OF CONTENTS

Page

LIST OF TABLES . . . . . I-xix
LIST OF FIGURES . . . . . I-xxvii
AUTHORS, CONTRIBUTORS, AND REVIEWERS . . . . . I-xlvii
U.S. ENVIRONMENTAL PROTECTION AGENCY SCIENTIFIC ADVISORY BOARD, CLEAN AIR SCIENTIFIC ADVISORY COMMITTEE . . . . . I-lv
U.S. ENVIRONMENTAL PROTECTION AGENCY PROJECT TEAM FOR DEVELOPMENT OF AIR QUALITY CRITERIA FOR PARTICULATE MATTER . . . . . I-lix

1. EXECUTIVE SUMMARY 1-1
   1.1 INTRODUCTION 1-1
      1.1.1 Purpose of the Document 1-1
      1.1.2 Organization of the Document 1-1
   1.2 AIR QUALITY AND EXPOSURE ASPECTS 1-2
      1.2.1 Chemistry and Physics of Atmospheric Particles 1-2
      1.2.2 Sources of Airborne Particles in the United States 1-3
      1.2.3 Atmospheric Transport and Fate of Airborne Particles 1-5
      1.2.4 Airborne Particle Measurement Methods 1-5
      1.2.5 Ambient U.S. Particulate Matter Concentrations: Regional Patterns and Trends 1-7
      1.2.6 Human Particulate Matter Exposure 1-8
   1.3 DOSIMETRY 1-10
   1.4 PARTICULATE MATTER HEALTH EFFECTS 1-11
      1.4.1 Epidemiology Findings 1-12
      1.4.2 Toxicology Findings 1-14
      1.4.3 Population Groups at Risk 1-16
   1.5 WELFARE EFFECTS 1-17
      1.5.1 Visibility Effects 1-18
      1.5.2 Climate Change 1-19
      1.5.3 Materials Damage 1-19
   1.6 KEY CONCLUSIONS 1-20

2. INTRODUCTION 2-1
   2.1 LEGISLATIVE REQUIREMENTS 2-1
   2.2 REGULATORY BACKGROUND 2-2
   2.3 SCIENTIFIC BASIS FOR THE EXISTING PARTICULATE MATTER STANDARDS 2-4
      2.3.1 Rationale for the Primary Standards 2-4
      2.3.2 Pollutant Indicator 2-5
      2.3.3 Averaging Time and Form of the Standards 2-7
         2.3.3.1 24-Hour Standard 2-7
         2.3.3.2 Annual Standard 2-7

TABLE OF CONTENTS (cont'd)

Page

2.3.4 Level of the Standards 2-8
2.3.4.1 Assessment of the Quantitative Epidemiological Studies 2-8
2.3.4.2 Identification of Margin of Safety Considerations 2-9
2.3.4.3 24-Hour Standard 2-10
2.3.4.4 Annual Standard 2-15
2.3.5 Welfare Effects 2-17
2.4 TOPICS/ISSUES OF CONCERN FOR CURRENT CRITERIA DEVELOPMENT 2-17
2.4.1 Air Quality and Exposure 2-18
2.4.1.1 Physics and Chemistry of Atmospheric Aerosols 2-18
2.4.1.2 Measurement Methodology 2-20
2.4.1.3 Ambient Levels 2-20
2.4.1.4 Cut Points 2-20
2.4.1.5 Exposure 2-21
2.4.2 Health Effects 2-22
2.4.2.1 Respiratory Tract Dosimetry 2-23
2.4.2.2 Epidemiology Studies 2-24
2.4.2.3 Toxicology of Particulate Matter Constituents 2-26
2.4.2.4 Sensitive Groups 2-27
2.4.3 Welfare Effects 2-28
2.4.3.1 Effects on Materials 2-28
2.4.3.2 Visibility Effects 2-28
2.4.3.3 Climate Change 2-29
2.4.3.4 Vegetation and Ecosystem Effects 2-29
2.5 DOCUMENT CONTENT AND ORGANIZATION 2-29
REFERENCES 2-32

3. PHYSICS AND CHEMISTRY OF PARTICULATE MATTER 3-1
3.1 INTRODUCTION 3-1
3.1.1 Overview 3-1
3.1.2 Atmospheric Aerosol Size Distributions 3-4
3.1.3 Definitions 3-7
3.1.3.1 Definitions of Particle Diameter 3-7
3.1.3.2 Definitions of Particle Size Fractions 3-9
3.1.3.3 Other Terminology 3-14
3.1.4 Major Chemical Constituents 3-14
3.1.5 Chemical Composition and Its Dependence on Particle Size 3-16
3.1.6 Particle-Vapor Partitioning 3-18
3.1.7 Single Particle Characteristics 3-20
3.1.8 Dry Deposition 3-21
3.1.9 Atmospheric Scavenging or Wet Deposition 3-21
3.2 PHYSICAL PROPERTIES AND PROCESSES 3-22
3.2.1 Aerosol Size Distributions 3-22

TABLE OF CONTENTS (cont'd)

Page

3.2.1.1 Particle Size Distribution Functions 3-22
3.2.1.2 Log-Normal Size Distributions 3-22
3.2.1.3 Ambient Aerosol Size Distributions 3-23
3.2.1.4 Coagulation of Spherical Particles 3-23
3.2.2 Particle Formation and Growth 3-25
3.2.2.1 Equilibrium Vapor Pressures 3-25
3.2.2.2 New Particle Formation 3-26
3.2.2.3 Particle Growth 3-27
3.2.2.4 Equilibria with Water Vapor 3-28
3.2.2.5 Particle Growth in Fogs and Clouds 3-31
3.2.3 Resuspension of Particulate Matter 3-32
3.2.3.1 Resuspension Mechanics 3-32
3.2.3.2 Applied Studies 3-33
3.2.3.3 Aerodynamic Resuspension 3-34
3.2.3.4 Mechanical Resuspension 3-34
3.2.3.5 Physical and Chemical Properties of Resuspended Particles 3-35
3.2.3.6 Levels of Production and Transport of Resuspended Aerosols 3-36
3.2.4 Particle Removal Mechanisms and Deposition 3-38
3.3 CHEMICAL COMPOSITION AND PROCESSES 3-41
3.3.1 Acid Aerosols and Particulate Sulfates 3-41
3.3.1.1 Aerosol Acidity 3-41
3.3.1.2 Sources of Sulfate 3-43
3.3.1.3 Gas-Phase Oxidation of Sulfur Dioxide 3-44
3.3.1.4 Aqueous-Phase Oxidation of Sulfur Dioxide 3-45
3.3.2 Particulate Nitrates 3-64
3.3.2.1 Sources 3-64
3.3.2.2 Major Gas-Phase Reaction 3-64
3.3.2.3 Major Aqueous-Phase Reaction 3-65
3.3.2.4 Other Reaction Mechanisms 3-66
3.3.2.5 Ammonium Nitrate Vaporization Equilibria 3-67
3.3.2.6 Sulfate/Nitrate Interaction 3-68
3.3.2.7 Ammonium Chloride Vaporization Equilibrium 3-69
3.3.3 Carbon-Containing Particulate Matter 3-70
3.3.3.1 Elemental Carbon 3-70
3.3.3.2 Organic Carbon 3-73
3.3.3.3 Semi-Volatile Organic Compounds 3-83
3.3.4 Metals and Other Trace Elements 3-89
3.4 FIELD STUDIES OF TRANSPORT AND TRANSFORMATIONS 3-96
3.4.1 Field Studies of Transport Processes 3-97
3.4.1.1 Field Measurements Related to Transport Modeling 3-99
3.4.1.2 Field Measurements Related to Dispersion Modeling . . 3-104
3.4.2 Field Studies of Transformations 3-106

TABLE OF CONTENTS (cont'd)

Page

3.4.2.1 Gas-to-Particle Conversion 3-106
3.4.2.2 Field Studies of Water Uptake By Atmospheric Aerosols 3-118
3.4.2.3 Pertinent Results of the Southern California Air Quality Study 3-123
3.5 DRY DEPOSITION 3-126
3.5.1 Theoretical Aspects of Dry Deposition 3-126
3.5.2 Field Studies of Dry Deposition 3-131
3.5.3 Measured Deposition Velocities 3-133
3.6 WET DEPOSITION 3-135
3.6.1 Introduction 3-135
3.6.2 Field Studies of Wet Deposition 3-137
3.6.3 Overview of Sulfur Dioxide and Nitrogen Oxide Wet Scavenging 3-143
3.7 PHYSICAL AND CHEMICAL CONSIDERATIONS IN SELECTING A SIZE CUT POINT FOR SEPARATING FINE AND COARSE PARTICULATE MATTER 3-144
3.7.1 Background 3-146
3.7.2 Size Measurements 3-147
3.7.3 Appropriate Display of Size-Distribution Data 3-148
3.7.4 Comparison of Particle-Counting and Particle-Collection Techniques 3-153
3.7.5 Review of Size-Distribution Data 3-156
3.7.5.1 Early Studies 3-156
3.7.5.2 Recent Work 3-156
3.7.6 Intermodal Region 3-162
3.7.6.1 Coarse Mode 3-162
3.7.6.2 Fine Mode 3-168
3.7.7 Conclusions 3-187
3.8 SUMMARY 3-187
REFERENCES 3-194

4. SAMPLING AND ANALYSIS METHODS FOR PARTICULATE MATTER AND ACID DEPOSITION 4-1
4.1 INTRODUCTION 4-1
4.2 SAMPLING FOR PARTICULATE MATTER 4-5
4.2.1 Background 4-5
4.2.2 Large Particle Separators 4-6
4.2.2.1 Cutpoint Considerations 4-6
4.2.2.2 Total Suspended Particulates 4-11
4.2.2.3 Total Inhalable Particles 4-12
4.2.2.4 PM_{10} 4-12
4.2.3 Fine Particle Separators 4-21
4.2.3.1 Cutpoint Considerations 4-21

TABLE OF CONTENTS (cont'd)

Page

4.2.3.2 Virtual Impactors 4-22
4.2.3.3 Cyclones 4-24
4.2.3.4 Impactors 4-25
4.2.4 Sampling Considerations 4-27
4.2.4.1 Siting Criteria 4-27
4.2.4.2 Averaging Time/Sampling Frequency 4-28
4.2.4.3 Collection Substrates 4-30
4.2.4.4 Chemical Speciation Sampling 4-31
4.2.4.5 Data Corrections/Analyses 4-34
4.2.5 Performance Specifications 4-35
4.2.5.1 Approaches 4-35
4.2.5.2 Performance Testing 4-37
4.2.6 Reference and Equivalent Method Program 4-41
4.2.7 Determination of Size Distribution 4-43
4.2.7.1 Cascade Impactors 4-43
4.2.7.2 Single Particle Samplers 4-49
4.2.8 Automated Sampling 4-51
4.2.8.1 Smoke Shade 4-52
4.2.8.2 Coefficient of Haze 4-54
4.2.8.3 Tapered Element Oscillating Microbalance® Sampler . . . 4-55
4.2.8.4 Beta Gauge 4-58
4.2.8.5 Nephelometer 4-60
4.2.9 Specialized Sampling 4-65
4.2.9.1 Personal Exposure Sampling 4-65
4.2.9.2 Receptor Model Sampling 4-68
4.2.9.3 Particle Acidity 4-69
4.2.10 Measurement Methods Comparisons 4-71
4.2.10.1 Nitrate 4-71
4.2.10.2 Carbonaceous Particulate Matter 4-75
4.3 ANALYSIS OF PARTICULATE MATTER 4-75
4.3.1 Mass Measurement Methods 4-79
4.3.2 Physical Analysis 4-80
4.3.2.1 X-Ray Fluorescence of Trace Elements 4-81
4.3.2.2 Particle Induced X-Ray Emission of Trace Elements 4-87
4.3.2.3 Instrumental Neutron Activation Analysis of Trace Elements 4-90
4.3.2.4 Microscopy Analysis of Particle Size, Shape, and Composition 4-91
4.3.3 Wet Chemical Analysis 4-93
4.3.3.1 Ion Chromatographic Analysis for Chloride, Nitrate, and Sulfate 4-94
4.3.3.2 Automated Colorimetric Analysis for Ammonium, Nitrate, and Sulfate 4-97

TABLE OF CONTENTS (cont'd)

Page

4.3.3.3 Atomic Absorption Spectrophotometric and Inductive Coupled Plasma Atomic Emission Spectrophotometry Analyses for Trace Elements 4-99
4.3.4 Organic Analysis 4-100
4.3.4.1 Analysis of Organic Compounds 4-100
4.3.4.2 Analysis of Organic and Elemental Carbon 4-103
4.3.4.3 Organic Aerosol Sampling Artifacts 4-105
4.3.5 Methods Validation 4-113
4.4 BIOAEROSOLS SAMPLING AND ANALYSIS 4-114
4.4.1 Analytical Methods 4-114
4.4.2 Sample Collection Methods 4-115
4.5 SUMMARY 4-116
4.5.1 PM_{10} Sampling 4-118
4.5.2 Fine Particle Sampling 4-119
4.5.3 Concentration Corrections to Standard Conditions 4-119
4.5.4 Performance Versus Design Specifications for Sampling Systems 4-120
4.5.5 Automated Sampling 4-120
4.5.6 Particulate Matter Samplers for Special Applications 4-121
REFERENCES 4-122

5. SOURCES AND EMISSIONS OF ATMOSPHERIC PARTICLES 5-1
5.1 INTRODUCTION 5-1
5.2 SOURCES OF PRIMARY PARTICULATE MATTER 5-4
5.2.1 Wind Erosion and Fugitive Dust 5-4
5.2.2 Stationary Sources 5-14
5.2.3 Mobile Sources 5-19
5.2.4 Biomass Burning 5-25
5.2.5 Sea-Salt Production and Other Natural Sources of Aerosol 5-27
5.3 SOURCES OF SECONDARY PARTICULATE MATTER (SULFUR DIOXIDE, NITROGEN OXIDES, AND ORGANIC CARBON) 5-29
5.4 EMISSIONS ESTIMATES FOR PRIMARY PARTICULATE MATTER AND SULFUR DIOXIDE, NITROGEN OXIDES, AND VOLATILE ORGANIC COMPOUNDS IN THE UNITED STATES 5-34
5.5 APPLICATIONS AND LIMITATIONS OF EMISSIONS INVENTORIES AND RECEPTOR MODELS 5-47
5.5.1 Uncertainties in Emissions Estimates 5-47
5.5.2 Receptor Modeling Methods 5-50
5.5.3 Source Contributions to Ambient Particles Derived by Receptor Models 5-59
5.6 SUMMARY AND CONCLUSIONS 5-66
REFERENCES 5-70

TABLE OF CONTENTS (cont'd)

Page

6. ENVIRONMENTAL CONCENTRATIONS 6-1
6.1 BACKGROUND, PURPOSE, AND SCOPE 6-1
6.1.1 Dimensionality and Structuring of the Aerosol Data Space 6-2
6.1.2 Spatial Pattern and Scales 6-3
6.1.3 Temporal Pattern and Scales 6-3
6.1.4 Space-Time Relationships 6-4
6.1.5 Particle Size Distribution 6-7
6.1.6 Aerosol Chemical Composition 6-8
6.2 GLOBAL AND CONTINENTAL SCALE AEROSOL PATTERN 6-9
6.3 U.S. NATIONAL AEROSOL PATTERN AND TRENDS 6-14
6.3.1 Nonurban National Aerosol Pattern 6-14
6.3.1.1 Nonurban $PM_{2.5}$ Mass Concentrations 6-15
6.3.1.2 Nonurban Particulate Matter Coarse Mass Concentrations 6-15
6.3.1.3 Nonurban PM_{10} Mass Concentrations 6-17
6.3.1.4 $PM_{2.5}/PM_{10}$ Ratio at Nonurban Sites 6-20
6.3.1.5 Nonurban Fine-Particle Chemistry 6-20
6.3.1.6 Seasonality of the Nonurban Chemistry 6-25
6.3.1.7 Background Concentrations of Particle Mass and Chemical Composition 6-32
6.3.2 Urban National Aerosol Pattern—Aerometric Information Retrieval System 6-46
6.3.2.1 National Pattern and Trend of Aerometric Information Retrieval System PM_{10} 6-48
6.3.2.2 Eastern U.S. PM_{10} Pattern and Trend 6-52
6.3.2.3 Western U.S. PM_{10} Pattern and Trend 6-54
6.3.2.4 Short-Term Variability of PM_{10} Concentrations 6-57
6.3.2.5 Aerometric Information Retrieval System $PM_{2.5}$ Concentrations. 6-60
6.3.2.6 Other National Surveys 6-60
6.3.3 Comparison of Urban and Nonurban Concentrations 6-63
6.4 REGIONAL PATTERNS AND TRENDS 6-67
6.4.1 Regional Aerosol Pattern in Eastern New York, New Jersey, and the Northeast 6-68
6.4.1.1 Nonurban Size and Chemical Composition in the Northeast 6-70
6.4.1.2 Urban Aerosols in the Northeast 6-71
6.4.2 Regional Aerosol Pattern in the Southeast 6-73
6.4.2.1 Nonurban Size and Chemical Composition in the Southeast 6-73
6.4.2.2 Urban Aerosols in the Southeast 6-76
6.4.3 Regional Aerosol Pattern in the Industrial Midwest 6-78
6.4.3.1 Nonurban Size and Chemical Composition in the Industrial Midwest 6-81

TABLE OF CONTENTS (cont'd)

Page

6.4.3.2 Urban Aerosols in the Industrial Midwest 6-82
6.4.4 Regional Aerosol Pattern in the Upper Midwest 6-84
6.4.4.1 Nonurban Size and Chemical Composition in the Upper Midwest 6-84
6.4.4.2 Urban Aerosols in the Upper Midwest 6-88
6.4.5 Regional Aerosol Pattern in the Southwest 6-90
6.4.5.1 Nonurban Size and Chemical Composition in the Southwest 6-90
6.4.5.2 Urban Aerosols in the Southwest 6-90
6.4.6 Regional Aerosol Pattern in the Northwest 6-94
6.4.6.1 Nonurban Size and Chemical Composition in the Northwest 6-96
6.4.6.2 Urban Aerosols in the Northwest 6-96
6.4.7 Regional Aerosol Pattern in Southern California 6-100
6.4.7.1 Nonurban Size and Chemical Composition in Southern California 6-100
6.4.7.2 Urban Aerosols in Southern California 6-102
6.5 SUBREGIONAL AEROSOL PATTERNS AND TRENDS 6-105
6.5.1 Subregional Aerosol Pattern in the Northeast 6-105
6.5.1.1 Shenandoah National Park 6-105
6.5.1.2 Washington, District of Columbia 6-108
6.5.1.3 Comparison of Nonurban to Urban Aerosols 6-110
6.5.1.4 New York City, New York 6-112
6.5.1.5 Philadelphia, Pennsylvania 6-116
6.5.1.6 Whiteface Mountain, New York 6-119
6.5.2 Subregional Aerosol Pattern in the Southeast 6-119
6.5.2.1 Atlantic Coast States 6-119
6.5.2.2 Texas and Gulf States 6-120
6.5.2.3 Atlanta 6-124
6.5.2.4 Great Smoky Mountains 6-124
6.5.3 Subregional Aerosol Pattern in the Industrial Midwest 6-124
6.5.3.1 Pittsburgh, Pennsylvania 6-125
6.5.3.2 St. Louis, Missouri 6-128
6.5.3.3 Chicago, Illinois 6-132
6.5.3.4 Detroit, Michigan 6-134
6.5.5 Subregional Aerosol Pattern in the Southwest 6-135
6.5.5.1 El Paso, Texas 6-135
6.5.5.2 Phoenix and Tucson, Arizona 6-137
6.5.5.3 Grand Canyon National Park 6-140
6.5.6 Subregional Aerosol Pattern in the Northwest 6-140
6.5.6.1 South Lake Tahoe 6-141
6.5.6.2 Salt Lake City, Utah, Subregion 6-143
6.5.6.3 Denver, Colorado 6-145
6.5.6.4 Northern Idaho-Western Montana Subregion 6-145

TABLE OF CONTENTS (cont'd)

Page

6.5.6.5 Washington-Oregon Subregion 6-148
6.5.6.6 Other Northwestern Locations 6-151
6.5.7 Subregional Aerosol Pattern in Southern California 6-151
6.5.7.1 San Joaquin Basin 6-151
6.5.7.2 Los Angeles-South Coast Air Basin-Southeastern Desert Air Basin 6-154
6.6 CHEMICAL COMPOSITION OF PARTICULATE MATTER AEROSOLS AT URBAN AND NONURBAN SITES 6-163
6.7 ACID AEROSOLS 6-168
6.7.1 Introduction 6-168
6.7.2 Geographical Distribution 6-169
6.7.3 Spatial Variation (Regional-Scale) 6-169
6.7.4 Spatial Variation (City-Scale) 6-172
6.7.5 Seasonal Variation 6-173
6.7.6 Diurnal Variation 6-174
6.7.7 Indoor and Personal Concentrations 6-176
6.8 NUMBER CONCENTRATION OF ULTRAFINE PARTICLES 6-177
6.8.1 Introduction 6-177
6.8.2 Ultrafine Particle Number-Size Distribution 6-177
6.8.3 Relation of Particle Number to Particle Mass 6-182
6.8.4 Conclusion 6-184
6.9 AMBIENT CONCENTRATIONS OF ULTRAFINE METALS 6-186
6.9.1 Introduction 6-186
6.9.2 Formation of Ultrafine Particles 6-187
6.9.3 Techniques for Collecting and Analyzing Ultrafine Metals 6-190
6.9.4 Observations of Very Fine Metals 6-193
6.9.4.1 Stack and Source-Enriched Aerosols 6-193
6.9.4.2 Ambient Aerosols 6-194
6.9.5 Conclusions 6-205
6.10 FINE AND COARSE PARTICULATE MATTER TRENDS AND PATTERNS 6-206
6.10.1 Daily and Seasonal Variability in $PM_{2.5}$ and PM_{10} 6-207
6.10.2 Fine and Coarse Particulate Matter Trends and Relationships 6-216
6.10.2.1 Visual Range/Haziness 6-216
6.10.2.2 Interagency Monitoring of Protected Visual Environments 6-219
6.10.2.3 Philadelphia 6-221
6.10.2.4 Harvard Six-Cities Study 6-223
6.10.2.5 Aerometric Information Retrieval System 6-228
6.10.2.6 California Sites 6-228
6.10.3 Interrelations and Correlations 6-228
6.10.3.1 Upper Range of Concentration for Various Particulate Matter Size Fractions 6-231

TABLE OF CONTENTS (cont'd)

Page

6.10.3.2 Relationships Among $PM_{2.5}$, $PM_{(10-2.5)}$, PM_{10}, and Total Suspended Particles in Philadelphia 6-242
6.10.3.3 Correlations Between $PM_{2.5}$, $PM_{(10-2.5)}$, and PM_{10} . . 6-249
6.10.3.4 Fine Fractions 6-249
6.11 SUMMARY AND CONCLUSIONS 6-251
REFERENCES 6-259

APPENDIX 6A: TABLES OF CHEMICAL COMPOSITION OF PARTICULATE MATTER 6A-1

7. HUMAN EXPOSURE TO PARTICULATE MATTER: RELATIONS TO AMBIENT AND INDOOR CONCENTRATIONS 7-1
7.1 INTRODUCTION 7-1
7.1.1 Ambient Particulate Matter Concentration as a Surrogate for Particulate Matter Dosage 7-3
7.1.2 General Concepts for Understanding Particulate Matter Exposure and Microenvironments 7-5
7.1.3 Summary of State-of-Knowledge in the 1982 Criteria Document 7-9
7.2 INDOOR CONCENTRATIONS AND SOURCES OF PARTICULATE MATTER 7-10
7.2.1 Introduction 7-10
7.2.2 Concentrations of Particles in Homes and Buildings 7-12
7.2.2.1 Particle Concentrations in Homes: Large-Scale Studies in the United States 7-12
7.2.2.2 Other Studies of Particulate Matter Indoors 7-44
7.2.2.3 Personal Exposures to Environmental Tobacco Smoke 7-55
7.2.2.4 The Fraction of Outdoor Air Particles Penetrating Indoors 7-56
7.2.2.5 Studies of Particulate Matter in Buildings 7-61
7.2.3 Indoor Air Quality Models and Supporting Experiments 7-67
7.2.3.1 Mass Balance Models 7-67
7.2.4 Summary of Indoor Particulate Matter Studies 7-68
7.2.5 Bioaerosols 7-70
7.2.5.1 Plant Aerosols 7-71
7.2.5.2 Animal Aerosols 7-74
7.2.5.3 Fungal Aerosols 7-76
7.2.5.4 Bacterial Aerosols 7-78
7.2.5.5 Viral Aerosols 7-79
7.2.5.6 Ambient and Indoor Air Concentrations of Bioaerosols 7-80

TABLE OF CONTENTS (cont'd)

Page

7.3 DIRECT METHODS OF MEASUREMENT OF HUMAN PARTICULATE MATTER EXPOSURE BY PERSONAL MONITORING 7-81
7.3.1 Personal Monitoring Artifacts 7-81
7.3.2 Characterization of Particulate Matter Collected by Personal Monitors 7-82
7.3.3 Microscale Variation and the Personal Cloud Effect 7-82
7.4 NEW LITERATURE ON PARTICLE EXPOSURES SINCE 1981 7-83
7.4.1 Personal Exposures in U.S. Studies 7-83
7.4.1.1 The Particle Total Exposure Assessment Methodology Study 7-88
7.4.2 Personal Exposures in International Studies 7-97
7.4.2.1 Personal Exposures in Tokyo (Itabashi Ward), Japan 7-99
7.4.2.2 Personal Exposures in the Netherlands 7-100
7.4.2.3 Reanalysis of Phillipsburg, New Jersey, Data 7-103
7.4.2.4 Overview of Comparison of Personal Exposure to Ambient Particulate Matter Concentrations 7-105
7.4.3 Personal Exposures to Constituents of Particulate Matter 7-105
7.5 INDIRECT MEASURES OF EXPOSURE 7-109
7.5.1 Time-Weighted-Averages of Exposure 7-109
7.5.2 Personal Exposure Models Using Time-Weighted Averages of Indoor and Outdoor Concentrations of Particulate Matter 7-110
7.6 DISCUSSION 7-114
7.6.1 Relation of Individual Exposures to Ambient Concentration 7-114
7.6.2 Relation of Community Particulate Matter Exposure to Ambient Particulate Matter Concentration 7-119
7.6.2.1 Methodology 7-120
7.6.3 U.S. Environmental Protection Agency Analysis of Data Sets 7-134
7.6.3.1 Tokyo, Japan, Data Set 7-134
7.6.3.2 Phillipsburg, New Jersey, Data Set 7-134
7.6.3.3 Beijing, China, Data Set 7-138
7.6.3.4 Riverside, California, Data Set 7-139
7.6.3.5 Azusa, California, Data Set 7-140
7.6.4 Discussion of Statistical Analyses: Mean Personal Exposure Monitor Versus Mean SAM 7-144
7.7 IMPLICATIONS FOR PARTICULATE MATTER AND MORTALITY MODELING 7-149
7.7.1 Relative Toxicity of Ambient Particulate Matter and Indoor Particulate Matter 7-151
7.7.2 Summary: Linkage of Ambient Concentrations of Particulate Matter to Personal Exposures to Particulate Matter 7-154

TABLE OF CONTENTS (cont'd)

Page

7.8 SUMMARY AND CONCLUSIONS 7-160
REFERENCES 7-166

LIST OF TABLES

Number		Page
3-1	Lognormal Parameters for Ambient Aerosols	3-24
3-2	Henry's Law Coefficients of Some Atmospheric Gases Dissolving in Liquid Water	3-47
3-3	Some Secondary Organic Compounds Identified in Ambient Particles in Urban Air	3-77
3-4	Predicted Percent Contribution to Secondary Organic Aerosol Concentrations at Los Angeles	3-79
3-5	Amount of Secondary Aerosol Produced in a Typical Los Angeles Smog Episode According to Functional Groups	3-79
3-6	Reactivity Scale for the Electrophilic Reactions of Polycyclic Aromatic Hydrocarbons	3-82
3-7	Values of Log P_L^o for Various Polycyclic Aromatic Hydrocarbons at 20 °C	3-87
3-8	m_p Values for Polycyclic Aromatic Hydrocarbons Sorbing to UPM in Osaka, Japan	3-87
3-9	Effects of Three Types of Artifacts on Volume-Averaged Values of ϕ Measured Using a Filter/Adsorbent Sampler	3-88
3-10	Concentration Ranges of Various Elements Associated with Particulate Matter in the Atmosphere	3-91
3-11	Compounds Observed in Aerosols by a Roadway at Argonne National Laboratory	3-93
3-12	Compounds Observed in Aerosols in a Forested Area, State College, Pennsylvania	3-93
3-13	Recent Field Studies of α-Mesoscale Transport and Trajectory Model	3-102
3-14	Scavenging Ratios	3-142
3-15	Comparison of Ambient Fine- and Coarse-Mode Particles	3-145
3-16	Relative Humidity of Deliquescence and Crystallization for Several Atmospheric Salts	3-170

LIST OF TABLES (cont'd)

Number		Page
3-17	Summary of Hygroscopic Growth Factors	3-175
3-18	Comparison of Sulfate Concentration and Mass Mean Diameters of Aerosols for Days with Higher and Lower Relative Humidity	3-181
4-1	U.S. Environmental Protection Agency-Designated Reference and Equivalent Methods for PM_{10}	4-44
4-2	Instrumental Detection Limits for Particles on Filters	4-77
4-3	Minimum Detectable Limits for X-Ray Fluorescence Analysis of Air Filters	4-84
4-4	Instrumental Neutron Activation Analysis Counting Scheme and Elements Measured	4-91
4-5	Overview of Analytical Methods	4-114
5-1A	Constituents of Atmospheric Fine Particles and Their Major Sources	5-2
5-1B	Constituents of Atmospheric Coarse Particles and Their Major Sources	5-3
5-2	Average Abundances of Major Elements in Soil and Crustal Rock	5-8
5-3	Composition of Fine Particles Released by Various Stationary Sources in the Philadelphia Area	5-15
5-4	Fractional Organic and Elemental Carbon Abundances in Motor Vehicle Emissions	5-21
5-5	Phoenix $PM_{2.5}$ Motor Vehicle Emissions Profiles	5-22
5-6	Nationwide Primary PM_{10} Emission Estimates from Mobile and Stationary Sources, 1985 to 1993	5-36
5-7	Miscellaneous and Natural Source Primary PM_{10} Emission Estimates, 1985 to 1993	5-37
5-8	Nationwide Sulfur Oxides Emission Estimates, 1984 to 1993	5-38
5-9	Nationwide Nitrogen Oxide Emission Estimates, 1984 to 1993	5-39
5-10	Nationwide Volatile Organic Compound Emission Estimates, 1984 to 1993	5-40

LIST OF TABLES (cont'd)

Number		Page
5-11	Projected Trends in Particulate Matter, Sulfur Dioxide, and Oxides of Nitrogen Emissions	5-43
5-12	Receptor Model Source Contributions to PM_{10}	5-62
6-1	Spatial Regions and Scales	6-3
6-2	Annual Average Concentrations and Chemical Composition from Interagency Monitoring of Protected Visual Environments Monitoring Sites	6-38
6-3	Annual Summer and Winter Concentrations from Interagency Monitoring of Protected Visual Environments Monitoring Sites	6-40
6-4	Summary of Annual and Seasonal Average Ranges of Background Concentration Levels of PM_{10} and $PM_{2.5}$	6-44
6-5	Maximum $SO_4^=$ and Hydrogen Ion Concentrations Measured at North American Sites	6-170
6-6	Regulated Metals and the Volatility Temperature	6-188
6-7	Composition of the Aerosols Present at Grand Canyon National Park in the Summer of 1984 for the Sulfate Episodes of August 15 and 16	6-197
6-8	Measurements of Fine and Very Fine Metals	6-198
6-9	Measurements of Fine and Very Fine Metals (Lead and Nickel)	6-201
6-10	Comparison of Selected Species at Shenandoah National Park; Washington, District of Columbia; San Gorgonio Wilderness, California; and Grand Canyon National Park During Summer 1993	6-204
6-11	Maximum Value; Second, Third, Fourth, and Fifth Highest Values; 98th and 95th Percentile Values; 50th Percentile Value; and the Difference Between the Median and the Maximum Values and the Number of Measurements Available from Eight California Air Resources Board Sites: $PM_{2.5}$, $PM_{(10-2.5)}$, and PM_{10}	6-240
6-12	Maximum Value; Second, Third, Fourth, and Fifth Highest Values; 98th and 95th Percentile Values; 50th Percentile Value; and the Difference Between the Median and the Maximum Values and the Number of Measurements Available for Sites in Philadelphia from 1979 to 1995: $PM_{2.5}$, $PM_{(10-2.5)}$, PM_{10}, and Total Suspended Particles	6-241

LIST OF TABLES (cont'd)

Number		Page
6-13	Relationships Between PM_x ($PM_{2.5}$ or PM_{10}) and Total Suspended Particles as a Function of Total Suspended Particle Concentration Levels for Several Sites in Philadelphia: Ratio of PM_x to Total Suspended Particles and Coefficient of Determination	6-248
6-14	Means and Standard Deviations for $PM_{2.5}$, $PM_{10-2.5)}$, and PM_{10} and Coefficients of Determination Between Pairs for Eight California Air Resources Board Sites During the Period 1989 to 1990	6-250
6-15	Means and Standard Deviations for $PM_{2.5}$, $PM_{(10-2.5)}$, PM_{10}, and Total Suspended Particles and Coefficients of Determination Between Pairs for Several Sites in Philadelphia During Periods from 1979 to 1995	6-251
6-16	$PM_{2.5}/PM_{10}$ (Fraction of PM_{10} Contributed by $PM_{2.5}$)	6-252
6A-1a	Summary of $PM_{2.5}$ Studies	6A-2
6A-1b	Summary of Coarse Fraction Studies	6A-3
6A-1c	Summary of PM_{10} Studies	6A-4
6A-2a	$PM_{2.5}$ Composition for the United States	6A-13
6A-2b	Coarse Particle Composition for the United States	6A-21
6A-2c	PM_{10} Composition for the United States	6A-29
6A-3	Selected Ratios of Particulate Matter Composition by Geographic Region	6A-37
6A-4a	Site-to-Site Variability of $PM_{2.5}$ Concentrations	6A-38
6A-4b	Site-to-Site Variability of PM_{10} Concentrations	6A-39
7-1	Concentrations of Particles in Homes of Children Participating in the Harvard Six-City Study	7-14
7-2a	Reconstructed Source Contributions to Indoor $PM_{2.5}$ Mass for Steubenville, Ohio	7-19
7-2b	Reconstructed Source Contributions to Indoor $PM_{2.5}$ Mass for Portage, Wisconsin	7-19

LIST OF TABLES (cont'd)

Number		Page
7-3	Weighted Summary Statistics by New York County for Respirable Suspended Particulate Concentrations	7-21
7-4	Weighted Analysis of Variance of Respirable Suspended Particulate Concentrations in the Main Living Area of Homes Versus Source Classification	7-22
7-5	Respirable Suspended Particulate Concentration in Homes by Source Category	7-22
7-6	Regressions of Indoor on Outdoor PM_{10} and $PM_{2.5}$ Concentrations: Particle Total Environmental Assessment Methodology Prepilot Study	7-25
7-7	Weighted Distributions of Personal, Indoor, and Outdoor Particle Concentrations	7-27
7-8	Weighted Distributions of $PM_{2.5}/PM_{10}$ Concentration Ratio	7-28
7-9	Stepwise Regression Results for Indoor Air Concentrations of PM_{10} and $PM_{2.5}$ Coefficients	7-34
7-10	Penetration Factors, Decay Rates, and Source Strengths: Nonlinear Estimates	7-36
7-11	Indoor-Outdoor Mean Concentrations of Fine Particles in Three Large-Scale Studies	7-42
7-12	Influence of Recent Cigarette Smoking on Indoor Concentrations of Particulate Matter	7-45
7-13	Indoor Average $PM_{2.5}$ and PM_{10} by Reported Smoking in the Home and Evaporative Cooler Use During Sampling Week for Tuscon, Arizona, Study	7-47
7-14	Regression of Indoor on Outdoor PM_{10} Concentrations: THEES Study, Phillipsburg, New Jersey	7-52
7-15	Median Values for Environmental Tobacco Smoke Markers	7-56
7-16	Fraction of Concentration of Outdoor Particles Estimated To Be Found Indoors at Equilibrium: Results from the Particle Total Exposure Assessment Methodology Study	7-62

LIST OF TABLES (cont'd)

Number		Page
7-17	Smoking, Nonsmoking, and Outdoor RSP Concentrations and Ratios	7-64
7-18	An Overview of Organisms, Aerosols, and Disease Agents	7-71
7-19	Quantile Description of Personal, Indoor, and Outdoor $PM_{3.5}$ Concentrations, by Location in Two Tennessee Communities	7-85
7-20	Regression Equation of Those Individuals Having Statistically Significant Relationships of Exposure with Outdoor Air Concentrations	7-87
7-21a	Particle Total Exposure Assessment Methodology Prepilot Study: 24-Hour PM_{10} Concentrations	7-90
7-21b	Particle Total Exposure Assessment Methodology Prepilot Study: 24-Hour $PM_{2.5}$ Concentrations	7-91
7-22	Regressions of Personal Exposure on Indoor and Outdoor PM_{10} and $PM_{2.5}$ Concentrations: Particle Total Exposure Assessment Methodoloy Prepilot Study	7-92
7-23	Population-Weighted Concentrations and Standard Errors, Particle Total Environmental Methodology Study	7-94
7-24	Summary of World Health Organization/United Nations Environment Programme Global Environment Monitoring System/Personal Exposure Pilot Study Results	7-99
7-25	Summary of Correlations Between PM_{10} Personal Exposures of Seven Tokyo Residents ant the PM_{10} Measured Outdoors Under the Eaves of Their Homes, and the Particulate Matter Measured at the Itabashi Monitoring Station	7-102
7-26	Comparison of Personal Exposure Monitor Exposure of Individuals to the Simultaneous Ambient Particulate Matter Concentration in Several U.S. and Foreign Cities	7-106
7-27	Forty-eight-Hour Personal Exposure to PM_{10}	7-121
7-28	Parameter Estimates for 48-Hour PM_{10} Personal Exposure Monitor Data Taken by Subjects Living Near a Main Road in Tokyo	7-124
7-29	Parameter Estimates for 48-Hour PM_{10} Perosonal Exposure Monitor Data Taken by Subjects Living Farther from the Same Tokyo Main Road Described in Table 7-28	7-125

LIST OF TABLES (cont'd)

Number		Page
7-30	Average Personal Exposure Data Compared with Itabashi Site Monitor	7-126
7-31	Results of Linear Regression Analysis, Assuming a Normal Error Using the Exposure Data from Japan	7-126
7-32	Results of Linear Regression Analysis, Assuming a Lognormal Error Using the Exposure Data from Japan	7-127
7-33	Results of an Orthogonal Regression Analysis to the Exposure Data from Japan	7-129
7-34	Results of an ANOVA Analysis of the Exposure Data from Japan	7-133
7-35	Covariance and Correlation Matrix for Average Personal Exposure and Ambient Exposures from Japan	7-134
7-36	Summary of Results of the Analysis of the Exposure Data from Japan	7-135
7-37	Personal Exposure Suspended Particulate Matter Data from Phillipsburg, New Jersey	7-136
7-38	Results of an ANOVA Analysis of the Personal Exposure Data of Phillipsburg, New Jersey	7-137
7-39	SAM Site Concentrations, PM_{10} Data, from Phillipsburg, New Jersey	7-137
7-40	Results of an ANOVA Analysis of the Site Exposure Data of Phillipsburg, New Jersey	7-138
7-41	Average Personal PM_{10} Exposure Data Compared with the Site Exposure Data for Phillipsburg, New Jersey	7-138
7-42	Results of the Analysis of the Exposure Data from Phillipsburg, New Jersey	7-140
7-43	Personal and Ambient Exposure Data for Beijing, China	7-141
7-44	Results of the Linear Regression Analysis for the Beijing, China, Exposure Data	7-141
7-45	Estimated Mean Vector, Covariance Matrix, and Correlation Matrix of Personal Exposure PM_{10} Data from Riverside, California	7-142

LIST OF TABLES (cont'd)

Number		Page
7-46	Results of an ANOVA Analysis of the Personal Exposure Data of Riverside, California	7-143
7-47	Results of the Analysis of the Exposure Data from Riverside, California	7-143
7-48	Average 24-Hour PM_{10} Personal Exposure Data Compared with the Personal Exposure Monitor-SAM Site Exposure Data for Riverside, California	7-145
7-49	Results of the Linear Regression Analysis of the Exposure Data from Azusa, California	7-146

LIST OF FIGURES

Number		Page
3-1	Number of particles as a function of particle diameter	3-5
3-2	Particle volume distribution as a function of particle diameter	3-6
3-3	An idealized distribution of ambient particulate matter showing fine- and coarse-mode particles and the fractions collected by size-selective samplers	3-10
3-4	Specified particle penetration through an ideal inlet for four different size-selective sampling criteria	3-13
3-5	Particle size related to relative humidity	3-15
3-6	Ion concentration as a function of particle size, measured in Claremont, California	3-18
3-7	Model dust emissions for the United States	3-37
3-8	Diffusion constants and settling velocities for particles	3-39
3-9	Particle deposition from wind tunnel studies	3-40
3-10	Sedimentation and inertia effects on large particle deposition	3-40
3-11	Comparison of observed hydrogen peroxide depletions and observed sulfate yields	3-61
3-12	Extrapolations from correlations of wind-tunnel-measured deposition velocities for z = 1 m, densities of 1, 4, and 11.5 g cm^{-3}	3-130
3-13	An example of histogram display and fitting to log-normal functions for particle-counting size-distribution data	3-149
3-14	An example of an effective display of impactor data	3-150
3-15	Size distributions of sulfate, Long Beach, June 1987, showing use of fitted log-normal distributions to describe diurnal variations in size and concentration	3-151
3-16	Effect of changing endpoints	3-152

LIST OF FIGURES (cont'd)

Number		Page
3-17	These size distributions, obtained during a U.S. Environmental Protection Agency study of the Denver brown cloud, represent one of the few efforts to compare particle-counting and particle-collection size-distribution measurements	3-154
3-18	Grand average volume-size distributions from the Aerosol Characterization Experiment in 1972	3-157
3-19	Volume-size distribution taken in the midwestern United States near the Cumberland Power Plant in Tennessee	3-158
3-20	Examples of size distribution histograms for total mass, sulfate, and iron obtained at two visibility levels using an Andersen impactor	3-159
3-21	Impactor size distribution measurement generated by Lundgren et al. with the Wide Range Aerosol Classifier: Philadelphia and Phoenix	3-160
3-22	Example of aged and fresh coarse-mode particle-size distributions	3-161
3-23	Size distributions reported by Noll and co-workers from the Chicago area using an Andersen impactor for the smaller particles and a Noll Rotary Impactor for the larger particles	3-163
3-24	Size distribution of dust generated by driving a truck over an unpaved test track	3-165
3-25	Size distribution of emissions from a pulverized-coal power plant and the particle size distributions remaining after several types of control devices	3-166
3-26	Size distributions from a fluidized-bed, pulverized coal combustor, after initial cleanup by a cyclone collector and after final cleanup by a baghouse	3-167
3-27	Particle growth curves showing fully reversible hygroscopic growth of sulfuric acid particles, deliquescent growth of ammonium sulfate particles at about 80% relative humidity, hygroscopic growth of ammonium sulfate solution droplets at relative humidity greater than 80%, and hysteresis until the crystallization point is reached	3-170
3-28	Theoretical predictions and experimental measurements of growth of NH_4HSO_4 and ammonium sulfate particles at relative humidity between 95 and 100%	3-172

LIST OF FIGURES (cont'd)

Number		Page
3-29	Tandem Differential Mobility Analyzer measurements of the sensitivity of particle size to relative humidity at Claremont, California	3-174
3-30	Example of growth in particle size due primarily to increases in relative humidity from Uniontown, Pennsylvania	3-176
3-31	Mass size distribution of nonvolatile aerosol material	3-178
3-32	Example of particle-counting volume distribution obtained in Claremont, California	3-180
3-33	Relative humidity versus sulfur, during the 1986 Carbonaceous Species Methods Comparison Study, for particles with D_{ae} greater than 0.56 μm	3-182
3-34	Data from the South Coast Air Quality Study	3-184
3-35	Log-log plot of sulfate mode concentration versus aerodynamic mode diameter from Claremont, California, during the summer South Coast Air Quality Study	3-185
3-36	Typical results of size-distribution measurements taken with a Berner impactor in a Vienna street with heavy automotive traffic	3-186
4-1	Characteristics of aerosol measurement instruments	4-3
4-2	American Conference of Governmental Industrial Hygienists, British Medical Research Council, and International Organization for Standardization size-selective sampling criteria	4-7
4-3	Sampling efficiency of Institute for Occupational Medicine ambient inhalable aerosol sampler for three different types of test aerosol	4-9
4-4	Liquid particle sampling effectiveness curves with solid particle points superimposed for the Wedding IP_{10} and the Andersen Samplers Model 321A inlets at eight kilometers per hour	4-14
4-5	Two-stage Sierra Andersen PM_{10} sampler	4-15
4-6	Sampling characteristics of two-stage size-selective inlet for liquid aerosols	4-16

LIST OF FIGURES (cont'd)

Number		Page
4-7	Penetration of particles for 16.67-liters-per-minute dichotomous sampler PM_{10} inlets	4-18
4-8	Collection performance variability illustrating the influence of wind speed for the Andersen 321A PM_{10} inlet	4-19
4-9	Aerosol separation and internal losses for a 2.5-micrometer dichotomous sampler virtual impactor	4-23
4-10	Percent collection as a function of aerodynamic diameter for the U.S. Environmental Protection Agency enhanced method glass cyclone	4-26
4-11	Performance of glass fiber filters compared to greased substrate	4-28
4-12	Schematic diagram of an annular denuder system	4-33
4-13	Measured calibration of the Andersen Cascade Dupactor as compared to that supplied by the manufacturer	4-47
4-14	Internal losses for the Micro-Orifice Uniform Deposit Impactor	4-48
4-15	Rupprecht and Patashnick Tapered Element Oscillating Microbalance® sampler	4-56
4-16	Andersen beta gauge sampler	4-59
4-17	Integrating nephelometer	4-61
4-18	Particle-scattering coefficient per volume concentration as a function of particle size for spherical particles of refractive index 1.5 illuminated by 550-nanometer light	4-62
4-19	Correlation of b_{sp} and fine fraction mass	4-64
4-20	Collection efficiency of the MSP personal aerosol sampler inlet	4-67
4-21	Modified dichotomous sampler	4-70
4-22	Comparison of $PM_{2.5}$ nitrate mass measurements from Teflon® filter versus denuded nylon filter sample collection for Los Angeles, California	4-73
4-23	Comparison of $PM_{2.5}$ nitrate mass measurements from Teflon® filter versus denuded nylon filter sample collection for Claremont, California	4-74

LIST OF FIGURES (cont'd)

Number		Page
4-24	Schematic of a typical X-ray fluorescence system	4-83
4-25	Example of an X-ray fluorescence spectrum	4-86
4-26	Schematic of a particle induced X-ray emission/PESA analysis system	4-89
4-27	Schematic representation of an ion chromatography system	4-95
4-28	Example of an ion chromatogram showing the separation of fluoride, chloride, nitrite, nitrate, phosphate, and sulfate ions	4-96
4-29	Schematic of a typical automated colorimetric system	4-98
4-30	Percent correction for vapor adsorption on quartz fiber filters for submicrometer particle sampling at a face velocity of 40 cm s-1 for 13 samples in Portland, Oregon	4-108
4-31	Two types of filter series used for adsorption artifact corrections	4-109
4-32	Schematic of the BYU Organic Sampling System	4-110
5-1	Size distribution of particles generated in a laboratory resuspension chamber	5-9
5-2	Size distribution of California source emissions, 1986	5-10
5-3	Chemical abundances for $PM_{2.5}$ emissions from paved-road dust in Denver, Colorado	5-12
5-4	Chemical abundances for $PM_{2.5}$ emissions from wood burning in Denver, Colorado	5-26
5-5	Estimates of primary PM_{10} emissions by U.S. Environmental Protection Agency region for 1992	5-46
5-6	Estimates of sulfur dioxide emissions by U.S. Enviromental Protection Agency region for 1992	5-46
6-1	Time scales for particle emissions	6-4
6-2	Relationship of spatial and temporal scales for coarse and fine particles	6-5

LIST OF FIGURES (cont'd)

Number		Page
6-3	Residence time in the lower troposphere for atmospheric particles from 0.1 to 1.0 μm	6-6
6-4	Space-time relationship in urban and mountainous areas	6-7
6-5	Continental scale pattern of aerosols derived from visibility observations over land and satellite monitoring over the oceans: North America	6-10
6-6	Global pattern of oceanic aerosols derived from satellite observations	6-11
6-7	Seasonal pattern of oceanic aerosols derived from satellite observations	6-13
6-8	Fine mass concentration derived from nonurban Interagency Monitoring of Protected Visual Environments/Northeast States for Coordinated Air Use Management networks	6-16
6-9	Coarse mass concentration derived from nonurban Interagency Monitoring of Protected Visual Environments/Northeast States for Coordinated Air Use Management networks	6-18
6-10	PM_{10} mass concentration derived from nonurban Interagency Monitoring of Protected Visual Environments/Northeast States for Coordinated Air Use Management networks	6-19
6-11	Fine fraction of PM_{10} derived from nonurban Interagency Monitoring of Protected Visual Environments/Northeast States for Coordinated Air Use Management networks	6-21
6-12	Yearly average absolute and relative concentrations for sulfate and nitrate	6-23
6-13	Yearly average absolute and relative concentrations for organic carbon and elemental carbon	6-24
6-14	Seasonal pattern of nonurban aerosol concentrations for the entire United States: monitoring locations; PM_{10}, $PM_{2.5}$, and PMCoarse; sulfate, soil, organic carbon, and elemental carbon fractions; and tracers	6-26
6-15	Seasonal pattern of nonurban aerosol concentrations for the eastern United States: monitoring locations; PM_{10}, $PM_{2.5}$, and PMCoarse; sulfate, soil, and organic carbon, and elemental carbon fractions; and tracers	6-29

LIST OF FIGURES (cont'd)

Number | Page

6-16 Seasonal pattern of nonurban aerosol concentrations for the western United States: monitoring locations; PM_{10}, $PM_{2.5}$, and PMCoarse; sulfate, soil, organic carbon, and elemental carbon fractions; and tracers 6-31

6-17 Trend of valid PM_{10} monitoring stations in the Aerometric Information Retrieval System database 6-47

6-18 Aerometric Information Retrieval System PM_{10} quarterly concentration maps using all available data 6-49

6-19 Aerometric Information Retrieval System PM_{10} and $PM_{2.5}$ concentration patterns for the conterminous United States 6-50

6-20 Aerometric Information Retrieval System concentration data for east of the Rockies: monitoring locations; PM_{10} concentration trends; PM_{10} and $PM_{2.5}$ relationship; and PM_{10}, $PM_{2.5}$, and PMCoarse seasonal pattern 6-53

6-21 Aerometric Information Retrieval System concentration data for west of the Rockies: monitoring trends; PM_{10} concentration trends; PM_{10} and $PM_{2.5}$ relationship; and PM_{10}, $PM_{2.5}$, and PMCoarse seasonal pattern 6-55

6-22 Short-term PM_{10} concentration time series for Missoula, Montana, and Knoxville, Tennessee 6-58

6-23 Geographic variation of the standard deviation of the lognormal distribution of PM_{10} concentrations from the Aerometric Information Retrieval System 6-59

6-24 Annual $PM_{2.5}$ concentration pattern obtained from Interagency Monitoring of Protected Visual Environments/Northeast States for Coordinated Air Use Management and Aerometric Information Retrieval System networks 6-61

6-25 Monthly mean concentrations in micrograms per cubic meter of PM_{15}, $PM_{2.5}$, PM_{15}-$PM_{2.5}$, and total sulfate as $(NH_4)_2SO_4$ in Portage, Wisconsin; Topeka, Kansas; Harriman, Tennessee; Watertown, Massachusetts; St. Louis, Missouri; and Steubenville, Ohio 6-62

6-26 Spatial maps of PM_{10} concentration difference between Aerometric Information Retrieval System and Interagency Monitoring of Protected Visual Environments/Northeast States for Coordinated Air Use Management networks 6-64

LIST OF FIGURES (cont'd)

Number		Page
6-27	Urban excess concentrations for the United States, the eastern United States, and the western United States	6-66
6-28	Aerosol regions of the conterminous United States	6-68
6-29	Interagency Monitoring of Protected Visual Environments/Northeast States for Coordinated Air Use Management concentration data for the Northeast: monitoring locations; PM_{10}, $PM_{2.5}$, and PMCoarse; sulfate, soil, organic carbon, and elemental carbon fractions; and tracers	6-69
6-30	Aerometric Information Retrieval System concentration data for the Northeast: monitoring locations; regional PM_{10} concentration trends; PM_{10} and $PM_{2.5}$ relationship; and PM_{10}, $PM_{2.5}$, and PMCoarse seasonal pattern	6-72
6-31	Short-term variation of PM_{10} average for the Northeast	6-74
6-32	Urban excess concentration for the Northeast	6-74
6-33	Interagency Monitoring of Protected Visual Environments/Northeast States for Coordinated Air Use Management concentration data for the Southeast: monitoring locations; PM_{10}, $PM_{2.5}$, and PMCoarse; sulfate, soil, organic carbon, and elemental carbon fractions; and tracers	6-75
6-34	Aerometric Information Retrieval System concentration data for the Southeast: monitoring locations; regional PM_{10} concentration trends; PM_{10} and $PM_{2.5}$ relationship; and PM_{10}, $PM_{2.5}$, and PMCoarse seasonal pattern	6-77
6-35	Short-term variation of PM_{10} average for the Southeast	6-79
6-36	Urban excess concentration for the Southeast	6-79
6-37	Interagency Monitoring of Protected Visual Environments/Northeast States for Coordinated Air Use Management concentration data for the industrial Midwest: monitoring locations; PM_{10}, $PM_{2.5}$, and PMCoarse; sulfate, soil, organic carbon, and elemental carbon fractions; and tracers	6-80
6-38	Aerometric Information Retrieval System concentration data for the industrial Midwest: monitoring locations; regional PM_{10} concentration trends; PM_{10} and $PM_{2.5}$ relationship; and PM_{10}, $PM_{2.5}$, and PMCoarse seasonal pattern	6-83
6-39	Short-term variation of PM_{10} average for the industrial Midwest	6-84

LIST OF FIGURES (cont'd)

Number		Page
6-40	Urban excess concentration for the industrial Midwest	6-85
6-41	Interagency Monitoring of Protected Visual Environments/Northeast States for Coordinated Air Use Management concentration data for the Upper Midwest: monitoring locations; PM_{10}, $PM_{2.5}$, and PMCoarse; sulfate, soil, organic carbon, and elemental carbon fractions; and tracers	6-86
6-42	Aerometric Information Retrieval System concentration data for the Upper Midwest: monitoring locations; regional PM_{10} monitoring trends; PM_{10} and $PM_{2.5}$ relationship; and PM_{10}, $PM_{2.5}$, and PMCoarse seasonal trends	6-87
6-43	Short-term variation of PM_{10} average for the Upper Midwest	6-89
6-44	Urban excess concentration for the Upper Midwest	6-89
6-45	Interagency Monitoring of Protected Visual Environments/Northeast States for Coordinated Air Use Management concentration data for the Southwest: monitoring locations; PM_{10}, $PM_{2.5}$, and PMCoarse; sulfate, soil, organic carbon, and elemental carbon fractions; and tracers	6-91
6-46	Aerometric Information Retrieval System concentration data for the Southwest: monitoring locations; regional PM_{10} monitoring trends; PM_{10} and $PM_{2.5}$ relationship; and PM_{10}, $PM_{2.5}$, and PMCoarse seasonal trends	6-92
6-47	Short-term variation of PM_{10} average for the Southwest	6-93
6-48	Urban excess concentration for the Southwest	6-94
6-49	Interagency Monitoring of Protected Visual Environments/Northeast States for Coordinated Air Use Management concentration data for the Northwest: monitoring locations; PM_{10}, $PM_{2.5}$, and PMCoarse; sulfate, soil, organic carbon, and elemental carbon fractions; and tracers	6-95
6-50	Aerometric Information Retrieval System concentration data for the Northwest: monitoring locations; regional PM_{10} monitoring; PM_{10} and $PM_{2.5}$ relationship; and PM_{10}, $PM_{2.5}$, and PMCoarse seasonal trend	6-97
6-51	Short-term variation of PM_{10} average for the Northwest	6-99
6-52	Urban excess concentration for the Northwest	6-99

LIST OF FIGURES (cont'd)

Number		Page
6-53	Interagency Monitoring of Protected Visual Environments/Northeast States for Coordinated Air Use Management concentration for Southern California: monitoring locations; PM_{10}, $PM_{2.5}$, and PMCoarse; sulfate, soil, organic carbon, and elemental carbon fractions; and tracers	6-101
6-54	Aerometric Information Retrieval System concentrations for Southern California: monitoring locations; regional PM_{10} monitoring trends; PM_{10} and $PM_{2.5}$ relationship; and PM_{10}, $PM_{2.5}$, and PMCoarse seasonal trend	6-103
6-55	Short-term variation of PM_{10} average for Southern California	6-104
6-56	Urban excess concentration for Southern California	6-104
6-57	Interagency Monitoring of Protected Visual Environments/Northeast States for Coordinated Air Use Management concentration for Shenandoah National Park: PM_{10}, $PM_{2.5}$, and PMCoarse; chemical fraction of sulfate, soil, organic carbon, and elemental carbon; and tracers	6-106
6-58	Interagency Monitoring of Protected Visual Environments/Northeast States for Coordinated Air Use Management concentration for Washington, District of Columbia: PM_{10}, $PM_{2.5}$, and PMCoarse; chemical fraction of sulfate, soil, organic carbon, and elemental carbon; and tracer concentrations	6-109
6-59	Excess aerosol concentration at Washington, District of Columbia, compared to Shenandoah National Park: PM_{10}, $PM_{2.5}$, and PMCoarse and concentration of sulfate, soil, organic carbon, and elemental carbon	6-111
6-60	Daily concentration of fine mass and fine sulfur at Washington, District of Columbia, and Shenandoah National Park	6-112
6-61	New York City region: aerosol concentration map, trend, and seasonal pattern	6-113
6-62	Fine, coarse, and PM_{10} particle concentrations at three New York City sites	6-115
6-63	Philadelphia region: aerosol concentration map, trend, and seasonal pattern	6-117
6-64	Seasonal particle concentrations at four Philadelphia sites	6-118

LIST OF FIGURES (cont'd)

Number		Page
6-65	PM_{10} concentration seasonality at Whiteface Mountain and neighboring low-elevation sites	6-120
6-66	Aerosol concentration patterns for Southeast Atlantic Coast states and sites in North Carolina and Florida: monitoring sites, trends, seasonal pattern, North Carolina sites, Florida sites, and seasonal pattern for Winston-Salem	6-121
6-67	Aerosol concentration pattern in Texas and Gulf states	6-122
6-68	Pittsburgh subregion: aerosol concentration map, trends, and seasonal pattern	6-126
6-69	Fine, coarse, and PM_{10} concentration at sites in or near Pittsburgh	6-127
6-70	St. Louis subregion: aerosol concentration map, trends, and seasonal pattern	6-129
6-71	Fine, coarse, and PM_{10} seasonal concentration patterns in or near St. Louis	6-131
6-72	Chicago subregion: aerosol concentration map, trends, and seasonal patterns	6-133
6-73	El Paso subregion: aerosol concentration map, trends, and seasonal pattern	6-136
6-74	Fine, coarse, and PM_{10} concentration patterns in El Paso and San Antonio	6-138
6-75	Phoenix-Tucson subregion: aerosol concentration map, trends, and seasonal pattern	6-139
6-76	Excess aerosol concentration and composition at South Lake Tahoe compared to Bliss State Park	6-142
6-77	Salt Lake City region: aerosol concentration map, trends, seasonal pattern, and seasonal patterns at sites in or near Salt Lake City	6-144
6-78	Northern Idaho-Northwestern Montana subregion: aerosol concentration map, trends, and seasonal pattern	6-146
6-79	PM_{10} concentration patterns at sites in Northern Idaho-Northwestern Montana subregion	6-147

LIST OF FIGURES (cont'd)

Number		Page
6-80	Aerosol concentration patterns in Washington State and Oregon	6-149
6-81	San Joaquin Valley: aerosol concentration map, trends, and seasonal pattern	6-152
6-82	Fine, coarse, and PM_{10} seasonal patterns in the San Joaquin Valley	6-153
6-83	Los Angeles: aerosol concentration map, trends, and seasonal pattern	6-155
6-84	Fine, coarse, and PM_{10} seasonal patterns near Los Angeles	6-157
6-85a	Major constituents of particles measured at sites in the eastern United States, as shown in Tables 6A-2a, 6A-2b, and 6A-2c	6-165
6-85b	Major constituents of particles measured at sites in the central United States, as shown in Tables 6A-2a, 6A-2b, and 6A-2c	6-166
6-85c	Major constituents of particles measured at sites in the western United States, as shown in Tables 6A-2a, 6A-2b, and 6A-2c	6-167
6-86	Mean air pollutant concentrations for days when winds were from the southerly direction, plotted versus population density	6-173
6-87	Average monthly aerosol strong acidity for Year 1 sites of the Harvard 24-City Study	6-174
6-88	Diurnal pattern of sulfate and hydrogen ion at Harriman, Tennessee, weekly pattern and daily average	6-175
6-89	Aerosol number and volume size distributions from an urban site at Long Beach, California	6-178
6-90	Aerosol number and volume size distributions from a background site in the Rocky Mountains, Colorado	6-179
6-91	Number concentrations as a function of time of day at Long Beach, California	6-180
6-92	Number and volume size distributions at the Rocky Mountain site, showing an intrusion of urban air	6-181
6-93	Number and volume and mass size distributions from Los Angeles, California, showing comparison of three measurement techniques	6-183

LIST OF FIGURES (cont'd)

Number		Page
6-94	Relationship between particle number and particle volume	6-185
6-95	Impact of treatment temperature on the enrichment of metals in the fly ash after the thermal treatment of soils from a Superfund site	6-189
6-96	Average normalized concentrations as a function of stage number, for selenium, sulfur, calcium, aluminum, silicon, potassium, molybdenum, tungsten, nickel, and chromium for five BLPI samples from a coal-fired power plant	6-194
6-97	Fine and very fine sulfur at Grand Canyon National Park, summer 1984	6-196
6-98	Concentration, in micrograms per cubic meter, of fine and very fine metals (nickel, selenium, and lead) in Long Beach, California, December 10 through 13, 1987, in four-hour increments	6-199
6-99	Patterns of zinc, arsenic, sulfur, and selenium in the United States	6-203
6-100	Apparent deposition of automotive lead aerosol in the respiratory tract of one of the authors as determined by cascade impactor and Proton-Induced X-ray Emissions as a function of aerodynamic diameter for greater than 4, 4 to 2, 2 to 1, 1 to 0.5, 0.5 to 0.25, and less than 0.25-μm particles of size classes 1 through 6, respectively	6-205
6-101	Concentrations of $PM_{2.5}$ measured at the PBY site in southwestern Philadelphia	6-208
6-102	Concentrations of PM_{10} measured at the PBY site in southwestern Philadelphia	6-209
6-103	Frequency distribution of $PM_{2.5}$ concentrations measured at the PBY site in southwestern Philadelphia	6-210
6-104	Frequency distribution of coarse mode mass derived by difference between PM_{10} and $PM_{2.5}$	6-210
6-105	Frequency distribution of PM_{10} concentrations measured at the PBY site in southwestern Philadelphia	6-211
6-106	Frequency distribution of $PM_{2.5}$ concentrations measured at the Riverside-Rubidoux site	6-212

LIST OF FIGURES (cont'd)

Number		Page
6-107	Frequency distribution of $PM_{(10-2.5)}$ concentrations measured at the Riverside-Rubidoux site	6-213
6-108	Frequency distribution of PM_{10} concentrations calculated as the sum of $PM_{2.5}$ and $PM_{(10-2.5)}$ masses measured at the Riverside-Rubidoux site	6-213
6-109	Concentrations of $PM_{2.5}$ measured at the Riverside-Rubidoux site	6-214
6-110	Concentrations of $PM_{(10-2.5)}$ measured at the Riverside-Rubidoux site	6-215
6-111	Concentrations of PM_{10} measured at the Riverside-Rubidoux site	6-215
6-112	United States trend maps for the 75th percentile extinction coefficient, B_{ext} for winter, spring, summer, and fall	6-218
6-113	Secular haze trends (1960 to 1992) for six eastern U.S. regions, summer and winter	6-220
6-114	Eastern U.S. regional background trend of sulfate indicated by seasonal trend data from Shenadoah and Great Smoky Mountains National Parks	6-222
6-115	Total suspended particle and $PM_{2.5}$ trend data for the city of Philadelphia from the Aerometric Information Retrieval System, IPN, and Harvard database	6-223
6-116	Comparison of fine and coarse particle parameters in Philadelphia in 1983 and 1993: $PM_{2.5}$ and $PM_{(10-2.5)}$ at South Broad Street site, 1983; $PM_{2.5}/PM_{10}$ at South Broad Street site, 1983; $PM_{2.5}$ and $PM_{(10-2.5)}$ at Presbyterian Home site, 1993; and $PM_{2.5}/PM_{10}$ at Presbyterian Home Site, 1993	6-224
6-117	Trend data from the Harvard Six-Cities Study: Steubenville, fine, coarse, PM_{15}, and total suspended particle means; Steubenville, fine, coarse, PM_{15}, and total suspended particle 90th percentiles; St. Louis, fine, coarse, PM_{15}, and total suspended particle means; and St. Louis, fine, coarse, PM_{10}, and total suspended particle 90th percentiles	6-225
6-118	Trend data from Harvard Six-Cities Study: Harriman, fine, coarse, PM_{15}, and total suspended particle means; Harriman, fine, coarse, PM_{15}, and total suspended particle 90th percentiles; Watertown, fine, coarse, PM_{15}, and total suspended particle means; and Watertown, fine, coarse, PM_{15}, and total suspended particle 90th percentiles	6-226

LIST OF FIGURES (cont'd)

Number		Page
6-119	Trend data from Harvard Six-Cities Study: Portage, fine, coarse, PM_{15}, and total suspended particle means; Portage, fine, coarse, PM_{15}, and total suspended particle 90th percentiles; Topeka, fine, coarse, PM_{15}, and total suspended particle means; and Topeka, fine, coarse, PM_{15}, and total suspended particle 90th percentiles	6-227
6-120	Trend data from Aerometric Information Retrieval System: New York City, Site 69, fine, coarse, and PM_{10} means; New York City, Site 69, fine, coarse, and PM_{10} 90th percentiles; New York City, Site 71, fine, coarse, and PM_{10} means; and New York City, Site 71, fine, coarse, and PM_{10} 90th percentiles	6-229
6-121	Trend data from Aerometric Information Retrieval System: Detroit, fine, coarse, and PM_{10} means; Detroit, fine, coarse, and PM_{10} 90th percentiles; St. Louis, fine, coarse, and PM_{10} means; and St. Louis, fine, coarse, and PM_{10} 90th percentiles	6-230
6-122	Trend data from Aerometric Information Retrieval System: Philadelphia, fine, coarse, and PM_{10} means and Philadelphia fine, coarse, and PM_{10} 90th percentiles	6-231
6-123	Trend data from San Jose from California Air Resources Board: fine, coarse, and total means; fine, coarse, and total 90th percentiles; every sixth-day fine and coarse mass for 1991; and fine and coarse mass as a fraction of PM_{10}	6-232
6-124	Trend data from Stockton-Hazelton from California Air Resources Board: fine, coarse, and total means; fine, coarse, and total 90th percentiles; every sixth-day fine and coarse mass for 1991; and fine and coarse mass as a fraction of PM_{10}	6-233
6-125	Trend data from Visalia from California Air Resources Board: fine, coarse, and total means; fine, coarse, and total 90th percentiles; every sixth-day fine and coarse mass for 1991; and fine and coarse mass as a fraction of PM_{10}	6-234
6-126	Trend data from Bakersfield from California Air Resources Board: fine, coarse, and total means; fine, coarse, and total 90th percentiles; every sixth-day fine and coarse mass for 1991; and fine and coarse mass as a fraction of PM_{10}	6-235

LIST OF FIGURES (cont'd)

Number		Page
6-127	Trend data from Azusa from California Air Resources Board: fine, coarse, and total means; fine, coarse, and total 90th percentiles; every sixth-day fine and coarse mass for 1991; and fine and coarse mass as a fraction of PM_{10}	6-236
6-128	Trend data from Riverside-Rubidoux from California Air Resources Board: fine, coarse, and total means; fine, coarse, and total 90th percentiles; every sixth-day fine and coarse mass for 1991; and fine and coarse mass as a fraction of PM_{10}	6-237
6-129	Trend data from Lone Pine from California Air Resources Board: fine, coarse, and total means; fine, coarse, and total 90th percentiles; every sixth-day fine and coarse mass for 1991; and fine and coarse mass as a fraction of PM_{10}	6-238
6-130	Trend data from El Centro from California Air Resources Board: fine, coarse, and total means; fine, coarse, and total 90th percentiles; every sixth-day fine and coarse mass for 1991; and fine and coarse mass as a fraction of PM_{10}	6-239
6-131	$PM_{2.5}$ and total suspended particle (TSP) relationships in Philadelphia, IPN Average, March 1979 to December 1983: comparison of $PM_{2.5}$ with TSP, frequency distribution of $PM_{2.5}$/TSP, comparison of $PM_{2.5}$/TSP with $PM_{2.5}$, and comparison of $PM_{2.5}$/TSP with TSP	6-243
6-132	$PM_{2.5}$ and total suspended particle (TSP) relationships in Philadelphia, IPN, South Broad Site, March 1982 to December 1983: comparison of $PM_{2.5}$ with TSP, frequency distribution of $PM_{2.5}$/TSP, comparison of $PM_{2.5}$/TSP with $PM_{2.5}$, and comparison of $PM_{2.5}$/TSP with TSP	6-244
6-133	$PM_{2.5}$ and total suspended particle (TSP) relationships in Philadelphia, Aerometric Information Retrieval System, 1987 to 1990: comparison of $PM_{2.5}$ with TSP, frequency distribution of $PM_{2.5}$/TSP, comparison of $PM_{2.5}$/TSP with $PM_{2.5}$, and comparison of $PM_{2.5}$/TSP with TSP	6-245
6-134	PM_{10} and total suspended particle (TSP) relationships in Philadelphia, IPN, South Broad Site, March 1982 to December 1983: comparison of PM_{10} with TSP, frequency distribution of PM_{10}/TSP, comparison of PM_{10}/TSP with PM_{10}, and comparison of PM_{10}/TSP with TSP	6-246
6-135	PM_{10} and total suspended particle (TSP) relationships in Philadelphia, Aerometric Information Retrieval System, 1987 to 1990: comparison of PM_{10} with TSP, frequency distribution of PM_{10}/TSP, comparison of PM_{10}/TSP with PM_{10}, and comparison of PM_{10}/TSP with TSP	6-247

LIST OF FIGURES (cont'd)

Number		Page
7-1	Sizes of various types of indoor particles	7-6
7-2	An example of personal exposure to respirable particles	7-11
7-3	The annual mean concentration of respirable particles for the highest and lowest site from the network of indoor and outdoor monitors in each city in the Harvard Six-City Study	7-14
7-4	Distribution percentiles for annual average concentrations of indoor respirable particulate matter by household smoking status and estimated number of cigarette packs smoked in the home during Phase 2 of the Harvard Six-City Study	7-17
7-5	$PM_{2.5}$ in smoking and nonsmoking homes in three of the Harvard Six-City Study sites	7-18
7-6	Cumulative frequency distribution of 24-hour personal, indoor, and outdoor PM_{10} concentrations in Riverside, California	7-29
7-7	Cumulative frequency distribution of 24-hour indoor and outdoor $PM_{2.5}$ concentrations in Riverside, California	7-30
7-8	Forty-eight-day sequence of PM_{10} and coarse particulate matter in Riverside, California, Particle Total Exposure Assessment Methodology study	7-30
7-9	Average indoor and outdoor 12-hour concentrations of PM_{10} during the Particle Total Exposure Assessment Methodology study in Riverside, California	7-32
7-10	Sources of fine particles and thoracic particles in all homes (Riverside, California)	7-38
7-11	Sources of fine particles and thoracic particles in homes with smokers (Riverside, California)	7-39
7-12	Sources of fine particles and thoracic particles for homes with cooking during data collection (Riverside, California)	7-40
7-13	Results of six penetration experiments in a test home	7-53
7-14	The change in suspended particle mass concentration versus time, as measured by optical particle counter, assuming spherical particles of unit density	7-53

LIST OF FIGURES (cont'd)

Number		Page
7-15	The ratio of the suspended particle concentration after a resuspension activity to the indoor concentration before that activity, by particle size	7-54
7-16	Fraction of indoor particulate matter from outdoor airborne particulate matter, under equilibrium conditions, as a function of air-exchange rate, for two different size fractions	7-61
7-17	Comparison of respirable particles in smoking and nonsmoking areas of 38 buildings in the Pacific Northwest	7-65
7-18	Chart of pollen prevalence	7-72
7-19	Chart of fungal spore prevalence in Kalamazoo, Michigan, for 1994	7-78
7-20	Residential outdoor monitors versus central-site mean of two dichotomous samplers in Riverside, California	7-95
7-21	Personal exposures versus residential outdoor PM_{10} concentrations in Riverside, California	7-95
7-22	Increased concentrations of elements in the personal versus the indoor samples	7-97
7-23	Source apportionment of Particle Total Exposure Assessment Methodology PM_{10} personal monitoring data	7-98
7-24	The relationship between PM_{10} in outdoor air and indoor air at each house in the study	7-101
7-25	Correlations between PM_{10} at the Itabashi monitoring station and PM_{10} in outdoor and personal exposure	7-102
7-26	Example of difference between serial correlation and cross-sectional correlation of personal exposure monitor (PEM) and SAM, showing how pooling of individuals can mask an underlying relationship of PEM and SAM	7-104
7-27	Personal versus outdoor $SO_4^=$	7-107
7-28	Estimated ("best fit" model) versus measured personal $SO_4^=$	7-107
7-29	Personal activity cloud and time-weighted average exposure	7-111

LIST OF FIGURES (cont'd)

Number		Page
7-30	Components of personal exposure	7-116
7-31	Plot of 48-hour average personal PM_{10} exposure and ambient PM_{10} data from Japan—linear regression	7-127
7-32	Plot of relationship between average personal PM_{10} exposure versus ambient PM_{10} monitoring data from Phillipsburg, New Jersey, and regression line calculated by U.S. Environmental Protection Agency	7-139
7-33	Plot of means of personal exposures and ambient PM_{10} from Beijing, China, and regression line calculated by U.S. Environmental Protection Agency	7-142
7-34	Particle Total Exposure Assessment Methodology mean 24-hour PM_{10} data compared for personal exposure monitor and SAM	7-144
7-35	Ambient and personal monitoring PM_{10} data from Azusa, California, and calculated (slightly negative slope) regression line, which becomes positive if single outlier value is deleted	7-146
7-36	Comparison of indoor and outdoor concentrations of lead in a home in Denver, October 1976, for one week, starting at 1600 hours	7-153
7-37	Venn diagram showing focusing of information to more completely specify toxicity of a given particulate matter mixture	7-154
7-38	Fraction of ambient particulate matter to which people are exposed as a function of fraction of time outdoors and air-exchange rate for fine and coarse particles	7-157
7-39	Conceptual representation of potential contributions of particulate matter of ambient origin and particulate matter generated indoors to total human exposure of a hypothetical individual	7-161

AUTHORS, CONTRIBUTORS, AND REVIEWERS

CHAPTER 1. EXECUTIVE SUMMARY

Principal Authors

Dr. Robert Chapman—National Center for Environmental Assessment (MD-52), U.S. Environmental Protection Agency, Research Triangle Park, NC 27711

Ms. Beverly Comfort—National Center for Environmental Assessment (MD-52), U.S. Environmental Protection Agency, Research Triangle Park, NC 27711

Mr. William Ewald—National Center for Environmental Assessment (MD-52), U.S. Environmental Protection Agency, Research Triangle Park, NC 27711

Dr. Lawrence J. Folinsbee—National Center for Environmental Assessment (MD-52), U.S. Environmental Protection Agency, Research Triangle Park, NC 27711

Dr. Lester D. Grant—National Center for Environmental Assessment (MD-52), U.S. Environmental Protection Agency, Research Triangle Park, NC 27711

Ms. Annie M. Jarabek—National Center for Environmental Assessment (MD-52), U.S. Environmental Protection Agency, Research Triangle Park, NC 27711

Dr. Dennis Kotchmar—National Center for Environmental Assessment (MD-52), U.S. Environmental Protection Agency, Research Triangle Park, NC 27711

Dr. David Mage—National Exposure Research Laboratory (MD-56), U.S. Environmental Protection Agency, Research Triangle Park, NC 27711

Dr. Allan Marcus—National Center for Environmental Assessment (MD-52), U.S. Environmental Protection Agency, Research Triangle Park, NC 27711

Dr. James McGrath—National Center for Environmental Assessment (MD-52), U.S. Environmental Protection Agency, Research Triangle Park, NC 27711

Dr. Joseph P. Pinto—National Center for Environmental Assessment (MD-52), U.S. Environmental Protection Agency, Research Triangle Park, NC 27711

Dr. William E. Wilson—National Center for Environmental Assessment (MD-52), U.S. Environmental Protection Agency, Research Triangle Park, NC 27711

Contributors and Reviewers

Dr. Judith Graham—National Exposure Research Laboratory (MD-75), U.S. Environmental Protection Agency, Research Triangle Park, NC 27711

Dr. Jeanette Wiltse—Office of Research and Development (8601), Waterside Mall, 401 M St. S.W., Washington, DC 20460

CHAPTER 2. INTRODUCTION

Principal Authors

Dr. Lester D. Grant—National Center for Environmental Assessment (MD-52), U.S. Environmental Protection Agency, Research Triangle Park, NC 27711

Dr. Dennis Kotchmar—National Center for Environmental Assessment (MD-52), U.S. Environmental Protection Agency, Research Triangle Park, NC 27711

CHAPTER 3. PHYSICS AND CHEMISTRY OF PARTICULATE MATTER

Principal Authors

Dr. Paul Altshuller—National Center for Environmental Assessment, U.S. Environmental Protection Agency, Research Triangle Park, NC 27711

Mr. William Ewald—National Center for Environmental Assessment (MD-52), U.S. Environmental Protection Agency, Research Triangle Park, NC 27711

Dr. Noor Gillani—Earth Systems Science Laboratory, University of Alabama, Huntsville, AL 35899

Dr. Dale Gillette—National Exposure Research Laboratory (MD-81), U.S. Environmental Protection Agency, Research Triangle Park, NC 27711

Dr. Susanne Hering—Aerosol Dynamics, Inc., 2329 Fourth Street, Berkeley, CA 94710

Dr. Paul J. Lioy—Environmental Occupational Health and Science Institute, Exposure Measurement and Assessment Division, 681 Frelinghuysen Road, Piscataway, NJ 08855-1179

Principal Authors (cont'd)

Dr. Kenneth Noll—Illinois Institute of Technology, Chicago, IL 60616

Dr. Spyros Pandis—Carnegie-Mellon University, Pittsburgh, PA 15146

Dr. James Pankow—Oregon Graduate Center, Beaverton, OR 97229-3678

Dr. Steven Schwartz—Brookhaven National Laboratory, Upton, NY 11934

Dr. William E. Wilson—National Center for Environmental Assessment (MD-52), U.S. Environmental Protection Agency, Research Triangle Park, NC 27711

Contributors and Reviewers

Dr. Michael Barnes—National Exposure Research Laboratory (MD-46), U.S. Environmental Protection Agency, Research Triangle Park, NC 27711

Dr. Thomas Cahill—University of California—Davis, Crocker Nuclear Lab., Davis, CA 95616

Ms. Beverly Tilton—National Center for Environmental Assessment (MD-52), U.S. Environmental Protection Agency, Research Triangle Park, NC 27711

Dr. Sheldon Friedlander—University of California, 5531 Boelter Hall, Los Angeles, CA 90095

Dr. Peter McMurray—University of Minnesota, Department of Mechanical Engineering, 111 Church Street, S.E., Minneapolis, MN 55455-0111

Dr. Sidney Soderholm—NIOSH, 1095 Willowdale Rd., Morgantown, WVA 26505

Dr. Barbara Turpin—Rutgers University, Box 231, New Brunswick, NJ 08903

CHAPTER 4. SAMPLING AND ANALYSIS METHODS FOR PARTICULATE MATTER AND ACID DEPOSITION

Principal Authors

Dr. Judith Chow—Desert Research Institute, P.O. Box 60220, Reno, NV 89506-0220

AUTHORS, CONTRIBUTORS, AND REVIEWERS (cont'd)

Principal Authors (cont'd)

Dr. Steven McDow—University of North Carolina at Chapel Hill, Chapel Hill, NC 27599

Dr. Susanne Hering—Aerosol Dynamics, Inc., 2329 Fourth Street, Berkeley, CA 94710

Dr. Charles Rodes—Research Triangle Institute, Center for Aerosol Technology, P.O. Box 12194, Research Triangle Park, NC 27709-2194

Contributors and Reviewers

Dr. Robert Burton—National Exposure Research Laboratory (MD-56), U.S. Environmental Protection Agency, Research Triangle Park, NC 27711

Dr. Thomas Cahill—University of California—Davis, Crocker Nuclear Laboratory, Davis, CA 95616

Dr. Delbert Eatough—Brigham Young University, Department of Chemistry, Provo, UT 84602

Mr. William Ewald—National Center for Environmental Assessment (MD-52), U.S. Environmental Protection Agency, Research Triangle Park, NC 27711

Dr. Sheldon Friedlander—University of California, Department of Chemical Engineering, 5531 Boelter Hall, Los Angeles, CA 90095

Dr. Peter McMurry—University of Minnesota, Department of Mechanical Engineering, 111 Church Street, S.E., Minneapolis, MN 55455-0111

Dr. Sidney Soderholm—National Institute of Occupational Safety and Health, 1095 Williowdale Road, Room 111, Morgantown, WV 26505

Dr. Barbara Turpin—Rutgers University, Environmental Sciences Building, Box 231, College Farm Road, New Brunswick, NJ 08903

Dr. Russell Wiener—National Exposure Research Laboratory (MD-77), U.S. Environmental Protection Agency, Research Triangle Park, NC 27711

Dr. Nancy Wilson—National Exposure Research Laboratory (MD-56), U.S. Environmental Protection Agency, Research Triangle Park, NC 27711

CHAPTER 5. SOURCES AND EMISSIONS OF ATMOSPHERIC PARTICLES

Principal Authors

Dr. Joseph P. Pinto—National Center for Environmental Assessment (MD-52), U.S. Environmental Protection Agency, Research Triangle Park, NC 27711

Contributors and Reviewers

Dr. Paul Altshuller—National Center for Environmental Assessment (MD-52), U.S. Environmental Protection Agency, Research Triangle Park, NC 27711

Dr. Judith Chow—Desert Research Institute, P.O. Box 60220, Reno, NV 89506-0220

Mr. William Ewald—National Center for Environmental Assessment (MD-52), U.S. Environmental Protection Agency, Research Triangle Park, NC 27711

Dr. Timothy Larson—University of Washington, Department of Civil Engineering, Seattle, WA 98195

Dr. John Seinfeld—California Institute of Technology, Department of Chemical Engineering, Pasadena, CA 91125

Dr. Barbara Turpin—Rutgers University, Environmental Sciences Building, Box 231, College Farm Road, New Brunswick, NJ 08903

Dr. John Watson—Desert Research Institute, P.O. Box 60220, Reno, NV 89506-0220

CHAPTER 6. ENVIRONMENTAL CONCENTRATIONS

Principal Authors

Dr. Paul Altshuller—National Center for Environmental Assessment (MD-52), U.S. Environmental Protection Agency, Research Triangle Park, NC 27711

Dr. Thomas Cahill—University of California—Davis, Crocker Nuclear Laboratory, Davis, CA 95616

Dr. Susanne Hering—Aerosol Dynamics, Inc., 2329 Fourth Street, Berkeley, CA 94710

AUTHORS, CONTRIBUTORS, AND REVIEWERS (cont'd)

Principal Authors (cont'd)

Dr. Rudolf Husar—Washington University, Center for Air Pollution and Impact and Trend Analyses, St. Louis, MO 63130

Dr. Joseph P. Pinto—National Center for Environmental Assessment (MD-52), U.S. Environmental Protection Agency, Research Triangle Park, NC 27711

Dr. Robert Stevens—National Exposure Research Laboratory (MD-47), U.S. Environmental Protection Agency, Research Triangle Park, NC 27711

Mr. Robert Willis—ManTech Environmental Technology, Inc., P.O. Box 12313, Research Triangle Park, NC 27709.

Dr. William E. Wilson—National Center for Environmental Assessment (MD-52), U.S. Environmental Protection Agency, Research Triangle Park, NC 27711

Dr. Michael Zelenka—National Exposure Research Laboratory (MD-75), U.S. Environmental Protection Agency, Research Triangle Park, NC 27711

Contributors and Reviewers

Dr. John Core—WESTAR Council, 1001 SW 5th Avenue, Suite 1100, Portland, OR 97204

Mr. William Ewald—National Center for Environmental Assessment (MD-52), U.S. Environmental Protection Agency, Research Triangle Park, NC 27711

Dr. Timothy Larson—University of Washington, Department of Civil Engineering, Seattle, WA 98195

Dr. Brian Leaderer—John B. Pierce Laboratory, 290 Congress Avenue, New Haven, CT 06519

Dr. Helen Suh—Harvard University, School of Public Health, 665 Huntington Avenue, Boston, MA 02115

AUTHORS, CONTRIBUTORS, AND REVIEWERS (cont'd)

CHAPTER 7. HUMAN EXPOSURE TO PARTICULATE MATTER: RELATIONS TO AMBIENT AND INDOOR CONCENTRATIONS

Principal Authors

Dr. Harriet Burge—Harvard School of Public Health, Environmental Science and Engineering, Boston, MA 02115

Dr. Dave Mage—National Exposure Research Laboratory (MD-56), U.S. Environmental Protection Agency, Research Triangle Park, NC 27711

Dr. Lance Wallace—National Exposure Research Laboratory, U.S. Environmental Protection Agency, Wallington, VA 22186

Dr. Robert Ziegenfus—Kutztown University, Department of Geography, Kutztown, PA 19550

Contributors and Reviewers

Dr. Gerald Akland—National Exposure Research Laboratory (MD-56), U.S. Environmental Protection Agency, Research Triangle Park, NC 27711

Dr. Timothy Buckley—National Exposure Research Laboratory (MD-56), U.S. Environmental Protection Agency, Research Triangle Park, NC 27711

Dr. Robert Burton—National Exposure Research Laboratory (MD-56), U.S. Environmental Protection Agency, Research Triangle Park, NC 27711

Mr. William Ewald—National Center for Environmental Assessment (MD-52), U.S. Environmental Protection Agency, Research Triangle Park, NC 27711

Dr. Paul J. Lioy—Environmental Occupational Health Science Institute, Exposure Measurement and Assessment Division, 681 Frelinghuysen Road, Piscataway, NJ 08855-1179

Dr. Peter McMurry—University of Minnesota, Department of Mechanical Engineering, 111 Church Street, SW, Minneapolis, MN 55455

Dr. William E. Wilson—National Center for Environmental Assessment (MD-52), U.S. Environmental Protection Agency, Research Triangle Park, NC 27711

U.S. ENVIRONMENTAL PROTECTION AGENCY
SCIENCE ADVISORY BOARD
CLEAN AIR SCIENTIFIC ADVISORY COMMITTEE

PARTICULATE MATTER CRITERIA DOCUMENT REVIEW

Chairman

Dr. George T. Wolff—General Motors Corporation, Environmental and Energy Staff, General Motors Bldg., 12th Floor, 3044 West Grand Blvd., Detroit, MI 48202

Members

Dr. Stephen Ayres—Office of International Health Programs, Virginia Commonwealth University, Medical College of Virginia, Box 980565, Richmond, VA 23298

Dr. Philip Hopke—Clarkson University, Box 5810, Pottsdam, NY 13699-5810

Dr. Jay Jacobson—Boyce Thompson Institute, Tower Road, Cornell University, Ithaca, NY 14853

Dr. Joseph Mauderly—Inhalation Toxicology Research Institute, Lovelace Biomedical and Environmental Research Institute, P.O. Box 5890, Albuquerque, NM 87185

Dr. Paulette Middleton—Science and Policy Associates, 3445 Penrose Place, Suite 140, Boulder, CO 80301

Dr. James H. Price, Jr.—Research and Technology Section, Texas Natural Resources Conservation Commission, P.O. Box 13087, Austin, TX 78711-3087

Invited Scientific Advisory Board Members

Dr. Morton Lippmann—Institute of Environmental Medicine, New York University Medical Center, Long Meadow Road, Tuxedo, NY 10987

Dr. Roger O. McClellan—Chemical Industry Institute of Toxicology, P.O. Box 12137, Research Triangle Park, NC 27711

Consultants

Dr. Petros Koutrakis—Harvard School of Public Health, 665 Huntington Avenue, Boston, MA 02115

U.S. ENVIRONMENTAL PROTECTION AGENCY
SCIENCE ADVISORY BOARD
CLEAN AIR SCIENTIFIC ADVISORY COMMITTEE
(cont'd)

Consultants (cont'd)

Dr. Kinley Larntz—Department of Applied Statistics, University of Minnesota, 352 COB, 1994 Buford Avenue, St. Paul, MN 55108-6042

Dr. Allan Legge—Biosphere Solutions, 1601 11th Avenue, N.W., Calgary, Alberta T2N 1H1, Canada

Dr. Daniel Menzel—Department of Community and Environmental Medicine, University of California—Irvine, 19172 Jamboree Boulevard, Irvine, CA 92717-1825

Dr. William R. Pierson—Energy and Environmental Engineering Center, Desert Research Institute, P.O. Box 60220, Reno, NV 89506-0220

Dr. Jonathan Samet—Johns Hopkins University, School of Hygiene and Public Health, Department of Epidemiology, 615 N. Wolfe Street, Baltimore, MD 21205

Dr. Christian Seigneur—Atmospheric and Environmental Research, Inc., 6909 Snake Road, Oakland, CA 94611

Dr. Carl M. Shy—Department of Epidemiology, School of Public Health, University of North Carolina, CB #7400 McGravran-Greenberg Hall, Chapel Hill, NC 27599-7400

Dr. Frank Speizer—Harvard Medical School, Channing Laboratory, 180 Longwood Avenue, Boston, MA 02115

Dr. Jan Stolwijk—Epidemiology and Public Health, Yale University, 60 College Street, New Haven, CT 06510

Dr. Mark J. Utell—Pulmonary Disease Unit, Box 692, University of Rochester Medical Center, 601 Elmwood Avenue, Rochester, NY 14642

Dr. Warren White—Washington University, Campus Box 1134, One Brookings Drive, St. Louis, MO 63130-4899

Designated Federal Official

Mr. Randall C. Bond—Science Advisory Board (1400), U.S. Environmental Protection Agency, 401 M Street, S.W., Washington, DC 20460

Designated Federal Official (cont'd)

Mr. A. Robert Flaak—Science Advisory Board (1400), U.S. Environmental Protection Agency, 401 M Street, S.W., Washington, DC 20460

Staff Assistant

Ms. Janice M. Cuevas—Science Advisory Board (1400), U.S. Environmental Protection Agency, 401 M Street, S.W., Washington, DC 20460

Secretary

Ms. Lori Anne Gross—Science Advisory Board (1400), U.S. Environmental Protection Agency, 401 M Street, S.W., Washington, DC 20460

Ms. Connie Valentine—Science Advisory Board (1400), U.S. Environmental Protection Agency, 401 M Street, S.W., Washington, DC 20460

U.S. ENVIRONMENTAL PROTECTION AGENCY
PROJECT TEAM FOR DEVELOPMENT OF AIR QUALITY CRITERIA
FOR PARTICULATE MATTER

Scientific Staff

Dr. Lester D. Grant—Director, National Center for Environmental Assessment (MD-52), U.S. Environmental Protection Agency, Research Triangle Park, NC 27711

Dr. Michael A. Berry—Deputy Director, National Center for Environmental Assessment, (MD-52), U.S. Environmental Protection Agency, Research Triangle Park, NC 27711

Dr. Dennis Kotchmar—Project Manager, Medical Officer, National Center for Environmental Assessment (MD-52), U.S. Environmental Protection Agency, Research Triangle Park, NC 27711

Ms. Beverly Comfort—Deputy Project Manager/Technical Project Officer, Health Scientist, National Center for Environmental Assessment (MD-52), U.S. Environmental Protection Agency, Research Triangle Park, NC 27711

Dr. Lawrence J. Folinsbee—Chief, Environmental Media Assessment Group, National Center for Environmental Assessment (MD-52), U.S. Environmental Protection Agency, Research Triangle Park, NC 27711

Dr. A. Paul Altshuller—Technical Consultant, Senior Atmospheric Scientist, National Center for Environmental Assessment (MD-52), U.S. Environmental Protection Agency, Research Triangle Park, NC 27711 (Retired)

Dr. Robert Chapman—Technical Consultant, Medical Officer, National Center for Environmental Assessment (MD-52), U.S. Environmental Protection Agency, Research Triangle Park, NC 27711

Mr. William Ewald—Technical Project Officer, Health Scientist, National Center for Environmental Assessment (MD-52), U.S. Environmental Protection Agency, Research Triangle Park, NC 27711

Mr. Norman Childs—Chief, Environmental Media Assessment Branch, National Center for Environmental Assessment (MD-52), U.S. Environmental Protection Agency, Research Triangle Park, NC 27711 (Retired)

Dr. Judith A. Graham—Associate Director for Health, National Exposure Research Laboratory (MD-77), U.S. Environmental Protection Agency, Research Triangle Park, NC 27711

U.S. ENVIRONMENTAL PROTECTION AGENCY
PROJECT TEAM FOR DEVELOPMENT OF AIR QUALITY CRITERIA
FOR PARTICULATE MATTER
(cont'd)

Scientific Staff (cont'd)

Ms. Annie M. Jarabek—Technical Project Officer, Toxicologist, National Center for Environmental Assessment (MD-52), U.S. Environmental Protection Agency, Research Triangle Park, NC 27711

Dr. Allan Marcus—Technical Project Officer, Statistician, National Center for Environmental Assessment (MD-52), U.S. Environmental Protection Agency, Research Triangle Park, NC 27711

Dr. James McGrath—Technical Project Officer, Visiting Senior Health Scientist, National Center for Environmental Assessment (MD-52), U.S. Environmental Protection Agency, Research Triangle Park, NC 27711

Dr. Joseph P. Pinto—Technical Project Officer, Physical Scientist, National Center for Environmental Assessment, U.S. Environmental Protection Agency, Research Triangle Park, NC 27711

Ms. Beverly Tilton—Technical Project Officer, Physical Scientist, National Center for Environmental Assessment (MD-52), U.S. Environmental Protection Agency, Research Triangle Park, NC 27711 (Retired)

Dr. William E. Wilson—Technical Consultant, Physical Scientist, National Center for Environmental Assessment (MD-52), U.S. Environmental Protection Agency, Research Triangle Park, NC 27711

Technical Support Staff

Mr. Douglas B. Fennell—Technical Information Specialist, National Center for Environmental Assessment (MD-52), U.S. Environmental Protection Agency, Research Triangle Park, NC 27711

Ms. Emily R. Lee—Management Analyst, National Center for Environmental Assessment (MD-52), U.S. Environmental Protection Agency, Research Triangle Park, NC 27711

Ms. Diane H. Ray—Program Analyst, National Center for Environmental Assessment (MD-52), U.S. Environmental Protection Agency, Research Triangle Park, NC 27711

U.S. ENVIRONMENTAL PROTECTION AGENCY
PROJECT TEAM FOR DEVELOPMENT OF AIR QUALITY CRITERIA
FOR PARTICULATE MATTER
(cont'd)

Technical Support Staff (cont'd)

Ms. Eleanor Speh—Office Manager, Environmental Media Assessment Branch, National Center for Environmental Assessment (MD-52), U.S. Environmental Protection Agency, Research Triangle Park, NC 27711

Ms. Donna Wicker—Administrative Officer, National Center for Environmental Assessment (MD-52), U.S. Environmental Protection Agency, Research Triangle Park, NC 27711

Mr. Richard Wilson—Clerk, National Center for Environmental Assessment (MD-52), U.S. Environmental Protection Agency, Research Triangle Park, NC 27711

Document Production Staff

Ms. Marianne Barrier—Graphic Artist, ManTech Environmental Technology, Inc., P.O. Box 12313, Research Triangle Park, NC 27709

Mr. John R. Barton—Document Production Coordinator, ManTech Environmental Technology, Inc., P.O. Box 12313, Research Triangle Park, NC 27709

Mr. Donald L. Duke—Project Director, ManTech Environmental Technology, Inc., P.O. Box 12313, Research Triangle Park, NC 27709

Ms. Shelia H. Elliott—Word Processor, ManTech Environmental Technology, Inc., P.O. Box 12313, Research Triangle Park, NC 27709

Ms. Sandra K. Eltz—Word Processor, ManTech Environmental Technology, Inc., P.O. Box 12313, Research Triangle Park, NC 27709

Ms. Sheila R. Lassiter—Word Processor, ManTech Environmental Technology, Inc., P.O. Box 12313, Research Triangle Park, NC 27709

Ms. Wendy B. Lloyd—Word Processor, ManTech Environmental Technology, Inc., P.O. Box 12313, Research Triangle Park, NC 27709

Ms. Carolyn T. Perry—Word Processor, ManTech Environmental Technology, Inc., P.O. Box 12313, Research Triangle Park, NC 27709

Ms. Terri D. Ragan—Personal Computer Technician, ManTech Environmental Technology, Inc., P.O. Box 12313, Research Triangle Park, NC 27709

U.S. ENVIRONMENTAL PROTECTION AGENCY
PROJECT TEAM FOR DEVELOPMENT OF AIR QUALITY CRITERIA
FOR PARTICULATE MATTER
(cont'd)

Document Production Staff (cont'd)

Mr. Derrick Stout—Local Area Network System Administrator, ManTech Environmental Technology, Inc., P.O. Box 12313, Research Triangle Park, NC 27709

Ms. Cheryl B. Thomas—Word Processor, ManTech Environmental Technology, Inc., P.O. Box 12313, Research Triangle Park, NC 27709

Technical Reference Staff

Ms. Ginny M. Belcher—Bibliographic Editor, ManTech Environmental Technology, Inc., P.O. Box 12313, Research Triangle Park, NC 27709

Mr. Robert D. Belton—Bibliographic Editor, Information Organizers, Inc., P.O. Box 14391, Research Triangle Park, NC 27709

Mr. John A. Bennett—Bibliographic Editor, ManTech Environmental Technology, Inc., P.O. Box 12313, Research Triangle Park, NC 27709

Ms. S. Blythe Hatcher—Bibliographic Editor, Information Organizers, Inc., P.O. Box 14391, Research Triangle Park, NC 27709

Ms. Susan L. McDonald—Bibliographic Editor, Information Organizers, Inc., P.O. Box 14391, Research Triangle Park, NC 27709

Ms. Deborah L. Staves—Bibliographic Editor, Information Organizers, Inc., P.O. Box 14391, Research Triangle Park, NC 27709

Ms. Patricia R. Tierney—Bibliographic Editor, ManTech Environmental Technology, Inc., P.O. Box 12313, Research Triangle Park, NC 27709

1. EXECUTIVE SUMMARY

1.1 INTRODUCTION

1.1.1 Purpose of the Document

The purpose of this document, Air Quality Criteria for Particulate Matter, is to present air quality criteria for particulate matter (PM) in accordance with Clean Air Act (CAA) Sections 108 and 109, which govern establishment, review, and revision of U.S. National Ambient Air Quality Standards (NAAQS).

- Section 108 directs the U.S. Environmental Protection Agency (EPA) Administrator to list pollutants that may reasonably be anticipated to endanger public health or welfare and to issue air quality criteria for them. The air quality criteria are to reflect the latest scientific information useful in indicating the kind and extent of all exposure-related effects on public health and welfare expected from the presence of the pollutant in ambient air.

- Section 109 directs the EPA Administrator to set and periodically revise, as appropriate, (a) primary NAAQS to protect against adverse health effects of listed criteria pollutants among sensitive population groups, with an adequate margin of safety, and (b) secondary NAAQS to protect against welfare effects (e.g., impacts on vegetation, crops, ecosystems, visibility, climate, man-made materials, etc.).

- To meet these CAA mandates, this document assesses the latest scientific information useful in deriving criteria as scientific bases for decisions on possible revision of current PM NAAQS. A separate EPA PM Staff Paper draws upon assessments in this document, together with other information, in delineating key information used to develop and present appropriate options for consideration by the EPA Administrator with regard to review of the PM NAAQS.

1.1.2 Organization of the Document

- This Executive Summary (Chapter 1) summarizes key points from ensuing chapters.

- Chapter 2 provides a general introduction, including an overview of the rationale underlying the current PM NAAQS, i.e., 150 $\mu g/m^3$ (24-h) and 50 $\mu g/m^3$ (annual average) as PM_{10} (particles $\leq$ 10 μm aerodynamic diameter, d_{ae}).

- Chapters 3 through 7 provide background information on air quality and exposure aspects, to help to place the succeeding discussions of PM effects into perspective.

- Chapter 8 deals with visibility and climate effects; and Chapter 9 assesses materials damage, as key types of welfare effects of concern for the current PM NAAQS review. Welfare effects of PM on vegetation, crops, and ecosystems are not assessed in the document.

- Chapters 10, 11, and 12, respectively, discuss PM dosimetry, toxicology and community epidemiology information. Chapter 13 provides an integrative synthesis of key points from those health chapters and other preceding air quality and exposure chapters.

1.2 AIR QUALITY AND EXPOSURE ASPECTS

The document's discussion of air quality and exposure aspects considers chemistry and physics of atmospheric PM; analytical techniques for measuring PM mass, size, and chemical composition; sources of ambient PM in the United States; temporal/spatial variability and trends in ambient U.S. PM levels; and human exposure relationships.

1.2.1 Chemistry and Physics of Atmospheric Particles

- Airborne PM is not a single pollutant, but rather is a mixture of many subclasses of pollutants with each subclass containing many different chemical species. Atmospheric PM occurs naturally as fine-mode and coarse-mode particles that, in addition to falling into different size ranges, differ in formation mechanisms, chemical composition, sources, and exposure relationships.

- Fine-mode PM is derived from combustion material that has volatilized and then condensed to form primary PM or from precursor gases reacting in the atmosphere to form secondary PM. New fine-mode particles are formed by the nucleation of gas phase species, and grow by coagulation (existing particles combining) or condensation (gases condensing on existing particles). Fine particles are composed of (a) freshly generated particles, in an ultrafine or nuclei mode, and (b) an accumulation mode, so called because particles grow into and remain in that mode.

- Coarse-mode PM, in contrast, is formed by crushing, grinding, and abrasion of surfaces, which breaks large pieces of material into smaller pieces. They are then suspended by the wind or by anthropogenic activity. Energy considerations limit the break-up of large particles and small particle aggregates generally to a minimum size of about 1 μm in diameter. Mining and agricultural activities are examples of anthropogenic sources of coarse-mode particles. Fungal spores, pollen, and plant and insect fragments are examples of natural bioaerosols also suspended as coarse-mode particles.

- Within atmospheric particle modes, the distribution of particle number, surface, volume, and mass by diameter is frequently approximated by lognormal distributions. Aerodynamic diameter, d_{ae}, which depends on particle density and is defined as the diameter of a particle with the same settling velocity as a spherical particle with unit density (1 g/cm^3) is often used to describe particle size. Typical values of the mass median aerodynamic diameter (MMAD) and geometric standard deviation (σ_g) of each size mode of an aerosol are:

- Nuclei mode:	MMAD=0.05 to 0.07 μm	σ_g = 1.8
- Accumulation mode:	MMAD= 0.3 to 0.7 μm	σ_g = 1.8
- Coarse mode:	MMAD= 6 to 20 μm	σ_g = 2.4

At high relative humidities or in air containing evaporating fog or cloud droplets, the accumulation mode may be split into a droplet mode (MMAD = 0.5 to 0.8 μm) and a condensation mode (MMAD = 0.2 to 0.3 μm).

- Research studies use (a) impactors to determine mass as a function of size over a wide range and (b) particle counting devices to determine number as a function of size. Such studies indicate an atmospheric bimodal distribution of fine and coarse particle mass with a minimum in the distribution between 1 and 3 μm d_{ae}. Routine monitoring studies, however, is generally limited to measuring TSP (total suspended particles) including both fine and coarse particles up to 40 or more μm d_{ae}; thoracic particles or PM_{10} (upper size limited by a 50% cut at 10 μm d_{ae}); fine particles or $PM_{2.5}$ (upper size limited by a 50% cut point at 2.5 μm d_{ae}), and the coarse fraction of PM_{10}, i.e., the difference between PM_{10} and $PM_{2.5}$ ($PM_{10-2.5}$). Cut points are not perfectly sharp for any of these PM indicators; some particles larger than the cutpoint are collected and some smaller-particles smaller than the cutpoint are not retained.

- The terms "fine" and "coarse" were originally intended to apply to the two major atmospheric particle distributions which overlap in the size range between 1 and 3 μm diameter. Now, fine has come to be often associated with the $PM_{2.5}$ fraction and coarse is often used to refer to $PM_{10-2.5}$. However, $PM_{2.5}$ may also contain, in addition to the fine-particle mode, some of the lower-size tail of the coarse particle mode between about 1 and 2.5 μm d_{ae}. Conversely, under high relative humidity conditions, the larger particles in the accumulation mode may also extend into the 1 to 3 μm d_{ae} range.

- Three approaches are used to classify particles by size: (1) modes, based on formation mechanisms and the modal structure observed in the atmosphere, e.g., nuclei and accumulation modes which comprise the fine particle mode and the coarse particle mode; (2) cut point, based on the 50% cut point of the specific sampling device, e.g., $PM_{2.5}$, $PM_{10-2.5}$, and PM_{10}; and (3) dosimetry, based on the ability of particles to enter certain regions of the respiratory tract.

1.2.2 Sources of Airborne Particles in the United States

- The chemical complexity of airborne particles requires that the composition and sources of a large number of primary and secondary components be considered. Major components of fine particles are: sulfate, strong acid, ammonium, nitrate, organic compounds, trace elements (including metals), elemental carbon, and water. Major sources of these fine mode substances are fossil fuel combustion by electric utilities, industry and motor vehicles; vegetation burning; and the smelting or other processing of metals.

- Sulfur dioxide (SO_2), nitrogen oxides (NO_x), and certain organic compounds are major precursors of fine secondary PM. NO reacts with ozone (O_3) to form NO_2. SO_2 and NO_2 react with hydroxy radical (OH) during the daytime to form sulfuric and nitric acid. During the nighttime NO_2 reacts with ozone and forms nitric acid through a sequence of reactions involving the nitrate radical (NO_3). These acids may react further with ammonia to form ammonium sulfates and nitrates. Some types of higher molecular weight organic compounds react with OH radicals, and olefinic compounds also react with ozone, to form

oxygenated organic compounds which can condense onto existing particles. SO_2 also dissolves in cloud and fog droplets where it may react with dissolved O_3, H_2O_2, or, if catalyzed by certain metals, with O_2, yielding sulfuric acid or sulfates, that lead to PM when the droplet evaporates.

- The formation of secondary PM depends on reactions involving OH, O_3, and H_2O_2, species which are normally present in the atmosphere but which are generated in higher concentrations during the photochemical smog formation process. Since smog formation increases with sunlight and temperature, secondary PM peaks during the summer in most U.S. areas.

- Background geogenic and biogenic emission sources include: wind blown dust from erosion and reentrainment; the long-range transport of dust from the Sahara desert; sea salt; particles formed from the oxidation of sulfur compounds emitted from oceans and wetlands; the oxidation of NO_x from natural forest fires and lightning; and the oxidation of hydrocarbons (such as terpenes) emitted by vegetation.

- Major components of coarse particles are aluminosilicates and other oxides of crustal elements (e.g., Fe, Ca, etc.) in soil dust; fugitive dust from roads, industry, agriculture, construction and demolition; fly ash from combustion of oil and coal; and additional contributions from plant and animal material.

- Fugitive dust constitutes about 90% of estimated PM_{10} emissions in the United States. Emissions are sporadic and widespread. Only a small percentage of this material is emitted in the fine particle size fraction.

- Uncertainties in emissions inventory estimates could range from about 10% for well defined sources (e.g., for SO_2) to an order of magnitude for widespread and sporadic sources (e.g., fugitive dust).

- There has been no clear trend in estimated emissions of fugitive dust and emissions from natural sources from 1984 to 1993. Estimated primary PM_{10} emissions from combustion sources have decreased by about 10%; estimated SO_2 emissions have decreased by about 6%; and there was no significant change in estimated NO_x emissions from 1984 to 1993.

- Receptor modeling has proven to be a useful method for identifying contributions of different types of sources especially for the primary components of ambient PM. Apportionment of secondary PM is more difficult because it requires consideration of atmospheric reaction processes and rates. Results from western U.S. sites indicate that fugitive dust, motor vehicles, and wood smoke are the major contributors to ambient PM samples there, while results from eastern U.S. sites indicate that stationary combustion and fugitive dust are major contributors to ambient PM samples in the East. Sulfate and organic carbon are the major secondary components in the East, while nitrates and organic carbon are the major secondary components in the West.

- Fine and coarse particles have distinctly different sources, both natural and anthropogenic. Therefore different control strategies are likely to be needed, depending on whether fine or coarse particles (or both) are selected for control.

1.2.3 Atmospheric Transport and Fate of Airborne Particles

- Dry deposition of fine particles is slow. Nuclei-mode (ultrafine) particles are rapidly removed by coagulation into accumulation-mode particles. Accumulation-mode particles are removed from the atmosphere primarily by forming cloud droplets and falling out in raindrops. Coarse particles are removed mainly by gravitational settling and inertial impaction.

- Primary and secondary fine particles have long lifetimes in the atmosphere (days to weeks) and travel long distances (hundreds to thousands of kilometers). They tend to be uniformly distributed over urban areas and larger regions, especially in the eastern United States. As a result, they are not easily traced back to their individual sources.

- Coarse particles normally have shorter lifetimes (minutes to hours) and only travel short distances (< 10's of km). Therefore, coarse particles tend to be unevenly distributed across urban areas and tend to have more localized effects than fine particles. (Dust storms occasionally cause long range transport of the smaller coarse-mode particles.)

1.2.4 Airborne Particle Measurement Methods

- Measurement of ambient PM mass and chemical composition is important for: source attribution; inventories of the observed mass; health and welfare effects studies; and determination of compliance with standards. A comprehensive approach requires a combination of analytical techniques to assess: (1) mass; (2) elemental composition; (3) water-soluble ionic species; and (4) organic compounds.

- Various sampling systems based on gravimetric (weight) measurements of collected particles yield direct measurements of airborne particle mass. The high volume (hi-vol) sampler, used extensively in the United States before establishment of PM_{10} as the indicator for the PM standard, collects and measures the mass of total suspended particulates (TSP), including both fine and coarse particles. Certain other samplers (e.g., dichotomous samplers or impactors) use one or more sampler heads or other separator devices to selectively collect and measure the mass of various size fractions of PM.

- There are no calibration standards for suspended particle mass; therefore, the accuracy of particle mass measurements cannot be determined. The precision of particle mass measurements can be estimated by comparing results from collocated samplers. When using different measurement techniques, samplers of different design or manufacturer, and, in some cases, when using identical systems of different age or cleanliness, substantial biases of 50% or more have been observed. Mass concentration measurements with a precision close to 10% have been obtained with collocated samplers of identical design and same time since cleaning.

- Available technology allows accurate ($\pm$10 to 15%) measurement of several of the major components of coarse and fine particles (minerals, sulfates, strong acids, and ammonium). However, collection and measurement technologies for elemental carbon, organic carbon, and nitrates are not as well established.

- Field studies of EPA Equivalent PM_{10} Reference Methods and reviews of field data from collocated PM_{10} samplers show substantial biases under certain conditions. These biases result from: (a) allowing a tolerance of $\pm$ 0.5 μm for the 10 μm cutpoint; (b) inadequate restrictions on internal particle bounce; (c) soiling of certain types of PM_{10} inlets; and the losses of semivolatile components.

- Semivolatile organic compounds and semivolatile ammonium compounds (such as NH_4NO_3) may be lost by volatilization during sampling. Such losses may be very important in woodsmoke impacted areas for organic compounds or in agricultural and other areas where low sulfate and high ammonia lead to high NH_4NO_3 concentrations.

- Beta attenuation, tapered element oscillating microbalance (TEOM), and optical monitoring methods have been extensively field tested. Although acceptable comparisons with EPA reference sampling methods have been reported in some collocated field studies, significant losses of semivolatile components may occur during and after sample collection. The presence of significant amounts of semivolatile particles at sampling locations in the western United States is a major concern.

- Certain older optical methods, which provided estimates of ambient PM levels used in epidemiology studies of the 1950s to 1970s, are still employed in some countries. These include (a) the black smoke (BS) method, based on light reflectance from particle stains on sample collection filters and extensively used in Britain and elsewhere in Europe; and (b) the coefficient of haze (COH) method, based on light transmission through the filter stain and used in some U.S. areas. Neither method directly measures the mass of collected particles; so credible estimates of particle concentrations (in $\mu g/m^3$) can only be made via site-specific calibration against mass measurements from collocated gravimetric sampling devices. BS and COH sampling devices typically have $\approx$4.5 μm cut points, collect mainly fine particles but also some coarse particles up to $\approx$10 μm, and are more comparable to $PM_{2.5}$ than PM_{10} or TSP measurements. BS and COH readings are especially sensitive to elemental carbon particle concentrations.

- Personal PM exposure samplers are desirable for evaluating individual exposures. Relatively unobtrusive personal samplers have been designed for several particle size cutpoints, and recent studies suggest that acceptable precision is possible, covering the size range from at least 0.1 to 10 μm d_{ae}.

- Physical elemental analysis methods for metals and other elements include x-ray fluorescence (XRF), particle-induced x-ray emission (PIXE), and instrumental neutron activation analysis (INAA). Atomic absorption spectrometry (AAS) is used for soluble ions such as sodium, magnesium, potassium, and calcium. Ion chromatography (IC) is used for nitrate and sulfate. Automated colorimetry (AC) is used to measure ammonium, chloride, nitrate, and sulfate.

- Accurate chemical speciation of organics, nitrates, and acidity requires comprehensive sampling system components, including gas stream denuders and sequential filter packs. Sampling artifacts can cause significant errors in measurement of organic PM. Some disagreement exists, however, about whether adsorption or volatilization artifacts are most important. Sampling artifacts may be introduced by changes in temperature or organic vapor concentration during sampling and/or storage. Organic aerosol sampling artifacts can cause large errors in particle mass measurements in areas where a large fraction of the PM mass is organic.

- Chemical analysis of the organic fraction of airborne PM is very costly and difficult because of the complex mixture of hundreds of compounds. Analyses of organic compounds have utilized high-performance liquid chromatography (HPLC) and gas-chromatography combined with mass spectroscopy (GC/MS), but only 10 to 20% of the organic mass has been identified as specific chemical compounds. It is now known that some organic vapors are adsorbed on quartz-fiber filters and that some semivolatile material evaporates during and after sampling. However, most information on organic, elemental, and carbonate carbon comes from samples collected on quartz-fiber filters.

- A variety of methods are now available for sampling or analysis of all types of bioaerosols, including fungal spores, bacteria, pollen, and plant or animal fragments. Analytical methods include: cell culture, microscopy, immunoassay, other bioassay methods, chemical assays, and molecular techniques for DNA/RNA-containing particles.

- Light and electron-microscopy analysis of particle morphology (size and shape) can also be used to help identify sources and transport mechanisms for airborne particles.

1.2.5 Ambient U.S. PM Concentrations: Regional Patterns and Trends

- Particle mass data have been collected at a number of rural, suburban, and urban sites across the United States by various local, state, and national programs. The data have been stored in the Aerometric Information Retrieval System (AIRS). Data have also been collected at remote sites as part of the IMPROVE and NESCAUM networks.

- Estimates of annual average biogenic and geogenic PM_{10} concentrations range from 5 to 11 $\mu g/m^3$ for the eastern United States and 4 to 8 $\mu g/m^3$ for the western United States. Annual average PM_{10} concentrations in national parks, wilderness areas, and national monuments in the western United States range from 5 to 10 $\mu g/m^3$ (based on data from IMPROVE). The lowest values in AIRS, obtained at remote sites, range from 4 to 10 $\mu g/m^3$. Annual average PM_{10} values representative of relatively clean suburban and rural areas reported in AIRS for 1993 ranged from 9 to 13 $\mu g/m^3$.

- The five cities with the highest annual mean PM_{10} concentrations for urban sites in the western United States, found in AIRS from 1990 to 1994, were Southern California cities in agricultural regions: Visalia, CA; Bakersfield, CA; Fresno, CA; Riverside, CA; and Stockton, CA. The average concentration in these five areas ranged from 44.8 to 60.4 $\mu g/m^3$.

- Annual average PM_{10} concentrations for most urban areas in the United States are typically greater than about 20 $\mu g/m^3$. Highest annual mean PM_{10} concentrations in the western United States are significantly higher than corresponding five year annual mean values of about 34 $\mu g/m^3$ in eastern U.S. urban areas (Atlanta, GA; Paterson, NJ; Roanoke, VA; Philadelphia, PA; and Atlantic City, NJ) and 36 $\mu g/m^3$ in central U.S. urban areas (St. Joseph, MO; Steubenville, OH; Cleveland, OH; Omaha, NE; and Chattanooga, TN). The lowest annual mean PM_{10} concentrations found at sites in U.S. populated areas (Penobscot Co., ME; Marquette, MI; and Lakeport, CA) averaged about 12 $\mu g/m^3$ during the period from 1990 to 1994.

- PM_{10} mass concentrations averaged over regions or by city, using sites in operation during 1988 to 1994, show a significant year to year decrease at most sites. Exceptions are Philadelphia and some locations in Southern California. The regional decreases at urban sites between 1988 and 1994 were: 20% for the contiguous United States; 18% for the eastern United States; and 28% for the western United States.

- Information on trends of $PM_{2.5}$ (fine) and $PM_{10-2.5}$ (coarse) have been examined. However, the data from Philadelphia, several AIRS sites, the Harvard Six-City sites, and California sites is generally not sufficient either in number of sites or number of years (2.5 to 10 years per site) to demonstrate differential trends in coarse PM and fine PM.

- Long time series for $PM_{2.5}$ and PM_{10} are available from a relatively few sites in Philadelphia and California. Typically, $PM_{2.5}$ to PM_{10} ratios are greater than 0.5 at these sites on an annually averaged basis. However, values of the ratio of $PM_{2.5}$ to PM_{10} are highly variable and can be much smaller than 0.5 on individual days. Because of these considerations, values of $PM_{2.5}$ should be inferred from PM_{10} only where some site-specific information is available. Seasonal or yearly estimates will be more reliable than daily estimates.

- Sulfate ($SO_4^=$) and strong acidity (H_2SO_4 plus HSO_4^-) are regional pollutants distributed relatively evenly over areas of the eastern United States during the summertime. However, in high density livestock areas and the centers of large urban areas, ammonia neutralizes part of the acidity.

- Data for assessing day-to-day variability in $PM_{2.5}$ and PM_{10} are only available from one site in Philadelphia. These data can be used to indicate the potential for daily changes in 24-hour average $PM_{2.5}$ and PM_{10} levels for risk analyses. During this study, average day-to-differences in $PM_{2.5}$ were 6.8 ± 6.5 $\mu g/m^3$ and 8.6 ± 7.5 $\mu g/m^3$ for PM_{10}. Maximum day-to-day differences were 54.7 $\mu g/m^3$ for $PM_{2.5}$ and 50.4 for PM_{10}.

1.2.6 Human PM Exposure

- The total personal exposure to PM consists of outdoor (ambient) and indoor exposures. Nonambient conditions, mainly indoors at home or at work, occupy the vast majority of a person's time. In the U.S., the average daily time spent indoors is 20 h/day, or 85% of the day. Some additional time, about 1.0 to 2.0 h (5%) of the day, is also spent in other nonambient microenvironments (e.g., in vehicles in transit)

- PM_{10} in ambient air penetrates into residential microenvironments and reaches an equilibrium approaching outdoor concentrations. Once indoors, PM of ambient origin decreases due to deposition on surfaces through gravitational settling and electrostatic attraction. The coarse PM has a much higher deposition rate than the fine PM.

- Human indoor activity (e.g., walking on carpets) tends to resuspend previously deposited PM > 5 μm and to stir up or suspend other material (such as tracked-in soil and a variety of biological material such as mold spores and insect debris). Such activity increases indoor PM_{10} but not indoor $PM_{2.5}$.

- In residential and occupational indoor microenvironments, PM is generated by indoor sources (cooking, smoking, vacuuming, dusting, etc.) and is also removed from the indoor air by gravitational deposition and mechanical means (air cleaners, filters, etc.).

- When a cross-sectional analysis is performed that compares ambient PM_{10} to individual personal exposures to PM_{10} for a group of subjects, the correlation often goes towards zero, because of the large influences of indoor sources and sinks that vary *between* the individuals. However, other types of analyses, as follow, indicate significant contributions of ambient particles to total human exposure.

- Because of the relative day-to-day consistency *within* any given residence for the indoor sources and sinks of PM_{10}, the longitudinal (time-series) correlation of personal exposure of a specific individual to total indoor PM_{10} (from outdoor *and* indoor sources) and ambient PM_{10} can be very high. Two analyses conducted to date on a limited number of subjects have yielded R^2 values above 0.9 when indoor sources are consistent from day-to-day.

- Experimental data on a cohort of elderly housewives (N=5) and retirees (N=2), purposefully chosen to have minimal sources of PM at home, shows that their personal exposures to PM_{10} are highly correlated both with the ambient PM_{10} immediately outside their homes ($0.77 < r < 0.96$) and at a nearby monitoring station ($0.75 < r < 0.96$). For the identical cohort of elderly housewives and retirees, their personal exposures to PM > 10 μm (TSP - PM_{10}) had virtually no correlation with the ambient PM > 10 μm ($r = -0.03$; $R^2 = 0.00$).

- Experimental data on personal exposures to sulfates, which are predominantly of outdoor origin and submicron size, show consistently high correlations of total personal exposures with ambient sulfate ($0.78 < R^2 < 0.92$).

- Both fine and coarse particles will enter homes and other microenvironments. However, because coarse particles are rapidly removed, the indoor concentration of ambient fine particles is more representative of the outdoor or ambient fine particle levels. Because fine particles are evenly distributed and remain suspended indoors, a centrally located ambient monitor may provide a fine-particle concentration that is representative of the community exposure to ambient fine particles, but this will usually not be the case for coarse particles.

- Because indoor sources typically do not generate fine mode particles of the same chemical composition as the most common fine particles of ambient origin (e.g., sulfates, metals, etc.), the presence of indoor PM sources will not change the relationships noted in the immediately preceding bullet. Also, the production of indoor-generated particles is controlled by daily indoor activities. Therefore, the exposure to indoor-generated particles will not be correlated with the concentration of ambient (outdoor-generated) particles, and time-series epidemiology based on ambient measurements will not identify health effects of indoor-generated particles.

- Therefore, the measurements of *daily* variations of *ambient* PM concentrations, as used in the *time-series* epidemiology studies of Chapter 12, have a plausible linkage to the daily variations of human exposures to PM from *ambient* sources, for the populations represented by the ambient monitoring stations. This linkage should be better for indicators of fine particles ($PM_{2.5}$) than for indicators of fine plus coarse particles (PM_{10} or TSP), which, in turn, should be better than indicators of coarse particles (PM_{10}-$PM_{2.5}$).

1.3 DOSIMETRY

For risk assessment purposes, exposure-dose-response models are useful in examining the effects of different host characteristics, activity patterns, and exposures on biological responses. Development of a comprehensive biologically based exposure-dose-response model to aid risk assessment requires more information on mechanisms of action of particles on respiratory tract tissues, including behavior of particles once inhaled or deposited (e.g., hygroscopic growth, disaggregation of aggregated particles), pathological processes affecting deposition and clearance of particles, and factors which influence the response of tissue to particle burden. Deposition and clearance models are useful in estimating average regional particle deposition and regional clearance as a function of major particle characteristics. Dosimetry models have also been useful to characterize average PM deposition patterns for humans as a function of age, gender, and activity pattern and may also ultimately be useful for extrapolating laboratory animal data to estimate concentrations that might be expected to be associated with effects in humans.

- Particles may be deposited in (a) the extrathoracic airways (i.e., mouth, nose, and larynx); (b) in airways of the tracheobronchial region; and (c) in the alveolar region where gas exchange occurs. There are differences in deposition mechanism and dose distribution in each of these areas that are dependent on particle size and airway geometry. The major mechanisms of particle deposition on airway surfaces in the respiratory tract are impaction, sedimentation, diffusion, interception, and electrostatic precipitation.

- Respiratory tract deposition patterns are primarily dependent on particle size and distribution (as indicated by the mass median aerodynamic diameter and the geometric standard deviation) within the inspired air. Biologic effects may be a function not only of particle mass deposition but also particle number or the total surface area of the particles.

- Various host factors have been shown to influence predicted particle deposition patterns including age, ventilation pattern, and the presence of obstructive or inflammatory airway disease. Higher overall ventilation increases total deposition. Increased mouth breathing increases the deposition of coarse particles in the tracheobronchial region. Obstructive airway disease, such as asthma, emphysema, and chronic bronchitis, results in increased deposition of particles in the lower respiratory tract.

- Acute effects of PM are probably best related to deposited dose, whereas chronic effects may be related to cumulative or retained dose. Retention of particles is a function of deposition site, clearance of particles by macrophages or the mucociliary system, and particle characteristics, especially solubility. Chronic effects may also arise from recurring cycles of pulmonary injury and repair.

- There are substantial differences among laboratory animal species with regard to the inhalability of different sized particles as well as quantitative and qualitative differences in airway geometry.

- With regard to PM, extrapolation of responses from laboratory animals to humans is hampered by limited development of models due to the lack of data characterizing differences in inhalability, airway geometry, and clearance mechanisms among species. In humans, some inhalable particles can exceed 15 μm d_{ae}, while in small laboratory animals, inhalable particles seldom exceed 4 μm d_{ae}.

- Respiratory tract dosimetry supports the choice of PM_{10} as an index of thoracic particles. However, dosimetric considerations do not provide insight into the selection of a size cut to characterize a fine particle mode.

1.4 PARTICULATE MATTER HEALTH EFFECTS

Many epidemiologic studies have shown statistically significant associations of ambient PM levels with a variety of human health endpoints, including mortality, hospital admissions, respiratory symptoms and illness measured in community surveys, and changes in pulmonary mechanical function. Associations of both short-term (usually days) and long-term (usually years) PM exposure with most of these endpoints have been consistently observed. The general internal consistency of the epidemiologic data base enhances the confidence accorded the reported results and has contributed to increasing public health concern. However, there remains uncertainty regarding the shapes of PM exposure-response relationships; the magnitude and variability of risk estimates for PM; the ability to attribute observed health effects to specific PM constituents; the time intervals over which PM health effects (e.g., shortening of life) are manifested; the extent to which findings in one location can be generalized to other locations; and the nature and magnitude of the overall public health risk imposed by ambient PM exposure. While the epidemiology data provide support for the associations mentioned above, understanding of underlying biologic mechanisms has not yet emerged.

1.4.1 Epidemiology Findings

The findings from the epidemiology studies are often expressed in terms of relative risk (RR), indicating the ratio of the probability of occurrence of a given effect between two different exposure conditions or exposure groups, or as an odds ratio, which is similar to RR for conditions that occur relatively infrequently (such as PM-mortality). Relative risks are often expressed for a specific increase in a PM indicator (e.g., a 50 $\mu g/m^3$ increase in PM_{10}) and provide an estimate of percentage increase in risk above baseline mortality or morbidity rates in the lowest exposure time periods or location per the stated increment of PM indicator concentration. For example, a RR = 1.05 per 50 $\mu g/m^3$ PM_{10} increase implies that an approximate 5% increase over background risk level is associated with a 50 $\mu g/m^3$ increase in PM_{10} over baseline in the particular study area, assuming linearity of dose-response relationships and the absence of a threshold.

Ambient PM Mortality Effects

- Early studies of severe air pollution episodes in Europe and the U.S. from the 1930's to 1950's indicated that exposure to high ambient levels of urban air pollution can produce marked increases above the expected numbers of daily deaths during severe episodes (e.g., in the Meuse Valley in 1930, in Donora in 1948, and in London in 1952). These observations left little doubt that exposures to ambient air containing high concentrations of particles and other copollutants such as SO_2 can be lethal, although underlying mechanisms have not yet been delineated.

- More than 20 time-series analyses published in the past 10 years demonstrate positive associations between daily mortality and 24-h concentrations of ambient particles indexed by various measures (BS, COH, TSP, PM_{10}, $PM_{2.5}$, H^+, $SO_4^=$) in numerous metropolitan areas of the U.S. and other countries. Relative risk (RR) estimates for daily mortality in relation to daily ambient PM concentration are generally positive and statistically significant across a variety of statistical modeling approaches and methods of adjustment for effects of relevant covariates such as season, weather, and co-pollutants.

- Numerous time-series analyses of TSP-mortality relationships have explored many methodological issues related to use of specific types of models (e.g., parametric, non-parametric, Poisson, GLM, LOESS, etc.), model specification (e.g., inclusion of only PM in analytical models or other copollutants as well), control for impacts of weather variables (temperature, humidity, synoptic weather patterns), and adjustments for other potentially confounding covariates. Several analyses of data from Philadelphia by various investigators have proven to be especially useful in confirming significant positive relationships between 24-h TSP concentrations and daily mortality, while also clarifying season-specific variations in the PM-mortality RR and the impacts of weather adjustments or other copollutants on the RR attributed to PM. Recent Health Effects Institute-sponsored analyses underscore the great complexity inherent in simultaneous statistical adjustment for health effects of multiple air pollutants. Overall, the analyses have produced basically robust results indicative of significant PM effects on mortality.

- RR estimates for total non-accidental mortality associated with a 50 $\mu g/m^3$ increase in 24-h average PM_{10} range from 1.015 to 1.085. With PM_{10} as the only pollutant index in

the model, RR = 1.025 to 1.085. In the studies testing multiple pollutant models (with copollutant(s) in the model), PM_{10} RR = 1.015 to 1.025. Higher relative risks are indicated for the elderly and for those with pre-existing respiratory conditions.

- The new time-series analyses clearly substantiate significant associations between daily mortality or morbidity and ambient 24-h PM_{10} concentrations typical of U.S. urban airsheds. Less extensive evidence points toward fine particles as likely being important contributors to the observed PM-associated mortality, based on studies showing positive associations of daily mortality with various fine particle indicators (e.g., $PM_{2.5}$, $SO_4^=$, H^+, etc.).

- Fine particles ($PM_{2.5}$) showed a consistent and statistically significant relationship to acute mortality in six U.S. cities, with relative risks ranging form 1.02 to 1.06 per 25 $\mu g/m^3$ $PM_{2.5}$. Coarse particles showed no significant relationship to excess mortality in five of the six cities. In Steubenville, $PM_{15-2.5}$ was more strongly related to mortality than was $PM_{2.5}$, but these two particle indicators were highly correlated.

- Recent chronic (annual average) PM exposure studies also indicate statistically significant positive associations between excess mortality and fine particle indicators. Relative risk estimates derived from such studies suggest greater percentage increases in mortality risk than do the short-term mortality RR estimates. However, the chronic exposure RR estimates are based on PM concentration during the 5 or 15 to 20 year study periods and do not necessary reflect the full impacts of longer past PM exposures (likely much higher in the most highly polluted cities). Thus, lower RR estimates than the published ones for mortality associated with chronic PM exposure are apt to apply.

Ambient PM Morbidity Effects

Numerous epidemiologic studies in the United States and elsewhere have also demonstrated significant associations between ambient PM exposures indexed by a variety of indicators (BS, TSP, PM_{10}, $PM_{2.5}$, $SO_4^=$, H^+) and various acute and chronic morbidity outcomes. Such outcomes include, for example, hospital admissions, increased respiratory symptoms, and decreased lung function.

- Studies of hospitalization for chronic obstructive pulmonary disease (COPD) and pneumonia show moderate, but statistically significant RR's in the range of 1.06 to 1.25 per increase of 50 $\mu g/m^3$ in PM_{10} (24-h). Most studies of hospitalizations for respiratory illnesses typically include patients $\geq$65 years of age. Increased hospital admissions for respiratory causes during London episodes suggested an association with sulfuric acid aerosols, as well as with BS and SO_2 levels. Recent studies also show associations between ambient acidic aerosols and summertime respiratory hospital admissions.

- Studies of PM associations with lower respiratory disease yielded odds ratios (OR) which ranged from 1.10 to 1.28, and studies of cough yielded odds ratios ranging from 0.98 to 1.29 for a 50 $\mu g/m^3$ increase in PM_{10} (24-h). Limited data were available relating PM exposure to asthma or respiratory symptoms in adults. Chronic cough, chest illness, and bronchitis showed positive associations with annual average PM concentrations.

- Pulmonary function studies of children suggest that short term effects result from PM exposure. Peak expiratory flow rates were decreased 30 to 40 ml/sec per 50 $\mu g/m^3$ increase in PM_{10} (24-h). Somewhat larger effects occurred in symptomatic groups, such as asthmatics. An estimate of the effect of PM on lung function in adults found a 29 ($\pm$10) ml decrease in FEV_1 per 50 $\mu g/m^3$ increase in PM_{10}, similar in magnitude to changes found in children. The chronic pulmonary function studies are less numerous than the acute studies and the results are inconclusive.

- Bronchitis symptoms and prevalence rates in children were found to be somewhat more closely associated with annual average H^+ concentrations than with other PM indicators. However, in studies demonstrating these effects, the acid levels were highly correlated with other fine-particle indicators.

- While numerous studies of PM related respiratory morbidity have been conducted using PM_{10} as an indicator, only a few studies have examined the effects of fine particle indicators, e.g., $PM_{2.5}$. Although different studies have suggested that one of these exposure indicators is a better predictor than the other for a specific endpoint, this issue is as yet unresolved. The $PM_{2.5}$ studies do show effects related to exposure to the fine fraction, but high correlations among $PM_{2.5}$, PM_{10}, and acid aerosols make it very difficult to attribute the effects to a single specific exposure indicator.

1.4.2 Toxicology Findings

The data on the potential toxicity of PM are derived from controlled human exposure, laboratory animal, and occupational studies. Each type of study has its own strengths and weaknesses. The studies vary in the populations examined (i.e., by age, health status, etc.), the duration of the study, and the exposure atmospheres (i.e., size distribution, concentration, chemical composition). The studies indicate that inhaled PM causes effects on the respiratory tract. The magnitude and character of the effects are dependent on the particle size distribution and exposure dose, as well as on the physiologic status of the host.

Acidic Aerosols

Most of the toxicology data on PM are derived from controlled exposure studies in humans and laboratory animals. These studies have most extensively focused on acidic aerosols, namely sulfuric acid aerosol and various sulfates and nitrates, and have included characterization of acid aerosol effects on pulmonary mechanical function, lung particle clearance mechanisms, and other lung defense mechanisms.

- Healthy subjects experience few, if any, decrements in lung function or altered airway responsiveness following single exposures to inhaled acid aerosols (H_2SO_4) at levels up to 2,000 $\mu g/m^3$ for 1 h. Mild lower respiratory symptoms (such as cough) occur at exposure concentrations in the >500 $\mu g/m^3$ range.

- A substantial portion of inhaled acid aerosols may be neutralized by airway ammonia or buffered by airway surface liquids.

- Acid aerosol exposures (>100 $\mu g/m^3$) can cause changes in mucociliary clearance, in healthy or asthmatic humans. Mucociliary clearance in laboratory animals is initially increased and then ultimately decreased by repeated exposures to 125 $\mu g/m^3$ H_2SO_4 aerosol. Chronic exposure of laboratory animals to higher acid levels (~ 250 $\mu g/m^3$) for 52 weeks alters clearance and is also associated with changes in the bronchial tree indicative of mucus hypersecretion.

- Asthmatic subjects are more sensitive than healthy subjects to the effects of acid aerosols on lung function. Responses in asthmatics are generally observed with acute (<3 h) exposures at concentrations of ~ 350 $\mu g/m^3$ and higher. Exposures in the 450 to 1000 $\mu g/m^3$ range in asthmatics can result in changes in airway responsiveness to bronchoconstrictor agents.

- Adolescent asthmatics may be more sensitive than adults and may experience small decrements in pulmonary mechanical function in response to acute exposures (<3 h) to H_2SO_4 at levels between 70 and 100 $\mu g/m^3$.

- Acute exposure (<24 h) of healthy laboratory animals to H_2SO_4 at concentrations above 1000 $\mu g/m^3$ can alter pulmonary mechanical function largely due to bronchoconstriction. In guinea pigs, 100 $\mu g/m^3$ of acid aerosol may produce small transient effects. Chronic exposure (weeks/months) to 500 $\mu g/m^3$ H_2SO_4 is also associated with alterations in pulmonary mechanical function.

- Submicron droplets of H_2SO_4 are effective in altering pulmonary mechanical function in laboratory animals. Aerosols larger than 2 to 4 μm have a low inhalability in small laboratory animals (e.g., mice, rats, etc.) However, acid aerosol studies in humans do not permit a clear distinction between responses to aerosols in the range of 0.1 to 20 μm.

- Lung defense mechanisms and resistance to bacterial infection may be altered by exposure to H_2SO_4 concentrations of about 1000 $\mu g/m^3$ in laboratory animal species; alveolar macrophage function may be affected at levels as low as 500 $\mu g/m^3$ H_2SO_4. Human exposure to acid aerosol (1000 $\mu g/m^3$) did not affect macrophage function.

- Low levels of H_2SO_4 (100 $\mu g/m^3$) have been shown to react synergistically with O_3. Exposure of healthy and asthmatic subjects to a mixture of H_2SO_4 and O_3 suggests that 100 $\mu g/m^3$ H_2SO_4 may slightly exacerbate O_3 lung function effects.

- Acid coating of ultrafine zinc oxide (ZnO) particles appears to enhance the effects of acid on some responses in the guinea pig, including permeability, inflammation, and diffusing capacity. Larger impacts on such endpoints occurred at lower concentrations of H_2SO_4 and ZnO with combined exposure than with separate exposures to each alone.

Other PM Constituents

Controlled human exposures to PM constituents other than acid aerosols are limited. Laboratory animal studies and occupational exposure studies provide information on other PM substances, including metals, diesel emissions, crystalline silica, and other miscellaneous

particles. Human studies of particles other than acid aerosols provide insufficient data to draw confident conclusions regarding health effects.

- Acute inhalation exposures of humans and laboratory animals to high levels (mg/m^3) or chronic exposures to lower concentrations of metal particles can have effects on the respiratory tract. The effective exposure levels in such studies are markedly higher than metal concentrations now generally present in the ambient U.S. atmosphere.

- Ultrafine particles occur in the ambient atmosphere in high numbers and have a high collective surface area. The presence of ultrafine particles in human alveolar macrophages suggests human exposure to ambient ultrafines or aggregates of ultrafine particles. Limited human studies indicate slower clearance of ultrafine than of larger inhalable particles. Laboratory animal studies suggest potential toxic effects of inhaled insoluble ultrafine particles, but the limited available data preclude quantitative estimates of any effective concentrations or doses for ambient ultrafine particle species.

- At very high concentrations ($> 1{,}000\ \mu g/m^3$) chronic exposures to diesel particles cause inflammatory, histological, and biochemical changes in laboratory animals. The toxicity of diesel emissions is considered to be associated with the particle rather than the gas phase. A no-adverse-effect level for chronic diesel particle exposure has been estimated at $155\ \mu g/m^3$. Thus, at current concentrations ($< 10\ \mu g/m^3$) typical for U.S. ambient air, diesel PM is not likely to exert significant health effects on healthy humans.

- Chronic exposure to crystalline silica has been shown to cause inflammation of the lung followed by silicosis, a fibrotic lung disease, in occupationally-exposed workers. Using a high estimate of 10% for the crystalline silica fraction in PM_{10}, current data suggests that, for healthy individuals not compromised by other respiratory ailments, maintenance of the $50\ \mu g/m^3$ annual NAAQS for PM_{10} would be adequate to protect against silicotic effects from ambient crystalline silica exposures.

1.4.3 Population Groups at Risk

Susceptibility can be affected by factors which influence dosimetry or the response of tissues to particle burdens. The mechanisms by which the various sizes and constituents of ambient PM could exert or modify health effects are not understood. Mechanistic studies to date have mainly focused attention on deposition and clearance mechanisms and less on the biological response to PM. Host factors that may increase the susceptibility to PM include both changes in physiologic factors affecting respiratory tract deposition and pathophysiologic factors affecting response. For example, asthmatics show increased response to acid aerosols or bioaerosols; COPD patients show increased PM deposition and impaired clearance; and airway inflammation or compromised immune status may alter tissue response to inhaled particles.

- Susceptible groups most clearly at special risk for PM effects include the elderly and those with cardiopulmonary disease, based on available epidemiology findings.

- Epidemiology studies indicate that mortality and hospitalization for respiratory causes are strongly related to ambient PM exposures. Several hypotheses have been advanced for possible underlying mechanisms. For example, PM may impair ventilation in COPD patients by causing airway narrowing and increasing the work of breathing. In addition, PM may lead to increased secretion and/or increased viscosity of mucus, possibly exacerbating airway narrowing. Also, some types of PM can cause inflammatory responses and epithelial cell damage in people with chronic respiratory disease.

- Epidemiologic findings indicate that ambient PM exposures are also associated with increased risk for mortality and hospitalization due to cardiovascular causes. Cardiac arrhythmia has been hypothesized as being involved in mortality due to acute PM exposure.

- Epidemiology findings indicate that risk of mortality and morbidity due to lower respiratory disease (e.g. pneumonia) is increased by ambient PM exposure. This may be due to exacerbation, by PM, of already existing respiratory disease. PM may also increase susceptibility to infectious disease by decreasing clearance, impairing macrophage function, or through other specific and nonspecific effects on the immune system. The epidemiologic findings also indicate that individuals with preexisting infectious respiratory disease (e.g. pneumonia) are at increased risk for PM effects.

- Smokers constitute a significant fraction (ca. 80%) of individuals with COPD and a smaller but notable portion of cardiovascular disease patients. Therefore, smokers are another population group at likely increased risk for PM health effects.

- Asthmatics are more responsive than non-asthmatics to acid aerosols in controlled exposure studies. Asthma exacerbations are well known to be associated with ambient and indoor bioaerosols. In epidemiological studies, asthma exacerbations, sometimes requiring medical attention have also been associated with ambient coarse PM dominated PM_{10} exposure.

- Children and adolescents may also be potentially susceptible to ambient PM effects due to their increased ventilatory frequency resulting in greater respiratory tract PM deposition. In children, epidemiologic studies reveal associations of PM exposure with increased bronchitis symptoms and small decreases in lung function.

1.5 WELFARE EFFECTS

Chapter 8 discusses visibility and climate change impacts of airborne particles as two key types of welfare effects associated with ambient airborne particulate matter. Chapter 9 discusses damage to materials due to PM and related pollutants. PM-related effects on vegetation, crops, and ecosystems are not covered in this document.

1.5.1 Visibility Effects

- Chapter 8 of this document includes information supplementary to several other significant reviews of the science of visibility, including the 1991 report of the National Acid Precipitation assessment Program, the National Research Council's *Protecting Visibility in National Parks and Wilderness Areas* (1993), and EPA's 1995 *Interim Findings on the Status of Visibility Research*. The following points are made in Chapter 8, and/or in the above referenced documents.

- The relationships between air quality and visibility are well understood. Ambient fine particles are the major cause of visibility impairment. Significant scientific evidence exists showing that reducing fine particle concentrations will improve visibility.

- The National Research Council defines visibility qualitatively as "the degree to which the atmosphere is transparent to visible light." This definition may be expressed quantitatively in terms of contrast transmittance. The EPA has defined visibility impairment as a reduction in visual range and atmospheric discoloration.

- Light, as it passes through the atmosphere from a scene to an observer, is both scattered and absorbed. The rate of loss of transmitted light intensity with distance is measured by the light-extinction coefficient which may be expressed as the sum of the coefficients for: (a) light scattering due to gases; (b) light scattering due to particles; (c) light absorption by gases, and; (d) light absorption by particles.

- Light scattering efficiency depends on particle size, falling off rapidly for particles below 0.3 or above 1.0 μm in diameter. Therefore, particles in the accumulation mode (of the fine particle mode) are most effective in scattering light and are more important in visibility degradation than either nuclei mode or coarse mode particles. Light absorption is not a strong function of particle size. Under exceptional circumstances, such as dust storms, coarse particles can dominate scattering.

- In addition to reducing the intensity of light carrying information about a scene (transmitted radiance), particles also scatter light into the observer's view. This extraneous light, called air light or path radiance, carries no information about the scene. The competition between these two sources of light, expressed as the ratio of transmitted radiance from the scene to path radiance, determines the contrast transmittance and the visual quality of the view.

- Visibility at any location is affected by air quality and non-air quality related effects. The visibility effects of atmospheric constituents are dependant upon not just the mass of pollutants, but on the size distribution and refractive index of particles, which are strongly influenced by relative humidity. Non-air quality effects include the angle between the sun and the observer's sight path, location of clouds, and reflectivity of the ground. These effects are independent of effects due to changes in atmospheric constituents. Lighting and scene effects can be accounted for by defining a range of these effects when estimating visibility changes due to air quality influences.

- The relationship between air pollution and the appearance of a scenic view is well understood. Models exist that, given an adequate description of the air quality and non-air quality variables, can produce a simulated photograph that accurately depicts a cloud-free scene as it would appear to a human observer.

- There are several potential quantitative indicators of visibility. Indicators such as contrast transmittance, which provide the most information on the appearance of a scenic view, provide little information that is helpful in developing control strategies to improve or protect visibility. Indicators such as fine particle mass and composition provide more information useful for control strategies but provide less information on visibility. Potential indicators include: (a) fine particle mass and composition (fine particle mass alone provides less of both types of information); (b) scattering by dried ambient particles; (c) scattering by particles under ambient conditions; (d) extinction (calculated from measurements of scattering plus absorption); (e) light extinction measured directly; and (f) contrast transmittance.

1.5.2 Climate Change

- Particles suspended in the atmosphere affect the earth's energy budget and thus exert an impact on climate: (a) directly by increasing the reflection of solar radiation by cloud-free portions of the atmosphere, and (b) indirectly by affecting cloud microphysical properties in ways that increase the brightness and stability of clouds.

- Estimates of atmospheric sulfate aerosol solar radiation effects (expressed as radiative forcing) range from -0.3 W m^{-2} to -1.1 W m^{-2} for direct effects and range from -0.4 to -1.6 W m^{-2} for indirect effects. These values may be compared to the estimated radiative forcing of +2.4 W m^{-2} due to the increase in concentrations of greenhouse gases from the pre-industrial era to 1994.

- Therefore, on a globally averaged basis, radiative cooling due to anthropogenic particles may have substantially offset the radiative heating due to increases in atmospheric concentrations of greenhouse gases such as carbon dioxide, methane, and chlorofluorocarbons.

- Aerosol lifetimes are also much shorter than the time required for global mixing, therefore, aerosol radiative effects are most likely to exert their influence on a regional rather than on a global basis.

- The lifetimes of particles in the troposphere are short (days to weeks) compared to the above greenhouse gases (years to over 100 years). Therefore, aerosol concentrations will respond more rapidly to variations in emissions than will the greenhouse gases.

1.5.3 Materials Damage

- Particle exposure results in the soiling of painted surfaces and other building materials, increasing the cleaning frequency for exposed surfaces and possibly reducing their useful lifetimes.

- Evidence suggests possible effects of particles on fabrics, electronics, and works of art.

- Building materials (metals, stones, wood, paints) undergo wear even in the absence of pollutant exposure through physical, chemical, and biological interactions involving moisture, temperature, oxygen, and various types of biological agents.

- Deposition of acid aerosols may increase the corrosion of metals by reacting directly with the metal or the metal corrosion film.

- Deliquescent or hygroscopic salts, deposited on metals, accelerate corrosion by decreasing the critical relative humidity. The decrease in the critical relative humidity results in an increase in the amount of moisture on the metal surface. Acid forming gases dissolve in the moisture layer, causing generation of corrosive acids and ionic species. Exposure to acid forming gases may also limit the life expectancy of paints and may damage various building stones and cement products beyond that resulting from natural weathering processes.

- There are insufficient data available to accurately estimate economic impacts of exposure of building materials to acid forming aerosols and particles.

1.6 KEY CONCLUSIONS

- Epidemiologic studies show consistent positive associations of exposure to ambient PM with health effects, including mortality and morbidity. The observed associations of ambient PM exposure with health effects must be adjusted for the effects of other environmental or demographic factors, depending on whether the effects are acute or chronic, in order to quantitatively assess the role that may be attributed to PM exposure. Estimates of PM health effects have shown reasonable quantitative consistency in different studies, with only modest sensitivity to different methods of analysis. However, a clear understanding of specific biologic mechanisms remains to be established.

- Individuals with cardiovascular or pulmonary disease, especially if they are elderly, are more likely to suffer severe health effects (mortality or hospitalization) related to PM exposure than are healthy young adults. Children and asthmatics are also susceptible to certain PM effects, e.g., increased respiratory symptoms and decreased lung function. Smokers also constitute a population group at increased risk for ambient PM exposure effects.

- Recent analyses continue to support the use of PM_{10} as an indicator of ambient particle exposures associated with human health effects. The consistent association of mortality and various morbidity end points with PM_{10} exposure clearly substantiates the earlier rationale underlying selection of this indicator and PM_{10} standard for protection of public health.

- Additional consideration of the subdivision of PM_{10} into fine and coarse components is also warranted. Indices of PM exposure that have been most consistently associated with health endpoints are by PM_{10} or PM_{15} and fine particle indicators. Less consistent relationships have been observed for TSP and the coarse fractions of $PM_{10-2.5}$.

- In human populations, the daily variation in the personal exposure to ambient fine particles is reflected by daily variation in ambient fine particle concentration measured at a central monitoring site better than total exposures to coarse particles are reflected by measurements of ambient coarse particles at community monitoring sites. This is consistent with the observed high correlations of personal sulfate exposures with ambient sulfate concentrations found experimentally. Therefore, central site measurements of fine particle indicators can be useful in PM epidemiology studies.

- Development of a comprehensive biologically-based exposure-dose-response model to aid health risk assessment requires further data characterizing differences in inhalability, airway geometry, and clearance rates among species. Information is also required on mechanism(s) of action, pathological processes affecting deposition and clearance of particles, and factors which influence the response(s) of respiratory tract tissues to particle burden.

- Estimation of public health impacts of ambient airborne particle exposures in the United States would most credibly require use of relative risk estimates derived for particular U.S. urban areas, in combination with estimates of exposures to ambient particle concentrations for the general population and/or specific susceptible subgroups (e.g., the elderly) within those particular areas. In view of geographic differences in ambient PM mixtures and demographics, broad generalization and application of some single "best estimate" of relative risk for a given increment in concentration of a given particle indicator (e.g., PM_{10}, $PM_{2.5}$, etc.) would be subject to much uncertainty.

- Epidemiological studies indicate increased health risks associated with exposure to PM, alone or in combination with other air pollutants. PM-related increases in individual health risks are small, but likely significant from an overall public health perspective because of the large numbers of individuals in susceptible risk groups that are exposed to ambient PM. PM_{10} and indicators of fine particles are more consistently associated with health risks than indicators of coarse particles.

- Aerosol effects on visibility and climate, through light scattering and changes in cloud microphysics, primarily arise from fine particles.

- Based on points discussed above, fine and coarse particles should be considered as separate subclasses of pollutants. Consideration of formation, composition, behavior, exposure relationships, and sources argue for monitoring fine and coarse particles separately. Because fine and coarse particles are derived from different sources, it is also necessary to quantify ambient levels of fine and coarse particles separately in order to plan effective control strategies.

2. INTRODUCTION

This document is an update revision of "Air Quality Criteria for Particulate Matter and Sulfur Oxides" published by the United States Environmental Protection Agency (EPA) in 1982, an Addendum to that document published in 1986, and an Acid Aerosols Issue Paper published in 1989, and it will serve as the basis for reevaluating the current National Ambient Air Quality Standard (NAAQS) for particulate matter (PM) set in 1987. The present document, Air Quality Criteria for Particulate Matter, critically assesses the latest scientific information relative to determining the health and welfare effects associated with exposure to various concentrations of PM in ambient air. The document is not intended as a complete and detailed literature review, but it does evaluate thoroughly information relevant to PM NAAQS criteria development based on pertinent literature available through February, 1996.

2.1 LEGISLATIVE REQUIREMENTS

Two sections (Sections 108 and 109, U.S. Code, 1991) of the U.S. Clean Air Act (CAA) govern the establishment, review, and revision of National Ambient Air Quality Standards (NAAQS). Section 108 directs the Administrator of the U.S. Environmental Protection Agency (EPA) to list pollutants that may reasonably be anticipated to endanger public health or welfare and to issue air quality criteria for them. The air quality criteria are to reflect the latest scientific information useful in indicating the kind and extent of all exposure-related effects on public health and welfare that may be expected from the presence of the pollutant in ambient air.

Section 109 directs the Administrator of EPA to propose and promulgate "primary" and "secondary" NAAQS for pollutants identified under Section 108. Section 109(b)(1) defines a primary standard as a level of air quality, the attainment and maintenance of which, in the judgment of the Administrator, based on the criteria and allowing for an adequate margin of safety, are requisite to protect the public health. Section 109(d) of the CAA requires the periodic review and, if appropriate, revision of existing criteria and standards. Under

Section 109(b) of the CAA, the Administrator must set secondary NAAQS that are based on the criteria and are requisite to protect the public welfare from any known or anticipated adverse effects associated with the presence of such pollutants. Welfare effects are impacts of air pollution not directly affecting human health, such as effects on vegetation, crops, soils, water, animals, manufactured materials, weather, visibility, and climate, as well as damage to and deterioration of property, hazards to transportation, and effects on economic value and personal comfort and well-being.

2.2 REGULATORY BACKGROUND

"Particulate matter" is the generic term for a broad class of chemically and physically diverse substances that exist as discrete particles (liquid droplets or solids) over a wide range of sizes. Particles originate from a variety of stationary and mobile sources. They may be emitted directly or formed in the atmosphere by transformation of gaseous emissions such as sulfur oxides (SO_x), nitrogen oxides (NO_x), and volatile organic substances. The chemical and physical properties of PM vary greatly with time, region, meteorology, and source category, thus complicating the assessment of health and welfare effects. Particles in ambient air usually occur in two somewhat overlapping bimodal size distributions: (1) fine (diameter less than 2.5 μm) and (2) coarse (diameter larger than 2.5 μm). The two size fractions tend to have different origins and composition.

On April 30, 1971 (Federal Register, 1971), EPA promulgated the original primary and secondary PM NAAQS under Section 109 of the CAA. The reference method for measuring attainment of these standards was the "high-volume" sampler (Code of Federal Regulations, 1986), which collects PM up to a nominal size of 25 to 45 μm (so-called "total suspended particulate" or "TSP"). Thus, TSP was the original indicator for the PM standards. The primary standards for PM (measured as TSP) were 260 $\mu g/m^3$, 24-h average not to be exceeded more than once per year, and 75 $\mu g/m^3$, annual geometric mean. The secondary standard (measured as TSP) was 150 $\mu g/m^3$, 24-h average not to be exceeded more than once per year.

On October 2, 1979 (Federal Register, 1979a), EPA announced that it was in the process of revising the Air Quality Criteria Document (AQCD) and reviewing the existing

PM NAAQS for possible revisions. External review drafts of that revised AQCD were made available for public comment and peer review by the Clean Air Scientific Advisory Committee (CASAC) of EPA's Science Advisory Board (SAB). CASAC prepared a "closure" memorandum to the Administrator indicating its satisfaction with the final draft of the AQCD. After closure, minor technical and editorial refinements were made to the AQCD (U.S. Environmental Protection Agency, 1982). The final draft of the document was issued simultaneously with the proposal of revisions to the PM standards.

On March 20, 1984 (Federal Register, 1984), EPA proposed a number of revisions to the primary and secondary PM standards. Following publication of the proposal, EPA held a public meeting in Washington, DC on April 30, 1984, to receive comments on the proposed standards revisions. After the close of the original public comment period (June 5, 1985), CASAC met on December 16 and 17, 1985, to review the proposal and to discuss the relevance of certain new scientific studies on the health effects of PM that had emerged since CASAC completed its review of the AQCD and staff paper in January 1982. Based on its preliminary review of these new studies, CASAC recommended that EPA prepare separate addenda to the AQCD and staff paper to evaluate relevant new studies and to discuss their potential implications for standard-setting. The EPA announced acceptance of these recommendations on April 1, 1986 (Federal Register, 1986a). On July 3, 1986, EPA announced (Federal Register, 1986b) the availability of an external review draft document, entitled Second Addendum to Air Quality Criteria for Particulate Matter and Sulfur Oxides (1982): Assessment of Newly Available Health Effects Information (U.S. Environmental Protection Agency, 1986). At the same time (on July 3 1986), EPA announced a supplementary comment period to provide the public an opportunity to comment on the implications of the new studies and addenda for the final standards. On October 15 and 16, 1986, the CASAC held a public meeting to review the AQCD addendum, at which time CASAC members and representatives of several organizations provided critical review comments on the subject addendum.

The CASAC sent a closure letter on the EPA AQCD addendum to the Administrator dated December 15, 1986, which stated that the 1986 addendum and the 1982 AQCD, previously reviewed by CASAC, represented a scientifically balanced and defensible summary of the extensive scientific literature on PM and SO_x (Lippmann, 1986b).

On July 1, 1987 (Federal Register, 1987), EPA published final revisions to the NAAQS for PM. The principal revisions in 1987 included (1) replacing TSP as the indicator for the ambient standards with a new indicator that includes only particles with an aerodynamic diameter less than or equal to a nominal 10 μm ("PM_{10}"), (2) replacing the 24-h primary TSP standard with a 24-h PM_{10} standard of 150 $\mu g/m^3$, (3) replacing the annual primary TSP standard with an annual PM_{10} standard of 50 $\mu g/m^3$, and (4) replacing the secondary TSP standard with 24-h and annual PM_{10} standards identical in all respects to the primary standards.

2.3 SCIENTIFIC BASIS FOR THE EXISTING PARTICULATE MATTER STANDARDS[1]

The following discussion describes the bases for the existing PM NAAQS set in 1987. The discussion includes the rationale for the primary standards, the pollutant indicator for particulate matter, the averaging time and form of the standard, and finally a discussion of EPA's assessment that led to the standard set in 1987.

2.3.1 Rationale for the Primary Standards

In selecting primary standards for PM, the Administrator must specify (1) the particle size fraction that is to be used as an indicator of particulate pollution, (2) the appropriate averaging times and form(s) of the standards, and (3) the numerical levels of the standards. Based on the assessment of relevant scientific and technical information in the earlier 1982 PM AQCD and addenda, the staff paper and staff paper addendum outlined a number of key factors considered in making decisions in each of these areas. The following discussion of the 1987 revisions of the standards focuses mainly on the considerations that were most influential in the Administrator's selection of particular options.

[1]Adapted from Federal Register (1987).

2.3.2 Pollutant Indicator

Based on the assessment of the available scientific information, EPA concluded in 1987 that (1) a separate PM standard (as opposed to a combination standard for PM and SO_x) remained a reasonable public health policy choice, and (2) given current scientific knowledge and uncertainties, a size-specific (rather than chemical-specific) indicator should be used. In assessing the information in the AQCD, EPA reached several conclusions summarized as follows:

(1) Health risks posed by inhaled particles are influenced by both the penetration and deposition of particles in the various regions of the respiratory tract and the biological responses to these deposited materials. Smaller particles penetrate furthest in the respiratory tract. The largest particles are deposited predominantly in the extrathoracic (head) region, with somewhat smaller particles depositing in the tracheobronchial region; still smaller particles can reach the deepest portion of the lung, the pulmonary region.

(2) The risks of adverse health effects associated with deposition of typical ambient fine and coarse particles in the thoracic region (tracheobronchial and pulmonary deposition) are markedly greater than those associated with deposition in the extrathoracic region. Maximum particle penetration to the thoracic region occurs during oronasal or mouth breathing.

(3) The size-specific indicator for primary standards should represent those particles small enough to penetrate to the thoracic region. The risks of adverse health effects from extrathoracic deposition of typical ambient PM are sufficiently low that particles depositing only in that region can safely be excluded from the indicator.

Considering the above conclusions, other information on air quality composition, the need to provide protection for sensitive individuals who may breathe by mouth or oronasally and the similar convention on particles penetrating the thoracic region adopted by the International Standards Organization (1981), EPA staff recommended that the size-specific indicator include particles of diameters less than or equal to a nominal 10 μm "cut point" generally referred to as "PM_{10}". In terms of collection efficiency, this represents a 50% cut point or diameter (D_{50}), the aerodynamic particle diameter for which the efficiency of particle collection is 50%. With such a cut point, larger particles are not excluded entirely but are collected with substantially decreasing efficiency, and smaller particles are collected with increasing (up to 100%) efficiency. Ambient samplers with this cut point provide a

reliable estimate of the total mass of suspended PM of aerodynamic size less than or equal to 10 μm. Such an indicator (PM_{10}) is conservative with respect to health protection in that it includes all of the particles small enough to penetrate to the sensitive pulmonary region and includes approximately the same proportion of the coarse-mode fraction that would be expected to reach the tracheobronchial region. It places substantially greater emphasis on controlling smaller particles than does a TSP indicator, but it does not completely exclude larger particles from all control.

The assessment of then-available information on respiratory tract deposition in the 1986 AQCD and staff paper addenda reinforced the conclusions reached in the original EPA assessment. In particular, (1) the data did not provide support for an indicator that excluded all particles larger than 10 μm in diameter; (2) the analysis used to support an alternative indicator with a nominal size cut point of 6 μm (Swift and Proctor, 1982) significantly underestimated thoracic deposition of particles larger than 6 μm in diameter under natural breathing conditions; (3) the PM_{10} indicator generally included a similar or larger fraction of the range of particles that can deposit in the tracheobronchial region, although it appeared to be somewhat less conservative in this regard than previously thought with respect to large (>10 μm) particle deposition under conditions of natural mouthbreathing; and (4) the studies of tracheobronchial deposition generally involved adult subjects (other information indicating even greater tracheobronchial deposition of particles in children than in adults provided an additional reason for an indicator that includes particles capable of penetration to the tracheobronchial region). Consideration of these and the earlier conclusions led EPA to reaffirm its recommendation for a PM_{10} indicator. The CASAC also restated its support for PM_{10} in its review of the proposal and the closure letter to the Administrator (Lippmann, 1986a,c).

In 1987 the Administrator accepted the recommendations of the staff and CASAC, as well as their underlying rationale, and decided to replace TSP as the particle indicator for the primary standards with a new indicator that included only those particles less than a nominal 10 μm in diameter (PM_{10}) as specified in the Federal Reference Method.

2.3.3 Averaging Time and Form of the Standards

The EPA's assessment at that time of scientific information available prior to 1987 confirmed the need for both short- and long-term primary standards for PM. The alternative of a single averaging time would not provide adequate protection against potential effects from both long- and short-term exposures without being unduly restrictive. The forms for the 24-h and annual standards are discussed below.

2.3.3.1 24-Hour Standard

The Environmental Protection Agency decided in 1987 that the 24-h standard should be stated in a statistical form that uses more than 1 year of data and accounts for variations in sampling frequency in order to predict the actual number of exceedances to be expected in an average year. When used with an appropriate standard level, the statistical form can provide improved health protection that is less sensitive to changes in sampling frequency than the deterministic form and can also offer a more stable target for control programs. Recognition of the limitations of the deterministic form also led EPA to promulgate a statistical form for the ozone standard (Federal Register, 1979b).

2.3.3.2 Annual Standard

The EPA Administrator decided to change the form of the annual standard in 1987 from the previous annual geometric mean form to a statistical form expressed as an expected annual arithmetic mean. The expected annual arithmetic mean is equivalent to the long-term arithmetic average concentration level, assuming no changes in underlying emissions. The expected arithmetic mean is more directly related to the available health effects information than is the annual geometric mean, which was the previous form of the standard. Because the arithmetic mean concentration is proportional to the sum of the daily means, it reflects the total cumulative exposure of PM to which an individual is exposed. Thus, it is an appropriate indicator to protect against any health effect that depends on chronic, cumulative PM exposure. It is also a reasonable indicator for protecting against health effects that depend on repeated short-term high concentrations (short-term peaks have an influence on the arithmetic mean that is proportional to their frequency, magnitude, and duration). The geometric mean, on the other hand, deemphasizes the effects of short-term peak

concentrations and is heavily influenced by days of relatively clean air. For these reasons, EPA staff and CASAC recommended the change to an arithmetic mean.

Under the statistical form, the expected annual arithmetic average is determined by averaging the annual arithmetic averages from 3 successive years of data. The prior deterministic form of the standard did not adequately take into account the random nature of meteorological variations. In general, annual mean PM concentrations vary from year to year, even if emissions remain constant, due to the random nature of meteorological conditions that affect the formation and dispersion of particles in the atmosphere. If only 1 year of data is considered, compliance with the standard and, consequently, emission control requirements, may be determined on the basis of a year with unusually adverse or unusually favorable weather conditions. The problem of year-to-year variability is, however, reduced by averaging 3 years of data.

2.3.4 Level of the Standards

The original Office of Air Quality Planning and Standards (OAQPS) PM Staff Paper and CASAC recommendations set forth a framework for determining the levels for the proposed PM standards that would protect public health with an adequate margin of safety. The Administrator's decision in 1987 relied heavily on that framework and on the supporting material in the staff paper and its addendum, as well as the CASAC closure letters. The essential steps in this framework are summarized here.

2.3.4.1 Assessment of the Quantitative Epidemiological Studies

The 1982 AQCD and its 1986 addendum identified a small number of community epidemiological studies that are useful in determining concentrations at which PM is likely to adversely impact public health. The EPA staff used these quantitative studies to examine concentration-response relationships and to develop numerical "ranges of interest" for possible PM_{10} standards.

A number of uncertainties associated with the use of these studies had to be considered in selecting an appropriate margin of safety. As discussed in the staff paper, the AQCD, and the addenda to those documents, epidemiological studies are generally limited in sensitivity and are subject to inherent difficulties involving control for covariates or confounders.

Moreover, many of the quantitative studies were conducted in times and places where pollutant composition may have varied considerably from current U.S. atmospheres. Also, most of the studies used British Smoke—British Smoke (BS) is a pseudo-mass indicator related to small particle (aerodynamic diameter less than a nominal 4.5 μm) darkness—or TSP as particle indicators. None of the published studies used the proposed PM_{10} indicator. Thus, assumptions had to be used to convert the various results to common (PM_{10}) units.

2.3.4.2 Identification of Margin of Safety Considerations

The 1982 AQCD and its addendum identified an additional substantial body of scientific literature that, although it did not provide reliable concentration-response relationships for ambient exposures, did provide important qualitative insights into the health risks associated with human exposure to particles. This literature included both quantitative and qualitative epidemiological studies, controlled human exposure experiments, and animal toxicological studies. The EPA staff assessed this literature to identify additional factors and uncertainties that should be considered in selecting the most appropriate margin of safety.

Experience had shown that it was difficult to identify, with confidence, the lowest pollution level at which an adverse effect would occur. Furthermore, in cases such as the present one, the evidence suggested that there is a continuum of effects, with the risk, incidence, or severity of harm decreasing, but not necessarily vanishing, as the level of pollution is decreased.

The requirement for an adequate margin of safety for primary standards addresses uncertainties associated with inconclusive scientific and technical information available at the time of standard setting. It also aims to provide a reasonable degree of protection against hazards that research has not yet identified. Both kinds of uncertainties are components of the risk associated with pollution at levels below those at which human health effects can be said to occur with reasonable scientific certainty. Thus, by selecting primary standards that provide an adequate margin of safety, the Administrator sought not only to prevent pollution levels that have been demonstrated to be harmful, but also to prevent lower pollutant levels that may pose an unacceptable risk of harm, even if that risk is not precisely identified as to nature or degree.

In the absence of clearly identified thresholds for health effects, the selection of a standard that provides an adequate margin of safety requires an exercise of informed judgment by the Administrator. The level selected will depend on the expected incidence and severity of the potential effects and on the size of the population at risk, as well as on the degree of scientific certainty that the effects will in fact occur at any given level of pollution.

The 1986 EPA staff paper recommended a range of potential standards for the Administrator's consideration. The recommended range was below the levels at which EPA staff, with the concurrence of CASAC, had concluded from the available data that adverse health effects were "likely", but in the domain where the data suggested that such effects were "possible". The Administrator proposed refined ranges of standard levels that were based on the 1984 staff and CASAC recommendations. After consideration of the then new scientific evidence contained in the AQCD addendum, the staff revised its recommended range of standards. The Administrator considered the revised EPA assessments and the CASAC recommendations (Lippmann, 1986b) in making the final decision on the standard levels. The rationales for the levels of the 24-h and annual standards are presented below.

2.3.4.3 24-Hour Standard

The 1987 assessment of the short-term epidemiological data expressed PM levels in both the BS or TSP and PM_{10} units. The term "effects likely" denoted concentration ranges derived from the 1982 AQCD and its addendum at or above which a consensus judgment suggested the greatest certainty that the effects studied would occur, at least under the conditions that occurred in the original studies. In the "effects possible" range, EPA found credible scientific evidence suggesting the existence of adverse health effects in sensitive populations, but substantial uncertainty existed regarding the conclusions to be drawn from such evidence.

The 1987 review of the data did not provide evidence of clear thresholds in exposed populations. Instead, they suggested a continuum of response for a given number of exposed individuals, with both the likelihood (risk) of any effects occurring and the extent (incidence and severity) of any potential effect decreasing with concentration (this was particularly true for the statistical analyses of daily mortality in London). Substantial agreement existed that

wintertime pollution episodes produced premature mortality in elderly and ill populations, but the range and nature of observed associations provided no clear bases for determining lowest effects-likely levels or for defining a concentration below which no association remained. The lung function studies in children also provided evidence of effects at concentrations over a range, but the relationships were not certain enough to derive effects-likely levels for PM_{10}. The lung function studies did, however, suggest levels below which detectable functional changes were unlikely to occur in exposed populations. Following CASAC recommendations, EPA used the combined range of effects-possible studies as a starting point for developing alternative standards.

The original range proposed by the Administrator, drawn from the 1984 staff analysis, was 150 to 250 $\mu g/m^3$ PM_{10} 24-h average, with no more than one expected exceedance per year. The lower bound of this range was derived from the original assessment of the London mortality studies. As a result of reanalyses of the London mortality data and the findings from the then current U.S. morbidity studies, the staff reduced the level of the lower bound of the range of interest to 140 $\mu g/m^3$, and noted that the difference between it and the original lower bound (150 $\mu g/m^3$) was within the range of uncertainty associated with converting the morbidity study results from TSP to PM_{10}.

At that time, the study of Lawther et al. (1970) was judged to provide evidence that health effects were likely at PM concentrations above 250 $\mu g/m^3$ (as BS). The effects observed in this study (related to aggravation of bronchitis) were of concern because of both their immediate impact and their potential for inducing longer term deterioration of health status in a significant sensitive group. Based on the uncertain conversion between smoke and PM_{10}, the lowest effects likely level derived from the Lawther study (250 $\mu g/m^3$ as BS) was judged to be in the range of 250 to 350 $\mu g/m^3$ in PM_{10} units.

The 1987 assessment of the Lawther et al. (1970) study formed the basis for the upper bound of the range of PM_{10} standards proposed by the Administrator in 1984. Considering this study alone, a PM_{10} standard of 250 $\mu g/m^3$ might have appeared to contain some margin of safety, even for the sensitive bronchitics studied, because it incorporated a conservative PM_{10} conversion factor and because of differences between exposure conditions in the British study and current U.S. air quality. Because persons with chronic bronchitis were identified as a group particularly sensitive to particulate pollution, a standard of 250 $\mu g/m^3$ (as PM_{10})

also might have provided some margin of safety for other, less sensitive groups. Nevertheless, this study of bronchitics in London had inherent limitations in sensitivity that precluded derivation of unequivocal "effects thresholds" at 250 $\mu g/m^3$ as BS and, by extension, PM_{10}. The 1982 AQCD noted that associations between pollution and health status persisted at lower BS concentrations in selected, more sensitive individuals. Although the lead author of the study objected to attaching any importance to these latter findings (Lawther, 1986), EPA, with CASAC concurrence, found no basis for asserting that this study demonstrated a population threshold at 250 $\mu g/m^3$.

In evaluating the margin of safety for a 24-h standard, it was also important to consider the London mortality studies. A standard at the upper portion of the proposed range (250 $\mu g/m^3$) would be well below the levels (500 to 1,000 $\mu g/m^3$ as BS) of the historical London episodes in which the scientific consensus indicated that pollution was responsible for excess mortality. The portions of the population at greatest risk of premature mortality associated with PM exposures in those episodes included the elderly and persons with preexisting respiratory or cardiac disease. Although the extent of life shortening could not be specified, the seriousness of the effect strongly justified a margin of safety for it (below the consensus effects levels) that was larger than that warranted for the effects on bronchitis.

The staff assessment at that time of several reanalyses of London mortality suggested, however, that the risk of premature mortality for sensitive individuals extended to concentrations substantially lower than those that occurred in the "episodes". Other analyses (Mazumdar et al., 1982; Ostro, 1984; Shumway et al., 1983) provided no objective support for a population threshold below which such a risk no longer existed. Although the risk to individuals may be small at concentrations of 250 $\mu g/m^3$ and below, the number of people exposed to lower concentrations, given U.S. levels, was substantially larger than the number exposed to higher levels. The increased number of individuals exposed increased the risk that effects would occur in the total population exposed.

Differences in the composition of particles and gases among U.S. cities and between U.S. conditions and London at the time that the mortality and morbidity data were gathered added to the complexity of assessing risk associated with PM in the United States. In the case of the mortality studies, however, the staff found that at least one study (Özkaynak and

Spengler, 1985) provided qualitative support for an association between daily mortality and particle concentrations in then nearly contemporary U.S. atmospheres.

The 1982 assessment of the mortality studies and related factors prompted the EPA Administrator to consider standard levels that extended from 250 $\mu g/m^3$ to the lower bound of the original staff range (150 $\mu g/m^3$) and even lower. Reanalyses of the London mortality data prior to 1987 provided additional evidence that serious adverse health effects may occur at PM concentrations below 250 $\mu g/m^3$. These analyses addressed a number of the uncertainties associated with the earlier studies and reinforced the Administrator's concern that a 24-h standard at the upper end of the proposed range may not provide an adequate margin of safety. However, given the uncertainties in converting from BS to PM_{10} measurements, particularly at lower concentrations and the possible differences in particle composition between London at the time the data were gathered and the contemporary United States, it was difficult to use these studies to set a precise level for a PM_{10} standard.

Given these difficulties, it was important to examine studies contemporary with the other studies that utilize gravimetric measurements of particulate concentrations. The staff found the studies of Dockery et al. (1982) and Dassen et al. (1986) to be useful. The Dockery study observed physiologically small but statistically significant decreases in lung function in a group of children exposed to peak PM_{10} levels of 140 to 250 $\mu g/m^3$. The decrements persisted for 2 to 3 weeks following the exposures. The study also suggested the possibility of larger responses in a subset of the children, including those with existing respiratory symptoms. The Dassen study recorded similar decrements in children in the Netherlands following exposure to PM_{10} levels estimated at 200 to 250 $\mu g/m^3$, but no observable effects 2 days after exposure to PM_{10} levels estimated at 125 $\mu g/m^3$. The particle composition, at least in the Dockery study, was more representative of contemporary U.S. cities in that time period, and the associated aerometry provided a more reliable estimate of PM_{10} levels than did the measurements used in the London studies. It was reasonable to expect the endpoints observed (small reversible reductions in lung function in children) to be, in most cases, more sensitive to air pollution than those observed in the London studies. These effects, *per se*, are of uncertain significance to health, but they may be associated with aggravation of respiratory symptoms in children with preexisting illness. Long-term examination of respiratory health in the same community studied by Dockery et al. (1982)

suggested that the children in that community had a higher incidence of respiratory illness and symptoms than children in communities with lower particle levels, but the data showed no evidence for any persistent reduction in lung function (Ware et al., 1986). Uncertainties with respect to the effects of other pollutants (e.g., sulfur dioxide), the consistency of the changes, and exposures precluded specifying unequivocal "effects likely" levels based on this study. The EPA assessment therefore suggested that short-term lung function effects in children were possible across a range of 140 to 250 $\mu g/m^3$ or more as PM_{10}.

In making a decision on a final standard level, the Administrator also considered information from the more qualitative studies of PM. These studies suggested increased risks for sensitive groups (asthmatics) and risks of potential effects (morbidity in adults) not demonstrated in the more quantitative epidemiological literature. The qualitative studies did not provide clear information on effect levels but did justify consideration of effects of PM that have not been sufficiently investigated.

Based on the 1982 assessment of the available scientific data, in 1984, the EPA Administrator expressed an inclination to select a 24-h level from the lower portion of the proposed range of 150 to 250 $\mu g/m^3$. The addendum to the 1982 assessment supported the original findings and, if anything, suggested an even wider margin of safety was warranted. The Administrator, therefore, decided to set the final standard at the lower bound of the range originally proposed (i.e., 150 $\mu g/m^3$). This standard provided a substantial margin of safety below the levels at which there was a scientific consensus that PM caused premature mortality and aggravation of bronchitis. Such a margin was judged to be necessary because of the seriousness of the effects and because the analyses of daily mortality studies suggested that adverse effects may occur at PM levels well below the consensus levels. The standard was in the lower portion of the range where sensitive, reversible physiological responses of uncertain health significance had been possibly, but not definitely, observed in children. Using a conservative assessment of the lung function/particle relationship from Dockery et al. (1982), a change in concentration from background levels (≈ 20 $\mu g/m^3$) to 150 $\mu g/m^3$ would produce lung function changes of at most 10 to 15% in less than 5% of exposed children. Based on the results of Dassen et al. (1986), it appeared unlikely that any functional changes would be detected 1 or 2 days following such exposures. Thus, the maximum likely changes in lung function appeared to present little risk of significant adverse

responses. Standards set at a somewhat higher level, however, would have presented an unacceptable risk of premature mortality and would have allowed the possibility of more significant functional changes. Furthermore, a standard level of 150 $\mu g/m^3$ was fully consistent with the recommendations of CASAC on the 24-h standard (Lippmann, 1986c).

2.3.4.4 Annual Standard

The long-term epidemiological studies examined in 1987 were subject to confounding variables that reduced the studies' sensitivity and made their interpretation difficult. No clear thresholds could be identified for the effects-likely levels, and evidence existed for effects at lower levels (the effects-possible levels); however, the evidence was inconclusive, and the effects were difficult to detect.

Based on an EPA assessment of PM_{10}/TSP ratios in areas with elevated TSP levels, the effects-likely levels from the Ferris et al. (1973) study were revised to 80 to 90 $\mu g/m^3$ as PM_{10}. Because of limitations in sampling duration and the conversion to PM_{10}, this estimate was particularly uncertain, with effects possible at lower concentrations. Of greatest concern was the possibility of long-term deterioration of the respiratory system in exposed populations, the potential for which was indicated by lung function (mechanical pulmonary) changes and increased incidence of respiratory disease. One set of studies (Ferris et al., 1973, 1976) provided some evidence for a "no-observed-effect level" for those effects at or below 60 to 65 $\mu g/m^3$ as PM_{10} (130 $\mu g/m^3$ as TSP), whereas another study (Bouhuys et al., 1978) suggested some possibility of symptomatic responses in adults at long-term median levels at or below about 50 to 55 $\mu g/m^3$ as PM_{10}. The importance of these symptomatic responses, which were unaccompanied by lung function changes, to long-term respiratory health was unclear.

The most important study of long-term effects at that time was an ongoing examination of six U.S. cities (Ware et al., 1986). The study indicated the possibility of increased respiratory symptoms and illnesses in children at multiyear levels across a range of 40 to more than 58 $\mu g/m^3$ as PM_{10} but found no evidence of reduced lung function at these concentrations. This study did not find similar gradients in symptoms and illness within some of the cities, which had somewhat smaller localized pollution gradients. The results of a separate series of studies of long- and intermediate-term (2- to 6-week) exposures in a

number of U.S. metropolitan areas (Ostro, 1987; Hausman et al., 1984) were more supportive of the possibility of effects within cities (respiratory-related activity restrictions in adults) at comparable U.S. exposure levels. The results of these studies were generally consistent with the earlier U.S. studies. In particular, the finding of symptomatic responses in children with no change in lung function (Ware et al., 1986) was consistent with similar findings in adults (Bouhuys et al., 1978) at estimated long-term PM_{10} levels down to 50 $\mu g/m^3$. However, the information available to support the existence of significant adverse effects at annual PM_{10} levels below 50 $\mu g/m^3$ (especially when 24-h levels are maintained below 150 $\mu g/m^3$) was quite limited and uncertain.

Because of the uncertainties and the limited scope and number of long-term quantitative studies available for review in 1987, it was important to examine the results of qualitative data from a number of epidemiological, animal, and ambient particle composition studies in determining what would constitute an adequate margin of safety for an annual standard. These studies justified concern for serious effects not directly evaluated in the above studies. Such effects included damage to lung tissues contributing to chronic respiratory disease, cancer, and premature mortality. Substantial segments of the population may be susceptible to one or more of these effects. Although the qualitative data did not provide evidence for major risks of these effects at the annual PM levels in most U.S. cities at that time, the Administrator believed that the seriousness of the potential effects and the large population at risk warranted caution in setting the standard.

Based on findings discussed in the 1982 AQCD, the EPA Administrator proposed in 1984 to select an annual standard level from a range of 50 to 65 $\mu g/m^3$. In the proposal, the Administrator favored a standard in the lower portion of the range. The evidence discussed in the 1986 addendum, although subject to substantial uncertainty, reinforced this inclination. In light of the 1986 assessment, and in accordance with CASAC recommendations, the Administrator decided to set the level of the annual standard at the lower bound of the original range (50 $\mu g/m^3$, expected annual arithmetic mean). This standard provided a reasonable margin of safety against long-term degradation in lung function, which was judged likely to occur at estimated PM_{10} levels above 80 to 90 $\mu g/m^3$ and for which there was some evidence at PM_{10} levels above 60 to 65 $\mu g/m^3$. Such a standard also provided reasonable protection against the less serious symptomatic effects (bronchitis) for which only

inconclusive evidence was available. Moreover, the staff and CASAC recommended that the combined protection afforded by both 24-h and annual NAAQS be considered in selecting the final standard level. In this regard, analyses of air quality data showed that implementation of the 24-h standard would reduce substantially the annual levels in many U.S. areas to below 50 $\mu g/m^3$, adding to the protection afforded by the annual standard in areas with higher 24-h peak-to-mean ratios. Based on the then available information on risks associated with annual exposures, the EPA Administrator believed that the annual and 24-h standards provided an adequate margin of safety.

2.3.5 Welfare Effects

No convincing evidence existed indicating significant adverse soiling and nuisance at TSP levels below 90 to 100 $\mu g/m^3$, and, on that basis, the Administrator concluded that secondary standards different from the primary standards were not requisite to protect the public welfare against soiling and nuisance. This conclusion was supported by CASAC's determination that there was no scientific support for a TSP-based secondary standard (Lippmann, 1986c). Therefore, the Administrator decided to set 24-h and annual secondary PM_{10} standards that are equal in all respects to the primary standards.

The other welfare effects of principal interest were impairment of visibility, potential modification of climate, and contribution to acidic deposition. All three of these effects were believed to be related to regional-scale levels of fine particles, and control programs designed to ameliorate them would likely involve region-wide reductions in emissions of sulfur oxides. The Administrator also concurred with the staff suggestions that a separate secondary particle standard was not needed to protect vegetation or to prevent adverse effects on personal comfort and well-being.

2.4 TOPICS/ISSUES OF CONCERN FOR CURRENT CRITERIA DEVELOPMENT

Based on the available scientific evidence, several critical topics and associated issues are addressed in this document, as part of the current CAA-mandated periodic review of

criteria and NAAQS for PM. Some of the most critical topics and issues addressed are as follows.

2.4.1 Air Quality and Exposure

2.4.1.1 Physics and Chemistry of Atmospheric Aerosols

The atmospheric aerosols of interest because of their potential health and welfare effects consist of two principal components: a gas phase ("air" in this case) and a solid or liquid particle phase in suspension. Fine particles in the atmosphere consist mainly of (1) sulfate, nitrate, ammonium ions, and water; (2) photochemically formed organic aerosols; and (3) carbon, organic matter, and metallic components emitted directly into the atmosphere. Coarse particles in the atmosphere are composed mainly of silica, calcium carbonate, clay minerals, soot, and, sometimes, organic substances. A general relationship exists between chemical composition and particle diameter, with particles of ≤ 2.5 μm in diameter containing most of the SO_4^{2-}, H^+, and NH_4^+, as well as a significant fraction of the NO_3^- and Cl^-. The particle volume (mass) frequency function is often multimodal. The fine-volume fraction may have two or more modes below 1.0. The coarse fraction generally has one mode within the range ≈ 5 to 50 μm. The particle volume frequency functions for the fine and coarse fractions often behave independently, (i.e., vary in relative proportion of the total ambient particle mix from location to location or from one time or season to another at the same location).

Previous documentation has shown that hydroxy, hydroperoxy, and alkoxy radicals are probably important in the oxidation of SO_2 to SO_3^-, although the rate constants for some of these reactions are not well established. The hydroxy radical dominates the gas-phase oxidation of SO_2 in the clean troposphere, and H_2O_2 is effective in the formation of SO_4^{2-} in particles, mists, fogs, and rain. Transition metals and soot have been shown to be effective catalysts for atmospheric oxidation of SO_2. Oxidation rates for NO and NO_3^- are known but have been considered too low to be important. The oxidation rate for NO_2^- is known, but the tropospheric concentration of HNO_2 is probably too low for this reaction to be important. Except for reactions of carbon (soot), solid surface reactions do not appear to be effective pathways for H_2SO_4 formation in the troposphere.

The physical properties of particles are physical configuration, bulk material properties, and surface properties. The bulk material properties that affect aerosol behavior include chemical composition, vapor pressure, hygroscopicity and deliquescence, and index of refraction. These properties control the physical state and growth of particles and result in scattering and absorption of light by tropospheric particles. Hygroscopicity, deliquescence, and efflorescence are critical properties in the growth of particles, but there is a paucity of thermodynamic data to permit prediction of deliquescence and hygroscopic behavior and vapor pressures of multicomponent systems, especially for relative humidities below about 90%. Few studies of desorption under atmospheric conditions have been reported; of more concern, desorption may prove to be important in biological systems. Shape, structure, and density are physical configuration properties that are important parameters in the equations of motion for particles. Because of irregularities in particle geometry or because the particles are agglomerates, the three configuration properties are usually defined in terms of an aerodynamic diameter. Surface properties of importance include electrostatic charging, adhesion, and the influence of surface films.

The physical properties of particles and their modal distributions are important considerations (1) in the sampling and analysis of atmospheric particles and (2) in predicting or determining the flux to biological and nonbiological materials and deposition in the human and laboratory animal respiratory tracts.

Advances in understanding the properties and behavior of atmospheric particulate matter have been made since publication of the previous criteria document (U.S. Environmental Protection Agency, 1982). In the current revision of the document, newer literature and data on the above topics are reviewed and discussed. For example, chemical pathways and rates of atmospheric particle formation and of removal from the atmosphere, by dry deposition and by precipitation scavenging, are examined. Likewise, the physical processes of nucleation, condensation, and coagulation by which condensible material is converted into particles are discussed, along with the size distribution of the resulting particles. The physical properties relevant to sampling considerations and deposition on surfaces, including those of the respiratory tract, are also discussed, including coverage of several newer areas of expanded research: aerosol equilibria, the unique properties of semi-volatile aerosols, and the role of particle-bound water.

2.4.1.2 Measurement Methodology

Techniques available for measurement of mass and specific components of aerosols are examined. Special attention is given to the suitability of current technology for measurement of aerosol mass with sufficient accuracy and precision to determine compliance with one or another possible type of a new PM standard (i.e., a PM_{10} standard with a lower level or a fine-particle standard). The need for continuous or daily PM measurements, the difficulty of removing particle-bound water without losing NH_4NO_3 or semivolatile organic matter, and problems in defining and maintaining a precise cut at 10 μm or lower (e.g., at 2.5 μm) are also assessed.

2.4.1.3 Ambient Levels

The present draft of the revised PM AQCD describes ambient PM data for the United States, with characterization as available by size (fine/coarse) and chemical composition. Data that focus on the current U.S. PM_{10} standard are emphasized, but information is also provided on $PM_{2.5}$, $PM_{2.5\text{-}10}$, and other similar cut points, as data are available. Ambient patterns are discussed, to include daily, seasonal, regional, etc. Acid aerosol data are also described as above as a separate aspect of PM. Key questions addressed include: What information is available on the distribution of PM with regard to: geographic, seasonal, diurnal, size, composition, sources, and trends? How important are uncertainties introduced by variations in the position and shape of the 10-μm cut point in various PM_{10} monitors? How important are measurement uncertainties due to volatilizable/condensible components (e.g., loss of ammonium nitrate and, possibly, other ammonium salts) or to the loss of semivolatile organics or retention of particle-bound water? How do these uncertainties vary geographically and seasonally? How do these uncertainties differ for filter collection and subsequent weighing as compared to continuous indicators?

2.4.1.4 Cut Points

Information helpful in evaluating the possible need for a new fine particle standard in addition to or instead of a PM_{10} NAAQS is presented. This information includes discussion of sources, sampling problems, composition, lung deposition, epidemiology, biochemistry, and toxicology of fine and coarse particles. Other considerations include techniques for

separating fine particles from coarse particles. Can fine and coarse particles be separated adequately by a single size cut-point in all areas of the country or will the optimal cut point differ in time and space, especially between very dry areas where coarse particles may be found below 2.5 μm and very humid areas where fine particles occur above 1.0 μm? If a single fine-particle cut point is chosen, which is best: 2.5 μm; 1.0 μm; or something in between? Is separation by size adequate or will chemical composition measurements also be needed?

2.4.1.5 Exposure

Particulate matter exposure estimates for most epidemiology studies are based on data from ambient monitoring sites. Relationships between such measurements and personal exposure are of interest in evaluating and interpreting epidemiology studies. Aspects assessed in the present document include: urban scale PM exposure models, indoor/outdoor PM characteristics and relationships, and the validity of ambient measurements to provide appropriate estimates to relate to health effect endpoints. Two exposure estimates are of concern, individual and population estimates of PM exposure. The type of epidemiology study determines which estimate is appropriate. Additionally, other factors (such as exposure durations) that may determine health effects are considered. Human exposure patterns to ambient and indoor air particles, including consideration of activity patterns and various microenvironments, are also characterized.

Actual human exposure differs from outdoor concentrations due to: the infiltration of ambient aerosols indoors; indoor sources; and human activity patterns. Human exposure can be determined through measurements and models. For PM, indoor and personal monitoring data show both higher than ambient and lower than ambient PM concentrations in indoor settings as a function of varying particle size and human activity patterns.

Coarse-mode particles (>2.5 μm), which are generally of nonanthropogenic origin (windblown dust, etc.), require turbulence to provide vertical velocity components greater than their settling velocity to allow them to remain suspended in the air. Outdoor particles enter into an indoor setting either (1) by bulk flow (e.g., through an open window) in which all particles can enter at the inlet condition or, (2) by diffusional flow (e.g., through cracks and fissures in the barrier of the building envelope). Current investigations suggest that both

fine and coarse particles penetrate indoors with high efficiency. However, indoor settings are usually quiescent, and the larger ambient particles that do enter indoors quickly settle out, leading to the presence of the familiar dust layers that require indoor settings to be cleaned constantly. Fine particles, which enter indoors, however, are not easily removed by settling or impaction and are more reflective of ambient fine particle concentrations than are coarse particles. Human activity in indoor settings does generate fine particles (<2.5 μm) from smoking, vacuuming, cooking, etc., and resuspends coarse particles that previously had settled out. Thus, indoor PM consists of both: (a) ambient particles which have penetrated indoors and remain suspended, and (b) particles generated indoors.

Two major factors influencing the relationship of ambient to indoor PM air quality are (1) the variability of indoor concentrations of PM compared to outdoor concentrations as a function of particle size (e.g., fine indoor $\geq$ fine outdoor and coarse indoor $<$ coarse outdoor) and (2) the variation of exposures of individuals related to the different activities that are involved with the local generation of particles in their immediate surroundings (smoking, traffic, dusting and vacuuming at home, etc.).

Long-term personal exposures to coarse-fraction PM (>2.5 μm) can be less than half the ambient concentrations. Long-term personal exposures to fine-fraction PM (<2.5 μm) of ambient origin may be estimated by ambient measurements of the <2.5 μm PM fraction. However, the concentration of particles generated indoors or due to personal activities would not be expected to vary in concert with ambient concentrations. Therefore, variations in ambient concentrations can serve as an indicator of variations in total exposure to ambient particles, experienced both outdoors and in various microenvironments.

2.4.2 Health Effects

A rapidly growing body of epidemiologic data examines associations between PM concentrations and human health effects, ranging from respiratory function changes and symptoms to exacerbation of respiratory disease and excess mortality. These effects appear to lie along an increasing gradient of severity of effects in different subpopulations. Although the exact biological mechanisms underlying such effects are poorly understood, the emerging pattern of findings points toward the plausibility that the observed associations likely reflect real relationships between ambient PM exposures and human health impacts.

This revised PM criteria document assesses evidence suggesting that this overall pattern of effects may extend to concentrations of PM_{10} below the current NAAQS or may be associated with other PM size fractions (e.g., fine particles < 2.5 μm). Controlled human exposure and laboratory animal studies are also evaluated, and the overall coherence and consistency of findings in relationship to the epidemiologic database is assessed. These include, for example: (1) studies of respiratory tract deposition and clearance of particles; (2) experimental studies (animal and human) evaluating mechanisms of action of various particles (by size, chemical composition, etc.) in order to evaluate biological plausibility of effects reported by epidemiology studies; and (3) other experimental studies that demonstrate various toxic effects of PM constituents in humans or in animal models.

2.4.2.1 Respiratory Tract Dosimetry

The biological endpoint or health effect of an aerosol exposure is likely more directly related to the quantitative pattern of deposition within the respiratory tract than just to the external exposure concentration. The regional deposition pattern determines not only the initial respiratory tract dose but also the specific pathways and rates by which the inhaled material is cleared and redistributed. Thus, in order to evaluate different toxic responses to inhaled particles across species and to accurately extrapolate such laboratory animal data to humans, or to evaluate differences that sex, age, or disease may have on human variability, the various physicochemical, anatomic, and physiologic factors described must be integrated to estimate a deposited dose or perhaps a retained dose (deposition − clearance = retention). Delineation of the dose to each respiratory tract region (extrathoracic, tracheobronchial, and pulmonary) is desired because each region has different dominant factors controlling deposition and clearance, and different defense mechanisms. A theoretical model to describe particle deposition and clearance would require detailed information on all the influential parameters mentioned above (e.g., respiratory rates, exact airflow patterns, complete measurements of the branching structure of the respiratory tract, pulmonary region mechanics) for men, women, children, and across the various species used in toxicity studies. An empirical model (i.e., equations fit to experimental data) may adequately describe regional deposition and require much less data to develop the model structure.

Within the dosimetry chapter, the anatomy of the respiratory tract and the physicochemical, anatomical, and physiological factors controlling particle deposition, clearance, and retention are reviewed. Other factors that modify deposition, including sex, age, disease state, and exposure to irritants also are discussed. The available human and laboratory data on deposition and clearance and their positive and negative attributes for use in quantitative model development are discussed. Available validated model structures to estimate deposition and clearance in humans and laboratory animals are described and evaluated. The application of these models to quantitative extrapolation of the human and animal toxicity data also are discussed. Consideration is given to uncertainties in input parameters and the variability of model predictions when evaluating the usefulness of models for quantitative dose extrapolation.

2.4.2.2 Epidemiology Studies

Epidemiologic analyses are expected to provide some of the most crucial information useful in deriving health criteria upon which to base Agency decisions regarding possible revision of the current PM standards, and such studies are accorded extensive attention in this document.

One useful distinction is to separate short- and long-term PM exposure effects. The short-term effects include changes in respiratory function, symptom indicators, hospital admissions associated with exacerbation of respiratory or cardiovascular disease, and excesses of daily death rates in urban areas associated with concurrent 24-h PM measurements on the same or preceding few days. The short-term effects studies are typically longitudinal in nature and are specific to a community or metropolitan area with reasonably homogeneous PM exposures. The analyses of data in short-term studies use time-series analysis methods. The long-term or chronic exposure effects studies typically use annual PM concentrations and annual symptom or death rates and are more likely to involve comparisons across several communities rather than within a single community. Although both kinds of epidemiologic analysis are useful, it is important to assess the consistency of conclusions based on different kinds of studies. Coherence of effects at lower concentrations is a useful criterion for assessing diverse studies with different endpoints or effects, different

populations, and different exposure metrics (Bates et al., 1990) and is considered as part of the evaluation of the available epidemiology literature.

Mortality Studies

Studies examining the relationship between ambient measures of PM and mortality were examined during the last review process (U.S. Environmental Protection Agency, 1982, 1986) and contributed to the key scientific bases underlying the current PM_{10} NAAQS. However, given the uncertainties in converting from British Smoke to PM_{10} measurements, particularly at lower concentrations, and the possible differences in particulate composition between London at the time the data were gathered and the contemporary United States, it was difficult to determine a precise level for a relationship between PM_{10} and mortality. Since that time, numerous contemporary U.S. mortality studies using either PM_{10} or TSP measurements have been published that examine short-term measurements. Also, long-term PM ambient measurements and mortality have been examined in some recent studies. These and other newly emerging PM-mortality studies are summarized and critically evaluated.

Issues of greatest concern so far relate primarily to the use and interpretation of the short-term mortality studies. Almost all analyses of the relationship between PM and excess mortality require statistical adjustment for mortality excesses associated with other potential confounding factors, including other environmental stressors such as temperature and relative humidity or other pollutants (co-pollutants) associated with PM and with mortality. For example, weather-related effects may be directly related to excess mortality, but may also be indirectly related when weather affects PM emissions and atmospheric concentrations. Statistical and conceptual approaches to estimating the direct and indirect effects of covariates or confounders and specification of statistical adjustments for possible confounding factors are evaluated in interpreting the PM effects on mortality calculated from each study. Studies using different exposure metrics are considered and differences in particle size distribution or particle composition between cities are considered as the data allow.

Specification of "exposure-effect" relationship(s) between mortality and PM is also important. A number of studies have reported no evident threshold for effects, even at relatively low concentrations, but the ability to carry out meaningful threshold evaluations may be greatly limited by the statistical power of the available studies. Estimates of the

relationship between PM and mortality may depend on differences in model specification. Even with similar model specifications (exposure-response relationship, adjustment for weather, copollutants, and other factors) there may be differences in the effects of PM at a given concentration, possibly related to differences in particle size/composition and/or climate or demographics among different cities. An important component of the health effects assessment in the criteria document is identification of susceptible subpopulations and other variables such as weather, climate, or other pollutants, potentially contributing to increased mortality risk.

Morbidity Studies

Decreased pulmonary function in predominantly healthy children was been reported in some earlier epidemiology studies. More recent studies add to this database. Earlier long-term exposure studies provided no evidence for an effect from PM exposure on level of pulmonary function, whereas some recent studies report reductions in pulmonary function associated with chronic exposure to particulate pollution. An evaluation of the epidemiologic database relating short-term (24-h) and long-term (annual) ambient measurement of PM_{10} and other measures of PM to changes in pulmonary function test results in children and adults is presented. The strength and consistency of epidemiologic databases that relate short-term (24-h) and long-term (annual) PM_{10} and other ambient PM indicator measurements to changes in the rate and/or severity of respiratory symptoms and disease are also critically reviewed. Studies examining exacerbation of respiratory (i.e., COPD and asthma) and cardiovascular diseases that lead to increased medical care utilization (such as emergency room visits and hospital admissions) in relation to ambient PM exposure are also evaluated. As appropriate, other factors and copollutants are also examined in relation to findings on each of the above types of health endpoints.

2.4.2.3 Toxicology of Particulate Matter Constituents

In addition to assessing epidemiologic studies of PM differentiated mainly in terms of various size indicators (TSP, PM_{10}, etc.), the toxicology of various major subclasses of PM constituents is also evaluated. That evaluation focuses on acid aerosols, metals, ultrafine particles, diesel particles, silica, bioaerosols, and other types of particles that make up

ambient air mixes of particles in the broad class designated in toto as "particulate matter". Animal inhalation toxicology and other types of studies are reviewed to ascertain information on several key health issues, e.g.: (1) the influence of particle size, number, and mass on health responses; (2) the differential influence of varying particle chemistry on the health effects observed; (3) the array of health effects that can be caused by specific PM constituents; (4) exposure-response relationships for various exposure durations (acute and chronic); (5) mechanisms of toxicity; and (6) pollutant interactions. Information from these studies relates to evaluation of the biological plausibility of the mortality and morbidity associations reported in epidemiological studies. The data on relationships among particle size, mass, number, and toxic effects may aid in determining the appropriateness of various exposure indicators of potential human effects.

Evaluation of the controlled human exposure (clinical) studies database concerning PM and health outcomes is presented as a subsection of the overall PM constituent toxicology chapter. This includes critical review of PM effects on pulmonary function in healthy and asthmatic individuals, pulmonary clearance mechanisms, airway reactivity, and immunologic defense especially in relation to particle size but only to a limited extent in relation to chemical composition. There remains an almost complete absence of controlled experiment data on exposure of humans to particles other than acid aerosols.

Human clinical studies of PM constituents have been almost completely limited to measuring effects on symptoms, lung function, and airway reactivity, in addition to a few studies of effects on mucociliary clearance. Few have used bronchoalveolar lavage to study PM effects on airway inflammation and host defense; nor have many examined effects of acid aerosols or other particle exposures on airway inflammation in asthmatic subjects or on exacerbation of effects of antigen challenge in allergic or asthmatic subjects.

2.4.2.4 Sensitive Groups

Available data are also evaluated for insight concerning human population groups potentially having increased susceptibility to ambient PM exposure. Preexisting respiratory or cardiovascular disease, in conjunction with advanced age, appear to be important factors contributing to increased susceptibility to PM mortality. For morbidity health endpoints,

children and asthmatic individuals may display increased sensitivity to PM exposure, and, as such, this topic is discussed.

2.4.3 Welfare Effects

2.4.3.1 Effects on Materials

All manmade materials exposed to the outdoor environment undergo degradation by heat, moisture, and some bacteria and fungi. For many years, air pollution has been suspected of accelerating the natural degradation processes. For example, acidic pollutants have been associated with accelerated degradation of paints such as water-based paint and alkyd coatings containing titanium dioxide, lead minium, or ferric oxide red. Other researchers have reported acidic pollution-related effects on automotive paint and steel coating. Particulate matter has also been reported to produce paint soiling. Also, acid aerosols and other particles containing acids also have been reported to affect building stones, cement, and concrete. Acidic or acid-forming aerosols change the physical characteristics of some stones, cement, and concrete by changing the chemical composition. Studies examining the effects on materials of PM pollution (primary and secondary particles and aerosol precursor gases) are reviewed and summarized; where possible, changes in material damage are correlated with changes in PM concentrations.

2.4.3.2 Visibility Effects

There are several definitions for visibility; however, visibility is generally defined as the degree to which the atmosphere is transparent to visible light or a reduction in visual range and atmosphere discoloration. In 1977, Congress amended the Clean Air Act (CAA) to address problems with visibility impairment resulting from manmade air pollution, particularly in Class I Federal areas (national parks and wilderness areas). Airborne PM in the form of varying amounts of sulfates, ammonium and nitrate ions, elemental carbon and organic carbon compounds, water and smaller amounts of soil dust, lead compounds, and other trace species reduce visibility, thereby affecting transportation safety and creating a loss in aesthetic appeal. The fundamentals of visibility impairment, including the effects of PM concentration, aerosol composition, and size and pollutant emission trends on visibility are evaluated. Indicators of visibility and air quality are also discussed.

2.4.3.3 Climate Change

It has been suggested that fine particles released into the atmosphere may alter the climate through a reduction in the amount of solar radiation reaching the earth's surface, thus cooling the surface while heating the aerosol layer. The scattering and absorbing properties of aerosols and their vertical distribution are briefly reviewed and reference made to other assessments of their effects on radiative balance and how changes in radiative balance may affect weather and climate. Aerosols also affect weather and climate through their role as cloud condensation nuclei. The concentration, composition, size, and number of aerosols can influence the structure, stability, and albedo of clouds, possible changing the location and amount of rainfall and the rate of global and regional warming due to greenhouse gases. Airborne particles also play an important role in influencing the penetration of ultraviolet light (e.g., UV-B) to the surface of the Earth due to stratospheric ozone depletion, as is also briefly discussed.

2.4.3.4 Vegetation and Ecosystem Effects

Extensive information also exists which indicates that ambient PM (especially wet and dry deposition of acidic particles) can damage both terrestrial and aquatic vegetation and ecosystems. Such information is thoroughly evaluated elsewhere (Irving, 1991; U.S. National Acid Precipitation Assessment Program, 1991) but is not assessed in the present document.

2.5 DOCUMENT CONTENT AND ORGANIZATION

The present document critically reviews and assesses relevant scientific literature on PM through February, 1996. The material selected for review and comment in the text generally comes from the more recent literature published since 1982, with emphasis on studies conducted at or near PM pollutant concentrations found in ambient air. Older literature cited in the previous 1982 EPA PM AQCD and its Addenda (U.S. Environmental Protection Agency, 1982, 1986) is generally not discussed. However, as appropriate, some limited discussion is included of older studies judged to be significant because of their potential usefulness in deriving a NAAQS. An attempt has been made to discuss key

literature in the text and present it in tables as well. Reports of lesser importance for the purposes of this document are typically only summarized in tables.

Generally, main emphasis is placed on consideration of published material that has undergone scientific peer review. However, in the interest of admitting new and important information, some material not yet fully published in the open literature but meeting other standards of scientific reporting may be included as reviewed by CASAC. As noted earlier, emphasis has been placed on studies in the range of current ambient levels. On this basis, studies in which the lowest concentration employed exceeded this level have been included if they contain unique data, such as documentation of a previously unreported effect or of mechanisms of effects, or if they were multiple-concentration studies designed to provide information on concentration-response relationships. In reviewing and summarizing the literature, an attempt is made to present alternative points of view where scientific controversy exists. As warranted, considerations bearing on the quality of studies are noted.

The present document consists of 13 chapters. The Executive Summary for the entire document is contained in Chapter 1, followed by this general introduction in Chapter 2. Chapters 3 through 7 provide background information on physical and chemical properties of PM and related compounds; sources and emissions; atmospheric transport, transformation, and fate of PM; methods for the collection and measurement of PM; and ambient air concentrations and factors affecting exposure of the general population. Chapter 8 describes effects on visibility and climate, whereas Chapter 9 describes damage to materials attributable to PM. Chapters 10 through 13 evaluate information concerning the health effects of PM. More specifically, Chapter 10 discusses dosimetry of inhaled particles in the respiratory tract, and Chapter 11 summarizes information on the toxicology of specific types of PM constituents, including laboratory animal studies and controlled human exposure studies. Chapter 12 discusses epidemiological studies, and Chapter 13 integrates key information on exposure, dosimetry, and critical health risk issues derived from studies reviewed in the prior chapters.

Neither control techniques nor control strategies for the abatement of PM are discussed in this document, although some topics covered may be incidentally relevant to abatement strategies. Technologies for controlling PM emissions are discussed in other documents issued by EPA's Office of Air Quality Policy and Standards (OAQPS). Likewise, issues

germane to the scientific basis for control strategies, but not pertinent to the development of criteria, are addressed in numerous other documents issued by OAQPS.

In addition, certain issues of direct relevance to standard setting are not explicitly addressed in this document, but are instead analyzed in documentation prepared by OAQPS as part of its regulatory analyses materials. Such analyses include (1) discussion of what constitutes an "adverse effect" and delineation of particular adverse effects that the primary and secondary NAAQS are intended to protect against, (2) exposure analyses and assessment of consequent risk, and (3) discussion of factors to be considered in determining an adequate margin of safety. Key points and conclusions from such analyses are summarized in a Staff Paper prepared by OAQPS and reviewed by CASAC. Although scientific data contribute significantly to decisions regarding the above issues, their resolution cannot be achieved solely on the basis of experimentally acquired information. Final decisions on items (1) and (3) are made by the Administrator, as mandated by the Clean Air Act.

A fourth issue directly pertinent to standard setting is identification of populations at risk, which is basically a selection by EPA of the subpopulation(s) to be protected by the promulgation of a given standard. This issue is addressed only partially in this document. For example, information is presented on factors, such as preexisting disease, that may biologically predispose individuals and subpopulations to adverse effects from exposures to PM. The identification of a population at risk, however, requires information above and beyond data on biological predisposition, such as information on levels of exposure, activity patterns, and personal habits. Such information is included in the Staff Paper developed by OAQPS and reviewed by CASAC as a separate item from this document.

REFERENCES

Bates, D. V.; Baker-Anderson, M.; Sizto, R. (1990) Asthma attack periodicity: a study of hospital emergency visits in Vancouver. Environ. Res. 51: 51-70.

Bouhuys, A.; Beck, G. J.; Schoenberg, J. B. (1978) Do present levels of air pollution outdoors affect respiratory health? Nature (London) 276: 466-471.

Code of Federal Regulations. (1986) Appendix B - reference method for the determination of suspended particulate matter in the atmosphere (high-volume method). C. F. R. 40: §50.

Dassen, W.; Brunekreef, B.; Hoek, G.; Hofschreuder, P.; Staatsen, B.; De Groot, H.; Schouten, E.; Biersteker, K. (1986) Decline in children's pulmonary function during an air pollution episode. J. Air Pollut. Control Assoc. 36: 1223-1227.

Dockery, D. W.; Ware, J. H.; Ferris, B. G., Jr.; Speizer, F. E.; Cook, N. R.; Herman, S. M. (1982) Change in pulmonary function in children associated with air pollution episodes. J. Air Pollut. Control Assoc. 32: 937-942.

Federal Register. (1971) National primary and secondary ambient air quality standards. F. R. (April 30) 36: 8186-8201.

Federal Register. (1979a) National ambient air quality standards; review of criteria and standards for particulate matter and sulfur oxides. F. R. (October 2) 44: 56730-56731.

Federal Register. (1979b) National primary and secondary ambient air quality standards: revisions to the national ambient air quality standards for photochemical oxidants. F. R. (February 8) 44: 8202-8221.

Federal Register. (1984) Proposed revisions to the national ambient air quality standards for particulate matter. F. R. (March 20) 49: 10408-10435.

Federal Register. (1986a) National ambient air quality standards; review of criteria and standards for particulate matter and sulfur oxides. F. R. (April 1) 51: 11058.

Federal Register. (1986b) National ambient air quality standards: review of criteria and standards for particulate matter and sulfur oxides. F. R. (July 3) 51: 24392-24393.

Federal Register. (1987) Revisions to the national ambient air quality standards for particulate matter. F. R. (July 1) 52: 24634-24669.

Ferris, B. G., Jr.; Higgins, I. T. T.; Higgins, M. W.; Peters, J. M. (1973) Chronic nonspecific respiratory disease in Berlin, New Hampshire, 1961 to 1967: a follow-up study. Am. Rev. Respir. Dis. 107: 110-122.

Ferris, B. G., Jr.; Chen, H.; Puleo, S.; Murphy, R. L. H., Jr. (1976) Chronic nonspecific respiratory disease in Berlin, New Hampshire, 1967 to 1973: a further follow-up study. Am. Rev. Respir. Dis. 113: 475-485.

Hausman, J. A.; Ostro, B. D.; Wise, D. A. (1984) Air pollution and lost work. Cambridge, MA: National Bureau of Economic Research; NBER working paper no. 1263.

International Standards Organization. (1981) Size definitions for particle sampling: recommendations of ad hoc working group appointed by Committee TC 146 of the International Standards Organization. Am. Ind. Hyg. Assoc. J. 42: A64-A68.

Irving, P., ed. (1991) Acidic deposition: state of science and technology: volumes I-IV. Washington, DC: The U.S. National Acid Precipitation Assessment Program.

Lawther, P. J. (1986) [Letter to John Bachmann]. Washington, DC: Office of Air Quality Planning and Standards; August 22. Available for inspection at: U.S. Environmental Protection Agency, Central Docket Section, Washington, DC; docket no. A-82-37, IV-D-319.

Lawther, P. J.; Waller, R. E.; Henderson, M. (1970) Air pollution and exacerbations of bronchitis. Thorax 25: 525-539.

Lippmann, M. (1986a) [Letter to EPA Administrator Lee Thomas]. Washington, DC: U.S. Environmental Protection Agency, Clean Air Scientific Advisory Committee; January 2. Available for inspection at: U.S. Environmental Protection Agency, Central Docket Section, Washington, DC; docket no. A-82-37, IV-D-315.

Lippmann, M. (1986b) [Letter to EPA Administrator Lee Thomas]. Washington, DC, U.S. Environmental Protection Agency, Clean Air Scientific Advisory Committee; December 15. Available for inspection at: U.S. Environmental Protection Agency, Central Docket Section, Washington, DC; docket no. A-82-37, IV-D-339.

Lippmann, M. (1986c) [Letter to EPA Administrator Lee Thomas]. Washington, DC: U.S. Environmental Protection Agency, Clean Air Scientific Advisory Committee; December 16. Available for inspection at: U.S. Environmental Protection Agency, Central Docket Section, Washington, DC; docket no. A-82-37, IV-D-338.

Mazumdar, S.; Schimmel, H.; Higgins, I. T. T. (1982) Relation of daily mortality to air pollution: an analysis of 14 London winters, 1958/59-1971/72. Arch. Environ. Health 37: 213-220.

Ostro, B. (1984) A search for a threshold in the relationship of air pollution to mortality: a reanalysis of data on London winters. Environ. Health Perspect. 58: 397-399.

Ostro, B. D. (1987) Air pollution and morbidity revisited: a specification test. J. Environ. Econ. Manage. 14: 87-98.

Özkaynak, H.; Spengler, J. D. (1985) Analysis of health effects resulting from population exposures to acid precipitation precursors. Environ. Health Perspect. 63: 45-55.

Shumway, R. H.; Tai, R. Y.; Tai, L. P.; Pawitan, Y. (1983) Statistical analysis of daily London mortality and associated weather and pollution effects. Sacramento, CA: California Air Resources Board; contract no. A1-154-33.

Swift, D. L.; Proctor, D. F. (1982) Human respiratory deposition of particles during oronasal breathing. Atmos. Environ. 16: 2279-2282.

U.S. Code. (1991) Clean Air Act, §108, air quality criteria and control techniques, §109, national ambient air quality standards. U. S. C. 42: §§7408-7409.

U.S. Environmental Protection Agency. (1982) Air quality criteria for particulate matter and sulfur oxides. Research Triangle Park, NC: Office of Health and Environmental Assessment, Environmental Criteria and Assessment Office; EPA report no. EPA-600/8-82-029aF-cF. 3v. Available from: NTIS, Springfield, VA; PB84-156777.

U.S. Environmental Protection Agency. (1986) Second addendum to air quality criteria for particulate matter and sulfur oxides (1982): assessment of newly available health effects information. Research Triangle Park, NC: Office of Health and Environmental Assessment, Environmental Criteria and Assessment Office; EPA report no. EPA-600/8-86-020F. Available from: NTIS, Springfield, VA; PB87-176574.

U.S. National Acid Precipitation Assessment Program. (1991) The U.S. National Acid Precipitation Assessment Program 1990 integrated assessment report. Washington, DC: The U.S. National Acid Precipitation Assessment Program.

Ware, J. H.; Ferris, B. G., Jr.; Dockery, D. W.; Spengler, J. D.; Stram, D. O.; Speizer, F. E. (1986) Effects of ambient sulfur oxides and suspended particles on respiratory health of preadolescent children. Am. Rev. Respir. Dis. 133: 834-842.

3. PHYSICS AND CHEMISTRY OF PARTICULATE MATTER

3.1 INTRODUCTION

3.1.1 Overview

Atmospheric particles originate from a variety of sources and possess a range of morphological, chemical, physical, and thermodynamic properties. Examples include combustion-generated particles such as diesel soot or fly ash, photochemically produced particles such as those found in urban haze, salt particles formed from sea spray, and soil-like particles from resuspended dust. Some particles are liquid, some are solid; others contain a solid core surrounded by liquid. Atmospheric particles contain inorganic ions and elements, elemental carbon, organic compounds, and crustal compounds. Some atmospheric particles are hygroscopic and contain particle-bound water. The organic fraction is especially complex, containing hundreds of organic compounds.

Particle diameters span more than four orders of magnitude, from a few nanometers to one hundred micrometers. Combustion-generated particles, such as those from power generation, from automobiles, and in tobacco smoke, can be as small as 0.003 μm and as large as 1 μm. Particles produced in the atmosphere by photochemical processes range in diameter from 0.003 to 2 μm. Fly ash produced by coal combustion ranges from 0.1 to 50 μm or more. Wind-blown dust, pollens, plant fragments, and cement dusts are generally above 2 μm in diameter. Particles as small as a few nanometers (Covert et al., 1992; Clarke, 1992) and as large as 100 μm have been measured in the atmosphere (Lin et al., 1993).

Particles are ubiquitous in the atmosphere. The lowest concentrations are found in background marine environments, where particle number concentrations range from 100/cm^3 to 400/cm^3. In background continental environments, particle concentrations vary from 100/cm^3 to 5,000/cm^3; while in urban areas of the United States concentrations may be as high as 4,000,000/cm^3 (Willeke and Whitby, 1975; Whitby and Sverdrup, 1980). Particles account for a mass of a few μg/m^3 near the surface over dry continental areas to several hundred μg/m^3 in polluted urban areas.

The composition and behavior of airborne particles are fundamentally linked with those of the surrounding gas. Aerosol is defined as a suspension of solid or liquid particles in air and includes both the particles and all vapor or gas phase components of air. However, the term aerosol is often used to refer to the suspended particles only. Particles may be solid or liquid or a mixture of both phases. Particulate is an adjective and should only be used as a modifier, as in particulate matter.

Particulate material can be primary or secondary. Primary particles are composed of material emitted directly into the atmosphere. This includes material emitted in particulate form such as wind-blown dust, sea salt, road dust, mechanically generated particles and combustion-generated particles such as fly ash and soot. It also includes particles formed from the condensation of high temperature vapors such as those formed during combustion. The concentration of primary particles depends on their emission rate, transport and dispersion, and removal rate from the atmosphere.

Secondary particles form from condensable vapors formed by chemical reaction involving gas-phase precursors or by other processes involving chemical reactions of free, adsorbed, or dissolved gases. Secondary formation processes can result in either the formation of new particles (Wiedensohler et al., 1994; Covert et al., 1992; Clarke et al., 1991, 1993; Frick and Hoppel, 1993; Hoppel et al., 1994; Weber et al., 1995) or the addition of particulate material to preexisting particles (Andreae et al., 1986; Wall et al., 1988; Wu and Okada, 1994). Most atmospheric sulfate particles are formed from atmospheric oxidation of sulfur dioxide. Atmospheric nitrate is also essentially secondary. Oxides of nitrogen react in the atmosphere to form nitric acid vapor which in turn may react with ammonia gas to form particulate ammonium nitrate. Nitric acid may also react with particles containing sodium chloride or calcium carbonate, releasing hydrochloric acid or carbon dioxide, and forming sodium nitrate or calcium nitrate which remains in the particle. A portion of the organic aerosol is also attributed to secondary processes (Hildemann et al., 1994a,b; Turpin and Huntzicker, 1991; Mylonas et al., 1991; Pickle et al., 1990; Gray et al., 1986). Secondary aerosol formation can depend on concentrations of other gaseous reactive species such as ozone, hydroxyl radical, or hydrogen peroxide; atmospheric conditions including solar radiation and relative humidity; and the interactions of precursors and preexisting particles within cloud or fog droplets (Meng and Seinfeld, 1994; McMurry

and Wilson, 1983; Hoppel and Frick, 1990). As a result, it is considerably more difficult to relate ambient concentrations of secondary species to sources of precursor emissions than it is to identify the sources of primary particles.

Airborne particulate matter can be anthropogenic or natural in origin. Both anthropogenic and natural particulate material can occur from either primary or secondary processes. Anthropogenic refers to particulate matter which is directly emitted, or formed from precursors which are emitted, as a result of human activity. Primary anthropogenic sources include fossil fuel combustion, fireplace emissions, and road dust. Secondary anthropogenic particulate material can be generated photochemically from anthropogenic SO_2, NO_x, or organic gases. Primary natural sources include wind blown dust from soil undisturbed by man, sea-salt, natural forest fires and biogenic sources such as pollen, mold spores, leaf waxes and fragments from plants (Simoneit and Mazurek, 1982). In addition, plants emit gaseous species such as terpenes (Lamb et al., 1987). Terpenes are photochemically reactive. In the presence of ozone or hydroxyl radicals they react to form secondary organic particles (Kamens et al., 1981; Pandis et al., 1991, 1993).

Volatilization and sorption processes also affect concentrations and compositions of airborne particles. Some aerosol constituents are semivolatile and exist in both gas and particle phases. Their gas-particle distribution depends on atmospheric conditions such as temperature, the concentrations of other aerosol species including water vapor, and the vapor pressure of the constituent. Some inorganic compounds such as ammonium nitrate (Stelson and Seinfeld, 1982a,b; Bassett and Seinfeld, 1983, 1984) and organic compounds, including many polycyclic aromatic hydrocarbons (Yamasaki et al., 1982; Ligocki and Pankow, 1989; Pankow, 1987, 1994a,b), are semivolatile. Diurnal temperature fluctuations can cause substantial changes in the particle-phase concentrations of semivolatile constituents as a result of gas-particle redistribution. Evidence exists suggesting that this volatilization-sorption cycle results in the redistribution of semivolatile material among particles of differing origins (Venkataraman and Hildemann, 1994).

A complete description of the atmospheric aerosol would include an accounting of the chemical composition, morphology, and size of each particle and the relative abundance of each particle type as a function of particle size (Friedlander, 1970). However, most often the physical and chemical characteristics of particles are measured separately. Number size

distributions are often determined by physical means, such as electrical mobility or light-scattering. Chemical composition is determined by analysis of collected samples. The mass size distribution and the average chemical composition of the aerosol as a function of size can be determined by collection of size-segregated samples (Countess et al., 1980; Hering and Friedlander, 1982; John et al., 1990; Sloane et al., 1991). Recent developments in single particle analysis techniques coupled with multivariate classification methods (Van Grieken and Xhoffer, 1992; Germani and Buseck, 1991; Mansoori et al., 1994) are bringing the description envisioned by Friedlander closer to reality. This introductory section describes some of the measurements that have been made on atmospheric particles, and the insights thus provided on the nature, origins, and atmospheric processes that affect particle composition.

3.1.2 Atmospheric Aerosol Size Distributions

Size is one of the most important parameters in determining the properties, effects and fate of atmospheric particles. The atmospheric deposition rates of particles, and therefore, their residence time in the atmosphere, are a strong function of particle size. Size also influences deposition patterns of particles within the lung. Light scattering is strongly dependent on particle size. Particle size distributions, therefore, have a strong influence on atmospheric visibility and through their effect on radiative balance on climate.

Atmospheric size distributions for averaged continental background, urban-influenced background, averaged urban, and freeway-influenced urban aerosols are shown in Figures 3-1. (Whitby and Sverdrup, 1980). Figure 3-1 describes the number of particles as a function of particle diameter. For the same data, the particle volume distribution is shown in Figures 3-2. Note that for the particle number distribution both the diameter and the number of particles are shown on a logarithmic scale. For the volume distribution, the volume is shown on an arithmetic scale and the distribution is plotted such that the volume of particles in a specified size range is proportional to the corresponding area under the curve. These distributions show that most of the particles are quite small, below 0.1 μm, while most of the particle volume (and therefore most of the mass) is found in particles > 0.1.

An important feature of atmospheric aerosol size distributions is their multimodal nature. Volume distributions, measured in ambient air in the United States, are almost

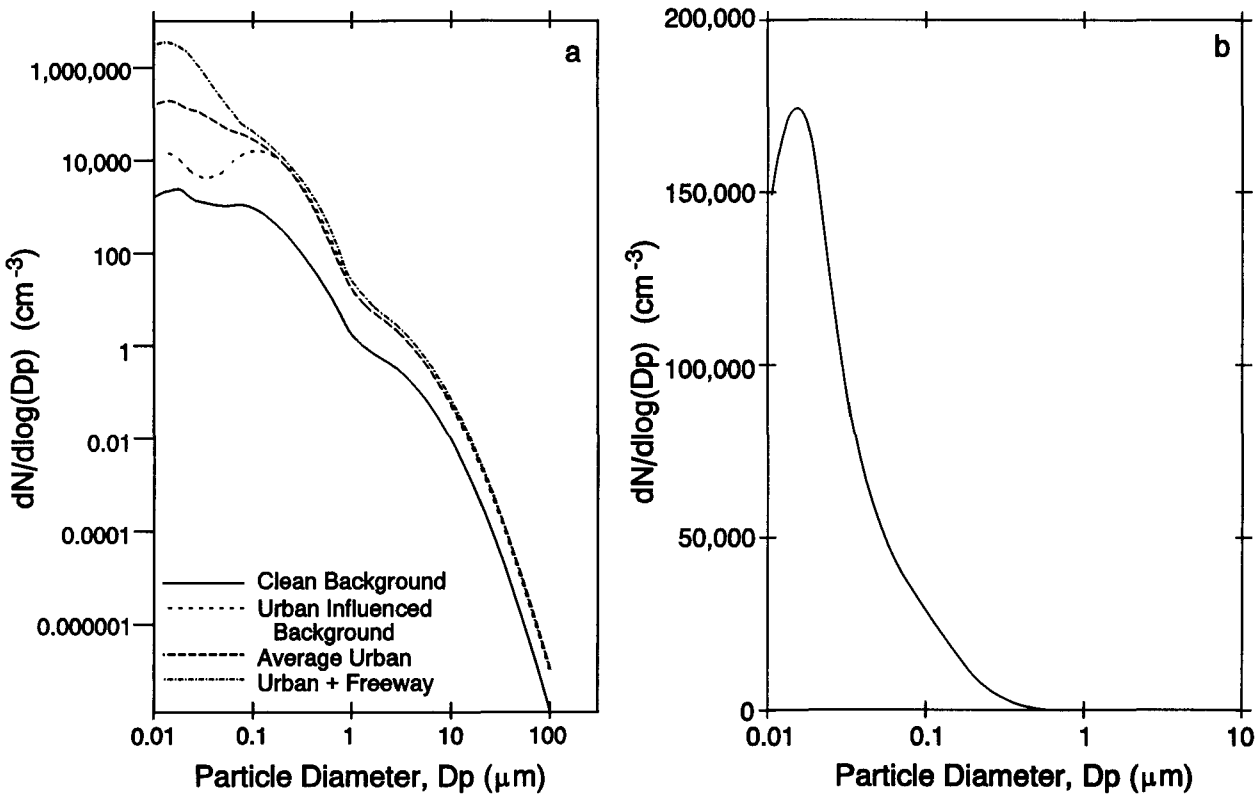

Figure 3-1. Number of particles as a function of particle diameter: (a) data are shown on a logarithmic scale to display the wide range in number concentrations from different sites; (b) averaged urban distribution are shown on a linear scale for which the area under the curve is proportional to particle number.

Source: Whitby and Sverdrup (1980).

always found to be bimodal, with a minimum between 1.0 and 3 μm. The distribution of particles that are mostly larger than the minimum is termed "coarse". The distribution of particles that are mostly smaller than the minimum is termed "fine". Whitby and Sverdrup (1980) and Willeke and Whitby (1975) identified three modes: nuclei, accumulation, and coarse. The three modes are most apparent in the freeway-influenced size distribution of Figure 3-2b. The smallest mode, corresponding to particles below about 0.1 μm, is the nuclei mode. The middle mode, from 0.1 to 1 or 2 μm, is the accumulation mode. Fine particles include both the accumulation and the nuclei modes. The largest mode, containing particles larger than 1 or 2 μm, is the coarse particle mode. Whitby and coworkers observed

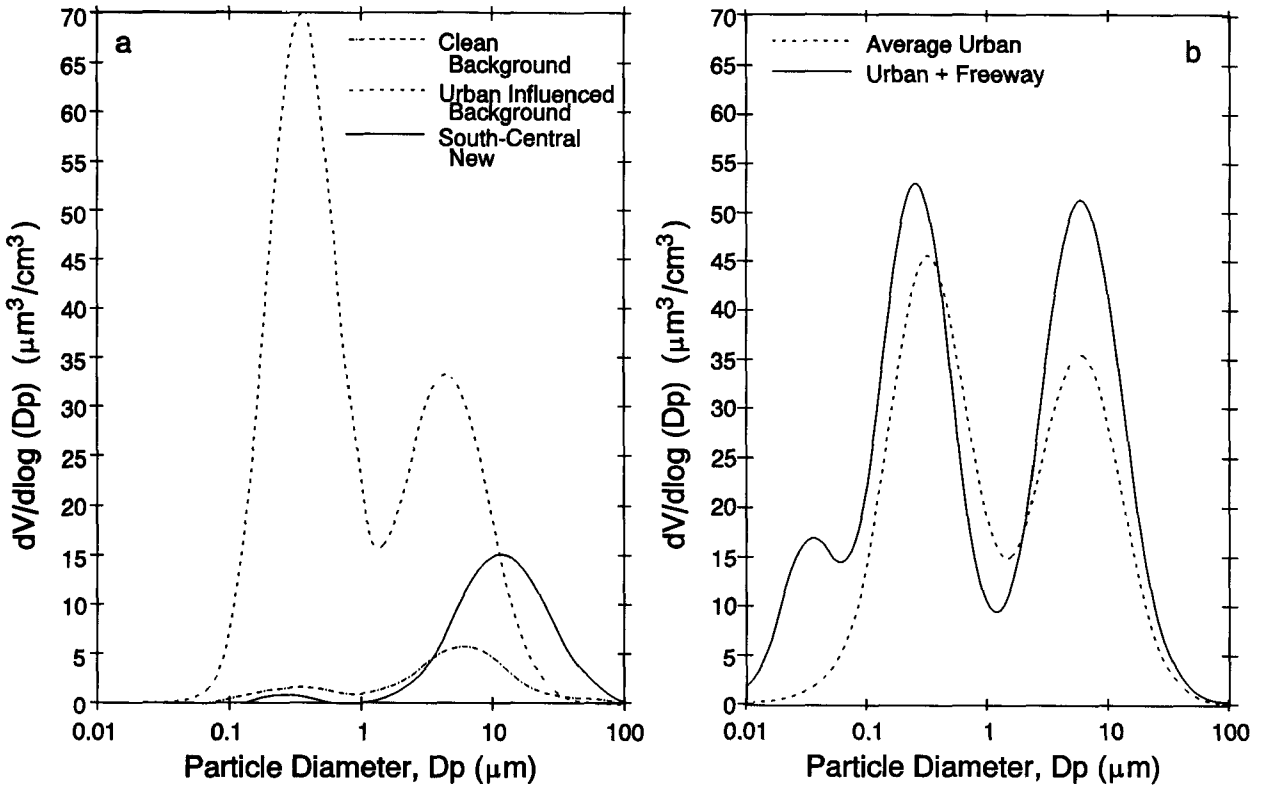

Figure 3-2. **Particle volume distribution as a function of particle diameter: (a) for the averaged background and urban-influenced background number distributions shown in Figure 3-1 and a distribution from south central New Mexico, and (b) for the averaged urban and freeway-influenced urban number distributions shown in Figure 3-1.**

Source: Whitby and Sverdrup (1980) and Kim et al. (1993c).

that continental background aerosols not influenced by sources have a small accumulation mode and no nuclei mode. For urban aerosols, the accumulation and coarse particles modes are comparable in volume. The nuclei mode is small in volume but, as discussed further in Section 6.8, dominates the number distributions of urban aerosols.

Many measurements indicate that the chemical compositions of coarse and fine particles are distinct. The processes that affect the formation and removal of these two size fractions of atmospheric aerosols are also distinct. Coarse particles are generated by mechanical processes and consist of soil dust, fly ash, sea spray, plant fragments, particles from tire wear, and emissions from rock-crushing operations. These particles are removed primarily by impaction and settling. Nuclei and accumulation mode particles contain primary particles

from combustion sources and secondary particles that result from condensation of low-volatility vapors formed from chemical reactions. Particles in the nuclei mode may be transferred into the accumulation mode by coagulation. Cloud coalescence and transformations in cloud droplets, followed by evaporation, are other processes that are important in atmospheric formation of accumulation mode particles. Accumulation mode particles do not ordinarily grow into the coarse mode, because number concentrations are too low for coagulation to be effective. Nuclei are readily removed by diffusion to surfaces. However, accumulation mode particles are not easily removed from the airstream. They have long atmospheric lifetimes and are able to penetrate deep into the lungs. The nuclei and accumulation modes are fairly independent of the coarse mode, both in formation and removal (Willeke and Whitby, 1975; Whitby and Sverdrup, 1980).

Fine and coarse particles are best differentiated by their formation mechanism (Wilson and Suh, 1996). Fine particles are formed by nucleation with gases while coarse particles are formed by mechanical processes from larger particles or bulk materials. The most appropriate size cut for separating fine from coarse particles is in the range of 1 to 3 μm in particle diameter; however, a precise size cut cannot be determined because of some size overlap between the fine and coarse particle modes.

3.1.3 Definitions

3.1.3.1 Definitions of Particle Diameter

The diameter of a particle may be determined geometrically, from optical or electron microscopy; by light scattering and Mie theory, or by its behavior, such as its electrical mobility, its settling velocity, or its aerodynamic behavior. Although atmospheric particles are often not spherical, their diameters are described by an "equivalent" diameter, that of a sphere which would have the same physical behavior. Two parameters that are often used are the Stokes diameter and the aerodynamic diameter. The Stokes diameter, D_p, describes particle size based on the aerodynamic drag force imparted on a particle when its velocity differs from that of the surrounding fluid. For a smooth, spherically shaped particle, D_p exactly equals the physical diameter of the particle. For irregularly shaped particles, D_p is the diameter of an equivalent sphere that would have the same aerodynamic resistance. Particles of equal Stokes diameters that carry the same electric charge will have the same

electrical mobility. Particles of equal density and equal Stokes diameter have the same settling velocity.

Aerodynamic diameter, D_a, depends on particle density and is defined as the diameter of a spherical particle with equal settling velocity but a material density of 1 g/cm^3. Particles with the same physical size and shape but different densities will have the same Stokes diameter but different aerodynamic diameters. For particles greater than about 0.5 μm, the aerodynamic diameter is generally the quantity of interest because it is the parameter that is important to particle transport, collection, and respiratory tract deposition. Respirable, thoracic, and inhalable particle sampling are based on particle aerodynamic diameter.

Aerodynamic diameter, D_a, is related to the Stokes diameter, D_p, by:

$$D_a = \left[\frac{\rho\, C}{C_a}\right]^{1/2} D_p \tag{3-1}$$

where ρ is the particle density, and C and C_a are the Cunningham slip factors evaluated for the particle diameters D_p and D_a respectively. The slip factor is a function of the ratio between particle diameter and mean free path of the suspending gas; it is given by the expression (Hinds, 1982):

$$C = 1 + \frac{\lambda}{D_p}\left\{2.514 + 0.800 \exp\left(-0.55 \frac{D_p}{\lambda}\right)\right\} \tag{3-2}$$

where λ is the mean free path of the air. C is an empirical factor that accounts for the reduction in the drag force on particles due to the "slip" of the gas molecules at the particle surface. It is important for particles less than 1 μm in diameter, for which the surrounding air cannot be modeled by a continuous fluid. At normal atmospheric conditions (temperature = 20 °C, pressure = 1 atmosphere) λ = 0.066 μm. For large particles (D_p > 5 μm) C = 1; while for smaller particles C > 1.

For particles with diameters greater than the mean free path, the aerodynamic diameter given by equation (3-1) is approximated by:

$$D_a = (\rho)^{1/2} D_p \qquad (D_p \gg \lambda) \tag{3-3}$$

This expression, which shows that aerodynamic diameter is directly proportional to the square root of the particle density, is often used for particles as small as 0.5 μm. For particles with diameters much smaller than the mean free path, the slip factor must be taken into account. In this case the aerodynamic diameter is directly proportional to the particle density [$D_a = (\rho) D_p$ for $D_p \ll \lambda$].

3.1.3.2 Definitions of Particle Size Fractions

In the preceding discussion several subdivisions of the aerosol size distribution were identified. The aerosol community uses three different approaches or conventions in the classification of particles by size: (1) modes, based on the observed size distributions and formation mechanisms; (2) dosimetry, based on the entrance into various compartments of the respiratory system; and (3) cut point, based on the 50% cut point of the specific sampling device.

Modal

The modal classification was first proposed by Whitby (1978). An idealized version is shown in Figure 3-3. A number of actual distributions are shown in Section 3.7. The observed modal structure is frequently approximated by several log-normal distributions.

Coarse Mode: The distribution of particles with diameters mostly greater than the minimum in the particle mass distribution, which generally occurs between 1 and 3 μm. These particles are usually mechanically generated.

Fine Mode: The distribution of particles with diameters mostly smaller than the minimum in the particle mass distribution, which generally occurs between 1 μm and 3 μm. These particles are usually formed from gases.

Accumulation Mode: That portion of the fine particle fraction with diameters above about 0.1 μm. Secondary particulate matter, formed from chemical reactions in the atmosphere, often "accumulates" in this size range. Accumulation-mode particles normally do not grow into the coarse mode.

Nuclei Mode: That portion of the fine particle fraction with diameters below about 0.1 μm. The nuclei mode can be observed as a separate mode only in clean or remote

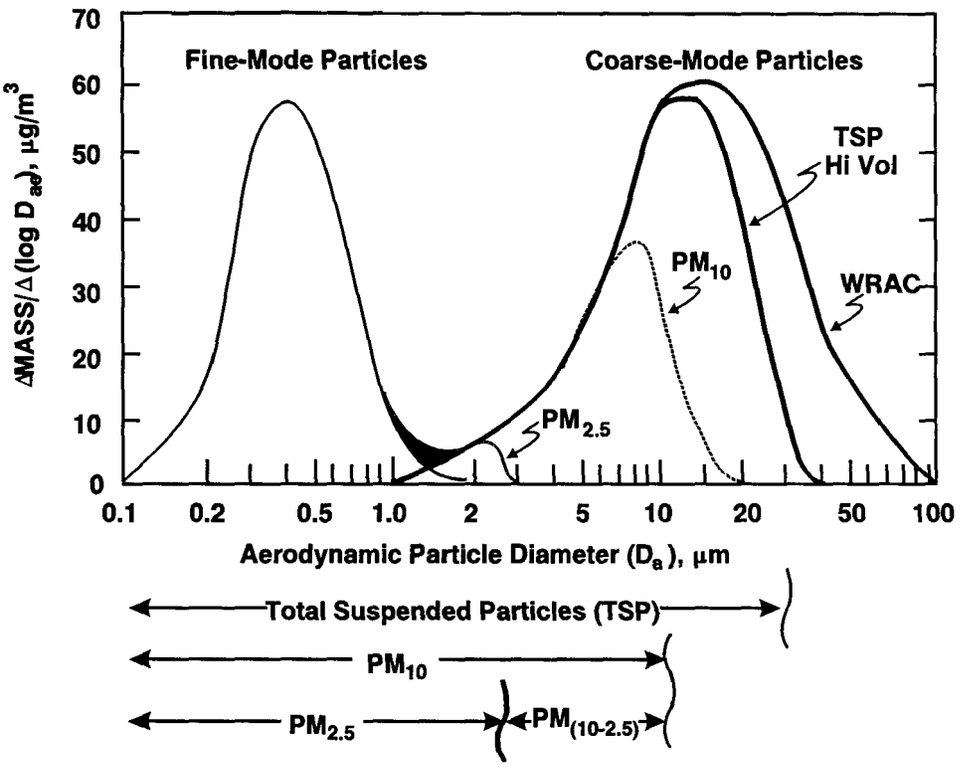

Figure 3-3. An idealized distribution of ambient particulate matter showing fine-mode particles and coarse-mode particles and the fractions collected by size-selective samplers.

Source: Adapted from Wilson and Suh (1996).

areas or near sources of new particle formation by nucleation. Nuclei-mode particles rapidly grow into the accumulation mode.

Over the years, the terms fine and coarse, as applied to particle sizes, have lost the precise meaning given in Whitby's (1978) definition. In any given article, therefore, the meaning of fine and coarse must be inferred from the author's usage. In this document, the term mode is used with fine and coarse when it is desired to specify the distribution of fine-mode particles or coarse-mode particles as shown in Figure 3-3.

Modes Within the Accumulation Mode: Aqueous-phase reactions may occur within cloud droplets, fog droplets or particles at very high relative humidity. The partial drying out of these particles may lead to a mode which is larger than the accumulation mode formed under drier conditions. This has been called the *droplet* mode. A smaller mode, perhaps

formed from non-hygroscopic material or formed after the relative humidity has decreased, may also be observed. This has been called the *condensation* mode (Hering and Friedlander, 1982; John et al., 1990). This phenomenon is discussed in greater detail in Section 3.7.

Modes Within the Nuclei Mode: Measurements over clean, remote areas (Hoppel et al., 1986; Hoppel and Frick, 1990; Covert et al., 1992; Wiedensohler et al., 1994) indicate that under some conditions two modes may be observed within the nuclei mode. Aerosol physicists distinguish these as:

> *Aitken Nuclei*: That portion of the nuclei mode which exhibits a local maximum in the number distribution above 15 nm; and the
>
> *Ultra-fine Nuclei*: That portion of the nuclei mode which exhibits a local maximum in the number distribution below 15 nm.

Ultra-fine Particles in a Biological Context: In the terminology of health scientists ultrafine is often used to characterize any size distribution, natural or laboratory-generated, which, under dry conditions, has a mass median diameter below about 0.1 μm. One hypothesis holds that such particles may cause inflammation and other health effects due to their physical size in addition to any chemically-induced effects (Oberdöster, 1995). Ultrafine particles, in the health effects usage, are closely related to the nuclei mode. In this document ultrafine will be used in the biological context and may include particles from the minimum size of about 3 nm to about 100 nm (100 nm = 0.1 μm).

Dosimetry

In a second approach, size fraction definitions are based on human health significance. This convention classifies particles into inhalable, thoracic, and respirable particles according to their entrance into the various compartments of the respiratory system. In a general sense, inhalable particles refer to those that enter the respiratory tract, including the head airways region. Thoracic particles refer to particles that reach the lung airways and the gas-exchange region of the lung, and respirable particles are those that reach the gas-exchange region. In the past exact definitions of these terms have varied among organizations. As of 1993 a unified set of definitions was adopted by the American Conference of Governmental Industrial Hygienists (ACGIH) (1994), the International Standards Organization (ISO), and the European Standardization Committee (CEN).

Sampler Cut Point

Another set of definitions of particle size fractions arises from considerations of size-selective sampling. Size-selective sampling refers to the collection of particles below or within a specified aerodynamic size range, usually defined by the 50% cut point size, and has arisen in an effort to measure particle size fractions with some special significance, e.g., health, visibility, source apportionment, etc. The PM_{10} standard set by the U.S. Environmental Protection Agency in 1987 is an example of size-selective sampling (Federal Register, 1987). The PM_{10} size cut was designed to focus regulatory concern on those particles small enough to enter the thoracic region. PM_{10} samplers, as defined in Appendix J to 40 Code of Federal Regulations (CFR) Part 50 (Federal Register, 1988), collect all of the fine particles and part of the coarse particles. The upper cut point is defined as having a 50% collection efficiency at 10 ± 0.5 μm diameter. The slope of the collection efficiency curve is defined in amendments to 40 CFR, Part 53. The curve which defines PM_{10}, and the curves which define inhalable, thoracic, and respirable particles, are shown in Figure 3-4.

Prior to the establishment of the PM_{10} standard, the particulate matter standard was based on total suspended particulate matter (TSP). TSP is defined by the design of the High Volume Sampler (hivol) which collects all of the fine particles but only part of the coarse particles. The upper cut off size of the hivol depends on the wind speed and direction, and may vary from 25 to 40 μm. Heroic measures, such as were undertaken with the Wide Range Aerosol Classifier (WRAC), are required to collect the entire coarse mode (Lundgren and Burton, 1995). Samplers with upper cut-points of 3.5, 2.5, 2.1 and 1.0 μm are also in use. Dichotomous samplers split the particles into smaller and larger fractions, which may be collected on separate filters.

An idealized distribution showing the normally observed division of ambient aerosols into fine-mode particles and coarse-mode particles, and the size fractions collected by TSP, PM_{10}, $PM_{2.5}$ and $PM_{(10-2.5)}$ samplers, is shown in Figure 3-3.

In an analysis reported in 1979, EPA scientists endorsed the need to measure fine and coarse particles separately (Miller et al., 1979). Based on the availability of a dichotomous sampler with a separation size of 2.5 μm, they recommended 2.5 μm as the cut point between fine and coarse particles. Because of the wide use of this cut point, the $PM_{2.5}$ fraction is frequently referred to as "fine" particles. However, while the $PM_{2.5}$ sample

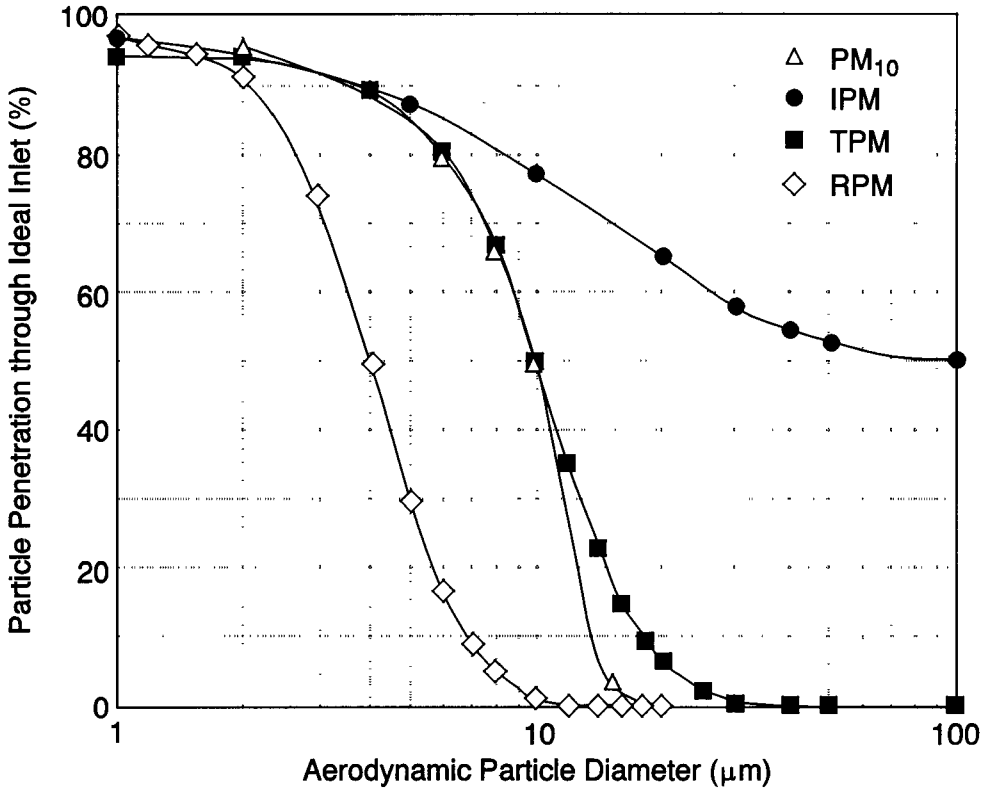

Figure 3-4. Specified particle penetration through an ideal inlet for four different size-selective sampling criteria. PM_{10} is defined in the Federal Register (1988). Curves for inhalable particulate matter (IPM), thoracic particulate matter (TPM) and respirable particulate matter (RPM) size cuts are computed from definitions given by American Conference of Governmental Industrial Hygienists (1994).

contains all of the fine particles it may, especially in dry areas or during dry conditions, collect a small fraction of the coarse particles. A PM_{10}-$PM_{2.5}$ size fraction may be obtained from a dichotomous sampler or by subtracting the mass on a $PM_{2.5}$ sampler from the mass on a PM_{10} sampler. The resulting PM_{10}-$PM_{2.5}$ mass, or $PM_{(10-2.5)}$, is sometimes called "coarse" particles. However, it would be more correct to call $PM_{2.5}$ an indicator of fine-mode particles, PM_{10} an indicator of thoracic particles, and PM(10-2.5) an indicator of the thoracic component of coarse-mode particles.

3.1.3.3 Other Terminology

Other terminology that has been introduced in this section is summarized below:

Primary Particles: material emitted into the atmosphere, either directly as particles or a vapor which rapidly forms particles by nucleation and/or condensation, from either natural sources or sources derived from human activity;

Secondary Particulate Material: material formed in the atmosphere as the result of chemical conversion of precursor gaseous species;

Internal Mixture: an aerosol for which the chemical composition of each individual particle is the same, that is, equal to the bulk composition;

External Mixture: an aerosol for which different chemical species comprise separate particles;

Anthropogenic: derived from human activities;

Biogenic: derived from plants;

Bioaerosols: airborne microorganisms and aeroallergens;

Fossil: derived from fossil fuel combustion; and

Contemporary carbon: derived from non-fossil fuel sources such as plants, wood burning, and cooking oils.

3.1.4 Major Chemical Constituents

The major constituents of atmospheric aerosol are sulfates, nitrates, carbonaceous compounds, water, hydrogen ions, ammonium ions, and materials of crustal origin. Average compositions vary with particle size, geographic location and season. Inorganic ions, including sulfate and nitrate, are typically analyzed by ion chromatography. Crustal elements are analyzed by x-ray fluorescence and/or proton-induced x-ray emission. The equilibrium models for inorganic ions predict that water is an important constituent of atmospheric particles, but measurements of particle-associated water are limited. McMurry and coworkers (McMurry and Stolzenburg, 1989; Zhang et al., 1993) measured the sensitivity of particle size to relative humidity for Los Angeles and Grand Canyon aerosols. They found that atmospheric particles of a single size exhibited two distinct hygroscopicities. These were described as "more" and "less" hygroscopic, as shown in Figure 3-5. For example, the diameters of more hygroscopic 0.2 μm particles humidified to approximately 90% relative

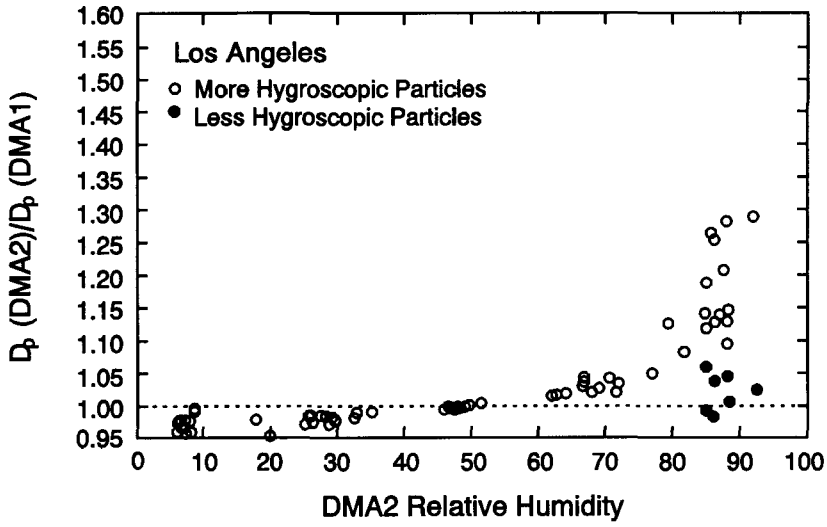

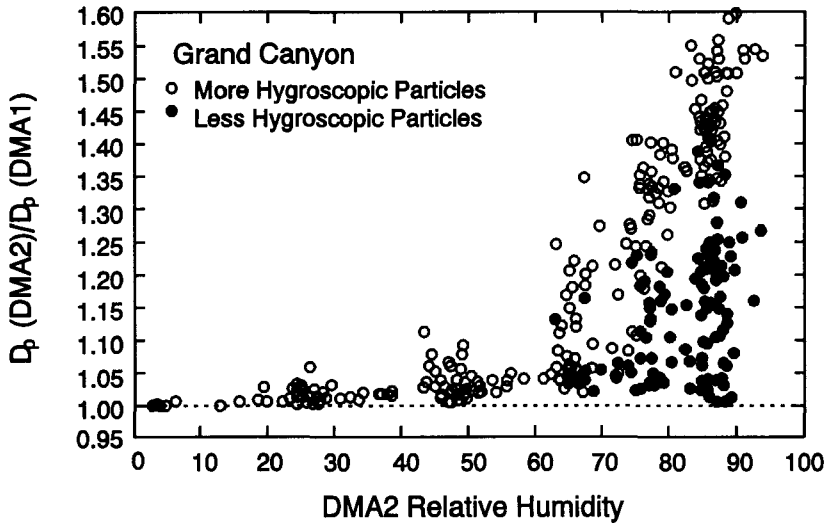

Figure 3-5. Particle size related to relative humidity.

Source: Zhang et al. (1993).

humidity increased by factors of 1.23 ± 0.08 and 1.49 ± 0.11 for Los Angeles and Grand Canyon particles, respectively. For relative humidities above 85 or 90%, water was the most abundant particulate species both in Los Angeles and at the Grand Canyon.

Because of the multitude of carbonaceous compounds present in atmospheric aerosols, carbonaceous material is often categorized as either organic carbon or elemental carbon.

Most measurements of aerosol carbon are made using one of a variety of thermal techniques that report particulate organic and elemental carbon concentrations (Johnson et al., 1981; Huntzicker et al., 1982; Mueller et al., 1982; Turpin et al., 1990). The split between organic and elemental carbon is somewhat operationally defined, but the term elemental generally refers to the nonvolatile,optically absorbing (black) portion of the carbon aerosol. Elemental carbon is associated with soot emissions from combustion. The remaining, more volatile portion is termed organic. Various methods of further classifying the organic fraction include: selective solvent extraction (Lioy and Daisey, 1986), functional group identification (Allen et al., 1994; Gordon et al., 1988), and division into neutral and acidic fractions (Hildemann et al., 1994a). Radiocarbon dating techniques have been used to distinguish fossil and contemporary carbon (Currie et al., 1994; Kaplan and Gordon, 1994; Hildemann et al., 1994a).

3.1.5 Chemical Composition and Its Dependence on Particle Size

Since the work of Whitby (1978), many studies have been conducted that provide chemical or elemental composition data on the coarse and fine fractions of the atmospheric aerosol. This has been done in several ways. The dichotomous sampler collects a $PM_{2.5}$ and a PM_{10}-$PM_{2.5}$ or coarse faction of PM_{10}. Alternately, a PM_{10} and a $PM_{2.5}$ sample may be collected and the $PM_{2.5}$ composition subtracted from the PM_{10} composition. Results from many such studies are presented in Section 6-6. More detailed information may be obtained by analysis of smaller size fractions obtained with cascade impactors (Figures 3-6, 20, Section 6-9). Studies conducted in most parts of the U.S. indicate that sulfate, ammonium, and hydrogen ions; elemental carbon and secondary organic carbon; and certain transition metals are found predominantly in the fine particles. Crustal materials such as calcium, aluminum, silicon, magnesium, and iron are found predominately in the coarse particles. Some organic material such as pollen, spores, and plant and animal debris is also found predominantly in the coarse mode. Some components such as potassium and nitrate may be found in both fine and coarse particles but from different sources or mechanisms. Potassium in coarse particles comes from soil, and in fine particles, comes from combustion of wood. Nitrate in fine particles comes primarily from the reaction of gas-phase nitric acid with gas-

phase ammonia to form particulate ammonium nitrate. Nitrate in coarse particles comes primarily from the reaction of gas-phase nitric acid with pre-existing coarse particles.

In the presence of cloud or fog droplets, or when sodium chloride particles from ocean spray or other sources are present, a mechanism is available for sulfate, nitrate, and ammonium ions to occur in the coarse mode. Detailed size distributions of the inorganic ions in Los Angeles are shown in Figure 3-6 (Wall et al., 1988; John et al., 1990). These data show two modes for sulfate and nitrate aerosols between 0.1 and 1 μm. Similar results for sulfate aerosols were reported by Hering and Freidlander (1982). The smaller mode, corresponding to particles near 0.2 μm in diameter, is attributed to gas-phase formation of condensible species and is referred to as the condensation mode. The larger mode has a peak near 0.6 μm and is called the droplet mode (Hering and Freidlander, 1982). Its existence is attributed to secondary formation through heterogeneous, aqueous-phase transformations. McMurry and Wilson (1983) found 0.6 μm sulfate particles in power plant plumes and attributed their existence to formation by heterogeneous processes. Further analysis of the data by Meng and Seinfeld (1994) indicates that these aqueous reactions most likely occur in cloud or fog droplets.

The data of Figure 3-6 in Los Angeles show that particulate nitrate is found in both coarse and fine particles. Nitrate near the coast was predominantly in the coarse mode. Coarse mode nitrate was less prominent for inland sites. Several investigators (Wall et al., 1988; John et al., 1990; Andreae et al., 1986) proposed that the coarse particle nitrate results from the heterogeneous reaction of nitric acid with sea salt. On the basis of single particle analysis by electron microscopy-energy dispersive XRF spectroscopy, Wu and Okada (1994) concluded that coarse-particle nitrate in a coastal region of Japan formed on sea salt. Coarse nitrate collected at an inland site was associated with soil dust. These data suggest that a heterogeneous chemical reaction on the surface of a mechanically generated, primary particle may provide a mechanism for adding secondary material to the coarse particle mode. They also show that secondary particulate material can be formed by the interaction of a natural constituent (sea salt) with a species derived from anthropogenic emissions (nitric acid).

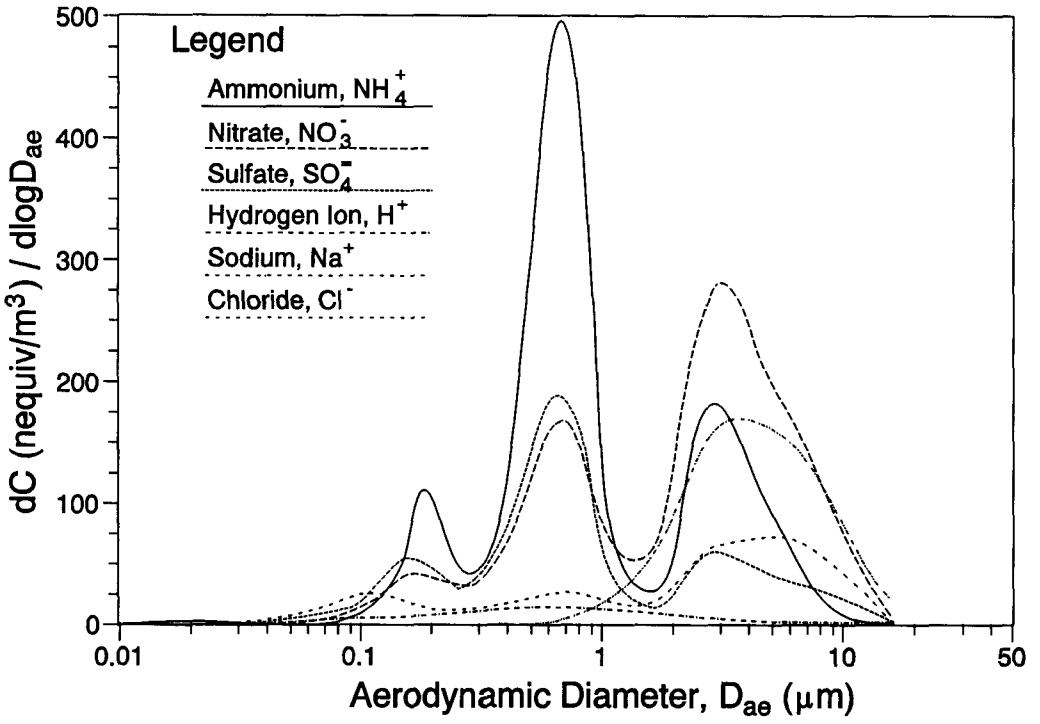

Figure 3-6. Ion concentration as a function of particle size, measured in Claremont, CA.

Source: Wall et al. (1988).

3.1.6 Particle-Vapor Partitioning

Several atmospheric aerosol species, such as ammonium nitrate and certain organic compounds, are semivolatile and are found in both gas and particle phases. The gas-particle distribution of semivolatile organic compounds depends on compound vapor pressure, total particle surface area, particle composition, and atmospheric temperature (Pankow, 1987; Junge, 1977; Bidleman, 1988). Junge (1977) modeled this relationship using a linear form of a Langmuir adsorption isotherm. Measurements of semivolatile organic compounds show that gas-particle distributions are highly correlated with total suspended particulate matter, temperature, and the sub-cooled liquid vapor pressure of the pure compound (Foreman and Bidleman, 1990; Ligocki and Pankow, 1989; Yamasaki et al., 1982). Yamasaki et al. (1982) used this information to model an empirical relationship between the gas-particle distribution, total suspended particulate matter and temperature. Pankow showed that the expressions of

Junge (1977) and Yamasaki et al. (1982) are consistent and continued the theoretical development of equilibrium gas-particle partitioning (Pankow, 1987; 1991; 1994a,b).

Although it is generally assumed that the gas-particle partitioning of semivolatile organics is in equilibrium in the atmosphere, the kinetics of redistribution are not well understood. Gerde and Scholander (1989) and Rounds and Pankow (1990) predicted that redistribution in the ambient air could take minutes to hours. Since changes in atmospheric conditions (i.e., temperature) will drive redistribution, it is not clear whether equilibrium conditions are maintained. However, the gas and particle data agree reasonably well with equilibrium theories. Hampton et al. (1983) report that the gas-particle partitioning of semi-volatile hydrocarbons from motor vehicle emissions can be described by Raoult's Law, i.e, the hydrocarbon species behave as solutes. The development of an understanding of gas-particle partitioning of semivolatile organic compounds is hampered by the difficulty associated with measuring the multitude of compounds, all present in small concentrations. Diurnal temperature fluctuations, which cause gas-particle partitioning to be dynamic on a time scale of a few hours, add to the measurement problems.

Stelson and Seinfeld (1982a) developed a thermodynamic model to predict the temperature and relative humidity dependence of the ammonium nitrate equilibrium dissociation constant. The model is supported by ambient data at inland sites in the Los Angeles Basin (Hildemann et al., 1984; Doyle et al., 1979). Bassett and Seinfeld extended the equilibrium model to include sulfates (1983) and the effect of particle size (1984). With the inclusion of sodium chloride in the equilibrium model, Pilinis and Seinfeld (1987) were able to predict observations at coastal sites. Atmospheric models based on equilibrium considerations have been successful in accounting for the gas-particle partitioning of inorganic species measured in Phoenix, Arizona (Watson et al., 1994a), and Uniontown, Pennsylvania (Saxena et al., 1993). Wexler and Seinfeld (1992) found that under some atmospheric conditions, such as cool, cold, or very clean air, the size distributions of ammonium ion and nitrate are not accurately predicted by equilibrium considerations alone, and that transport kinetics can be important. The dynamic changes in gas-particle partitioning, caused by changes in temperature or total concentration, both in the atmosphere and after collection, cause sampling problems which are discussed in Chapter 4.

3.1.7 Single Particle Characteristics

The "mixing characteristics" of the aerosol describes the distribution of chemical species among particles. An aerosol in which all particles contain the same homogeneous blend of chemical species is internally mixed. In an externally mixed aerosol each chemical species is found in a distinct set of particles. Experiments measuring atmospheric aerosol properties for single-particle size ranges (Hering and McMurry, 1991; Covert et al., 1990; Zhang et al., 1993) and single-particle analyses (De Bock et al., 1994; Sheridan et al., 1993; Van Borm et al., 1989; Anderson et al., 1988) indicate that atmospheric aerosols are to some degree both internally and externally mixed. Single particle analyses provide descriptions of individual particle compositions. These are then categorized either manually or through multivariate methods such as cluster analysis (Kim and Hopke, 1988) to give an accounting of the relative number of particles of each chemically defined particle type. Morphological information can also be included in particle type definitions.

Single-particle composition and morphology provide insights into the sources and atmospheric processes affecting airborne particles. For example, a priori one expects that particles emitted from different sources would in fact be distinct. However, Andreae et al. (1986) observed that over remote ocean areas between 80 and 90% of silicon-rich particles (presumably originating from silicate mineral particles) were also rich in sodium, chlorine, and variable amounts of potassium, magnesium, calcium, and sulfur (attributed to sea salt particles). The internal mixing of silicates with sea salt, particles originating from different sources and externally mixed when emitted into the atmosphere, suggested the processing of aerosol particles within clouds (see Section 3.2.2.5). The hypothesis was that a single cloud droplet could take up two or more particles and that these particles would remain together after droplet evaporation. Other mechanisms of particle coalescence, such as differential settling, Brownian coagulation, and electrostatic attraction, were considered too slow to account for the large fraction of internal mixing observed. Andreae et al. (1986) also found enrichment of sulfur (presumably sulfate) on sea salt particles. This also was attributed to the interaction of clouds with particles. Gas-to-particle conversion in cloud droplets or by condensation can also lead to mixtures of aerosol species.

Particle morphology has many effects on atmospheric particle properties and processes. Chain agglomerates, for example, have much larger surface areas on which adsorption and

chemical reactions can take place than spherical particles of identical volumes. In addition, the atmospheric lifetime is longer, and the optical absorption per unit mass is greater for chain agglomerates than for more compact particles. Combustion-generated soot particles are often chain agglomerates composed of a large number of small primary spherules. Laboratory experiments conducted by Huang et al. (1994) and Colbeck et al. (1990) demonstrated that condensation-evaporation processes can cause chain agglomerates to become more compact. Colbeck et al. (1990) also showed that the collapse of the soot aggregates resulting from humidification results in a decrease in both the optical scattering and extinction of the particles.

3.1.8 Dry Deposition

Dry deposition is the process whereby, in the absence of precipitation, airborne gases and particles are transported down to the surface of the earth where they are removed. Atmospheric turbulent mixing continually brings airborne gases and particles into close proximity to the earth's surface, where they may diffuse across a thin layer of stagnant air to the surface itself. Actual removal at the surface depends on the affinity between the airborne substance and the surface element (ground, body of water, vegetation surface, etc.). Dry deposition is a complex process but it is represented as occurring in three steps: (1) transport down to the vicinity of the earth by turbulent mixing processes; (2) diffusion across a thin quasi-laminar layer of air; and (3) attachment to the surface itself. Dry deposition of particles is a strong function of particle size, atmospheric conditions and terrain physiography. For large particles (e.g., above 10 μm in diameter), gravitation also contributes significantly to the overall dry deposition process.

3.1.9 Atmospheric Scavenging or Wet Deposition

Atmospheric gases are scavenged directly by absorption in droplets and by chemical reactions in clouds. The direct absorption of gases in falling droplets depends on the solubility of the gas in water, and may be affected by the presence of other species in solution (Seinfeld, 1986). Particles are scavenged in clouds when they serve as nuclei for the formation of cloud droplets (cloud condensation nuclei). This process is especially important for fine particles. Particles are also scavenged below clouds when they are

intercepted by falling hydrometeors, e.g., rain, snow, etc. This process is more important for coarse particles than fine particles. Because fine particles tend to follow air motions, they move out of the way and are not impacted by falling rain drops. The wet removal of particles depends on the air trajectories through clouds, the supersaturation to which the air mass is exposed, and the time for which droplets are present before arriving at the ground.

3.2 PHYSICAL PROPERTIES AND PROCESSES

3.2.1 Aerosol Size Distributions

3.2.1.1 Particle Size Distribution Functions

The distribution of particles with respect to size is perhaps the most important physical parameter governing their behavior. The concentration of the number of particles as a function of their diameter is given by a particle number distribution.

Because atmospheric particles cover several orders of magnitude in particle size, size distributions are often expressed in terms of the logarithm of the particle diameter, on the X-axis, and the differential concentration on the Y-axis: $dN/d(\log D_p)$ = the number of particles per cm^3 of air having diameters in the size range from $\log D_p$ to $\log(D_p + dD_p)$. It is not proper formally to take the logarithm of a dimensional quantity. However, one can think of the distribution as a function of $\log(D_p/D_{p0})$, where the reference diameter $D_{p0} = 1\ \mu m$ is not explicitly stated. If $dN/d(\log D_p)$ is plotted on a linear scale, the number of particles between D_p and $D_p + dD_p$ is proportional to the area under the curve of $dN/d(\log D_p)$ versus $\log D_p$. Similar considerations apply to distributions of surface, volume, and mass.

3.2.1.2 Log-Normal Size Distributions

Under some conditions, atmospheric aerosol size distributions may be approximated by a sum of log-normal distributions. Although such log-normal representations are not always an accurate description of the actual aerosol size distributions, they have been found, in many cases, to be convenient mathematical constructs to represent aerosol size distributions. The use of log-normal approximations to aerosol size distributions was first introduced by Foitzik (1950) and later expanded to a wide range of atmospheric data by Whitby and

co-workers (e.g., Whitby and Sverdrup, 1980; Willeke and Whitby, 1975). A log-normal distribution is a specific form of the size distribution function for which the population of particles follows a Gaussian distribution function with respect to the logarithm of the particle diameter. The logarithm of the geometric standard deviation, σ_g, is the standard deviation of the quantity $\log D_p$ and defines the width of the distribution. For a monodisperse aerosol, that is, one for which all particles are the same diameter, $\sigma_g = 1$. For polydisperse aerosols, $\sigma_g > 1$. Typical values for one of the modes of the atmospheric aerosol, such as the accumulation mode discussed above, are $1.8 < \sigma_g < 2.8$. For log-normal distributions, 84.1% of the particles are below the size $\sigma_g \cdot D_{gn}$, 84.1% lie above the size D_{gn}/σ_g, and 95% of the particles lie within two standard deviations of the mean, that is, the range from $D_{gn}/2\sigma_g$ to $D_p \cdot 2\sigma_g$.

One of the properties of the log-normal distribution is that if the number distribution is log-normal, the surface and volume distributions are also log-normal, and their geometric standard deviation σ_g is the same as for the number distribution.

3.2.1.3 Ambient Aerosol Size Distributions

Log-normal parameters which describe ambient aerosol size distributions are listed in Table 3-1. These parameters are the geometric number mean diameter, D_{gn}, geometric standard deviation, σ_g, and number concentration, N, for each mode. Also given are the parameters of the lognormal volume distributions, geometric mean diameters, D_{gv}, and the corresponding total particle volume for each mode, V. The tables include data from Sverdrup and Whitby (1980) and results from more recent measurements in a nonurban area of New Mexico (Kim et al., 1993c). Note that the volume geometric mean diameters for the accumulation mode vary from 0.2 μm to 0.4 μm and those for the coarse mode from 5 to 12 μm. The standard deviations for the coarse particle mode tend to be larger than for the accumulation mode.

3.2.1.4 Coagulation of Spherical Particles

Many processes affect the size distribution of an aerosol, including addition of volume by gas-to-particle conversion, and losses by deposition. Even without these processes, under conditions in which the total volume of an aerosol is conserved, the number of particles will

TABLE 3-1. LOGNORMAL PARAMETERS FOR AMBIENT AEROSOLS

A. Parameters of the Number Distribution

Site of Measurement	Nuclei Mode Num. (cm^3)	Nuclei Mode Dgn (μm)	Nuclei Mode σ_g	Accumulation Mode Num. (cm^3)	Accumulation Mode Dgn (μm)	Accumulation Mode σ_g	Coarse Mode Num. (cm^3)	Coarse Mode Dgn (μm)	Coarse Mode σ_g	Reference
Clean continental background	N: 1,000	0.016	1.6	800.00	0.067	2.1	0.72	0.93	2.2	(1)
Average continental background	N: 6,400	0.015	1.7	2,300.00	0.076	2.0	3.2	1.02	2.16	(1)
Urban influenced background	N: 6,600	0.014	1.6	9,600.00	0.120	1.84	7.2	0.83	2.12	(1)
Urban average	N: 106,000	0.014	1.8	32,000.00	0.054		5.4	0.86	2.25	(1)
Urban and freeway	N: 2,120,000	0.013	1.74	37,000.00	0.032	1.98	4.9	1.08	2.13	(1)
South central NM - February 1989	N: not reported			706.00	0.13	1.72	0.42	2.45	1.91	(2)
South central NM - July 1989	N: not reported			253.00	0.13	1.71	0.72	1.59	2.27	(2)

B. Parameters of the Volume Distribution

Site of Measurement	Nuclei Mode Volume (μm^3 cm^3)	Nuclei Mode Dgv (μm)	Nuclei Mode σ_g	Accumulation Mode Volume (μm^3 cm^3)	Accumulation Mode Dgv (μm)	Accumulation Mode σ_g	Coarse Mode Volume (μm^3 cm^3)	Coarse Mode Dgv (μm)	Coarse Mode σ_g	Reference
Clean continental background	V: 0.01	0.030	1.6	1.50	0.35	2.1	5.0	6.0	2.0	(1)
Average continental background	V: 0.04	0.034	1.7	4.45	0.32	2.0	25.9	6.04	2.16	(1)
Urban influenced background	V: 0.03	0.028	1.6	44.00	0.36	1.84	27.4	4.51	2.12	(1)
Urban average	V: 0.63	0.038	1.8	38.40	0.32	2.16	30.8	5.7	2.25	(1)
Urban and freeway	V: 9.20	0.032	1.74	37.50	0.25	1.98	42.7	6.0	2.13	(1)

Sources: (1) Whitby and Sverdrup (1980), (2) Kim et al. (1993c).

decrease by coagulation while the average volume per particle increases. The coalescence of two particles always reduces the total surface area and therefore is favored thermodynamically. Thus, in this sense, aerosols are inherently unstable. In some cases coagulation leads to the formation of chain agglomerates, such as for soot and some metals.

3.2.2 Particle Formation and Growth

A significant portion of the fine atmospheric aerosol is secondary, i.e., material added to the particle phase as the result of gas-to-particle conversion processes. For example, fine sulfate and nitrate particles are mostly formed by secondary processes. One mechanism of gas-to-particle conversion is homogeneous gas-phase chemical reactions to form a condensible species, such as the oxidation of sulfur dioxide to form sulfuric acid. Condensible species can either nucleate to form a new particle (nucleation), or can condense onto the surface of an existing particle (condensation). Another important class of gas-to-particle conversion mechanisms is heterogeneous chemical reactions, which are chemical reactions involving both gas-phase and particle-phase constituents. Transformation on the surface of particles, such as the uptake of nitric acid on the surface of calcium carbonate particles to produce calcium nitrate, is one type of heterogeneous reaction. Aqueous-phase chemical reactions, such as the dissolution of sulfur dioxide into a hygroscopic particle or fog or cloud droplet, followed by oxidation of the dissolved sulfur dioxide to sulfate and evaporation of the fog or cloud droplets back to aerosol size, provide an important mechanism for conversion of gases to particles. Heterogeneous reactions lead to addition of aerosol material to existing particles. Nucleation results in an increase in particle number as well as an increase in particle mass. Condensation leads only to an increase of aerosol mass and surface area, but does not affect the total number of particles. In this section the physical aspects of these gas-to-particle conversion mechanisms, and their effects on the particle size distribution, are discussed.

3.2.2.1 Equilibrium Vapor Pressures

An important parameter in particle nucleation and in particle growth by condensation is the saturation ratio S, defined as the ratio of the partial pressure of a species, p, to its equilibrium vapor pressure above a flat surface, p_o: $S = p/p_o$. For either condensation or

nucleation to occur, the species vapor pressure must exceed its equilibrium vapor pressure. For particles, the equilibrium vapor pressure is not the same as p_0. Two effects are important: (1) the Kelvin effect, which is an increase in the equilibrium vapor pressure above the surface due to its curvature; thus very small particles have higher vapor pressures and will not be stable to evaporation until they attain a critical size and (2) the solute effect, which is a decrease in the equilibrium vapor pressure due to the presence of other compounds.

For an aqueous solution of a nonvolatile salt, the presence of the salt decreases the equilibrium vapor pressure of the drop. This effect is in the opposite direction as the Kelvin effect, which increases the equilibrium vapor pressure above a droplet because of its curvature.

3.2.2.2 New Particle Formation

When the vapor concentration of a species exceeds its equilibrium concentration (expressed as its equilibrium vapor pressure), it is considered condensible. Condensible species can either condense on the surface of existing particles or can form new particles. The relative importance of nucleation versus condensation depends on the rate of formation of the condensible species and on the surface area of existing particles. An analytical relation for the relative importance of each pathway is dependent on the ratio of the square of the available surface area to the rate of formation (McMurry and Friedlander, 1979).
In urban environments, the available particle surface area is sufficient to rapidly scavenge the newly formed condensible species. New particle formation is usually not important except near sources of condensible species. Wilson et al. (1977) report observations of the nuclei mode in traffic. New particle formation can also be observed in cleaner, remote regions. Bursts of new particle formation in the atmosphere under clean conditions correspond to low aerosol surface area concentrations (Covert et al., 1992). The highest concentrations of volatile ultrafine particles occur in regions corresponding to the lowest particle mass concentrations, indicating that new particle formation is inversely related to the available aerosol surface area (Clarke, 1992). In contrast to continental aerosols, where sulfate particles are the result of conversion of sulfur dioxide, the sulfate particles over the oceans

are the result of the conversion of dimethylsulfide emitted by phytoplankton (Charlson et al., 1987).

3.2.2.3 Particle Growth

When material is added to the particle phase by condensation or by particle-phase chemical reactions, particles of different sizes may grow at different rates, depending on the mechanism involved. Condensational growth can have a different effect on the size distribution of the aerosol than the effect of heterogeneous conversion through chemical reactions within a droplet. The relative rates at which the size of particles change depend on whether the rate-limiting step in the growth process is transport to the particle, chemical reactions at the surface of the particle, or chemical reactions within the particle. These are referred to as transport-limited, surface-reaction rate-limited or volume-reaction rate-limited. These different physical mechanisms give rise to a different form of the growth law for the particle. Growth laws are the expressions for dv/dt or dD_p/dt as a function of particle size (where v is single particle volume and D_p is particle diameter).

For condensational growth, the rate-limiting step relevant to the rate at which particles of different size grow is transport of condensible species to the particle surface. For particles much smaller than the mean free path of air (free molecule regime), transport is governed by single molecular bombardment of the surface, and the volume (or mass) of these particles grows in proportion to their surface area. For particles larger than the mean free path (continuum regime), transport is governed by diffusion. In this regime the loss of diffusing species at the surface of the particle causes a gradient in the concentration of the diffusing species near the surface of the particle such that the volume of the particle grows in proportion to particle diameter rather than surface area.

For heterogeneous chemical reactions, the rate limiting step for growth may not be the transport of the reacting species to the particle, but the rate of reaction on or within the particle. For reactions at the surface of the particle, the rate of growth is controlled by the particle surface area; for droplet-phase reactions, it depends on the volume of the particle. In summary, the aerosol growth laws show that in the continuum regime the particle size dependence of the rate of change of particle volume varies from a dependence on D_p for condensation by diffusion, to D_p^2 for surface reactions, to D_p^3 for droplet reactions.

Condensation by diffusion varies as D_p^2 in the free molecule regime, in the transition regime, intermediate between the free molecule and continuum regimes, condensation by diffusion varies between a dependence on D_p^2 for small particles to a dependence on D_p for larger particles.

3.2.2.4 Equilibria with Water Vapor

The principal equilibrium of concern pertinent to ambient aerosols is that with water vapor. This equilibrium is important as it influences the size of the particles and in turn their aerodynamic properties (important for deposition to the surface, to airways, following inhalation, and to sampling instrumentation) and their light scattering properties. This section reviews recent work describing this equilibrium as it pertains to ambient aerosols.

Briefly the interaction of particles with water vapor may be described as follows. As relative humidity increases, crystalline soluble salts in aerosol particles undergo a phase transition to become aqueous solution aerosols. According to the phase rule, for particles consisting of a single component, this phase transition is abrupt, taking place at a relative humidity that corresponds to the vapor pressure of water above the saturated solution (the deliquescence point). With further increase in relative humidity the particle growth is such that the vapor pressure of the solution (concentration of which decreases as additional water is accredited) is maintained equal to that of the surrounding relative humidity; the particle thus tends to follow the equilibrium growth curve. As relative humidity decreases, the particle follows the equilibrium curve to the deliquescence point. However, rather than crystallizing at the deliquescence relative humidity, the particle remains a solution (supersaturated solution) to considerably lower relative humidities. Ultimately the particle abruptly loses its water vapor (efflorescence), returning typically to the initial, stable crystalline form. This behavior has been amply demonstrated in numerous laboratory studies (Tang and Munkelwitz, 1977; Tang, 1980). Recently Tang and Munkelwitz (1994) have presented data for water activity (equilibrium relative humidity) as a function of composition for several sulfate salts.

For particles consisting of more than one component, the solid to liquid transition will take place over a range of relative humidities, with an abrupt onset at the lowest deliquescence point of the several components, and with subsequent growth as crystalline

material in the particle dissolves according to the phase diagram for the particular multicomponent system. Under such circumstances a single particle may undergo several more or less abrupt phase transitions until the soluble material is fully dissolved.
At decreasing relative humidity such particles tend to remain in solution to relative humidities well below the several deliquescence points; such behavior has been amply demonstrated. In the case of the sulfuric acid-ammonium sulfate-water system the phase diagram is fairly completely worked out. Mixed anion systems containing nitrate are more difficult due to the equilibrium between particulate NH_4NO_3 and gaseous NH_3 and HNO_3 (Tang et al., 1978, 1981; Spann and Richardson, 1985). Spann and Richardson also give the compositional dependence of the relative humidity of efflorescence. For particles of composition intermediate between NH_4HSO_4 and $(NH_4)_2SO_4$ this transition occurs in the range from 40% to below 10%, indicating that for certain compositions the solution cannot be dried in the atmosphere. At low relative humidities particles of this composition would likely be present in the atmosphere as supersaturated solution droplets (liquid particles) rather than as solid particles, thus they would exhibit hygroscopic rather than deliquescent behavior during relative humidity cycles.

Evidence of the interaction of ambient aerosol particles with water vapor has been obtained by several investigators. Koutrakis et al. (1989) found systematically increasing aerosol mean diameter with increasing relative humidity, which they attributed to water accretion on sulfates. Rood et al. (1989) examined the response of light scattering coefficient of ambient aerosols to increase in temperature and attributed the decrease in light scattering upon heating to loss of liquid water associated with the particles. However, heating can also cause the loss of NH_4NO_3 and semi-volatile organic material. More detailed information regarding the size dependence of hygroscopic properties has been obtained by examining the change in particle size of a monodisperse size cut selected with a mobility analyzer, subjecting that aerosol to an increase or decrease in relative humidity, and reanalyzing the size at the new humidity. Studies of this phenomenon in the Los Angeles area indicate this phenomenon, but also frequently indicate the presence of externally mixed aerosol, in which some of the aerosol exhibits the growth expected of soluble salts, where another, apparently hydrophobic, fraction does not exhibit such growth (McMurry and Stolzenburg, 1989). Such bimodal growth with relative humidity was exhibited by particles present at Hopi Point,

Arizona (Pitchford and McMurry (1994). In the latter study the relative humidity dependence of the size of the more hygroscopic fraction was found to be consistent with that expected for sulfate salts. Such external mixtures have also been commonly observed in European aerosols (Svenningsson et al., 1994). Saxena et al. (1995) have shown that the presence of organic compounds in particles may lead to more water condensation on particles (as shown by data collected in Arizona) or to less water condensation, probably because of the formation of an organic film that isolates inorganic salts from the ambient gas-phase (as shown by data collected in Los Angeles).

The time constant that characterizes the rate of exchange of water vapor between the gas phase and a solution droplet is of interest relative to the rate of response of particles to changes in relative humidity in the ambient environment, especially in the vicinity of surfaces, and relative to changes experienced by particles following inhalation or during sampling. It is generally assumed that the rate of this water exchange is rapid. The characteristic time for diffusional growth in response to a change in relative humidity was calculated by Pilinis et al. (1989) to be about 1×10^{-7} s. However Khlystov et al. (1993) noted that this estimate was erroneously low by several orders of magnitude. The latter investigators examined the characteristic time for establishment of phase equilibrium in response to a change in relative humidity for $(NH_4)_2SO_4$ aerosol particles (dry radius 0.5 μm). The characteristic time increases from ca 1 ms at 8% relative humidity to 1.6 s at 99% relative humidity. Above 99% relative humidity the characteristic time can become much longer because of the large change in droplet radius at such relative humidities. These calculations indicate that the water equilibrium can be expected to be rapidly achieved in the ambient environment. A possible but important exception is near 100% relative humidity, pertinent to dry deposition of particles to vegetation or to water, where the equilibrium size might not be reached in the time required for the particle to traverse the diffusive layer adjacent to the surface.

The lability of water associated with ambient aerosol has been evidenced in comparisons by Malm et al. (1994) of measured particulate light scattering coefficient obtained with an integrating nephelometer with values reconstructed from aerosol composition, taking into account the relative humidity dependence of light scattering coefficients of the aerosol components. The reconstructed values were found to

systematically exceed the measured value. However when in the reconstruction the relative humidity was taken as that in the nephelometer chamber (invariably lower than ambient because of heating in the chamber) the reconstruction was markedly improved.

3.2.2.5 Particle Growth in Fogs and Clouds

Several measurements of the aerosol mass distributions in urban areas have shown that two distinct modes can exist in the 0.1 to 1 μm diameter range (Hering and Friedlander, 1982; McMurry and Wilson, 1983; Wall et al., 1988; John et al., 1990). These are referred to as the condensation mode (approximate aerodynamic diameter 0.2 μm) and the droplet mode (aerodynamic diameter around 0.7 μm). Hering and Friedlander (1982) and John et al. (1990) postulated that the larger mode could result from aqueous-phase chemistry. Meng and Seinfeld (1994) proposed that growth of condensation mode particles by accretion of water vapor or by gas-phase or aerosol-phase sulfate production cannot explain the existence of the droplet mode. Activation of condensation mode particles, formation of cloud/fog drops followed by aqueous-phase chemistry, and aqueous droplet evaporation was shown by these authors to be a plausible mechanism for formation of the urban and regional aerosol droplet mode. The sulfate formed during fog/cloud processing of an air mass favors the aerosol particles that had access to most of the fog/cloud liquid water content, which are usually the particles with dry diameters around 1 μm (Pandis et al., 1990b). These two submicron mass-distribution modes have been also observed in non-urban continental locations (McMurry and Wilson, 1983; Hobbs et al., 1985; Radke et al., 1989), but the frequency of their co-existence remains unknown. Thus, cloud processing of an air parcel can clearly affect the scattering efficiency and in general the radiative properties of the corresponding aerosol (Hegg et al., 1992; Bower and Choularton, 1993).

The aerosol distribution is also modified during in-cloud processing by collision-coalescence of droplets and impaction scavenging of aerosols (Pruppacher and Klett, 1980). The aerosol scavenging by droplets is a relatively slow process, and collision coalescence among droplets of different sizes causes a redistribution of aerosol mass in such a manner that the main aerosol mass is associated with the main water mass (Flossmann et al., 1985). The processing of the remote aerosol distribution by clouds has been clearly demonstrated in a series of field studies (Frick and Hoppel, 1993). This multiple processing of remote

aerosol by nonprecipitating clouds results in an extra mode in the aerosol number distribution (Hoppel et al., 1986; Frick and Hoppel, 1993).

Clouds and fogs can influence the atmospheric aerosol number and mass concentration and chemical composition, the shape of the aerosol size distribution, the aerosol acidity and radiative properties. These effects can be important in all environments (urban, rural and remote) and all seasons. Our qualitative understanding of the aerosol-cloud interactions has improved significantly, but, with few exceptions, the quantification of these effects remains uncertain (Altshuller, 1987; Kelly et al., 1989; Pandis et al., 1992b).

3.2.3 Resuspension of Particulate Matter

The resuspension of deposited material as well as the suspension of material which has not been previously airborne can be an important source of particulate contamination (Gillette, 1980). This discussion will use "resuspension" to include both resuspension and suspension. Surface contamination may result from the atmospheric deposition of a number of materials; for some of these (e.g., plutonium), resuspension has been considered to be the most important exposure pathway. Likewise, resuspended soil particles have the greatest atmospheric mass over continents of any single particle type (Peterson and Junge, 1971). Despite this importance, the literature shows relatively few experimental or theoretical studies for the resuspension mechanism compared to other aerosol generation mechanisms. The following summarizes work on the physics of resuspension, physical/chemical properties of resuspension generated particles, and levels of production and transport of resuspended particles.

3.2.3.1 Resuspension Mechanics

Resuspension studies may be divided into applied research and detailed studies of mechanisms. Applied studies are usually motivated by atmospheric deposition of hazardous substances (i.e., radionuclides from the Chernobyl 1982 accident [Cambray, 1989]) and the need to predict the spreading of contamination and the lifetime of hazardous air concentrations. Resuspension experiments have been conducted over a wide range of surface types. Many experiments have been conducted in dry or arid regions, simply because many contamination events have occurred in such locations (i.e., the Nevada Test Site). Of the

experiments conducted over vegetation, most have been related to short grass. Alternately, applied studies may be motivated by mitigation efforts for soil erosion by wind or by need for measurement of high atmospheric particulate concentrations caused by resuspension, so-called "fugitive dust". Experiments concerning wind erosion have largely occurred in locations where wind erosion is prevalent, e.g., in the "Dust Bowl" area of the central United States.

3.2.3.2 Applied Studies

Resuspension can occur due to the action of wind or by mechanical stresses. Applied research considers resuspension factors, K (air concentration divided by surface concentration) (units of length^{-1}) and resuspension rates (flux of contaminant divided by surface concentration) (unit of time^{-1}). Mechanical stresses, such as disturbances by traffic or agricultural operations, might result in large amounts of resuspension over short intervals in specific localities. For example, Sehmel (1984) quotes K values of 4×10 m^{-1} (for beryllium particles by vigorous sweeping in an unventilated room) to 7×10^{-3} m^{-1} for plutonium particles in extensive traffic at the Nevada Test Site to 3×10^{-7} m^{-1} for gamma-radioactive-fallout by walking on the deposit in an Australian desert.

Wind generated resuspension is considered to be of major importance because it can be relatively continuous and can occur over large regions. Resuspension has been found to increase as a power of wind speed (with the resuspension rate being related to the second or third power of wind speed). Examples of resuspension factors from wind stresses quoted by Sehmel (1984) range from 3×10^{-4} m^{-1} for uranium at Maralinga trials to 9×10^{-11} m^{-1} for yttrium chloride on a cleared, sandy soil. Part of the range of Ks quoted above might be caused by the aging of deposits, although a lack of understanding of the mechanisms dominant in the resuspension process has precluded identifying any reasons for the wide range of results.

Nicholson's (1988) data verify previous work, giving an approximate 1/time decrease of the resuspension rate. Makhon'ko's (1986) data for resuspension from grass suggest a relationship between relative resuspension rate K' versus phytomass m in grams per square meter, $K' = 2.9 \times 10^{-8}\ m^{-1.4}\ [sec^{-1}]$.

3.2.3.3 Aerodynamic Resuspension

Aerodynamic models include (1) balance of forces models and (2) statistical mechanisms. Balance of forces models account for forces holding the particles to the surfaces versus those forces acting to remove the particles from the surfaces. Experimental studies of particle motions show that particles being entrained into a turbulent fluid tend to move vertically into the stream with unsteady motions (Sutherland, 1967). Braaten et al. (1989) and Braaten and Paw U (1992) stressed the importance of bursts of a sweeping eddy having the characteristics of large shear stress near the wall where particles are sparsely deposited, breaking up the viscous sublayer and transporting fluid forces to the particles. This mechanism removes particles from a surface in short bursts followed by periods of little resuspension activity. Observations of Lycopodium spores placed on the flat floor of a wind tunnel were used to verify the model.

Reeks et al. (1988) proposed a different aerodynamic mechanism that would account for sudden random injections of particles into the air, the injections taking place more randomly in time than in the above force balance model. Their mechanism calls for the individual particles to accumulate energy from the turbulent stream (most efficiently at a resonant frequency for the particle). Accumulation of energy takes place because energy dissipation is limited by the local fluid and substrate. Once sufficient energy has accumulated to overcome the potential energy well holding it in place, the particle is resuspended. Slow motion movies of saltating sand surfaces showed such a vibrating motion of a particle before it becomes airborne (Willetts, 1992).

3.2.3.4 Mechanical Resuspension

The importance of mechanical disturbance is seen in the differences of resuspension factors given by Sehmel (1984) for mechanical activities over contaminated soil versus those for wind. Another example of the comparison of resuspension by mechanical disturbance with resuspension by the wind was given by Garland (1979) as a two-order-of-magnitude increase of the resuspension factor for the mechanical disturbance of a full 5-liter bottle dragged along the grass 20 times in 5 minutes in wind compared to the 10 m/s wind alone. Sehmel (1984) conducted experiments to determine the fraction of tracer particles resuspended by driving cars and trucks through the deposited tracer or near the deposited

tracer. The fraction increases with speed and size of vehicle. The fraction resuspended per vehicle pass increased as the first power of vehicle speed for the truck driven through the tracer, the fourth power of vehicle speed for a car driven through the tracer, and the third power of the vehicle speed for a car driven near the tracer.

The emission of PM_{10} particles in wind erosion is driven by the mechanical process of sandblasting, although Shinn et al. (1983) have pointed out the importance of direct aerodynamic emission for low emission rates below erosion threshold. Threshold velocities for particles smaller than 10 micrometer diameter are several times greater than that for 100 micrometer particles (Bagnold, 1941). Nonetheless, one observes submicrometer to 10-micrometer particles in wind erosion events for winds very much below the threshold velocity for the above mentioned particles. Gillette and Walker (1977) interpreted this to be caused by the mechanical suspension (sandblasting) of fine particles by more-easily-eroded sand particles. Shao et al. (1993) showed that sand-grain bombardment (saltation) is the overwhelmingly dominant mechanism in maintaining fine particle emissions from the surface. To derive an expression for the emission of dust, Shao et al. (1993) assumed that the number of dust particles dislodged from a surface per sand grain impact was proportional to the ratio for the kinetic energy loss of the impacting sand grain to the binding potential energy holding a dust particle to the surface. This assumption led to the prediction that the dust flux is proportional to the sand grain mass flux, which was in turn proportional to the friction velocity cubed. Dust emission is highly sporadic. After the wind stress threshold is surpassed, the vertical flux increases with the third power of friction velocity.

3.2.3.5 Physical and Chemical Properties of Resuspended Particles

The physical and chemical properties of resuspended particles depend partly on the properties of the particles that were deposited on the surface in the initial stage of resuspension. But, "the deposited particles probably lose their individual identity by becoming attached to host (soil) particles. When the pollutant particle is transported downwind, it is usually attached (aggregated) to this host particle" (Sehmel, 1973). Furthermore, the host particle is most likely an aggregate itself. Studies of the cross section of particles, mineralogy, and scanning electron microscope analysis of dust samples show

that particles suspended from the soil are aggregated. For these reasons, this section describes physical properties of the aggregated (host plus pollutant) particles.

The size distribution of resuspended soil particles may be described as lognormal bimodal with one mode at 2 to 5 micrometers and another mode at 30 to 60 micrometers (Sviridenkov et al., 1993; Patterson and Gillette, 1977a,b; Gillette and Nagamoto, 1992; Gillette, 1974). Because the mass mode of the distribution for particles smaller than 10 micrometers is roughly at 2.5 micrometers, a rough approximation is that half the PM_{10} mass is smaller than 2.5 micrometers and half is larger. The ratio

$$\frac{v_{sed}}{u_*} < 0.1 \tag{3-4}$$

defines the upper size of suspended dust, where v_{sed} is the sedimentation velocity of the upper size limit, and u_* is friction velocity. Data from Pinnick et al. (1985) show that very similar size distributions result from resuspension by traffic.

The mineralogical components of dust collected in Texas dust storms, given in order of abundance, are: for particles 1 to 10 micrometers: quartz, mica, kaolinite, mixed layer phyllosilicates and feldspars; for particles smaller than 1 micrometers: mica, kaolinite, quartz, and mixed layer phyllosilicates (Gillette et al., 1978). Studies of elemental composition show that composition of the resuspended material, compared to that of the total sediment, is enriched in elements associated with the smallest particles (i.e., titanium) and impoverished in elements associated with the coarsest materials (i.e., silicon).

3.2.3.6 Levels of Production and Transport of Resuspended Aerosols

Airborne dust measurements in the southern and central Great Plains states of the United States were made in the early 1970's. The total mass of dust produced by individual dust storms was 0.3 to 0.5 $\times$ 10^{12}g (Gillette et al., 1978). Individual dust storm production rates may be compared to the global production rate estimated by d'Alameida (1989) of 1,800 to 2,000 $\times$ 10^{12}g per year. The Great Plains study, part of a severe storm study, showed that the dust storms were typically associated with vigorous frontal activity, and that the dust travels great distances (many 100's of km) as tracked by jet aircraft. Estimates of

transport distance for dust of well over 1,000 km (from West Texas dust storms to deposition sites in northern Minnesota) were supported by isentropic trajectories, positions of rainclouds and elevated concentrations of calcium in collections of rainwater in the National Acid Deposition Program/National Trends Network. Even greater transport distances of resuspended dust are shown by oxygen isotopic 18 to 16 ratios (δ^{18}) in quartz (parts per thousand). By matching the δ^{18} value for deposited quartz and source areas for the quartz (wind erodible soils) the following long-range transport paths were found: Asian deserts to Hawaii; Sahara desert to the Caribbean, South America, and Florida; and U.S. sources to Greenland and northern Europe (Jackson et al., 1973).

A model developed for national acid rain and desertification/paleoclimate studies (Gillette and Passi, 1988) expressed the emission of dust for a given study area as an integral over friction velocity (expressing the forcing function), and the threshold friction velocity (expressing the resistance of the soil and environment to ablation). Results from the model for the contiguous United States (Figure 3-7) show a strong agreement of the model dust emissions with known emissions from dusty areas (Gillette and Hanson, 1989). Predicted alkaline emissions also agree in many respects with observed wet deposition patterns of alkaline elements (Gillette et al., 1992). A considerable fraction of wind emitted dust is from dust devils (Gillette and Sinclair, 1990).

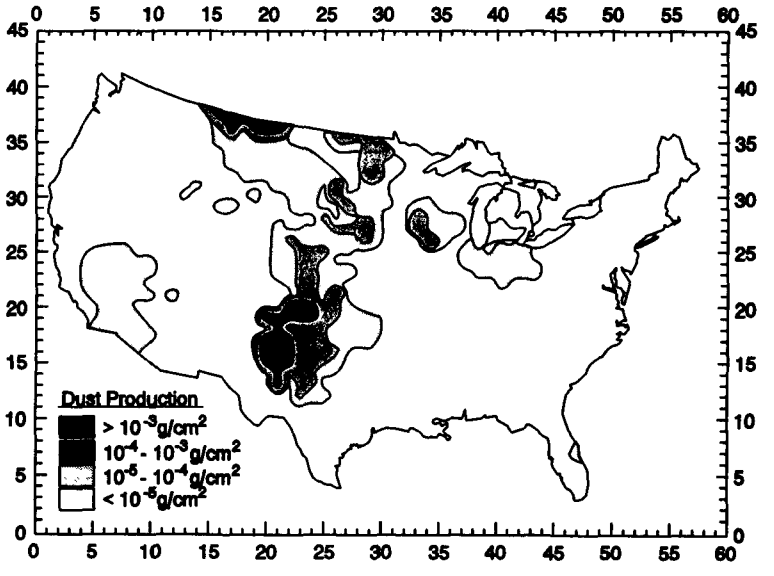

Figure 3-7. Model dust emissions for the United States.

Source: Gillette and Hanson (1989).

3.2.4 Particle Removal Mechanisms and Deposition

Particles in the air are in constant motion. They are subject to Brownian motion, which is the constant random movement along an irregular path caused by the bombardment by surrounding air molecules. This process is most important for small particles, and is related to the particle diffusion coefficient. Particles are also subject to the earth's gravitational force, as characterized by a sedimentation velocity. Gravitational settling is most important for larger particles. Both of these processes involve the motion of the particle relative to its surrounding air medium.

A particle subject to any constant external force will reach a terminal velocity called the drift velocity. The proportionality between the particle drift velocity (V_{drift}) and the external force (F_{ext}) is called the particle mobility, B, and is defined by:

$$B = \frac{V_{drift}}{F_{ext}} = \frac{C}{3\pi\mu D_p} \tag{3-5}$$

where C is the Cunningham correction factor and μ is the particle velocity. The Cunningham correction factor must be introduced because when the particle diameter, D_p, approaches the same order as the mean free path of air, the resistance to particle motion becomes less than that predicted by continuum theory. The Cunningham correction factor increases as the particle size decreases. When the external force is that due to gravity (F_{ext} = mg), the drift velocity is the settling (sedimentation) velocity ($V_{drift} = V_{TS}$ = Bmg). If the external force is an electric field, then the drift velocity equals qEB where q is the electric charge on the particle and E is the electric field. Small particles are the most mobile. For particle diameters much smaller than the mean free path ($D_p \ll 0.066$ μm for air at standard conditions), B varies as the inverse square of the particle diameter. For large particles, B varies inversely with particle diameter. The particle diffusion coefficient is related to particle mobility by D = BKT.

Brownian diffusion is important for small particles, whereas gravitational settling is important for large ones. During a time period of 1 s a 0.1 μm particle will travel a total distance of about 40 μm due to Brownian motion, while it will fall about 1 μm due to gravity. In the same 1 s time period, a 1 μm particle will travel a total distance of about 8 μm due to Brownian motion and will fall 35 μm due to gravity. Note that the diffusion

constant is directly proportional to the particle mobility B, while the settling velocity depends on the product of particle mass and mobility, mB. Diffusion constants and settling velocities are plotted in Figure 3-8.

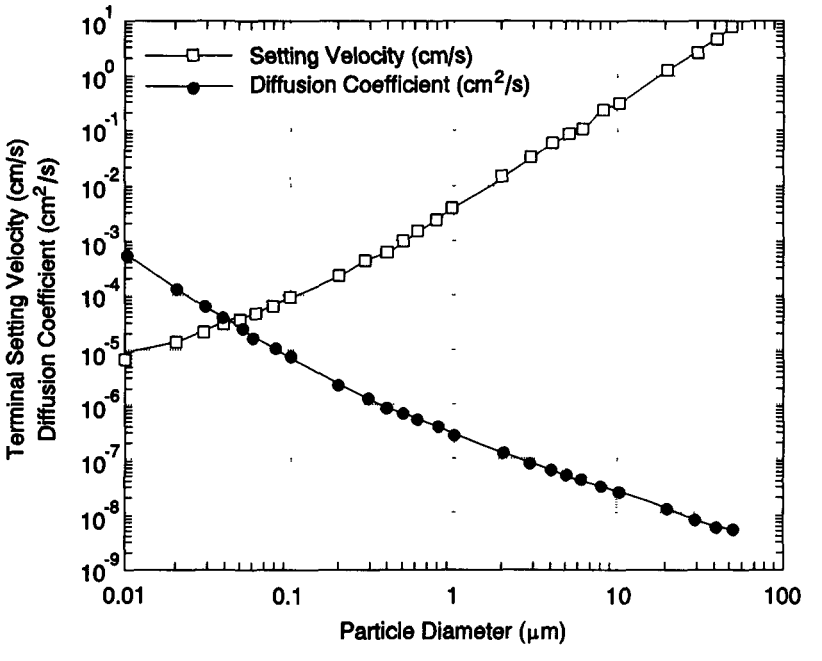

Figure 3-8. Diffusion constants and settling velocities for particles.

The deposition of particles in the atmosphere is not easily modeled, and is characterized by a deposition velocity, which is defined as the ratio of the flux of particles to the surface to the ambient concentration. Results from wind tunnel studies, shown in Figure 3-9, show characteristic minima. Small particles are collected by diffusion, larger particles are collected by impaction and sedimentation. Deposition models which account for these mechanisms are given by Sehmel (1980), Fernandez de la Mora and Friedlander (1982) and Fernandez de la Mora (1986). Atmospheric data from Lin et al. (1994), shown in Figure 3-10, show that inertial mechanisms, as well as sedimentation, are important for the deposition of large particles. As can be seen in Figure 3-9, these various removal mechanisms are least effective for particles in the 0.1 to 1.0 μm diameter size range. Therefore, accumulation mode particles, which occur mainly in this size range, have long

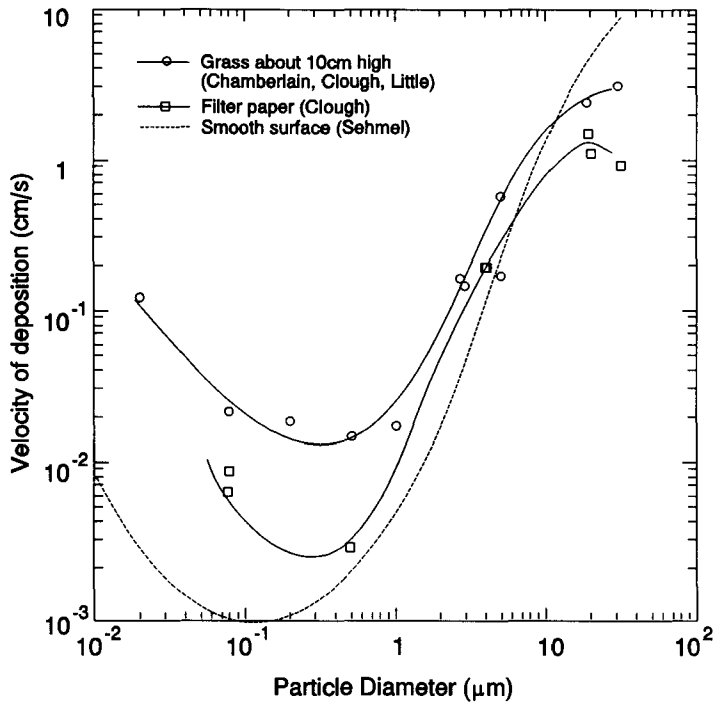

Figure 3-9. Particle deposition from wind tunnel studies.

Source: Chamberlain (1983).

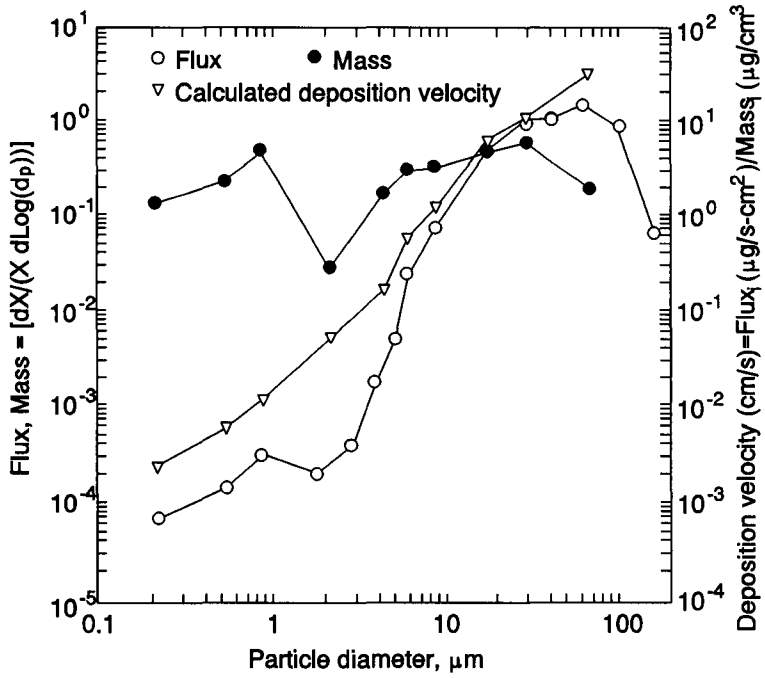

Figure 3-10. Sedimentation and inertia effects on large particle deposition.

Source: Lin et al. (1994).

lifetimes in the atmosphere. Such particles act as nuclei for the formation of cloud droplets and are removed when the cloud droplets grow large enough to fall as rain. Falling rain drops also remove larger particles by impaction and smaller particles by diffusion. More details on removal processes may be found in Sections 3.5 and 3.6.

3.3 CHEMICAL COMPOSITION AND PROCESSES

3.3.1 Acid Aerosols and Particulate Sulfates

Sulfuric acid and its neutralization products with ammonia constitute a major anthropogenic contribution to fine particle aerosol. This section reviews recent advances in understanding of the sources, removal processes, loadings and properties of tropospheric sulfate aerosols. Emphasis is given to properties and processes pertinent to these aerosols in regions influenced by anthropogenic emissions as distinguished from remote locations influenced primarily by natural sources.

3.3.1.1 Aerosol Acidity

Aerosol acidity can occur in suspended particulate matter (liquid or solid) or in the gas phase. The concept of aerosol acidity includes both the actual acid dissociation and the H^+ potentially available for reaction when the gas or particle contacts a liquid or solid surface (Waldman et al., 1995). With respect to pulmonary surfaces and fluids, many components in the air are acidic. The extent and location of acid deposition in the airways is greatly affected by whether exposure is to gaseous or particulate acids and also varies according to the size of particles.

The principal acids found in the atmosphere are related to mineral acids: particulate sulfuric acid (H_2SO_4) and bisulfate (HSO_4^-) and gaseous nitric (HNO_3), nitrous (HNO_2), and hydrochloric (HCl) acids. Organic acids (such as carboxylic and dicarboxylic acids) can also be found in the particulate and gaseous forms. Formic and acetic acids are the most abundant of organic acid compounds. As weak acids, these tend to exist in the nondissociated form and will often be volatile. In the atmosphere, the magnitude of particle acidity contributed from organic acids is generally found to be minor compared to particle strong acids (Lawrence and Koutrakis, 1994). However, organic and inorganic acids may be generated indoors (Zhang et al., 1994).

Particle strong acidity (PSA) has recently been reviewed by Waldman et al. (1995). The primary source of PSA is sulfuric acid, formed largely by oxidation of SO_2. When the acid is formed in the gas phase, it rapidly condenses to very small particles; these grow in the atmosphere by condensation and coagulation. When formed within cloud or fog droplets, the acidic sulfates are also found in the accumulation mode after the droplets evaporate. Measurements in southern Ontario for aerosols in several size ranges indicated that the vast majority of PSA was in the range of 0.2-2 μm (Koutrakis et al., 1989). The contribution to PSA from nuclei mode (<0.1 μm) particles is not substantial; acidic particles in this size range either grow or are neutralized rapidly. Particles larger than 2 μm contain little sulfate, but include wind-blown materials, in which there is often an abundance of alkaline materials.

The form of PSA is rarely pure sulfuric acid; H_2SO_4 can be partially neutralized to forms that are still acidic. A variety of crystalline forms intermediate in acidity between H_2SO_4 and $(NH_4)_2SO_4$ may be observed in the solid state. However, in the atmosphere, sulfate salts will usually be present in solutions containing H^+, NH_4^+, HSO_4^-, and $SO_4^=$. PSA is defined, in terms of molar or equivalent concentrations, as the sum of H^+ and HSO_4^-. Some writers have recommended that PSA be defined as the concentration of free H^+ ions in the particles as they exist in the atmosphere (Saxena et al., 1993). In this definition HSO_4^- would not be counted as contributing to the PSA. There are several disadvantages to this definition. The water associated with a particle increases as the relative humidity increases; as the solution becomes more dilute, more HSO_4^- dissociates and the PSA increases. Thus for this definition PSA varies with relative humidity and must be calculated from equilibrium theory. As a particle enters the lung the relative humidity increases to near 100% relative humidity and the PSA will also increase. If deposited in the lung all of the H^+ in HSO_4^- will be available for reaction. Therefore, it seems most useful for health effects purposes to define PSA as $[H^+] + [HSO_4^-]$ (Schlesinger, 1994; Saxena, 1994).

In practice PSA is measured by extracting collected particles and determining H^+ from a measurement of the pH of the solution. One technique uses a pH=4 solution of perchloric acid ($HCLO_4$), which prevents dissociation of weak acids but dilutes the solution sufficiently to allow dissociation of HSO_4^- (Koutrakis et al., 1988a,b; Suh et al., 1994a). PSA may also be measured by extracting the collected particles with water, titrating with base, and using

the Gran titration technique to determine strong acidity separate from weak acidity (Brosset et al., 1975).

Theory predicts a very fast neutralization reaction between PSA and atmospheric ammonia, which limited laboratory experiments with pure compounds appear to confirm (Huntzicker et al., 1980). However, measurements seem to indicate that neutralization is slower under field conditions and that some amount of PSA may persist even with ammonia present (Brauer et al., 1991; Liang and Waldman, 1992; Harrison and Kitto, 1992). Measurements of PSA and ammonia are normally averages over time periods of several to 24 h. Thus, it is possible that nonzero concentrations occur in different time intervals and only appear to be coincident. Recent research has evaluated the possibility that organic compounds retard the rate of neutralization (Daumer et al., 1992). Attenuation of regional PSA levels in central city locations has been observed to varying degrees. People and their activities generate ammonia, and in areas with higher population densities, ambient ammonia concentrations are generally higher. A study in Philadelphia showed daily decreases, in the city center relative to the suburbs, as high as 60%, although these were during a summer with pollution levels notably lower than the previous and subsequent summers (Suh et al., 1995). PSA levels are also attenuated indoors due to ammonia generated by people (Suh et al., 1992, 1994b).

The recent articles by Spengler et al. (1989) and Thompson et al. (1991) on the Harvard 24-cities study PSA results and Thurston et al. (1992) report data for daily (or alternate-day) sampling over the entire year at fixed sites. These have shown that the largest PSA exposures occur in the warmer months. The highest levels are specifically associated with summertime, regional stagnation periods. Frequently, PSA episodes are coincident with photochemical smog and high ozone levels, although the converse is not always the case. Simultaneous measurements on a regional scale have confirmed the spatial homogeneity in PSA levels over large areas. Good correlations for daily PSA concentrations among suburban sites 100 km apart were observed in New York (Thurston et al., 1992).

3.3.1.2 Sources of Sulfate

Knowledge of the sources of sulfates is important to understanding the processes responsible for the observed loading, composition, and size distribution of sulfates and to

developing effective methods to control sulfate concentration. Ambient sulfate may be either primary or secondary. Primary refers to material emitted into the atmosphere as particulate sulfate or as gas-phase SO_3 or H_2SO_4, species which readily nucleate and condense to form particles. Secondary refers to material that is formed by gas to particle conversion following the chemical reaction of SO_2, or other sulfur containing gases, to form SO_3, H_2SO_4, or $SO_4^=$ in solution. Most sulfate in the troposphere is secondary sulfate formed from SO_2.

Atmospheric oxidation of SO_2 takes place both by gas-phase reaction and by aqueous-phase reaction. The principal gas-phase mechanism is thought to be the OH-initiated reaction. The principal aqueous-phase reactions are thought to be oxidation by H_2O_2, O_2 (when catalyzed by trace metals), and O_3. Aqueous-phase reactions followed by cloud evaporation can result in formation of aerosol. Evaporation can be a major production route for atmospheric sulfate aerosols. The relative proportion of sulfate aerosol produced by the aqueous and gas-phase routes is not well established.

3.3.1.3 Gas-Phase Oxidation of Sulfur Dioxide

Gas phase oxidation of SO_2 is thought to occur largely, if not entirely, by a sequence of reactions initiated by the reaction of OH with SO_2.

$$SO_2 + OH + M \rightarrow HSO_3 + M \tag{3-6}$$

$$HSO_3 + O_2 \rightarrow SO_3 + HO_2 \tag{3-7}$$

$$SO_3 + H_2O \rightarrow H_2SO_4 \tag{3-8}$$

The gaseous H_2SO_4 subsequently adds to existing particles or may nucleate to form new particles.

Until recently the evidence for the occurrence of this reaction in the atmosphere has relied on modeled OH concentrations and on laboratory-determined reaction rate coefficient (Gleason et al., 1987) for the OH + SO_2 reaction. However, recent measurements of OH and H_2SO_4 in the atmosphere provide empirical evidence for this mechanism (Eisele and Bradshaw, 1993; Eisele and Tanner, 1993; Eisele et al., 1994). Simultaneous measurements

of OH and SO_2 allow the gas-phase reaction production rate of H_2SO_4 to be calculated at the time and location of the measurement. Likewise, measurements of particle size distribution allow the effective first-order rate coefficient for diffusive uptake of H_2SO_4 monomer by aerosol particles to be calculated, and measurement of the concentration of H_2SO_4 monomer allows the loss rate by this mechanism to be calculated. Comparison of the calculated production and loss rates of H_2SO_4 monomer show them to be equal, consistent with the observed steady state concentration of this species. This study lends substantial confidence to the applicability of the laboratory mechanism and rate to evaluation of the rate of sulfuric acid formation in the ambient atmosphere.

The reaction of SO_3 has recently been reexamined by Kolb et al. (1994), who find that the reaction is second order in water vapor and propose that the reaction takes place by interaction of SO_3 with water vapor dimer:

$$SO_3 + (H_2O)_2 \rightarrow H_2SO_4 + H_2O \tag{3-9}$$

The investigators note that it is probable that sufficient water dimer exists in the atmosphere to allow the reaction to efficiently form sulfuric acid vapor.

3.3.1.4 Aqueous-Phase Oxidation of Sulfur Dioxide

Aqueous-Phase Equilibria

The liquid water content of the atmosphere, w_L, is usually expressed either in g of water per m^3 of air or as a dimensionless volume fraction L (e.g., m^3 of liquid water per m^3 of air). Typical liquid water content values are 0.1 to 1 g m^{-3} ($L = 10^{-7} - 10^{-6}$) for clouds, 0.05 to 0.5 g m^{-3} ($L = 5 \times 10^{-7} - 5 \times 10^{-6}$) for fogs, and only 10^{-5} to 10^{-4}g m^{-3} ($L = 10^{-11}$-10^{-10}) for aerosols. Cloud chemistry has been reviewed by Schwartz (1984a, 1986a). Aqueous-phase oxidation of SO_2 has recently been reviewed by Martin (1994).

For dilute solutions the equilibrium distribution of a reagent gas A between the gas and aqueous phases is given by Henry's law

$$[A] = H_A p_A \tag{3-10}$$

where p_A is the partial pressure of A in the gas-phase, $[A]$ is the equilibrium aqueous-phase concentration of A and H_A is the Henry's law coefficient for species A. The customary units of H_A are mole l^{-1} atm^{-1}. H_A can be viewed as the equilibrium constant of the reaction

$$A(g) \leftrightarrows A(aq) \tag{3-11}$$

Table 3-2 gives the Henry's law coefficients of some atmospheric gases in liquid water at 298 K. The values given reflect only the physical solubility of the gas regardless of the subsequent fate of the dissolved species A. Some of the species included in Table 3-2 dissociate after dissolution or react with water. Henry's law constants do not account for these processes, and the modifications necessary will be discussed in the next paragraph. Henry's law coefficients generally decrease for increasing temperatures, reflecting the lower solubilities of gases at higher temperatures (Seinfeld, 1986).

Several gases, after dissolving in the aqueous-phase, ionize and establish an aqueous-phase chemical equilibrium system. For example for SO_2,

$$SO_2(g) \leftrightarrows SO_2 \cdot H_2O \tag{3-12}$$

$$SO_2 \cdot H_2O \leftrightarrows HSO_3^- + H^+ \tag{3-13}$$

$$HSO_3^- \leftrightarrows SO_4^= + H^+ \tag{3-14}$$

with

$$H_{SO_2} = \frac{[SO_2 \cdot H_2O]}{p_{SO_2}}, \quad K_{s1} = \frac{[HSO_3^-][H^+]}{[SO_2 \cdot H_2O]}, \quad K_{s2} = \frac{[SO_4^=][H^+]}{[HSO_3^-]} \tag{3-15}$$

K_{s1} and K_{s2} are the first and second dissociation constants for SO_2. It is convenient to

TABLE 3-2. HENRY'S LAW COEFFICIENTS OF SOME ATMOSPHERIC GASES DISSOLVING IN LIQUID WATER

Species	H (M/atm) (298 K)
O_2	1.3×10^{-3}
NO	1.9×10^{-3}
C_2H_4	4.8×10^{-3}
NO_2	1.0×10^{-2}
O_3	1.2×10^{-2}
N_2O	2.5×10^{-2}
CO_2	3.4×10^{-2}
H_2S	0.12
SO_2	1.23
CH_3ONO_2	2.6
OH	55.
HNO_2	49.
NH_3	57.
HO_2	2.0×10^{3}
HCOOH	5.6×10^{3}
HCHO	6.3×10^{3}
CH_3COOH	8.7×10^{3}
H_2O_2	1×10^{5}
HNO_3	2.1×10^{5}

Source: Schwartz (1986a).

consider the total dissolved sulfur in oxidation state IV as a single entity and refer to it as S(IV),

$$[S(IV)] = [SO_2 \cdot H_2O] + [HSO_3^-] + [SO_4^=] \tag{3-16}$$

The three sulfur species are in rapid equilibrium and therefore [S(IV)] changes only when SO_2 is transferred between the gas and aqueous phases. The total dissolved sulfur, S(IV), can be expressed as a function of only the pH and the partial pressure of SO_2 over the solution by:

$$[S(IV)] = H_{SO_2} p_{SO_2} \left[1 + \frac{K_{s1}}{[H^+]} + \frac{K_{s1}K_{s2}}{[H^+]^2} \right] \tag{3-17}$$

The above equation can be expressed in a form similar to Henry's law as

$$[S(IV)] = H^*_{S(IV)} p_{SO_2} \tag{3-18}$$

where $H^*_{S(IV)}$ is the effective (or modified) Henry's law coefficient given for S(IV) by

$$H^*_{S(IV)} = H_{SO_2} \left[1 + \frac{K_{s1}}{[H^+]} + \frac{K_{s1}K_{s2}}{[H^+]^2} \right] \tag{3-19}$$

The modified Henry's law coefficient relates the total dissolved S(IV) (not only $SO_2 \cdot H_2O$) with the SO_2 vapor pressure over the solution. The effective Henry's law coefficient always exceeds the Henry's law coefficient, indicating that the dissociation of a species enhances its solubility in the aqueous phase.

Several of the species that are in rapid equilibrium can be also considered as single entities:

$$[S(VI)] = [H_2SO_4(aq)] + [HSO_4^-] + [SO_4^=] \tag{3-20}$$

$$[N(V)] = [HNO_3(aq)] + [NO_3^-] \tag{3-21}$$

$$[NO_2^T] = [HNO_2(aq)] + [NO_2^-] \tag{3-22}$$

$$[HCHO^T] = [HCHO] + [H_2C(OH)_2] \tag{3-23}$$

Equations relating the total concentrations of these aqueous-phase species with the corresponding equilibrium concentrations of the gas-phase species can be derived similarly to those for S(IV).

Aqueous-Phase Reaction Mechanisms

The aqueous-phase conversion of dissolved SO_2 to sulfate is thought to be the most important chemical transformation in cloudwater. Dissolution of SO_2 in water results in the formation of three chemical species: hydrated SO_2 ($SO_2 \cdot H_2O$), the bisulfite ion (HSO_3^-) and the sulfite ion ($SO_3^=$). At the pH range of atmospheric interest (pH =2-7) most of the S(IV) is in the form of HSO_3^-, whereas at low pH (pH <2), all of the S(IV) occurs as $SO_2 \cdot H_2O$. At higher pH values (pH >7), ($SO_3^=$) is the preferred S(IV) state (Seinfeld, 1986). The individual dissociations are fast, occurring on timescales of milliseconds or less (Martin, 1984; Schwartz and Freiberg, 1981; Seinfeld, 1986). Therefore, during a reaction consuming one of the three species, $SO_2 \cdot H_2O$, HSO_3^-, or $SO_3^=$, the corresponding aqueous-phase equilibria are re-established instantaneously. The dissociation of dissolved SO_2 enhances its aqueous solubility. The total amount of dissolved S(IV) is quite pH dependent but always exceeds that predicted by Henry's law for SO_2 alone. The Henry's law coefficient for SO_2 alone, H_{SO_2}, is 1.23 M atm^{-1} at 298 K, while for the same temperature, the effective Henry's law coefficient for S(IV), $H^*_{S(IV)}$, is 16.4 M atm^{-1} for pH=3, 152 M atm^{-1} for pH=4 and 1,524 M atm^{-1} for pH=5. Equilibrium S(IV) concentrations for SO_2 gas-phase concentrations of 0.2-200 ppb, and over a pH range of 1 to 6 vary approximately from 0.001 to 1000 mM.

Several pathways for S(IV) transformation to S(VI) have been identified involving reactions of S(IV) with O_3, H_2O_2, O_2 (catalyzed by Mn^{2+} and Fe^{3+}), OH, SO_5^-, HSO_5^- SO_4^-, PAN, CH_3OOH, $CH_3C(O)OOH$, HO_2, NO_3, NO_2, N(III), HCHO and Cl_2^- (Pandis and Seinfeld, 1989a; Martin, 1994).

Although ozone reacts very slowly with SO_2 in the gas phase, the aqueous-phase reaction is rapid. The possible importance of O_3 as an aqueous-phase oxidant for S(IV) was first suggested by Penkett (1972) and the kinetics of

$$S(IV) + O_3 \rightarrow S(VI) + O_2 \qquad (3\text{-}24)$$

have been studied by several investigators (Erickson et al., 1977; Penkett et al., 1979; Maahs, 1983). Hoffmann and Calvert (1985), after a detailed investigation of existing

experimental kinetic and mechanistic data, suggested the following expression for the rate of the reaction of S(IV) with dissolved ozone:

$$R_1 = -\frac{d[S(IV)]}{dt} = (k_0[SO_2 \cdot H_2O] + k_1[HSO_3^-] + k_2[SO_3^=])[O_3] \qquad (3\text{-}25)$$

recommending the values $k_0 = 2.4 \times 10^4\ M^{-1}\ s^{-1}$, $k_1 = 3.7 \times 10^5\ M^{-1}\ s^{-1}$ and, $k_2 = 1.5 \times 10^9\ M^{-1}\ s^{-1}$. They also proposed that this reaction proceeds by nucleophilic attack on ozone by $SO_2 \cdot H_2O$, HSO_3^-, and $SO_3^=$. An increase in the aqueous-phase pH results in an increase of all three, $[SO_2 \cdot H_2O]$, $[HSO_3^-]$ and $[SO_3^=]$, equilibrium concentrations and therefore in an increase of the overall reaction rate. For an ozone gas-phase mixing ratio of 30 ppb, the reaction rate varies from less than 0.001 mM h^{-1} (ppb $SO_2)^{-1}$ at pH=2 (or less than 0.01% SO_2 (g) h^{-1} (g water /m^3 air)$^{-1}$) to 3,000 mM h^{-1} (ppb $SO_2)^{-1}$ at pH=6 (7,000% SO_2 (g) h^{-1} (g water /m^3 air)$^{-1}$). The gas-phase SO_2 oxidation rate is of the order of 1% h^{-1} and therefore the S(IV) heterogeneous oxidation by ozone is significant for pH values greater than 4. The strong positive dependence of the reaction rate on the pH renders this reaction self limiting. The production of sulfate by this reaction lowers the pH and effectively decreases the rate of further reaction. The availability of atmospheric ozone guarantees that this reaction will play an important role both as a sink of gas-phase SO_2 and as a cause of cloudwater acidification as long as the pH of the atmospheric aqueous phase exceeds 4.

Hydrogen peroxide, H_2O_2, is one of the most effective oxidants of S(IV) in clouds and fogs (Pandis and Seinfeld, 1989a; Jacob and Hoffmann, 1983; Chameides, 1984; Schwartz, 1986a; Seigneur and Saxena, 1988; Nair and Peters, 1989; Bott and Carmichael, 1993). H_2O_2 is very soluble in water and under typical ambient conditions its aqueous-phase concentration is approximately six orders of magnitude higher than that of ozone. This reaction has been studied in detail by several investigators (Hoffmann and Edwards, 1975; Penkett et al., 1979; Martin and Damschen, 1981; Cocks et al., 1982; Kunen et al., 1983; McArdle and Hoffmann, 1983) and the reproducibility of the measurements suggests a lack of susceptibility of this reaction to influence of trace constituents. The proposed rate expression is (Hoffmann and Calvert, 1985)

$$R_2 = -\frac{d[S(IV)]}{dt} = \frac{k[H^+][H_2O_2][HSO_3^-]}{1 + K[H^+]} \tag{3-26}$$

with k=7.45 × 10^7 M^{-1} s^{-1} and K=13 M^{-1} at 298 K. Noting that H_2O_2 is a very weak electrolyte; that $[H^+]$ $[HSO_3^-]$ = $H_{SO_2}K_{s1}p_{SO_2}$ (Equation 3-15); and that for pH > 2, $1 + K[H^+] \simeq 1$, one concludes that the rate of this reaction is practically pH independent in the pH range of atmospheric interest. For a H_2O_2(g) mixing ratio of 1 ppb the rate is roughly 300 mM h^{-1} (ppb $SO_2)^{-1}$ (700% SO_2(g)h^{-1} (g water /m^3 air)$^{-1}$). The near pH independence can also be viewed as the result of the cancellation of the pH dependence of the S(IV) solubility and the reaction rate constant. The reaction is very fast and indeed both field measurements (Daum et al., 1984a) and theoretical studies (Pandis and Seinfeld, 1989b) have suggested that H_2O_2(g) and SO_2(g) rarely coexist in clouds and fogs. The species with the lowest concentration before the cloud or fog formation is the limiting reactant, and is rapidly depleted inside the cloud or fog layer.

The fastest, aqueous-phase, atmospheric reaction of SO_2 is believed to be with hydrogen peroxide, and with ozone at higher pH values. However, results of a study by Hofmann and Jacob (1984) show that in heavily polluted atmospheric water droplets, such as those found in urban fogs, metal-catalyzed oxidation by O_2 contributes significantly to formation of sulfate in the liquid phase, and in such situations may be more important than oxidation by hydrogen peroxide. Organic peroxides have been also proposed as potential aqueous-phase oxidants of dissolved sulfur (Graedel and Goldberg, 1983; Lind and Lazrus, 1983; Hoffmann and Calvert, 1985). However, simulations for typical continental clouds suggest that these reactions are of minor importance for the S(IV) oxidation and represent only small sinks for the gas-phase methylhydroperoxide (0.2% CH_3OOH h^{-1}) and peracetic acid (0.7% $CH_3C(O)OOH$ h^{-1}).

The S(IV) oxidation by O_2 is known to be catalyzed by Fe^{3+} and Mn^{2+}

$$S(IV) + 1/2\ O_2 \xrightarrow{Mn^{2+},\ Fe^{3+}} S(VI) \tag{3-27}$$

This reaction has been the subject of considerable interest (Hoffmann and Boyce, 1983; Martin, 1984, 1994; Martin et al., 1991; Hoffmann and Jacob, 1984; Hoffmann and Calvert, 1985; Clarke and Radojevic, 1987) and significantly different measured reaction rates, rate laws and pH dependencies have been reported (Hoffmann and Jacob, 1984). Martin and Hill (1987a,b) have demonstrated that this reaction is inhibited as ionic strength increases. They explained most of the literature discrepancies by differences in these factors during the various laboratory studies.

In the presence of oxygen, iron in the ferric state, Fe(III), catalyzes the oxidation of S(IV) in aqueous solutions. Fe(II) appears not to catalyze the reaction directly but must be first oxidized to Fe(III) before S(IV) oxidation can begin (Huss et al., 1982a,b). The recent review by Martin (1994) gives a comprehensive discussion of the oxidation of SO_2 by O_2 in the presence of iron.

For pH values from 0 to 3.6 the iron-catalyzed S(IV) oxidation rate is first order in iron, first order in S(IV) and is inversely proportional to $[H^+]$ (Martin and Hill, 1987a),

$$R = -\frac{d[S(IV)]}{dt} = k_1 \frac{[Fe^{3+}][S(IV)]}{[H^+]} \tag{3-28}$$

This reaction is inhibited by ionic strength and sulfate and these effects are described by:

$$k_1 = k_1^* \times 10^{\frac{-2\, I^{1/2}}{1 + I^{1/2}}} \tag{3-29}$$

and

$$k_1 = k_1^* \frac{1}{1 + 150[S(VI)]^{2/3}} \tag{3-30}$$

where I is the ionic strength of the solution and [S(VI)] is in M. A rate constant $k_1^* = 6\ s^{-1}$ has been recommended by Martin and Hill (1987a). Sulfite appears to be almost as equally inhibiting as sulfate.

The rate expression for the same reaction changes completely above pH 3.6. This suggests that the mechanism of the reaction differs in the two pH regimes, and is probably a

free radical chain at high pH and a non radical mechanism at low pH (Martin et al., 1991). The low solubility of Fe(III) above pH 3.6 presents special experimental problems. At high pH the reaction rate depends on the amount of iron in solution, rather than on the total amount of iron present. At this range the reaction is second order in dissolved iron (zero order above the solution iron saturation point) and first order in S(IV). The reaction is still not very well understood and Martin et al. (1991) proposed the following phenomenological expressions (in M s^{-1})

$$\text{pH4.0: } -\frac{d[S(IV)]}{dt} = 1\times10^{9}[S(IV)][Fe^{3+}]^{2} \tag{3-31}$$

$$\text{pH5.0-6.0: } \frac{d[S(IV)]}{dt} = 1\times10^{-3}[S(IV)] \tag{3-32}$$

$$\text{pH7.0: } -\frac{d[S(IV)]}{dt} = 1\times10^{-4}[S(IV)] \tag{3-33}$$

for the following conditions:

$$[S(IV)] \simeq 10\mu M, [Fe^{3+}] > 0.1\mu M,\ I < 0.01M,\ [S(VI)] < 100M, \text{ and } T = 298K.$$

Note that iron does not appear in the pH 5-7 rates because it is assumed that a trace of iron will be present under normal atmospheric conditions. This reaction is important in this high pH regime (Pandis and Seinfeld, 1989a,b; Pandis et al., 1992b).

Martin et al. (1991) also found that non-complexing organic molecules (e.g., acetate, trichloroacetate, ethyl alcohol, isopropyl alcohol, formate, allyl alcohol, etc.) are highly inhibiting at pH values of 5 and above, and are not inhibiting at pH values of 3 and below. They calculated that, for remote clouds, formate would be the main inhibiting organic, but by less than 10%. In contrast, near urban areas formate could reduce the rate of the catalyzed oxidation by a factor of 10-20 in the high pH regime.

The manganese catalyzed S(IV) oxidation was initially thought to be inversely proportional to the H^{+} concentration. Martin and Hill (1987b) suggested that ionic strength,

not hydrogen ion, accounts for the pH dependence of the rate. These authors were also able to explain some unusual behavior described in the literature on this reaction and to partially reconcile some of the literature rates. The manganese catalyzed reaction obeys zero-order kinetics in S(IV) in the concentration regime above 100 mM S(IV),

$$-\frac{d[S(IV)]}{dt} = k_0[Mn^{2+}]^2 \tag{3-34}$$

$$k_0 = k_0^* \times 10^{\frac{-4.07\ I^{1/2}}{1 + I^{1/2}}} \tag{3-35}$$

with $k_0^* = 680\ M^{-1}\ s^{-1}$ (Martin and Hill, 1987b). For S(IV) concentrations below 1 mM the reaction is first order in S(IV),

$$-\frac{d[S(IV)]}{dt} = k_0[Mn^{2+}][S(IV)] \tag{3-36}$$

$$k_0 = k_0^* \times 10^{\frac{-4.07\ I^{1/2}}{1 + I^{1/2}}} \tag{3-37}$$

with $k_0^* = 1{,}000\ M^{-1}\ s^{-1}$ (Martin and Hill, 1987b). It is still not clear which rate law is appropriate for use in atmospheric calculations, although Martin and Hill (1987b) suggested the provisional use of the first order, low S(IV) rate.

When both Fe^{3+} and Mn^{2+} are present in atmospheric droplets, the overall rate of the S(IV) reaction is enhanced over the sum of the two individual rates. Martin (1984) reported that the rates measured were 3 to 10 times higher than expected from the sum of the independent rates. Martin et al. (1991) obtained at pH 3.0 and for [S(IV)] < 10 mM the following rate law

$$-\frac{d[S(IV)]}{dt} = 750[Mn(II)][S(IV)] + 2600[Fe(III)][S(IV)] + 1.0\times10^{10}[Mn(II)][Fe(III)][S(IV)] \tag{3-38}$$

and a similar expression for pH 5.0 in agreement with the work of Ibusuki and Takeuchi (1987).

Free radicals, such as OH and HO_2, either heterogeneously scavenged by the aqueous phase or produced in the aqueous phase, participate in a series of aqueous phase reactions (Graedel and Weschler, 1981; Chameides and Davis, 1982; Graedel and Goldberg, 1983; Schwartz, 1984b; Jacob, 1986; Pandis and Seinfeld, 1989a).

Pandis and Seinfeld (1989a) proposed that under typical remote continental conditions there are two main radical pathways resulting in the conversion of S(IV) to S(VI):

$$S(IV)(+OH) \rightarrow SO_5^- \ (+O_2^-\ ) \rightarrow HSO_5^- \ \ (+HSO_3^-\ ) \rightarrow S(VI) \qquad (3\text{-}39)$$

$$S(IV)(+OH) \rightarrow SO_5^- \ \rightarrow SO_4^- \ (+Cl^-, HSO_3^- \ \rightarrow S(VI) \qquad (3\text{-}40)$$

with the first of these two pathways typically being faster that the second.

Nitrogen dioxide has a low water solubility and therefore its low resulting aqueous-phase concentrations suggests that its oxidation of S(IV)

$$2NO_2 \ + HSO_3^- \xrightarrow{H_2O} 3H^+ + 2NO_2^- + SO_4^= \qquad (3\text{-}41)$$

should be of minor importance in most cases. This reaction has been studied by Lee and Schwartz (1983) at pH 5.0, 5.8 and 6.4 and was described as a reaction that is first order in NO_2 and first order in S(IV), with a pH-dependent rate constant. The evaluation of this rate expression (3-41) was considered tentative by Lee and Schwartz (1983), in view of evidence for the formation of a long-lived intermediate species. The apparent rate constant was found to increase with pH. This reaction is considered of secondary importance at the concentrations and pH values representative of clouds. However, Pandis and Seinfeld (1989b) reported that for fogs occurring in urban polluted areas with high NO_2 concentrations this reaction could be a major pathway for the S(IV) oxidation, if the atmosphere has enough neutralizing capacity, e.g. high NH_3 (g) concentrations.

Sulfite and bisulfite can form complexes with various dissolved aldehydes. One important example is the reaction of sulfite or bisulfite with formaldehyde to produce hydroxymethanesulfonate ion (HMS) (Boyce and Hoffmann, 1984; Munger et al., 1984, 1986; Olson and Hoffman, 1989; Facchini et al., 1992).

The HMS formed acts as a S(IV) reservoir protecting it from further oxidation, and its formation has been advanced to explain high S(IV) concentrations that have been observed in clouds, fogs, and dew (Pierson and Brachaczek, 1990). The rates of S(IV) complexation and oxidation are highly dependent on cloud pH and on the concentrations of HCHO and oxidants. Characteristic times for S(IV) depletion through complexation and oxidation can be compared for typical ranges of HCHO, H_2O_2, and pH. At pH values below about 4, the rate of complex formation is several orders of magnitude slower than the reaction of S(IV) with dissolved H_2O_2. Thus, in this range oxidation predominates over complexation. The characteristic times of the two reactions become approximately comparable at pH around 5 so that complexation with HCHO becomes competitive with oxidation by H_2O_2. When pH exceeds 6, the reactions of S(IV) with HCHO became more important than reaction with H_2O_2. HMS formation can inhibit S(IV) oxidation if the S(IV) complexation rate is comparable to, or greater than, the S(IV) oxidation rate and the rate of SO_2 mass transport into the drop controls the rate of S(IV) oxidation. The effectiveness of HMS as a S(IV) reservoir depends critically on its resistivity to OH attack.

Formation of Sulfates in Clouds

The atmospheric aqueous phase (clouds, fogs) can be viewed as a processor of the aerosol size/composition distribution (Pandis et al., 1990a,b). Precipitating clouds are well known to be the major removal mechanism of aerosol particles from the atmosphere. At the same time, the liquid droplets provide the reacting medium for aqueous-phase reactions (Graedel and Weschler, 1981; Chameides and Davis, 1982; Graedel and Goldberg, 1983; Jacob and Hoffmann, 1983; Munger et al., 1983; Chameides, 1984; Seigneur and Saxena, 1984; Hoffmann and Jacob, 1984; Fuzzi et al., 1984; Hong and Carmichael, 1986a; Hill et al., 1986; Jacob, 1986; Jacob et al., 1985, 1986a,b; Johnson et al., 1987; Fuzzi et al., 1988; Dlugi, 1989; Pandis and Seinfeld, 1989a,b; Munger et al., 1990; Forkel et al., 1990; Bott, 1991; Joos and Baltensperger, 1991; Barth, 1994; De Valk, 1994). Several gaseous species dissolve in cloudwater and react giving products that remain in the aerosol phase after the cloud dissipates; for example, the dissolution of SO_2, its ionization, and subsequent oxidation to sulfate. These species can attract additional gaseous species, such as ammonia and water into the aerosol phase and thereby increase further the aerosol mass. Therefore, aerosol

processing by nonprecipitating clouds represents a mechanism by which atmospheric particles can grow during their residence time in the atmosphere. A detailed review of the state of science in 1990 has been presented by United States National Acid Precipitation Assessment Program (U.S. NAPAP) (1991).

A cyclical relationship between the occurrence of smog and fog in polluted areas has been proposed by Munger et al. (1983) and was termed the smog-fog-smog cycle. In a polluted atmosphere with high aerosol concentration, the formation of late night and early morning fogs is augmented enhancing smog production, visibility reduction, and aerosol sulfate the next day (Cass, 1979; Cass and Shair, 1984; Pandis et al., 1990a,b). Processing of aerosol by clouds can result in similar cyclical relationships and enhanced contribution of the aerosol produced in clouds to ground-level particulate concentrations (Altshuller, 1987). This processing cycle accelerates the production of atmospheric acidity through aqueous-phase reactions (Schwartz, 1989).

Cloud Effects on Particle Number Concentration

There has been a series of observations of enhanced aerosol number concentrations in the vicinity of clouds (Saxena and Hendler, 1983; Hegg et al., 1990; Radke and Hobbs, 1991; Hegg et al., 1991). Saxena and Hendler (1983) suggested that the observed high aerosol number concentrations near clouds could be due to the shattering of rapidly evaporating droplets. Hegg et al. (1991) proposed that the high actinic radiation fluxes near cloud tops could lead to high OH concentrations and nucleation of new H_2SO_4/H_2O particles. The high relative humidity areas around clouds often have total particle number concentrations about twice those in the air at the same level but well removed from the cloud boundaries (Radke and Hobbs, 1991). Kerminen and Wexler (1994a,b) have demonstrated that there is high nucleation probability associated with these high relative humidity areas, especially near relatively clean clouds. All these speculated mechanisms for production of new particles produce negligible new aerosol mass, but may influence the shape of the aerosol distribution, especially in remote regions. Aqueous-phase reactions producing sulfate and nitrate increase the aerosol mass, but do not influence directly the aerosol number concentration, unless some cloud droplets shatter into many smaller droplets. The removal

of gas-phase SO_2, H_2SO_4, and NH_3, due to their transfer to the aqueous-phase, indirectly slows down the production of new particles in the vicinity of the cloud.

Cloud Effects on Aerosol Mass Concentration

Significant production of sulfate has been detected in clouds and fogs in different environments (Lazrus et al., 1983; Hegg and Hobbs, 1987, 1988; Pandis and Seinfeld, 1989b; Husain et al., 1991; Swozdziak and Swozdziak, 1990; Pandis et al., 1992b; De Valk, 1994; Liu et al., 1993). The detection of sulfate-producing reactions is often hindered by the variability of cloud liquid water content and the temporal instability and spatial variability in concentrations of reagents and product species (Kelly et al., 1989). The production of sulfate has also been detected and investigated in laboratory clouds (Hansen et al., 1991). Aqueous-phase oxidation of HSO_3^- by H_2O_2 is particularly fast, as illustrated by the mutual exclusivity of SO_2 and H_2O_2 observed in clouds (Daum et al., 1984a,b, 1987). Other reactions, including oxidation of dissolved SO_2 by ozone and oxidation by O_2 catalyzed by Fe^{3+} and Mn^{2+}, may also contribute, significantly in some cases, to sulfate production (Pandis et al., 1990b; Barth et al., 1992; Barth, 1994). During aqueous-phase sulfate production the reactants including SO_2, H_2O_2, O_3, and OH are transferred from the gas phase to the cloud droplets. This transport includes a series of steps (gas-phase diffusion, transport across the gas-liquid interface, dissociation and aqueous-phase diffusion) that ultimately couple the gas and aqueous phases and in some cases control the overall sulfate production rate (Schwartz, 1988).

The formation of sulfate in raining and non-raining clouds has been modeled (Seigneur et al, 1984; Seigneur and Saxena, 1988; Seigneur and Wegrecki, 1990). The results have been compared to experimental measurements of cloud chemistry. Contributions to sulfate formation from gas-phase reactions and from various aqueous phase mechanisms during daytime and nighttime can be compared.

Hydrogen peroxide is the most important oxidant for the conversion of SO_2 in cloud water at pH 4.5 or lower (Calvert et al., 1985) and dominates the aqueous sulfate formation pathways (McHenry and Dennis, 1994) in the northeastern United States. The measured H_2O_2 gas-phase mixing ratio over the northeastern and central United States has been reported to vary from 0.2 to 6.7 ppb (Sakugawa et al., 1990) with the highest values during

the summer and the lowest during the winter months. The H_2O_2 concentrations usually increase with decreasing latitude and increasing altitude (Sakugawa et al., 1990). The availability of hydrogen peroxide may be the limiting factor in sulfate formation in clouds. This limitation is more pronounced near SO_2 sources and during the winter months. The seasonal contribution of clouds to sulfate levels depends on both the availability of oxidants and on the cloud cover. In cases where the sulfate cloud production is oxidant limited, changes in aerosol sulfate levels will be less than proportional to SO_2 emission changes, with the relationship being more nonlinear in winter than in spring or summer (U.S. NAPAP, 1991).

Evaluations of the rate of the SO_2-H_2O_2 reaction in cloudwater indicate that the characteristic time for this reaction is a few minutes to an hour, depending on conditions (Schwartz, 1984a; Meagher et al., 1990). Since such a reaction time is shorter than the lifetime of stratiform clouds in the troposphere it is anticipated that the reaction of SO_2 and H_2O_2 will proceed to completion in liquid water stratiform clouds. Evidence of this occurring would be that only one or the other of these species would be present in such clouds, but not both at the same time. This expectation has been borne out in field measurements supporting the inference of rapid reaction given by the model estimates. Daum and colleagues (Daum et al., 1984a; Daum, 1988) have presented results of simultaneous aircraft measurements of H_2O_2 in collected cloudwater samples and SO_2 in air (filter pack measurements) in nonprecipitating stratiform clouds indicating that in almost all instances either one or the other species was at very low concentrations, and by inference that the reaction has proceeded essentially to completion in the clouds. A rather different set of results was reported by Husain et al. (1991) who conducted measurements of gas-phase SO_2 and H_2O_2 during cloud events at Whiteface Mountain, NY. Although a general negative correlation between the two species concentrations was exhibited, the data indicated substantial periods of apparent coexistence of these species.

There is the possibility of spatial inhomogeneities in the clouds that are not resolved in the sampling period (typically 30 min in the Daum studies; an hour or more for the Husain studies), in which one region was H_2O_2 rich and another SO_2 rich. In such instances a lack of coexistence of the two species would be masked by the extended duration of sampling. Such spatial inhomogeneities might also account for the few instances reported by Daum in

which SO_2 and H_2O_2 apparently coexisted in clouds. Additionally, local patches of subsaturated air in the clouds during the sampling period might also account for these observations, although Daum took efforts to exclude such instances from their data base. Yet another possible explanation of the Husain results is that the cloud was relatively newly formed, and the material had not had time to react. An obvious improvement in this approach is to measure the species, as well as cloud liquid water content, with greater time resolution. Burkhard et al. (1994) have reported aircraft measurements of gas-phase SO_2 and H_2O_2 during in-cloud flights; traces of liquid water content are also shown. These data support a strong anticorrelation of SO_2 and H_2O_2 in clouds on various time (location) scales, with numerous instances of peaks of SO_2 coincident with valleys of H_2O_2 and vice versa.

A quantitative estimate of the amount of cloudwater sulfate that is formed by in-cloud reaction can be gained by inferring the amount of cloudwater sulfate that derives from preexisting sulfate aerosol. Husain et al. (1991) has used selenium as a tracer to allow such inferences to be drawn. By measuring the sulfate to selenium ratio in clear air aerosol that is representative of the aerosol that is the pre-cloud aerosol of the clouds under investigation, and by assuming that the fractional incorporation of the sulfate and selenium into cloudwater is identical (and/or by measuring this ratio), it is possible to infer the amount of cloudwater sulfate derived from preexisting sulfate aerosol and, by difference, the amount formed by in-cloud reaction. A series of such studies carried out at Whiteface Mountain, NY, indicates that the assumption of identical scavenging of sulfate and selenium is valid (1.04 ± 0.29; 1.04 ± 0.19 in two separate cloud systems). Evidence of enhanced sulfate in cloudwater, attributed to sulfate formed by in-cloud reaction, was found in five of six cloud systems studied; amounts formed were consistent with ambient SO_2 concentrations. Examination of the pH dependence of the concentration of in-cloud produced sulfate inferred by this technique indicated that sulfate was produced by in-cloud reaction only at pH values below 4.0, consistent with oxidation by H_2O_2, but not with oxidation by O_3.

Recently Snider and Vali (1994) reported studies of oxidation of SO_2 in winter orographic clouds in which SO_2 was released and the extent of increased concentrations of sulfate in cloudwater (relative to the unperturbed cloud) were compared to decreased concentrations of H_2O_2 (sum of gaseous plus aqueous, inferred from aqueous concentrations). Despite considerable scatter, the data fall fairly close to the one-to-one line, indicative of the

expected stoichiometry of reaction, Figure 3-11. The investigators also modeled the reaction kinetics. The rate of reaction is sensitive to the liquid water content (LWC) of the cloud during the time between the point of cloud condensation to the point of sampling. Since this profile was not known the investigators assumed a linear profile for LWC versus time. The resulting model predictions agreed closely with the extent of reaction inferred from changes in H_2O_2 and sulfate concentrations, supporting the applicability of the model.

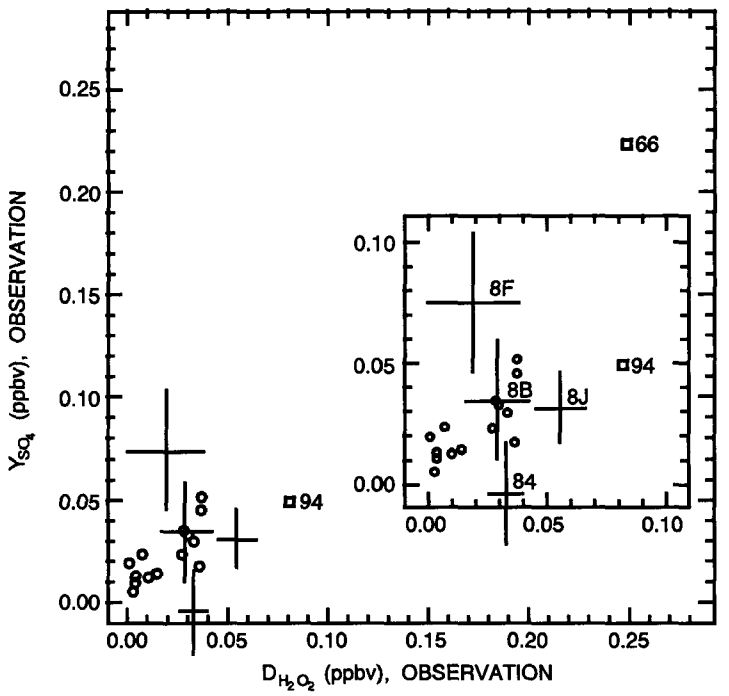

Figure 3-11. Comparison of observed hydrogen peroxide (H_2O_2) depletions ($D_{H_2O_2}$, abscissa) and observed sulfate yields (Y_{SO4}, ordinate). Errors associated with experiments 84, 8B, 8F, and 8J are indicated and data values from these experiments are labeled in the inset figure. Data values corresponding to experiments 94 and 66 are also labeled. The slope of the best fit line, forced through the origin, and calculated using only those data values indicated by circles is 1.21 ($\pm$0.13).

Source: Snider and Vali (1994).

In contrast to the H_2O_2 reaction, oxidation of SO_2 by O_3 exhibits a strong pH dependence. The reaction is quite rapid at high pH ($\sim$6) but is expected to greatly slow

down as strong acid is produced in the course of the reaction. However, if concentrations of NH_3 or other basic materials are sufficiently high to maintain a pH above 5, the reaction can continue to proceed at a high rate.

Walcek et al. (1990) calculated that, during the passage of a midlatitude storm system, over 65% of the sulfate in the troposphere over the northeastern United States was formed in cloud droplets via aqueous-phase chemical reactions. The same authors indicated that, during a 3-day springtime period, chemical reactions in clouds occupying 1 to 2% of the tropospheric volume were responsible for sulfate production comparable to the gas-phase reactions throughout the entire tropospheric volume under consideration. McHenry and Dennis (1994) estimated that annually more than 60% of the ambient sulfate in Central and Eastern United States is produced in clouds with the non-precipitating cloud production dominating over precipitating cloud production. Spatial variability of emissions and ambient H_2O_2 concentrations induces spatial variability in the contribution of in-cloud sulfate production, making it highest in the south. These conclusions are in quantitative agreement with similar calculations of Dennis et al. (1993) and Karamchandani and Venkatram (1992). Aqueous-phase oxidation in clouds is also the most important pathway for the conversion of SO_2 to sulfate on the global scale (Hegg, 1985; Langner and Rodhe, 1991).

Clouds could under some conditions also be a significant source of aerosol nitrate during the night. Choularton et al. (1992) and Colvile et al. (1994) observed production of around 0.5 $\mu g\ m^{-3}$ of nitrate during the processing of an air parcel by a hill cap cloud. They speculated that the sources of this nitrate were gaseous N_2O_5 and NO_3.

Chemical heterogeneities in the droplet population affect significantly the overall sulfate production rate and the produced sulfate size distribution (Seidl, 1989; Twohy et al., 1989; Lin and Chameides, 1991; Pandis et al., 1990a,b; Ayers and Larson, 1990; Hegg and Larson, 1990; Bower et al., 1991; Ogren and Charlson, 1992; Roelofs, 1992a,b; 1993; Carter and Borys, 1993; Bott and Carmichael, 1993; Collett et al., 1993b). Neglecting these chemical concentration differences could result in significant underestimations of the sulfate production rates in some cases (Hegg and Larson, 1990; Roelofs, 1993). Ice-related microphysical processes can also have a significant impact on cloud chemistry (Taylor, 1989; Wang and Chang, 1993; Collett et al., 1993a).

Fogs in polluted environments have the potential to increase aerosol sulfate concentrations by droplet phase reactions but at the same time to cause reductions in the aerosol concentrations of nitrate, chloride, ammonium and sodium, as well as in the total aerosol mass concentration, because of the more rapid deposition of larger fog droplets compared to smaller particles (Pandis et al., 1990a). Pandis et al. (1992b) calculated that more than half of the sulfate in a typical Los Angeles air pollution episode was produced inside a fog layer the previous night. This heterogeneously produced sulfate represented 5 to 8% of the measured PM_{10} mass.

Aqueous-Phase Oxidation of Sulfur Dioxide in Aerosols

Until recently it was thought that the low amount of liquid water associated with particles (volume fraction on the order of 1×10^{-10}, compared to clouds, for which the volume fraction is the order of 1×10^{-7}) precluded significant aqueous-phase conversion of SO_2 in such droplets. However, field studies (McMurry, et al., 1981; McMurry and Wilson, 1982, 1983) of aerosol growth as a function of size suggest the occurrence of aqueous-phase reactions. Model studies (Saxena and Seigneur, 1987) indicate that conversion of SO_2 to sulfate in aerosols at 90% relative humidity can contribute perhaps 10% to the total sulfate formation (90% due to the gas-phase reaction of SO_2 with OH). At night the conversion rate is lower, 10% of the daytime rate, and is almost all due to aqueous-phase reactions. At higher relative humidities and/or lower temperatures the aqueous-phase contribution would be expected to increase.

Sievering and colleagues (1991) have also called attention to the possibility of rapid oxidation of SO_2 by O_3 in aqueous sea-salt aerosols, which are buffered by the alkalinity of sea salt particles,. Indeed, it appears that such a rate may initially be quite rapid, 1 $\mu M\ s^{-1}$ corresponding to 8% h^{-1}, in the example given by Sievering et al. (1991) for liquid water content 50 $\mu g\ m^{-3}$ and SO_2 concentration 2 n mol m^{-3} (mixing ratio 0.05 ppb). Despite this rapid initial rate, it would appear that the extent of such oxidation may be quite limited. For the example given by Sievering et al. (1991), the sea-salt sodium concentration is given as 100 n mol m^{-3}. Based on the concentrations of (HCO_3^- + $CO_3^=$) and Na^+ in seawater (2.25 and 454 m mol kg^{-1}, respectively), the alkalinity of the sea salt aerosol is expected to be 0.5 n mol m^{-3}. Consequently, after only 0.25 n mol m^{-3} of SO_2 is taken up in solution

and oxidized (i.e., 12% of the initial SO_2), the initial alkalinity would be exhausted, and the reaction rapidly quenched.

Sievering et al. (1994) have presented field measurements over Lake Michigan of coarse-mode sulfate (diameter 5-20 μm), which they ascribe at least in part to oxidation of SO_2 in such particles derived from wind driven spray of lake water, in which the pH is maintained high by alkalinity present in the lake water. Calculations were carried out for liquid water volume fraction of 13×10^{-12} (13 μg m^{-3}). The alkalinity was inferred from the measured cation minus anion difference (cations NH_4^+ , Mg^{++}, Ca^{++}; anions $SO_4^=$, NO_3^-) in the coarse mode, which averaged 26 neq m^{-3}, corresponding to an aqueous alkalinity of 2×10^{-5} M. In the absence of mass transport limitation the rate of the aqueous-phase O_3-SO_2 reaction was calculated to be $7 \pm 3 \times 10^{-4}$ M s^{-1}; however, mass transport limitation reduced this rate by a factor of 20 to 40 at pH 7. The conversion rate referred to gas-phase SO_2 was calculated as 0.5 to 1.7% h^{-1}. The investigators concluded that this mechanism is a significant contributor to the SO_2 oxidation under these conditions. Again, however, concern may be raised with that conclusion, namely that the indicated oxidation rate, 2×10^{-5} M s^{-1} after taking mass transport limitation into account, would quickly produce an acidity equal to the initial alkalinity, thereby quenching the reaction.

3.3.2 Particulate Nitrates

3.3.2.1 Sources

By analogy to the sulfur system, sources of aerosol nitrates might be distinguished into primary, gas-phase, and aqueous-phase. However, as primary nitric acid emissions are considered to be small, the present discussion focuses on in situ production mechanisms in the atmosphere. Once nitric acid has been formed its reaction with ammonia in the gas phase may lead to the formation of particulate ammonium nitrate. Nitric acid may also react with salts of chloride or carbonate, releasing the corresponding acid, and forming a particulate salt or a solution.

3.3.2.2 Major Gas-Phase Reaction

The principal mechanism for gas-phase production of nitrates is reaction of OH with NO_2 to form HNO_3.

$$OH + NO_2 + M \rightarrow HNO_3 \tag{3-42}$$

Here, as with SO_2, the mechanism and rate of the gas-phase reaction is well established from laboratory studies (see Hicks et al., 1991), and the principal source of uncertainty in describing the reaction rate is the concentrations of the reagent species, mainly OH.

The reaction of OH with NO_2 is approximately 10 times as fast as the reaction of OH with SO_2 (Equation 3-6) (Finlayson-Pitts and Pitts, 1986). Therefore, NO_2 is preferentially converted to HNO_3 and the conversion of SO_2 to H_2SO_4 is delayed until much of the NO_2 has reacted (Gillani and Wilson, 1983).

3.3.2.3 Major Aqueous-Phase Reaction

A second key pathway for formation of nitric acid is the reaction sequence:

$$NO_2 + O_3 \rightarrow NO_3 + O_2 \tag{3-43}$$

$$NO_3 + NO_2 \rightleftarrows N_2O_5 \tag{3-44}$$

$$N_2O_5 + H_2O(l) \rightarrow 2HNO_3(aq) \tag{3-45}$$

The reaction of N_2O_5 with water vapor is thought to be slow, but reaction with condensed water, in cloud or fog droplets, or in or on the surface of wet particles, is thought to be fast (Tuazon et al., 1983). Other reactions of NO_3 and/or N_2O_5, for example N_2O_5 with aromatics (Pitts et al., 1985a,b) must also be considered. Reaction of N_2O_5 with liquid water appears to be rapid and irreversible. Studies of the uptake of N_2O_5 on aqueous sulfuric droplets give mass accommodation coefficients of about 0.1 (Mozurkewich and Calvert, 1988; Van Doren et al., 1990; Fried et al., 1994) . Thus the overall rate and yield of this reaction can be evaluated from the pertinent gas-phase rate constants and the mass transfer rate constant for uptake of N_2O_5 by aqueous aerosol or cloud droplets (Finlayson-Pitts and Pitts, 1986).

3.3.2.4 Other Reaction Mechanisms

Reactions of NO_3 other than Equation 3-39 must be considered. In daytime NO_3 may undergo photolysis.

$$NO_3 \xrightarrow{h\nu} NO + O_2 \tag{3-46}$$

However, during the night NO_3 concentration can build up sufficiently that formation of HNO_3 by hydrogen abstraction from alkanes and aldehydes may become significant (Finlayson-Pitts and Pitts, 1986).

The aqueous-phase reactions of NO and NO_2 to yield HNO_3 also need to be considered. Field measurements comparing the chemical composition of cloud droplets and rain with that of the surrounding air suggest the conversion of nitrogen oxides to nitric acid in the aqueous phase (Lazrus et al., 1983; Colvile et al., 1994). The aqueous-phase conversion of NO_2 to nitric acid,

$$2NO_2 + H_2O(l) \rightarrow 2H^+ + NO_2^- + NO_3^- \tag{3-47}$$

has been proposed. However, laboratory studies indicate that this reaction in pure water is too slow to be an important source of HNO_3 in clouds (Schwartz, 1986b). Measurements in smog chambers and indoor environments, however, suggest that a heterogeneous analog of Equation 3-43 may be occurring.

Aqueous phase reactions of NO_2 with O_2, O_3, and H_2O_2 are also though to be insignificant under representative atmospheric conditions (Schwartz, 1986b). The chemical kinetics of the aqueous-phase oxidation of NO by O_2 has been reexamined by two groups (Lewis and Deen, 1994; Pires et al.,1994). Evaluation of the rate of this reaction in cloudwater confirms that the reaction rate is negligible under atmospheric conditions, as indicated earlier by Schwartz and White (1983).

3.3.2.5 Ammonium Nitrate Vaporization Equilibria

In the sulfate system the vapor pressure of H_2SO_4 is negligible, so that all sulfate may be considered present in the particles. Also, at least for acidic sulfates (that is, not fully neutralized) the vapor pressure of NH_3 is likewise negligible. Even for fully neutral $(NH_4)_2SO_4$ any hydrolysis of NH_4^+ to form NH_3 that might escape to the vapor phase is suppressed by the resultant acidity. In contrast, nitrates in aerosols are distinguished from sulfates because of the volatility of NO_3^- (as HNO_3) and of NH_4NO_3 (as NH_3 + HNO_3). The equilibrium

$$NH_4NO_3 \text{ (s) or (aq)} \rightleftarrows NH_3(g) + HNO_3(g) \tag{3-48}$$

is such that at ambient conditions the partial pressures of NH_3 and/or HNO_3 are appreciable above crystalline NH_4NO_3 and likewise above solutions containing NH_4^+ and NO_3^- ions (of not necessarily equal concentrations). It is thus necessary to consider these equilibria not just for the crystalline material but also for solutions, in the latter case as a function of concentration or, equivalently, water activity. Such a treatment has been given in detail by Stelson and Seinfeld (1982a,b), and that study is the basis for much subsequent interpretation of field measurements.

As an example of such a study, Harrison and Msibi (1994) compare the measured concentration product of HNO_3 and NH_3 versus the equilibrium constant for the reaction. Agreement is found roughly within a factor of 2 or so based on assumption of equilibrium with pure NH_4NO_3 (crystal or solution). However, when the observations were stratified by relative humidity, no strong trend of measured concentration product with relative humidity was evidenced.

As noted above, the time scale of reaching this equilibrium is of interest, for example as it may influence dry deposition or accommodation to changing gaseous environments, as in human airways. Wexler and Seinfeld (1990) modeled the time dependence of achieving this equilibrium and concluded that equilibrium is generally reached within seconds to minutes for typical aerosol loadings. By evaluating the time scales for equilibrium of vapor-phase species with a population of aerosol particles, Wexler et al. (1992) found that ammonium salts in the gas and aerosol phases are not always in equilibrium, especially under

less polluted and cooler conditions. Thus, both transport and thermodynamic properties of the aerosol population govern the distribution of ammonium salts. At low temperatures and low aerosol loadings the time constant for achieving this equilibrium could be a day or more.

An important implication of the high vapor pressure of ammonium nitrate (as NH_3 + HNO_3) is that ammonia will distill from any ammonium nitrate if there is an acidic site present, for example acidic sulfate that is less than fully neutralized by ammonia. As a consequence ammonium nitrate aerosol cannot exist indefinitely in the presence of acidic sulfate aerosol (Gebhart et al., 1994).

A further consequence of this equilibrium is the influence it may exert on dry deposition. Sievering et al. (1994) reported steep gradients of NH_4NO_3 concentration with height above forest canopies, and inferred high rates of deposition of particulate nitrate, 2 to 9 cm s^{-1}, comparable to those of gaseous HNO_3. They attribute this to the large particle size of the nitrate, 2 to 2.5 μm mean diameter, citing calculation of Peters and Eiden (1992). An alternative explanation of the observations, which does not appear to be ruled out, is that the deposition is actually of HNO_3. The deposition of HNO_3 may perturb the equilibrium of NH_4NO_3 with NH_3 + HNO_3, leading to a decrease of NH_4NO_3 in the vicinity of the surface and giving the appearance of enhanced deposition of the particulate species.

3.3.2.6 Sulfate/Nitrate Interaction

In the eastern United States enough H_2SO_4 is usually formed to react with the available NH_3. Indeed, the sulfate is frequently acidic, the average composition in the summer being approximately NH_4HSO_4. Since appreciable concentrations of NH_3 and HNO_3 are present in equilibrium with NH_4NO_3, while the vapor pressure of NH_3 in equilibrium with $(NH_4)_2SO_4$ or NH_4HSO_4 is very low, NH_4NO_3 is not stable in the presence of NH_4HSO_4 and transformations produce $(NH_4)_2SO_4$ and HNO_3. However, if SO_2 emissions are reduced and less H_2SO_4 is formed, some NH_3 may be left over after all H_2SO_4 has been converted to $(NH_4)_2SO_4$. Particulate NH_4NO_3 will form if the concentrations of HNO_3 and excess NH_3 are sufficient to exceed the equilibrium constant of Equation 3-38, $K_p = [HNO_3][NH_3]$, which at 17°C, is 4 ppb^2 over the solid and 1 ppb^2 over the solution droplet at 85% relative humidity (Harrison and Msibi, 1994).

If the H_2SO_4 formed in the atmosphere is insufficient to react with all available NH_3, i.e. $1/2[H_2SO_4] < [NH_3]$, the concentration of sulfate plus nitrate may be controlled by the amount of NH_3 available (until the concentration of sulfate plus nitrate is less than the amount needed to react with NH_3, i.e., $1/2[H_2SO_4] + [HNO_3] < [NH_3]$. Thus, as SO_2 emissions are reduced, NH_4NO_3 may replace $(NH_4)_2SO_4$.

NH_4NO_3 would not be expected to have as long a lifetime in the atmosphere as $(NH_4)_2SO_4$. It is likely that HNO_3 will have a very high dry deposition rate. As HNO_3 is removed by dry deposition, NH_4NO_3 will evaporate to maintain the $[HNO_3][NH_3]$ concentration product. Modeling studies have not addressed this issue, perhaps because of lack of certainty in the necessary parameters: the NH_4NO_3 equilibrium constant, the NH_4NO_3 evaporation rate, the HNO_3 dry deposition rate, and the atmospheric concentrations of NH_3.

Sampling problems caused by the volatility of NH_4NO_3 are discussed in Chapter 4, Section 4.2.10.1. Reliable measurements of NH_4NO_3 require special techniques, e.g. denuders to remove gas-phase HNO_3 and nylon filters to absorb any HNO_3 vapors that evaporate from collected NH_4NO_3 (Benner et al., 1992; Koutrakis et al., 1992). Large concentrations of NH_4NO_3, observed in areas of California where NH_3 is high and SO_2 emissions are low (Hering et al., 1988; Benner et al., 1991), suggest that replacement of $(NH_4)_2SO_4$ by NH_4NO_3 as SO_2 emissions are reduced is a possibility.

3.3.2.7 Ammonium Chloride Vaporization Equilibrium

Although particulate chloride is not a major component of the atmospheric ambient aerosol, it is of interest because it is involved in some particulate formation processes. For example, sea salt contains NaCl that may react with HNO_3 to lead to $NaNO_3$ coarse particles and a release of HCl. HCl could react with NH_3 to form particulate ammonium chloride (NH_4Cl). However, the concentrations of NH_3 and HCl are typically too low and the volatility of NH_4Cl too high, to lead to NH_4Cl condensation. However, in stack plumes with high concentrations of HCl and NH_3 (NH_3 may be emitted from a stack with a selective catalytic reduction system), NH_4Cl particles could be formed. Therefore, it is important to include NH_4Cl in formulations of aerosol equilibria (see e.g., Wexler and Seinfeld, 1990, 1991; Seigneur and Wu, 1992).

3.3.3 Carbon-Containing Particulate Matter

The carbonaceous fraction of ambient particulate matter consists of both elemental (EC) and organic carbon (OC). Elemental carbon, also called black carbon or graphitic carbon, has a chemical structure similar to impure graphite and is emitted directly into the atmosphere predominantly during combustion. Organic carbon is either emitted directly by sources (primary OC) or can be formed *in situ* by condensation of low volatility products of the photooxidation of hydrocarbons (secondary OC). Soot is sometimes used to refer to the primary carbonaceous aerosol (sum of primary EC and OC) but soot has no firmly established definition. Small additional quantities of aerosol carbon may exist either as carbonates (e.g., $CaCO_3$) or CO_2 adsorbed onto particulate matter (Appel et al., 1989; Clarke and Karani, 1992).

3.3.3.1 Elemental Carbon

Elemental carbon is a strong absorber of visible radiation and is the major species responsible for light absorption by atmospheric particles (Novakov, 1984; Goldberg, 1985; Finlayson-Pitts and Pitts, 1986; Japar et al., 1986; Sloane et al., 1991; Hamilton and Mansfield, 1991). Elemental carbon found in atmospheric particles is a complex three dimensional array of carbon with small amounts of other elements such as oxygen, nitrogen, and hydrogen incorporated in its graphitic hexagonal structure (Chang et al., 1982).

Wood-burning fireplaces and diesels are major sources of EC (Mulhbaier and Williams, 1982; Dasch and Cadle, 1989; Brown et al., 1989; Dod et al., 1989; Hansen and Rosen, 1990; Burtscher, 1992). In areas where wood burning is significant, more particulate graphitic carbon is expected in winter than in summer. Tracer techniques have been developed for the calculation of the source contribution to the EC concentrations, including use of K as a woodsmoke tracer (Currie et al., 1994) and use of the carbon isotopic tracers ^{14}C and ^{12}C (Lewis et al., 1988; Klouda et al., 1988; Currie et al., 1989). Around 47% of the EC in Detroit, 93% in Los Angeles and 30 to 60% in a rural area in Pennsylvania has been attributed to motor vehicle sources (Wolff and Korsog, 1985; Pratsinis et al., 1988; Keeler et al., 1990). The corresponding contribution of diesel emissions to EC concentrations in Western Europe is estimated to be 70 to 90% (Hamilton and Mansfield, 1991). Elemental carbon was also a major constituent of the Kuwait oil fires, with

concentrations as high as 178 mg m^{-3} inside the plume (Cofer et al., 1992; Daum et al., 1993; and references therein). Global emissions of EC were estimated by Penner et al. (1993) to be 12.6 to 24 Tg C yr^{-1}, while the EC emission for the US was 0.4 to 1.1 Tg yr^{-1} and for the rest of North America 0.2 Tg yr^{-1}.

Elemental carbon also scatters light (Appel et al., 1985) although its light scattering efficiency is smaller than the efficiencies of the other aerosol principal components (Sloane et al., 1991). Because EC both absorbs and scatters light, its contribution to total light extinction exceeds its contribution to fine particle mass. For example, in Los Angeles, EC was found to represent 8.5 to 10% of the fine particulate mass, but to account for 14 to 21% of the total light extinction (Pratsinis et al., 1984). A significant fraction of the dark colored fine EC particles is able to penetrate the indoor atmosphere of buildings and may constitute a soiling hazard of objects like works of art (Ligocki et al., 1993).

The concentration of EC varies with location and season. Elemental carbon concentrations in rural and remote areas usually vary from 0.2 to 2.0 μg m^{-3} (Wolff, 1981; Clarke et al., 1984; Goldberg, 1985; Cadle and Dasch, 1988; Japar et al., 1986; Shah et al., 1986; Pinnick et al., 1993) and from 1.5 to 20 μg m^{-3} in urban areas (Wolff, 1981; Delumyea and Kalivretenos, 1987; Pratsinis et al., 1984, 1988; Grosjean, 1984a; Heintzenberg and Winkler, 1984; Goldberg, 1985; Shah et al., 1986; Rau, 1989). The concentration of EC over the remote oceans is approximately 5 to 20 ng m^{-3} (Clarke, 1989). Average EC concentration values are around 1.3 and 3.8 μg m^{-3} for U.S. rural and urban sites respectively (Shah et al., 1986). Average PM_{10} EC values exceeding 10 μg m^{-3} are common for some urban locations (Chow et al., 1994). The ratio of EC to total carbon has been observed to vary from 0.15 to 0.20 in rural areas, to 0.2 to 0.6 in urban areas (Wolff et al., 1982; Gray et al., 1984; Grosjean, 1984a; Pratsinis et al., 1984; Chow et al., 1993a). The annual mean of this ratio was approximately 0.4 for the Los Angeles basin in 1982 (Gray et al., 1986), while this ratio in the same area decreases to 0.2 during summer midday periods (Larson et al., 1989; Wolff et al., 1991). Aging of an air mass results in lowering of the EC fraction of the aerosol due to its mixing with non-combustion particles or by condensation of material from the gas phase (Burtscher et al., 1993).

The distribution of EC emitted by automobiles is unimodal with over 85% of the mass in particles smaller than 0.12 μm aerodynamic diameter (Venkataraman et al., 1994). The

ambient distribution of EC is bimodal with peaks in the 0.05 to 0.12 μm (mode I) and 0.5 to 1.0 μm (mode II) size ranges (Nunes and Pio, 1993; Venkataraman and Friedlander, 1994). The creation of mode II is mainly the result of accumulation of secondary aerosol products on primary aerosol particles.

The degree of mixing of EC particles with other aerosol components is controversial. Particles emitted from spark-ignition engines have been found to consist of a core of EC covered with a layer of PAHs and an outermost shell of volatile compounds (Steiner et al., 1992). Ambient carbonaceous aerosol in urban areas has been found to consist of aggregated spherules, with a range of carbon structures from amorphous (OC) to graphitic (EC) within aggregates (Katrinak et al., 1992). These aggregates are often (especially during summer months) coated with sulfates and nitrates (Katrinak et al., 1992, 1993). However, often sulfate and EC are externally mixed (Covert and Heintzenberg, 1984). Coating of EC with organic compounds may alter its hygroscopicity and its lifetime in the atmosphere (Andrews and Larson, 1993). Noone et al. (1992a) reported that the interstitial aerosol inside urban fogs is enriched in EC, something that would tend to increase its lifetime in the atmosphere with respect to other species like sulfate or OC (Nunes and Pio, 1993). However, the degree of incorporation of EC in droplets is highly variable (0 to 80%) and its behavior appears to vary from hygroscopic to hydrophobic (Hansen and Novakov, 1989). Our lack of understanding of the processes, where by EC changes from hydrophobic to hygroscopic, makes a quantitative estimate of the atmospheric lifetime of EC problematic.

The participation of EC and soot in atmospheric chemical reactions with SO_2, O_3 and NO_2 has been the subject of a series of studies (Baldwin, 1982; Dlugi and Güsten, 1983; Akhter et al., 1984, 1985; Jassim et al., 1986; Sergides et al., 1987; Gundel et al., 1989; Chughtai et al., 1991). The strong dependence of the often conflicting results of these studies on the nature of the samples inhibits the extrapolation of their conclusions to the atmosphere. Chughtai et al. (1991) reported that oxidation and hydrolysis of accessible reactive sites on the soot surface result in particle solubilization and accelerated particle removal from the atmosphere. DeSantis and Allegrini (1992) suggested that NO_2 reactions in the presence of SO_2 on carbon-containing particles could be a source of HNO_2 in the urban environment. The reaction of soot with ozone is faster than its reaction with NO_2, which in turn is faster than its reaction with SO_2 (Smith et al., 1989). The review by Hoffmann and

Calvert (1985) concludes that the reaction of soot with SO_2 is not a major atmospheric pathway for sulfate formation.

3.3.3.2 Organic Carbon

The organic component of ambient aerosol both in polluted and remote areas is a complex mixture of hundreds of organic compounds (Cass et al., 1982; Seinfeld, 1986; Rogge et al., 1993d; Hahn, 1980; Simoneit and Mazurek, 1982; Zafiriou et al., 1985; Graedel, 1986; Gray et al., 1986). Only 10 to 20% of the organic material has been characterized in terms of molecular structure. Compounds identified in the ambient aerosol include n-alkanes, n-alkanoic acids, n-alkanals, aliphatic dicarboxylic acids, diterpenoid acids and retene, aromatic polycarboxylic acids, polycyclic aromatic hydrocarbons, polycyclic aromatic ketones and quinones, steroids, N-containing compounds, regular steranes, pentacyclic triterpanes, iso- and anteiso-alkanes, etc. (Graedel, 1986; Mazurek et al., 1989; Hildemann et al., 1991, 1993, 1994; Rogge et al., 1993d). OC does not strongly absorb light, but its light scattering efficiency in urban hazes is similar to that of nitrate and sulfate (McMurray et al., 1995; Lowenthal et al., 1995).

Aerosol OC measurements are often subject to sampling artifacts due to adsorption of organic vapors on the filters used or evaporation of the collected mass. These sampling problems are discussed in Section 3.3.3.1. Wolff et al. (1991) found that this sampling error represented roughly 20% of the measured OC under urban polluted conditions. McMurry and Zhang (1989) observed in ambient and smog chamber measurements that a consistently large fraction of the OC (40 to 70%) was collected on the quartz filters following their impactors. The strong possibility of sampling artifacts in the laboratory and field measurements presented below, increases the uncertainty of our current knowledge about aerosol OC. Most of the investigators report the OC concentration as concentration of carbon. These values neglect the contribution to the aerosol mass of the other elements (namely oxygen, hydrogen and nitrogen) of the organic aerosol compounds. Measured OC values have been multiplied by 1.5 (Wolff et al.. 1991) or 1.4 (White and Macias, 1989) to estimate the total organic mass.

The concentration of OC is around 3.5 μg C m^{-3} in rural locations (Stevens et al., 1984) and 5 to 20 μg C m^{-3} in polluted atmospheres (Grosjean, 1984a; Wolff et al., 1991).

Wolff et al. (1991) and Chow et al. (1994) summarizing measurements during the summer and fall of 1987 in the Los Angeles basin, reported that OC represented on average 10 to 18% of the PM_{10} mass and 11 to 24% of the $PM_{2.5}$ mass during the summer and 15 to 25% of the PM_{10} and 16 to 25% of the $PM_{2.5}$ during the fall. Wolff et al. (1991) suggested that these values should be reduced by roughly 20% to correct for the sampling bias and then multiplied by 1.5 to account for the non-carbon mass of the organic aerosol compounds (an overall increase by roughly a factor of 1.3). In rural areas of the western U.S. particulate OC concentrations are comparable to sulfate (White and Macias, 1989). In other areas OC contributes roughly 10 to 15% of the $PM_{2.5}$ and PM_{10} mass (Stevens et al., 1984). Organic compounds accumulate mainly in the submicrometer aerosol size range (Finlayson-Pitts and Pitts, 1986; McMurry and Zhang, 1989) and their mass distribution is typically bimodal with the first peak around diameter of 0.2 μm and the second around 1 μm (Pickle et al., 1990; Mylonas et al., 1991).

The contribution of the primary and secondary components of aerosol OC have been difficult to quantify. The lack of a direct chemical analysis method for the identification of either of these OC components has led researchers to the employment of several indirect methods. These methods include the use of tracer compounds for either the primary or the secondary OC (Larson et al., 1989; Turpin and Huntzicker, 1991, 1995; Turpin et al., 1991), the use of models describing the emission and dispersion of primary OC (Gray, 1986; Gray et al., 1986; Larson et al., 1989; Hildemann, 1990) and the use of models describing the formation of secondary OC (Pilinis and Seinfeld, 1988; Pandis et al., 1992a; Pandis et al., 1993). The above studies concluded that the secondary OC contribution is maximized in the early afternoon of summer days, varying from 30 to 60% of the total OC depending on location. The yearly averaged contribution of secondary OC is smaller, 10 to 40%.

The interactions of the OC compounds with each other and the inorganic aerosol species are poorly understood. The compounds have the potential to form organic films around the inorganic and EC core of the aerosol (Gill et al., 1983). Goschnick et al. (1993) provided evidence for such formation by reporting that carbon compounds and organic hydrogen were enriched within the particles' outer layer, while inorganics like NH_4NO_3 were enriched inside the particles. The presence of such films can inhibit the transport of water and other inorganic components between the gas and aerosol phases (Otani and Wang, 1984;

Rubel and Gentry, 1984). However, atmospheric OC may be water-soluble and hygroscopic as well as water-insoluble (Saxena et al., 1995) and organic particles may serve as cloud-condensation-nuclei (Novakov and Penner, 1993).

Primary Organic Carbon

Primary carbonaceous particles (OC) are produced by combustion (pyrogenic), chemical (commercial products), geological (fossil fuels), and natural (biogenic) sources. The complexity of the molecular composition of OC is such that tracer compounds are still necessary to decouple the contributions of the various sources. Rogge et al. (1991) suggested that fine aerosol cholesterol could be used as a tracer for meat smoke. An alternative proposed meat smoke tracer set consists of myristic acid (n-tetradecanoic acid), palmitic acid (n-hexadecanoic acid), stearic acid (n-octadecanoic acid), oleic acid (cis-9-octadecenoic acid), nonanal and 2-decanone (Rogge et al., 1991). Benzothiazole has been used as a tracer for tire wear contributions to ambient aerosol (Kim et al., 1990; Rogge et al., 1993b). Steranes and pentacyclic triterpanes (hopanes) can be used as tracer compounds for the vehicular sources (Rogge et al., 1993a). The odd carbon number n-alkanes ranging from C_{27} to C_{33} can serve as a molecular tracer assemblage for biogenic primary OC (green, dead, and degraded plant wax material directly emitted or resuspended from soil and road dust) (Mazurek and Simoneit, 1984; Simoneit, 1989; Rogge et al., 1993c). The iso- and anteiso-alkanes can be used to trace the cigarette smoke contribution to the outdoor atmosphere (Rogge et al., 1994),

Primary biogenic organic matter consists predominantly of lipids, humic and fulvic acids, and often represents a major fraction of the carbonaceous aerosol mass (Duce et al., 1983; Gagosian et al., 1987; Mazurek et al., 1989, 1991; Simoneit, 1984, 1986, 1989). Mamane et al. (1990) reported that most coarse OC in the Great Lakes region is of biologic origin while most fine OC is anthropogenic.

Secondary Organic Carbon

Secondary organic aerosol material is formed in the atmosphere by the condensation on already existing particles of low vapor pressure products of the oxidation of organic gases.

As the hydrocarbons are oxidized in the gas-phase by species such as the hydroxyl radical (OH), ozone (O_3) and the nitrate radical (NO_3), their oxidation products accumulate in the gas phase. If the concentration of such a product is smaller than its saturation concentration, the species remains mainly in the gas phase. Small amounts of the species can be adsorbed on aerosol surfaces or dissolved in the aerosol phase at this stage (Yamasaki et al., 1982; Pankow, 1987; Ligocki and Pankow, 1989; Pankow and Bidleman, 1991; Pankow, 1994a,b; Pandis et al., 1992a). If the gas-phase concentration of a species exceeds its saturation concentration, the species condenses on the available aerosol surface so that at equilibrium its gas-phase concentration equals its saturation concentration. If this gas-phase concentration is reduced to less than the saturation value as a result of dilution, deposition or chemical reaction, the aerosol species evaporates in an effort to maintain thermodynamic equilibrium (Pilinis and Seinfeld, 1988). Many volatile organic compounds (VOC) do not form aerosol under atmospheric conditions due to the high vapor pressure of their products (Grosjean and Seinfeld, 1989). These VOC include all alkanes with up to six carbon atoms (from methane to hexane isomers), all alkenes with up to six carbon atoms (from ethylene to hexene isomers), benzene and many low-molecular-weight carbonyls, chlorinated compounds and oxygenated solvents.

Organic aerosols formed by gas-phase photochemical reactions of hydrocarbons, ozone and nitrogen oxides have been identified in both urban and rural atmospheres (Grosjean, 1977). Most of these species are di- or poly-functionally substituted alkane derivatives. These compounds include aliphatic organic nitrates (Grosjean and Friedlander, 1975), dicarboxylic acids (adipic and glutaric acids) (O'Brien et al., 1975), carboxylic acids derived from aromatic hydrocarbons (benzoic and phenylacetic acids), polysubstituted phenols and nitroaromatics from aromatic hydrocarbons (Kawamura et al., 1985; Satsumakayashi et al., 1989, 1990). Some species that have been identified in ambient aerosol and are believed to be secondary in nature are depicted in Table 3-3. Despite the above studies, the available information about the molecular composition of atmospheric secondary OC and about the composition of the OC produced during the oxidation of specific hydrocarbons remains incomplete. The reaction mechanisms leading to the observed products are to a great extent speculative at present (Finlayson-Pitts and Pitts, 1986).

TABLE 3-3. SOME SECONDARY ORGANIC COMPOUNDS IDENTIFIED IN AMBIENT PARTICLES IN URBAN AIR

Compound	n
$HOOC(CH_2)_nCOOH$	1-8
$HOOC(CH_2)_nCHO$	3-5
$HOOC(CH_2)_nCH_2OH$	3-5
$HOOC(CH_2)_nCH_2ONO$ or $CHO(CH_2)_nCH_2ONO_2$	3-5
$CHO(CH_2)_nCH_2OH$	3-5
$CHO(CH_2)_nCHO$	3-5
$HOOC(CH_2)_nCOONO$ or $CHO(CH_2)_nCOONO_2$	3-5
$CHO(CH_2)_nCOONO$	3-4
$HOOC(CH_2)_nCOONO$	3-4
$HOOC(CH_2)_nCOONO_2$	4-5
$HOOC(CH_2)_nCH_2ONO_2$	3-4
$(C_6H_5)\text{-}(CH_2)_nCOOH$	1-3
$HOOC\text{-}(C_6H_4)\text{-}(CH_2)_nCH_3$	1-2

Source: Schuetzle et al. (1975), Cronn et al. (1977).

Natural hydrocarbons like the monoterpenes ($C_{10}H_{16}$) and isoprene (C_5H_8) are emitted by various types of trees and plants. In the United States the biogenic hydrocarbon sources are estimated to produce 30 to 60 Mt of carbon per year (isoprene and monoterpenes combined) whereas anthropogenic hydrocarbon sources have been estimated to account for 27 Mt of carbon per year (Lamb et al., 1987; Zimmerman, 1979; Altshuller, 1983). Laboratory investigations have indicated that biogenic hydrocarbons are very reactive under typical atmospheric conditions (Arnts and Gay, 1979). The aerosol forming potential of biogenic hydrocarbons has been investigated in a series of smog chamber studies (Kamens et al., 1981, 1982; Hatakeyama et al., 1989; 1991; Pandis et al., 1991; Zhang et al., 1992). These studies demonstrate that isoprene photooxidation does not contribute to the production of secondary aerosol under ambient conditions. On the other hand, pinenes and other monoterpenes form secondary aerosol in their reactions with O_3 and OH and have the

potential to contribute significantly to aerosol in areas with high vegetation coverage. Monoterpenes were estimated to contribute around 15% of the secondary organic aerosol (SOA) in urban areas with low vegetation like Los Angeles, while they are expected to dominate the SOA in areas with high vegetation coverage like Atlanta (Pandis et al., 1991, 1992a).

The chemical composition of the majority of the aerosol products of the monoterpene photooxidation remains unknown or is speculative (Pandis et al., 1991; Palen et al., 1992). The few products that have been identified include nopinone, pinanediol, pinonic acid and 5-(1-hydroxy-1-methylethyl)-2-methyl-2-cyclohexen-1-one. Several investigators have studied the SOA formation from selected anthropogenic hydrocarbons. The literature data up to 1976 have been reviewed by Grosjean (1977). Other studies focused on toluene and other aromatic hydrocarbons (Leone et al., 1985; Stern et al., 1987; Gery et al., 1985, 1987; Izumi and Fukuyama, 1990), styrenes (Izumi and Fukuyama, 1990), cyclic olefins (Hatakeyama et al., 1985, 1987; Izumi et al., 1988), cresols and nitrocresols (Grosjean, 1985) and alkenes with more than six carbon atoms (Grosjean, 1984b; McMurry and Grosjean, 1985; Wang et al., 1992a,b). Measured and estimated aerosol yields from a variety of SOA precursors have been tabulated by Grosjean and Seinfeld (1989) and Pandis et al. (1992a).

The calculated contribution of the main individual secondary organic aerosol precursors to the secondary organic aerosol concentration in Los Angeles on August 28, 1987 is presented in Table 3-4 (Grosjean and Seinfeld, 1989; Pandis et al., 1992a). Toluene, the nonmethane hydrocarbon with the highest emission rate in the Los Angeles area (165 t d^{-1}) was predicted to contribute 28% of the secondary organic aerosols. Differences were attributed to sampling artifacts and calibration uncertainties during the interpretation of the ambient data.

Grosjean (1992) calculated the daily production rates of various chemical functionalities of the secondary organic aerosol formed *in situ* during a smog episode in Los Angeles using the precursor hydrocarbon emission inventory and the results of smog chamber studies. His estimates are presented in Table 3-5. These predictions were compared with the available measurements of ambient OC functional group relative abundances (Grosjean, 1992).

TABLE 3-4. PREDICTED PERCENT CONTRIBUTION TO SECONDARY ORGANIC AEROSOL CONCENTRATIONS AT LOS ANGELES

	Contribution	
Species	Grosjean and Seinfeld (1989)	Pandis et al. (1992a)
Aromatics	58	65
Biogenic Hydrocarbons	10	16
Alkanes	21	15
Olefins	11	4

TABLE 3-5. AMOUNT OF SECONDARY AEROSOL PRODUCED IN A TYPICAL LOS ANGELES SMOG EPISODE ACCORDING TO FUNCTIONAL GROUPS

	Aerosol produced (kg day^{-1})			
Precursor	Carbonyls	Aliphatic Acids	Nitrophenols	Aliphatic Nitrate
Alkenes	-	608	-	-
Cyclic olefins	62	131	-	9
Terpenes	295	623	-	41
Alkanes	243	-	-	121
Cycloalkanes	72	-	-	72
Aromatics	-	-	3118	-
TOTAL	672	1362	3118	243

Source: Grosjean (1992).

Pickle et al. (1990) and Mylonas et al. (1991) argued that the SOA mass size distribution in urban areas like Los Angeles is typically bimodal with maxima in the 0.1 and 1.0 μm size ranges. Our understanding of the mechanisms of creation of these two modes remains tentative (Pandis et al., 1993). The effect of relative humidity in the SOA partitioning between gas and aerosol phases is generally not understood. Thibodeaux et al. (1991) developed a theoretical model based on classical adsorption theory and predicted that as air relative humidity increases (remaining less than 60%) the equilibrium secondary

organic carbon content on the aerosol particles decreases due to competition for adsorption sites with water molecules. This theoretical result seems to be supported by the little available experimental information, but the necessary experimental data for the incorporation of these relative humidity effects on SOA partitioning into an aerosol model do not exist. Knowledge of the saturation concentrations of the organic condensable species remains incomplete. These concentrations are expected to vary significantly with temperature. The few available relevant measurements include the saturation vapor concentrations of monocarboxylic and dicarboxylic acids (Tao and McMurry, 1989) and the β-pinene aerosol products (Pandis et al., 1991). The saturation vapor concentrations of condensable products from the oxidation of some aromatic hydrocarbons (toluene, m-xylene, and 1,3,5-trimethylbenzene) were estimated to lie in the range 3 to 30 ppt (Seinfeld et al., 1987). McMurry and Grosjean (1985) estimated saturation vapor concentrations for condensable products from the oxidation of 1-heptene (0.14 to 1.28 ppb), o-cresol (0.06 to 1.6 ppb) and nitrocresol (1.7 to 2.2 ppb).

Polycyclic Aromatic Hydrocarbons

Polycyclic aromatic hydrocarbons (PAHs) are formed during the incomplete combustion of organic matter, for example, coal, oil, wood and gasoline fuel (National Research Council, 1983; Bjorseth and Olufsen, 1983). Stationary sources (residential heating, industrial processes, open burning, power generation) are estimated to account for roughly 80% of the annual total PAH emissions in the U.S. Mobile sources only account for 20% of the annual total PAH emissions in the U.S., however, they are the major contributors in urban areas (National Research Council, 1983; Freeman and Cattell, 1990). More than one hundred PAH compounds have been identified in urban air. The PAH observed in the atmosphere range from bicyclic species such as naphthalene, present mainly in the gas phase, to PAH containing seven or more fused rings, such as coronene, which are present exclusively in the aerosol phase (Finlayson-Pitts and Pitts, 1986). Intermediate PAH such as pyrene and anthracene are distributed in both the gas and aerosol phases (see also Section 3.3.3.4).

Measurements of the size distribution of PAH indicate that while they are found exclusively in the 0.01 to 0.5 μm diameter mode of fresh combustion emissions

(Venkataraman et al., 1994) they exhibit a bi-modal distribution in ambient urban aerosol, with an additional mode in the 0.5 to 1.0 μm diameter range (Venkataraman and Friedlander, 1994). The growth of nuclei-mode particles by condensation of secondary aerosol species like nitrate, sulfate and secondary organic aerosol has been proposed as an explanation of this distribution.

Polycyclic aromatic hydrocarbons adsorbed on the surfaces of combustion generated particles are released into an atmosphere containing gaseous co-pollutants including O_3, NO_2, SO_2, HNO_3, PAN, radicals and are exposed to sunlight. Under these conditions PAH undergo chemical transformations that might lead to significant degradation and formation of products more polar than the parent PAH (National Research Council, 1983). Several studies have focused on the reaction rates and products of reactions of PAH adsorbed on specific substrates and exposed in the dark or in the light to other pollutants. However, the extrapolation of these laboratory results to real atmospheric conditions remains difficult.

Benzo(a)pyrene (BaP) and other PAH on a variety of aerosol substrates react with gaseous NO_2 and HNO_3 to form mono- and dinitro-PAH (Finlayson-Pitts and Pitts, 1986). The presence of HNO_3 along with NO_2 is necessary for PAH nitrification. The reaction rate depends strongly on the nature of the aerosol substrate (Ramdahl et al., 1982, 1984), but the qualitative composition of the products does not. The aerosol water is also a favorable medium for heterogeneous PAH nitration reactions (Nielsen et al., 1983). Nielsen (1984) proposed a reactivity classification of PAH based on chemical and spectroscopic parameters (Table 3-6). The PAH nitration rate under typical urban conditions remains poorly understood. Bjorseth et al. (1979) observed a lack of significant PAH reactions during their transport from central to northern Europe and suggested that these reactions are slow in most environments. However, this may not be the case in heavily polluted areas with high NO_2 and HNO_3 concentrations and acidic particles (Finlayson-Pitts and Pitts, 1986). Reactions of fluoranthene and pyrene with NO_2 in the gas phase and condensation the 2-nitro-PAH derivatives on the aerosol surface have been proposed as an alternative reaction pathway for the production of the observed aerosol nitro-PAH (Pitts et al., 1985a).

Nitrogen oxide (N_2O_5) has been proposed as an additional nitrating agent for certain PAH during nighttime (Kamens et al., 1990). Pitts et al. (1985b) exposed six PAH to N_2O_5

TABLE 3-6. REACTIVITY SCALE FOR THE ELECTROPHILIC REACTIONS OF POLYCYCLIC AROMATIC HYDROCARBONS (REACTIVITY DECREASES IN THE ORDER I TO VI)

I	Benzo(a)tetracene, dibenzo(a,h)pyrene, pentacene, tetracene
II	Anthanthrene, anthracene, benzo(a)pyrene, cyclopenta(cd)pyrene, dibenzo(a,l)pyrene, dibenzo(a,i)pyrene, dibenzo(a,c)tetracene, perylene
III	Benz(a)anthracene, benzo(g)chrysene, benzo(ghi)perylene, dibenzo(a,e)pyrene, picene, pyrene
IV	Benzo(c)chrysene, benzo(c)phenanthrene, benzo(e)pyrene, chrysene, coronene, dibenzanthracene, dibenzo(e,l)pyrene
V	Acenaphthylene, benzofluoranthenes, fluranthene, indeno(1,2,3-cd)fluoranthene, indeno(1,2,3-cd)pyrene, naphtalene, phenanthrene, triphenylene
VI	Biphenyl

Source: Finlayson-Pitts and Pitts (1986).

and proposed the following reactivity order: pyrene > fluoranthene > BaP > benz(a)anthracene > perylene > chrysene. Nitro-PAH photodecompose into quinones and possibly phenolic derivatives. For example 6-NO_2-BaP on silica gel photolyses to the 1,6-, 3,6-, and 6,12- isomers of BaP quinones and a host of other oxy-PAH (Finlayson-Pitts and Pitts, 1986). These reactions are expected to depend strongly on the chemical composition and structure of the aerosol substrate and are not well understood for ambient particles.

Aerosol PAH react with O_3 to produce oxidized PAH. Pyrene, BaP and anthracenes react rapidly and the benzofluoranthenes slowly (Finlayson-Pitts and Pitts, 1986; Alebic-Juretic et al., 1990). Reaction rates of 15 to 30% hr^{-1} were observed for the most reactive PAH adsorbed on filters during exposure to 200 ppb of O_3 (Pitts et al., 1986). However, other researchers (Atkinson and Aschmann, 1987; Coutant et al., 1988; De Raat et al., 1990) have suggested that the PAH-O_3 reaction is of negligible importance for typical atmospheric conditions. Relatively little is known about the full ranges of products and the mechanisms of their formation. Polycyclic aromatic hydrocarbons exposed to sunlight have been found to photodegrade in a series of laboratory studies (Valerio et al., 1984; Behymer and Hites, 1988). The photodegradation rates depend strongly on the chemical composition

and the pH of the aerosol substrate (Dlugi and Güsten, 1983; Valerio et al., 1984; Behymer and Hites, 1988). Polycyclic aromatic hydrocarbons appear to be more stable when adsorbed on ambient aerosol than when present in pure form or in solution or on artificial surfaces (Baek et al., 1991). The occurrence of PAH-SO_x reactions remains uncertain (Baek et al., 1991).

3.3.3.3 Semi-Volatile Organic Compounds

General

Species that may exist in the atmosphere either in the gas phase or the condensed phase, and that may change back and forth between phases as a function of temperature, concentration, or other atmospheric variables, are known as semi-volatile substances. They present special sampling and measurement problems, discussed in Chapter 4, Sections 4.2.10.2 and 4.3.4.3.

Semi-volatile organic compounds (SOCs) may be defined as organic compounds whose saturation vapor pressures (p_L^o) are in the range of 10^{-2} to 10^{-9} torr, intermediate between solids and gases. Understanding the factors controlling the relative amounts of SOCs and semi-volatile inorganic materials in the gaseous (G) and aerosol particulate (P) phases is important for sampling and health reasons.

Several processes may lead to partitioning of atmospheric species between the gasphase and the condensed phase (Saxena and Hildemann, 1996). These include normal equilibrium vapor pressure, adsorption, absorption, and chemical reaction.

Equilibrium Vapor Pressure

A specific organic compound may be characterized by a temperature-dependent saturation vapor concentration that represents, under equilibrium conditions, the maximum capacity of the air for this species. If the gas-phase concentration of the compound exceeds this saturation concentration, the species can homogeneously nucleate or condense on available aerosol surfaces such that at equilibrium its gas-phase concentration equals the saturation concentration. If the gas-phase concentration of the species is less than this saturation concentration, it will not condense into the liquid phase of the pure compound. If the concentration of a species in the gas phase is reduced to less than the saturation

concentration as a result of dilution, deposition, or chemical reaction, the condensed-phase component will evaporate to maintain thermodynamic equilibrium.

Adsorption (Condensation on Solid Surfaces)

A gas-phase species can be adsorbed on available aerosol particles even if its concentration is less than its saturation concentration (Pankow, 1987). The phase distribution is estimated by a temperature-dependent equilibrium constant and the relationship is called an adsorption isotherm (Adamson, 1976; Hänel, 1976). Several investigators have applied adsorption theory to study the partitioning of relatively nonpolar compounds such as PAHs and pesticides to atmospheric aerosol and fog systems (e.g., Jung, 1977; Yamasaki et al., 1982; Pankow, 1987; Storey and Pankow, 1992; Valsaraj et al., 1993). Such an adsorption process has been found to be significant for polycyclic aromatic hydrocarbons (Ligocki and Pankow, 1989) but the extent of this process for other secondary organic aerosol species is uncertain (Pankow, 1994).

Absorption (Condensation on Existing Droplets)

If aqueous aerosol particles, cloud or fog droplets are already present (e.g., sea-salt particles in marine environments; inorganic particles containing sulfate and nitrate in continental air masses), then a water-soluble organic compound would distribute between the vapor and liquid phases according to its air-water equilibrium constant and the relative volumes of the two phases. No threshold gas-phase concentration is needed: absorption, i.e., condensation onto, or solution into, existing droplets, would take place at all partial pressures.

Similar considerations would hold for absorption on or into liquid organic particles (or components of particles). Some information is available on the partitioning of organic and inorganic gases with respect to water (Henry's Law, Table 3-2). However, the properties for other specific adsorbate and adsorbent pairs are not widely known and the process of absorption into complex mixtures is not well understood. In comparison to absorption, adsorption remains poorly understood. Absorptive phase partitioning of primary organic emissions (Turpin et al., 1991) and secondary organic species formed by reactions in the

atmosphere (Pandis et al., 1992a) has been studied. Organic gases may also dissolve into aerosol particles containing plant wax (Pankow, 1994a,b).

Chemical Reaction

If a gas-phase species reacts with another gas-phase species to form a compound with a lower saturation vapor pressure, condensed-phase material may form by nucleation or condensation. A gas may also react with an existing condensed-phase particle to add to it or to replace another species. Such processes are known for inorganic species, e.g., $NH_3(g) + HNO_3(g) \rightleftarrows NH_4NO_3(s)$. However, similar reactions are possible with organic species.

Theory

A useful parameterization of G/P partitioning is (Yamasaki et al., 1982; Pankow, 1991)

$$K_p = \frac{F / TSP}{A} \tag{3-49}$$

where: K_p ($m^3\ \mu g^{-1}$) = partitioning constant; TSP ($\mu g\ m^{-3}$) = concentration of total suspended particulate matter; and F ($ng\ m^{-3}$) and A ($ng\ m^{-3}$) = the P-associated and G concentrations of the compound of interest, respectively. The symbols F and A originate in the common usage of a filter followed by an adsorbent to collect the P and G portions, respectively. With urban particulate matter, a given SOC at a given temperature T tends to exhibit similar K_p values from sampling event to sampling event. The fraction ϕ of the total compound that is on/in the P phase is given by

$$\phi = \frac{F}{A + F} = \frac{K_p\, TSP}{K_p\, TSP + 1} \tag{3-50}$$

Though not yet used in practice, it may also prove useful to define $K_{p,10} = (F_{10} / PM10) / A$ where $PM10$ ($\mu g\ m^{-3}$) = concentration of particles with aerodynamic diameters smaller than 10 μm, and F_{10} ($ng\ m^{-3}$) = $PM10$-associated concentration of the compound of interest.

Theory (Pankow, 1994a) predicts that the values of K_p for a given compound class will be given by a relation of the form $K_p = [C_1 + C_2] / p_L^o$, where C_1/p_L^o and C_2/p_L^o represent the adsorptive and absorptive contributions to K_p, respectively. Log K_p values measured

under given conditions (*e.g.*, T) for a compound class such as the polycyclic aromatic hydrocarbons (PAHs) will thus tend to be linearly correlated with the corresponding log p_L^o values according to $\log K_p = m_r \log p_L^o + b_r$. For PAHs sorbing to urban particulate matter in Osaka, Japan, $m_r \approx -1.028$ and $b_r \approx -8.11$ (Pankow and Bidleman, 1992). (Table 3-7 gives p_L^o values for several PAHs at 20 °C.) This correlation allows K_p to be predicted for a compound that is within the compound class of interest, but was not examined in a given study. K_p for a given compound depends on T (Kelvin) according to $\log K_p = m_p/T + b_p$ where m_p depends on the enthalpy of desorption; values of the intercept b_p will be similar within a given compound class (Table 3-8). Increasing the relative humidity from 40 to 90% appears to cause K_p values to decrease by a factor of about two for PAHs sorbing to urban particulate matter (Pankow et al., 1993).

For constant K_p, then ϕ will increase as *TSP* increases. For constant *TSP* and T, as volatility increases (*i.e.*, as p_L^o increases), then K_p and ϕ will decrease. When $\phi \approx 0$, one can sample just the G phase when determining the atmospheric concentration of an SOC; when $\phi \approx 1$, one can sample just the P phase; when ϕ is between 0 and 1, one must sample both phases.

Sampling Methods and Associated Sampling Artifacts

Atmospheric SOCs have been determined using a *filter* followed by an *adsorbent*. These collect the P and G portions, respectively. Filter types include glass fiber filters (GFFs), quartz fiber filters (QFFs), and teflon membrane filters (TMFs). Adsorbent types includes polyurethane foam (PUF), Tenax, and XAD resins. Safe sampling volumes for G-phase SOCs on Tenax and PUF can be predicted based on studies of retention volumes on these adsorbents (Pankow, 1988 and 1989). *Volatilization losses from particles* (*i.e.*, "blow-off") can occur from a filter/adsorbent when T increases during sampling, when the general level of air contamination decreases during sampling, and/or when a large pressure drop develops across the filter (Zhang and McMurry, 1991). In the first case, K_p for a given compound and the already-filtered particles will decrease, leading to desorption from the sampled P-phase. In the second case, even with T constant, if A in the air being sampled decreases, then desorption losses from the collected particles can occur.

TABLE 3-7. VALUES OF LOG P_L^o FOR VARIOUS PAHS AT 20 °C

Compound	log p_L^o (torr)
Fluorene	-2.72
Phenanthrene	-3.50
Anthracene	-3.53
Fluoranthene	-4.54
Pyrene	-4.73
Benzo[a]fluorene	-5.24
Benzo[b]fluorene	-5.22
Benz[a]anthracene	-6.02
Chrysene	-6.06
Triphenylene	-6.06
Benzo[b]fluoranthene	-7.12
Benzo[k]fluoranthene	-7.13
Benzo[a]pyrene	-7.33
Benzo[e]pyrene	-7.37

Source: Pankow (1994a).

TABLE 3-8. m_p VALUES FOR PAHS SORBING TO UPM IN OSAKA, JAPAN. (Obtained by Fitting to a Common *Y*-intercept B_P of −18.48)

Compound	m_p
Phenanthrene and Anthracene	4,124
Methylphenanthrene and Methylanthracene	4,240
Fluoranthene	4,412
Pyrene	4,451
Benzo[a]fluorene and Benzo[b]fluorene	4,549
Benz[a]anthracene, Chrysene, and Triphenylene	4,836
Benzo[b]fluoranthene and Benzo[k]fluoranthene	5,180
Benzo[a]pyrene and Benzo[e]pyrene	5,301

Source: Pankow (1991).

Volatilization is of particular concern with long sampling times since large overnight T cycles and/or large changes in the level of contamination are then more likely. Material volatilized from the filter will be collected on the adsorbent following the filter. *Adsorption gains to particles* from the gas phase due to decreases in T and/or increases in A during sampling is a second possible artifact type with filter/adsorbent samplers. *Adsorption to the filter* from the G phase is a third artifact type. In this last case, a portion of the value of A for an SOC of interest sorbs directly to the filter and so incorrectly contributes to the measured value of F for the compound. It is difficult to generalize regarding the magnitudes of the first two artifact types. One can attempt to correct for the third artifact type through the use of a backup-filter (Hart and Pankow, 1994). For sampling of urban particulate matter in Portland, Oregon, Hart and Pankow (1994) estimated that failure to correct for gas adsorption to the filter caused F values for PAHs to be overestimated by a factor of ~ 1.4. Correction of the G-adsorption effect through the use of a backup filter is subject to two possible confounding effects: 1) the atmospheres to which the front and back filters are exposed may differ, making for different G-adsorption to the two filters; 2) organic compounds sorbed to a backup filter could have in part volatilized from the front filter. Table 3-9 summarizes how the three artifact types act to cause measured values of F, A, and ϕ to deviate from the true, volume-averaged values.

TABLE 3-9. EFFECTS OF THREE TYPES OF ARTIFACTS ON VOLUME-AVERAGED VALUES OF ϕ MEASURED USING A FILTER/ADSORBENT SAMPLER

	Artifact Effect	
Artifact	On A	On F and ϕ
Volatilization from collected particles	Too large	Too small
Adsorption to collected particles	Too small	Too large
Gas adsorption to filter itself	Too small	Too large

A sampler employing a *diffusion denuder* may avoid some of the artifact problems of filter/adsorbent samplers. Air drawn into a diffusion denuder can be stripped of G-phase

SOCs by a sorbent that coats the walls of the denuder: G-phase SOCs diffuse from the core of the air flow toward the walls. Sorbent coatings that have been used include silicones, gas chromatographic stationary phases (Krieger and Hites, 1992 and 1994), finely divided XAD resin (Gundel et al., 1995; Kamens et al., 1995), and carbon impregnated filter paper (Eatough et al., 1995). The majority of the P-phase SOCs do not deposit on the walls of the denuder because aerosol particles have much smaller diffusion coefficients than do gaseous molecules. The particles exiting the denuder are collected on a filter. Because the air stream flowing onto the filter has been largely stripped of G-phase SOCs, some desorption of the filtered P-phase SOCs can occur, and so an adsorbent is often placed after the filter to collect any such desorbed SOCs. F for a given compound is taken as the sum of the amounts on the filter and the subsequent adsorbent. Analysis of the denuder sorbent provides A. When the denuder sorbent cannot be analyzed (as with silicone rubber), A can be determined by difference using a second, total ($A + F$) determination for SOCs (Lane et al., 1988; Coutant et al., 1988 and 1992; and Eatough et al., 1989 and 1993). Although sampling artifacts are not often discussed for denuder-based samplers, artifacts cannot be assumed to be absent. *In the denuder section*, less than 100% efficiency for G-phase collection will tend to make measured A values too small and F and ϕ values too large; greater than 0% efficiency for P-phase collection will tend to make measured A values too large and F and ϕ values too small. Turpin et al. (1993) have presented a new denuder design which does not use a sorbent-coated wall. Rather, a laminar flow separator is used to separate a portion of the G phase from a mixed G+P flow; collection of the G-phase compounds on a sorbent like PUF allows determination of the G-phase concentrations. P-phase concentrations are determined by difference. Other sampling and analysis issues and a more detailed discussion of the diffusion denuder technique are presented in Chapter 4 of this document.

3.3.4 Metals and Other Trace Elements

The major components of fine particles are sulfate, nitrate, organic and elemental carbon, ammonium ions and a variety of trace elements (Godish, 1985; Finlayson-Pitts and Pitts, 1986). Trace elements that are found predominantly in the fine particle size range are Pb, Zn, Cd, As, Sb, Ag, In, La, Mo, I, and Sm. Elements which are found in both fine and

coarse modes are Na, K, Fe, V, Cr, Co, Ni, Mn, Cu, Se, Ba, Cl, Ga, Cs, Eu, W, and Au. Elements found primarily within large particle size range are Ca, Al, Ti, Mg, Sc, La, Lu, Hf, and Th (Klee, 1984; Bernstein and Rahn, 1979). The concentrations and the relative proportions of these species in the various particle size ranges depend on a number of factors such as the nature of the emissions, the photochemical activity and the meteorology (Finlayson-Pitts and Pitts, 1986). The concentration ranges of various elements associated with particulate matter in the atmosphere are shown in Table 3-10. For most elements the range in concentrations is greater than three orders of magnitude. This reflects the different sources and the different pollution control strategies that exist in each area. This information was compiled by Schroeder et al. (1987), and includes a large number of studies from the United States, and abroad, which indicates the need to complete site specific evaluations for high end concentrations (references can be found in the original paper by Schroeder et al., 1987).

In general, remote areas recorded measurable concentrations of some elements associated with crustal origin, as well as some elements indicative of anthropogenic sources. This supports hypotheses which suggest that long range transport occurs in these remote areas (Schroeder et al., 1987). The urban data (Table 3-10) reflect elemental concentrations in different parts of the world. Elements such as lead, iron, and copper are measured in greatest abundance in particulate matter from all locations, while elements such as cobalt, mercury and antimony are found in the smallest quantities (Schroeder et al., 1987).

Potential sources of trace metals found in fine airborne particles are primarily anthropogenic and include combustion of coal and oil, wood burning, waste incineration, and metal smelting operations. Biomass burning which includes residential wood combustion and forest fires, is another source for the release of trace elements in the atmosphere. In a profile of biomass burning, zinc was the characteristic trace element present in the fine particles in concentration ($0.0866 \pm 0.0355\%$) of primary mass emitted. Other trace elements present were Cl ($1.9083 \pm 0.6396\%$), K ($3.9926 \pm 1.2397\%$) and S ($0.5211 \pm 0.1761\%$) (Chow et al., 1992).

The chemical composition of particulate matter analyzed in New Jersey as part of the Airborne Toxic Element and Organic Substances project (ATEOS), identified the trace elements Pb, Fe, Zn, V and As (Daisey, 1987; Morandi et al., 1991). The main source for

TABLE 3-10. CONCENTRATION RANGES OF VARIOUS ELEMENTS ASSOCIATED WITH PARTICULATE MATTER IN THE ATMOSPHERE (ng/m^3)

Elements	Remote	Rural	Urban (USA)
As	0.007 - 1.9	1.0 - 28	2 - 2,320
Cd	0.003 - 1.1	0.4 - 1,000	0.2 - 7,000
Ni	0.01 - 60.0	0.6 - 78	1 - 328
Pb	0.007 - 64	2 - 1,700	30 - 96,270
V	0.001 - 14	2.7 - 97	0.4 - 1,460
Zn	0.03 - 460	11 - 403	15 - 8,328
Co	0.001 - 0.9	0.08 - 10.1	0.2 - 83
Cr	0.005 - 11.2	1.1 - 44	2.2 - 124
Cu	0.029 - 12	3 - 280	3 - 5,140
Fe	0.62 - 4,160	55 - 14,530	130 - 13,800
Hg	0.005 - 1.3	0.05 - 160	0.58 -458
Mn	0.01 - 16.7	3.7 - 99	4 - 488
Se	0.0056 - 0.19	0.01 - 3.0	0.2 - 30
Sb	0.0008 - 1.19	0.6 - 7.0	0.5 - 171

Source: Schroeder et al. (1987).

atmospheric lead concentration is the combustion of leaded gasoline in motor vehicles. However with increased use of unleaded gasoline, levels of atmospheric lead have been reduced, and other sources of lead tend now to be more significant components of the residual lead. Morandi (1985) has reported evidence of contributions to airborne lead from resuspended soil, oil burning and small scale smelting, which taken together accounted for more than half of the airborne lead at a New Jersey site. Vanadium levels were derived from oil burning for space heating and power production, while Zn is attributed to a zinc smelter in the area (Daisey, 1987).

Road dust aerosols are analyzed for trace elements in a variety of studies (Barnard et al., 1987, 1988; Warren and Birch, 1987). Recent source apportionment studies, in California's South Coast Air Basin, provide additional information on trace element

concentrations in roadside dusts as well as in motor vehicle exhaust for particle sizes $< 2.5\ \mu m$ (Watson et al., 1994b). In addition to elemental carbon, Al, Si, K, Ca, Ti and Fe were present in paved road dust in abundances which exceeded 1%. Elevated concentrations of Pb and Br were detected, which illustrated the deposition from the tailpipe exhaust from vehicles that burned leaded fuels (Watson et al., 1994b; Chow et al., 1992, 1993b). Significant amounts of $SO_4^=$, Br^-, Cl^-, and Pb were detected in the motor vehicle exhaust profile, though Pb levels were much lower than those reported in earlier tests (Watson et al., 1994d; Pierson and Brachaczek, 1983).

Ambient measurements of the mass and chemical composition of PM_{10} and $PM_{2.5}$, and associated source profiles have been taken through the years. Data base summaries identify locations, sampling times and chemical species of data available since 1988, complementing previous existing databases (Watson and Chow, 1992; Lioy et al., 1980). Size specific measurements show that over 90% of the mass from geological material is in the coarse particle size fraction, while the combustion related source categories contained ~90% of their mass concentrations in the $PM_{2.5}$ size fraction (Chow et al., 1992, 1993b). In a municipal incinerator profile, elements in the fine particle fraction include Cu, Zn, As, Cd, Sb, Pb and Ba, while trace elements in the coarse particle fraction include Ca, Cr, Mn, and Ni (Olmez et al., 1988). In an oil-fired power plant, trace elements such as V, Ni, Co, Ba and Cu are present in both fine and coarse particles (Olmez et al., 1988).

Although a knowledge of the elemental and ionic composition of ambient particles is necessary in order to understand their sources and chemistry, the chemical forms in which important species exist are not known. For example, sulfate, nitrate and ammonium ions, which are the main constituents of fine particles, may exist in forms other than simple ammonium salts (Finlayson-Pitts and Pitts, 1986). Table 3-11 lists some compounds identified in aerosols by a roadway at Argonne National Laboratory, and Table 3-12 lists compounds observed in aerosols in a forested area, at State College, Pennsylvania (Tani et al., 1983). However, there are uncertainties associated with the compounds shown in Tables 3-11 and 3-12. Tani et al. pointed out that both physical and chemical changes may occur during or following impaction of aerosol particles on a collector, which would lead to the formation of compounds not initially present in the ambient aerosols (Tani et al., 1983).

TABLE 3-11. COMPOUNDS OBSERVED IN AEROSOLS BY A ROADWAY AT ARGONNE NATIONAL LABORATORY

SiO_2	$K_2Sn(SO_4)_2$
$CaCO_3$	$(NH_4)_2Co(SO_4)_2 \cdot 6H_2O$
$CaMg(CO_3)_2$	$(NH_4)_3H(SO_4)_2$ (letovicite)
$CaSO_4.2H_2O$	$3(NH_4NO_3).(NH_4)_2SO_4$
$(NH_4)_2Pb(SO_4)_2$	$2(NH_4NO_3).(NH_4)_2SO_4$
$(NH_4)_2Ca(SO_4)_2.H_2O$	$NH_4MgCl_3.6H_2O$
$(NH_4)HSO_4$	NaCl
$(NH_4)_2SO_4$	$(NH_4)_2Ni(SO_4)_2 \cdot 6H_2O$

Source: Tani et al. (1983).

TABLE 3-12. COMPOUNDS OBSERVED IN AEROSOLS IN A FORESTED AREA, STATE COLLEGE, PA

$(NH_4)_2SO_4$
$(NH_4)_3H(SO_4)_2$ (letovicite)
NH_4HSO_4
$2(NH_4NO_3).(NH_4)_2SO_4$
$(NH_4)_2Pb(SO_4)_2$

Source: Tani et al. (1983).

Metals such as Al, Ca, Fe, Mg and Pb known to be present in atmospheric aerosols, also exist in uncertain chemical forms (Finlayson-Pitts and Pitts, 1986). This is partially due to the use of analytical techniques that normally provide information on total metal content (Schroeder et al., 1987). It is generally assumed that many of the elements, especially from combustion sources, are present in the form of oxides (Olmez et al., 1988), while trace elements in incinerator emissions may be in the form of chlorides (Schroeder et al., 1987). Data from Los Angeles indicate that arsenic may be present in two chemical forms in atmospheric aerosols, as arsenite and arsenate. Both forms were identified in both the fine and coarse particle fractions (Rabano et al., 1989). Fe_2O_3, Fe_3O_4, Al_2O_3, and $AlPO_4$ have been identified in roadside particulate matter (Biggins and Harrison, 1980). Ca and Mg may exist in the form of oxides (i.e., CaO, MgO), although in the presence of water, Stelson and Seinfeld (1981) suggest that, on equilibrium considerations, CaO and MgO should react to

form their hydroxides, $Ca(OH)_2$ and $Mg(OH)_2$, respectively. Similarly the oxides Na_2O and K_2O should form NaOH and KOH when water is present. Lead has been observed in roadside particulate matter in a wide variety of forms, such as $PbSO_4$, Pb_3O_4, $PbSO_4.(NH_4)_2SO_4$, $PbO.PbSO_4$, $2PbCO_3.Pb(OH)_2$, $2PbBrCl.NH_4Cl$, PbBrCl, $(PbO)_2PbBrCl$, $3Pb_3(PO_4)_2.PbBrCl$, and elemental lead (Biggins and Harrison, 1980; Post and Buseck, 1985). Cr is present in the atmosphere in both the hexavalent and the trivalent forms. However, in the atmosphere the hexavalent form tends to be reduced to the less toxic trivalent form (Seigneur and Constantinou, 1995). Information is also available on the atmospheric compounds of Ni (Schmidt and Andren, 1980) and Se (Ross, 1984).

Heterogeneous oxidation of sulphur dioxide in air can be catalyzed by species such as iron, manganese (Barrie and Georgii, 1976) and cadmium, while vanadium is suspected to catalyze the formation of sulfuric acid during oil combustion. Oxides of iron, manganese and lead are reported to absorb SO_2 (Schroeder et al., 1987).

It has been suggested that the elements arsenic, cadmium, manganese, nickel, lead, antimony, selenium, vanadium and zinc volatilize at high temperatures during fossil fuel combustion and condense uniformly on surfaces of entrained fly ash particles as the temperature falls beyond the combustion zone (Linton et al., 1976). Accumulation of trace metals in the fine fraction of airborne dust sampled in iron foundries showed Pb and Zn localized on the surface of the fine particles (Michaud et al., 1993). From the viewpoint of toxicity, such emissions are more important than natural sources where trace elements are usually bound within the matrix of natural aerosols and thus less mobile and bioavailable (Schroeder et al., 1987).

Trace metal compounds found in road dust can accumulate from anthropogenic or natural sources. Subsequently these can become re-entrained in the atmosphere. In such samples lead and zinc were found to be strongly associated with carbonate and iron-manganese oxide phases, with small amounts being associated with an organic phase. Half of cadmium was associated with carbonate and iron-manganese oxide phases, while copper was mainly associated with the organic phase. These associations influence the relative mobility and bioavailability of trace metals in the environment (Harrison et al., 1981).

Resuspension of particles from contaminated surfaces may also contribute to an increase in the toxic trace elements in airborne particles (Kitsa et al., 1992; Kitsa and Lioy,

1992; Pastuszka and Kwapulinski, 1988; Falerios et al., 1992). Kitsa et al. (1992) measured elemental concentrations in particles resuspended from a waste site in New Jersey. Close to the resuspension source, coarse particles were dominant, but farther downwind from the site, fine particles were prevailing. The fine particles were enriched in chromium and lead, indicating the potential for elevated human exposure through inhalation. Chromium may exist in different valence states, but the most stable and abundant are the trivalent and hexavalent states. Hexavalent chromium is classified as a known respiratory carcinogen in humans.

Oxidation of the species present in aerosols results from interaction with various atmospheric oxidants, such as molecular oxygen, ozone or hydrogen peroxide. The presence of oxides of As, Cd, Co, Cr, Cu, Hg, Mn, Ni, Pb, Sb, Se, V and Zn has been measured in emissions of cement plants, blast furnace and sintering operations, secondary iron foundries, non-ferrous smelting of arsenic-bearing ores, zinc and lead smelters and many other sources (Schroeder et al., 1987).

Sulphation, and possibly nitration, of metallic oxides can be surmised to be an important transformation as particles age. A statistical assessment of multielemental measurements in a study in the rural and urban atmospheres of Arizona showed strong correlations of lead, copper, cadmium and zinc with sulfates in the rural atmosphere and moderate correlation of lead and copper with sulfates and nitrates in urban atmosphere (Moyers et al., 1977). Nickel has also great affinity for sulfur which may lead to the emission of nickel sulfate containing particles from combustion sources. In the absence of sulfur, nickel oxides or complex metal oxides containing nickel may form (U.S. Environmental Protection Agency, 1986a).

Lead was formerly emitted in the air from automobiles as lead halides and as double salts with ammonium halides (e.g. $PbBrCl.2NH_4Cl$). From mines and smelters, the dominant species are $PbSO_4$, $PbO.PbSO_4$, and PbS. In the atmosphere lead is present as sulfate with minor amounts of halides. Lead sulfide is the main constituent of samples associated with ore handling and fugitive dust from open mounds of ore concentrate. The major constituents from sintering and blast furnace operations appeared to be $PbSO_4$ and $PbO.PbSO_4$ respectively (U.S. Environmental Protection Agency, 1986b).

3.4 FIELD STUDIES OF TRANSPORT AND TRANSFORMATIONS

Appropriate and reliable field measurements play a central role in shaping our understanding of atmospheric processes, in providing key model inputs, and in the evaluation of models. Real-world observations are all the more important in the case of atmospheric aerosols, which, on the one hand, are the end product of many complex processes and, on the other hand, are key precursors of important microphysical cloud processes. Field studies include short-term, three dimensional, high-resolution intensive research campaigns, as well as longer-term surface and upper-air monitoring programs (in routine mode, or in more comprehensive and higher-resolution research mode). Research studies are generally mechanistic (targeted at understanding of process rates and mechanisms), and/or diagnostic (aimed at development and testing of individual process modules or subgrid-scale parameterizations for use in complex models). Routine monitoring studies are aimed more at operational evaluation of overall model performance, or at generation of model input data including those (e.g., meteorological) which, through dynamic assimilation into the computations, can improve the realism of the simulations. Since atmospheric fine particles are substantially of secondary origin, measurements of their gaseous precursors and other reactants are also important. In North America, most of the anthropogenic emissions of fine particles and their precursors are from large point sources (power plants and smelters) and from urban-industrial complexes including vehicle emissions. Consequently, special attention is given in this section to measurements in the plumes of such emissions.

In the 1970s, many field studies were plume studies or urban-scale studies, and most models were Lagrangian and limited to linearized treatment of chemistry and other non-linear processes. Some of these field studies, along with regional visibility information and back-trajectories from local pollution episodes, pointed to the existence of long range transport and to the regional nature of air pollution and haze (Hall et al., 1973; Gillani and Husar, 1976; Wolff et al., 1977). In response, some of the major field studies in the 1980s had a regional scope with focus on acidic depositions, oxidants, or aerosols and visibility. That decade also saw major strides in measurement technology and in the development of increasingly sophisticated Eulerian air quality models with explicit treatment of non-linear processes. In these models, however, the treatment of plumes, particularly point-source plumes, was grossly distorted by varying degrees depending on the spatial resolution of the grid. New

interest also began to emerge in global climate change, global data, and global modeling. In the decade of the 1990s, the principal interests in modeling and measurements appear to be in two areas: global-scale issues, with particular focus on clouds and aerosols; and, regional and sub-regional issues, with special interests in comprehensive linked study of oxidants, aerosols and acidic depositions, and in multi-scale interactions (e.g., nested gridding and the treatment of subgrid-scale processes related to plumes, clouds, and air-surface interactions).

Topics related to field measurements are also covered in other parts of this document: methodologies for sampling and analysis of PM and acidic deposition in Chapter 4; ambient air measurements of PM concentrations and properties in Chapter 6; and field studies of visibility and PM in Chapter 8. The focus in this section is on North American field studies of the past 15 years or so, particularly as they relate to the following objectives: better understanding of atmospheric transport and transformation processes which *modify* the concentration, size and composition of PM; evaluation of source- or receptor- oriented models of PM air quality; and generation of model inputs.

3.4.1 Field Studies of Transport Processes

Except for the gravitational settling of coarse particles (included in dry deposition), the transport of PM is similar to that of gases. Following their emissions, gases and fine aerosols rise due to buoyancy effects, are advected downwind by the prevailing mean flow field, and are dispersed horizontally and vertically by ambient turbulence, wind-shear effects, and cloud processes. These dispersive mechanisms result from the interaction of large air masses, or from the disturbance of the larger-scale flow in a given air mass by insolation-driven surface fluxes of heat and moisture, and by surface drag effects. The influence of these surface effects is largely confined to the atmospheric boundary layer (ABL), the height of which varies diurnally and seasonally, peaking typically at between 1 and 3 km on summer afternoons over the continental U.S.A. Pollutant emissions may be within the ABL or above it (depending on emission height, momentum, and buoyancy), and their dispersion is markedly different in the two cases, being much more rapid and vigorous in the daytime convective boundary layer (CBL) than in the stable layers aloft or in the stable nocturnal boundary layer. Quantitative study of these transport and dispersion processes requires,

ideally, simultaneous measurements of a large number of variables related to insolation and clouds, surface characteristics and surface fluxes of heat and moisture, and dynamic 3-D fields of flow, temperature, humidity and concentrations of trace pollutants in the ambient atmosphere. Transport and dispersion processes also have a critical influence on plume chemistry and dry deposition, which are often diffusion-limited. Meteorological measurements must therefore be an integral part of any plume study, even when the focus is on chemistry or deposition. The shift to Eulerian grid modeling in the 1980s did not, in general, include adequate measures, particularly at the regional scale, to preserve the essence of the sub-grid-scale features of plumes, which were instantaneously dispersed over the entire emission grid cell (a volume of $\approx 10^{12}$ m^3 in RADM with 80 km horizontal resolution), thereby also grossly distorting plume chemistry, aerosol formation, and pollutant budgets. There is growing awareness now of the need for more realistic treatment of plumes in grid models. Two other sub-grid-scale issues which are receiving increasing attention pertain to pollutant redistribution by clouds (e.g., Hong and Carmichael, 1986b) and surface fluxes of heat and momentum related to inhomogeneous land use within a grid cell (e.g., Avissar and Pielke, 1989).

A large body of literature exists on studies (including field studies) of ABL structure and dynamics, and on the characteristics of the wind, temperature and moisture fields in the ABL and, to a lesser extent, in the free troposphere aloft. Those studies are outside the present scope. Some of the recent major advances in the knowledge about the ABL are reviewed by Briggs and Binkowski (1985). This discussion is limited to field studies of the transport and dispersion of PM and their precursors (e.g., SO_x and NO_x). Prior to 1975, most such field studies were limited to the behavior of point-source plumes in the γ-mesoscale range ($\lesssim$20 km), i.e., on plume rise and short-range dispersion. Such behavior is well understood qualitatively; quantitatively, it is well enough represented in models at the time scales characteristic of most commonly-used plume dispersion models ($\approx$1 h), but not at the much shorter time scales of relevance to plume chemistry and plume visibility. In this near-source range, instantaneous plume behavior is very different from the larger scale average behavior. In an intercomparison of four plume visibility models, it was concluded that much of the variation in visibility observed in the Navajo power plant plume in northern Arizona was probably due to fluctuations in source emissions and plume dispersion at scales

below those resolvable by the models (White et al., 1985). Since the atmospheric residence of fine PM in the lower troposphere is on the order of days, our interest here is more on the transport and dispersion of plumes over the β- and α- mesoscale ranges ($\approx$20 to 200 and 200 to 2,000 km). Quantitative determination of transport over the mesoscale requires special field studies with controlled tracer releases. Such studies are relatively recent and very few, and they represent only a few isolated meteorological scenarios.

3.4.1.1 Field Measurements Related to Transport Modeling

Routine meteorological field measurements include surface weather observations of a broad variety of meteorological variables made every three hours at several thousand sites across the country by the National Weather Service, as well as upper-air soundings (radiosondes) of wind, temperature and relative humidity twice a day (noon and midnight) at a much more limited number of sites which, on average, are about 400 km apart. These data constitute the principal raw meteorological information used in regional transport models, which are either Lagrangian trajectory models or dynamic three dimensional (3D) Eulerian grid models. Most trajectory models are two-dimensional, with atmospheric flow patterns being analyzed on isobaric or terrain-following surfaces, or in bulk transport layers confined to the mixed boundary layer. These simplifying assumptions concerning vertical motions lead to large transport errors on the regional scale (Kuo et al., 1985). The vertical velocity can be calculated at grid points in a regional model domain from the continuity equation, but the temporal and spatial resolutions of the radiosonde data are so coarse in most areas that the result would be a gross approximation only. 3D flows may be best simulated by moist adiabatic trajectories, but since analysis methods cannot always resolve the stratified nature of the required moisture fields, the most reasonable practical simulations of 3D transport are probably dry adiabatic (isentropic) trajectories. Danielsen (1961) presented a case study showing a separation of $\approx$1,300 km after only 12 h of transport as simulated by isobaric and isentropic trajectories. It was probably an extreme case. The gridded wind field in regional Eulerian air quality models is typically generated by the application of dynamic 3D mesoscale meteorological models such as PSU/NCAR-MM5 (Grell et al., 1994) and CSU-RAMS (Pielke et al., 1992), which incorporate the routine NWS observations through a dynamic Four Dimensional Data Assimilation (FDDA)

technique. The NWS surface weather database also includes a measure of prevailing visibility as determined by human observers. A number of field studies have established the reliability of such subjective visibility observations (e.g., Horvath and Noll, 1969; Hoffmann and Kuehnemann, 1979). They have proved to be a very useful indicator of regional haze and its long-range transport (Gillani and Husar, 1976), and have been used to study the long-term trends of the spatial-temporal variability of regional haze and air quality in the eastern U.S. over many decades (Husar et al., 1981; Sloane, 1982).

Special field studies of transport and dispersion are based on observations of the transport of pressurized (constant density) balloons (called tetroons if their shape is tetrahedral), and of the evolution of plumes resulting from pollutant emissions or controlled releases of artificial tracers. Balloons have been used in mesoscale studies in three ways: as isolated Lagrangian markers of pollutant emissions (e.g., Clarke et al., 1983); in sequential releases to provide one-particle diffusion estimates (e.g., Thomas and Vogt, 1990); and in cluster releases to study relative diffusion (e.g., Er-El and Peskin, 1981). Tetroons generally carry a transponder which permits continuous tracking with a radar, thus providing the complete detailed 3D trajectory. The range of the tetroon experiment is normally limited by the tracking range of the radar (<100 km). This range can be extended to the full range of tetroon transport by including a tag which the finder can return with information, at least, about the terminal location. In some studies (e.g., Clarke et al., 1983), tetroons have been tracked continuously over much longer ranges by sequential tracking from the network of FAA radars used in support of aviation. Studies based on tracers and air pollutants also provide information about plume dispersion. Most early tracer studies were limited to a range of about 100 km due to the nature of the tracers then available and limitations of technology. Development of new tracers (e.g., the PFTs or perfluorocarbon tracers) and new sampling and analysis techniques have not only extended the range in more recent experiments by more than an order of magnitude, but the new data are also more reliable.

Pack et al. (1978) presented a detailed review of many early studies in which observations of the transport of pollutant plumes, tracers, or balloons were compared with results of diagnostic trajectory calculations. The models commonly used then were based on the kinematic approach (using objectively-analyzed wind fields based on measured winds) and a single transport layer. The observed winds were used as input in different ways: for

example, surface winds or adjusted surface winds representing average winds in the whole transport layer; or, upper air winds averaged over the transport layer. The adjustment of surface winds included enhancement of the speed by as much as a factor of two, and a veer of the wind direction by as much as 40°, to account for the real-world wind speed shear and directional veer with height. The advantage of using surface winds was due to their much higher spatial and temporal resolution, compared to the much coarser resolution of the upper-air radiosonde winds. The early results of comparisons of calculated and observed trajectories evidenced a broad range of discrepancy (10 to 54% of the trajectory length after only 100 km, and 55 to 60% after 650 km), and also the presence of large systematic errors, not always in the same direction, depending on the presence of complex flows due to fronts, complex terrain, etc. The best simulations were often obtained by the use of adjusted surface winds, and such adjustments varied between studies. The errors were found to be lowest for transport in the daytime CBL, and substantially larger for transport in stably-stratified layers.

Moran (1992) has tabulated (his Table 2-4) basic information about a number of formal β- and α- mesoscale tracer experiments since 1973, in which the release was at surface level and the measured transport range was at least 25 km (and up to 3,000 km). Table 3-13 summarizes, in chronological order, some of the major field studies of the past 20 years with measurements and modeling of transport extending into the α-mesoscale. It includes the major tracer studies as well as air quality and tetroon studies. The transport models in these studies were driven either by routine meteorological observations or by additional measurements made as part of the field studies. The following important observations are based on the studies listed in Table 3-13:

- The routine data of the radiosonde network (with resolution of $\approx$400 km, 12 h) are too coarse both spatially (Kahl and Samson, 1986, 1988) and temporally (Rolph and Draxler, 1990; Kuo et al., 1985) for accurate simulation of long range transport.

- The error in calculated trajectories is greatest under conditions of high speeds which generally accompany complex mesoscale systems (Rolph and Draxler, 1990).

- Initial errors in trajectory simulations (both in direction and vertical spread) play a critical role in overall model uncertainty (Draxler et al., 1991).

- Single-layer Lagrangian trajectory models do not spread the "plume" adequately, while Eulerian models spread it too much. Multi-layer Lagrangian models perform the best in terms of dispersion of point-source emissions (Clark and Cohn, 1990).

TABLE 3-13. RECENT FIELD STUDIES OF α-MESOSCALE TRANSPORT AND TRAJECTORY MODEL

Study	Period	Tracer(s)	Release Sites(s)	Tracking/Sampling	Maximum Range (Airshed)	Model Comparison(s)	Ref(s)	Comments
INEL Study Idaho Nat'l Eng. Lab	Feb-May 74	Kr-85	INEL (Idaho) fuel reprocessing plant (76 m stack)	Samplers at 11 Midwestern NWS sites; 10-h day and night samples.	~1,500 km	NOAA-ARL trajectory model with 300 m vertical resolution	Draxler (1982)	Small signal above b/g; 300 m layered approach to permit spread by wind dir'l shear necessary.
MISTT Midwest Interstate Sulfur Transport and Transformation Study	Summer 75 Summer 76	Plume sulfur	Labadie Power Plant near St. Louis, MO	In-situ aircraft measurements.	~300 km	Simple particle trajectory model	Gillani et al. (1978) Gillani (1986)	Quasi-Lagrangian pibal measurements of winds along plume transport.
VISTTA Visibility Impairment due to Sulfur Transport and Transformation in the Atmosphere	Jun, Jul, Dec-79	Anthropogenic aerosol, ozone	Los Angeles Basin	Detailed air quality and aerosol measurements at a Grand Canyon site.	~750 km	CAPITA Monte Carlo particle transport model	Macias et al. (1981)	Evidence also of long-range impact of Copper smelter plumes.
TPS Tennessee Plume Study	Aug-78	Tetroons (1 cu. m) with transponder	TVA Cumberland Steam Plant, TN	Radar to ~75 km; terminal point based on return tag.	~1,000 km (KY,IN,OH,ONT)	• NOAA-ATAD • NCAR isentropic • CAPITA Monte Carlo model	Clarke et al. (1983)	Part of a large plume transport/ chemistry study, including aircraft measts.
	15-Aug-78	"	"	"	~300 km (KY)	3D reg'l dyn. model	Warner (1981)	
NEROS Northeast Regional Oxidant Study	Summer 79 Summer 80	Tetroons (6 cu. m) Tetroons (1 and 6 cu. m)	MD, OH, PA, TN Columbus, OH	Continued FAA radars Radar and return tag.	~500 km to NE ~1,500 km to NE	NOAA, NCAR, CAPITA, as above	Clarke et al. (1983)	Part of a large urban and reg'l oxidant study.
Mt. Isa Smelters Plume Study	Jul-79	Excess plume S and Aitken Nuclei Count (ANC)	Mt. Isa, Australia (Sulphide smelters, ~0.6 km apart)	Aircraft measts. of Total S, ANC, COSPEC-SO2.	~1,000 km (Semi-arid region in N. Australia)	Simple layered wind trajectory model;	Carras and Williams (1981)	Exceptionally clean plume b/g.
Great Plains Mesoscale Tracer Expt.	Jul-80	Two PFTs (PMCH and PDCH) and two heavy methanes (ME-20, ME-21)	Norman, OK (1 m AGL)	Surface samplers: 17 on arc at 100 km 38 on arc at 600 km and aircraft sampling.	600 km to N NE	Different 3D regional models	Ferber et al. (1981) Moran (1992)	Important role of wind shear effects of nocturnal jet.
CAPTEX Cross-Appalachian Tracer Expt.	Sep/Oct 83	PFT (PMCH)	Dayton, OH Sudbury, ONT	Surface array of >80 samplers at arcs from 300-1,100 km and aircraft sampling.	~1,100 km (NE U.S.)	Different 3D regional models; also MESOPUFF II	Ferber et al. (1986) Moran (1992) Godowitch (1989)	Terrain-effects found important. Enhanced upper air met measts.
ANATEX Across North America Tracer Expt.	Jan-Mar 87	3 PFTs (PMCP, PMCH, PDCH)	Glasgow, MT St. Cloud, MN	Surface network (77); Towers (5); and aircraft sampling.	~3,000 km (Eastern U.S.)	3 single-layer LAGR, 6 multi-layer LAGR, 2 multi-layer Eulerian	Draxler et al. (1991) Rolph and Draxler (1990) Clark and Cohn (1990)	Enhanced upper air met measts.
MISERS GOLD	1-Jun-89	Indium oxide (vapor deposits on particles)	White Sands Missile Range, NM	In-situ aircraft: filter samples analyzed for tracer and particles.	~1,400 km NM to MO	Gifford's random-force diffusion theory	Kahl et al. (1991) Mason and Gifford (1992)	Dust plume from a military test explosion.

- Vertical information about tracer trajectories, based on continuously-tracked tetroons and aircraft measurements, contains much useful information not captured by surface sampling alone (Clarke et al., 1983). There is, for example, evidence of cloud venting of ABL pollutants into the free troposphere, where their residence time is longer and the flow field may be quite different.

- Terrain-induced effects played an important role in CAPTEX, and effects related to the nocturnal jet were important in the Great Plains Experiment (Moran, 1992). Nocturnal wind directional shear plays a major role in effectively dispersing plumes which have been dispersed vertically during the preceding daytime CBL.

- Directional wind shear plays an important role in plume dispersion even in the CBL during β-mesoscale transport (Gillani, 1986).

The issue of substantial overdispersion by Eulerian models is important because the state-of-the-art as well as the future direction in mesoscale modeling (meteorological/air quality/aerosol) appear to favor the Eulerian approach. A significant source of the problem must be related to the gross initial overdispersion of plumes in regional Eulerian models, particularly of elevated point-source plumes (carriers of most of the U.S. anthropogenic emissions of sulfur). The instantaneous false dilution of fresh emissions of NO_x into the NO_x-limited surrounding environment (e.g., in the eastern U.S.) greatly distorts plume chemistry and aerosol formation. Proper sub-grid-scale treatment of plumes remains an important outstanding issue in regional modeling. Other sub-grid-scale effects in need of more attention pertain to complex mesoscale flows (e.g., storms, fronts, cloud venting, complex terrain effects, etc.). They too are an important source of model errors. A few special field studies have been carried out to investigate such flows: for example, VENTEX (Ching and Alkezweeny, 1986) and PRESTORM (Dickerson et al., 1987) for cloud venting, and ASCOT (Allwine, 1993) and the NGS Visibility Study (Richards et al., 1991) for flows over complex terrain. Thermal effects and drainage flows also evidently play an important role in influencing particulate air quality, as in the occurrence of the Denver "brown cloud" phenomenon (Sloane and Groblicki, 1981).

There is considerable field evidence also for synoptic scale transport ($\lesssim$2,000 km) of airborne particles (see, for example, Gordon, 1991). The impact of such transport is important on the global scale. That subject is beyond the present scope.

3.4.1.2 Field Measurements Related to Dispersion Modeling

Gaussian semi-empirical models have been the basis of most applied diffusion modeling since their development around 1960. These models were based on Taylor's diffusion theory of stationary homogeneous turbulence (Taylor, 1922), and were built on a few field experiments that were quite limited in scope and technology. The results have been extrapolated far beyond the intended range of downwind distance and ambient conditions. Some of the extrapolations were guided by statistical theory, but most were freehand extrapolations (Briggs and Binkowski, 1985). Many research-grade field studies of atmospheric dispersion have since been performed, but most have been limited to the γ-mesoscale range. These have been reviewed by Draxler (1984), Irwin (1983), Briggs and Binkowski (1985) and others. β- and α-mesoscale studies, based on observations of the dispersion of pollutant and tracer plumes have been reviewed by Moran (1992).

Pollutant plumes remain vertically narrow in stable flows (e.g., elevated power plant plumes released at night), but rapidly fill up the CBL after fumigation in the daytime (see, for example, Gillani et al., 1984). Information about spreads of plumes in the elevated stable layers is particularly limited. The most common basis for estimation of such spreads (expressed as σ_y and σ_z, the RMS variances of lateral and vertical plume spreads) over distances under 100 km or so is the well-known Pasquill-Gifford (P-G) curves for different stability classes (Gifford, 1961), which make use of the routine meteorological measurements to determine applicable stability class. The P-G curves were developed mostly from data collected within the mixing layer. Another set of parameterizations of elevated plume spreads was developed by TVA (Carpenter et al., 1971) based on twenty years of experience in plume observations and aerial monitoring. These require the temperature profile to establish atmospheric stability. More recently, Smith (1981) analyzed aircraft measurements in elevated power plant plumes in different parts of the U.S., mostly in stable layers with small directional wind shear effects, and determined that the P-G curves overestimated plume spread in stable layers quite substantially both vertically and horizontally. Bergstrom et al. (1981) analyzed a smaller set of data in stable layers in which there was significant directional shearing of the plume, and found the P-G curves to underestimate horizontal plume spread. The TVA approach tended to underestimate the horizontal spread, but possibly overestimate the vertical spread. Evidently, there continues to be uncertainty about

plume spreads even at distances under 100 km. Of particular interest is horizontal plume dispersion, both because it is generally far greater over the mesoscale, and because it is highly variable. Close to the source, plume spread is largely by progressively larger turbulent eddies, but after the plume dimension substantially exceeds the scale of these eddies (typically less than 1 km), dispersion is increasingly by directional wind shear with height (Carras and Williams, 1981; Pasquill and Smith, 1983; McNider et al., 1988), and possibly also by other mechanisms involving the diurnal cycle of PBL stability changes and inertial oscillations (Pasquill, 1974; McNider et al., 1988). Directional wind shear is relatively small for the vertically thin nocturnal plume, moderate for the plume in the CBL, but maximum for the daytime plume which, after maximum vertical spread in the CBL, enters the nocturnal regime which is often characterized by strong directional shear effects (Gillani et al., 1984). Such a nocturnally sheared and stratified plume subsequently becomes vertically well-mixed following fumigation into the next day's mixing layer. The average crosswind spread rates of plumes from a large tall stack power plant emitted within the CBL on summer days in the Midwest were observed to be in the range 0.25 to 1.0 km per km of downwind transport until the plume attained a width of about 30 km (Gillani and Pleim, 1995). Direct observations of the three-dimensional nocturnal shearing of well-mixed daytime plumes are extremely sparse.

A common approach in Lagrangian studies of dispersion over long distances has been to use semi-empirical "mesoscale" dispersion coefficients by analogy with parameterizations of microscale turbulent spread. An important consequence of Taylor's statistical theory was that, in stationary homogeneous turbulence, σ_y grew linearly with time at first for $t \approx T_L$ (the Lagrangian time scale, ≈ 1 to 2 min in the CBL), and then asymptotically as $t^{1/2}$ within a few kilometers. Observations of a few α-mesoscale field studies have been interpreted to suggest that the regime of linear time dependence may apply also at long distances (see, for example, Pack et al., 1978), with the characteristic time scale (T_L) here being related to the diurnal and/or inertial scale (≈ 24 h). Others have proposed parameterizations of mesoscale σ_y which use powers of t ranging from 0.85 to 1.5 (see, for example, Carras and Williams, 1988). Thus, there is no consensus about simplistic modeling of mesoscale diffusion over scales exceeding 24 h. Given the wide range of conditions that plumes can experience during long range transport in different air masses, over a variety of terrain types, and over

multiple diurnal cycles during different seasons, such a controversy is not surprising. For transport in the first 24 h, the time and height of emission are critical influencing variables. Thus, for example, crosswind spreads after 24 h of transport of two plumes released from the same tall-stack power plant at 0800 and 2000 on a given day are likely to be very different. During the next diurnal cycle, however, these spreads, as a fraction of downwind distance travelled, are likely to converge. Alternate approaches of representing mesoscale plume dispersion include simulation of relative dispersion of hypothetical co-emitted conservative particles (McNider et al., 1988; Uliasz, 1993). In conjunction with instantaneous wind data (e.g., pibal soundings), such models have proved to be satisfactory over β-mesoscale distances (e.g., Gillani, 1986), but more work is needed to establish their application over long distances based on hourly-average gridded wind data such as are produced by the meteorological preprocessors of regional Eulerian models. Overall, based on field evidence, particulate air quality is significantly influenced by regional transport and dispersion, but quantitative simulation of these processes is still subject to considerable error.

3.4.2 Field Studies of Transformations

This section has three subsections. The first two subsections are focussed on the two most important transformation processes related to PM, viz., gas-to-particle conversion (chemical transformation) and the growth of hygroscopic aerosols by condensation of water on them (physical transformation). The latter process is important in clouds, fogs and other humid environments, and has important implications for atmospheric radiation, chemistry and pollutant scavenging. The third subsection is devoted entirely to what was possibly the most comprehensive field study of the past decade related to PM, the Southern California Air Quality Study (SCAQS).

3.4.2.1 Gas-to-Particle Conversion

A number of field studies of gas-to-particle conversion have been conducted in the plumes of large point-sources of SO_x and NO_x (e.g., coal- and oil-fired power plants and metal smelters). Fewer studies have focused on urban-industrial plumes. A number of studies pertain to the regional background. These studies have focused principally on quantifying the rates of aerosol formation and, to a lesser extent, on investigating the

mechanisms. Mechanistic studies are more difficult, particularly when multiple mechanisms are co-active, as is commonly the case.

Point-Source Plume Studies

In the NAPAP emissions inventory for base year 1985 (Placet et al., 1991), about 70% of the U.S. anthropogenic emissions of SO_2, and about 25% of the corresponding emissions of NO_x, were attributed to large point-sources with stack heights exceeding 120 m (probably less than 150 individual sources). The contribution of such sources is even higher in the eastern U.S., particularly in the Ohio and Tennessee River Valleys. Clearly, these large emissions are very important in the context of regional aerosols. Fortunately, many of these sources are located in rural areas, and their plume chemistry can be studied in isolation from the complications of interactions with other plumes. Much of the remaining anthropogenic emissions of SO_x and NO_x are contributed by urban-industrial area sources.

Point-source and urban plume studies of SO_2-to-sulfate transformations published before 1980 have been reviewed by Newman (1981) and in the earlier 1982 PM/SO_x Air Criteria Document (U.S. Environmental Protection Agency, 1982). Only a brief overview of those studies is provided here; the main focus here is on plume studies published after 1980. Since the plume mass is airborne, the most meaningful plume studies are based on measurements made from instrumented aircraft. Early studies (pre-1975) often reported SO_2 oxidation rates as high as 50% h^{-1}. They are now generally considered to be flawed due to limitations in the measurement technology then available. This technology has made major strides since. For example, the development of the filter pack (Forrest and Newman, 1973) has proved to be a useful method of simultaneous collection of high-volume samples of SO_2 and particulate sulfur. Such samples, however, only provide average concentrations over entire plume cross-sections or, at best, over long crosswind plume traverses. The development of continuous monitors for both SO_2 and particulate sulfur (Huntzicker et al., 1978; Cobourn et al., 1978) made it possible to study sulfate formation with crosswind plume detail. Such detail during a single plume traverse contains a nearly instantaneous snapshot of the full spectrum of chemistry between the high-NO_x regime in plume core to the low-NO_x regime at plume edge (Gillani and Wilson, 1980). With cross-sectionally averaged measurements, such a spectrum can only be discerned in measurements ranging from near-source to far

downwind. The technology of continuous measurements of nitrogen species with high sensitivity has also evolved greatly since 1980.

The period between 1974 and 1981 was very active in terms of plume studies focused particularly on estimating the rate of oxidation of SO_2. Studies by Brookhaven National Laboratory (Newman et al., 1975a,b; Forrest and Newman, 1977a,b) and TVA (Meagher et al., 1978) in coal- and oil-fired power plant plumes as well as a nickel smelter plume generally yielded low oxidation of SO_2 (seldom exceeding 5% over 50 km and several hours of plume transport, with an uncertainty of about a factor of two). These investigators found the oxidation rate to be highest close to the source, where it appeared to be correlated with plume particulate loading, and interpreted the oxidation to be due to a heterogeneous second-order mechanism which became quenched as the plume diluted (Schwartz and Newman, 1978). These results were in sharp contrast to those of Husar et al. (1976) for a coal-fired power plant plume, also over about 50 km of plume transport, which showed the oxidation rate to be slow during an early induction period, increasing thereafter to as much as 5% h^{-1}. No mechanistic interpretation was proposed by these authors.

This controversy was resolved by the subsequent findings of Gillani et al. (1978) resulting from two case studies which were remarkable for their coverage of downwind range exceeding 300 km and 10 to 12 h of transport of a coal-fired power plant plume during daylight as well as dark. The authors found the oxidation rate of SO_2 to be strongly correlated with sunlight, and also with the extent of plume dilution, and background ozone concentration (considered to be a surrogate for background reactivity). Maximum measured particulate sulfur as a fraction of total plume sulfur ranged as high as 18%. The daytime conversion rate in the plume was slow at first, but increased as the plume diluted, reaching maximum values on the two days of 1.8 and 3.0% h^{-1} in the afternoon. Such rates are consistent with theoretical rates based on the SO_2-OH reaction (Calvert et al., 1978; Höv and Isaksen, 1981). The entire plume transport on both occasions was in fairly dry environment (relative humidity $< 70\%$). Presumably, the mixing of plume NO_x and background VOC led to photochemistry which generated the necessary oxidants for gas-phase oxidation of SO_2. The measurements of VOC in the background were both sparse and of limited reliability. The study also found the formation of substantial excess of ozone in aged plumes. The interpretation based on plume-background interaction satisfactorily explained the results of

the BNL and TVA studies in which the measurements of low oxidation of SO_2 were all in coherent stable elevated plumes during early morning and evening hours (low sunlight and little plume dilution), as well as of Husar et al. (1976) whose measurements were in the more polluted and convective summer daytime CBL.

As of the end of the 1970s, a number of factors had been implicated as being relevant to plume sulfur chemistry. Gillani and Wilson (1980) conducted a systematic investigation of the dependence of ozone and aerosol formation in power plant plumes on a variety of possible influencing factors, based on the plume data of five case studies. They found that temperature variations in the range 28 to 33 °C, and R.H. variations in the range 50 to 80% did not have an appreciable influence; the importance of sunlight, plume dilution and background composition was reconfirmed. Eatough et al. (1981, 1982) have observed a positive temperature dependence of a linear SO_2 oxidation rate in power plant and smelter plumes in western U.S. in the temperature range 0 to 30 °C.

Gillani and Wilson (1980) also presented direct evidence and interpretation of the role of plume-background interactions in plume photochemistry within the context of a common pattern of diffusion-limited plume chemical evolution through three stages in a moderately polluted environment. In the "early" stage, the plume is narrow and dominated by a high-NO_x regime in which ozone and other oxidants are sharply depleted by reaction with plume NO and SO_2; the VOC-NO_x chemistry, SO_2 oxidation, and aerosol formation are inhibited in the plume in this stage. As the plume spreads and dilutes with a background characterized by relatively high VOC/NO_x ratio, the VOC/NO_x ratio increases also in plume edges. This "intermediate" stage of plume chemistry is characterized by rapid formation of ozone and aerosols in plume edges, leading to an observed excess there of ozone over the background (ozone "wings") while the plume core still has an ozone deficit. Sharp "wings" of Aitken nuclei concentration have also been observed in plume edges at times, indicating directly the nucleation of new aerosol (Wilson, 1978; Gillani et al., 1981). With continuing dilution, the plume ultimately develops a condition of low-NO_x, high VOC/NO_x ratio and, in the summer, an ozone "bulge" throughout. In this "mature" stage, the rate of oxidation of SO_2 to sulfates (and presumably also of NO_x to secondary products) reaches its peak.

Gillani et al. (1981) provided a quantitative interpretation of the above observations by developing an empirical parameterization of the gas-phase conversion rate of SO_2 to sulfate

in terms of measured variables representing sunlight, mixing and background reactivity. The parameterization was verified based on the "dry" data of three different power plant plumes over ten days of measurements in two different summer periods. Crosswind-resolved reactive plume models capable of facilitating plume-background interactions and including detailed simulation of chemical kinetics have been developed and applied by Höv and Isaksen (1981), Stewart and Liu (1981), Seigneur (1982), Gillani (1986) and Hudischewskyj and Seigneur (1989). The reactive plume models of Seigneur and collaborators also include simulation of aerosol dynamics. These models can depict the observed behavior of ozone in the three plume stages. Their applications have shown that the evolution of OH in the plume (a measure of oxidation potential) mimics the above description of ozone evolution (Höv and Isaksen, 1981), and that plume oxidant and aerosol formation are very sensitive to background VOC and their ingestion into the plume (Gillani, 1986). However, these models continue to remain unevaluated adequately owing to a continuing lack of data characterizing the composition of plume background (especially VOC) and the crosswind detail of important intermediate and secondary species (e.g., OH, HO_2, HNO_3, etc.). Reactive plume models that describe the formation of oxidants and secondary particulate matter, as well as the evolution of the aerosol size distribution, have been developed and evaluated with available data (Eltgroth and Hobbs, 1979; Seigneur, 1982; Hudischewskyj and Seigneur, 1989). The most comprehensive model performance and evaluation available to date is that conducted by Hudischewskyj and Seigneur (1989). For example, they conclusively demonstrated that SO_2 oxidation occurs at a faster rate in smelter plumes than in power plant plumes, because in power plant plumes NO_2 competes effectively with SO_2 for OH radicals.

A number of plume studies have verified the sunlight dependence of the SO_2 oxidation process, observing higher seasonal conversion rates during summer, and higher diurnal rates during midday (Husar et al., 1978; Lusis et al., 1978; Roberts and Williams, 1979; Meagher et al., 1981; Hegg and Hobbs, 1980; Gillani et al., 1981; Forrest et al., 1981; Williams et al., 1981; Wilson, 1981; Wilson and McMurry, 1981; Liebsch and de Pena, 1982). In these studies, the peak daytime conversion rate was typically between 1 and 5% h^{-1} in the summer (higher under humid conditions), and much lower in winter. Wilson (1981) reviewed the data of twelve power plant and smelter plumes in the U.S., Canada and Australia, covering measurements during day and night, and summer and winter. The main

conclusion was that diurnally, midday conversion rates were relatively high and quite variable (1 to 10% h^{-1}), while the nighttime conversion rates were generally low (under 0.5% h^{-1}). Also, the rates were found to be lower in winter than in summer. Geographically, the measured plume conversion rates in the arid and relatively clean southwestern U.S. environment were found to be particularly low (0.5% h^{-1}) at all times, including summer midday. Williams et al. (1981) also found the rates to be low in a smelter plume in the arid, clean environment of north central Australia ($\approx$0.15% h^{-1} averaged over 24 h of transport).

Gillani et al. (1981) were able to formulate the parameterization of the gas-phase conversion rate by isolating case studies performed entirely in dry conditions when liquid-phase contributions were negligible. They also observed that for all cases when the plume had any history of wet exposure (clouds, fogs or high humidity), the oxidation of SO_2 invariably proceeded at a rate faster than that predicted by the gas-phase parameterization. Whereas the typical range of the peak summer daytime conversion rate was 1 to 5% h^{-1} in Project MISTT (Missouri, Illinois), it was closer to 1 to 10% h^{-1} in the more humid conditions of the Tennessee Plume Study (Tennessee, Kentucky). In the wetter daytime situations, evidently, liquid-phase chemistry was superposed over the underlying gas-phase chemistry. Gillani and Wilson (1983) focused their study on the plume data of such "wet" situations. They attributed to liquid-phase chemistry the part of the total measured conversion rate which was in excess of the rate estimated by the gas-phase parameterization. The liquid phase was found to be due to clouds, fogs and light rain, or due to wetted aerosols under conditions of high ambient humidity (relative humidity > 75%). The liquid-phase contribution to the conversion rate was found to be in excess of 40% of the total in two-thirds of the cases analyzed, being as high as 8% h^{-1} averaged over the whole plume over 6 h of transport in the most extreme case (clouds and light rain). Similar increases in conversion rates in power plant plumes interacting with high humidity have also been observed by others (e.g., Dittenhoefer and de Pena, 1978; Eatough et al., 1984; Richards et al., 1985).

Determination of the liquid-phase conversion rate involves quantification not only of the kinetics, but also of the discrete and variable extent of plume-cloud interaction. Gillani et al. (1983) formulated a parameterization of the conversion rate for plume-cloud interaction in

which the physical extent of such interaction was represented probabilistically, and the higher liquid-phase conversion rate was applied only for the in-cloud portion of the plume. The application of the parameterization to a case study corresponding to summer daytime plume transport within the CBL, in patchy contact with fair-weather cumulus above, permitted estimation of the average in-cloud conversion rate averaged over 7 h (1000 to 1700) to be 12% h^{-1}. Considering that the corresponding average liquid water content in the clouds was certainly less than 1 g m^{-3} (1 ppm), much higher actual oxidation rates within individual droplets are indicated. Gas-phase photochemistry at a much slower rate was concurrently quite active in the more extensive drier parts of the plume below, producing ozone and other oxidants which contributed to gas-phase as well as liquid-phase sulfur chemistry. It was not possible to relate the in-cloud kinetic rate to the critical variables controlling it, such as cloud liquid water content, H_2O_2 concentration, or droplet pH, because such measurements were not made. The role of concurrent gas-phase photochemistry is indeed essential to provide the oxidizing agents of liquid-phase chemistry. Clark et al. (1984) found the contribution of liquid-phase chemistry in a power plant plume to be negligible during long-range transport over water in a shallow stratocumulus-filled boundary layer, with limited plume dilution, low insolation, and little photochemistry.

A quite different approach based on aerosol growth laws applied to aerosol size distribution data was taken by McMurry et al. (1981) and McMurry and Wilson (1982) to study relative contributions of the principal mechanisms of gas-to-particle conversion. Theory predicts different growth laws for different chemical mechanisms of aerosol formation. The authors examined the functional dependence of calculated particle diameter growth rate on particle diameter. By matching field data with theoretical growth laws, it was possible to differentiate between mechanisms. Application of this approach indicated gas-phase chemistry and condensation of the product to be the predominant mechanism of aerosol formation in several power plant plumes in eastern and western U.S., with increasing contribution of heterogeneous mechanisms with increasing humidity (McMurry et al., 1981); in a case study of the urban plume of St. Louis, 75% and 25% of the aerosol formation were attributed to homogeneous and heterogeneous mechanisms, respectively, while most of the aerosol formation in the ambient air in the Great Smoky Mountains where relative humidities

were high (up to 95%) was attributed to the droplet-phase mechanism (McMurry and Wilson, 1982).

In an overview of empirical parameterizations of sulfur transformations in power plant plumes, Gillani (1985) estimated that on a 24-h average basis, sulfate formation rates in a large power plant plume in the U.S. Midwest in July 1976 were likely to be $0.8 \pm 0.3\%\ h^{-1}$ by gas-phase reactions (midday peak $\approx 2.6\%\ h^{-1}$) and at least half as much by liquid-phase reactions. Winter rates were estimated to be an order of magnitude lower than the summer rates for the gas-phase mechanism, but comparable for the liquid-phase mechanism. Since 1981, no new field studies of chemistry in large point-source plumes have been conducted in the eastern U.S. A comprehensive plume study with state-of-the-art aircraft measurements of primary and secondary sulfur and nitrogen species, as well as VOC and ozone, is planned to occur in the summer of 1995 as part of the Southern Oxidant Study (SOS) Nashville Field Measurement Program.

Smelter plume chemistry is different from that of power plant plumes in some significant ways. Based on aircraft measurements made in 1981 in two Arizona smelter plumes, Richards et al. (1982a,b,c) reported markedly higher SO_2 oxidation rates in these plumes compared to those observed in power plant plumes in similar arid and relatively clean environments. The authors also demonstrated that the oxidation mechanism was predominantly gas-phase, in spite of the relatively high primary aerosol (including iron and manganese) and water loading of those smelter plumes. They attributed the higher SO_2 oxidation rates in smelter plumes to the fact that these plumes contain little or no NO_x emissions, in sharp contrast to the high NO_x emissions in fresh power plant plumes. As a result of the absence of NO_x, there is no initial depletion of OH in the plume (and the associated inhibition of SO_2 oxidation), nor is there any competition to SO_2 oxidation by OH from NO_2. It is useful to note also that a major downward change has occurred since 1981 in the contribution of smelters nationally to atmospheric PM. The number of operational smelters has dropped from 18 to 7; in those still operational, SO_2 emissions have been reduced by more than an order of magnitude as a result of improvements in control technology; finally, the primary emissions of aerosols and water have also been sharply reduced. Unfortunately, no new detailed field studies of smelter plumes have been conducted since those reported in 1982.

Information about field measurements of nitrate formation in point-source combustion plumes is much more meager. Summertime plume measurements suggest that nitrate formation is principally in the form of nitric acid vapor (Hegg and Hobbs, 1979; Richards et al., 1981), and that oxidation of NO_x to HNO_3 may proceed about three times faster than the rate of oxidation of SO_2 (Richards et al., 1981; Forrest et al., 1979, 1981). Richards et al. (1981) observed that along the transport of the Navajo Generating Station in Arizona, there was adequate ammonia to neutralize the sulfate formed in the plume, but not enough to form ammonium nitrate. Forrest et al. (1981) found $NH_4^+/SO_4^=$ to increase with downwind distance and was mostly less than 2 (not enough to fully neutralize the sulfate), but sometimes more than 2, indicating a possibility of the formation of some ammonium nitrate. Eatough et al. (1981) observed that in the western desert region, the neutralization of sulfuric acid in plumes was due not only to ammonia, but also to other basic material (e.g., metal oxides and $CaCO_3$).

Urban Plume Studies

Field information about secondary formations in urban plumes is scantier than for power plant plumes for sulfur compounds, but possibly slightly more for nitrogen compounds. White et al. (1976, 1983) reported slow formation of ozone and aerosols at first in the St. Louis urban plume, but faster rates farther downwind. Average sulfate formation rates between successive downwind measurement locations on summer days were estimated at 2 to 4% h^{-1}. Isaksen et al. (1978) applied a reactive plume model to a subset of the St. Louis data, and estimated peak rates for the formation of sulfuric and nitric acid of 5 and 20% h^{-1}, respectively. Based on the same data set, Whitby (1980) estimated that about 1,000 tons of secondary fine aerosol may be produced in the plume in one summer irradiation day. Alkezweeny and Powell (1977) estimated peak sulfate formation rates in the St. Louis plume at 10 to 14% h^{-1}. Miller and Alkezweeny (1980) reported sulfate formation rates in the Milwaukee urban plume on two summer days in very different air masses to range from 1% h^{-1} (clean background) to 11% h^{-1} (polluted background). The most extensive studies of NO_x chemistry in urban plumes have been reported by Spicer and co-workers. They have reported results for the Los Angeles, Phoenix, Boston and Philadelphia urban plumes. In the Los Angeles studies, the transformation rate of NO_2-to-

products was estimated at 5 to 15% h^{-1} (Spicer, 1977a,b) and 5 to 10% h^{-1} (Spicer et al., 1979). The sum of transformation plus removal rates was estimated for the Phoenix and Boston plumes at <5% h^{-1} and 14 to 24% h^{-1}, respectively. The low rate for Phoenix was attributed partly to thermal decomposition of PAN after its formation in the plume. In a study of the Detroit plume, Kelly (1987) estimated the NO_x transformation rate at 10% h^{-1}, with 67 to 84% of the products being in the form of HNO_3. Measured concentrations of nitric acid, however, were much lower because of its higher removal rate. All of the above urban plume studies, and most of the power plant plume studies, have been daytime studies. Field measurements of nighttime chemistry of nitrogen oxides in plumes are almost non-existent.

Background Field Studies

Attention is now focused on studies of aerosol formation in background air. The plume studies have shown that the *rates* of oxidation of SO_2 and NO_x in the background represent approximately the upper limit of the conversion rates in the plume. In non-humid, moderately polluted conditions, the rates typically range between 1 and 5% h^{-1} for midday SO_2 oxidation in summer in the eastern U.S. (depending on the composition of volatile organic compounds (VOC) and the variability of VOC/NO_x, and up to 1% h^{-1} in the cleaner parts of the Western U.S. Winter rates are about an order of magnitude lower. By contrast, observed NO_x to nitrate conversion rates are about three times faster in summer than in winter (Parrish et al., 1986). Aerosol nitrate formation depends strongly on availability of NH_3 and on temperature. Background aerosol is generally more aged and its acidity more neutralized than plume aerosol.

The situation is more complex in humid conditions. Field measurements of the compositions of cloudwater, rainwater and the precursor clear-air aerosol have shown that strong acidity is substantially greater in cloud and rain water than in the clear-air aerosol (Daum et al., 1984b; Lazrus et al., 1983; Weathers et al., 1988). This is indicative of the contribution of aqueous-phase chemistry to cloudwater acidity in excess of that due to scavenged aerosol. Based on climatological data of clouds and SO_2 distribution, and assuming aqueous-phase oxidation of SO_2 by ozone, Hegg (1985) estimated contribution of the aqueous mechanism to global tropospheric sulfate production to be at least 10 to 15 times

greater than that due to the gas-phase mechanisms. Applications of more comprehensive global models have given estimated aqueous-phase contributions of 40 to 95% of the total sulfate production (Langner and Rodhe, 1991 and references therein). Regional models for North America suggest 50 to 80% of the sulfate deposited in precipitation to be formed in clouds (Fung et al., 1991; McHenry and Dennis, 1991).

A number of ambient studies have attempted to study aqueous chemistry based on in situ measurements in clouds. Determination of the rates and mechanisms of aqueous-phase chemistry is particularly ambiguous for several reasons. First, it is difficult to distinguish between the contributions of in situ chemistry and aerosol scavenging to the observed concentration of the solute in the droplet phase. Also, aqueous chemistry rate depends not only on the change in concentration, but also on the change in time. It is difficult enough to determine the difference in concentration of even one reactant or product species, but determining the corresponding *time* difference is even more difficult (Schwartz, 1987; Gervat et al., 1988; Kelly et al., 1989). In stratiform clouds, in particular, it is not always possible to determine what constitutes pre-cloud air corresponding to specific cloud water samples (Gillani et al., 1995). Finally, it is difficult, based on field data, to attribute the inferred chemistry to specific mechanisms (oxidation by H_2O_2 or O_3, etc.). The conclusions regarding rates and mechanisms of aqueous chemistry based on measurements in clouds are therefore quite uncertain, and have been a source of considerable controversy (e.g., Hegg and Hobbs, 1982, 1983a,b versus Schwartz and Newman, 1983). One important finding in support of in-cloud oxidation of SO_2 by H_2O_2 , however, is the almost universal mutual exclusion of these two species in non-precipitating stratiform clouds (Daum et al., 1984a; Daum, 1988). In such clouds, there is generally enough time available for the species to react fully until the one with the lower concentration in the precursor air is depleted. The implication is that the aqueous-phase oxidation of SO_2 by H_2O_2 takes precedence over other competing reactions.

Most field studies have been limited to estimating the amount or fraction of sulfate formed by the aqueous pathway, rather than the rate of formation. Liu et al. (1993) have summarized the results of a number of cloud studies between 1979 and 1991. In these studies, a number of different approaches have been used to resolve the contributions of aerosol scavenging and in situ chemistry to the observed cloudwater sulfate. The study of

Liu et al. (1993), which was part of the first intensive (summer 1988) of the Eulerian Model Evaluation Field Study (EMEFS), used three different approaches for estimating the scavenged fraction of observed sulfate, and attributed 27 to 55% of cloudwater sulfate to in situ production. The inferred results for the aqueous-phase production of sulfate in the collective studies vary widely. In winter studies, such production is low (e.g., Strapp et al., 1988), while in summer studies, it is generally higher (e.g., Mohnen and Kadlecek, 1989). Many studies implicate H_2O_2 as the principal oxidant (e.g., Van Valin et al., 1990), while others implicate ozone (e.g., Hegg and Hobbs, 1986).

There is a variety of evidence for and against the formation of HNO_3 in the cloud environment (e.g., Lazrus et al., 1983; Daum et al., 1984b; Hegg and Hobbs, 1986; Leaitch et al., 1986a). The heterogeneous mechanism involving N_2O_5 has received attention mostly as the "nighttime" mechanism (Lazrus et al., 1983; Richards, 1983) owing to the short life of the NO_3 radical (precursor of N_2O_5) in sunlight. To account for the comparable measured amounts of sulfate and nitrate deposited in winter storms in Ontario, Barrie (1985) suggested the possibility of the N_2O_5 mechanism for wintertime formation of nitrate in clouds. Leaitch et al. (1988) found substantial enhancement of NO_3^- in and near clouds on 8 of 12 days of winter measurements in central Ontario under freezing conditions and low insolation. On these occasions, variations in $NO_3^-/SO_4^=$ were associated with $H^+/SO_4^=$ in the cloud water, implicating HNO_3. Also, the observed levels of NO_3^- could not be simulated in a model without invoking the N_2O_5 mechanism. Based on a detailed examination of the nighttime behavior of the NO_3 radical, Noxon (1983) concluded that there was a significant loss of NO_3 compared to N_2O_5 by an unknown scavenger (wet particles?). In measurements at a rural site in central Ontario in August 1988 as part of EMEFS, Li et al. (1993) observed a gradual increase in the concentration of aerosol nitrate (NO_3^-) from 1800 to midnight, and then a gradual decrease. In a diagnostic model study, they concluded that the observations could be explained by heterogeneous reactions of NO_3 and N_2O_5 on wet particles. They attributed more than 80% of the NO_3^- formation to NO_3 and about 10% to N_2O_5, and less than 5% to HNO_3.

3.4.2.2 Field Studies of Water Uptake by Atmospheric Aerosols

Water is an important ingredient of atmospheric aerosols. The water content of atmospheric aerosols and the behavior of atmospheric aerosols with respect to changes in ambient humidity are of great importance in the global water cycle, the global energy budget, and also in atmospheric chemistry and optics. Understanding the relationship between atmospheric aerosols and water has proven to be a difficult problem. Most of the water associated with atmospheric aerosol is "unbound" (Pilinis et al., 1989) i.e., it can increase or decrease with ambient humidity in a non-linear manner. This non-linear relationship depends on particle size and composition, indeed on size-dependent composition. More recent studies have included monitoring of particle size distributions (either directly, or indirectly through light scattering and use of Mie theory) and size-dependent chemical composition under controlled relative humidity (e.g., Covert and Heintzenberg, 1984; Rood et al., 1985). Such studies have presented increasing evidence in favor of external mixtures in particles. Covert and Heintzenberg (1984) found that size spectra of sulfur-bearing species were sensitive to relative humidity while those of EC were not, and concluded that sulfur and EC are, to some extent, externally mixed. Harrison (1985) segregated the particles into CCN (cloud condensation nuclei) and non-CCN fractions and measured their chemical compositions. Both fractions contained sulfate, nitrate and soot, but sulfate was 15% of the CCN mass and only 5.8% of the non-CCN mass. Again, this was taken as evidence of external mixture to some extent. The differential mobility analyzer has been a useful tool permitting study of particle properties for monodispersed size classes. Using this instrument, Covert et al. (1990) and Hering and McMurry (1991) showed that monodispersed particles scatter varying amounts of light in a single particle optical counter, indicating different refractive indices, and hence, different chemical composition. Using a tandem differential mobility analyzer, McMurry and Stolzenberg (1989) showed that hygroscopic and hydrophobic particles of the same size co-exist frequently in Los Angeles, again an indication of external mixing.

In visibility studies, the water content of aerosols is of crucial importance. The estimation of visibility impairment involves use of models in conjunction with ambient data of both aerosols and relative humidity. Frequently, both sets of data are not available concurrently for all stations in a monitoring network such as IMPROVE (Interagency Monitoring of PROtected Visual Environments). In such cases, gaps in information must be

filled by the use of empirical relationships between average visibility impairment caused by soluble aerosols and average relative humidity derived from the available concurrent data. Such an application based on data at the 36 national IMPROVE sites is described by Sisler and Malm (1994).

Another important area which critically involves water uptake by soluble aerosols relates to aerosol-cloud interactions. Such interactions are a critical link in cloud formation and the global water cycle, in cloud optics and the global energy budget, in pollutant redistribution by clouds, in pollutant wet removal from the atmosphere, and in atmospheric chemistry. Of particular importance is the process of aerosol incorporation in clouds. Interstitial aerosols in clouds may become incorporated into cloud droplets by "activation" (droplet nucleation), Brownian diffusion, inertial impaction, coalescence, and phoretic effects. Of these microphysical cloud processes, aerosol activation is by far the most important. A soluble particle (the CCN) is activated when water vapor supersaturation around it (S) exceeds a critical value (S_c) which depends principally on particle dry size (D_0) and composition (commonly expressed in terms of the water-soluble solute fraction, ε). The works of Köhler (1936), Junge and McLaren (1971) and Hänel (1976) provide the underlying theory for condensation of water on aerosols based on assumptions of internally mixed aerosols. Based on properties of representative continental and marine CCN, Junge and McLaren predicted that S_c would be sensitive to CCN size, but to CCN composition only for $\lesssim 0.1$. Fitzgerald (1973) confirmed the insensitivity to ε in the range 0.15 to 0.35 based on simultaneous measurements of CCN size, ϵ and CCN activation spectra (functional dependence of activated fraction of aerosol on S) for S between 0.35 and 0.75%.

More recently, based on extensive year-long measurements of CCN spectra for continental aerosols (representative of eastern U.S. background), separated into narrow size bands within the accumulation mode, Alofs et al. (1989) derived a simple semi-empirical expression relating S_c to D_0 and ε applicable down to $S = 0.014\%$. They also showed, based on their own data and a literature review, that for continental aerosols in industrialized regions, $\varepsilon \approx 0.5$ is a reasonable approximation, indicating that the activation of such aerosols is unlikely to be sensitive to particle composition. Based on their expression for S_c and using $\varepsilon = 0.5$, a supersaturation of about 0.1% (characteristic for stratiform clouds) would be adequate to activate most of the accumulation mode particles exposed to a cloud.

Cumuliform clouds with higher S would activate many Aitken mode particles also. In cumulus clouds, peak supersaturation is typically attained near cloud base, which is where maximum activation is likely to occur. The cloud module of the Regional Acid Deposition Model (RADM) is based primarily on a cumulus parameterization, and makes the assumption of 100% cloud scavenging efficiency for sulfates formed from the oxidation of SO_2 (Chang et al., 1991).

The principal interest in quantitative field studies of aerosol-cloud interactions is the scavenging of acidic aerosol mass by clouds. The focus of measurements in these studies (from aircraft or at fixed mountain sites) was on gross spatial averages (over 10s of km) of species mass concentrations (mostly of sulfate and nitrate) based on batch samples collected in cloud water, and in cloud and clear air (Scott and Laulainen, 1979; Sievering et al., 1984; Daum et al., 1984b, 1987; Hegg et al., 1984; Hegg and Hobbs, 1986; Leaitch et al., 1986b; Pueschel et al., 1986). In some studies, continuous measurements of aerosol size spectra were used to derive spatially-averaged aerosol volume concentrations (Leaitch et al., 1983; Hegg et al., 1984; Heintzenberg et al., 1989) based on which, aerosol volume scavenging efficiency was inferred. In one study, continuous measurements of light scattering coefficient were used as a surrogate for aerosol mass concentration (ten Brink et al., 1987). In these studies, inferences of the efficiency of aerosol scavenging were generally based on comparisons of species mass or volume concentrations (or their surrogates) in cloud water and/or cloud interstitial air with those in putative pre-cloud air. Such inferences can be confounded by incorrect identification of pre-cloud air, non-Lagrangian sampling, extended sampling periods and resultant averaging of spatial inhomogeneities (including clear air pockets within clouds), and inadequately resolved contributions of aqueous-phase chemistry. Not surprisingly, the results of the above studies varied quite widely. Most commonly, however, mass scavenging efficiency was found to be high (>0.8).

The above studies based on spatially-averaged particle *mass* concentrations could not address the issue of main concern with respect to radiative transfer, namely, the partitioning of cloud particles between droplets and interstitial aerosol in terms of their local *number* concentrations. Field studies focused on aerosol scavenging based on particle number concentrations are relatively scarce. In the study of Leaitch et al. (1986b) for stratiform and cumuliform clouds, the authors took special care to ensure Lagrangian adiabatic

interpretation by comparing the instantaneous cloud droplet number concentration at a single location within the adiabatic updraft core near cloud base with the below-cloud aerosol number concentration. They found that activation efficiencies so defined were generally high when pre-cloud AMP concentrations were less than about 750 cm^{-3}, but dropped off non-linearly at higher particle loading. Raga and Jonas (1993) made a similar observation when comparing droplet concentrations near cloud top with the sub-cloud aerosol concentrations on the assumption that the latter represented the pre-cloud condition.

Gillani et al. (1995) demonstrated that such an assumption was not generally valid in stratiform clouds which are layered and may include sharp inversions decoupling the layers from each other and from the sub-cloud layer. For such clouds, the adiabatic assumption made in 1-D cloud models is not generally valid. To circumvent this difficulty with respect to identification of pre-cloud air, Gillani et al. defined fractional activation (F) in terms of local variables only, as the ratio of cloud droplet concentration (activated particles) to total particle concentration (droplet concentration + concentration of unactivated accumulation-mode particles, 0.17 to 2.07 μm diameter). In their study (aircraft measurements in and near stratiform clouds near Syracuse, NY in the Fall of 1984), continuous *in situ* measurements were available for particle number concentrations in 15 size classes each for the droplets and for dried (by heating the probe inlet air) interstitial aerosols. Thus, they were able to determine F at a high spatial resolution throughout the clouds studied (continental stratiform). It was determined that accumulation-mode particles larger than 0.37 μm were efficiently activated in the cloud under all measurement conditions, but that particles in the range 0.17 to 0.37 μm were often activated only partially. Partial activation generally correlated with high local total particle concentration (>600 cm^{-3}) and with low temperature lapse rate (surrogate for cooling rate with ascent, $dT/dt = w.\ dT/dz$, where $w=$ the mean long-wave updraft speed), the two conditions most responsible for limiting supersaturation. It is important to note that w is a most difficult quantity to measure, and is not generally available in field measurements. Under the most polluted conditions in a stable stratus, fractional activation of the accumulation-mode particles was as low as 0.1 in the core of the cloud. Statistically, based on ten days of measurements in the Syracuse study, it exceeded 0.9 in 36% of the data in cloud interior, but was below 0.6 in 28% of such data. It was generally

quite low in cloud edges. Evidently, the assumption made in RADM of total activation is questionable for stratiform clouds.

Simple parameterizations of fractional activation in clouds have been developed based on 1-D adiabatic Lagrangian models (e.g., Twomey, 1959; Ghan et al., 1994), and generally highlight the significance of particle loading and updraft speed (model calculated). The 1-D adiabatic approach is useful near cloud base and in updraft cores, but it breaks down near cloud edges and in the upper portions of clouds where entrainment and mixing effects are substantial. It is also questionable in the presence of additional complexities such as cloud layering (Gillani et al., 1995) and lifting and sinking motions (Baker and Latham, 1979; Pruppacher and Klett, 1980). These complex effects result in three-dimensional spatial inhomogeneities and multi-modal droplet size spectra which are uncharacteristic of the simple adiabatic model.

Noone et al. (1992b) studied activation in ground fogs. They were able to infer size-segregated volume and number scavenging efficiencies of aerosols (using a counterflow virtual impactor) in the fog under conditions of very high particle loading and extremely low supersaturations. For such highly-polluted fog conditions, they found high activation efficiencies (>0.8) only for particles larger than 0.8 μm.

In most cloud and fog studies which include considerations of particle composition, use is made of the concept of water-soluble mass fraction (ε). This implicitly assumes internally mixed particles. As was shown by Zhang et al. (1993), there may really be two ε's, one (ε_m) for the "more" hygroscopic particles, and one (ε_l) for the "less" hygroscopic aerosols. In the diagnostic modeling study of Pitchford and McMurry (1994), the two-ε concept was implemented. For clouds and fogs, this implies that S_c may be different for different particles in the same size range.

The interaction between aerosols and clouds modifies not only the clouds, but also the aerosols. The condensation-evaporation cycling of aerosols through non-precipitating clouds generally results in growth of the nuclei due to microphysical and chemical processes during their in-cloud residence (Hoppel, 1988; Hoppel et al., 1990).

3.4.2.3 Pertinent Results of the Southern California Air Quality Study

A separate section is devoted here to the Southern California Air Quality Study (SCAQS) because it was perhaps the most comprehensive and sophisticated field study related to PM conducted in the past decade. It was a major measurement and modeling program conducted during 1985 to 1990 under the sponsorship of a number of local/state/federal government agencies and industrial organizations to study the air quality, including PM_{10}, of the Southern California Air Basin (SoCAB). It was a remarkably comprehensive study in terms of participating scientists and organizations, pollutants studied, and measurements made. Evaluation of measurement methods was one of its stated major objectives. Accordingly, the main field studies of summer and fall 1987 were preceded in the summers of 1985 and 1986, respectively, by the Nitrogen Species Methods Comparison Study (overview and results published in a number of papers in Atmos. Environ. 22: 1517- , 1988) and the Carbonaceous Species Methods Comparison Study (overview and results published in a number of papers in the special issue of Aerosol Sci. Technol. 12(1), 1990). An overview of the study is contained in Lawson (1990), which also includes a summary of preliminary results of the 1987 field study presented at the 82nd Annual Meeting of the Air & Waste Management Association. A SCAQS data analysis meeting was held in Los Angeles in July 1992, the proceedings of which are available from AWMA as well as the California Air Resources Board (CARB). CARB has also compiled a listing of the principal publications resulting from SCAQS, and has produced a brief unpublished document entitled "SCAQS Summary of Goals and Conclusions". What follows is a brief overview of some of the principal findings of the SCAQS particulate and related measurements and analyses as they pertain to the subject of transformations. It is based on the CARB document summarizing goals and conclusions. No attempt is made here to identify the specific research studies which have generated these conclusions.

The SCAQS 1987 intensive field measurements were made during summer (11 days) and fall (6 days), when a wide range of air quality measurements were made at up to 36 surface sites. These were augmented by measurements from up to three instrumented aircraft, surface and upper air meteorological measurements at a number of sites, and other special measurements including photography. Some of the principal findings were as follows:

Source Characterization

Primary geological material was the major contributor to PM_{10} during summer at the eastern sites in SoCAB. Its contribution was generally lower in fall. There was a positive gradient from the coast inland, where it constituted about 30% of PM_{10}. Primary motor vehicle exhaust was generally the second largest contributor during the summer, with the largest fractional contribution (24% of PM_{10}) in downtown Los Angeles. Industrial facilities, vegetative burning and biogenic emissions were not major contributors.

Concentration, Size, and Composition

Concentrations of PM_{10} (24-h average) were highest in fall (> 200 $\mu g/m^3$); highest concentrations in summer were around 120 $\mu g/m^3$. The most abundant PM_{10} species at all sites were nitrate, sulfate, ammonium, OC, EC, calcium, sodium, chloride and iron. $PM_{2.5}$ constituted 1/2 to 2/3 of PM_{10} at all sites, being a higher fraction in fall than in summer. Average mass fractions of $PM_{2.5}$ were 15-30% OC, 4-9% EC (peaking during the morning traffic period), 12-36% nitrates (large site-to-site variation and midday peak preceding the ozone peak by about two hours), and 3-30% sulfate (large seasonal variation). About 20% of the total $PM_{2.5}$ were estimated to be due to non-fossil fuel combustion (modern C). Aerosols occurred in the local atmosphere in three size modes with relative maxima around 0.2, 0.7 and ~5 μm diameter. The predominant modes for sulfate and ammonium were around 0.7 μm, and for nitrate around 0.7 and 4-5 μm.

Ammonium Nitrate and Ammonium Sulfate

Ammonium nitrate concentrations were lowest at Hawthorne (1% of PM_{10}) closer to the coast, and highest at Riverside (24% of PM_{10}) downwind of a large source of ammonia near Rubidoux. For ammonium sulfate, the reverse was true, with the highest concentration at Hawthorne (31%) and the lowest at Riverside (8%). Together, the two species constituted about 1/2 to 2/3 of $PM_{2.5}$. In summer, ammonium nitrate was 5-10 times larger at Riverside than at other sites, its formation apparently being ammonia-limited at the other sites. In fall, it was the second highest contributor to PM_{10} at all sites, and it could not be determined if its formation was NH_3-limited or HNO_3-limited. Ammonium sulfate was rather uniformly

distributed over all sites during both seasons, with concentrations in fall being about half of those in summer.

Secondary Organic Carbon

Secondary OC was contributed significantly to peak 2-h PM_{10} during several episodes, being as high as 70% of total OC and 14 $\mu gC/m^3$, and its diurnal peak lagged the ozone peak by up to 2 h. Interestingly, its highest concentrations occurred on Saturdays.

Hygroscopic Nature of the Aerosol

As has been pointed out before, based on TDMA and MOUDI measurements, there were indications that the particles were to some extent externally mixed, with "more" hygroscopic and "less" hygroscopic components in monodisperse size classes, with a pattern of relationship to sulfate-to-carbon ratio.

A number of other findings with implications for aerosol formation and growth also resulted from SCAQS. Some of the principal ones are highlighted below:

- Measured concentration ratios VOC/NO_x in the morning traffic period were found to be 2 to 2.5 times higher than the corresponding values based on emission inventories. SCAQS tunnel studies indicated that this discrepancy may be due to an underestimation in the emission inventories of VOC and CO for motor vehicles by a factor of about 2. This finding had major potential implications not only for Los Angeles and California, but for the whole nation, because similar mobile-source emission models are used throughout the nation. This uncertainty is relevant to ozone formation as well as aerosol formation. Urban airshed model simulations were found to be in better agreement with ozone measurements when the VOC emission estimates were doubled.

- Nitrous acid, directly emitted as well as presumably formed by nighttime reactions involving NO_x, water and aerosols, may be the single largest source of OH radicals in the morning.

- Biogenic VOC were found to be relatively negligible in the SoCAB.

- Urban airshed model applications to SCAQS episodes were found to underpredict NO_x oxidation products. Also, the models did not satisfactorily simulate observed layers of ozone and other secondary pollutants near the top of the daytime mixed layer. The sources of these errors may be related to model formulation (terrain-following coordinate system), meteorological inputs, and transport simulation.

3.5 DRY DEPOSITION

3.5.1 Theoretical Aspects of Dry Deposition

Dry deposition is commonly parameterized by the deposition velocity, V_d (m s^{-1}) which is defined as the coefficient relating the pollutant deposition flux F (g $m^{-2}s^{-1}$) and the pollutant concentration c (g/m^3) at a certain reference height above the surface, i.e.,

$$F = V_d c \tag{3-51}$$

The deposition velocity can be expressed as the inverse of a sum of "resistances" in three layers adjacent to the surface (Sehmel, 1980; Hicks, 1984):

1. The aerodynamic layer (i.e., the layer in which atmospheric turbulent fluxes are constant [typically extending to about 20 m above the ground]). In this layer, pollutant transfer, whether gas or particle, is controlled by atmospheric turbulence.

2. The surface (or quasi-laminar) layer, a thin layer ($\sim$1 mm) just above the surface in which transport occurs by molecular diffusion. In this layer, gases transfer to the surface by molecular diffusion and particles undergo Brownian diffusion and inertial impaction.

3. The earth/canopy/vegetation surface, at which the pollutant gas molecule or particle is removed from the air by attachment to the surface.

For gases, the deposition velocity is a function of these three types of resistance as follows:

$$V_d = (r_a + r_s + r_c)^{-1} \tag{3-52}$$

where r_a is the atmospheric resistance through the aerodynamic layer, r_s is the surface layer resistance, and r_c is the canopy/vegetation resistance. All resistances are in units of s m^{-1}.

The aerodynamic resistance r_a can be expressed (Wesely and Hicks, 1977) by:

$$r_a = \frac{1}{ku*}[\ln(z_s/z_o) - \varnothing_h] \tag{3-53}$$

where z_s is the reference height (m) ($\sim$10 m), z_o is the roughness length (m), k is the von Kármán constant (0.4), u_* is the friction velocity (m s^{-1}), and $\varnothing_h$ is the stability correction factor. Roughness lengths vary from about 10^{-5} m for very smooth surfaces (ice, mud flats) to 0.1 m for fully grown root crops, to 1 m for a forested area, to 5-10 m for an urban core (Seinfeld, 1986).

The surface layer resistance can be parameterized as a function of the Schmidt number Sc = v/D, where v is the kinematic viscosity of air (m^2/s) and D is the molecular diffusivity (m^2/s) of the species, as

$$r_s = d_1 \frac{Sc^{d_2}}{ku*} \tag{3-54}$$

where d_1, d_2 are empirical parameters ($d_1 \simeq 1.6$ - 16.7, and d_2 = 0.4 - 0.8, with a suggested choice of d_1 = 5, d_2 = 0.66).

The canopy resistance is the resistance for gases in the vegetation layer. There are three main pathways for uptake/reaction of the pollutant within the vegetation or surface: (1) transfer through the stomatal pore and dissolution or reaction in the mesophyll cell; (2) reaction with or transfer through the leaf cuticle; (3) transfer into the ground/water surface. In the resistance model, these pathways are treated as three resistances in parallel. The canopy resistance r_c for a gaseous species may be parameterized (Yamartino et al., 1992) as:

$$r_c = [LAI/r_f + LAI/r_{cut} + 1/r_g]^{-1} \tag{3-55}$$

where LAI is the leaf area index (i.e., the ratio of leaf surface area divided by ground surface area), r_f is the internal foliage resistance, r_{cut} is the cuticle resistance, and r_g is the ground or water surface resistance. Values for r_f are discussed by O'Dell et al. (1977). The resistance r_{cut} is parameterized by Pleim et al. (1984).

For gaseous pollutants, solubility and reactivity are the major factors affecting surface resistance and net deposition velocity. For particles, the factor most strongly influencing the deposition velocity is the particle mass or, assuming similar densities, the particle size. Particles are transported toward the surface by turbulent diffusion, which for larger particles is enhanced by gravitational settling. Across the quasi-laminar surface layer very small particles (< 0.05 μm diameter) are transported primarily by Brownian diffusion, analogous to the molecular diffusion of gases. The larger particles possess inertia, which may enhance the flux through the quasi-laminar sublayer.

The downward pollutant flux is the sum of the turbulent diffusive flux and a flux due to gravitational settling, i.e.,

$$F(z) = F_d + V_g C = V_d C \tag{3-56}$$

where V_g is the gravitational settling velocity of the particle. Whereas in the formulation of the algorithm for gases the analogy with electrical resistance is straightforward, it is less so for particles. This is because at any height within the aerodynamic layer and surface layer the flux of trace gases is diffusive only and hence a function of the concentration gradient. Consequently, when equating the fluxes through each layer under the steady-state assumption, the deposition velocity may be cast in a form proportional to the inverse of a sum of resistances. Nevertheless, the electrical resistance analogy can still be employed for particles. The gravitational settling velocity is merely represented by the reciprocal of an additional resistance acting in parallel with the diffusive resistance.

As noted earlier, for particles, the resistance in the vegetation layer (r_c) is usually assumed to be zero, since particles that penetrate the surface layer are assumed to stick to the surface. The expression for deposition velocity in terms of the resistances, modified to include gravitational settling, is

$$V_d = (r_a + r_s + r_a r_s V_g)^{-1} + V_g \tag{3-57}$$

Therefore, the deposition velocity of particles may be viewed in terms of electrical resistance as the reciprocal of three resistances in series (r_a, r_s, and $r_a r_s V_g$) and one in parallel ($1/V_g$). The third resistance in series is denoted here as a virtual resistance in view of the fact that it is a mathematical artifact of the equation manipulation and not a physical resistance. Equation 3-57 is usually implemented with r_a (particles) equal to r_a (gases), in which r_a is computed by Equation 3-53, and the surface layer resistance is

$$r_s = (Sc^{-2/3} + 10^{-3/St})^{-1} (u*)^{-1} \tag{3-58}$$

where Sc is the Schmidt number based on D, the Brownian diffusivity of the particle in air, and St is the Stokes number, $St=V_g(u^*)^2/gv$, where u* is the friction velocity, g is the gravitational constant and v is the air kinematic viscosity. The surface layer resistance incorporates the effects of both Brownian diffusion, through the Schmidt number, and inertial impaction effects, through the Stokes number.

The gravitational settling velocity V_g is a function of the particle size, shape and density. For spherical particles (Seinfeld, 1986),

$$V_g = \frac{d_p^2 g(\rho_p - \rho_a)C}{18\mu} \tag{3-59}$$

where d_p is the particle diameter (m), ρ_p is the particle density (g /m^3), ρ_a is density of the air (g /m^3), μ is the viscosity of air (g m^{-1}s^{-1}), and C is the slip correction factor

$$C = 1 + (2\lambda / d_p)[1.257 + 0.4\exp(-0.55 d_p / \lambda)] \tag{3-60}$$

where λ is the mean free path of air molecules (λ = 6.53 x 10^{-6} cm at 298K)

Figure 3-12 shows particle deposition velocities based on wind tunnel measurements. Deposition velocities are presented as a function of particle diameter, particle density, and surface roughness height. Particle deposition velocities exhibit a characteristic minimum as a function of particle size. For the smallest particles, deposition velocity increases as particle size decreases because diffusion by Brownian motion increases as particles get smaller. For the largest particles, gravitational settling becomes important as particles get larger so the deposition velocity increases as particles increase in size. A characteristic minimum in deposition velocity results in the range of 0.1 to 1.0 μm diameter where neither Brownian diffusion nor gravitational settling is strong enough to control removal.

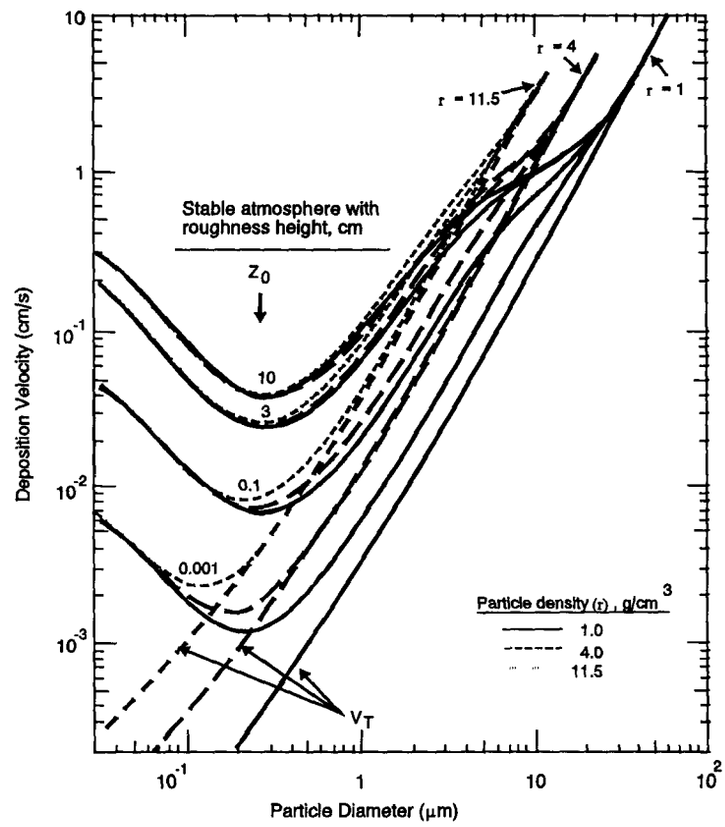

Figure 3-12. Extrapolations from correlations of wind-tunnel measured deposition velocities for z = 1 m, densities of 1, 4, and 11.5 g cm^{-3}. V_T represents terminal settling velocity.

Source: Sehmel (1980) as presented by Nicholson (1988).

It is possible to obtain a rapid estimate of the atmospheric lifetime of particles with respect to removal by dry deposition. If the aerosol can be assumed to have a uniform concentration between the ground and a height h, then the residence time relative to removal by dry deposition is h/V_d. For example, for a 1000 m atmospheric layer, and a particle deposition velocity of 0.1 cm/s, the estimated residence time is 11.5 days.

3.5.2 Field Studies of Dry Deposition

In spite of many field measurements and considerable progress since 1980 in our understanding of dry deposition processes and their quantification, uncertainties remain substantial. The problem is extremely complex involving a large multiplicity of factors, and their complex interactions, which influence dry deposition of atmospheric particles and their precursors (see, for example, a tabulation of some of these in Davidson and Wu, 1990). These factors relate to characteristics of the atmosphere, nature of the deposition surface, and properties of the depositing species. It is impossible in field studies to measure all the pertinent variables over large enough spatial and temporal domains. In essence, knowledge of dry deposition is limited by the inability to make the necessary measurements in other than special circumstances. This was a key statement of the NAPAP Workshop on Dry Deposition in Harpers Ferry, West Virginia (Hicks et al., 1986). The Workshop report also noted that there is presently a lack of fundamental knowledge concerning the chemical and biological processes influencing dry deposition, and there are serious hazards associated with scaling input information down from grid level to local, and scaling up the results of local measurements to broader domains. Information contained in the Workshop report and in subsequent research publications on the subject were reviewed by Davidson and Wu (1990). That review summarizes the results of a large number of field studies published since earlier reviews by McMahon and Denison (1979), Sehmel (1980), Hosker and Lindberg (1982) and Galloway et al. (1982). It also includes summaries of dry deposition processes, wind tunnel studies and empirical models, techniques for measuring deposition in the field, and comparisons of field data and model results. The summary presented in this section is based largely on Davidson and Wu (1990).

Many techniques have been used to measure dry deposition. They are generally grouped into two classes: surface analysis methods, which are based on examination of

contaminant accumulations on natural or surrogate surfaces, and atmospheric flux methods, which involve ambient measurements of the species of interest and other related variables. These methods provide the deposition flux out of which the deposition velocity is inferred. *Surface analysis methods* include foliar extraction (by washing individual leaves), throughfall and stemflow (wet measurements above and within the canopy), watershed mass balance, tracer techniques, snow sampling, collection on surrogate surfaces, etc. These methods may provide useful data on the flux of coarse particles, but fail to simulate the physical processes which control the deposition of sub-micron particles to natural surfaces, and to give meaningful data on trace gas deposition. Deposition on surrogate surfaces may not mimic that on natural surfaces. *Atmospheric flux methods* include micrometeorological methods (eddy correlation and vertical gradients), aerometric mass balance in a box over the depositing surface, tracer techniques, etc. Micrometeorological methods also include what has come to be known as the inferential approach in which measured concentrations are combined with specified or calculated deposition velocities based on meteorological data and surface information. This approach is used in long-term monitoring programs in which only simple measurements are possible at remote sites (e.g. weekly average species concentrations and routine meteorological measurements). For details of the various methods, see Davidson and Wu (1990) and the report from NAPAP Workshop on Dry Deposition (Hicks et al., 1986).

Estimates of flux in the surface layer have historically been inferred from measurements of the vertical gradients of mean quantities such as concentration or horizontal wind speed under conditions that the gradient-transport theory was assumed to be valid. Calculations are modified by corrections of departures from neutral stability. However, with fast response instruments it is possible to directly measure the correlation of fluctuations in velocity and transported quantities of interest such as pollutants, water vapor or heat. For direct measurement of flux, the eddy correlation method is widely used. In this case, pollutant flux and aerodynamic resistance can be measured with appropriate fast sensors with matched time response. A discussion of these methods may be found in Hubbe (1989).

Several limitation of the methods presently being implemented should be noted. For example, the aerometric mass balance technique is essentially inferential, relying heavily on the accurate measurements of air concentrations and on the evaluation of accurate deposition

velocities. The dominant limitations are probably those associated with the ability to evaluate appropriate deposition velocities. The knowledge on which any interpretive scheme for deposition can be based is quite limited. Most information on gas transfer either deals with average uptake in laboratory conditions (chambers, wind-tunnel, etc.), or is derived from short-term micrometerological measurements at selected field sites. Ongoing research programs are addressing these problems. However, a major task, confronting all attempts to monitor dry deposition, is to assess the magnitude of errors arising from the need to apply poorly-known relationships.

3.5.3 Measured Deposition Velocities

Measurements of dry deposition in the field and in chambers have primarily involved six categories of contaminants: sulfur species, nitrogen species, chloride species, ozone, trace elements and atmospheric particles. The results of many of these studies published between 1978 and 1987 are reviewed in Davidson and Wu (1990), which includes extensive tabulations of the studies and their results. Of the reported studies on sulfur species, 20 pertain to SO_2. They give deposition velocities ranging from nearly 0 to 3.4 cm/s. The variations are due to differences in seasonal and diurnal conditions, aerodynamic transfer, surface characteristics (especially stomatal resistance), measurement methods, etc. Daytime values are generally higher, as expected (lower aerodynamic and stomatal resistances). Micrometeorological methods were used in 16 studies whose average values of v_d gave a grand average of 0.95 ± 0.62 cm/s. Four studies provided an average value of 0.13 ± 0.09 cm/s for deposition velocity on snow. For particulate sulfur, 34 studies are included, with 10 also including particle size measurements. A graph also includes results of earlier studies, and gives values of v_d in the range 0.01 to 10 cm/s. Results for v_d in cm/s based on different methods are as follows: 0.55 ± 0.65 for micromet methods, 0.26 ± 0.25 for surrogate surface exposures, 0.23 ± 0.24 for foliar extraction, and 1.00 ± 0.41 for throughfall. Since the micromet method is believed to be more specific for submicron particles while the surrogate surface method is biased in favor of larger particles, the difference in the results of those methods is opposite to that expected. The surrogate surface and foliar extraction results are close, but each has a large variance. Throughfall values are

the largest probably partly because they include deposition of SO_2. Evidently, measurement methods themselves are an important variable because they do not measure the same thing.

Twenty two species are reported for nitrogen species, including NO_2, NO_x, HNO_3, NO_3^-, NH_3, and NH_4^+. The inferred values of v_d (cm/s) are: 0.012 to 0.5 for NO_2 (2 studies), -2.6 to 0.3 for NO_x (4 studies), 0 to 2.9 for HNO_3 (4 studies), 0.13 to 1.3 for NO_3^- (7 studies), 1.9 $\pm$ 1.55 for NH_3 (1 study), and 0.06 to 1.0 for NH_4^+ (4 studies). The zero value for nitric acid was for snow in a chamber study; otherwise, the values for nitric acid are the highest, indicating low surface resistance. The values for particulate nitrate are somewhat larger than for sulfate; this may reflect larger particle size associated with nitrate. Davidson and Wu (1990) report four studies for chloride-containing particles, giving values of 1.0 to 5.1 cm/s; and one study for HCl gas giving a value for HCl of 0.73 cm/s on dew. The highest values for chloride were in winter, related to road salt. Deposition velocities to dew were measured for a number of species including HNO_3, NO_2, SO_2, and aerosol $SO_4^=$ and NH_4^+ in southwest Pennsylvania (Pierson et al., 1986) and in the Los Angeles basin (Pierson et al., 1988; Pierson and Brachaczek, 1990). Low values were obtained, consistent with the high atmospheric stability required for dew formation. Based on 11 studies using micromet methods, v_d of ozone on vegetation ranged between nearly 0 and 1.5 cm/s (average of 15 values = 0.39 $\pm$ 0.21). Nighttime values were lower, but the day-night difference was less for ozone than for NO_2.

Results of 19 studies included measurements for 21 trace elements, with particle size data in 15 studies. For these data, crustal element enrichment factors (EF) were determined. Values of EF $\approx$ 1 indicate crustal sources, while EF $\gg$ 1 (enriched) indicate non-crustal sources such as anthropogenic, natural combustion (volcanism, forest fires), biogenic, sea-spray, etc.. Large enrichment factors were found for Ag, As, Cd, Cu, In, Pb, Sb, Se and Zn. Ni and V were marginally enriched. Other elements were mainly soil-derived. v_d for these elements were generally higher (>1 cm/s), while they were generally less than 1 cm/s for the enriched elements (smaller, submicron particles). A figure including these as well as data of earlier studies is presented, showing a positive correlation between v_d and MMD (mass median diameter). For Pb, the values ranged between 0.1 and 1.0 cm/s. Friedlander et al. (1986) have used CO as a tracer for automobile emissions to estimate the deposition velocity for Pb, by comparing the ratio Pb/CO in ambient air to that in a tunnel.

They found the former to be lower, indicating deposition compared to its value in fresh emission (tunnel). Based on these data, they estimated v_d for Pb to be 0.26 cm/s, which is consistent with the range given above. Davidson and Wu (1990) also report the results of 5 other field studies with micromet measurements of dry deposition for submicron particles, and particle size measurements also. v_d was generally less than 1 cm/s, in general agreement with results for sulfate and the enriched trace elements.

Davidson and Wu (1990) have also presented results of comparisons between measured values of v_d with predicted values based on six model calculations. These results are from published studies with size distribution data for aerosol sulfate and trace elements. The measured values of v_d are for the full size range; the model value is the concentration-weighted average of the calculated values for all size classes. For sulfate, the predicted values were generally smaller than the measured values. Good agreement was, however, not expected because of differences in ambient conditions and surface conditions between values used in the model compared to the corresponding measured values. Similar comparisons for 24 trace elements were also tenuous: out of 11 of the 24 elements for which more than one or two data points only were available, the measured values were in the predicted range; for Al, Ca and Fe, the predictions were low, while for Zn, the predictions were too high. For the other 13 elements with sparse measured data, the agreement was generally much poorer.

3.6 WET DEPOSITION

3.6.1 Introduction

Although detailed physico-chemical models are needed to describe the details of in-cloud and below-cloud scavenging of particles, there has been a benefit in using comparatively simple formulations of precipitation scavenging that provide a convenient picture of the process as a whole. These simple methods are not designed to explain detailed variations in wet deposition with time or space, but they are useful in describing average deposition rates over large areas. Two alternative techniques have become popular. The first relates concentrations of material in precipitation to the quantity available in the air, thus describing the overall efficiency of precipitation as a removal path. By relating concentrations in precipitation to those in the air, dimensionless scavenging ratios can be

determined. The second common method is based on the first-order removal of airborne gases or particles as rain falls through the atmosphere. Concentrations in the air will decrease exponentially and a scavenging rate can then be determined.

Below-cloud scavenging rates for particles of about 3×10^{-5} s^{-1} appear to be typical; in-cloud scavenging leads to rates typically ten times larger (Hicks and Meyers, 1989). Hygroscopic particles are scavenged more readily than hydrophobic ones.

Based on the wet flux W, the wet deposition velocity may be defined as

$$V_w = \frac{W}{c(x,y,0,t)} \simeq \bar{\Lambda} h \tag{3-61}$$

where $\bar{\Lambda}$ is the vertically averaged scavenging rate. The last equality assumes that the pollutant is uniformly distributed between $z = 0$ and $z = h$. The wet deposition velocity V_w can be computed by

$$V_w = w_r p_o \tag{3-62}$$

where w_r is the washout ratio (i.e., the dimensionless ratio of the concentration of material in surface-level precipitation to the concentration of the material in surface-level air) and p_o is the precipitation intensity (mm hr^{-1}). For example, if $w_r = 10^6$ and $p_o = 1$ mm h^{-1}, then $V_w = 28$ cm s^{-1}, which gives, for $h = 1{,}000$ m, $\bar{\Lambda} = 2.8 \times 10^{-4}$ s^{-1}. Seinfeld (1986) provides a detailed discussion of precipitation scavenging of particles, including the calculation of collision efficiencies and scavenging rates.

Scavenging ratios relate concentrations in precipitation to those in air. Although such ratios depend on many factors, they provide a simple way to include wet deposition processes in air quality models. The washout (or "scavenging") ratio is

$$w_r = \frac{[c]_{rain}\rho_a}{[c]_{aerosol}} \tag{3-63}$$

with $[c]_{rain}$ in mg g^{-1}, $[c]_{aerosol}$ in mg m^{-3}, and ρ_a (=1,200 g m^{-3}), the density of air. The definition of this ratio presumes that the aerosol measured at ground level is vertically uniform and that there are no factors limiting the collection of aerosol by the droplets, such as solubility. Scavenging ratios of about 400 appear to be appropriate in the case of particles well mixed in the lower atmosphere but originating near the surface, while values of about 800 appear characteristic of material derived from the free troposphere (Hicks and Meyers, 1989).

3.6.2 Field Studies of Wet Deposition

Removal of accumulation mode aerosol particles from the atmosphere occurs largely by the precipitation process (e.g., Slinn, 1983). These particles are the dominant particles on which cloud droplets form (cloud condensation nuclei, CCN). Once a cloud droplet (of diameter of a few up to about 20 micrometers) is formed, it is much more susceptible to scavenging and removal in precipitation than is the original submicrometer particle. The fraction of aerosol particles incorporated in cloud droplets on cloud formation is the subject of active current research, which has been reviewed in Section 3.4.2.2.

The dominance of precipitation removal processes for accumulation mode particles results in high variability in temporal patterns of aerosol loadings, that may be attributed to the episodicity of precipitation events and synoptic scale meteorology that delivers air of differing origins to a given location (e.g., Waldman et al., 1990). This variability leads to difficulties in attempts to estimate mean residence times based on budget considerations (Junge, 1963; Schwartz, 1979). A unique approach to estimation of the mean residence time of accumulation mode aerosol particles was presented by measurement of the decay of atmospheric concentrations of ^{137}Ce at several mid-latitude surface stations in Europe and Asia in the weeks following the Chernobyl accident (Cambray et al., 1987); the ^{137}Ce was present largely in this size range. This study led to an estimate for the mean residence time of 7 days, consistent with other estimates. It may be noted, however, that this residence

time is applicable to particles in the free troposphere, where the ^{137}Ce was mainly present during the several week period. The mean residence time of accumulation mode particles in the boundary layer is expected to be somewhat less (Benkovitz et al., 1994).

Wet deposition measurements are made principally to meet three objectives: (1) to determine the regional spatial-temporal distribution and chemistry of wet deposition; (2) to study pathways and mechanisms of pollutant wet removal from the atmosphere; and, (3) to generate data for diagnostic evaluations of precipitation scavenging modules. The first of these objectives is best studied based on data of routine monitoring programs. These were reviewed in detail by NAPAP (Sisterson et al., 1991) and are not covered here. The focus here is on recent research field studies aimed at objectives (2) and (3) above.

A significant effort in NAPAP in the 1980s was devoted to development of wet removal characterizations that directly reflected the cloud physics, attachment, reaction, and precipitation processes (Hales, 1991). The PLUVIUS II models, prepared under the auspices of NAPAP, was a reactive storm model based on multi-phase material balance, and served as the basis for the development of the one-dimensional RADM Scavenging Module, RSM. A parallel activity in NAPAP was DOE's PRECP (Processing of Emissions by Clouds and Precipitation) field measurements program which comprised a series of six individual intensive field studies with the objective of systematically measuring scavenging characteristics for different classes of storm systems important to regional acid deposition. In these, studies, the emphasis was on *in situ* aircraft measurements. What follows is a brief review of such research field studies. It is based substantially on Hales (1991). In the context of precipitation scavenging studies, it is useful to bear in mind that pollutant particles, on average, undergo a number of repeated cycles in and out of non-precipitating clouds before finally being removed by precipitation.

In situ aircraft measurements in clouds and precipitation are of crucial importance in mechanistic/diagnostic studies. Current technology permits continuous aircraft measurements of NO, NO_2, NO_y, HNO_3, PAN, SO_2, O_3, H_2O_2, liquid water content (LWC), and size-segregated aerosol and cloud/rain droplet concentrations with quite high sensitivity and precision. In addition, filter samples and cloudwater samples can provide mass concentrations of the major ions in aerosols and droplets at a temporal resolution of a few minutes. Ground monitoring of precipitation in recent studies has included use of the

NAPAP-developed Computer-Controlled Automated Rain Sampler (CCARS) which is a combination rain gauge and sequential precipitation chemistry sampler, controlled and monitored by a programmable microprocessor. Such samplers permit capture of statistically valid footprints (multiple sequential event samples) of deposition during the course of a storm. Upper-air meteorological measurements with fine vertical resolution of wind components, temperature and moisture are also important. These can be made using radar profilers and doppler radars.

Field studies have been conducted in and below point-source plumes (meso-γ scale) and urban plumes (meso-β scale). In the former, precipitation scavenging of S and N compounds was found to be minimal (Granat and Soderland, 1975; Dana et al., 1976; Drewes and Hales, 1982), indicating low precipitation scavenging efficiency for SO_2 and NO_x from fresh plumes. Hales and Dana (1979) found appreciable removal of S and N compounds from the urban plume of St. Louis by summer convective storms. Patrinos and Brown (1984), Patrinos (1985) and Patrinos et al. (1989) found efficient scavenging of these compounds from the urban plumes of Philadelphia and Washington, DC by frontal storms. H_2O_2 data in rain showed considerable spatial variability in the plumes.

The major regional-scale field studies include OSCAR (Oxidation and Scavenging by April Rains, April 1981), PRECP (mid-1980s), and the DOE-FBS (Frontal Boundary Study). OSCAR (Chapman et al., 1987) included a nested array of ground level sampling (an extended regional precipitation chemistry network in northeastern United States, with an embedded high-density network in northeast Indiana) as well as three research aircraft. The focus was on scavenging by extratropical cyclonic storms. The aircraft made clear air measurements before and after frontal passage, as well as measurements within the storm, in the vicinity of the high-density network. Measurements were made during four storms. OSCAR data have been used for regional model development and evaluation.

The six PRECP studies, conducted between 1984 and 1988, were targeted at scavenging measurements in different types of storm systems. Three studies were focussed on convective storms (II, V, and VI) in summer, and the other three on extratropical cyclonic and frontal storms during other seasons; five were conducted east of the Mississippi River, and one in the Oklahoma-Kansas-Colorado area. All of them included two or more research aircraft, and all also included at least limited area precipitation chemistry networks (PRECP

IV had three multiscale networks ranging from a coastal "rain-band" network to a truly regional scale network). The network in PRECP VI was a highly-density network within an 80-km RADM grid cell, designated to provide information about regional sub-grid scale variability. Two of the studies were conducted jointly with other meteorology-focussed measurement programs; PRECPII with the NSF PRESTORM study, and PRECP IV with the NSF-NASA-NOAA Genesis of Atlantic Lows Experiment (GALE). Such synergism resulted in particularly strong meteorological data in these two studies. PRECP I was intended to be an exploratory study, but generated a database of which at least one storm has been extensively studied (Saylor, 1989). PRECP VI, on the other hand was designed as the grand finale aimed at generating a definitive database for evaluation of the RADM Scavenging Module, but failed to meet its main objective owing to the extreme drought of the summer of 1988.

Overall, the studies have developed a substantial database of mechanistic-diagnostic information suitable for diagnostic model studies. PRECP II definitively demonstrated the cloud venting phenomenon transporting boundary layer pollutants to considerable heights in the free troposphere (Dickerson et al., 1987). PRECP III provided a significant new mechanistic insight regarding scavenging in orographically enhanced storms, e.g., the observation of an unexpected entrainment mechanism that occurs as orographic lifting occurs, and which enhances chemical wet removal appreciably (Hales, 1991). PRECP V, focussed on studying vertical profiles of chemical species in and around convective storms, resulted in one study (Daum et al., 1990) which showed that while SO_2 was more concentrated in the lower parts of the ABL, H_2O_2 was concentrated near the top, underscoring the importance of mixing in facilitating aqueous-phase of SO_2 by H_2O_2. The same study also found that in the low-NO_x background, H_2O_2 was correlated with humidity.

The Frontal Boundary Study (DOE) was conducted in fall 1989 as part of a global study of the fate of energy-related pollutants. The focus was on pollutant redistribution and removal by stable frontal storms occurring subsequent to pollution episodes associated with high-pressure stagnation. Aircraft soundings ahead of, within, and following the passage of the front showed considerable spatial variability in precipitation amount and composition (Hales, 1991).

The data of the above studies constitute a substantial mechanistic-diagnostic database for model evaluation. In addition to these research studies, a number of research-grade precipitation chemistry networks were also operated in the 1980s. They include the Canadian CAPMON, and the U.S. MAP3S and UAPSP, as well as the shorter-term EPRI-OEN and the EPA-ME35. Applications of the research network measurements for source-receptor pathway studies are discussed by Hales et al. (1987).

Jaffrezo and Colin (1988) studied the wet removal of trace elements in a year-long study in Paris. They reported their results in terms of the scavenging ratio, along with corresponding information from a number of earlier studies (Table 3-14). The scavenging coefficient and the scavenging ratio, in common use in the Lagrangian models of the 1970s, represent highly lumped representations of the complex of processes involved in wet removal. They are empirical entities which, by themselves, contain little mechanistic information. While reporting their measurements of scavenging ratio during a year-long study in Paris, Jaffrezo and Colin (1988) included a table (Table 3-14) which summarized not only their own data but also those of other earlier studies. The various results are not directly comparable owing, at least partly, to differences in measurement methods.
Of particular interest in their study is the interpretation of elemental composition data. They were able to separate the measured elements into three groups which differed in terms of their solubility and also, by the mechanisms of their scavenging. The measured concentrations in precipitation and in air were nearly proportional for the insoluble species Al, Si, and Fe; this was interpreted to imply that their scavenging was mostly a local mechanism (below-cloud impaction). At the other extreme, the local concentrations of the very soluble species Na and Cl in the two phases were least correlated, indicating a more complex and progressive process of enrichment of one medium relative to the other (in-cloud processes). The remaining soluble species ($SO_4^=$, K, Ca, Zn, and Mg) showed an intermediate behavior. Earlier data at the same site of the relationship between scavenging ratio and particle mass median diameter (MMD), which showed a minimum in the scavenging ratio for MMD = 1 to 2 μm (reported as Figure 6-1), were judged to be supportive of the above interpretation.

TABLE 3-14. SCAVENGING RATIOS
(Dimensionless)[a]

Reference	n	G.M.	Med. (1)	S.D.	A.M.	A.M. (2)	G.M. (3)	G.M. (4)	A.M. (5)	A.M. (6)	G.M. (7)	A.M. (8)	A.M. (9)	A.M. (10)
Cl	78	2,941	2,917	4.73	7,710	600	350	1,400				2,300	4,100	
S	82	743	753	1.98	940	700			1,000					370[b]
Na	81	444	530	3.17	744	560	360	2,100				2,900	5,500	490
K	82	951	970	2.30	1,325	620	300	2,000		548				
Mg	81	596	682	2.39	816	850	400			457				
Ca	82	1,048	1,097	2.49	1,579	1,890	320	1,100		352		2,100		
Zn	69	767	707	2.65	1,226		790		820	179	612	1,050	1,030	
Al	82	291	283	2.72	459		580	1,300			756	620	430	
Si	82	373	405	2.35	533									
Fe	82	184	194	2.51	267		390	600		253	468	890	270	2
Ti	9	305		1.30	378									
Mn	7	146		1.36	171		250	2,100	3,600	370	756	760		

1. Jaffrezo and Colin (1988).
2. Harrison and Pio (1983).
3. Arimoto et al. (1985).
4. Buat-Menard and Duce (1986).
5. Lindberg (1982).
6. Gatz (1977).
7. Chan et al. (1986).
8. Peirson et al. (1973).
9. Cawse (1981).
10. Savoie et al. (1987).

[a]G.M. = Geometric mean.
A.M. = Arithmetic mean.
Med. = Median.
S.D. = Geometric standard deviation.
[b]Non-sea sulfate.

3.6.3 Overview of Sulfur Dioxide and Nitrogen Oxide Wet Scavenging

Hales (1991) has presented a useful overview of our understanding of SO_2 and NO_x wet scavenging based on field measurements which is very pertinent here, and is recapped below. SO_x: SO_2 is emitted principally from point sources. It is moderately soluble in water, and its solubility decreases with increasing acidity of the solution. It is not efficiently scavenged from concentrated fresh plumes, but this efficiency improves as the plumes dilute. It is essentially insoluble in ice and cold snows, but tends to be more efficiently scavenged by wet slushy snow and snows composed of graupel formed by rimming of supercooled cloud water. Only a small fraction of the SO_2 emission is removed as unreacted S(IV) which constitutes about 20% of S in precipitation in the eastern U.S. in sold seasons (significantly in the form of hydroxymethane sulfonate ions), and virtually none in summer (high acidity of droplets). Sulfate removal is also small from fresh plumes (not much there), but increases substantially with plume dilution as more is formed in the plume. It is scavenged efficiently by clouds and rain. Roughly 1/3 of the S emitted annually in North America is believed to be removed by precipitation.

NO_x: Point sources are a relatively smaller contributor of NO_x, but still quite substantial. Both NO and NO_2 have low solubility in water. Virtually no NO_x is removed from fresh plumes. HNO_3 formed by gas-phase oxidation of NO_2 is very soluble in water and is the principal source of NO_3^- in precipitation. NO_3, N_2O_5, and HO_2NO_2 are also believed to be significant intermediates. Since all of the intermediates are secondary products, NO_x scavenging increases with plume dilution and oxidation. Mesoscale studies show much variation in the efficiency of wet scavenging of SO_x and NO_x, depending on storm type and history of plume chemistry. About 1/3 of the anthropogenic NO_x emissions in the U.S. are estimated to be removed by wet deposition. The distinct seasonal character of SO_x wet deposition is absent in the case of NO_x wet deposition. Some likely reasons are as follows: HNO_3 has a strong affinity for ice as well as liquid water; its formation has no direct dependence on H_2O_2 which peaks in summer; and, there are mechanisms for the formation of HNO_3 in low winter sunlight.

3.7 PHYSICAL AND CHEMICAL CONSIDERATIONS IN SELECTING A SIZE CUT-POINT FOR SEPARATING FINE AND COARSE PARTICULATE MATTER

Particulate matter is not a single pollutant but a mixture of many classes of pollutants that differ in sources; formation mechanisms; composition; size; and chemical, physical and biological properties. One of the most fundamental divisions is the natural separation into a fine particle mode and a coarse particle mode as shown in Figure 3-6. (The term "fine" and "coarse" are used in this section to refer to particles in the fine or coarse particle distribution or modes. It is understood that the two distribution overlap between 1 and 3 μm aerodynamic diameter, D_{ae}. Fine is also used to refer to particles with a upper cut point of 3.5, 2.5, 2.1, or 1.0 μm D_{ae}. Coarse is also used to refer to particles between 2.5 and 10 μm D_{ae} or particles collected by the high volume samples as well as the entire coarse mode.) Some of the many differences between fine and coarse particles are summarized in Table 3-15. Because of these many differences it may be advantageous to treat fine and coarse PM as separate pollutants.

As will be discussed in Chapter 5, fine and coarse particles have different sources. Therefore, in order to devise a cost effective control program it is necessary to know, as a minimum, the relative amount of fine and coarse particles in order to know what types of sources to target for control. Source apportionment analysis, i.e., studies of particle composition and other properties to determine the contributions of specific types of sources, is most effective if fine and coarse particles are collected and analyzed separately.

Fine and coarse particles may be anticipated to have different biological properties as well as different physical and chemical properties. As discussed later in Chapters 10 through 13, many of the current hypotheses for health effects at PM concentration levels near or below the current standard are increasingly focusing attention on components of fine particles. Most of the particle strong acidity, sulfate, transition metals, toxic elements, and all of the ultrafine particles are found in the fine particle mode or distribution. On the other hand, much of the airborne biological material, such as pollen, mold spores and insect parts, are found in the coarse particle mode or distribution. Because of the potential for different types of biological effects from fine and coarse particles, it may be useful to separate out relative contributions of each to observed or projected health risks and to balance controls for one or both sizes/types of particles accordingly.

TABLE 3-15. COMPARISON OF AMBIENT FINE AND COARSE MODE PARTICLES

	Fine	Coarse
Formed from:	Gases	Large solids/droplets
Formed by:	Chemical reaction Nucleation Condensation Coagulation Evaporation of fog and cloud droplets in which gases have dissolved and reacted	Mechanical disruption (crushing, grinding, abrasion of surfaces, etc.) Evaporation of sprays Suspension of dusts
Composed of:	Sulfate, $SO_4^=$ Nitrate, NO_3^- Ammonium, NH_4^+ Hydrogen ion, H^+ Elemental carbon, Organic compounds (e.g., PAHs, PNAs) Metals, (e.g., Pb, Cd, V, Ni, Cu, Zn, Mn, Fe) Particle-bound water	Resuspended dust (Soil dust, street dust) Coal and oil fly ash Oxides of crustal elements, (Si, Al, Ti, Fe) $CaCO_3$, NaCl, sea salt Pollen, mold, fungal spores Plant/animal fragments Tire wear debris
Solubility:	Largely soluble, hygroscopic and deliquescent	Largely insoluble and non-hygroscopic
Sources:	Combustion of coal, oil, gasoline, diesel fuel, wood Atmospheric transformation products of NO_x, SO_2, and organic compounds including biogenic organic species, e.g., terpenes High temperature processes, smelters, steel mills, etc.	Resuspension of industrial dust and soil tracked onto roads and streets Suspension from disturbed soil, e.g., farming, mining, unpaved roads Biological sources Construction and demolition, coal and oil combustion, ocean spray
Atmospheric half-life:	Days to weeks	Minutes to hours
Travel distance:	100s to 1000s of km	<1 to 10s of km

Source: Adapted from Wilson and Suh (1996).

Considerations of the relationships between the concentrations measured at a control site and the personal exposure of individuals, discussed in detail in Chapter 7, suggest that a central site monitor may serve as a useful indicator of community exposure to fine particles. A central monitor is a poor indicator of exposure to coarse particles and other PM components with localized sources. Thus for epidemiological or personal exposure studies it will be useful to have separate measurements of fine and coarse particles.

Visibility degradation is due primarily to fine particles since particles with diameters near the wavelengths of visible light (0.4 to 0.7 μm) are much more effective in scattering light on a unit mass basis than larger particles (Chapter 8). On the other hand soiling is more closely related to coarse particles (Chapter 9). Again, these differences provide additional reasons to treat fine and coarse particles separately.

3.7.1 Background

In 1979 EPA scientists, in a paper entitled "Size Considerations for Establishing a Standard for Inhalable Particles" recommended that total suspended particulate matter (TSP), as defined by the high volume sampler, be replaced by the fraction obtained with a sampler having a precise upper cut-point (originally 15 μm D_{ae}, but later changed to 10 μm D_{ae}); and that "a second particle size cut-point of $\leq$ 2.5 μm D_{ae} be incorporated in the air sampling devices" (Miller et al., 1979). This study found that "the existence of a bimodal distribution with fine and coarse modes has been clearly demonstrated by.... mass-size distribution studies and by number distribution studies. These size distribution studies suggest 1 to 3 μm D_{ae} as the most appropriate range for a cut-point for fine and coarse aerosols. However, practical considerations of reducing plugging of impactor orifices indicate that 2.5 μm D_{ae} is a more appropriate cut-point, especially for particle size fractionating devices such as the dichotomous sampler" (Miller et al., 1979).

The cut-point of 2.5 μm D_{ae}, which has been used in many studies since 1979, was chosen not because it was ideal but because it was the smallest cut-point deemed feasible for a dichotomous sampler at that time. Current technology has demonstrated the feasibility of dichotomous samplers with cut-points at 1 μm D_{ae}, or even lower if desired. Impactor and cyclone technology can also be used for cut-points below 2.5 μm D_{ae}. Therefore, it is appropriate at this time to review existing data on size distribution of ambient aerosols so

that policy makers may consider whether a change to a smaller cut-point should be considered. This is especially important in view of the possibility of a major increase in both research measurements, exposure assessment, and regulatory monitoring of fine particles, as well as of PM_{10}.

3.7.2 Size Measurements

Information on the size of fine and coarse particles comes from two basic techniques, (1) particle-counting techniques that measure the size of individual particles and convert the particle number distribution to a particle volume distribution and (2) particle-collecting techniques that use aerodynamic separation, collection of material in specific size ranges, and gravimetric or chemical analysis to determine the total mass or the mass of specific components in the size ranges collected. Particle counting has the potential advantages of not causing as much disturbance to the gas/particle equilibrium. However, considerable care must be taken to avoid heating the sample or diluting it with clean or drier air than that present in the atmosphere. With particle counting techniques it may also be possible to avoid problems of particle bounce. However, several expensive and complex instruments are required to cover the desired range of 0.001 to 100 μm. Because sizes can be measured very precisely, the size ranges covered can be very small and an almost continuous function of number versus size can be obtained.

Particle collecting techniques have the advantage of obtaining size-differentiated samples for chemical analysis. The equipment used is simpler and less expensive. However, aerodynamic separation does not provide as distinct a classification by size. Large particles may bounce from their intended collection surface and be counted in smaller size ranges. Also, the requirement for long sampling times may result in averages of distributions that change with time. Particle collection techniques provide a limited number of size cuts and yield discontinuous functions of mass versus particle size.

Both techniques, however, clearly indicate the natural division of ambient air particles into fine and coarse modes with a minimum between 1.0 and 3.0 μm diameter. Size distributions obtained with particle counting techniques tend to show a lower, broader, and more distinct minimum than distributions obtained with particle collection techniques such as impactors. The position of the minimum between the accumulation and coarse mode may

vary from study to study. The peak of the fine particle mode tends to increase in size with increasing concentration and with increasing relative humidity. Several good reviews of particle size distribution are available: physical properties of sulfur aerosols (Whitby, 1978), urban aerosols (Lippmann, 1980), trace elements (Milford and Davidson, 1985), particulate sulfate and nitrate in the atmosphere (Milford and Davidson, 1987), and coarse mode aerosol (Lundgren and Burton, 1995).

3.7.3 Appropriate Display of Size-Distribution Data

Size-distribution data, if not properly displayed, can give misleading information on the position and shape of peaks and valleys and can lead to incorrect conclusions, especially in regard to the position, width, and separation of fine and coarse modes. For this reason many workers use a histogram display obtained as follows. The mass, number, surface, or volume in each size range is divided by the difference of the logarithms of the diameters at the upper D_i and the lower D_{i-1} ends of the size range, and plotted as rectangles of width log D_i-log D_{i-1} and height, i.e. mass/ (log D_u-log D_e) on a log diameter scale. This is normally shown as $\Delta C/\Delta$ log D, dM/d log D, or normalized, for example, as $\Delta M/M*\Delta$ log D. Such histogram plots are especially useful for impactor data, which normally yield fewer size intervals than particle-counting techniques. Examples of such displays are shown in Figure 3-13 (Wilson et al., 1977) and Figure 3-14a (John et al., 1990). D_{ae} is typically used when the data is presented as aerodynamic diameter and D_p when the data is presented as geometric diameter.

It is frequently desirable to draw a smooth line through the data in order to identify modes and the mass median diameters (MMD) and widths (σ_g) of modes. This can be done by fitting the data to two or more lognormal distributions, as was done in Figure 3-13 (also see Hasan and Dzubay, 1987; and Whitby-DISFIT (TSI, 1993). It is better to use an inversion process, such as originally developed by Twomey, to construct a continuous curve to represent the measurement data as shown in Figure 3-14b (John et al., 1990; Winklmayr et al., 1990). The continuous curve may then be fit to one or more log-normal distributions as shown in Figure 3-14c. However, one must be aware that log-normal distributions may not always provide good fit to actual data (see Figure 3-16). In this type of presentation the area in each rectangle or the area under a portion of a curve is proportional to the mass in

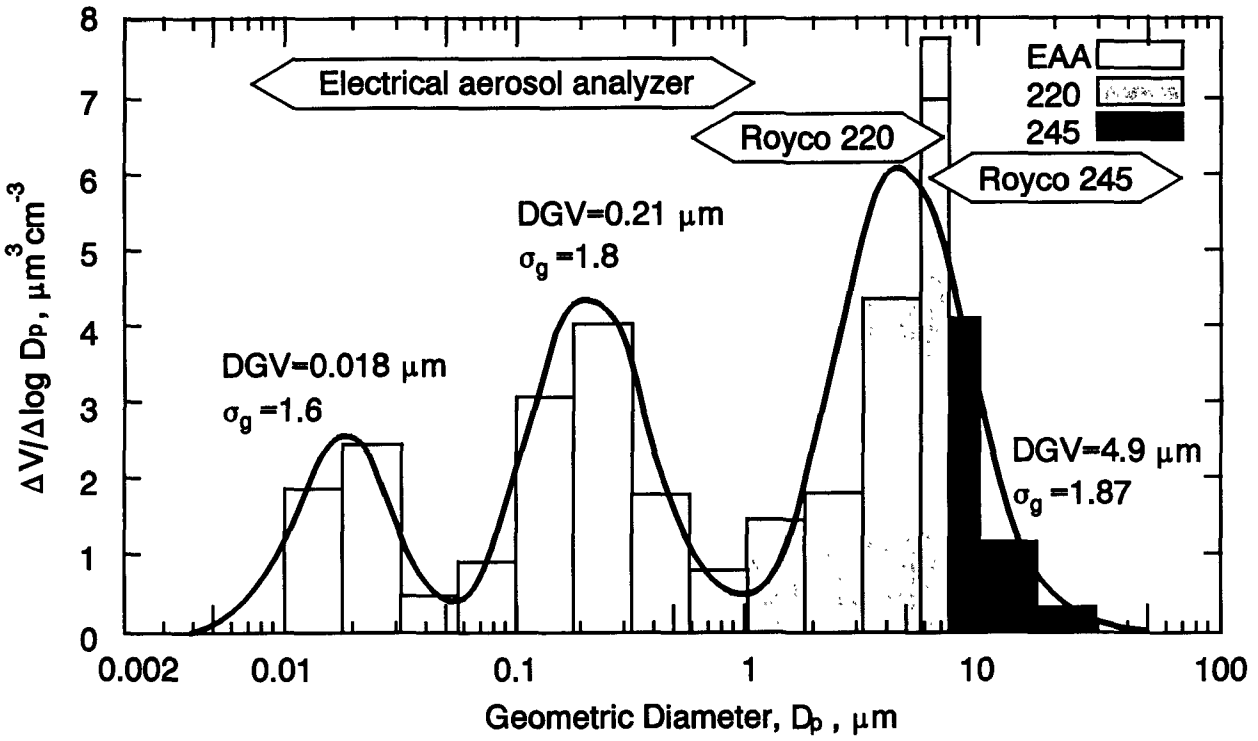

Figure 3-13. An example of histogram display and fitting to log-normal functions for particle-counting size distribution data. Instruments used and the range covered by each are shown. Counts are combined into reasonably-sized bins and displayed. Lognormal functions, fitted to the data, are shown with geometric mean diameter (DGV, equivalent to volume median diameter) of each mode and the width (σ_g) of each mode. Note the clear separation of the nuclei mode (OGV = 0.018 μm), the accumulation mode (OGV = 0.21 μm) and coarse mode (OGV = 4.9 μm). Fine particles, as defined by Whitby (1978), include the nuclei and accumulation mode.

Source: Wilson et al. (1977).

that size range (or the quantity of any other parameter plotted on a linear scale). Plotting mass per impactor stage versus impactor stage number, or drawing lines connecting the midpoints of size range at the heights of the mass in each size range, does not provide such quantitative information. Once the characteristics of the impactor have been demonstrated, and once good fits to lognormal distributions have been obtained, repeated measurements of the same species may be shown by curves fitted to inversion or lognormal distributions such as the example in Figure 3-15 (John et al., 1990).

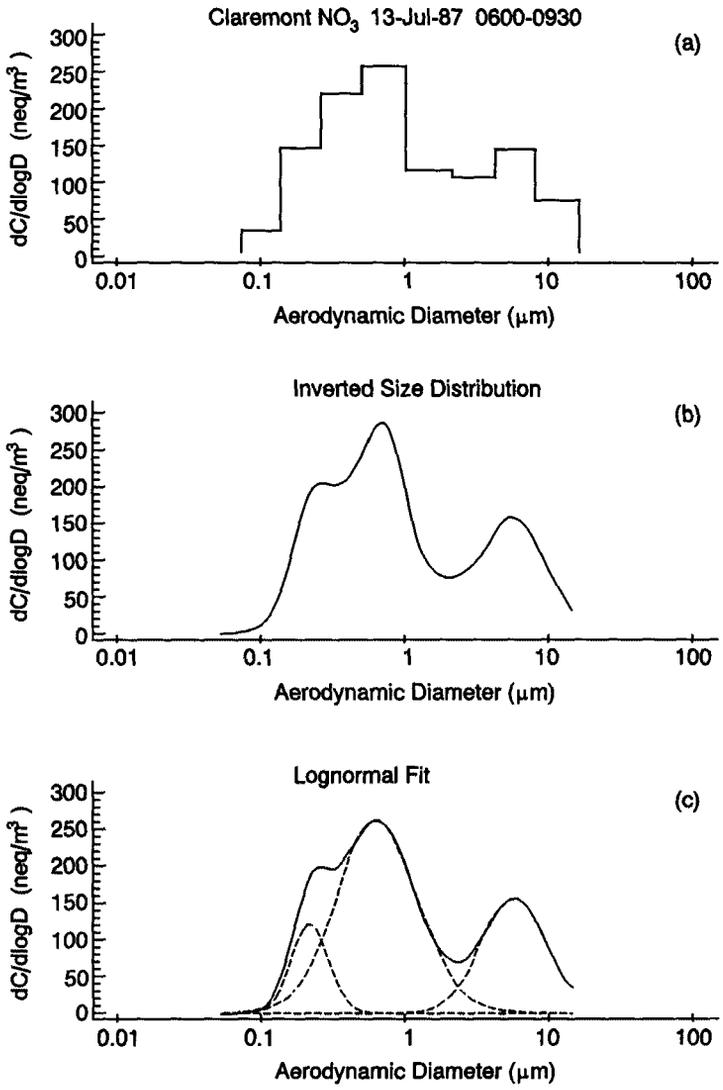

Figure 3-14. An example of an effective display of impactor data: (a) histograph showing mass found on each impactor stage and upper and lower cut points of each stage, (b) inverted size distribution, (i.e., a smooth distribution that would give the observed distribution considering the actual efficiency of each stage; cut points are not exact; each stage allows some large particles, which it should collect, to pass through to the next stage and collects some small particles which it should pass on to the next stage), (c) the solid line is the distribution obtained by fitting a sum of several lognormal functions to the inverted distribution. The dashed lines show the lognormal functions obtained from the fitting process. In this case, the use of log-normal distributions provides a reasonably good fit to the data.

Source: John et al. (1990).

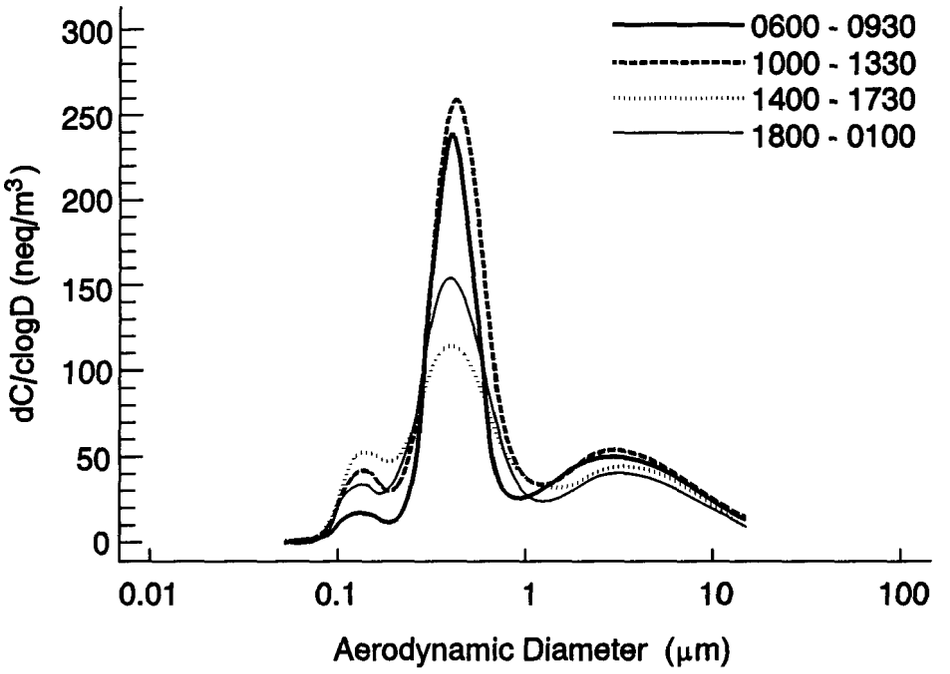

Figure 3-15. Size distributions of sulfate, Long Beach, June, 1987, showing use of fitted log-normal distributions to describe diurnal variations in size and concentration.

Source: John et al. (1990).

In impactor measurements, the maximum size of the upper stage and the minimum size of the lower stage (or after filter) are not well defined. Therefore, an arbitrary choice must be made in order to define the $\Delta \log D_{ae}$. This choice can have a remarkable influence on the perceptions of the positions, height, and width of modes. A particularly dramatic example is shown in Figure 3-16, from Šega and Fugaš (1984). The authors chose 0.1 μm for the lower limit and 20 μm for the upper limit, suggesting a bimodal distribution with a fine mode MMAD at about 1.5 μm, and a coarse mode MMAD at about 10.5 μm. However, if 0.4 μm is chosen for the lower limit and 10 μm for the upper limit, the display suggests a fine mode MMAD of about 0.7 μm and a coarse mode MMAD of about 8 μm.

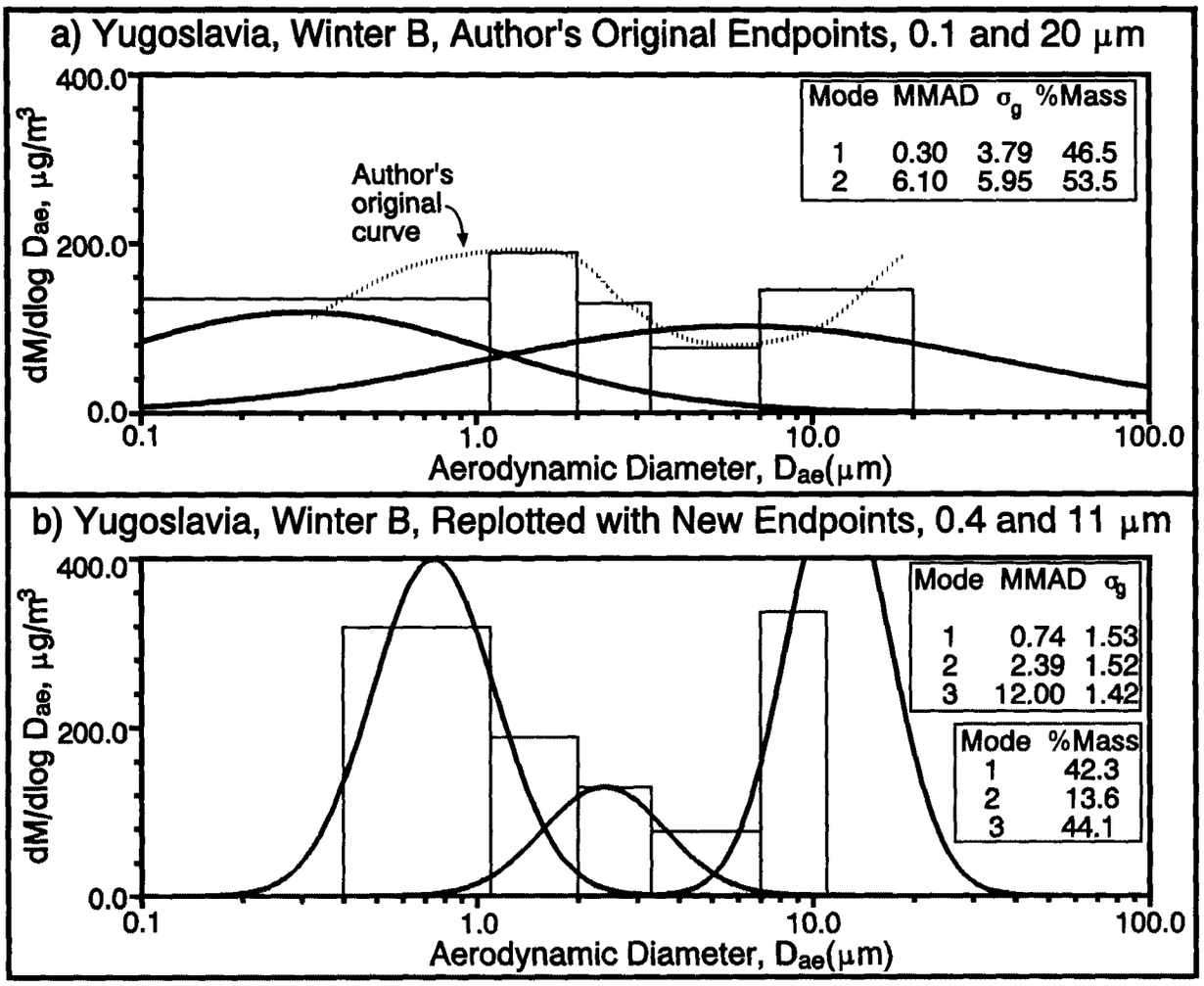

Figure 3-16. Effect of changing endpoints. This example of impactor data shows how the lack of a well-defined upper and lower size limit can affect the perception of the location of fine and coarse particle modes. A histogram with an upper limit of 20 μm and a lower limit of 0.1 μm diameter, along with the curve drawn by authors of the report, is shown in Figure 3-16a. In Figure 3-16b a histogram with a lower limit of 0.4 μm and an upper limit of 10 μm is shown. The author's free hand curve suggests a fine particle MMAD around 1.5 μm diameter. A quite different idea of the location of the modes is given when different endpoints are chosen. Much of the material found between 1.0 and 5.0 μm is probably smaller particles caught on the glass fiber impactor stages which have very poor separation efficiencies. The data has been fitted to a 3-lognormal mode distribution; however, log-normal distributions do not provide a good fit to this data.

Source: Šega and Fugaš (1984).

3.7.4 Comparison of Particle-Counting and Particle-Collection Techniques

Unfortunately, there have been few efforts to compare results of the two particle-sizing techniques. One such effort is shown in Figure 3-17 (Durham et al., 1975). The differences between the two techniques, as evident in the figure, are qualitatively observed in individual studies using either of the two techniques. Particle counting techniques usually give a lower and wider minimum. Typically particle counting leads to volume distributions plotted versus geometric size (or more properly, geometric size inferred from mobility or optical size); whereas impactor separations give mass versus aerodynamic size. In Figure 3-17 both geometric and aerodynamic scales are given. This figure illustrates the problems involved in defining particle "size" and serves as a reminder that each particle sizing technique gives a different "size". The upper scale, used for impactor data, is given in aerodynamic diameter. The aerodynamic diameter of a particle is the diameter of a particle of density, $\rho=1.0$, which would behave similarly with respect to impaction as the particle in question. For spheres in the coarse mode, the aerodynamic diameter, D_a, equals $\sqrt{\rho}\ D_p$, where ρ is the density of the particle and D_p is the geometric diameter. Since coarse particles are expected to have a greater density than fine particles, converting the volume, geometric-size distribution to a mass, aerodynamic-size distribution would increase the apparent size of the volume distribution above 1 μm and widen the minimum. For small particles, below 0.5 μm, or at reduced pressures where the mean free path of the gas molecules is of the same order, or larger than the particle diameter, the Stokes diameter, which is more closely related to the diffusion coefficient, is a more useful parameter. The relationships between Stokes, aerodynamic and geometric diameter are discussed in Section 3.1.3.1.

The particle size distribution shown on the bottom of the graph was derived from a combination of a mobility counter and several optical counters. The "mobility size", obtained from the electrical aerosol analyzer (EAA) in earlier studies and the differential mobility analyzer (DMA) in more recent studies is dependent on the particle shape but not the density. For irregularly shaped particles the "mobility" size gives the Stokes diameter, which is the geometric diameter of a sphere with the same aerodynamic drag. For a sphere the Stokes diameter and the geometric diameter are the same. By comparing the mobility or Stokes diameter to the aerodynamic diameter it is possible to measure the density of spherical particles (Stein et al., 1994).

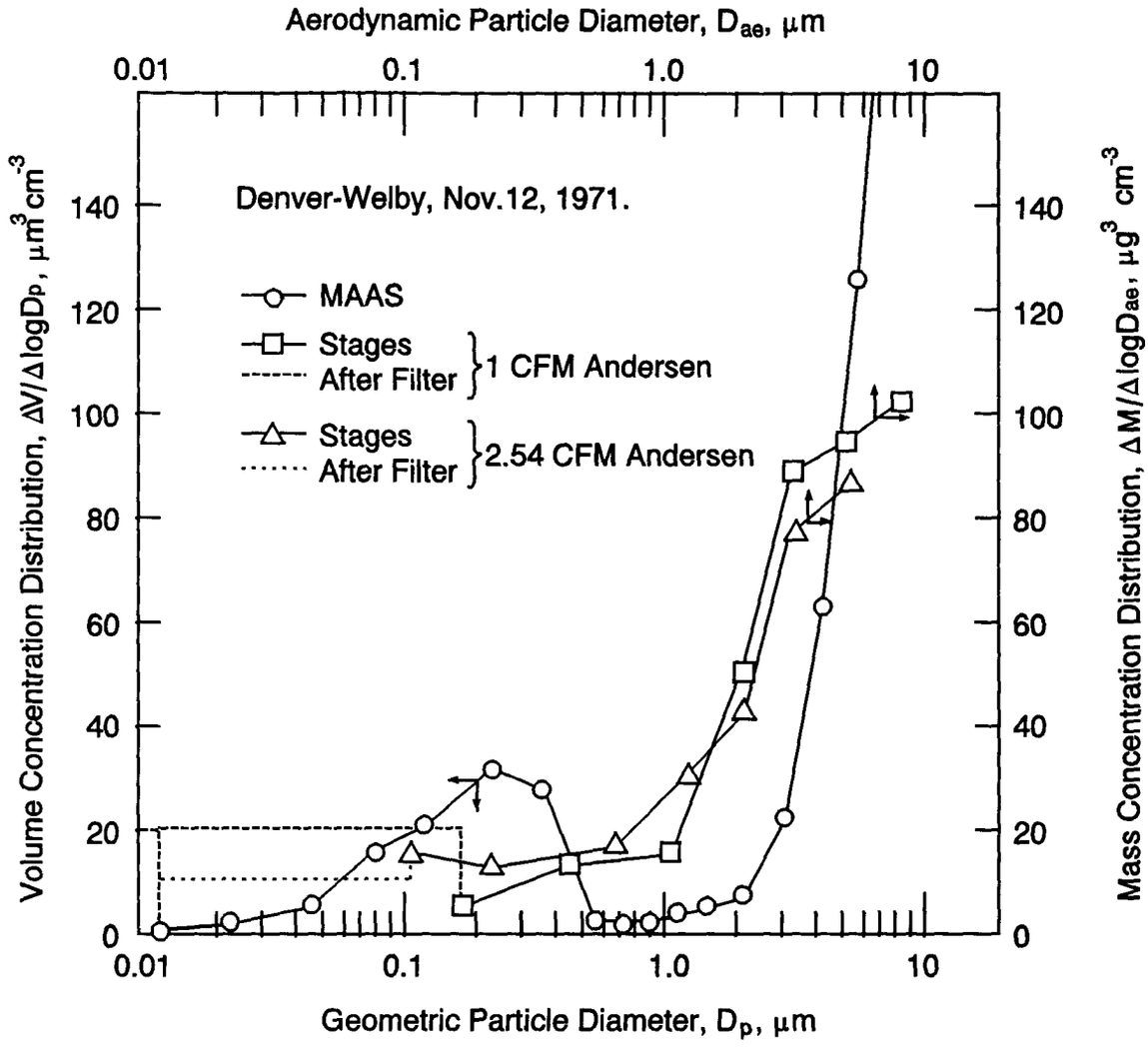

Figure 3-17. These size distributions, obtained during an EPA study of the Denver brown cloud represent one of the few efforts to compare particle-counting and particle-collection size-distribution measurements. Note that impactor data is given in aerodynamic diameter, D_{ae}, and particle-counting data is given in geometric diameter, D_p, derived from the number distribution and estimated density.

Source: Durham et al. (1975).

The "optical" size of a particle depends on the particles shape and refractive index, and on the characteristics of the optical counter. The amount of light scattered by a particle at a wavelength near the particle size varies rapidly with changes in size, wavelength, refractive index, and scattering angle. Therefore, several different optical counters may be needed to cover the range of atmospheric particle sizes. Because of non-linearities in the response of

laser or narrow wavelength optical counters to size changes it is especially difficult to measure particles in the 0.5 to 1.0 size range (Hering and McMurry, 1991; Kim, 1995). Since the amount of scattered light depends strongly on the refractive index it would be useful to calibrate optical counters with particles of the same refractive index as those in the atmosphere. Hering and McMurry (1991) used a differential mobility analyzer to select particles of a uniform geometric diameter. The light scattering of these monodispersed atmospheric particles, as measured by a Particle Measuring System LAS-X optical counter, was compared to that of spheres of polystyrene latex (a substance frequently used to calibrate optical counters) and oleic acid of the same geometric diameter. The atmospheric aerosols scattered less light than polystyrene latex sphere (refractive index = 1.9 - 0.0i), but about the same amount of light as oleic acid spheres (refractive index = 1.46 - 0.0i) of the same geometric size. Relating the variety of sizes measured by particle counters and impactors, and displaying them together on an aerodynamic diameter scale, or other scale, is a major task which has not yet been adequately addressed.

The greater width of the coarse modes, as measured by the impactor in Figure 3-17, may be attributed to the use of glass fiber filter paper for the impactor surface. It is now recognized that the use of glass fiber filter material, as contrasted to a flat surface, causes a severe reduction in the effectiveness of the cut. Large particles bounce off the glass fiber (Vanderpool et al., 1987) giving much reduced collection efficiencies; whereas fine particles penetrate into the fiber and some are captured in stages that should have near zero collection efficiencies (Rao and Whitby, 1978). Many studies that used the Anderson High Volume Fractionating Sampler also used glass fiber filters. The use of glass fiber filters as impaction collection surfaces causes any given size range to contain both larger and smaller particles than predicted and thus tends to spread out the modes and fill in the minima. An example of the smoothing effect of glass fiber collection surfaces, and especially the collection of fine particles on upper stages, can be seen in Figure 3-16. Nevertheless, the bimodal nature of the ambient aerosol is still captured.

3.7.5 Review of Size-Distribution Data

3.7.5.1 Early Studies

In 1978, when EPA scientists debated the best cut-point to separate fine particles from coarse particles, there was limited information available. Particle-counting data from California studies had been summarized by Whitby and Sverdrup (1980) and are shown in Figure 3-18. With the exception of one distribution from Pomona, all distributions showed a minimum near 1 μm and indications of significant amounts of coarse particle material between 1.0 and 2.5 μm. (The region between 1 and 2.5 μm will be referred to as the intermodal region.) Other studies of size distribution (McMurry et al., 1981) in the Southeastern United States, provided similar information (Figure 3-19).

Results from several impactor studies were also available, some of which suggested two modes. However, much of the impactor data were considered unreliable in regard to the existence and position of modes (Whitby et al., 1974). However, one of the more extensive and reliable studies available (Patterson and Wagman, 1977) provided confirmation of the Whitby bimodal observations. In this study, mass and composition measurements were made for four different levels of visibility. The histograms for mass, sulfate, and iron for two levels of visibility are shown in Figure 3-20. It is clear that the major portion of the fine mass is below 0.6 μm and the major portion of the coarse mass is greater than 3 μm in diameter. These impactor data, coupled with the more extensive number-size distributions data of Whitby and Sverdrup (1980) led to a preference for a 1 μm cut-point but an acceptance of 2.5 μm on the assumption, then considered to be the case, that 2.5 μm represented the minimum cut-point that was attainable with a dichotomous sampler (Miller et al., 1979).

3.7.5.2 Recent Work

In the intervening 15 years, there has been very little additional work in which particle-counting techniques, covering the entire size range, have been used to measure ambient aerosols. Most of the particle-counting studies have focused on fine and ultrafine particles, diameter <1.0 μm. There have however been a number of impactor studies that provide insight into the size of the fine and coarse modes and into what material is found between them.

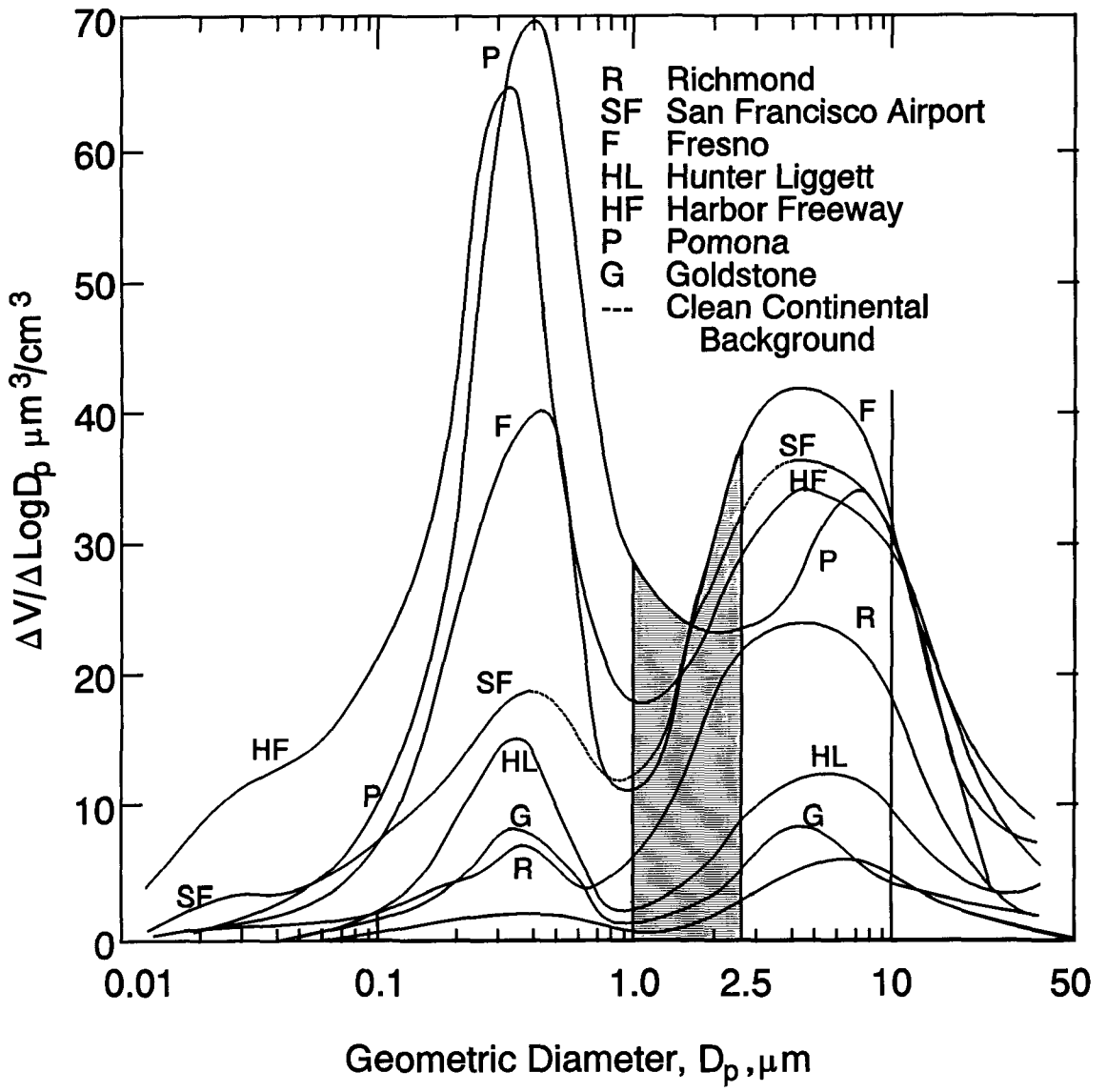

Figure 3-18. Grand average volume-size distributions from the Aerosol Characterization Experiment (ACHEX) in 1972. A size distribution for clean continental aerosol is shown for comparison. Note that with the exception of the Pomona size distribution, all distributions show a distinct minima near 1.0 μm diameter. A line has been added at 1.0 μm, 2.5 μm, and 10 μm diameter to indicate how much of the coarse particle mode is observed between 1.0 and 2.5 μm diameter.

Source: Whitby and Sverdrup (1980).

There are only a few impactor size distribution studies that cover the full size range from 0.01 to 100 μm (Lundgren and Hausknecht, 1982a,b; Lundgren et al., 1984; Burton and Lundgren, 1987; Vanderpool et al., 1987). Lundgren and co-workers used a mobile

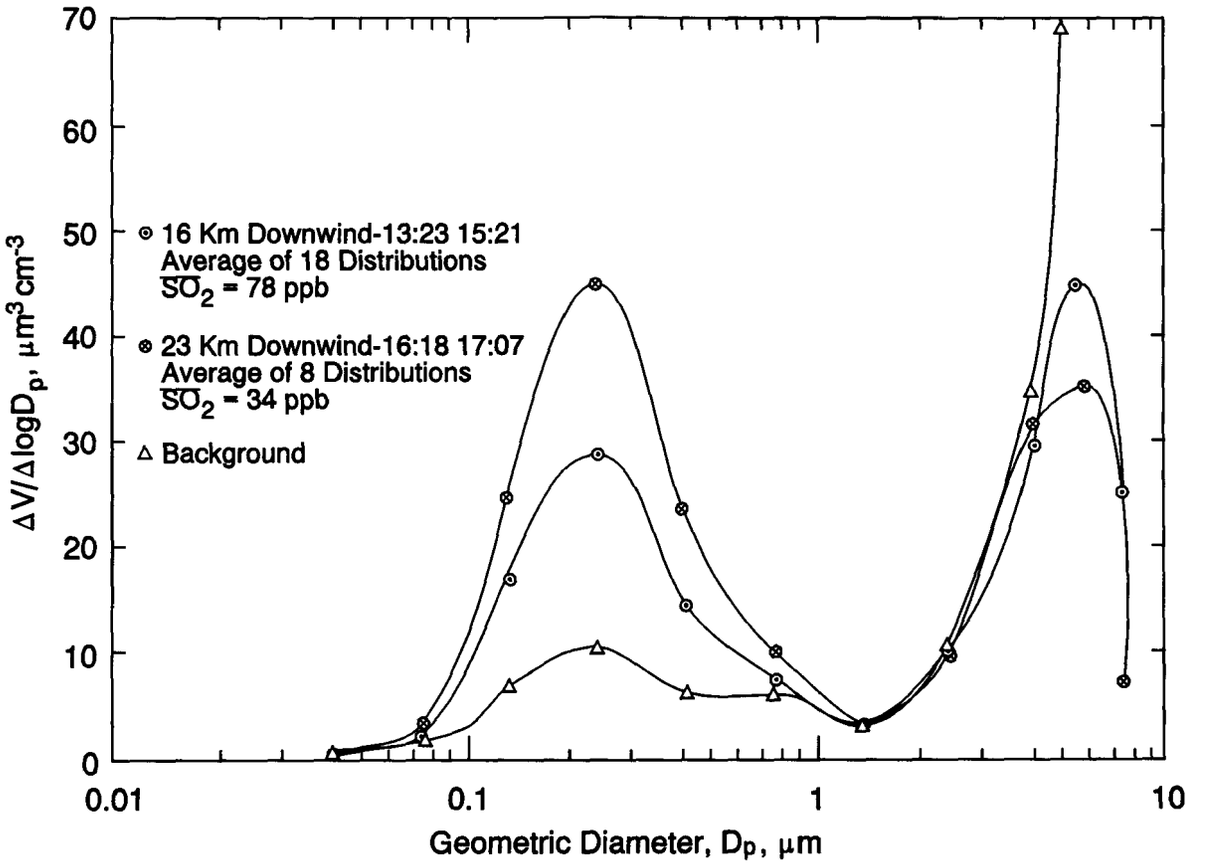

Figure 3-19. Volume-size distribution taken in the midwestern United States near the Cumberland Power Plant in Tennessee. Note that coarse mode decreases and fine mode increased as the mobile sampling van moved downwind farther from urban influence but allowing more time for reaction as the power plant plume mixed with background air and SO_2 was converted to sulfate and NO_x to nitrate.

Source: McMurry et al. (1981).

unit, the wide range aerosol classifier (WRAC), to measure mass-size distribution in ten size ranges from <0.4 to >50 μm. Two distributions, averages for Philadelphia and Phoenix, are shown in Figure 3-21. Both clearly indicate a fine particle mode with an MMAD near 0.5 μm for Philadelphia and below 0.3 μm for Phoenix. Both show a coarse particle mode with an MMAD near 20 μm in diameter. However, there is a significant amount of material found in the intermodal region, 1 to 2.5 μm. Although the intermodal mass is not a significant fraction of the total suspended particulate mass or even of TSP, as would be measured by a high-volume sample (upper cut-point around 25 μm), it does represent a

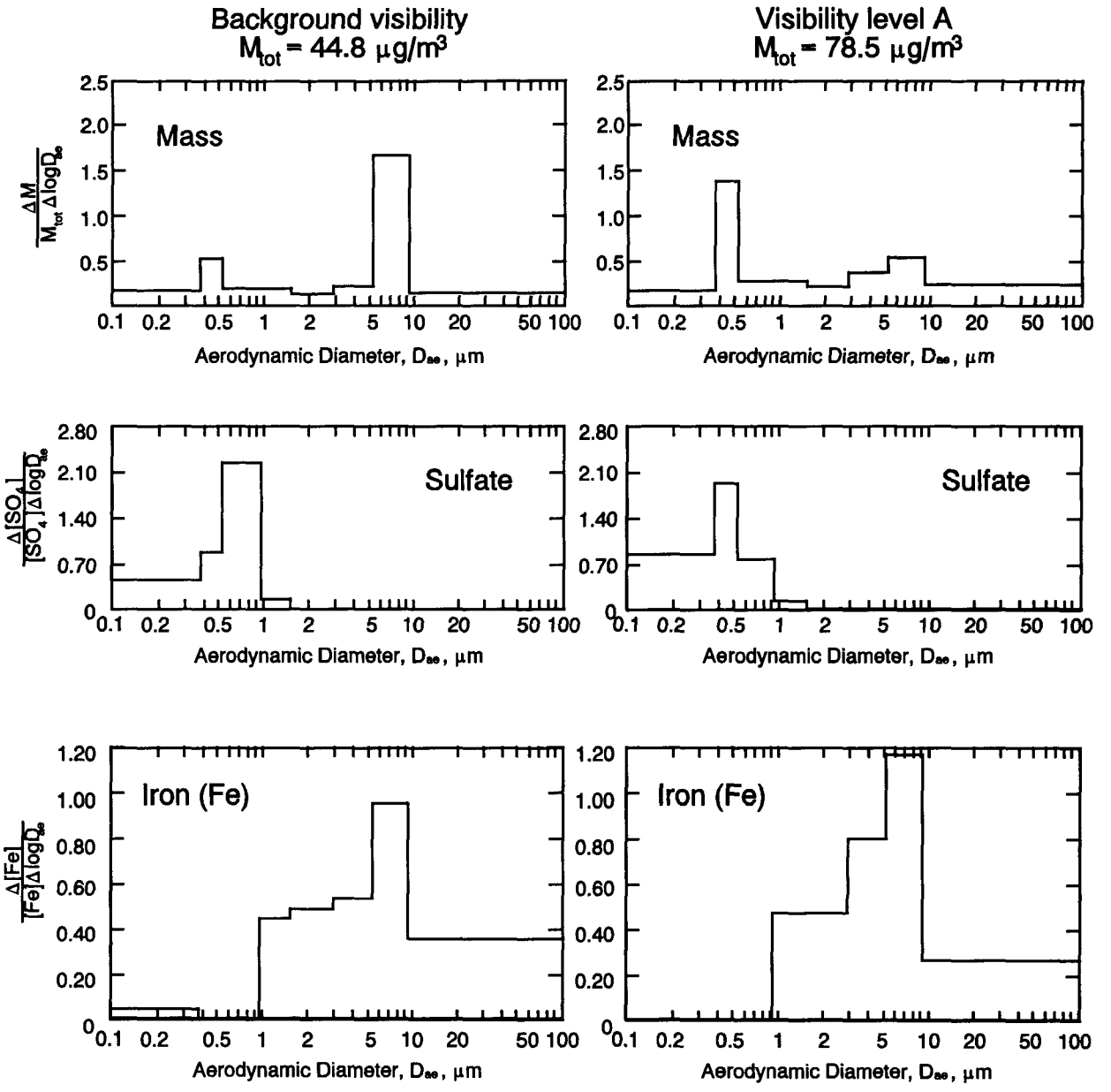

Figure 3-20. Examples of size distribution histograms for total mass, sulfate, and iron obtained at two visibility levels using an Andersen impactor. Arbitrary choice of 0.1 and 100 for lower and upper limits cause the extreme rectangles to be long and low. Note the separation into fine and coarse modes in mass and that sulfate and iron clearly belong in the fine and coarse mode respectively.

Source: Patterson and Wagman (1977).

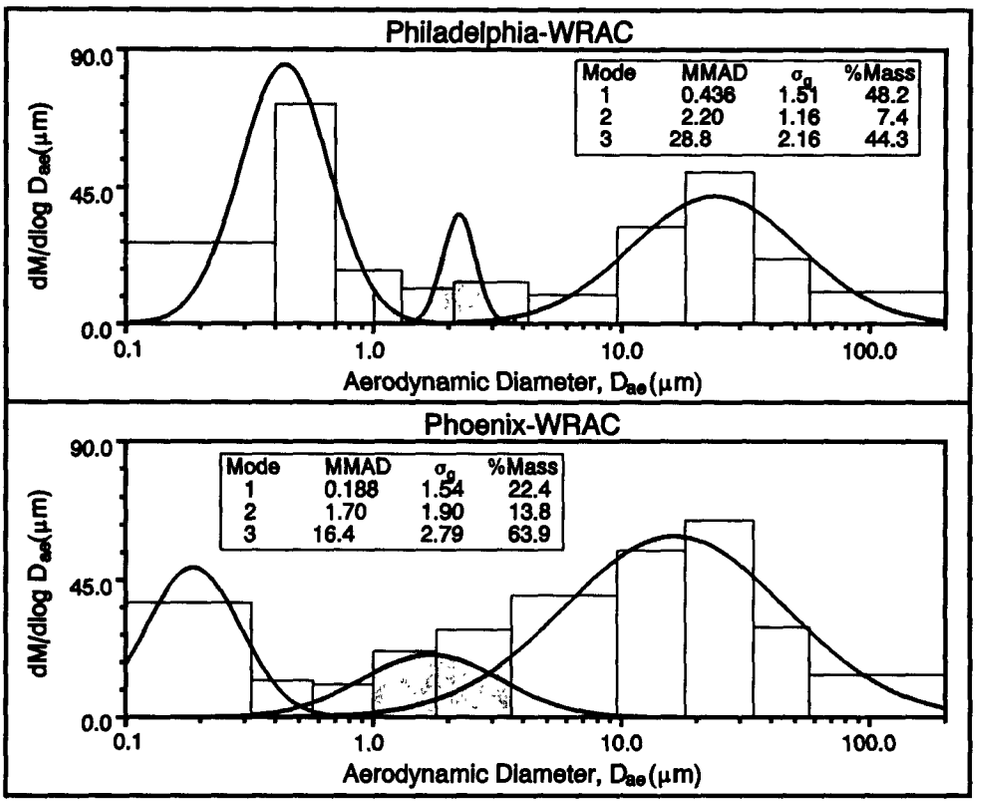

Figure 3-21. Impactor size distribution measurement generated by Lundgren et al. with the Wide Range Aerosol Classifier: (a) Philadelphia and (b) Phoenix. Note the presence of more coarse mode particles in the size range 1 to 2.5 μm, in the dryer environment of Phoenix.

Source: Adapted from Lundgren and Hausknecht, 1982b.

major portion of the coarse fraction of PM_{10}. An attempt has been made to fit the distribution with three, log-normal distributions. In this case, the fit is poor. In the Phoenix case the accumulation mode cannot be defined other than that the MMAD is below 0.2 μm. The coarse particle fractions are very wide suggesting the possibility of two or more modes (Figure 3-24). The material between 1 and 2.5 μm is not a new mode but an indication of either an artifact due to particle bounce, or a long-lasting tail of the coarse distribution.

The existing size-distribution data were recently reviewed by Lundgren and Burton (1995), with emphasis on the coarse mode. They concluded that the coarse mode could be reasonably well described by a lognormal distribution with a mass median aerodynamic diameter (MMAD) of 15 to 25 μm and a mode spread (σ_g) of approximately two. This allows one to calculate, for a freshly-generated coarse mode aerosol, that about 1% of the

mass would be less than 2.5 μm and only about 0.1% would be less than 1.0 μm in diameter. This conclusion is confirmed by data from Whitby in which a wind change allowed a measurement of fresh coarse mode aerosol (National Research Council, 1979). As can be seen in Figure 3-22, the intermodal mass, 1.0 to 2.5 μm, was not affected, even though the mass at 20 μm increased substantially.

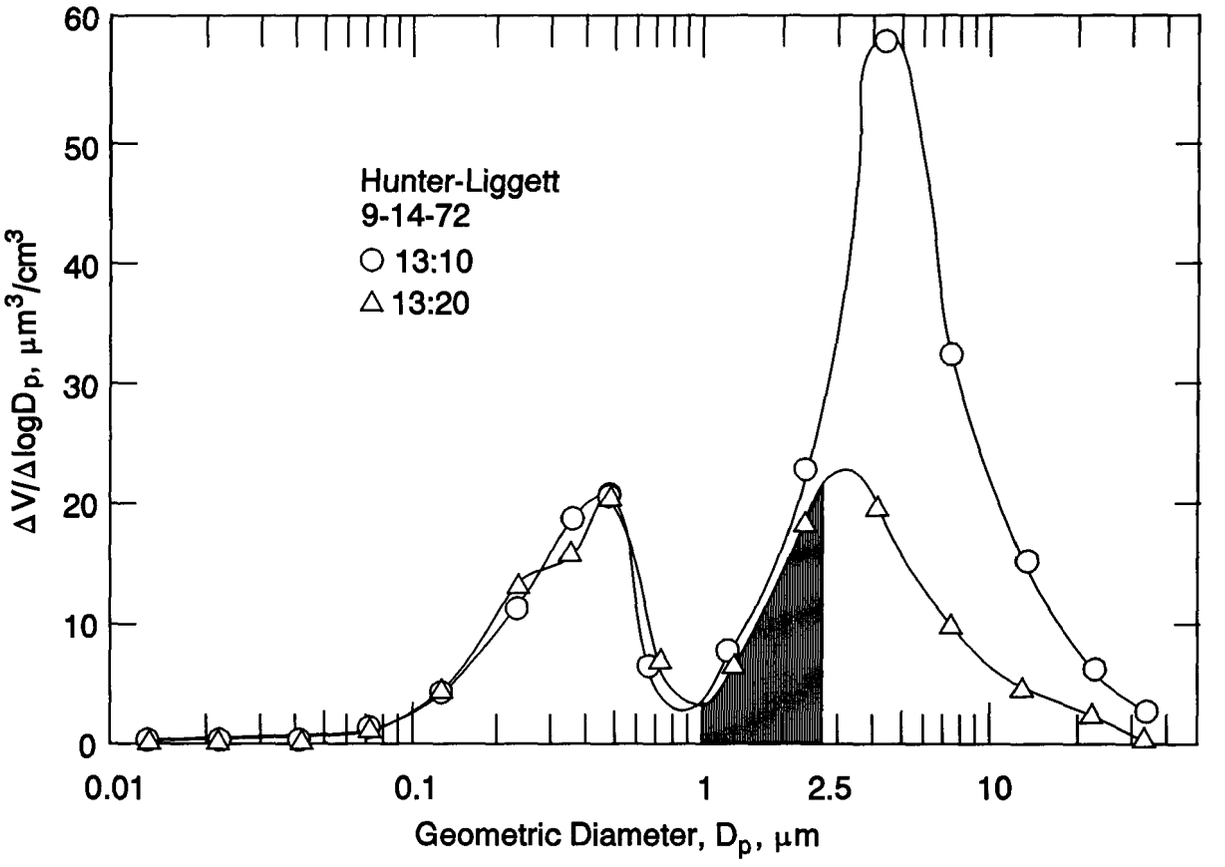

Figure 3-22. Example of aged and fresh coarse mode particle size distributions. A sudden wind change brought fresh wind-blown dust to the sampler, operated as part of the South Coast Air Quality Study. Note that there is only a very small change in the intermodal mass, 1.0 to 2.5 μm diameter, although there is a major increase in the mass between 2.5 and 10 μm in diameter.

Source: National Research Council (1979).

Another extensive set of studies covering the full size range, but limited to the Chicago area, has been reported by Noll and coworkers (Lin et al., 1993, 1994). They used an Andersen impactor for smaller particles and a Noll Rotary Impactor for larger particles. Results of Lin et al. also indicate a bimodal mass distribution. For the shorter time interval measurements (8 or 16 h), the average MMAD for the fine mode was 0.42 μm, with a σ_g around two. The average MMAD of the coarse mode was 26 ± 8 μm, with a σ_g varying from 2.0 to 3.5. As shown in Figure 3-23, the results of Noll and coworkers (Lin et al., 1993, 1994) also suggest that in some instances little coarse mode material is found in the intermodal region, 1.0 to 2.5 μm. Lin et al. (1993) combined material on the 0.65 to 1.0 μm and the 1.0 to 2.0 μm stages before weighing. Therefore, the MMAD of the accumulation mode is not as well defined as it might be, and could be smaller than that given by the fitting process. Therefore, these results cannot be used to show that some fine PM is found above 1.0 μm. When fitted to two log-normal distributions the fit is poor and the coarse mode is very wide. The fit with three log-normal distributions is used to show the possibility of particle bounce or a second mode within the coarse particle size range contributing to mass in the intermodal (1-2.5 μm) region.

3.7.6 Intermodal Region

3.7.6.1 Coarse Mode

The question then arises, what portion of the coarse mode material found in the intermodal region is real and what portion is artifact? As discussed in Section 3.3.3.2.4, the optical size may differ from the geometric or aerodynamic size. Optical counters are normally calibrated with latex particles, or other particles of a specific refractive index. Atmospheric particles with different refractive indices would be incorrectly sized if the difference in refractive index resulted in a difference in the amount of light scattered by the particles (Wilson et al., 1988; Liu et al., 1992; Hering and McMurry, 1991). For particle counters using lasers, particles of different sizes within the 0.5 to 1.0 μm range may give the same light scattering (Hering and McMurry, 1991; Kim 1995).

In the case of impactors, it is possible that an artifact may arise from particle bounce, from fragmentation of larger agglomerates, or from loosening of material from other surfaces by impacting particles. The problem of particle bounce in impactors has been treated

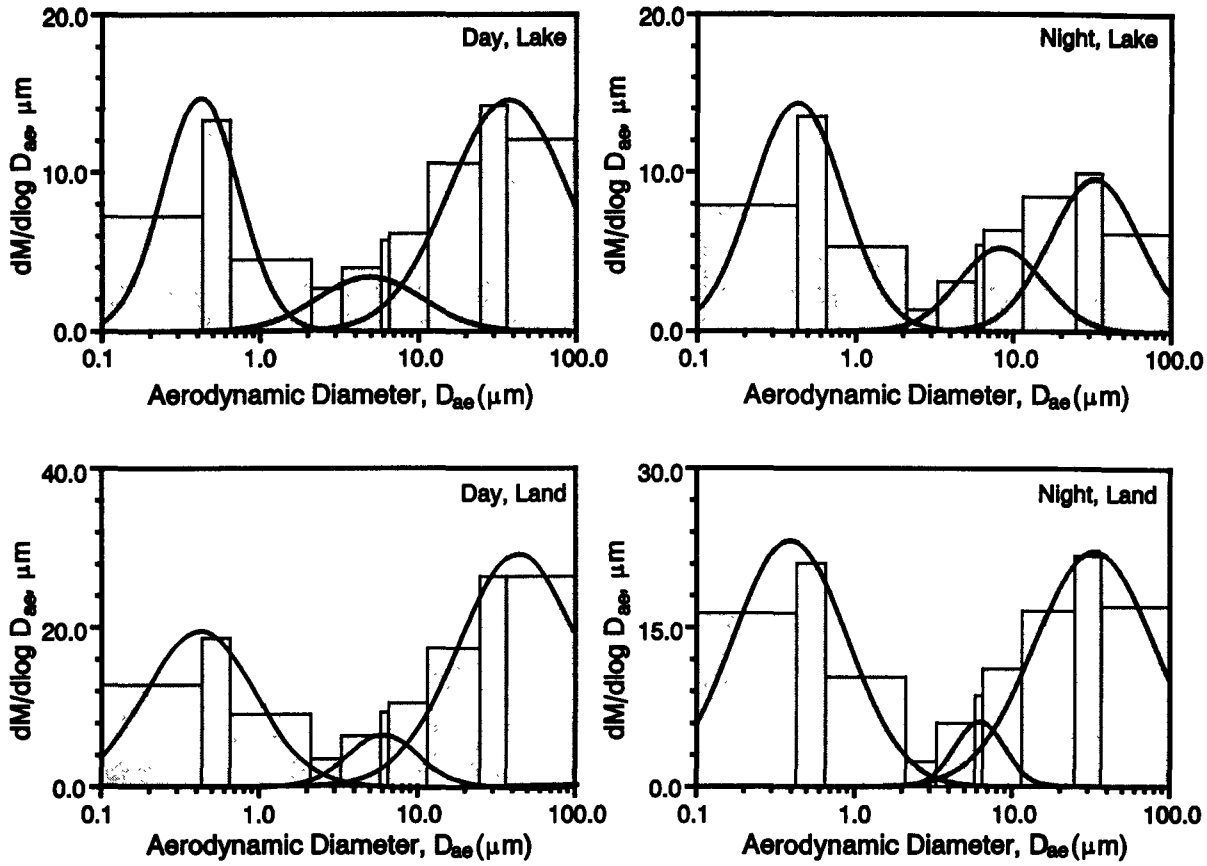

Figure 3-23. Size distributions reported by Noll and co-workers from the Chicago area using an Anderson impactor for the smaller particles and a Noll Rotary Impactor for the larger particles.

Source: Lin et al. (1993).

theoretically and practically in many studies (Wang and John, 1987, 1988). Most workers coat the coarse particle stages with a grease or oil to reduce bounce. However, as the surface becomes covered with aerosols, a particle may impact another particle instead of the surface and either bounce to a lower stage or cause deagglomeration and reentrainment of previously collected particles (John et al., 1991; John and Sethi, 1993). As impactor collection plates become loaded or as inlet upper size cut surfaces become dirty, the magnitude of the effect increases (Ranade et al., 1990; John and Wang, 1991). One result is a lowering of the effective cut point of the inlet and the impactor stages. Thus, it is uncertain how much of the mass found in the intermodal size range is real and how much is due to artifacts.

There are several reasons to believe, however, that some of the intermodal mass may be real. For example, Lundgren and Burton (1995) point out that the lifetime of particles in the atmosphere is a strong function of their aerodynamic size. Thus, while freshly generated coarse mode aerosol may have a MMAD of 20 μm, with only 1% below 2.5 μm, as the aerosol ages the larger particles will rapidly fall out, leaving a distribution enriched with particles in the small-size tail of the distribution.

A second explanation has to do with the possible multimodal nature of dust generated by wind or vehicular traffic. A study by the U.S. Army (Pinnick et al., 1985) measured the size distribution of dust generated by heavy vehicles driven on unpaved roadways in the arid southwestern United States. A variety of light-scattering instruments were used and were recalibrated for the refractive index of the soil particles. The occurrence of strong surface winds (gusts of 15 to 20 m s^{-1}) during the study permitted, in addition to the vehicular-generated dust, some measurements of windblown dust. There were some differences between sandy soil and silty soil, and between dust generated by vehicular traffic and by wind. However, all situations produced a bimodal size distributions. The upper mode had an MMAD that ranged from 35 to 53 μm, with σ_g from 1.37 to 1.68. Of particular interest, however, was a second mode having an MMAD that varied from 6.2 to 9.6 μm, with a σ_g from 1.95 to 2.20. (One measurement in silty soil had an MMAD of 19.4 μm.) The MMADs of the smaller coarse particle modes are significantly smaller than those coarse mode MMADs observed by Lundgren or Noll. An example of vehicular generated dust is shown in Figure 3-24. Note that the differential mass is plotted on a logarithmic scale. These results suggest that in arid areas, significant soil material, generated by traffic or wind, may be found in the intermodal region.

A third reason for believing that the intermodal mass is real has to do with the relative size efficiency of particle removal equipment used on power plants and other large industrial facilities. Older control devices, which may still be used in some applications, allow significant particle mass to escape. Overall mass efficiencies are approximately 80% for cyclones and 94% for scrubbers. Modern control devices have very high overall efficiencies, 99.2% for electrostatic precipitators (ESP) and 99.8% for baghouses. However, all of these devices have efficiencies for coarse particles that decrease with decreasing size. Efficiencies typically reach a minimum between 0.1 and 1 μm and increase for particles

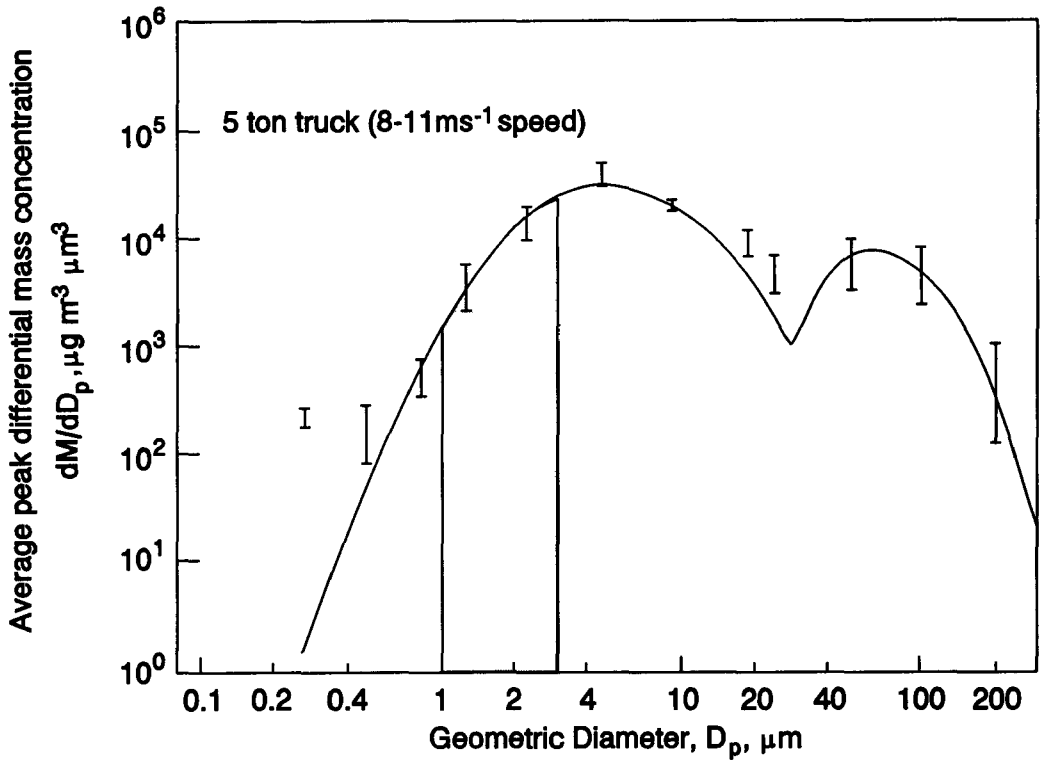

Figure 3-24. Size distribution of dust generated by driving a truck over an unpaved test track. "Error bars" show the range of distributions from individual tests. The curves shown are log-normal fits to the average distribution. The original data were plotted as log radius but have been replotted versus log diameter. The shaded bar between lines at diameters of 1.0 and 2.5 μm indicates how the smaller size mode of this dust can contribute to the intermodal mass found in arid areas (see Figures 3-21 and 3-23).

Source: Pinnick et al. (1985).

smaller than 0.1 μm. Thus, although most of the particulate mass is captured, the particles that do escape are in the smaller size range. Data from U.S. EPA, plotted in Figure 3-25, (U.S. Environmental Protection Agency, 1995) show the size distribution of fly ash from a pulverized coal power plant and the size distribution of the material escaping from the various control devices. The small-size tail of the coarse mode escapes preferentially and may possibly contribute material to the intermodal region.

Cheng et al. (1985) reported experimental measurements from an atmospheric fluidized-bed coal combustor. Size distribution measurements, made downstream of a cyclone and again downstream from baghouse filtration of the material leaving the cyclone, are shown in

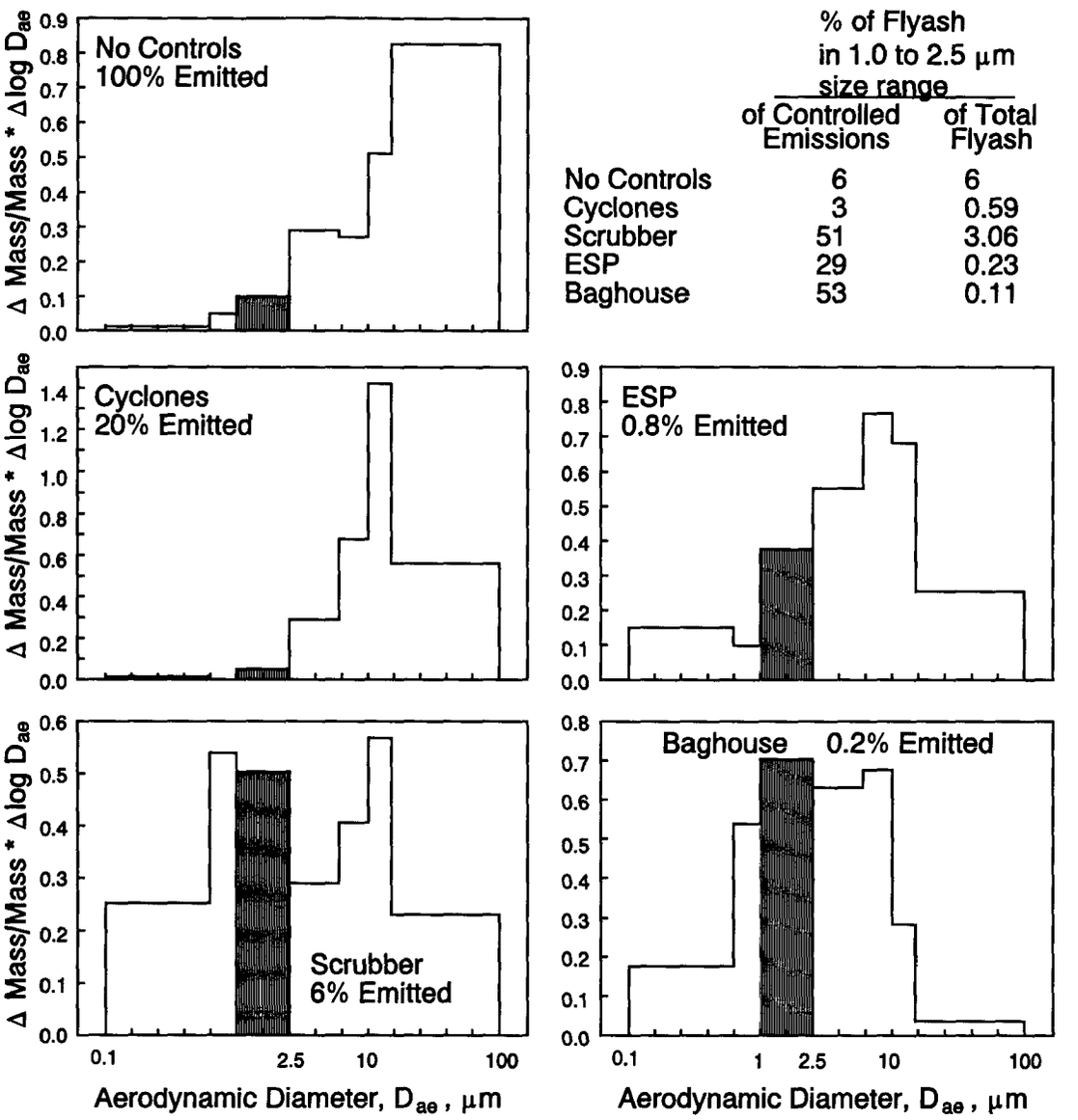

	% of Flyash in 1.0 to 2.5 μm size range of Controlled Emissions	% of Flyash in 1.0 to 2.5 μm size range of Total Flyash
No Controls	6	6
Cyclones	3	0.59
Scrubber	51	3.06
ESP	29	0.23
Baghouse	53	0.11

Figure 3-25. Size distribution of emissions from a pulverized-coal power plant and the particle size distributions remaining after several types of control devices.

Source: U.S. Environmental Protection Agency (1995).

Figure 3-26 (Cheng et al., 1985). Electron microscope photographs confirmed a fine particle mode of spherical particles between 0.1 and 0.25 μm, presumably formed from evaporation and condensation of volatile species from the coal matrix; and irregular-shaped chunks from the coarse mode with a peak concentration between 1 and 3 μm in diameter.

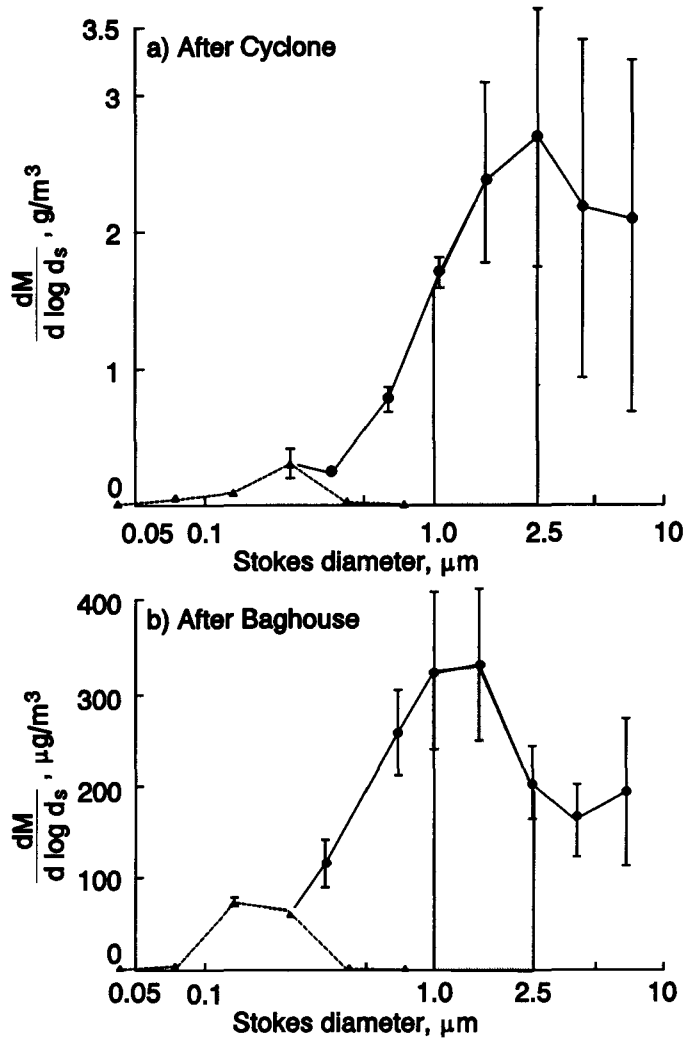

Figure 3-26. Size distributions from a fluidized-bed, pulverized coal combustor, (a) after initial cleanup by a cyclone collector and (b) after final cleanup by a baghouse.

Source: Cheng et al. (1985).

A fourth piece of evidence comes from studies in which measurements are made of the elemental composition of $PM_{2.5}$ and PM_{10} or the coarse fraction of PM_{10}. Elements representative of soil type material have been found in the $PM_{2.5}$ fraction. In a study in Philadelphia that used dichotomous samplers, an amount of soil-type material equal to 5% of the coarse mode fraction of PM_{10} was found in the $PM_{2.5}$ fraction (Dzubay et al., 1988). Since the virtual impactor used in the dichotomous sampler minimizes particle bounce and reintrainment, this would appear to be the small-size tail of the coarse mode in the 1 to

2.5 μm size range. Similar results have been reported from the IMPROVE network (Eldred et al., 1994). Elemental analysis suggested that soil-derived material, equal to 20% of the coarse fraction of the PM_{10} sample, was found in the $PM_{2.5}$ sample.

Thus, one can conclude that coarse mode material is found in the intermodal region. There are reasons to suspect that a portion of this material is an artifact but that a portion is real coarse mode material having an aerodynamic diameter between 1.0 and 2.5 μm. In either event, this can lead to a misunderstanding of the source of the particles, to inappropriate control strategies, or to exposure studies that fail to differentiate correctly between fine and coarse particles.

3.7.6.2 Fine Mode

This section discusses the source of fine mode material found in the intermodal region. Early particle-counting data suggested that, with a few exceptions, significant mass of fine mode material would not be found above 1 μm (see Figures 3-13, 3-18, 3-19, and 3-20). However, impactor studies, on some occasions, have observed significant mass on stages with a cut point of 1 μm. In some instances, the MMAD of the fine mode was as large as 1 μm (John et al., 1990). The change in relative humidity produced by a few degrees change in temperature can significantly modify the MMAD of an ambient aerosol size distribution. As the RH approaches 100%, accumulation mode aerosols, with dry sizes below 1.0 μm in diameter, may grow larger than 2.5 μm in diameter, be rejected by $PM_{2.5}$ samples, and be counted as coarse particles.

Before examining additional field data demonstrating the effect of relative humidity on particle size, it is useful to review some basic information on the interaction of water vapor with the components of fine particles. Sulfuric acid (H_2SO_4) is a hygroscopic substance. When exposed to water vapor a H_2SO_4 droplet will absorb water vapor and grow in size until an equilibrium exists between the liquid water concentration in the H_2SO_4 solution droplet and the water vapor concentration in the air. The amount of water in the sulfuric acid droplet will increase and decrease smoothly as the RH increases and decreases. Ammonium sulfate, $(NH_4)_2SO_4$, however, is deliquescent. If initially a crystal in dry air, it will remain a crystal until a certain RH is reached; at this point it will absorb water and become a solution droplet. The RH at which this happens, $\approx$ 80% RH in the case of

$NH_4)_2SO_4$, is called the deliquescent point. At RH's above the deliquescent point the $(NH_4)_2SO_4$ droplets are hygroscopic, gaining or losing water reversibly as the RH increases or decreases. If the RH decreases below the deliquescent point the solution droplet becomes supersaturated and unstable to crystallization. However, sub-micron sized droplets will remain supersaturated until a significantly lower RH, known as the crystallization or efflorescent point is reached. The crystallization point decreases with decreasing droplet size and decreasing purity (Whitby, 1984). Thus, for a deliquescent substance, a plot of droplet diameter or water content as a function of RH will have two lines, one for increasing RH and another for decreasing RH. An example of this phenomenon, known as hysteresis, is shown in Figure 3-27. Table 3-16 shows the RH at the deliquescent and crystallization points for some compounds found in the atmosphere.

Much experimental and theoretical effort has gone into understanding this process. The basic theory was elucidated by Hänel (1976). Much experimental work has been done on atmospheric species (e.g., Tang and Munkelwitz, 1977, 1993; Richardson and Spann, 1984). The electrodynamic balance, by which single particles can be studied, has advanced the understanding of particle-water vapor equilibrium, especially for particles in metastable states, e.g., the supersaturated solution particles which are responsible for the hysteresis loop shown in Figure 3-27 (Cohen et al., 1987a,b; Chan et al., 1992; Kim et al., 1994). Ammonium nitrate, NH_4NO_3, because of its volatility, is difficult to handle but has been studied successfully by Richardson and Hightower (1987). The aerosol equilibria models developed by Seinfeld and co-workers allow calculation of the water content of bulk solution as a function of relative humidity (Kim and Seinfeld). The model SCAPE (Kim et al., 1993a,b) has been used to estimate the contribution of water to suspended aerosol mass in the California South Coast Air Basin using particle composition data from the 1987 Southern California Air Quality Study (Meng et al., 1995). From midnight to early morning, when the temperature is low and relative humidity is high, water was usually the predominant aerosol substance. Particulate water in the winter was estimated to be considerably larger than in the summer at each of the four sites studied.

The water content of a sub-micron sized droplet, and therefore its size, depends not only on the dry size but is a result of a balance between surface tension and solute concentration (Li et al., 1992). Pure water is in equilibrium with its vapor when the RH

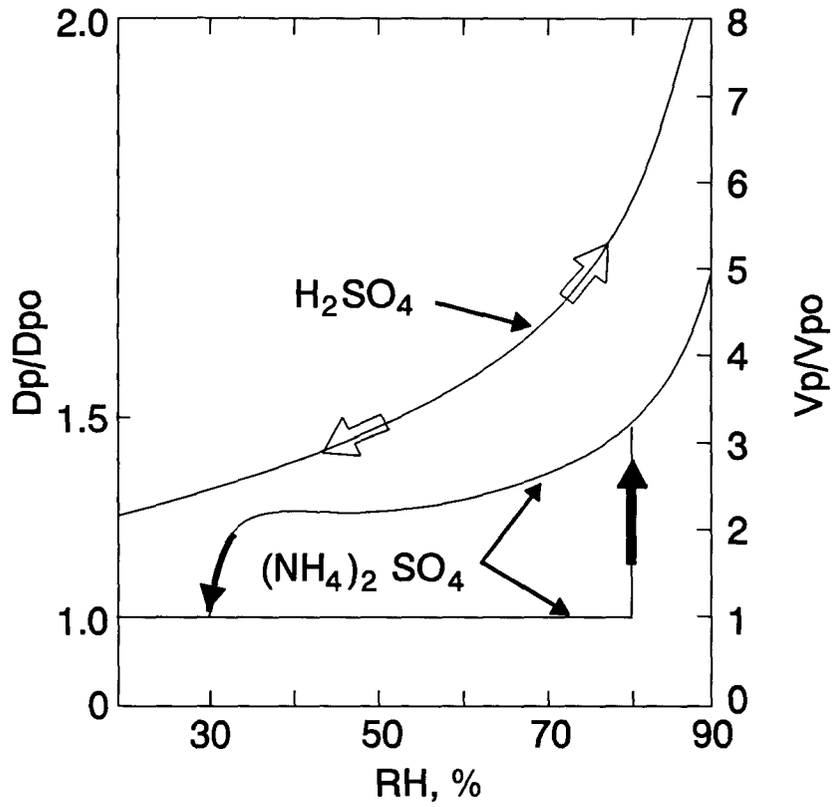

Figure 3-27. Particle growth curves showing fully reversible hygroscopic growth of sulfuric acid (H_2SO_4) particles, deliquescent growth of ammonium sulfate [$(NH_4)_2$ SO_4] particles at about 80% relative humidity (RH), hygroscopic growth of ammonium sulfate solution droplets at RH greater than 80%, and hysteresis (the droplet remains supersaturated as the RH decreases below 80%) until the crystallization point is reached.

Source: National Research Council (1993) adapted from Tang (1980).

TABLE 3-16. RELATIVE HUMIDITY OF DELIQUESCENCE AND CRYSTALLIZATION FOR SEVERAL ATMOSPHERIC SALTS[a]

Compound	Deliquescence	Crystallization[c]
$(NH_4)_2SO_4$	79.9 ± 0.5	37 ± 2
NH_4HSO_4	39.0 ± 0.5[b]	
NH_4NO_3	61.8	
NaCl	75.3 ± 0.1	42

[a]Taken from Tang and Munkelwitz (1993) unless otherwise indicated.
[b]Tang and Munkelwitz (1977).
[c]Shaw and Rood (1990) and references therein.

equals 100% and is therefore, stable, i.e. the rate of evaporation equals the rate of condensation. The water in a solution will be in equilibrium with water vapor at a lower water vapor concentration because the presence of solute molecules or ions lower the rate of evaporation. Therefore, a solution will absorb water and become more dilute, increasing the water vapor concentration needed for equilibrium until the solution water vapor concentration required for equilibrium matches the ambient water vapor concentration or RH. As the droplet size decreases the surface tension increases and the vapor pressure of water required to maintain equilibrium increases. Therefore, the smaller the dry size of the particle, the less the amount of growth as RH increases.

Theoretical calculations of the growth of various sizes of ammonium sulfate particles and an experimental verification of such calculations, using a simulation of the humidification process in the human lung, are shown in Figure 3-28. Note the very rapid increase in the amount of water and in the diameter of the aerosol particle as the relative humidity approaches 100% RH. Considering the difficulty of measuring relative humidity accurately between 99 and 100%, theory and experiment are in reasonable agreement. As can be seen the effect of surface tension is most important for particles with dry size less than 100 nm (0.1 μm). This phenomenon may be of importance in considering the biological effect of water-soluble pollutants. Accumulation mode particles will be diluted when exposed to humidification in the lungs. Ultrafine or nuclei mode particles will not be diluted as much. In the atmospheric aerosol the number distribution will almost always be dominated by particles below 100 nm (see Section 3.1.2). However, aerosols generated in the laboratory for exposure studies probably lack the smaller particles found in the atmosphere. This provides a hypothesis for the difference in effects observed in epidemiological studies and laboratory exposure studies. The importance of this more concentrated, ultrafine droplet component of the atmospheric aerosol may have been neglected because most of the experimental studies of hygroscopicity have used near-micron-sized particles. However, in the modeling of deposition of hygroscopic particles, workers, such as Martonen (1993), have corrected the experimental curves of particle size as a function of RH, based on measurements of near micron-sized particles, to account for the effects of surface tension on ultrafine particles.

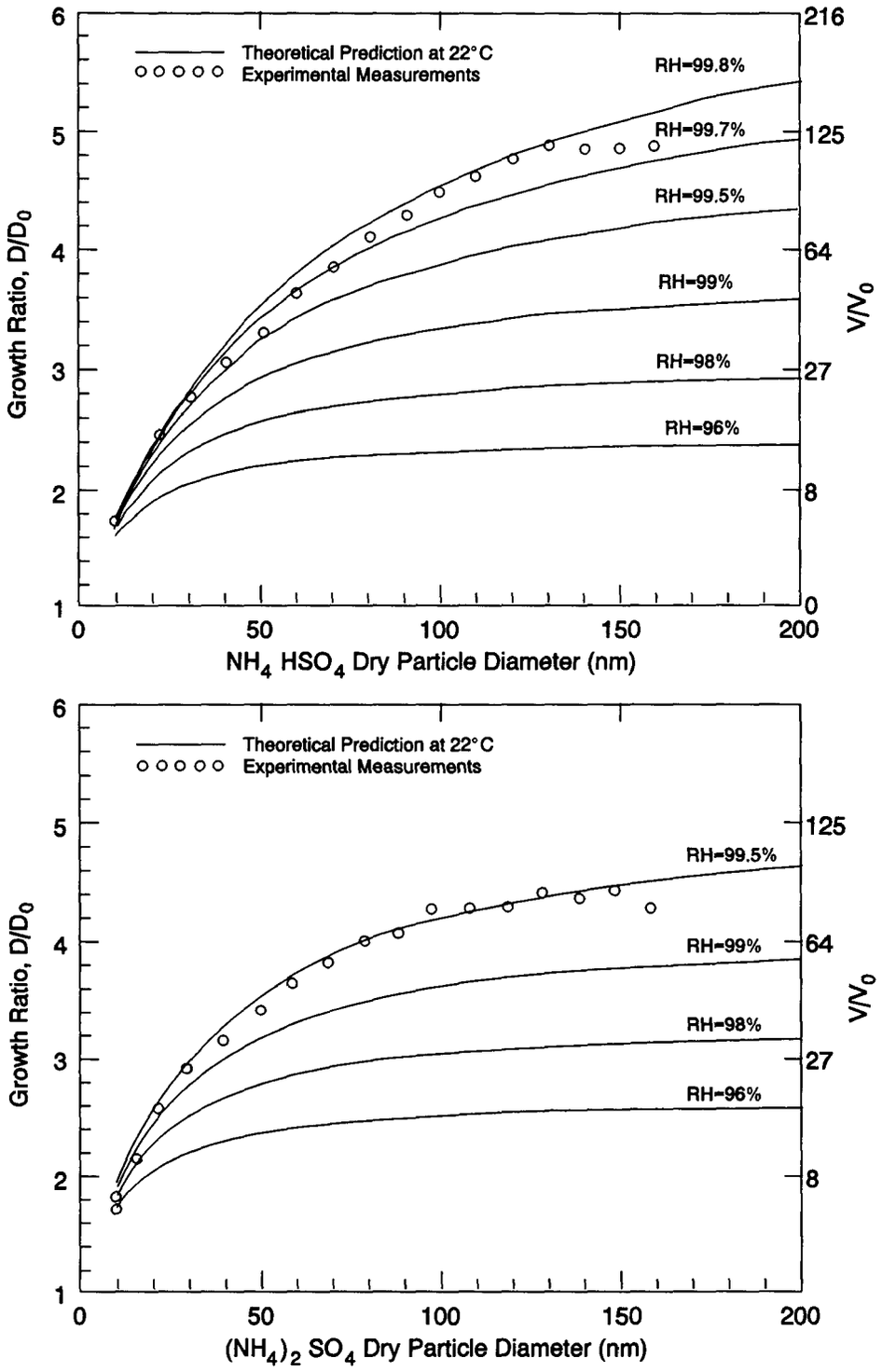

Figure 3-28. Theoretical predictions and experimental measurements of growth of NH_4HSO_4 and $(NH_4)_2SO_4$ particles at relative humidity between 95 and 100%.

Source: Li et al. (1992).

In addition to the laboratory studies discussed above there are some measurements on the effect of RH changes on atmospheric aerosol. McMurry and co-workers have made use of a Tandem Differential Mobility Analyzer (TDMA) system (Rader and McMurry, 1986) to measure the change in particle size with changes in relative humidity at Claremont, CA, as part of the Southern California Air Quality Study (SCAQS) (McMurry and Stolzenberg, 1989) and at the Grand Canyon National Park, AZ, as part of the Navajo Generating Station Visibility Study (Zhang et al., 1993; Pitchford and McMurry, 1994). One mobility analyzer is used to isolate a narrow size distribution. After humidification the size distribution of this fraction is measured. An example is shown in Figure 3-29. Note that Figure 3-29 is a number size distribution not a mass size distribution. Particle growth with increasing RH is evident. However, between 70 and 91% RH the distribution splits into less-hygroscopic and more-hygroscopic components. Pitchford and McMurry (1994) attribute this splitting to external mixing, i.e. there are two relatively distinct classes of particles, both containing some soluble and some non-soluble material, with the more hygroscopic component containing significantly more soluble and hygroscopic material. A summary of the results of these studies is given in Table 3-17 (Zhang et al., 1993). The difference in growth rates may be due both to size and to variation in composition as a function of size. The lower growth factor for 0.2 μm particles in Claremont relative to the Grand Canyon may be due to a higher concentration of non-soluble organic material in Claremont.

While there is a significant amount of information on the hygroscopic properties of inorganic compounds, much less is known about the hygroscopic properties of organic components of the atmospheric aerosol. Saxena et al. (1995) have examined the hygroscopic properties of several organic species and noted that water soluble organics may be hygroscopic or deliquescent. Using concurrent cascade impactor samples, they determined the composition of the Grand Canyon and Claremont aerosol, whose size distribution as a function of relative humidity was discussed above. They compared the observed water content at the higher relative humidity with the water content calculated for the inorganic components. They concluded "that the aggregate hygroscopic properties of inorganic particles are altered when organics are also present. Furthermore, the alterations can be positive or negative. The findings are consistent with the expectation that organics are

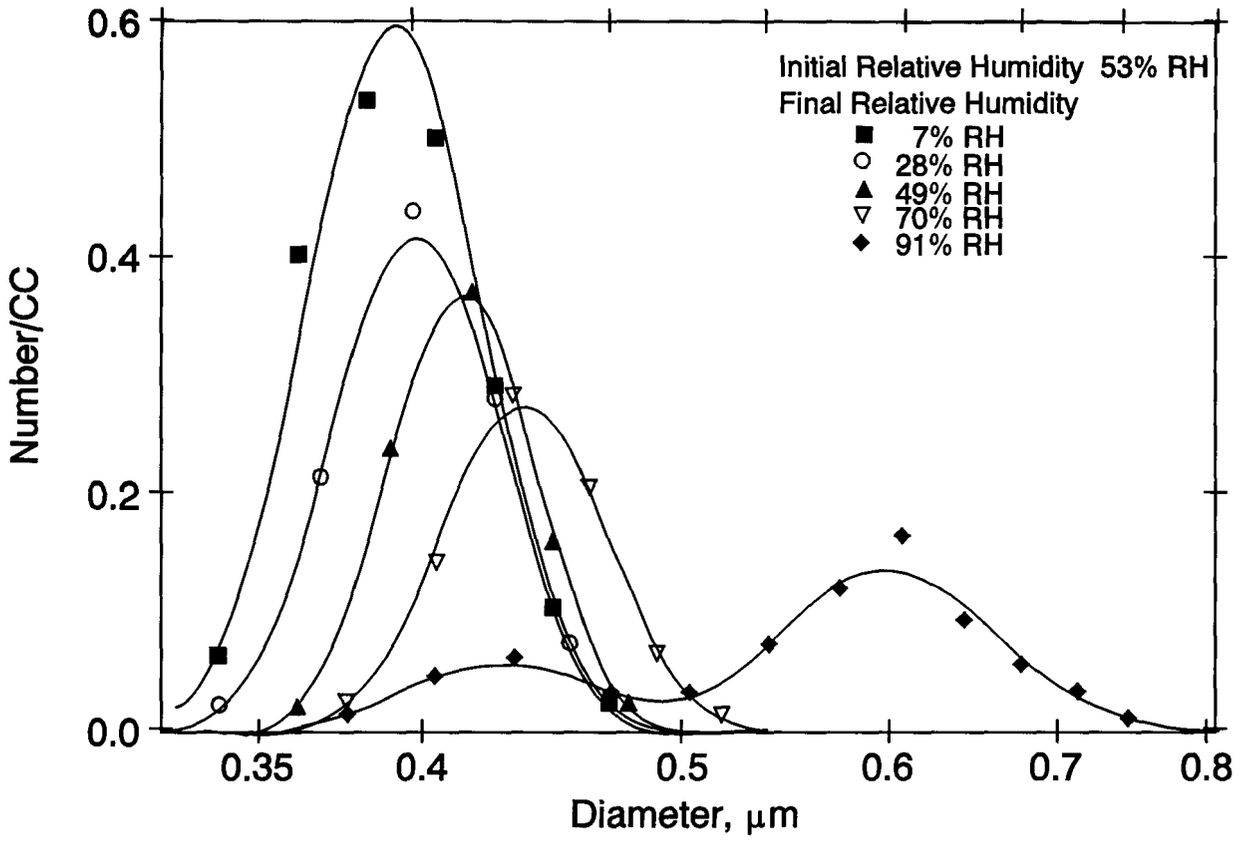

Figure 3-29. Tandem Differential Mobility Analyzer measurements of the sensitivity of particle size to relative humidity at Claremont, CA. Particle number concentrations varied during the measurement, therefore changes in relative size with humidity are meaningful but changes in number concentration are not.

Source: McMurry and Stolzenberg (1989).

predominantly secondary (and thus likely to be hydrophilic) in nonurban areas and predominantly primary (and hence hydrophobic) in urban areas".

Some experimental examples of the significant effect of relative humidity on ambient aerosol size distributions are shown in Figure 3-30 (Lowenthal et al., 1995). In this work, impactor collection and ion chromatographic analysis were used to measure sulfate size distributions over short enough periods to demonstrate the effects of changing relative humidities. The results suggest that the lognormal distribution is preserved as relative humidity increases, but that the MMAD increases. This effect is especially pronounced as the relative humidity approaches 100%.

TABLE 3-17. SUMMARY OF HYGROSCOPIC GROWTH FACTORS[a]

	1987 SCAQS, Claremont, CA	
Dry Size (μm)	More Hygroscopic Peak $\frac{D_p(90 \pm 3\%\ RH)}{D_p(0\%\ RH)}$	Less Hygroscopic Peak $\frac{D_p(87 \pm 2\%\ RH)}{D_p(0\%\ RH)}$
0.05	1.14 ± 0.05	1.03 ± 0.03
0.2	1.23 ± 0.08	1.02 ± 0.02
0.4	1.63 ± 0.11	1.04 ± 0.05
0.5	1.59 ± 0.08	1.07 ± 0.03

	1990 NGS Visibility Study, Grand Canyon, AZ	
Dry Size (μm)	More Hygroscopic Peak $\frac{D_p(89 \pm 4\%\ RH)}{D_p(0\%\ RH)}$	Less Hygroscopic Peak $\frac{D_p(89 \pm 4\%\ RH)}{D_p(0\%\ RH)}$
0.05	1.36 ± 0.08	1.14 ± 0.10
0.10	1.42 ± 0.08	1.17 ± 0.09
0.20	1.49 ± 0.11	1.17 ± 0.10
0.30	1.51 ± 0.09	1.14 ± 0.10
0.40	1.43 ± 0.10	1.07 ± 0.03

[a]Values are mean ± standard deviations.

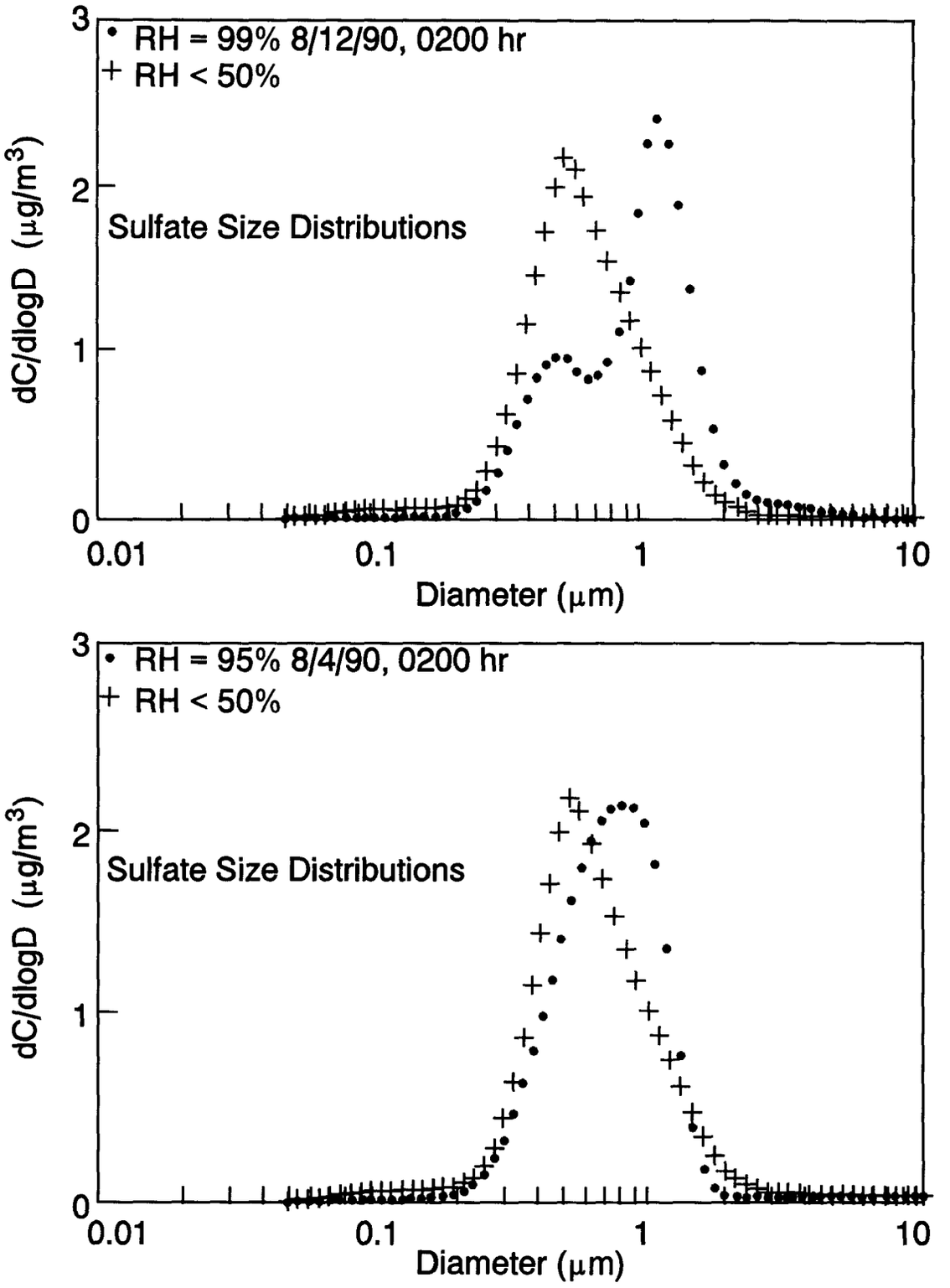

Figure 3-30. Example of growth in particle size due primarily to increases in relative humidity from Uniontown, PA.

Source: Lowenthal et al. (1995).

There are also studies of the behavior of ambient aerosols as the relative humidity is reduced by heating the sampled air. Shaw and Rood (1990) report a study using a heated integrating nephelometer in which crystallization RHs of 4 to 67% were observed. Similar studies in Washington, D.C. by Fitzgerald et al. (1982) found no evidence of crystallization or efflorescence when RH was reduced to 30% RH.

Further experimental evidence of the effect of decreasing relative humidity on aerosol size distribution is provided by impactor data reported by Berner (1989) and is shown in Figure 3-31. One impactor sampled aerosol in its humidified state directly from the atmosphere. The inlet of a second impactor was warmed ≈ 7 °C above the ambient temperature of ≈ 5 °C in order to evaporate most of the particle-bound water before collecting the aerosol. The water and other volatile material in both the "wet" and the "dry" samples would evaporate in the laboratory prior to weighing the impactor stages. As can be seen, in the ambient air most of the non-volatile mass was above 1.0 μm with significant amounts above 2.5 μm. However, after heating the size of the aerosol was reduced so that most of the non-volatile mass was below 1.0 μm. Berner treated the distributions as monomodal and derived growth factors of 4.9 for fog and 4.1 for haze. If the observations are treated as multimodal, good bimodal, or as shown in Figure 3-31, trimodal fits are obtained. This splitting into "more" and "less" hygroscopic modes at high relative humidity has been observed by McMurry and co-workers (McMurry and Stolzenberg, 1989; Zhang et al., 1993) (Figure 3-29) and Lowenthal et al. (1995) (Figure 3-30). In some cases, reported by Pitchford and McMurry (1994), splitting into three modes of varying hygroscopicity was observed. However, the separation into two "more" hygroscopic modes may represent, as suggested by Berner, variations in relative humidity extremes during different parts of the overnight sampling period.

In measuring light scattering with the integrating nephelometer, the aerosol community has been very concerned about the difference in relative humidity and temperature in the ambient air and in the volume of air in which particle scattering is actually measured (Covert et al., 1972; Fitzgerald et al., 1982). Temperature differences between the measurement volume and ambient air of 1 or 2 °C can change the relative humidity and change the observed light scattering. Great efforts have been made to minimize this temperature

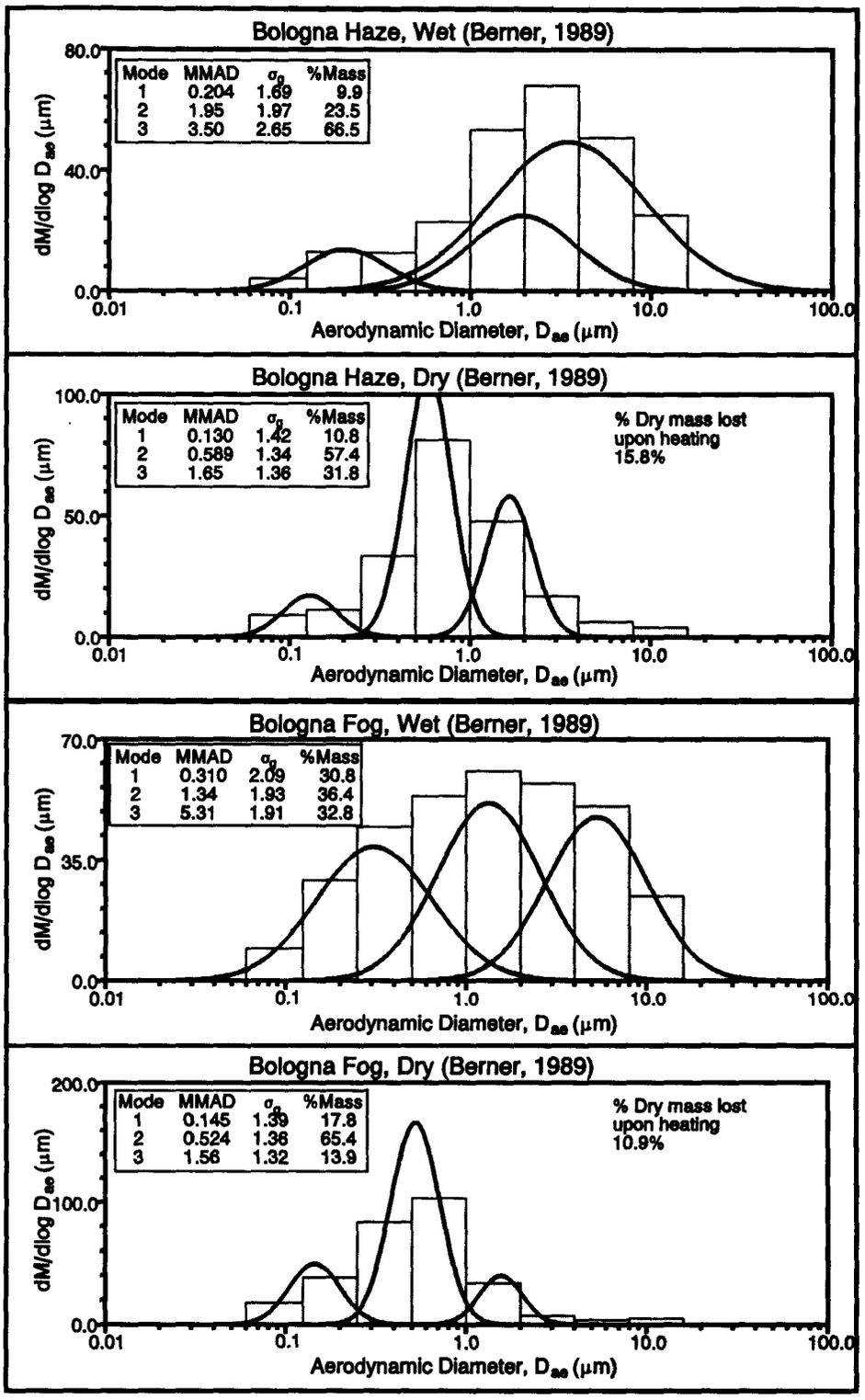

Figure 3-31. Mass size distribution of non-volatile aerosol material. The aerosol was collected at ambient conditions, "wet", or after evaporation of water, "dry".

Source: Berner (1989).

difference. However, researchers have not been nearly as careful in considering temperature and relative humidity effects when measuring size distribution, either with impactors or particle counters, even though effects have been reported in the early literature (Wagman et al., 1967; Sverdrup and Whitby, 1980).

A recent paper by Cass and coworkers (Eldering et al., 1994) provides some insight into how differences in RH resulting from heating can cause differences between particle-counting distributions and impactor distributions. Particle size distributions were obtained by counting particles by mobility (electrical aerosol analyzer) and light scattering (optical particle counter). An example is shown in Figure 3-32. Almost no particles were found between 1.0 and 2.5 μm diameter. When these particle number data were converted to total expected light scattering, they agreed with measurements made by a heated, but not an unheated, integrating nephelometer; and when converted to expected mass, agreed with filter measurements of dry mass. Eldering et al. (1994) conclude that even the moderate heating occurring in mobility and optical counters was enough to change the size of the particles, especially when the ambient air was close to 100% RH. It seems likely that most particle counting systems produce some heating of the aerosol, and thus some reduction of the measured particle size from that existing in the ambient air. On the other hand, if particle-size measuring devices were located in air conditioned or heated trailers or laboratories, the temperature of the sampled air would be changed and the measured particle size distribution would be different from that existing in the ambient air (Sverdrup and Whitby, 1980).

During the high relative humidities that occur at nighttime, growth of hygroscopic components can result in the growth of some fine mode aerosol to diameters greater than 1.0 μm and perhaps even above 2.5 μm. As can be seen in Figure 3-28, dry ammonium sulfate particles having a dry diameter of 0.5 μm will grow to $\approx$2.5 μm at a relative humidity between 99 and 100%. When the relative humidity actually reaches 100%, the particles will continue to grow to maintain the relative humidity at 100%, and eventually become fog droplets that are large enough to be collected in the fraction larger than 2.5 μm. Ammonium sulfate particles with dry sizes greater than 0.5 μm would also grow into the larger than 2.5 μm size range.

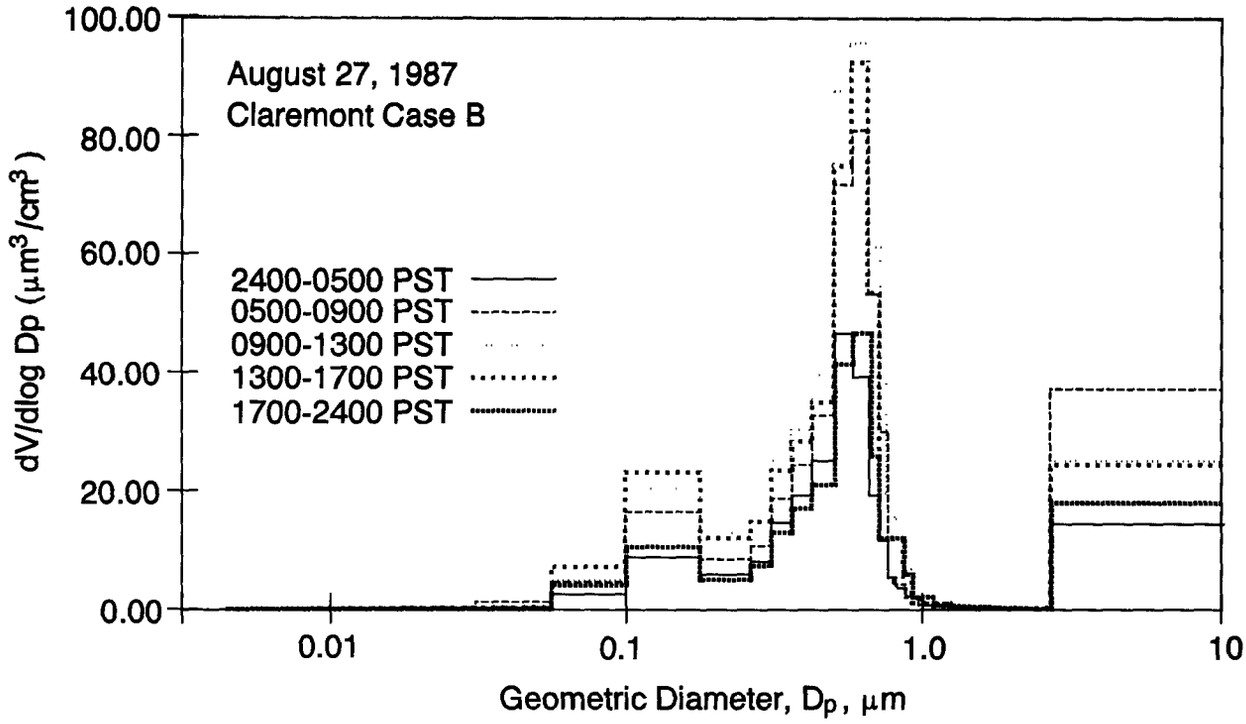

Figure 3-32. Example of particle-counting volume distribution obtained in Claremont, CA. Compare to Figures 3-14 and 3-31. Heating of the sampled air by the mobility and optical counters are believed to have resulted in a distribution representative of a lower than ambient relative humidity.

Source: Eldering et al. (1994).

The addition of water to hygroscopic particles, discussed in the previous section, is a reversible process. Particles absorb water and grow as RH increases; as RH decreases some of the particle-bound water evaporates and the particles shrink. However, the large amount of liquid water associated with hygroscopic particles at high relative humidity provides a medium for liquid phase transformation process. A number of atmospheric process, which convert SO_2 to sulfate or NO_x to nitrate, can take place in water solutions but not in the gas phase. These processes are not reversible but lead to an accumulation of sulfate or nitrate and lead to an increase in the dry size of the particle. Of course as more sulfate or nitrate is added to the particle it will absorb more water so that the wet size will also increase.

The first observation and clear discussion of these combined effects of relative humidity on growth and SO_2 conversion to sulfate are given by Hering and Friedlander (1982) as

shown in Table 3-18. Using a low pressure impactor, they observed that days with higher relative humidity had higher sulfate concentration and higher MMAD's compared to days with lower relative humidity. Hering and Friedlander (1982) named the small mode the condensation mode and suggested that it was formed by the gas phase conversion of SO_2 to sulfate and subsequent nucleation, coagulation, and growth by condensation. They named the larger mode the droplet mode and discussed possible formation mechanisms. This mode is now believed to result from the reaction of SO_2 in fog or cloud droplets (Meng and Seinfeld, 1994).

TABLE 3-18. COMPARISON OF SULFATE CONCENTRATION AND MASS MEAN DIAMETERS OF AEROSOLS FOR DAYS WITH HIGHER AND LOWER RELATIVE HUMIDITY

	Low RH Days	High RH Days
Minimum RH, %	17 - 35	26 - 66
Maximum RH, %	45 - 68	69 - 100
Sulfate concentration, $\mu g/m^3$	3 - 9	3 - 52
Mass median aerodynamic diameter, μm	0.20 ± 0.02	0.54 ± 0.07

Source: Hering and Friedlander (1982).

In a series of papers McMurry and co-workers make use of the aerosol growth law, originally developed by Heisler and Friedlander (1977), to study the mechanism and rates of sulfate formation in ambient air (McMurry et al., 1981; McMurry and Wilson, 1982, 1983). They were able to apportion growth to condensation and droplet mechanisms and observed droplet growth in particles up to 3 μm in diameter.

A process of aerosol growth due to increasing relative humidity (Figure 3-33) has also been utilized by Cahill et al. (1990) to explain observations of sulfate size changes during the 1986 Carbonaceous Species Methods Comparison Study in Glendora, CA. Cahill used a DRUM sampler to measure sulfate in nine size ranges. By tracking the mass of sulfate in the 0.56 to 1.15 μm size range Cahill et al. could follow the expansion and contraction of aerosol particles containing sulfate. Because of the relative high time resolution of the DRUM sampler (4 h except for an 8-h increment each night from midnight to 8 a.m.),

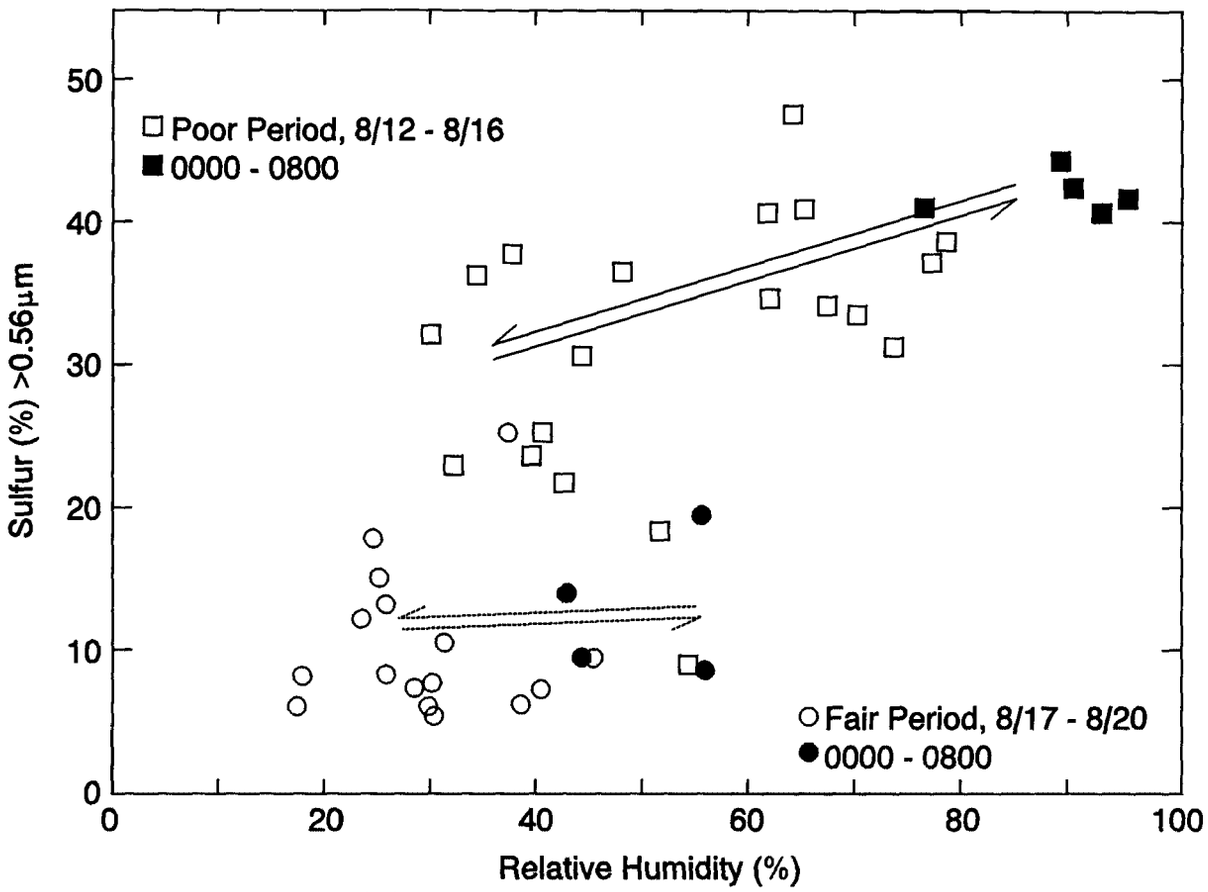

Figure 3-33. Relative humidity versus sulfur, during the 1986 Carbonaceous Species Methods Comparison Study, for particles with $D_{ae} > 0.56$ μm. The approximate trajectories followed during each day by the $D_{ae} > 0.56$ μm sulfur size fraction are shown for period P and period F. Note that even when the humidities are low, 30 to 50 %, the period P aerosols remain coarser by a factor of three than those of period F. The water content incorporated in the aerosols during the 0000- to 0800-h time periods is lost only slowly, giving a strong hysteresis effect in sulfur size.

Source: Cahill et al. (1990).

Cahill et al. (1990) could follow this process as the relative humidity increased during the night and decreased during the day. These data indicate that during the "Poor Period" (low visibility) particles grow as relative humidity increases. However, they did not return to the smaller size observed during the "Fair Period" (good visibility). This could be due to a combination of growth due to reaction of SO_2 to sulfate within the particles or failure of the droplet to crystallize thus maintaining particle-bound water in a supersaturated state.

John et al. (1990), in studies in the Los Angeles area, observed a number of sulfate size distributions with MMAD near 1.0 μm. A histogram of the sulfate MMADs from his study is shown in Figure 3-34. John et al. (1990) have provided a qualitative explanation to account for these large MMADs for fine mode aerosol. In analyzing their data John et al. plotted sulfate mass as a function of sulfate MMAD and found two distinct regions, as shown in Figure 3-35. Distributions with particles near 0.2 μm diameter are probably still dry; the particles have not reached their deliquescent point. As the relative humidity increases they reach their deliquescent point and grow rapidly into the 0.5 to 0.7 μm size range. During the formation of fog, the hygroscopic particles act as fog condensation nuclei, and with relative humidity at 100%, grow into 1 to 10 μm fog droplets. Sulfur dioxide dissolves in the fog droplets and is rapidly oxidized to sulfate by atmospheric oxidants such as H_2O_2 or O_3, or by catalysis by Fe or Mn. These particles lose some of their water as the relative humidity decreases below 100% RH, but will have substantially more sulfate than prior to activation. Similar processes occur in clouds (Schwartz, 1984a, 1986a).

This type of process probably accounts for the large size of the fine mode observed in Vienna (Berner et al., 1979; Berner and Lürzer, 1980). Winter and summer size distributions are shown in Figure 3-36. Berner et al. reported that fog occurred during the night time during the winter study. In this European study, as in American studies, instances of fine mode size distributions with MMADs near or above 1 μm seem to occur only when fog or very high relative humidity conditions have been present. Two log-normal distributions are fit to the accumulation mode to suggest the separation, at high relative humidity, into hygroscopic and hydrophobic components. No distribution was fit to the coarse mode because only a fraction of the coarse size range was measured.

Similar results have been observed in sampling with dichotomous samplers. A large humidity driven shift of normally fine mode material into the coarse mode was observed by Keeler et al. (1988). In the extreme case, 60% of the $SO_4^=$ and 50% of the $PM_{2.5}$ mass was shifted to the coarse fraction. Such occurrences were not rare, occurring in 12 out of 83 several-hour sampling periods.

In an analysis of data from the IMPROVE network Cahill and co-workers (Eldred et al., 1994) report that 20% of the total sulfate is found in the coarse fraction of PM_{10}. Studies in Philadelphia using dichotomous samplers have also reported that 20% of the total

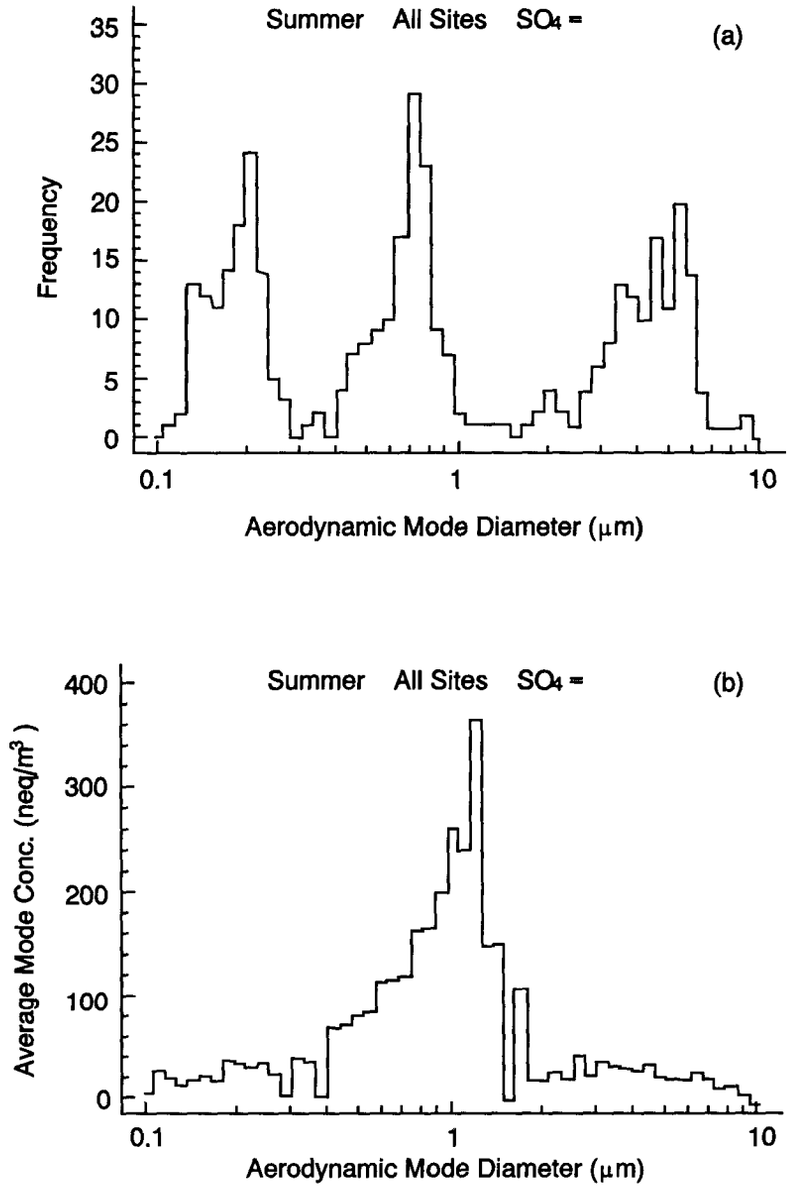

Figure 3-34. **Data from the South Coast Air Quality Study (John et al., 1990). Plots show (a) frequency of sulfate modes of various sizes as a function of mode diameter and (b) average sulfate mode concentration as a function of mode diameter. Note that although there are only a few instances when the mode diameter is near 1.0 μm, it is these situations that give rise to the highest sulfate concentrations. Modes with diameters above 2.5 μm may be due to collection of fog droplets containing sulfate or reaction of SO_2 in liquid droplets of NaCl due to NaCl sea spray droplets in which SO_2 has dissolved and reacted to form sulfate and release HCl gas.**

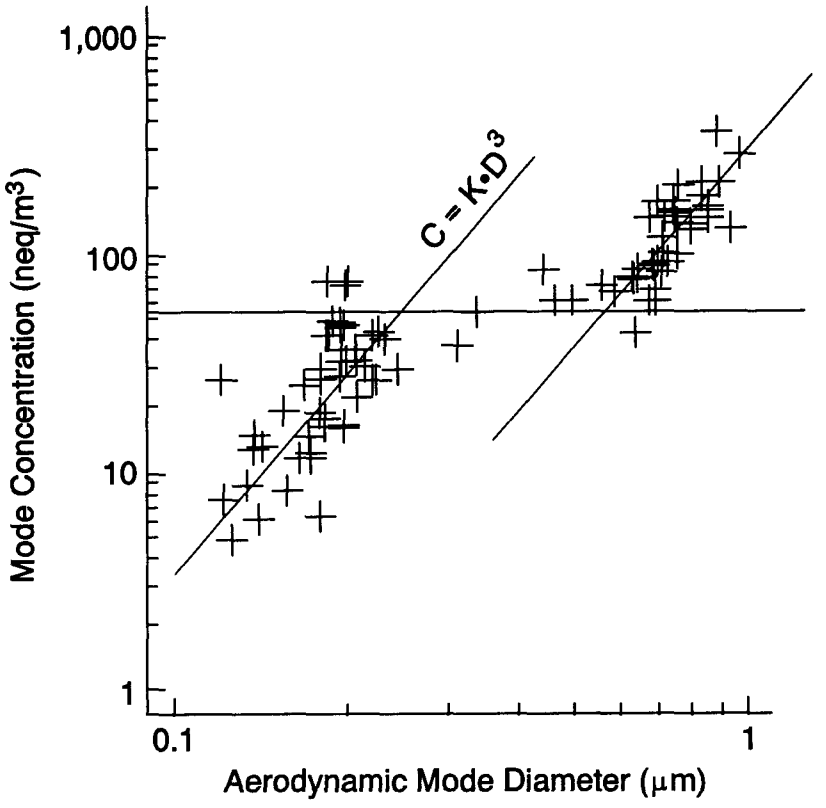

Figure 3-35. Log-log plot of sulfate mode concentration versus aerodynamic mode diameter from Claremont, CA, during the summer SCAQS (John et al., 1990). The solid lines have slopes corresponding to mode concentration increasing with the cube of the mode diameter. A transition between the two modes is believed to occur at approximately the sulfate mode concentration indicated by the horizontal dashed line.

sulfate is found in the coarse fraction (Dzubay et al., 1988). Cahill and coworkers suggest that sulfate particles may grow larger than 2.5 μm in diameter and thus be sampled in the PM_{10} fraction but not the $PM_{2.5}$ fraction. It is possible for SO_2 to react with basic carbonate coarse particles to form a sulfate coating or to dissolve in wet NaCl particles, from oceans, lakes, or salt placed on streets to dissolve ice, and be converted to sulfate with the release of HCl. However, there also is substantial evidence that some fine sulfate, and therefore possibly other fine mode material, may be found in the size range above 1.0 μm and even

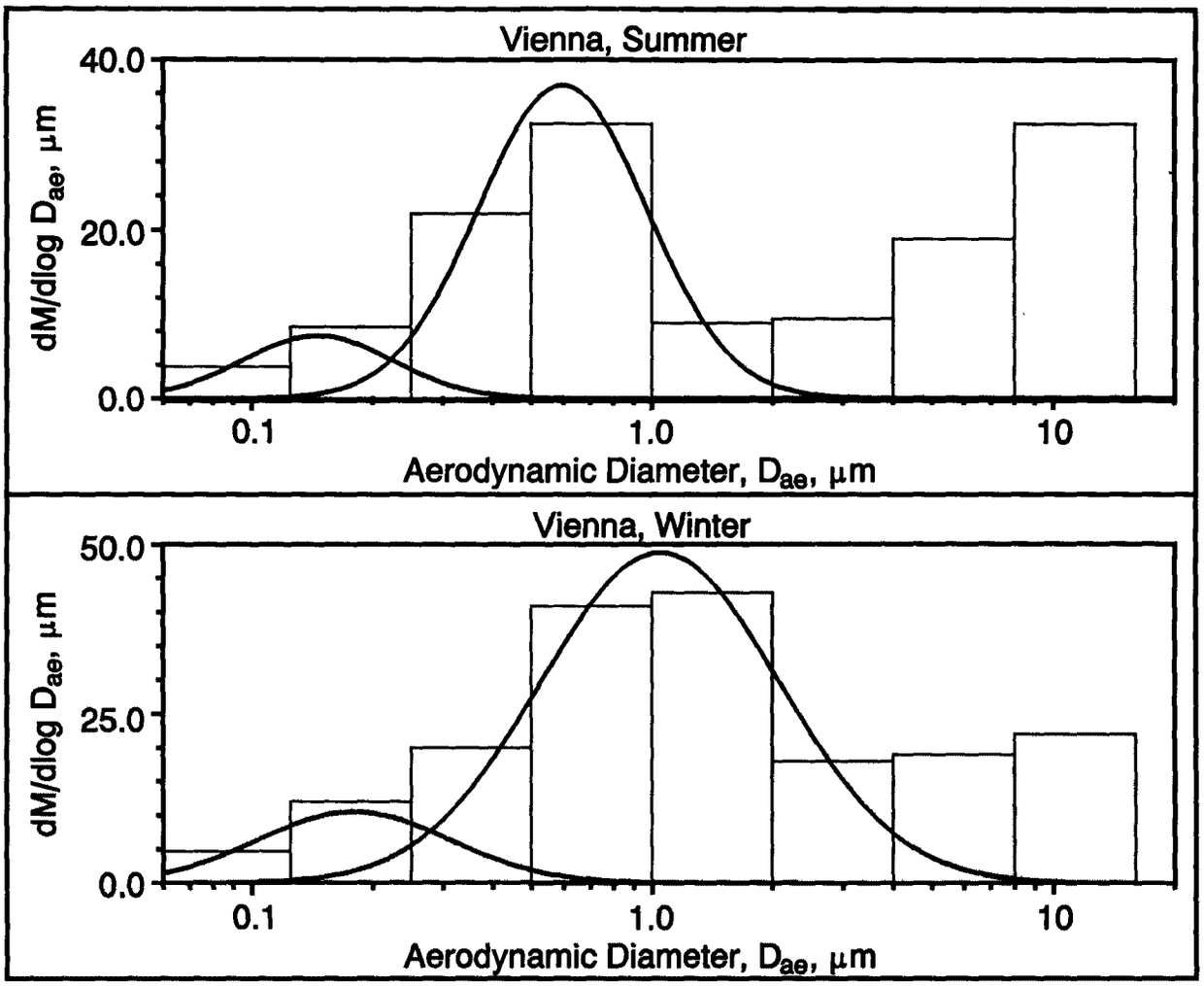

Figure 3-36. Typical results of size-distribution measurements taken with a Berner impactor in a Vienna street with heavy automotive traffic: (a) measurements taken during summer at three different elevations, (b) measurements taken during winter at three different elevations, fog was frequently present during the winter sampling period.

Source: Berner and Lürzer (1980).

above 2.5 μm diameter, due to the growth of hygroscopic particles at very high relative humidity.

These observations, indicating that, during near 100% relative humidity conditions, significant amounts of normally fine mode material will be found in the coarse fractions (>2.5 μm diameter), have broader implications than selection of a cut point to separate fine

and coarse particles. Such shifts could cause problems for receptor modeling using chemical mass balance or factor analysis, for interpretation of exposure data in epidemiological studies, and in estimated removal of particulate matter by deposition.

3.7.7 Conclusions

This review of atmospheric particle-size-distributions was undertaken to provide information which could be used to determine what cut-point; 1.0 μm, 2.5 μm, or something in between; would give the best separation between the fine and coarse particle modes. The data do not provide a clear or obvious answer. Depending on conditions, a significant amount of either fine or coarse mode material may be found in the intermodal region between 1.0 and 3 μm. However, the analysis does demonstrate the important role of relative humidity in influencing the size of the fine particle mode and indicates that significant fine mode material is found above 1.0 μm only during periods of very high relative humidity.

Thus, a $PM_{2.5}$ sample will contain most of the fine mode material, except during periods of RH near 100 %. However, especially in conditions of low RH, it may contain 5 to 20 % of the coarse mode material below 10 μm in diameter. A $PM_{1.0}$ sample will prevent misclassification of coarse mode material as fine but under high RH conditions will result in some of the fine mode material being misclassified as coarse.

A reduction in RH, either intentionally or inadvertently, will reduce the size of the fine mode. A sufficient reduction in RH will yield a dry fine particle mode with very little material above 1.0 μm. However, reducing the RH by heating will result in loss of semivolatile components such as ammonium nitrate and semivolatile organic compounds. No information was found on techniques designed to remove particle-bound water without loss of other semivolatile components.

3.8 SUMMARY

Atmospheric particulate matter (PM) refers to solid or liquid particles suspended in air. The term atmospheric aerosol refers to both the suspended particles and the air (including gaseous pollutants) in which the particles are suspended. However, the term aerosol is

frequently used to refer only to the suspended particles. The terms particulate matter and particles will be used most frequently in this document.

Particulate matter is not a single pollutant but rather a mixture of many classes of pollutants. The components of PM differ in sources; formation mechanisms; composition; size; and chemical, physical, and biological properties. Particle diameters span more than four orders of magnitude, ranging from a few nanometers (nm) to one hundred micrometers (μm). Because of this wide size range, plots of particle-size distribution are almost always plotted versus the logarithm of the particle diameter. Diameter usually refers to the aerodynamic diameter, defined as the diameter of a spherical particle with an equal settling velocity but a density of 1 g/cm^3. This normalizes particles of different shapes and densities.

One of the most fundamental divisions of atmospheric particles is the naturally occurring separation into a fine particle mode and a coarse particle mode as shown in Figure 3-3. The terms fine mode particles and coarse mode particles are used to refer to particles in the fine or coarse particle distributions. The two distributions overlap between 1 and 3 μm aerodynamic diameter.

Particles may also be defined by the size cut of the collection or measuring device. A frequently used descriptor is the 50% cut point. This is the aerodynamic diameter at which the efficiency of the device for particle collection is 50%. As particles increase in size above the 50% cut point, they are collected with decreasing efficiency, eventually reaching 0%; as particles decrease in size below the 50% cut point, they are collected with increasing efficiency, eventually reaching 100%. The indicator for the current particle standard is PM_{10} (i.e. particles with a 50% cut point of 10 μm aerodynamic diameter). However, PM_{10} contains some particles larger than 10 μm and does not contain all particles below 10 μm. Fine is also used to refer to particles with an upper cut point of 3.5, 2.5 ($PM_{2.5}$), 2.1, or 1.0 μm. Coarse is also used to refer to particles between 2.5 and 10 μm ($PM_{(10-2.5)}$) or particles collected by the high volume sampler as well as the entire coarse mode.

Size fractions may also be characterized in terms of their entrance into various compartments of the body. Thus, inhalable particles enter the respiratory tract, including the head airways. Thoracic particles travel past the larynx and reach the lung airways and the gas-exchange regions of the lung. Respirable particles reach the gas-exchange region of the

lung. PM_{10} is an indicator of thoracic particles; $PM_{2.5}$ is an indicator of fine mode particles; and $PM_{(10-2.5)}$ is an indicator of the thoracic component of coarse mode particles.

The fine and coarse particle distributions are frequently approximated by log-normal distributions. However, finer distinctions can be made. The fine particles consist of a nuclei mode, composed of particles recently formed from gases, and an accumulation mode, into which the nuclei grow and accumulate (Figure 3-6). Ultrafine particles, defined in this document as distributions with mass median diameters below 0.1 μm, are associated with the nuclei mode (Figures 3-1, 3-2, and 3-13). In the presence of fogs or clouds, the accumulation mode may split into a smaller, less hygroscopic mode and a larger droplet mode. The latter is formed by gases dissolving in the fog or cloud droplets, reacting, and forming particles when the water of the droplets evaporates (Figure 3-14). There may also be several modes within the coarse particle distribution or mode but these are usually less distinct.

The terms primary and secondary, anthropogenic and biogenic, outdoor and indoor microenvironment have significant applications to particulate matter. Primary fine particles are emitted from sources, either directly as particles or as vapors which rapidly condense to form particles. Primary coarse particles are usually formed by mechanical processes. Secondary fine particles are formed within the atmosphere as the result of gas-phase or aqueous-phase chemical reactions. Anthropogenic particles may be formed by primary or secondary processes. Similarly, biogenic particles include primary particles of biological origin, including bioallergens, as well as secondary particles formed from biogenic precursors such as terpenes emitted into the atmosphere. The term outdoor refers to community atmospheres. These are the atmospheres which are usually monitored for particulate matter. Indoor microenviroments include homes, apartments, schools, office buildings and other indoor work places, large enclosed areas such as malls, vehicles used for commuting, etc.

Some general classes of particles, such as organic particles, can occur not only as fine or coarse particles, but can be of either anthropogenic and biogenic origin, and can be produced both in outdoor and indoor microenvironments. Organic particles also can be present in air as primary fine particles from combustion processes or as secondary fine particles formed as a result of atmospheric reactions involving higher molecular weight

volatile anthropogenic alkenes and aromatics or from the atmospheric reactions of volatile biogenic compounds such as terpenes. Therefore, there is considerable overlap for chemical species among the categories listed above.

A substantial fraction of the fine particle mass, especially during the warmer months of the year, is secondary PM, formed as a result of atmospheric reactions. Such reactions involve the gas phase conversion of SO_2 to H_2SO_4 by OH radicals and aqueous-phase reactions of SO_2 with H_2O_2, O_3, or O_2 (catalyzed by Fe and Mn). The NO_2 portion of NO_x can be converted to HNO_3 by reaction with OH radicals during the day. During nighttime NO_2 is converted into HNO_3 by a series of reactions involving O_3 and the nitrate radical (NO_3). Both H_2SO_4 and HNO_3 react with atmospheric ammonia (NH_3). Gaseous NH_3 reacts with gaseous HNO_3 to form particulate NH_4NO_3. Gaseous NH_3 reacts with H_2SO_4 to form acidic HSO_4^- and neutral $(NH_4)_2SO_4$. A number of volatile organic compounds can react with O_3 and/or OH radical to form fine organic particles. In addition, acid gases such as SO_2 and HNO_3 may react with coarse particles such as $CaCO_3$ and NaCl to form coarse particles of different chemical composition.

The concentrations of OH radicals, O_3, and H_2O_2, formed by gas phase reactions involving volatile organic compounds and NO_x, depend on the concentrations of the reactants, and on meteorological conditions including temperature, solar radiation, wind speed, mixing volume and passage of high pressure systems. Therefore, formation of a substantial fraction of fine particles can depend on the gas phase reactions which also produce O_3 and a variety of other volatile products.

The fine particle fraction, in addition to $SO_4^=$ and NO_3^-, contains elemental carbon (EC), organic carbon (OC), H^+ (hydrogen ions or acidity) and a number of metal compounds at lower concentrations. Species such as $SO_4^=$, NO_3^- and some organic species are associated with substantial amounts of particle-bound water. NH_4NO_3 is in equilibrium with HNO_3 and NH_3 so it can vaporize from particles. Organic particles can also be in equilibrium with their vapor. Such species are called semi-volatile. A number of trace elements including, but not necessarily limited to, Pb, Zn, Ni, Cd, Na, Cl, Br, Se and As have been measured in the $PM_{2.5}$ fraction of fine particles. The coarse particles are largely composed of the crustal elements Si, Ca, Al, and Fe. However, a considerable number of elements are found in both the fine and coarse fractions.

Chemical reactions of SO_2 and NO_x within plumes are an important source of H^+, $SO_4^=$ and NO_3^-. These conversions can occur by gas-phase and aqueous-phase mechanisms.

In point-source plumes emitting SO_2 and NO_x, the gas-phase chemistry depends on plume dilution, sunlight and background volatile organic compounds mixed into the diluting plume. For the conversion of SO_2 to H_2SO_4, the gas-phase rate in such plumes during summer midday conditions in the eastern United States typically varies between 1 and 3% h^{-1} but in the cleaner western United States rarely exceeds 1% h^{-1}. For the conversion of NO_x to HNO_3, the gas-phase rates appear to be approximately three times faster than the SO_2 conversion rates. Winter rates for SO_2 conversion were approximately an order of magnitude lower than the summer rates.

The contribution of aqueous-phase chemistry to particle formation in point-source plumes is highly variable, depending on the availability of the aqueous phase (wetted aerosols, clouds, fog, and light rain) and the photochemically generated gas-phase oxidizing agents, especially H_2O_2 for SO_2 chemistry. The in-cloud conversion rates of SO_2 to $SO_4^=$ can be several times larger than the gas-phase rates given above. Overall, it appears that SO_2 oxidation rates to $SO_4^=$ by gas-phase and aqueous-phase mechanisms may be comparable in summer, but aqueous phase chemistry may dominate in winter.

In the western United States, markedly higher SO_2 conversion rates have been reported in smelter plumes than in power plant plumes. The conversion is predominantly by a gas-phase mechanism. This result is attributed to the lack of NO_x in smelter plumes. In power plant plumes NO_2 depletes OH and competes with SO_2 for OH.

In urban plumes, the upper limit for the gas-phase SO_2 conversion rate appears to be about 5% h^{-1} under the more polluted conditions. For NO_2, the rates appear to be approximately three times faster than the SO_2 conversion rates. Conversion rates of SO_2 and NO_x in background air are comparable to the peak rates in diluted plumes. Neutralization of H_2SO_4 formed by SO_2 conversion increases with plume age and background NH_3 concentration. If the NH_3 concentrations are more than sufficient to neutralize H_2SO_4 to $(NH_4)_2SO_4$, the HNO_3 formed from NO_x conversions may be converted to NH_4NO_3.

The lifetimes of particles vary with size. Coarse particles can settle rapidly from the atmosphere within hours, and normally travel only short distances. However, when mixed high into the atmosphere as in dust storms the smaller sized coarse mode particles may have

longer lives and travel distances. Nuclei mode particles rapidly grow into the accumulation mode. However, the accumulation mode does not grow into the coarse mode. Accumulation-mode fine particles are kept suspended by normal air motions and have very low deposition rates to surfaces. They can be transported thousands of km and remain in the atmosphere for a number of days. Both accumulation-mode and nuclei-mode (or ultrafine) particles have the ability to penetrate deep into the lungs. Dry deposition rates are expressed in terms of a deposition velocity which varies as the particle size, reaching a minimum between 0.1 and 1.0 μm aerodynamic diameter. Accumulation-mode particles are removed from the atmosphere primarily by cloud processes. Fine particles, especially particles with a hygroscopic component, grow as the relative humidity increases, serve as cloud condensation nuclei, and grow into cloud droplets. If the cloud droplets grow large enough to form rain, the particles are removed in the rain. Falling rain drops impact coarse particles and remove them. Ultrafine or nuclei mode particles are small enough to diffuse to the falling drop and be removed. Falling rain drops, however, are not effective in removing accumulation-mode particles.

There are many reasons for wanting to collect fine and coarse particles separately. However, because fine-mode particles and coarse-mode particles overlap in the size range between 1.0 and 3 μm diameter, it is not clear what 50% cut point will give the best separation.

A review of atmospheric particle-size-distribution data did not provide a clear or obvious answer. Depending on conditions, a significant amount of either fine or coarse mode material may be found in the intermodal region between 1.0 and 3 μm. However, the analysis of the existing data did demonstrate the important role of relative humidity in influencing the size of the fine particle mode and indicated that significant fine mode material is found above 1.0 μm only during periods of very high relative humidity.

Thus, a $PM_{2.5}$ sample will contain most of the fine mode material, except during periods of RH near 100 %. However, especially in conditions of low RH, it may contain 5 to 20 % of the coarse mode material below 10 μm in diameter. A $PM_{1.0}$ sample will prevent misclassification of coarse mode material as fine but under high RH conditions will result in some of the fine mode material being misclassified as coarse.

A reduction in RH, either intentionally or inadvertently, will reduce the size of the fine mode. A sufficient reduction in RH will yield a dry fine particle mode with very little material above 1.0 μm. However, techniques to reduce the RH without loss of semivolatile components such as ammonium nitrate and semivolatile organic compounds have not yet been developed.

REFERENCES

Adamson, A. W. (1976) Physical chemistry of surfaces New York, NY: John Wiley & Sons, Inc.

Akhter, M. S.; Chughtai, A. R.; Smith, D. M. (1984) Reaction of hexane soot with NO_2/N_2O_4. J. Phys. Chem. 88: 5334-5342.

Akhter, M. S.; Chughtai, A. R.; Smith, D. M. (1985) The structure of hexane soot I: spectroscopic studies. Appl. Spectrosc. 39: 143-153.

Aleic-Juretic, A.; Cvitas, T.; Klasinc, L. (1990) Heterogeneous polycyclic aromatic hydrocarbon degradation with ozone on silica gel carrier. Environ. Sci. Technol 24: 62-66.

Alkezweeny, A.; Powell, D. (1977) Estimation of transformation rate of SO_2 to SO_4 from atmospheric concentration data. Atmos. Environ. 11: 179-182.

Allen, D. T.; Palen, E. J.; Haimov, M. I.; Hering, S. V.; Young, J. R. (1994) Fourier transform infrared spectroscopy of aerosol collected in a low pressure impactor (LPI / FTIR): method development and field calibration. Aerosol Sci. Technol. 21: 325-342.

Allwine, K. J. (1993) Atmospheric dispersion and tracer ventilation in a deep mountain valley. J. Appl. Meteorol. 32: 1017-1037.

Alofs, D. J.; Hagen, D. E.; Trueblood, M. B. (1989) Measured spectra of the hygroscopic fraction of atmospheric aerosol particles. J. Appl. Meteorol. 28: 126-136.

Altshuller, A. P. (1983) Review: natural volatile organic substances and their effect on air quality in the United States. Atmos. Environ. 17: 2131-2165.

Altshuller, A. P. (1987) Potential contribution of sulfate production in cumulus cloud droplets to ground level particle sulfur concentrations. Atmos. Environ. 21: 1097-1105.

American Conference of Governmental Industrial Hygienists (ACGIH). (1994) Appendix D: particle size-selective sampling criteria for airborne particulate matter. In: 1994-1995 threshold limit values for chemical substances and physical agents and biological exposure indices. Cincinnati, OH: American Conference of Governmental Industrial Hygienists; pp. 43-46.

Anderson, J. R.; Aggett, F. J.; Buseck, P. R.; Germani, M. S.; Shattuck, T. W. (1988) Chemistry of individual aerosol particles from Chandler, Arizona, an arid urban environment. Environ. Sci. Technol. 22: 811-818.

Andreae, M. O.; Charlson, R. J.; Bruynseels, F.; Storms, H.; Van Grieken, R.; Maenhaut, W. (1986) Internal mixture of sea salt, silicates, and excess sulfate in marine aerosols. Science (Washington, DC) 232: 1620-1623.

Andrews, E.; Larson, S. M. (1993) Effect of surfactant layers on the size changes of aerosol particles as a function of relative humidity. Environ. Sci. Technol. 27: 857-865.

Appel, B. R.; Tokiwa, Y.; Hsu, J.; Kothny, E. L.; Hahn, E. (1985) Visibility as related to atmospheric aerosol constituents. Atmos. Environ. 19: 1525-1534.

Appel, B. R.; Cheng, W.; Salaymeh, F. (1989) Sampling of carbonaceous particles in the atmosphere—II. Atmos. Environ. 23: 2167-2175.

Arimoto, R.; Duce, R. A.; Ray, B. J.; Unni, C. K. (1985) Atmospheric trace elements at Enewetak Atoll: 2. transport to the ocean by wet and dry deposition. J. Geophys. Res. [Atmos.] 90: 2391-2408.

Arnts, R. R.; Gay, B. W., Jr. (1979) Photochemistry of some naturally emitted hydrocarbons. Research Triangle Park, NC: U.S. Environmental Protection Agency, Environmental Sciences Research Laboratory; EPA report no. EPA-600/3-79-081. Available from: NTIS, Springfield, VA; PB80-131980.

Atkinson, R.; Aschmann, S. M. (1987) Kinetics of the gas-phase reactions of alkylnaphthalenes with O_3, N_2O_5 and OH radicals at 298$\pm$2 K. Atmos. Environ. 21: 2323-2326.

Avissar, R.; Pielke, R. A. (1989) A parameterization of heterogeneous land surfaces for atmospheric numerical models and its impact on regional meteorology. Mon. Weather Rev. 117: 2113-2136.

Ayers, G. P.; Larson, T. V. (1990) Numerical study of droplet size dependent chemistry in oceanic, wintertime stratus clouds at southern mid-latitudes. J. Atmos. Chem. 11: 143-167.

Baek, S. O.; Field, R. A.; Goldstone, M. E.; Kirk, P. W.; Lester, J. N.; Perry, R. (1991) A review of atmospheric polycyclic aromatic hydrocarbons: sources, fate and behavior. Water Air Soil Pollut. 60: 279-300.

Bagnold, R. A. (1941) The physics of blown sand and desert dunes. London, United Kingdom: Methuen & Co.

Baker, M. B.; Latham, J. (1979) The evolution of droplet spectra and the rate of production of embryonic raindrops in small cumulus clouds. J. Atmos. Sci. 36: 1612-1615.

Baldwin, A. C. (1982) Heterogeneous reactions of sulfur dioxide with carbonaceous particles. Int. J. Chem. Kinet. 14: 269-277.

Barnard, W. R.; Gatz, D. F.; Stensland, G. J. (1987) Chemical characterization of aerosols emitted from vehicle traffic on unpaved roads. Presented at: 80th annual meeting of the Air Pollution Control Association; June; New York, NY. Pittsburgh, PA: Air Pollution Control Association; paper no. 87-14.3.

Barnard, W. R.; Stansland, G. J.; Gatz, D. F. (1988) Flux of alkaline materials from unpaved roads in the southwestern United States. In: Particulate matter/fugitive dusts: measurement and control in western arid regions. Proccedings of an Air Pollution Control Association meeting. Pittsburgh, PA: Air Pollution Control Association; pp. 27-39.

Barrie, L. A. (1985) Scavenging ratios, wet deposition, and in-cloud oxidation: an application to the oxides of sulphur and nitrogen. J. Geophys. Res. [Atmos.] 90: 5789-5799.

Barrie, L. A.; Georgii, H. W. (1976) An experimental investigation of the absorption of sulphur dioxide by water drops containing heavy metal ions. Atmos. Environ. 10: 743-749.

Barth, M. C. (1994) Numerical modeling of sulfur and nitrogen chemistry in a narrow cold-frontal rainband: the impact of meteorological and chemical parameters. J. Appl. Meteorol. 33: 855-868.

Barth, M. C.; Hegg, D. A.; Hobbs, P. V. (1992) Numerical modeling of cloud and precipitation chemistry associated with two rainbands and some comparisons with observations. J. Geophys. Res. [Atmos.] 97: 5825-5845.

Bassett, M.; Seinfeld, J. H. (1983) Atmospheric equilibrium model of sulfate and nitrate aerosols. Atmos. Environ. 17: 2237-2252.

Bassett, M. E.; Seinfeld, J. H. (1984) Atmospheric equilibrium model of sulfate and nitrate aerosols - II. particle size analysis. Atmos. Environ. 18: 1163-1170.

Behymer, T. D.; Hites, R. A. (1988) Photolysis of polycyclic aromatic hydrocarbons adsorbed on fly ash. Environ. Sci. Technol. 22: 1311-1319.

Benkovitz, C. M.; Berkowitz, C. M.; Easter, R. C.; Nemesure, S.; Wagener, R.; Schwartz, S. E. (1994) Sulfate over the North Atlantic and adjacent continental regions: evaluation for October and November 1986 using a three-dimensional model driven by observation-derived meteorology. J. Geophys. Res. [Atmos.] 99: 20,725-20,756.

Benner, C. L.; Eatough, D. J.; Eatough, N. L.; Bhardwaja, P. (1991) Comparison of annular denuder and filter pack collection of HNO_3 (g), HNO_2 (g), SO_2 (g), and particulate-phase nitrate, nitrite and sulfate in the south-west desert. Atmos. Environ. Part A 25: 1537-1545.

Bergstrom, R. W.; Seigneur, C.; Babson, B. L.; Holman, H.-Y.; Wojcik, M. A. (1981) Comparison of the observed and predicted visual effects caused by power plant plumes. Atmos. Environ. 15: 2135-2150.

Berner, A. (1989) Haze and its relation to atmospheric accumulation aerosol. Sci. Total Environ. 86: 251-263.

Berner, A.; Lürzer, C. (1980) Mass size distributions of traffic aerosols at Vienna. J. Phys. Chem. 84: 2079-2083.

Berner, A.; Lürzer, Ch.; Pohl, F.; Preining, O.; Wagner, P. (1979) The size distribution of the urban aerosol in Vienna. Sci. Total Environ. 13: 245-261.

Bernstein, D. M.; Rahn, K. A. (1979) New York Summer Aerosol Study: trace element concentrations as a function of particle size. In: Kneip, T. J.; Lippmann, M., eds. The New York Summer Aerosol Study, 1976. Ann. N. Y. Acad. Sci. 322: 87-97.

Bidleman, T. F. (1988) Atmospheric processes. Environ. Sci. Technol. 22: 361-367.

Biggins, P. D. E.; Harrison, R. M. (1980) Chemical speciation of lead compounds in street dusts. Environ. Sci. Technol. 14: 336-339.

Bjørseth, A.; Olufsen, B. S. (1983) Long-range transport of polycyclic aromatic hydrocarbons. In: Bjørseth, A., ed. Handbook of polycyclic aromatic hydrocarbons. New York, NY: Marcel Dekker, Inc.; pp. 507-524.

Bjørseth, A.; Lunde, G.; Lindskog, A. (1979) Long-range transport of polycyclic aromatic hydrocarbons. Atmos. Environ. 13: 45-53.

Bott, A. (1991) On the influence of the physico-chemical properties of aerosols on the life cycle of radiation fogs. Boundary Layer Meteorol. 56: 1-31.

Bott, A.; Carmichael, G. R. (1993) Multiphase chemistry in a microphysical radiation fog model—a numerical study. Atmos. Environ. Part A 27: 503-522.

Bower, K. N.; Choularton, T. W. (1993) Cloud processing of the cloud condensation nucleus spectrum and its climatological consequences. Q. J. R. Meteorol. Soc. 119: 655-679.

Bower, K. N.; Hill, T. A.; Coe, H.; Choularton, T. W. (1991) SO_2 oxidation in an entraining cloud model with explicit microphysics. Atmos. Environ. Part A 25: 2401-2418.

Boyce, S. D.; Hoffmann, M. R. (1984) Kinetics and mechanism of the formation of hydroxymethanesulfonic acid at low pH. J. Phys. Chem. 88: 4740-4746.

Braaten, D. A.; Paw U, K. T. (1992) A stochastic particle resuspension and deposition model. In: Schwartz, S. E.; Slinn, W. G. N., eds. Precipitation scavenging and atmosphere-surface exchange: proceedings of the fifth international conference, v. 2: the Semonin volume: atmosphere-surface exchange processes; July 1991; Richland, WA. Washington, DC: Hemisphere Publishing Corporation; pp. 1143-1152.

Braaten, D. A.; Paw U, K. T.; Shaw, R. H. (1989) Particles resuspension in a turbulent boundary layer—observed and modeled. J. Aerosol Sci. 21: 613-628.

Brauer, M.; Koutrakis, P.; Keeler, G. J.; Spengler, J. D. (1991) Indoor and outdoor concentrations of inorganic acidic aerosols and gases. J. Air Waste Manage. Assoc. 41: 171-181.

Briggs, G. A.; Binkowski, F. S. (1985) Research on diffusion in atmospheric boundary layers: a position paper on status and needs. Research Triangle Park, NC: U.S. Environmental Protection Agency, Atmospheric Sciences Research Laboratory; EPA report no. EPA/600/3-85/072. Available from: NTIS, Springfield, VA; PB86-122587.

Brosset, C.; Andreasson, K.; Ferm, M. (1975) The nature and possible origin of acid particles observed at the Swedish west coast. Atmos. Environ. 9: 631-642.

Brown, N. J.; Dod, R. L.; Mowrer, F. W.; Novakov, T.; Williamson, R. B. (1989) Smoke emission factors from medium-scale fires: part 1. Aerosol Sci. Technol. 10: 2-19.

Buat-Ménard, P.; Duce, R. A. (1986) Precipitation scavenging of aerosol particles over remote marine regions. Nature (London) 321: 508-510.

Burkhard, E. G.; Dutkiewicz, V. A.; Husain, L. (1994) A study of SO_2, SO_4^{2-} and trace elements in clear air and clouds above the midwestern United States. Atmos. Environ. 28: 1521-1533.

Burton, R. M.; Lundgren, D. A. (1987) Wide range aerosol classifier: a size selective sampler for large particles. Aerosol Sci. Technol. 6: 289-301.

Burtscher, H. (1992) Measurement and characteristics of combustion aerosols with special consideration of photoelectric charging and charging by flame ions. J. Aerosol Sci. 23: 549-595.

Burtscher, H.; Leonardi, A.; Steiner, D.; Baltensperger, U.; Weber, A. (1993) Aging of combustion particles in the atmosphere - results from a field study in Zürich. Water Air Soil Pollut. 68: 137-147.

Cadle, S. H.; Dasch, J. M. (1988) Wintertime concentrations and sinks of atmospheric particulate carbon at a rural location in northern Michigan. Atmos. Environ. 22: 1373-1381.

Cahill, T. A.; Surovik, M.; Wittmeyer, I. (1990) Visibility and aerosols during the 1986 Carbonaceous Species Methods Comparison Study. Aerosol Sci. Technol. 12: 149-160.

Calvert, J. G.; Su, F.; Bottenheim, J. W.; Strausz, O. P. (1978) Mechanism of the homogeneous oxidation of sulfur dioxide in the troposphere. In: Sulfur in the atmosphere: proceedings of the international symposium; September 1977; Dubrovnik, Yugoslavia. Atmos. Environ. 12: 197-226.

Calvert, J. G.; Lazrus, A.; Kok, G. L.; Heikes, B. G.; Walega, J. G.; Lind, J.; Cantrell, C. A. (1985) Chemical mechanisms of acid generation in the troposphere. Nature (London) 317: 27-35.

Cambray, R. S. (1989) Radioactive fallout in air and rain: results to the end of 1987. Harwell, United Kingdom: Atomic Energy Establishment; report no. AERE-R 13226.

Cambray, R. S.; Cawse, P. A.; Garland, J. A.; Gibson, J. A. B.; Johnson, P.; Lewis, G. N. J.; Newton, D.; Salmon, L.; Wade, B. O. (1987) Observations on radioactivity from the Chernobyl accident. Nucl. Energy (Br. Nucl. Energy Soc.) 26: 77-101.

Carpenter, S. B.; Montgomery, T. L.; Leavitt, J. M.; Colbaugh, W. C.; Thomas, F. W. (1971) Principal plume dispersion models: TVA power plants. J. Air Pollut. Control Assoc. 21: 491-495.

Carras, J. N.; Williams, D. J. (1981) The long-range dispersion of a plume from an isolated point source. Atmos. Environ. 15: 2205-2217.

Carras, J. N.; Williams, D. J. (1988) Measurements of relative σ_y up to 1800 km from a single source. Atmos. Environ. 22: 1061-1069.

Carter, E. J.; Borys, R. D. (1993) Aerosol-cloud chemical fractionation: enrichment factor analysis of cloud water. J. Atmos. Chem. 17: 277-292.

Cass, G. R. (1979) On the relationship between sulfate air quality and visibility with examples in Los Angeles. Atmos. Environ. 13: 1069-1084.

Cass, G. R.; Shair, F. H. (1984) Sulfate accumulation in a sea breeze/land breeze circulation system. J. Geophys. Res. [Atmos.] 89: 1429-1438.

Cass, G. R.; Boone, P. M.; Macias, E. S. (1982) Emissions and air quality relationships for atmospheric carbon particles in Los Angeles. In: Wolff, G. T.; Klimisch, R. L., eds. Particulate carbon: atmospheric life cycle. New York, NY: Plenum Press; pp. 207-243.

Cawse, P. A. (1981) Trace elements in the atmosphere of the United Kingdom. Presented at: ESNA meeting; September-October; Aberdeen, Scotland.

Chamberlain, A. C. (1983) Deposition and resuspension. In: Pruppacher, H. R.; Semonin, R. G.; Slinn, W. G. N., eds. Precipitation scavenging, dry deposition, and resuspension, v. 2: dry deposition and resuspension: proceedings of the fourth international conference; November-December 1982; Santa Monica, CA. New York, NY: Elsevier; pp. 731-751.

Chameides, W. L. (1984) The photochemistry of a remote marine stratiform cloud. J. Geophys. Res. [Atmos.] 89: 4739-4755.

Chameides, W. L.; Davis, D. D. (1982) The free radical chemistry of cloud droplets and its impact upon the composition of rain. J. Geophys. Res. C: Oceans Atmos. 87: 4863-4877.

Chan, W. H.; Tang A. J. S.; Chung, D. H. S.; Lusis, M. A. (1986) Concentration and deposition of trace metals in Ontario - 1982. Water Air Soil Pollut. 29: 373-389.

Chan, C. K.; Flagan, R. C.; Seinfeld, J. H. (1992) Water activities of $NH_4NO_3/(NH_4)_2SO_4$ solutions. Atmos. Environ. Part A 26: 1661-1673.

Chang, S. G.; Brodzinsky, R.; Gundel, L. A.; Novakov, T. (1982) Chemical and catalytic properties of elemental carbon. In: Wolff, G. T.; Klimisch, R. L., eds. Particulate carbon: atmospheric life cycle. New York, NY: Plenum Press; pp. 158-181.

Chang, J. S.; Middleton, P. B.; Stockwell, W. R.; Walcek, C. J.; Pleim, J. E.; Lansford, H. H.; Madronich, S.; Binkowski, F. S.; Seaman, N. L.; Stauffer, D. R. (1991) The regional acid deposition model and engineering model. In: Irving, P. M., ed. Acidic deposition: state of science and technology, volume I: emissions, atmospheric processes, and deposition. Washington, DC: The U.S. National Acid Precipitation Assessment Program. (State of science and technology report no. 4).

Chapman, E. G.; Luecken, D. J.; Dana, M. T.; Easter, R. C.; Hales, J. M.; Laulainen, N. S.; Thorp, J. M. (1987) Inter-storm comparisons from the OSCAR high-density network experiment. Atmos. Environ. 21: 531-549.

Cheng, Y.-S.; Carpenter, R. L.; Barr, E. B.; Hobbs, C. H. (1985) Size distribution of fine particle emissions from a steam plant with a fluidized-bed coal combustor. Aerosol Sci. Technol. 4: 175-189.

Ching, J. K. S.; Alkezweeny, A. J. (1986) Tracer study of vertical exchange by cumulus clouds. J. Clim. Appl. Meteorol. 25: 1702-1711.

Choularton, T. W.; Wicks, A. J.; Downer, R. M.; Gallagher, M. W.; Penkett, S. A.; Bandy, B. J.; Dollard, G. J.; Jones, B. M. R.; Davies, T. D.; Gay, M. J.; Tyler, B. J.; Fowler, D.; Cape, J. N.; Hargreaves, K. J. (1992) A field study of the generation of nitrate in a hill cap cloud. Environ. Pollut. 75: 69-73.

Chow, J. C.; Watson, J. G.; Lowenthal, D. H.; Solomon, P. A.; Magliano, K. L.; Ziman, S. D.; Richards, L. W. (1992) PM10 source apportionment in California's San Joaquin Valley. Atmos. Environ. Part A 26: 3335-3354.

Chow, J. C.; Watson, J. G.; Pritchett, L. C.; Pierson, W. R.; Frazier, C. A.; Purcell, R. G. (1993a) The DRI thermal/optical reflectance carbon analysis system: description, evaluation and applications in U.S. air quality studies. In: Lodge, J. P., Jr. Fourth international conference on carbonaceous particles in the atmosphere; April 1991; Vienna, Austria. Atmos. Environ. Part A 27: 1185-1201.

Chow, J. C.; Watson, J. G.; Lowenthal, D. H.; Solomon, P. A.; Magliano, K. L.; Ziman, S. D.; Richards, L. W. (1993b) PM_{10} and $PM_{2.5}$ compositions in California's San Joaquin Valley. Aerosol Sci. Technol. 18: 105-128.

Chow, J. C.; Watson, J. G.; Fujita, E. M.; Lu, Z.; Lawson, D. R.; Ashbaugh, L. L. (1994) Temporal and spatial variations of $PM_{2.5}$ and PM_{10} aerosol in the Southern California Air Quality Study. Atmos. Environ. 28: 2061-2080.

Chughtai, A. R.; Jassim, J. A.; Peterson, J. H.; Stedman, D. H.; Smith, D. M. (1991) Spectroscopic and solubility characteristics of oxidized soots. Aerosol Sci. Technol. 15: 112-126.

Clark, T. L.; Cohn, R. D. (1990) The Across North America Tracer Experiment (ANATEX) model evaluation study. Research Triangle Park, NC: U.S. Environmental Protection Agency, Atmospheric Research and Exposure Assessment Laboratory; EPA report no. EPA/600/3-90/051. Available from: NTIS, Springfield, VA; PB90-261454.

Clark, P. A.; Fletcher, I. S.; Kallend, A. S.; McElroy, W. J.; Marsh, A. R. W.; Webb, A. H. (1984) Observations of cloud chemistry during long-range transport of power plant plumes. Atmos. Environ. 18: 1849-1858.

Clarke, A. D. (1989) Aerosol light absorption by soot in remote environments. Aerosol Sci. Technol. 10: 161-171.

Clarke, A. D. (1992) Atmospheric nuclei in the remote free-troposphere. J. Atmos. Chem. 14: 479-488.

Clarke, A. D. (1993) Atmospheric nuclei in the Pacific midtroposphere—their nature, concentration, and evolution. J. Geophys. Res. [Atmos.] 98: 20,633-20,647.

Clarke, A. G.; Karani, G. N. (1992) Characterisation of the carbonate content of atmospheric aerosols. J. Atmos. Chem. 14: 119-128.

Clarke, A. G.; Radojevic, M. (1987) Oxidation of SO_2 in rainwater and its role in acid rain chemistry. Atmos. Environ. 21: 1115-1123.

Clarke, J. F.; Clark, T. L.; Ching, J. K. S.; Haagenson, P. L.; Husar, R. B.; Patterson, D. E. (1983) Assessment of model simulation of long-distance transport. Atmos. Environ. 17: 2449-2462.

Clarke, A. D.; Weiss, R. E.; Charlson, R. J. (1984) Elemental carbon aerosols in the urban, rural and remote-marine troposphere and in the stratosphere: interferences from light absorption data and consequences regarding radiative transfer. Sci. Total Environ. 36: 97-102.

Cobourn, W. G.; Husar, R. B.; Husar, J. D. (1978) Continuous *in situ* monitoring of ambient particulate sulfur using flame photometry and thermal analysis. In: Husar, R. B.; Lodge, J. P., Jr.; Moore, D. J., eds. Sulfur in the atmosphere: proceedings of the international symposium; September 1977; Dubrovnik, Yugoslavia. Atmos. Environ. 12: 89-98.

Cocks, A. T.; McElroy, W. L.; Wallis, P. G. (1982) The oxidation of sodium sulphite solutions by hydrogen peroxide. Central Electricity Research Laboratories; report no. RD/L/2215N81.

Cofer, W. R., III; Stevens, R. K.; Winstead, E. L.; Pinto, J. P.; Sebacher, D. I.; Abdulraheem, M. Y.; Al-Sahafi, M.; Mazurek, M. A.; Rasmussen, R. A.; Cahoon, D. R.; Levine, J. S. (1992) Kuwaiti oil fires: compositions of source smoke. J. Geophys. Res. [Atmos.] 97: 14,521-14,525.

Cohen, M. D.; Flagan, R. C.; Seinfeld, J. H. (1987a) Studies of concentrated electrolyte solutions using the electrodynamic balance. 1. Water activities for single-electrolyte solutions. J. Phys. Chem. 91: 4563-4574.

Cohen, M. D.; Flagan, R. C.; Seinfeld, J. H. (1987b) Studies of concentrated electrolyte solutions using the electrodynamic balance. 2. Water activities for mixed-electrolyte solutions. J. Phys. Chem. 91: 4575-4582.

Colbeck, I.; Appleby, L.; Hardman, E. J.; Harrison, R. M. (1990) The optical properties and morphology of cloud-processed carbonaceous smoke. J. Aerosol Sci. 21: 527-538.

Collett, J. L., Jr.; Oberholzer, B.; Mosimann, L.; Staehelin, J.; Waldvogel, A. (1993a) Contributions of cloud processes to precipitation chemistry in mixed phase clouds. Water Air Soil Pollut. 68: 43-57.

Collett, J., Jr.; Oberholzer, B.; Staehelin, J. (1993b) Cloud chemistry in Mt. Rigi Switzerland: dependence on drop size and relationship to precipitation chemistry. Atmos. Environ. Part A 27: 33-42.

Colvile, R. N.; Choularton, T. W.; Gallagher, M. W.; Wicks, A. J.; Downer, R. M.; Tyler, B. J.; Storeton-West, K. J.; Fowler, D.; Cape, J. N.; Dollard, G. J.; Davies, T. J.; Jones, B. M. R.; Penkett, S. A.; Bandy, B. J.; Burgess, R. A. (1994) Observation on Great Dun Fell of the pathways by which oxides of nitrogen are converted to nitrate. Atmos. Environ. 28: 397-408.

Countess, R. J.; Wolff, G. T.; Cadle, S. H. (1980) The Denver winter aerosol: a comprehensive chemical characterization. J. Air Pollut. Control Assoc. 30: 1194-1200.

Coutant, R. W.; Brown, L.; Chuang, J. C.; Riggin, R. M.; Lewis, R. G. (1988) Phase distribution and artifact formation in ambient air sampling for polynuclear aromatic hydrocarbons. Atmos. Environ. 22: 403-409.

Coutant, R. W.; Callahan, P. J.; Chuang, J. C.; Lewis, R. G. (1992) Efficiency of silicone-grease-coated denuders for collection of polynuclear aromatic hydrocarbons. Atmos. Environ. Part A 26: 2831-2834.

Covert, D. S.; Heintzenberg, J. (1984) Measurement of the degree of internal/external mixing of hygroscopic compounds and soot in atmospheric aerosols. Sci. Total Environ. 36: 347-352.

Covert, D. S.; Charlson, R. J.; Ahlquist, N. C. (1972) A study of the relationship of chemical composition and humidity to light scattering by aerosols. J. Appl. Meteorol. 11: 968-976.

Covert, D. S.; Heintzenberg, J.; Hansson, H.-C. (1990) Electro-optical detection of external mixtures in aerosols. Aerosol Sci. Technol. 12: 446-456.

Covert, D. S.; Kapustin, V. N.; Quinn, P. K.; Bates, T. S. (1992) New particle formation in the marine boundary layer. J. Geophys. Res. [Atmos.] 97: 20,581-20,589.

Cronn, D. R.; Charlson, R. J.; Knights, R. L.; Crittenden, A. L.; Appel, B. R. (1977) A survey of the molecular nature of primary and secondary components of particles in urban air by high-resolution mass spectrometry. Atmos. Environ. 11: 929-937.

Currie, L. A.; Stafford, T. W.; Sheffield, A. E.; Klouda, G. A.; Wise, S. A.; Fletcher, R. A.; Donahue, D. J.; Jull, A. J. T.; Linick, T. W. (1989) Microchemical and molecular dating. Radiocarbon 31: 448-463.

Currie, L. A.; Sheffield, A. E.; Riederer, C.; Gordon, G. E. (1994) Improved atmospheric understanding through exploratory data analysis and complementary modeling: the urban K-Pb-C system. Atmos. Environ. 28: 1359-1369.

Daisey, J. M. (1987) Chemical composition of inhalable particulate matter—seasonal and intersite comparisons. In: Lioy, P. J.; Daisey, J. M., eds. Toxic air pollution: a comprehensive study of non-criteria air pollutants. Chelsea, MI: Lewis Publishers, Inc.; pp. 45-65.

D'Almeida, G. A. (1989) Desert aerosol: characteristics and effects on climate. In: Leinen, M.; Sarnthein, M. Paleoclimatology and paleometeorology: modern and past patterns of global atmospheric transport. Boston, MA: Kluwer Academic Publishers; pp. 311-338. (NATO ASI series. Series C, mathematical and physical sciences: v. 282).

Dana, M. T.; Drewes, D. R.; Glover, D. W.; Hales, J. M. (1976) Precipitation scavenging of fossil-fuel effluents. Research Triangle Park, NC: U.S. Environmental Protection Agency, Environmental Sciences Research Laboratory; report no. EPA-600/4-76-031. Available from: NTIS, Springfield, VA; PB-256649.

Danielsen, E. F. (1961) Trajectories: isobaric, isentropic and actual. J. Meteorol. 18: 479-486.

Dasch, J. M.; Cadle, S. H. (1989) Atmospheric carbon particles in the Detroit urban area: wintertime sources and sinks. Aerosol Sci. Technol. 10: 236-248.

Daum, P. H. (1988) Processes determining cloudwater composition: inferences from field measurements. In: Unsworth, M. H.; Fowler, D., eds. Acid deposition at high elevation sites. Dordrecht, The Netherlands: Kluwer; pp. 139-153.

Daum, P. H.; Kelly, T. J.; Schwartz, S. E.; Newman, L. (1984a) Measurements of the chemical composition of stratiform clouds. Atmos. Environ. 18: 2671-2684.

Daum, P. H.; Schwartz, S. E.; Newman, L. (1984b) Acidic and related constituents in liquid water stratiform clouds. J. Geophys. Res. [Atmos.] 89: 1447-1458.

Daum, P. H.; Kelly, T. J.; Strapp, J. W.; Leaitch, W. R.; Joe, P.; Schemenauer, R. S.; Isaac, G. A.; Anlauf, K. G.; Wiebe, H. A. (1987) Chemistry and physics of a winter stratus cloud layer: a case study. J. Geophys. Res. [Atmos.] 92: 8426-8436.

Daum, P. H.; Kleinman, L. I.; Hills, A. J.; Lazrus, A. L.; Leslie, A. C. D.; Busness, K.; Boatman, J. (1990) Measurement and interpretation of concentrations of H_2O_2 and related species in the upper midwest during summer. J. Geophys. Res. [Atmos.] 95: 9857-9871.

Daum, P. H.; Al-Sunaid, A.; Busness, K. M.; Hales, J. M.; Mazurek, M. (1993) Studies of the Kuwait oil fire plume during midsummer 1991. J. Geophys. Res. [Atmos.] 98: 16,809-16,827.

Däumer, B.; Niessner, R.; Klockow, D. (1992) Laboratory studies of the influence of thin organic films on the neutralization reaction of H_2SO_4 aerosol with ammonia. J. Aerosol Sci. 23: 315-325.

Davidson, C. I.; Wu, Y.-L. (1990) Dry deposition of particles and vapors. In: Lindberg, S. E.; Page, A. L.; Norton, S. A., eds. Acidic precipitation: v. 3, sources, deposition, and canopy interactions. New York, NY: Springer-Verlag; pp. 103-216.

De Bock, L. A.; Van Malderen, H.; Van Grieken, R. E. (1994) Individual aerosol particle composition variations in air masses crossing the North Sea. Environ. Sci. Technol. 28: 1513-1520.

Delumyea, R. D.; Kalivretenos, A. (1987) Elemental carbon and lead content of fine particles from American and French cities of comparable size and industry, 1985. Atmos. Environ. 21: 1643-1647.

Dennis, R. L.; McHenry, J. N.; Barchet, W. R.; Binkowski, F. S.; Byun, D. W. (1993) Correcting RADM's sulfate underprediction: discovery and correction of model errors and testing the corrections through comparisons against field data. Atmos. Environ. Part A 27: 975-997.

De Raat, W. K.; Bakker, G. L.; de Meijere, F. A. (1990) Comparison of filter materials used for sampling of mutagens and polycyclic aromatic hydrocarbons in ambient airborne particles. Atmos. Environ. Part A 24: 2875-2887.

De Santis, F.; Allegrini, I. (1992) Heterogeneous reactions of SO_2 and NO_2 on carbonaceous surfaces. Atmos. Environ. Part A 26: 3061-3064.

De Valk, J. P. J. M. M. (1994) A model for cloud chemistry: a comparison between model simulations and observations in stratus and cumulus. Atmos. Environ. 28: 1665-1678.

Dickerson, R. R.; Huffman, G. J.; Luke, W. T.; Nunnermacker, L. J.; Pickering, K. E.; Leslie, A. C. D.; Lindsey, C. G.; Slinn, W. G. N.; Kelly, T. J.; Daum, P. H.; Delany, A. C.; Greenberg, J. P.; Zimmerman, P. R.; Boatman, J. F.; Ray, J. D.; Stedman, D. H. (1987) Thunderstorms: an important mechanism in the transport of air pollutants. Science (Washington, DC) 235: 460-465.

Dittenhoefer, A. C.; de Pena, R. G. (1978) A study of production and growth of sulfate particles in plumes from a coal-fired power plant. Atmos. Environ. 12: 297-306.

Dlugi, R. (1989) Chemistry and deposition of soot particles in moist air and fog. Aerosol Sci. Technol. 10: 93-105.

Dlugi, R.; Güsten, H. (1983) The catalytic and photocatalytic activity of coal fly ashes. Atmos. Environ. 17: 1765-1771.

Dod, R. L.; Brown, N. J.; Mowrer, F. W.; Novakov, T.; Williamson, R. B. (1989) Smoke emission factors from medium-scale fires: part 2. Aerosol Sci. Technol. 10: 20-27.

Doyle, G. J.; Tuazon, E. C.; Graham, R. A.; Mischke, T. M.; Winer, A. M.; Pitts, J. N., Jr. (1979) Simultaneous concentrations of ammonia and nitric acid in a polluted atmosphere and their equilibrium relationship to particulate ammonium nitrate. Environ. Sci. Technol. 13: 1416-1419.

Draxler, R. R. (1982) Measuring and modeling the transport and dispersion of Krypton-85 1500 km from a point source. Atmos. Environ. 16: 2763-2776.

Draxler, R. R. (1984) Diffusion and transport experiments. In: Randerson, D., ed. Atmospheric science and power production. Washington, DC: U.S. Department of Energy, Office of Scientific and Technical Information; pp. 367-422; report no. DOE/TIC-27601. Available from: NTIS, Springfield, VA; DE84-005177.

Draxler, R. R.; Dietz, R.; Lagomarsino, R. J.; Start, G. (1991) Across North America Tracer Experiment (ANATEX): sampling and analysis. Atmos. Environ. Part A 25: 2815-2836.

Drewes, D. R.; Hales, J. M. (1982) SMICK—a scavenging model incorporating chemical kinetics. Atmos. Environ. 16: 1717-1724.

Duce, R. A.; Mohnen, V. A.; Zimmerman, P. R.; Grosjean, D.; Cautreels, W.; Chatfield, R.; Jaenicke, R.; Ogren, J. A.; Pellizzari, E. D.; Wallace, G. T. (1983) Organic material in the global troposphere. Rev. Geophys. Space Phys. 21: 921-952.

Durham, J. L.; Wilson, W. E.; Ellestad, T. G.; Willeke, K.; Whitby, K. T. (1975) Comparison of volume and mass distributions for Denver aerosols. Atmos. Environ. 9: 717-722.

Dzubay, T. G.; Stevens, R. K.; Gordon, G. E.; Olmez, I.; Sheffield, A. E.; Courtney, W. J. (1988) A composite receptor method applied to Philadelphia aerosol. Environ. Sci. Technol. 22: 46-52.

Eatough, D. J.; Richter, B. E.; Eatough, N. L.; Hansen, L. D. (1981) Sulfur chemistry in smelter and power plant plumes in the western U.S. In: White, W. H.; Moore, D. J.; Lodge, J. P., Jr., eds. Plumes and visibility: measurements and model components: proceedings of the symposium; November 1980; Grand Canyon National Park, AZ. Atmos. Environ. 15: 2241-2253.

Eatough, D. J.; Christensen, J. J.; Eatough, N. L.; Hill, M. W.; Major, T. D.; Mangelson, N. F.; Post, M .E.; Ryder, J. F.; Hansen, L. D.; Meisenheimer, R. G.; Fischer, J. W. (1982) Sulfur chemistry in a copper smelter plume. Atmos. Environ. 16: 1001-1015.

Eatough, D. J.; Arthur, R. J.; Eatough, N. L.; Hill, M. W.; Mangelson, N. F.; Richter, B. E.; Hansen, L. D.; Cooper, J. A. (1984) Rapid conversion of SO_2(g) to sulfate in a fog bank. Environ. Sci. Technol. 18: 855-859.

Eatough, D. J.; Sedar, B.; Lewis, L.; Hansen, L. D.; Lewis, E. A.; Farber, R. J. (1989) Determination of semivolatile organic compounds in particles in the Grand Canyon area. Aerosol Sci. Technol. 10: 438-449.

Eatough, D. J.; Wadsworth, A.; Eatough, D. A.; Crawford, J. W.; Hansen, L. D.; Lewis, E. A. (1993) A multiple-system, multi-channel diffusion denuder sampler for the determination of fine-particulate organic material in the atmosphere. Atmos. Environ. Part A 27: 1213-1219.

Eatough, D. J.; Tang, H.; Cui, W.; Machir, J. (1995) Determination of the size distribution and chemical composition of fine particulate semi-volatile organic material in urban environments using diffusion denuder technology. In: Phalen, R. F.; Bates, D. V., eds. Proceedings of the colloquium on particulate air pollution and human mortality and morbidity, part II; Janaury 1994; Irvine, CA. Inhalation Toxicol. 7: 691-710.

Eisele, F. L.; Bradshaw, J. D. (1993) The elusive hydroxyl radical: measuring OH in the atmosphere. Anal. Chem. 65: 927A-939A.

Eisele, F. L.; Tanner, D. J. (1993) Measurement of the gas phase concentration of H_2SO_4 and methane sulfonic acid and estimates of H_2SO_4 production and loss in the atmosphere. J. Geophys. Res. [Atmos.] 98: 9001-9010.

Eldering, A.; Cass, G. R.; Moon, K. C. (1994) An air monitoring network using continuous particle size distribution monitors: connecting pollutant properties to visibility via Mie scattering calculations. Atmos. Environ. 28: 2733-2749.

Eldred, R. A.; Cahill, T. A.; Flocchini, R. G. (1994) Comparison of PM_{10} and $PM_{2.5}$ aerosols in the IMPROVE network. In: Proceedings of an international specialty conference on aerosol and atmospheric optics: radiative balance and visual air quality, volume A. Pittsburgh, PA: Air and Waste Management Association. Air Waste: submitted.

Eltgroth, M. W.; Hobbs, P. V. (1979) Evolution of particles in the plumes of coal-fired power plants—II. A numerical model and comparisons with field measurements. Atmos. Environ. 13: 953-975.

Er-El, J.; Peskin, R. L. (1981) Relative diffusion of constant-level balloons in the southern hemisphere. J. Atmos. Sci. 38: 2264-2274.

Erickson, R. E.; Yates, L. M.; Clark, R. L.; McEwen, D. (1977) The reaction of sulfur dioxide with ozone in water and its possible atmospheric significance. Atmos. Environ. 11: 813-817.

Facchini, M. C.; Fuzzi, S.; Lind, J. A.; Fierlinger-Oberlinninger, H.; Kalina, M.; Puxbaum, H.; Winiwarter, W.; Arends, B. G.; Wobrock, W.; Jaeschke, W.; Berner, A.; Kruisz, C. (1992) Phase-partitioning and chemical reactions of low molecular weight organic compounds in fog. Tellus Ser. B 44B: 533-544.

Falerios, M.; Schild, K.; Sheehan, P.; Paustenbach, D. (1992) Airborne concentrations of trivalent and hexavalent chromium from contaminated soils at unpaved partially paved commercial/industrial sites. J. Air Waste Manage. Assoc. 42: 40-48.

Ferber, G. J.; Telegadas, K.; Heffter, J. L.; Dickson, C. R.; Dietz, R. N.; Krey, P. W. (1981) Demonstration of a long-range atmospheric tracer system using perfluorocarbons. Silver Springs, MD: National Oceanic and Atmospheric Administration; NOAA report no. NOAA TM ERL ARL-101.

Ferber, G. J.; Heffter, J. L.; Draxler, R. R.; Lagomarsino, R. J.; Thomas, F. L.; Dietz, R. N.; Benkovitz, C. M. (1986) Cross-Appalachian Tracer Experiment (CAPTEX-83) final report. Silver Springs, MD: National Oceanic and Atmospheric Administration; NOAA report no. NOAA TM ERL ARL-142.

Fernandez de la Mora, J. (1986) Inertia and interception in the deposition of particles from boundary layers. Aerosol Sci. Technol. 5: 261-266.

Fernandez de la Mora, J.; Friedlander, S. K. (1982) Aerosol and gas deposition to fully rough surfaces: filtration model for blade-shaped elements. Int. J. Heat Mass Transfer 25: 1725-1735.

Finlayson-Pitts, B. J.; Pitts, J. N., Jr. (1986) Atmospheric chemistry: fundamentals and experimental techniques. New York, NY: John Wiley & Sons; pp. 783-1007.

Fitzgerald, J. W. (1973) Dependence of the supersaturation spectrum of CCN on aerosol size distribution and composition. Presented at: the second international workshop on condensation and ice nuclei; August 1970; Fort Collins, CO. J. Atmos. Sci. 30: 628-634.

Fitzgerald, J. W.; Hoppel, W. A.; Vietti, M. A. (1982) The size and scattering coefficient of urban aerosol particles at Washington, DC as a function of relative humidity. J. Atmos. Sci. 39: 1838-1852.

Flossmann, A. I.; Hall, W. D.; Pruppacher, H. R. (1985) A theoretical study of the wet removal of atmospheric pollutants. Part I: The redistribution of aerosol particles captured through nucleation and impaction scavenging by growing cloud drops. J. Atmos. Sci. 42: 583-606.

Foitzik, L. (1950) Zur meteorologischen Optik von Dunst und Nebel: Teil II [The meteorological optics of haze and fog: part II]. Z. Meteorol. 4: 321-329.

Foreman, W. T.; Bidleman, T. F. (1990) Semivolatile organic compounds in the ambient air of Denver, Colorado. Atmos. Environ. Part A 24: 2405-2416.

Forkel, R.; Seidl, W.; Dlugi, R.; Deigele, E. (1990) A one-dimensional numerical model to simulate formation and balance of sulfate during radiation fog events. J. Geophys. Res. [Atmos.] 95: 18,501-18,515.

Forrest, J.; Newman, L. (1973) Sampling and analysis of atmospheric sulfur compounds for isotope ratio studies. Atmos. Environ. 7: 561-573.

Forrest, J.; Newman, L. (1977a) Further studies on the oxidation of sulfur dioxide in coal-fired power plant plumes. Atmos. Environ. 11: 465-474.

Forrest, J.; Newman, L. (1977b) Oxidation of sulfur dioxide in the Sudbury smelter plume. Atmos. Environ. 11: 517-520.

Forrest, J.; Garber, R.; Newman, L. (1979) Formation of sulfate, ammonium and nitrate in an oil-fired power plant plume. Atmos. Environ. 13: 1287-1297.

Forrest, J.; Garber, R. W.; Newman, L. (1981) Conversion rates in power plant plumes based on filter pack data: the coal-fired Cumberland plume. Atmos. Environ. 15: 2273-2282.

Freeman, D. J.; Cattell, F. C. R. (1990) Woodburning as a source of atmospheric polycyclic aromatic hydrocarbons. Environ. Sci. Technol. 24: 1581-1585.

Frick, G. M.; Hoppel, W. A. (1993) Airship measurements of aerosol size distributions, cloud droplet spectra, and trace gas concentrations in the marine boundary layer. Bull. Am. Meteorol. Soc. 74: 2195-2202.

Fried, A.; Henry, B. E.; Calvert, J. G.; Mozurkewich, M. (1994) The reaction probability of N_2O_5 with sulfuric acid aerosols at stratospheric temperatures and compositions. J. Geophys. Res. [Atmos.] 99: 3517-3532.

Friedlander, S. K. (1970) The characterization of aerosols distributed with respect to size and chemical composition. J. Aerosol Sci. 1: 295-307.

Friedlander, S. K.; Turner, J. R.; Hering, S. V. (1986) A new method for estimating dry deposition velocities for atmospheric aerosols. J. Aerosol Sci. 17: 240-244.

Fung, C. S.; Misra, P. K.; Bloxam, R.; Wong, S. (1991) A numerical experiment on the relative importance of H_2O_2 and O_3 in aqueous conversion of SO_2 to SO_4^{2-}. Atmos. Environ. Part A 25: 411-423.

Fuzzi, S.; Castillo, R. A.; Jiusto, J. E.; Lala, G. G. (1984) Chemical composition of radiation fog water at Albany, New York, and its relationship to fog microphysics. J. Geophys. Res. [Atmos.] 89: 7159-7164.

Fuzzi, S.; Orsi, G.; Nardini, G.; Facchini, M. C.; McLaren, S.; McLaren, E.; Mariotti, M. (1988) Heterogeneous processes in the Po Valley radiation fog. J. Geophys. Res. [Atmos.] 93: 11,141-11,151.

Gagosian, R. B.; Peltzer, E. T.; Merrill, J. T. (1987) Long-range transport of terrestrially derived lipids in aerosols from the south Pacific. Nature (London) 325: 800-803.

Galloway, J. N.; Thornton, J. D.; Norton, S. A.; Volchok, H. L.; McLean, R. A. N. (1982) Trace metals in atmospheric deposition: a review and assessment. Atmos. Environ. 16: 1677-1700.

Garland, J. A. (1979) Resuspension of particulate matter from grass and soil. Harwell, United Kingdom: Atomic Energy Research Establishment; report no. AERE-R9452. Available from: NTIS, Springfield, VA.; AERE-R9452.

Gatz, D. F. (1977) Scavenging ratio measurements in METROMEX. In: Semonin, R. G.; Beadle, R. W., eds. Precipitation scavenging (1974): proceedings of a symposium; October 1974; Champaign, IL. Oak Ridge, TN: Energy Research and Development Administration; pp. 71-87. Available from: NTIS, Springfield, VA; CONF-741003. (ERDA symposium series no. 41).

Gebhart, K. A.; Malm, W. C.; Day, D. (1994) Examination of the effects of sulfate acidity and relative humidity on light scattering at Shenandoah National Park. Atmos. Environ. 28: 841-849.

Gerde, P.; Scholander, P. (1989) Mass transfer rates of polycyclic aromatic hydrocarbons between micron-size particles and their environment—theoretical estimates. Environ. Health Perspect. 79: 249-258.

Germani, M. S.; Buseck, P. R. (1991) Automated scanning electron microscopy for atmospheric particle analysis. Anal. Chem. 63: 2232-2237.

Gervat, G. P.; Clark, P. A.; Marsh, A. R. W.; Choularton, T. W.; Gay, M. J. (1988) Controlled chemical kinetic experiments in cloud: a review of the CERL/UMIST Great Dun Fell project. In: Unsworth, M. H.; Fowler, D., eds. Acid deposition at high elevation sites: proceedings of the NATO advanced research workshop; September 1986; Edinburgh, United Kingdom. Dordrecht, The Netherlands: Kluwer Academic Publishers; pp. 283-298. (NATO ASI series C: mathematical and physical sciences v. 252).

Gery, M. W.; Fox, D. L.; Jeffries, H. E.; Stockburger, L.; Weathers, W. S. (1985) A continuous stirred tank reactor investigation of the gas-phase reaction of hydroxyl radicals and toluene. Int. J. Chem. Kinet. 17: 931-955.

Gery, M. W.; Fox, D. L.; Kamens, R. M.; Stockburger, L. (1987) Investigation of hydroxyl radical reactions with o-xylene and m-xylene in a continuous stirred tank reactor. Environ. Sci. Technol. 21: 339-348.

Ghan, S. J.; Chuang, C. C.; Penner, J. E. (1993) A parameterization of cloud droplet nucleation, part I: single aerosol type. Atmos. Res. 30: 198-221.

Gifford, F. A., Jr. (1961) Use of routine meteorological observations for estimating atmospheric dispersion. Nucl. Saf. 2: 47-51.

Gill, P. S.; Graedel, T. E.; Wechsler, C. J. (1983) Organic films on atmospheric aerosol particles, fog droplets, cloud droplets, raindrops and snowflakes. Rev. Geophys. Space Phys. 21: 903-920.

Gillani, N. V. (1985) Modeling of chemical transformations of SO_x and NO_x in the polluted atmosphere—an overview of approaches and current status. In: De Wispelaere, C., ed. Air pollution modeling and its application IV. New York, NY: Plenum Publishers; pp. 163-192.

Gillani, N. V. (1986) Ozone formation in pollutant plumes: a reactive plume model with arbitrary crosswind resolution. Research Triangle Park, NC: U.S. Environmental Protection Agency, Atmospheric Sciences Research Laboratory; EPA report no. EPA/600/3-86/051. Available from: NTIS, Springfield, VA; PB86-236973.

Gillani, N. V.; Husar, R. B. (1976) Synoptic-scale haziness over the eastern US and its long range transport. Presented at: 4th National AMS/SAF conference on fire and forest meteorology; Boston, MA.

Gillani, N. V.; Pleim, J. E. (1995) Subgrid-scale features of anthropogenic emissions of VOC and NOx in the context of regional Eulerian models. Atmos. Environ.: in press.

Gillani, N. V.; Wilson, W. E. (1980) Formation and transport of ozone and aerosols in power plant plumes. Ann. N. Y. Acad. Sci. 338: 276-296.

Gillani, N. V.; Wilson, W. E. (1983) Gas-to-particle conversion of sulfur in power plant plumes—II. observations of liquid-phase conversions. Atmos. Environ. 17: 1739-1752.

Gillani, N. V.; Husar, R. B.; Husar, J. D.; Patterson, D. E.; Wilson, W. E., Jr. (1978) Project MISTT: kinetics of particulate sulfur formation in a power plant plume out to 300 km. Atmos. Environ. 12: 589-598.

Gillani, N. V.; Kohli, S.; Wilson, W. E. (1981) Gas-to-particle conversion of sulfur in power plant plumes—I. parametrization of the conversion rate for dry, moderately polluted ambient conditions. Atmos. Environ. 15: 2293-2313.

Gillani, N. V.; Colby, J. A.; Wilson, W. E. (1983) Gas-to-particle conversion of sulfur in power plant plumes—III. parameterization of plume-cloud interactions. Atmos. Environ. 17: 1753-1763.

Gillani, N. V.; Shannon, J. D.; Patterson, D. E. (1984) Transport processes. In: Altshuller, A. P.; Linthurst, R. A., eds. The acidic deposition phenomenon and its effects: critical assessment review papers, v. 1: atmospheric sciences. Washington, DC: U.S. Environmental Protection Agency, Office of Research and Development; report no. EPA/600/8-83/016AF. Available from: NTIS, Springfield, VA; PB85-100030.

Gillani, N. V.; Schwartz, S. E.; Leaitch, W. R.; Strapp, J. W.; Isaac, G. A. (1995) Field observations in continental stratiform clouds: partitioning of cloud particles between droplets and unactivated interstitial aerosols. J. Geophys. Res. [Atmos.] 100: 18,687-18,706.

Gillette, D. A. (1974) On the production of soil wind erosion aerosols having the potential for long range transport. J. Rech. Atmos. 8: 735-744.

Gillette, D. (1980) Major contributions of natural primary continental aerosols: source mechanisms. In: Kniep, T. J.; Lioy, P. J., eds. Aerosols: anthropogenic and natural, sources and transport. Ann N. Y. Acad. Sci. 338: 348-358.

Gillette, D. A.; Hanson, K. J. (1989) Spatial and temporal variability of dust production caused by wind erosion in the United States. J. Geophys. Res. [Atmos.] 94: 2197-2206.

Gillette, D.; Nagamoto, C. (1992) [Size distribution and single particle composition for two dust storms in Soviet Central Asia in September 1989 and size distributions and chemical composition of local soil]. In: Golitsyn, G., ed. Soviet-American experiment for the investigation of arid aerosols. St. Petersburg, USSR: Typhoon; pp. 130-140.

Gillette, D. A.; Passi, R. (1988) Modeling dust emission caused by wind erosion. J. Geophys. Res. [Atmos.] 93: 14,233-14,242.

Gillette, D. A.; Sinclair, P. C. (1990) Estimation of suspension of alkaline material by dust devils in the United States. Atmos. Environ. Part A 24: 1135-1142.

Gillette, D. A.; Walker, T. R. (1977) Characteristics of airborne particles produced by wind erosion of sandy soil, high plains of west Texas. Soil Sci. 123: 97-110.

Gillette, D. A.; Clayton, R. N.; Mayeda, T. K.; Jackson, M. L.; Sridhar, K. (1978) Tropospheric aerosols from some major dust storms of the southwestern United States. J. Appl. Meteorol. 17: 832-845.

Gillette, D. A.; Stensland, G. J.; Williams, A. L.; Barnard, W.; Gatz, D.; Sinclair, P. C.; Johnson, T. C. (1992) Emissions of alkaline elements calcium, magnesium, potassium, and sodium from open sources in the contiguous United States. Global Biogeochem. Cycles 6: 437-457.

Gleason, J. F.; Sinha, A.; Howard, C. J. (1987) Kinetics of the gas-phase reaction $HOSO_2 + O_2 \rightarrow HO_2 + SO_3$. J. Phys. Chem. 91: 719-724.

Godish, T. (1985) Air quality. Chelsea, MI: Lewis Publishers, Inc.

Godowitch, J. M. (1989) Evaluation and sensitivity analyses results of the MESOPUFF II model with CAPTEX measurements. Research Triangle Park, NC: U.S. Environmental Protection Agency, Atmospheric Research and Exposure Assessment Laboratory; EPA report no. EPA/600/3-89/056. Available from: NTIS, Springfield, VA; PB89-198253.

Goldberg, E. D. (1985) Black carbon in the environment: properties and distribution. New York, NY: John Wiley & Sons. (Metcalf, R. L.; Stumm, W., eds. Environmental science and technology series).

Gordon, G. E. (1991) Airborne particles on global and regional scales. Environ. Sci. Technol. 25: 1822-1828.

Gordon, R. J.; Trivedi, N. J.; Singh, B. P.; Ellis, E. C. (1988) Characterization of aerosol organics by diffuse reflectance Fourier transform infrared spectroscopy. Environ. Sci. Technol. 22: 672-677.

Goschnick, J.; Fichtner, M.; Lipp, M.; Schuricht, J.; Ache, H. J. (1993) Depth-resolved chemical analysis of environmental microparticles by secondary mass spectrometry. Appl. Surf. Sci. 70/71: 63-67.

Graedel, T. E.; Goldberg, K. I. (1983) Kinetic studies of raindrop chemistry: 1. inorganic and organic processes. J. Geophys. Res. C: Oceans Atmos. 88: 10,865-10,882.

Graedel, T. E.; Weschler, C. J. (1981) Chemistry within aqueous atmospheric aerosols and raindrops. Rev. Geophys. Space Phys. 19: 505-539.

Graedel, T. E.; Hawkins, D. T.; Claxton, L. D. (1986) Atmospheric chemical compounds: sources, occurrence, and bioassay. Orlando, FL: Academic Press, Inc.

Granat, L.; Soderland, R. (1975) Atmospheric deposition due to long and short distance sources with special reference to wet and dry deposition of sulfur. Stockholm, Sweden: Stockholm University, Meteorological Institute; report no. MISU-A32.

Gray, H. A. (1986) Control of atmospheric fine primary carbon particle concentration [Ph.D. thesis]. Pasadena, CA: California Institute of Technology; EQL report no. 23.

Gray, H. A.; Cass, G. R.; Huntzicker, J. J.; Heyerdahl, E. K.; Rau, J. A. (1984) Elemental and organic carbon particle concentrations: a long-term perspective. Sci. Total Environ. 36: 17-25.

Gray, H. A.; Cass, G. R.; Huntzicker, J. J.; Heyerdahl, E. K.; Rau, J. A. (1986) Characteristics of atmospheric organic and elemental carbon particle concentrations in Los Angeles. Environ. Sci. Technol. 20: 580-589.

Grell, G. A.; Dudhia, J.; Stauffer, D. R. (1994) A description of the fifth-generation Penn State/NCAR mesoscale model (MM5). Boulder, CO: National Center for Atmospheric Research; technical note no. NCAR/TN-398+STR.

Grosjean, D. (1977) Aerosols. In: Ozone and other photochemical oxidants. Washington, DC: National Academy of Sciences; pp. 45-125.

Grosjean, D. (1984a) Particulate carbon in Los Angeles air. Sci. Total Environ. 32: 133-145.

Grosjean, D. (1984b) Photooxidation of 1-heptane. Sci. Total Environ. 37: 195-211.

Grosjean, D. (1985) Reactions of *o*-cresol and nitrocresol with NO_x in sunlight and with ozone-nitrogen dioxide mixtures in the dark. Environ. Sci. Technol. 19: 968-974.

Grosjean, D. (1992) *In situ* organic aerosol formation during a smog episode: estimated production and chemical functionality. Atmos. Environ. Part A 26: 953-963.

Grosjean, D.; Friedlander, S. K. (1975) Gas-particle distribution factors for organic and other pollutants in the Los Angeles atmosphere. J. Air Pollut. Control Assoc. 25: 1038-1044.

Grosjean, D.; Seinfeld, J. H. (1989) Parameterization of the formation potential of secondary organic aerosols. Atmos. Environ. 23: 1733-1747.

Gundel, L. A.; Guyot-Sionnest, N. S.; Novakov, T. (1989) A study of the interaction of NO_2 with carbon particles. Aerosol Sci. Technol. 10: 343-351.

Gundel, L. A.; Lee, V. C.; Mahanama, K. R. R.; Stevens, R. K.; Daisey, J. M. (1995) Direct determination of the phase distributions of semi-volatile polycyclic aromatic hydrocarbons using annular denuders. Atmos. Environ. 29: 1719-1733.

Hahn, J. (1980) Organic constituents of natural aerosols. Ann. N. Y. Acad. Sci. 338: 359-376.

Hales, J. M. (1991) Atmospheric processes research and process model development. Section 4. Precipitation scavenging. In: Irving, P. M., ed. Acidic deposition: state of science and technology, volume I: emissions, atmospheric processes, and deposition. Washington, DC: The U.S. National Acid Precipitation Assessment Program; pp. 2-109 - 2-168. (State of science and technology report no. 2).

Hales, J. M.; Dana, M. T. (1979) Precipitation scavenging of urban pollutants by convective storm systems. J. Appl. Meteorol. 18: 294-316.

Hales, J. M.; Hicks, B. B.; Miller, J. M. (1987) The role of research measurement networks as contributors to federal assessments of acid deposition. Bull. Am. Meteorol. Soc. 68: 216-225.

Hall, F. P., Jr.; Duchon, C. E.; Lee, L. G.; Hagan, R. R. (1973) Long-range transport of air pollution: a case study, August 1970. Mon. Weather Rev. 101: 404-411.

Hamilton, R. S.; Mansfield, T. A. (1991) Airborne particulate elemental carbon: its sources, transport and contribution to dark smoke and soiling. Atmos. Environ. Part A 25: 715-723.

Hampton, C. V.; Pierson, W. R.; Schuetzle, D.; Harvey, T. M. (1983) Hydrocarbon gases emitted from vehicles on the road. 2. Determination of emission rates from diesel and spark-ignition vehicles. Environ. Sci. Technol. 17: 699-708.

Hänel, G. (1976) The properties of atmospheric aerosol particles as functions of the relative humidity at thermodynamic equilibrium with the surrounding moist air. In: Landsberg, H. E.; Van Mieghem, J., eds. Advances in geophysics: v. 19. New York, NY: Academic Press; pp. 73-188.

Hansen, A. D. A.; Novakov, T. (1989) Real-time measurements of the size fractionation of ambient black carbon aerosols at elevated humidities. Aerosol Sci. Technol. 10: 106-110.

Hansen, A. D. A.; Rosen, H. (1990) Individual measurements of the emission factor of aerosol black carbon in automobile plumes. J. Air Waste Manage. Assoc. 40: 1654-1657.

Hansen, A. D. A.; Benner, W. H.; Novakov, T. (1991) Sulfur dioxide oxidation in laboratory clouds. Atmos. Environ. Part A 25: 2521-2530.

Harrison, L. (1985) The segregation of aerosols by cloud-nucleating activity. Part II: Observation of an urban aerosol. J. Clim. Appl. Meteorol. 24: 312-321.

Harrison, R. M.; Kitto, A.-M. N. (1992) Estimation of the rate constant for the reaction of acid sulphate aerosol with NH_3 gas from atmospheric measurements. J. Atmos. Chem. 15: 133-143.

Harrison, R. M.; Msibi, I. M. (1994) Validation of techniques for fast response measurement of HNO_3 and NH_3 and determination of the $[NH_3][HNO_3]$ concentration product. Atmos. Environ. 28: 247-255.

Harrison, R. M.; Pio, C. A. (1983) A comparative study of the ionic composition of rainwater and atmospheric aerosols: implications for the mechanism of acidification of rainwater. Atmos. Environ. 17: 2539-2543.

Harrison, R. M.; Laxen, D. P. H.; Wilson, S. J. (1981) Chemical associations of lead, cadmium, copper, and zinc in street dusts and roadside soils. Environ. Sci. Technol. 15: 1378-1383.

Hart, K. M.; Pankow, J. F. (1994) High-volume air sampler for particle and gas sampling. 2. Use of backup filters to correct for the adsorption of gas-phase polycyclic aromatic hydrocarbons to the front filter. Environ. Sci. Technol. 28: 655-661.

Hasan, H.; Dzubay, T. G. (1987) Size distributions of species in fine particles in Denver using a microorifice impactor. Aerosol Sci. Technol. 6: 29-39.

Hatakeyama, S.; Tanonaka, T.; Weng, J.; Bandow, H.; Takagi, H.; Akimoto, H. (1985) Ozone-cyclohexene reaction in air: quantitative analysis of particulate products and the reaction mechanism. Environ. Sci. Technol. 19: 935-942.

Hatakeyama, S.; Ohno, M.; Weng, J.; Takagi, H.; Akimoto, H. (1987) Mechanism for the formation of gaseous and particulate products from ozone-cycloalkene reactions in air. Environ. Sci. Technol. 21: 52-57.

Hatakeyama, S.; Izumi, K.; Fukuyama, T.; Akimoto, H. (1989) Reactions of ozone with α-pinene and β-pinene in air: yields of gaseous and particulate products. J. Geophys. Res. [Atmos.] 94: 13,013-13,024.

Hatakeyama, S.; Izumi, K.; Fukuyama, T.; Akimoto, H.; Washida, N. (1991) Reactions of OH with α-pinene and β-pinene in air: estimate of global CO production from the atmospheric oxidation of terpenes. J. Geophys. Res. [Atmos.] 96: 947-958.

Hegg, D. A. (1985) The importance of liquid-phase oxidation of SO_2 in the troposphere. J. Geophys. Res. [Atmos.] 90: 3773-3779.

Hegg, D. A.; Hobbs, P. V. (1979) Some observations of particulate nitrate concentrations in coal-fired power plant plumes. Atmos. Environ. 13: 1715-1716.

Hegg, D. A.; Hobbs, P. V. (1980) Measurements of gas-to-particle conversion in the plumes from five coal-fired electric power plants. Atmos. Environ. 14: 99-116.

Hegg, D. A.; Hobbs, P. V. (1982) Measurements of sulfate production in natural clouds. Atmos. Environ. 16: 2663-2668.

Hegg, D. A.; Hobbs, P. V. (1983a) Errata [Hegg and Hobbs (1982)]. Atmos. Environ. 17: 1059.

Hegg, D. A.; Hobbs, P. V. (1983b) Author's reply: measurements of sulfate production in natural clouds. Atmos. Environ. 17: 2632-2633.

Hegg, D. A.; Hobbs, P. V. (1986) Sulfate and nitrate chemistry in cumuliform clouds. Atmos. Environ. 20: 901-909.

Hegg, D. A.; Hobbs, P. V. (1987) Comparisons of measured sulfate production due to ozone oxidation in clouds with a kinetic rate equation. Geophys. Res. Lett. 14: 719-721.

Hegg, D. A.; Hobbs, P. V. (1988) Comparisons of sulfate and nitrate production in clouds on the mid-Atlantic and Pacific Northwest Coasts of the United States. J. Atmos. Chem. 7: 325-333.

Hegg, D. A.; Larson, T. V. (1990) The effects of microphysical parameterization on model predictions of sulfate production in clouds. Tellus Ser. B 42B: 272-284.

Hegg, D. A.; Hobbs, P. V.; Radke, L. F. (1984) Measurements of the scavenging of sulfate and nitrate in clouds. Atmos. Environ. 18: 1939-1946.

Hegg, D. A.; Radke, L. F.; Hobbs, P. V. (1990) Particle production associated with marine clouds. J. Geophys. Res. [Atmos.] 95: 13,917-13,926.

Hegg, D. A.; Radke, L. F.; Hobbs, P. V. (1991) Measurements of Aitken nuclei and cloud condensation nuclei in the marine atmosphere and their relation to the DMS-cloud-climate hypothesis. J. Geophys. Res. [Atmos.] 96: 18,727-18,733.

Hegg, D. A.; Yuen, P.-F.; Larson, T. V. (1992) Modeling the effects of heterogeneous cloud chemistry on the marine particle size distribution. J. Geophys. Res. [Atmos.] 97: 12,927-12,933.

Heintzenberg, J.; Winkler, P. (1984) Elemental carbon in the urban aerosol: results of a seventeen month study in Hamburg, FRG. Sci. Total Environ. 36: 27-38.

Heintzenberg, J.; Ogren, J. A.; Noone, K. J.; Gärdneus, L. (1989) The size distribution of submicrometer particles within and about stratocumulus cloud droplets on Mt. Åreskutan, Sweden. Atmos. Res. 24: 89-101.

Heisler, S. L.; Friedlander, S. K. (1977) Gas-to-particle conversion in photochemical smog - aerosol growth laws and mechanisms for organics. Atmos. Environ. 11: 157-168.

Hering, S. V.; Friedlander, S. K. (1982) Origins of aerosol sulfur size distributions in the Los Angeles basin. Atmos. Environ. 16: 2647-2656.

Hering, S. V.; McMurry, P. H. (1991) Optical counter response to monodisperse atmospheric aerosols. Atmos. Environ. Part A 25: 463-468.

Hering, S. V.; Lawson, D. R.; Allegrini, I.; Febo, A.; Perrino, C.; Possanzini, M.; Sickles, J. E., II; Anlauf, K. G.; Wiebe, A.; Appel, B. R.; John, W.; Ondo, J.; Wall, S.; Braman, R. S.; Sutton, R.; Cass, G. R.; Solomon, P. A.; Eatough, D. J.; Eatough, N. L.; Ellis, E. C.; Grosjean, D.; Hicks, B. B.; Womack, J. D.; Horrocks, J.; Knapp, K. T.; Ellestad, T. G.; Paur, R. J.; Mitchell, W. J.; Pleasant, M.; Peake, E.; MacLean, A.; Pierson, W. R.; Brachaczek, W.; Schiff, H. I.; Mackay, G. I.; Spicer, C. W.; Stedman, D. H.; Winer, A. M.; Biermann, H. W.; Tuazon, E. C. (1988) The nitric acid shootout: field comparison of measurement methods. Atmos. Environ. 22: 1519-1539.

Hicks, B. B. (1984) Dry deposition processes. In: Altshuller, A. P.; Linthurst, R. A., eds. Acidic deposition phenomenon and its effects: critical assessment review papers, volume I, atmospheric sciences. Washington, DC: U.S. Environmental Protection Agency, Office of Research and Development; pp. 7-1 to 7-70; EPA report no. EPA/600/8-83/016AF. Available from: NTIS, Springfield, VA; PB85-100030.

Hicks, B. B.; Meyers, T. P. (1989) Atmosphere-surface exchange processes. Presented at: 82nd annual meeting of the Air & Waste Management Association; June; Anaheim, CA. Pittsburgh, PA: Air & Waste Management Association; paper no. 89-113.4.

Hicks, B. B.; Wesely, M. L.; Lindberg, S. E.; Bromberg, S. M., eds. (1986) Proceedings of the NAPAP workshop on dry deposition; March; Harpers Ferry, WV. Oak Ridge, TN: National Oceanic and Atmospheric Administration.

Hicks, B. B.; Draxler, R. R.; Dodge, M.; Hales, J. M.; Albritton, D. L.; Schwartz. S. E.; Meyers, T. P.; Fehsenfeld, F. C.; Tanner, R. L.; Vong, R. J. (1991) Atmospheric processes research and process model development. In: Irving, P. M., ed. Acidic deposition: state of science and technology, volume I: emissions, atmospheric processes, and deposition. Washington, DC: The U.S. National Acid Precipitation Assessment Program. (State of science and technology report no. 2).

Hildemann, L. M. (1990) A study of the origin of atmospheric organic aerosols [Ph.D. thesis]. Pasadena, CA: California Institute of Technology. Available from: University Microfilms, Ann Arbor, MI; order no. AAC90-14378.

Hildemann, L. M.; Russell, A. G.; Cass, G. R. (1984) Ammonia and nitric acid concentrations in equilibrium with atmospheric aerosols: experiment vs theory, Atmos. Environ. 18: 1737-1750.

Hildemann, L. M.; Cass, G. R.; Mazurek, M. A.; Simoneit, B. R. T. (1993) Mathematical modeling of urban organic aerosol: properties measured by high-resolution gas chromatography. Environ. Sci. Technol. 27: 2045-2055.

Hildemann, L. M.; Klinedinst, D. B.; Klouda, G. A.; Currie, L. A.; Cass, G. R. (1994a) Sources of urban contemporary carbon aerosol. Environ. Sci. Technol. 28: 1565-1576.

Hildemann, L. M.; Mazurek, M. A.; Cass, G. R.; Simoneit, B. R. T. (1994b) Seasonal trends in Los Angeles ambient organic aerosol observed by high-resolution gas chromatography. Aerosol Sci. Technol. 20: 303-317.

Hill, T. A.; Choularton, T. W.; Penkett, S. A. (1986) A model of sulphate production in a cap cloud and subsequent turbulent deposition onto the hill surface. Atmos. Environ. 20: 1763-1771.

Hinds, W. C. (1982) Aerosol technology. New York, NY: John Wiley and Sons.

Hobbs, P. V.; Bowdle, D. A.; Radke, L. F. (1985) Particles in the lower troposphere over the high plains of the United States. Part I: size distributions, elemental compositions and morphologies. J. Clim. Appl. Meteorol. 24: 1344-1356.

Hoffmann, M. R.; Boyce, S. D. (1983) Catalytic autooxidation of aqueous sulfur dioxide in relationship to atmospheric systems. Adv. Environ. Sci. Technol. 12: 147-189.

Hoffmann, M. R.; Calvert, J. G. (1985) Chemical transformation modules for Eulerian acid deposition models: volume II, the aqueous-phase chemistry. Research Triangle Park, NC: U.S. Environmental Protection Agency, Atmospheric Sciences Research Laboratory; EPA report no. EPA/600/3-85/036. Available from: NTIS, Springfield, VA; PB85-198653/AS.

Hoffmann, M. R.; Edwards, J. O. (1975) Kinetics of the oxidation of sulfite by hydrogen peroxide in acidic solution. J. Phys. Chem. 79: 2096-2098.

Hoffmann, M. R.; Jacob, D. J. (1984) Kinetics and mechanisms of the catalytic oxidation of dissolved sulfur dioxide in aqueous solution: an application to nighttime fog water chemistry. In: Calvert, J. G., ed. SO_2, NO and NO_2 oxidation mechanisms: atmospheric considerations. Boston, MA: Butterworth Publishers; pp. 101-172. (Teasley, J. I., ed. Acid precipitation series: v. 3).

Hoffmann, H. E.; Kuehnemann, W. (1979) Comparison of the results of two measuring methods determining the horizontal standard visibility with the visual visibility range. Atmos. Environ. 13: 1629-1634.

Holsen, T. M.; Noll, K. E.; Fang, G.-C.; Lee, W.-J.; Lin, J.-M.; Keeler, G. J. (1993) Dry deposition and particle size distributions measured during the Lake Michigan Urban Air Toxics Study. Environ. Sci. Technol. 27: 1327-1333.

Hong, M.-S.; Carmichael, G. R. (1986a) An investigation of sulfate production in an orographic storm using a detailed transport/chemistry model coupled with a detailed cloud scavenging model. Atmos. Environ. 20: 1989-1997.

Hong, M.-S.; Carmichael, G. R. (1986b) Examination of a subgrid-scale parameterization for the transport of pollutants in a nonprecipitating cumulus cloud ensemble. Atmos. Environ. 20: 2205-2217.

Hoppel, W. A. (1988) The role of non-precipitating cloud cycles and gas-to-particle conversion in the maintainence of the submicron aerosol size distribution over the tropical oceans. In: Hobbs, P. V.; McCormick, M. P., eds. Aerosols and climate. Hampton, VA: A. Deepak Publishers; pp. 9-19.

Hoppel, W. A.; Frick, G. M. (1990) Submicron aerosol size distributions measured over the tropical and South Pacific. Atmos. Environ. Part A 24: 645-659.

Hoppel, W. A.; Frick, G. M.; Larson, R. E. (1986) Effect of nonprecipitating clouds on the aerosol size distribution in the marine boundary layer. Geophys. Res. Lett. 13: 125-128.

Hoppel, W. A.; Fitzgerald, J. W.; Frick, G. M.; Larson, R. E.;, et al. (1990) Aerosol size distributions and optical properties found in the marine boundary layer over the Atlantic Ocean. J. Geophys. Res. [Atmos.] 95: 3659-3686.

Hoppel, W. A.; Frick, G. M.; Fitzgerald, J.; Larson, R. E. (1994) Marine boundary layer measurements of new particle formation and the effects nonprecipitating clouds have on aerosol size distribution. J. Geophys. Res. [Atmos.] 99: 14,443-14,459.

Horvath, H.; Noll, K. E. (1969) The relationship between atmospheric light scattering coefficient and visibility. Atmos. Environ. 3: 543-550.

Hosker, R. P., Jr.; Lindberg, S. E. (1982) Review: atmospheric deposition and plant assimilation of gases and particles. Atmos. Environ. 16: 889-910.

Hov, O.; Isaksen, I. S. A. (1981) Generation of secondary pollutants in a power plant plume: a model study. Atmos. Environ. 15: 2367-2376.

Huang, P.-F.; Turpin, B. J.; Pipho, M. J.; Kittelson, D. B.; McMurry, P. H. (1994) Effects of water condensation and evaporation on diesel chain-agglomerate morphology. J. Aerosol Sci. 25: 447-459.

Hubbe, J. M. (1989) Assessing procedures for estimating deposition rates for pollutants of interest. Sacramento, CA: California Air Resources Board, San Joaquin Valley Air Pollution Study Agency; San Joaquin Valley Air Quality Study technical support study no. 8.

Hudischewskyj, A. B.; Seigneur, C. (1989) Mathematical modeling of the chemistry and physics of aerosols in plumes. Environ. Sci. Technol. 23: 413-421.

Huntzicker, J. J.; Hoffman, R. S.; Ling, C.-S. (1978) Continuous measurement and speciation of sulfur-containing aerosols by flame photometry. Atmos. Environ. 12: 83-88.

Huntzicker, J. J.; Cary, R. A.; Ling, C.-S. (1980) Neutralization of sulfuric acid aerosol by ammonia. Environ. Sci. Technol. 14: 819-824.

Huntzicker, J. J.; Johnson, R. L.; Shah, J. J.; Cary, R. A. (1982) Analysis of organic and elemental carbon in ambient aerosols by a thermal-optical method. In: Wolff, G. T.; Klimisch, R. L., eds. Particulate carbon - atmospheric life cycle: proceedings of an international symposium; October 1980; Warren, MI. New York, NY: Plenum Press; pp. 79-88.

Husain, L.; Dutkiewicz, V. A.; Hussain, M. M.; Khwaja, H. A.; Burkhard, E. G.; Mehmood, G.; Parekh, P. P.; Canelli, E. (1991) A study of heterogeneous oxidation of SO_2 in summer clouds. J. Geophys. Res. [Atmos.] 96: 18,789-18,805.

Husar, R. B.; Gillani, N. V.; Husar, J. D. (1976) Particulate sulfur formation in power plant: urban and regional plumes. Presented at: Symposium on aerosol science and technology at the 82nd national meeting of the AIChE; August-September; Atlantic City, MD.

Husar, R. B.; Patterson, D. E.; Husar, J. D.; Gillani, N. V.; Wilson, W. E., Jr. (1978) Sulfur budget of a power plant plume. In: Husar, R. B.; Lodge, J. P., Jr.; Moore, D. J., eds. Sulfur in the atmosphere: proceedings of the international symposium; September 1977; Dubrovnik, Yugoslavia. Atmos. Environ. 12: 549-568.

Husar, R. B.; Holloway, J. M.; Patterson, D. E.; Wilson, W. E. (1981) Spatial and temporal pattern of eastern U.S. haziness: a summary. Atmos. Environ. 15: 1919-1928.

Huss, A., Jr.; Lim, P. K.; Eckert, C. A. (1982a) Oxidation of aqueous sulfur dioxide. 1. Homogeneous manganese(II) and iron(II) catalysis at low pH. J. Phys. Chem. 86: 4224-4228.

Huss, A., Jr.; Lim, P. K.; Eckert, C. A. (1982b) Oxidation of aqueous sulfur dioxide. 2. High-pressure studies and proposed reaction mechanisms. J. Phys. Chem. 86: 4229-4233.

Ibusuki, T.; Takeuchi, K. (1987) Sulfur dioxide oxidation by oxygen catalyzed by mixtures of manganese(II) and iron(III) in aqueous solutions at environmental reaction conditions. Atmos. Environ. 21: 1555-1560.

Irwin, J. S. (1983) Estimating plume dispersion—a comparison of several sigma schemes. J. Clim. Appl. Meteorol. 22: 92-114.

Isaksen, I. S. A.; Hov, O.; Hesstvedt, E. (1978) Ozone generation over rural areas. Environ. Sci. Technol. 12: 1279-1284.

Izumi, K.; Fukuyama, T. (1990) Photochemical aerosol formation from aromatic hydrocarbons in the presence of NO_x. Atmos. Environ. Part A 24: 1433-1441.

Izumi, K.; Murano, K.; Mizuochi, M.; Fukuyama, T. (1988) Aerosol formation by the photooxidation of cyclohexene in the presence of nitrogen oxides. Environ. Sci. Technol. 22: 1207-1215.

Jackson, M. L.; Gillette, D. A.; Danielsen, E. F.; Blifford, I. H.; Bryson, R. A.; Syers, J. K. (1973) Global dustfall during the quaternary as related to environments. Soil Sci. 116: 135-145.

Jacob, D. J. (1986) Chemistry of OH in remote clouds and its role in the production of formic acid and peroxymonosulfate. J. Geophys. Res. [Atmos.] 91: 9807-9826.

Jacob, D. J.; Hoffmann, M. R. (1983) A dynamic model for the production of H^+, NO_3^-, and SO_4^{2-} in urban fog. J. Geophys. Res. C: Oceans Atmos. 88: 6611-6621.

Jacob, D. J.; Waldman, J. M.; Munger, J. W.; Hoffmann, M. R. (1985) Chemical composition of fogwater collected along the California coast. Environ. Sci. Technol. 19: 730-736.

Jacob, D. J.; Munger, J. W.; Waldman, J. M.; Hoffmann, M. R. (1986a) The H_2SO_4-HNO_3-NH_3 system at high humidities and in fogs: 1. spatial and temporal patterns in the San Joaquin Valley of California. J. Geophys. Res. [Atmos.] 91: 1073-1088.

Jacob, D. J.; Waldman, J. M.; Munger, J. W.; Hoffmann, M. R. (1986b) The H_2SO_4-HNO_3-NH_3 system at high humidities and in fogs: 2. comparison of field data with thermodynamic calculations. J. Geophys. Res. [Atmos.] 91: 1089-1096.

Jaffrezo, J.-L.; Colin, J.-L. (1988) Rain-aerosol coupling in urban area: scavenging ratio measurement and identification of some transfer processes. Atmos. Environ. 22: 929-935.

Japar, S. M.; Brachaczek, W. W.; Gorse, R. A., Jr.; Norbeck, J. M.; Pierson, W. R. (1986) The contribution of elemental carbon to the optical properties of rural atmospheric aerosols. Atmos. Environ. 20: 1281-1289.

Jassim, J. A.; Lu, H. P.; Chughtai, A. R.; Smith, D. M. (1986) The origin of infrared absorption bands of soot in the region 750 to 900 cm^{-1}. Appl. Spectrosc. 40: 113-116.

John, W.; Sethi, V. (1993) Threshold for resuspension by particle impaction. Aerosol Sci. Technol. 19: 69-79.

John, W.; Wang, H.-C. (1991) Laboratory testing method for PM-10 samplers: lowered effectiveness from particle loading. Aerosol Sci. Technol. 14: 93-101.

John, W.; Wall, S. M.; Ondo, J. L.; Winklmayr, W. (1990) Modes in the size distributions of atmospheric inorganic aerosol. Atmos. Environ. Part A 24: 2349-2359.

John, W.; Winklmayr, W.; Wang, H.-C. (1991) Particle deagglomeration and reentrainment in a PM-10 sampler. Aerosol Sci. Technol. 14: 165-176.

Johnson, R. L.; Shah, J. J.; Cary, R. A.; Huntzicker, J. J. (1981) An automated thermal-optical method for the analysis of carbonaceous aerosol. In: Macias, E. S.; Hopke, P. K., eds. Atmospheric aerosol: source/air quality relationships; based on a symposium jointly sponsored by the Divisions of Nuclear Chemistry and Technology at the 180th national meeting of the American Chemical Society; August 1980; Las Vegas, NV. Washington, DC: American Chemical Society; pp. 223-233. (Comstock, M. J., ed. ACS symposium series: 167).

Johnson, C. A.; Sigg, L.; Zobrist, J. (1987) Case studies on the chemical composition of fogwater: the influence of local gaseous emissions. Atmos. Environ. 21: 2365-2374.

Joos, F.; Baltensperger, U. (1991) A field study on chemistry, S(IV) oxidation rates and vertical transport during fog conditions. Atmos. Environ. Part A 25: 217-230.

Junge, C. E. (1963) Air chemistry and radioactivity. New York, NY: Academic Press. (Van Mieghem, J.; Hales, A. L., eds. International geophysics series: v. 4).

Junge, C. E. (1977) Basic considerations about trace constituents in the atmosphere as related to the fate of global pollutants. In: Suffet, I. H., ed. Fate of pollutants in the air and water environments: part I, mechanism of interaction between environments and mathematical modeling and the physical fate of pollutants, papers from the 165th national American Chemical Society meeting; April 1975; Philadelphia, PA. New York, NY: John Wiley & Sons; pp. 7-25. (Advances in environmental science and technology: v. 8).

Junge, C.; McLaren, E. (1971) Relationship of cloud nuclei spectra to aerosol size distribution and composition. J. Atmos. Sci. 28: 382-390.

Kadowaki, S. (1994) Characterization of carbonaceous aerosols in the Nagoya urban area. 2. Behavior and origin of particulate *n*-alkanes. Environ. Sci. Technol. 28: 129-135.

Kahl, J. D.; Samson, P. J. (1986) Uncertainty in trajectory calculations due to low resolution meteorological data. J. Clim. Appl. Meteorol. 25: 1816-1831.

Kahl, J. D.; Samson, P. J. (1988) Trajectory sensitivity to rawinsonde data resolution. Atmos. Environ. 22: 1291-1299.

Kahl, J. D.; Schnell, R. C.; Sheridan, P. J.; Zak, B. D.; Church, H. W.; Mason, A. S.; Heffter, J. L.; Harris, J. M. (1991) Predicting atmospheric debris transport in real-time using a trajectory forecast model. Atmos. Environ. Part A 25: 1705-1713.

Kamens, R. M.; Jeffries, H. E.; Gery, M. W.; Wiener, R. W.; Sexton, K. G.; Howe, G. B. (1981) The impact of α-pinene on urban smog formation: an outdoor smog chamber study. Atmos. Environ. 15: 969-981.

Kamens, R. M.; Gery, M. W.; Jeffries, H. E.; Jackson, M.; Cole, E. I. (1982) Ozone-isoprene reactions: product formation and aerosol potential. Int. J. Chem. Kinet. 14: 955-975.

Kamens, R.; Odum, J.; Fan, Z.-H. (1995) Some observations on times to equilibrium for semivolatile polycyclic aromatic hydrocarbons. Environ. Sci. Technol. 29: 43-50.

Kaplan, I. R.; Gordon, R. J. (1994) Non-fossil-fuel fine-particle organic carbon aerosols in Southern California determined during the Los Angeles Aerosol Characterization and Source Apportionment Study. Aerosol Sci. Technol. 21: 343-359.

Karamchandani, P.; Venkatram, A. (1992) The role of non-precipitating clouds in producing ambient sulfate during summer: results from simulations with the Acid Deposition and Oxidant Model (ADOM) Atmos. Environ. Part A 26: 1041-1052.

Katrinak, K. A.; Rez, P.; Buseck, P. R. (1992) Structural variations in individual carbonaceous particles from an urban aerosol. Environ. Sci. Technol. 26: 1967-1976.

Katrinak, K. A.; Rez, P.; Perkes, P. R.; Buseck, P. R. (1993) Fractal geometry of carbonaceous aggregates from an urban aerosol. Environ. Sci. Technol. 27: 539-547.

Kawamura, K.; Ng, L.-L.; Kaplan, I. R. (1985) Determination of organic acids (C_1-C_{10}) in the atmosphere, motor exhausts, and engine oils. Environ. Sci. Technol. 19: 1082-1086.

Keeler, G. J.; Brachaczek, W. W.; Gorse, R. A., Jr.; Japar, S. M.; Pierson, W. R. (1988) Effect of ambient humidity on dichotomous sampler coarse/fine ratios. Atmos. Environ. 22: 1715-1720.

Keeler, G. J.; Japar, S. M.; Brachaczek, W. W.; Gorse, R. A., Jr.; Norbeck, J. M.; Pierson, W. R. (1990) The sources of aerosol elemental carbon at Allegheny Mountain. Atmos. Environ. Part A 24: 2795-2805.

Kelly, N. A. (1987) The photochemical formation and fate of nitric acid in the metropolitan Detroit area: ambient, captive-air irradiation and modeling results. Atmos. Environ. 21: 2163-2177.

Kelly, T. J.; Schwartz, S. E.; Daum, P. H. (1989) Detectability of acid producing reactions in natural clouds. Atmos. Environ. 23: 569-583.

Kerminen, V. M.; Wexler, A. S. (1994a) Particle formation due to SO_2 oxidation and high relative humidity in the remote marine boundary layer. J. Geophys. Res. [Atmos.] 99: 25607-25625.

Kerminen, V.-M.; Wexler, A. S. (1994b) Post-fog nucleation of H_2SO_4-H_2O particles in smog. Atmos. Environ. 28: 2399-2406.

Khlystov, A.; ten Brink, H. M.; Wyers, G. P. (1993) Hygroscopic growth rates of aerosols at high relative humidity. Petten, The Netherlands: Netherlands Energy Research Foundation ECN; report no. ECN-C-93-011.

Kim, Y. J. (1995) Response of the Active Scattering Aerosol Spectrometer Probe (ASASP-100X) to particles of different chemical composition. Aerosol Sci. Technol. 22: 33-42.

Kim, D.; Hopke, P. K. (1988) Classification of individual particles based on computer-controlled scanning electron microscopy data. Aerosol Sci. Technol. 9: 133-151.

Kim, Y. P.; Seinfeld, J. H. (1995) Atmospheric gas-aerosol equilibrium: III. Thermodynamics of crustal elements Ca^{2+}, K^+, and Mg^{2+}. Aerosol Sci. Technol. 22: 93-110.

Kim, M. G.; Yagawa, K.; Inoue, H.; Lee, Y. K.; Shirai, T. (1990) Measurement of tire tread in urban air by pyrolysis-gas chromatography with flame photometric detection. Atmos. Environ. Part A 24: 1417-1422.

Kim, Y. P.; Seinfeld, J. H.; Saxena, P. (1993a) Atmospheric gas-aerosol equilibrium: I. thermodynamic model. Aerosol Sci. Technol. 19: 157-181.

Kim, Y. P.; Seinfeld, J. H.; Saxena, P. (1993b) Atmospheric gas-aerosol equilibrium: II. analysis of common approximations and activity coefficient calculation methods. Aerosol Sci. Technol. 19: 182-198.

Kim, Y. J.; Boatman, J. F.; Gunter, R. L.; Wellman, D. L.; Wilkison, S. W. (1993c) Vertical distribution of atmospheric aerosol size distribution over south-central New Mexico. Atmos. Environ. Part A 27: 1351-1362.

Kim, Y. P.; Pun, B. K.-L.; Chan, C. K.; Flagan, R. C.; Seinfeld, J. H. (1994) Determination of water activity in ammonium sulfate and sulfuric acid mixtures using levitated single particles. Aerosol Sci. Technol. 20: 275-284.

Kitsa, V.; Lioy, P. J. (1992) Near field dispersion of mechanically resuspended dust from an unpaved road. Transactions AWMA 1: 199-210.

Kitsa, V.; Lioy, P. J.; Chow, J. C.; Watson, J. G.; Shupack, S.; Howell, T.; Sanders, P. (1992) Particle-size distribution of chromium: total and hexavalent chromium in inspirable, thoracic, and respirable soil particles from contaminated sites in New Jersey. Aerosol Sci. Technol. 17: 213-229.

Klee, A. J. (1984) Source control - municipal solid waste incinerators. In: Calvert, S.; Englund, H. M., eds. Handbook of air pollution technology. New York, NY: John Wiley & Sons; pp. 513-550.

Klouda, G. A.; Currie, L. A.; Verkouteren, R. M.; Einfeld, W.; Zak, B. D. (1988) Advances in microradiocarbon dating and the direct tracing of environmental carbon. J. Radioanal. Nucl. Chem. 123: 191-197.

Koenig, L. R.; Murray, F. W. (1976) Ice-bearing cumulus cloud evolution: numerical simulation and general comparison against observations. J. Appl. Meteorol. 15: 747-762.

Köhler, H. (1936) The nucleus in and the growth of hygroscopic droplets. Trans. Faraday Soc. 32: 1152-1161.

Kolb, C. E.; Jayne, J. T.; Worsnop, D. R.; Molina, M. J.; Meads, R. F.; Viggiano, A. A. (1994) Gas phase reaction of sulfur trioxide with water vapor. J. Am. Chem. Soc. 116: 10314-10315.

Koutrakis, P.; Wolfson, J. M.; Slater, J. L.; Brauer, M.; Spengler, J. D.; Stevens, R. K.; Stone, C. L. (1988a) Evaluation of an annular denuder/filter pack system to collect acidic aerosols and gases. Environ. Sci. Technol. 22: 1463-1468.

Koutrakis, P.; Wolfson, J. M.; Spengler, J. D. (1988b) An improved method for measuring aerosol strong acidity: results from a nine-month study in St. Louis, Missouri and Kingston, Tennessee. Atmos. Environ. 22: 157-162.

Koutrakis, P.; Wolfson, J. M.; Spengler, J. D.; Stern, B.; Franklin, C. A. (1989) Equilibrium size of atmospheric aerosol sulfates as a function of the relative humidity. J. Geophys. Res. [Atmos.] 94: 6442-6448.

Koutrakis, P.; Thompson, K. M.; Wolfson, J. M.; Spengler, J. D.; Keeler, G. J.; Slater, J. L. (1992) Determination of aerosol strong acidity losses due to interactions of collected particles: results from laboratory and field studies. Atmos. Environ. Part A 26: 987-995.

Krieger, M. S.; Hites, R. A. (1992) Diffusion denuder for the collection of semivolatile organic compounds. Environ. Sci. Technol. 26: 1551-1555.

Krieger, M. S.; Hites, R. A. (1994) Measurement of polychlorinated biphenyls and polycyclic aromatic hydrocarbons in air with a diffusion denuder. Environ. Sci. Technol. 28: 1129-1133.

Kunen, S. M.; Lazrus, A. L.; Kok, G. L.; Heikes, B. G. (1983) Aqueous oxidation of SO_2 by hydrogen peroxide. J. Geophys. Res. C: Oceans Atmos. 88: 3671-3674.

Kuo, Y.-H.; Skumanich, M.; Haagenson, P. L.; Chang, J. S. (1985) The accuracy of trajectory models as revealed by the observing system simulation experiments. Mon. Weather Rev. 113: 1852-1867.

Lamb, B.; Guenther, A.; Gay, D.; Westberg, H. (1987) A national inventory of biogenic hydrocarbon emissions. Atmos. Environ. 21: 1695-1705.

Lane, D. A.; Johnson, N. D.; Barton, S. C.; Thomas, G. H. S.; Schroeder, W. H. (1988) Development and evaluation of a novel gas and particle sampler for semivolatile chlorinated organic compounds in ambient air. Environ. Sci. Technol. 22: 941-947.

Langner, J.; Rodhe, H. (1991) A global three-dimensional model of the tropospheric sulfur cycle. J. Atmos. Chem. 13: 225-263.

Larson, S. M.; Cass, G. R. (1989) Characteristics of summer midday low-visibility events in the Los Angeles area. Environ. Sci. Technol. 23: 281-289.

Larson, S. M.; Cass, G. R.; Gray, H. A. (1989) Atmospheric carbon particles and the Los Angeles visibility problem. Aerosol Sci. Technol. 10: 118-130.

Lawrence, J. E.; Koutrakis, P. (1994) Measurement of atmospheric formic and acetic acids: methods evaluation and results from field studies. Environ. Sci. Technol. 28: 957-964.

Lawson, D. R. (1990) The Southern California Air Quality Study. J. Air Waste Manage. Assoc. 40: 156-165.

Lazrus, A. L.; Haagenson, P. L.; Kok, G. L.; Huebert, B. J.; Kreitzberg, C. W.; Likens, G. E.; Mohnen, V. A.; Wilson, W. E.; Winchester, J. W. (1983) Acidity in air and water in a case of warm frontal precipitation. Atmos. Environ. 17: 581-591.

Leaitch, W. R.; Strapp, J. W.; Wiebe, H. A.; Isaac, G. A. (1983) Measurements of scavenging and transformation of aerosol inside cumulus. In: Pruppacher, H. R.; Semonin, R. G.; Slinn, W. G. N., eds. Precipitation scavenging, dry deposition, and resuspension: proceedings of the fourth international conference, v. 1: precipitation scavenging; November-December 1982; Santa Monica, CA. New York, NY: Elsevier; pp. 53-69.

Leaitch, W. R.; Strapp, J. W.; Wiebe, H. A.; Anlauf, K. G.; Isaac, G. A. (1986a) Chemical and microphysical studies of nonprecipitating summer cloud in Ontario, Canada. J. Geophys. Res. [Atmos.] 91: 11,821-11,831.

Leaitch, W. R.; Strapp, J. W.; Isaac, G. A.; Hudson, J. G. (1986b) Cloud droplet nucleation and cloud scavenging of aerosol sulphate in polluted atmospheres. Tellus Ser. B 38B: 328-344.

Leaitch, W. R.; Bottenheim, J. W.; Strapp, J. W. (1988) Possible contribution of N_2O_5 scavenging to HNO_3 observed in winter stratiform cloud. J. Geophys. Res. [Atmos.] 93: 12,569-12,584.

Lee, Y.-N.; Schwartz, S. E. (1983) Kinetics of oxidation of aqueous sulfur(IV) by nitrogen dioxide. In: Pruppacher, H. R.; Semonin, R. G.; Slinn, W. G. N., eds. Precipitation scavenging, dry deposition, and resuspension: proceedings of the fourth international conference, v. 1: precipitation scavenging; November-December 1982; Santa Monica, CA. New York, NY: Elsevier; pp. 453-470.

Leone, J. A.; Flagan, R. C.; Grosjean, D.; Seinfeld, J. H. (1985) An outdoor smog chamber and modeling study of toluene-NO_x photooxidation. Int. J. Chem. Kinet. 17: 177-216.

Lewis, R. S.; Deen, W. M. (1994) Kinetics of the reaction of nitric oxide with oxygen in aqueous solutions. Chem. Res. Toxicol. 7: 568-574.

Lewis, C. W.; Baumgardner, R. E.; Stevens, R. K.; Claxton, L. D.; Lewtas, J. (1988) Contribution of woodsmoke and motor vehicle emissions to ambient aerosol mutagenicity. Environ. Sci. Technol. 22: 968-971.

Li, W.; Montassier, N.; Hopke, P. K. (1992) A system to measure the hygroscopicity of aerosol particles. Aerosol Sci. Technol. 17: 25-35.

Li, S.-M.; Anlauf, K. G.; Wiebe, H. A. (1993) Heterogeneous nighttime production and deposition of particle nitrate at a rural site in North America during summer 1988. J. Geophys. Res. [Atmos.] 98: 5139-5157.

Liang, C. S. K.; Waldman, J. M. (1992) Indoor exposures to acidic aerosols at child and elderly care facilities. Indoor Air 2: 196-207.

Liebsch, E. J.; de Pena, R. G. (1982) Sulfate aerosol production in coal-fired power plant plumes. Atmos. Environ. 16: 1323-1331.

Ligocki, M. P.; Pankow, J. F. (1989) Measurements of the gas/particle distributions of atmospheric organic compounds. Environ. Sci. Technol. 23: 75-83.

Ligocki, M. P.; Salmon, L. G.; Fall, T.; Jones, M. C.; Nazaroff, W. W.; Cass, G. R. (1993) Characteristics of airborne particles inside southern California museums. Atmos. Environ. Part A 27: 697-711.

Lin, X.; Chameides, W. L. (1991) Model studies of the impact of chemical inhomogeneity on SO_2 oxidation in warm stratiform clouds. J. Atmos. Chem. 13: 109-129.

Lin, J.-M.; Fang, G.-C.; Holsen, T. M.; Noll, K. E. (1993) A comparison of dry deposition modeled from size distribution data and measured with a smooth surface for total particle mass, lead and calcium in Chicago. Atmos. Environ. Part A 27: 1131-1138.

Lin, J. J.; Noll, K. E.; Holsen, T. M. (1994) Dry deposition velocities as a function of particle size in the ambient atmosphere. Aerosol Sci. Technol. 20: 239-252.

Lind, J. A.; Lazrus, A. L. (1983) Aqueous phase oxidation of sulfur IV by some organic peroxides [abstract]. EOS Trans. 64: 670.

Lindberg, S. E. (1982) Factors influencing trace metal, sulfate and hydrogen ion concentrations in rain. Atmos. Environ. 16: 1701-1709.

Linton, R. W.; Loh, A.; Natusch, D. F. S.; Evans, C. A., Jr.; Williams, P. (1976) Surface predominance of trace elements in airborne particles. Science (Washington, DC) 191: 852-854.

Lioy, P. J.; Daisey, J. M. (1986) Airborne toxic elements and organic substances. Environ. Sci. Technol. 20: 8-14.

Lioy, P. J.; Watson, J. G., Jr. ; Spengler, J. D. (1980) APCA specialty conference workshop on baseline data for inhalable particulate matter. J. Air Pollut. Control Assoc. 30: 1126-1130.

Lippmann, M. (1980) Size distributions in urban aerosols. In: Kneip, T. J.; Lioy, P. J., eds. Aerosols: anthropogenic and natural, sources and transport. Ann. N. Y. Acad. Sci. 338: 1-12.

Liu, P. S. K.; Leaitch, W. R.; Strapp, J. W.; Wasey, M. A. (1992) Response of particle measuring systems airborne to ASASP and PCASP to NaCl and latex particles. Aerosol Sci. Technol. 16: 83-95.

Liu, P. S. K.; Leaitch, W. R.; Macdonald, A. M.; Isaac, G. A.; Strapp, J. W.; Wiebe, H. A. (1993) Sulphate production in summer cloud over Ontario, Canada. Tellus Ser. B 45B: 368-389.

Lowenthal, D. H.; Rogers, C. F.; Saxena, P.; Watson, J. G.; Chow, J. C. (1995) Sensitivity of estimated light extinction coefficients to model assumptions and measurement errors. Atmos. Environ. 29: 751-766.

Lundgren, D. A.; Burton, R. M. (1995) Effect of particle size distribution on the cut point between fine and coarse ambient mass fractions. In: Phalen, R. F.; Bates, D. V., eds. Proceedings of the colloquium on particulate air pollution and human mortality and morbidity; January 1994; Irvine, CA. Inhalation Toxicol. 7: 131-148.

Lundgren, D. A.; Hausknecht, B. J. (1982a) Ambient aerosol mass distribution of 1 to 100 μm particles in five cities. Presented at: 75th annual meeting of the Air Pollution Control Association; June; New Orleans, LA. Pittsburgh, PA: Air Pollution Control Association; paper no. 82-45.4.

Lundgren, D. A.; Hausknecht, B. J. (1982b) Ambient aerosol size distribution determination using a mobile wide range aerosol classifier. Research Triangle Park, NC: U.S. Environmental Protection Agency, Environmental Monitoring Systems Laboratory; EPA contract no. CR-808606-01-1.

Lundgren, D. A.; Hausknecht, B. J.; Burton, R. M. (1984) Large particle size distribution in five U.S. cities and the effect on a new ambient particulate matter standard (PM_{10}). Aerosol Sci. Technol. 7: 467-473.

Lusis, M. A.; Anlauf, K. G.; Barrie, L. A.; Wiebe, H. A. (1978) Plume chemistry studies at a northern Alberta power plant. Atmos. Environ. 12: 2429-2437.

Maahs, H. G. (1983) Kinetics and mechanism of the oxidation of S(IV) by ozone in aqueous solution with particular reference to SO_2 conversion in nonurban tropospheric clouds. J. Geophys. Res. C: Oceans Atmos. 88: 10,721-10,732.

Macias, E. S.; Zwicker, J. O.; White, W. H. (1981) Regional haze case studies in the southwestern U.S.—II. source contributions. In: White, W. H.; Moore, D. J.; Lodge, J. P., Jr., eds. Plumes and visibility: measurements and model components: proceedings of the symposium; November 1980; Grand Canyon National Park, AZ. Atmos. Environ. 15: 1987-1997.

Makhonko, K. P. (1986) Wind dust lift from the grass surface. Meteorol. Gidrol. 10: 61-65.

Malm, W. C.; Gebhart, K. A.; Molenar, J.; Cahill, T.; Eldred, R.; Huffman, D. (1994) Examining the relationship between atmospheric aerosols and light extinction at Mount Rainier and North Cascades National Parks. Atmos. Environ. 28: 347-360.

Mamane, Y.; Stevens, R. K.; Dzubay, T. G. (1990) On the sources of fine and coarse carbon particles in the Great Lakes. J. Aerosol Sci. 21(suppl. 1): S353-S356.

Mansoori, B. A.; Johnston, M. V.; Wexler, A. S. (1994) Quantitation of ionic species in single microdroplets by on-line laser desorption/ionization. Anal. Chem. 66: 3681-3687.

Martin, L. R. (1984) Kinetic studies of sulfite oxidation in aqueous solution. In: Calvert, J. G., ed. SO_2, NO and NO_2 oxidation mechanisms: atmospheric considerations. Boston, MA: Butterworth Publishers; pp. 63-100. (Teasley, J. I., ed. Acid precipitation series: v. 3).

Martin, L. R. (1994) Aqueous sulfur(IV) oxidation revisited. In: Nriagu, J. O.; Simmons, M. S., eds. Environmental oxidants. New York, NY: John Wiley & Sons, Inc.; pp. 221-268. (Nriagu, J. O., ed. Advances in environmental science and technology: v. 28).

Martin, L. R.; Damschen, D. E. (1981) Aqueous oxidation of sulfur dioxide by hydrogen peroxide at low pH. Atmos. Environ. 15: 1615-1621.

Martin, L. R.; Hill, M. W. (1987a) The iron catalyzed oxidation of sulfur: reconciliation of the literature rates. Atmos. Environ. 21: 1487-1490.

Martin, L. R.; Hill, M. W. (1987b) The effect of ionic strength on the manganese catalyzed oxidation of sulfur(IV). Atmos. Environ. 21: 2267-2270.

Martin, L. R.; Hill, M. W.; Tai, A. F.; Good, T. W. (1991) The iron catalyzed oxidation of sulfur(IV) in aqueous solution: differing effects of organics at high and low pH. J. Geophys. Res. [Atmos.] 96: 3085-3097.

Martonen, T. B. (1993) Mathematical model for the selective deposition of inhaled pharmaceuticals. J. Pharm. Sci. 82: 1191-1199.

Mason, A. S.; Gifford, F. A. (1992) Atmospheric tracer dispersion over a 24-h time span. Atmos. Environ. Part A 26: 3203-3205.

Mazurek, M. A.; Simoneit, B. R. T. (1984) Characterization of biogenic and petroleum-derived organic matter in aerosols over remote, rural and urban areas. In: Keith, L. H., ed. Identification and analysis of organic pollutants in air: [papers from a symposium at the 184th national American Chemical Society meeting]; September 1982; Kansas City, MO. Woburn, MA: Butterworth Publishers; pp. 353-370.

Mazurek, M. A.; Cass, G. R.; Simoneit, B. R. T. (1989) Interpretation of high-resolution gas chromatography / mass spectrometry data aquired from atmospheric organic aerosol samples. Aerosol Sci. Technol. 10: 408-420.

Mazurek, M. A.; Cass, G. R.; Simoneit, B. R. T. (1991) Biological input to visibility-reducing aerosol particles in the remote arid southwestern United States. Environ. Sci. Technol. 25: 684-694.

McArdle, J. V.; Hoffmann, M. R. (1983) Kinetics and mechanism of the oxidation of aquated sulfur dioxide by hydrogen peroxide at low pH. J. Phys. Chem. 87: 5425-5429.

McHenry, J. N.; Dennis, R. L. (1991) Partitioning of the sulfate budget into gas- and aqueous-phase components in the regional acid deposition model (RADM). In: Proceedings of the 7th joint AMS-AWMA conference: applications of air pollution meteorology; New Orleans, LA; pp. 143-147.

McHenry, J. N.; Dennis, R. L. (1994) The relative importance of oxidation pathways and clouds to atmospheric ambient sulfate production as predicted by the Regional Acid Deposition Model. J. Appl. Meteorol. 33: 890-905.

McMahon, T. A.; Denison, P. J. (1979) Empirical atmospheric deposition parameters—a survey. Atmos. Environ. 13: 571-585.

McMurry, P. H.; Friedlander, S. K. (1979) New particle formation in the presence of an aerosol. Atmos. Environ. 13: 1635-1651.

McMurry, P. H.; Grosjean, D. (1985) Photochemical formation of organic aerosols: growth laws and mechanisms. Atmos. Environ. 19: 1445-1451.

McMurry, P. H.; Stolzenburg, M. R. (1989) On the sensitivity of particle size to relative humidity for Los Angeles aerosols. Atmos. Environ. 23: 497-507.

McMurry, P. H.; Wilson, J. C. (1982) Growth laws for the formation of secondary ambient aerosols: implications for chemical conversion mechanisms. Atmos. Environ. 16: 121-134.

McMurry, P. H.; Wilson, J. C. (1983) Droplet phase (heterogeneous) and gas phase (homogeneous) contributions to secondary ambient aerosol formation as functions of relative humidity. J. Geophys. Res. 88: 5101-5108.

McMurry, P. H.; Zhang, X. Q. (1989) Size distributions of ambient organic and elemental carbon. Aerosol Sci. Technol. 10: 430-437.

McMurry, P. H.; Rader, D. J.; Stith, J. L. (1981) Studies of aerosol formation in power plant plumes—I. growth laws for secondary aerosols in power plant plumes: implications for chemical conversion mechanisms. In: White, W. H.; Moore, D. J.; Lodge, J. P., Jr., eds. Plumes and visibility: measurements and model components: proceedings of the symposium; November 1980; Grand Canyon National Park, AZ. Atmos. Environ. 15: 2315-2327.

McMurry, P. H.; Zhang, X.; Lee, C.-T. (1996) Issues in aerosol measurement. J. Geophys. Res. [Atmos.]: in press.

McNider, R. T.; Moran, M. D.; Pielke, R. A. (1988) Influence of diurnal and inertial boundary-layer oscillations on long-range dispersion. Atmos. Environ. 22: 2445-2462.

Meagher, J. F.; Stockburger, L.; Bailey, E. M.; Huff, O. (1978) The oxidation of sulfur dioxide to sulfate aerosols in the plume of a coal-fired power plant. Atmos. Environ. 12: 2197-2203.

Meagher, J. F.; Stockburger, L., III; Bonanno, R. J.; Bailey, E. M.; Luria, M. (1981) Atmospheric oxidation of flue gases from coal-fired power plants—a comparison between conventional and scrubbed plumes. Atmos. Environ. 15: 749-762.

Meagher, J. F.; Olszyna, K. J.; Weatherford, F. P.; Mohnen, V. A. (1990) The availability of H_2O_2 and O_3 for aqueous phase oxidation of SO_2. The question of linearity. Atmos. Environ. Part A 24: 1825-1829.

Meng, Z.; Seinfeld, J. H. (1994) On the source of the submicrometer droplet mode of urban and regional aerosols. Aerosol Sci. Technol. 20: 253-265.

Meng, Z.; Seinfeld, J. H.; Saxena, P.; Kim, Y. P. (1995) Contribution of water to particulate mass in the South Coast Air Basin. Aerosol Sci. Technol. 22: 111-123.

Michaud, D.; Baril, M.; Perrault, G. (1993) Characterization of airborne dust from cast iron foundries by physico-chemical methods and multivariate statistical analyses. Air Waste 43: 729-735.

Milford, J. B.; Davidson, C. I. (1985) The sizes of particulate trace elements in the atmosphere—a review. J. Air Pollut. Control Assoc. 35: 1249-1260.

Milford, J. B.; Davidson, C. I. (1987) The sizes of particulate sulfate and nitrate in the atmosphere—a review. JAPCA 37: 125-134.

Miller, D. F.; Alkezweeny, A. J. (1980) Aerosol formation in urban plumes over Lake Michigan. In: Kneip, T. J.; Lioy, P. J., eds. Aerosols: anthropogenic and natural, sources and transport. Ann. N. Y. Acad. Sci. 338: 219-232.

Miller, F. J.; Gardner, D. E.; Graham, J. A.; Lee, R. E., Jr.; Wilson, W. E.; Bachmann, J. D. (1979) Size considerations for establishing a standard for inhalable particles. J. Air Pollut. Control Assoc. 29: 610-615.

Mohnen, V. A.; Kadlecek, J. A. (1989) Cloud chemistry research at Whiteface Mountain. Tellus Ser. B 41B: 79-91.

Moran, M. D. (1992) Numerical modeling of mesoscale atmospheric dispersion [Ph.D. dissertation]. Ft. Collins, CO: Colorado State University, Department of Atmospheric Science.

Morandi, M. T. (1985) Development of source apportionment models for inhalable particulate matter and its extractable organic fractions in urban areas of New Jersey [Ph.D. dissertation]. Syracuse, NY: New York University. Available from: University Microfilms, Ann Arbor, MI; order no. AAC85-10516.

Morandi, M. T.; Lioy, P. J.; Daisey, J. M. (1991) Comparison of two multivariate modeling approaches for the source apportionment of inhalable particulate matter in Newark, NJ. Atmos. Environ. Part A 25: 927-937.

Moyers, J. L.; Ranweiler, L. E.; Hopf, S. B.; Korte, N. E. (1977) Evaluation of particulate trace species in southwest desert atmosphere. Environ. Sci. Technol. 11: 789-795.

Mozurkewich, M.; Calvert, J. G. (1988) Reaction probability of N_2O_5 on aqueous aerosols. J. Geophys. Res. [Atmos.] 93: 15,889-15,896.

Mueller, P. K.; Fung, K. K.; Heisler, S. L.; Grosjean, D.; Hidy, G. M. (1982) Atmospheric particulate carbon observations in urban and rural areas of the United States. In: Wolff, G. T.; Klimisch, R. L., eds. Particulate carbon: atmospheric life cycle: proceedings of an international symposium; October 1980; Warren, MI. New York, NY: Plenum Press; pp. 343-370.

Mulhbaier, J. L.; Williams, R. L. (1982) Fireplaces, furnaces and vehicles as emission sources of particulate carbon. In: Wolff, G. T.; Klimisch, R. L., eds. Particulate carbon: atmospheric life cycle. New York, NY: Plenum Press; pp. 185-205.

Munger, J. W.; Jacob, D. J.; Waldman, J. M.; Hoffmann, M. R. (1983) Fogwater chemistry in an urban atmosphere. J. Geophys. Res. C: Oceans Atmos. 88: 5109-5121.

Munger, J. W.; Jacob, D. J.; Hoffmann, M. R. (1984) The occurrence of bisulfite-aldehyde addition products in fog- and cloudwater. J. Atmos. Chem. 1: 335-350.

Munger, J. W.; Collett, J., Jr.; Daube, B., Jr.; Hoffmann, M. R. (1990) Fogwater chemistry at Riverside, California. Atmos. Environ. Part B 24: 185-205.

Mylonas, D. T.; Allen, D. T.; Ehrman, S. H.; Pratsinis, S. E. (1991) The sources and size distributions of organonitrates in Los Angeles aerosol. Atmos. Environ. Part A 25: 2855-2861.

Nair, S. K.; Peters, L. K. (1989) Studies on non-precipitating cumulus cloud acidification. Atmos. Environ. 23: 1399-1423.

National Research Council. (1979) Airborne particles. Baltimore, MD: University Park Press.

National Research Council. (1983) Polycyclic aromatic hydrocarbons: evaluation of sources and effects. Washington, DC: National Academy Press.

National Research Council. (1993) Protecting visibility in national parks and wilderness areas. Washington, DC: National Academy Press. 3v.

Newman, L. (1981) Atmospheric oxidation of sulfur dioxide: a review as viewed from power plant and smelter plume studies. Atmos. Environ. 15: 2231-2239.

Newman, L.; Forrest, J.; Manowitz, B. (1975a) The application of an isotopic ratio technique to a study of the atmospheric oxidation of sulfur dioxide in the plume from an oil-fired power plant. Atmos. Environ. 9: 959-968.

Newman, L.; Forrest, J.; Manowitz, B. (1975b) The application of an isotopic ratio technique to a study of the atmospheric oxidation of sulfur dioxide in the plume from a coal fired power plant. Atmos. Environ. 9: 969-977.

Nicholson, K. W. (1988) The dry deposition of small particles: a review of experimental measurements. Atmos. Environ. 22: 2653-2666.

Nielsen, T. (1984) Reactivity of polycyclic aromatic hydrocarbons toward nitrating species. Environ. Sci. Technol. 18: 157-163.

Nielsen, T.; Ramdahl, T.; Bjørseth, A. (1983) The fate of airborne polycyclic organic matter. Environ. Health Perspect. 47: 103-114.

Noone, K. J.; Ogren, J. A.; Hallberg, A.; Hansson, H.-C.; Wiedensohler, A.; Swietlicki, E. (1992a) A statistical examination of the chemical differences between interstitial and scavenged aerosol. Tellus Ser. B 44B: 581-592.

Noone, K. J.; Ogren, J. A.; Hallberg, A.; Heintzenberg, J.; Ström, J.; Hansson, H.-C.; Svenningsson, B.; Wiedensohler, A.; Fuzzi, S.; Facchini, M. C.; Arends, B. G.; Berner, A. (1992b) Changes in aerosol size- and phase distributions due to physical and chemical processes in fog. Tellus Ser. B 44B: 489-504.

Novakov, T. (1984) The role of soot and primary oxidants in the atmospheric chemistry. Sci. Total Environ. 36: 1-10.

Novakov, T.; Penner, J. E. (1993) Large contribution of organic aerosols to cloud-condensation-nuclei concentrations. Nature (London) 365: 823-826.

Noxon, J. F. (1983) NO_3 and NO_2 in the mid-Pacific troposphere. J. Geophys. Res. C: Oceans Atmos. 88: 11,017-11,021.

Nunes, T. V.; Pio, C. A. (1993) Carbonaceous aerosols in industrial and coastal atmospheres. Atmos. Environ. Part A 27: 1339-1346.

Oberdörster, G. (1995) Lung particle overload: implications for occupational exposures to particles. Regul. Toxicol. Pharmacol. 27: 123-135.

O'Brien, R. J.; Crabtree, J. H.; Holmes, J. R.; Hoggan, M. C.; Bockian, A. H. (1975) Formation of photochemical aerosol from hydrocarbons: atmospheric analysis. Environ. Sci. Technol. 9: 577-582.

O'Dell, R. A.; Taheri, M.; Kabel, R. L. (1977) A model for uptake of pollutants by vegetation. J. Air Pollut. Control Assoc. 27: 1104-1109.

Ogren, J. A.; Charlson, R. J. (1992) Implications for models and measurements of chemical inhomogeneities among cloud droplets. Tellus Ser. B 44B: 208-225.

Olmez, I.; Sheffield, A. E.; Gordon, G. E.; Houck, J. E.; Pritchett, L. C.; Cooper, J. A.; Dzubay, T. G.; Bennett, R. L. (1988) Compositions of particles from selected sources in Philadelphia for receptor modeling applications. JAPCA 38: 1392-1402.

Olson, T. M.; Hoffman, M. R. (1989) Hydroxyalkylsulfonate formation: its role as a S(IV) reservoir in atmospheric water droplets. Atmos. Environ. 23: 985-997.

Otani, Y.; Wang, C. S. (1984) Growth and deposition of saline droplets covered with a monolayer of surfactant. Aerosol Sci. Technol. 3: 155-166.

Pack, D. H.; Ferber, G. J.; Heffter, J. L.; Telegadas, K.; Angell, J. K.; Hoecker, W. H.; Machta, L. (1978) Meteorology of long-range transport. Atmos. Environ. 12: 425-444.

Palen, E. J.; Allen, D. T.; Pandis, S. N.; Paulson, S. E.; Seinfeld, J. H.; Flagan, R. C. (1992) Fourier transform infrared analysis of aerosol formed in the photo-oxidation of isoprene and β-pinene. Atmos. Environ. Part A 26: 1239-1251.

Pandis, S. N.; Seinfeld, J. H. (1989a) Sensitivity analysis of a chemical mechanism for aqueous-phase atmospheric chemistry. J. Geophys. Res. [Atmos.] 94: 1105-1126.

Pandis, S. N.; Seinfeld, J. H. (1989b) Mathematical modeling of acid deposition due to radiation fog. J. Geophys. Res. [Atmos.] 94: 12,911-12,923.

Pandis, S. N.; Seinfeld, J. H.; Pilinis, C. (1990a) The smog-fog-smog cycle and acid deposition. J. Geophys. Res. [Atmos.] 95: 18,489-18,500.

Pandis, S. N.; Seinfeld, J. H.; Pilinis, C. (1990b) Chemical composition differences in fog and cloud droplets of different sizes. Atmos. Environ. Part A 24: 1957-1969.

Pandis, S. N.; Paulson, S. E.; Seinfeld, J. H.; Flagan, R. C. (1991) Aerosol formation in the photooxidation of isoprene and β-pinene. Atmos. Environ. Part A 25: 997-1008.

Pandis, S. N.; Harley, R. A.; Cass, G. R.; Seinfeld, J. H. (1992a) Secondary organic aerosol formation and transport. Atmos. Environ. Part A 26: 2269-2282.

Pandis, S. N.; Seinfeld, J. H.; Pilinis, C. (1992b) Heterogeneous sulfate production in an urban fog. Atmos. Environ. Part A 26: 2509-2522.

Pandis, S. N.; Wexler, A. S.; Seinfeld, J. H. (1993) Secondary organic aerosol formation and transport—II. predicting the ambient secondary organic aerosol size distribution. Atmos. Environ. Part A 27: 2403-2416.

Pankow, J. F. (1987) Review and comparative analysis of the theories on partitioning between the gas and aerosol particulate phases in the atmosphere. Atmos. Environ. 21: 2275-2283.

Pankow, J. F. (1988) Gas phase retention volume behavior of organic compounds on the sorbent poly(oxy-*m*-terphenyl-2'-5'-ylene). Anal. Chem. 60: 950-958.

Pankow, J. F. (1989) Overview of the gas phase retention volume behavior of organic compounds on polyurethane foam. Atmos. Environ. 23: 1107-1111.

Pankow, J. F. (1991) Common *y*-intercept and single compound regressions of gas-particle partitioning data vs. $1/T$. Atmos. Environ. Part A 25: 2229-2239.

Pankow, J. F. (1994a) An absorption model of gas/particle partitioning of organic compounds in the atmosphere. Atmos. Environ. 28: 185-188.

Pankow, J. F. (1994b) An absorption model of the gas/aerosol partitioning involved in the formation of secondary organic aerosol. Atmos. Environ. 28: 189-193.

Pankow, J. F.; Bidleman, T. F. (1991) Effects of temperature, *TSP* and per cent non-exchangeable material in determining the gas-particle partitioning of organic compounds. Atmos. Environ. Part A 25: 2241-2249.

Pankow, J. F.; Bidleman, T. F. (1992) Interdependence of the slopes and intercepts from log-log correlations of measured gas-particle partitioning and vapor pressure - I. theory and analysis of available data. Atmos Environ. Part A 26: 1071-1080.

Pankow, J. F.; Storey, J. M. E.; Yamasaki, H. (1993) Effects of relative humidity on gas/particle partitioning of semivolatile organic compounds to urban particulate matter. Environ. Sci. Technol. 27: 2220-2226.

Parrish, D. D.; Fahey, D. W.; Williams, E. J.; Liu, S. C.; Trainer, M.; Murphy, P. C.; Albritton, D. L.; Fehsenfeld, F. C. (1986) Background ozone and anthropogenic ozone enhancement at Niwot Ridge, Colorado. J. Atmos. Chem. 4: 63-80.

Pasquill, F. (1974) Atmospheric diffusion. New York, NY: John Wiley and Sons.

Pasquill, F.; Smith, F. B. (1983) Atmospheric diffusion. 3rd ed. New York, NY: Jóhn Wiley.

Pastuszka, J. S.; Kwapulinski, J. (1988) The change in mass size distribution of aerosol near dumps as a result of resuspension of dust. Presented at: 81st annual meeting of Air Pollution Control Association; June; Dallas, TX. Pittsburgh, PA: Air Pollution Control Association; paper no. 88-151.3.

Patrinos, A. A. N. (1985) The impact of urban and industrial emissions on mesoscale precipitation quality. J. Air Pollut. Control Assoc. 35: 719-727.

Patrinos, A. A. N.; Brown, R. M. (1984) Mesoscale wetfall chemistry around Philadelphia during frontal storms. Geophys. Res. Lett. 11: 561-564.

Patrinos, A. A. N.; Leach, M. J.; Brown, R. M.; Tanner, R. L.; Binkowski, F. S. (1989) An acid rain study in the Washington, D.C. area. J. Appl. Meteorol. 28: 948-968.

Patterson, E. M.; Gillette, D. A. (1977a) Commonalities in measured size distributions for aerosols having a soil-derived component. J. Geophys. Res. 82: 2074-2082.

Patterson, E. M.; Gillette, D. A. (1977b) Measurements of visibility vs. mass-concentration for airborne soil particles. Atmos. Environ. 11: 193-196.

Patterson, R. K.; Wagman, J. (1977) Mass and composition of an urban aerosol as a function of particle size for several visibility levels. J. Aerosol Sci. 8: 269-279.

Peirson, D. H.; Cawse, P. A.; Salmon, L.; Cambray, R. S. (1973) Trace elements in the atmospheric environment. Nature (London) 241: 252-256.

Penkett, S. A. (1972) Oxidation of SO_2 and other atmospheric gases by ozone in aqueous solution. Nature (London) 240: 105-106.

Penkett, S. A.; Jones, B. M. R.; Brice, K. A.; Eggleton, A. E. J. (1979) The importance of atmospheric ozone and hydrogen peroxide in oxidising sulphur dioxide in cloud and rainwater. Atmos. Environ. 13: 123-137.

Penner, J. E.; Eddleman, H.; Novakov, T. (1993) Towards the development of a global inventory for black carbon emissions. Atmos. Environ. Part A 27: 1277-1295.

Peters, K.; Eiden, R. (1992) Modelling the dry deposition velocity of aerosol particles to a spruce forest. Atmos. Environ. Part A 26: 2555-2564.

Peterson, J. T.; Junge, C. E. (1971) Sources of particulate matter in the atmosphere. In: Matthews, W. H.; Kellogg, W. W.; Robinson, G. D., eds. Man's impact on the climate. Cambridge, MA: MIT Press.

Pickle, T.; Allen, D. T.; Pratsinis, S. E. (1990) The sources and size distributions of aliphatic and carbonyl carbon in Los Angeles aerosol. Atmos. Environ. Part A 24: 2221-2228.

Pielke, R. A.; et al. (1992) A comprehensive mesoscale modeling system - RAMS. Meteorol. Atmos. Phys. 49: 69-91.

Pierson, W. R.; Brachaczek, W. W. (1983) Particulate matter associated with vehicles on the road. II. Aerosol Sci. Technol. 2: 1-40.

Pierson, W. R.; Brachaczek, W. W. (1990) Dew chemistry and acid deposition in Glendora, California, during the 1986 Carbonaceous Species Methods Comparison Study. Aerosol Sci. Technol. 12: 8-27.

Pierson, W. R.; Brachaczek, W. W.; Gorse, R. A., Jr.; Japar, S. M.; Norbeck, J. M. (1986) On the acidity of dew. J. Geophys. Res. [Atmos.] 91: 4083-4096.

Pierson, W. R.; Brachaczek, W. W.; Japar, S. M.; Cass, G. R.; Solomon, P. A. (1988) Dry deposition and dew chemistry in Claremont, California, during the 1985 Nitrogen Species Methods Comparison Study. Atmos. Environ. 22: 1657-1663.

Pilinis, C.; Seinfeld, J. H. (1987) Continued development of a general equilibrium model for inorganic multicomponent atmospheric aerosols. Atmos. Environ. 21: 2453-2466.

Pilinis, C.; Seinfeld, J. H. (1988) Development and evaluation of an Eulerian photochemical gas-aerosol model. Atmos. Environ. 22: 1985-2001.

Pilinis, C.; Seinfeld, J. H.; Grosjean, D. (1989) Water content of atmospheric aerosols. Atmos. Environ. 23: 1601-1606.

Pinnick, R. G.; Fernandez, G.; Hinds, B. D.; Bruce, C. W.; Schaefer, R. W.; Pendleton, J. D. (1985) Dust generated by vehicular traffic on unpaved roadways: sizes and infrared extinction characteristics. Aerosol Sci. Technol. 4: 99-121.

Pinnick, R. G.; Fernandez, G.; Martinez-Andazola, E.; Hinds, B. D.; Hansen, A. D. A.; Fuller, K. (1993) Aerosol in the arid southwestern United States: measurements of mass loading, volatility, size distribution, absorption characteristics, black carbon content, and vertical structure to 7 km above sea level. J. Geophys. Res. [Atmos.] 98: 2651-2666.

Pires, M.; Rossi, M. J.; Ross, D. S. (1994) Kinetic and mechanistic aspects of the NO oxidation by O_2 in aqueous phase. Int. J. Chem. Kinet. 26: 1207-1227.

Pitchford, M. L.; McMurry, P. H. (1994) Relationship between measured water vapor growth and chemistry of atmospheric aerosol for Grand Canyon, Arizona, in winter 1990. Atmos. Environ. 28: 827-839.

Pitts, J. N., Jr.; Atkinson, R.; Sweetman, J. A.; Zielinska, B. (1985a) The gas-phase reaction of naphthalene with N_2O_5 to form nitronaphthalenes. Atmos. Environ. 19: 701-705.

Pitts, J. N., Jr.; Zielinska, B.; Sweetman, J. A.; Atkinson, R.; Winer, A. M. (1985b) Reaction of adsorbed pyrene and perylene with gaseous N_2O_5 under simulated atmospheric conditions. Atmos. Environ. 19: 911-915.

Pitts, J. N., Jr.; Paur, H.-R.; Zielinska, B.; Arey, J.; Winer, A. M.; Ramdahl, T.; Mejia, V. (1986) Factors influencing the reactivity of polycyclic aromatic hydrocarbons adsorbed on filters and ambient POM with ozone. Chemosphere 15: 675-685.

Placet, M.; Battye, R. E.; Fehsenfeld, F. C.; Bassett, G. W. (1991) Emissions involved in acidic deposition processes. In: Irving, P. M., ed. Acidic depostion: state of science and technology, volume I: emissions, atmospheric processes, and deposition. Washington, DC: The U.S. National Acid Precipitation Assessment Program. (State of science and technology report no. 1).

Pleim, J.; Venkatram, A.; Yamartino, R. J. (1984) The dry deposition model, v. 4. Rexdale, ON, Canada: Ontario Ministry of the Environment, ADOM/TADAP Model Development Program.

Post, J. E.; Buseck, P. R. (1985) Quantitative energy-dispersive analysis of lead halide particles from the Phoenix urban aerosol. Environ. Sci. Technol. 19: 682-685.

Pratsinis, S.; Ellis, E. C.; Novakov, T.; Friedlander, S. K. (1984) The carbon containing component of the Los Angeles aerosol: source apportionment and contributions to the visibility budget. J. Air Pollut. Control Assoc. 34: 643-650.

Pratsinis, S. E.; Zeldin, M. D.; Ellis, E. C. (1988) Source resolution of the fine carbonaceous aerosol by principal component-stepwise regression analysis. Environ. Sci. Technol. 22: 212-216.

Pruppacher, H. R.; Klett, J. D. (1980) Microphysics of clouds and precipitation. Boston, MA: D. Reidel Publishing Company.

Pueschel, R. F.; Van Valin, C. C.; Castillo, R. C.; Kadlecek, J. A.; Ganor, E. (1986) Aerosols in polluted versus nonpolluted air masses: long-range transport and effects on clouds. J. Clim. Appl. Meteorol. 25: 1908-1917.

Rabano, E. S.; Castillo, N. T.; Torre, K. J.; Solomon, P. A. (1989) Speciation of arsenic in ambient aerosols collected in Los Angeles. JAPCA 39: 76-80.

Rader, D. J.; McMurry, P. H. (1986) Application of the tandem differential mobility analyzer to studies of droplet growth or evaporation. J. Aerosol Sci. 17: 771-787.

Radke, L. F.; Hobbs, P. V. (1991) Humidity and particle fields around some small cumulus clouds. J. Atmos. Sci. 48: 1190-1193.

Radke, L. F.; Brock, C. A.; Lyons, J. H.; Hobbs, P. V.; Schnell, R. C. (1989) Aerosol and lidar measurements of hazes in mid-latitude and polar airmasses. Atmos. Environ. 23: 2417-2430.

Raga, G. B.; Jonas, P. R. (1993) On the link between cloud-top radiative properties and sub-cloud aerosol concentrations. Q. J. R. Meteorol. Soc. 119: 1419-1425.

Ramdahl, T. (1983) Polycyclic aromatic ketones in environmental samples. Environ. Sci. Technol. 17: 666-670.

Ramdahl, T.; Becher, G.; Bjrsøeth, A. (1982) Nitrated polycyclic aromatic hydrocarbons in urban air particles. Environ. Sci. Technol. 16: 861-865.

Ramdahl, T.; Bjørseth, A.; Lokensgard, D.; Pitts, J. N., Jr. (1984) Nitration of polycyclic aromatic hydrocarbons adsorbed to different carriers in a fluidized bed reactor. Chemosphere 13: 527-534.

Ranade, M. B. (Arun); Woods, M. C.; Chen, F.-L.; Purdue, L. J.; Rehme, K. A. (1990) Wind tunnel evaluation of PM_{10} samplers. Aerosol Sci. Technol. 13: 54-71.

Rao, A. K.; Whitby, K. T. (1978) Non-ideal collection characteristics of inertial impactors—I. single-stage impactors and solid particles. J. Aerosol Sci. 9: 77-86.

Rau, J. A. (1989) Composition and size distribution of residential wood smoke particles. Aerosol Sci. Technol. 10: 181-192.

Reeks, M. W.; Reed, J.; Hall, D. (1988) On the resuspension of small particles by a turbulent flow. J. Phys. D: Appl. Phys. 21: 574-589.

Richards, L. W. (1983) Comments on the oxidation of NO_2 to nitrate - day and night. Atmos. Environ. 17: 397-402.

Richards, L. W.; Anderson, J. A.; Blumenthal, D. L.; Brandt, A. A.; McDonald, J. A.; Waters, N.; Macias, E. S.; Bhardwaja, P. S. (1981) The chemistry, aerosol physics, and optical properties of a western coal-fired power plant plume. Atmos. Environ. 15: 2111-2134.

Richards, L. W.; Anderson, J. A.; Blumenthal, D. L.; McDonald, J. A. (1982a) Nitrogen and sulfur chemistry and aerosol formation in plumes. Presented at: 75th annual meeting of the Air Pollution Control Association; June; New Orleans, LA. Pittsburgh, PA: Air Pollution Control Association; paper no. 82-24.6.

Richards, L. W.; Anderson, J. A.; Blumenthal, D. L.; McDonald, J. A. (1982b) Comparison of the optical properties of particles in smelter and western power plant plumes [poster presentation]. Presented at: 75th annual meeting of the Air Pollution Control Association; June; New Orleans, LA. Pittsburgh, PA: Air Pollution Control Association; poster presentation no. 82-7P.5

Richards, L. W.; Blumenthal, D. L.; Bergstrom, R. W.; Seigneur, C.; Smith, T. B.; Macias, E. S.; Hering, S. V.; Bhardwaja, P. S.; Wilson, W. E. (1982c) VISTTA authors' reply. Atmos. Environ. 16: 2363-2365.

Richards, L. W.; Anderson, J. A.; Blumenthal, D. L.; McDonald, J. A.; Macias, E. S.; Hering, S. V.; Wilson, W. E., Jr. (1985) Chemical, aerosol and optical measurements in the plumes of three midwestern coal-fired power plants. Atmos. Environ. 19: 1685-1704.

Richards, L. W.; Blanchard, C. L.; Blumenthal, D. L. (1991) Navajo generating station visibility study, draft #2. Santa Rosa, CA: Sonoma Technology, Inc.; final report STI-90200-1124-FRD2.

Richardson, C. B.; Hightower, R. L. (1987) Evaporation of ammonium nitrate particles. Atmos. Environ. 21: 971-975.

Richardson, C. B.; Spann, J. F. (1984) Measurement of the water cycle in a levitated ammonium sulfate particle. J. Aerosol Sci. 15: 563-571.

Roberts, D.; Williams, D. (1979) The kinetics of oxidation of sulphur dioxide within the plume from a sulphide smelter in a remote region. Atmos. Environ. 13: 1485-1499.

Roelofs, G. J. H. (1992a) Drop size dependent sulfate distribution in a growing cloud. J. Atmos. Chem. 14: 109-118.

Roelofs, G. J. H. (1992b) On the drop and aerosol size dependence of aqueous sulfate formation in a continental cumulus cloud. Atmos. Environ. Part A 26: 2309-2321.

Roelofs, G. J. H. (1993) A cloud chemistry sensitivity study and comparison of explicit and bulk cloud model performance. Atmos. Environ. Part A 27: 2255-2264.

Rogge, W. F.; Hildemann, L. M.; Mazurek, M. A.; Cass, G. R.; Simoneit, B. R. T. (1991) Sources of fine organic aerosol. 1. Charbroilers and meat cooking operations. Environ. Sci. Technol. 25: 1112-1125.

Rogge, W. F.; Hildemann, L. M.; Mazurek, M. A.; Cass, G. R.; Simoneit, B. R. T. (1993a) Sources of fine organic aerosol. 2. Noncatalyst and catalyst-equipped automobiles and heavy-duty diesel trucks. Environ. Sci. Technol. 27: 636-651.

Rogge, W. F.; Hildemann, L. M.; Mazurek, M. A.; Cass, G. R.; Simoneit, B. R. T. (1993b) Sources of fine organic aerosol. 3. Road dust, tire debris, and organometallic brake lining dust: roads as sources and sinks. Environ. Sci. Technol. 27: 1892-1904.

Rogge, W. F.; Hildemann, L. M.; Mazurek, M. A.; Cass, G. R.; Simoneit, B. R. T. (1993c) Sources of fine organic aerosol. 4. Particulate abrasion products from leaf surfaces of urban plants. Environ. Sci. Technol. 27: 2700-2711.

Rogge, W. F.; Mazurek, M. A.; Hildemann, L. M.; Cass, G. R.; Simoneit, B. R. T. (1993d) Quantification of urban organic aerosols at a molecular level: identification, abundance and seasonal variation. Atmos. Environ. Part A 27: 1309-1330.

Rogge, W. F.; Hildemann, L. M.; Mazurek, M. A.; Cass, G. R.; Simoneit, B. R. T. (1994) Sources of fine organic aerosol. 6. Cigarette smoke in the urban atmosphere. Environ. Sci. Technol. 28: 1375-1388.

Rolph, G. D.; Draxler, R. R. (1990) Sensitivity of three-dimensional trajectories to the spatial and temporal densities of the wind field. J. Appl. Meteorol. 29: 1043-1054.

Rood, M. J.; Larson, T. V.; Covert, D. S.; Ahlquist, N. C. (1985) Measurement of laboratory and ambient aerosols with temperature and humidity controlled nephelometry. Atmos. Environ. 19: 1181-1190.

Rood, M. J.; Shaw, M. A.; Larson, T. V.; Covert, D. S. (1989) Ubiquitous nature of ambient metastable aerosol. Nature (London) 337: 537-539.

Rounds, S. A.; Pankow, J. F. (1990) Application of a radial diffusion model to describe gas/particle sorption kinetics. Environ. Sci. Technol. 24: 1378-1386.

Rubel, G. O.; Gentry, J. W. (1984) Measurement of the kinetics of solution droplets in the presence of adsorbed monolayers: determination of water accommodation coefficients. J. Phys. Chem. 88: 3142-3148.

Sakugawa, H.; Kaplan, I. R.; Tsai, W.; Cohen, Y. (1990) Atmospheric hydrogen peroxide: does it share a role with ozone in degrading air quality? Environ. Sci. Technol. 24: 1452-1462.

Satsumabayashi, H.; Kurita, H.; Yokouchi, Y.; Ueda, H. (1989) Mono- and di-carboxylic acids under long-range transport of air pollution in central Japan. Tellus Ser. B 41B: 219-229.

Satsumakayashi, H.; Kurita, H.; Yokouchi, Y.; Ueda, H. (1990) Photochemical formation of particulate dicarboxylic acids under long-range transport in central Japan. Atmos. Environ. Part A 24: 1443-1450.

Savoie, D. L.; Prospero, J. M.; Nees, R. T. (1987) Washout ratios of nitrate, non-sea-salt sulfate and sea-salt on Virginia Key, Florida and on American Samoa. Atmos. Environ. 21: 103-112.

Saxena, P. (1994) Authors' response to comments on "Coupling thermodynamic theory with measurements to characterize acidity of atmospheric particles." Aerosol Sci. Technol. 20: 287-288.

Saxena, V. K.; Hendler, A. H. (1983) In-cloud scavenging and resuspension of cloud active aerosols during winter storms over Lake Michigan. In: Pruppacher, H. R.; Semonin, R. G.; Slinn, W. G. N., eds. Precipitation scavenging, dry deposition, and resuspension, v. 1: precipitation scavenging: proceedings of the fourth international conference; November-December 1982; Santa Monica, CA. New York, NY: Elsevier; pp. 91-101.

Saxena, P.; Hildemann, L. M. (1996) Water-soluble organics in atmospheric particles: a critical review of the literature and applications of thermodynamics to identify candidate compounds. J. Atmos. Chem.: accepted.

Saxena, P.; Seigneur, C. (1987) On the oxidation of SO_2 to sulfate in atmospheric aerosols. Atmos. Environ. 21: 807-812.

Saxena, P.; Mueller, P. K.; Kim, Y. P.; Seinfeld, J. H.; Koutrakis, P. (1993) Coupling thermodynamic theory with measurements to characterize acidity of atmospheric particles. Aerosol Sci. Technol. 19: 279-293.

Saxena, P.; Hildemann, L. M.; McMurry, P. H.; Seinfeld, J. H. (1995) Organics alter hygroscopic behavior of atmospheric particles. J. Geophys. Res. [Atmos.]: in press.

Saylor, R. D. (1989) A study of mesoscale acid deposition in the lower Ohio River Valley [Ph.D. dissertation]. Lexington, KY: University of Kentucky, Chemical Engineering Department.

Schlesinger, R. B. (1994) Comments on "Coupling thermodynamic theory with measurements to characterize acidity of atmospheric particles" by P. Saxena et al. Aerosol Sci. Technol. 20: 285-286.

Schmidt, J. A.; Andren, A. W. (1980) The atmospheric chemistry of nickel. In: Nriagu, J. O., ed. Nickel in the environment. New York, NY: John Wiley & Sons, Inc.; pp. 93-135.

Schroeder, W. H.; Dobson, M.; Kane, D. M.; Johnson, N. D. (1987) Toxic trace elements associated with airborne particulate matter: a review. JAPCA 37: 1267-1285.

Schuetzle, D.; Cronn, D.; Crittenden, A. L.; Charlson, R. J. (1975) Molecular composition of secondary aerosol and its possible origin. Environ. Sci. Technol. 9: 838-845.

Schwartz, S. E. (1979) Residence times in reservoirs under non-steady-state conditions: application to atmospheric SO_2 and aerosol sulfate. Tellus 31: 530-547.

Schwartz, S. E. (1984a) Gas-aqueous reactions of sulfur and nitrogen oxides in liquid-water clouds. In: Calvert, J. G., ed. SO_2, NO and NO_2 oxidation mechanisms: atmospheric considerations. Boston, MA: Butterworth Publishers; pp. 173-208. (Teasley, J. I., ed. Acid precipitation series: v. 3).

Schwartz, S. E. (1984b) Gas- and aqueous-phase chemistry of HO_2 in liquid water clouds. J. Geophys. Res. [Atmos.] 89: 11,589-11,598.

Schwartz, S. E. (1986a) Chemical conversions in clouds. In: Lee, S. D.; Schneider, T.; Grant, L. D.; Verkerk, P., eds. Aerosols: research, risk assessment and control strategies, proceedings of the second U.S.-Dutch international symposium; May 1985; Williamsburg, VA. Chelsea, MI: Lewis Publishers, Inc.; pp. 349-375.

Schwartz, S. E. (1986b) Mass-transport considerations pertinent to aqueous-phase reactions of gases in liquid-water clouds. In: Jaeschke, W., ed. Chemistry of multiphase atmospheric systems. Berlin, Federal Republic of Germany: Springer-Verlag; pp. 415-471. (NATO advanced science institutes series G: ecological sciences v. 6).

Schwartz, S. E. (1987) Both sides now: the chemistry of clouds. Ann. N. Y. Acad. Sci. 502: 83-144.

Schwartz, S. E. (1988) Mass-transport limitation to the rate of in-cloud oxidation of SO_2: re-examination in the light of new data. Atmos. Environ. 22: 2491-2499.

Schwartz, S. E. (1989) Acid deposition: unraveling a regional phenomenon. Science (Washington, DC) 243: 753-763.

Schwartz, S. E.; Freiberg, J. E. (1981) Mass-transport limitation to the rate of reaction of gases in liquid droplets: application to oxidation of SO_2 in aqueous solutions. Atmos. Environ. 15: 1129-1144.

Schwartz, S. E.; Newman, L. (1978) Processes limiting oxidation of sulfur dioxide in stack plumes. Environ. Sci. Technol. 12: 67-73.

Schwartz, S. E.; Newman, L. (1983) Measurements of sulfate production in natural clouds [discussion of Hegg and Hobbs (1982)]. Atmos. Environ. 17: 2629-2632.

Schwartz, S. E.; White, W. H. (1983) Kinetics of reactive dissolution of nitrogen oxides into aqueous solution. In: Schwartz, S. E., ed. Trace atmospheric constituents: properties, transformations, and fates. New York, NY: John Wiley & Sons; pp. 1-116. (Advances in environmental science and technology: v. 12).

Scott, B. C.; Laulainen, N. S. (1979) On the concentration of sulfate in precipitation. J. Appl. Meteorol. 18: 138-147.

Šega, K.; Fugaš, M. (1984) Seasonal and spatial differences in mass concentration levels and particle size distribution of aerosols over an urban area. Atmos. Environ. 18: 2433-2437.

Sehmel, G. A. (1973) Particle resuspension from an asphalt road caused by car and truck traffic. Atmos. Environ. 7: 291-309.

Sehmel, G. A. (1980) Particle and gas dry deposition: a review. Atmos. Environ. 14: 983-1011.

Sehmel, G. A. (1984) Deposition and resuspension. In: Randerson, D., ed. Atmospheric science and power production. Washington, DC: U.S. Department of Energy, Office of Scientific and Technical Information; report no. DOE/TIC-27601; pp. 533-583. Available from: NTIS, Springfield, VA; DE84-005177.

Seidl, W. (1989) Ionic concentrations and initial S(IV)-oxidation rates in droplets during the condensational stage of cloud. Tellus Ser. B 41B: 32-50.

Seigneur, C. (1982) A model of sulfate aerosol dynamics in atmospheric plumes. Atmos. Environ. 16: 2207-2228.

Seigneur, C.; Constantinou, E. (1995) Chemical kinetic mechanism for atmospheric chromium. Environ. Sci. Technol. 29: 222-231.

Seigneur, C.; Saxena, P. (1984) A study of atmospheric acid formation in different environments. Atmos. Environ. 18: 2109-2124.

Seigneur, C.; Saxena, P. (1988) A theoretical investigation of sulfate formation in clouds. Atmos. Environ. 22: 101-115.

Seigneur, C.; Wegrecki, A. M. (1990) Mathematical modeling of cloud chemistry in the Los Angeles basin. Atmos. Environ. Part A 24: 989-1006.

Seigneur, C.; Saxena, P.; Roth, P. M. (1984) Computer simulations of the atmospheric chemistry of sulfate and nitrate formation. Science (Washington, DC) 225: 1028-1030.

Seinfeld, J. H.; Flagan, R. C.; Petti, T. B.; Stern, J. E.; Grosjean, D. (1987) Aerosol formation in aromatic hydrocarbon-NOx systems. Pasadena, CA: California Institute of Technology; project no. AP-6.

Sergides, C. A.; Jassim, J. A.; Chughtai, A. R.; Smith, D. M. (1987) The structure of hexane soot. Part III: Ozonation studies. Appl. Spectrosc. 41: 482-492.

Shah, J. J.; Johnson, R. L.; Heyerdahl, E. K.; Huntzicker, J. J. (1986) Carbonaceous aerosol at urban and rural sites in the United States. J. Air Pollut. Control Assoc. 36: 254-257.

Shao, Y.; Raupach, M. R.; Findlater, P. A. (1993) Effect of saltation bombardment on the entrainment of dust by wind. J. Geophys. Res. [Atmos.] 98: 12,719-12,726.

Shaw, M. A.; Rood, M. J. (1990) Measurement of the crystallization humidities of ambient aerosol particles. Atmos. Environ. Part A 24: 1837-1841.

Sheridan, P. J.; Schnell, R. C.; Kahl, J. D.; Boatman, J. F.; Garvey, D. M. (1993) Microanalysis of the aerosol collected over south-central New Mexico during the ALIVE field experiment, May-December 1989. Atmos. Environ. Part A 27: 1169-1183.

Shinn, J. H.; Homan, D. N.; Gay, D. D. (1983) Plutonium aerosol fluxes and pulmonary exposure rates during resuspension from bare soils near a chemical separation facility. In: Pruppacher, H. R.; Semonin, R. G.; Slinn, W. G. N., eds. Precipitation scavenging, dry deposition, and resuspension, v. 2: dry deposition and resuspension: proceedings of the fourth international conference; November-December 1982; Santa Monica, CA. New York, NY: Elsevier; pp. 1131-1143.

Sievering, H.; Van Valin, C. C.; Barrett, E. W.; Pueschel, R. F. (1984) Cloud scavenging of aerosol sulfur: two case studies. Atmos. Environ. 18: 2685-2690.

Sievering, H.; Boatman, J.; Galloway, J.; Keene, W.; Kim, Y.; Luria, M.; Ray, J. (1991) Heterogeneous sulfur conversion in sea-salt aerosol particles: the role of aerosol water content and size distribution. Atmos. Environ. Part A 25: 1479-1487.

Sievering, H.; Gorman, E.; Kim, Y.; Ley, T.; Seidl, W.; Boatman, J. (1994) Heterogeneous conversion contribution to the sulfate observed over Lake Michigan. Atmos. Environ. 28: 367-370.

Simoneit, B. R. T. (1984) Organic matter of the troposphere—III. characterization and sources of petroleum and pyrogenic residues in aerosols over the western United States. Atmos. Environ. 18: 51-67.

Simoneit, B. R. T. (1986) Characterization of organic constituents in aerosols in relation to their origin and transport: a review. Presented at: the 2nd workshop on chemistry analysis of hydrocarbons in the environment; November 1985; Barcelona, Spain. Int. J. Environ. Anal. Chem. 23: 207-237.

Simoneit, B. R. T. (1989) Organic matter of the troposphere - V: application of molecular marker analysis to biogenic emissions into the troposphere for source reconciliations. Presented at: the international symposium on biosphere-atmosphere exchange; March 1986; Mainz, Federal Republic of Germany. J. Atmos. Chem. 8: 251-275.

Simoneit, B. R. T.; Mazurek, M. A. (1982) Organic matter of the troposphere—II. natural background of biogenic lipid matter in aerosols over the rural western United States. Atmos. Environ. 16: 2139-2159.

Sisler, J. F.; Malm, W. C. (1994) The relative importance of soluble aerosols to spatial and seasonal trends of impaired visibility in the United States. Atmos. Environ. 28: 851-862.

Sisterson, D. L.; Bowersox, V. C.; Olsen, A. R.; Meyers, T. P.; Olsen, A. R.; Vong, R. L. (1991) Deposition monitoring: methods and results. In: Irving, P. M., ed. Acidic deposition: state of science and technology, volume I: emissions, atmospheric processes, and depostition. Washington, DC: The U.S. National Acid Precipitation Assessment Program. (State of science and technology report no. 6).

Slinn, W. G. N. (1983) Air-to-sea transfer of particles. In: Liss, P. S.; Slinn, W. G. N., eds. Air-sea exchange of gases and particles. Boston, MA: D. Reidel Publishing Company; pp. 299-405. (NATO ASI series. Series C, mathematical and physical sciences; no. 108).

Sloane, C. S. (1982) Visibility trends—II. mideastern United States 1948-1978. Atmos. Environ. 16: 2309-2321.

Sloane, C. S.; Groblicki, P. J. (1981) Denver's visibility history. Atmos. Environ. 15: 2631-2638.

Sloane, C. S.; Watson, J.; Chow, J.; Pritchett, L.; Richards, L. W. (1991) Size-segregated fine particle measurements by chemical species and their impact on visibility impairment in Denver. Atmos. Environ. Part A 25: 1013-1024.

Smith, T. B. (1981) Some observations of pollutant transport associated with elevated plumes. Atmos. Environ. 15: 2197-2203.

Smith, D. M.; Akhter, M. S.; Jassim, J. A.; Sergides, C. A.; Welch, W. F.; Chughtai, A. R. (1989) Studies of the structure and reactivity of soot. Aerosol Sci. Technol. 10: 311-325.

Snider, J. R.; Vali, G. (1994) Sulfur dioxide oxidation in winter orographic clouds. J. Geophys. Res. [Atmos.] 99: 18,713-18,733.

Spann, J. F.; Richardson, C. B. (1985) Measurement of the water cycle in mixed ammonium acid sulfate particles. Atmos. Environ. 19: 819-825.

Spengler, J. D.; Keeler, G. J.; Koutrakis, P.; Ryan, P. B.; Raizenne, M.; Franklin, C. A. (1989) Exposures to acidic aerosols. In: Symposium on the health effects of acid aerosols; October 1987; Research Triangle Park, NC. Environ. Health Perspect. 79: 43-51.

Spicer, C. W. (1977a) Photochemical atmospheric pollutants derived from nitrogen oxides. Atmos. Environ. 11: 1089-1095.

Spicer, C. W. (1977b) The fate of nitrogen oxides in the atmosphere. In: Pitts, J. N., Jr.; Metcalf, R. L.; Lloyd, A. C., eds. Advances in environmental science and technology: v. 4. New York, NY: John Wiley and Sons, Inc.; pp. 163-261.

Stein, S. W.; Turpin, B. J.; Cai, X.; Huang, P.-F.; McMurry, P. H. (1994) Measurements of relative humidity-dependent bounce and density for atmospheric particles using the DMA-impactor technique. Atmos. Environ. 28: 1739-1746.

Steiner, D.; Burtscher, H.; Gross, H. (1992) Structure and disposition of particles from a spark-ignition engine. Atmos. Environ. Part A 26: 997-1003.

Stelson, A. W.; Seinfeld, J. H. (1981) Chemical mass accounting of urban aerosol. Environ. Sci. Technol. 15: 671-679.

Stelson, A. W.; Seinfeld, J. H. (1982a) Relative humidity and temperature dependence of the ammonium nitrate dissociation constant. Atmos. Environ. 16: 983-992.

Stelson, A. W.; Seinfeld, J. H. (1982b) Relative humidity and pH dependence of the vapor pressure of ammonium nitrate-nitric acid solutions at 25°C. Atmos. Environ. 16: 993-1000.

Stern, J. E.; Flagan, R. C.; Grosjean, D.; Seinfeld, J. H. (1987) Aerosol formation and growth in atmospheric aromatic hydrocarbon photooxidation. Environ. Sci. Technol. 21: 1224-1231.

Stevens, R. K.; Dzubay, T. G.; Lewis, C. W.; Shaw, R. W., Jr. (1984) Source apportionment methods applied to the determination of the origin of ambient aerosols that affect visibility in forested areas. Atmos. Environ. 18: 261-272.

Stewart, D. A.; Liu, M.-K. (1981) Development and application of a reactive plume model. Atmos. Environ. 15: 2377-2393.

Storey, J. M. E.; Pankow, J. F. (1992) Gas-particle partitioning of semi-volatile organic compounds to model atmospheric particulate materials—I. Sorption to graphite, sodium chloride, alumina, and silica particles under low humidity conditions. Atmos. Environ. Part A 26: 435-443.

Strapp, J. W.; Leaitch, W. R.; Anlauf, K. G.; Bottenheim, J. W.; Joe, P.; Schemenauer, R. S.; Wiebe, H. A.; Isaac, G. A.; Kelly, T. J.; Daum, P. H. (1988) Winter cloud water and air composition in Central Ontario. J. Geophys. Res. [Atmos.] 93: 3760-3772.

Suh, H. H.; Spengler, J. D.; Koutrakis, P. (1992) Personal exposures to acid aerosols and ammonia. Environ. Sci. Technol. 26: 2507-2517.

Suh, H. H.; Allen, G. A.; Aurian-Blăjeni, B.; Koutrakis, P.; Burton, R. M. (1994a) Field method comparison for the characterization of acid aerosols and gases. Atmos. Environ. 28: 2981-2989.

Suh, H. H.; Koutrakis, P.; Spengler, J. D. (1994b) The relationship between airborne acidity and ammonia in indoor environments. J. Exposure Anal. Environ. Epidemiol. 4: 1-23.

Suh, H. H.; Allen, G. A.; Koutrakis, P.; Burton, R. M. (1995) Spatial variation in acidic sulfate and ammonia concentrations within metropolitan Philadelphia. J. Air Waste Manage. Assoc. 45: 442-452.

Sutherland, A. J. (1967) Proposed mechanism for sediment entrainment by turbulent flows. J. Geophys. Res. 72: 6183-6194.

Svenningsson, B.; Hansson, H.-C.; Wiedensohler. A.; Noone, K.; Ogren, J.; Hallberg, A.; Calvile, R. (1994) Hygroscopic growth of aerosol particles and its influence on nucleation scavenging in cloud: experimental results from Kleiner Feldberg. J. Atmos. Chem. 19: 129-152.

Sverdrup, G. M.; Whitby, K. T. (1980) The effect of changing relative humidity on aerosol size distribution measurements. In: Hidy, G. M.; Mueller, P. K.; Grosjean, D.; Appel, B. R.; Wesolowski, J. J., eds. The character and origins of smog aerosols: a digest of results from the California Aerosol Characterization Experiment (ACHEX). New York, NY: John Wiley & Sons; pp. 527-558. (Advances in environmental science and technology: v. 10).

Sviridenkov, M. A.; Gillette, D. A.; Isakov, A. A.; Sokolik, I. N.; Smirnov, V. V.; Belan, B. D.; Pachenko, M. V.; Andronova, A. V.; Kolomiets, S. M.; Zhukov, V. M.; Zhukovsky, D. A. (1993) Size distributions of dust aerosol measured during the Soviet-American experiment in Tadzhikistan, 1989. Atmos. Environ. Part A 27: 2481-2486.

TSI. (1993) Model 390045 DISTFIT™ aerosol data fitting software. St. Paul and Golden Valley, MN: TSI, Inc. and Chimera Software.

Tang, I. N. (1980) Deliquescence properties and particle size change of hygroscopic aerosols. In: Willeke, K., ed. Generation of aerosols and facilities for exposure experiments. Ann Arbor, MI: Ann Arbor Science; pp. 153-167.

Tang, I. N.; Munkelwitz, H. R. (1977) Aerosol growth studies—III. ammonium bisulfate aerosols in a moist atmosphere. J. Aerosol Sci. 8: 321-330.

Tang, I. N.; Munkelwitz, H. R. (1993) Composition and temperature dependence of the deliquescence properties of hygroscopic aerosols. Atmos. Environ. Part A 27: 467-473.

Tang, I. N.; Munkelwitz, H. R. (1994) Water activities, densities, and refractive indices of aqueous sulfates and sodium nitrate droplets of atmospheric importance. J. Geophys. Res. [Atmos.] 99: 18,801-18,808.

Tang, I. N.; Munkelwitz, H. R.; Davis, J. G. (1978) Aerosol growth studies - IV. phase transformation of mixed salt aerosols in a moist atmosphere. J. Aerosol Sci. 9: 505-511.

Tang, I. N.; Wong, W. T.; Munkelwitz, H. R. (1981) The relative importance of atmospheric sulfates and nitrates in visibility reduction. Atmos. Environ. 15: 2463-2471.

Tani, B.; Siegel, S.; Johnson, S. A.; Kumar, R. (1983) X-ray diffraction investigation of atmospheric aerosols in the 0.3-1.0 μm aerodynamic size range. Atmos. Environ. 17: 2277-2283.

Tao, Y.; McMurry, P. H. (1989) Vapor pressures and surface free energies of C14-C18 monocarboxylic acids and C5 and C6 dicarboxylic acids. Environ. Sci. Technol. 23: 1519-1523.

Taylor, G. I. (1922) Diffusion by continuous movements. Proc. London Math. Soc. 20: 196-212.

Taylor, G. R. (1989) Sulfate production and deposition in midlatitude continental cumulus clouds. Part II: Chemistry model formulation and sensitivity analysis. J. Atmos. Sci. 46: 1991-2007.

Ten Brink, H. M.; Schwartz, S. E.; Daum, P. H. (1987) Efficient scavenging of aerosol sulfate by liquid-water clouds. Atmos. Environ. 21: 2035-2052.

Thibodeaux, L. J.; Nadler, K. C.; Valsaraj, K. T.; Reible, D. D. (1991) The effect of moisture on volatile organic chemical gas-to-particle partitioning with atmospheric aerosols—competitive adsorption theory predictions. Atmos. Environ. Part A 25: 1649-1656.

Thomas, P.; Vogt, S. (1990) Mesoscale atmospheric dispersion experiments using tracer and tetroons. Atmos. Environ. Part A 24: 1271-1284.

Thompson, K. M.; Koutrakis, P.; Brauer, M.; Spengler, J. D.; Wilson, W. E.; Burton, R. M. (1991) Measurements of aerosol acidity: sampling frequency, seasonal variability, and spatial variation. Presented at: 84th annual meeting and exhibition of the Air & Waste Management Association; June; Vancouver, BC, Canada. Pittsburgh, PA: Air & Waste Management Association; paper no. 91-89.5.

Thurston, G. D.; Gorczynski, J. E., Jr.; Jaques, P.; Currie, J.; He, D. (1992) An automated sequential sampling system for particulate acid aerosols: description, characterization, and field sampling results. J. Exposure Anal. Environ. Epidemiol. 2: 415-428.

Tuazon, E. C.; Atkinson, R.; Plum, C. N.; Winer, A. M.; Pitts, J. N., Jr. (1983) The reaction of gas phase N_2O_5 with water vapor. Geophys. Res. Lett. 10: 953-956.

Turpin, B. J.; Huntzicker, J. J. (1991) Secondary formation of organic aerosol in the Los Angeles basin: a descriptive analysis of organic and elemental carbon concentrations. Atmos. Environ. Part A 25: 207-215.

Turpin, B. J.; Huntzicker, J. J. (1995) Identification of secondary organic aerosol episodes and quantitation of primary and secondary organic aerosol concentrations during SCAQS. Atmos. Environ. 29: 3527-3544.

Turpin, B. J.; Cary, R. A.; Huntzicker, J. J. (1990) An in situ, time-resolved analyzer for aerosol organic and elemental carbon. Aerosol Sci. Technol. 12: 161-171.

Turpin, B. J.; Huntzicker, J. J.; Larson, S. M.; Cass, G. R. (1991) Los Angeles summer midday particulate carbon: primary and secondary aerosol. Environ. Sci. Technol. 25: 1788-1793.

Turpin, B. J.; Liu, S.-P.; Podolske, K. S.; Gomes, M. S. P.; Eisenreich, S. J.; McMurry, P. H. (1993) Design and evaluation of a novel diffusion separator for measuring gas/particle distributions of semivolatile organic compounds. Environ. Sci. Technol. 27: 2441-2449.

Twohy, C. H.; Austin, P. H.; Charlson, R. J. (1989) Chemical consequences of the initial diffusional growth of cloud droplets: a clean marine case. Tellus Ser. B 41B: 51-60.

Twomey, S. (1959) The nuclei of natural cloud formation: part II: the supersaturation in natural clouds and the variation of cloud droplet concentration. Geofis. Pura Appl. 43: 243-249.

U.S. Environmental Protection Agency. (1982) Air quality criteria for particulate matter and sulfur oxides. Research Triangle Park, NC: Office of Health and Environmental Assessment, Environmental Criteria and Assessment Office; EPA report no. EPA-600/8-82-029aF-cF. 3v. Available from: NTIS, Springfield, VA; PB84-156777.

U.S. Environmental Protection Agency. (1986a) Health assessment document for nickel and nickel compounds. Research Triangle Park, NC: Environmental Criteria and Assessment Office; report no. EPA/600/8-83/012FF. Available from: NTIS, Springfield, VA; PB86-232212.

U.S. Environmental Protection Agency. (1986b) Air quality criteria for lead. Research Triangle Park, NC: Office of Health and Environmental Assessment, Environmental Criteria and Assessment Office; EPA report no. EPA-600/8-83/028aF-dF. 4v. Available from: NTIS, Springfield, VA; PB87-142378.

U.S. Environmental Protection Agency. (1995) Compilation of air pollutant emission factors, v. I: stationary point and area sources. 5th ed. Research Triangle Park, NC: Office of Air Quality Planning and Standards; sections 1.1 and 1.2; report no. AP-42.

Uliasz, M. (1993) The atmospheric mesoscale dispersion modeling system. J. Appl. Meteorol. 32: 139-149.

Valerio, F.; Bottino, P.; Ugolini, D.; Cimberle, M. R.; Tozzi, G. A.; Frigerio, A. (1984) Chemical and photochemical degradation of polycyclic aromatic hydrocarbons in the atmosphere. Sci. Total Environ. 40: 169-188.

Valsaraj, K. T.; Thoma, G. J.; Reible, D. D.; Thibodeaux, L. J. (1993) On the enrichment of hydrophobic organic compounds in fog droplets. Atmos. Environ. Part A 27: 203-210.

Van Borm, W. A.; Adams, F. C.; Maenhaut, W. (1989) Characterization of individual particles in the Antwerp aerosol. Atmos. Environ. 23: 1139-1151.

Vanderpool, R. W.; Lundgren, D. A.; Marple, V. A.; Rubow, K. L. (1987) Cocalibration of four large-particle impactors. Aerosol Sci. Technol. 7: 177-185.

Van Doren, J. M.; Watson, L. R.; Davidovits, P.; Worsnop, D. R.; Zahniser, M. S.; Kolb, C. E. (1990) Temperature dependence of the uptake coefficients of HNO_3, HCl, and N_2O_5 by water droplets. J. Phys. Chem. 94: 3265-3272.

Van Grieken, R.; Xhoffer, C. (1992) Microanalysis of individual environmental particles. J. Anal. At. Spectrom. 7: 81-88.

Van Valin, C. C.; Luria, M.; Ray, J. D.; Boatman, J. F. (1990) Hydrogen peroxide and ozone over the northeastern United States in June 1987. J. Geophys. Res. [Atmos.] 95: 5689-5695.

Venkataraman, C.; Friedlander, S. K. (1994) Size distributions of polycyclic aromatic hydrocarbons and elemental carbon. 2. Ambient measurements and effects of atmospheric processes. Environ. Sci. Technol. 28: 563-572.

Venkataraman, C.; Hildemann, L. M. (1994) Factors affecting the distribution of primary semivolatile organic compounds of urban aerosol particles. Environ. Sci. Technol.: submitted.

Venkataraman, C.; Lyons, J. M.; Friedlander, S. K. (1994) Size distributions of polycyclic aromatic hydrocarbons and elemental carbon. 1. Sampling, measurement methods, and source characterization. Environ. Sci. Technol. 28: 555-562.

Wagman, J.; Lee, R. E., Jr.; Axt, C. J. (1967) Influence of some atmospheric variables on the concentration and particle size distribution of sulfate in urban air. Atmos. Environ. 1: 479-489.

Walcek, C. J.; Stockwell, W. R.; Chang, J. S. (1990) Theoretical estimates of the dynamic, radiative and chemical effects of clouds on tropospheric trace gases. Atmos. Res. 25: 53-69.

Waldman, J. M.; Lioy, P. J.; Thurston, G. D.; Lippmann, M. (1990) Spatial and temporal patterns in summertime sulfate aerosol acidity and neutralization within a metropolitan area. Atmos. Environ. Part B 24: 115-126.

Waldman, J. M.; Koutrakis, P.; Allen, G. A.; Thurston, G. D.; Burton, R. M.; Wilson, W. E. (1995) Human exposures to particle strong acidity. In: Phalen, R. F.; Bates, D. V., eds. Proceedings of the colloquium on particulate air pollution and human mortality and morbidity, part II; January 1994; Irvine, CA. Inhalation Toxicol. 7: 657-669.

Wall, S. M.; John, W.; Ondo, J. L. (1988) Measurement of aerosol size distributions for nitrate and major ionic species. Atmos. Environ. 22: 1649-1656.

Wang, C.; Chang, J. S. (1993) A three-dimensional numerical model of cloud dynamics, microphysics, and chemistry: 4. cloud chemistry and precipitation chemistry. J. Geophys. Res. [Atmos.] 98: 16,799-16,808.

Wang, H.-C.; John, W. (1987) Comparative bounce properties of particle materials. Aerosol Sci. Technol. 7: 285-299.

Wang, H.-C.; John, W. (1988) Characteristics of the Berner impactor for sampling inorganic ions. Aerosol Sci. Technol. 8: 157-172.

Wang, S.-C.; Paulson, S. E.; Grosjean, D.; Flagan, R. C.; Seinfeld, J. H. (1992a) Aerosol formation and growth in atmospheric organic/NO_x systems—I. Outdoor smog chamber studies of C_7- and C_8- hydrocarbons. Atmos. Environ. Part A 26: 403-420.

Wang, S.-C.; Flagan, R. C.; Seinfeld, J. H. (1992b) Aerosol formation and growth in atmospheric organic/NO_x systems—II. aerosol dynamics. Atmos. Environ. Part A 26: 421-434.

Warner, T. T. (1981) Verification of a three-dimensional transport model using tetroon data from Project STATE. Atmos. Environ. 15: 2219-2222.

Warren, R. S.; Birch, P. (1987) Heavy metal levels in atmospheric particulates, roadside dust and soil along a major urban highway. Sci. Total Environ. 59: 253-256.

Watson, J. G.; Chow, J. C. (1992) Data bases for PM_{10} and $PM_{2.5}$ chemical compositions and source profiles. Transactions AWMA 1: 61-91.

Watson, J. G.; Chow, J. C.; Lurmann, F. W.; Musarra, S. P. (1994a) Ammonium nitrate, nitric acid, and ammonia equilibrium in wintertime Phoenix, Arizona. Air Waste 44: 405-412.

Watson, J. G.; Chow, J. C.; Lu, Z.; Fujita, E. M.; Lowenthal, D. H.; Lawson, D. R.; Ashbaugh, L. L. (1994b) Chemical mass balance source apportionment of PM_{10} during the Southern California Air Quality Study. Aerosol Sci. Technol. 21: 1-36.

Weathers, K. C.; Likens, G. E.; Bormann, F. H.; Bicknell, S. H.; Bormann, B. T.; Daube, B. C., Jr.; Eaton, J. S.; Galloway, J. N.; Keene, W. C.; Kimball, K. D.; McDowell, W. H.; Siccama, T. G.; Smiley, D.; Tarrant, R. A. (1988) Cloudwater chemistry from ten sites in North America. Environ. Sci. Technol. 22: 1018-1026.

Weber, R. J.; McMurry, P. H.; Eisele, F. L.; Tanner, D. J. (1995) Measurement of expected nucleation precursor species and 5 to 500 nm diameter particles at Mauna Loa, Hawaii. J. Atmos. Sci. 52: 2242-2257.

Wesely, M. L.; Hicks, B. B. (1977) Some factors that affect the deposition rates of sulfur dioxide and similar gases on vegetation. J. Air Pollut. Control Assoc. 27: 1110-1116.

Wexler, A. S.; Seinfeld, J. H. (1990) The distribution of ammonium salts among a size and composition dispersed aerosol. Atmos. Environ. Part A 24: 1231-1246.

Wexler, A. S.; Seinfeld, J. H. (1992) Analysis of aerosol ammonium nitrate: departures from equilibrium during SCAQS. Atmos. Environ. Part A 26: 579-591.

Wexler, A. S.; Eldering, A.; Pandis, S. N.; Cass, G. R.; Seinfeld, J. H.; Moon, K. C.; Hering, S. (1992) Modeling aerosol processes and visibility based on the SCAQS data. Final report. Sacramento, CA: California Air Resources Board; contract no. A932-054.

Whitby, K. T. (1978) The physical characteristics of sulfur aerosols. Atmos. Environ. 12: 135-159.

Whitby, K. T. (1980) Aerosol formation in urban plumes. Ann. N. Y. Acad. Sci. 338: 258-275.

Whitby, K. T. (1984) Physical and optical behavior of sulfate-nitrate aerosols in equilibrium with atmospheric water vapor, ammonia and nitric acid. In: Ruhnke, L. H.; Deepak, A., eds. Hygroscopic aerosols: technical proceedings of the workshop on hygroscopic aerosols in the planetary boundary layer; April 1982; Vail, CO. Hampton, VA: A. Deepak Publishing; pp. 45-63.

Whitby, K. T.; Sverdrup, G. M. (1980) California aerosols: their physical and chemical characteristics. In: Hidy, G. M.; Mueller, P. K.; Grosjean, D.; Appel, B. R.; Wesolowski, J. J., eds. The character and origins of smog aerosols: a digest of results from the California Aerosol Characterization Experiment (ACHEX). New York, NY: John Wiley & Sons, Inc.; pp. 477-517. (Advances in environmental science and technology: v. 9).

Whitby, K. T.; Husar, R. B.; Liu, B. Y. H. (1972) The aerosol size distribution of Los Angeles smog. J. Colloid Interface Sci. 39: 177-204.

Whitby, K. T.; Charlson, R. E.; Wilson, W. E.; Stevens, R. K. (1974) The size of suspended particle matter in air. Science (Washington, DC) 183: 1098-1099.

White, W. H.; Macias, E. S. (1989) Carbonaceous particles and regional haze in the western United States. Aerosol Sci. Technol. 10: 111-117.

White, W. H.; Anderson, J. A.; Blumenthal, D. L.; Husar, R. B.; Gillani, N. V.; Husar, J. D.; Wilson, W. E., Jr. (1976) Formation and transport of secondary air pollutants: ozone and aerosols in the St. Louis urban plume. Science (Washington, DC) 194: 187-189.

White, W. H.; Patterson, D. E.; Wilson, W. E. (1983) Urban exports to the nonurban troposphere: results from Project MISTT. J. Geophys. Res. 88: 10,745-10,752.

White, W. H.; Seigneur, C.; Heinold, D. W.; Eltgroth, M. W.; Richards, L. W.; Roberts, P. T.; Bhardwaja, P. S.; Conner, W. D.; Wilson, W. E., Jr. (1985) Predicting the visibility of chimney plumes: an intercomparison of four models with observations at a well-controlled power plant. Atmos. Environ. 19: 515-528.

Wiedensohler, A.; Aalto, P.; Covert, D.; Heintzenberg, J.; McMurry, P. H. (1994) Intercomparison of four methods to determine size distributions of low-concentration ($\sim$ 100 cm^{-3}), ultrafine aerosols ($3 < D_p < 10$ nm) with illustrative data from the Artic. Aerosol Sci. Technol. 21: 95-109.

Willeke, K.; Whitby, K. T. (1975) Atmosperic aerosols: size distribution interpretation. J. Air Pollut. Control Assoc. 25: 529-534.

Willetts, B. (1992) [Personal communication]. Aberdeen, Scotland: University of Aberdeen.

Williams, D. J.; Carras, J. N.; Milne, J. W.; Heggie, A. C. (1981) The oxidation and long-range transport of sulphur dioxide in a remote region. Atmos. Environ. 15: 2255-2262.

Wilson, W. E. (1978) Sulfates in the atmosphere: a progress report on project MISTT. Atmos. Environ. 12: 537-547.

Wilson, W. E., Jr. (1981) Sulfate formation in point source plumes: a review of recent field studies. Atmos. Environ. 15: 2573-2581.

Wilson, J. C.; McMurry, P. H. (1981) Studies of aerosol formation in power plant plumes—II. secondary aerosol formation in the Navajo generating station plume. In: White, W. H.; Moore, D. J.; Lodge, J. P., eds. Plumes and visibility: measurements and model components: proceedings of the symposium; November 1980; Grand Canyon National Park, AZ. Atmos. Environ. 15: 2329-2339.

Wilson, W. E.; Suh, H. H. (1996) Fine and coarse particles: concentration relationships relevant to epidemiological studies. J. Air Waste Manage. Assoc.: accepted.

Wilson, W. E.; Spiller, L. L.; Ellestad, T. G.; Lamothe, P. J.; Dzubay, T. G.; Stevens, R. K.; Macias, E. S.; Fletcher, R. A.; Husar, J. D.; Husar, R. B.; Whitby, K. T.; Kittelson, D. B.; Cantrell, B. K. (1977) General Motors sulfate dispersion experiment: summary of EPA measurements. J. Air Pollut. Control Assoc. 27: 46-51.

Wilson, J. C.; Gupta, A.; Whitby, K. T.; Wilson, W. E. (1988) Measured aerosol light scattering coefficients compared with values calculated from EAA and optical particle counter measurements: improving the utility of the comparison. Atmos. Environ. 22: 789-793.

Winklmayr, W.; Wang, H.-C.; John, W. (1990) Adaptation of the Twomey algorithm to the inversion of cascade impactor data. Aerosol Sci. Technol. 13: 322-331.

Wolff, G. T. (1981) Particulate elemental carbon in the atmosphere. J. Air Pollut. Control Assoc. 31: 935-938.

Wolff, G. T.; Korsog, P. E. (1985) Estimates of the contributions of sources to inhalable particulate concentrations in Detroit. Atmos. Environ. 19: 1399-1409.

Wolff, G. T.; Lioy, P. J.; Wight, G. D.; Meyers, R. E.; Cederwall, R. T. (1977) An investigation of long-range transport of ozone across the midwestern and eastern United States. Atmos. Environ. 11: 797-802.

Wolff, G. T.; Groblicki, P. J.; Cadle, S. H.; Countess, R. J. (1982) Particulate carbon at various locations in the United States. In: Wolff, G. T.; Klimsch, R. L., eds. Particulate carbon: atmospheric life cycle. New York, NY: Plenum Press; pp. 297-315.

Wolff, G. T.; Ruthkosky, M. S.; Stroup, D. P.; Korsog, P. E. (1991) A characterization of the principal PM-10 species in Claremont (summer) and Long Beach (fall) during SCAQS. Atmos. Environ. Part A 25: 2173-2186.

Wu, P.-M.; Okada, K. (1994) Nature of coarse nitrate particles in the atmosphere—a single particle approach. Atmos. Environ. 28: 2053-2060.

Yamartino, R. J.; Scire, J. S.; Carmichael, G. R.; Chang, Y. S. (1992) The CALGRID mesoscale photochemical grid model—I. Model formulation. Atmos. Environ. Part A 26: 1493-1512.

Yamasaki, H.; Kuwata, K.; Miyamoto, H. (1982) Effects of ambient temperature on aspects of airborne polycyclic aromatic hydrocarbons. Environ. Sci. Technol. 16: 189-194.

Zafiriou, O. C.; Gagosian, R. B.; Peltzer, E. T.; Alford, J. B.; Loder, T. (1985) Air-to-sea fluxes of lipids at Enewetak Atoll. J. Geophys. Res. [Atmos.] 90: 2409-2423.

Zhang, X.; McMurry, P. H. (1991) Theoretical analysis of evaporative losses of adsorbed or absorbed species during atmospheric aerosol sampling. Environ. Sci. Technol. 25: 456-469.

Zhang, S.-H.; Shaw, M.; Seinfeld, J. H.; Flagan, R. C. (1992) Photochemical aerosol formation from α-pinene and β-pinene. J. Geophys. Res. [Atmos.] 97: 20,717-20,729.

Zhang, X. Q.; McMurry, P. H.; Hering, S. V.; Casuccio, G. S. (1993) Mixing characteristics and water content of submicron aerosols measured in Los Angeles and at the Grand Canyon. Atmos. Environ. Part A 27: 1593-1607.

Zhang, J.; Wilson, W. E.; Lioy, P. J. (1994) Indoor air chemistry: formation of organic acids and aldehydes. Environ. Sci. Technol. 28: 1975-1982.

Zimmerman, P. R. (1979) Testing of hydrocarbon emissions from vegetation, leaf litter and aquatic surfaces, and development of a methodology for compiling biogenic emission inventories: final report. Research Triangle Park, NC: U.S. Environmental Protection Agency, Office of Air Quality Planning and Standards; EPA report no. EPA-450/4-79-004. Available from: NTIS, Springfield, VA; PB-296070.

Zwozdziak, J. W.; Zwozdziak, A. B. (1990) Sulphate aerosol production in the upper parts of the Sudety Range, Poland. J. Aerosol Sci. 21(suppl. 1): S369-S372.

4. SAMPLING AND ANALYSIS METHODS FOR PARTICULATE MATTER AND ACID DEPOSITION

4.1 INTRODUCTION

Assessment of health risks associated with airborne aerosols implies that measurements be made defining the aerosol characteristics, concentrations and exposures that contribute to, or simply correlate with, adverse health effects. The proper selection of an aerosol sampling or analysis methodology to accomplish such measurements requires that rationales be applied that consider how the resulting data will be used and interpreted, in addition to the data quality required. As an example, treatment of a sample to remove particle-associated liquid water, either by heating the sample during the collection process or by equilibrating the sample at a low relative humidity subsequent to collection, may lead to changes in the character of the collected particles, relative to the dispersed particles, in addition to the removal of water (e.g. Meyer et al., 1995). Similarly, integrated collection of acidic fine aerosols, without selectively removing the larger, more basic particles, will cause neutralization (i.e., modification) of the sample on the substrate (Stevens et al., 1978). The same logic applies to the selective removal of gas phase components during sampling that might react with the deposited aerosol sample, in a manner inconsistent with naturally occurring transformation processes. The assumption that fixed-location measurements are representative of inhalation exposure implies that the effects of local spatial and temporal gradients are understood and appropriately applied to the sampler siting criteria (Spengler et al., 1994). Development of relationships between aerosol characteristics and health or ecological responses requires that the aerosol sampling and analysis processes are truly representative and adequately defined.

The application of sampling and analytical systems for aerosols must recognize that particles exist modally as size distributions generated by distinctively different source categories and having distinctly different chemistries, as discussed in Chapter 3. Two important reasons for making size-specific aerosol measurements are (a) to relate the in situ aerosol character to the potential deposition sites, and thus toxicity, of the respiratory system, and (b) separation of the size distribution modes to identify sources, transformation processes

or aerosol chemistry. The interpretation of particle size must be made based on the diameter definition inherent in the measurement process. Since the respiratory system classifies particles of unknown shapes and densities based on aerodynamic diameter, elucidation of aerosol relationships with health responses requires that sampling techniques either incorporate inertial aerodynamic sizers or provide mechanisms to accurately convert the measured diameters (e.g., optical) to an aerodynamic basis. All particle diameters described in this chapter are aerodynamic, unless otherwise specified.

Friedlander (1977) provided the descriptive matrix shown in Figure 4-1 for placing measurement techniques that define aerosol characteristics into perspective, in terms of their particle sizing capabilities, resolution times and chemical identification attributes. This approach defined these characteristics by resolution (single particle or greater), discretizing ability, and averaging process. The author notes that the "perfect" aerosol sampler would characterize particle size with "perfect" resolution, determine the chemistry of each particle "perfectly", and operate in real-time with no "lumping" of classes. These characteristics could be amended in "real-world" terms by suggesting that the "perfect" sampler would also have minimal cost and operator intervention. Also, if the aerosol measurement design goal is to mimick the respiratory system, physiological averaging characteristics must be considered. Size-specific, integrated aerosol measurements have improved significantly and their capabilities are better characterized since the 1987 PM_{10} NAAQS, but a "perfect" aerosol sampling system has not been devised. As discussed below, the methodologies required to adequately define the performance specifications of aerosol samplers have yet to be devised.

Many recent developmental efforts in aerosol measurement technologies have addressed the need to perfect the chemical characterization of reactive or volatile species collected on filtration substrates (e.g., Lamb et al., 1980; Koutrakis et al., 1988). Some of the most significant recent advances in aerosol measurement technologies have come in the form of analysis system "protocols", rather than individual pieces of hardware. Recognizing that there is no single "perfect" sampler, these protocols attempt to merge several aerosol sampling and analysis technologies into an adaptable and analytically versatile system. System attributes typically include one or more size-specific aerosol inlets, subsequent fractionators to separate the fine and coarse particle modes, and denuders and/or sequential filter packs to selectively account for reactive gas phase species. Examples include EPA's

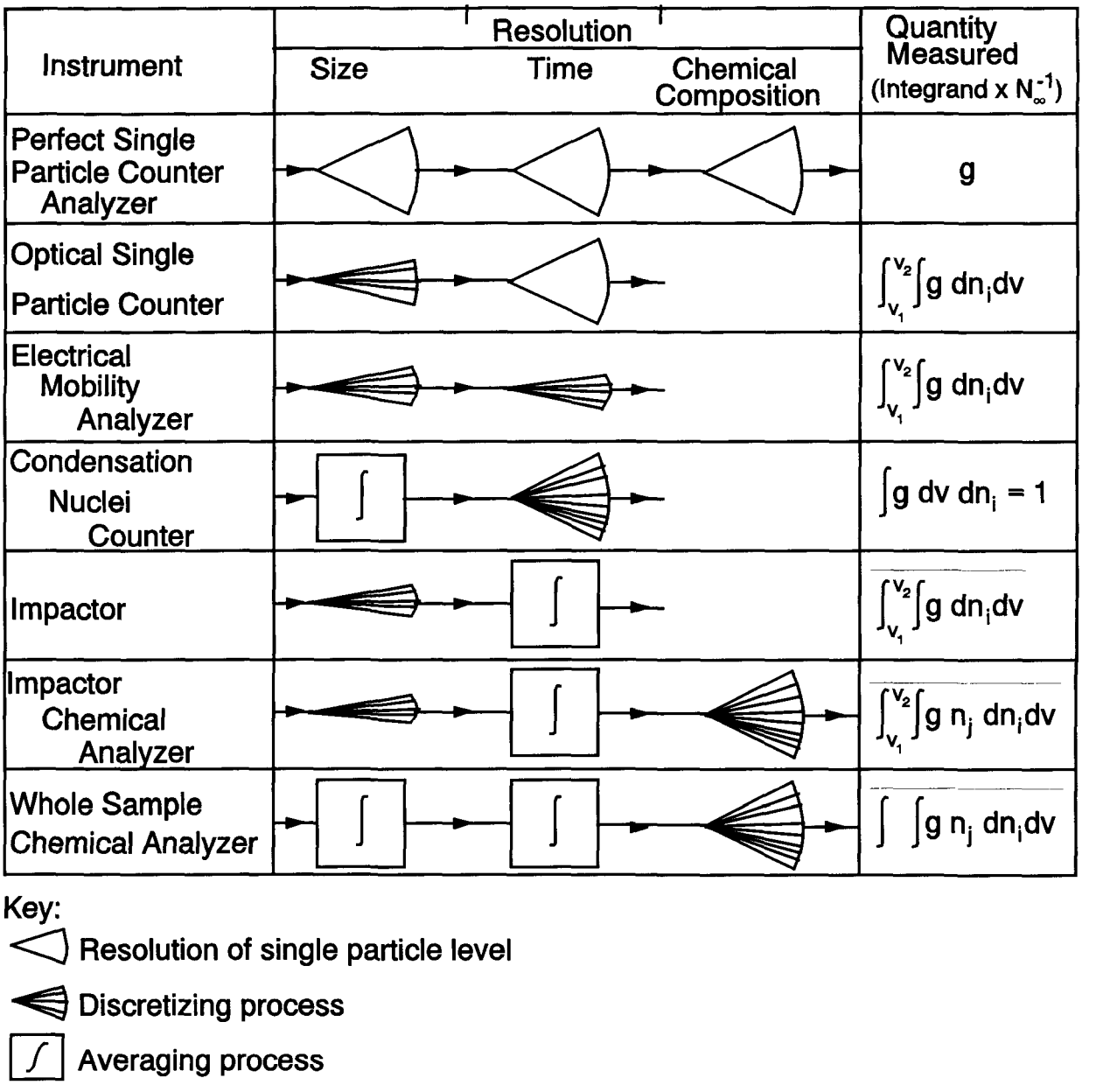

Figure 4-1. Characteristics of aerosol measurement instruments.

Source: Friedlander (1977).

Versatile Air Pollution Sampler (VAPS) (Conner et al., 1993), the Southern California Air Quality Study (SCAQS) sampler (Fitz et al., 1989) and the Interagency Monitoring of PROtected Visual Environments (IMPROVE) sampler (Malm et al., 1994).

Recognizing that personal exposure concentrations for aerosols may differ from classical outdoor fixed-location measurements has produced much smaller and less obtrusive

samplers using the same sizing techniques for application indoors, or even to be worn on the body during normal activities. Miniaturization of aerosol separators stretches the limits of current technologies to maintain required sampling precisions and accuracies. One of the most significant limitations imposed by the low flowrates inherent in personal exposure samplers is the extremely small sample size available for chemical analysis.

This chapter briefly describes the technical capabilities and limitations of aerosol sampling and analytical procedures in Sections 4.2 and 4.3, respectively, focusing on (1) those that were used to collect data supporting other sections in this document, (2) those supporting the existing PM_{10}, TSP[1] and Pb regulations, (3) those that were used to support health and welfare response studies, (4) those having application in development of a possible fine particle standard, and (5) discussing the attributes of several new technologies. The discussion of aerosol separation technologies is divided between (a) devices used to mimic the larger particle (>10 μm) penetration rationales for the upper airways, and (b) those devices generally used to mimic smaller particle penetration ($<$ 10 μm) to the thoracic regions. These device descriptions are followed by sampling considerations for their applications. The applications of performance specifications to define these measurement systems for regulatory purposes are discussed, along with a number of critical observations suggesting that the current specification process does not always ensure the accuracy or representativeness necessary in the field. The EPA program designating PM_{10} reference and equivalent sampling systems is then briefly described, along with a current list of designated devices. Selected measurement systems used to provide more detailed characterization of aerosol properties for research studies are discussed, with a focus on the determination of particle size distributions.

Aerosol sampling systems for specialty applications, including automated samplers, personal exposure samplers and the sampling systems used in aerosol apportionment studies are briefly described. The chapter then presents a short section (4.4) on sampling and analysis of bioaerosols Nevalainen et al. (1992). Also, Nevalainen et al. (1993), and Qian et al. (1995) provide excellent summaries of the principles involved in bioaerosol sampling and the most commonly used techniques.

---

[1]Subsequent identifications in this chapter: "TSP" for Total Suspended Particulates by high volume sampler, "PM_{10}" for the fraction less than 10 μm, "fine" for the fraction less than 2.5 μm.

4.2 SAMPLING FOR PARTICULATE MATTER

4.2.1 Background

The development of relationships between airborne particulate matter and human or ecological effects requires that the aerosol[2] measurement process be accurately, precisely and representatively defined. Improvements in sampling methodologies since the 1982 Air Quality Criteria Document for Particulate Matter and Sulfur Oxides (U.S. Environmental Protection Agency, 1982)[3] was released, have resulted from improved sensor technologies, and more importantly, a better understanding of the aerosol character in situ[4]. Additionally, health studies and atmospheric chemistry research in the past decade have focused more closely on smaller, better-defined aerosol size fractions of known integrity, collected specifically for subsequent chemical characterization.

The system of aerosols in ambient air is a continuum of particle sizes in a gas phase carrier formed as the summation of all size distributions produced by individual sources and secondary transformations. Portions of the composite distributions are often found to exist lognormally (Baron and Willeke, 1993; see also Chapter 3, Section 3.3.3). Aerosol systems also exist as a continuum of particle "ages", resulting from loss and transformation mechanisms such as agglomeration, settling, volatilization, gas-particle reaction, and rain-out affecting freshly generated particles. The chemical compositions of the various portions (modes) of the aerosol size distribution are more discreet, and sampling strategies must consider a specific range of sizes for a given chemical class. The constantly changing character of the atmosphere (or of indoor air) places a premium on sampling strategies both to collect representative aerosol samples from the air and to protect their integrity until analyzed.

The 1982 Criteria Document provided basic descriptions of many aerosol measurement techniques still used today. These included both older optically-based techniques, such as "Black Smoke" or "British Smoke" (BS) or "coefficient of haze" (COH) methods and certain

---

[2]Consistent with recent literature (e.g., see Willeke and Baron, 1993), the term "aerosol" will refer to the continuum of suspended particles and the carrier gas.

[3]Referred to in the text subsequently as an entity as the "1982 Criteria Document".

[4]The in situ characteristics of particles in the ambient air medium can be substantially modified by the sampling and analysis processes. For example, a particle counter which draws particles through a restrictive or heated inlet before they reach the sensing volume, may perceive the particle properties (e.g. scattering coefficients, size distributions) differently from those that existed in the ambient.

other now lesser used gravimetric methods, that are only briefly mentioned here but not described in detail. Instead the reader is referred to the earlier Criteria Document (U.S. Environmental Protection Agency, 1982) for more information on those methods not extensively covered here. This section mainly highlights the more recent peer-reviewed research on aerosol measurement technologies since 1982 and notes salient points that should be considered in their application. The aerosol sampling section is not intended to be an exhaustive treatise, but is structured to highlight important concepts and technologies relevant to the development of aerosol measurement/response relationships, or supporting existing and potential EPA aerosol regulations. Ancillary reference texts, describing basic aerosol mechanics (e.g., Hinds, 1982; Reist, 1984) and applied aerosol mechanics and measurements (e.g., Willeke and Baron, 1993; Hering, 1989; Lundgren et al., 1979; Liu, 1976) should be consulted for more fundamental details.

4.2.2 Large Particle Separators

4.2.2.1 Cutpoint Considerations

The collection of an aerosol sample is defined by the penetration characteristics of the inlet, overlaid on the existing in situ size distribution. Cooper and Guttrich (1981) describe this process mathematically, and they estimate the influences of non-ideal penetration characteristics. Miller et al. (1979) described the considerations for the possible selection of 15 μm (designated "inhalable") as a standard for size-selective particle sampling with upper airway respiratory deposition as the primary consideration. The selection of the most appropriate aerodynamic criteria for ambient aerosol sampling was only partially resolved by the 1987 EPA designation (U.S. Environmental Protection Agency, 1987) of a 10 μm (PM_{10}) cutpoint. The "ideal" PM_{10} inlet was referenced to the thoracic penetration model of Lippmann and Chan (1979). Ogden (1992) noted that the standardization for aerosol cutpoint sizes and separation sharpness is still under debate across settings (ambient air, occupational) and across national and international governmental entities. As shown in Figure 4-2 (from Jensen and O'Brien, 1993), the international conventions for cutpoints have been roughly categorized as Respirable, Thoracic and Inhalable (previously, Inspirable). These cutpoints are related to the penetration, respectively, to the gas exchange region of the lung, the larynx, and the nasal/oral plane. The influences of physiological variables on these

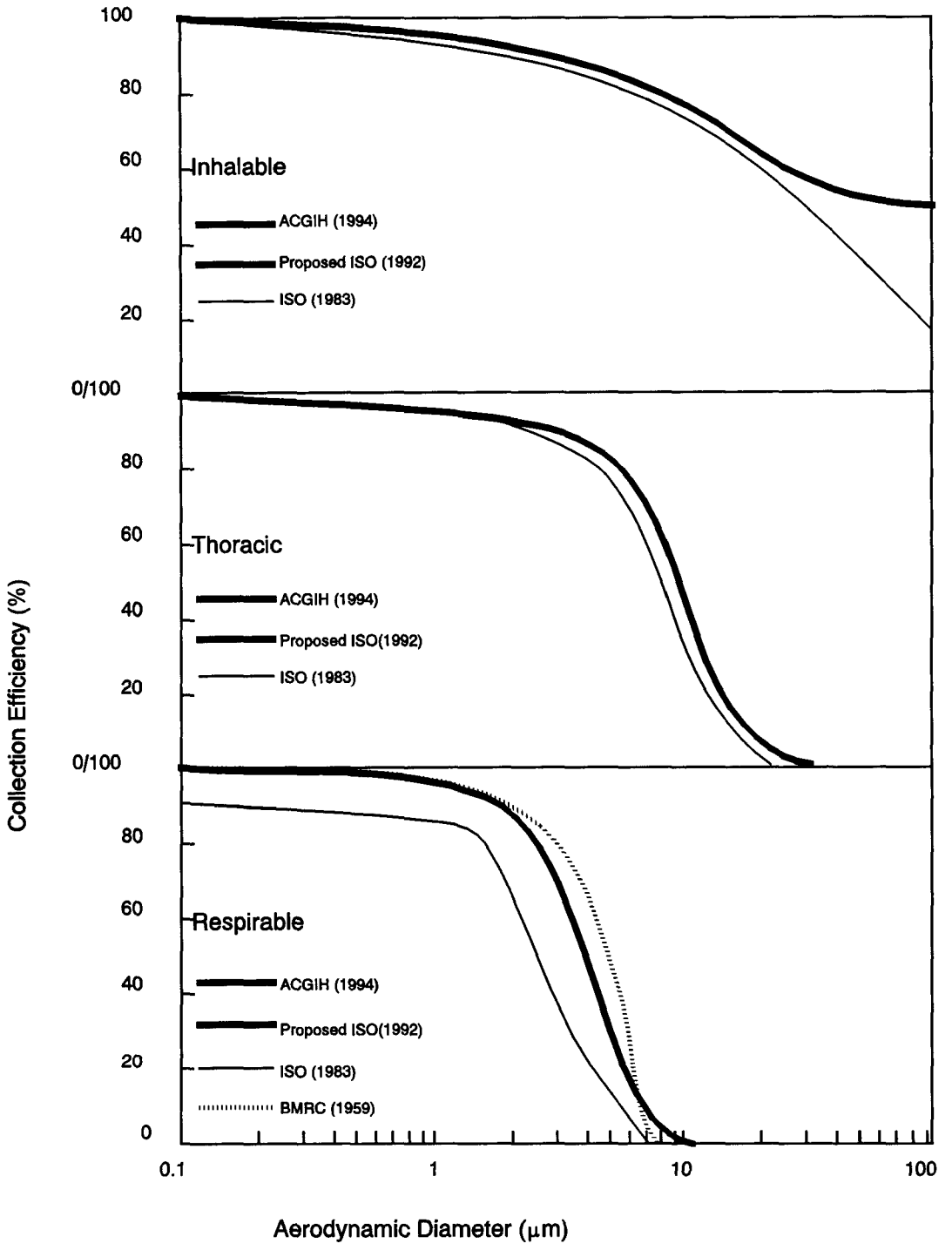

Figure 4-2. American Conference of Governmental Industrial Hygienists (ACGIH), British Medical Research Council (BMRC), and International Organization for Standardization (ISO) size-selective sampling criteria.

Source: Jensen and O'Brien (1993).

cutpoints are described by Soderholm (1989). The British Standard EN 481 (CEN [European Committee for Standardization], 1993) describes size fraction definitions for workplace aerosol sampling, and identifies inhalable "conventions" relative to thoracic, respirable, extra-thoracic and tracheobronchial penetration (but not necessarily deposition) in the respiratory system. They define a thoracic cumulative lognormal distribution with a median of 11.64 μm and a geometric standard deviation of 1.5, such that 50% of airborne particles with D_a = 10 μm are in the thoracic region. The American Conference of Governmental and Industrial Hygienists (ACGIH, 1994) also adopted these convention definitions. Owen et al. (1992) provides an extensive list of the outdoor and indoor particles by type and source category that are found in or overlap these ranges. Willeke et al. (1992) describe the sampling efficiencies and test procedures for bioaerosol monitors.

The concept of using an inlet or separator that has the same sampling (penetration) characteristics as portions of the respiratory system has been discussed by a number of researchers, including Marple and Rubow (1976), Lippmann and Chan (1979), Vincent and Mark (1981), Soderholm (1989), Lidén and Kenny (1991) and John and Wall (1983). They describe sampler design considerations for matching penetration models for respirable, thoracic and inhalable fractions that have been proposed by a number of governing bodies. Since all models proposed for the same fraction do not necessarily coincide, given the variability and differences in interpretation of respiratory system data, Soderholm (1989) proposed compromise conventions for each fraction. Watson et al. (1983), Wedding and Carney (1983), and van der Meulen (1986) mathematically evaluated the influences of inlet design parameters on collection performance relative to proposed sampling criteria. These analyses suggested that factors such as extremes in wind speed and coarse particle concentration could pose significant problems in meeting performance specifications.

An analysis of the human head as an aerosol sampler was discussed by Ogden and Birkett (1977), who noted that breathing is an anisokinetic sampling process. The concept of a "total inhalable" fraction that passes the oral and nasal entry planes was refined by Mark and Vincent (1986) with the development of a personal aerosol sampling inlet that mimicked this penetration as a function of aerodynamic size. The inlet was designated the IOM for the Institute for Occupational Medicine in Edinburgh, Scotland, where it was developed with the cutpoint as a function of wind speed and aerosol type shown in Figure 4-3. The total

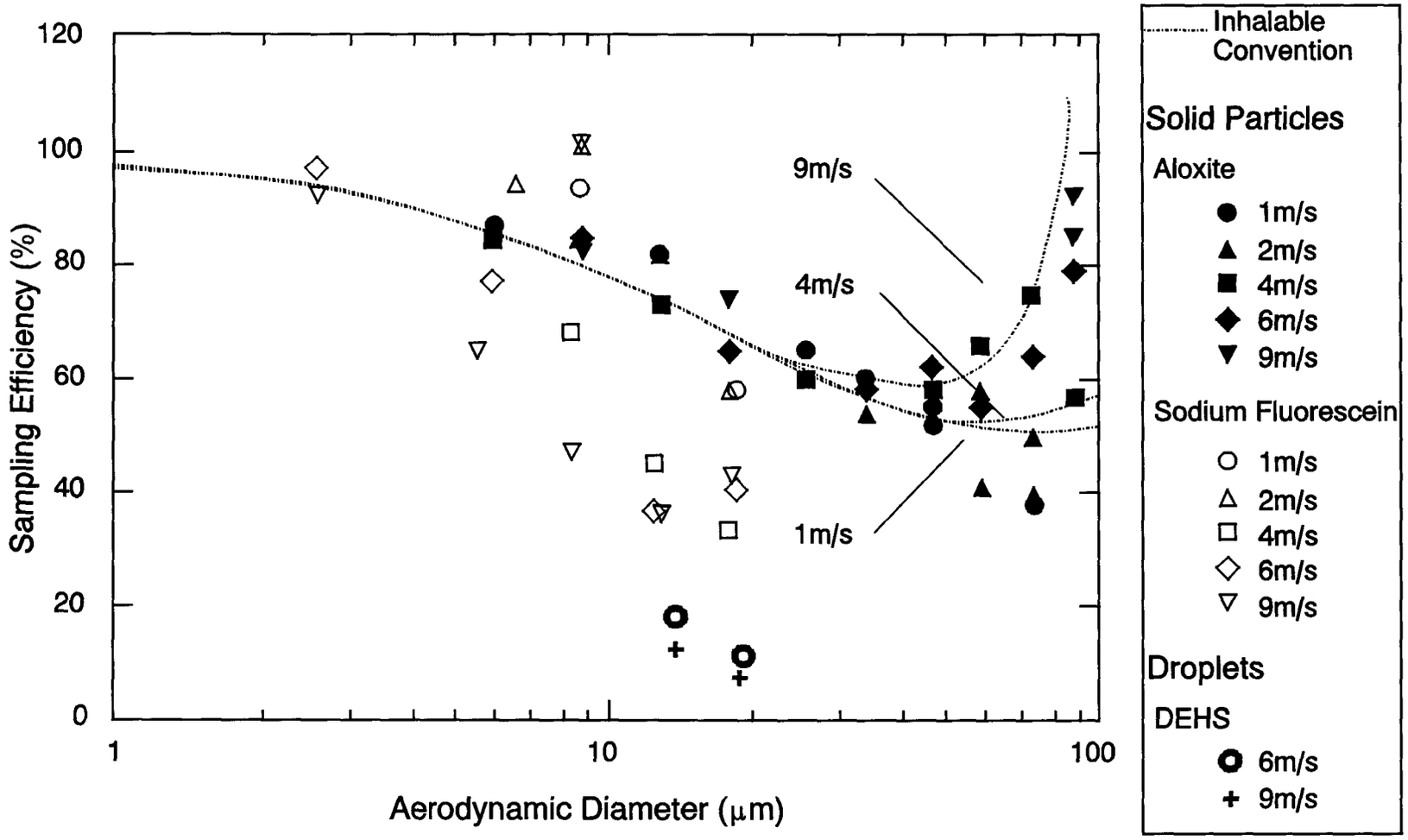

Figure 4-3. Sampling efficiency of IOM ambient inhalable aerosol sampler for three different types of test aerosol.

Source: Mark et al. (1992).

inhalable approach has been adopted by the International Standards Organization (ISO, 1993), European Committee for Standardization (CEN, 1993) and by the American Conference on Governmental and Industrial Hygienists (ACGIH, 1985; ACGIH, 1994) for workplace aerosol sampling. The ACGIH (1985) reference provides a detailed rationale for the selection of various cut sizes. The total inhalable fraction using the IOM inlet was selected for a total human exposure study (Pellizzari et al., 1995) to provide the total body burden for metals (lead and arsenic) by the air exposure route.

Similar thoracic penetration conventions have been adopted by ISO, CEN, ACGIH and EPA, each with D_{50} values of 10.0 μm (ISO, 1993; CEN, 1993; ACGIH, 1994; and U.S. EPA, 1987). The EPA definition was based primarily on the data of Chan and Lippmann (1980). The exact shapes of each efficiency curve were mathematically defined by Soderholm (1989) and are slightly different for each convention.

The respirable conventions have had D_{50} values ranging from 3.5 to 5.0 μm, but a compromise convention has been accepted internationally by several organizations. It has a D_{50} of 4.0 μm (Soderholm, 1989). ISO (1993) calls this the "healthy adult respirable convention". Lidén and Kenny (1992) discuss the performance of currently available respirable samplers. EPA's emphasis on the 2.5 μm cutpoint was more closely associated with separating the fine and coarse atmospheric aerosol modes, rather than mimicking a respiratory deposition convention. The exact location of this minimum in the atmospheric size distribution is currently under debate. It is noteworthy that ISO (1993) defines a "high risk" respirable convention which is claimed to relate to the deposition of particles in the lungs of children and adults with certain lung diseases. The respirable "high risk" convention has a D_{50} of 2.4 μm, so it could be identified closely with the EPA samplers having a cutpoint of 2.5 μm.

The PM_{10} size fraction has become nearly universal for ambient air sampling in the U.S., with the implementation of the 1987 standard (U.S. Environmental Protection Agency, 1987). The setting of performance specifications, even with their limitations, has provided a more consistent PM_{10} data base, with better definition of the data quality. As additional information becomes available on the sources of biases in aerosol collection methodologies, further characterizations of older methods may be needed to better define the quality of collected data. Factors that affect bias, and especially representativeness, should be

identified and their influences determined as a function of particle size. As examples, Appel et al. (1984) studied gas/particle and particle/substrate interactions for sulfates and nitrates, volatilization losses of nitrates were reported by Zhang and McMurry (1992), while losses for organics were reported by Eatough et al. (1993). Because of the prevalence of these chemical classes in the fine fraction, the effect of the losses on larger fractions (e.g., PM_{10}, TSP) would be proportionately smaller and can now be estimated. The losses of larger particles through aerosol inlet sampling lines (Anand et al., 1992) has a substantial influence on PM_{10} coarse fraction samples. This was demonstrated for the British smoke shade sampler inlet line by McFarland et al. (1982). Inlet losses would be expected to play only a minor role in sampling the fine particle fraction (<2.5 μm). Biases in concentration for samplers with large particle cutpoints are exacerbated by the large amount of mass present near the cutpoints and the steep slope of mass versus aerodynamic size. Thus, small changes in cutpoint can give significant and hard-to-predict mass biases.

4.2.2.2 Total Suspended Particulates

The TSP high volume sampler has remained essentially unchanged since the sampler's identification as a reference ambient sampling device in 1971 (Federal Register, 1971). The sampling performance (e.g., wind speed and direction sensitivity) was described in detail in the 1982 Criteria Document, and the TSP sampler was shown by McFarland and Ortiz (1979) to collect particles with aerodynamic diameters exceeding 40 μm. More importantly, its particle collection characteristics were shown to be significantly sensitive to wind speed (2 to 24 km/h) and wind direction. Only minor technical updates have been incorporated in commercially available units, such as in the types of available sequence and elapsed timers (mechanical, electronic) and in the types of flow controllers (mass flow, volumetric). Also, cassettes are now available that protect the fragile glass or quartz fiber filters during handling and transport. Size fractionating inlets for smaller size cutpoints (e.g., 2.5, 6.0 and 10.0 μm) and cascade impactors have been developed. Similar to the Pb strategy of using the TSP high volume sampler to collect a "total" sample, asbestos sampling utilizes an aerosol inlet that attempts to collect a "total" sample, by using an open-faced filter holder with a conductive inlet cowling. Baron (1993) discusses the potential anisokinetic problems

that can occur with such a simple inlet, but notes that the small Stokes number for typical asbestos fibers provides efficiencies close to 100%.

4.2.2.3 Total Inhalable Particles

The toxicity of contaminants such as lead poses health concerns as total body burdens, suggesting that penetration of all aerosols inhaled into the nose and mouth must be considered, rather than just thoracic penetration. The TSP sampler for atmospheric lead is thought (Federal Register, 1978) to more closely capture this larger size fraction than would a PM_{10} counterpart, but was not specifically designed to mimic inhalability. The ISO "inhalable" draft sampling convention (ISO, 1993) is intended to apply to such situations, defining collection of all particles passing the oral/nasal entry planes. The total inhalable cutpoint is currently available only in a personal sampler version. Mark and Vincent (1986) described the development of an inhalable particle inlet (designated as the IOM) meeting the ISO (1992), CEN (1993) and ACGIH (1994) conventions for inspirable dust. This inlet was improved by Upton et al. (1992) and tested by Mark et al. (1992) and shown to satisfy the ACGIH criteria for wind speeds of 0.5 and 1.0 m/s.

4.2.2.4 PM_{10}

The penetration of ambient aerosols through a size-fractionating inlet to the collection substrate must be characterized over the ranges of operating conditions (meteorology and aerosol types) that may be encountered. The range of conditions currently required by EPA PM_{10} performance specifications was given in U.S. Environmental Protection Agency (1987). Ranade et al. (1990) and John and Wall (1983) described the required testing, which specifies a controlled flow wind tunnel, monodispersed fluorescently-tagged wet and dry aerosols, and an isokinetic nozzle aerosol sampling reference to determine aerodynamic penetration through candidate PM_{10} inlets.

Marple and Rubow (1976) placed inertial impactors on the inlet of an optical particle counter to provide an aerodynamic calibration of the optical readout for non-ideal particles. Buettner (1990) noted that an aerodynamically calibrated optical particle counter could in turn be used to test the sampling performance of other devices only if the particle shape and refractive index of the test aerosol were consistent between calibrations. Maynard (1993)

used this approach to determine the penetration of a respirable cyclone to polydisperse glass micro-spheres, using the TSI, Inc. Aerodynamic Particle Sizer (APS). John and Wall (1983) noted that inaccurate inlet sizing results may be obtained using poly-disperse AC test dust, as the result of agglomeration. Kenny and Lidén (1991) used the APS to characterize personal sampler inlets and observed that, on theoretical grounds, calm air sampling would be expected to provide unity aspiration efficiencies for particles below about 8 μm. Tufto and Willeke (1982) used an optical particle counter (OPC) to monitor monodisperse aerosols in a wind tunnel setting to determine the performance of aerosol sampling inlets relative to an isokinetic nozzle. Yamada (1983) proposed using electron microscopy to determine the size distributions of polydispersed particles using manual counting techniques before and after a candidate aerosol separator. Penetration data from this technique were found to be significantly less precise and more difficult to interpret compared with data for the same separators using fluorometric methods.

The aerosol cutpoint performance of two PM_{10} samplers that have met the EPA performance specifications is illustrated (see Figure 4-4) by the data for the Andersen 321A and Wedding IP_{10} high volume sampler inlets at 8 km/h from Ranade et al. (1990). The data show that the cutpoint requirements, defined as a D_{50} of 10.0 μm $\pm$ 0.5 μm and mimicking a modeled cutpoint sharpness (σ_g), were met for each of the tested wind speeds. These performance results were verified by repeating the tests in wind tunnels located at two other research facilities. A diagram (U.S. Environmental Protection Agency, 1992) of the two-stage Sierra-Andersen PM_{10} high volume sampler inlet with a design flowrate of 1.13 m^3/min is shown in Figure 4-5. The buffer chamber of this inlet serves to dampen the particle-laden air stream passing through two sets of acceleration nozzles, which deposit particles larger than PM_{10} on internal collection surfaces. The PM_{10} fraction is typically collected by a glass fiber filter. An oiled impaction shim was incorporated into the first stage fractionator of the 321A to minimize reentrainment of deposited particles during field sampling. This modified version (Sierra-Andersen 321B) was designated as an EPA reference method for PM_{10} in 1987. A subsequent single-stage fractionator (Sierra-Andersen 1200) was developed[5] and designated as an EPA reference method, with a D_{50} of 9.5 μm and a hinged design to facilitate cleaning and oiling of the oiled impaction shim.

---

[5]Graseby-Andersen, Inc., Atlanta, GA.

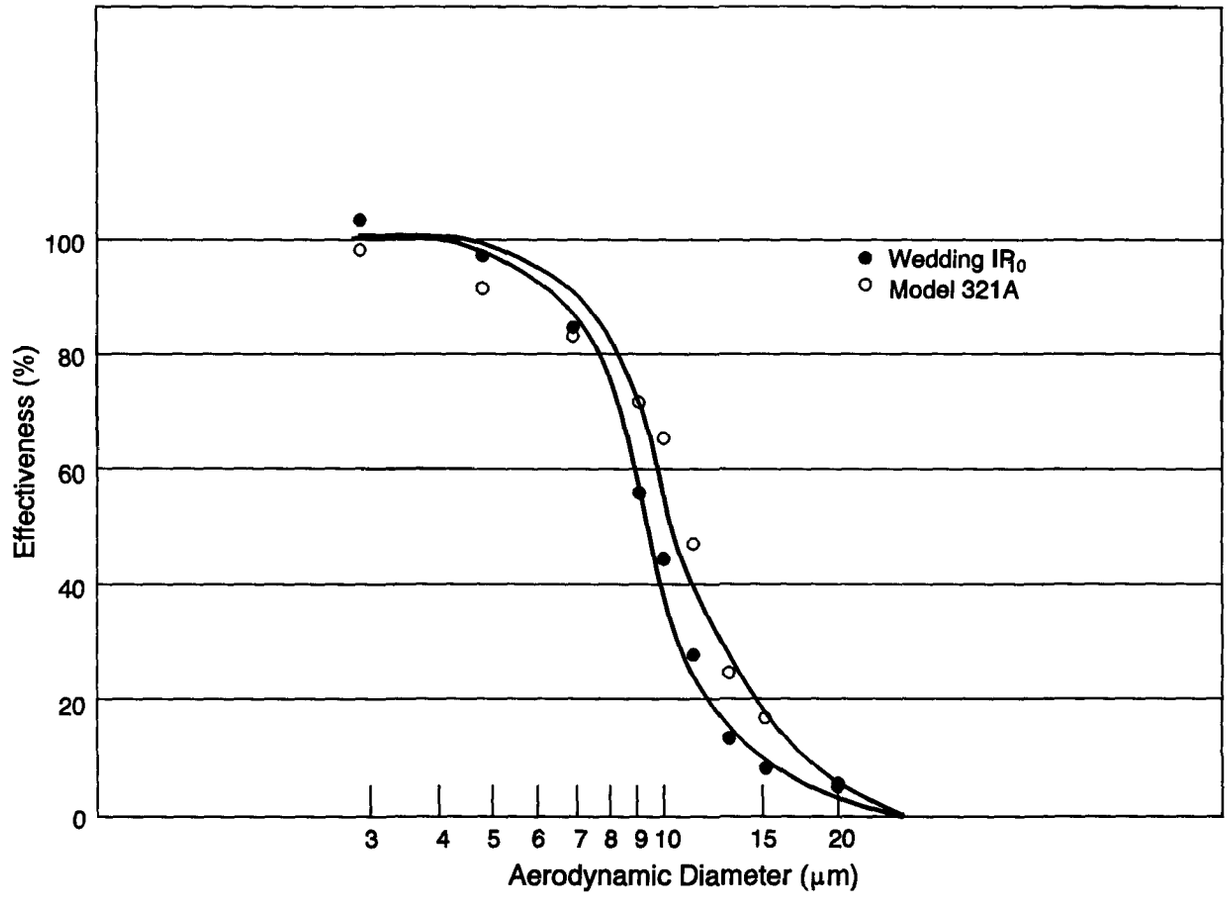

Figure 4-4. Liquid particle sampling effectiveness curves with solid particle points superimposed for the Wedding IP_{10} (•) and the Andersen Samplers Model 321A inlets at 8 km/h.

Source: U.S. Environmental Protection Agency (1992).

A diagram of the cyclone-based Wedding[6] PM_{10} high volume sampler inlet (U.S. Environmental Protection Agency, 1990) with a design flowrate of 1.13 m^3/min is shown in Figure 4-6. This inlet uses an omni-directional cyclone to accelerate the particle-laden air stream to deposit particles larger than PM_{10} on an oiled collection surface. Two additional turns are made to alter the flow into a downward trajectory toward the collection filter. A brush is used to clean the deposited aerosol from the absorber surface through an access port. This inlet was designated as an EPA reference method for PM_{10} in 1987.

[6]Wedding and Associates, Fort Collins, CO.

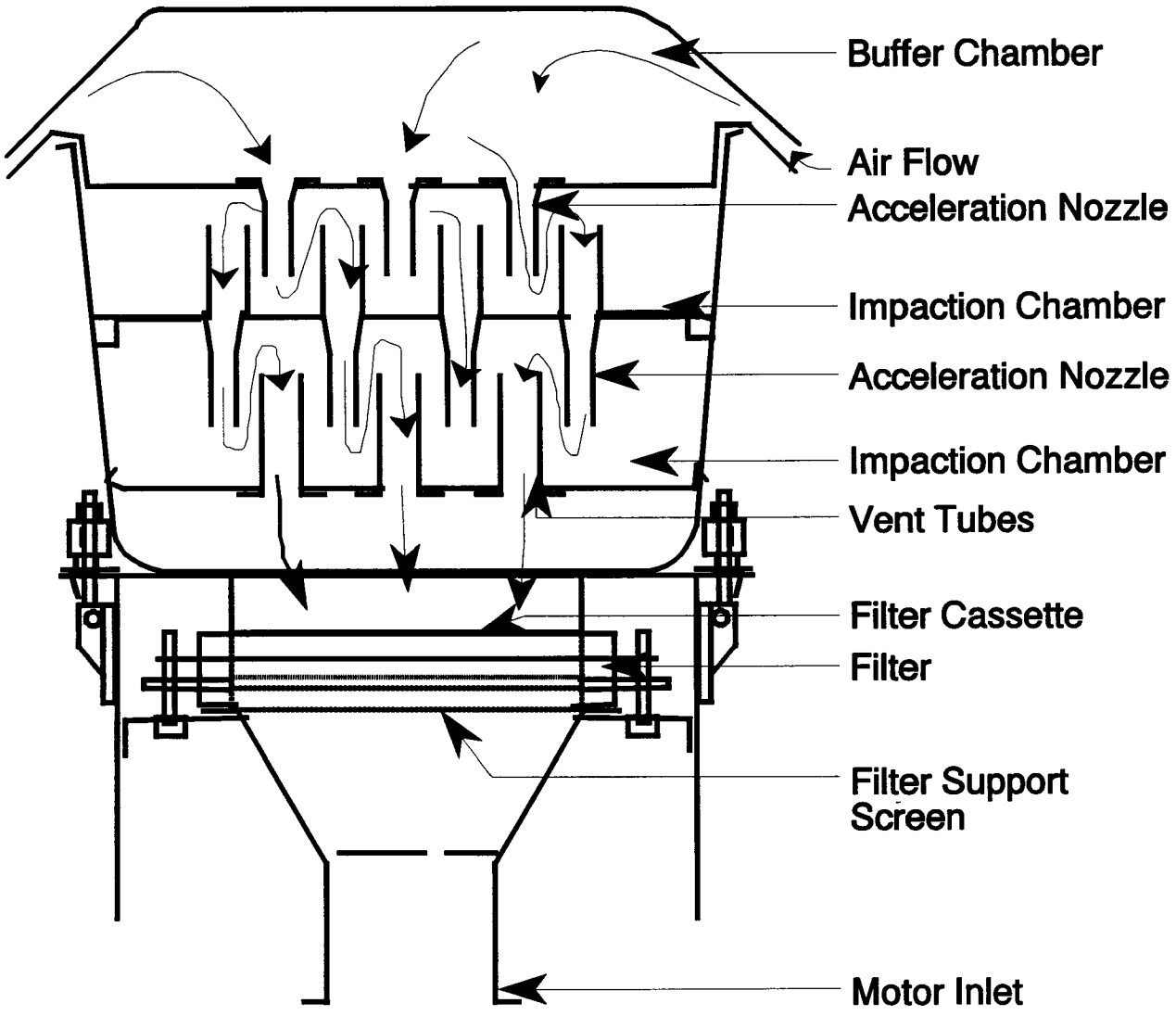

Figure 4-5. Two-stage Sierra Andersen PM_{10} sampler.

Source: U.S. Environmental Protection Agency (1992).

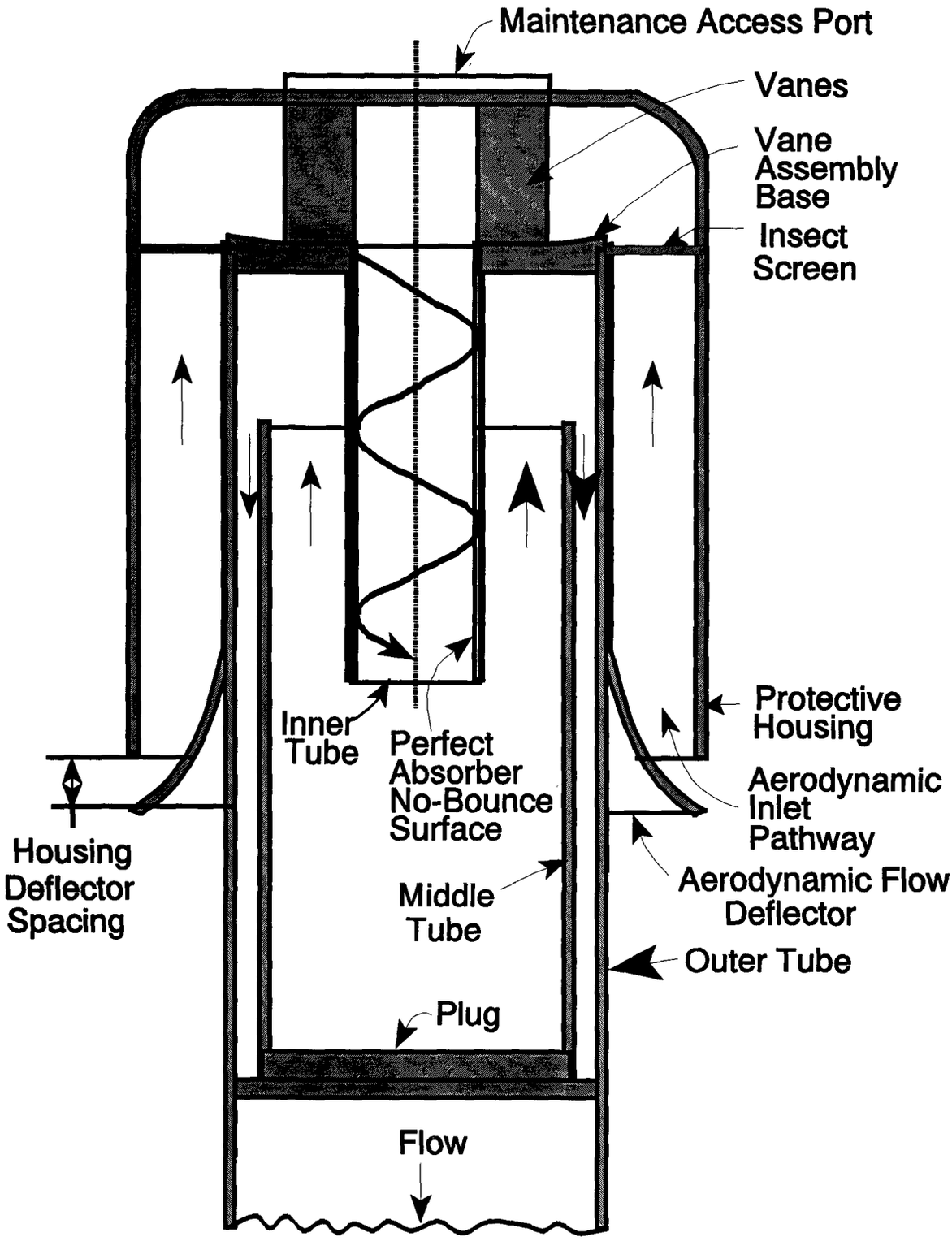

Figure 4-6. Sampling characteristics of two-stage size-selective inlet for liquid aerosols.

Source: U.S. Environmental Protection Agency (1992).

The aerosol collection performances for 16.67 lpm PM_{10} inlets for the dichotomous sampler are described by Wedding et al. (1982) and McFarland and Ortiz (1984) and are illustrated by the penetration data in Figure 4-7. The variability of the performance as a function of wind speed for the Andersen 321A PM_{10} inlet is shown in Figure 4-8 from data by McFarland et al. (1984). This is a dramatic improvement over the variability shown by the TSP high volume sampler (McFarland and Ortiz, 1979) for the same wind speed range. An attempt to simplify the complexity and improve the availability of wind tunnels to test PM_{10} inlets was addressed by Teague et al. (1992), who describe a compact tunnel 6 m long by 1.2 m high that is capable of testing inlets against the EPA PM_{10} specifications.

Watson and Chow (1993) noted that the EPA PM_{10} performance specifications allowed a tolerance range around the D_{50} that permitted inlets to be undesirably "fine tuned" to provide a cutpoint on the lower or upper end of the range. Since a significant amount of mass in the atmospheric aerosol may be associated with particles in the allowable tolerance range, a "reduction" in reported concentrations could be achieved by simply using a lower (e.g., 9.6 μm) cutpoint inlet that is still within the acceptable D_{50} range. The biases between acceptable samplers have been apparent in the data from field aerosol comparison studies (e.g., Rodes et al., 1985; Purdue et al., 1986; Thanukos et al., 1992). Most of the reported biases between samplers were less than 10%, although some differences greater than 30% were reported. The data suggested that the collection efficiency of the high volume sampler PM_{10} inlets based on cyclonic separation (Wedding, 1985) were consistently lower, while those based on low velocity impaction (McFarland et al., 1984) were consistently higher. Sweitzer (1985) reported results of a field comparison of these two high volume sampler types at an industrial location and reported average biases of 15%. It was noted that this amount of bias was unacceptable for compliance monitoring and more stringent performance requirements should be used. Rodes et al. (1985) observed that the PM_{10} concentration data from the dichotomous sampler (regardless of the inlet design) gave the most predictable results.

Wang and John (1988) were critical of the EPA PM_{10} performance specification on allowable particle bounce (U.S. Environmental Protection Agency, 1987), stating that the criteria can lead to a 30% overestimation of mass under worst-case conditions. In a related paper, John et al. (1991) reported that although reentrainment by air flow alone of particles

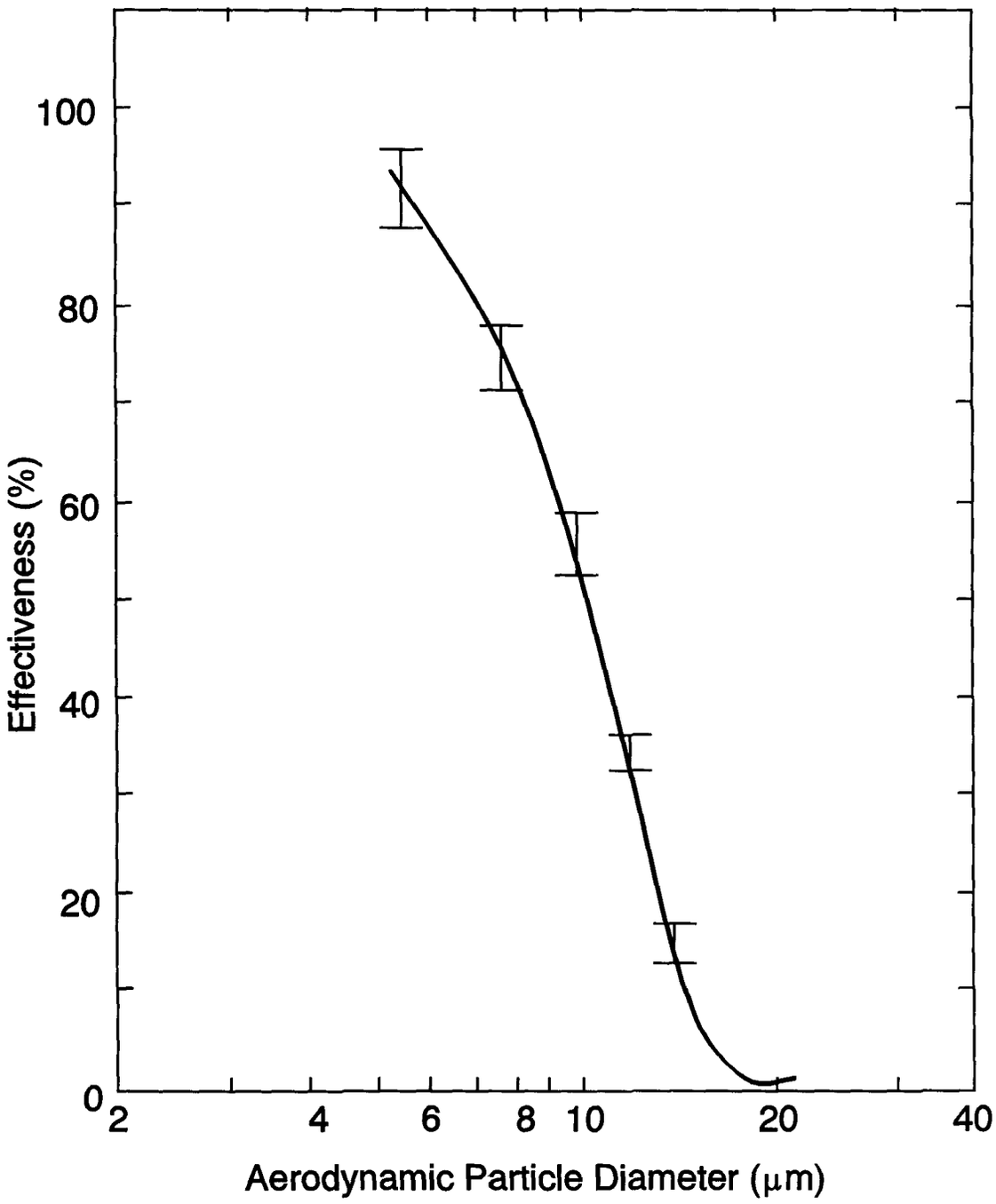

Figure 4-7. Penetration of particles for 16.67 lpm dichotomous sampler PM_{10} inlets.

Source: McFarland et al. (1984).

deposited in an aerosol inlet is typically negligible, reentrainment caused from subsequent particle deagglomeration caused by "bombardment" can be substantial. John and Wang (1991) suggested that particle loading on oiled deposition surfaces can bias the collection

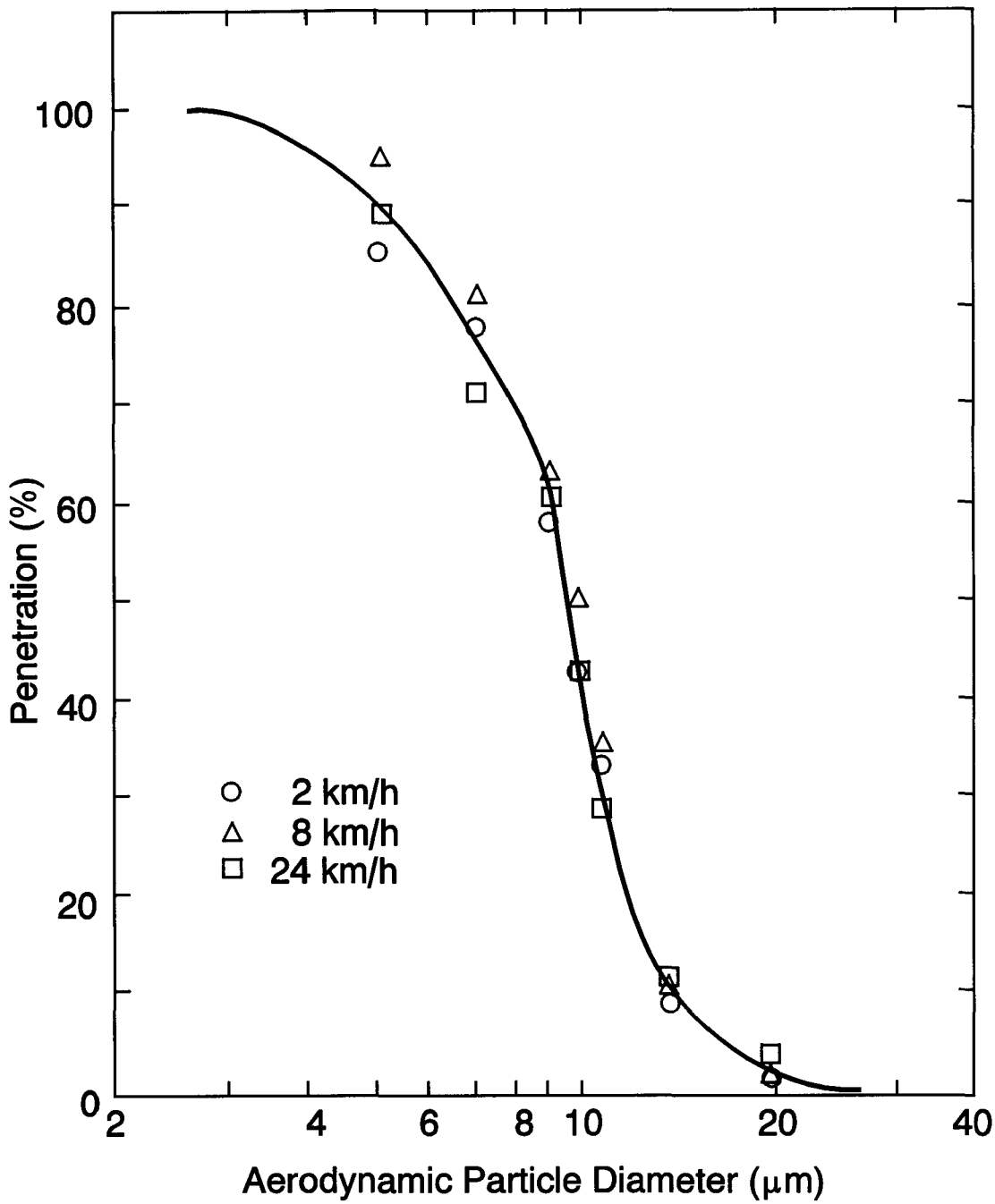

Figure 4-8. Collection performance variability illustrating the influence of wind speed for the Andersen 321A PM_{10} inlet.

Source: McFarland et al. (1984).

(2.2%/gram deposited) and strongly suggested that periodic cleaning and re-oiling should be required for PM_{10} inlets. Özkaynak et al. (1993) observed that immediately after inlets of

the Wedding (1985) design were cleaned, an underestimation (compared to the dichotomous sampler) occurred of 14%. This bias was followed by a steady "recovery" period of 2 days, until the expected performance returned. They also observed a strong influence of diurnal temperature change on the ratios of concentrations between the Wedding (1985) design samplers and other PM_{10} samplers. This influence could not be attributed to a physical phenomenon.

The EPA PM_{10} performance specification program should be considered successful (John and Wall, 1983) in providing consistent aerosol collection results during field sampling. As noted by Thanukos et al. (1992), the cases of greatest concern were those where the measured concentrations were near an exceedance level. Wiener et al. (1994) noted that EPA was scrutinizing the current performance of designated reference and equivalent sampling methods for PM_{10} in light of reassessment of the existing standard. A review of the current PM_{10} performance requirements and possible amendments of the existing specifications may be appropriate, given the information base now available.

Laboratory and field testing reported in the literature since 1987 suggest that the EPA PM_{10} Federal Reference Method (FRM) specifications and test requirements have not adequately controlled the differences observed in collocated ambient PM_{10} sampling. The most significant performance flaws have combined to produce excessive (up to 60%) mass concentration biases. These biases apparently resulted from the combined factors of (1) allowing a cutpoint tolerance (10 ± 0.5 μm), (2) an inadequate restriction placed on internal particle bounce, and (3) a degradation of particle separation performance as certain technology PM_{10} inlets became soiled. Particle bounce or soiling problems have not been reported for the PM_{10} inlets for the dichotomous sampler.

A cutpoint tolerance of ± 0.5 μm was required to account for expected differences between different wind tunnel laboratories testing the same hardware. The between-sampler bias from this tolerance limit alone is predictable and should provide PM_{10} concentration differences significantly less than $\pm 10\%$ in most cases. Particle bounce allowances are not as predictable, but design practices (primarily surface coatings with viscous oil, as suggested by John et al. [1991]) to minimize the penetration caused by bounce and resuspension have been shown to be very effective when properly serviced. The influences of internal surface soiling on PM_{10} inlet performance were not recognized when the FRM was established in

1987, but were found to have severe consequences for some separation technologies. The magnitude of biases from soiling is also not readily predicted, but can be ameliorated by not allowing the inlet to become excessively dirty during operation by routine cleaning prior to sampling.

Although the EPA test procedures have not been formally amended since 1987, the manufacturers of the designated PM_{10} reference methods (see section 4.2.6) have voluntarily modified their hardware designs and instruction procedures to accommodate particle bounce and soiling concerns. The SA-321b and SA-321c PM_{10} inlets were voluntarily withdrawn from the market by the vendor because of excessive biases attributed to particle bounce. The manufacturer now sells the SA1200 inlet which provides oiled surfaces to eliminate particle bounce and access screws to facilitate cleaning. The manufacturer also amended the instruction manuals to require a routine cleaning schedule. Similarly, the manufacturer for the Wedding PM_{10} inlet now provides an access port in the inlet and a cleaning procedure that can be applied prior to the collection of each sample. Based on our current understanding of the PM_{10} sampling process, it could be expected that sampling systems can be designed and concentration measurements made that are within 10% of the true concentrations.

4.2.3 Fine Particle Separators

4.2.3.1 Cutpoint Considerations

Although a particle separation at 2.5 μm has been utilized by the dichotomous sampler for a number of years, the 1987 standard reassessment (U.S. Environmental Protection Agency, 1987) did not specifically require routine monitoring for fine particles. It has become apparent (see Chapters 8 and 12) that certain health and ecological responses are most strongly correlated with fine particles, significantly smaller than 10 μm, and their related chemistry. Since the mass of a particle is proportional to the cube of its diameter, larger particles (especially above 10 μm) can totally dominate the mass of PM_{10} and TSP samples. The 2.5 μm cutpoint generally occurs near a minimum in the mass distribution, minimizing mass concentration differences between samplers with cutpoint biases. The development of control strategies based on mass concentrations from a smaller cutpoint

standard must be carefully constructed, especially if large particle interference problems (e.g., particle bounce) cannot be appropriately minimized.

Practical considerations would be the time and expense required to develop separators with 1.0 μm cutpoints that meet required specifications, conduct validation testing, and retrofit existing samplers. A virtual impaction "trichotomous" sample was described by Marple and Olson (1995) that uses a PM_{10} inlet and separators for both 2.5 and 1.0 μm cutpoints. They also noted that technology was not a limiting factor in providing a fine particle separator. Given the body of data available at 2.5 μm, a focused effort may prove practical that defines the characteristics of the particle mass and chemistry between 1.0 and 2.5 μm. This would add to the technical knowledge base, allow interpretive corrections between cutpoints to be made, and permit continued sampling at 2.5 μm with a minimum of additional resources.

4.2.3.2 Virtual Impactors

The dichotomous sampler utilizes virtual impaction to separate the fine (<2.5 μm) and coarse (2.5 to 10 μm) fractions into two separate flowstreams (see, for example, Novick and Alvarez, 1987) for collection on filters. The calibration of a nominal 2.5 μm impactor, including wall loss data, is shown in Figure 4-9 (from Loo and Cork, 1988). The current separator design was shown to provide a relatively sharp cutpoint with minimal internal losses. A virtual impactor has been designed with a 1.0 μm cutpoint (Marple et al., 1989), and for cutpoints as small as 0.12 μm (Sioutas et al., 1994). After a cross-channel correction factor for the coarse mode is applied, the mass concentrations of each fraction and the total mass (using a PM_{10} inlet) can be determined gravimetrically. An inherent consideration with virtual separation is contamination of the coarse fraction by a portion of the fine fraction, equivalent to the ratio of the coarse channel flow to the total flow (typically 10%). Although a straightforward mathematical correction can account for the particle mass between channels, this can influence subsequent chemical and physical characterizations, if significant differences exist between the chemistry of each fraction (e.g., acidic fine fraction and basic coarse fraction). Stevens et al. (1993) utilized this limited addition of fine particles to the coarse fraction to advantage in the SEM analysis of samples collected on Nuclepore

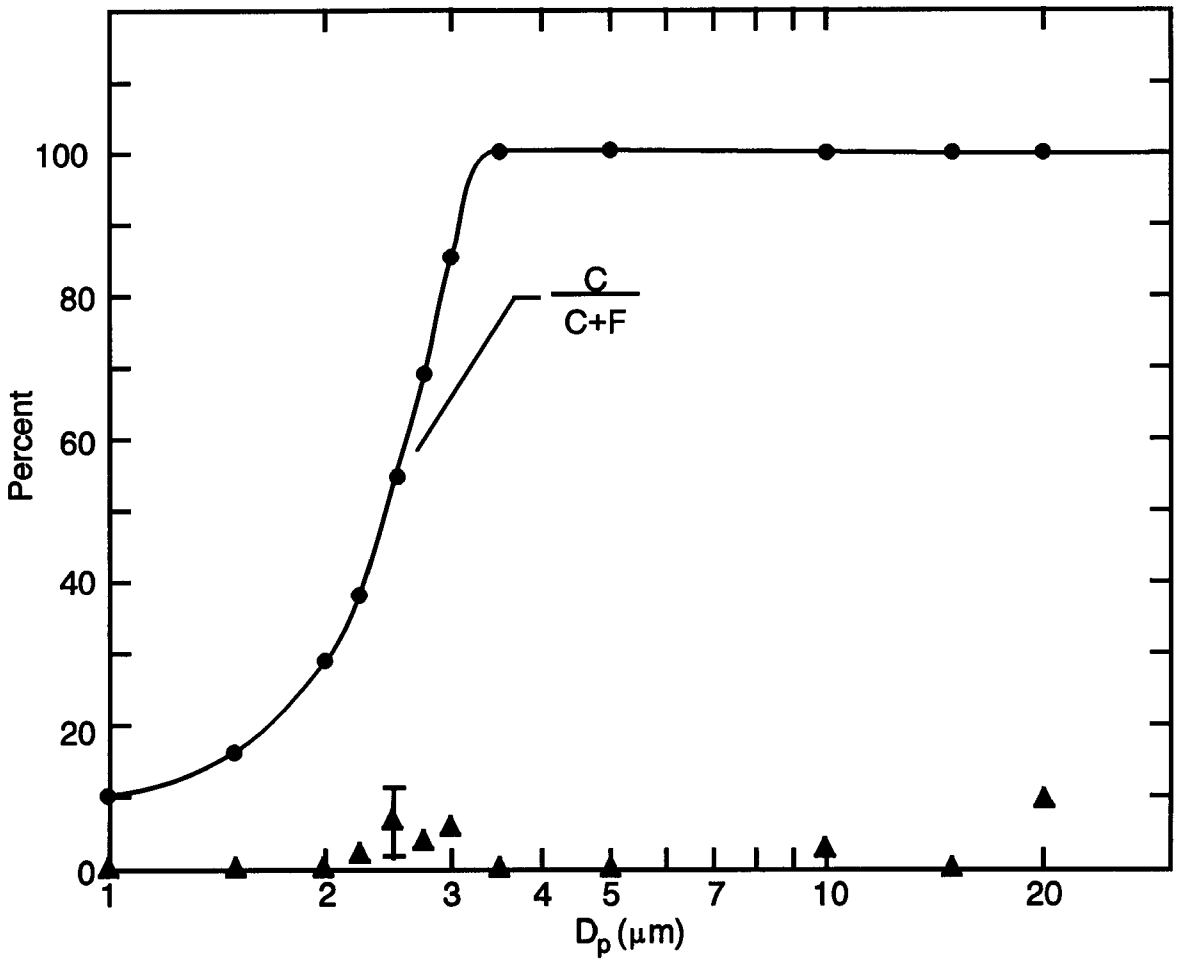

Figure 4-9. Aerosol separation and internal losses for a 2.5-μm dichotomous sampler virtual impactor.

Source: Loo and Cork (1988).

filters. Keeler et al. (1988) showed that the growth of fine aerosols at elevated relative humidities can significantly alter the ratio of fine to coarse collection for the dichotomous sampler. During early morning periods when the humidity approached 100%, an apparent loss of up to 60% of the fine mass (to the coarse channel) was observed. Keeler et al. (1988) concluded that analyzing only the fine fraction of the measured aerosol may not be appropriate, especially for short integration intervals.

A high volume (1.13 m^3/min) virtual impactor assembly was developed by Marple, et al. (1990) that can be placed on an existing high volume sampler to permit larger total collections than the dichotomous sampler for chemical speciation by size fraction.

By placing a number of virtual impactors in parallel, a separation can be achieved at higher flows, while reducing the total pressure drop. Marple et al. (1993) provide a list of commercially available virtual impactors by flowrate and available cutpoints. They also note that virtual separators inherently concentrate the particles in the coarse fraction (typically by a factor of 10), making them useful as pre-concentrators for sensors with marginal sensitivities. John et al. (1983) found that an oiled Nuclepore filter with a nominal 8 μm porosity could provide a D_{50} cutpoint of 2.5 μm, similar to that of a virtual impactor, if operated at the appropriate face velocity and for a sampling period short enough to minimize overloading.

4.2.3.3 Cyclones

Cyclones have been used as aerosol separators in personal exposure sampling in occupational settings for many years. Lippmann and Chan (1979) summarized the cyclones for sampling aerosol sizes below 10 μm and noted that the aerosol penetration through a cyclone can be designed to closely mimic respiratory deposition. An intercomparison of three cyclone-based personal exposure samplers under occupational conditions (concentrations typically > 1 mg/m^3) was described by Groves et al. (1994). They reported that even though the cyclones were reportedly designed to mimic similar respirable conventions, biases as large as a factor of two were noted, possibly attributable to overloading problems. Marple et al. (1993) provided a list of commercially available air sampling cyclones, by sampling flowrate and D_{50} range. Cyclones can be used individually or in a cascade arrangement to provide a size distribution. Bartley and Breuer (1982) describe methods to reduce biases when using a 10 mm (diameter) personal air sampling cyclone, especially as related to cutpoint shifts caused by flowrate changes. Saltzman (1984) provided a similar analysis for atmospheric sampling cyclones. Sass-Kortsak et al. (1993) observed that substantial uniformity-of-deposition problems can occur on the filters downstream of personal sampling cyclones. Wedding and Weigand (1983) used a cyclone within a high volume aerosol inlet to provide a $PM_{6.0}$ cutpoint for ambient sampling that did not allow penetration of particles greater than 10.0 μm.

The simplicity of cyclones has prompted their use as inlets and subsequent separators in samplers designed to fractionate the aerosol sample for chemical analysis. The "Enhanced

Method" employed by EPA for sampling acidic aerosols uses a glass cyclone with a 2.5 μm cutpoint as the sampler inlet (U.S. EPA, 1992). The percent collection as a function of aerodynamic diameter is shown in Figure 4-10 (Winberry et al., 1993). The modest cutpoint sharpness exhibited by some cyclones should be considered when attempting to separate particle size fractions that may interact chemically. Hering et al. (1990) describe several validated aerosol systems for sampling carbonaceous particles that utilize cyclones with 2.5 μm cutpoints to sample the fine fraction on either Teflon or quartz substrates. Spagnolo and Paoletti (1994) describe a dual cyclone ambient aerosol sampler with a 15 μm inlet (described by Liu and Piu, 1981). This sampler was designed to collect a 20 to 15 μm fraction, a 20 to 4.0 μm fraction, and a 0 to 2.5 μm fraction. Malm et al. (1994) describe a sampling system with a PM_{10} inlet and three parallel channels following a 2.5 μm cutpoint cyclone that was used for the 40 site IMPROVE network. Over 120,000 fine particle filter substrates of Teflon®, nylon and quartz were collected for chemical analysis over a 6 year period.

4.2.3.4 Impactors

Impactors have been developed for a wide range of cutpoints and flowrates. In cascade arrangements (see Section 4.2.7.1.1) with a characterized inlet, impactors provide particle distribution information over a range of aerodynamic sizes. Impactors used as components of inlets or as in-line fractionators stop and retain the aerosol on a surface (e.g., oil-soaked, sintered metal or glass) that provides consistent performance (primarily minimal bounce) over the entire sampling interval. Recovery and analysis of the deposited particles in these situations are usually not considerations. Koutrakis et al. (1990) described the design of 2.1 μm cutpoint impactor for a single stage annular denuder system that exhibited internal losses of less than 3%. Marple (1978) described the use of multiple nozzle impactors in a single stage to emulate selected respiratory penetration curves.

Marple et al. (1993) noted that the three primary limitations of impactors are particle bounce, overloading of collection stages and interstage losses. Particles can bounce from a stage after impaction if the surface forces are not adequate for their retention. Wang and John (1988) described the effects of surface loading and relative humidity on particle bounce and growth, and they noted that if less than 6% of the impact area was covered by deposited

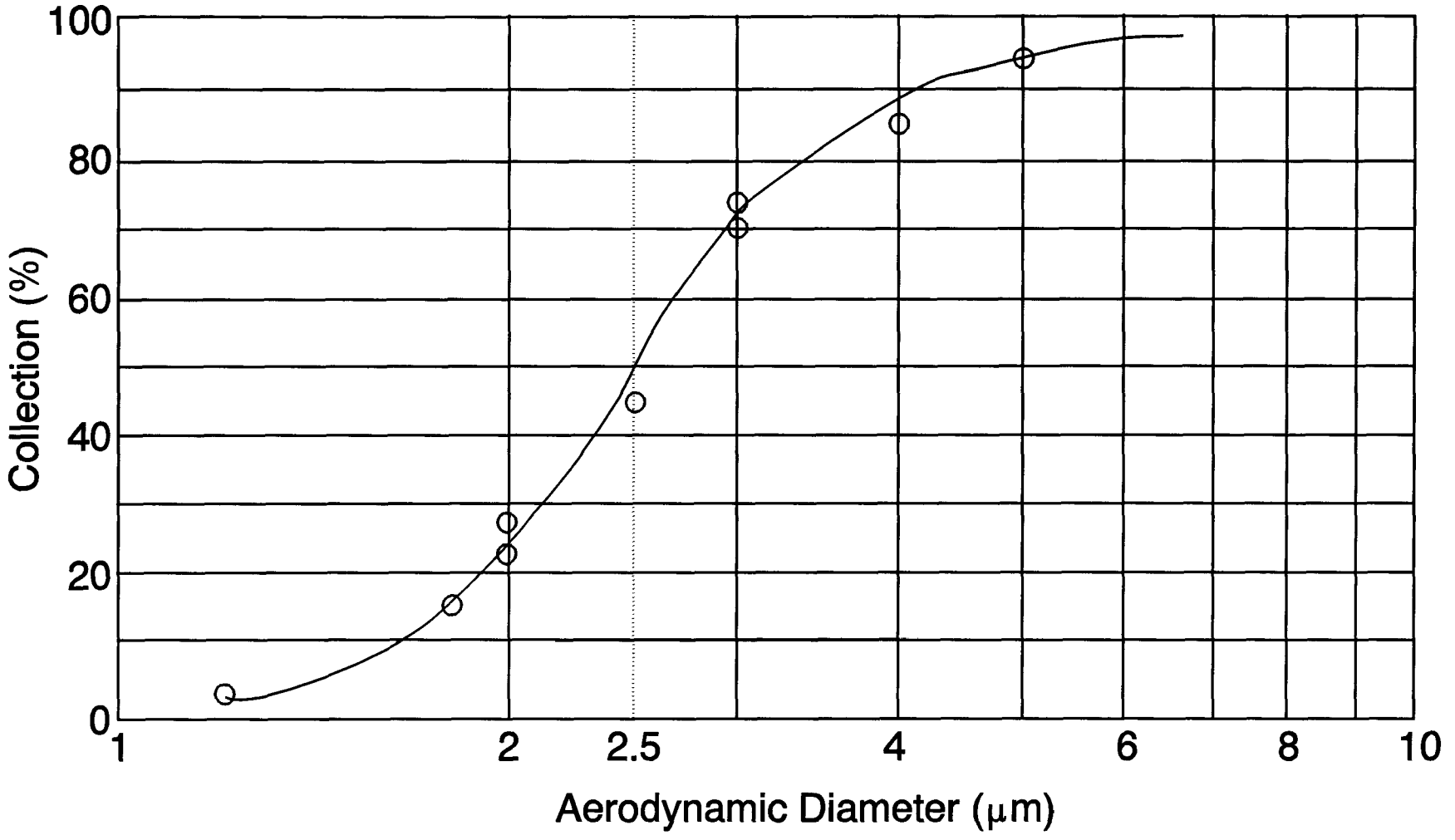

Figure 4-10. Percent collection as a function of aerodynamic diameter for the U.S. Environmental Protection Agency enhanced method glass cyclone.

Source: Winberry et al. (1993).

particles, particle-to-particle collisions (and bounce) could be neglected. They also showed that ammonium sulfate aerosol growth with increasing humidity resulted in a 25% shift in cutpoint as the relative humidity increased to 64%. Biswas et al. (1987) showed that, especially in low pressure zones, the relative humidity and temperature can change rapidly within a cascade impactor, potentially altering cutpoints and losses. Wang and John (1988) in subsequent work did not observe these shifts, noting that the transit time in a jet is only on the order of 10 μs. Turner and Hering (1987) noted that the stage substrate materials (Mylar®, stainless steel and glass) with the same grease (Vaseline®) could produce substantially different particle adhesion characteristics. Vanderpool et al. (1987) showed that using glass fiber filters as impactor surfaces can produce drastically reduced performance as compared to a greased substrate (see Figure 4-11). Markowski (1987) suggested that adding a duplicate (same cutpoint) serial impactor stage can permit reasonable bounce and re-entrainment corrections to be made.

4.2.4 Sampling Considerations

4.2.4.1 Siting Criteria

Selection of aerosol sampling locations is partially guided by siting criteria under the 1987 PM_{10} regulation (U.S. Environmental Protection Agency, 1987), which provided limited guidance for Pb and PM_{10} samplers. The details behind these guidelines for PM_{10} are provided in a guidance document (U.S. Environmental Protection Agency, 1987), which relates physical and chemical characteristics of aerosols to the spatial scales (regional, urban, neighborhood, middle and micro) required to define the influences of sources on various populations. Guidance was also provided on the influences of nearby point, line and area sources on sampling location as a general function of particle size. Only limited information was noted to be available on specific influences of local obstructions and topography (e.g., trees, buildings) on measured aerosol concentrations. The primary focus was establishment of the degree that a sampling location was representative of a specific scale.

The high purchase cost, and occasionally physical size, of aerosol samplers have restricted the number of sampling sites used in air monitoring studies. This may pose problems if the selected sites are not truly representative of the exposures for the populations at risk. To address the biases resulting from too few aerosol samplers in a field study, a

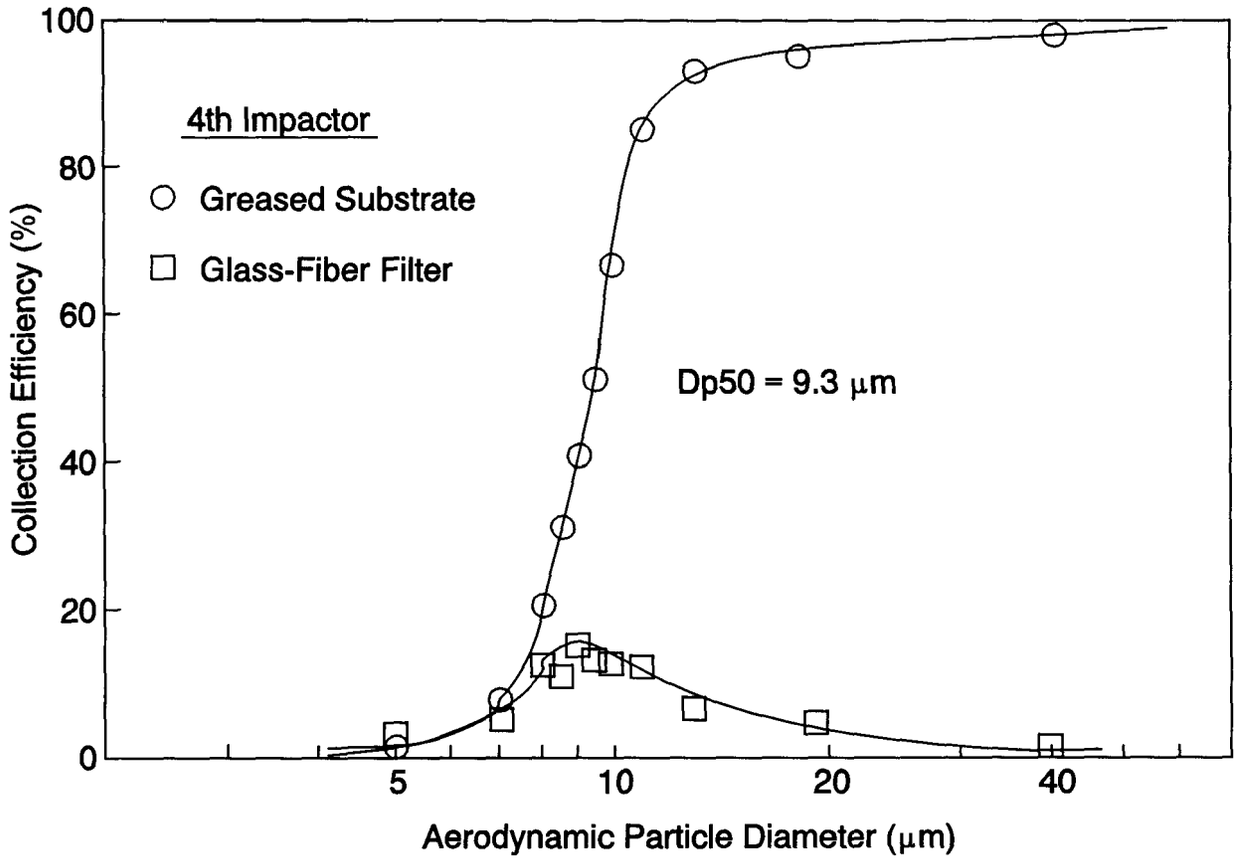

Figure 4-11. Performance of glass fiber filters compared to greased substrate.

Source: Vanderpool et al. (1987).

"saturation" sampler approach has been used, utilizing an inexpensive, miniature and battery-powered PM_{10} sampler that can be deployed at a large number of sites. Phillips et al. (1994) reported application of this approach, using 15 PM_{10} saturation samplers in conjunction with one dichotomous sampler to study the contribution of diesel emissions to total PM levels in Philadelphia. Although the mean for PM_{10} concentrations of the saturation samplers was essentially identical to that of the dichotomous sampler, the saturation data showed site-to-site mean differences of up to 30 $\mu g/m^3$.

4.2.4.2 Averaging Time/Sampling Frequency

The collection frequency for samples to support the EPA PM_{10} NAAQS has typically been on an every-6th-day schedule. Shaw et al. (1982) raised a statistically-based concern

that infrequent collection increases the coefficient of variation about the overall mean concentration value; that is, the variability of computed fine mass concentration means increased as the square root of the number of intervals between individual measurements. Symanski and Rappaport (1994), using time series analyses, described the influences of autocorrelation and non-stationary behavior in occupational settings on concentration distributions constructed from infrequent sampling. They recommended a random sampling design where a sufficient number of locations are sampled repeatedly over an adequate period of time to account for the full range of exposure possibilities. Hornung and Reed (1990) described a method of estimating non-detectable (or missing) values to lessen variance about the estimate of the geometric mean, by assuming that the concentration distribution is log-normal.

Insufficient sample collections can be remedied by more frequent operation of manual samplers. The recent PM_{10} equivalency designations (see section 4.2.5) of two beta gauge samplers and the TEOM sampler can provide the necessary information, with hourly rather than daily resolution. The initial cost of an automated sampler is typically 2-3 times that of a manual, single channel PM_{10} sampler, but can be offset by savings in operator labor costs. If inherent biases described in section 4.2.3.4 for the beta and TEOM samplers can be overcome (and they are field reliable), these approaches should prove very useful in routine regulatory and research monitoring studies. Potential also exists for the integrating nephelometer to be an acceptable exceedance monitor[7], using site specific calibrations relating the measured scattering coefficient, b_{sp}, to fine aerosol mass concentrations (e.g., Larson et al., 1992).

Another consideration for defining sampling intervals is the setting of start and stop clock times. Daily 24-h sampling is most often done from midnight-to-midnight, but occasionally from noon-to-noon to either reduce the number of samplers required or to reduce operator burden. Sampling locations with highly variable diurnal aerosol concentration patterns (e.g., from night time wood smoke influence or day time traffic dust), or marked differences between week days and weekend days may require special consideration. These influences can be especially significant for <24-h sampling periods.

---

[7]A Pollutant Standard Index (PSI) monitor used to estimate when a pre-determined exceedance level has been reached or exceeded, to potentially trigger the operation of an equivalent PM_{10} gravimetrically-based sampler.

4.2.4.3 Collection Substrates

The selection of a filtration substrate for integrated collection of particles must be made with some knowledge of the expected particle characteristics and a pre-determined analytical protocol. The expected sampled size distribution places a requirement on the porosity of the filter media to effectively trap a reasonably high percentage of the particles with a minimum of pressure drop. The most common filter types used in air sampling are fiber and membrane. Fiber filters tend to be less expensive than membrane filters, have low pressure drops, and have high efficiencies for all particle sizes. They are most commonly available in glass fiber, Teflon coated glass fiber and quartz materials. Membrane filters retain the particles on the surface for non-depth analyses (e.g., X-Ray Fluorescence), can have specific porosity's, and are available in a wide variety of materials. Teflon is a popular membrane material because of its inertness, but is 2 to 4 times as expensive as more common materials. Liu et al. (1978) summarize the effective penetration characteristics as a function of particle size and pressure drops for a wide variety of fiber and membrane filters. The selection of filter diameter for a given flowrate influences the face velocity and the loading capacity before the pressure drop becomes unacceptable. A 47mm filter provides a surface area that is 60% larger than that of a 37mm filter. Polycarbonate filters with well defined porosities (e.g., Nuclepore®) have been used in "stacked" arrangements as fine particle separators. John et al. (1983) describe using an 8 μm porosity filter in series with a back-up filter to effectively provide a 3.5 μm separation of fine and coarse particles in a small, inexpensive package. Samplers based on this principle were widely used in the early 1980's (Cahill et al., 1990) and their performance under field conditions was shown to be equivalent to later cyclone based $PM_{2.5}$ samplers in the IMPROVE network.

The reactivities of filter substrates with the aerosol have been reported extensively. A common problem with glass fiber filters used on high volume samplers is the basic pH of the glass material and its effective conversion of SO_2 to particulate sulfates (e.g., Pierson et al., 1976). Appel et al. (1984) also reported similar conversions of nitrogen oxides to particulate nitrates on glass fiber filters. Witz et al. (1990) reported losses of particulate nitrates, chlorides and ammonium (19, 51 and 65%, respectively) from quartz fiber filters during storage. No significant losses of sulfates were reported from quartz filters. Similarly, Zhang and McMurry (1992) reported the anomalous loss of fine particle nitrates

from Teflon filters and noted that predictive loss theories were insufficiently accurate to permit corrections. Lipfert (1994) also observed that nitrate artifacts on glass fiber filters were difficult to quantify on a routine basis. Measurements of particulate nitrate using nylon filters by the IMPROVE protocols show, however, that such effects are minor except in California (Malm et al., 1994). Eatough et al. (1993) found significant losses of particulate organic compounds on quartz filters due to volatilization, such that ambient concentrations of particulate carbon may be underestimated substantially. Lipfert (1994) investigated filter artifacts in a field study in New York and concluded that positive sulfate artifacts inflated PM_{10} values from glass fiber filters by 6 $\mu g/m^3$. It was noted that the combination of sulfate and nitrate artifacts on glass fiber filters may inflate TSP measurements by as much as 10 to 20 $\mu g/m^3$.

4.2.4.4 Chemical Speciation Sampling

The collection of aerosol samples for chemical speciation analysis adds another dimension to the complexity of the sampling protocol (also see Section 4.3). The simplest approach utilizes a characterized inlet or separator to define a size fraction, provides an aerosol collection substrate compatible with the analytical technique, and collects an adequate quantity of sample for analysis. This approach is applicable for relatively nonreactive and stable components such as heavy metals. An important consideration is the potential reactivity of the sampling substrate with either the collected aerosols or the gas phase. Appel et al. (1984) predicted effects of filter alkalinity on conversion of acid gases to sulfates and nitrates and provided an upper limit estimate for artifact sulfate formation (added mass) for TSP high volume sampling of 8-15 $\mu g/m^3$ for a 24-h sample.

Analyses for semi-volatile organics found in both the particle and vapor phases must be collected by adding a vapor trap (e.g., polyurethane foam plug) downstream of the sampling filter. Arey et al. (1987) noted that this arrangement of sequential sampling reservoirs may account for the total mass of organics, but not accurately describe their phase distribution in situ, due to "blow-off" from the filter during sampling. Van Vaeck et al. (1984) measured the volatilization "blow-off" losses of organic species from cascade impactor sampling to be up to 30%, while the loss of total mass was only 10%. McDow and Huntzicker (1990) characterized the face velocity dependence for organic carbon sampling and provided

correction models, based on adsorption losses to a backup filter. Turpin et al. (1994) examined organic aerosol sampling artifacts and highlighted the distinction between "organic carbon" and individual organic species. They observed that organic carbon sampled from the atmosphere is unlikely to attain equilibrium between that in the gas phase and that adsorbed on a quartz fiber back-up filter. They also noted that under typical sampling conditions, adsorption is the dominant artifact in the sampling of particulate organic carbon, and longer sampling periods reduce the percentage of collected material that is adsorbed vapor. It was recommended that collection of aerosols for carbon analyses be made on a pre-fired quartz filter, with estimates of the adsorption artifact made from a quartz filter placed behind a Teflon filter in a parallel sampler.

For more highly reactive and unstable species, the recognition of the in situ character of the aerosol in the air must be identified and preserved during all facets of the sampling process to provide a representative and accurate sample. Durham et al. (1978) described a denuder to remove sulfur dioxide while sampling for sub-micron aerosols. Spicer and Schumacher (1979) observed that many artifact reactions may occur if stripping of nitric acid, sulfuric acid and ammonia is not performed during speciated aerosol sampling. Appel et al. (1988a) described the various loss mechanisms that apply to the aerosol and vapor phases while sampling for nitric acid. They noted that residence time, surface material compositions, and conditioning prior to sampling were the predominant variables affecting transmission efficiency.

The determination of strong acidity for atmospheric aerosols (U.S. Environmental Protection Agency, 1992) describes an "enhanced" method that recognizes the inter-relationships between the vapor and aerosol phases for each constituent and the potential interferences. An inlet cyclone or impactor is used to provide a 2.5 μm cutpoint to exclude the higher pH aerosols found in the coarse fraction of PM_{10}. As shown in Figure 4-12, denuders are used in the flowstream which selectively remove gas phase components with minimal, characterized losses of aerosol. Ye et al. (1991) determined the aerosol losses through an 10 lpm annular denuder system as a function of particle size. They noted that total particle losses were less than a few percent whether the denuders were coated or uncoated. Also, using parallel annular denuders, Forrest et al. (1982) found aerosol losses of only 0.2 to 2.2% for 0.3 to 0.6 μm particles and 4 to 5% for 1 to 2 μm particles.

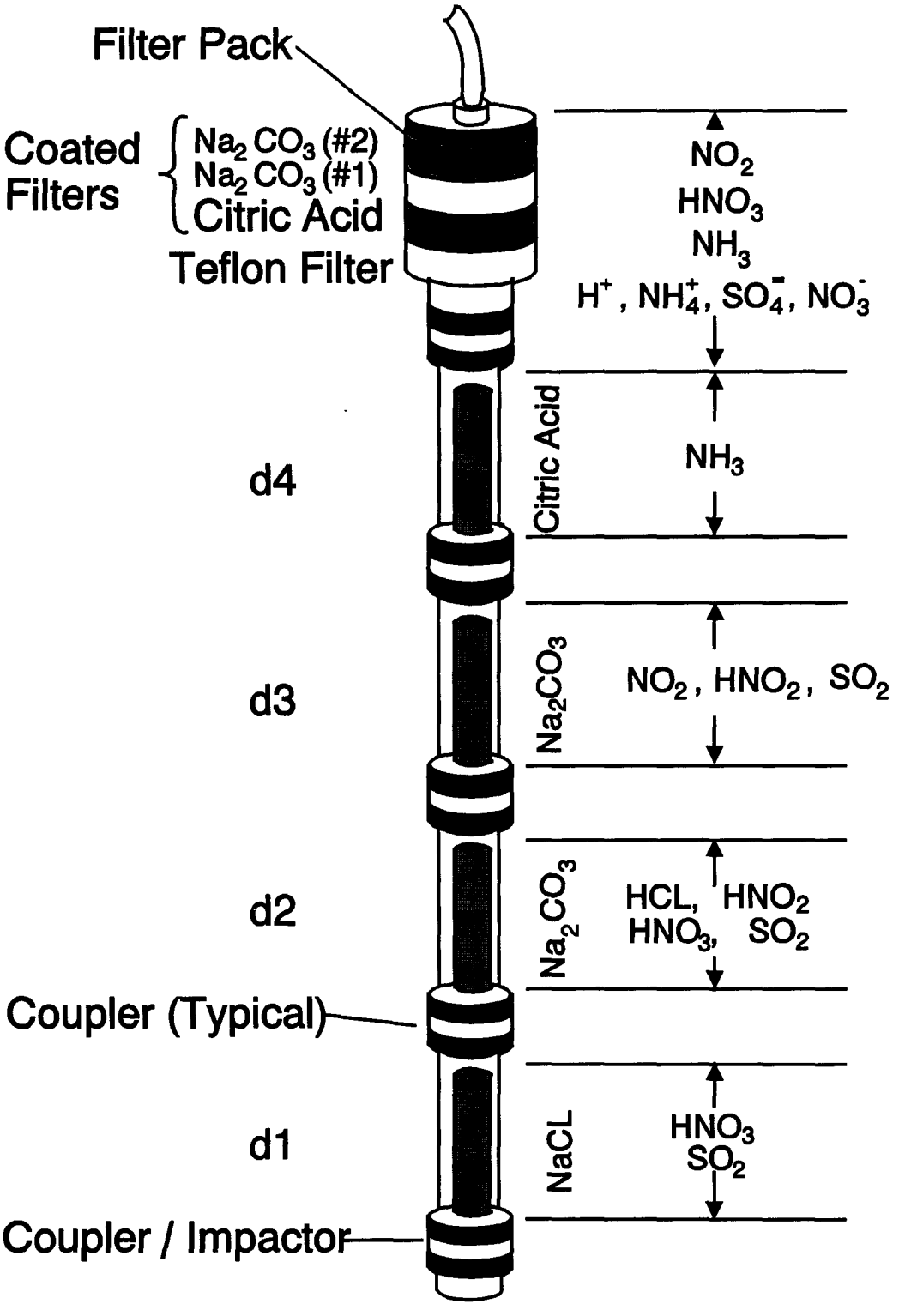

Figure 4-12. Schematic diagram of an annular denuder system.

Source: U.S. Environmental Protection Agency (1992).

Filter packs have been developed, consisting of a sandwich of filters and collection media of various types in series, to collect aerosols and selectively trap gases and aerosol volatilization products. Benner et al. (1991) described an annular denuder sampling system using Teflon and nylon filter packs and annular denuders to quantitatively collect the distributed ammonium nitrate, nitric acid and ammonia in the vapor and aerosol species. They observed that volatile nitrates were 71% $\pm$ 27% of the total nitrates during the day and 55% $\pm$ 30% at night in arid, southwestern U. S. locations. Masia et al. (1994) described the anomalous uptake of ammonia on the nylon filters, which were expected to collect only the gas phase nitric acid. Wang and John (1988) reported volatilization losses of ammonium nitrate in the Berner impactor of 7% under hot, dry (18% Rh) conditions.

Vossler et al. (1988) reported the results of improvements in an annular denuder system, including Teflon coating of the internal glass surfaces. They found an apparent particle bounce problem with the cyclone inlets (with or without Teflon coating) and proposed adding an additional in-line, greased impactor. John et al. (1988) found that anodized aluminum surfaces absorb nitric acid efficiently and irreversibly. Several method comparison studies have been reported for systems utilizing annular denuder/filter pack technologies, including Harrison and Kitto (1990), Sickles et al. (1990), and Benner et al. (1991).

4.2.4.5 Data Corrections/Analyses

Aerosol concentration data are reported in units of mass per volume (e.g., $\mu g/m^3$). The current EPA regulations for sampling TSP, PM_{10} and Pb require that sampler flowrates be controlled and the sampled volumes be standardized to 760 mm Hg and 25 °C. These requirements may pose problems in the interpretation of concentrations from aerosol samplers. Wedding (1985) notes that the flowrate through inertial impactors should be maintained at "local" temperatures and pressures to retain the separator's aerodynamic calibration. Mass flow controllers may significantly affect the separator flow velocity during large diurnal temperature changes, excessively biasing the resulting cutpoint diameter.

Subsequent correction of the sampled aerosol volume to "standard" conditions by mathematically compensating for average meteorological conditions may improperly report the aerosol concentration measurement. If the rationale for aerosol sampling was to mimic

respiratory penetration (which occurred at local conditions), a correction after-the-fact may not be appropriate. These corrections are typically small (less than a few percent) except in locations at higher altitudes and those with large diurnal or seasonal temperature changes. The basis for mandating flowrate controller performance for aerosol samplers is sound, but the subsequent requirements for concentration corrections for temperature and pressure are complex. Although the issue of sampled volume correction for local temperature and pressure is beyond the scope of this document, the scientific bases should be reassessed for aerosol sampling to determine if this requirement is consistent with EPA goals.

The matching of aerosol measurement capabilities with data quality requirements is discussed by Baron and Willike (1993). They note that although aerosol sampler precision can be determined from collocated measurements, field sampling accuracy is more difficult to define. Generation of mono- or polydisperse calibration aerosols are rarely done in field settings because of the complexity of the calibration process. Typically, only the aerosol sampler flowrate accuracy is determined in the field. Biases between the means from collocated aerosol samplers using different separation techniques, may result from sampler operational errors, or from inadequacies in determining the performance specifications during laboratory testing.

4.2.5 Performance Specifications

4.2.5.1 Approaches

A significant step in the standardization process for aerosol sampling was the EPA definition (U.S. Environmental Protection Agency, 1987) of the PM_{10} size fraction, based on the aerodynamic diameter of particles capable of penetrating to the thoracic region of the respiratory system. This definition was followed by implementation of the PM_{10} provisions of EPA's Ambient Air Monitoring Reference and Equivalent Methods regulation (U.S. Environmental Protection Agency, 1987). The format of the latter regulation included adoption of performance specifications for aerosol samplers, based on controlled wind tunnel testing with mono-dispersed aerosols. Controlled laboratory testing is followed by limited field testing, including tests of candidate equivalent methods to demonstrate comparability to designated reference methods. The stringency of the field testing to elucidate potential

sampling biases is strongly influenced by the local sampling site environment, including factors such as wind speed, nearby point sources, and the probability of fugitive dust events.

This approach was chosen, rather than the design specification approach taken in 1971 (Federal Register, 1971), which identified the high volume sampler and associated operational procedures as the reference method for Total Suspended Particulates (TSP). The 1971 regulation had no provisions for the use of alternative or equivalent methods, and subsequent to this design designation, significant problems of the TSP high volume sampler, such as wind speed and direction dependency (McFarland et al., 1979) and off-mode collection (Sides and Saiger, 1976), were reported. These inherent biases complicated the interpretation of TSP concentration data (U.S. Environmental Protection Agency, 1982) and weakened correlations with other measures. The problems were estimated to have induced biases of less than 10% for most situations, but occasionally as high as 30%. The subsequent development of aerosol testing programs for size selective aerosol samplers (e.g., McFarland and Ortiz, 1979; Wedding, 1980; John and Wall, 1983; Ranade et al., 1990; Hall et al., 1992) more rapidly identified weaknesses in existing technologies and facilitated the development of better methods.

No reference standard exists for aerosol concentration measurements in air. The calibration of aerosol samplers relies primarily on characterizations under controlled conditions of the sampler sub-systems, including the size selective inlet, sample conditioning and transmission system, the flow control system, and, if used, subsequent size separators, sample collection and storage elements, and sensors and associated electronics. Although the precision of an aerosol sampler is readily obtained by using replicate, collocated samplers, the accuracy can only be estimated by comparison with either designated "reference" samplers or with computations of expected aerosol mass collections. Performance specification limits are used to control the overall aerosol sampling accuracy. As noted by John and Wall (1983) the selection of a comprehensive list of sampling elements requiring inclusion and the setting of the performance limits for each element is a difficult task, especially when the range of "real-world" sampling situations is considered.

Performance specifications were utilized for the PM_{10} standard to allow the broadest spectrum of measurement technologies, hopefully encouraging the development of new and better methods. A research program was implemented by EPA in parallel with preparation

and review of the 1982 Criteria Document to identify the critical specifications and understand the inter-relationships among the parameters influencing the aerosol sampling process. Studies of the influences of factors such as wind velocity, particle character, flow rate stability, particle bounce and wall losses on precision and accuracy substantially advanced the science of large particle sampling. The performance specification approach was a significant improvement over the design specification approach used for the TSP high volume sampler, in that it fostered the development of new information and technologies and provided for the use of alternative methods. In retrospect, the primary weakness of the design specification approach for the TSP reference method was not the process per se, but the technical inadequacy of the development and testing program that produced the high volume sampler design.

The utilization of a performance specification approach requires that a minimum level of knowledge be available about the measurement process and the associated test procedures. Some significant drawbacks subsequently observed in the performance specification approach for PM_{10} included the complexity, expense and scarcity of aerosol wind tunnel test facilities, and the difficulty in defining comprehensive specifications that considered all of the nuances of aerosol sampling. Wind tunnel evaluation and limited field tests do not always identify sampler related problems encountered during extended periods of ambient sampling (e.g., John and Wang, 1991). Future performances tests should ideally include extended field testing, for example, to evaluate performance in different geographic regions and seasons, as well as under different meteorological conditions.

4.2.5.2 Performance Testing

Since the 1982 Criteria Document (U.S. Environmental Protection Agency, 1982a), aerosol sampling research studies have identified numerous factors that influence the precision and accuracy of samplers in both wind tunnel and field performance testing. Rodes et al. (1985), Purdue et al. (1986), and Cook et al. (1995) showed, in field evaluations under a variety of sampling situations, that PM_{10} samplers meeting the EPA performance specifications provide aerosol concentration measurements with a precision of 10% or less when samplers of the same model were compared. However, significant biases were evident when different types of samplers were compared. The Andersen SA-321A PM_{10} sampler

was found to collect an average of 58% more mass than a collocated Wedding PM_{10} sampler (Perdue et al., 1986). This was partly attributed to the (predicted) bias associated with cutpoint differences between the inlets. A more significant bias (not predicted) was associated with degraded performances in opposite directions (Andersen over-sampling, Wedding under-sampling) due to soiling of the separators during extended sampling periods. Rodes et al. (1985) noted that sampler precisions (coefficients of variation) were better than $\pm 10\%$, with several samplers better than $\pm 5\%$. Cook et al. (1995) reported good agreement (variability less than 15%) among several types of $PM_{2.5}$ samplers. Other sampler types showed significant biases. Under the conditions of the study, high concentrations of NH_4NO_3 and organic carbon (winter in Bakerfield, CA), samplers which heated the collected particles to 30 °C or 50 °C during sampling gave lower mass values than filter samples which were collected at ambient conditions and equilibrated for 24 hours at 23 $\pm$ 3 °C and 40 $\pm$ 5% relative humidity. Coefficient of Haze (COH) measurements by an American Iron and Steel (AISI) tape sampler and light scattering (b_{scat}) measured by an intergrating nephelometer heated to 17 °C correlate well with $PM_{2.5}$ measurments (COH, $r = 0.82$ to 0.91; b_{scat}, $r = 0.91$ to 0.98).

Mark et al. (1992) reviewed the attributes of wind tunnel testing, and noted that tests using controlled conditions are a necessity to determine whether an aerosol sampler meets a basic set of established performance specifications. Hollander (1990) suggested that sampler performance criteria should be evaluated in controlled outdoor tests, given the inability of wind tunnels to accurately mimic the influences of outdoor meteorological conditions on sampling. The current EPA PM_{10} performance testing requires field tests to demonstrate sampler precision and flow rate stability, and the comparability of equivalent methods to designated reference methods. The stringency of such tests are highly dependent on the sampling location chosen, local aerosol sources, the existing meteorology and the season.

Kenny and Lidén (1991) noted that the EPA PM_{10} sampler performance specifications (U.S. Environmental Protection Agency, 1987) provided inadequate consideration for defining the uncertainty in each parameter, and they suggested that bias mapping approaches be considered. Bias mapping relates the allowable precision of a parameter to the critical values of expected bias that just meet the specifications. A similar but less robust procedure is used in the EPA performance specifications. Botham et al. (1991) recommended that the

wind tunnel test system duplicate the expected field sampling scenarios as closely as possible, including characteristic flow obstructions. They described the wind tunnel testing of personal aerosol samplers mounted on an anthropogenically consistent (e.g., breathing, heated) mannequin. Hoffman et al. (1988) and John et al. (1991) described the adverse influence of internal surface soiling on aerosol collection performance during extended field operation, and noted that the existing EPA PM_{10} performance specifications only considered clean samplers. Mark et al. (1992) noted that even though wind tunnel performance testing cannot exactly emulate outdoor turbulence scales, testing in the controlled tunnel environment is a necessity to adequately characterize particle samplers.

Significant new innovations in aerosol sensing technologies that meet the PM_{10} performance specification and have earned designations as equivalent methods (see Section 4.2.6) have occurred since the 1982 Criteria Document. These indirect[8] methods include automated beta attenuation monitors (e.g., Merrifield, 1989; Wedding and Weigand, 1993), and the automated Tapered Element Oscillating Microbalance (TEOM®) technology (Patashnick and Rupprecht, 1991). The TEOM® sampler does not use gravimetric analysis on a balance, but computes mass based on the frequency shift as particles are deposited on an oscillating element. These designations added automated sampling capabilities to the previously all-manual list of sampling methods. Recent field tests of both the beta and TEOM methodologies suggest that biases compared to gravimetrically-based samplers may exist that were not identified by the EPA performance test requirements. Arnold et al. (1992) provide data suggesting that the mass concentration data from a Wedding beta gauge averaged 19% lower than a collocated Wedding PM_{10} gravimetric sampler. Several researchers reported that the TEOM can yield mass concentrations that are either lower or higher than those observed in reference method measurements (Hering, et al., 1994; Meyer, et al., 1992; Meyer et al., 1995). The TEOM operates at an elevated temperature (30 °C or 50 °C) during the collection and measurement process in order to ensure the removal of liquid water associated with particles. In the reference method, the particle-associated water is removed during an equilibration period in a specified temperature and relative humidity range. Both techniques are subject to loss of semivolatile materials such as NH_4NO_3 and

[8]An alternate technology used instead of direct gravimetric analysis to infer mass concentrations from developed relationships.

some organic components. The TEOM may lose semivolatile material that is volatilized due to the higher than ambient sampling temperatures. The reference method may lose semivolatile material during sampling (if concentrations decrease or temperature increases during the sampling period). The reference method is also subject to loss of semivolatile materials during equilibration and storage prior to weighing. These processes, in areas or times during which semivolatile aerosol components are a significant component of the ambient aerosol mass, can cause either technique to yield a significant under-estimation of the mass of particulate matter in the ambient air. This also applies to some degree to any integrated sample collected on a substrate. Devising comprehensive performance specifications and test procedures for aerosol samplers, given the complexities of aerosol chemistry, physics, and mechanics, is a demanding task.

The size-selective, gravimetrically-based, 24-h manual aerosol concentration measurement has been the mainstay of compliance sampling for at least two decades. Although several new sensor technologies have been designated as Equivalent methods for PM_{10} by EPA, no superior technology has been developed that is a better reference method than that based on collection of a discreet aerosol sample followed by gravimetric analysis. Improvements have been made since 1982 in the accuracy and precision of integrated, manual aerosol sampling. Some of the most significant advances have occurred in aerosol size separation technologies, improved performance characterization test methods, and speciation sampling techniques.

As discussed by Lippmann (1993), there may be no threshold for health responses down to the lowest aerosol concentrations. This implies that the precision and lower detection limit requirements will continue to be important for aerosol measurements across the concentration spectrum. These factors become even more critical as the size fraction of interest becomes smaller and fewer total particles are collected. At low concentrations (especially with small size fractions), normally insignificant factors can become important contributors to biases. Witz et al. (1990) reported rapid and substantial losses of nitrates, chlorides and ammonium ion (19, 65 and 51%, respectively) from quartz high volume sampler filters during storage periods of one week prior to analyses. Transformations can also occur on glass fiber substrates during sampling, as reported by Sickles and Hodson (1989) for the rapid conversion of collected nitrites to nitrates in the presence of ozone.

Zhang and McMurry (1992) showed that nearly complete evaporative losses of Fine particle nitrate can occur during sampling on Teflon filters. Lioy et al. (1988), in a study using PM_{10} samplers, reported 25 to 34% lower concentration values resulting from losses of glass fibers from the filter to the filter holder gasket during sampling. Feeney et al. (1984) reported weight gains in Teflon filters used in contaminated ring cassettes, that posed significant problems for light aerosol loadings. Grinshpun et al. (1993) suggest that if unavoidable changes in the aerosol occur during sampling, development of a model that permits back-calculation of the in situ characteristics can be considered.

4.2.6 Reference and Equivalent Method Program

Ambient air PM_{10} measurements are used (among other purposes) to determine whether defined geographical areas are in attainment or non-attainment with the National Ambient Air Quality Standards (NAAQS) for PM_{10}. These measurements are obtained by the States in their state and local air monitoring station (SLAMS) networks as required under 40 CFR Part 58. Further, Appendix C of Part 58 requires that the ambient air monitoring methods used in these EPA-required SLAMS networks must be methods that have been designated by the EPA as either reference or equivalent methods.

Monitoring methods for particulate matter (i.e., PM_{10}) are designated by the EPA as reference or equivalent methods under the provisions of 40 CFR Part 53, which was amended in 1987 to add specific requirements for PM_{10} methods. Part 53 sets forth functional specifications and other requirements that reference and equivalent methods for each criteria pollutant must meet, along with explicit test procedures by which candidate methods or samplers are to be tested against those specifications. General requirements and provisions for reference and equivalent methods are also given in Part 53, as are the requirements for submitting an application to the EPA for a reference or equivalent method determination. The distinction between reference and equivalent methods is a technical one. On one hand, it provides for detailed, explicit specification of a selected measurement technology for reference methods. On the other hand, it allows alternative (including innovative and potentially improved) methodologies for equivalent methods, based only on meeting specified requirements for functional performance and for comparability to the reference method. For purposes of determining attainment or non-attainment with the

NAAQS, however, the distinction between reference and equivalent methods is largely, if not entirely, immaterial.

Under the Part 53 requirements, *reference methods* for PM_{10} must be shown to use the measurement principle and meet the other specifications set forth in 40 CFR 50, Appendix J (Code of Federal Regulations, 1991). They must also include a PM_{10} sampler that meets the requirements specified in Subpart D of 40 CFR 53. Appendix J specifies a measurement principle based on extracting an air sample from the atmosphere with a powered sampler that incorporates inertial separation of the PM_{10} size range particles followed by collection of the PM_{10} particles on a filter over a 24-h period. The average PM_{10} concentration for the sample period is determined by dividing the net weight gain of the filter over the sample period by the total volume of air sampled. Other specifications are prescribed in Appendix J for flow rate control and measurement, flow rate measurement device calibration, filter media characteristics and performance, filter conditioning before and after sampling, filter weighing, sampler operation, and correction of sample volume to EPA reference temperature and pressure. Also, sampler performance requirements in Subpart D of Part 53 include wind tunnel tests for "sampling effectiveness" (the efficacy of the PM_{10} particle size separation capability) at each of three wind speeds and "50 percent cutpoint" (the accuracy of the primary 10-micron particle size separation). Field tests for sampling precision and flow rate stability are also specified. In spite of the instrumental nature of the sampler, this method is basically a manual procedure, and all designated reference methods for PM_{10} are therefore defined as manual methods.

Equivalent methods for PM_{10}, alternatively, need not be based on the measurement principle specified in Appendix J nor meet the other Appendix J requirements. Instead, equivalent methods must meet the "sampler" performance specifications set forth in Subpart D of Part 53 and demonstrate *comparability* to a reference method as required by Subpart C of Part 53. The provisions of Subpart C specify that a candidate equivalent method must produce PM_{10} measurements that agree with measurements produced by collocated reference method samplers at each of two field test sites. For this purpose, agreement means a regression slope of 1 ± 0.1, a regression intercept of $0 \pm 5\ \mu g/m^3$, and a correlation >0.97. These requirements allow virtually any type of PM_{10} measurement

technique, and therefore an equivalent method for PM_{10} may be either a manual method or a fully automated instrumental method (i. e., analyzer).

As of this writing, the EPA has designated seven reference methods and three equivalent methods for PM_{10}, as listed in Table 4-1. The reference methods include four methods featuring high-volume samplers from two manufacturers, with one using a cyclone-type size separator and the others using an impaction-type separator. The other reference methods include a low-volume sampler (from a third manufacturer), a low-volume sampler featuring a secondary size separation at 2.5 microns (dichotomous sampler), and a medium-volume, non-commercial sampler. The three designated equivalent methods are all automated PM_{10} analyzers and include two operating on the beta-attenuation principle and one based on a tapered element oscillating microbalance (TEOM™). It should be noted that although these latter three automated PM_{10} analyzers may be capable of providing continuous or semi-continuous PM_{10} concentration measurements, only 24-h average PM_{10} measurements are recognized as approved under their equivalent method designations.

4.2.7 Determination of Size Distribution

The determination of aerosol size distributions can be a powerful research tool when studying source contributions and transformation processes. A number of techniques are available as described by texts such as Willeke and Baron (1993) to make near real-time, single particle aerosol measurement in addition to cascade impactors.

4.2.7.1 Cascade Impactors

In cascade applications, the aerosol is impacted and trapped onto a series of removable, coated substrates (e.g., greased foils), including a final total stage collection on a filter for gravimetric analysis. Marple et al. (1993) list over 30 single stage and cascade impactors that are either commercially available or still commonly used. The design and calibration of a miniature eight-stage cascade impactor for personal air sampling in occupational settings is described by Rubow et al. (1987), operating at 2.0 lpm. Evaluations of the most commonly used cascade impactor systems have been reported by Vaughan (1989) for the Andersen MK1 and MK2 7-stage cascade impactors, Marple et al. (1991) for the 10-stage Micro-Orifice Uniform Deposit Impactor (MOUDI), and Wang and John (1988) and Hillamo and

TABLE 4-1. U.S. ENVIRONMENTAL PROTECTION AGENCY-DESIGNATED REFERENCE AND EQUIVALENT METHODS FOR PM_{10}

Method No.	Identification	Description	Type	Date
RFPS-1087-062	Wedding & Associates PM_{10} Critical Flow High-Volume Sampler.	High-volume (1.13 m^3/min) sampler with cyclone-type PM_{10} inlet; 203 x 254 cm (8 x 10 in) filter.	Manual reference method	10/06/87
RFPS-1287-063	Sierra-Andersen or General Metal Works Model 1200 PM_{10} High-Volume Air Sampler System	High-volume (1.13 m^3/min) sampler with impaction-type PM_{10} inlet; 203 x 254 cm (8 x 10 in) filter.	Manual reference method	12/01/87
RFPS-1287-064	Sierra-Andersen or General Metal Works Model 321-B PM_{10} High-Volume Air Sampler System	High-volume (1.13 m^3/min) sampler with impaction-type PM_{10} inlet; 203 x 254 cm (8 x 10 in) filter. (No longer available.)	Manual reference method	12/01/87
RFPS-1287-065	Sierra-Andersen or General Metal Works Model 321-C PM_{10} High-Volume Air Sampler System	High-volume (1.13 m^3/min) sampler with impaction-type PM_{10} inlet; 203 x 254 cm (8 x 10 in) filter. (No longer available.)	Manual reference method	12/01/87
RFPS-0389-071	Oregon DEQ Medium Volume PM_{10} Sampler	Non-commercial medium-volume (110 L/min) sampler with impaction-type inlet and automatic filter change; two 47-mm diameter filters.	Manual reference method	3/24/89
RFPS-0789-073	Sierra-Andersen Models SA241 or SA241M or General Metal Works Models G241 and G241M PM_{10} Dichotomous Samplers	Low-volume (16.7 L/min) sampler with impaction-type PM_{10} inlet; additional particle size separation at 2.5 micron, collected on two 37-mm diameter filters.	Manual reference method	7/27/89
EQPM-0990-076	Andersen Instruments Model FH62I-N PM_{10} Beta Attenuation Monitor	Low-volume (16.7 L/min) PM_{10} analyzers using impaction-type PM_{10} inlet, 40 mm filter tape, and beta attenuation analysis.	Automated equivalent method	9/18/90

TABLE 4-1 (cont'd). U.S. ENVIRONMENTAL PROTECTION AGENCY-DESIGNATED REFERENCE AND EQUIVALENT METHODS FOR PM_{10}

Method No.	Identification	Description	Type	Date
EQPM-1090-079	Rupprecht & Patashnick TEOM Series 1400 and Series 1400a PM_{10} Monitors	Low-volume (16.7 L/min) PM_{10} analyzers using impaction-type PM_{10} inlet, 12.7 mm diameter filter, and tapered element oscillating microbalance analysis.	Automated equivalent method	10/29/90
EQPM-0391-081	Wedding & Associates PM_{10} Beta Gauge Automated Particle Sampler	Low-volume (16.7 L/min) PM_{10} analyzer using cyclone-type PM_{10} inlet, 32 mm filter tape, and beta attenuation analysis.	Automated equivalent method	3/5/91
RFPS-0694-098	Rupprecht & Patashnick Partisol Model 2000 Air Sampler	Low-volume (16.7 L/min) PM_{10} samplerwith impaction-type inlet and 47 mm diameter filter.	Manual reference method	7/11/94

Kauppinen (1991) for the 6-stage Berner, low pressure cascade impactor. The smallest particle stages of these impactors can have very small diameter jets and/or very low total pressures to achieve the sub-micron separations. The MOUDI impactor has 2000 holes on the lowest cutpoint stage. Raabe et al. (1988) describe an 8 stage cascade slit impactor with slowly rotating impactor drums instead of flat plates. This arrangement, in combination with a PIXIE analyzer, permitted aerodynamic sizing of elemental components, with temporal resolution. The skill and care required in the operation of cascade impactors suggests that they are research rather than routine samplers.

The importance of the aerosol calibration of a cascade impactor is illustrated by Vaughan (1989) in Figure 4-13, which compares the experimental data with the manufacturer's calibrations and indicates biases as large as 1.0 μm. Marple et al. (1991) provided a similar type of stage calibration for the MOUDI impactor and included data on the internal particle losses (see Figure 4-14). These loss data showed that an improperly designed inlet to the impactor, combined with the inertial and interception losses of the larger particle sizes, can substantially bias the first stage collections. This was also demonstrated for the inlet to the Andersen impactor by McFarland et al. (1977). Cascade impactors that cover wide particle size ranges inherently require design compromises among competing factors, including cutpoint sharpness, internal stage losses and the physical size of the device.

Cascade impactors can be used to construct distributions of mass and speciated constituents as a function of aerodynamic diameter. These distributions can be constructed graphically or using matrix inversion techniques. Marple et al. (1993) notes that impactor stage calibrations which do not demonstrate sharp cutoffs can cause significant between-stage sizing errors if not accommodated. John et al. (1990) measured distributions over the 0.08 to 16 μm range for mass and inorganic ions for several sites in Southern California. They identified the standard coarse mode and two separate, previously unreported modes in the 0.1 to 1.0 μm range. This latter range was referred to by Whitby (1978) as a single "accumulation" mode. John et al. (1990) described a "condensation" mode at 0.2 $\pm$ 0.1 μm containing gas phase reaction products, and a "droplet" mode at 0.7 $\pm$ 0.2 μm which grows from the "condensation" mode by the addition of water and sulfates. Fang et al. (1991) described the effects of flow-inducted relative humidity changes on the sizing of acid aerosols in the MOUDI impactor. They noted that it may not be possible to measure size

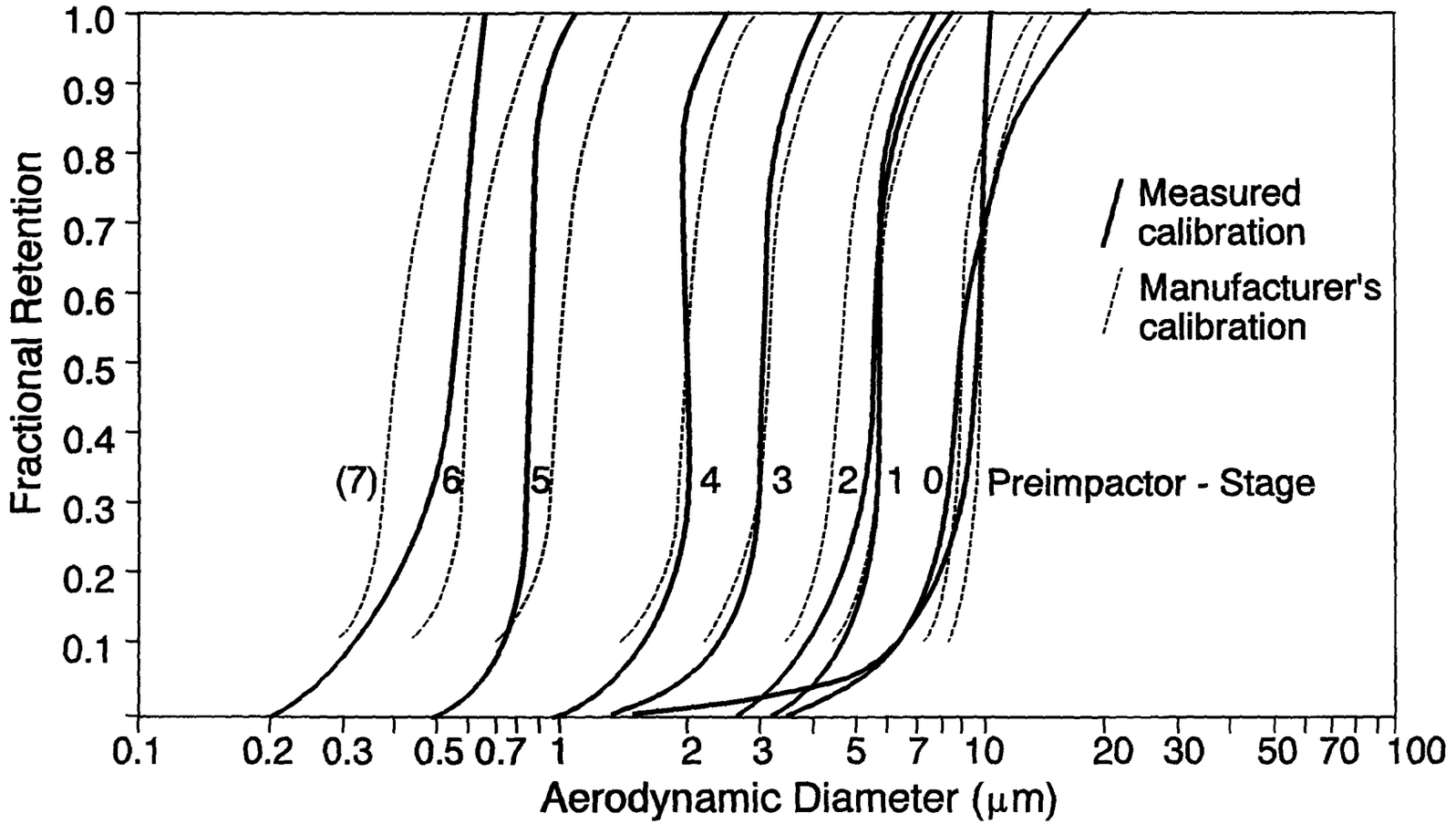

Figure 4-13. Measured calibration of the Andersen Cascade Dupactor as compared to that supplied by the manufacturer.

Source: Vaughan (1989).

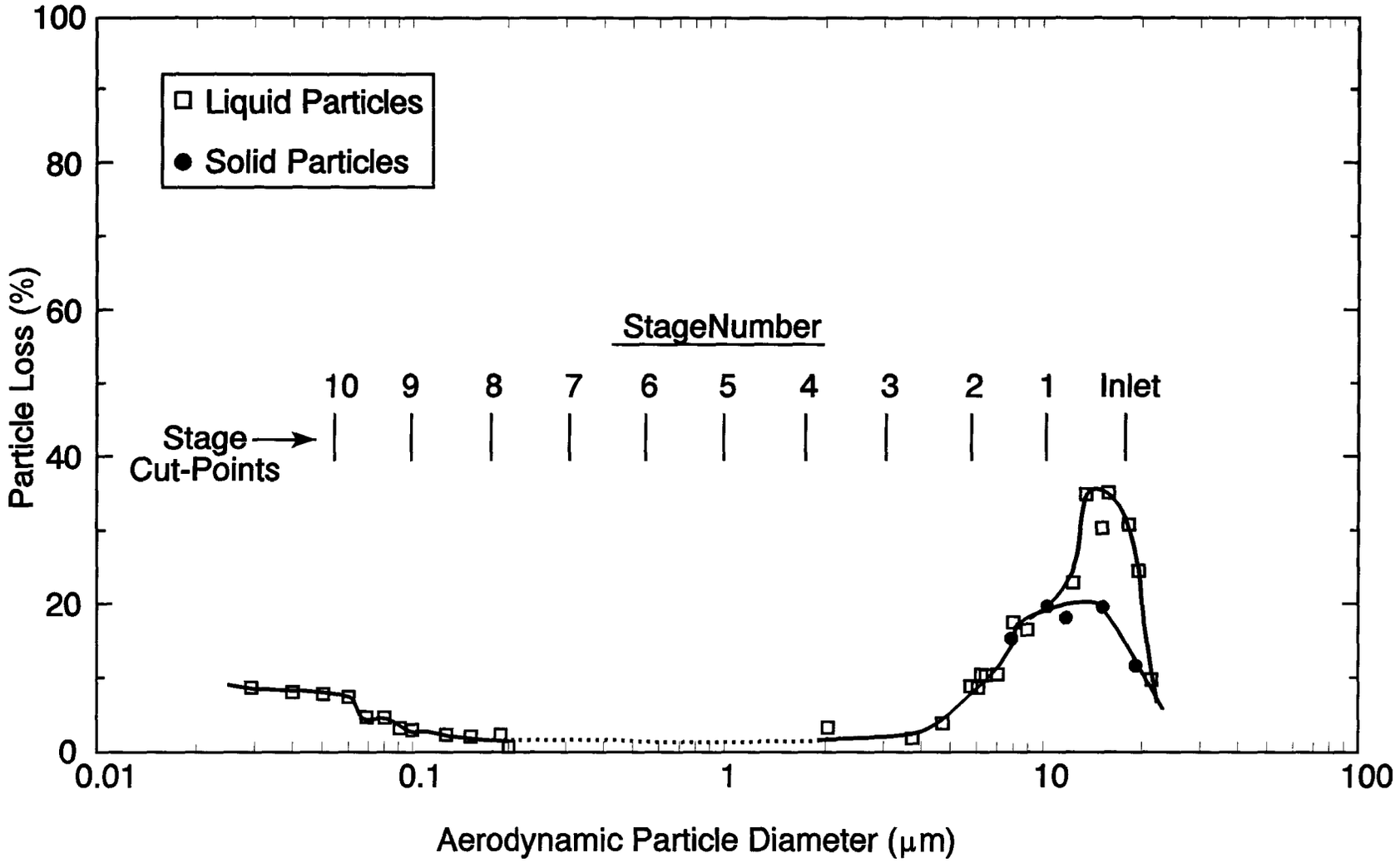

Figure 4-14. Internal losses for the MOUDI impactor.

Source: Marple et al. (1991).

distributions of small (less than about 0.2 to 0.5 μm) particles with impactors at relative humidities exceeding 80%.

4.2.7.2 Single Particle Samplers

Aerosol size distribution data are useful for studies of particle transport and transformation processes, source characterization, and particle sizing and collection device performance. In addition to cascade impactors, a number of real time or near real time sizing instruments are available and described in texts such as Willeke and Baron (1993). While cascade impactors provide distributions in terms of aerodynamically sized mass, single particle sampling devices can produce optically sized distributions as a function of particle number (count), with surface area and volume distributions computed during the data reduction, assuming spherical particles. Particle density and shape information as a function of size are required to convert from volume distributions to an estimated mass basis. Individual particle sizing and counting instruments are generally limited to a particle detection range of a decade or so, but several devices can overlap to cover the range of approximately 0.001 to 10 μm. The principle of detection of an instrument restricts the particle sizes which can be detected. For example, instruments using electrical mobility analysis are limited to particle sizes less than about 1 μm. Optical methods are typically used to measure particles larger than about 0.1 to 0.3 μm. Inlet and transport system losses of coarse particles above about 2 μm, prior to the sensing volume, must be factored into reported size distributions.

The three most commonly used single particle sampler types are aerodynamic particle sizers, electrical mobility analyzers and optical particle counters (OPC's). Aerodynamic particle sizers use laser doppler anemometry to measure the velocity of particles in a jet. The acceleration of the particle is related to the aerodynamic particle diameter. This technique is typically applied to particles larger than about 0.5 μm. In electrical mobility analysis, aerosol with a known charge distribution flows through an electric field. The particles migrate according to their mobility which can be related to size. The original TSI electrical aerosol analyzer (EAA) performed this separation in an integrated manner over the total size distribution and detected the particles by unipolar diffusion charging. A more versatile approach, the differential mobility analyzer or DMA (Liu et al., 1978), is able to

examine a narrow slice of the size distribution in an equilibrium charge state, detected by a condensation nucleus counter (CNC). Differential mobility analyzers have been employed in pairs (Tandem Differential Mobility Analyzer, or TDMA) to examine both (a) particle characteristics such as NH_3 and H_2SO_4 reaction rates (McMurry et al., 1983) and (b) the sensitivity of the size distributions of Los Angeles aerosol to relative humidity (McMurry and Stolzenburg, 1989). The latter research used the first DMA to select particles of known mobility from the input aerosol, a humidification system to condition the selected particles, and the second DMA to determine mobility changes. Optical particle counters pass a jet of aerosol through an optical system. Light scattered from individual particles is detected and the signal in processed in a multi-channel analyzer. Discreet signals are counted and sorted by intensity and by optical size. One example of a forward-scattering counter with an open sensing volume (for use on aircraft) is the Particle Measuring Systems, Inc., FSSP-300, which can provide high resolution (31 channel) count distributions over the size range of 0.3 to 20 μm (Rader and O'Hern, 1993). Gebhart (1993) described currently available OPC's and their counting efficiencies over a range of diameters.

Single particle samplers have common considerations, as dicussed below.

Calibration: They are calibrated with reference aerosol either by the manufacture or by the user. If the properties of the aerosol measured are quite different than the calibration, the indicated size distribution may be quite different than actual distribution. Brockman et al. (1988) demonstrated that the APS calibration can vary significantly with the type of test aerosol and showed substantial response biases between oleic acid and polystyrene latex spheres above 10 μm. Wang and John (1989) described a procedure to correct the APS response for aerosol particle density. Particle shape can also provide serious sizing errors, and specific calibrations are needed for particles with shape factors significantly different from unity (spherical). Yeh (1993) commented that the calculated geometric standard deviations (σ_g) determined by the EAA and DMA are generally larger than 1.3, even if the correct value is significantly closer to unity. Woskie et al. (1993) observed, as did Willeke and Degarmo (1988), that optical particle counting devices must be appropriately calibrated using realistic aerosols, especially for low concentration applications. Harrison and Harrison (1982) suggested that the ratio of fine particle mass concentration to optical scattering

extinction will be more variable when a significant contribution is made by irregular (shaped) particles - an event likely to occur when the mean mass diameter exceeds 1 μm.

Particle Concentration Effects: Gebhart (1993) noted that the response of single particle counters may be influenced by extremely high particle concentrations. Wake (1989) and Heitbrink et al. (1991) described the coincidence problems of the APS when sampling high total particle concentrations, especially for sizes greater than 1 μm. Baron et al. (1993) reported that the concentration levels giving 1% coincidence in an aerodynamic particle sizer for 0.8, 3 and 10 μm particles, respectively, are the relatively low values of 558, 387 and 234 particles/cm^3. Optical particle counters can experience coincidence errors (two particles are detected as a single particle) and counter saturation at high particle concentrations. Hinds and Kraske (1986) described the performance of the PMS, Inc. LAS-X and noted a sizing accuracy of ± 2 channel widths, with coincidence errors of less than 10% for concentrations below 10,000 particles/cm^3. Clearly, typical particle concentrations found in the atmosphere may produce significant errors if sample dilution is not utilized.

4.2.8 Automated Sampling

Automated methods to provide measures of aerosol concentrations in the air have existed for decades in an attempt to provide temporal definition of suspended particles and enhance every-sixth-day sampling schedules with a minimum labor expense. Arnold et al. (1992) collected daily 24-h PM_{10} samples with an automated monitor and noted that 80% of the highest 10 daily concentrations between 1989 and 1990 were not encountered by the every-sixth-day sampling schedule. Some of the automated samplers (e.g., British Smoke Shade and AISI tape samplers) described in the 1982 Criteria Document were indicator measures of aerosol concentration, using calibrations relating aerosol concentrations to reflected or absorbed light. Tape samplers were used in the U. S. primarily as exceedance (index) monitors.

The beta attenuation and integrating nephelometer techniques described in the 1982 Criteria Document primarily were research methods. Since that time, the beta gauge sampling approach has been refined and a new approach, based on the Tapered Element Oscillating Microbalance (TEOM) principle, has been developed. Samplers based on these techniques have been designated as equivalent methods for PM_{10}.

Although one could be readily constructed, there are presently no commercially available, automated high volume (> 1 m^3/min flowrate) aerosol samplers, excluding the possibility of the timed operation of an array of manual samplers. The physical size of such a sampling system using 8 x 10 inch filters is impractical. The dichotomous sampler is currently the only low volume, gravimetrically-based sampler commercially available in an automated version.

4.2.8.1 Smoke Shade (British Smoke, Black Smoke)

Historically, the British smoke shade sampler was one of the earliest ambient PM sampling devices to be developed and to gain widespread use as an automated optical PM monitoring method. Key features and limitations of the British or black smoke (BS) method were discussed in EPA's 1982 Criteria Document. As indicated in Chapters 3 and 14 of that Criteria Document, the BS method typically involves use of a sampler that draws ambient air through an inverted funnel and approximately 3m of plastic tubing to deposit collected particles on white filter paper. The amount of PM deposited during a given time period (e.g., 1-h during severe episodes, or more typically, 24-h) is determined by measuring the blackness of the stain on the filter paper. An automated version of the sampler can collect daily samples sequentially for up to eight days.

It is important to note, as described in the 1982 Criteria Document, that the BS method and its variations (e.g., the OECD version) in routine use typically employ standard monitoring equipment with a D_{50} cutpoint $\cong$4.5 μm, which mainly allows fine-mode particles and small coarse mode particles (some ranging up to ~8 to 10 μm) to be collected. Thus, regardless of whether larger particles are present in the atmosphere, the BS method collects predominately small particles. Also, the BS method neither directly measures mass nor determines chemical composition of the collected PM. Rather, it measures light absorption of particles as indicated by reflectance from the stain formed by the particles collected on the filter paper, which depends both on the density of the stain, or amount of PM collected, and the optical properties of the collected PM. Smoke particles composed of elemental carbon, found in incomplete fossil-fuel combustion products, typically make the greatest contribution to the darkness of the stain, especially in urban areas. Thus, the amount of elemental carbon, but not organic carbon, present in the stain tends to be most highly correlated with

BS reflectance readings. Other nonblack, noncarbon particles also have optical properties such that they can affect the reflectance readings, although their contribution to optical absorption is usually negligible.

Since the relative proportions of atmospheric carbon and noncarbon PM can vary greatly from site to site or from one time to another at the same site, the same absolute BS reflectance reading can be associated with markedly different amounts (or mass) of collected particles or, in unusual circumstances, even with markedly different amounts of carbon. Site-specific calibrations of reflectance readings against actual mass measurements obtained by collocated gravimetric monitoring devices are therefore necessary to obtain estimates of atmospheric concentrations of particulate matter based on the BS method. A single calibration curve relating mass or atmospheric concentration (in $\mu g/m^3$) of particulate matter to BS reflectance readings obtained at a given site may serve as a basis for crude estimates of the levels of PM (mainly small particles) at that site over time, so long as the chemical composition and relative proportions of elemental carbon and noncarbon PM do not change substantially. However, the actual mass or smoke concentrations present at a particular site may differ markedly (by factors of two or more) from the values calculated from a given reflectance reading on either of the two most widely used standard curves (the British and OECD standard smoke curves)[9]. Thus, great care must be taken in interpreting the meaning of any BS value reported in terms of $\mu g/m^3$, especially as employed in the British and other European epidemiological studies discussed in Chapter 12 of this document.

There has existed long standing interest with regard to relationships between ambient PM concentrations indexed by BS readings (based on conversion of reflectance values to estimated $\mu g/m^3$ concentrations by means of standard calibration curves) and those obtained by gravimetric methods. The 1982 Criteria Document noted that Ball and Hume (1977) and Waller (1963) found that such relationships are site, season, and particle-source dependent. Also, Lee et al. (1972) noted, from collocated TSP hi-vol and smoke shade sampler

---

[9]For this reason, smoke data reported in $\mu g/m^3$ based on either the British or OECD Standard curve are appropriately interpreted in terms of "nominal" $\mu g/m^3$ smoke units and cannot be accepted as accurate estimates of airborne PM mass unless corroborated by local site-specific gravimetric calibrations. In other words, unless based on local site-specific calibrations, smoke readings in $\mu g/m^3$ cannot yield quantitative estimates of atmospheric PM concentrations. In the absence of such calibrations, smoke readings only allow for rough qualitative (i.e., $<$; $=$; or $>$) comparisons of amounts of PM present at a given time versus another time at the same site and do not permit meaningful comparisons between PM levels at different geographic areas having airborne PM of different chemical composition (especially in terms of relative proportions of elemental carbon).

comparisons made at various sites in England, that the overall correlation coefficients between these measurements for all sites was 0.618. However, the individual coefficients ranged from 0.936 (good correlation) to 0.072 (no correlation). Bailey and Clayton (1980) showed that smoke shade measurements correlated more closely with soot (elemental carbon) content than with gravimetric mass. Other work by Paschel and Egner (1981) and Clayton and Wallin (1982) showed consistently higher TSP values than BS readings (converted to $\mu g/m^3$) from collocated samplers in various U.S. and U.K. cities, respectively (as would be expected given that the BS measurements of fine and small coarse mode particles typically represent only some fraction of the wider range of particles sampled by TSP measurements). Clayton and Wallin (1982), not surprisingly, also found widely variable ratios of TSP to BS readings from different U.K. cities reflecting the varying proportions of small particles present in the total ambient mix of particles at different sites. Likewise, varying (site- and season-dependent) relationships between BS measurements and ambient PM measurements made by various gravimetric methods have been reported in the Federal Republic of Germany (Laskus, 1983) and in the semi-arid climate of Baghdad, Iraq (Kanbour et al., 1990). Lastly, Muir and Laxton (1995) reported that, for Bristol (a moderate size U.K. city), daily average BS (averaged over six urban background sites) appears to be a reasonable predictor of daily average PM_{10} and daily 1-h peak PM_{10} values; but different relationships apply for winter versus summer, indicating that BS and PM_{10} measure different components of airborne PM (i.e., BS may be a better index of fine-mode particles than PM_{10}, which has a D_{50} cutpoint of $\cong 10$ μm).

Only limited examples exist of derivation of models of interrelationships between BS readings and gravimetric measurements for particular time periods in a given location. For example, see Mage (1995) for discussion of an empirical model relating BS to TSP values during London winters of the 1950s and 1960s.

4.2.8.2 Coefficient of Haze (AISI/ASTM Tape Sampler)

The 1982 Criteria Document also described a second type of automated optical PM measurement methods. Developed before 1940, the American Iron and Steel Institute (AISI) light transmittance method is similar in approach to the BS technique and has been employed for routine monitoring in some American cities. The instrument collects particles with a D_{50}

cutpoint of ≅5.0 μm aerodynamic diameter and uses an air intake similar to that of the BS method. Ambient PM is collected on a filter-paper tape that is periodically advanced to allow accumulation of another stain. Opacity of the stain is determined by transmittance of light through the deposited material and the tape. The results are expressed in terms of optical density or coefficient of haze (CoH) units per 1,000 linear feet of air sampled (rather than in mass units). Readings in CoH units are somewhat more responsive to noncarbon particles than are BS measurements; but, again, the AISI method neither directly measures mass nor determines chemical composition of the PM collected. Any attempt to relate CoHs to $\mu g/m^3$ requires site-specific calibration of CoH readings against mass measurements determined by a collocated gravimetric device, but the accuracy of such mass estimates are still subject to question.

Few attempts have been reported on calibration of COH measurements versus results from collocated gravimetric devices. One notable attempt (Ingram, 1969; Ingram and Golden, 1973) was reported for New York City, but the results are of very limited applicability to New York City aerometric data of the 1960's. Also, Regan et al. (1979) showed that CoH readings correlate favorably with gravimetric measurements limited to smaller particle sizes. Edwards (1980) and Edwards et al. (1983) have also shown that BS reflectance measurements can be related to the absorption coefficient of the atmosphere and that BS measurements can be converted to approximate CoH measurements made by AISI tape sampler using the absorption coefficient relationships. As several investigators noted, (e.g., Lodge, et al., 1981), if a relationship could be developed between optical and gravimetric measurements, it would be site specific, but still variable because of seasonal and long-term differences in the sources of collected particle size fractions and their carbon content.

4.2.8.3 TEOM® Sampler

The Tapered Element Oscillating Microbalance (R & P, Inc.) sensor, as described by Patashnick and Rupprecht (1991), consists of an oscillating tapered tube with a filter on its free end (see the diagram in Figure 4-15). The change in mass of the filter and collected aerosol produces a shift in the oscillation frequency of the tapered tube that is directly related to mass. Rupprecht et al. (1992) suggested that the filter can be archived after sampling for

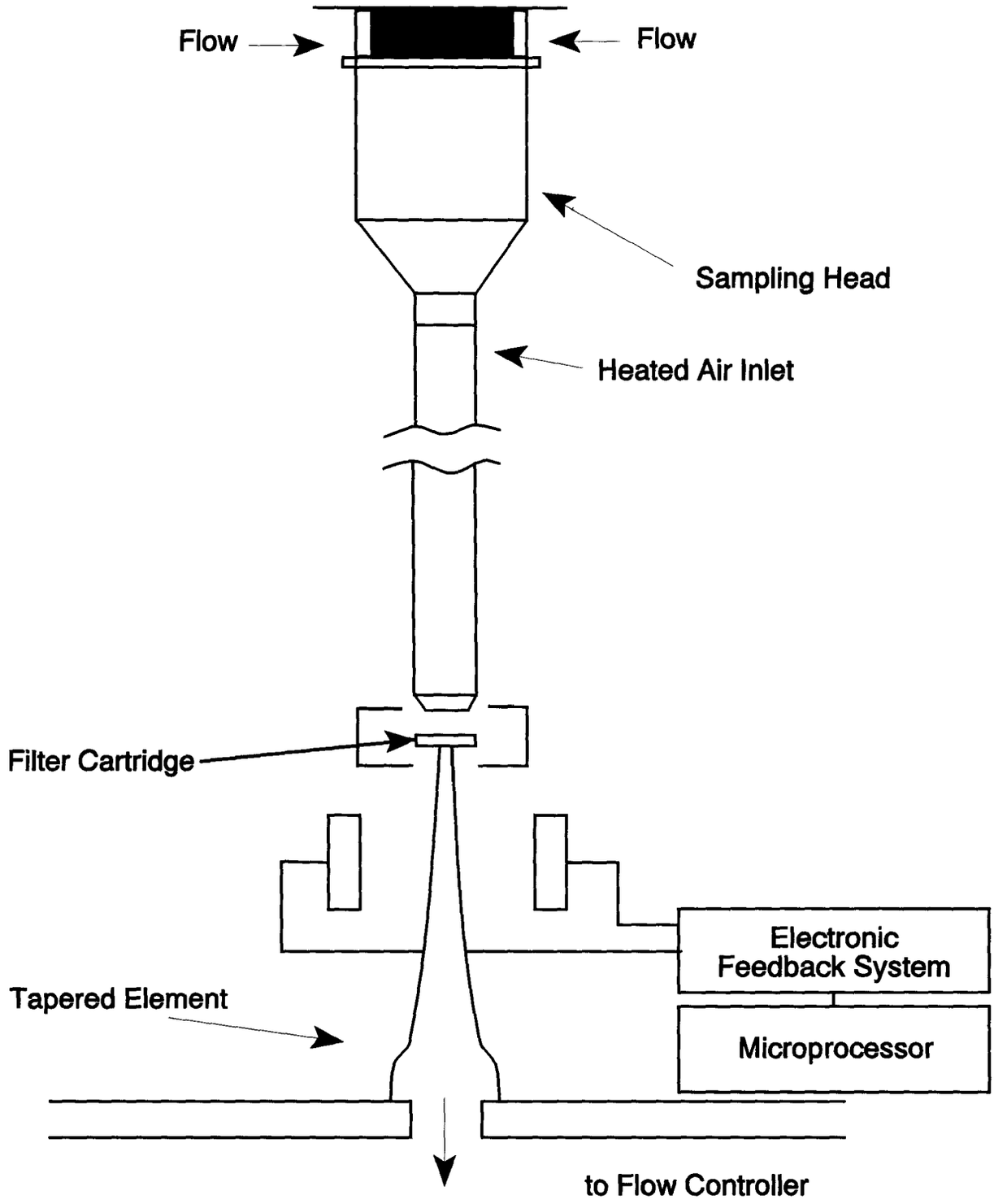

Figure 4-15. Rupprecht and Patashnick TEOM® sampler.

Source: Patashnick and Rupprecht (1991).

subsequent analysis. The sampler inlet has a PM_{10} cutpoint and operates at 16.67 lpm. A flow splitter samples a 3 lpm portion of this flow to be filtered. Since the fraction of volatile species (e.g., water, nitrates, organics) in the aerosol is a function of ambient temperature, the TEOM® sampler heats the inlet air stream to a constant 30 or 50 °C to keep moisture in the vapor phase. The mass transducer is also heated to 50 °C to stabilize the measurement process. Operation with the flow stream heated to a lower temperature (e.g., 30 °C) is possible, but care must be taken to avoid moisture condensation that will confound the measurement. The transducer is also heated to 50 °C to stabilize the mass measurement. A factory calibration regression is used to electronically correct the computed mass from the TEOM® sampler to that measured by a reference PM_{10} sampler.

Although several studies (e.g. Patashnick and Rupprecht, 1991; Kalthoff and Crumpler, 1990) have shown consistent and linear relationships between the TEOM® sampler and gravimetric PM_{10} samplers, a number of studies have shown biases under certain conditions. Several researchers, including Cahill et al. (1994), Hering (1994) and Meyer et al. (1992) have reported that the modification of the aerosol by the elevated operating temperature appears to have a significant effect (loss) on mass concentration. Meyer et al. (1992) collocated a TEOM® sampler with an PM_{10} SA1200 gravimetric sampler in Mammoth Lakes, CA during a winter heating season (heavy wood stove usage). The regressions between the TEOM® sampler and PM_{10} sampler gave strong correlations ($r^2 > 0.98$), with slopes of 0.55 for operation at 50 °C, and 0.66 for operation at 30 °C. The negative bias of the TEOM was attributed primarily to losses of semi-volatile organics from the filter. Cahill et al. (1994) reported that the TEOM® sampler showed biases on the order of 30% low and poor correlations with PM_{10} samplers in dry, dusty conditions. The reasons for this discrepancy were unknown. The field comparison data of Patashnick and Rupprecht (1990) showed near unity (1 ± 0.06) regression slopes for the TEOM with the Wedding IP_{10} and Sierra-Andersen dichotomous samplers in El Paso, TX and Birmingham, AL. Since aerosol composition is highly dependent on local sources and meteorology, volatilization losses could be expected to be site- and season-dependent. This could significantly affect the rigor of collocated field sampling. A WESTAR (1995) council report summarizes the relationships between TEOM® monitors and other direct gravimetric samplers in at least 10 states in the western U.S. This report concluded that on average the TEOM® sampler concentrations

were 21.8% lower than other collocated PM_{10} samplers for concentrations > 50 $\mu g/m^3$. This would significantly affect the TEOM® sampler's ability to be used as a "trigger" monitor for control strategy plans. More data are needed to determine the implications of these problems on the ability of the TEOM® sampler to be used in a regulatory setting. Although it is clear that the TEOM® sampler can provide PM_{10} data comparable to the existing reference method samplers, the specific field sampling conditions where excessive bias might be expected to occur have not been completely defined. A portion of the bias is undoubtedly due to concomitant variabilities in the associated gravimetric measurements.

4.2.8.4 Beta Gauge

The Andersen FH 62I-N beta attenuation sampler was described by Merrifield (1989) and uses a 30 mCi Krypton-85 source and detector to determine the attenuation caused by deposited aerosols on a filter (see diagram in Figure 4-16). To improve the stability over time, a reference reading is periodically made of a foil with an attenuation similar to that of the filter and collected aerosol. The Wedding beta attenuation sampler was described by Wedding and Weigand (1993) and uses a 100 mCi ^{14}C source. Both samplers have inlets with a PM_{10} cutpoint, with the Andersen sampler operating at 16.67 lpm and the Wedding at 18.9 lpm. The filter material is contained on a roll and advances automatically on a time sequence, or when a preset aerosol loading is reached. An automatic beta gauge sampler was also described by Spagnolo (1989), using a 15 μm inlet and a ^{14}C source. The calibration of a beta gauge is site specific, and a calibration regression must be processed electronically to provide accurate mass readings. Rupprecht et al. (1992) suggested that the closer link between deposited mass and frequency shift for the TEOM principle should provide less site-specific response, compared to the aerosol compositional sensitivity of the beta gauge technique.

Arnold et al. (1992) provided data over a 2 year period in Denver, CO for the mass concentration regression data from a Wedding beta gauge, showing a range of correlations (r^2 from 0.72 to 0.86), varying by sampler and season. The authors suggested that installation of a newer technology beta gauge accounted for the higher correlations, but noted that unexplained outliers resulted in poorer than expected results. The regression slopes between the two sampler types showed that the beta gauge averaged 19% lower than a

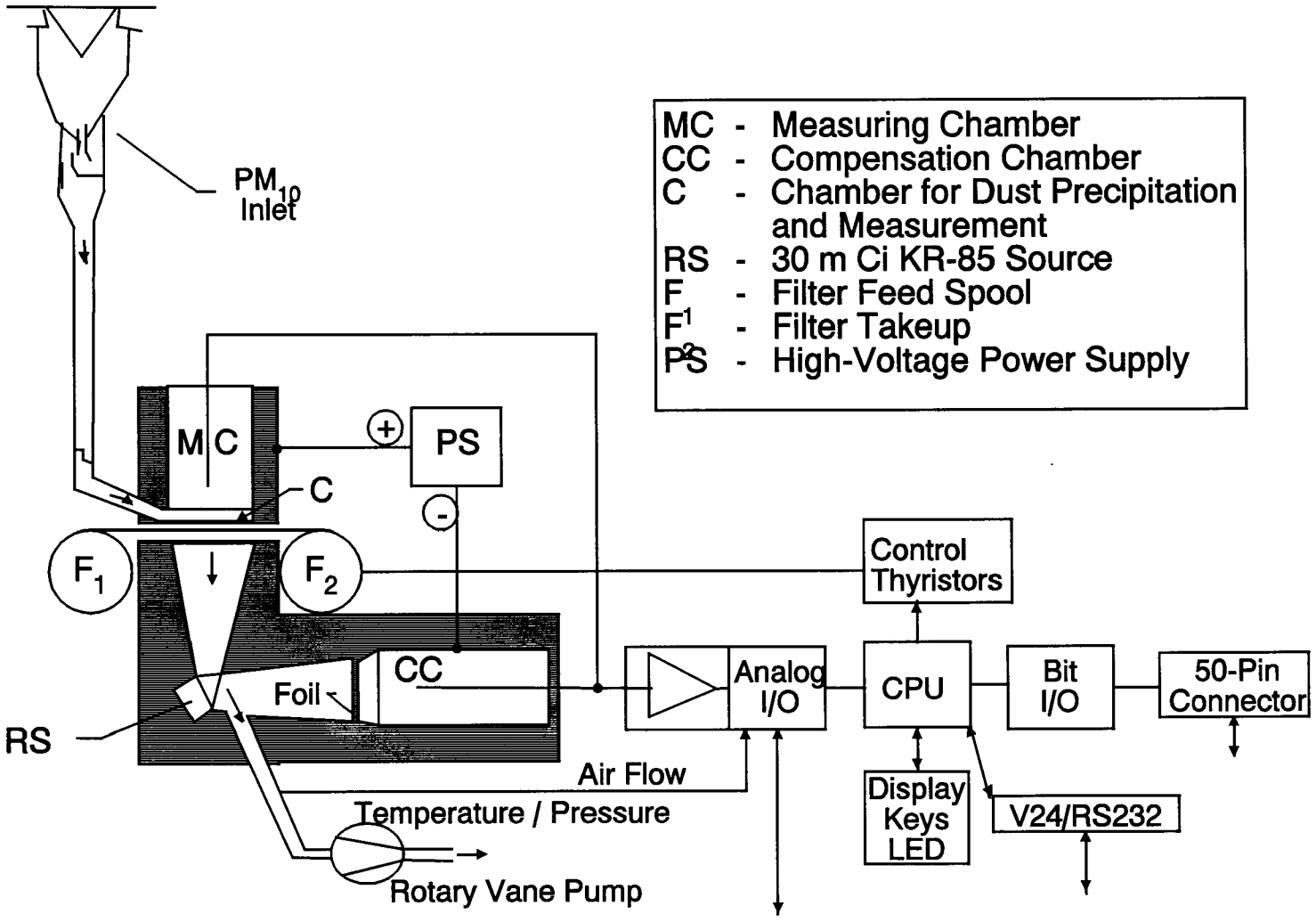

Figure 4-16. Andersen beta gauge sampler.

collocated Wedding PM_{10} gravimetric sampler. It should be noted that the Wedding PM_{10} inlet has typically been reported (see Section 4.2.2.4) to be 10 to 15% lower in collocated field tests with Sierra-Andersen PM_{10} inlets. A WESTAR (1995) council report summarizes the relationships between beta gauge monitors and other direct gravimetric samplers in at least five states in the western U.S. This report concluded that on average beta gauge concentrations were 8.6% lower than other collocated PM_{10} samplers for concentrations $> 20\ \mu g/m^3$. Field data from Wedding and Weigand (1993) at two sites (Fort Collins, CO and Cleveland, OH) using the same samplers produced regressions exhibiting strong correlations ($r^2 = 0.99$) with no apparent outliers and a composite slope of 1.00. Arnold et al. (1992) operated the PM_{10} high volume samplers on the required every-6th-day schedule and the beta attenuation monitors continuously, and noted that only 22.5% of the exceedance days, as measured by the beta monitor, were operational days for the high volume samplers.

4.2.8.5 Nephelometer

The integrating nephelometer is commonly used as a visibility monitor; it measures the light scattered by aerosols, integrated over as wide a range of angles as possible. A schematic diagram of the integrating nephelometer is shown in Figure 4-17 (from Hinds, 1982). The measured scattering coefficient of particles, b_{sp}, can be summed with the absorption coefficient, b_{ap}, and the comparable coefficients for the gas phase to compute the overall atmospheric extinction coefficient, b_{ext}. Methods for estimating absorption and extinction for atmospheric particles are discussed in 8.2.2. The atmospheric extinction has been related to visibility as visual range. The particle scattering coefficient is dependent upon particle size, index of refraction and illumination wavelength, as shown by Charlson et al. (1968) in Figure 4-18, while the absorption coefficient is relatively independent of size. The field calibration of nephelometers has historically been based on the refractive index of Freon-12 (and occasionally carbon dioxide), but newer calibration procedures using atomized sugar aerosols have been proposed (Horvath and Kaller, 1994) as more environmentally conscious. Nephelometry over a narrow wavelength band or at a selected wavelength can be applied to measure the laser light scattered from a volume of aerosol containing a number of

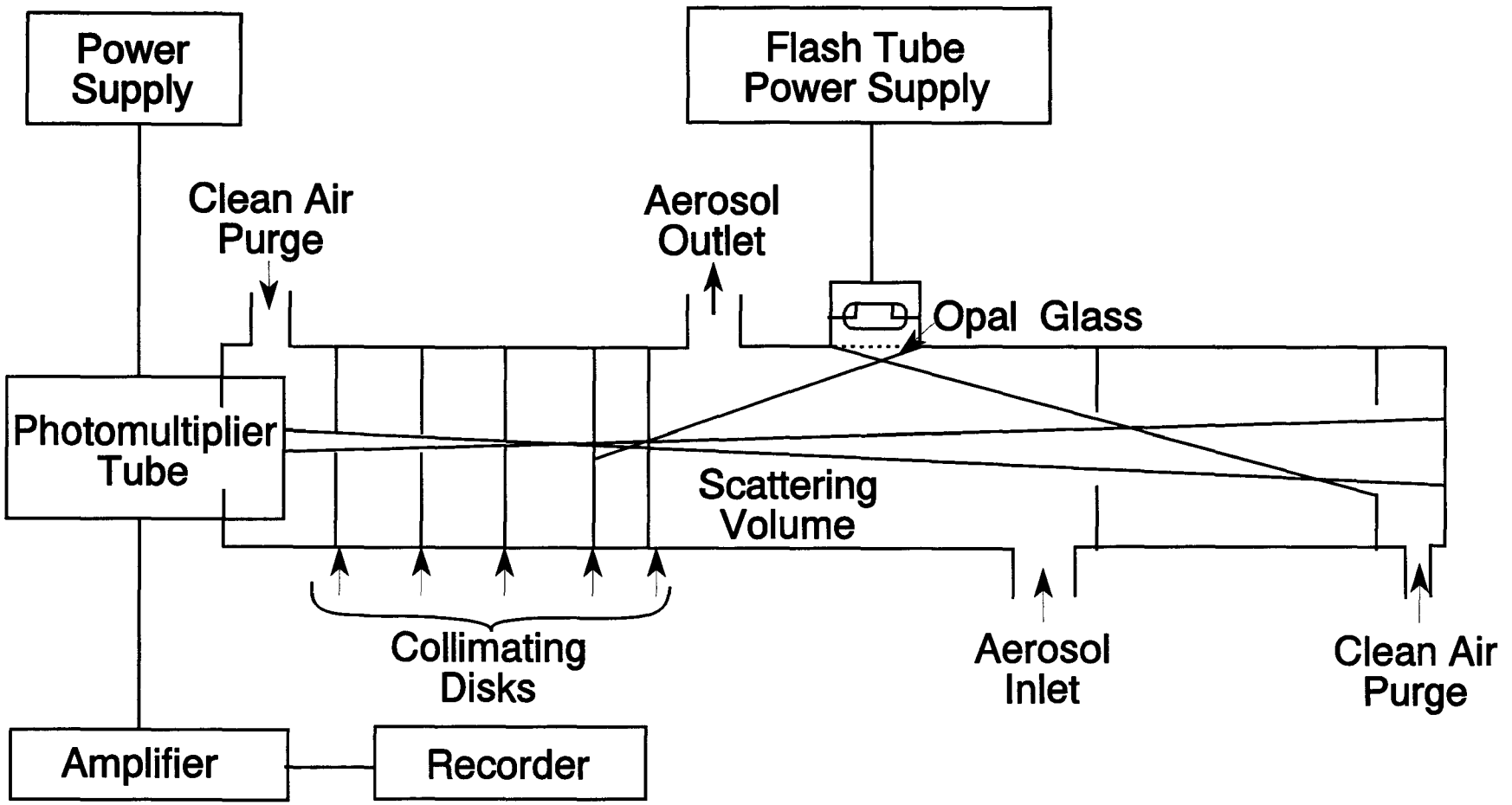

Figure 4-17. Integrating nephelometer.

Source: Hinds (1982).

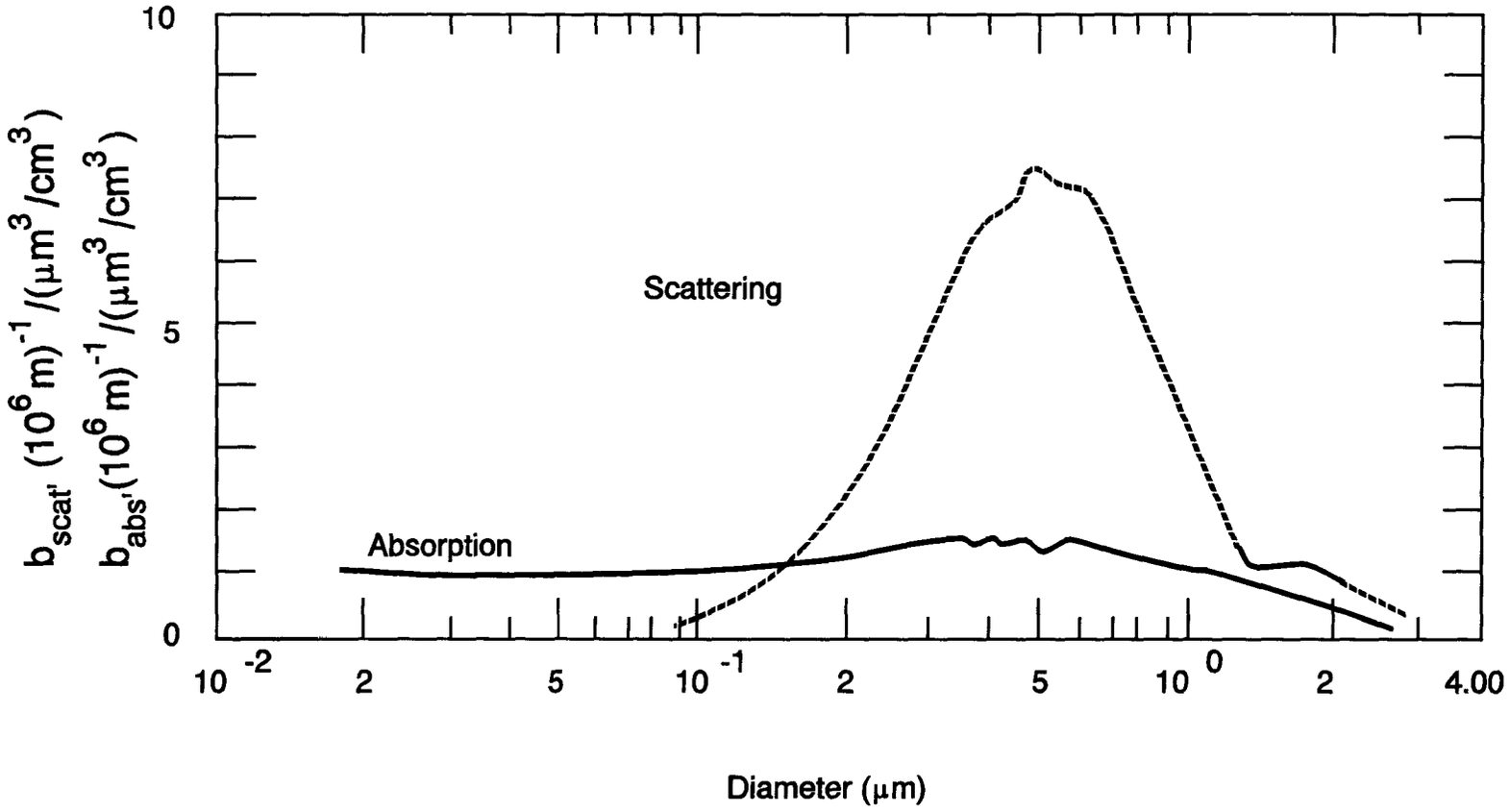

Figure 4-18. Particle-scattering coefficient per volume concentration as a function of particle size for spherical particles of refractive index 1.5 illuminated by 550 nm light.

Source: Charlson et al. (1968).

particles. Gebhart (1993) described devices such as the MIE, Inc.[10]. MINIRAM, often used in portable applications to estimate real-time aerosol concentrations. Cantrell et. al. (1993) showed that MINIRAM calibration was significantly different for diesel and mine aerosols. Woskie et al. (1993) described the performance of a MINIRAM (using the manufacturer's calibration) against gravimetric borate concentrations for particles as large as 30 μm, and found significant biases (a regression slope = 4.48). This bias was expected, since the large mass median particle diameters were substantially outside the respirable particle range recommended by the manufacturer.

The relative insensitivity of the nephelometer to particles above ~ 2 μm results in poor correlations with PM_{10} mass. Larson et al. (1992) showed strong correlations ($r^2 = 0.945$) between b_{sp} and fine fraction mass (see Figure 4-19) for a woodsmoke impacted neighborhood near Seattle, WA, with a slope of 4.89 m^2/g. They noted that this slope fell within the range of values reported by others and was predicted by Mie scattering theory. The slope of the Larson et al. (1992) data could be compared with other site-specific calibrations, such as the data of Waggoner and Weiss (1980), which gave a composite slope of 3.13 m^2/g, characterized by the authors as representative of a "wide range" of sites. Lewis (1981) provided an analysis of the relationships of the features of the ambient size distribution to b_{sp}. The inlet air stream to the nephelometers for the latter data was heated from 5 to 15 °C above background. Rood et al. (1987) conducted a controlled comparison of the influence of aerosol properties on b_{sp} in Riverside, CA and reported a regression slope against fine mass (defined as less than 2.0 μm) of 2.1 m^2/g with an r^2 value of 0.92. In this experiment, the relative humidity for b_{sp} determinations was controlled to less than 35% and the gravimetric filter substrate was nylon. The authors attributed the smaller than normal slope reading to possible nitrate evaporation from the filtered aerosol and artifact reactions with the nylon substrate material. Thomas et al. (1993) demonstrated that the influence of relative humidity on the relationship between photometer response and collocated gravimetric particle concentrations can be predicted.

The data scatter in Figure 4-19 (if assumed to be typical of such comparisons) would suggest that fine particle mass concentration estimates from b_{sp} values were typically within 5 to 7 $\mu g/m^3$ of the gravimetrically determined values. To be useful as a surrogate measure

[10]Bedford, MA.

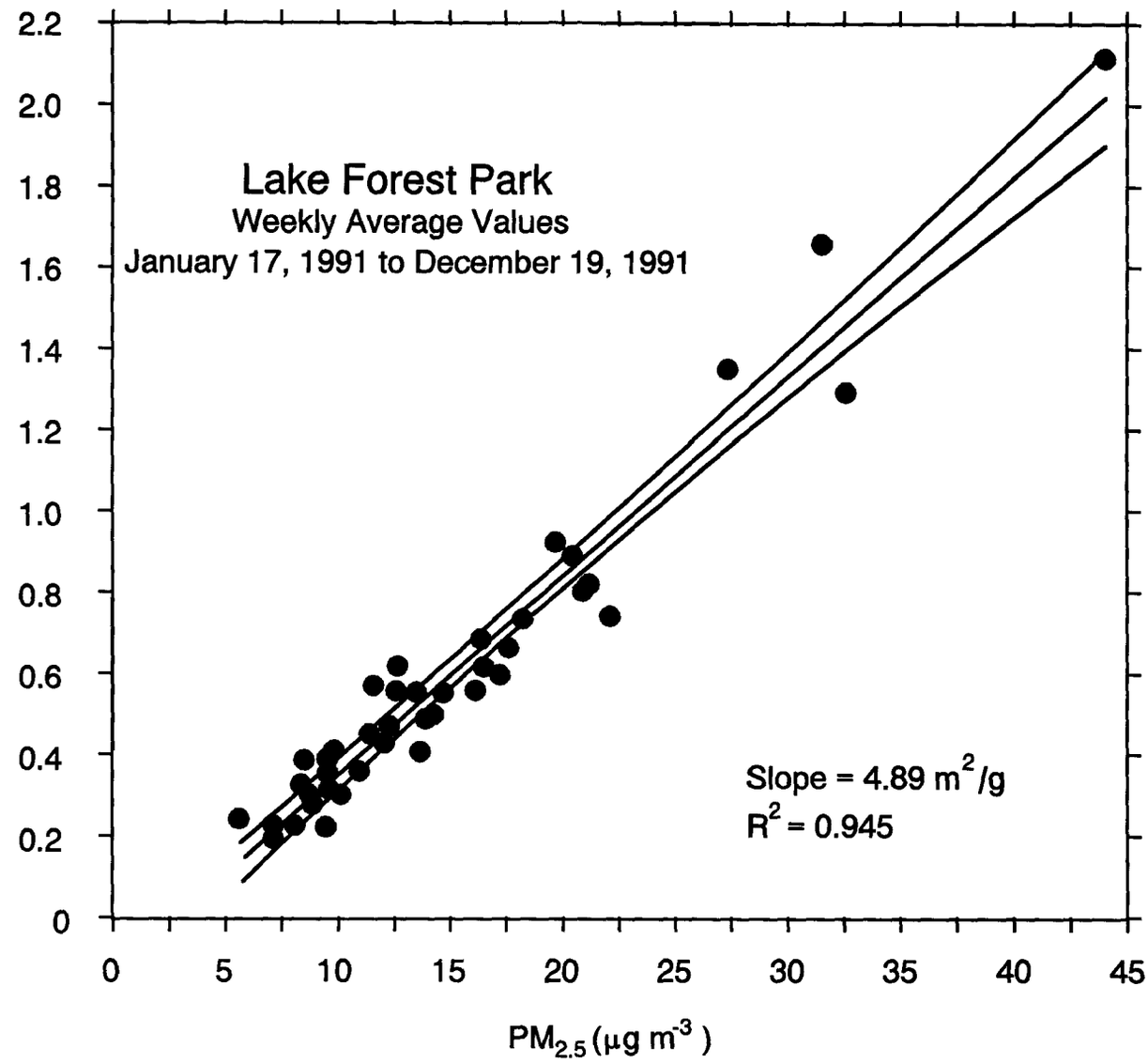

Figure 4-19. Correlation of b_{sp} and fine fraction mass.

Source: Larson et al. (1992).

for mass concentration, the site-specific nephelometer calibration should be valid for a wide range of situations, especially during episodes where the concentration levels approach or exceed an action limit. The scattergram of b_{sp} versus fine particle mass provided by Rood et al. (1987) showed much greater variability, with a given b_{sp} value providing an estimated 20 to 25 $\mu g/m^3$ concentration range. They noted that metastable H_2O contributed 5 to 20% of the total particle light scattering coefficient, especially during the late afternoon and early evening. The precisions and biases of the dependent and independent variables between b_{sp}

and fine mass concentration are not constants, since at least one factor - moisture content of the aerosol - affects both measures. The gravimetric sample filters are typically equilibrated to a specific relative humidity range (e.g., 40 to 60%) to normalize the tare weighings.

Sloane (1986) and others have noted that light scattering from particles is not solely a function of mass but are also very dependent on a summation of the scattering coefficients of each species. The scattering cross section of a particle is dependent on the water content, and, hence, the relative humidity in situ. Pre-heating of the inlet air of the nephelometer normalizes the response to water content, but biases the reading relative to the in situ case. Sloane (1986) also gave the computed and measured scattering coefficients for ammonium sulfate and noted that chemical interactions can cause a two-fold variation in scattering response to a change in the mass of hygroscopic constituents. It was also observed that the light scattering efficiency of an aerosol such as ammonium acid sulfate is not a constant, but varies with the overall aerosol composition. Eldering et al. (1994) developed and validated a predictive model for b_{sp} in Southern California. This model used composite size distributions constructed from a TSI, Inc.[11] EAA, a PMS, Inc.[12] LAS-X and a Climet, Inc.[13] multi-channel OPC, and filter-based estimates of refractive indices for ammonium sulfate, ammonium nitrate, organic carbon, elemental carbon and residual aerosol mass concentrations as independent variables. The quality of their comparisons with nephelometer data suggested that this approach could be used to test models that predict visual range from source emissions. Further research is needed to determine the effectiveness of the integrating nephelometer as a predictor of fine particle mass concentrations.

4.2.9 Specialized Sampling

4.2.9.1 Personal Exposure Sampling

The application of aerosol measurement technologies to smaller and less obtrusive samplers have resulted in devices used as fixed-location indoor aerosol samplers and personal exposure monitors (PEMs) worn on the body to estimate exposure. The reduction in physical size of personal aerosol sampling systems to reduce participant burden sometimes

[11]Minneapolis, MN.
[12]Boulder, CO.
[13]Redlands, CA.

results in poorer aerosol collection performance as compared to the outdoor counterparts. Wiener and Rodes (1993) noted that personal sampling systems generally have poorer precisions than outdoor aerosol samplers, due to the smaller sampler collections (from lower flowrates) and poorer flow controllers. Özkaynak et al. (1993) reported that the precisions of collocated PEMs in the PTEAM study operating at 4.01 pm for a 12-h period were 3 to 4% (RSD). Wallace et al. (1994) reported biases for the Particle Total Exposure Assessment Methodology study averaging a factor of two between personal exposure measurements and fixed location PM_{10} concentrations. He was unable to completely account for the biases, but attributed portions to proximity to indoor sources, a difference in inlet cutpoints (11.7 μm versus 10.0 μm) and the collection of aerosols from the "personal cloud" caused by body dander. Rodes et al. (1991) showed that the ratio of personal to indoor aerosol measurements for the EPA PTEAM study appeared to be log-normally distributed with a median value of 1.98 and an unexpectedly high value of 3.7 at the 90th ("most exposed") percentile. Ingham and Yan (1994) suggested that the performance of a personal aerosol sampling inlet in an isolated mode (without mounting on a representative humanoid bluff body) can result in substantial under-sampling for larger particles. The relationship between measured aerosol exposure at some external location on the body and actual uptake through oral and nasal entry is very complex.

Buckley et al. (1991) described the collection efficiency of an MSP, Inc.[14] personal aerosol sampler at 4.0 lpm as shown in Figure 4-20. They evaluated this sampler in a field comparison study with collocated PM_{10} high volume and dichotomous samplers. The precision for the personal sampler was found to be very good (CV = $\pm 3.2\%$) with strong correlations ($r^2 = 0.970$) with the dichotomous samplers. Lioy et al. (1988) described a similar comparison for a 10 lpm Air Diagnostics and Engineering, Inc.[15] indoor air sampler, with a PM10 inlet characterized by Marple et al. (1987). Correlations against the PM10 dichotomous sampler were also described as very strong ($r^2 > 0.970$), but noted a substantial bias caused by the loss of fragments from indoor air sampler's glass fiber filters. They recommended that exposure studies using samplers that collect small total volumes should utilize filters with greater integrity, such as Teflon. Colome et al. (1992) describe an

[14]Minneapolis, MN.
[15]Naples, ME.

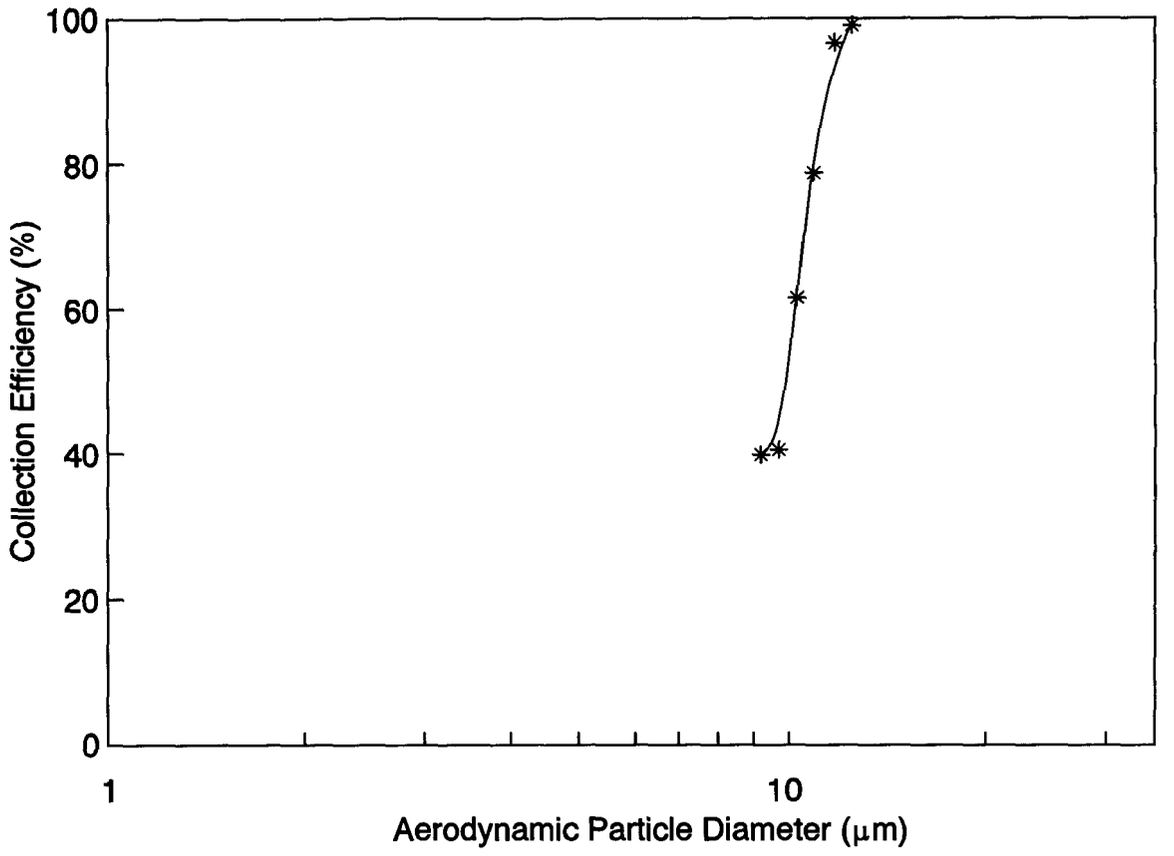

Figure 4-20. Collection efficiency of the MSP personal aerosol sampler inlet.

Source: Buckley et al. (1991).

indoor/outdoor sampling study using an impactor characterized by Marple et al. (1987) with a PM_{10} cutpoint that had duplicate impactors with the same cutpoint in series. This sequential arrangement, in combination with a coating of 100 μl of light oil, was used to minimize particle bounce at 4.0 lpm for 24 h period.

Personal aerosol sampler systems have typically been characterized as burdensome (excessive weight, size, noise). The success of passive detector badges for gaseous pollutants has recently prompted research into passive aerosol samplers. Brown et al. (1994) described a prototype aerosol sampler utilizing electrostatic charge to move the particles to a collection substrate. They noted that preliminary results are encouraging, but the effective sampling rate and size-selectivity of the sampler was dependent on the electrical mobility of the aerosol. This posed calibration problems for real aerosols with a distribution of electrical

mobility's. Holländer (1992) described a passive pulsed-corona sampler that has similar collection characteristics as a PM_{10} inlet, with only modest wind speed dependence.

The performance characterization of PEMs has been considered for occupational settings by Kenny and Lidén (1989), who reviewed the ACGIH, National Institute for Occupational Safety and Health (NIOSH), and EPA PM_{10} aerosol sampler performance programs. They proposed that an international consensus be reached on the basic principles underlying the experimental protocols for testing personal samplers, as an essential prerequisite to the setting of standards. An ISO working group has made progress in developing such a consensus (Kenny, 1992). As EPA becomes more focused on exposure assessment and personal exposure sampling, it will become even more important for the agency to consider establishing performance specifications for personal aerosol samplers.

Models have become powerful tools in understanding aerosol behavior in the vicinity of personal exposure samplers. This is demonstrated by particle trajectory models that can predict the influences of the geometries and flow field on aerosol capture and losses (e.g., Okazaki and Willeke, 1987, Ingham and Yan, 1994, and Tsai and Vincent, 1993). These models have not only permitted more rapid design changes to accommodate new cutpoints and flowrates, but have added insights as to the influence of air flow obstructions on sampling efficiencies. Vincent and Mark (1982) suggested that there is a critical particle trajectory that determines whether a particle is sampled or rejected by an inlet worn on the body. An extension of this model applicable to personal exposure sampling by Ingham and Yan (1994) suggested that testing the performance of a personal aerosol sampling inlet in an isolated mode (without mounting the inlet on a representative bluff body) can result in under-sampling for larger particles by a factor of two. Validation of this model may explain a portion of the bias reported by Wallace et al. (1994) between personal and indoor sampler measurements.

4.2.9.2 Receptor Model Sampling

Receptor modeling has become an established tool to relate ambient concentrations of pollutants to major source categories, by apportioning the components in collected ambient aerosol samples using complimentary source "signatures". Various approaches developed for constructing source/receptor relationships were described by Henry et al. (1984), who also

provided a review of modeling fundamentals. They listed the advantages and disadvantages of multivariate models and discussed multi-collinearity problems associated with the presence of two or more sources with nearly identical signatures. Javitz et al. (1988) described the basic Chemical Mass Balance (CMB) approach and showed the influence of the variance in identifying a component in the source signature sample on the projected apportionment. Dzubay et al. (1984) described aerosol source and receptor collection schemes that permitted the separation of ambient samples into fine and coarse fractions for mass, elemental and volatile carbon, and metals analyses. Stevens and Pace (1984) suggested the addition of Scanning Electron Microscopy to permit additional categorization using x-ray diffraction analysis. The most widely used aerosol receptor model is the EPA CMB 7.0 model described by Watson et al. (1990). This paper describes the structure of the model and computer code and the data requirements to evaluate the validity of the estimates. Numerous papers have been published describing the applications of receptor models to the apportionment of the sources of aerosols, with the receptor modeling conference summary by Watson et al. (1989b) descriptive of the state-of-the-art.

Stevens et al. (1993) described (see Figure 4-21) a modified dichotomous sampler with a PM_{10} inlet, two Fine channels operating at 15 lpm and one coarse channel operating at 2.0 lpm, designated as the Versatile Air Pollution Sampler (VAPS). The additional fine fraction channel permitted sampling on a 47 mm Teflon filter for elemental analysis and a 47-mm quartz filter for carbon speciation (elemental and volatile). A Nuclepore filter was used on the Coarse channel for Scanning Electron Microscopy (SEM) evaluation and energy dispersive x-ray diffraction analysis for selected particles.

4.2.9.3 Particle Acidity

An emphasis was placed on sampling sulfuric acidic aerosols in the 1982 Criteria Document. This was followed by a number of research efforts (e.g., Ferm, 1986; Koutrakis et al., 1988; Pierson et. al., 1989) to identify and study the in situ rate reactions, develop sampling strategies to representatively remove the acid particle from the air, identify the co-existing reactive species (e.g., ammonia, nitric acid, aerosol sulfates and nitrates), and protect the collected aerosol prior to analysis. A "Standard" and an "Enhanced" method were subsequently described (U.S. Environmental Protection Agency, 1992) for the

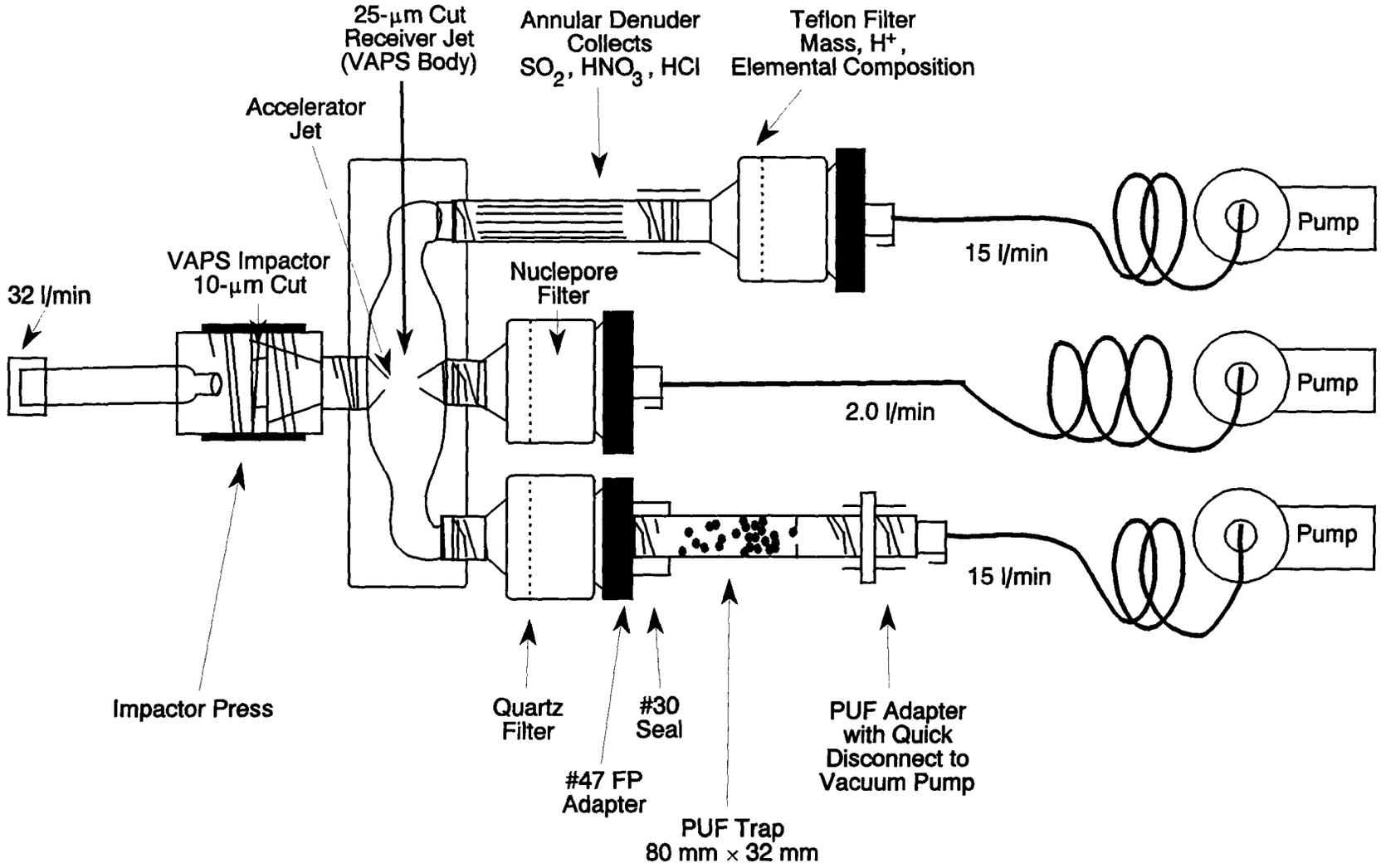

Figure 4-21. Modified dichotomous sampler (VAPS).

Source: Stevens et al. (1993).

determination of aerosol acidity (titratable H+) using annular denuder technology. The "Standard" method did not account for potential interferences from nitric acid, ammonium nitrate aerosol, or other ammonium salts. The "Enhanced" method added an additional denuder prior to filtration, with nylon and treated glass fiber backup filters to account for these species. These sampling technologies utilized either an inlet impactor or a cyclone with 2.5 μm cutpoints to sample the fine fraction. This technology has recently been extended to other reactive aerosol systems, including semi-volatile organics (e.g., Vossler et al., 1988). Bennett et al. (1994) describe a $PM_{2.5}$ cyclone-based, filter pack sampling system designed for fine particle network sampling and acidity measurements, as part of the Acid MODES program. The sampler operated at 8.8 lpm, and was designed to selectively remove ammonia, speciate gas and particle phase sulfur compounds, as well as collect gas phase nitric acid. An intercomparison of 18 nitric acid measurement methods was reported by Hering et al. (1988), who noted that measurements differed by as much as a factor of four and biases increased as nitric acid loadings increased. In general the filter pack systems reported the highest acidity measurements, while the denuder-difference techniques reported significantly lower measurements. Benner et al. (1991) in a comparison of the SCENES filter pack sampler with a denuder-based sampler found excellent agreement between sampler types for both nitric acid and total nitrates. They attributed the close agreement to limited positive artifact formation, since the test field site had high nitric acid gas to particulate nitrate ratios. John et al. (1988) noted that internal aluminum sampler surfaces denude nitric acid, and describe the design of an aluminum denuder for the inlet of a commercially available dichotomous sampler to quantitatively remove nitric acid for extended periods.

Brauer et al. (1989) describe the design of a miniature personal sampler to collect acid aerosols and gases. A significant finding was the lower than expected personal acidity levels, attributed to the "personal cloud" production of ammonia by the body. Personal exposure levels of acid aerosols were reported to be lower than indoor measurements.

4.2.10 Measurement Method Comparisons

4.2.10.1 Nitrate

Methods for measuring particle nitrate and gaseous nitric acid were compared in the field as part of the 1985 Nitrogen Species Methods Comparison Study conducted over an

8-day period in the summer of 1985 in Claremont, CA (Hering et al., 1988). Particle nitrate methods included sampling with filter packs (teflon and nylon filters operated in series), sampling with nylon or impregnated filters operated downstream of a denuder to remove vapor nitric acid (Possanzini et al., 1983; Shaw et al., 1982; Appel et al., 1981), and sampling with an impactor (Wall et al., 1988). Results from that study showed that the precision for identical samplers was about 4% (Anlauf et al., 1988; Solomon et al., 1988). Denuded nylon filter methods were used in 6 different samplers operated by 4 different groups (Appel et al., 1988; John et al., 1988; Pierson et al., 1988; Solomon et al., 1988). Data from these 6 methods show no systematic bias among samplers. The average measurement precision (coefficient of variation) was 11%. Impactor results were also in agreement with that from the denuded nylon filters (Wall et al., 1988). In contrast, fine particle nitrate values from teflon filter of the filter packs were 43 to 59% lower than those measured by denuded nylon filters, with higher discrepancies for longer sampling times (Soloman et al., 1988). The lower results on filter pack sampling are due to the volatilization of nitrate particles from the filter. The vaporized nitrate is measured as nitric acid on the backup filter (Hering et al., 1988; Solomon et al., 1988). To summarize, sampling with denuded nylon filters or with impactors gave equivalent values for fine particle nitrate, whereas teflon filter sampling was biased low due to the volatilization losses.

The results of the 1985 Nitrogen Species Methods Comparison Study were confirmed by data collection as part of the 1987 Southern California Air Quality Study (Chow et al., 1994). In this study, sampling times were 4 to 7 h. Samples were retrieved immediately, within 30 minutes of the end of sampling. Fine particle samples were collected by teflon filters, by denuded nylon filters and by impactors. Results, stratified by time of day and season, are illustrated in Figures 4-22 and 4-23 for central Los Angeles, CA and Claremont, CA, respectively. Losses from the teflon filters are greatest in the summer, especially for daytime samples (10 a.m. to 2 p.m., and 2 p.m. to 6 p.m.). Over 11 summer sampling days at 8 basin locations for Claremont, CA, an average of 79% or 9.9$\mu g/m^3$ of the fine particle nitrate was volatilized from the teflon filters for summer daytime sampling. For nighttime and morning samples, 40% was lost. The percentage losses are smaller for winter samples, but the absolute magnitude remains high at 8.9 $\mu g/m^3$ for daytime samples. Impactor data are in much closer agreement with those from the denuded nylon filter than the teflon filter.

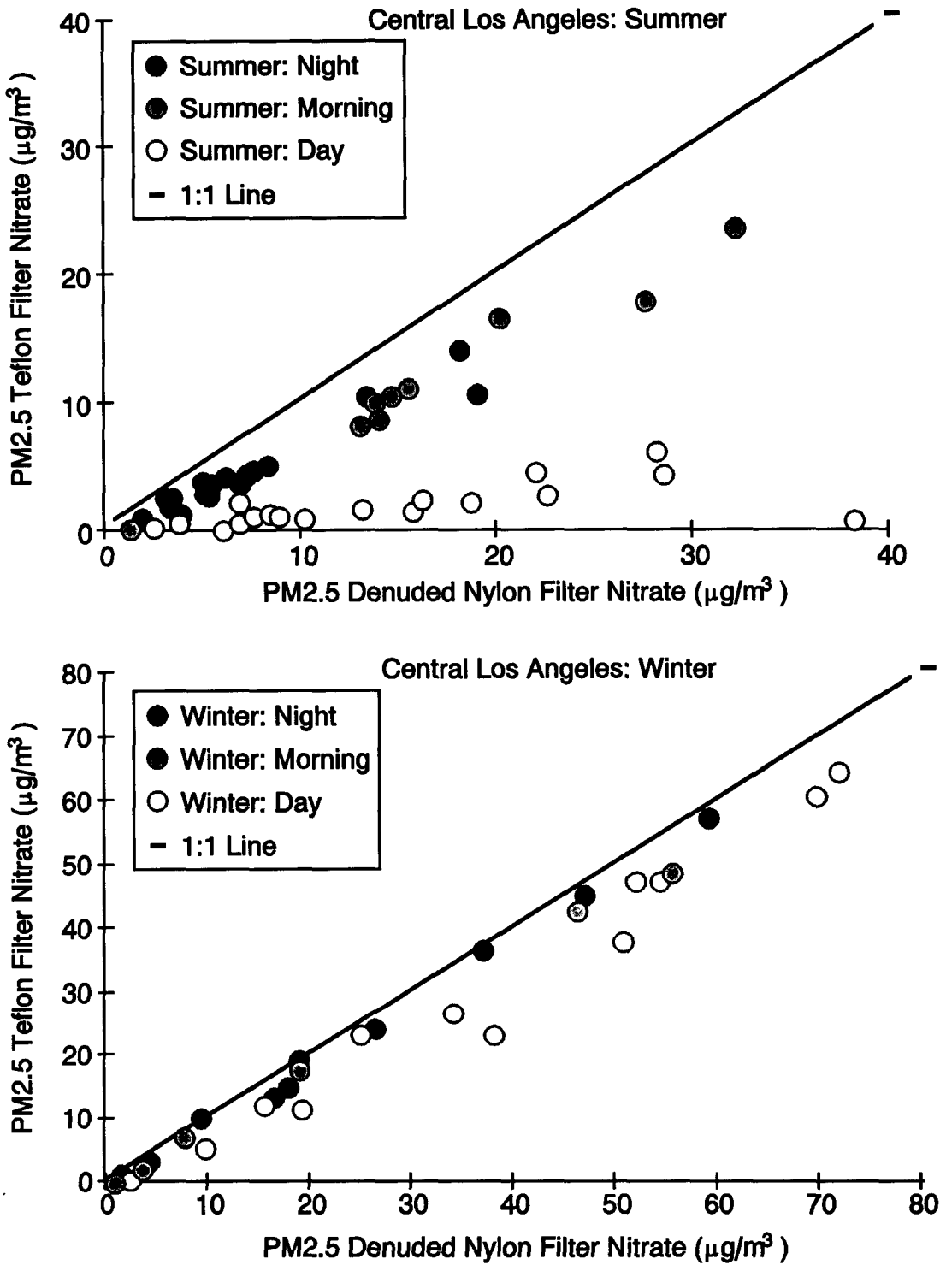

Figure 4-22. Comparison of $PM_{2.5}$ nitrate mass measurements from Teflon® filter versus denuded nylon filter sample collection for Los Angeles, CA.

Source: Chow, et al. (1994).

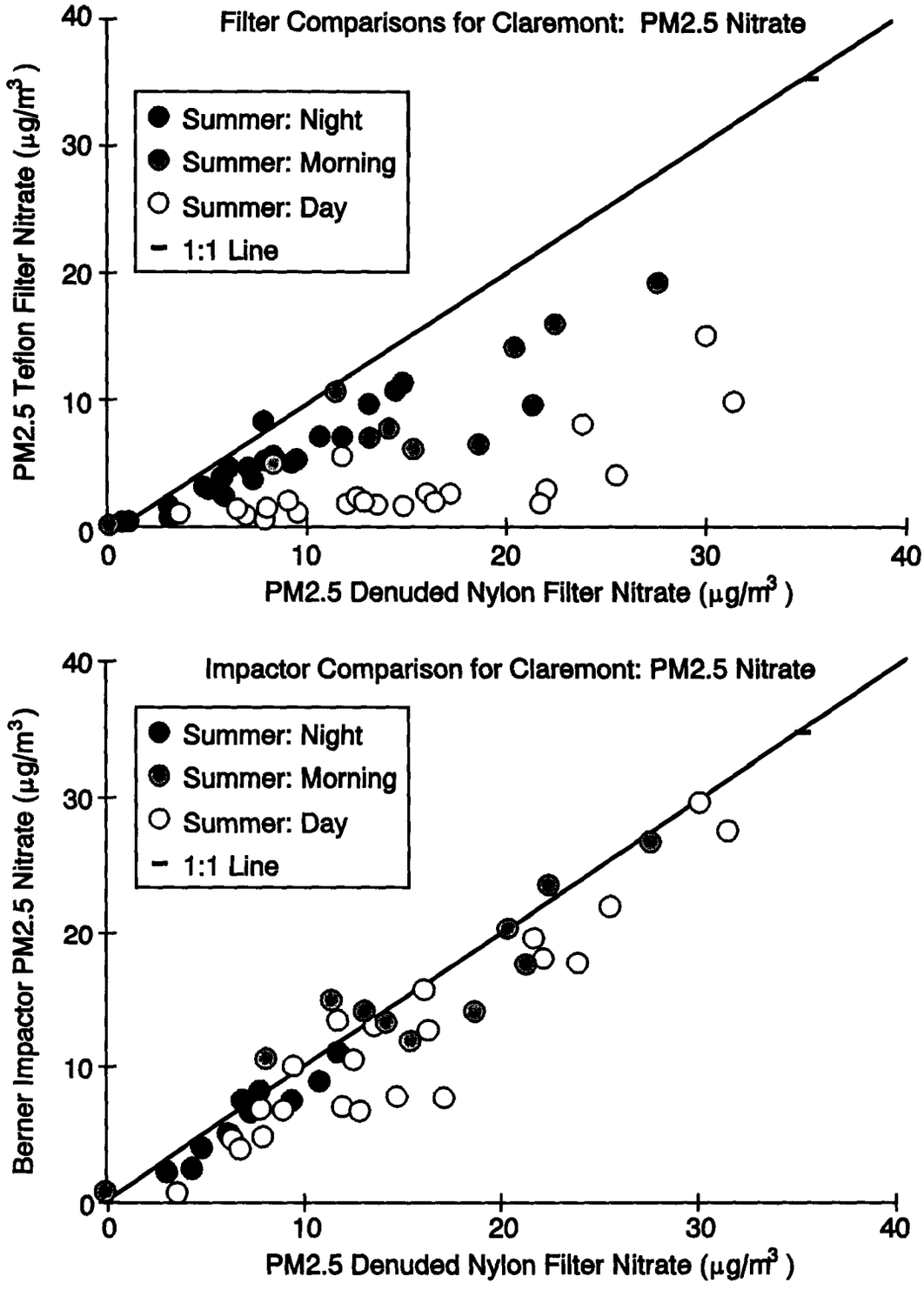

Figure 4-23. Comparison of $PM_{2.5}$ nitrate mass measurements from Teflon® filter versus denuded nylon filter sample collection for Claremont, CA.

Source: Chow, et al. (1994).

4.2.10.2 Carbonaceous Particulate Matter

Methods for measuring carbonaceous aerosol, classified as either "organic" or "black" carbon, were compared in a similar study conducted in the summer of 1986 in Glendora, CA (Hering et al., 1990). In that study, analytical methods were compared, as were differences in simultaneous ambient sampling of $PM_{2.5}$ aerosol with quartz filters, adsorption-corrected quartz filters and two types of impactors. The results showed generally good agreement among analytical methods for total carbon, with 5 of the 6 laboratories reporting values within 9% of each other. In contrast, ambient sampling results showed variations among methods. Quartz filter results, whether or not corrected for carbon vapor adsorption were within 40% of each other. Concentrations from impactors, exclusive of after-filter, were lower than the mean from the filter samplers by as much as 50%. Addition of the after-filter carbon brought impactor values to within 10% of the mean, but the lack of "black" carbon on these after-filters leads to the conclusion that vapor adsorption led to a positive bias for quartz filter sampling on these days. Similar results were found for the 1987 Southern California Air Quality Study, for which impactor measurements of carbon were systematically lower than filter measurements (Chow, et al., 1994).

4.3 ANALYSIS OF PARTICULATE MATTER

The interest in the composition of aerosol particles lies in the areas of: (1) explaining and inventorying the observed mass, (2) establishing the effect of aerosols on health and welfare, and (3) attributing ambient aerosols to pollution sources. While any compositional measurement will address one or more of these goals, certain methods excel for specific tasks. In general, no single method can measure all chemical species, and comprehensive aerosol characterization programs use a combination of methods to address complex needs. This allows each method to be optimized for its objective, rather than be compromised to achieve goals unsuitable to the technique. Such programs also greatly aid quality assurance objectives, since confidence may be placed in the accuracy of a result when it is obtained by two or more methods on different substrates and independent samplers.

In the sections that follow, some of the more commonly used methods that address the goals stated above are described. The sections are designed to be illustrative rather than

exhaustive, since new methods are constantly appearing as old methods are being improved. These chemical analysis methods for the following section are divided into four categories: (1) mass, (2) elements, (3) water-soluble ions, and (4) organics. Material balance comparing the sum of the chemical species to the PM mass concentrations show that elements, water soluble ions, and organic and elemental carbon typically explain 65 to 85% of the measured mass and are adequate to characterized the chemical composition of measured mass for filter samples collected in most urban and non-urban areas. Some of these chemical analysis methods are non-destructive, and these are preferred because they preserve the filter for other uses. Methods which require destruction of the filter are best performed on a section of the filter to save a portion of the filter of other analyses or as a quality control check on the same analysis method. Table 4-2 identifies the elements and chemical compounds commonly found in air using these methods with typical detection limits.

Less common analytical methods, which are applied to a small number of specially-taken samples, include isotopic abundances (Jackson, 1981; Currie, 1982; Hirose and Sugimura, 1984); mineral compounds (Davis, 1978, 1980; Schipper et al., 1993); and functional groups (Mylonas et al., 1991; Palen et al., 1992; 1993; Allen et al., 1994). Recent advances in infrared optics and detectors have resulted in the quantitative determination of the major functional groups (e.g., sulfate, nitrate, aliphatic carbons, carbonyl carbons, organonitrates, and alcohols) in the atmospheric aerosol (Allen et al., 1994). The advantages of functional analysis in source apportionment are that the number of functional groups is much less than the number of organic compounds to be classified. The cited references provide information on sampling and analysis methods for these highly-specialized methods.

The following section focuses on:

- Physical analysis of elements and single particle size, shape, and composition,
- Wet chemical analysis of anions and cations, and
- Organic analysis of organic compounds and elemental/organic carbon.

TABLE 4-2. INSTRUMENTAL DETECTION LIMITS FOR PARTICLES ON FILTERS

	Minimum Detection Limit in ng/m^3[a]								
	ICP/ AES[b,d]	AA Flame[b,d]	AA Furnace[b]	INAA[b,f]	PIXE[g]	XRF[c]	IC[b]	AC[b]	TOR[b]
Be	0.06	2[d]	0.05	NA[h]	NA	NA	NA	NA	NA
Na	NA	0.2[d]	< 0.05	2	60	NA	NA	NA	NA
Mg	0.02	0.3	0.004	300	20	NA	NA	NA	NA
Al	20	30	0.01	24	12	5	NA	NA	NA
Si	3	85	0.1	NA	9	3	NA	NA	NA
P	50	100,000	40	NA	8	3	NA	NA	NA
S	10	NA	NA	6,000	8	2	NA	NA	NA
Cl	NA	NA	NA	5	8	5	NA	NA	NA
K	NA	2[d]	0.02	24	5	3	NA	NA	NA
Ca	0.04	1[d]	0.05	94	4	2	NA	NA	NA
Sc	0.06	50	NA	0.001	NA	NA	NA	NA	NA
Ti	0.3	95	NA	65	3	2	NA	NA	NA
V	0.7	52	0.2	0.6	3	1	NA	NA	NA
Cr	2	2	0.01	0.2	2	1	NA	NA	NA
Mn	0.1	1	0.01	0.12	2	0.8	NA	NA	NA
Fe	0.5	4	0.02	4	2	0.7	NA	NA	NA
Co	1	6[d]	0.02	0.02	NA	0.4	NA	NA	NA
Ni	2	5	0.1	NA	1	0.4	NA	NA	NA
Cu	0.3	4	0.02	30	1	0.5	NA	NA	NA
Zn	1	1	0.001	3	1	0.5	NA	NA	NA
Ga	42	52	NA	0.5	1	0.9	NA	NA	NA
As	50	100	0.2	0.2	1	0.8	NA	NA	NA
Se	25	100	0.5	0.06	1	0.6	NA	NA	NA
Br	NA	NA	NA	0.4	1	0.5	NA	NA	NA
Rb	NA	NA	NA	6	2	0.5	NA	NA	NA
Sr	0.03	4	0.2	18	2	0.5	NA	NA	NA
Y	0.1	300	NA	NA	NA	0.6	NA	NA	NA
Zr	0.6	1000	NA	NA	3	0.8	NA	NA	NA
Mo	5	31	0.02	NA	5	1	NA	NA	NA
Pd	42	10	NA	NA	NA	5	NA	NA	NA
Ag	1	4	0.005	0.12	NA	6	NA	NA	NA
Cd	0.4	1	0.003	4	NA	6	NA	NA	NA
In	63	31	NA	0.006	NA	6	NA	NA	NA
Sn	21	31	0.2	NA	NA	8	NA	NA	NA

TABLE 4-2 (cont'd). INSTRUMENTAL DETECTION LIMITS FOR PARTICLES ON FILTERS

	Minimum Detection Limit in ng/m^3[a]								
Species	ICP/ AES[b,d]	AA Flame[b,d]	AA Furnace[b]	INAA[b,f]	PIXE[g]	XRF[c]	IC[b]	AC[b]	TOR[b]
Sb	31	31	0.2	0.06	NA	9	NA	NA	NA
I	NA	NA	NA	1	NA	NA	NA	NA	NA
Cs	NA	NA	NA	0.03	NA	NA	NA	NA	NA
Ba	0.05	8[d]	0.04	6	NA	25	NA	NA	NA
La	10	2,000	NA	0.05	NA	30	NA	NA	NA
Au	2.1	21	0.1	NA	NA	2	NA	NA	NA
Hg	26	500	21	NA	NA	1	NA	NA	NA
Tl	42	21	0.1	NA	NA	1	NA	NA	NA
Pb	10	10	0.05	NA	3	1	NA	NA	NA
Ce	52	NA	NA	0.06	NA	NA	NA	NA	NA
Sm	52	2,000	NA	0.01	NA	NA	NA	NA	NA
Eu	0.08	21	NA	0.006	NA	NA	NA	NA	NA
Hf	16	2,000	NA	0.01	NA	NA	NA	NA	NA
Ta	26	2,000	NA	0.02	NA	NA	NA	NA	NA
W	31	1,000	NA	0.2	NA	NA	NA	NA	NA
Th	63	NA	NA	0.01	NA	NA	NA	NA	NA
U	21	25,000	NA	NA	NA	1	NA	NA	NA
Cl-	NA	NA	NA	NA	NA	NA	50	NA	NA
NO_3^-	NA	NA	NA	NA	NA	NA	50	NA	NA
$SO_4^=$	NA	NA	NA	NA	NA	NA	50	NA	NA
NH_4^+	NA	NA	NA	NA	NA	NA	NA	50	NA
OC	NA	NA	NA	NA	NA	NA	NA	NA	100
EC	NA	NA	NA	NA	NA	NA	NA	NA	100

[a]Minimum detection limit is three times the standard deviation of the blank for a filter of 1 mg/cm^2 areal density.
ICP/AES = Inductively Coupled Plasma with Atomic Emission Spectroscopy.
AA = Atomic Absorption Spectrophotometry.
PIXE = Proton Induced X-ray Emissions Spectrometry.
XRF = Non-Dispersive X-ray Fluorescence Spectrometry.
INAA = Instrumental Neutron Activation Analysis.
IC = Ion Chromatography.
AC = Automated Colorimetry.
TOR = Thermal Optical Reflectance.
[b]Concentration is based on the extraction of 1/2 of a 47 mm quartz-fiber filter in 15 ml of deionized-distilled water, with a nominal flow rate of 20 L/min for 24-h samples.
[c]Concentration is based on 13.8 cm^2 deposit area for a 47 mm ringed teflon-membrane filter, with a nominal flow rate of 20 L/min for 24-h samples with 100 sec radiation time.
[d]Harman (1989).
[e]Fernandez de la Mora (1989).
[f]Olmez (1989).
[g]Eldred et al. (1993).
[h]Not Available.

4.3.1 Mass Measurement Methods

Particulate mass concentration is the most commonly made measurement on aerosol samples. It is used to determine compliance with PM_{10} standards and to select certain samples for more detailed, and more expensive, chemical analyses. As noted in Section 2, the beta attenuation and inertial microbalance methods have been incorporated into in situ measurement systems which acquire real-time mass measurements. Gravimetric analysis is used almost exclusively to obtain mass measurements of filters in a laboratory environment. The U.S. Environmental Protection Agency (1976) has published detailed procedures for mass analyses associated with 20.32 cm × 25.40 cm fiber filters, but the guidance for other types of filters used for chemical analyses is less well documented.

Gravimetry measures the net mass on a filter by weighing the filter before and after sampling with a balance in a temperature- and relative humidity-controlled environment. PM_{10} reference methods require that filters be equilibrated for 24 h at a constant (within ±5%) relative humidity between 20 and 40% and at a constant (within ±3 °C) temperature between 15 and 30 °C. These are intended to minimize the liquid water associated with soluble compounds and to minimize the loss of volatile species. Nominal values of 30% RH and 15 to 20 °C best conserve the particle deposits during sample weighing.

Balances used to weigh 20.32 cm × 25.40 cm filters from high volume PM_{10} samples must have a sensitivity of at least 100 μg. Balances used for medium volume PM_{10} samples should have a sensitivity of at least 10 μg, and those used for low-volume PM_{10} samples should have a sensitivity of at least 1 μg. Modifications to the balance chamber are sometimes needed to accommodate filters of different sizes. All filters, even those from high-volume PM_{10} samplers, should be handled with gloved hands when subsequent chemical analyses are a possibility.

Balance calibrations should be established before and after each weighing session using Class M and Class S standards, and they should be verified with a standard mass every 10 filters. Approximately one out of ten filters should be re-weighed by a different person at a later time. These re-weights should be used to calculate the precision of the measurement as outlined by Watson et al. (1989a).

Feeney et al. (1984) examined the gravimetric measurement of lightly loaded membrane filters and obtained excellent precision and accuracy. The sensitivity of the electrobalance is

about ± 0.001 mg, though tolerances on re-weights of Teflon-membrane filters are typically ± 0.010 mg. The main interference in gravimetric analysis of filters results from electrostatic effects. Engelbrecht et al. (1980) found that residual charge on a filter could produce an electrostatic interaction between the filter on the pan and the metal casing of the electrobalance. This charge can be removed by exposing the filter to a radioactive polonium source before and during sample weighing.

Beta attenuation methods have been applied in the laboratory as well as in the field, and the results are comparable to those of gravimetric measurements. The precision of beta-gauge measurements has been shown to be ± 5 $\mu g/m^3$ or better for counting intervals of one minute per sample, which translates into ± 32 μg/filter for 37 mm diameter substrates. This is substantially higher than the ± 6 μg/filter precision determined by gravimetric analysis using an electrobalance (Feeney et al., 1984). Jaklevic et al. (1981) found equivalent accuracy and precision for both techniques as they were used in that study. Courtney et al. (1982) found beta attenuation and gravimetric mass measurements to differ by less than $\pm 5\%$. Patashnick and Rupprecht (1991) examine results from TEOM samplers operated alongside filter-based PM_{10} samplers, and Shimp (1988) reports comparisons with beta attenuation field monitors; these comparisons all show good agreement for mass measurements.

4.3.2 Physical Analysis

The most common interest in elemental composition derives from concerns about health effects and the utility of these elements to trace the sources of suspended particles. Instrumental neutron activation analysis (INAA), photon-induced x-ray fluorescence (XRF), particle-induced x-ray emission (PIXE), atomic absorption spectrophotometry (AAS), inductively-coupled plasma with atomic emission spectroscopy (ICP/AES), and scanning electron microscopy with x-ray fluorescence (SEM/XRF) have all been applied to elemental measurements of aerosol samples. AAS and ICP/AES are also appropriate for ion measurements when the particles are extracted in deionized-distilled water (DDW). Since air filters contain very small particle deposits (20 to 100 $\mu g/cm^2$), preference is given to methods that can accommodate small sample sizes. XRF and PIXE leave the sample intact after analysis so that it can be submitted to additional examinations by other methods. Excellent

agreement was found for the intercomparison of elements acquired form the XRF and PIXE analyses (Cahill, 1980). The analytical measurement specifications of air filter samples for the different elemental analysis is shown in Table 4-2.

4.3.2.1 X-Ray Fluorescence of Trace Elements

In x-ray fluorescence (XRF) (Dzubay and Stevens, 1975; Hammerle and Pierson, 1975; Jaklevic et al., 1977; Torok and Van Grieken, 1994), the filter deposit is irradiated by high energy x-rays that eject inner shell electrons from the atoms of each element in the sample. When a higher energy electron drops into the vacant lower energy orbital, a fluorescent x-ray photon is released. The energy of this photon is unique to each element, and the number of photons is proportional to the concentration of the element. Concentrations are quantified by comparing photon counts for a sample with those obtained from thin-film standards of known concentration.

XRF methods can be broadly divided into two categories: wavelength dispersive x-ray fluorescence (WDXRF), which utilizes crystal diffraction for observation of fluorescent x-rays, and energy dispersive x-ray fluorescence (EDXRF), which uses a silicon semiconductor detector. The WDXRF method is characterized by high spectral resolution, which minimizes peak overlaps. It requires high power excitation to overcome low sensitivity, resulting in excessive sample heating and potential degradation. Conversely, EDXRF features high sensitivity but less spectral resolution, requiring complex spectral deconvolution procedures.

XRF methods can be further categorized as direct/filtered excitation, where the x-ray beam from the tube is optionally filtered and then focused directly on the sample, or secondary target excitation, where the beam is focused on a target of material selected to produce x-rays of the desired energy. The secondary fluorescent radiation is then used to excite the samples. The direct/filtered approach has the advantage of delivering higher incident radiation flux to the sample for a given x-ray tube power, since about 99% of the incident energy is lost in a secondary fluorescence. However, the secondary fluorescence approach, produces a more nearly monochromatic excitation that reduces unwanted scatter from the filter, thereby yielding better detection limits.

XRF is usually performed on Teflon-membrane filters for a variety of trace elements. A typical XRF system is schematically illustrated in Figure 4-24. The x-ray output stability should be within $\pm 0.25\%$ for any 8-h period within a 24-h duration. Typically, analyses are controlled, spectra are acquired, and elemental concentrations are calculated by software on a computer that is interfaced to the analyzer. Separate XRF analyses are conducted on each sample to optimize detection limits for the specified elements. A comparison of the minimum detectable limits of Teflon-membrane and quartz-fiber filters is listed in Table 4-3. Figure 4-25 shows an example of an XRF spectrum.

Three types of XRF standards are used for calibration, performance testing, and auditing: (1) vacuum-deposited thin-film elements and compounds (Micromatter); (2) polymer films (Dzubay et al., 1981); and (3) National Institute of Science and Technology (NIST, formerly NBS) thin-glass films. The thin film standards cover the largest number of elements and are used to establish calibration curves, while the polymer film standards are used to verify the accuracy of the thin film standards. The NIST standards are used to validate the accuracy of the calibration curves. NIST produces the definitive standard reference materials, but these are only available for the species of aluminum, silicon, calcium, iron, cobalt, copper, manganese, and uranium (SRM 1832), and silicon, potassium, titanium, iron, zinc, and lead (SRM 1833). One or more separate Micromatter thin-film standards are used to calibrate the system for each element.

Sensitivity factors (number of x-ray counts per $\mu g/cm^2$ of the element) are determined for each excitation condition. These factors are then adjusted for absorption of the incident and emitted radiation in the thin film. These sensitivity factors are plotted as a function of atomic number and a smooth curve is fitted to the experimental values. The calibration sensitivities are then read from these curves for the atomic numbers of each element in each excitation condition. NIST standards are analyzed on a periodic basis to verify the sensitivity factors. A multi-layer thin film standard prepared by Micromatter is analyzed with each set of samples to check the stability of the instrument response. When deviations from specified values are greater than $\pm 5\%$, the system should be re-calibrated.

The sensitivity factors are multiplied by the net peak intensities yielded by ambient samples to obtain the $\mu g/cm^2$ deposit for each element. The net peak intensity is obtained

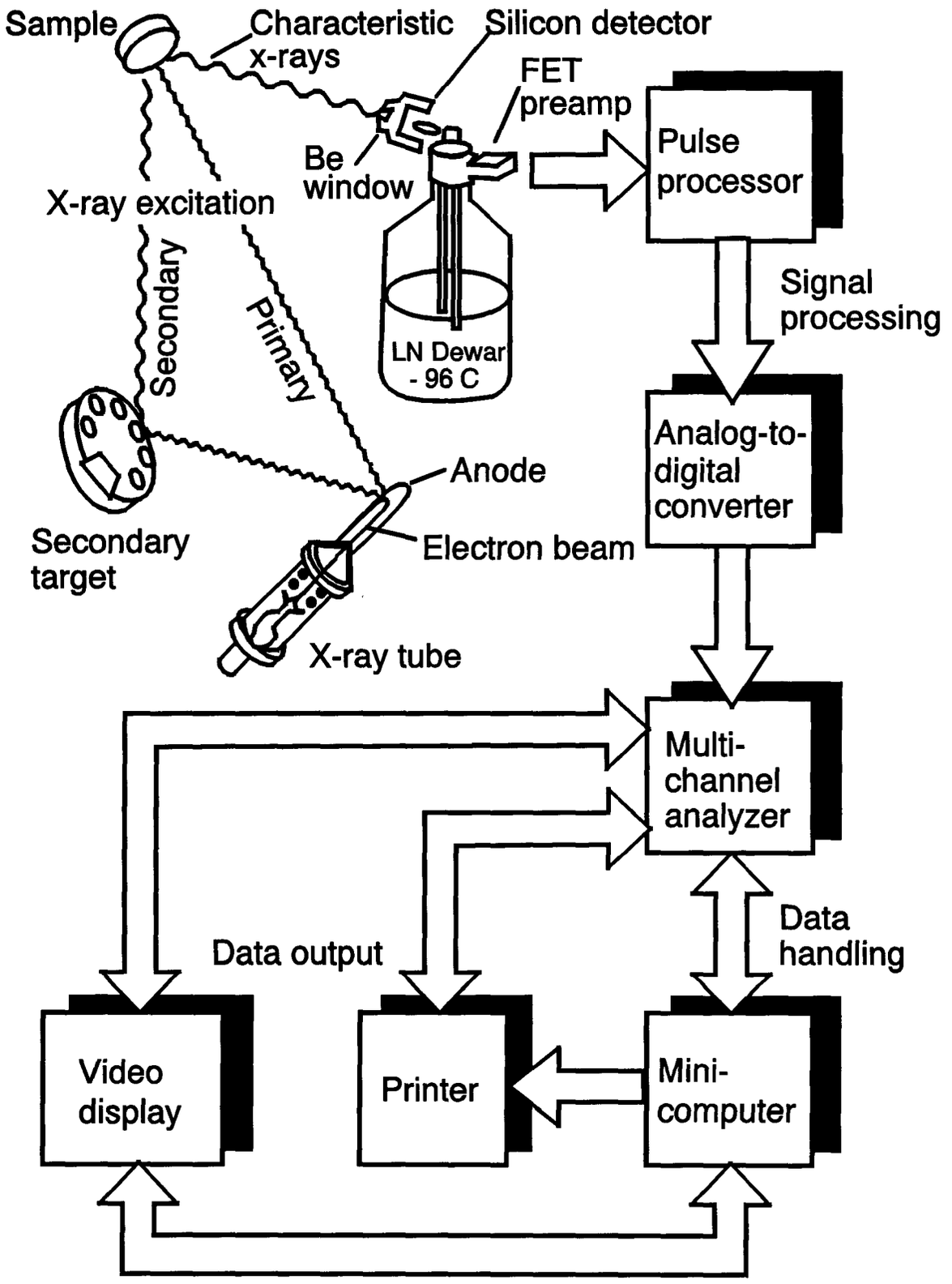

Figure 4-24. Schematic of a typical X-ray fluorescence system.

TABLE 4-3. MINIMUM DETECTABLE LIMITS[a] FOR X-RAY FLUORESCENCE ANALYSIS OF AIR FILTERS

		Quartz-Fiber Filter[b]	Teflon Membrane Filter[c]			
Element	Condition Number[d]	Protocol QA-A ng/cm^2 [e]	Protocol A ng/cm^2 [d]	Protocol B ng/cm^2	Protocol C ng/cm^2	Protocol D ng/cm^2
Al	5	NA[f]	10	7.2	3.6	2.5
Si	5	NA	6.3	4.4	2.2	1.4
P	5	NA	5.6	4.0	2.0	1.4
S	5	40[g]	5.0	3.5	1.8	1.2
Cl	4	30	10	7.4	3.7	2.6
K	4	40	6.1	4.3	2.2	1.5
Ca	4	100	4.5	3.2	1.6	1.1
Ti	3	50	2.9	2.1	1.0	0.73
V	3	20	2.5	1.7	0.87	0.62
Cr	3	8	1.9	1.4	0.67	0.48
Mn	3	7	1.6	1.1	0.56	0.40
Fe	3	15	1.5	1.1	0.54	0.38
Co	3	5	0.88	0.62	0.31	0.22
Ni	3	4	0.89	0.63	0.31	0.22
Cu	3	4	1.1	0.76	0.38	0.27
Zn	3	6	1.1	0.76	0.38	0.27
Ga	2	8	1.9	1.4	0.68	0.48
As	2	9	1.6	1.1	0.56	0.39
Se	2	5	1.2	0.86	0.43	0.31
Br	2	5	1.0	0.72	0.36	0.25
Rb	2	5	1.0	0.68	0.34	0.24
Sr	2	8	1.1	0.78	0.39	0.28
Y	2	8	1.3	0.92	0.46	0.33
Zr	2	10	1.7	1.2	0.59	0.42
Mo	4	20	2.7	1.9	0.95	0.67
Pd	1	20	11	7.6	3.8	2.7
Ag	1	20	12	8.6	4.3	3.0
Cd	1	25	12	8.6	4.3	3.0
In	1	30	13	9.5	4.8	3.4

TABLE 4-3 (cont'd). MINIMUM DETECTABLE LIMITS[a] FOR X-RAY FLUORESCENCE ANALYSIS OF AIR FILTERS

		Quartz-Fiber Filter[b]	Teflon Membrane Filter[c]			
Element	Condition Number[d]	Protocol QA-A ng/cm^2 [e]	Protocol A ng/cm^2 [d]	Protocol B ng/cm^2	Protocol C ng/cm^2	Protocol D ng/cm^2
Sn	1	40	17	12	6.2	4.4
Sb	1	50	18	13	6.4	4.5
Ba	1	170	52	37	18	13
La	1	190	62	44	22	16
Au	2	NA	3.1	2.2	1.1	0.77
Hg	2	20	2.6	1.8	0.91	0.65
Tl	2	NA	2.5	1.8	0.88	0.62
Pb	2	14	3.0	2.2	1.1	0.76
U	2	NA	2.3	1.7	0.83	0.59

[a]MDL defined as three times the standard deviation of the blank for a filter of 1 mg/cm^2 areal density.
[b]Analysis times are 100 sec. for Conditions 1 and 4, and 400 sec. for Conditions 2 and 3. Actual MDL's for quartz filters vary from batch to batch due to elemental contamination variability.
[c]Standard protocol, developed at the Desert Research Institute, University and Community College System of Nevada, Reno, NV, analysis times are 100 sec. for Conditions 1, 4 and 5, and 400 sec. for Conditions 2 and 3 for Protocol A; 200 sec. for Conditions 1, 4 and 5 and 800 sec. for Conditions 2 and 3 for Protocol B; 800 sec. for Conditions 1,4 and 5 and 3,200 sec. for Conditions 2 and 3 for Protocol C; and 1600 sec. for Conditions 1, 4 and 5 and 6400 sec. for Conditions 2 and 3 for Protocol D.
[d]Condition 1 is direct mode excitation with a primary excitation filter of 0.15 mm thick Mo. Tube voltage is 50 KV and tube current is 0.6 mA. Condition 2 is direct mode excitation with a primary excitation filter of 0.13 mm thick Rh. Tube voltage is 35 KV and tube voltage is 2.0 mA. Condition 3 uses Ge secondary target excitation with the secondary excitation filtered by a Whatman 41 filter. Tube voltage is 30 KV and tube current is 3.3 mA. Condition 4 uses Ti secondary target excitation with the secondary excitation filtered by 3.8 μm thick mylar film. Tube voltage is 30 KV and tube current is 3.3 mA. Condition 5 uses direct mode excitation with a primary excitation filter consisting of 3 layers of Whatman 41 filters. Tube voltage is 8 KV and tube current os 0.6 mA. Multi-channel analyzer energy range is 0 to 40 KeV for condition 1, 0 - 20 KeV for condition 2, and 0 to 10 KeV for conditions 3, 4, and 5.
[e]Typical exposed area is 406 cm^2 for standard high-volume filters; 6.4 cm^2 for 37 mm ringed Teflon-membrane filters; and 13.8 cm^2 for 47 mm ringed Teflon-membrane filters.
[f]Information not available.
[g]For condition 4.

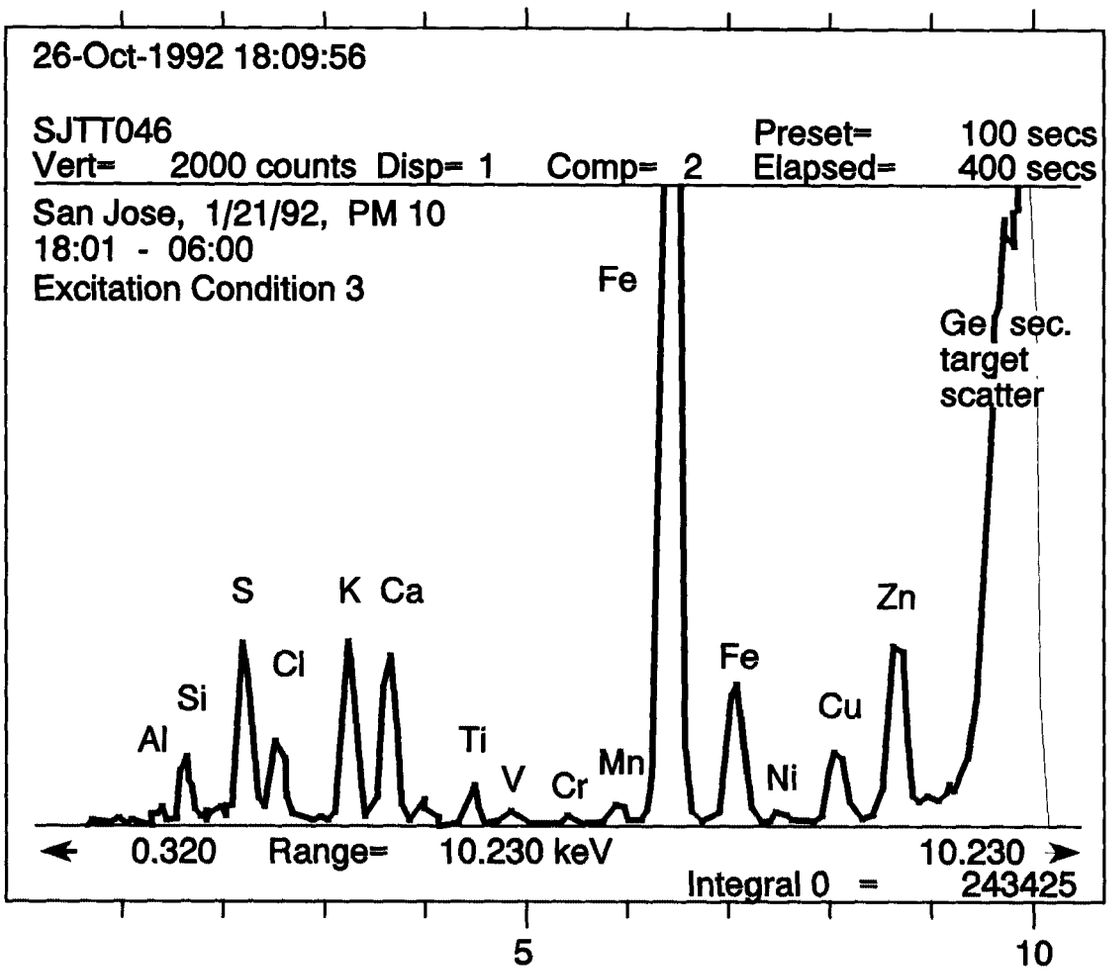

Figure 4-25. Example of an X-ray fluorescence spectrum.

Source: Chow and Watson (1994).

by: (1) subtracting background radiation; (2) subtracting spectral interferences; and (3) adjusting for x-ray absorption.

XRF analysis of air particulate samples has had widest application to samples collected on membrane-type filters such as Teflon- or polycarbonate-membrane filter substrates. These membrane filters collect the deposit on their surfaces, which eliminates biases due to absorption of x-rays by the filter material. These filters also have a low areal density which minimizes the scatter of incident x-rays, and their inherent trace element content is very low.

Quartz-fiber filters used for high-volume aerosol sampling do not exhibit these features. As noted earlier, blank elemental concentrations in quartz-fiber filters that have not undergone acceptance testing can be several orders of magnitude higher than the

concentrations in the particulate deposits. The concentrations vary substantially among the different types of quartz-fiber filters and even within the same filter type and manufacturing lot. Blank impurity concentrations and their variabilities decrease the precision of background subtraction from the XRF spectral data, resulting in higher detection limits. Impurities observed in various types of glass- and quartz-fiber filters include aluminum, silicon, sulfur, chlorine, potassium, calcium, iron, nickel, copper, zinc, rubidium, strontium, molybdenum, barium, and lead. Concentrations for aluminum, silicon, phosphorus, sulfur, and chlorine cannot be determined for quartz-fiber filters because of the large silicon content of the filters.

Quartz-fiber filters also trap particles within the filter matrix, rather than on the surface. This causes absorption of X rays within the filter fibers yielding lower concentrations than would otherwise be measured. The magnitude of this absorption increases exponentially as the atomic number of the measured element decreases and varies from sample to sample. Absorption factors generally are "1.2" or less for iron and heavier elements, but can be from "2" to "5" for sulfur.

Quartz-fiber filters are much thicker than membrane filters resulting in an increased scattering of x-rays and a consequent increase in background and degradation of detection limits. The increased x-ray scatter also overloads the x-ray detector which requires samples to be analyzed at a lowered x-ray intensity. These effects alone can result in degradation of detection limits by up to a factor of 10 with respect to Teflon-membrane substrates.

Larger particles collected during aerosol sampling have sufficient size to cause absorption of x-rays within the particles. Attenuation factors for fine particles ($PM_{2.5}$, particles with aerodynamic diameters equal to or less than 2.5 μm) are generally negligible (Criss, 1976), even for the lightest elements, but these attenuations can be significant for coarse fraction particles (particles with aerodynamic diameters from 2.5 to 10 μm). Correction factors for XRF have been derived using the theory of Dzubay and Nelson (1975) and should be applied to coarse particle measurements.

4.3.2.2 Particle Induced X-Ray Emission of Trace Elements

Particle Induced X-Ray Emission (PIXE) is another form of elemental analysis based on the characteristics of x-rays and the nature of x-ray detection (Cahill et al., 1987; 1989).

PIXE uses beams of energetic ions, consisting of protons at an energy level of 2 to 5 MeV, to create inner electron shell vacancies. As inner electron shell atomic vacancies are filled by outer electrons, the emitted characteristics of x-rays can be detected by wavelength dispersion (which is scattering from a crystal) or by energy dispersion (which involves direct conversion of x-rays). The development of focusing energetic proton beams (proton microprobes) has expanded the application of PIXE from environmental and biological sciences to geology and material sciences. Figure 4-26 illustrates a typical PIXE setup in a thin target mode (Cahill, et al., 1989). PIXE analysis is often used for impactor samples or small filter substrates, since proton beams can be focused to a small area with no loss of sensitivity (Cahill and Wakabayashi, 1993).

Very thick filters or thick particle deposits on filter substrates scatter the excitation protons and lower the signal-to-noise ratio for PIXE. X-ray analysis methods, such as PIXE and XRF, require particle size diameter corrections (for low atomic number targets) associated with a spherical particle of a given diameter (typically particles with aerodynamic diameters >2.5 μm) and compositions typical in ambient aerosol studies. These analyses also require correction for sample loadings that reflect the passage of x-rays through a uniform deposit layer. Procedures for instrument calibration, spectrum process, and quality assurance are similar to those documented in Section 4.3.1.2 for XRF.

PIXE analysis can provide information on one of the widest range of elements in a single analysis, since x-ray results require two or three separate anodes. However, attempts to improve sensitivity of PIXE analysis may result in damage to Teflon-membrane filters. Recent developments (Malm et al., 1994) using PIXE analysis at moderate sensitivity plus single anode XRF analysis at high sensitivity for transition/heavy metals have achieved the minimum detectable limits of less than 0.01 ng/m^3. With the addition of hydrogen analysis (a surrogate for organic matter), almost all gravimetric mass concentrations can be explained (Cahill, et al., 1987).

XRF and PIXE are the most commonly used elemental analysis methods owing to their nondestructive multi-element capabilities, relatively low cost, high detection limits, and preservation of the filter for additional analyses. XRF sometimes needs to be supplemented with INAA when extremely low detection limits are needed, but the high cost of INAA precludes this method from being applied to large numbers of samples. AAS is a good

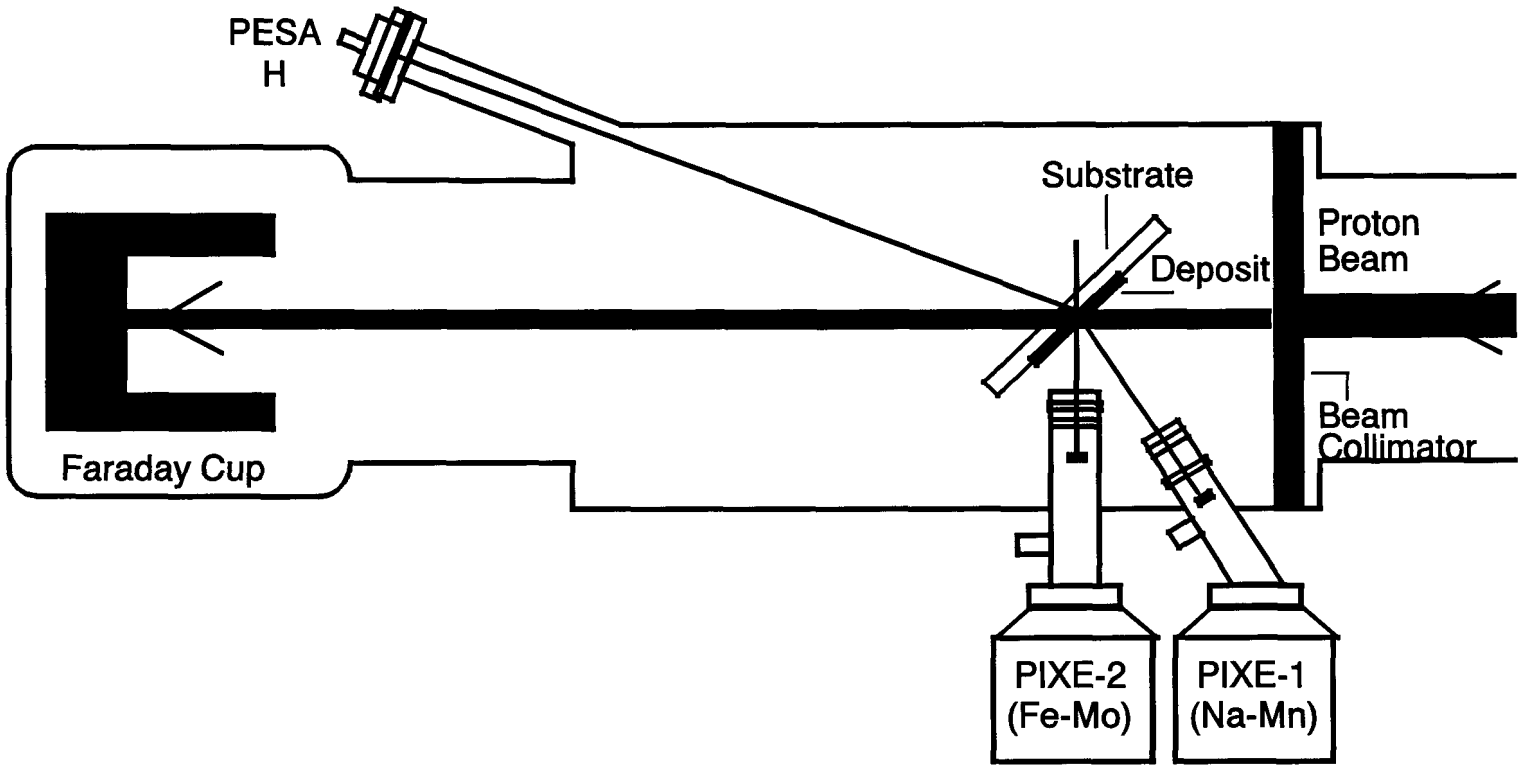

Figure 4-26. Schematic of a PIXE/PESA analysis system.

alternative for water-soluble species, especially for low atomic number. ICP/AES analysis is a viable alternative, but it is less desirable because of the sample extraction elements such as sodium and magnesium, but it requires large dilution factors to measure many different elements expense and the destruction of the filter.

4.3.2.3 Instrumental Neutron Activation Analysis of Trace Elements

Instrumental neutron activation analysis (INAA) (Dams et al., 1970; Zoller and Gordon, 1970; Olmez, 1989; Ondov and Divita, 1993) basically involves irradiation of a thin membrane filter sample in the core of a nuclear reactor for periods ranging from a few minutes to several hours. Bombardment of the sample with neutrons induces a nuclear reaction of the stable isotopes in the sample. The energies of the gamma rays emitted by the decay of this induced radioactivity are used to identify them, and therefore, their parents. With the use of prepared elemental standards, the amount of parent element in the sample can be determined since the intensity of these gamma rays are proportional to their number.

The gamma-ray spectra of radioactive species are usually collected with a high resolution germanium detector utilizing commercially available amplifiers and multi-channel analyzers. Typical detector efficiencies range from 10 to 40% relative to a 3 $\times$ 3 in. sodium iodide detector. Detector system resolution, measured as the full-width at half-maximum for Table 4-4, the 1,332 KeV gamma-ray peak of ^{60}Co, should be less than 2.3 KeV in order to provide adequate resolution between isotopes of neighboring energies.

In order to obtain a full suite of elemental analysis results (often over 40 elements), multiple counting periods and irradiations are performed on the same sample (e.g., two irradiations would produce elements separated into short- and long-lived decay products). An example of the elements determined from multiple irradiations and counting periods and the irradiation, cooling, and counting times used for ambient particulate samples collected on Teflon-membrane filter material are summarized in Table 4-4 (Divita, 1993). These irradiations were performed at the 20-MW NIST Research Reactor operated at 15-MW (neutron flux of 7.7×10^{13} and 2.7×10^{13} neutron/cm^2 $\times$ s).

The power of INAA is that it is not generally subject to interferences like XRF or PIXE due to a much better ratio of gamma ray peak widths to total spectral width, by a factor of about 20. INAA does not quantify some of the abundant species in ambient

TABLE 4-4. INSTRUMENTAL NEUTRON ACTIVATION ANALYSIS COUNTING SCHEME AND ELEMENTS MEASURED

Counting Period	Irradiation Time	Cooling Time	Counting Time	Elements Measured
Short-Lived 1	10 min	5 min	5 min	Mg, Al, S, Ca, Ti, V, Cu
Short-Lived 2		20 min	20 min	Na, Mg, Cl, K, Ca, Mn, Zn, Ga, Br, Sr, In, I, Ba
Long-Lived 1	4-6 h	3-4 days	6-8 h	Na, K, Ga, As, Br, Mo, Cd, Sb, La, Nd, Sn, Yb, Lu, W, Au, U
Long-Lived 2		30 days	12-24 h	Sc, Cr, Fe, Co, Zn, Se, Sr, Ag, Sb, Cs, Ba, Ce, Nd, Eu, Gd, Tb, Lu, Hf, Ta, Th

particulate matter such as silicon, nickel, tin, cadmin, mercury, and lead. While INAA is technically nondestructive, sample preparation involves folding the samples tightly and sealing it in plastic, and the irradiation process makes the filter membrane brittle and radioactive. These factors limit the use of the sample for subsequent analyses by other methods. The technique also suffers from the fact that a nuclear reactor is usually used as a source of neutrons. However, since the advent of high-resolution gamma-ray detectors, individual samples can be analyzed for numerous elements simultaneously, most at remarkably trace levels without the need for chemical separation. This greatly diminishes the danger of contamination due to excessive sample handling and introduction of chemical reagents used for separation procedures.

4.3.2.4 Microscopy Analysis of Particle Size, Shape, and Composition

Morphological and chemical features of particles can be used to identify the sources and transport mechanism of airborne particles. The chemical analysis of individual particles allows the attribution of specific pollution sources more straightforward while the abundance of a specific group is a representative of the source strength. Both light (optical) and scanning electron microscopy have been applied in environmental studies to examine the

single particles (e.g., Casuccio et al., 1983; Bruynseels et al., 1988; Van Borm and Adams, 1988; Van Borm et al., 1989; Cornille et al., 1990; Hopke and Casuccio, 1991; Turpin et al., 1993a).

Light microscopy has been used for providing particle size information regarding the morphology of microscopic features (Crutcher, 1982). The practical resolution of optical microscopes is limited by the wavelengths associated with light of the visible spectrum. When features of interest occur in micron and submicron size ranges, detailed resolution cannot be obtained. The practical resolution of light microscopy is typically 1 to 2 μm (Meyer-Arendt, 1972).

The use of accelerated electrons in electron microscopy (a) allows for the formation of magnified images and an increased depth of field and (b) provides the resolution of a few angstroms (10^{-4} μm). Electron microscopy has now evolved to include: (1) the transmission electron microscope (TEM); (2) the scanning electron microscope (SEM), and; (3) the scanning transmission electron microscope (STEM) (Hearle et al. 1972; Lee et al., 1979; Lee and Fisher, 1980; Lee and Kelly, 1980; Lee et al., 1981; Johnson et al., 1981; McIntyre and Johnson, 1982; Casuccio et al., 1983; Wernisch, 1985, 1986; Kim et al., 1987; Kim and Hopke, 1988; Dzubay and Mamane, 1989; Schamber, 1993).

The SEM and STEM use accelerated electrons to strike the sample. As the electron beam strikes the samples, various signals (e.g., secondary, backscattered, and Anger electrons, characteristic x-rays, photons, and cathodoluminescence) are generated. These signals can be collected to provide highly detailed information on a point-by-point basis. The secondary electron signal yields a sample image with three-dimensional prospective, high depth of field, and illuminated appearance. Back scattered electron images are used to separate phases containing elements of different atomic number.

The information obtained from light and scanning microscopy analyses are usually considered to be qualitative, due to the limited number of particles counted. To achieve a quantitative analysis, a sufficient number of particles must be properly sized and identified by morphology and/or chemistry to represent the entire sample. The selection of filter media, optimal particle loadings, and sample handling methods are also of importance. In this manner, the microscopic characteristics can be directly and reliably related to the bulk or macroscopic properties of the sample (Casuccio et al., 1983).

Microscopic analysis requires a high degree of skill and extensive quality assurance to provide quantitative information. The techniques is complex and expensive when quantitative analysis is required. The evolution of computer technology has allowed for quantitative analysis of particle samples of an entire population of features. With advanced pattern recognition methods, data from individual particle features can be sorted and summarized by size and composition, permitting improved quantitative source apportionment (Bruynseels et al., 1988; Hopke and Casuccio, 1991). Casuccio et al. (1983) summarized the pros and cons of automatic scanning electron microscopy.

Recent development of the SEM/XRF allows analysis of elemental compositions and morphological information on small quantities of material (Bruynseels et al., 1988). Coupled with statistical data analysis, computer controlled scanning electron microscopy shows great promise for identifying and quantifying complex pollution sources in the field of receptor modeling source apportionment (e.g., Griffin and Goldberg, 1979; Janocko et al., 1982; Johnson et al., 1982; Massart and Kaufman, 1983; Hopke, 1985; Derde et al., 1987, Saucy et al., 1987; Mamane, 1988; Dzubay and Mamane, 1989).

4.3.3 Wet Chemical Analysis

Aerosol ions refer to chemical compounds that are soluble in water. The water-soluble portion of suspended particles associates itself with liquid water in the atmosphere when relative humidity increases, thereby changing the light scattering properties of these particles. Different emissions sources may also be distinguished by their soluble and non-soluble fractions. Gaseous precursors can also be converted to their ionic counterparts when they interact with chemicals impregnated on the filter material.

Several simple ions, such as soluble sodium, magnesium, potassium, and calcium are best quantified by atomic absorption spectrometry (AAS) as described above. In practice, AAS has been very useful for measuring water-soluble potassium and sodium, which are important in apportioning sources of vegetative burning and sea salt, respectively. Polyatomic ions such as sulfate, nitrate, ammonium, and phosphate must be quantified by other methods such as ion chromatography (IC) and automated colorimetry (AC). Simple ions, such as chloride, chromium III, and chromium IV, may also be measured by these methods along with the polyatomic ions.

All ion analysis methods require filters to be extracted in DDW and then filtered to remove the insoluble residue. The extraction volume needs to be as small as possible, lest the solution become too dilute to detect the desired constituents. Each square centimeter of filter should be extracted in no more than 2 ml of solvent for typical sampler flow rates of 20 to 30 L/min and sample durations of 24 h. This often results in no more than 20 ml of extract that can be submitted to the different analytical methods, thereby giving preference to those methods which require only a small sample volume. Sufficient sample deposit must be acquired to account for the dilution volume required by each method.

When other analyses are to be performed on the same filter, the filter must first be sectioned using a precision positioning jig attached to a paper cutter. For rectangular filters (typically 20.32 cm by 25.40 cm), a 2.0 cm by 20.32 cm wide strip is cut from the center two-thirds of the filter. Circular filters of 25-, 37-, and 47-mm diameters are usually cut in half for these analyses, so the results need to be multiplied by two to obtain the deposit on the entire filter. Filter materials that can be easily sectioned without damage to the filter or the deposit must be chosen for these analyses.

4.3.3.1 Ion Chromatographic Analysis for Chloride, Nitrate, and Sulfate

Ion chromatography (IC) can be used for both anions (fluoride [F^-], chloride [Cl^-], nitrite [NO_2^-], bromide [Br^-], nitrate [NO_3^-], phosphate [PO_4^{-3}], sulfate [$SO_4^{=}$]) and cations (soluble potassium [K^+], ammonium [NH_4^+], soluble sodium [Na^+]) with separate columns. Applied to aerosol samples, the anions are most commonly analyzed by IC with the cations being analyzed by a combination of atomic absorption spectrophotometry (AAS) and automated colorimetry (AC) (U.S. EPA, 1994). In IC (Small et al., 1975; Mulik et al., 1976; Butler et al., 1978) the sample extract passes through an ion-exchange column that separates the ions in time for individual quantification, usually by a electroconductivity detector. Figure 4-27 shows a schematic representation of the IC system. Prior to detection, the column effluent enters a suppressor column where the chemical composition of the eluent is altered, resulting in a lower background conductivity. The ions are identified by their elution/retention times and are quantified by the conductivity peak area or peak height. IC is especially desirable for particle samples because it provides results for several ions with a single analysis and it uses a small portion of the filter extract with low detection limits.

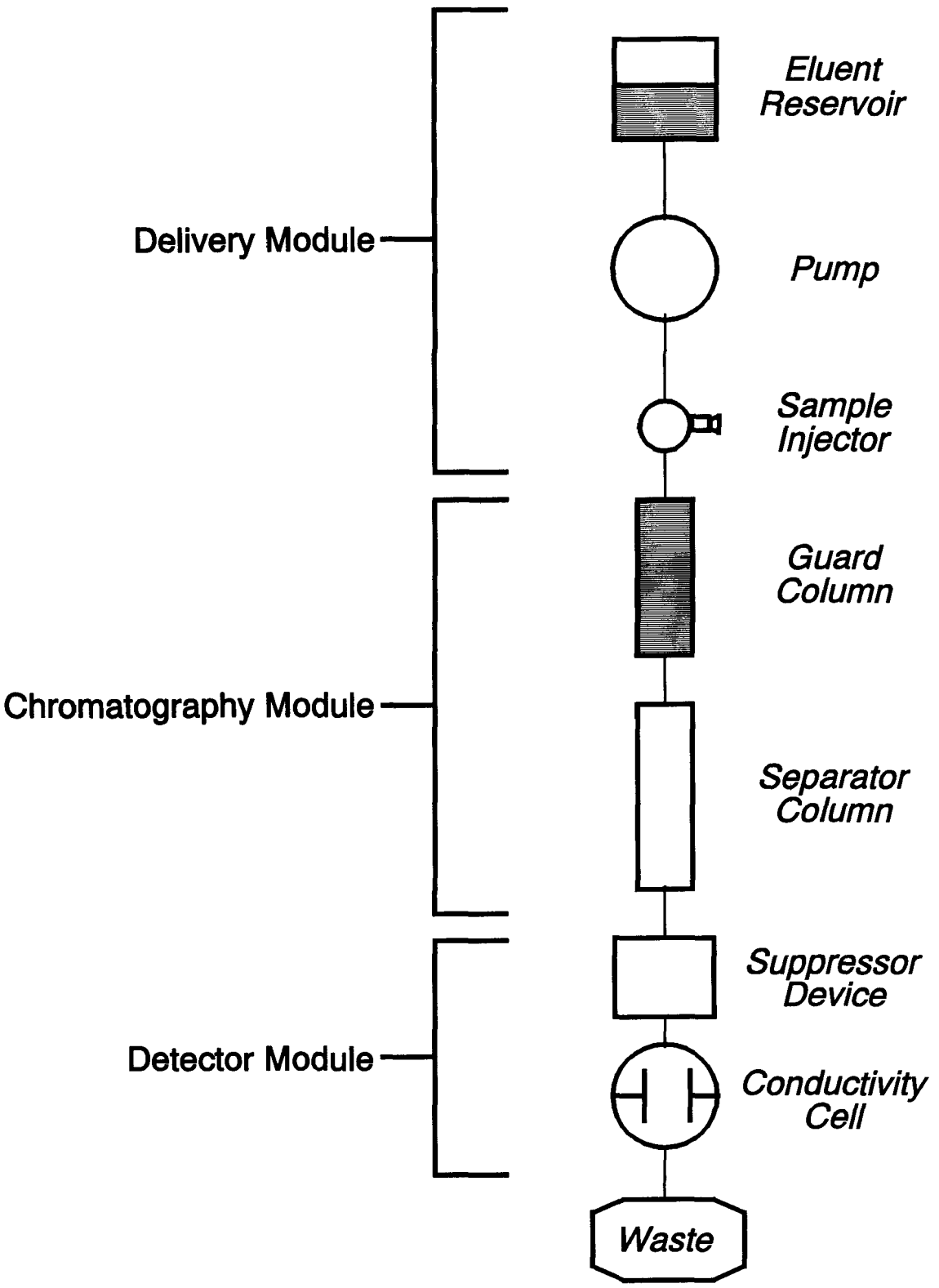

Figure 4-27. Schematic representation of an ion chromatography system.

Water-soluble chloride (Cl^-), nitrate (NO_3^-), and sulfate ($SO_4^=$) are the most commonly measured anions in aerosol samples. Figure 4-28 shows an example of an IC anion chromatogram. IC analyses can be automated by interfacing to an automatic sampler that can conduct unattended analysis of as many as 400 samples (Tejada et al., 1978).

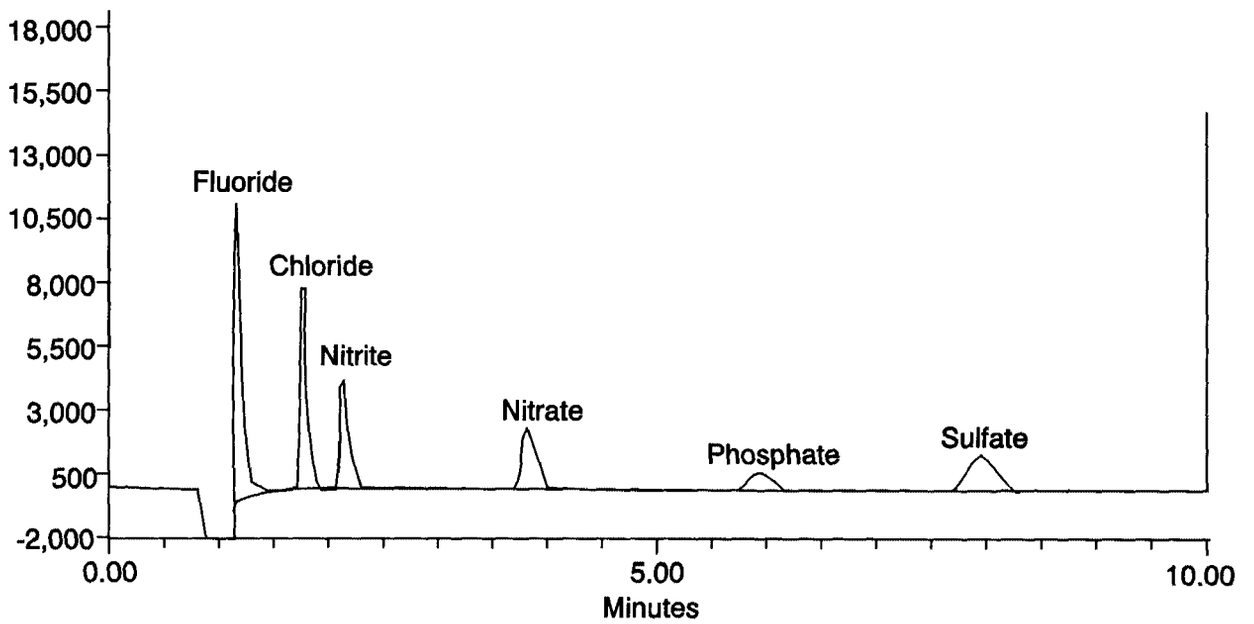

Figure 4-28. Example of an ion chromatogram showing the separation of fluoride, chloride, nitrite, nitrate, phosphate, and sulfate ions.

Several independent quality assurance (QA) standards should be used to check the calibration curve. The standards that are traceable to NIST simulated rainwater standards are: Environmental Resource Associates (ERA, Arvada, CA) custom standards containing the anions measured at a concentration of 100 μg/ml, ERA Waste Water Nutrient Standard, ERA Waste Water Mineral Standard, and Alltech individual standards at 200 μg/ml. The QA standards are diluted in DDW to concentrations that are within the range of the calibration curve.

Calibration curves are performed weekly. Chemical compounds are identified by matching the retention time of each peak in the unknown sample with the retention times of

peaks in the chromatograms of the standards. The QA standards are analyzed at the beginning of each sample run to check calibrations. A DDW blank is analyzed after every 20 samples and a calibrations standard is analyzed after every 10 samples. These quality control (QC) checks verify the baseline and calibration respectively.

4.3.3.2 Automated Colorimetric Analysis for Ammonium, Nitrate, and Sulfate

Automated Colorimetry (AC) applies different colorimetric analyses to small sample volumes with automatic sample throughput. The most common ions measured are ammonium, chloride, nitrate, and sulfate (Butler et al., 1978; Fung et al., 1979). Since IC provides multi-species analysis for the anions, ammonium is most commonly measured by AC.

The AC system is illustrated schematically in Figure 4-29. The heart of the automated colorimetric system is a peristaltic pump, which introduces air bubbles into the sample stream at known intervals. These bubbles separate samples in the continuous stream. Each sample is mixed with reagents and subjected to appropriate reaction periods before submission to a colorimeter. The ion being measured usually reacts to form a colored liquid. The liquid absorbance is related to the amount of the ion in the sample by Beer's Law. This absorbance is measured by a photomultiplier tube through an interference filter specific to the species being measured.

The standard AC technique can analyze ≈ 60 samples per hour per channel, with minimal operator attention and relatively low maintenance and material costs. Several channels can be set up to simultaneously analyze several ions. The methylthymol-blue (MTB) method is applied to analyze sulfate. The reaction of sulfate with MTB-barium complex results in free ligand, which is measured colorimetrically at 460 nm. Nitrate is reduced to nitrite that reacts with sulfanilamide to form a diazo compound. This compound is then reacted to an azo dye for colorimetric determination at 520 nm. Ammonium is measured with the indophenol method. The sample is mixed sequentially with potassium sodium tartrate, sodium phenolate, sodium hypochlorite, sodium hydroxide, and sodium nitroprusside. The reaction results in a blue-colored solution with an absorbance measured at 630 nm. The system determines carry-over by analysis of a low concentration standard

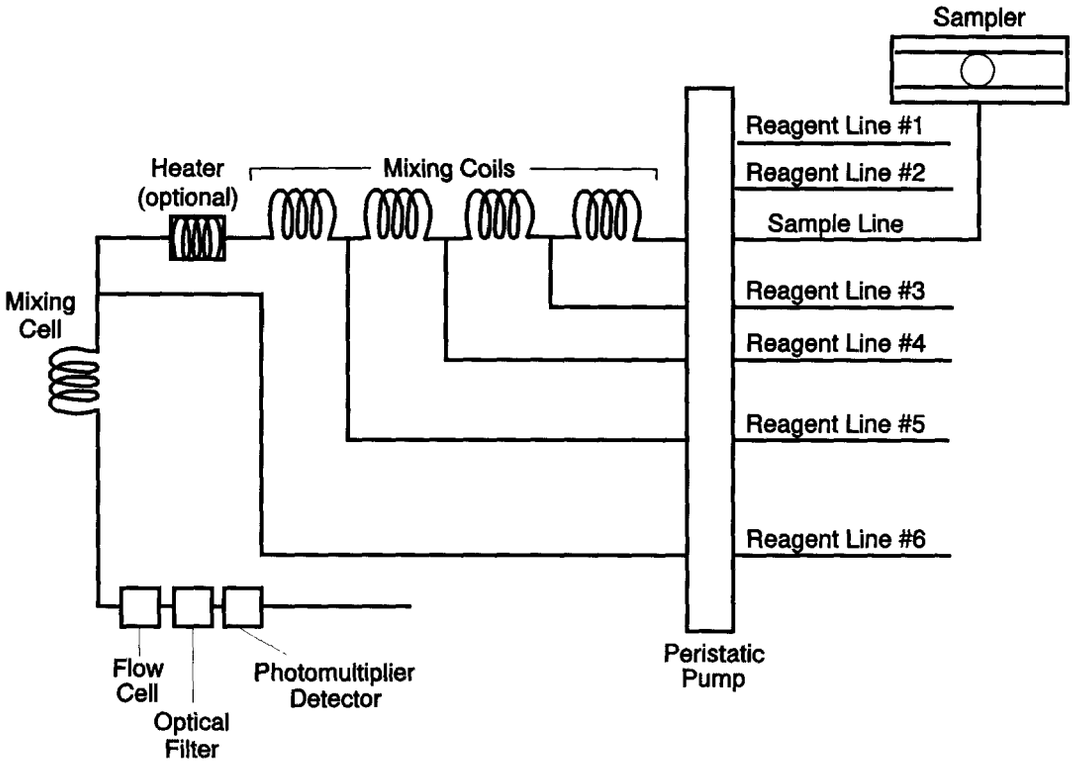

Figure 4-29. Schematic of a typical automated colorimetric system.

following a high concentration. The percent carry-over is then automatically calculated and can be applied to the samples analyzed during the run.

Intercomparison studies between AC and IC have been conducted by Butler et al. (1978) and Fung et al. (1979). Butler et al. (1978) found excellent agreement between sulfate and nitrate measurements by AC and IC. The accuracy of both methods is within the experimental errors, with higher blank values observed for AC techniques. Comparable results were also obtained between the two methods by Fung et al. (1979). The choice between the two methods for sample analysis is dictated by sensitivity, scheduling, and cost constraints.

Two milliliters of extract in sample vials are placed in an autosampler that is controlled by a computer. Five standard concentrations (e.g., $(NH_4)_2SO_4$, Na_2SO_4, $NaNO_3$) are prepared from American Chemical Society reagent-grade chemicals following the same procedure as that for IC standards. Each set of samples consists of two DDW blanks to establish a baseline, five calibration standards and a blank, then sets of ten samples followed by analysis of one of the standards and a replicate from a previous batch. The computer

control allows additional analysis of any filter extract to be repeated without the necessity of loading the extract into more than one vial.

4.3.3.3 Atomic Absorption Spectrophotometric (AAS) and Inductive Coupled Plasma Atomic Emission Spectro (ICP/AES) Photometry Analyses for Trace Elements

In atomic absorption spectrophotometric (AAS) analysis (Fernandez de la Mora, 1989), the sample is first extracted in a strong solvent to dissolve the solid material; the filter or a portion thereof is also dissolved during this process. A few milliliters of this extract are introduced into a flame where the elements are vaporized. Most elements absorb light at certain wavelengths in the visible spectrum, and a light beam with wavelengths specific to the elements being measured is directed through the flame to be detected by a monochrometer. The light absorbed by the flame containing the extract is compared with the absorption from known standards to quantify the elemental concentrations. AAS requires an individual analysis for each element, and a large filter or several filters are needed to obtain concentrations for a large number of the elements specified in Table 4-3. AAS is a useful complement to other methods, such as XRF and PIXE, for species such as beryllium, sodium, and magnesium that are not well-quantified by XRF and PIXE. Airborne particles are chemically complex and do not dissolve easily into complete solution, regardless of the strength of the solvent. There is always a possibility that insoluble residues are left behind and soluble species may co-precipitate on them or on container walls.

In inductive coupled plasma atomic emission spectrophotometric (ICP/AES), (Lynch et al., 1980; Harman, 1989), the dissolved sample is introduced into an atmosphere of argon gas seeded with free electrons induced by high voltage from a surrounding Tesla coil. The high temperatures in the induced plasma raise valence electrons above their normally stable states. When these electrons return to their stable states, a photon of light is emitted which is unique to the element which was excited. This light is detected at specified wavelengths to identify the elements in the sample. ICP/AES acquires a large number of elemental concentrations using small sample volumes with acceptable detection limits for atmospheric samples. As with AAS, this method requires complete extraction and destruction of the sample.

4.3.4 Organic Analysis

4.3.4.1 Analysis of Organic Compounds

Organic compounds comprise a major portion of airborne particles in the atmosphere, thus contributing to visibility degradation, and affecting the properties of clouds into which these particles are scavenged. Specific groups of organic compounds (e.g., polycyclic aromatic hydrocarbons, PAHs) have also been implicated in human health effects. However, due to the very complex composition of the organic fraction of atmospheric aerosols, the detailed composition and atmospheric distributions of organic aerosol constituents are still not well understood.

Sampling techniques for atmospheric particulate matter have been extensively investigated, resulting in the development of collection methods suspended in a wide range of sizes. Particles are most frequently collected on glass or quartz-fiber filters that have been specially treated to achieve low "carbon blanks". Ambient organic particulate matter has also been collected on a variety of particle sizing devices, such as low pressure impactors and Micro Oriface Uniforms Deposit Impactors("MOUDI"). Very recently, diffusion denuder based samplers have been used as well (Tang et al., 1994). However, the task of sampling organic compounds in airborne particles is complicated by the fact that many of these compounds have equilibrium vapor pressures (gaseous concentrations) that are considerably larger than their normal ambient concentrations. This implies a temperature- and concentration-dependent distribution of such organics between particulate and vapor phases. It also suggests that artifacts may occur due to volatilization during the sampling process (Coutant et al., 1988). Such volatilization would cause the under-estimation of the particle-phase concentrations of organics. Conversely, the adsorption of gaseous substances on deposited particles or on the filter material itself, a process driven by the lowered vapor pressure over the sorbed material, would lead to over-estimation of the particle-phase fraction (Bidleman et al., 1986; Ligocki and Pankow, 1989; McDow and Huntzicker, 1990). In addition, several studies have suggested that chemical degradation of some organics may occur during the sampling procedure (Lindskog et al., 1985; Arey et al., 1988; Parmar and Grosjean, 1990).

The partitioning of semi-volatile organic compounds (SOC) between vapor and particle phases has received much attention (Cautreels and Cauwenberghe, 1978; Broddin et al.,

1980; Hampton et al., 1983; Ligocki and Pankow, 1989; Cotham and Bidleman, 1992; Lane et al., 1992; Kaupp and Umlauf, 1992; Pankow, 1992; Turpin et al., 1993b, 1996). Most estimates of partition have relied on high-volume (hi-vol) sampling, using a filter to collect particles followed by a solid adsorbent trap to collect the gaseous portion of SOC (e.g., Kaupp and Umlauf, 1992, Foreman and Bidleman, 1990). Kaupp and Umlauf (1992) recently reported that this approach, although not absolutely free from sorption and desorption artifacts, produces reliable results. The maximum differences observed between hi-vol filter-solid adsorbent sampling and impactor sampling (the latter believed to be less susceptible to these sampling artifacts) did not exceed a factor of two.

There is good theoretical and experimental evidence that use of a diffusion denuder technique significantly improves measurements of vapor-particle phase partitioning (Coutant et al., 1988, 1989, 1992; Lane et al., 1988). However, at the present state of their technological development, the reliability of denuders for investigation of atmospheric partitioning of non-polar SOC needs to be improved, as suggested by contradictions in published field data (e.g., Kaupp and Umlauf, 1992). Gundel et al. (1992) used a proprietary XAD-4-coated tube for vapor collection, followed by filter collection of organic aerosol particles and a sorbent bed to quantitatively retain desorbed (volatilized) organic vapors. Denuders that remove ozone from the air before it reaches the filter reduce the potential for artifact formation on the captured particulate material during sampling (Williams and Grosjean, 1990).

Since the organic fraction of airborne particulate matter is typically a complex mixture of hundreds to thousands of compounds distributed over many organic functional groups, its chemical analysis is an extremely difficult task (Appel et al., 1977; Simoneit, 1984; Flessel et al., 1991; Hildemann et al., 1991; Li and Kamens, 1993; Rogge et al., 1993a, 1993b, 1993c). Analyses of organics generally begin with solvent extraction of the particulate sample. A variety of solvents and extraction techniques have been used in the past. One common method is sequential extraction with increasingly polar solvents, which typically separates the organic material into nonpolar, moderately polar, and polar fractions (Daisey et al., 1982). This step is usually followed by further fractionation using open-column liquid chromatography and/or high-performance liquid chromatography (HPLC) in order to obtain several less complicated fractions (e.g., Schuetzle and Lewtas, 1986; Atkinson et al., 1988).

These fractions can then be analyzed further with high resolution capillary-column gas chromatography (GC), combined with mass spectrometry (GC/MS), Fourier transform infrared (GC/FTIR/MS) or other selective detectors.

Much of the recent work on the identification of nonpolar and semi-polar organics in airborne samples has used bioassay-directed chemical analysis (Scheutzle and Lewtas, 1986), and has focused on identification of fractions and compounds that are most likely to be of significance to human health. In particular, PAHs and their nitro-derivatives (nitroarenes) attracted considerable attention due to their mutagenic and, in some cases, carcinogenic properties. More than 100 PAHs have been identified in the $PM_{2.5}$ fraction of ambient particulate matter (Lee et al., 1981). While most of the nitroarenes found in ambient particles are also present in primary combustion-generated emissions, some are formed from their parent PAH in the atmospheric nitration reactions (e.g., Arey et al., 1986; Zielinska et al., 1989, Ramdahl et al., 1986).

Little work has been done to date to chemically characterize the polar fraction in detail, even though polar material accounts for up to half the mass and mutagenicity of soluble ambient particulate organic matter (Atherholt et al., 1985; Gundel et al., 1994). Until recently the polar fraction has remained analytically intractable, since very polar and labile species interact with conventional fractionation column packing materials and cannot be recovered quantitatively. Recently, very polar particulate organic matter has been successfully fractionated using cyanopropyl-bonded silica (Gundel et al., 1994), with good recovery of mass and mutagenicity (Kado et al., 1989). However, ambient particulate polar organic material cannot be analyzed with conventional GC/MS because of GC column losses resulting from adsorption, thermal decomposition, and chemical interactions. New analytical techniques, such as HPLC/MS and MS/MS, need to be applied if the chemical constituents of polar particulate organic matter are to be identified and quantified.

Most of the recent work on the identification of particulate organic matter has focused on mutagenic and carcinogenic compounds that are of significance to human health. Relatively little work has been done to characterize individual compounds or classes of compounds that are specific to certain sources of organic aerosol. In urban and rural atmospheres, as well as in the remote troposphere, organic composition corresponding to chemical source profiles for of plant waxes, resin residues, and long-chain hydrocarbons

from petroleum residues have been found (e.g., Gagosian et al., 1981; Simoneit, 1984; Mazurek et al., 1987, 1989, 1991; Simoneit et al., 1991). However, a variety of smaller, multi-functional compounds characteristic of gas-to-particle conversion have also been observed (e.g., Finlayson-Pitts and Pitts, 1986). These compounds tend to be present in the polar fraction of ambient organic aerosol particles, having been formed from atmospheric chemical reactions of less polar precursors. Little is currently known about the chemical composition of this polar fraction due to the serious analytical difficulties mentioned above.

4.3.4.2 Analysis of Organic and Elemental Carbon

Three classes of carbon are commonly measured in aerosol samples collected on quartz-fiber filters: (1) organic, volatile, or non-light absorbing carbon; (2) elemental or light-absorbing carbon; and 3) carbonate carbon. Carbonate carbon (i.e., K_2CO_3, Na_2CO_3, $MgCO_3$, $CaCO_3$) can be determined on a separate filter section by measurement of the carbon dioxide (CO_2) evolved upon acidification (Chow et al., 1993b; Johnson et al., 1981). Though progress has been made in the quantification of specific organic chemical compounds in suspended particles (e.g., Rogge et al., 1993a,b,c), sampling and analysis methods have not yet evolved for use in practical monitoring situations.

Many methods have been applied to the separation of organic and elemental carbon in ambient and source particulate samples (Mueller et al., 1971; Lin et al., 1973; Gordon, 1974; Grosjean, 1975; Smith et al., 1975; Appel et al., 1976, 1979; Kukreja and Bove, 1976; Dod et al., 1979; Johnson and Huntzicker, 1979; Macias et al., 1979; Malissa, 1979; Weiss et al., 1979; Cadle et al., 1980a; Johnson et al., 1981b; Daisey et al., 1981; Novakov, 1982; Cadle and Groblicki, 1982; Gerber, 1982; Huntzicker et al., 1982; Stevens et al., 1982; Wolff et al., 1982; Japar et al., 1984; Chow et al., 1993b). Comparisons among the results of the majority of these methods show that they yield comparable quantities of total carbon in aerosol samples, but the distinctions between organic and elemental carbon are quite different (Countess, 1990; Hering et al., 1990).

The definitions of organic and elemental carbon are operational and reflect the method and purpose of measurement. Elemental carbon is sometimes termed "soot", "graphitic carbon," or "black carbon." For studying visibility reduction, light-absorbing carbon is a more useful concept than elemental carbon. For source apportionment by receptor models,

several consistent but distinct fractions of carbon in both source and receptor samples are desired, regardless of their light-absorbing or chemical properties. Differences in ratios of the carbon concentrations in these fractions form part of the source profile that distinguishes the contribution of one source from the contributions of other sources.

Light-absorbing carbon is not entirely constituted by graphitic carbon, since there are many organic materials that absorb light (e.g., tar, motor oil, asphalt, coffee). Even the "graphitic" black carbon in the atmosphere has only a poorly developed graphitic structure with abundant surface chemical groups. "Elemental carbon" is a poor but common description of what is measured. For example, a substance of three-bond carbon molecules (e.g., pencil lead) is black and completely absorbs light, but four-bond carbon in a diamond is completely transparent and absorbs very little light. Both are pure, elemental carbon.

Chow et al. (1993b) document several variations of the thermal (T), thermal/optical reflectance (TOR), thermal/optical transmission (TOT), and thermal manganese oxidation (TMO) methods for organic and elemental carbon. The TOR and TMO methods have been most commonly applied in aerosol studies in the United States.

The TOR method of carbon analysis developed by Huntzicker et al. (1982) has been adapted by several laboratories for the quantification of organic and elemental carbon on quartz-fiber filter deposits. While the principle used by these laboratories is identical to that of Huntzicker et al. (1982), the details differ with respect to calibration standards, analysis time, temperature ramping, and volatilization/combustion temperatures. In the TOR method (Chow et al., 1993b), a filter is submitted to volatilization at temperatures ranging from ambient to 550°C in a pure helium atmosphere, then to combustion at temperatures between 550 to 800°C in a 2% oxygen and 98% helium atmosphere with several temperature ramping steps. The carbon that evolves at each temperature is converted to methane and quantified with a flame ionization detector. The reflectance from the deposit side of the filter punch is monitored throughout the analysis. This reflectance usually decreases during volatilization in the helium atmosphere owing to the pyrolysis of organic material. When oxygen is added, the reflectance increases as the light-absorbing carbon is combusted and removed. Organic carbon is defined as that which evolves prior to re-attainment of the original reflectance, and elemental carbon is defined as that which evolves after the original reflectance has been re-attained. By this definition, "organic carbon" is actually organic carbon that does not

absorb light at the wavelength (632.8 nm) used, and "elemental carbon" is light-absorbing carbon (Chow et al., 1993b). The TOT method applies the same thermal/optical carbon analysis method except that transmission through instead of reflectance off of the filter punch is measured. Thermal methods apply no optical correction and define elemental carbon as that which evolves after the oxidizing atmosphere is introduced.

The TMO method (Fung, 1990) uses manganese dioxide (MnO_2), present and in contact with the sample throughout the analysis, as the oxidizing agent, and temperature is relied upon to distinguish between organic and elemental carbon. Carbon evolving at 525°C is classified as organic carbon, and carbon evolving at 850°C is classified as elemental carbon.

Carbon analysis methods require a uniform filter deposit because only a small portion of each filter is submitted to chemical analysis. The blank filter should be white for light reflection methods, and at least partially transparent for light transmission methods. The filter must also withstand very high temperatures without melting during combustion.

Since all organic matter contains hydrogen as the most common elemental species, analysis of hydrogen by proton elastic scattering analysis (PESA) has been developed by Cahill et al. (1989). A correction must be made for hydrogen in sulfates and nitrates, but since the analysis is done in a vacuum, water is largely absent. PESA has excellent sensitivity which is approximately 20 times better than combustion techniques. This method requires knowledge of the chemical state of sulfates, nevertheless, reasonable agreement was found as compared to the combustion techniques.

4.3.4.3 Organic Aerosol Sampling Artifacts

Sampling artifacts contribute to inaccuracies in mass measurements of particulate organic matter collected by filtration. They can generally be classified into two types: (1) adsorption on filters or collected particulate matter of organic gases normally in the vapor phase causes particulate organic mass to be overestimated, and (2) volatilization of collected organic material during sampling leads to an underestimate of particulate organic mass. These artifacts can cause significant errors in particle mass measurements in areas where a large fraction of the particulate mass is organic.

Vaporization Artifact

Significant loss of organic mass from filter samples occurs when clean air or nitrogen is pumped through them after collection (Commins, 1962; Rondia, 1965; Van Vaeck et al., 1984). This has frequently been referred to as "blow-off" or "volatilization artifact" (Broddin et al., 1980; Konig et al., 1980; Van Vaeck et al., 1984). Van Vaeck et al. (1984) found up to 70% of some n-alkanes volatilized from the filter on exposure to a clean air stream. Coutant et al. (1988) reported that the amount of fluoranthene and pyrene lost through the volatilization artifact for a set of ambient samples ranged from 7 to 62% and 16 to 83%, respectively. Eatough et al. (1989) concluded that 40 to 80% of the organic material was lost after collection from samples at Hopi Point in the Southwestern United States. It has been proposed that an upper limit for the volatilization artifact is reached if the concentration of the volatilizing species reaches its equilibrium vapor concentration in the air exiting the filter, but that actual loss from the filter can be substantially lower because of slow volatilization kinetics or strong adsorption on particulate matter (Pupp et al., 1974). The volatilization artifact has been offered as a possible explanation for frequently observed variations in concentrations of particulate organic matter with flow rate, face velocity and sampling period duration (Della Fiorentina et al., 1975; Appel et al., 1979; Schwartz et al., 1981). An increase in pressure drop across the filter during sampling can also promote volatilization artifact if enough particulate matter is collected (Van Vaeck et al., 1984). However, pressure drop does not appear to explain artifact behavior under typical sampling conditions if the pressure drop across the filter does not change during sampling (McDow and Huntzicker, 1990; Turpin et al., 1994).

Adsorption Artifact

Other workers have been more concerned with adsorption of the gas-phase organics. Cadle et al. (1983) reported that adsorbed vapor accounted for an average of 15% of the organic carbon collected on quartz fiber filters. In the recent Carbonaceous Species Methods Intercomparison Study it was estimated that organic vapor adsorption on filters caused organic aerosol concentrations to be overestimated by 14 to 53% (Hering et al., 1990). Significant adsorption of organic vapors has also been observed on backup filters from a variety of different primary aerosol sources (Hildemann et al., 1991). The adsorption

artifact appears to be inversely related to particulate organic matter concentration, so that artifact correction becomes more important at lower concentrations of particulate organic matter as shown in Figure 4-30 (McDow and Huntzicker, 1990). Adsorption artifact also varies with face velocity (McDow and Huntzicker, 1990; Turpin et al., 1993b) and sampling duration (McDow and Huntzicker, 1993), and significant amounts of adsorbed vapor volatilizes when clean air flows across the filter (McDow and Huntzicker, 1993). Because of this, it is not possible to distinguish between adsorption and volatilization artifacts either by blowing clean air across a filter or by a simple comparison of variations of collected organic mass with face velocity or sampling duration. Adsorption occurs to a greater extent on filters which have already collected organics on the filter surface during sampling than on clean filters not previously used for sampling, suggesting that the filter becomes an increasingly better adsorbent as adsorbed vapors build up on the filter (Cotham and Bidleman, 1992).

The following compounds have been observed to be adsorbed on quartz or glass fiber filters: n-alkanes (Eichmann et al., 1979; Hart and Pankow, 1990), PAH (Ligocki and Pankow, 1989), and formaldehyde (Klippel and Warneck, 1980). Appel et al. (1989) analyzed backup filters for carbonate and ruled out carbon dioxide as a major contributor to adsorption artifact in Los Angeles on the basis of these analyses.

Artifact Correction

Appel et al. (1989) advocated a simple backup filter correction procedure described by Equation 4-1:

$$Cp = QQ1 - QQ2 \tag{4-1}$$

where Cp is artifact corrected particulate concentration, QQ1 represents the mass collected on filter QQ1 and QQ2 represents the mass collected on downstream backup filter QQ2 (Figure 4-31). In some cases a modified backup filter correction procedure described by Equation 4-2 appears to be more accurate (McDow and Huntzicker, 1990):

$$Cp = QQ1 - TQ2 \tag{4-2}$$

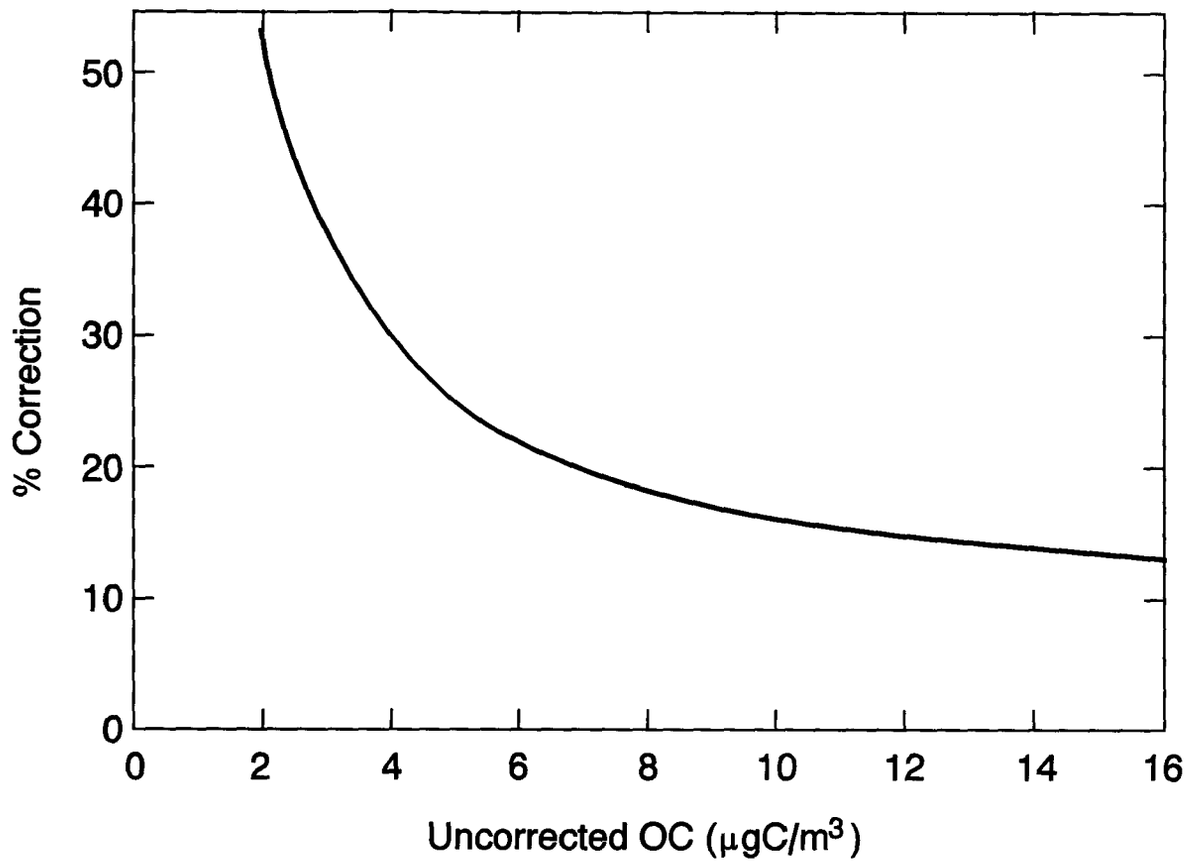

Figure 4-30. Percent correction for vapor adsorption on quartz fiber filters for submicrometer particle sampling at a face velocity of 40 cm s-1 for 13 samples in Portland, OR.

Source: McDow and Huntzicker (1990).

where Cp is artifact corrected particulate concentration, QQ1 represents the mass collected on filter QQ1 in Figure 4-31, and TQ2 represents the mass collected from filter TQ2, the backup filter behind a Teflon filter in a parallel sampling port.

Several approaches have been used to attempt to determine the relative importance of the adsorption and volatilization artifacts. Using quartz fiber denuders to remove vapors upstream of filter samples, Appel et al., (1989) found 59% and Fitz (1990) found 80% on average of the organic mass adsorbed on the backup filter could be removed by the denuder, indicating that the 41% or 20% of the organic mass adsorbed on the backup filter was volatilized from the collected particulate matter.

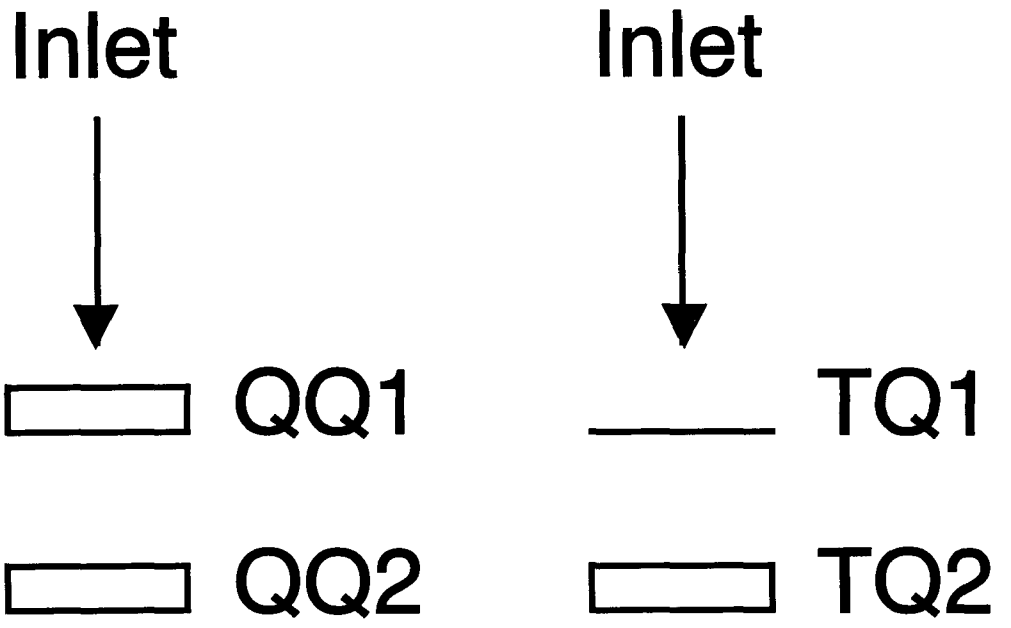

Figure 4-31. Two types of filter series used for adsorption artifact corrections. QQ1 is a quartz fiber filter, and QQ2 is a quartz fiber backup filter to a quartz filter. TQ1 is a Teflon membrane filter, and TQ2 is a quartz fiber backup filter to a Teflon filter.

Source: McDow and Huntzicker (1990).

McDow and Huntzicker (1990) used Equation 4-3 to correct for adsorption artifacts in samples simultaneously collected at three different face velocities. They found that in four experiments more than 80% of the observed difference in organic carbon mass was eliminated by this correction procedure. In contrast, if the organic carbon mass on the backup filter was added to that of the front filter the difference between samples collected at different face velocities was significantly greater. This suggests that adsorption artifact is more likely to account for observed face velocity differences than volatilization artifact.

Eatough et al. (1989, 1993) felt that both the adsorption and the volatilization artifacts were important. Eatough concluded that the backup filter, either QQ2 or TQ2 in Figure 4-32, would adsorb both organic material from the gas phase and organic vapors volatilized from the collected particulate matter. In order to obtain a correct measure of the

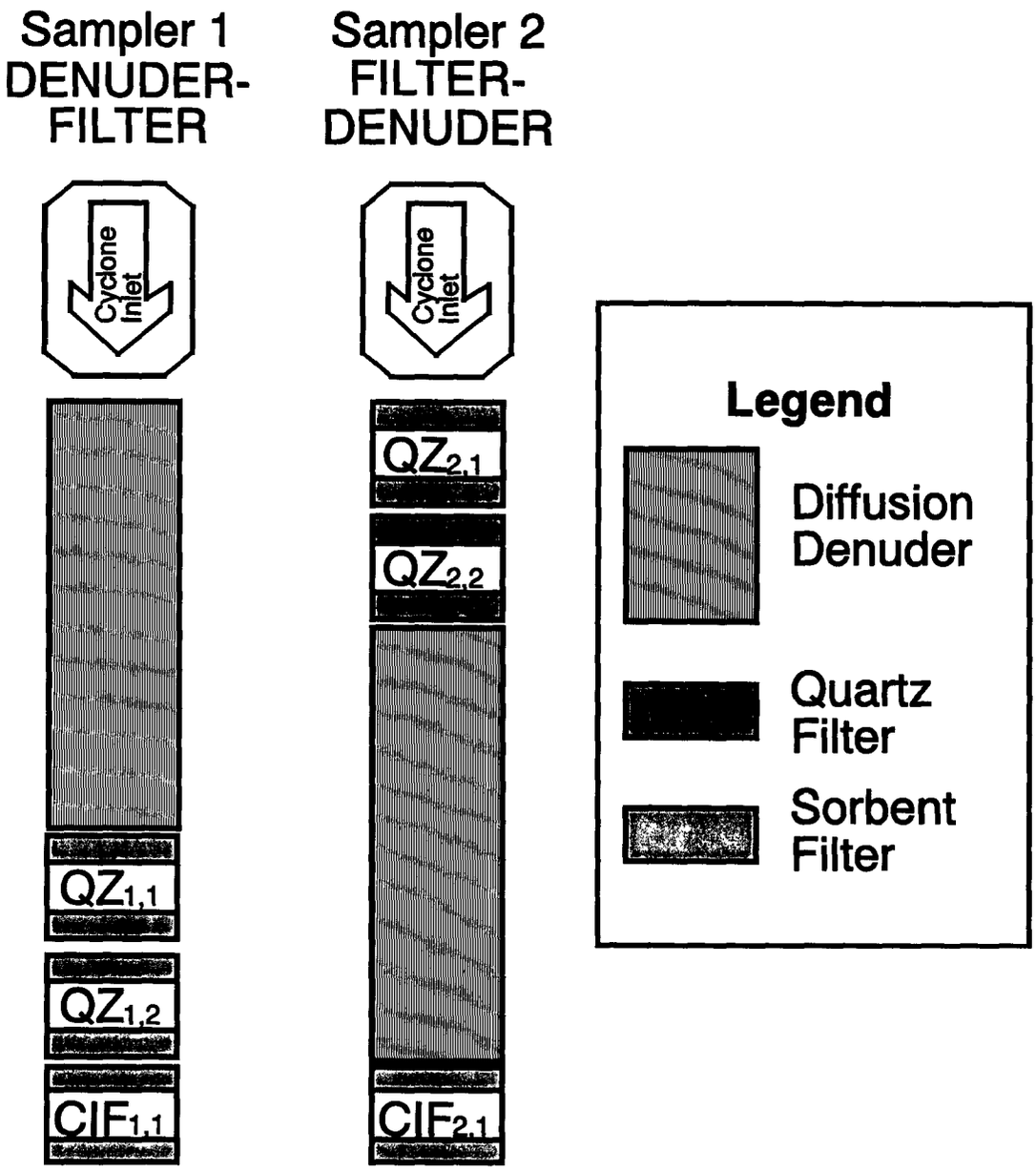

Figure 4-32. Schematic of the BYU Organic Sampling System. Sampler 1 (denuder/filter) and sampler 2 (filter/denuder).

Source: Eatough (1995).

organic particulate matter, present in the ambient air in particulate form, it would be necessary to eliminate the adsorption artifact and add back the volatilization artifact. Accordingly, Eatough collected particulate matter using two parallel sampling trains described in Figure 4-32 (Eatough et al., 1989, 1993; Eatough, 1995) and proposed as an artifact correction equation:

$$Cp = Q1,1 + Q1,2 + CIF1,1/E - CIF2,1/E \tag{4-3}$$

where: Cp is artifact corrected particulate concentration; Q1,1 and Q1,2 are the organic carbon masses collected on the first and second filters following the denuder in sampler 1 of Figure 4-32, respectively; CIF1,1 and CIF2,1 are the carbon masses collected on the sorbent samplers, carbon impregnated filters (CIF) in samplers 1 and 2 in Figure 4-32, respectively; and E is the vapor collection efficiency of the denuder. Eatough (1995) demonstrated that the denuder, made from carbon impregnated filter paper (CIF), removed all of the gas phase organic that could be adsorbed on the quartz fiber filter material. Thus, the organic material on Q1,2 would be due to the volatilization artifact only and Q2,2 - Q1,2 would give an indication of the adsorption artifact (assuming independent adsorption of both artifacts). Any organic material volatilized from the organic particles collected on Q1,1 and not adsorbed on Q1,1 or Q1,2 would be adsorbed on CIF1,1. While the denuder is 100% efficient in removing organic material that would adsorb on quartz fiber filters, it is not 100% efficient for adsorbing the organic material that would be adsorbed by the carbon impregnated filters. Therefore, assuming that all of the organic material vaporized from particles collected on Q2,1 would be adsorbed on Q2,1, Q2,2 or the denuder in Sampler 2, CIF2,1 may be used to correct CIF2,2 for any organic material which passed through the denuder on sampler 1 and was adsorbed on CIF1,2. Since the carbon impregnated filters in the denuders are not 100% efficient they are each corrected for their efficiency (measured separately by comparing the organic mass on several carbon impregnated filters in series).

Several types of samplers have also been designed to reduce sampling artifacts. Van Vaeck et al. (1984) designed a sampler which automatically replaced filters after short time intervals. This prevented large increases in pressure drop across the filter observed during the relatively long sampling periods they typically used. Several denuder systems have also

been designed to reduced sampling artifacts (Appel, et al., 1989; Coutant et al., 1988; Eatough et al., 1989, 1993; Fitz, 1990). Turpin et al. (1993b) developed a laminar flow separator, which also utilizes differences in diffusion rates between vapors and particles to reduce sampling artifacts.

Little is known concerning the chemical species responsible for sampling artifacts, with the exception of the few species reported here. Volatile organic compounds (VOCs) such as formaldehyde make a contribution to the adsorption artifact. Semi-volatile organic compounds (SVOCs), those compounds such as n-alkanes and polycyclic aromatic hydrocarbons, which are generally distributed between the vapor phase and particulate matter in the atmosphere, play a role in both types of artifacts.

Equilibrium partitioning of SVOCs between condensed phase, vapor phase and adsorbed phase depends on their temperature- dependent vapor pressure, the surface area of the collection material, and their concentration. (Section 3.3.3; Junge, 1977; Yamasaki et al., 1982; Pankow, 1987). Some examples of possible causes of SVOC phase equilibrium shifts leading to sampling artifacts are (1) changes in temperature, either if the air temperature changes during sampling, if the sampler is cooled or heated, or if samples are allowed to stand in room air with a different temperature than during sampling, (2) changes in surface area, either in ambient aerosol surface area, or the increase in available surface area for adsorption experienced when an SVOC encounters additional filter surface area, (3) changes in SVOC concentration, which can also occur during sampling or after sample collection if samples are exposed to room air. Thus SVOCs can vaporize during the temperature and relative humidity conditioning prescribed by the Federal Reference Method for measuring particulate mass.

Conclusions

The following conclusions can be drawn from this literature review. (1) There is general agreement that sampling artifacts can cause significant errors in the measurement of particulate organic mass. (2) Disagreement exists about whether adsorption artifact or volatilization artifact are the most important sampling artifact to consider. It is not clear to what extent disagreements between studies are caused by differences in the aerosol sampled, sampling procedures used, or interpretation of sampling results. (3) Little is known about

the causes of sampling artifacts or the individual species involved. (4) Sampling artifacts may be strongly influenced by changes in temperature or organic vapor concentration during sampling and storage. Procedures which do not take these factors into consideration are likely to contribute to sampling artifact errors. (5) Organic aerosol sampling artifacts can cause significant errors in particle mass measurements in areas where a large fraction of the particulate mass is organic.

4.3.5 Methods Validation

The use of multiple methods and parallel samplers achieves both optimum performance and quality assurance. While this has been a part of major research studies since the 1970s, its extension to long-term monitoring of aerosols was most extensively introduces in the SCENES and IMPROVE visibility programs (Eldred and Cahill, 1984). The concept was labeled, "Integral Redundancy," and was recently adopted by the United Nation's Global Atmospheric Watch Program.

The internal consistency checks applied to the IMPROVE network are listed as follows:

(1) Mass (gravimetric) is compared to the sum of all elements on the Teflon-membrane filter of Channel A (PIXE, PESA, XRF analysis; Internally XRF and PIXE are compared for elements around iron). This was pioneered in the SCENES program and is now the standard practice for many aerosol studies.

(2) Sulfate, by ion chromatography on Channel B's nylon filter, after an acidic vapor denuder, is compared to sulfur (X3) from Channel A's Teflon-membrane filter by PIXE. Agreement is excellent, except for summer.

(3) Organic matter, by combustion on Channel C's quartz-fiber filter stack, is compared to organic matter via PESA analysis of hydrogen on Channel A's Teflon-membrane filter. This is an exceptionally sever test due to the nature of organics. These comparisons are made for every IMPROVE analysis, yielding about 25,000 comparisons to date (Malm et al., 1994).

These types of data validation checks should be carried out in every PM measurement program to ensure the accuracy, precision, and validity of the chemical analysis data.

4.4 BIOAEROSOLS SAMPLING AND ANALYSIS

4.4.1 Analytical Methods

Because of the complexity of the particles contained in the term "bioaerosols" no single analytical method is available that will allow assessment of all of the potential biologically-derived particle in an aerosol. Table 4-5 is an overview of the available analytical methods, examples of the kinds of agents detected, and some sampling considerations.

TABLE 4-5. OVERVIEW OF ANALYTICAL METHODS

	Kinds of Agents	Examples	Sampling Considerations
Culture	culturable organisms	fungal spores, yeasts, bacteria, viruses (rarely used)	viability must be protected
Microscopy	recognizable particles	pollen, fungal spores, bacteria	good optical quality is required
Immunoassay	agents that stimulate antibodies	allergens, aflatoxin, glucan	agents must be elutable from sampling medium. Activity must be preserved
Bioassay	agents exerting observable effects in a biological system	endotoxin, cytotoxins	same as immunoassay
Chemical assays	chemicals with recognized characteristics	trichothecene toxins	same as immunoassay
Molecular techniques	DNA or RNA-containing particles	specific organisms	

A good principle to guide the kind of analysis for use in detecting a particular bioaerosol is to use the approach that best characterizes the agent of disease rather than the

agent-bearing particle. Thus, while culture is appropriate where infectious disease is of concern, or where you know that allergens are only released as a spore germinates, it is likely to be only a poor indicator for mycotoxin exposure. Culture always underestimates actual levels of any viable aerosol because no culture conditions are appropriate for all cells. The extent of the underestimate can be very large if an aerosol is damaged or consists primarily of non-living cells. The reason culture is not the best approach for evaluating mycotoxins is because it is unlikely that viability is a necessary requirement for mycotoxin release from spores (although this has not been studied).

Microscopy allows direct counts of identifiable particles. Light microscopy will reveal particles as small as 1.5 μm reliably. Identification of the type of particle requires either some morphological characteristic unique to the particle, or some factor that can be labelled with a visible dye. Most pollens and many fungal spores can be placed in relevant groupings by microscopy alone. Bacteria, on the other hand, can only be counted. Specific techniques to enhance visibility based on specific immune responses or DNA polymerization techniques have yet to be developed.

Immunoassays detect the actual agent of hypersensitivity disease. Two types are commonly used: one based on a mixture of polyclonal antibodies that detects a relatively wide range of allergens, and the other based on monoclonal antibodies that detects only the single allergen to which the antibody is detected. Endotoxin is measured using a bioassay that involves dose-dependant clotting of lysate from the amoebocytes of horseshoe crabs. This is not only an agent-specific assay, but actually measures biological activity of the endotoxin rather than simply the number of molecules.

4.4.2 Sample Collection Methods

Bioaerosol particles follow the principles of physics like any other particle type, and are collected from aerosols by equipment that use these common physical principles. Bioaerosol sampling devices were recently reviewed in depth by Macher et al., 1995. The most commonly used bioaerosol samplers are suction sieve impactors that collect particles directly on culture media. The second most commonly used types are slit impactors that collect particles either on rotating plates of agar, or on grease-coated surfaces. Rotating arm impactors are often used for the collection of pollen in clinical allergy practices across the

country (American Academy of Allergy and Immunology, 1994). In addition to the impactors, bioaerosols are also collected using filtration, either with filters mounted in cassettes or on large sheets of filter material mounted in high-volume suction samplers. Liquid impingers are also used under research conditions.

Analysis of culture plate samples is more or less restricted to static culture, although one group has developed a procedure for suspending the catch in a liquid, and using dilution culture to increase the upper level of sensitivity. For static culture, the maximum number of fungal colonies on a 100 mm petri plate that does not result in inhibition between colonies is about 30. The number of bacteria is much higher (~ 100). Sieve plate impactors have a limited number of sites available for deposition, so that above some given number than depends on the number of holes in the sieve plate, multiple impactions occur. For biological aerosols, this means that only one colony of one organism is likely to appear at each site although several different kinds of organisms might have been collected. Rotating slit culture samplers do not present this constraint, although the upper limit to prevent competition losses remains in effect.

Analysis of samples collected on greased surfaces is generally limited to microscopy, although some attempts have been to transfer allergens to nitrocellulose membranes and analyze by immunoassay (immunoblotting). Filtration samples can be analyzed by culture, microscopy, and by elution followed by immuno- or bioassay. Obviously these are the most versatile devices. However, cultural counts made from filter collections may severely underestimate actual levels because of desiccation on the filter. Microscopic analysis requires large numbers of particles on the filter, so that, unless long sampling times are used, the sensitivity can be poor. Filter collections have been the choice for samples to be analyzed by immunoassay (e.g., cat allergens) and bioassay (e.g., Endotoxin).

4.5 SUMMARY

Though much of the discussion in the preceding sub-sections has been specific to different sampling and analysis methods, several generalizations can be drawn.

First, it is found that samples taken to determine compliance with air quality standards are often used for other purposes, such as source apportionment, personal exposure, and

chemical characterization. Different sampling systems that are more closely coupled to the intended analysis methods may be needed to attain additional monitoring objectives.

Second, though off-site gravimetric analysis of filter samples is straightforward and relatively inexpensive in terms of equipment, more costly in-situ monitors have the potential to provide higher time resolution, more frequent sampling intervals, and possibly reduced manpower requirements. The mass concentrations obtained may not always be comparable between the manual and automated methods, owing to differences in particle volatilization and liquid water content of off-site and in situ measurements.

Third, technology is now proven and available to measure the major chemical components of suspended particles, e.g. many separate elements, organic carbon, elemental carbon, sulfate, nitrate, ammonium, and H+ ions. With reasonable assumptions regarding oxide and hydrocarbon forms, most of the measured mass at many locations can be accounted for by these chemical measurements. This technology could be applied more routinely than it has in the past to better characterize particles to determine compliance with future air quality standards.

Fourth, since ambient particle size distributions contain fine and coarse particle modes, with a minimum between them in the 1 to 3 μm size range, shifts in inlet cut-points near the 2.5 μm size range are not expected to have a large effect on the mass collected owing to the low proportion of particles with sizes near this cut-point. This contrasts to the sensitivity of PM_{10} mass concentrations to small shifts in the cutpoints of PM_{10} inlets, where the maximum of the coarse mode occurs between 6 and 25 μm (Lundgren and Burton, 1995).

Fifth, concentrations of volatile chemicals (such as ammonium nitrate or certain organic compounds) and liquid water may change during sampling, during sample transport and storage, and during sample analysis. Liquid water may be removed by lowering the relative humidity surrounding the sample by heating the sampled air stream, or by selectively denuding the airstream of water vapor. Several sampling systems involving diffusion denuders and absorbing substrates operating in series and in parallel have been demonstrated to quantify volatilized particles, but these are not practical for sustained, long-term monitoring on limited budgets.

Finally, collocated studies show substantial differences between mass concentration measurements acquired by different sampling systems. They also show differences for

similar sampling systems for which procedures are somewhat different. Inlet maintenance, filter handling and storage, laboratory analyses, and quality control procedures are just as important variables as sampler design in explaining these differences. Inlet characteristics and particle volatilization properties are the most important variables that cause mass concentrations to differ. The lack of common calibration standards is one of the major reasons for differences between certain chemical analysis results.

This chapter also briefly describes the technical capabilities and limitations of specific aerosol sampling procedures, focusing on those that (1) were used to collect data supporting other sections in this document, (2) supported the existing PM_{10}, TSP and Pb regulations, and (3) have application in development of a possible fine particle standard. The discussion of aerosol separation technologies is divided between devices used to mimic the larger particle penetration rationales for the upper airways, and those used to mimic smaller particle penetration to the sub-thoracic regions. The applications of performance specifications to define these measurement systems for regulatory purposes are discussed with observations suggesting that the current specification process has not always assured the necessary sampling accuracy. Particle sampling systems for specialty applications, including automated samplers and personal exposure monitors, are briefly described.

4.5.1 PM_{10} Sampling

Laboratory and field testing reported in the literature since 1987 suggest that the EPA specifications and test requirements for PM_{10} samplers have not adequately controlled the differences observed in collocated ambient sampling. The most significant performance flaws have combined to produce mass concentration biases as large as 60%. These biases appear to have resulted from the combined factors of (1) allowing a cutpoint tolerance of 10 ± 0.5 μm, (2) placing an inadequate restriction on internal particle bounce, and (3) allowing a degradation of particle separation performance as certain technology PM_{10} inlets became soiled. The between-sampler bias from a ± 0.5 μm tolerance limit is predictable and should provide PM_{10} concentration differences significantly less than $\pm 10\%$ in almost all cases. Design practices (primarily surface coatings with viscous oil) to minimize the penetration caused by bounce and resuspension have been shown to be very effective. The magnitude of biases from soiling events can be accommodated by not

allowing the inlet to become excessively dirty during operation through routine cleaning prior to sampling. Particle bounce or soiling problems have not been reported for the PM_{10} inlets for the dichotomous sampler.

Based on the current understanding of the PM_{10} sampling process, it could be expected that sampling systems can now be designed and concentration measurements made that are within 10% of the true concentration. This range poses the greatest concern where the measured concentrations are near a standard exceedance level. A review by EPA of the current PM_{10} performance requirements and possible amendments of the existing specifications may be appropriate, given the information base now available.

4.5.2 Fine Particle Sampling

The technology is available to provide an accurate Fine particle cutpoint (e.g. 1.0 or 2.5 μm) for routine sampling. Virtual impactors and cyclones have been shown to be the most trouble-free and versatile methodologies. The exclusion of larger particles using a scalping inlet eliminates many of the transport and loss problems encountered during PM_{10} sampling. The absence of the Coarse particle fraction, however, exaggerates the problems inherent with Fine particle chemistry, such as particle-substrate interactions and sublimation losses. Although it could be expected that Fine particle mass concentration measurements can be made within 10% of the true concentration, accurate chemical speciation may require more comprehensive sampling system components, including gas stream denuders and sequential filter packs.

4.5.3 Concentration Corrections to Standard Conditions

The appropriateness of the correction of particulate concentrations to a reference temperature and pressure is currently under review at EPA. Aerodynamic sampling requires incorporation of local conditions to provide the correct velocities for accurate particle size separation. Correcting the collection volume to standard conditions may improperly influence interpretations of the developed relationships between particle concentration and adverse health responses. It appears to be more appropriate to compute particle concentrations at site conditions and provide temperature and barometric pressure data subsequently, as needed for data interpretation.

4.5.4 Performance Versus Design Specifications for Sampling Systems

The current EPA PM_{10} Reference and Equivalent Method program established in 1987 is based on providing the necessary data quality by using sampling performance specifications. Several research studies have recently reported that key elements of the sampling process were inadequately considered when the original performance specifications were developed. The observations from these controlled studies have been bolstered by reviews of field data from collocated PM_{10} samplers that showed substantial biases under certain conditions. The particle sampling process *is* complex. Obtaining an acceptable bias level using performance standards is difficult, but not impossible, if the appropriate developmental research is identified and implemented. The alternative approach of defining sampling systems by design specifications seems attractive, but may ultimately pose more problems than are solved without producing better quality data. Additionally, specification of a sampling system by design would have the undesirable attribute of virtually eliminating further new technology research. The approach for specifying particle sampling systems is currently under review at EPA.

4.5.5 Automated Sampling

The performances of two sampling methods that are currently designated as Equivalent PM_{10} methods by EPA - beta attenuation and the TEOM sampler - have been evaluated extensively in field settings. Although acceptable comparisons with EPA Reference sampling methods are reported in collocated field studies, attention must be paid to situations where significant biases existed. These biases have been attributed to a number of factors, but focused on the treatment of the particle sample during and after collection. The presence of highly reactive or unstable particles at sampling locations in the western U.S. appears to cause the greatest concern, because of a higher proportion of these species. These bias issues are significant because they complicate the use of automated samplers as "triggers" for control strategy actions, and they question the adequacy of the existing performance specifications for equivalent PM_{10} sampling systems.

4.5.6 PM Samplers for Special Applications

Reviews of typical U.S. personal activity patterns suggest that personal exposure sampling for particulates should also be considered in developing population risk assessments. Relatively unobtrusive personal sampling systems have been designed for a number of particle size cutpoints, and recent studies suggest that acceptable accuracies and precisions are possible. The collection of particle size distribution data can assist in identifying particulate sources and subsequent studies of particle transport and fate. Well characterized cascade impactors are available that cover the aerodynamic size range from at least 0.1 to 10 μm. More automated optical systems are also available, providing either optical or aerodynamic diameter ranges from about 0.5 to 10 μm. Source apportionment sampling systems are available to assist in relating the chemical attributes of ambient particulate matter to the chemical "signatures" from various source categories. This is accomplished by using sampling system components and collection substrates designed to collect specific chemical classes (e.g., a suite of individual metals, speciated carbon) in defined particle size categories.

REFERENCES

Allen, D. T.; Palen, E. J.; Haimov, M. I.; Hering, S. V.; Young, J. R. (1994) Fourier transform infrared spectroscopy of aerosol collected in a low pressure impactor (LPI/FTIR): method development and field calibration. Aerosol Sci. Technol. 21: 325-342.

American Academy of Allery & Immunology. (1994) Aeroallergen Monitoring Network 1994 pollen and spore report. Milwaukee, WI: American Academy of Allery & Immunology.

American Conference of Governmental Industrial Hygienists (ACGIH). (1985) Particle size-selective sampling in the workplace: report of the ACGIH technical committee on air sampling procedures. Cincinnati, OH: American Conference of Governmental Industrial Hygienists.

American Conference of Governmental Industrial Hygienists (ACGIH). (1994) 1994-1995 threshold limit values for chemical substances and physical agents and biological exposure indices. Cincinnati, OH: American Conference of Governmental Industrial Hygienists.

Anand, N. K.; McFarland, A. R.; Kihm, K. D.; Wong, F. S. (1992) Optimization of aerosol penetration through transport lines. Aerosol Sci. Technol. 16: 105-112.

Anlauf, K. G.; MacTavish, D. C.; Wiebe, H. A.; Schiff, H. I.; Mackay, G. I. (1988) Measurement of atmospheric nitric acid by the filter method and comparisons with the tuneable diode laser and other methods. Atmos. Environ. 22: 1579-1586.

Appel, B. R.; Colodny, P.; Wesolowski, J. J. (1976) Analysis of carbonaceous materials in southern California atmospheric aerosols. Environ. Sci. Technol. 10: 359-363.

Appel, B. R.; Hoffer, E. M.; Haik, M.; Wall, S. M.; Kothny, E. L.; Knights, R. L.; Wesolowski, J. J. (1977) Characterization of organic particulate matter. Final report. Sacramento, CA: California Air Resources Board; report no. ARB-R-5-682-77-72. Available from: NTIS, Springfield, VA; PB-279209.

Appel, B. R.; Hoffer, E. M.; Kothny, E. L.; Wall, S. M.; Haik, M.; Knights, R. L. (1979) Analysis of carbonaceous material in southern California atmospheric aerosols. 2. Environ. Sci. Technol. 13: 98-104.

Appel, B. R.; Tokiwa, Y.; Haik, M. (1981) Sampling of nitrates in ambient air. Atmos. Environ. 15: 283-289.

Appel, B. R.; Tokiwa, Y.; Haik, M.; Kothny, E. L. (1984) Artifact particulate sulfate and nitrate formation on filter media. Atmos. Environ. 18: 409-416.

Appel, B. R.; Povard, V.; Kothny, E. L. (1988a) Loss of nitric acid within inlet devices intended to exclude coarse particles during atmospheric sampling. Atmos. Environ. 22: 2535-2540.

Appel, B. R.; Tokiwa, Y.; Kothny, E. L.; Wu, R.; Povard, V. (1988b) Evaluation of procedures for measuring atmospheric nitric acid and ammonia. Atmos. Environ. 22: 1565-1573.

Appel, B. R.; Cheng, W.; Salaymeh, F. (1989) Sampling of carbonaceous particles in the atmosphere—II. Atmos. Environ. 23: 2167-2175.

Arey, J.; Zielinska, B.; Atkinson, R.; Winer, A. M.; Ramdahl, T.; Pitts, J. N., Jr. (1986) The formation of nitro-PAH from the gas-phase reactions of fluoranthene and pyrene with the OH radical in the presence of NO_x. Atmos. Environ. 20: 2339-2345.

Arey, J.; Zielinska, B.; Atkinson, R.; Winer, A. M. (1987) Polycyclic aromatic hydrocarbon and nitroarene concentrations in ambient air during a wintertime high-NO_x episode in the Los Angeles basin. Atmos. Environ. 21: 1437-1444.

Arey, J.; Zielinska, B.; Atkinson, R.; Winer, A. M. (1988) Formation of nitroarenes during ambient high-volume sampling. Environ. Sci. Technol. 22: 457-462.

Arnold, S.; Hague, W.; Pierce, G.; Sheetz, R. (1992) The use of beta gauge monitors for PSI and every day SIP monitoring: an overview of the Denver experience. In: Chow, J. C.; Ono, D. M., eds. PM_{10} standards and nontraditional particulate source controls, an A&WMA/EPA international specialty conference, v. I; January; Scottsdale, AZ. Pittsburgh, PA: Air & Waste Management Association; pp. 13-23. (A&WMA transactions series no. 22).

Atherholt, T. B.; McGarrity, G. J.; Louis, J. B.; McGeorge, L. J.; Lioy, P. J.; Daisey, J. M.; Greenberg, A.; Darack, F. (1985) Mutagenicity studies of New Jersey ambient air particulate extracts. In: Waters, M. D.; Sandhu, S. S.; Lewtas, J.; Claxton, L.; Strauss, G.; Nesnow, S., eds. Short-term bioassays in the analysis of complex environmental mixtures IV. New York, NY: Plenum Press; pp. 211-231. (Environmental science research: v. 32).

Atkinson, R.; Arey, J.; Winer, A. M.; Zielinska, B. (1988) A survey of ambient concentrations of selected polycyclic aromatic hydrocarbons (PAH) at various locations in California [final report]. Sacramento, CA: California Air Resources Board; contract no. A5-185-32.

Bailey, D. L. R.; Clayton, P. (1980) The measurement of suspended particulate and carbon concentrations in the atmosphere using standard smoke shade methods. Stevenage, Hertfordshire, United Kingdom: Warren Spring Laboratory; report no. LR 325 (AP).

Ball, D. J.; Hume, R. (1977) The relative importance of vehicular and domestic emissions of dark smoke in greater London in the mid-1970s, the significance of smoke shade measurements, and an explanation of the relationship of smoke shade to gravimetric measurements of particulate. Atmos. Environ. 11: 1065-1073.

Baron, P. A. (1993) Measurement of asbestos and other fibers. In: Willeke, K.; Baron, P. A., eds. Aerosol measurement: principles, techniques, and applications. New York, NY: Van Nostrand Reinhold; pp. 560-590.

Baron, P. A.; Willeke, K. (1993) Aerosol fundamentals. In: Willeke, K.; Baron, P. A., eds. Aerosol measurement: principles, techniques, and applications. New York, NY: Van Nostrand Reinhold; pp. 8-22.

Baron, P. A.; Mazumder, M. K.; Cheng, Y. S. (1993) Direct-reading techniques using optical particle detection. In: Willeke, K.; Baron, P. A., eds. Aerosol measurement: principles, techniques, and applications. New York, NY: Van Nostrand Reinhold; p. 381-409.

Bartley, D. L.; Breuer, G. M. (1982) Analysis and optimization of the performance of the 10 mm cyclone. Am. Ind. Hyg. Assoc. J. 43: 520-528.

Benner, C. L.; Eatough, D. J.; Eatough, N. L.; Bhardwaja, P. (1991) Comparison of annular denuder and filter pack collection of HNO_3 (g), HNO_2 (g), SO_2 (g), and particulate-phase nitrate, nitrite and sulfate in the south-west desert. Atmos. Environ. Part A 25: 1537-1545.

Bennett, R. L.; Stockburger, L.; Barnes, H. M. (1994) Comparison of sulfur measurements from a regional fine particle network with concurrent acid modes network results. Atmos. Environ. 28: 409-419.

Bidleman, T. F.; Billings, W. N.; Foreman, W. T. (1986) Vapor-particle partitioning of semivolatile organic compounds: estimates from field collections. Environ. Sci. Technol. 20: 1038-1043.

Biswas, P.; Jones, C. L.; Flagan, R. C. (1987) Distortion of size distributions by condensation and evaporation in aerosol instruments. Aerosol Sci. Technol. 7: 231-246.

Botham, R. A.; Hughson, G. W.; Vincent, J. H.; Mark, D. (1991) The development of a test system for investigating the performances of personal aerosol samplers under actual workplace conditions. Am. Ind. Hyg. Assoc. J. 52: 423-427.

Brauer, M.; Koutrakis, P.; Spengler, J. D. (1989) Personal exposures to acidic aerosols and gases. Environ. Sci. Technol. 23: 1408-1412.

Brockmann, J. E.; Yamano, N.; Lucero, D. (1988) Calibration of the aerodynamic particle sizer 3310 (APS-3310) with polystyrene latex monodisperse spheres and oleic acid monodisperse particles. Aerosol Sci. Technol. 8: 279-281.

Broddin, G.; Cautreels, W.; Van Cauwenberghe, K. (1980) On the aliphatic and polyaromatic hydrocarbon levels in urban and background aerosols from Belgium and the Netherlands. Atmos. Environ. 14: 895-910.

Brown, R. C.; Wake, D.; Thorpe, A.; Hemingway, M. A.; Roff, M. W. (1994) Preliminary assessment of a device for passive sampling of airborne particulate. Ann. Occup. Hyg. 38: 303-318.

Bruynseels, F.; Storms, H.; Van Grieken, R.; Van der Auwera, L. (1988) Characterization of North Sea aerosols by individual particle analysis. Atmos. Environ. 22: 2593-2602.

Buckley, T. J.; Waldman, J. M.; Freeman, N. C. G.; Lioy, P. J.; Marple, V. A.; Turner, W. A. (1991) Calibration, intersampler comparison, and field application of a new PM-10 personal air-sampling impactor. Aerosol Sci. Technol. 14: 380-387.

Buettner, H. (1990) Measurement of the size of fine nonspherical particles with a light-scattering particle counter. Aerosol Sci. Technol. 12: 413-421.

Butler, F. E.; Jungers, R. H.; Porter, L. F.; Riley, A. E.; Toth, F. J. (1978) Analysis of air particulates by ion chromatography: comparison with accepted methods. In: Sawicki, E.; Mulik, J. D.; Wittgenstein, E., eds. Ion chromatographic analysis of environmental pollutants. Ann Arbor, MI: Ann Arbor Science Publishers, Inc.; pp. 65-76.

CEN (European Committee for Standardization). (1993) Workplace atmospheres—size fraction definitions for measurement of airborne particles. London, United Kingdom: British Standards Institution; publication no. BS EN 481: 1993; BS 6069: section 3.5: 1993.

Cadle, S. H.; Groblicki, P. J. (1982) An evaluation of methods for the determination of organic and elemental carbon in particulate samples. In: Wolff, G. T.; Klimisch, R. L., eds. Particulate carbon: atmospheric life cycle. New York, NY: Plenum Press; pp. 89-109.

Cadle, S. H.; Groblicki, P. J.; Stroup, D. P. (1980a) Automated carbon analyzer for particulate samples. Anal. Chem. 52: 2201-2206.

Cadle, S. H.; Nebel, G. J.; Williams, R. L. (1980b) Measurements of unregulated emissions from General Motors' light-duty vehicles. SAE Trans. 88: 2381-2401.

Cadle, S. H.; Groblicki, P. J.; Mulawa, P. A. (1983) Problems in the sampling and analysis of carbon particles. Atmos. Environ. 17: 593-600.

Cahill, T. A. (1980) Proton microprobes and particle-induced X-ray analytical systems. Annu. Rev. Nucl. Part. Sci. 30: 211-252.

Cahill, T. A.; Wakabayashi, P. (1993) Compositional analysis of size-segregated aerosol samples. In: Newman, L., ed. Measurement challenges in atmospheric chemistry. Washington, DC: American Chemical Society; pp. 211-228. (Advances in chemistry series no. 232).

Cahill, T. A.; Eldred, R. A.; Kusko, B. H.; Feeney, P. J.; Malm, W. C. (1987) Concentrations of natural hydrocarbon particles at National Park Service sites as derived from mass/hydrogen/sulfur correlations. In: Bhardwaja, P. S., ed. Visibility protection: research and policy aspects, an APCA international specialty conference; September 1986; Grand Teton National Park, WY. Pittsburgh, PA: Air Pollution Control Association; pp. 407-417. (APCA transactions series no. TR-10).

Cahill, T. A.; Eldred, R. A.; Motallebi, N.; Malm, W. C. (1989) Indirect measurement of hydrocarbon aerosols across the United States by nonsulfate hydrogen-remaining gravimetric mass correlations. Aerosol Sci. Technol. 10: 421-429.

Cahill, T. A.; Eldred, R. A.; Feeney, P. J.; Beveridge, P. J.; Wilkinson, L. K. (1990) The stacked filter unit revisited. In: Mathai, C. V., ed. Visibility and fine particles: an A&WMA/EPA international specialty conference; October 1989; Estes Park, CO. Pittsburgh, PA: Air & Waste Management Association; pp. 213-221. (A&WMA transactions series no. TR-17).

Cahill, T. A.; Gill, T. E.; Gillette, D. A.; Gearhart, E. A.; Reid, J. S.; Yau, M.-L. (1994) Generation, characterization and transport of Owens (Dry) Lake dusts [final report]. Sacramento, CA: California Air Resources Board; contract no. A132-105.

Cantrell, B. K.; Williams, K. L.; Watts, W. F., Jr.; Jankowski, R. A. (1993) Mine aerosol measurement. In: Willeke, K.; Baron, P. A., eds. Aerosol measurement: principles, techniques, and applications. New York, NY: Van Nostrand Reinhold; pp. 591-611.

Casuccio, G. S.; Janocko, P. B.; Lee, R. J.; Kelly, J. F.; Dattner, S. L.; Mgebroff, J. S. (1983) The use of computer controlled scanning electron microscopy in environmental studies. J. Air Pollut. Control Assoc. 33: 937-943.

Cautreels, W.; Van Cauwenberghe, K. (1978) Experiments on the distribution of organic pollutants between airborne particulate matter and the corresponding gas phase. Atmos. Environ. 12: 1133-1141.

Chan, T. L.; Lippmann, M. (1980) Experimental measurements and empirical modelling of the regional deposition of inhaled particles in humans. Am. Ind. Hyg. Assoc. J. 41: 399-409.

Charlson, R. J.; Ahlquist, N. C.; Horvath, H. (1968) On the generality of correlation of atmospheric aerosol mass concentration and light scatter. Atmos. Environ. 2: 455-464.

Chow, J. C.; Watson, J. G. (1994) Contemporary source profiles for geological material and motor vehicle emissions [final report]. Research Triangle Park, NC: U.S. Environmental Protection Agency, Office of Air Quality Planning and Standards.

Chow, J. C.; Watson, J. G.; Ono, D. M.; Mathai, C. V. (1993a) PM_{10} standards and nontraditional particulate source controls: a summary of the A&WMA/EPA international specialty conference. J. Air Waste Manage. Assoc. 43: 74-84.

Chow, J. C.; Watson, J. G.; Pritchett, L. C.; Pierson, W. R.; Frazier, C. A.; Purcell, R. G. (1993b) The DRI thermal/optical reflectance carbon analysis system: description, evaluation and applications in U.S. air quality studies. In: Lodge, J. P., Jr. Fourth international conference on carbonaceous particles in the atmosphere; April 1991; Vienna, Austria. Atmos. Environ. Part A 27: 1185-1201.

Chow, J. C.; Fujita, E. M.; Watson, J. G.; Lu, Z.; Lawson, D. R.; Ashbaugh, L. L. (1994) Evaluation of filter-based aerosol measurements during the 1987 Southern California Air Quality Study. Environ. Monit. Assess. 30: 49-80.

Clayton, P.; Wallin, S. C. (1982) Comparison of ambient suspended particulate matter concentrations as measured by the British smoke sampler and the high volume sampler. Atmos. Environ. 16: 2031-2032.

Code of Federal Regulations. (1991) Appendix J to Part 50—reference method for the determination of particulate matter as PM_{10} in the atmosphere. C. F. R. 40: §50.

Colome, S. D.; Kado, N. Y.; Jaques, P.; Kleinman, M. (1992) Indoor-outdoor air pollution relations: particulate matter less than 10 μm in aerodynamic diameter (PM_{10}) in homes of asthmatics. Atmos. Environ. Part A 26: 2173-2178.

Commins, B. T. (1962) Interim report on the study of techniques for determination of polycyclic aromatic hydrocarbons in air. In: Sawicki, E.; Cassel, K., Jr., eds. Analysis of carcinogenic air pollutants: [proceedings of a symposium]; August 1961; Cincinnati, OH. Bethesda, MD: U.S. Department of Health, Education, and Welfare, Public Health Service, National Cancer Institute; pp. 225-233. (National Cancer Institute monograph no. 9).

Conner, T. L.; Miller, J. L.; Willis, R. D.; Kellogg, R. B.; Dann, T. F. (1993) Source apportionment of fine and coarse particles in southern Ontario, Canada. Presented at: 86th annual meeting & exhibition of the Air & Waste Management Association; June; Denver, CO. Pittsburgh, PA: Air & Waste Management Association; paper no. 93-TP-58.05.

Cook, J. P.; Oslund, W. E.; Frank, N. (1995) Evaluation of fine particulate samplers ($PM_{2.5}$) in an area of volatile constituents. In: Particulate matter: health and regulatory issues: proceedings of an international specialty conference; April; Pittsburgh, PA. Pittsburgh, PA: Air & Waste Management Association; pp. 277-296. (A&WMA publication VIP-49).

Cooper, D. W.; Guttrich, G. L. (1981) A study of the cut diameter concept for interpreting particle sizing data. Atmos. Environ. 15: 1699-1707.

Cornille, P.; Maenhaut, W.; Pacyna, J. M. (1990) Sources and characteristics of the atmospheric aerosol near Damascus, Syria. Atmos. Environ. Part A 24: 1083-1093.

Cotham, W. E.; Bidleman, T. F. (1992) Laboratory investigations of the partitioning of organochlorine compounds between the gas phase and atmospheric aerosols on glass fiber filters. Environ. Sci. Technol. 26: 469-478.

Countess, R. J. (1990) Interlaboratory analyses of carbonaceous aerosol samples. Aerosol Sci. Technol. 12: 114-121.

Courtney, W. J.; Shaw, R. W.; Dzubay, T. G. (1982) Precision and accuracy of a β gauge for aerosol mass determinations. Environ. Sci. Technol. 16: 236-239.

Coutant, R. W.; Brown, L.; Chuang, J. C.; Riggin, R. M.; Lewis, R. G. (1988) Phase distribution and artifact formation in ambient air sampling for polynuclear aromatic hydrocarbons. Atmos. Environ. 22: 403-409.

Coutant, R. W.; Callahan, P. J.; Kuhlman, M. R.; Lewis, R. G. (1989) Design and performance of a high-volume compound annular denuder. Atmos. Environ. 23: 2205-2211.

Coutant, R. W.; Callahan, P. J.; Chuang, J. C.; Lewis, R. G. (1992) Efficiency of silicone-grease-coated denuders for collection of polynuclear aromatic hydrocarbons. Atmos. Environ. Part A 26: 2831-2834.

Criss, J. W. (1976) Particle size and composition effects in x-ray fluorescence analysis of pollution samples. Anal. Chem. 48: 179-186.

Crutcher, E. R. (1982) Light microscopy as an analytical approach to receptor modeling. In: A specialty conference on: receptor models applied to contemporary pollution problems; October; Danvers, MA. Pittsburgh, PA: Air Pollution Control Association; pp. 266-284. (SP-48).

Currie, L. A. (1982) Contemporary particulate carbon. In: Wolff, G. T.; Klimisch, R. L., eds. Particulate carbon: atmospheric life cycle. New York, NY: Plenum Press; pp. 245-260.

Daisey, J. M.; McCaffrey, R. J.; Gallagher, R. A. (1981) Polycyclic aromatic hydrocarbons and total extractable particulate organic matter in the Arctic aerosol. Atmos. Environ. 15: 1353-1363.

Daisey, J. M.; Hershman, R. J.; Kneip, T. J. (1982) Ambient levels of particulate organic matter in New York City in winter and summer. Atmos. Environ. 16: 2161-2168.

Dams, R.; Robbins, J. A.; Rahn, K. A.; Winchester, J. W. (1970) Nondestructive neutron activation analysis of air pollution particulates. Anal. Chem. 42: 861-867.

Davis, B. L. (1978) Additional suggestions for X-ray quantitative analysis of high-volume filter samples. Atmos. Environ. 12: 2403-2406.

Davis, B. L. (1980) "Standardless" X-ray diffraction quantitative analysis. Atmos. Environ. 14: 217-220.

Della Fiorentina, H.; De Wiest, F.; De Graeve, J. (1975) Determination par spectrometrie infrarouge de la matiere organique non volatile associee aux particules en suspension dans l'air—II. Facteurs influencant l'indice aliphatique. [Determination of the nonvolatile organic matter associated with suspended particles by infrared spectrometry—II. Factors influencing the aliphatic index]. Atmos. Environ. 9: 517-522.

Derde, M.-P.; Buydens, L.; Guns, C.; Massart, D. L.; Hopke, P. K. (1987) Comparison of rule-building expert systems with pattern recognition for the classification of analytical data. Anal. Chem. 59: 1868-1871.

Divita, F., Jr. (1993) Size distributions and sources of submicrometer atmospheric particles in Washington, D.C. and Philadelphia, PA [Ph.D. dissertation]. College Park, MD: University of Maryland. Available from: University Microfilms, Ann Arbor, MI; publication no. AAC94-25018.

Dod, R. L.; Rosen, H.; Novakov, T. (1979) Atmospheric aerosol research annual report for 1977-1978. Berkeley, CA: Lawrence Berkeley Laboratories; document no. 8696.

Durham, J. L.; Wilson, W. E.; Bailey, E. B. (1978) Application of an SO_2-denuder for continuous measurement of sulfur in submicrometric aerosols. Atmos. Environ. 12: 883-886.

Dzubay, T. G.; Mamane, Y. (1989) Use of electron microscopy data in receptor models for PM-10. Atmos. Environ. 23: 467-476.

Dzubay, T. G.; Nelson, R. O. (1975) Self absorption corrections for X-ray fluorescence analysis of aerosols. Adv. X-Ray Anal. 18: 619-631.

Dzubay, T. G.; Stevens, R. K. (1975) Ambient air analysis with dichotomous sampler and X-ray fluorescence spectrometer. Environ. Sci. Technol. 9: 663-668.

Dzubay, T. G.; Morosoff, N.; Whitaker, G. L.; Yasuda, H. (1981) Evaluation of polymer films as standards for X-ray fluorescence spectrometers. In: Electron microscopy and X-ray applications to environmental and occupational health analysis. Ann Arbor, MI: Ann Arbor Science Publishers, Inc.

Dzubay, T. G.; Stevens, R. K.; Balfour, W. D.; Williamson, H. J.; Cooper, J. A.; Core, J. E.; De Cesar, R. T.; Crutcher, E. R.; Dattner, S. L.; Davis, B. L.; Heisler, S. L.; Shah, J. J.; Hopke, P. K.; Johnson, D. L. (1984) Interlaboratory comparison of receptor model results for Houston aerosol. Atmos. Environ. 18: 1555-1566.

Eatough, D. J. (1995) BOSS, the Brigham Young University Organic Sampling System: determination of particulate carbonaceous material using diffision denuder sampling technology. In: Lane, D., ed. Gas/phase partition measurements of atmospheric organic compounds. New York, NY: Gordon and Breach Science Publishers; in press.

Eatough, D. J.; Sedar, B.; Lewis, L.; Hansen, L. D.; Lewis, E. A.; Farber, R. J. (1989) Determination of semivolatile organic compounds in particles in the Grand Canyon area. Aerosol Sci. Technol. 10: 438-449.

Eatough, D. J.; Wadsworth, A.; Eatough, D. A.; Crawford, J. W.; Hansen, L. D.; Lewis, E. A. (1993) A multiple-system, multi-channel diffusion denuder sampler for the determination of fine-particulate organic material in the atmosphere. Atmos. Environ. Part A 27: 1213-1219.

Edwards, J. D. (1980) A comparison of the British smoke shade method and the intergrating plate method [Ph.D thesis]. Seattle, WA: University of Washington.

Edwards, J. D.; Ogren, J. A.; Weiss, R. E.; Charlson, R. J. (1983) Particulate air pollutants: a comparison of British "Smoke" with optical absorption coefficient and elemental carbon concentration. Atmos. Environ. 17: 2337-2341.

Eichmann, R.; Neuling, P.; Ketseridis, G.; Hahn, J.; Jaenicke, R.; Junge, C. (1979) *n*-alkane studies in the troposphere—I. Gas and particulate concentrations in North Atlantic air. Atmos. Environ. 13: 587-599.

Eldering, A.; Cass, G. R.; Moon, K. C. (1994) An air monitoring network using continuous particle size distribution monitors: connecting pollutant properties to visibility via Mie scattering calculations. Atmos. Environ. 28: 2733-2749.

Eldred, R. A.; Cahill, T. A. (1994) Trends in elemental concentrations of fine particles at remote sites in the United States of America. Atmos. Environ. 28: 1009-1019.

Eldred, R. A.; Cahill, T. A.; Feeney, P. J. (1993) Comparison of independent measurements of sulfur and sulfate in the IMPROVE network. Presented at: 86th annual meeting and exhibition of the Air & Waste Management Association; June; Denver, CO. Pittsburgh, PA: Air & Waste Management Association; paper no. 93-RA-110.02.

Engelbrecht, D. R.; Cahill, T. A.; Feeney, P. J. (1980) Electrostatic effects on gravimetric analysis of membrane filters. J. Air Pollut. Control Assoc. 30: 391-392.

Fang, C. P.; McMurry, P. H.; Marple, V. A.; Rubow, K. L. (1991) Effect of flow-induced relative humidity changes on size cuts for sulfuric acid droplets in the microorifice uniform deposit impactor (MOUDI). Aerosol Sci. Technol. 14: 266-277.

Federal Register. (1971) National primary and secondary ambient air quality standards. F. R. (April 30) 36: 8186-8201.

Federal Register. (1978) Reference method for the determination of lead in suspended particulate matter collected from ambient air. F. R. (October 5) 43: 46258.

Feeney, P.; Cahill, T.; Olivera, J.; Guidara, R. (1984) Gravimetric determination of mass on lightly loaded membrane filters. J. Air Pollut. Control Assoc. 31: 376-378.

Ferm, M. (1986) Concentration measurements and equilibrium studies of ammonium, nitrate and sulphur species in air and precipitation [Ph.D. thesis]. Göteborg, Sweden: Göteborg University, Department of Inorganic Chemistry. Available from: Library of Congress, Washington, DC; call no. QC879/.6/.F47/1986.

Fernandez de la Mora, J. (1986) Inertia and interception in the deposition of particles from boundary layers. Aerosol Sci. Technol. 5: 261-266.

Finlayson-Pitts, B. J.; Pitts, J. N., Jr. (1986) Atmospheric chemistry: fundamentals and experimental techniques. New York, NY: John Wiley & Sons; pp. 783-1007.

Fitz, D. R. (1990) Reduction of the positive organic artifact on quartz filters. Aerosol. Sci. Technol. 12: 142-148.

Fitz, D.; Chan, M.; Cass, G.; Lawson, D.; Ashbaugh, L. (1989) A multi-component size-classifying aerosol and gas sampler for ambient air monitoring. Presented at: 82nd annual meeting of the Air & Waste Management Association; June; Anaheim, CA. Pittsburgh, PA: Air & Waste Management Association; paper no. 89-140.1.

Flessel, P.; Wang, Y. Y.; Chang, K.-I.; Wesolowski, J. J.; Guirguis, G. N.; Kim, I.-S.; Levaggi, D.; Siu, W. (1991) Seasonal variations and trends in concentrations of filter-collected polycyclic aromatic hydrocarbons (PAH) and mutagenic activity in the San Francisco Bay Area. J. Air Waste Manage. Assoc. 41: 276-281.

Foreman, W. T.; Bidleman, T. F. (1990) Semivolatile organic compounds in the ambient air of Denver, Colorado. Atmos. Environ. Part A 24: 2405-2416.

Forrest, J.; Spandau, D. J.; Tanner, R. L.; Newman, L. (1982) Determination of atmospheric nitrate and nitric acid employing a diffusion denuder with a filter pack. Atmos. Environ. 16: 1473-1485.

Friedlander, S. K. (1977) Smoke, dust and haze: fundamentals of aerosol behavior. New York, NY: John Wiley & Sons.

Fung, K. (1990) Particulate carbon speciation by MnO_2 oxidation. Aerosol Sci. Technol. 12: 122-127.

Fung, K. K.; Heisler, S. L.; Price, A.; Nuesca, B. V.; Mueller, P. K. (1979) Comparison of ion chromatography and automated wet chemical methods for analysis of sulfate and nitrate in ambient particulate filter samples. In: Mulik, J. D.; Sawicki, E., eds. Ion chromatographic analysis of environmental pollutants: volume 2. Ann Arbor, MI: Ann Arbor Science Publishers Inc.; pp. 203-209.

Gagosian, R. B.; Peltzer, E. T.; Zafiriou, O. C. (1981) Atmospheric transport of continentally derived lipids to the tropical North Pacific. Nature (London) 291: 312-314.

Gebhart, J. (1993) Optical direct-reading techniques: light intensity systems. In: Willeke, K.; Baron, P. A., eds. Aerosol measurement: principles, techniques, and applications. New York, NY: Van Nostrand Reinhold; pp. 313-344.

Gerber, H. E. (1982) Optical techniques for the measurement of light absorption by particulates. In: Wolff, G. T.; Klimisch, R. L., eds. Particulate carbon: atmospheric life cycle. New York, NY: Plenum Press; pp. 145-158.

Gordon, R. J. (1974) Solvent selection in extraction of airborne particulate matter. Atmos. Environ. 8: 189-191.

Griffin, J. J.; Goldberg, E. D. (1979) Morphologies and origin of elemental carbon in the environment. Science (Washington, DC) 206: 563-565.

Grinshpun, S.; Willeke, K.; Kalatoor, S. (1993) A general equation for aerosol aspiration by thin-walled sampling probes in calm and moving air. Atmos. Environ. Part A 27: 1459-1470.

Grosjean, D. (1975) Solvent extraction and organic carbon determination in atmospheric particulate matter: the organic extraction-organic carbon analyzer (OE-OCA) technique. Anal. Chem. 47: 797-805.

Groves, W. A.; Hahne, R. M. A.; Levine, S. P.; Schork, M. A. (1994) A field comparison of respirable dust samplers. Am. Ind. Hyg. Assoc. J. 55: 748-755.

Gundel, L. A.; Stevens, R. K.; Daisey, J. M.; Lee, V.; Mahanama, K. R. R. (1992) Annular denuders for sampling semi-volatile polycyclic aromatic hydrocarbons and other organic species. Presented at: 11th annual meeting of the American Association for Aerosol Research; October; San Francisco, CA.

Gundel, L. A.; Mahanama, K. R. R.; Daisey, J. M. (1994) Fractionation of polar organic extracts of airborne particulate matter using cyanopropyl-bonded silica in solid-phase extraction. J. Chromatogr. 629: 75-82.

Hall, D. J.; Mark, D.; Upton, S. L. (1992) A new large wind tunnel for dust and aerosol studies. J. Aerosol Sci. 23(suppl. 1): S591-S594.

Hammerle, R. H.; Pierson, W. R. (1975) Sources and elemental composition of aerosol in Pasadena, Calif., by energy-dispersive X-ray fluorescence. Environ. Sci. Technol. 9: 1058-1068.

Hampton, C. V.; Pierson, W. R.; Schuetzle, D.; Harvey, T. M. (1983) Hydrocarbon gases emitted from vehicles on the road. 2. Determination of emission rates from diesel and spark-ignition vehicles. Environ. Sci. Technol. 17: 699-708.

Harman, J. N., Chairman. (1989) Inductively coupled plasma emission spectroscopy. In: Lodge, J. P., Jr., ed. Methods of air sampling and analysis. 3rd ed. Chelsea, MI: Lewis Publishers, Inc.; pp. 89-92.

Harrison, L.; Harrison, H. (1982) A comparison of optical and aerodynamic aerosol sizes: the effects of inhomogeneous particles. Atmos. Environ. 16: 293-300.

Harrison, R. M.; Kitto, A.-M. N. (1990) Field intercomparison of filter pack and denuder sampling methods for reactive gaseous and particulate pollutants. Atmos. Environ. Part A 24: 2633-2640.

Hart, K. M.; Pankow, J. F. (1990) Comparison of *n*-alkane and PAH concentrations collected on quartz fiber and Teflon membrane filters in an urban environment. J. Aerosol Sci. 21(suppl. 1): S377-S380.

Hearle, J. W. S.; Sparrow, J. T.; Cross, P. M. (1972) The use of the scanning electron microscope. New York, NY: Pergamon Press.

Heitbrink, W. A.; Baron, P. A.; Willeke, K. (1991) Coincidence in time-of-flight aerosol spectrometers: phantom particle creation. Aerosol Sci. Technol. 14: 112-126.

Henry, R. C.; Lewis, C. W.; Hopke, P. K.; Williamson, H. J. (1984) Review of receptor model fundamentals. Atmos. Environ. 18: 1507-1515.

Hering, S. V., ed. (1989) Air sampling instruments for evaluation of atmospheric contaminants. 7th ed. Cincinnati, OH: American Conference of Governmental Industrial Hygienists.

Hering, S. V.; Lawson, D. R.; Allegrini, I.; Febo, A.; Perrino, C.; Possanzini, M.; Sickles, J. E., II; Anlauf, K. G.; Wiebe, A.; Appel, B. R.; John, W.; Ondo, J.; Wall, S.; Braman, R. S.; Sutton, R.; Cass, G. R.; Solomon, P. A.; Eatough, D. J.; Eatough, N. L.; Ellis, E. C.; Grosjean, D.; Hicks, B. B.; Womack, J. D.; Horrocks, J.; Knapp, K. T.; Ellestad, T. G.; Paur, R. J.; Mitchell, W. J.; Pleasant, M.; Peake, E.; MacLean, A.; Pierson, W. R.; Brachaczek, W.; Schiff, H. I.; Mackay, G. I.; Spicer, C. W.; Stedman, D. H.; Winer, A. M.; Biermann, H. W.; Tuazon, E. C. (1988) The nitric acid shootout: field comparison of measurement methods. Atmos. Environ. 22: 1519-1539.

Hering, S. V.; Appel, B. R.; Cheng, W.; Salaymeh, F.; Cadle, S. H.; Mulawa, P. A.; Cahill, T. A.; Eldred, R. A.; Surovik, M.; Fitz, D.; Howes, J. E.; Knapp, K. T.; Stockburger, L.; Turpin, B. J.; Huntzicker, J. J.; Zhang, X.-Q.; McMurry, P. H. (1990) Comparison of sampling methods for carbonaceous aerosols in ambient air. Aerosol Sci. Technol. 12: 200-213.

Hering, S. V.; Roberts, P. T.; Taylor, C. A. (1994) Particle measurements for the Children's Health Study: development of a two-week sampler [abstract]. Presented at: Sixth conference of the International Society for Environmental Epidemiology/fourth conference of the International Society for Exposure Analysis; September; Research Triangle Park, NC. Chapel Hill, NC: University of North Carolina, School of Public Health; p. 260.

Hildemann, L. M.; Markowski, G. R.; Cass, G. R. (1991) Chemical composition of emissions from urban sources of fine organic aerosol. Environ. Sci. Technol. 25: 744-759.

Hillamo, R. E.; Kauppinen, E. I. (1991) On the performance of the Berner low pressure impactor. Aerosol Sci. Technol. 14: 33-47.

Hinds, W. C. (1982) Aerosol technology. New York, NY: John Wiley and Sons.

Hinds, W. C.; Kraske, G. (1986) Performance of PMS model LAS-X optical particle counter. J. Aerosol Sci. 17: 67-72.

Hirose, K.; Sugimura, Y. (1984) Excess ^{228}Th in the airborne dust: an indicator of continental dust from the east Asian deserts. Earth Planet. Sci. Lett. 70: 110-114.

Hoffman, A. J.; Purdue, L. J.; Rehme, K. A.; Holland, D. M. (1988) 1987 PM_{10} sampler intercomparison study. In: Mathai, C. V.; Stonefield, D. H., eds. PM-10: implementation of standards, an APCA/EPA international specialty conference; February; San Francisco, CA. Pittsburgh, PA: Air Pollution Control Association; pp. 138-149. (APCA transactions series TR-13).

Holländer, W. (1990) Proposed performance criteria for samplers of total suspended particulate matter. Atmos. Environ. Part A 24: 173-177.

Holländer, W. (1992) Ambient aerosol sampling without pumps. J. Aerosol Sci. 23(suppl. 1): S619-S622.

Hopke, P. K. (1985) Receptor modeling in environmental chemistry. New York, NY: John Wiley & Sons.

Hopke, P. K.; Casuccio, G. S. (1991) Scanning electron microscopy. In: Hopke, P. K., ed. Receptor modeling for air quality management: v. 7. Amsterdam, The Netherlands: Elsevier; pp. 149-212.

Hornung, R. W.; Reed, L. D. (1990) Estimation of average concentration in the presence of nondetectable values. Appl. Occup. Environ. Hyg. 5: 46-51.

Horvath, H.; Kaller, W. (1994) Calibration of integrating nephelometers in the post-halocarbon era. Atmos. Environ. 28: 1219-1223.

Huntzicker, J. J.; Johnson, R. L.; Shah, J. J.; Cary, R. A. (1982) Analysis of organic and elemental carbon in ambient aerosols by a thermal-optical method. In: Wolff, G. T.; Klimisch, R. L., eds. Particulate carbon - atmospheric life cycle: proceedings of an international symposium; October 1980; Warren, MI. New York, NY: Plenum Press; pp. 79-88.

Ingham, D. B.; Yan, B. (1994) The effect of a cylindrical backing body on the sampling efficiency of a cylindrical sampler. J. Aerosol Sci. 25: 535-541.

Ingram, W. T. (1969) Smoke curve calibration. New York, NY: New York University, School of Engineering and Science; PHS contract no. PH-86-68-66.

Ingram, W. T.; Golden, J. (1973) Smoke curve calibration. J. Air Pollut. Control Assoc. 23: 110-115.

International Standards Organization (ISO). (1983) Air quality: particle size fraction definitions for health-related sampling. Geneva, Switzerland: International Standards Organization; technical report ISO/TR7708-1983.

International Standards Organization (ISO). (1992) Air quality—particle size fraction definitions for health-related sampling (draft revision of ISO/TR 7708:1983). Geneva, Switzerland: International Organization for Standardization; draft international standard no. ISO/DIS 7708.

International Standards Organization (ISO). (1993) Air quality—particle size fraction definitions for health-related sampling (revision of ISO/TR 7708:1983). Geneva, Switzerland: International Organization for Standardization; approved international standard no. ISO/DIS 7708.

Jaklevic, J. M.; Loo, B. W.; Goulding, F. S. (1977) Photon-induced X-ray fluorescence analysis using energy-dispersive detector and dichotomous sampler. In: Dzubay, T. G., ed. X-ray fluorescence analysis of environmental samples. Ann Arbor, MI: Ann Arbor Science Publishers, Inc.; pp. 3-18.

Jaklevic, J. M.; Gatti, R. C.; Goulding, F. S.; Loo, B. W. (1981) A β-gauge method applied to aerosol samples. Environ. Sci. Technol. 15: 680-686.

Janocko, P. B.; Casuccio, G. S.; Dattner, S. L.; Johnson, D. L.; Crutcher, E. R. (1982) The El Paso airshed; source apportionment using complementary analyses and receptor models. In: A specialty conference on: receptor models applied to contemporary pollution problems; October; Danvers, MA. Pittsburgh, PA: Air Pollution Control Association; pp. 249-265. (SP-48).

Japar, S. M.; Szkarlat, A. C.; Gorse, R. A., Jr.; Heyerdahl, E. K.; Johnson, R. L.; Rau, J. A.; Huntzicker, J. J. (1984) Comparison of solvent extraction and thermal-optical carbon analysis methods: application to diesel vehicle exhaust aerosol. Environ. Sci. Technol. 18: 231-234.

Javitz, H. S.; Watson, J. G.; Robinson, N. (1988) Performance of the chemical mass balance model with simulated local-scale aerosols. Atmos. Environ. 22: 2309-2322.

Jensen, P. A.; O'Brien, D. (1993) Industrial hygiene. In: Willeke, K.; Baron, P. A., eds. Aerosol measurement: principles, techniques, and applications. New York, NY: Van Nostrand Reinhold; pp. 537-559.

John, W.; Wall, S. M. (1983) Aerosol testing techniques for size-selective samplers. J. Aerosol Sci. 14: 713-727.

John, W.; Wang, H.-C. (1991) Laboratory testing method for PM-10 samplers: lowered effectiveness from particle loading. Aerosol Sci. Technol. 14: 93-101.

John, W.; Hering, S.; Reischl, G.; Sasaki, G.; Goren, S. (1983) Characteristics of Nuclepore filters with large pore size—II. filtration properties. Atmos. Environ. 17: 373-382.

John, W.; Wall, S. M.; Ondo, J. L. (1988) A new method for nitric acid and nitrate aerosol measurement using the dichotomous sampler. Atmos. Environ. 22: 1627-1635.

John, W.; Wall, S. M.; Ondo, J. L.; Winklmayr, W. (1990) Modes in the size distributions of atmospheric inorganic aerosol. Atmos. Environ. Part A 24: 2349-2359.

John, W.; Winklmayr, W.; Wang, H.-C. (1991) Particle deagglomeration and reentrainment in a PM-10 sampler. Aerosol Sci. Technol. 14: 165-176.

Johnson, R. L.; Huntzicker, J. J. (1979) Analysis of volatilizable and elemental carbon in ambient aerosols. In: Novakov, T., ed. Proceedings: carbonaceous particles in the atmosphere; March 1978; Berkeley, CA. Berkeley, CA: University of California, Lawrence Berkeley Laboratory; pp. 10-13; report no. LBL-9037.

Johnson, D. L.; McIntyre, B. L.; Fortmann, R.; Stevens, R. K.; Hanna, R. B. (1981a) A chemical element comparison of individual particle analysis and bulk analysis methods. Scanning Electron Microsc. 1: 469-476.

Johnson, R. L.; Shah, J. J.; Cary, R. A.; Huntzicker, J. J. (1981b) An automated thermal-optical method for the analysis of carbonaceous aerosol. In: Macias, E. S.; Hopke, P. K., eds. Atmospheric aerosol: source/air quality relationships; based on a symposium jointly sponsored by the Divisions of Nuclear Chemistry and Technology at the 180th national meeting of the American Chemical Society; August 1980; Las Vegas, NV. Washington, DC: American Chemical Society; pp. 223-233. (Comstock, M. J., ed. ACS symposium series: 167).

Junge, C. E. (1977) Basic considerations about trace constituents in the atmosphere as related to the fate of global pollutants. In: Suffet, I. H., ed. Fate of pollutants in the air and water environments: part I, mechanism of interaction between environments and mathematical modeling and the physical fate of pollutants, papers from the 165th national American Chemical Society meeting; April 1975; Philadelphia, PA. New York, NY: John Wiley & Sons; pp. 7-25. (Advances in environmental science and technology: v. 8).

Kado, N. Y.; Kozmicky, P. A.; Hsieh, D. P. H.; Gundel, L. A.; Daisey, J. M.; Mahanama, K. R. R.; Schuetzle, D. (1991) Mutagenic activity of the polar organic matter and its fractions from airborne particles. Presented at: AAAR meeting; October; Traverse City, MI.

Kalthoff, K.; Crumpler, J. (1990) PM_{10} methods comparison test report [unpublished material]. Sacramento, CA: California Air Resources Board, Instrumentation and Operations Support Section.

Kanbour, F. I.; Altai, F. A.; Yassin, S.; Harrison, R. M.; Kitto, A.-M. N. (1990) A comparison of smoke shade and gravimetric determination of suspended particulate matter in a semi-arid climate (Baghdad, Iraq). Atmos. Environ. Part A 24: 1297-1301.

Kaupp, H.; Umlauf, G. (1992) Atmospheric gas-particle partitioning of organic compounds: comparison of sampling methods. Atmos. Environ. Part A 26: 2259-2267.

Keeler, G. J.; Brachaczek, W. W.; Gorse, R. A., Jr.; Japar, S. M.; Pierson, W. R. (1988) Effect of ambient humidity on dichotomous sampler coarse/fine ratios. Atmos. Environ. 22: 1715-1720.

Kenny, L. C. (1992) Report of progress towards the development of a performance standard for aerosol sampling instruments used in occupational hygiene. J. Aerosol Sci. 23: 773-779.

Kenny, L. C.; Lidén, G. (1989) The application of performance standards to personal airborne dust samplers. Ann. Occup. Hyg. 33: 289-300.

Kenny, L. C.; Lidén, G. (1991) A technique for assessing size-selective dust samplers using the APS and polydisperse test aerosols. J. Aerosol Sci. 22: 91-100.

Kim, D.; Hopke, P. K. (1988) Classification of individual particles based on computer-controlled scanning electron microscopy data. Aerosol Sci. Technol. 9: 133-151.

Kim, D. S.; Hopke, P. K.; Massart, D. L.; Kaufman, L.; Casuccio, G. S. (1987) Multivariate analysis of CCSEM auto emission data. Sci. Total Environ. 59: 141-155.

Klippel, W.; Warneck, P. (1980) The formaldehyde content of the atmospheric aerosol. Atmos. Environ. 14: 809-818.

König, J.; Funcke, W.; Balfanz, E.; Grosch, B.; Pott, F. (1980) Testing a high volume air sampler for quantitative collection of polycyclic aromatic hydrocarbons. Atmos. Environ. 14: 609-613.

Koutrakis, P.; Wolfson, J. M.; Slater, J. L.; Brauer, M.; Spengler, J. D.; Stevens, R. K.; Stone, C. L. (1988) Evaluation of an annular denuder/filter pack system to collect acidic aerosols and gases. Environ. Sci. Technol. 22: 1463-1468.

Koutrakis, P.; Wolfson, J. M.; Brauer, M.; Spengler, J. D. (1990) Design of a glass impactor for an annular denuder/filter pack system. Aerosol Sci. Technol. 12: 607-612.

Kukreja, V. P.; Bove, J. L. (1976) An enrichment method for polycyclic aromatic hydrocarbons (PAH's) collected on glass fiber filters using hydrofluoric acid. J. Environ. Sci. Health Part A 11: 517-524.

Lamb, S. I.; Petrowski, C.; Kaplan, I. R.; Simoneit, B. R. T. (1980) Organic compounds in urban atmospheres: a review of distribution, collection and analysis. J. Air Pollut. Control Assoc. 30: 1098-1115.

Lane, D. A.; Johnson, N. D.; Barton, S. C.; Thomas, G. H. S.; Schroeder, W. H. (1988) Development and evaluation of a novel gas and particle sampler for semivolatile chlorinated organic compounds in ambient air. Environ. Sci. Technol. 22: 941-947.

Lane, D. A.; Johnson, N. D.; Hanley, M.-J. J.; Schroeder, W. H.; Ord, D. T. (1992) Gas- and particle-phase concentrations of α-hexachlorocyclohexane, γ-hexachlorocyclohexane, and hexachlorobenzene in Ontario air. Environ. Sci. Technol. 26: 126-133.

Larson, T. V.; Yuen, P. F.; Maykut, N. N. (1992) Weekly composite sampling of PM_{10} for total mass and trace elemental analysis. In: Chow, J. C.; Ono, D. M., eds. PM_{10} standards and nontraditional particulate source controls, an A&WMA/EPA international specialty conference, v. I; January; Scottsdale, AZ. Pittsburgh, PA: Air & Waste Management Association; pp. 39-50. (A&WMA transactions series no. 22).

Laskus, L. (1983) Comparative measurements of suspended particulates using several gravimetric methods and the British smoke sampler. Sci. Total Environ. 31: 23-40.

Lee, R. J.; Fisher, R. M. (1980) Quantitative characterization of particulates by scanning and high voltage electron microscopy. Washington, DC: National Bureau of Standards; special publication.

Lee, R. J.; Kelly, J. F. (1980) Overview of SEM-based automated image analysis. Scanning Electron Microsc. 1: 303-310.

Lee, R. E., Jr.; Caldwell, J. S.; Morgan, G. B. (1972) The evaluation of methods for measuring suspended particulates in air. Atmos. Environ. 6: 593-622.

Lee, R. J.; Fasiska, E. J.; Janocko, P.; McFarland, D.; Penkala, S. (1979) Electron-beam particulate analysis. Ind. Res. Dev. (June): 105-108.

Lee, R. J.; Spitzig, W. A.; Kelly, J. F.; Fisher, R. M. (1981) Quantitative metallography by computer-controlled scanning electron microscopy. J. Met. 33(3): 20-25.

Lewis, C. W. (1981) On the proportionality of fine mass concentration and extinction coefficient for bimodal size distributions. Atmos. Environ. 15: 2639-2646.

Li, C. K.; Kamens, R. M. (1993) The use of polycyclic aromatic hydrocarbons as source signatures in receptor modeling. Atmos. Environ. Part A 27: 523-532.

Lidén, G.; Kenny, L. C. (1991) Comparison of measured respirable dust sampler penetration curves with sampling conventions. Ann. Occup. Hyg. 35: 485-504.

Lidén, G.; Kenny, L. C. (1992) The performance of respirable dust samplers: sampler bias, precision and inaccuracy. Ann. Occup. Hyg. 36: 1-22.

Ligocki, M. P.; Pankow, J. F. (1989) Measurements of the gas/particle distributions of atmospheric organic compounds. Environ. Sci. Technol. 23: 75-83.

Lin, C.; Baker, M.; Charlson, R. J. (1973) Absorption coefficient of atmospheric aerosol: a method for measurement. Appl. Opt. 12: 1356-1363.

Lindskog, Å.; Brorström-Lundén, E.; Sjödin, A. (1985) Transformation of reactive PAH on particles by exposure to oxidized nitrogen compounds and ozone. Environ. Int. 11: 125-130.

Lioy, P. J.; Wainman, T.; Turner, W.; Marple, V. A. (1988) An intercomparison of the indoor air sampling impactor and the dichotomous sampler for a 10-μm cut size. JAPCA 38: 668-670.

Lipfert, F. W. (1994) Filter artifacts associated with particulate measurements: recent evidence and effects on statistical relationships. Atmos. Environ. 28: 3233-3249.

Lippmann, M. (1993) Environmental toxicology and exposure limits for ambient air. Appl. Occup. Environ. Hyg. 8: 847-858.

Lippmann, M.; Chan, T. L. (1979) Cyclone sampler performance. Staub Reinhalt. Luft 39: 7-11.

Liu, B. Y. H., ed. (1976) Fine particles: aerosol generation, measurement, sampling, and analysis. New York, NY: Academic Press, Inc.

Liu, B. Y. H.; Pui, D. Y. H. (1981) Aerosol sampling inlets and inhalable particles. Atmos. Environ. 15: 589-600.

Liu, B. Y. H.; Pui, D. Y. H.; Rubow, K. L.; Kuhlmey, G. A. (1978) Progress report: research on air sampling filter media. Minneapolis, MN: University of Minnesota, Mechanical Engineering Department, Particle Technology Laboratory; publication no. 366.

Lodge, J. P., Jr.; Waggoner, A. P.; Klodt, D. T.; Crain, C. N. (1981) Non-health effects of airborne particulate matter. Atmos. Environ. 15: 431-482.

Loo, B. W.; Cork, C. P. (1988) Development of high efficiency virtual impactors. Aerosol Sci. Technol. 9: 167-176.

Lundgren, D. A.; Burton, R. M. (1995) Effect of particle size distribution on the cut point between fine and coarse ambient mass fractions. In: Phalen, R. F.; Bates, D. V., eds. Proceedings of the colloquium on particulate air pollution and human mortality and morbidity; January 1994; Irvine, CA. Inhalation Toxicol. 7: 131-148.

Lundgren, D. A.; Lippmann, M.; Harris, F. S., Jr.; Clark, W. E.; Marlow, W. H.; Durham, M. D., eds. (1979) Aerosol measurement: [papers from a workshop]; March 1976; Gainesville, FL. Gainesville, FL: University Presses of Florida.

Lynch, A. J.; McQuaker, N. R.; Brown, D. F. (1980) ICP/AES analysis and the composition of airborne and soil materials in the vicinity of a lead/zinc smelter complex. J. Air Pollut. Control Assoc. 30: 257-260.

Macher, J.; Chatigny, M. A.; Burge, H. A. (1995) Sampling airborne microorganisms and aeroallergens. In: Air sampling instruments. 8th ed. Cincinnati, OH: American Conference of Governmental Industrial Hygienists.

Macias, E. S.; Blumenthal, D. L.; Anderson, J. A.; Cantrell, B. K. (1979) Characterization of visibility-reducing aerosols in the Southwest. Project VISTTA. Progress report no. 1 (final report). Research Triangle Park, NC: U.S. Environmental Protection Agency, Environmental Sciences Research Laboratory; EPA report no. EPA-600/7-79-243. Available from: NTIS, Springfield, VA; PB80-139041.

Mage, D. T. (1995) The relationship between total suspended particulate matter (TSP) and British Smoke measurements in London: development of a simple model. J. Air Waste Manage. Assoc. 45: 737-739.

Malissa, H. (1979) Some analytical approaches to the chemical characterization of carbonaceous particulates. In: Novakov, T., ed. Proceedings: carbonaceous particles in the atmosphere; March 1978; Berkeley, CA. Berkeley, CA: University of California, Lawrence Berkeley Laboratory; pp. 3-9; report no. LBL-9037.

Malm, W. C.; Sisler, J. F.; Huffman, D.; Eldred, R. A.; Cahill, T. A. (1994) Spatial and seasonal trends in particle concentration and optical extinction in the United States. J. Geophys. Res. [Atmos.] 99: 1347-1370.

Mamane, Y. (1988) Estimate of municipal refuse incinerator contribution to Philadelphia aerosol—I. source analysis. Atmos. Environ. 22: 2411-2418.

Mark, D.; Vincent, J. H. (1986) A new personal sampler for airborne total dust in workplaces. Ann. Occup. Hyg. 30: 89-102.

Mark, D.; Lyons, C. P.; Upton, S. L.; Hall, D. J. (1992) A review of the rationale of current methods for determining the performance of aerosol samplers. J. Aerosol Sci. 23(suppl. 1): S611-S614.

Markowski, G. R. (1987) On identifying and correcting for reentrainment in cascade impactor measurements. Aerosol Sci. Technol. 7: 143-159.

Marple, V. A. (1978) Simulation of respirable penetration characteristics by inertial impaction. J. Aerosol Sci. 9: 125-134.

Marple, V. A.; Olson, B. A. (1995) A high volume $PM_{10}/PM_{2.5}/PM_{1.0}$ trichotomous sampler. In: Particulate matter: health and regulatory issues: proceedings of an international specialty conference; April; Pittsburgh, PA. Pittsburgh, PA: Air & Waste Management Association; pp. 237-261. (A&WMA publication VIP-49).

Marple, V. A.; Rubow, K. L. (1976) Aerodynamic particle size calibration of optical particle counters. J. Aerosol Sci. 7: 425-433.

Marple, V. A.; Rubow, K. L.; Turner, W.; Spengler, J. D. (1987) Low flow rate sharp cut impactors for indoor air sampling: design and calibration. JAPCA 37: 1303-1307.

Marple, V. A.; Liu, B. Y. H.; Olson, B. A. (1989) Evaluation of a cleanroom concentrating aerosol sampler. In: Proceedings of the 35th annual meeting of the Institute of Environmental Sciences. Anaheim, CA: Institute of Environmental Sciences; pp. 360-363.

Marple, V. A.; Liu, B. Y. H.; Burton, R. M. (1990) A high volume dichotomous sampler: design and evaluation. Presented at: 83rd annual meeting & exhibition of the Air & Waste Management Association; June; Pittsburgh, PA. Pittsburgh, PA: Air & Waste Management Association; paper no. 90-84.2.

Marple, V. A.; Rubow, K. L.; Behm, S. M. (1991) A microorifice uniform deposit impactor (MOUDI): description, calibration, and use. Aerosol Sci. Technol. 14: 434-446.

Marple, V. A.; Rubow, K. L.; Olson, B. A. (1993) Inertial, gravitational, centrifugal, and thermal collection techniques. In: Willeke, K.; Baron, P. A., eds. Aerosol measurement: principles, techniques, and applications. New York, NY: Van Nostrand Reinhold; pp. 206-232.

Masia, P.; Di Palo, V.; Possanzini, M. (1994) Uptake of ammonia by nylon filters in filter pack systems. Atmos. Environ. 28: 365-366.

Massart, D. L.; Kaufman, L. (1983) The interpretation of analytical chemical data by the use of cluster analysis. New York, NY: John Wiley & Sons (Elving, P. J.; Winefordner, J. D., eds. Chemical analysis: a series of monographs on analytical chemistry and its applications: v. 65).

Maynard, A. D. (1993) Respirable dust sampler characterisation: efficiency curve reproducibility. J. Aerosol Sci. 24(suppl. 1): S457-S458.

Mazurek, M. A.; Simoneit, B. R. T.; Cass, G. R.; Gray, H. A. (1987) Quantitative high-resolution gas chromatography and high-resolution gas chromatography/mass spectrometry analyses of carbonaceous fine aerosol particles. Int. J. Environ. Anal. Chem. 29: 119-139.

Mazurek, M. A.; Cass, G. R.; Simoneit, B. R. T. (1989) Interpretation of high-resolution gas chromatography/ mass spectrometry data aquired from atmospheric organic aerosol samples. Aerosol Sci. Technol. 10: 408-420.

Mazurek, M. A.; Cass, G. R.; Simoneit, B. R. T. (1991) Biological input to visibility-reducing aerosol particles in the remote arid southwestern United States. Environ. Sci. Technol. 25: 684-694.

McDow, S. R.; Huntzicker, J. J. (1990) Vapor adsorption artifact in the sampling of organic aerosol: face velocity effects. Atmos. Environ. Part A 24: 2563-2571.

McDow, S. R.; Huntzicker, J. J. (1993) Vapor adsorption artifact in the sampling of organic aerosol. In: Winegar, E. D.; Keith, L. H., eds. Sampling and analysis of airborne pollutants. Boca Raton, FL: Lewis Publishers, Inc.; pp. 191-208.

McFarland, A. R.; Ortiz, C. A. (1979) Aerosol characterization of ambient particulate samplers used in environmental monitoring studies. College Station, TX: Texas A&M Research Foundation; contract no. 68-02-2720.

McFarland, A. R.; Ortiz, C. A. (1984) Characterization of Sierra-Andersen model 321a μm size selective inlet for hi-vol samplers. College Station, TX: Texas A&M University, Department of Civil Engineering, Air Quality Laboratory; report no. 4716/01/02/84/ARM.

McFarland, A. R.; Wedding, J. B.; Cermak, J. E. (1977) Wind tunnel evaluation of a modified Andersen impactor and an all weather sampler inlet. Atmos. Environ. 11: 535-539.

McFarland, A. R.; Ortiz, C. A.; Rodes, C. E. (1979) Characteristics of aerosol samplers used in ambient air monitoring. Presented at: 86th national meeting of the American Institute of Chemical Engineers; April; Houston, TX. College Station, TX: Texas A & M University.

McFarland, A. R.; Ortiz, C. A.; Rodes, C. E. (1982) Wind tunnel evaluation of the British smoke shade sampler. Atmos. Environ. 16: 325-328.

McFarland, A. R.; Ortiz, C. A.; Bertch, R. W., Jr. (1984) A 10 μm cutpoint size selective inlet for hi-vol samplers. J. Air Pollut. Control Assoc. 34: 544-547.

McIntyre, B. L.; Johnson, D. L. (1982) A particle class balance receptor model for aerosol apportionment in Syracuse, NY. In: Dattner, S. L.; Hopke, P. K., eds. A specialty conference on receptor models applied to contemporary pollution problems; October; Danvers, MA. Pittsburgh, PA: Air Pollution Control Association. (SP-48).

McMurry, P. H.; Stolzenburg, M. R. (1989) On the sensitivity of particle size to relative humidity for Los Angeles aerosols. Atmos. Environ. 23: 497-507.

McMurry, P. H.; Takano, H.; Anderson, G. R. (1983) Study of the ammonia (gas)-sulfuric acid (aerosol) reaction rate. Environ. Sci. Technol. 17: 347-352.

Merrifield, T. (1989) The measurement of PM-10 by β-absorption. Presented at: 82nd annual meeting and exhibition of the Air & Waste Management Association; June; Anaheim, CA. Pittsburgh, PA: Air & Waste Management Association; paper no. 89-66A.2.

Meyer, M. B.; Lijek, J.; Ono, D. (1992) Continuous PM_{10} measurements in a woodsmoke environment. In: Chow, J. C.; Ono, D. M., eds. PM_{10} standards and nontraditional particulate source controls, an A&WMA/EPA international specialty conference, v. I; January; Scottsdale, AZ. Pittsburgh, PA: Air & Waste Management Association; pp. 24-38. (A&WMA transactions series no. 22).

Meyer, M. B.; Rupprecht, E.; Patashnick, H. (1995) Considerations for the sampling and measurement of ambient particulate matter. In: Particulate matter: health and regulatory issues: proceedings of an international specialty conference; April; Pittsburgh, PA. Pittsburgh, PA: Air & Waste Management Association; pp. 204-210. (A&WMA publication VIP-49).

Meyer-Arendt, J. R. (1972) Introduction to classical and modern optics. Englewood Cliffs, NJ: Prentice Hall, Inc.

Miller, F. J.; Gardner, D. E.; Graham, J. A.; Lee, R. E., Jr.; Wilson, W. E.; Bachmann, J. D. (1979) Size considerations for establishing a standard for inhalable particles. J. Air Pollut. Control Assoc. 29: 610-615.

Mueller, P. K.; Mosley, R. W.; Pierce, L. B. (1971) Carbonate and noncarbonate carbon in atmospheric particles = carbon, carbonate et non carbonate, dans les particules atmospherique. In: Englund, H. M.; Beery, W. T., eds. Proceedings of the second international clean air congress; December 1970; Washington, DC. New York, NY: Academic Press, Inc.; pp. 532-539.

Muir, D.; Laxen, D. P. H. (1995) Black smoke as a surrogate for PM_{10} in health studies? Atmos. Environ. 29: 959-962.

Mulik, J.; Puckett, R.; Williams, D.; Sawicki, E. (1976) Ion chromatographic analysis of sulfate and nitrate in ambient aerosols. Anal. Lett. 9: 653-663.

Mylonas, D. T.; Allen, D. T.; Ehrman, S. H.; Pratsinis, S. E. (1991) The sources and size distributions of organonitrates in Los Angeles aerosol. Atmos. Environ. Part A 25: 2855-2861.

Nevalainen, A.; Pastuszka, J.; Liebhaber, F.; Willeke, K. (1992) Performance of bioaerosol samplers: collection characteristics and sampler design considerations. Atmos. Environ. Part A 26: 531-540.

Nevalainen, A.; Willeke, K.; Liebhaber, F.; Pastuszka, J.; Burge, H.; Henningson, E. (1993) Bioaerosol sampling. In: Willeke, K.; Baron, P. A., eds. Aerosol measurement: principles, techniques, and applications. New York, NY: Van Nostrand Reinhold; pp. 471-492.

Novakov, T. (1982) Soot in the atmosphere. In: Wolff, G. T.; Klimisch, R. L., eds. Particulate carbon: atmospheric life cycle. New York, NY: Plenum Press; pp. 19-41.

Novick, V. J.; Alvarez, J. L. (1987) Design of a multistage virtual impactor. Aerosol Sci. Technol. 6: 63-70.

Ogden, T. L. (1992) Inhalable and respirable dust - moving from aerosol science to legislation. J. Aerosol Sci. 23(suppl. 1): S445-S448.

Ogden, T. L.; Birkett, J. L. (1977) The human head as a dust sampler. In: Walton, W. H., ed. Inhaled particles IV, part 1: proceedings of an international symposium; September 1975; Edinburgh, Scotland. Oxford, United Kingdom: Pergamon Press; pp. 93-105.

Olmez, I. (1989) Trace element signatures in groundwater pollution. In: Watson, J. G., ed. Receptor models in air resources management: an international specialty conference; February 1988; San Francisco, CA. Pittsburgh, PA: Air & Waste Management Association; pp. 3-11. (APCA transactions series: no. 14).

Olmez, I.; Harman, J. N. (1989) Instrumental neutron activation analysis of atmospheric particulate matter. In: Lodge, J. P., Jr., ed. Methods of air sampling and analysis. 3rd ed. Chelsea, MI: Lewis Publishers, Inc.; pp. 143-150.

Ondov, J. M.; Divita, F., Jr. (1993) Size spectra for trace elements in urban aerosol particles by instrumental neutron activation analysis. J. Radioanal. Nucl. Chem. 167: 247-258.

Owen, M. K.; Ensor, D. S.; Sparks, L. E. (1992) Airborne particle sizes and sources found in indoor air. Atmos. Environ. Part A 26: 2149-2162.

Özkaynak, H.; Xue, J.; Weker, R.; Butler, D.; Spengler, J. (1993) The particle TEAM (PTEAM) study: analysis of the data, volume III [draft final report]. Research Triangle Park, NC: U.S. Environmental Protection Agency; EPA contract no. 68-02-4544.

Palen, E. J.; Allen, D. T.; Pandis, S. N.; Paulson, S. E.; Seinfeld, J. H.; Flagan, R. C. (1992) Fourier transform infrared analysis of aerosol formed in the photo-oxidation of isoprene and β-pinene. Atmos. Environ. Part A 26: 1239-1251.

Palen, E. J.; Allen, D. T.; Pandis, S. N.; Paulson, S.; Seinfeld, J. H.; Flagan, R. C. (1993) Fourier Transform Infrared analysis of aerosol formed in the photo-oxidation of 1-octene. Atmos. Environ. Part A 27: 1471-1477.

Pankow, J. F. (1987) Review and comparative analysis of the theories on partitioning between the gas and aerosol particulate phases in the atmosphere. Atmos. Environ. 21: 2275-2283.

Pankow, J. F. (1992) Application of common *y*-intercept regression parameters for log K_p vs $1/T$ for predicting gas-particle partitioning in the urban environment. Atmos. Environ. Part A 26: 2489-2497.

Parmar, S. S.; Grosjean, D. (1990) Laboratory tests of KI and alkaline annular denuders. Atmos. Environ. Part A 24: 2695-2698.

Pashel, G.; Egner, D. (1981) A comparison of ambient suspended particulate matter concentrations as measured by the British smoke sampler and the high volume sampler at 16 sites in the United States. Atmos. Environ. 15: 919-927.

Patashnick, H.; Rupprecht, E. G. (1990) Continuous PM-10 measurements using the tapered element oscillating microbalance. Presented at: 83rd annual meeting and exhibition of the Air & Waste Management Association; June; Pittsburgh, PA. Pittsburgh, PA: Air & Waste Management Association; paper no. 90-84.1.

Patashnick, H.; Rupprecht, E. G. (1991) Continuous PM-10 measurements using the tapered element oscillating microbalance. J. Air Waste Manage. Assoc. 41: 1079-1083.

Pellizzari, E.; Lioy, P.; Quackenboss, J.; Whitmore, R.; Clayton, A.; Freeman, N.; Waldman, J.; Thomas, K.; Rodes, C.; Wilcosky, T. (1995) Population-based exposure measurements in EPA Region 5: Phase I field study in support of the National Human Exposure Assessment Survey. J. Exposure Anal. Environ. Epidemiol. 5: 327-358.

Phillips, B.; Lumpkin, T.; Pleasant, M. (1994) Philadelphia diesel particulate matter monitoring study. In: Measurement of toxic and related air pollutants: proceedings of the U.S. EPA/A&WMA international symposium; May; Durham, NC. Pittsburgh, PA: Air Waste Manage. Assoc.; pp. 640-645. (A&WMA specialty conference VIP-39).

Pierson, W. R.; Hammerle, R. H.; Brachaczek, W. W. (1976) Sulfate formed by interaction of sulfur dioxide with filters and aerosol deposits. Anal. Chem. 48: 1808-1811.

Pierson, W. R.; Brachaczek, W. W.; Japar, S. M.; Cass, G. R.; Solomon, P. A. (1988) Dry deposition and dew chemistry in Claremont, California, during the 1985 Nitrogen Species Methods Comparison Study. Atmos. Environ. 22: 1657-1663.

Pierson, W. R.; Brachaczek, W. W.; Gorse, R. A., Jr.; Japar, S. M.; Norbeck, J. M.; Keeler, G. J. (1989) Atmospheric acidity measurements on Allegheny Mountain and the origins of ambient acidity in the northeastern United States. Atmos. Environ. 23: 431-459.

Possanzini, M.; Febo, A.; Liberti, A. (1983) New design of a high-performance denuder for the sampling of atmospheric pollutants. Atmos. Environ. 17: 2605-2610.

Pupp, C.; Lao, R. C.; Murray, J. J.; Pottie, R. F. (1974) Equilibrium vapour concentrations of some polycyclic aromatic hydrocarbons, As_4O_6 and SeO_2 and the collection efficiencies of these air pollutants. Atmos. Environ. 8: 915-925.

Purdue, L. J.; Rodes, C. E.; Rehme, K. A.; Holland, D. M.; Bond, A. E. (1986) Intercomparison of high-volume PM_{10} samplers at a site with high particulate concentrations. J. Air Pollut. Control Assoc. 36: 917-920.

Qian, Y.; Willeke, K.; Ulevicius, V.; Grinshpun, S. A.; Donnelly, J. (1995) Dynamic size spectrometry of airborne microorganisms: laboratory evaluation and calibration. Atmos. Environ. 29: 1123-1129.

Raabe, O. G.; Braaten, D. A.; Axelbaum, R. L.; Teague, S. V.; Cahill, T. A. (1988) Calibration studies of the drum impactor. J. Aerosol Sci. 19: 183-195.

Rader, D. J.; O'Hern, T. J. (1993) Optical direct-reading techniques: *in situ* sensing. In: Willeke, K.; Baron, P. A., eds. Aerosol measurement: principles, techniques, and applications. New York, NY: Van Nostrand Reinhold; pp. 345-380.

Ramdahl, T.; Zielinska, B.; Arey, J.; Atkinson, R.; Winer, A. M.; Pitts, J. N., Jr. (1986) Ubiquitous occurrence of 2-nitrofluoranthene and 2-nitropyrene in air. Nature (London) 321: 425-427.

Ranade, M. B. (Arun); Woods, M. C.; Chen, F.-L.; Purdue, L. J.; Rehme, K. A. (1990) Wind tunnel evaluation of PM_{10} samplers. Aerosol Sci. Technol. 13: 54-71.

Regan, G. F.; Goranson, S. K.; Larson, L. L. (1979) Use of tape samplers as fine particulate monitors. J. Air Pollut. Control Assoc. 29: 1158-1160.

Reist, P. C. (1984) Introduction to aerosol science. New York, NY: Macmillan Publishing Company.

Rodes, C. E.; Holland, D. M.; Purdue, L. J.; Rehme, K. A. (1985) A field comparison of PM_{10} inlets at four locations. J. Air Pollut. Control Assoc. 35: 345-354.

Rodes, C. E.; Kamens, R. M.; Wiener, R. W. (1991) The significance and characteristics of the personal activity cloud on exposure assessment measurements for indoor contaminants. Indoor Air 2: 123-145.

Rogge, W. F.; Hildemann, L. M.; Mazurek, M. A.; Cass, G. R.; Simoneit, B. R. T. (1993a) Sources of fine organic aerosol. 2. Noncatalyst and catalyst-equipped automobiles and heavy-duty diesel trucks. Environ. Sci. Technol. 27: 636-651.

Rogge, W. F.; Mazurek, M. A.; Hildemann, L. M.; Cass, G. R.; Simoneit, B. R. T. (1993b) Quantification of urban organic aerosols at a molecular level: identification, abundance and seasonal variation. Atmos. Environ. Part A 27: 1309-1330.

Rogge, W. F.; Hildemann, L. M.; Mazurek, M. A.; Cass, G. R.; Simoneit, B. R. T. (1993c) Sources of fine organic aerosol. 3. Road dust, tire debris, and organometallic brake lining dust: roads as sources and sinks. Environ. Sci. Technol. 27: 1892-1904.

Rondia, D. (1965) Sur la volatilite des hydrocarbures polycycliques [Volatility of polycyclic hydrocarbons]. Int. J. Air Water Pollut. 9: 113-121.

Rood, M. J.; Covert, D. S.; Larson, T. V. (1987) Hygroscopic properties of atmospheric aerosol in Riverside, California. Tellus Ser. B 39B: 383-397.

Rubow, K. L.; Marple, V. A.; Olin, J.; McCawley, M.A. (1987) A personal cascade impactor: design, evaluation and calibration. Am. Ind. Hyg. Assoc. J. 48: 532-538.

Rupprecht, E.; Meyer, M.; Patashnick, H. (1992) The tapered element oscillating microbalance as a tool for measuring ambient particulate concentrations in real time. J. Aerosol Sci. 23(suppl. 1): S635-S638.

Saltzman, B. E. (1984) Generalized performance characteristics of miniature cyclones for atmospheric particulate sampling. Am. Ind. Hyg. Assoc. J. 45: 671-680.

Sass-Kortsak, A. M.; O'Brien, C. R.; Bozek, P. R.; Purdham, J. T. (1993) Comparison of the 10-mm nylon cyclone, horizontal elutriator, and aluminum cyclone for silica and wood dust measurements. Appl. Occup. Environ. Hyg. 8: 31-37.

Saucy, D. A.; Anderson, J. R.; Buseck, P. R. (1987) Cluster analysis applied to atmospheric aerosol samples from the Norwegian Arctic. Atmos. Environ. 21: 1649-1657.

Schamber, F. H. (1993) SEM for nontraditional users. Am. Lab. 25(9): 34, 36-38.

Schipper, L. B., III; Chow, J. C.; Frazier, C. A. (1993) Particulate air toxic emission estimation of the PM_{10} fraction in natural aggregate processing facilities. Presented at: 86th annual meeting and exhibition of the Air & Waste Management Association; June; Denver, CO. Pittsburgh, PA: Air Waste Manage. Assoc.; paper no. 93-MP-6.03.

Schuetzle, D.; Lewtas, J. (1986) Bioassay-directed chemical analysis in environmental research. Anal. Chem. 58: 1060A-1076A.

Schwartz, G. P.; Daisey, J. M.; Lioy, P. J. (1981) Effect of sampling duration on the concentration of particulate organics collected on glass fiber filters. Am. Ind. Hyg. Assoc. J. 42: 258-263.

Shaw, R. W., Jr.; Stevens, R. K.; Bowermaster, J.; Tesch, J. W.; Tew, E. (1982) Measurements of atmospheric nitrate and nitric acid: the denuder difference experiment. Atmos. Environ. 16: 845-853.

Shimp, D. R. (1988) Field comparison of beta attenuation PM-10 sampler and high-volume PM-10 sampler. In: Mathai, C. V.; Stonefield, D. H., eds. PM10: implementation of standards, an APCA/EPA international specialty conference; February; San Francisco, CA. Pittsburgh, PA: Air Pollution Control Association; pp. 171-178. (APCA transactions series TR-13).

Sickles, J. E., II; Hodson, L. L. (1989) Fate of nitrous acid on selected collection surfaces. Atmos. Environ. 23: 2321-2324.

Sickles, J. E., II; Grohse, P. M.; Hodson, L. L.; Salmons, C. A.; Cox, K. W.; Turner, A. R.; Estes, E. D. (1990) Development of a method for the sampling and analysis of sulfur dioxide and nitrogen dioxide from ambient air. Anal. Chem. 62: 338-346.

Sides, J. O.; Saiger, H. F. (1976) Effects of prolonged static exposures of filters to ambient air on high volume sampling results. Topeka, KS: Department of Health and Environment.

Simoneit, B. R. T. (1984) Organic matter of the troposphere—III. characterization and sources of petroleum and pyrogenic residues in aerosols over the western United States. Atmos. Environ. 18: 51-67.

Simoneit, B. R. T.; Sheng, G.; Chen, X.; Fu, J.; Zhang, J.; Xu, Y. (1991) Molecular marker study of extractable organic matter in aerosols from urban areas of China. Atmos. Environ. Part A 25: 2111-2129.

Sioutas, C.; Koutrakis, P.; Olson, B. A. (1994) Development and evaluation of a low cutpoint virtual impactor. Aerosol Sci. Technol. 21: 223-235.

Sloane, C. S. (1986) Effect of composition on aerosol light scattering efficiencies. Atmos. Environ. 20: 1025-1037.

Small, H.; Stevens, T. S.; Bauman, W. C. (1975) Novel ion exchange chromatographic method using conductimetric detection. Anal. Chem. 47: 1801-1809.

Smith, R. G.; Bryan, R. J.; Feldstein, M.; Locke, D. C.; Warner, P. O. (1975) Tentative method for the determination of carbon monoxide (detector tube method). Health Lab. Sci. 12: 171-172.

Soderholm, S. C. (1989) Proposed international conventions for particle size-selective sampling. Ann. Occup. Hyg. 33: 301-320.

Solomon, P. A.; Larson, S. M.; Fall, T.; Cass, G. R. (1988) Basinwide nitric acid and related species concentrations observed during the Claremont Nitrogen Species Comparison Study. Atmos. Environ. 22: 1587-1594.

Spagnolo, G. S. (1989) Automatic instrument for aerosol samples using the beta-particle attenuation. J. Aerosol Sci. 20: 19-27.

Spagnolo, G. S.; Paoletti, D. (1994) Automatic system for three fractions sampling of aerosol particles in outdoor environments. J. Air Waste Manage. Assoc. 44: 702-706.

Spengler, J.; Schwab, M.; Ryan, P. B.; Colome, S.; Wilson, A. L.; Billick, I.; Becker, E. (1994) Personal exposure to nitrogen dioxide in the Los Angeles Basin. J. Air Waste Manage. Assoc. 44: 39-47.

Spicer, C. W.; Schumacher, P. M. (1979) Particulate nitrate: laboratory and field studies of major sampling interferences. Atmos. Environ. 13: 543-552.

Stevens, R. K.; Pace, T. G. (1984) Overview of the mathematical and empirical receptor models workshop (Quail Roost II). Atmos. Environ. 18: 1499-1506.

Stevens, R. K.; Dzubay, T. G. ; Russwurm, G.; Rickel, D. (1978) Sampling and analysis of atmospheric sulfates and related species. Atmos. Environ. 12: 55-68.

Stevens, R. K.; McClenny, W. A.; Dzubay, T. G.; Mason, M. A.; Courtney, W. J. (1982) Analytical methods to measure the carbonaceous content of aerosols. In: Wolff, G. T.; Klimisch, R. L., eds. Particulate carbon: atmospheric life cycle. New York, NY: Plenum Publishing Corp.; pp. 111-129.

Stevens, R.; Pinto, J.; Mamane, Y.; Ondov, J.; Abdulraheem, M.; Al-Majed, N.; Sadek, M.; Cofer, W.; Ellenson, W.; Kellogg, R. (1993) Chemical and physical properties of emissions from Kuwaiti oil fires. Water Sci. Technol. 27: 223-233.

Stott, W. R.; Chatfield, E. J. (1979) A precision SEM image analysis system with full feature EDXA characterization. Scanning Electron Microsc. 2: 53-60.

Sweitzer, T. A. (1985) A field evaluation of two PM_{10} inlets in an industrialized area of Illinois. J. Air Pollut. Control Assoc. 35: 744-746.

Symanski, E.; Rappaport, S. M. (1994) An investigation of the dependence of exposure variability on the interval between measurements. Ann. Occup. Hyg. 38: 361-372.

Tang, H.; Lewis, E. A.; Eatough, D. J.; Burton, R. M.; Farber, R. J. (1994) Determination of the particle size distribution and chemical composition of semi-volatile organic compounds in atmospheric fine particles with a diffusion denuder sampling system. Atmos. Environ. 28: 939-947.

Teague, S. V.; Raabe, O. G.; Eldred, R. A. (1992) A bench top wind tunnel for testing PM_{10} sampling inlets. In: Chow, J. C.; Ono, D. M., eds. PM_{10} standards and nontraditional particulate source controls, an A&WMA/EPA international specialty conference, v. I; January; Scottsdale, AZ. Pittsburgh, PA: Air & Waste Management Association; pp. 2-12. (A&WMA transactions series no. 22).

Tejada, S. B.; Zweidinger, R. B.; Sigsby, J. E., Jr.; Bradow, R. L. (1978) Modification of an ion chromatograph for automated routine analysis: applications to mobile source emissions. In: Sawicki, E.; Mulik, J. D.; Wittgenstein, E., eds. Ion chromatographic analysis of environmental pollutants. Ann Arbor, MI: Ann Arbor Science Publishers, Inc.; pp. 111-124.

Thanukos, L. C.; Miller, T.; Mathai, C. V.; Reinholt, D.; Bennett, J. (1992) Intercomparison of PM_{10} samplers and source apportionment of ambient PM_{10} concentrations at Rillito, Arizona. In: Chow, J. C.; Ono, D. M., eds. PM_{10} standards and nontraditional particulate source controls, an A&WMA/EPA international specialty conference, v. I; January; Scottsdale, AZ. Pittsburgh, PA: Air & Waste Management Association; pp. 244-261. (A&WMA transactions series no. 22).

Thomas, A.; Gebhart, J.; Müller, J. (1993) Effect of relative humidity on light scattering of atmospheric aerosols. J. Aerosol Sci. 24(suppl. 1): S117-S118.

Török, S. B.; Van Grieken, R. E. (1994) X-ray spectrometry. Anal. Chem. 66: 186R-206R.

Tsai, P.-J.; Vincent, J. H. (1993) Impaction model for the aspiration efficiencies of aerosol samplers at large angles with respect to the wind. J. Aerosol Sci. 24: 919-928.

Tufto, P. A.; Willeke, K. (1982) Dynamic evaluation of aerosol sampling inlets. Environ. Sci. Technol. 16: 607-609.

Turner, J. R.; Hering, S. V. (1987) Greased and oiled substrates as bounce-free impaction surfaces. J. Aerosol Sci. 18: 215-224.

Turpin, B. J.; Huang, P.-F.; Roos, A.; McMurry, P. H. (1993a) Elemental analysis of single atmospheric particles influencing visibility at the Grand Canyon. In: Bailey, G. W.; Rieder, C. L., eds. Proceedings of the 51st annual meeting of the Microscopy Society of America; August; Cincinnati, OH. San Francisco, CA: San Francisco Press, Inc.; pp. 1124-1125.

Turpin, B. J.; Liu, S.-P.; Podolske, K. S.; Gomes, M. S. P.; Eisenreich, S. J.; McMurry, P. H. (1993b) Design and evaluation of a novel diffusion separator for measuring gas/particle distributions of semivolatile organic compounds. Environ. Sci. Technol. 27: 2441-2449.

Turpin, B. J.; Huntzicker, J. J.; Hering, S. V. (1994) Investigation of organic aerosol sampling artifacts in the Los Angeles basin. Atmos. Environ. 28: 3061-3071.

Turpin, B. J.; Huang, P.-F.; McMurry, P. H.; Hawkins, D. M.; Hering, S. V.; Casuccio, G. S. (1996) Description of a cluster analysis technique to characterize single particle compositions and application to Grand Canyon aerosols. Aerosol Sci. Technol.: submitted.

U.S. Environmental Protection Agency. (1976) Laboratory procedures for the analysis of ammonia in particulates collected by means of HI-VOL samplers-Technicon autoanalyzer II procedures. Research Triangle Park, NC: Analytical Chemistry Branch.

U.S. Environmental Protection Agency. (1982) Air quality criteria for particulate matter and sulfur oxides: v. II. Research Triangle Park, NC: Office of Health and Environmental Assessment, Environmental Criteria and Assessment Office; report no. EPA-600/8-82-029bF. Available from: NTIS, Springfield, VA; PB84-120419.

U.S. Environmental Protection Agency. (1987) PM_{10} SIP development guideline. Research Triangle Park, NC: U.S. Environmental Protection Agency, Office of Air Quality Planning and Standards; EPA report no. EPA-450/2-86-001. Available from: NTIS, Springfield, VA; PB87-206488.

U.S. Environmental Protection Agency. (1992) Determination of the strong acidity of atmospheric fine-particles (<2.5 μm) using annular denuder technology. Washington, DC: Atmospheric Research and Exposure Assessment Laboratory; EPA report no. EPA/600/R-93/037.

U.S. Environmental Protection Agency. (1994) Guidelines for PM-10 sampling and analysis applicable to receptor modeling. Research Triangle Park, NC: Office of Air Quality Planning and Standards; report no. EPA/452/R-94/009. Available from: NTIS, Springfield, VA; PB94-177441.

Upton, S. L.; Mark, D.; Hall, D. J. (1992) Improvements to the design and performance of an ambient inhalable aerosol sampler. J. Aerosol Sci. 23(suppl. 1): S595-S598.

Van Borm, W. A.; Adams, F. C. (1988) Cluster analysis of electron microprobe analysis data of individual particles for source apportionment of air particulate matter. Atmos. Environ. 22: 2297-2307.

Van Borm, W. A.; Adams, F. C.; Maenhaut, W. (1989) Characterization of individual particles in the Antwerp aerosol. Atmos. Environ. 23: 1139-1151.

Van der Meulen, A. (1986) The relationship between PM_{10} and thoracic particle sampling. J. Air Pollut. Control Assoc. 36: 383-387.

Vanderpool, R. W.; Lundgren, D. A.; Marple, V. A.; Rubow, K. L. (1987) Cocalibration of four large-particle impactors. Aerosol Sci. Technol. 7: 177-185.

Van Vaeck, L.; Van Cauwenberghe, K.; Janssens, J. (1984) The gas-particle distribution of organic aerosol constituents: measurements of the volatilisation artefact in hi-vol cascade impactor sampling. Atmos. Environ. 18: 417-430.

Vaughan, N. P. (1989) The Andersen impactor: calibration, wall losses and numerical simulation. J. Aerosol Sci. 20: 67-90.

Vincent, J. H.; Mark, D. (1981) The basis of dust sampling in occupational hygiene: a critical review. Ann. Occup. Hyg. 24: 375-390.

Vincent, J. H.; Mark, D. (1982) Applications of blunt sampler theory to the definition and measurement of inhalable dust. Ann. Occup. Hyg. 26: 3-19.

Vossler, T. L.; Stevens, R. K.; Paur, R. J.; Baumgardner, R. E.; Bell, J. P. (1988) Evaluation of improved inlets and annular denuder systems to measure inorganic air pollutants. Atmos. Environ. 22: 1729-1736.

WESTAR Council. (1995) Comparative data review of manual and continuous PM_{10} sampling methods. Seattle, WA: U.S. Environmental Protection Agency, Region 10; July.

Waggoner, A. P.; Weiss, R. E. (1980) Comparison of fine particle mass concentration and light scattering extinction in ambient aerosol. Atmos. Environ. 14: 623-626.

Wake, D. (1989) Anomalous effects in filter penetration measurements using the aerodynamic particle sizer (APS 3300). J. Aerosol Sci. 20: 13-17.

Wall, S. M.; John, W.; Ondo, J. L. (1988) Measurement of aerosol size distributions for nitrate and major ionic species. Atmos. Environ. 22: 1649-1656.

Wallace, L. A.; Duan, N.; Ziegenfus, R. (1994) Can long-term exposure distributions be predicted from short-term measurements? Risk Anal. 14: 75-85.

Waller, R. E. (1963) Acid droplets in town air. Int. J. Air Water Pollut. 7: 773-778.

Wang, H.-C.; John, W. (1988) Characteristics of the Berner impactor for sampling inorganic ions. Aerosol Sci. Technol. 8: 157-172.

Wang, H.-C.; John, W. (1989) A simple iteration procedure to correct for the density effect in the aerodynamic particle sizer. Aerosol Sci. Technol. 10: 501-505.

Watson, J. G.; Chow, J. C.; Shah, J. J.; Pace, T. G. (1983) The effect of sampling inlets on the PM-10 and PM-15 to TSP concentration ratios. J. Air Pollut. Control Assoc. 33: 114-119.

Watson, J. G.; Bowen, J. L.; Chow, J. C.; Rogers, C. F.; Ruby, M. G.; Rood, M. J.; Egami, R. T. (1989a) High-volume measurement of size classified particulate matter. In: Lodge, J. P., Jr., ed. Methods of air sampling and analysis. 3rd ed. Chelsea, MI: Lewis Publishers, Inc.; pp. 427-439.

Watson, J. G.; Chow, J. C.; Mathai, C. V. (1989b) Receptor models in air resources management: a summary of the APCA international specialty conference. JAPCA 39: 419-426.

Watson, J. G.; Robinson, N. F.; Chow, J. C.; Henry, R. C.; Kim, B. M.; Pace, T. G.; Meyer, E. L.; Nguyen, Q. (1990) The USEPA/DRI chemical mass balance receptor model, CMB 7.0. Environ. Software 5: 38-49.

Wedding, J. B. (1980) Ambient aerosol sampling: history, present thinking and a proposed inlet for inhalable particulate matter. Presented at: 73rd annual meeting of the Air Pollution Control Association; June; Montreal, PQ, Canada. Pittsburgh, PA: Air Pollution Control Association; paper no. 80-38.1.

Wedding, J. B. (1985) Errors in sampling ambient concentrations with instruments employing setpoint temperature compensated mass flow transducers. Atmos. Environ. 19: 1219-1222.

Wedding, J. B.; Carney, T. C. (1983) A quantitative technique for determining the impact of non-ideal ambient sampler inlets on the collected mass. Atmos. Environ. 17: 873-882.

Wedding, J. B.; Weigand, M. A. (1983) Preliminary communication: a thoracic particle inlet (d50 = 6 μm, do = 1 μm) for the high-volume sampler. Atoms. Environ. 17: 1203-1204.

Wedding, J. B.; Weigand, M. A. (1993) An automatic particle sampler with beta gauging. J. Air Waste Manage. Assoc. 43: 475-479.

Wedding, J. B.; Weigand, M. A.; Carney, T. C. (1982) A 10 μm cutpoint inlet for the dichotomous sampler. Environ. Sci. Technol. 16: 602-606.

Wedding, J. B.; Weigand, M. A.; Lodge, J. P., Jr. (1983) A thoracic particle inlet (d_{50} = 6 μm, d_o = 10 μm) for the high-volume sampler. Atmos. Environ. 17: 1203-1204.

Weiss, R. E.; Waggoner, A. P.; Charlson, R. J.; Thorsell, D. L.; Hall, J. S.; Riley, L. A. (1979) Studies of the optical, physical & chemical properties of light absorbing aerosols. In: Novakov, T., ed. Proceedings: carbonaceous particles in the atmosphere; March 1978; Berkeley, CA. Berkeley, CA: University of California, Laurence Berkeley Laboratory; pp. 257-262; report no. LBL-9037.

Wernisch, J. (1985) Quantitative electron microprobe analysis without standard samples. X-ray Spectrom. 14: 109-119.

Wernisch, J. (1986) Application of different Φ (ρz) distributions in quantitative electron probe microanalysis without standard samples. Radex Rundsch. 2/3: 110-113.

Whitby, K. T. (1978) The physical characteristics of sulfur aerosols. Atmos. Environ. 12: 135-159.

Wiener, R. W.; Rodes, C. E. (1993) Indoor aerosols and aerosol exposure. In: Willeke, K.; Baron, P. A., eds. Aerosol measurement: principles, techniques, and applications. New York, NY: Van Nostrand Reinhold; pp. 659-689.

Wiener, R. W.; Rehme, K. A.; Eisner, A.; Vanderpool, R. W. (1994) Review and comparison of PM_{10} sampler performance. Presented at: Fourth international aerosol conference; August; Los Angeles, CA.

Willeke, K.; Degarmo, S. J. (1988) Passive versus active aerosol monitoring. Appl. Ind. Hyg. 3: 263-266.

Willeke, K.; Baron, P. A., eds. (1993) Aerosol measurement: principles, techniques and applications. New York, NY: Van Nostrand Reinhold Publishers.

Willeke, K.; Grinshpun, S. A.; Chang, C.-W.; Juozaitis, A.; Liebhaber, F.; Nevalainen, A.; Thompson, M. (1992) Inlet sampling efficiency of bioaerosol samplers. J. Aerosol Sci. 23(suppl. 1): S651-S654.

Williams, E. L., II; Grosjean, D. (1990) Removal of atmospheric oxidants with annular denuders. Environ. Sci. Technol. 24: 811-814.

Winberry, W. T., Jr.; Forehand, L.; Murphy, N. T.; Ceroli, A.; Phinney, B.; Evans, A. (1993) Determination of reactive acidic and basic gases and particulate matter in indoor air (annular denuder technique). In: Methods for determination of indoor air pollutants: EPA methods. Park Ridge, NJ: Noyes Data Corporation.

Witz, S.; Eden, R. W.; Wadley, M. W.; Dunwoody, C.; Papa, R.; Torre, K. J. (1990) Rapid loss of particulate nitrate, chloride and ammonium on quartz fiber filters during storage. J. Air Waste Manage. Assoc. 40: 53-61.

Wolff, G. T.; Groblicki, P. J.; Cadle, S. H.; Countess, R. J. (1982) Particulate carbon at various locations in the United States. In: Wolff, G. T.; Klimsch, R. L., eds. Particulate carbon: atmospheric life cycle. New York, NY: Plenum Press; pp. 297-315.

Woskie, S. R.; Shen, P.; Finkel, M.; Eisen, E. A.; Smith, T. J.; Smith, R.; Wegman, D. H. (1993) Calibration of a continuous-reading aerosol monitor (Miniram) to measure borate dust exposures. Appl. Occup. Environ. Hyg. 8: 38-45.

Yamada, Y. (1983) A new method for the determination of collection efficiency of an aerosol sampler by electron microscopy. Atmos. Environ. 17: 369-372.

Yamasaki, H.; Kuwata, K.; Miyamoto, H. (1982) Effects of ambient temperature on aspects of airborne polycyclic aromatic hydrocarbons. Environ. Sci. Technol. 16: 189-194.

Ye, Y.; Tsai, C.-J.; Pui, D. Y. H.; Lewis, C. W. (1991) Particle transmission characteristics of an annular denuder ambient sampling system. Aerosol Sci. Technol. 14: 102-111.

Yeh, H.-C. (1993) Electrical techniques. In: Willeke, K.; Baron, P. A., eds. Aerosol measurement: principles, techniques, and applications. New York, NY: Van Nostrand Reinhold; pp. 410-426.

Zhang, X.; McMurry, P. H. (1992) Evaporative losses of fine particulate nitrates during sampling. Atmos. Environ. Part A 26: 3305-3312.

Zielinska, B.; Arey, J.; Atkinson, R.; Winer, A. M. (1989) The nitroarenes of molecular weight 247 in ambient particulate samples collected in southern California. Atmos. Environ. 23: 223-229.

Zoller, W. H.; Gordon, G. E. (1970) Instrumental neutron activation analysis of atmospheric pollutants utilizing Ge(Li) γ-ray detectors. Anal. Chem. 42: 257-265.

5. SOURCES AND EMISSIONS OF ATMOSPHERIC PARTICLES

5.1 INTRODUCTION

Unlike gaseous criteria pollutants (SO_2, NO_2, CO, O_3), which are well defined chemical entities, atmospheric particles comprise a complex mixture of chemical constituents. Because of this fact, sources of each constituent of the atmospheric aerosol must be considered in turn. Since particulate matter (PM) is composed of both primary and secondary constituents, emissions of both the primary components and the gaseous precursors must be considered. The chemical composition of ambient aerosols was treated in general terms in Chapter 3. Information on ambient concentrations of particles of various sizes (PM_{10}, $PM_{2.5}$) and their chemical composition, based on specific field studies, is presented in Chapter 6.

Tables 5-1A and 5-1B summarize anthropogenic and natural sources for the major primary and secondary aerosol constituents of fine and coarse particles. Anthropogenic sources can be further divided into stationary and mobile sources. Stationary sources include fuel combustion for electrical utilities and industrial processes; construction and demolition; metals, minerals, petrochemicals and wood products processing; mills and elevators used in agriculture; erosion from tilled lands; waste disposal and recycling; and fugitive dust from paved and unpaved roads. Mobile, or transportation related, sources include direct emissions of primary PM and secondary PM precursors from highway and off-highway vehicles and nonroad sources. Also shown are sources for precursor gases whose oxidation forms secondary particulate matter. In general, the nature of sources of particulate matter shown in Table 5-1A is very different from that for particulate matter shown in Table 5-1B. A large fraction of the mass in the fine size fraction is derived from material that has been volatilized in combustion chambers and then recondensed to form primary fine PM, or has been formed in the atmosphere from precursor gases as secondary PM. Since precursor gases and fine particulate matter are capable of travelling great distances, it is difficult to identify individual sources of constituents shown in Table 5-1A. The PM constituents shown in Table 5-1B

TABLE 5-1A. CONSTITUENTS OF ATMOSPHERIC FINE PARTICLES (<2.5 μm) AND THEIR MAJOR SOURCES

	Sources			
	Primary		Secondary	
Aerosol species	Natural	Anthropogenic	Natural	Anthropogenic
$SO_4^{=}$	Sea spray	Fossil fuel combustion	Oxidation of reduced sulfur gases emitted by the oceans and wetlands; and SO_2 and H_2S emitted by volcanism and forest fires	Oxidation of SO_2 emitted from fossil fuel combustion
NO_3^-	—	Motor vehicle exhaust	Oxidation of NO_x produced by soils, forest fires, and lighting	Oxidation of NO_x emitted from fossil fuel combustion; and in motor vehicle exhaust
Minerals	Erosion, re-entrainment	Fugitive dust; paved, unpaved roads; agriculture and forestry	—	—
NH_4^+	—	Motor vehicle exhaust	Emissions of NH_3 from wild animals, undisturbed soil	Emissions of NH_3 from animal husbandry, sewage, fertilized land
Organic carbon (OC)	Wild fires	Open burning, wood burning, cooking, motor vehicle exhaust, tire wear	Oxidation of hydrocarbons emitted by vegetation, (terpenes, waxes); wild fires	Oxidation of hydrocarbons emitted by motor vehicles, open burning, wood burning
Elemental carbon	Wild fires	Motor vehicle exhaust, wood burning, cooking	—	—
Metals	Volcanic activity	Fossil fuel combustion, smelting, brake wear	—	—
Bioaerosols	Viruses, bacteria	—	—	—

TABLE 5-1B. CONSTITUENTS OF ATMOSPHERIC COARSE PARTICLES (>2.5 μm) AND THEIR MAJOR SOURCES

	Sources			
	Primary		Secondary	
Aerosol species	Natural	Anthropogenic	Natural	Anthropogenic
Minerals	Erosion, re-entrainment	Fugitive dust; paved, unpaved road dust, agriculture and forestry	—	—
Metals	Erosion, re-entrainment, organic debris	—	—	—
Miscellaneous ions	Sea spray	Road salting	—	—
Organic carbon	—	Tire and asphalt wear	—	—
Organic debris	Plant, insect fragments	—	—	—
Bioaerosols	Pollen, fungal spores, bacterial agglomerates	—	—	—

have shorter lifetimes in the atmosphere, so their impacts tend to be more localized. Only major sources for each constituent are listed in Tables 5-1A and 5-1B.

Natural sources of primary PM include windblown dust from undisturbed land, sea spray, and plant and insect debris. The oxidation of a fraction of terpenes emitted by vegetation and reduced sulfur species from anaerobic environments leads to secondary PM formation. Ammonium (NH_4^+) ions which are crucial for regulating the pH of particles are derived from emissions of ammonia (NH_3) gas. Source categories for NH_3 have been divided into emissions from undisturbed soils (natural) and emissions which are related to human activities (e.g., fertilized lands, domestic and farm animal waste). It is difficult to describe emissions from biomass burning as either natural or anthropogenic. Clearly, fuel wood burning is an anthropogenic source of PM, whereas wildfires would be a natural source. Forest fires have been included as a natural source, because of the lack of information on the amount of prescribed burning or accidental fires caused by humans.

Similar considerations apply to the biogenic emissions of trace metals which may be remobilized from anthropogenic inputs.

Although a large number of potential source contributions have been listed for particulate matter and gaseous precursors in Tables 5-1A and 5-1B, it should be noted that emissions inventories have been compiled for only a limited number of entries for either aerosol constituents or source categories. The remainder of the chapter includes discussion of the processes responsible for the most important sources of primary and secondary PM in Sections 5.2 and 5.3, respectively, followed by discussion of emissions estimates for the United States in Section 5.4. Applications of emissions inventories and other techniques, such as receptor modeling for inferring sources of ambient particulate matter, are then discussed in Section 5.5.

5.2 SOURCES OF PRIMARY PARTICULATE MATTER

This section discusses processes responsible for the emissions of primary particulate matter. The order of sources roughly follows their estimated relative source strengths for the United States to be presented in Section 5.4. Emissions of mineral particles produced as the result of natural wind erosion and human activities are discussed in 5.2.1. Sources of primary particulate matter produced by fossil fuel combustion and other stationary anthropogenic sources are discussed in 5.2.2, while sources of secondary particulate matter are discussed in section 5.3. Motor vehicle emissions are discussed in 5.2.3. Vegetation burning in woodstoves and forest fires is discussed as a source of particulate matter in 5.2.4. Sea salt aerosol production, the suspension of organic debris, and the production of trace metals by natural processes are discussed in 5.2.5. Data for the chemical composition and particle size distribution for each of these sources of particulate matter are included where available along with information about techniques for measuring source compositions and emissions rates.

5.2.1 Wind Erosion and Fugitive Dust

Windblown dust constitutes a major component of the atmospheric aerosol, especially in arid and semi-arid areas of the world. Windblown dust represents the largest single category

in global emissions inventories, constituting about 50% of the total global source of primary and secondary particulate matter (IPCC, 1995). Since the next major category is sea-salt aerosol production, which is estimated to constitute about 40% of total emissions, it can be seen that about 70% of non-sea-salt aerosol emitted is in the form of mineral dust. If one-half of the dust is assumed to be emitted in the PM_{10} size range, then it can be seen that 54% of non-sea-salt PM_{10} emitted globally is dust, less than about 10% of which originates in the United States.

Many areas of the western United States are classified as arid or semi-arid, potentially leading to a larger contribution of dust to the mass of the ambient aerosol there compared to the eastern United States. Large-scale dust events are generally associated with semi-arid regions where marginal lands are used for agriculture and herding. During times of drought, the denuded and broken soil surface is easily carried away, periodically forming "dust bowl" conditions as in the midwestern U.S. (Prospero, 1995).

Emission rates of mineral aerosols are found to be strongly dependent on meteorological parameters such as wind velocity and precipitation. Wind tunnel experiments (Bagnold, 1941; Chepil, 1945) have shown that the motion of loose particles on the surface is initiated when the surface wind stress (The wind stress acting on the surface is supplied by the downward transport of momentum from the mean winds. In micrometeorological applications, u^*, or the square root of the ratio of the wind stress to the air density is used.) acting on erodible particles exceeds the downward force of gravity and the interparticle cohesion forces acting on the particles. Particle motion occurs when u^* exceeds the threshold friction velocity, u^*_t, which is dependent on particle properties. Values of u^*_t are strongly size dependent, with a minimum for particles having diameters of about 60 μm (Bagnold, 1941). Individual smaller particles are held by cohesive forces and larger particles are constrained by the force of gravity. Measurements of u^*_t are available for a number of different soil types (e.g., Gillette et al., 1980).

Three types of particle motion were characterized in the early wind tunnel experiments: suspension, saltation, and creeping. Suspension refers to the upward transport of dust ($d < 60$ μm) by turbulent eddies; saltation to the horizontal motion of particles ($60 < d < 2000$ μm) which can reach heights of up to a meter above the surface before they fall back;

creeping to particles too massive ($d > 2000\ \mu m$) to be lifted from the surface so they roll along.

Because of strong cohesive forces in soil crusts and rock surfaces, particles are not suspended directly by the transfer of momentum from the wind but by sandblasting and abrasion by saltating particles. The impact of saltating grains then results in the emission of smaller particles (Shao et al., 1993). The flux of saltating particles increases rapidly with wind speed, and varies as $(u^*)^2(u^*-u^*_t)$. The size distribution of the suspended aerosol is then controlled by the aerosol microphysical processes of coagulation and sedimentation.

Non-erodible elements on natural surfaces cut down on the surface area available for erosion, and they take up wind momentum which would otherwise be available for erosion. Soil moisture, salts, and organic matter mainly affect soil cohesion (e.g., Gillette et al., 1982) and thus the size distribution of soil particle aggregates. Chepil (1956), Belly (1964), Bisal and Hsieh (1966), and Svasek and Terwindt (1974) show that substantially greater wind forces are needed when soil surface moisture is increased by less than 1% from its dry state. The moisture content of soils will vary throughout the year depending on the frequency and intensity of precipitation events, irrigation, and the relative humidity and temperature of the surrounding air. Large amounts of rain falling during 1 mo of a year will not be as effective in stabilizing dust as the same amount of rain interspersed at intervals throughout the year.

An operational difficulty arises because u^* is derived from anemometers placed at a height of 5 or 10 m above the surface and requires assumptions about the wind profile down to the surface. The challenge is to derive values for wind stress acting on erodible elements (Alfaro and Gomes, 1995) which are valid for large areas. Alfaro and Gomes (1995) have derived relations between wind velocity measurements made at conventional heights and surface wind stresses using radar imagery to characterize surface roughness. Surface roughness is determined by the presence of vegetation, structures, rocks and boulders, topographic irregularities and surface obstructions. Marticorena and Bergametti (1995) have developed parameterizations including these physical considerations suitable for use in large scale models.

Apart from the large-scale, mean flow small-scale atmospheric vortices are also capable of suspending dust. Dust devils, so-called because of the dust they entrain, may be found in arid areas along roads or where the surface has been disturbed by human activity (Hall,

1981; Snow and McClelland, 1990). Hall (1981) proposed that dust devils could constitute the major source of suspended dust on hot summer days with light winds and convectively unstable conditions, as an example in Pima Co., AZ demonstrates. Hall (1981) estimated that large scale winds could raise 171 kg km^{-2} day^{-1} and motor vehicles could raise 48 kg km^{-2} day^{-1} on an annually averaged basis, while dust devils could raise up to 250 kg km^{-2} day^{-1} of dust (in all size ranges) on hot summer days. Atmospheric vortices are not a source component currently treated in emissions inventories.

Apart from sources within the continental United States, an additional source of windblown dust involves the long-range transport of dust from the Sahara desert westward across the Atlantic Ocean. Individual dust storms have been tracked across the Atlantic, after emerging from the northwest coast of Africa, to the east coast of the United States (Ott et al., 1991). Saharan dust is carried into the Miami area, capable of producing dense hazes during the summer (Prospero et al., 1987). While summertime monthly mean dust concentrations are about 10 $\mu g/m^3$ (Prospero et al., 1993), dust events are highly sporadic and of short duration. In a one-year study of Saharan dust deposition in Miami, Prospero et al. (1987) found that 22% of the annual deposition occurred in one day and 68% in rain events that occurred during two dust episodes spread over a total of four days. Gatz (1995) has found evidence suggesting that Saharan dust has reached as far as central Illinois in at least one episode which occurred during the summer of 1979. Up to 20 $\mu g/m^3$ of the ambient aerosol may have originated in the Sahara desert and the Sahel during this episode. These dust events are highly sporadic and more work needs to be done to characterize the frequency, magnitude, and variability of these events. Similar dust transport may also occur from the deserts of Asia across the Pacific Ocean (Prospero, 1995), but it is not clear to what extent any of this dust reaches the United States (See Chapter 6 for more information on long distance transport of dust particles into the United States from Africa or Asia.)

The compositions of soils and average crustal material are shown in Table 5-2 (adapted from Warneck, 1988). Two entries are shown as representations of average crustal material. Differences from the mean soil composition shown can result from local geology and climate conditions. Major elements in both soil and crustal profiles are Si, Al, and Fe which are found in the form of various minerals. In addition, organic matter constitutes a few percent,

TABLE 5-2. AVERAGE ABUNDANCES OF MAJOR ELEMENTS IN SOIL AND CRUSTAL ROCK

	Elemental Abundances (ppmw)		
		Crustal Rock	
Element	Soil (a)	(b)	(c)
Si	330,000	277,200	311,000
Al	71,300	81,300	77,400
Fe	38,000	50,000	34,300
Ca	13,700	36,300	25,700
Mg	6,300	20,900	33,000
Na	6,300	28,300	31,900
K	13,600	25,900	29,500
Ti	4,600	4,400	4,400
Mn	850	950	670
Cr	200	100	48
V	100	135	98
Co	8	25	12

Source: (a) Vinogradov (1959); (b) Mason (1966); (c) Turekian (1971), Model A; as quoted in Warneck (1988).

on average, of soils. In general, the soil profile is similar to the crustal profiles, except for the depletion of soluble elements such as Ca, Mg, and Na.

Because of the enormous difficulties encountered in developing theoretical estimates of windblown dust emissions, most current estimates rely on the results of empirical studies. These studies typically involve the placement of wind tunnels over natural surfaces and then measuring emission rates and size distributions for different wind conditions. The emissions of fugitive dust raised as the result of human activities are also extremely difficult to quantify. Fugitive dust emissions arise from paved and unpaved roads, building construction and demolition, storage piles, and agricultural tilling in addition to wind erosion.

Figure 5-1 shows examples of size distributions in dust from paved and unpaved roads, agricultural soil, sand and gravel, and alkaline lake bed sediments which were measured in a

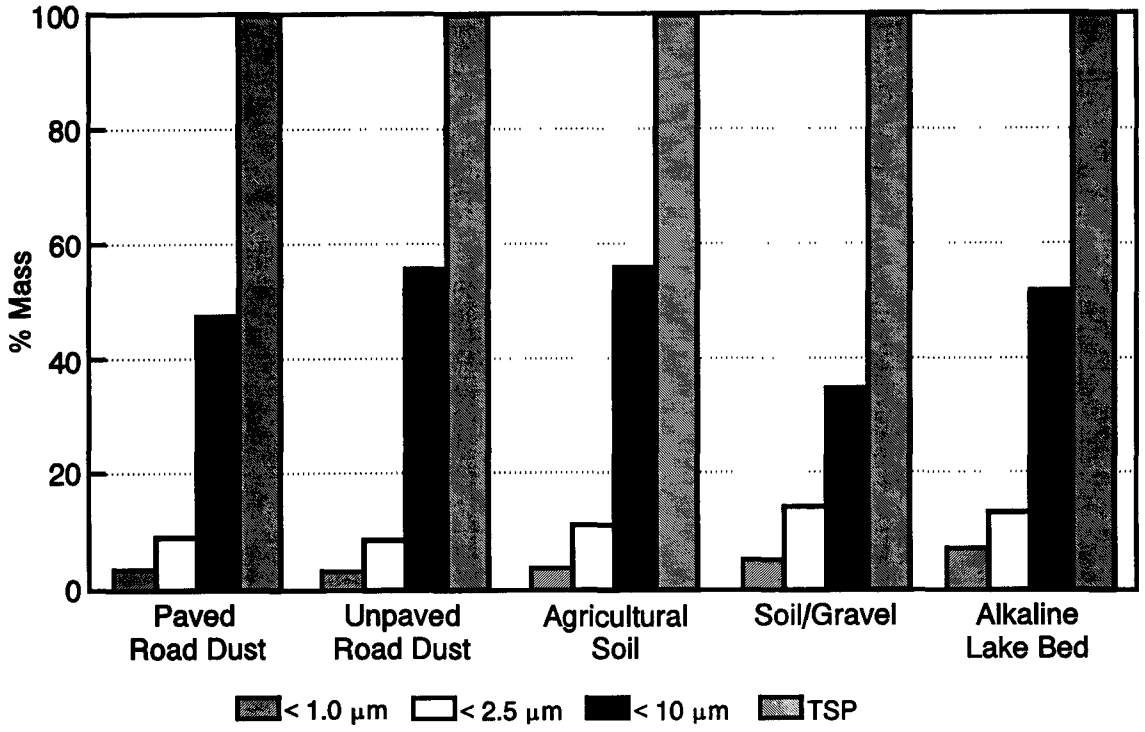

Figure 5-1. Size distribution of particles generated in a laboratory resuspension chamber.

Source: Chow et al. (1994).

laboratory resuspension chamber as part of a study in California (Chow et al., 1994). This figure shows substantial variation in particle size among some of these fugitive dust sources. The $PM_{1.0}$ abundance (6.9%) in the alkaline lake bed dust is twice its abundance in paved and unpaved road dust. Approximately 10% of TSP is in the $PM_{2.5}$ fraction and approximately 50% of TSP is in the PM_{10} fraction. The sand/gravel dust sample shows that 65% of the mass is in particles larger than the PM_{10} fraction. The $PM_{2.5}$ fraction of TSP is approximately 30% to 40% higher in alkaline lake beds and sand/gravel than in the other soil types. The tests were performed after seiving and with a short (<1 min) waiting period prior to sampling. It is expected that the fraction of $PM_{1.0}$ and $PM_{2.5}$ would increase with distance from a fugitive dust emitter as the larger particles deposit to the surface at a larger velocity than the smaller particles. Additional data shown in Figure 5-2 (Houck et al., 1989, 1990) were obtained in a study characterizing particle sources in California.

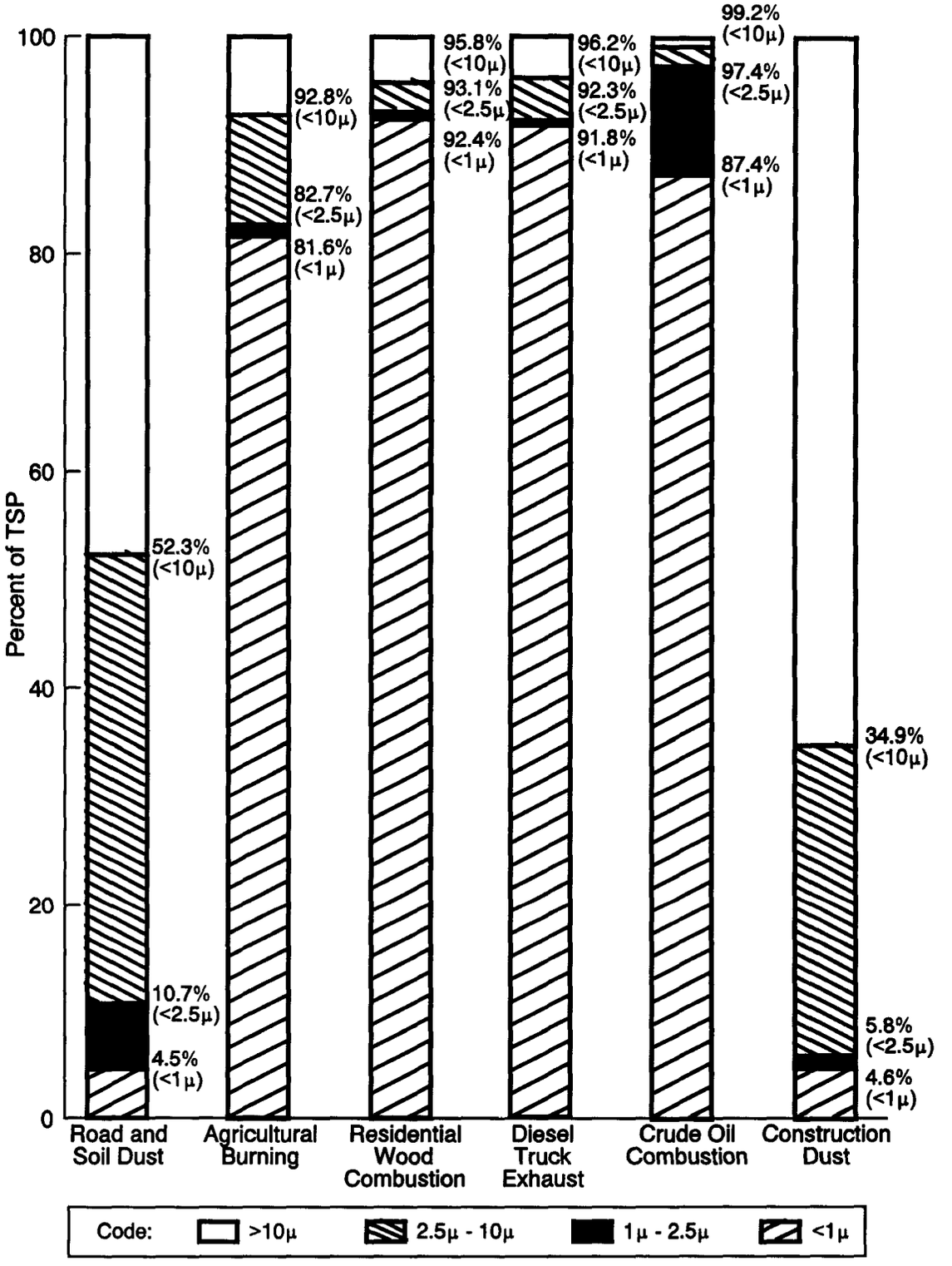

Figure 5-2. Size distribution of California source emissions, 1986.

Source: Houck et al. (1989, 1990).

Unpaved roads and other unpaved areas with vehicular activity are essentially unlimited reservoirs of dust loading when vehicles are moving. These surfaces are always being disturbed, and wind erosion seldom has an opportunity to increase their surface roughness sufficiently to inhibit particle suspension. The U.S. EPA AP-42 emission factor (U.S. Environmental Protection Agency, 1995a) for unpaved road dust emissions contains variables which account for silt loading, mean vehicle speed, mean vehicle weight, mean number of wheels, and number of days with detectable precipitation, to determine annual PM_{10} dust emissions for each vehicle-kilometer traveled. Dust loadings on a paved road surface build up by being tracked out from unpaved areas such as construction sites, unpaved roads, parking lots, and shoulders; by spills from trucks carrying dirt and other particulate materials; by transport of dirt collected on vehicle undercarriages; by wear of vehicle components such as tires, brakes, clutches, and exhaust system components; by wear of the pavement surface; by deposition of suspended particles from many emissions sources; and by water and wind erosion from adjacent areas. Moisture causes dust to adhere to vehicle surfaces so that it can be carried out of unpaved roads, parking lots, and staging areas. Carryout also occurs when trucks exit heavily watered construction sites. This dust is deposited on paved roadway surfaces as it dries, where it is available for suspension far from its point of origin. Fugitive dust emissions from paved roads are often higher after rainstorms in areas where unpaved accesses are abundant, even though the rain may have flushed existing dust from many of the paved streets.

The size distribution of samples of paved road dust obtained from a source characterization study in California is shown in Figure 5-2. As might be expected, most of the emissions are in the coarse size mode. The chemical composition of paved road dust obtained in Denver, CO, during the winter of 1987-1988 is shown in Figure 5-3. The chemical composition of paved road dust is much like an ambient PM_{10} sample, which consists of a complex mixture of particulate matter from a wide variety of sources. Hopke et al. (1980) found that the inorganic composition of urban roadway dust in samples from Urbana, IL could be described in terms of contributions from natural soil, automobile exhaust, rust, tire wear, and salt. Automobile contributions arose from exhaust emissions enriched in Pb; from rust as Fe; tire wear particles enriched in Zn; brake linings enriched in Cr, Ba, and Mn; and cement particles derived from roadways by abrasion. The complexity

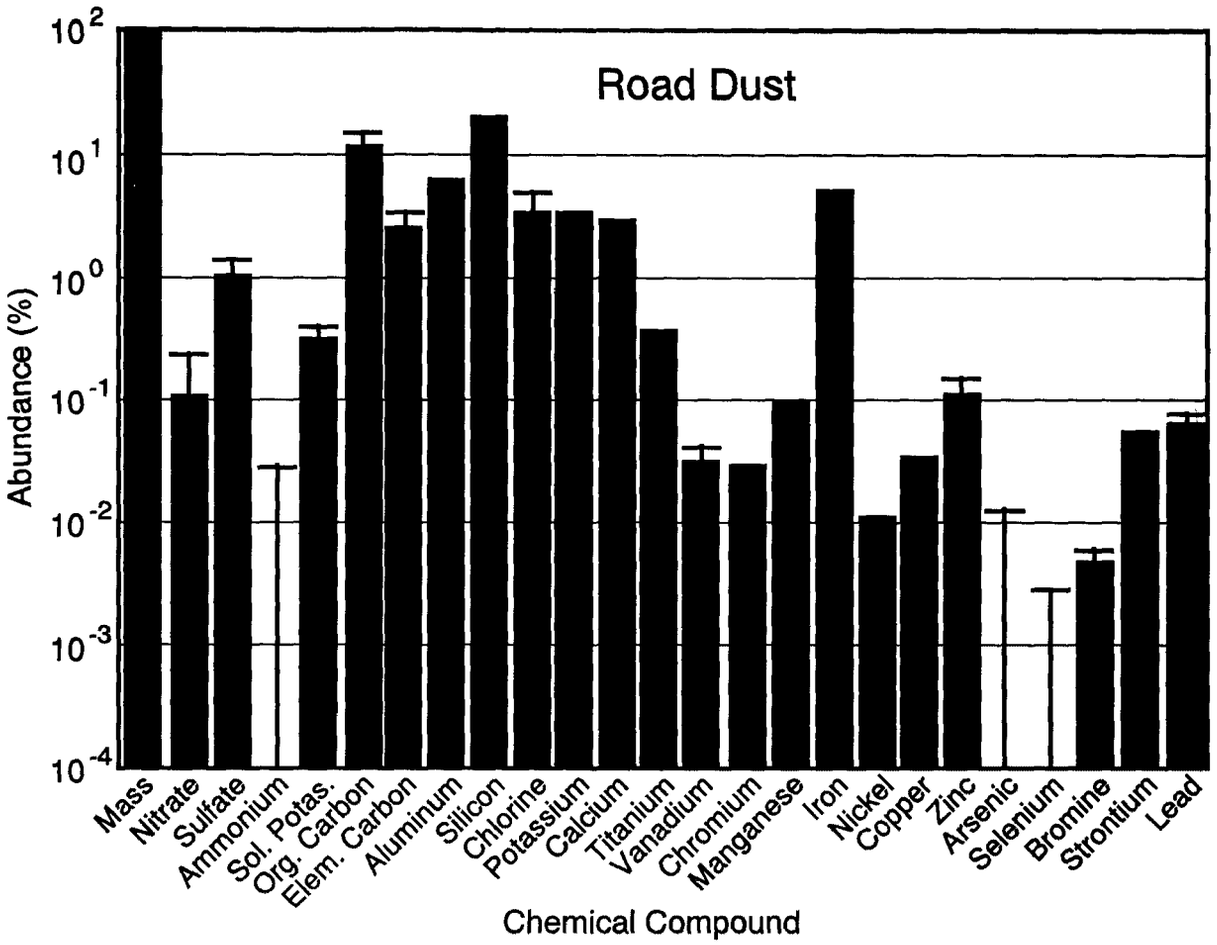

Figure 5-3. Chemical abundances for $PM_{2.5}$ emissions from paved road dust in Denver, CO. Solid bars represent fractional abundances, and the error bars represent variability in species abundances. Error bars represent detection limits when there are no solid bars.

Source: Watson and Chow (1994).

of paved road dust is also evident in the comparison of a paved road dust profile reported by Chow et al. (1991) for Phoenix, AZ, with profiles from other geological sources in the area. Chow et al. (1991) noted that the abundance of organic carbon in the profile was $11 \pm 9\%$, larger and more variable than its abundance in profiles from agricultural land, construction sites, and vacant lots. The presence of particles produced by automotive emissions, tire wear, organic detritus, and engine oils may account for this enrichment for organic carbon.

The abundances of Pb and Br in Phoenix paved road dust were more than double the concentrations in the other geological profiles, indicating the presence of tailpipe exhaust

from vehicles burning leaded fuels. The contribution of tire wear could have been from 4 to 45% of that of motor vehicle exhaust, based on the results of Pierson and Brachaczek (1974). Enrichments in species from clutch and brake wear were not detectable in the Phoenix paved road dust profiles. These are often composed of asbestos and/or semi-metal carbon composites. Cooper et al. (1987) examined the elemental composition of semi-metal brake shoes and found abundances of ~45% Fe, ~2% Cu, ~0.5% Sn, ~3% Ba, and ~0.5% Mo. None of these species were found in the Phoenix paved road dust profiles at levels significantly in excess of their abundances in other geological sub-types.

Many fugitive dust sources are episodic rather than continuous emitters. Though windblown dust emissions are low on an annual average, they can be quite large during those few episodes when wind speeds are high. In Coachella Valley, CA, the South Coast Air Quality Management District (1994) calculated 24-h emissions based on a worst windy day. On a day when wind gust speeds exceeded 96 km/h, fugitive dust emissions could account for 20% of the entire annual emissions. Since the rate of dust suspension varies as the cube of the wind speed for large wind speeds, estimates of windblown dust emissions use highest wind speeds quoted in National Weather Service Local Climatological Summaries. Construction activities are also episodic in nature. Reeser et al. (1992) reported that fugitive dust emissions during wintertime in Denver, CO, were 44% higher than those found in the annual inventory using standard emissions inventory methods.

Finally, the spatial disaggregation for fugitive dust emissions is poorer than that for all other source categories. Whereas most mobile sources are confined to established roadways and most area sources are located in populated regions, suspendable dust sources are everywhere. Most fugitive dust emissions are compiled on a county-wide basis and are not allocated to specific fields, streets, unpaved roads, and construction sites possibly contributing to high airborne PM concentrations. Several of these limitations may be impossible to overcome, but many result from old methods being applied to the problem.

The inherent variability of fugitive dust emissions may preclude absolute emissions estimates. Nevertheless, this examination of physical processes shows that better knowledge of the locations of these emissions, the joint frequencies of activities and different meteorological conditions, and more site specific measurements of key parameters could provide much better absolute emissions rates than are now available.

5.2.2 Stationary Sources

The combustion of fossil fuels, such as coal and oil, leads to the formation of both primary and secondary particulate matter. Fossil fuels are mainly composed of a mixture of the remnants of plant matter and surrounding soils which have been processed at elevated temperatures and pressures over periods of up to three hundred million years. The process of coal formation results in a matrix of high molecular weight, highly cross-linked polyaromatic carbocyclic and heterocyclic ring compounds containing C, H, O, N, P, and S, and crustal materials. The hydrogen, nitrogen and phosphorus contents of coal are lower than the original biomass, reflecting losses by microbial utilization and thermal processing. Petroleum consists of long chain straight and branched alkanes with high carbon numbers (i.e., C_{25}-C_{50}), alkenes and aromatic hydrocarbons. The trace element content of these fuels reflects the trace element content of the initial organic matter and soil, subsequent hydrothermal alteration during diagenesis and industrial processing. Because of the inherent variability in each of these factors, the trace element content of fossil fuels is highly variable.

Coal combustion in the high temperature combustion zones of power plants results in the melting and volatilization of refractory crustal components, such as aluminosilicate minerals which condense to form spherical fly ash particles. Fly ash is enriched with metals compared to ordinary crustal material by the condensation of metal vapors. The sulfur content of fossil fuels ranges from fractions of a percent to about 4%. The sulfur in the fuel is released primarily as SO_2 along with smaller amounts of sulfate. Ratios of sulfate S to total S range from about 1% for modern coal fired power plants to several percent in residential, commercial and industrial boilers (Goklany et al., 1984).

The elemental composition of primary particulate matter emitted in the fine fraction from a variety of power plants and industries in the Philadelphia area is shown in Table 5-3 as a representative example of emissions from stationary fossil combustion sources (Olmez et al., 1988). Entries for the coal fired power plant show that Si and Al followed by sulfate are the major primary constituents produced by coal combustion, while fractional abundances of elemental carbon were much lower and organic carbon species were not detected. Sulfate is the major particulate constituent released by the oil fired power plants examined in this study; and, again, elemental and organic carbon are not among the major species emitted. Olmez et al. (1988) also compared their results to a number of similar studies and concluded

TABLE 5-3. COMPOSITION OF FINE PARTICLES RELEASED BY VARIOUS STATIONARY SOURCES IN THE PHILADELPHIA AREA

Species (Units)	Eddystone Coal-Fired Power Plant	N	Oil-Fired Power Plants				Secondary Al Plant	N	Fluid Cat. Cracker	N	Municipal Incinerator	N
			Eddystone	N	Schuylkill	N						
C-v (%)	ND		2.7 ± 1.2	3	0.75 ± 0.63	4	1.6 ± 1.5	2	ND		0.57 ± 0.26	4
C-e (%)	0.89 ± 0.12	3	7.7 ± 1.5	3	0.22 ± 0.17	4	0.18 ± 0.10	2	0.16 ± 0.05	3	3.5 ± 0.2	4
NH_4 (%)	1.89 ± 0.19	3	3.5 ± 1.6	3	3.7 ± 1.7	4	2.2 ± 0.9	2	0.43 ± 0.22	3	0.36 ± 0.07	4
Na (%)	0.31 ± 0.03	3	3.0 ± 0.8	3	3.3 ± 0.8	3	16.3 ± 0.8	1	0.38 ± 0.05	3	6.6 ± 3.5	3
Al (%)	14 ± 2	3	0.45 ± 0.09	3	0.94 ± 0.08	3	1.74 ± 0.09	1	6.8 ± 1.2	3	0.25 ± 0.10	3
Si (%)	21.8 ± 1.6	9	1.9 ± 0.6	9	2.6 ± 0.4	11	3.1 ± 2.2	2	9.8 ± 20.0	9	1.7 ± 0.3	10
P (%)	0.62 ± 0.10	9	1.5 ± 0.4	9	1.0 ± 0.2	11	0.45 ± 0.27	2	ND		0.63 ± 0.12	10
S (%)	3.4 ± 0.6	9	11 ± 2	9	13 ± 1	11	3 ± 4	2	4.2 ± 12.6	9	2.9 ± 0.8	10
SO_4 (%)	11.9 ± 1.2	3	40 ± 4	3	45 ± 7	4	5.9 ± 2	2	38 ± 4	3	6.8 ± 2.3	4
Cl (%)	0.022 ± 0.11	3	0.019 ± 0.009	2	ND		21 ± 4	1	ND		29 ± 5	3
K (%)	1.20 ± 0.09	9	0.16 ± 0.05	9	0.21 ± 0.03	11	10.9 ± 1.5	2	0.031 ± 0.005	9	7.6 ± 2.3	10
Ca (%)	1.4 ± 0.5	3	3.6 ± 1.0	3	2.3 ± 1.0	3	0.12 ± 0.09	2	0.030 ± 0.004	9	0.23 ± 0.10	10
Sc (ppm)	42 ± 2	3	0.17 ± 0.02	3	0.47 ± 0.02	3	0.092 ± 0.039	1	2.7 ± 0.4	3	0.11 ± 0.02	1
Ti (%)	1.1 ± 0.2	3	0.040 ± 0.044	9	0.12 ± 0.02	11	0.024 ± 0.003	2	0.38 ± 0.1	3	0.030 ± 0.015	10
V (ppm)	550 ± 170	3	11500 ± 3000	3	20000 ± 3000	3	36 ± 7	1	250 ± 70	3	8.6 ± 5.3	2
Cr (ppm)	390 ± 120	3	235 ± 10	3	230 ± 70	3	410 ± 20	1	59 ± 8	3	99 ± 31	3
Mn (ppm)	290 ± 15	3	380 ± 40	3	210 ± 50	3	120 ± 15	1	14 ± 3	3	165 ± 40	3
Fe (%)	7.6 ± 0.4	3	1.6 ± 0.2	3	1.7 ± 0.4	3	0.31 ± 0.02	1	0.20 ± 0.03	9	0.22 ± 0.05	3
Co (ppm)	93 ± 10	3	790 ± 150	3	1100 ± 200	3	13 ± 2	1	15 ± 2	3	3.7 ± 0.8	3
Ni (ppm)	380 ± 50	9	15000 ± 5000	9	19000 ± 2000	11	300 ± 100	2	220 ± 30	9	290 ± 40	10

TABLE 5-3 (cont'd). COMPOSITION OF FINE PARTICLES RELEASED BY VARIOUS STATIONARY SOURCES IN THE PHILADELPHIA AREA

Species (Units)	Eddystone Coal-Fired Power Plant	N	Oil-Fired Power Plants				Secondary Al Plant	N	Fluid Cat. Cracker	N	Municipal Incinerator	N
			Eddystone	N	Schuylkill	N						
Cu (ppm)	290 ± 20	9	980 ± 320	9	1100 ± 500	11	450 ± 200	2	14 ± 8	9	1300 ± 500	3
Zn (%)	0.041 ± 0.005	3	1.3 ± 0.3	3	0.78 ± 0.30	3	0.079 ± 0.006	1	0.0026 ± 0.0007	3	10.4 ± 0.5	3
As (ppm)	640 ± 80	3	33 ± 6	1	50 ± 16	3	15 ± 6	1	ND		64 ± 34	3
Se (ppm)	250 ± 20	3	26 ± 9	3	23 ± 7	3	66 ± 3	1	15 ± 1	3	42 ± 16	3
Br (ppm)	35 ± 8	3	90 ± 60	9	45 ± 17	11	630 ± 70	2	5.6 ± 1.8	9	2300 ± 800	10
Rb (ppm)	190 ± 80	1	ND		ND		97 ± 38	1	ND		230 ± 50	2
Sr (ppm)	1290 ± 60	9	160 ± 50	9	280 ± 70	11	ND		36 ± 6	9	87 ± 14	10
Zr (ppm)	490 ± 190	9	140 ± 180	9	100 ± 120	11	ND		130 ± 50	2	ND	
Mo (ppm)	170 ± 60	2	930 ± 210	3	1500 ± 300	3	ND		ND		240 ± 130	10
Ag (ppm)	ND		ND		ND		ND		ND		71 ± 15	3
Cd (ppm)	ND		ND		ND		ND		ND		1200 ± 700	3
In (ppm)	0.71 ± 0.04	2	ND		ND		ND		ND		4.9 ± 1.4	3
Sn (ppm)	ND		320 ± 230	9	200 ± 80	11	550 ± 540	2	ND		6700 ± 1900	10
Sb (ppm)	(a)		370 ± 410	3	1020 ± 90	3	6100 ± 300	1	7.7 ± 1.5	3	1300 ± 1000	3
Cs (ppm)	9.2 ± 0.9	2	ND		ND		ND		ND		5.9 ± 3.0	3
Ba (ppm)	ND		1960 ± 100	3	2000 ± 500	3	ND		290 ± 90	2	ND	
La (ppm)	120 ± 10	3	130 ± 30	3	450 ± 30	3	19 ± 2	1	3300 ± 500	3	1.1 ± 0.5	1
Ce (ppm)	180 ± 10	2	89 ± 23	3	360 ± 20	3	ND		2700 ± 400	3	ND	
Nd (ppm)	80 ± 26	3	28 ± 5	2	230 ± 20	3	ND		1800 ± 250	3	ND	
Sm (ppm)	23 ± 2	3	3.7 ± 0.7	3	20.5 ± 1.5	3	ND		170 ± 20	3	ND	

TABLE 5-3 (cont'd). COMPOSITION OF FINE PARTICLES RELEASED BY VARIOUS STATIONARY SOURCES IN THE PHILADELPHIA AREA

Species (Units)	Eddystone Coal-Fired Power Plant	N	Oil-Fired Power Plants: Eddystone	N	Oil-Fired Power Plants: Schuylkill	N	Secondary Al Plant	N	Fluid Cat. Cracker	N	Municipal Incinerator	N
Eu (ppm)	5.1 ± 0.5	3	ND		0.65 ± 0.23	3	ND		4.9 ± 0.7	3	ND	
Gd (ppm)	ND		ND		ND		ND		71 ± 10	3	ND	
Tb (ppm)	3.3 ± 0.3	3	ND		0.90 ± 0.29	3	ND		8.9 ± 1.3	3	ND	
Yb (ppm)	10.3 ± 0.5	1	ND		ND		ND		3.7 ± 0.4	3	ND	
Lu (ppm)	ND		ND		ND		ND		0.59 ± 0.17	3	ND	
Hf (ppm)	5.8 ± 0.8	3	0.39 ± 0.07	1	ND		ND		0.99 ± 0.08	3	ND	
Ta (ppm)	ND		ND		ND		ND		0.56 ± 0.10	3	ND	
W (ppm)	20 ± 8	1	60 ± 5	2	ND		ND		ND		ND	
Au (ppm)	ND		0.054 ± 0.017	2	ND		ND		ND		0.56 ± 0.27	3
Pb (%)	0.041 ± 0.004	9	1.8 ± 0.6	9	1.0 ± 0.2	11	0.081 ± 0.014	2	0.0091 ± 0.0021	9	5.8 ± 1.2	10
Th (ppm)	24 ± 2	3	1.9 ± 0.5	2	ND		ND		6.2 ± 0.7	3	ND	
% mass	24 ± 2	6	93.5 ± 2.5	6	96 ± 2	6	81 ± 10	2	97 ± 2	7	89 ± 2	7

N = Number of samples.
ND = Not detected.
The "% mass" entries give the average percentage of the total emitted mass found in the fine fraction.
(a) Omitted because of sample contamination.

Source: Adapted from Olmez et al. (1988).

that their data could have much wider applicability to receptor model studies in other areas with some of the same source types. The high temperature of combustion in power plants results in the almost complete oxidation of the carbon in the fuel to CO_2 and very small amounts of CO. A number of trace elements are greatly enriched over crustal abundances (in different fuels), such as Se in coal and V and Ni in oil. In fact, the higher V content of the fuel oil than in coal could help account for the higher sulfate seen in the profiles from the oil-fired power plant compared to the coal-fired power plant since V is known to catalyze the oxidation of reduced sulfur species. Although Table 5-3 only gives values of the fine particle composition, measurements of coarse particle composition were also reported by Olmez et al. (1988) which were qualitatively similar.

The composition of the organic carbon produced by stationary sources has not been well characterized. Information is available for the composition of polycyclic aromatic hydrocarbons, or PAH's (Daisey et al., 1986), while data for the composition of other classes of organic compounds are sparse. In addition, the phase distribution of a number of PAH's and other organic compounds will depend strongly on ambient atmospheric conditions. It may be expected that the composition of emissions in systems operating at low temperatures (e.g., residential coal combustion) will reflect that of the unburned fuel.

Emissions from stationary sources are determined mainly by stack sampling with a variety of techniques. All these techniques rely on measurements of stack flow rates and concentrations of pollutants to determine emissions. Method 5 (Federal Register, 1977) consists of a sampling train which is commonly used to measure emissions of various trace metals. The method is cumbersome and is limited in the number of species that can be sampled. Based on the realization that direct sampling of hot undiluted stack gases may not yield an accurate representation of the chemical composition and size distribution of particles leaving the stack, dilution sampling has also been used (e.g., Olmez et al., 1988). Condensation, coagulation, and chemical reactions occur as stack gases are cooled and diluted. In dilution sampling, stack gases are diluted with filtered ambient air in an attempt to partially simulate processes occurring in upper portions of the stack and in the plume leaving the stack. Another advantage in the use of dilution systems is that the same sampling substrates and analytical techniques used in ambient sampling can be used. As a result, a wider variety of constituents can be sampled than in conventional direct sampling techniques

and biases resulting from the use of separate sampling systems in source apportionment studies are eliminated. Remote monitoring methods (e.g., differential optical absorption spectroscopy) have also been used to determine emissions of species such as Hg. The size distribution of particles emitted by burning crude oil is shown in Figure 5-2. As can be seen, almost all of the mass is in the fine fraction.

Apart from emissions in the combustion of fossil fuels, trace elements are emitted as the result of various industrial processes such as steel and iron manufacturing and non-ferrous metal production (e.g., for Pb, Cu, Ni, Zn, and Cd) as may be expected, emissions factors for various trace elements are highly source-specific (Nriagu and Pacyna, 1988). Inspection of Table 5-3 reveals that the emissions from the catalytic cracker and the oil-fired power plant are greatly enriched in rare-earth elements such as La compared to other sources.

Emissions from municipal waste incinerators are dominated by Cl arising mainly from the combustion of plastics and metals that form volatile chlorides. The metals can originate from cans or other metallic objects and some metals such as Zn and Cd are also additives in plastics or rubber. Many elements such as S, Cl, Zn, Br, Ag, Cd, Sn, In, and Sb are enormously enriched compared to their crustal abundances. A comparison of the trace elemental composition of incinerator emissions in Philadelphia, PA (shown in Table 5-3) with the composition of incinerator emissions in Washington D.C., and Chicago, IL, (Olmez et al., 1988) shows agreement for most constituents to better than a factor of two. High levels of Hg associated with emissions from medical waste incinerators from discarded thermometers, mercurials, mercury batteries, etc., have been declining because of reductions in the use of Hg for medical purposes (Walker and Cooper, 1992). A sizable fraction of the Hg may be particulate Hg(II) as opposed to gas phase Hg^0.

5.2.3 Mobile Sources

Particulate matter from motor vehicles originates from tailpipe exhaust and from friction acting on individual components such as tires and brakes. Both diesel and gasoline fueled vehicles are sources of primary and secondary particulate matter. The rates of emission and the composition of particles emitted by motor vehicles have been measured using dynamometers with samples collected directly in the exhaust of individual vehicles

(e.g., Lang et al., 1982) or at the vents of inspection facilities (e.g., Watson et al., 1994a); or in tunnels and along open roadways (e.g., Pierson and Brachaczek, 1983; Szkarlat and Japar, 1983). Each approach has its merits and limitations and each approach is best used to augment the other. The principal components emitted by diesel and gasoline fueled vehicles are organic carbon (OC) and elemental carbon (EC) as shown in Table 5-4. As can be seen, the variability among entries for an individual fuel type is large and overlaps that found between different fuel types. On average, the abundance of elemental carbon is larger than that of organic carbon in the exhaust of diesel vehicles, while organic carbon is the dominant species in the exhaust of gasoline fueled vehicles. There appears to be a tendency for emissions of elemental carbon to increase relative to emissions of organic carbon for gasoline fueled vehicles as simulated driving conditions are changed from a steady 55 km /hr to those in the Federal Test Procedures (FTP's). Also shown are the results of sampling from mixed vehicle types along roadsides and in tunnels.

The results shown in Table 5-4 were obtained during the late 1980's, and, so, the results may not be entirely representative of current vehicles. Examples of data for the trace element composition of motor vehicle emissions obtained in Phoenix, AZ are shown in Table 5-5. SO_2 emissions are also shown in relation to the mass of fine particles emitted. As can be seen, small quantities of soluble ions such as $SO_4^=$ and NH_4^+ are emitted. The ammonium may be emitted as the result of an improperly functioning catalytic converter, or may simply be the result of contamination during sample handling and analysis. Four fractions are given for the organic carbon fraction and three for elemental carbon. These refer to abundances measured at different temperatures in a thermographic analysis. Temperatures for OC1, OC2, OC3, and OC4 are 120 °C, 250 °C, 450 °C, and 550 °C, respectively; and, for EC1, EC2, EC3, they are 550 °C, 700 °C, and 800 °C, respectively, in He/2% O_2. The abundances of trace elements are all quite low, with most being less than 1%. It is not clear what the source of the small amount of Pb seen in the auto exhaust profile is. It is extremely difficult to find suitable tracers for automotive exhaust since Pb has been removed from gasoline. However, it should also be remembered that restrictions in the use of leaded gasoline have resulted in a dramatic lowering of ambient Pb levels. Huang et al. (1994) attempted to identify marker elements in motor vehicle emissions, based on sampling the exhaust of 49 automobiles. They proposed that the combination of Zn, Br, and

TABLE 5-4. FRACTIONAL ORGANIC AND ELEMENTAL CARBON ABUNDANCES IN MOTOR VEHICLE EMISSIONS

Fuel Type	Organic Carbon	Elemental Carbon	N[e]	Sources
Diesel				
Denver, CO[a]	23 ± 8%	74 ± 21%	3	1, 2
Los Angeles, CA[a]	36 ± 3%	52 ± 5%	2	3, 4, 5, 6
Bakersfield, CA[b]	49 ± 13%	43 ± 8%	3	7
Phoenix, AZ[b]	40 ± 7%	33 ± 8%	8	8
Unleaded gasoline				
Denver, CO[a]	76 ± 29%	18 ± 11%	8	1, 2
Los Angeles, CA[c]	93 ± 52%	5 ± 7%	11	3, 4, 5, 6
Los Angeles, CA[a]	49 ± 10%	39 ± %	11	3, 4, 5, 6
Phoenix, AZ[b]	30 ± 12%	14 ± 8%	9	8
Leaded gasoline				
Denver, CO[a]	67 ± 23%	16 ± 7%	3	1, 2
Los Angeles, CA[c]	52 ± 4%	13 ± 1%	3	3, 4, 5, 6
Los Angeles, CA[a]	31 ± 20%	15 ± 2%	3	3, 4, 5, 6
Mixed (tunnel and roadside)				
Denver, CO	50 ± 24%	28 ± 19%		1, 2
Los Angeles, CA[d]	38 ± 6%	38 ± 5%	3	3
Phoenix, AZ	39 ± 19%	36 ± 11%		8

Sources: (1) Watson et al. (1990a), (2) Watson et al. (1990b), (3) Cooper et al. (1987), (4) NEA (1990a), (5) NEA (1990b), (6) NEA (1990c), and (7) Houck et al. (1989), cited in (8) Watson et al. (1994a).

Notes: (a) Modified Federal Test Procedures followed in dynamometer tests; (b) Roof monitoring at inspection station; (c) 55 km/hr steady speed in dynamometer tests; (d) Rt. 1 tunnel at LA airport, (e) N = Number of samples.

Sb could be used for this purpose. However, the relative abundances of these species in automobile exhaust were shown to be highly variable, implying that other sources of these elements may limit their usefulness as automotive tracers in some locations. To minimize

TABLE 5-5. PHOENIX $PM_{2.5}$ MOTOR VEHICLE EMISSIONS PROFILES (% MASS)

Chemical Species	Auto	Diesel
NO_3^-	3.9 ± 2.9	0.31 ± 0.40
SO_4^{2-}	2.3 ± 1.3	2.4 ± 1.0
NH_4^+	1.7 ± 1.0	0.87 ± 0.13
OC	30.1 ± 12.3	40.1 ± 6.6
OC1	11.3 ± 3.5	21.0 ± 6.3
OC2	9.2 ± 6.8	9.1 ± 1.9
OC3	4.6 ± 2.2	5.9 ± 1.3
OC4	3.5 ± 1.5	4.0 ± 1.5
EC	13.5 ± 8.0	32.9 ± 8.0
EC1	11.7 ± 7.2	4.4 ± 1.3
EC2	3.1 ± 1.6	27.9 ± 5.6
EC3	0.15 ± 0.30	0.69 ± 0.82
Al	0.41 ± 0.20	0.17 ± 0.12
Si	1.64 ± 0.88	0.46 ± 0.18
P	0.11 ± 0.07	0.06 ± 0.06
S	1.01 ± 0.48	1.24 ± 0.28
Cl	0.34 ± 0.32	0.03 ± 0.06
K	0.25 ± 0.14	0.04 ± 0.03
Ca	0.71 ± 0.41	0.16 ± 0.06
Ti	0.07 ± 0.13	0.00 ± 0.15
Cr	0.02 ± 0.01	0.00 ± 0.01
Mn	0.10 ± 0.04	0.01 ± 0.01
Fe	0.68 ± 0.42	0.16 ± 0.07
Cu	0.07 ± 0.06	0.01 ± 0.01
Zn	0.27 ± 0.22	0.07 ± 0.02
Sb	0.02 ± 0.13	0.01 ± 0.14
Ba	0.06 ± 0.40	0.14 ± 0.47
La	0.15 ± 0.51	0.18 ± 0.59
Pb	0.16 ± 0.07	0.01 ± 0.03
SO_2[a]	32.8 ± 13.9	66.9 ± 24.0

Source: Watson et al. (1994a).

Note: Elemental abundances ≤0.01% (V, Co, Ni, Ga, As, Se, Br, Rb, Sr. Y, Zr, Mo, Pd, Ag, Cd, In, Sn, Au, Hg, Tl, U) in XRF analyses excluded; OC = organic carbon; EC = elemental carbon.
[a]Relative to total $PM_{2.5}$.

errors arising from the loss of Br from filters, samples should be analyzed as soon as possible after collection (O'Connor et al., 1977).

The chemical mechanisms responsible for the formation of carbonaceous particles in diesel engines are not well established but are thought to involve the intermediate formation of polycyclic aromatic hydrocarbons, or PAH's (U.S. Environmental Protection Agency, 1993). Elemental carbon particles may be formed by the polymerization of gaseous intermediates adsorbed on a core of refractory material. The particles are in the form of chain or cluster agglomerates at temperatures above 500 °C. At temperatures below 500 °C, high molecular weight organic compounds condense on the carbon chain agglomerates. Roughly 10-40% of particulate emissions from diesels are extractable into organic solvents (National Research Council, 1982). In a typical profile, 50% of the extract is composed of aliphatic hydrocarbons with 14-35 C atoms and alkyl substituted benzenes; 4% are PAH's and heterocycles; and about 6% are PAH oxidation products including a small fraction of nitro-PAH's. The highly polar fraction of the organic emissions has not been as well characterized (Johnson, 1988). Inorganic compounds such as sulfuric acid are also produced in diesel engines (Truex et al., 1980).

Particulate matter is also formed in internal combustion engines as the result of the incomplete combustion of gasoline with contributions from engine oil. The particles consist essentially of a solid carbon core with a coating of organic compounds, sulfate, and trace elements. The composition of PAH's, oxy-PAH's and their alkyl homologues in tailpipe emissions from gasoline fueled vehicles is similar to that produced in diesel engines (Behymer and Hites, 1984). Particles produced by gasoline fueled vehicles range from 0.01 to 0.1 μm in diameter with a peak at around 0.02 μm, while the majority of particles in diesel exhaust range from 0.1 to 1.0 μm with a peak at around 0.15 μm (U.S. Environmental Protection Agency, 1993).

The concentrations of particulate matter and total hydrocarbons in the exhaust of gasoline fueled vehicles were found to be roughly correlated with each other by Hammerle et al. (1992). Emission factors for particulate matter in the exhaust of gasoline fueled vehicles range from 0.011 g/km for light duty vehicles to 0.12 g/km for heavy duty gasoline vehicles, and from 0.23 g/km in the exhaust of diesel passenger vehicles to 1.20 g/km for

heavy duty diesel vehicles (Radwan, 1995). These values are based on characteristics of the motor vehicle fleet in 1990.

As mentioned before, the composition of automotive emissions is sampled using individual vehicles on chassis dynamometers or by collecting aerosol samples along roadsides or in tunnels. The control over operating characteristics by using dynamometers allows the development of models which can predict emissions on the basis of variables such as vehicle make and age and driving cycle. The representativeness of dynamometer test data can be questioned if volunteered vehicles, as opposed to randomly selected vehicles, are sampled. In addition, measuring emissions from individual vehicles is also costly and the sample numbers are usually small, as reflected in the small number of samples shown in Table 5-4. Moreover, a number of driving practices are not reflected in the Federal Test Procedures leading to significant underestimates of emissions of CO and hydrocarbons (Calvert et al., 1993). It is still not clear what effects superemitters and off-cycle driving practices have on particle emissions rates. If the relation between particulate matter and hydrocarbon emissions discussed above is representative of the vehicle fleet, the effects could be substantial. Hansen and Rosen (1990) measured the ratio of light-absorbing carbon to CO_2 in the exhausts of 60 gasoline fueled vehicles. They found a factor of 250 difference between the highest and lowest ratios measured. Larger scale studies designed to assess the variability of particulate emissions from motor vehicles are lacking.

Roadside and tunnel measurements sample large numbers of vehicles of different types and have demonstrated their potential for validating the predictions of emissions models. However, the extent to which traffic conditions in the tunnel reflect those in the situation under study must be defined for the results to be considered representative. The same considerations can be extended to dynamometer studies and to open-road studies along road segments. Results from some tunnel studies are of limited usefulness because they have been obtained under highway driving conditions which may not be representative of the conditions found in most urban and suburban areas. Additional uncertainties result from resuspended dust in using tunnel and roadside studies to characterize motor vehicle emissions. However, methods are available for estimating contributions from tire wear (Pierson and Brachaczek, 1974, 1976). Remote measurements of elemental carbon in the exhaust plumes of individual

vehicles (Hansen and Rosen, 1990) can overcome many of these difficulties, but the method cannot yet be applied to aerosol constituents other than elemental carbon.

5.2.4 Biomass Burning

In addition to fossil fuels, biomass in the form of wood may be burned in forest fires or as fuel for heating or cooking. At first glance these two broad categories might seem to serve to distinguish between natural and anthropogenic sources. However, many forest fires result from human intervention, either deliberately through prescribed burning in forest management or accidentally through the improper disposal of flammable material or fugitive sparks (e.g., Andreae, 1991). On the other hand, human intervention also suppresses lightning triggered fires. Not enough data is available to assess the effects of humans on forest fires, except for land clearing for agriculture. In contrast to the mobile and stationary sources discussed earlier, emissions from biomass burning in woodstoves and forest fires are strongly seasonal and can be highly episodic within their peak emissions seasons. Burning fuelwood is confined mainly to the winter months and is acknowledged to be a major source of ambient air particulate matter in the northwestern United States during the heating season. Forest fires mainly occur during the driest seasons of the year in different areas of the country and are especially prevalent during prolonged droughts.

An example of the composition of fine particles ($PM_{2.5}$) produced by woodstoves is shown in Figure 5-4. These data were obtained in Denver during the winter of 1987-1988 (Watson and Chow, 1994). As was the case for motor vehicle emissions, organic and elemental carbon are the major components of particulate emissions from wood burning. It should be remembered that the relative amounts shown for organic carbon and elemental carbon will vary with the type of stove, the stage of combustion and the type and condition of the fuelwood. Potassium (K) is by far the major trace element found in woodstove emissions (Watson and Chow, 1994), making it suitable for use as a tracer for vegetation burning (Lewis et al., 1988). Fine particles are dominant in studies of wood burning emissions. For instance, the mass median diameter of wood-smoke particles was found to be about 0.17 μm in a study of the emissions from burning hardwood, softwood and synthetic logs (Dasch, 1982).

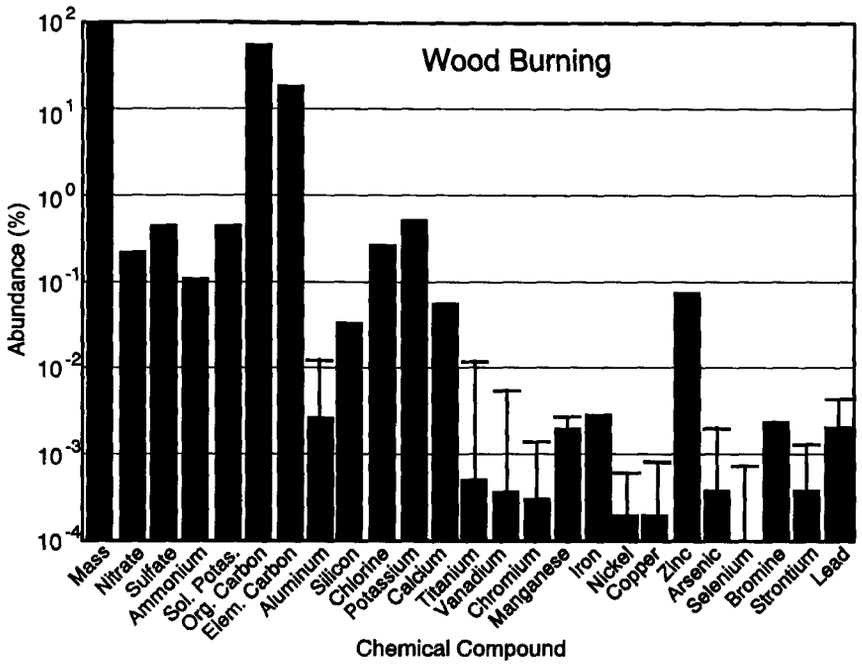

Figure 5-4. Chemical abundances for $PM_{2.5}$ emissions from wood burning in Denver, CO. Solid bars represent fractional abundances, and the error bars represent variability in species abundances. Error bars represent detection limits when there are no solid bars.

Source: Watson and Chow (1994).

Measurements of aerosol composition, size distributions, and aerosol emissions factors have been made in biomass burning plumes either on towers (Susott et al., 1991) or aloft on fixed wing aircraft (e.g., Radke et al., 1991) or on helicopters (e.g., Cofer et al., 1988). As was found for woodstove emissions, the composition of biomass burning emissions is strongly dependent on the stage of combustion (i.e., flaming, smoldering, or mixed), and the type of vegetation (e.g., forest, grassland, scrub). Over 90% of the dry mass in particulate biomass burning emissions is composed of organic carbon (Mazurek et al., 1991). Ratios of organic carbon to elemental carbon are highly variable ranging from 10:1 to 95:1, with the highest ratio found for smoldering conditions and the lowest for flaming conditions. Ambient particle concentrations were about two mg/m^3 during the measurement period. Available measurements suggest that K is by far the most abundant trace element in biomass burning plumes. Although there is considerable inter-sample variation, results from tower

samples also suggest that S, Cl, and K are highest during flaming stages, while Al, Si, Ca, and Fe tend to increase during the smoldering phase (Susott et al., 1991). Emissions factors for total particulate emissions increase by factors of two to four in going from flaming to smoldering stages in the individual fires studied by Susott et al. (1991). These measurements were made when ambient particle concentrations ranged from 15 to 40 mg/m^3.

Particles in biomass burning plumes from a number of different fires were found to have three distinguishable size modes, namely a nucleation mode, an accumulation mode, and a coarse mode (Radke et al., 1991). Based on an average of 81 samples, approximately 70% of the mass was found in particles < 3.5 μm in aerodynamic diameter. The fine particle composition was found to be dominated by tarlike, condensed hydrocarbons and the particles were usually spherical in shape. Additional information for the size distribution of particles produced by vegetation burning was shown in Figure 5-2.

5.2.5 Sea-Salt Production and Other Natural Sources of Aerosol

Although sea-salt aerosol production is confined to salt water bodies, it is included here because many marine aerosols can exert a strong influence on the composition of the ambient aerosol in coastal areas. In some respects, the production of sea-salt aerosols is like that of windblown dust in that both are produced by wind agitation of the surface. The difference between the two categories arises because sea-salt particles are produced from the bursting of air bubbles rising to the sea surface. Air bubbles are formed by the entrainment of air into the water by breaking waves. The surface energy of a collapsing bubble is converted to kinetic energy in the form of a jet of water which can eject drops above the sea surface. The mean diameter of the jet drops is about 15% of the bubble diameter (Wu, 1979). Bubbles in breaking waves range in size from a few μm to several mm in diameter. Field measurements by Johnson and Cooke (1979) of bubble size spectra show maxima in diameters at around 100 μm, with the bubble size distribution varying as $(d/d_0)^{-5}$ with $d_0 = 100$ μm.

Since the water jet receives its water from the surface layer, which is enriched in organic compounds, the aerosol drops are composed of this organic material in addition to sea salt (about 3.5% by weight in sea water). Na^+ (30.7%),Cl^- (55.0%), $SO_4^=$ (7.7%), Mg^{2+} (3.6%), Ca^{2+} (1.2%), K^+ (1.1%), HCO_3^- (0.4%), and Br^- (0.2%) are the major ionic

species by mass in sea water (Wilson, 1975). The composition of the marine aerosol also reflects the occurrence of displacement reactions which enrich sea-salt particles in SO_4^- and NO_3^- while depleting them of Cl^- and Br^-. As the drops travel upward above the water surface, they encounter lower relative humidities and lose water until they come into equilibrium with their environment. The resulting marine aerosol size distribution reflects the processes of coagulation, coalescence, and sedimentation.

Seasalt is concentrated in the coarse size mode with a mass median diameter of about 7 μm for samples collected in Florida, the Canary Islands and Barbados (Savoie and Prospero, 1982). The size distribution of sulfate is distinctly bimodal. Sulfate in the coarse mode is derived from sea water but sulfate in the submicron aerosol arises from the oxidation of dimethyl sulfide (CH_3SCH_3) or DMS. DMS is produced during the decomposition of marine micro-organisms. DMS is oxidized to MSA (methane sulfonic acid) a large fraction of which is oxidized to sulfate (e.g., Hertel et al., 1994).

Apart from sea spray, other natural sources of particles include the suspension of organic debris and volcanism. Particles are released from plants in the form of seeds, pollen, spores, leaf waxes and resins, ranging in size from 1 to 250 μm (Warneck, 1988). Fungal spores and animal debris such as insect fragments are also to be found in ambient aerosol samples in this size range. While material from all the foregoing categories may exist as individual particles, bacteria are usually found attached to other dust particles .(Warneck, 1988). Smaller bioaerosol particles include viruses, individual bacteria, protozoa, and algae (Matthias-Maser and Jaenicke, 1994). In addition to natural sources, other sources of bioaerosol include industry (e.g., textile mills), agriculture, and municipal waste disposal (Spendlove, 1974).

Trace metals are emitted to the atmosphere from a variety of sources such as sea spray, wind blown dust, volcanoes, wild fires and biotic sources (Nriagu, 1989). Biologically mediated volatilization processes (e.g., biomethylation) are estimated to account for 30-50% of the worldwide total Hg, As, and Se emitted annually, whereas other metals are derived principally from pollens, spores, waxes, plant fragments, fungi, and algae. It is not clear, however, how much of the biomethylated species are remobilized from anthropogenic inputs. Median ratios of the natural contribution to globally averaged total sources for trace metals are estimated to be 0.39 (As), 0.15 (Cd), 0.59 (Cr), 0.44 (Cu), 0.41 (Hg), 0.35 (Ni),

0.04 (Pb), 0.41 (Sb), 0.58 (Se), 0.25 (V), and 0.34 (Zn), suggesting a not insignificant natural source for many trace elements. It should be noted though that these estimates are based on emissions estimates which have uncertainty ranges of an order of magnitude.

5.3 SOURCES OF SECONDARY PARTICULATE MATTER (SULFUR DIOXIDE, NITROGEN OXIDES, AND ORGANIC CARBON)

Secondary particulate matter is an important contributor to suspended particle mass. Sulfate is formed by the oxidation of SO_2, nitrate by the oxidation of NO_2, and aerosol organic carbon species by the oxidation of a large number of precursors. Thus, the formation rate of a substantial fraction of aerosol mass is given by a complex function of both emission rates of precursor gases and the rates of photochemical processes in the atmosphere. In order to use precursor emissions estimates effectively, however, it is necessary to understand the nature of the processes that cause them to convert to particulate matter. Mechanisms for the oxidation of SO_2 to $SO_4^{=}$, and NO_2 to NO_3^{-}, have been discussed in Chapter 3. Both species are oxidized during daytime in the gas phase by hydroxyl (OH) radicals. At night, NO_x is also oxidized to nitric acid by a sequence of reactions initiated by O_3, that include nitrate radicals (NO_3) and dinitrogenpentoxide (N_2O_5). SO_2 is also oxidized by heterogeneous reactions occurring in films of atmospheric particles and in cloud and fog droplets. Data for primary and secondary components of aerosol mass at a number of locations across the United States can be found in Chapter 6.

While the mechanisms and pathways for forming inorganic secondary particulate matter are fairly well known, those for organic secondary aerosol are not well understood. Numerous precursors participate in these conversions, and the rates at which these convert from gas to particles are highly dependent on the concentrations of other pollutants and meteorological conditions. Pandis et al. (1992) identified three mechanisms for secondary organic PM formation: (1) condensation of oxidized end-products of photochemical reactions (e.g., ketones, aldehydes, organic acids, and hydroperoxides); (2) adsorption of organic gases onto existing solid particles (e.g., polycyclic aromatic hydrocarbons); and (3) dissolution of soluble gases which can undergo reactions in particles (e.g., aldehydes). The first and third mechanisms are expected to be of major importance during the

summertime when photochemistry is at its peak. The second pathway can be driven by diurnal and seasonal temperature and humidity variations at any time of the year. Turpin and Huntzicker (1991) and Turpin et al. (1991) provided strong evidence that secondary PM formation occurs during periods of photochemical ozone formation in Los Angeles.

Haagen-Smit (1952) first demonstrated that hydrocarbons irradiated in the presence of NO_x produce light scattering aerosols. Results of later studies summarized by Altshuller and Bufalini (1965) indicated that aerosols are produced by the irradiation of mixtures of NO_x and numerous six-carbon and higher molecular weight acyclic and cyclic olefins and aromatic hydrocarbons. Cyclic olefins were shown to be more effective in aerosol formation than acyclic olefins of similar molecular weight by Stevenson et al. (1965). The possibility that aerosols might be formed from biogenic hydrocarbon emissions was investigated by Went (1960) and Rasmussen and Went (1965). Analyses of the aerosol produced from the photooxidation of α-pinene and NO_x mixtures indicated the presence of pinonic acid and norpinonic acid (Wilson et al., 1972).

Numerous smog chamber studies of the formation of secondary organic aerosol from the photooxidation of terpene precursors have been performed since these earlier studies. A study of the reaction of α-pinene and β-pinene with O_3 by Hatakeyama et al. (1989) obtained aerosol carbon yields (mass of aerosol carbon produced per mass of C reacted), or ACY's, of 18% and 14%, respectively, for HC levels ranging from 10-120 ppb C. In this study, pinonaldehyde, pinenic acid, nor-pinonaldehyde, and nor-pinonic acid accounted for less than 10% of the aerosol yield from the reaction of α-pinene. Hatakeyama et al. (1991) subsequently obtained ACY's of 56 $\pm$ 4% and 79 $\pm$ 8% following the reaction of α-pinene and β-pinene, respectively, for initial HC levels of 820-3170 ppb C and NO_x levels of 210-2550 ppb. Pandis et al. (1991) obtained ACY's ranging from 0.1 to 8% for the oxidation of β-pinene for HC levels ranging from 20-250 ppb C and NO_x levels ranging from 39 to about 700 ppb. Zhang et al. (1992) obtained ACY's ranging from 0 to 5.3% for HC levels ranging from 37-582 ppb C and NO_x levels ranging from 31-380 ppb for the oxidation of α-pinene. Results from the above studies showed that aerosol yields strongly depend on the initial concentration of terpenes and the ratio of hydrocarbons (HC) to NO_x in the reaction chamber. However, Hooker et al. (1985) did not find a significant dependence of aerosol yield on initial HC abundance for HC levels ranging from 3.1-50 ppb C. Their

approach differed from that used in all of the above studies because they used ^{14}C-α-pinene. Of the ^{14}C-α-pinene which reacted, 38-68% was found in aerosol products, 6-20% was found in gas phase products, and 11-29% was lost to the walls of their reaction chamber.

After reaction of the α-pinene with OH radicals or O_3, the radical product will add O_2 to form a peroxy radical. Zhang et al. (1992) proposed that the peroxy radical may react with NO initiating a series of reactions forming pinonaldehyde, which may condense depending on its concentration, or the peroxy radical may react with HO_2 or other free radicals to form aerosol products. The inhibition of the second pathway by the addition of NO was proposed by Zhang et al. (1992) to explain the decrease of aerosol yield with added NO. They also suggested that the dependence of aerosol yield on initial HC concentration arises because the concentration of pinonaldehyde can more easily exceed its saturation value and the rate of formation of aerosol products in the other pathway will also increase.

Pandis et al. (1991) found no aerosol products formed in the photooxidation of isoprene, although they and Zhang et al. (1992) found that the addition of isoprene to reaction mixtures increased the reactivity of the systems studied. Based on their experimental results and the high ratio of terpene to NO_x concentration ratios found in rural and remote areas, Zhang et al. (1992) suggested that the upper limits for aerosol yields they obtained should be used in estimating the aerosol yields from the oxidation of biogenic hydrocarbons.

The aerosol forming potentials of a wide variety of individual anthropogenic and biogenic hydrocarbons were compiled by Pandis et al. (1992) based mainly on estimates made by Grosjean and Seinfeld (1989) and data from Pandis et al. (1991) for β-pinene and Izumi and Fukuyama (1990) for aromatic HC's. The estimates given by Pandis et al. (1992) were converted to aerosol carbon yields below. Examples of compounds with zero ACY's are all C_1-C_7 alkanes, all C_2-C_6 acyclic alkenes, benzene, and aldehydes; examples of compounds with lowest ACY's (< 2.0%) are C_8-C_{10} alkanes, C_6-C_8 cycloalkanes, C_7-C_9 acyclic alkenes, C_5 cyclic alkenes and p-xylene; examples of compounds with intermediate values (2.0%-4.0%) are C_{11}-C_{14} alkanes, C_9-C_{10} cycloalkanes, alkyl benzenes other than p-xylene, C_{10}-C_{13} alkenes and C_6^+ cycloalkenes; and examples of compounds with high values (>4.0%) are C_{15}^+ alkanes, C_{11}^+ cycloalkanes, C_{14}^+ cyclic alkenes and monoterpenes.

Studies of the production of secondary OC in ambient air have focussed on the Los Angeles Basin. Based on aerosol yields shown above, Pandis et al. (1991) suggested that about 1-4 tons day^{-1} of secondary OC in the Los Angeles basin is formed from the oxidation of monoterpenes which are emitted at the rate of 10-40 tons day^{-1}. This estimate may be compared to the secondary OC production rate of 7.5 tons day^{-1} estimated to result from the oxidation of anthropogenic hydrocarbons which are emitted at the rate of 1200 tons day^{-1} (Grosjean and Seinfeld, 1989). The overall yield of secondary OC from anthropogenic sources in this example is about 0.6%. Pandis et al. (1991) also proposed that most of the secondary OC in highly vegetated urban areas such as Atlanta is produced by the oxidation of monoterpenes.

As part of the Southern California Air Quality Study (SCAQS), Turpin and Huntzicker (1991) measured elemental and organic carbon at Claremont, CA in the summer of 1987 with an in situ carbon analyzer with 2 hour time resolution. During an air pollution episode centered on August 28, 1987, airmass trajectories arriving at Claremont were directed eastward (i.e., inland from the coast), allowing the entrainment of substantial hydrocarbon precursors during transit. Peak OC concentrations (23 $\mu g/m^3$) and highest OC to EC ratios (4.6 ± 0.4) occurred together at Claremont from about 1500 to 1700 PDT. In addition, correlations between EC and OC were low throughout the day ($R^2 = 0.38$). Turpin and Huntzicker (1991) also measured OC and EC concentrations at Long Beach in November of 1987 with the same instrumentation. On the basis of these data, they suggested that OC to EC ratios of 2.2 ± 0.7 are characteristic of primary OC in the Los Angeles area.

Pandis et al. (1992) constructed a Lagrangian trajectory model to simulate the chemical formation, transport and deposition of secondary OC during the August episode. They used estimates of aerosol yields from HC oxidation compiled by Grosjean and Seinfeld (1989), updated as necessary (e.g., Pandis et al., 1991) along with estimates of daily emissions, to predict that 28% of the peak secondary OC on Aug. 28 at Claremont resulted from the oxidation of toluene, 38% from other aromatic HC's, 9% from biogenic HCs, 21% from alkanes and cycloalkanes, and the remaining 4% from other species. Values were somewhat different on a daily average basis (19% from toluene, 46% from other aromatic HC's, 16% from biogenic HC's, 15% from alkanes, and 4% from alkenes). There was reasonable agreement with the data of Turpin and Huntzicker (1991) throughout most of the day, but

calculated peak secondary OC levels ($\sim 5\ \mu g/m^3$) were about half those inferred by Turpin and Huntzicker (1991). A combination of factors could have contributed to this underprediction including errors in emissions, deposition rates, chemical reaction rate data and aerosol yields. In general, the calculated secondary OC represented 15-27% of the daily average total OC at inland locations (Burbank, Claremont, Azusa, and Rubidoux) on August 28, 1987 and 5-19% of the average total OC at coastal sites.

Attempts were made during SCAQS to determine the composition of the organic carbon fraction of the ambient aerosol. Organic nitrates were measured on size segregated samples collected on zinc selenide disks which were later analyzed by transmission FTIR by Mylonas et al. (1991). Concentrations of organic nitrates in the particle phase ranged from 0.8 to 4.0 $\mu g/m^3$, with maximum mass loadings in the 0.05 to 0.075 μm and 0.12 to 0.26 μm size ranges. Concurrently, Pickle et al. (1990) used infrared spectroscopy to measure the total abundance of compounds containing carbonyl groups and aliphatic compounds. Maximum absorption at wavelengths characteristic of carbonyl groups was observed for particles in the 0.12 to 0.26 μm and 0.5 to 1.0 μm size ranges. These results suggest that carbonyl compounds are largely of secondary origin and that IR absorption by aliphatic compounds in particles smaller than 0.12 μm was correlated directly with automotive emissions.

Kao and Friedlander (1995) examined the statistical properties of a number of PM components in the South Coast Air Basin. They found that the concentrations of non-reactive, primary components of PM_{10} have approximately log normal frequency distributions and constant values of geometric standard deviations (GSDs) regardless of source type and location within their study area. However, aerosol constituents of secondary origin (e.g., $SO_4^{=}$, NH_4^{+}, and NO_3^{-}) were found to have much higher GSD's. Surprisingly, the GSD's of organic (1.87) and elemental (1.74) carbon were both found to be within 1σ (0.14) of the mean GSD (1.85) for non-reactive primary species, compared to GSD's of 2.1 for sulfate, 3.5 for nitrate, and 2.6 for ammonium. These results suggest that most of the OC seen in ambient samples is of primary origin. Pinto et al. (1995) found similar results for data obtained during the summer of 1994. Further studies are needed to determine if these relations are valid at other locations and to determine to what extent the results might be influenced by the evaporation of volatile constituents after sampling.

It must be emphasized that the inferences drawn from field studies in the Los Angeles Basin are unique to that area and cannot be extrapolated to other areas of the country. In addition, there is a high degree of uncertainty associated with all aspects of the calculation of secondary OC concentrations which is compounded by the volatilization of OC during and after sampling. Grosjean and Seinfeld (1989) derived a factor of five range in estimates of production rates of secondary OC in the Los Angeles area by comparison of results obtained from four different methods. Aerosol yields from the oxidation of individual hydrocarbons reported by different investigators vary by an order of magnitude (Grosjean and Seinfeld, 1989). Significant uncertainties always arise in the interpretation of smog chamber data because of wall reactions. Limitations also exist in extrapolating the results of smog chamber studies to ambient conditions found in urban airsheds and forest canopies. Concentrations of terpenes and NO_x are much lower in forest canopies (Altshuller, 1983) than are commonly used in smog chamber studies. The identification of aerosol products of terpene oxidation has not been a specific aim of field studies, making it difficult to judge the results of model calculations of secondary OC formation. Uncertainties may also arise because of the methods used to measure biogenic hydrocarbon emissions. Khalil and Rasmussen (1992) found much lower ratios of terpenes to other hydrocarbons (e.g., isoprene) in forest air than were expected, based on their relative emissions strengths and rate coefficients for reaction with OH radicals and O_3. They offered two explanations, either the terpenes were being rapidly removed by some heterogeneous process or emissions were artificially enhanced by feedbacks caused by the bag enclosures they used. If the former consideration is correct, then the production of aerosol carbon from terpene emissions could be substantial; if the latter is correct, then terpene emissions could have been overestimated by the techniques used.

5.4 EMISSIONS ESTIMATES FOR PRIMARY PARTICULATE MATTER AND SO_2, NO_x, AND VOCs IN THE UNITED STATES

The emissions of a pollutant can be expressed by the following equation:

$$E = \sum_i A_i \cdot F_i \cdot (1-C_{eff,i}) \qquad (5\text{-}1)$$

where E is the total emissions rate from all sources; A_i is the activity rate for source i; F_i is the emissions factor for the production of the pollutant by source i; and $C_{eff,i}$ is the fractional efficiency of control devices used by source i. Activity rates relevant to the entries shown in Tables 5-6 to 5-10 might refer to the electricity generated by power plants, the amount of coke produced by a coke oven, the distance travelled by motor vehicles, the amount of biomass consumed by forest fires per year, etc. The mass of pollutant emitted per unit activity of a source is then expressed in terms of an emissions factor (e.g., amount of NO_x emitted per kw-hour of energy generated or per vehicle mile travelled). Emissions factors are given in compilations (e.g., AP-42 [U.S. Environmental Protection Agency, 1995a]) or are calculated by emissions models, which include a number of variables which can affect emissions. Examples include the U.S. Environmental Protection Agency's PART5 model for estimating particulate motor vehicle emissions, and BEIS which is used to calculate emissions of hydrocarbons from vegetation (Geron et al., 1994). The product of $A_i \times F_i$ yields an estimate of the uncontrolled emissions from a particular source i. These are then multiplied by a factor incorporating the effects of any control devices that might be used. It is acknowledged that control equipment breaks down, and its efficiency might not be maintained over its lifetime of operation. Therefore, the optimum efficiencies of control devices are multiplied by a rule effectiveness factor. The default value for the rule effectiveness factor is taken to be 0.8 in the inventory calculations, unless a better factor can be justified (U.S. Environmental Protection Agency, 1989). Equation 5-1 was used in the preparation of the emissions inventories shown in Tables 5-6 through 5-10. Further details about collection and reporting methods may be found in the National Emissions Inventory Trends data base (U.S. Environmental Protection Agency, 1994).

Table 5-6 shows the primary PM_{10} emissions estimated for the period of 1985 through 1993 using the National Emissions Inventory Trends data base (U.S. Environmental Protection Agency, 1994). Emissions are shown in the original units used in their calculation. A short ton is equal to 2,000 pounds or 9.08×10^5 gm. Between 1985 and 1993, PM_{10} emissions from stationary and mobile sources decreased almost 10 percent. During this period, contributions from highway vehicles decreased by 27 percent, reflecting emissions controls on diesel vehicles. Contributions from industrial fuel production

TABLE 5-6. NATIONWIDE PRIMARY PM_{10} EMISSION ESTIMATES FROM MOBILE AND STATIONARY SOURCES, 1985 TO 1993

	(Thousands short tons/year)								
Source Category	1985	1986	1987	1988	1989	1990	1991	1992	1993
Fuel Combustion - Electric Utilities	284	289	282	278	278	291	253	255	270
Fuel Combustion - Industrial	234	231	226	230	229	228	229	223	219
Fuel Combustion - Other	896	902	910	918	922	930	942	819	723
Chemical and Allied Product Manufacturing	67	68	68	73	74	74	72	75	75
Metals Processing	147	137	131	141	142	140	136	137	141
Petroleum and Related Industries	32	31	30	29	28	28	28	27	26
Other Industrial Processes	317	321	314	314	308	306	300	303	311
Solvent Utilization	2	2	2	2	2	2	2	2	2
Storage and Transport	57	56	54	54	54	54	53	53	55
Waste Disposal and Recycling	279	275	265	259	251	242	245	246	248
Highway Vehicles	271	265	261	256	253	239	223	210	197
Off-Highway	368	372	350	387	372	372	367	379	395
Total	2,953	2,949	2,893	2,942	2,909	2,907	2,849	2,729	2,661

Note: The sums of sub-categories may not equal total due to rounding (1 short ton = 9.08×10^5 gms).

Source: U.S. Environmental Protection Agency (1994).

TABLE 5-7. MISCELLANEOUS AND NATURAL SOURCE PRIMARY PM_{10} EMISSION ESTIMATES, 1985 TO 1993

	(Thousands short tons/year)								
Source Category	1985	1986	1987	1988	1989	1990	1991	1992	1993
Fugitive Dust									
Unpaved roads	14,719	14,672	13,960	15,626	15,346	15,661	14,267	14,540	14,404
Paved roads	6,299	6,555	6,877	7,365	7,155	7,299	7,437	7,621	8,164
Construction/mining and quarrying	13,009	12,139	12,499	12,008	11,662	10,396	10,042	10,899	11,368
Agriculture and Forestry									
Agricultural crops	6,833	6,899	7,008	6,090	6,937	6,999	6,965	6,852	6,842
Agricultural livestock	275	285	330	376	397	381	363	386	394
Other Combustion									
Wildfires	142	142	142	142	142	717	457	341	418
Managed burning	523	530	536	555	549	546	537	547	549
Other	59	59	59	59	59	59	59	59	59
Natural Sources wind erosion	3,565	9,390	1,457	17,509	11,862	4,192	10,054	4,655	628
Total	45,424	50,671	42,868	60,730	54,073	46,250	50,181	45,900	42,826

Note: The sums of sub-categories may not equal total due to rounding (1 short ton = 9.08×10^5 gms).

Source: U.S. Environmental Protection Agency (1994).

TABLE 5-8. NATIONWIDE SULFUR OXIDES EMISSION ESTIMATES, 1984 TO 1993

	(Thousands short tons/year)									
Source Category	1984	1985	1986	1987	1988	1989	1990	1991	1992	1993
Fuel Combustion - Electric Utilities	16,023	16,273	15,701	15,715	15,990	16,218	15,898	15,784	15,417	15,836
Fuel Combustion - Industrial	2,723	3,169	3,116	3,068	3,111	3,086	3,106	3,139	2,947	2,830
Fuel Combustion - Other	728	578	611	663	660	623	597	608	600	600
Chemical and Allied Product Manufacturing	229	456	432	425	449	440	440	442	447	460
Metals Processing	1,387	1,042	888	616	702	657	578	544	557	580
Petroleum and Related Industries	707	505	469	445	443	429	440	444	417	409
Other Industrial Processes	923	425	427	418	411	405	401	391	401	413
Solvent Utilization	0	1	1	1	1	1	1	1	1	1
Storage and Transport	0	4	4	4	5	5	5	5	5	5
Waste Disposal and Recycling	25	34	35	35	36	36	36	36	37	37
Highway Vehicles	445	446	449	457	468	480	480	478	483	438
Off-Highway	198	208	221	233	253	267	265	266	273	278
Miscellaneous	9	7	7	7	7	7	14	11	10	11
Total	23,396	23,148	22,361	22,085	22,535	22,653	22,261	22,149	21,592	21,888

Note: The sums of sub-categories may not equal the totals, due to rounding (1 short ton = 9.08×10^5 gms).

Source: U.S. Environmental Protection Agency (1994).

TABLE 5-9. NATIONWIDE NO_x[a] EMISSION ESTIMATES, 1984 TO 1993

	(Thousands short tons/year)									
Source Category	1984	1985	1986	1987	1988	1989	1990	1991	1992	1993
Fuel Combustion - Electric Utilities	7,268	6,916	9,909	7,128	7,530	7,607	7,516	7,482	7,473	7,782
Fuel Combustion - Industrial	3,415	3,209	3,065	3,063	3,187	3,209	3,256	3,309	3,206	3,176
Fuel Combustion - Other	670	701	694	710	737	730	732	745	735	732
Chemical and Allied Product Manufacturing	161	374	381	371	398	395	399	401	411	414
Metals Processing	54	87	80	76	82	83	81	79	80	82
Petroleum and Related Industries	70	124	109	101	100	97	100	103	96	95
Other Industrial Processes	203	327	328	320	315	311	306	298	305	314
Solvent Utilization	0	2	3	3	3	3	2	2	3	3
Storage and Transport	0	2	2	2	2	2	2	2	3	3
Waste Disposal and Recycling	90	87	87	85	85	84	82	81	83	84
Highway Vehicles	8,387	8,089	7,773	7,662	7,661	7,662	7,488	7,373	7,440	7,437
Off-Highway	2,644	2,734	2,777	2,664	2,914	2,844	2,843	2,796	2,885	2,966
Miscellaneous	210	201	202	203	206	205	384	305	272	296
Total	23,172	22,853	22,409	22,386	23,221	23,250	23,192	22,977	22,991	23,402

[a]Emissions calculated as NO_2.

Note: The sums of sub-categories may not equal total due to rounding (1 short ton = 9.08×10^5 gms).

Source: U.S. Environmental Protection Agency (1994).

TABLE 5-10. NATIONWIDE VOLATILE ORGANIC COMPOUND EMISSION ESTIMATES, 1984 TO 1993

	(Thousands short tons/year)									
Source Category	1984	1985	1986	1987	1988	1989	1990	1991	1992	1993
Fuel Combustion - Electric Utilities	45	32	34	34	37	37	36	36	35	36
Fuel Combustion - Industrial	156	248	254	249	271	266	266	270	271	271
Fuel Combustion - Other	917	508	499	482	470	452	437	426	385	341
Chemical and Allied Product Manufacturing	1,620	1,579	1,640	1,633	1,752	1,748	1,771	1,778	1,799	1,811
Metals Processing	182	76	73	70	74	74	72	69	72	74
Petroleum and Related Industries	1,253	797	764	752	733	731	737	745	729	720
Other Industrial Processes	227	439	445	460	479	476	478	475	482	486
Solvent Utilization	6,309	5,779	5,710	5,828	6,034	6,053	6,063	6,064	6,121	6,249
Storage and Transport	1,810	1,836	1,767	1,893	1,948	1,856	1,861	1,868	1,848	1,861
Waste Disposal and Recycling	687	2,310	2,293	2,256	2,310	2,290	2,262	2,217	2,266	2,271
Highway Vehicles	9,441	9,376	8,874	8,201	8,290	7,192	6,854	6,499	6,072	6,094
Off-Highway	1,973	2,008	2,039	2,038	2,106	2,103	2,120	2,123	2,160	2,207
Miscellaneous	951	428	435	440	458	453	1,320	937	780	893
Total	25,572	25,417	24,826	24,338	24,961	23,731	24,276	23,508	23,020	23,312

Note: The sums of sub-categories may not equal total due to rounding (1 short ton = 9.08×10^5 gms).

Source: U.S. Environmental Protection Agency (1994).

decreased by 6 percent, leading to an overall decrease of about 10% in emissions from all of these categories from 1985 to 1993.

Table 5-7 shows PM_{10} emissions from natural and miscellaneous sources for 1985 to 1994. Fugitive dust is the largest source in the miscellaneous category. No clear trend is evident in overall fugitive dust emissions, because increases in paved road dust are offset by decreases in the mining and quarrying and construction categories. The large year-to-year variability in wind erosion reflects changes in precipitation and regional soil conditions. For instance, the values for 1993 reflect the flooding and extremely wet conditions that occurred in the midwestern United States.

Tables 5-8 through 5-10 show nationwide emissions for sulfur dioxide, oxides of nitrogen, and VOC's, which are all precursors for secondary aerosol formation, for the period from 1984 through 1993. Electric utilities account for the largest fraction of sulfur dioxide, nearly 70% of total emissions in 1993 (Table 5-8). Estimates of sulfur dioxide emissions from industrial fuel combustion increased by approximately 16% from 1984 to 1985, and decreased by 11% between 1985 and 1993. Sulfur dioxide emissions from chemical manufacturing doubled between 1984 and 1985, with emissions leveling off between 0.42 and 0.46 million short tons/year after 1985. Sulfur dioxide emissions from highway vehicles were estimated to have increased by 8% from 1984 to 1989, then levelling off and then decreasing by about 10% from 1992 to 1993, reflecting the introduction of regulations for the desulfurization of diesel fuel. Off-highway vehicle emissions increased from 0.20 million short tons per year in 1984 to 0.28 million short tons per year in 1993. Major sulfur dioxide emissions reductions were observed for petroleum processing and other industrial processes, with decreases of 40% to 50% over the ten-year period. In total, however, sulfur dioxide emissions estimates in 1993 decreased by 6% from those given for 1984.

Table 5-9 shows no significant variations in total nitrogen oxides emissions over the 10-year period. Electric utility and motor vehicle emissions each account for about one-third of total emissions. Emissions from (a) industrial and other fuel combustion and (b) from off-highway vehicles each account for about one-sixth of total emissions. There is little change in total emissions from 1984 to 1993. Moderate increases are seen in the electric utility, industrial and other fuel combustion, and off-highway vehicles categories with much

larger relative increases for chemical manufacturing and metals processing. These increases are offset by decreases in fuel combustion by industry and on-highway vehicles.

Volatile organic compound (VOC) emissions in Table 5-10 are dominated by highway vehicles and solvent use. These two sources together account for 50 to 60% of total emissions. Off-highway vehicles, petroleum-related industries, chemical manufacturing, and petroleum storage and transport account for most of the remaining amounts. VOC emissions from highway vehicles were reduced between 1984 and 1993 by 35%, in spite of increased vehicle mileage. Most of this decrease is due to the presumed effectiveness of emissions controls on newer vehicles. VOC emissions from petroleum industries also were reduced by 43% between 1984 and 1993. Total VOC emissions decreased by 9% between 1984 and 1993. It should be noted that emissions from natural sources are not reflected in the above discussion.

Although total emissions of gaseous precursors (SO_2, NO_x, and VOC's) are shown in Tables 5-8, 5-9, and 5-10, it should be remembered that these values cannot be directly translated into production rates of particulate matter. Dry deposition and precipitation scavenging of some of these gases can occur before they are oxidized to aerosols in the atmosphere. In addition, some fraction of these gases are transported outside of the domain of the continental United States before being oxidized. Likewise, emissions of these gases from areas outside the United States can result in the transport of their oxidation products into the United States. While the chemical oxidation of SO_2 will lead quantitatively to the formation of $SO_4^{=}$, the formation of aerosol from the oxidation of VOC's will be much less because only a small fraction of VOC's react to form particles, and those that do have efficiencies less than 10% (c.f. Section 5.3). The oxidation of NO_2 will yield HNO_3, some of which may dry deposit or be scavenged by precipitation, and the remainder will form particulate nitrate.

Projections of future emissions of primary PM_{10}, SO_2, and NO_x are shown in Table 5-11. Controls mandated by the Clean Air Act Amendments of 1990 are expected to reduce PM_{10} emissions in nonattainment areas. However, because emissions in nonattainment areas constitute a small subset of total emissions, overall emissions are projected as still likely to increase. Fugitive dust sources contribute the major share of the increase. Changes in emissions after 1996 solely reflect activity level changes with the

TABLE 5-11. PROJECTED TRENDS IN PARTICULATE MATTER (PM_{10}), SULFUR DIOXIDE (SO_2), AND OXIDES OF NITROGEN (NO_x) EMISSIONS (10^6 short tons yr^{-1})

	PM_{10} Source Categories										
			Fuel Combustion[a]			Mobile[a]					
	Natural[a]	Misc.[a,b]	Electric Utilities	Industrial	Other	OS[c]	On-Road	Nonroad	Total[a]	SO_2[d]	NO_x[d]
1990	4.36	36.3	0.28	0.24	0.55	0.90	0.36	0.37	43.3	22.4	23.0
1993	1.98	37.9	0.26	0.23	0.54	0.91	0.32	0.40	42.5	21.5	23.3
1996	4.36	43.6	0.31	0.21	0.66	0.89	0.15	0.44	50.6	18.1	21.9
1999	4.36	48.5	0.33	0.20	0.59	0.93	0.13	0.47	55.9	17.6	21.8
2000	4.36	49.8	0.34	0.20	0.66	0.94	0.12	0.48	56.9	17.4	20.5
2002	4.36	51.8	0.35	0.19	0.59	0.97	0.13	0.50	59.0	17.1	20.5
2005	4.36	54.9	0.37	0.19	0.64	1.01	0.13	0.53	62.2	16.7	20.8
2008	4.36	57.4	0.40	0.18	0.69	1.04	0.13	0.55	64.7	16.1	21.3
2010	4.36	59.0	0.42	0.18	0.73	1.06	0.12	0.56	66.4	15.7	21.6

[a]Same categories as used in Tables 5-6 and 5-7.
[b]The miscellaneous category includes fugitive dust from unpaved and paved roads, and other sources; wildfires and managed burning; and agricultural and forestry related emissions.
[c]OS refers to other stationary sources such as chemical manufacturing, metal processing, petroleum refining, other industrial processes, solvent utilization, storage and transport, waste disposal and recycling.
[d]Only total emissions are shown.

Source: U.S. Environmental Protection Agency (1995b).

exception of on-road vehicles. Emission factors for on-road vehicles are expected to decrease mainly because of stringent standards for diesel emissions. Diesel vehicle emissions are expected to decrease nationwide by about 70% from 1990 to 2010 (U.S. Environmental Protection Agency, 1993). This decrease results mainly from a roughly 90% decrease in emissions factors which are partially offset by an increase in total diesel vehicle miles travelled. As can be seen from Table 5-11, emissions from non-road sources (e.g., marine vessels, railroads, aircraft, vehicles used in construction, industry, agriculture, airport services, and landscaping) are projected to exceed those from on-road vehicles from 1990 to 2010.

Emissions of SO_2 from fossil fuel combustion by electric utilities show an expected continued decline through 2010. Emissions from all other categories in Table 5-7 show a slight increase from 1993 to 2002 and then level off to the year 2010. Total NO_x emissions show a decrease of over 10% from 1993 to 2002, then increase by about 5% by the year 2010. This pattern reflects projected emissions for the major categories of fuel combustion by electric utilities and on-road vehicles.

Emissions of ammonia and ammonium are not included in the U.S. Environmental Protection Agency inventories for criteria pollutants. Dentener and Crutzen (1994) have constructed a global inventory of NH_3 emissions. Anthropogenic sources (animals kept for human use, fertilizer applications, and biomass burning) and natural sources (wild animals, vegetation, and the oceans) were included. Emissions from sewage were not included, though.

Vegetation was found to be either a source or a sink for NH_3 depending on ambient concentrations and vegetation type. Animals kept for human use represent the largest single source category. Highest emission rates in North America were found in the central United States. Matthews (1994) found that about 75% of U.S. NH_3 emissions from the application of nitrogenous fertilizers occur in the central United States, with the remainder about evenly divided between the eastern and western United States. Emissions of approximately 0.51 Tg NH_3-N yr^{-1} were calculated for the United States. The Dentener and Crutzen (1994) estimate of NH_3 emissions for North America of 5.2 Tg N yr^{-1} may be compared to a wet deposition rate of NH_4^+ in the United States of 3 -4.5 Tg N yr^{-1}, and three separate emission inventories yielding values of 1.2, 8.8, and 2.8 Tg N yr^{-1} for the U.S. (Placet et al., 1991).

While emissions of organic carbon (OC) and elemental carbon (EC) are included implicitly in the emissions inventories for PM_{10}, it is still useful to consider independent estimates. Zhang et al. (1992) estimated the total production of secondary organic aerosol to be about 1.2 Tg yr^{-1} in the United States. Liousse et al. (1996) have constructed OC and EC emissions inventories for use in a global scale chemical tracer model. They estimate OC emissions of 0.80 Tg OC yr^{-1} from live biomass combustion, 1.4 Tg OC yr^{-1} from fossil fuel combustion, and 0.59 Tg OC yr^{-1} from the oxidation of naturally emitted terpenes assuming a fractional aerosol yield of 5%. Carbon values for OC sources have been multiplied by a factor of 1.2 to account for the presence of oxidized species. EC emissions from the combustion of live biomass and fossil fuels are estimated to be 0.11 Tg EC yr^{-1} and 0.30 Tg C yr^{-1}, respectively. These estimates are roughly 8% of total particulate emissions shown in Tables 5-6 and 5-7. Comparisons of model results with observations from the IMPROVE/NESCAUM network by Liousse et al. (1996) suggest that both the OC and EC emissions derived for their model may be systematically underestimated by at least a factor of two.

The regional nature of total primary particulate matter emissions is illustrated in Figure 5-5. At least 80% of the emissions in any single region arises from fugitive dust sources and wind erosion. SO_2 regional emissions are shown in Figure 5-6 as a reminder that they are highest in the eastern United States and that the oxidation of SO_2 to $SO_4^=$ can constitute a substantial fraction of the aerosol mass in the eastern United States. It can also be seen that the ratio of SO_2 to primary PM_{10} emissions tends to be much higher in the eastern than in the western United States.

Annual averages do not reflect the seasonality of certain emissions. Residential wood burning in fireplaces and stoves, for example, is a seasonal practice which reaches its peak during cold weather. Cold weather also affects motor vehicle exhaust particulate emissions, both in terms of chemical composition and emission rates (e.g., Watson et al., 1990b; Huang et al., 1994). Planting, fertilizing, and harvesting are also seasonal activities. Forest fires occur mainly during the local dry season and during periods of drought.

Several of the sources in Tables 5-6 through 5-10 are episodic rather than continuous in nature. This is especially true of prescribed and structural fires and fugitive dust emissions. Although windblown dust emissions are low on an annual average, they are likely to be quite

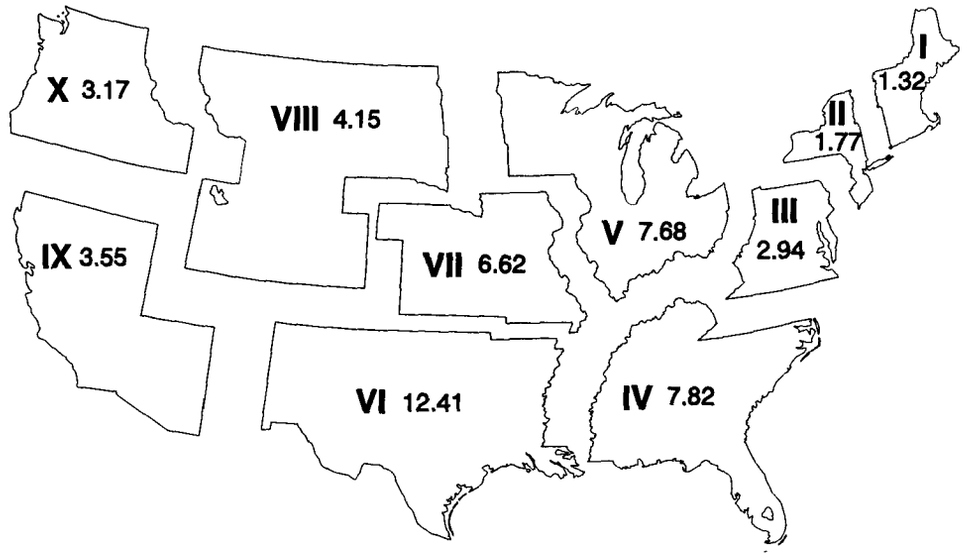

Figure 5-5. Estimates of primary PM_{10} emissions by U.S. Environmental Protection Agency region for 1992.

Units = 10^6 short tons/yr (1 short ton = 9.08×10^5 gms).

Source: U.S. Environmental Protection Agency (1993).

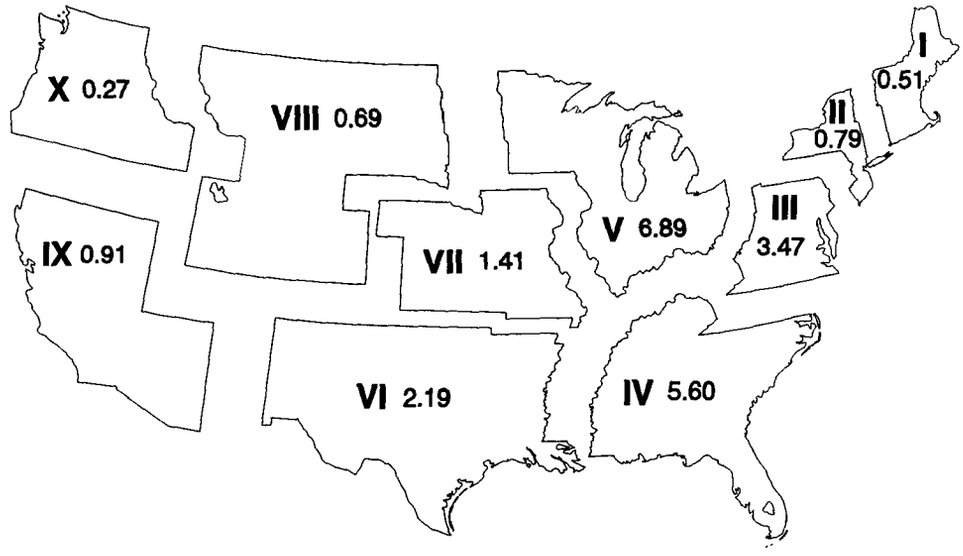

Figure 5-6. Estimates of sulfur dioxide emissions by U.S. Environmental Protection Agency region for 1992.

Units = 10^6 short tons/yr (1 short ton = 9.08×10^5 gms).

Source: U.S. Environmental Protection Agency (1993).

large during those few episodes when wind speeds are high. The transport of Saharan dust to the continental United States is also highly episodic.

5.5 APPLICATIONS AND LIMITATIONS OF EMISSIONS INVENTORIES AND RECEPTOR MODELS

This section examines requirements for the design and construction of emissions inventories and potential areas of uncertainty and limitations in their use. Receptor modeling methods to apportion sources to mass components in ambient aerosol measurements, and results for a number of aerosol monitoring studies, will then be presented. Some general considerations of the relative strengths and weaknesses of using emissions inventories and receptor models to assign sources to particulate matter components in ambient samples will then be discussed. Finally, results from specific receptor modeling studies in the eastern and western United States will be discussed.

5.5.1 Uncertainties in Emissions Estimates

It is difficult to assign uncertainties quantitatively to entries in emissions inventories. Methods that can be used to verify or place constraints on emissions inventories are sparse. In general, the overall uncertainty in the emissions of a given pollutant includes contributions from all of the terms on the right hand side of Eq. 5-1 (activity rates, emissions factors, and control device efficiencies). Additional uncertainties can arise during the compilation of an emissions inventory because of missing sources and arithmetical errors. The variability of emissions can cause errors when annual average emissions are applied to applications involving shorter time scales.

Activity rates for well-defined point sources (e.g., power plants) should have the smallest uncertainty associated with their use, since accurate production records need to be kept. On the other hand, activity rates for a number of areally dispersed fugitive sources are extremely difficult to quantify. Emissions factors for easily measured fuel components which are quantitatively released during combustion (e.g., CO_2 and SO_2) should be the most reliable. Emissions of components formed during combustion are more difficult to characterize as the emissions rates are dependent on factors specific to individual combustion

units and on combustion stage (i.e., smoldering or active). Although the AP-42 emissions factors (U.S. Environmental Protection Agency, 1995a) contain extensive information for a large number of source types, these data are very limited in the number of sources sampled. The efficiency of control devices is determined by their age, their maintenance history, and operating conditions. It is virtually impossible to assign uncertainties in control device performance due to these factors. It should be noted that the largest uncertainties occur for those devices which have the highest efficiencies (>90%). This occurs because the efficiencies are subtracted from one and small errors in assigning efficiencies can lead to large errors in emissions.

Ideally an emissions inventory should include all major sources of a given pollutant. This may be an easy task for major point sources, but becomes problematic for poorly characterized area sources. As an example, it was recently realized that meat cooking could be a significant source of organic carbon (Hildemann et al., 1991). Further research is needed to better characterize the sources of pollutants in order to reduce this source of uncertainty. Errors can arise from the misreporting of data, and arithmetic errors can occur in the course of compiling entries from thousands of individual sources. A quality assurance program is required to check for outliers and arithmetic errors.

Because of the variability in emissions rates, there can be errors in the application of inventories developed on an annually averaged basis (as are the inventories shown in Tables 5-6 to 5-10) to episodes occurring on much shorter time scales. As an example, most modeling studies of air pollution episodes are carried out for periods of a few days.

Uncertainties in annual emissions were estimated to range from 4 to 9% for SO_2 and from 6 to 11% for NO_x in the 1985 NAPAP inventories for the United States (Placet et al., 1991). Uncertainties in these estimates increase as the emissions are disaggregated both spatially and temporally. The uncertainties quoted above are conservative estimates and refer only to random variability about the mean, assuming that the variability in emissions factors was adequately characterized and that extrapolation of emissions factors to sources other than those for which they were measured is valid. The estimates do not consider the effects of weather or variations in operating and maintenance procedures. Fugitive dust sources, as mentioned above, are extremely difficult to quantify, and stated emission rates may only represent order-of-magnitude estimates. As rough estimates, uncertainties in emissions

estimates could be as low as 10% for the best characterized source categories, while emissions figures for windblown dust should be regarded as order-of-magnitude estimates. Given (a) uncertainties in the deposition of SO_2 and its oxidation rate, (b) the variability seen in OC and EC emissions from motor vehicles along with the findings from past verification studies for NMHC and CO to NO_x ratios, (c) ranges of values found among independent estimates for emissions of individual species (NH_3, OC), and (d) the predominance of fugitive emissions, PM emissions rates should be regarded as order-of-magnitude estimates.

There have been few field studies designed to test emissions inventories observationally. The most direct approach would be to obtain cross-sections of pollutants upwind and downwind of major urban areas from aircraft. The computed mass flux through a cross section of the urban plume can then be equated to emissions from the city chosen. This approach has been attempted on a few occasions. Results have been ambiguous because of contributions from fugitive sources, non-steady wind flows, and general logistic difficulties.

Greater success, albeit on a smaller scale, has been achieved in studies that tested predictions of the State of California EMFAC emissions model. An ambient-air study in the Los Angeles basin (Fujita et al., 1992) showed that motor vehicle emissions of CO and nonmethane hydrocarbons (NMHC) were being systematically underpredicted in the emissions model by a factor of about 2.5, assuming that NO_x emissions were much better known; i.e., the CO to NO_x and NMHC to NO_x ratios were underpredicted by the model. A study performed in a tunnel in the Los Angeles basin (Ingalls, 1989; Pierson et al., 1990) showed that motor vehicle NO_x emission rates (g/mi) were predicted approximately correctly but that the CO and NMHC emission rates were systematically underpredicted in the emissions model by factors of two to three. Similar tests need to be performed for particulate matter emissions from motor vehicles.

A completely different approach to obtaining area-wide emissions of pollutants relies on the construction of inversion algorithms applied in the context of atmospheric transport models (Brown, 1993). Emissions of a pollutant that are required to produce a specified distribution of surface concentrations are solved for by using model-derived transport and chemical loss terms. Uncertainties in the emissions fields are then generated in terms of specified uncertainties in the observed data and in the model transport and chemistry fields.

A number of factors limit the ability of an emissions inventory driven, chemical tracer model to determine the effects of various sources on particle samples obtained at a particular location apart from uncertainties in the inventories given above. Air pollution model predictions represent averages over the area of a grid cell, which in the case of the Urban Airshed Model typically has been 25 km^2 (5 km $\times$ 5 km). The contributions of sources to pollutant concentrations at a monitoring site are strongly controlled by local conditions which cannot be resolved by an Eulerian grid-cell model. Examples would be the downward mixing of tall stack emissions and deviations from the mean flow caused by buildings. The impact of local sources may not be accurately predicted, because their emissions would be smeared over the area of a grid cell or if the local wind flow were in the wrong direction during sampling.

For these reasons, receptor models have been used to determine source contributions to particulate matter at individual monitoring sites. Receptor models are strictly diagnostic in their application and do not have the prognostic, or predictive, capability of chemical transport models. In addition, receptor models have been developed for apportioning sources of primary particulate matter and are not formulated to include the processes of secondary particulate matter formation which are explicitly included in the chemical transport models.

5.5.2 Receptor Modeling Methods

Receptor models relate source contributions to ambient concentrations based on composition analysis of ambient particulate samples. They depend on the assumption of mass conservation and the use of a mass balance. As an example, assume that the total concentration of particulate lead measured at a site can be considered to be the sum of contributions from a number of independent sources,

$$Pb_{total} = Pb_{motor\ vehicles} + Pb_{soil} + Pb_{smelter} + \ . \ . \ . \qquad (5\text{-}2)$$

Since most sources emit particles that contain a number of chemical elements or compounds, the atmospheric concentration of an element can be considered to be the product of the abundance of the element of interest (ng/mg) in the effluent and the mass concentration of particles from that source in the atmosphere (mg/m^3). For lead from motor vehicles, for example,

$$Pb_{motor\ vehicles} = a_{Pb,\ mv} f_{mv} \tag{5-3}$$

where $a_{Pb,mv}$ is the abundance of lead in motor vehicle emissions, and f_{mv} is the mass concentration of motor vehicle emitted particles in the atmosphere. Extending this idea to m chemical elements, n samples, and p independent sources,

$$x_{ij} = \sum_{k=1}^{p} a_{ik} f_{kj} \tag{5-4}$$

where x_{ij} is the ith elemental concentration measured in the jth sample (ng m^{-3}), a_{ik} is the gravimetric abundance of the ith element in material from the kth source (ng mg^{-1}), and f_{kj} is the airborne mass concentration of material from the kth source contributing to the jth sample (mg m^{-3}). The f_{kj} are the quantities to be determined from Equation 5-4. To distinguish the contributions of one source type from another using receptor models, the chemical and physical characteristics must be such that (1) they are present in different proportions in different source emissions, (2) these proportions remain relatively constant for each source type, and (3) changes in these proportions between source and receptor are negligible or can be empirically represented.

A number of specialty conference proceedings, review articles, and books have been published to provide greater detail about source apportionment receptor models (Cooper and Watson, 1980; Watson et al., 1981; Macias and Hopke, 1981; Dattner and Hopke, 1982; Pace, 1986; Watson et al., 1989; Gordon, 1980, 1988; Stevens and Pace, 1984; Hopke, 1985, 1991; Javitz et al., 1988). Watson et al. (1994b) present data analysis plans which include receptor models as an integral part of visibility and PM_{10} source apportionment and control strategy development.

The first step in attempting to relate ambient particulate matter measured at a particular location to source contributions is typically data evaluation. The objectives for data evaluation are: (1) to summarize the accuracy and precision of measurements; (2) to identify and investigate extreme and inconsistent values; (3) to perform data comparisons and investigate discrepancies; and (4) to estimate the equivalence of measurements of the same variable by different methods.

Even with the most stringent quality assurance, it is prudent to perform several straightforward analyses to identify the presence of any discrepancies in atmospheric

particulate data and to correct, flag, or eliminate them. Investigating the equivalence of different measurement methods for the same variable is especially important for particulate chemical measurements, which may show substantial differences in concentration depending upon how they were made. Data evaluation activities include: (1) plotting and examining pollutant time series data to identify spikes and outliers for investigation; (2) comparing the sum of chemical species with PM_{10} mass measurements; and (3) comparing measurements of the same variables at the same or nearby sites using different measurement devices and procedures.

After data evaluation the next step in an analysis of particulate air quality in a region is a process that can be termed a descriptive air quality analysis. The objectives of a descriptive air quality analysis are: (1) to identify similarities and differences in air quality at different sampling sites; and (2) to depict temporal and spatial variations in particulate and gaseous precursor measurements. Descriptive air quality analysis includes: (1) statistical summaries of median and extreme values of air quality variables for different sites, episodes, and times of day; (2) time series plots of PM_{10} and selected chemical components; (3) spatial pie plots of particulate chemical composition; and (4) spatial and temporal correlations between PM_{10} and chemical composition measurements. The product of this analysis is a quantitative overview of particulate concentrations during the period of interest.

Performed at the same time as a descriptive air quality analysis, a descriptive meteorological analysis is carried out to: (1) describe the spatial structure, temporal variability, and statistical distribution of meteorological conditions; (2) describe the transport and mixing patterns in the study domain; and (3) identify relationships between meteorology and atmospheric particulate concentrations. Data normally available would include wind speed, wind direction, temperature, relative humidity, and solar radiation at ground level and aloft (if available).

Descriptive meteorological analysis activities include: (1) statistical summaries of meteorological variables; (2) time series and spatial plots of meteorological variables, including wind vectors, with examination for phenomena such as inter-basin transport, stagnation, slope flows, convergence zones, and recirculation; (3) identification of layers and orographic phenomena that change with elevation; (4) tabulations of fog occurrences,

frequencies, locations, and intensities; and (5) meteorological descriptions and comparisons with meteorology during high PM_{10} episodes from prior years.

The product of these analyses is a conceptual understanding of how meteorological phenomena influence atmospheric particulate concentrations in a particular region.

The next step in receptor modeling for particulate matter is a source profile compilation. The objectives of source profile compilation analysis are: (1) to combine profiles from individual samples into composite profiles; and (2) to assign source profiles to source categories based on their degree of similarity or difference. Data needed for this study are the chemical measurements on samples from representative source types that are expected to contribute to airborne particulate matter during study periods. Major source types include, for example: (1) suspended geological material from roads and from agricultural and unpaved areas; (2) primary particle exhaust from gasoline- and diesel-powered vehicles; (3) industrial sources; (4) residual oil combustion; and (5) secondary ammonium sulfate and ammonium nitrate originating from gaseous precursors. Source profile compilations include: (1) tables and plots of individual profiles and their uncertainties; (2) calculation of averages and standard deviations for category profiles; and (3) calculation of weighted composite profiles for source categories which are found for the source apportionment modeling described below. It is important to emphasize that source and ambient samples must be analyzed using the same protocols and methods (U.S. Environmental Protection Agency, 1994).

The chemical mass balance (CMB) receptor model is the model most commonly used for particulate matter source apportionment. The CMB model uses the chemical and physical characteristics of gases and particles measured at source and receptor to both identify the presence of, and quantify source contributions to, the receptor (Friedlander, 1973).

The CMB consists of an effective variance least-squares solution to the set of linear equations (5-4) that expresses each concentration of a chemical species at a receptor site as a linear sum of products of source profile species and source contributions. The source profile species, i.e., the fractional amount of the species in the emissions from each source type, and the receptor concentrations, with appropriate uncertainty estimates, serve as input data to the CMB model. The output consists of: (1) the source contribution estimates of

each source type; (2) the standard errors of these source contribution estimates; and (3) the amount contributed by each source type to each chemical species. The model calculates values for the contributions from each source type and the uncertainties associated with those values. Input data uncertainties are used both to weight the importance of input data values in the solution and to calculate the uncertainties of the source contributions. The CMB model assumptions are: (1) compositions of source emissions are constant over the period of ambient and source sampling; (2) chemical species do not react with each other, i.e., they add linearly; (3) all sources with a potential for significantly contributing to the receptor have been identified and their emissions have been characterized; (4) the source compositions are linearly independent of each other; (5) the number of sources or source categories is less than or equal to the number of chemical species; and (6) measurement uncertainties are random, uncorrelated, and normally distributed. Assumptions 1 through 6 for the CMB model are fairly restrictive and will never be completely satisfied in actual practice. Fortunately, the CMB model can tolerate reasonable deviations from these assumptions, although these deviations increase the stated uncertainties of the source contribution estimates.

The CMB modeling procedure requires: (1) identification of the contributing source types; (2) selection of chemical species to be included; (3) estimation of the fraction of each of the chemical species which is contained in each source type (i.e., the source compositions); (4) estimation of the uncertainty in both ambient concentrations (including artifacts during sampling and storage such as gas absorption or volatilization in filter samples) and source compositions; (5) estimation of differential losses during transport from source to receptor; (6) solution of the chemical mass balance equations; and (7) validation and reconciliation. Each of these steps requires different types of data. Uncertainties in the modeling results can be noticeably reduced by obtaining source profile measurements which correspond to the period of ambient measurements (Glover et al., 1991; Dzubay et al., 1988; and Olmez et al., 1988). Stratifying data according to wind direction can also increase the number of source types that can be resolved as shown in the above studies.

Emissions inventories are examined to determine the types of sources that are most likely to influence a receptor. These emissions inventories for particulate matter are

frequently far from complete, however, and other measures are needed to infer the influence of uninventoried sources. The Principal Components Analysis and Empirical Orthogonal Function models described below can aid in this identification. Once these sources have been identified, profiles acquired from similar sources can be examined to select the chemical species to be measured. The more species measured, the better the precision of the CMB apportionment.

The Principal Components Analysis (PCA) receptor model classifies variables into groups identifiable as causes of particulate matter levels measured at receptors. Typical causes are emissions sources, chemical interactions, or meteorological phenomena. The PCA model uses ambient concentrations of chemical species and meteorological data as inputs. PCA does not use source emissions measurements, as does the CMB model, but it may require 50 or more measurements of many species from different time periods at a single receptor site.

The PCA procedure is as follows: (1) select the chemical species and measurement cases to be included; (2) calculate the correlation coefficients between the species; (3) calculate the eigenvectors and eigenvalues of the correlation matrix; (4) select eigenvectors to be retained; (5) rotate these eigenvectors into a more physically meaningful space; and (6) interpret the rotated vectors as air pollution sources based on the chemical species with which they are highly correlated. Freeman et al. (1989) describe the computer software and methods required to use the PCA model for PM_{10} source assessment. See also Henry (1991).

The PCA model assumptions are: (1) compositions of source emissions are constant over the period of ambient and source sampling; (2) chemical species concentrations add linearly; (3) measurement errors are random and uncorrelated; (4) the case-to-case variability of actual source contributions is much larger than the variability due to other causes, such as measurement uncertainty or changes in source profiles due to process and fuel changes; (5) causes of variability that affect all sources equally (such as atmospheric dispersion) have much smaller effects than causes of variability for individual source types (such as wind direction or emission rate changes); (6) the number of cases exceeds the number of variables in the PCA model to an extent that statistical stability is achieved; and (7) eigenvector rotations are physically meaningful.

There are a number of examples of the application of PCA models. Photochemical factors were found to influence particulate matter measurements from Los Angeles, CA, New York, NY (Henry and Hidy, 1979), St. Louis, MO (Henry and Hidy, 1982), Lewisburg, WV (Lioy et al., 1982), and Detroit, MI (Wolff et al., 1985a). These photochemical factors were consistently associated with daily average and maximum ozone (O_3), maximum temperatures, and absolute humidity. The photochemical factors found for Los Angeles data (Henry and Hidy, 1979) were highly correlated with daily maximum and minimum relative humidity measurements. Local source factors were found for Salt Lake City (Henry and Hidy, 1982) and Los Angeles (Henry and Hidy, 1979) and were highly correlated with sulfur dioxide (SO_2) and the wind direction frequency distributions. Dispersion/stagnation factors were found for St. Louis, Salt Lake City, and Lewisburg. The variables correlated with the dispersion/stagnation factor were nitric oxide (NO), nitrogen dioxide (NO_2), wind speed at midnight and noon, average wind speed, morning mixing height, maximum hourly precipitation, and average precipitation. PCA has also been used to identify sources which may not be inventoried (Wolff and Korsog, 1985; Cheng et al., 1988; Henry and Kim, 1989; Koutrakis and Spengler, 1987; Zeng and Hopke, 1989).

The PCA procedure as outlined above provides only a qualitative assessment of air pollution sources. In some circumstances, however, the procedure can be extended to produce quantitative estimates of the source impacts. For example, a chemical species strongly associated with a single PCA group may be suitable as a source tracer for use in a subsequent multiple linear regression receptor model (Kleinman et al., 1980)

The Empirical Orthogonal Function (EOF) receptor model is applied to a spatially dense network of measurements to identify the locations of emissions sources and to estimate the net fluxes (emissions minus deposition) of those pollutants. The EOFs manifest themselves as isopleth maps of flux density. When a major point source is the emitter, such as a coal-fired power plant, the EOFs have been shown (Gebhardt et al., 1990) to surround that source. EOFs have been applied to air pollution measurements by Peterson (1970), Ashbaugh et al. (1984), Wolff et al. (1985b), and Henry et al. (1990). Henry et al. (1990) were the first researchers to place this method on a firm theoretical foundation and to demonstrate that EOFs reproduce the net fluxes used as input to a dispersion model.

In prior studies, the EOF model was applied to single chemical constituents, such as sulfur dioxide, sulfate, and total particulate mass concentrations. In a recent study (Watson et al., 1991), the EOF model was applied to the source contribution estimates calculated for each sample from the CMB modeling described above. In this way, source-type specific patterns of net flux were determined. For example, the geological source contributions may be represented as a linear sum of EOFs which correspond to a dirt road, a construction site, and an area of intense agricultural activity. The motor vehicle exhaust source contributions may be represented by a linear sum of EOFs which correspond to a major highway, a large truck stop, or an urban core area. The EOF model may also be applied to specific chemical species which are identified as potential markers for uninventoried sources.

The EOF procedure is similar to the PCA procedure: (1) select the source contribution estimates and measurement cases to be included; (2) calculate the covariance coefficients between the species measured at the same time at several sites; (3) calculate the eigenvectors and eigenvalues of the covariance matrix; (4) select eigenvectors to be retained; (5) rotate these eigenvectors into a more physically meaningful space; and (6) interpolate between the values of these eigenvectors to supply the net flux patterns. The main difference between PCA and EOF is that PCA operates on many samples from a single site taken over an extended time period, while EOF operates on many samples from many sites taken over a single time period.

The formulation of Henry et al. (1990), termed Source Identification Through Empirical Orthogonal Functions (SITEOF), uses wind velocities as input in addition to the spatially distributed source contribution estimates. The SITEOF assumptions are: (1) net fluxes of spatially-distributed pollutants add linearly; (2) pollutants are homogeneously distributed vertically in the mixed layer; (3) measurement errors are random and uncorrelated; (4) the number of sampling sites exceeds the number of source locations to an extent that statistical stability is achieved; and (5) measurement locations are located in positions to maximize spatial gradients from major source emissions. The major unknown concerning the SITEOF model is the extent to which assumptions 4 and 5 can be met in actual practice. Motor vehicle exhaust is confined to specific areas (e.g., roads and parking lots), and it is a straightforward task to locate monitors close to and far from these known locations. Fugitive dust, on the other hand, can be emitted from many locations.

The SITEOF model is one of a class of procedures referred to as "hybrid receptor models". Such models make use of not only the ambient species concentration measurements that form the input data for a pure receptor model, but in addition source emission rates or atmospheric dispersion or transformation information characteristic of dispersion models. By exploiting simultaneously the strengths of the two complementary approaches their individual weaknesses should be minimized. A survey of hybrid receptor models is available (Lewis and Stevens, 1987).

Ashbaugh et al., (1985) developed the concept of the potential source contribution function (PSCF) for performing the apportionment of secondary species, for combining air parcel back trajectories from a receptor site with chemical data at the site to infer possible source locations. The PSCF is an estimate of the conditional probability that a trajectory which passed through a given cell in the emissions grid (g_{ij}) contributed a concentration greater than some threshold value to ambient concentrations at the receptor site. Gao et al. (1993) extended the PSCF analysis to provide an apportionment of secondary species. By multiplying the PSCF by the emissions rate in g_{ij}, an estimate of the maximum contribution of sources in g_{ij} to the concentrations measured at the receptor site is obtained. Further research is needed to quantify the uncertainties associated with this method. These uncertainties are related to unidentified sources, background sources, emissions estimates at the time of calculation, the differential loss of species (e.g., by deposition), and mixing of air parcels from different cells during transit from source to receptor. Gao et al. (1993) have applied PSCF's along with emissions estimates to the apportionment of SO_2 and $SO_4^=$ at sites in the South Coast Air Basin, and Cheng et al. (1996) have also applied this technique to the apportionment of NO_x and NH_3 in this area.

The use of ^{14}C isotopic analysis has been used to distinguish between fossil fuel and biomass sources of carbon in aerosol samples. An example would be to determine the fraction of ambient aerosol mass concentration in wintertime samples originating from woodburning. This method has been particularly useful in validating less expensive receptor methods of achieving the same goal (Wolff et al., 1981; Lewis et al., 1988).

The preceding sections have dealt with receptor models that rely on chemical information obtained from bulk samples. It is worth noting that in addition there are powerful receptor modeling methods which also use the morphology and composition of

individual particles to provide clues to their source origin (Dzubay and Mamane, 1989). Scanning electron microscopy (SEM) along with energy dispersive X-ray analysis (EDX) has allowed the size distribution of particles to be characterized according to shape and elemental composition. This technique has proven to be extremely useful for distinguishing between fly ash and soil derived particles; both types of particles have similar composition, but fly ash particles are spherical while soil particles are irregularly shaped.

Manually performing SEM/EDX analyses of the large number individual particles necessary to characterize a size distribution is extremely time consuming. Automated methods have been developed for the rapid characterization of the shapes of hundreds of particles in aerosol samples (Xie et al., 1994a, 1994b). The morphology data can then be used along with EDX data to assign particles to clusters related to specific source types (Van Espen, 1984).

5.5.3 Source Contributions to Ambient Particles Derived by Receptor Models

Receptor modeling has been used for obtaining information about the nature of sources of ambient aerosol samples. The results of several studies will be discussed to provide an indication of different sources of particulate matter across the United States. First, results obtained by using the CMB approach for estimating contributions to $PM_{2.5}$ and $PM_{(10-2.5)}$ from different source categories at monitoring sites in the United States east of the Mississippi River will be discussed. Estimated contributions from a number of source categories to PM_{10} in ambient samples, obtained mainly at sites west of the Mississippi River, will then be discussed.

Dzubay et al. (1988) estimated source category contributions to 24-hour $PM_{2.5}$ and $PM_{(10-2.5)}$ samples obtained by a dichotomous sampler at three widely separated sites in the Philadelphia, PA area (NE airport in Philadelphia, PA; Camden, NJ; and a site about 30 km to the SW of Camden, NJ) during the summer of 1982. They used a composite of CMB, multiple linear regression (MLR), and wind trajectory receptor models. Source compositions shown in Table 5-3 were obtained partly to provide input to this study (Olmez et al., 1988). Ambient concentrations of individual species used by Dzubay et al. (1988) are shown in Table 6A-2a (Chapter 6, Appendix A). Sulfate, associated NH_4+ and water

constituted about 70% of $PM_{2.5}$. Since the mean fractional abundances of $PM_{2.5}$ to PM_{10} was 0.75, it can be seen that sulfate components contributed approximately 53% of PM_{10}. Coal- and oil-fired power plants located east of the Mississippi River were found to contribute 50 ± 6% and 11 ± 4% of $PM_{2.5}$, by using Se as a tracer for coal combustion and V and Ni as tracers for oil combustion, based on an MLR analysis.

The study was performed during a period (summer of 1982) when the Pb content of gasoline was declining markedly, and so Pb could not be used as a unique tracer of motor vehicle emissions. CMB was used to determine nonvehicular Pb, which was subtracted from the measured Pb concentration to yield a tracer for vehicle exhaust. Motor vehicle exhaust was then found to contribute about 8%, on average, to $PM_{2.5}$. Local sources of sulfate (determined from the MLR intercept) were found to contribute 13%, on average, with smaller contributions from local industrial sources, incinerators, and crustal matter to $PM_{2.5}$.

Crustal matter constituted about 76%, on average, of $PM_{(10-2.5)}$. Sulfate and associated NH_4^+ and water constituted only about 7% of $PM_{(10-2.5)}$. Other contributions to $PM_{(10-2.5)}$ were found to arise from sea-salt and incinerators. In a study of the Philadelphia aerosol in the summer of 1994, Pinto et al. (1995) found close agreement with Dzubay et al. (1988) both in measured concentrations and in the magnitude of the inferred fractional contribution of regional sulfate sources.

Glover et al. (1991) estimated the contributions of different source categories to 24-hour $PM_{2.5}$ and $PM_{(10-2.5)}$ samples obtained with a dichotomous sampler at a site in Granite City, IL. Again, sulfate was the major constituent of $PM_{2.5}$, constituting from 59% of $PM_{2.5}$ with SSW winds to 86.6% of $PM_{2.5}$ with NNW winds. Inferred contributions from specific source types were also shown to be strongly dependent on wind direction. Inferred contributions from iron works ranged from 3.4% with NNW winds to 16.4% with SSE winds. Inferred contributions from a Pb smelter ranged from 2.8% with WNW winds to 11.6% with SSW winds. Inferred contributions from other sources (e.g., motor vehicles, incinerators, other smelters, and soil) were all typically a few per cent.

Sulfate was a relatively minor constituent (< 10%) of $PM_{(10-2.5)}$ samples. Major inferred contributions were from iron works, ranging from 5.7% with WNW winds to 53.8% with ENE winds; soil, ranging from 4.2% with WSW winds to 35.8% with ESE

winds; street dust, ranging from 1.4% SSE winds to 45.6% with WNW winds; with generally smaller contributions from the other sources listed for $PM_{2.5}$.

These results demonstrate the different nature of $PM_{2.5}$ and $PM_{(10-2.5)}$ sources (i.e., $PM_{2.5}$ was derived from regional sources, while $PM_{(10-2.5)}$ was derived from local industries); the utility of wind sectoring to help locate sources; and the need to obtain site-specific source composition profiles. The use of site-specific source profiles instead of profiles culled from the literature resulted in decreases in predicted error values, especially for fugitive dust.

Results obtained at a number of monitoring sites in the central and western United States obtained by using the CMB model are shown in Table 5-12 for PM_{10}. The sampling sites represent a variety of different source characteristics within different regions of Arizona, California, Colorado, Idaho, Illinois, Nevada and Ohio. Several of these are background sites, specifically Estrella Park, Gunnery Range, Pinnacle Peak, and Corona de Tucson, AZ, and San Nicolas Island, CA. Definitions of source categories also vary from study to study. In spite of these differences, several features can be observed from the values in this table.

Fugitive dust (geological material) from roads, agriculture and erosion appears as a highly variable contributor to PM_{10} at nearly all sampling sites shown in Table 5-12, contributing about 40% of the average PM_{10} mass concentration. The average fugitive dust source contribution is highly variable among sampling sites within the same urban areas, as seen by differences between the Central Phoenix (33 $\mu g/m^3$) and Scottsdale (25 $\mu g/m^3$) sites in Arizona, and it is also seasonally variable, as evidenced by the summer and fall contributions at Rubidoux, CA. These studies found that the source profiles for fugitive dust were chemically similar, even though the dust came from different emitters, so that further apportionment into sub-categories was not possible by the CMB model alone. Road sand often contains salts that allow it to be distinguished from other fugitive dust sources. It is usually the only exposed fugitive dust source when other sources are covered by snowpack. Dust from some construction activities and cement plants can also be separated from other sources due to enrichments in calcium content of these emissions, as seen in studies at Rubidoux, CA, Rillito, AZ (near cement plants), and Pocatello, ID (near chemical and fertilizer production plants).

TABLE 5-12. RECEPTOR MODEL SOURCE CONTRIBUTIONS TO PM_{10}

		$\mu g/m^3$										
Sampling Site	Time Period	Primary Geological	Primary Construction	Primary Motor Vehicle Exhaust	Primary Vegetative Burning	Secondary Ammonium Sulfate	Secondary Ammonium Nitrate	Misc. Source 1	Misc. Source 2	Misc. Source 3	Misc. Source 4	Measured PM_{10} Concentration
Central Phoenix, AZ (Chow et al., 1991)	Winter 1989-1990	33.0	0.0	25.0	2.3	0.2	2.8	0.0	0.0	0.0	0.0	64.0
Craycroft, AZ (Chow et al., 1992a)	Winter 1989-1990	13.0	0.0	8.3	0.0	0.7	0.6	1.2[a]	0.0	0.0	0.0	23.4
Hayden 1, AZ (Garfield) (Ryan et al., 1988)	1986	5.0	2.0[b]	0.0	0.0	4.0	0.0	74.0[c]	5.0[d]	1.0[e]	0.0	105.0
Hayden 2, AZ (Jail) (Ryan et al., 1988)	1986	21.0	4.0[b]	0.0	0.0	4.0	0.0	28.0[c]	0.0	1.0[e]	0.0	59.0
Phoenix, AZ (Estrella Park) (Chow et al., 1991)	Winter 1989-1990	37.0	0.0	10.0	0.9	1.6	0.0	0.0	0.0	0.0	0.0	55.0
Phoenix, AZ (Gunnery Rg.) (Chow et al., 1991)	Winter 1989-1990	20.0	0.0	5.5	0.0	1.0	0.0	0.0	0.0	0.0	0.0	27.0
Phoenix, AX (Pinnacle Pk.) (Chow et al., 1991)	Winter 1989-1990	7.0	0.0	2.9	1.0	0.9	0.0	0.0	0.0	0.0	0.0	12.0
Rillito, AZ (Thanukos et al., 1992)	1988	42.7	13.8[b]	1.2[f]	0.0	0.0	0.0	11.6[g]	0.0	0.0	0.0	79.5
Scottsdale, AZ (Chow et al., 1991)	Winter 1989-1990	25.0	0.0	19.0	7.4	0.6	3.6	0.0	0.0	0.0	0.0	55.0
West Phoenix, AZ (Chow et al., 1991)	Winter 1989-1990	30.0	0.0	25.0	10.0	0.4	3.1	0.0	0.0	0.0	0.0	69.0
Bakersfield, CA (Magliano, 1988)	1986	27.4	3.0	5.5	9.6[l]	5.6	0.0	0.5[j]	0.0	0.0	0.0	67.6
Bakerfield, CA (Chow et al., 1992b)	1988-1989	42.9	1.6	7.7	6.5	5.5	12.7	1.0[m]	1.5[n]	0.6[k]	0.0	79.6
Crows Landing, CA (Chow et al., 1992b)	1988-1989	32.2	0.0	2.2	3.4	2.8	6.5	0.5[m]	1.5[n]	1.2[k]	0.0	52.5
Fellows, CA (Chow et al., 1992b)	1988-1989	29.0	1.4	2.1	3.4	5.1	7.5	7.0[m]	1.4[n]	1.4[k]	0.0	54.6
Fresno, CA (Magliano, 1988)	1986	17.1	0.7	4.0	9.2[l]	1.8	0.0	0.1[j]	0.0	0.0	0.0	48.1
Fresno, CA (Chow et al., 1992b)	1988-1989	31.8	0.0	6.8	5.1	3.6	10.4	0.3[m]	1.0[n]	0.1[k]	0.0	71.5
Indio, CA (Kim et al., 1992)		33.0	3.0	4.4	7.1	3.6	4.1	0.2[j]	1.0[h]	0.0	0.0	58.0
Kern Wildlife Refuge, CA (Chow et al., 1992b)	1988-1989	15.1	2.0	2.2	4.0	3.3	1.5	0.5[m]	1.5[n]	0.7[k]	0.0	47.8
Long Beach, CA (Gray et al., 1988)	1986	20.7	0.0	5.1[i]	0.0	8.0	9.2	0.1[j]	2.0[h]	6.4[k]	0.0	51.9
Long Beach, CA (Summer) (Watson et al., 1994b)	Summer 1987	11.1	0.0	6.3	0.0	10.9	0.8	0.1[j]	2.2[h]	0.0	0.0	46.1
Long Beach, CA (Fall) (Watson et al., 1994b)	Fall 1987	11.3	0.0	42.8	0.0	3.8	23.2	0.0[j]	2.7[h]	0.0	0.0	96.1
Riverside, CA (Chow et al., 1992c)	1988	32.6	0.0	7.0	0.0	4.8	21.4	0.3[j]	1.3[h]	1.1[o]	0.0	64.0
Rubidoux, CA (Gray et al., 1988)	1986	43.1	4.0[j]	5.6[i]	0.0	6.4	21.3	0.3[j]	1.0[h]	5.9[k]	0.0	87.4
Rubidoux, CA (Summer) (Watson et al., 1994b)	Summer 1987	34.9	4.5	17.3	0.0	9.5	27.4	0.0[j]	5.1[h]	0.0	0.0	114.8
Rubidoux, CA (Fall) (Watson et al., 1994b)	Fall 1987	19.2	16.1	30.3	0.0	2.1	31.6	0.0[j]	1.1[h]	0.0	0.0	112.0
Rubidoux, CA (Chow et al., 1992c)	1988	48.0	0.0	10.2	0.0	5.3	21.7	0.4[j]	1.5[h]	5.7[o]	0.0	87.0
San Nicolas Island, CA (Summer) (Watson et al., 1994b)	Summer 1987	1.6	0.0	0.9	0.0	3.7	0.5	0.0[j]	4.3[h]	0.0	0.0	17.4

TABLE 5-12 (cont'd). RECEPTOR MODEL SOURCE CONTRIBUTIONS TO PM_{10}

		$\mu g/m^3$										
Sampling Site	Time Period	Primary Geological	Primary Construction	Primary Motor Vehicle Exhaust	Primary Vegetative Burning	Secondary Ammonium Sulfate	Secondary Ammonium Nitrate	Misc. Source 1	Misc. Source 2	Misc. Source 3	Misc. Source 4	Measured PM_{10} Concentration
Stockton, CA (Chow et al., 1992b)	1989	34.4	0.5	5.2	4.8	3.1	7.0	0.7[m]	1.8[n]	0.0[k]	0.0	62.4
Pocatello, ID (Houck et al., 1992)	1990	8.3	7.5[q]	0.1	0.0	0.0	0.0	0.0	0.0	84.1[r]	0.0	100.0
S. Chicago, IL (Hopke et al., 1988)	1986	27.2	2.4	2.8	0.0	15.4[s]	--	15.1[t]	2.2[u]	0.0	0.0	80.1
S.E. Chicago, IL (Vermette et al., 1992)	1988	14.7[v]	0.0	0.9[f]	0.0	7.7	--	0.8[t]	0.3[h]	1.1[w]	7.7[g]	41.0
Reno, NV (Chow et al., 1988)	1986-1987	14.9	0.0	10.0	1.9	1.3	0.6	0.0	0.0	0.0	0.0	30.0
Sparks, NV (Chow et al., 1988)	1986-1987	15.1	0.0	11.6	13.4	2.7	0.9	0.0	0.0	0.2[k]	0.0	41.0
Follansbee, WV (Skidmore et al., 1992)	1991	10.0	0.0	35.0	0.0	16.0	--	9.3[t]	0.0	0.0	0.0	66.0
Mingo, OH (Skidmore et al., 1992)	1991	12.0	0.0	14.0	4.1	15.0	--	3.4[t]	11.0[x]	0.0	0.0	60.0
Steubenville, OH (Skidmore et al., 1992)	1991	8.3	0.0	14.0	0.8	14.0	--	3.8[t]	5.0[x]	0.0	0.0	46.0

[a]Smelter background aerosol.
[b]Cement plant sources, including kiln stacks, gypsum pile, and kiln area.
[c]Copper ore.
[d]Copper tailings.
[e]Copper smelter building.
[f]Heavy-duty diesel exhaust emission.
[g]Background aerosol.
[h]Marine aerosol, road salt, and sea salt plus sodium nitrate.
[i]Motor vehicle exhaust from diesel and leaded gasoline.
[j]Residual oil combustion.
[k]Secondary organic carbon.
[l]Biomass burning.
[m]Primary crude oil.
[n]$NaCl + NaNO_3$.
[o]Lime.
[p]Road sanding material.
[q]Asphalt industry.
[r]Phosphorus/phosphate industry.
[s]Regional sulfate.
[t]Steel mills.
[u]Refuse incinerator.
[v]Local road dust, coal yard road dust, steel haul road dust.
[w]Incineration.
[x]Unexplained mass.

Dust sources constitute 88% of the annual average PM_{10} National Emissions Inventory (U.S. Environmental Protection Agency, 1994), but they average more than 50% of the contribution to average PM_{10} concentrations in only about 40% of the entries shown in Table 5-12. The reasons for this apparent discrepancy are not clear. In addition to errors in inventories or source apportionments, weather-related factors (wind speed and ground wetness) and the dominance of local sources on spatial scales too small to be captured in inventories may be involved. It should be remembered that dust emissions are widely dispersed and highly sporadic. Dust particles also have short atmospheric residence times and as a result their dominance in emissions inventories may not be reflected in samples collected near specific sources. The contributions from primary motor vehicle exhaust, residential wood combustion, and industrial sources would be underestimated if values from the National Emissions Inventory Trends data base (U.S. Environmental Protection Agency, 1994) were used. Some of these deficiencies, such as fugitive dust emissions, are probably intractable, and the best that can be done is to estimate the uncertainties in these emissions and to value the data accordingly when decisions are made.

In Table 5-12, primary motor vehicle exhaust contributions account for up to 40% of average PM_{10} at many of the sampling sites. Vehicle exhaust contributions are also variable at different sites within the same study area. The mean value and the variability of motor vehicle exhaust contributions reflects the proximity of sampling sites to roadways and traffic conditions during the time of sampling. Vegetation burning, which includes agricultural fires, wildfires, prescribed burning, and residential wood combustion, was found to be significant at residential sampling sites such as: Craycroft, Scottsdale, and West Phoenix, AZ; Fresno, Bakersfield, and Stockton, CA; Sparks, NV; and Mingo, OH. The predominance of these contributions during winter months and the local rather than regional coverage indicates that residential wood combustion was the major sub-category, even though chemical profiles are too similar to separate residential combustion from other vegetative burning sources. For example, Chow et al. (1988) show substantial differences between the residential Sparks, NV and urban-commercial Reno, NV burning contributions even though these sites are separated by less than 10 km. Sites near documented industrial activity show evidence of that activity, but not necessarily involving primary particles emitted by point sources. Hayden, AZ, for example, contains a large smelter, but the major

smelter contributions appear to arise from fugitive emissions of copper tailings rather than stack emissions. Secondary sulfate contributions at Hayden were low, even though SO_2 emissions from the stack were substantial during the time of the study. Fellows, CA is in the midst of oilfield facilities that burn crude oil for tertiary oil extraction. These have been converted to natural gas since the 1988 to 1989 study period. The Follansbee, WV, Mingo, OH, and Steubenville, OH sites are all close to each other in the Ohio River Valley and show evidence of the widespread steel mill emissions in that area.

Marine aerosol is found, as expected, at coastal sites such as Long Beach (average 3.8% of total mass), and San Nicolas Island (25%). These contributions are relatively variable and are larger at the more remote sites. Individual values reflect proximity to local sources. Of great importance are the contributions from secondary ammonium sulfate and ammonium nitrate in the western United States. These are especially noticeable at sites in California's San Joaquin Valley (Bakersfield, Crows Landing, Fellows, Fresno, Kern Wildlife, and Stockton) and in the Los Angeles area.

In addition to these commonly measured components, it is possible that isotopic ratios in source emissions may vary in an informative way with the nature of the combustion process and with the geologic age and character of the source input material. Carbon-14, for example, has been used to separate contemporary carbon due to vegetative burning from carbon emitted by fossil fuel combustion (Currie et al., 1984). Organic compounds (Rogge et al., 1991, 1993a, 1993b, 1993c, 1993d, 1993e; Lowenthal et al., 1994; Hildemann et al., 1991, 1993) show great promise for further differentiation among sources, but measurement methods need to be standardized and made more cost-effective to take advantage of extended chemical source profiles.

Several aspects of the data in Table 5-12 limit the generalizations that can be drawn from it:

- The source contribution estimates for the receptor sites shown are for different years and different times of year. The results, therefore, do not show the temporal variability which may exist in relative source contributions and should not be used to infer differences between sites.

- Samples selected for chemical analysis are often biased toward the highest PM_{10} mass concentrations in these studies, so average source contribution estimates are probably not representative of annual averages.

- Many studies were conducted during the late 1980s, when a portion of the vehicle fleet still used leaded gasoline. While the lead and bromine in motor vehicle emissions facilitated the distinction of motor vehicle contributions from other sources, it was also associated with higher emission rates than vehicles using unleaded fuels. Lead has been virtually eliminated from vehicle fuels.

- Uncertainties of source contribution estimates are not usually reported with the average values summarized in Table 5-12. Estimates of standard errors are calculated in source apportionment studies, and typically range from 15 to 30% of the source contribution estimate. They are much higher when the chemical source profiles for different sources are highly uncertain or too similar to distinguish one source from another.

- Different measurement sites within the same airshed show different proportions of contributions from the same sources. Most often, the sites in close proximity to an emitter show a much larger contribution from that emitter than sites that are distant from that emitter, even by distances as short as 10 km (e.g., Chow et al., 1988; 1992c).

- Given the mass, trace element, ion, and carbon components measured in source and receptor samples in most of the studies from Table 5-12, greater differentiation among sources (e.g., diesel and gasoline vehicle exhaust, meat cooking and other organic carbon sources, different sources of fugitive dust, and secondary aerosol precursors) is not possible for the studies shown in Table 5-12.

5.6 SUMMARY AND CONCLUSIONS

Ambient particulate matter contains both primary and secondary components. Due to the complexity of the composition of ambient PM_{10}, sources are best discussed in terms of individual constituents of both primary and secondary PM_{10}. Each of these constituents can have anthropogenic and natural sources, as shown in Tables 5-1A and 5-1B. The distinction between natural and anthropogenic sources is not always obvious. While windblown dust might seem to be the result of natural processes, highest emission rates are associated with agricultural activities in areas that are susceptible to periodic drought. Examples include the dust bowl region of the midwestern United States and the Sahel of Africa. Most forest fires in the United States may ultimately be of human origin, either through prescribed burning or accident.

Windblown dust from whatever source represents the largest single source of PM in U.S. and global emissions inventories. Although dust emissions (88% of total U.S. PM_{10})

are far in excess of any other source of primary or secondary PM_{10} in any region of the country, measurements of soil constituents in ambient samples suggest that the overall contribution from this source could be much lower. The reasons for this apparent discrepancy are not clear. In addition to errors in inventories or source apportionments, weather-related factors (wind speed and ground wetness) and the dominance of local sources on spatial scales too small to be captured in inventories may be involved. It should be remembered that dust emissions are widely dispersed and highly sporadic. Dust particles also have short atmospheric residence times and, as a result, their dominance in emissions inventories may not be reflected in samples collected near specific sources.

There is a great deal of spatial and temporal variability which is still not reflected in emissions inventories. Apart from seasonal variability, many of the sources discussed in this chapter are highly episodic even within their peak emissions seasons. Examples include the long-range transport of Saharan dust to the United States, regional dust storms, volcanism, and forest fires. Their spatial variability is also evident. Annual estimates for an area can easily be exceeded in a few days by unusual events involving these sources. Less dramatic examples of strong seasonal variability, such as wood burned for home heating in the northwestern United States, may be the major source of winter PM there.

It might be thought that enough data are available to adequately characterize mobile and stationary source emissions. However, data characterizing the variability of PM emissions from mobile sources are quite sparse. Available data suggest that elemental carbon followed by organic carbon species are the major components of diesel particulate emissions, while organic carbon emissions are larger than elemental carbon emissions in the case of gasoline fueled vehicles.

Emissions from biomass burning are also composed mainly of organic carbon species and elemental carbon, although the ratio of organic carbon to elemental carbon is much higher than in motor vehicle emissions. Power plant emissions are not significant sources of aerosol carbon. The fractional yield of secondary organic carbon from the oxidation of natural and anthropogenic hydrocarbons is highly uncertain. Yields from the oxidation of anthropogenic hydrocarbons are probably less than a few percent, and larger yields are found in the oxidation of terpenes emitted by vegetation.

As seen in Table 5-1B, emissions of surface dust, organic debris, and sea spray are concentrated mainly in the coarse fraction of PM_{10} (> 2.5 μm aero. diam.). A small fraction of this material is in the $PM_{2.5}$ size range (< 2.5 μm aero. diam., c.f. Figure 5-1). Nevertheless, concentrations of crustal material can be appreciable especially during dust events. It should also be remembered that all of the Saharan dust reaching the United States is in the $PM_{2.5}$ size range. Emissions from combustion sources (mobile and stationary sources, biomass burning) are predominantly in the $PM_{2.5}$ size range.

As shown in Table 5-6, estimated primary PM_{10} emissions decreased by about 10% from 1985 through 1993. A high degree of variability is evident for emissions from miscellaneous (fugitive dust, biomass burning, and agriculture) and natural (wind erosion of natural surfaces) categories shown in Table 5-7. Estimated SO_2 emissions decreased by several per cent from 1984 through 1993 as shown in Table 5-8. Estimated emissions of NO_x show little variation over the same time period as shown in Table 5-9. Emissions of primary PM_{10} are projected to increase to the year 2010 mainly because of increases in fugitive dust emissions, while emissions of SO_2 and NO_x are expected to decrease over the same time period.

Uncertainties in emissions inventories are difficult to quantify. They may be as low as 10% for well-defined sources (e.g., for SO_2) and may range up to a factor of 10 or so for windblown dust. As a rule, total PM emissions rates should be regarded as order-of-magnitude estimates. Because of the large uncertainty associated with emissions of suspended dust, trends of total PM_{10} emissions should be viewed with caution and emissions from specific source categories are best discussed on an individual basis.

Emissions inventories are generally not the most appropriate way to apportion material in ambient samples. Receptor modeling has proven to be an especially valuable tool in this regard. Compositional profiles developed for receptor modeling applications are perhaps the most accessible and reliable means to characterize the composition of emissions. Quoted uncertainties in source apportionments of constituents in ambient aerosol samples typically range from 15 to 30%. Receptor modeling studies in the western United States have found that motor vehicles and fugitive dust are major sources of PM_{10}. Likewise, a limited number of studies in the eastern United States have found that fossil fuel combustion and fugitive dust are major sources of PM_{10}. Techniques are currently being

developed to use receptor modeling techniques along with ambient data to refine emissions inventory estimates. Because of the site-specific nature of receptor modeling results, more rigorous methods for determining site locations and methods for applying receptor model results to larger spatial scales are needed for this purpose. Again, it should be emphasized that, because of limitations in receptor modeling methods in treating secondary components, these efforts are more likely to be successful for primary components, although it should be mentioned that methods are being developed to apportion secondary constituents.

REFERENCES

Alfaro, S. C.; Gomes, L. (1995) Improving the large-scale modeling of the saltation flux of soil particles in presence of nonerodible elements. J. Geophys. Res. [Atmos.] 100: 16,357-16,366.

Altshuller, A. P. (1983) Review: natural volatile organic substances and their effect on air quality in the United States. Atmos. Environ. 17: 2131-2165.

Altshuller, A. P.; Bufalini, J. J. (1965) Photochemical aspects of air pollution: a review. Photochem. Photobiol. 4: 97-146.

Andreae, M. O. (1991) Biomass burning: its history, use, and distribution and its impact on environmental quality and global climate. In: Levine, J. S., ed. Global biomass burning: atmospheric, climatic, and biospheric implications. Cambridge, MA: MIT Press; pp. 1-21.

Ashbaugh, L. L.; Myrup, L. O.; Flocchini, R. G. (1984) A principal component analysis of sulfur concentrations in the western United States. Atmos. Environ. 18: 783-791.

Ashbaugh, L. L.; Malm, W. C.; Sadeh, W. Z. (1985) A residence time probability analysis of sulfur concentrations at Grand Canyon National Park. Atmos. Environ. 19: 1263-1270.

Bagnold, R. A. (1941) The physics of blown sand and desert dunes. London, United Kingdom: Methuen & Co.

Behymer, T. D.; Hites, R. A. (1984) Similarity of some organic compounds in spark-ignition and diesel engine particulate extracts. Environ. Sci. Technol. 18: 203-206.

Belly, P.-Y. (1964) Sand movement by wind. Washington, DC: U.S. Army Corps of Engineers, Coastal Engineering Research Center; technical memorandum no. 1.

Bisal, F.; Hsieh, J. (1966) Influence of moisture on erodibility of soil by wind. Soil Sci. 102: 143-146.

Brown, M. (1993) Deduction of emissions of source gases using an objective inversion algorithm and a chemical transport model. J. Geophys. Res. [Atmos.] 98: 12,639-12,660.

Calvert, J. G.; Heywood, J. B.; Sawyer, R. F.; Seinfeld, J. H. (1993) Achieving acceptable air quality: some reflections on controlling vehicle emissions. Science 261: 37-45.

Cheng, M.-D.; Lioy, P. J.; Opperman, A. J. (1988) Resolving PM 10 data collected in New Jersey by various multivariate analysis techniques. In: Mathai, C. V.; Stonefield, D. H., eds. PM-10: implementation of standards, an APCA/EPA international specialty conference; February; San Francisco, CA. Pittsburgh, PA: Air Pollution Control Association; pp. 472-483. (APCA transactions series TR-13).

Cheng, M.-D.; Gao, N.; Hopke, P. K. (1996) Source apportionment study of nitrogen species measured in sourthern California in 1987. J. Environ. Eng. (N. Y.) 122: in press.

Chepil, W. S. (1945) Dynamics of wind erosion. Soil Sci. 60: 305-320.

Chepil, W. S. (1956) Influence of moisture on erodibility of soil by wind. Soil Sci. Soc. Am. Proc. 20: 288-292.

Chow, J. C.; Watson, J. G.; Frazier, C. A.; Egami, R. T.; Goodrich, A.; Ralph, C. (1988) Spatial and temporal source contributions to PM_{10} and $PM_{2.5}$ in Reno, NV. In: Mathai, C. V.; Stonefield, D. H., eds. PM-10: implementation of standards, an APCA/EPA international specialty conference; February; San Francisco, CA. Pittsburgh, PA: Air Pollution Control Association; pp. 438-457. (APCA transactions series TR-13).

Chow, J. C.; Watson, J. G.; Richards, L. W.; Haase, D. L.; McDade, C.; Dietrich, D. L.; Moon, D.; Sloane, C. (1991) The 1989-90 Phoenix PM_{10} study, v. II: source apportionment [final report]. Phoenix, AZ: Arizona Department of Environmental Quality; report no. 8931.6F1; Table 3-1.

Chow, J. C.; Watson, J. G.; Lowenthal, D. H.; Frazier, C. A.; Hinsvark, B. A.; Prichett, L. C.; Neuroth, G. R. (1992a) Wintertime PM_{10} and $PM_{2.5}$ chemical compositions and source contributions in Tucson, Arizona. In: Chow, J. C.; Ono, D. M., eds. PM_{10} standards and nontraditional particulate source controls, an A&WMA/EPA international specialty conference, v. I; January; Scottsdale, AZ. Pittsburgh, PA: Air & Waste Management Association; pp. 231-243. (A&WMA transactions series no. 22).

Chow, J. C.; Watson, J. G.; Lowenthal, D. H.; Solomon, P. A.; Magliano, K. L.; Ziman, S. D.; Richards, L. W. (1992b) PM10 source apportionment in California's San Joaquin Valley. Atmos. Environ. Part A 26: 3335-3354.

Chow, J. C.; Liu, C. S.; Cassmassi, J.; Watson, J. G.; Lu, Z.; Pritchett, L. C. (1992c) A neighborhood-scale study of PM_{10} source contributions in Rubidoux, California. Atmos. Environ. Part A 26: 693-706.

Chow, J. C.; Watson, J. G.; Houck, J. E.; Pritchett, L. C.; Rogers, C. F.; Frazier, C. A.; Egami, R. T.; Ball, B. M. (1994) A laboratory resuspension chamber to measure fugitive dust size distributions and chemical compositions. Atmos. Environ. 28: 3463-3481.

Cofer, W. R.; Levine, J. S.; Sebacher, D. I.; Winstead, E. L.; Riggan, P. J.; Brass, J. A.; Ambrosia, V. G. (1988) J. Geophys. Res. [Atmos.] 93: 5207-5212.

Cooper, J. A.; Watson, J. G., Jr. (1980) Receptor oriented methods of air particulate source apportionment. J. Air Pollut. Control Assoc. 30: 1116-1125.

Cooper, J. A.; Redline, D. C.; Sherman, J. R.; Valdovinos, L. M.; Pollard, W. L.; Scavone, L. C.; Badgett-West, C. (1987) PM_{10} source composition library for the South Coast Air Basin: volume I, source profile development documentation final report. El Monte, CA: South Coast Air Quality Management District; July 15.

Currie, L. D.; Gerlach, R. W.; Lewis, C. W.; Balfour, W. D.; Cooper, J. A.; Dattner, S. L.; De Cesar, R. T.; Gordon, G. E.; Heisler, S. L.; Hopke, P. K.; Shah, J. J.; Thurston, G. D.; Williamson, H. J. (1984) Interlaboratory comparison of source apportionment procedures: results for simulated data sets. Atmos. Environ. 18: 1517-1537.

Daisey, J. M.; Cheney, J. L.; Lioy, P. J. (1986) Profiles of organic particulate emissions from air pollution sources: status and needs for receptor source apportionment modeling. J. Air Pollut. Control Assoc. 36: 17-33.

Dasch, J. M. (1982) Particulate and gaseous emissions from wood-burning fireplaces. Environ. Sci. Technol. 16: 639-645.

Dattner, S. L.; Hopke, P. K. (1982) Receptor models applied to contemporary pollution problems: an introduction. In: Frederick, E. R., ed. A specialty conference on: receptor models applied to contemporary pollution problems; October; Danvers, MA. Pittsburgh, PA: Air Pollution Control Association; pp. 1-5. (APCA specialty conference proceedings SP-48).

Dentener, F. J.; Crutzen, P. J. (1994) A three-dimensional model of the global ammonia cycle. J. Atmos. Chem. 19: 331-369.

Dzubay, T. G.; Mamane, Y. (1989) Use of electron microscopy data in receptor models for PM-10. Atmos. Environ. 23: 467-476.

Dzubay, T. G.; Stevens, R. K.; Gordon, G. E.; Olmez, I.; Sheffield, A. E.; Courtney, W. J. (1988) A composite receptor method applied to Philadelphia aerosol. Environ. Sci. Technol. 22: 46-52.

Federal Register. (1977) Method 5 - determination of particulate emissions from stationary sources. F. R. (August 18) 42: 41776-41783.

Freeman, D. L.; Chow, J. C.; Egami, R. T.; Watson, J. G. (1989) A receptor and dispersion modeling software package. In: Watson, J. G., ed. Receptor models in air resources management: an international specialty conference; February 1988; San Francisco, CA. Pittsburgh, PA: Air & Waste Management Association; pp. 243-268. (APCA transactions series: no. 14).

Friedlander, S. K. (1973) Chemical element balances and identification of air pollution sources. Environ. Sci. Technol. 7: 235-240.

Fujita, E. M.; Croes, B. E.; Bennett, C. L.; Lawson, D. R.; Lurmann, F. W.; Main, H. H. (1992) Comparison of emission inventory and ambient concentration ratios of CO, NMOG, and NO_x in California's south coast air basin. J. Air Waste Manage. Assoc. 42: 264-276.

Gao, N.; Cheng, M.-D.; Hopke, P. K. (1993) Potential source contribution function analysis and source apportionment of sulfur species measured at Rubidoux, CA during the Southern California Air Quality Study, 1987. Anal. Chim. Acta 277: 369-380.

Gatz, D. F. (1995) A large silicon-aluminum aerosol plume in central Illinois: Saharan Desert dust? Atmos. Environ.: accepted.

Gebhart, K. A.; Lattimer, D. A.; Sisler, J. F. (1990) Empirical orthogonal function analysis of the particulate sulfate concentrations measured during WHITEX. In: Mathai, C. V., ed. Visibility and fine particles: an A&WMA/EPA international specialty conference; October 1989; Estes Park, CO. Pittsburgh, PA: Air & Waste Management Association; pp. 860-871. (A&WMA transactions series no. TR-17).

Geron, C. D.; Guenther, A. B.; Pierce, T. E. (1994) An improved model for estimating emissions of volatile organic compounds from forests in the eastern United States. J. Geophys. Res. [Atmos.] 99: 12,773-12,791.

Gillette, D. A.; Adams, J.; Endo, A.; Smith, D.; Kihl, R. (1980) Threshold velocities for input of soil particles into the air by desert soils. J. Geophys. Res. C: Oceans Atmos. 85: 5621-5630.

Gillette, D. A.; Adams, J.; Muhs, D. R.; Khil, R. (1982) Threshold friction velocities and rupture moduli for crusted desert soils for the input of soil particles into the air. J. Geophys. Res. B 87: 9003-9015.

Glover, D. M.; Hopke, P. K.; Vermette, S. J.; Landsberger, S.; D'Auben, D. R. (1991) Source apportionment with site specific source profiles. J. Air Waste Manage. Assoc. 41: 294-305.

Goklany, I. M.; Hoffnagle, G. F.; Brackbill, E. A. (1984) Acidic and total primary sulfates: development of emission factors for major stationary combustion sources. J. Air Pollut. Control Assoc. 34: 124-134.

Gordon, G. E. (1980) Receptor models. Environ. Sci. Technol. 14: 792-800.

Gordon, G. E. (1988) Receptor models. Environ. Sci. Technol. 22: 1132-1142.

Gray, H. A.; Landry, B.; Liu, C. S.; Henry, R. C.; Cooper, J. A.; Sherman, J. R. (1988) Receptor modeling for PM10 source apportionment in the South Coast Air Basin of California. In: Mathai, C. V.; Stonefield, D. H., eds. PM-10: implementation of standards, an APCA/EPA international specialty conference; February; San Francisco, CA. Pittsburgh, PA: Air Pollution Control Association; pp. 399-418. (APCA transactions series TR-13).

Grosjean, D.; Seinfeld, J. H. (1989) Parameterization of the formation potential of secondary organic aerosols. Atmos. Environ. 23: 1733-1747.

Haagen-Smit, A. J. (1952) Chemistry and physiology of Los Angeles smog. Ind. Eng. Chem. 44: 1342-1346.

Hall, F. F., Jr. (1981) Visibility reductions from soil dust in the western U.S. In: White, W. H.; Moore, D. J.; Lodge, J. P., Jr., eds. Plumes and visibility: measurements and model components: proceedings of the symposium; November 1980; Grand Canyon National Park, AZ. Atmos. Environ. 15: 1929-1933.

Hammerle, R. H.; Korniski, T. J.; Weir, J. E.; Chladek, E.; Glerczak, C. A.; Chase, R. E.; Hurley, R. G. (1992) Effect of mileage accumulation on particulate emissions from vehicles using gasoline with methylcyclopentadienyl manganese tricarbonyl. Presented at: International congress & exposition; February; Detroit, MI. Warrendale, PA: Society of Automotive Engineers; SAE technical paper no. 920731.

Hansen, A. D. A.; Rosen, H. (1990) Individual measurements of the emission factor of aerosol black carbon in automobile plumes. J. Air Waste Manage. Assoc. 40: 1654-1657.

Hatakeyama, S.; Izumi, K.; Fukuyama, T.; Akimoto, H. (1989) Reactions of ozone with α-pinene and β-pinene in air: yields of gaseous and particulate products. J. Geophys. Res. [Atmos.] 94: 13,013-13,024.

Hatakeyama, S.; Izumi, K.; Fukuyama, T.; Akimoto, H.; Washida, N. (1991) Reactions of OH with α-pinene and β-pinene in air: estimate of global CO production from the atmospheric oxidation of terpenes. J. Geophys. Res. [Atmos.] 96: 947-958.

Henry, R. C. (1991) Multivariate receptor models. In: Hopke, P. K., ed. Receptor modeling for air quality management. Amsterdam, The Netherlands: Elsevier; pp. 117-147.

Henry, R. C.; Hidy, G. M. (1979) Multivariate analysis of particulate sulfate and other air quality variables by principal components—part I: annual data from Los Angeles and New York. Atmos. Environ. 13: 1581-1596.

Henry, R. C.; Hidy, G. M. (1982) Multivariate analysis of particulate sulfate and other air quality variables by principal components—II: Salt Lake City, Utah and St. Louis, Missouri. Atmos. Environ. 16: 929-943.

Henry, R. C.; Kim, B. M. (1989) A factor analysis receptor model with explicit physical constraints. In: Watson, J. G., ed. Receptor models in air resources management: an international specialty conference; February 1988; San Francisco, CA. Pittsburgh, PA: Air & Waste Management Association; pp. 214-225. (APCA transactions series: no. 14).

Henry, R. C.; Wang, Y.-J.; Gebhart, K. A. (1990) The relationship between empirical orthogonal functions and sources of air pollution. Atmos. Environ. Part A 24: 503-509.

Hertel, O.; Christensen, J.; Hov, Ø, (1994) Modelling of the end products of the chemical decomposition of DMS in the marine boundary layer. Atmos. Environ. 28: 2431-2449.

Hildemann, L. M.; Markowski, G. R.; Jones, M. C.; Cass, G. R. (1991) Submicrometer aerosol mass distributions of emissions from boilers, fireplaces, automobiles, diesel trucks, and meat-cooking operations. Aerosol Sci. Technol. 14: 138-152.

Hildemann, L. M.; Cass, G. R.; Mazurek, M. A.; Simoneit, B. R. T. (1993) Mathematical modeling of urban organic aerosol: properties measured by high-resolution gas chromatography. Environ. Sci. Technol. 27: 2045-2055.

Hooker, C. L.; Westberg, H. H.; Sheppard, J. C. (1985) Determination of carbon balances for smog chamber terpene oxidation experiments using a ^{14}C tracer technique. J. Atmos. Chem. 2: 307-320.

Hopke, P. K. (1985) Receptor modeling in environmental chemistry. New York, NY: John Wiley & Sons.

Hopke, P. K., ed. (1991) Receptor modeling for air quality management. New York, NY: Elsevier Science Publishing Company, Inc. (Vandeginste, B. G. M.; Kvalheim, O. M., eds. Data handling in science and technology: v. 7).

Hopke, P. K.; Lamb, R. E.; Natusch, D. F. S. (1980) Multielemental characterization of urban roadway dust. Environ. Sci. Technol. 14: 164-172.

Hopke, P. K.; Wlaschin, W.; Landsberger, S.; Sweet, C.; Vermette, S. J. (1988) The source apportionment of PM10 in south Chicago. In: Mathai, C. V.; Stonefield, D. H., eds. PM-10: implementation of standards, an APCA/EPA international specialty conference; February; San Francisco, CA. Pittsburgh, PA: Air Pollution Control Association; pp. 484-494. (APCA transactions series TR-13).

Houck, J. E.; Chow, J. C.; Watson, J. G.; Simons, C. A.; Pritchett, L. C.; Goulet, J. M.; Frazier, C. A. (1989) Determination of particle size distribution and chemical composition of particulate matter from selected sources in California: volume I and executive summary (final report). Sacramento, CA: California Air Resources Board.

Houck, J. E.; Goulet, J. M.; Chow, J. C.; Watson, J. G.; Pritchett, L. C. (1990) Chemical characterization of emission sources contributing to light extinction. In: Mathai, C. V., ed. Visibility and fine particles: an A&WMA/EPA international specialty conference; October 1989; Estes Park, CO. Pittsburgh, PA: Air & Waste Management Association; pp. 437-446. (A&WMA transactions series no. TR-17).

Houck, J. E.; Rau, J. A.; Body, S.; Chow, J. C. (1992) Source apportionment: Pocatello, Idaho PM_{10} nonattainment area. In: Chow, J. C.; Ono, D. M., eds. PM_{10} standards and nontraditional particulate source controls, an A&WMA/EPA international specialty conference, v. I; January; Scottsdale, AZ. Pittsburgh, PA: Air & Waste Management Association; pp. 219-230. (A&WMA transactions series no. 22).

Huang, X.; Olmez, I.; Aras, N. K.; Gordon, G. E. (1994) Emissions of trace elements from motor vehicles: potential marker elements and source composition profile. Atmos. Environ. 28: 1385-1391.

Ingalls, M. N. (1989) On-road vehicle emission factors from measurements in a Los Angeles area tunnel. Presented at: 82nd annual meeting & exhibition of the Air and Waste Management Association; June; Anaheim, CA. Pittsburgh, PA: Air and Waste Management Association; paper no. 89-137.3.

Intergovernmental Panel on Climate Change. (1995) Climate change 1995: the science of climate change: draft summary for policymakers (SPM) of the draft contribution of Working Group I to the IPCC second assessment report. Geneva, Switzerland: World Meteorological Association, IPCC Secretariat; November.

Izumi, K.; Fukuyama, T. (1990) Photochemical aerosol formation from aromatic hydrocarbons in the presence of NO_x. Atmos. Environ. Part A 24: 1433-1441.

Javitz, H. S.; Watson, J. G.; Guertin, J. P.; Mueller, P. K. (1988) Results of a receptor modeling feasibility study. JAPCA 38: 661-667.

Johnson, J. H. (1988) Automotive emissions. In: Watson, A. Y.; Bates, R. R.; Kennedy, D., eds. Air pollution, the automobile, and public health. Washington, D.C.: National Academy Press; pp. 39-76.

Johnson, B.; Cooke, R. C. (1979) Bubble populations and spectra in coastal waters: a photographic approach. J. Geophys. Res. C: Oceans Atmos. 84: 3763-3766.

Kao, A. S.; Friedlander, S. K. (1995) Frequency distributions of PM_{10} chemical components and their sources. Environ. Sci. Technol. 29: 19-28.

Khalil, M. A. K.; Rasmussen, R. A. (1992) Forest hydrocarbon emissions: relationships between fluxes and ambient concentrations. J. Air Waste Manage. Assoc. 42: 810-813.

Kim, B. M.; Zeldin, M. D.; Liu, C. S. (1992) Source apportionment study for state implementation plan development in the Coachella Valley. In: Chow, J. C.; Ono, D. M., eds. PM10 standards and nontraditional particulate source controls, an A&WMA/EPA international specialty conference, v. II; January; Scottsdale, AZ. Pittsburgh, PA: Air & Waste Management Association; pp. 979-991. (A&WMA transactions series no. 22).

Kleinman, M. T.; Pasternack, B. S.; Eisenbud, M.; Kneip, T. J. (1980) Identifying and estimating the relative importance of sources of airborne particulates. Environ. Sci. Technol. 14: 62-65.

Koutrakis, P.; Spengler, J. D. (1987) Source apportionment of ambient particles in Steubenville, OH using specific rotation factor analysis. Atmos. Environ. 21: 1511-1519.

Lang, J. M.; Snow, L.; Carlson, R.; Black, F.; Zweidinger, R.; Tejada, S. (1982) Characterization of particulate emissions from in-use gasoline-fueled motor vehicles. Warrendale, PA: Society of Automotive Engineers; SAE technical paper no. 811186.

Lewis, C. W.; Stevens, R. K. (1987) Hybrid receptor models. In: Johnson, R. W.; Gordon, G. E.; Calkins, W.; Elzerman, A. Z., eds. The chemistry of acid rain: sources and atmospheric processes; developed from a symposium sponsored by the Divisions of Petroleum Chemistry, Inc., Nuclear Chemistry and Technology, Environmental Chemistry, and Fuel Chemistry at the 191st meeting of the American Chemical Society; April 1986; New York, NY. Washington, DC: American Chemical Society; pp. 58-65. (ACS symposium series: 349).

Lewis, C. W.; Baumgardner, R. E.; Stevens, R. K.; Claxton, L. D.; Lewtas, J. (1988) Contribution of woodsmoke and motor vehicle emissions to ambient aerosol mutagenicity. Environ. Sci. Technol. 22: 968-971.

Liousse, C.; Penner, J. E.; Chuang, C.; Walton, J. J.; Eddleman, H.; Cachier, H. (1996) A global three-dimensional model study of carbonaceous aerosols. J. Geophys. Res. [Atmos.] 101: in press.

Lioy, P. J.; Mallon, R. P.; Lippmann, M.; Kneip, T. J.; Samson, P. J. (1982) Factors affecting the variability of summertime sulfate in a rural area using principal component analysis. J. Air Pollut. Control Assoc. 32: 1043-1047.

Lowenthal, D. H.; Zielinska, B.; Chow, J. C.; Watson, J. G.; Gautam, M.; Ferguson, D. H.; Neuroth, G. R.; Stevens, K. D. (1994) Characterization of heavy-duty diesel vehicle emissions. Atmos. Environ. 28: 731-743.

Macias, E. S.; Hopke, P. K., eds. (1981) Atmospheric aerosol: source/air quality relationships; based on a symposium jointly sponsored by the Divisions of Nuclear Chemistry and Technology at the 180th national meeting of the American Chemical Society; August 1980; Las Vegas, NV. Washington, DC: American Chemical Society. (Comstock, M. J., ed. ACS symposium series: 167).

Magliano, K. L. (1988) Level 1 PM_{10} assessment in a California air basin. In: Mathai, C. V.; Stonefield, D. H., eds. PM-10: implementation of standards, an APCA/EPA international specialty conference; February; San Francisco, CA. Pittsburgh, PA: Air Pollution Control Association; pp. 508-517. (APCA transactions series TR-13).

Marticorena, B.; Bergametti, G. (1995) Modeling the atmospheric dust cycle: I. design of a soil-derived dust emission scheme. J. Geophys. Res. [Atmos.] 100: 16,415-16,430.

Mason, B. (1966) Principles of geochemistry. 3rd ed. New York, NY: John Wiley & Sons, Inc.

Matthews, E. (1994) Nitrogenous fertilizers: global distribution of consumption and associated emissions of nitrous oxide and ammonia. Global Biogeochem. Cycles 8: 411-439.

Matthias-Maser, S.; Jaenicke, R. (1994) Examination of atmospheric bioaerosol particles with radii > 0.2 μm. J. Aerosol Sci. 25: 1605-1613.

Mazurek, M. A.; Cofer, W. R., III; Levine, J. S. (1991) Carbonaceous aerosols from prescribed burning of a boreal forest ecosystem. In: Levine, J. S., ed. Global biomass burning: atmospheric, climatic, and biospheric implications. Cambridge, MA: MIT Press; pp. 258-263.

Mylonas, D. T.; Allen, D. T.; Ehrman, S. H.; Pratsinis, S. E. (1991) The sources and size distributions of organonitrates in Los Angeles aerosol. Atmos. Environ. Part A 25: 2855-2861.

NEA. (1990a) Enhancement of the south coast air basin source profile library for chemical mass balance receptor model applications: volume I, final report. Beaverton, OR: NEA.

NEA. (1990b) Enhancement of the south coast air basin source profile library for chemical mass balance receptor model applications: volume II, source profile library supplement. Beverton, OR: NEA.

NEA. (1990c) Enhancement of the south coast air basin source profile library for chemical mass balance receptor model applications: volume III, appendices. Beverton, OR: NEA.

National Research Council. (1982) Diesel cars: benefits, risks and public policy: final report of the Diesel Impacts Study Committee. Washington, DC: National Academy Press.

Nriagu, J. O. (1989) A global assessment of natural sources of atmospheric trace metals. Nature (London) 338: 47-49.

Nriagu, J. O.; Pacyna, J. M. (1988) Quantitative assessment of worldwide contamination of air, water and soils by trace metals. Nature (London) 333: 134-139.

O'Connor, B. H.; Kerrigan, G. C.; Hinchliffe, P. (1977) The loss of Br from thin-film samples during X-ray fluorescence analysis. X-Ray Spectrom. 6: 83-85.

Olmez, I.; Sheffield, A. E.; Gordon, G. E.; Houck, J. E.; Pritchett, L. C.; Cooper, J. A.; Dzubay, T. G.; Bennett, R. L. (1988) Compositions of particles from selected sources in Philadelphia for receptor modeling applications. JAPCA 38: 1392-1402.

Ott, S.-T.; Ott, A.; Martin, D. W.; Young, J. A. (1991) Analysis of a trans-Atlantic saharan dust outbreak based on satellite and GATE data. Mon. Weather Rev. 119: 1832-1850.

Pace, T. G., ed. (1986) Receptor methods for source apportionment: real world issues and applications, an APCA international specialty conference; March 1985; Williamsburg, VA. Pittsburgh, PA: Air Pollution Control Association. (APCA transactions no. TR-5).

Pandis, S. N.; Paulson, S. E.; Seinfeld, J. H.; Flagan, R. C. (1991) Aerosol formation in the photooxidation of isoprene and β-pinene. Atmos. Environ. Part A 25: 997-1008.

Pandis, S. N.; Harley, R. A.; Cass, G. R.; Seinfeld, J. H. (1992) Secondary organic aerosol formation and transport. Atmos. Environ. Part A 26: 2269-2282.

Peterson, J. T. (1970) Distribution of sulfur dioxide over metropolitan St. Louis, as described by empirical eigenvectors, and its relation to meteorological parameters. Atmos. Environ. 4: 501-518.

Pickle, T.; Allen, D. T.; Pratsinis, S. E. (1990) The sources and size distributions of aliphatic and carbonyl carbon in Los Angeles aerosol. Atmos. Environ. Part A 24: 2221-2228.

Pierson, W. R.; Brachaczek, W. W. (1974) Airborne particulate debris from rubber tires. Presented at: Joint meeting of the American Chemical Society, Rubber Division, and the Chemical Institute of Canada, Macromolecular Science Division; May; Toronto, Ontario, Canada. Rubber Chem. Technol. 47: 1275-1299.

Pierson, W. R.; Brachaczek, W. W. (1976) Particulate matter associated with vehicles on the road. Presented at: SAE automotive engineering congress and exposition; February; Detroit, MI. Warrendale, PA: Society of Automotive Engineers; SAE technical paper no. 760039.

Pierson, W. R.; Brachaczek, W. W. (1983) Particulate matter associated with vehicles on the road. II. Aerosol Sci. Technol. 2: 1-40.

Pierson, W. R.; Gertler, A. W.; Bradow, R. L. (1990) Comparison of the SCAQS tunnel study with other on-road vehicle emission data. J. Air Waste Manage. Assoc. 40: 1495-1504.

Pinto, J. P.; Pleasant, M.; Kellogg, R.; Torok, Sz.; Stiles, D.; Willis, R. D.; Koutrakis, P.; Allen, G. A. (1995) Chemical characterization of the ambient aerosol in Philadelphia. Presented at: Particulate matter: health and regulatory issues: an A&WMA international specialty conference; April; Pittsburgh, PA. Pittsburgh, PA: Air & Waste Management Association; submitted abstract.

Placet, M.; Battye, R. E.; Fehsenfeld, F. C.; Bassett, G. W. (1991) Emissions involved in acidic deposition processes. In: Irving, P. M., ed. Acidic depostion: state of science and technology, volume I: emissions, atmospheric processes, and deposition. Washington, DC: The U.S. National Acid Precipitation Assessment Program. (State of science and technology report no. 1).

Prospero, J. M. (1995) The atmospheric transport of particles to the ocean. In: Ittekkot, V.; Honjo, S.; Depetris, P. J., eds. SCOPE report: particle flux in the ocean. New York, NY: John Wiley & Sons, Ltd.; in press.

Prospero, J. M.; Nees, R. T.; Uematsu, M. (1987) Deposition rate of particulate and dissolved aluminum derived from Saharan dust in precipitation at Miami, Florida. J. Geophys. Res. [Atmos.] 92: 14,723-14,731.

Prospero, J. M.; Savoie, D. L.; Arimoto, R.; Huang, F. (1993) Long-term trends in African mineral dust concentrations over the western North Atlantic: relationship to North African rainfall. EOS Trans. Am. Geophys. Union 74: 146.

Radke, L. F.; Hegg, D. A.; Hobbs, P. V.; Nance, J. D.; Lyons, J. H.; Laursen, K. K.; Weiss, R. E.; Riggan, P. J.; Ward, D. E. (1991) Particulate and trace gas emissions from large biomass fires in North America. In: Levine, J. S., ed. Global biomass burning: atmospheric, climatic, and biospheric implications. Cambridge, MA: MIT Press; pp. 209-224.

Radwan, C. (1995) Particulate emissions trends predicted in the PART5 model. In: Particulate matter: health and regulatory issues: proceedings of an international specialty conference; April; Pittsburgh, PA. Pittsburgh, PA: Air & Waste Management Association; pp. 599-607. (A&WMA publication VIP-49).

Rasmussen, R. A.; Went, F. W. (1965) Volatile organic material of plant origin in the atmosphere. Proc. Natl. Acad. Sci. U. S. A. 53: 215-220.

Reeser, W. K.; Zimmer, R. A.; Cummins, P.; Briggs, K. R. (1992) An episodic PM_{10} emissions inventory for Denver, Colorado. In: Chow, J. C.; Ono, D. M., eds. PM_{10} standards and nontraditional particulate source controls, an A&WMA/EPA international specialty conference, v. I; January; Scottsdale, AZ. Pittsburgh, PA: Air & Waste Management Association; pp. 131-145. (A&WMA transactions series no. 22).

Rogge, W. F.; Hildemann, L. M.; Mazurek, M. A.; Cass, G. R.; Simoneit, B. R. T. (1991) Sources of fine organic aerosol. 1. Charbroilers and meat cooking operations. Environ. Sci. Technol. 25: 1112-1125.

Rogge, W. F.; Hildemann, L. M.; Mazurek, M. A.; Cass, G. R.; Simoneit, B. R. T. (1993a) Sources of fine organic aerosol. 2. Noncatalyst and catalyst-equipped automobiles and heavy-duty diesel trucks. Environ. Sci. Technol. 27: 636-651.

Rogge, W. F.; Hildemann, L. M.; Mazurek, M. A.; Cass, G. R.; Simoneit, B. R. T. (1993b) Sources of fine organic aerosol. 5. Natural gas home appliances. Environ. Sci. Technol. 27: 2736-2744.

Rogge, W. F.; Hildemann, L. M.; Mazurek, M. A.; Cass, G. R.; Simoneit, B. R. T. (1993c) Sources of fine organic aerosol. 4. Particulate abrasion products from leaf surfaces of urban plants. Environ. Sci. Technol. 27: 2700-2711.

Rogge, W. F.; Hildemann, L. M.; Mazurek, M. A.; Cass, G. R.; Simoneit, B. R. T. (1993d) Sources of fine organic aerosol. 3. Road dust, tire debris, and organometallic brake lining dust: roads as sources and sinks. Environ. Sci. Technol. 27: 1892-1904.

Rogge, W. F.; Mazurek, M. A.; Hildemann, L. M.; Cass, G. R.; Simoneit, B. R. T. (1993e) Quantification of urban organic aerosols at a molecular level: identification, abundance and seasonal variation. Atmos. Environ. Part A 27: 1309-1330.

Ryan, W. M.; Badgett-West, C. R.; Holtz, D. R.; Peters, T. A.; Cooper, J. A.; Ono, D. (1988) Reconciliation of receptor and dispersion modeling impacts of PM_{10} in Hayden, Arizona. In: Mathai, C. V.; Stonefield, D. H., eds. PM-10: implementation of standards, an APCA/EPA international specialty conference; February; San Francisco, CA. Pittsburgh, PA: Air Pollution Control Association; pp. 419-429. (APCA transactions series TR-13).

Savoie, D. L.; Prospero, J. M. (1982) Particle size distribution of nitrate and sulfate in the marine atmosphere. Geophys. Res. Lett. 9: 1207-1210.

Shao, Y.; Raupach, M. R.; Findlater, P. A. (1993) Effect of saltation bombardment on the entrainment of dust by wind. J. Geophys. Res. [Atmos.] 98: 12,719-12,726.

Skidmore, L. W.; Chow, J. C.; Tucker, T. T. (1992) PM_{10} air quality assessment for the Jefferson County, Ohio air quality control region. In: Chow, J. C.; Ono, D. M., eds. PM_{10} standards and nontraditional particulate source controls, an A&WMA/EPA international specialty conference, v. II; January; Scottsdale, AZ. Pittsburgh, PA: Air and Waste Management Association; pp. 1016-1031. (A&WMA transactions series no. 22).

Snow, J. T.; McClelland, T. M. (1990) Dust devils at White Sands Missile Range, New Mexico: 1. temporal and spatial distributions. J. Geophys. Res. [Atmos.] 95: 13,707-13,721.

South Coast Air Quality Management District. (1994) State implementation plan for PM10 in the Coechella Valley: 1994 "BACM" revision. Diamond Bar, CA: South Coast Air Quality Management District.

Spendlove, J. C. (1974) Industrial, agricultural, and municipal microbial aerosol problems. In: Current problems in aerobiology: proceedings of the thirtieth general meeting of the Society for Industrial Microbiology; August 1973; Evanston, IL. Dev. Ind. Microbiol. 15: 20-27.

Stevens, R. K.; Pace, T. G. (1984) Overview of the mathematical and empirical receptor models workshop (Quail Roost II). Atmos. Environ. 18: 1499-1506.

Stevenson, H. J. R.; Sanderson, D. E.; Altshuller, A. P. (1965) Formation of photochemical aerosols. Int. J. Air Water Pollut. 9: 367-375.

Susott, R. A.; Ward, D. E.; Babbitt, R. E.; Latham, D. J. (1991) The measurement of trace emissions and combustion characteristics for a mass fire. In: Levine, J. S., ed. Global biomass burning: atmospheric, climatic, and biospheric implications. Cambridge, MA: MIT Press; pp, 245-257.

Svasek, J. N.; Terwindt, J. H. J. (1974) Measurements of sand transport by wind on a natural beach. Sedimentology 21: 311-322.

Szkarlat, A. C.; Japar, S. M. (1983) Optical and chemical properties of particle emissions from on-road vehicles. J. Air Pollut. Control Assoc. 33: 592-597.

Thanukos, L. C.; Miller, T.; Mathai, C. V.; Reinholt, D.; Bennett, J. (1992) Intercomparison of PM10 samplers and source apportionment of ambient PM10 concentrations at Rillito, Arizona. In: Chow, J. C.; Ono, D. M., eds. PM_{10} standards and nontraditional particulate source controls, an A&WMA/EPA international specialty conference, v. I; January; Scottsdale, AZ. Pittsburgh, PA: Air & Waste Management Association; pp. 244-261. (A&WMA transactions series no. 22).

Truex, T. J.; Pierson, W. R.; McKee, D. E. (1980) Sulfate in diesel exhaust. Environ. Sci. Technol. 14: 1118-1121.

Turekian, K. K. (1971) Elements, geochemical distribution of. In: Encyclopedia of science and technlogy, v. 4. New York, NY: McGraw-Hill Book Company; pp. 627-630.

Turpin, B. J.; Huntzicker, J. J. (1991) Secondary formation of organic aerosol in the Los Angeles basin: a descriptive analysis of organic and elemental carbon concentrations. Atmos. Environ. Part A 25: 207-215.

Turpin, B. J.; Huntzicker, J. J.; Larson, S. M.; Cass, G. R. (1991) Los Angeles summer midday particulate carbon: primary and secondary aerosol. Environ. Sci. Technol. 25: 1788-1793.

U.S. Environmental Protection Agency. (1989) Procedures for estimating and applying rule effectiveness in post-1987 base year emission inventories for ozone and carbon monoxide state implementation plans. Research Triangle Park, NC: Office of Air Quality Planning and Standards.

U.S. Environmental Protection Agency. (1993) Motor vehicle-related air toxics study. Ann Arbor, MI: Office of Mobile Sources; EPA report no. EPA/420/R-93/005. Available from: NTIS, Springfield, VA; PB93-182590/XAB.

U.S. Environmental Protection Agency. (1994) National air quality and emissions trends report, 1993. Research Triangle Park, NC: Office of Air Quality Planning and Standards; EPA report no. EPA 454/R-94-026.

U.S. Environmental Protection Agency. (1995a) Compilation of air pollutant emission factors, volume I: stationary point and area sources. 5th ed. Research Triangle Park, NC: Office of Air Quality Planning and Standards; report no. AP-42.

U.S. Environmental Protection Agency. (1995b) National air pollutant emission trends, 1900 - 1994. Research Triangle Park, NC: Office of Air Quality Planning and Standards; report no. EPA-454/R-95-011.

Van Espen, P. (1984) A program for the processing of analytical data (DPP). Anal. Chim. Acta 165: 31-49.

Vermette, S. J.; Williams, A. L.; Landsberger, S. (1992) PM_{10} source apportionment using local surface dust profiles: examples from Chicago. In: Chow, J. C.; Ono, D. M., eds. PM_{10} standards and nontraditional particulate source controls, an A&WMA/EPA international specialty conference, v. I; January; Scottsdale, AZ. Pittsburgh, PA: Air & Waste Management Association; pp. 262-278. (A&WMA transactions series no. 22).

Vinogradov, A. P. (1959) The geochemistry of rare and dispersed chemical elements in soils. 2nd ed. New York, NY: Consultants Bureau, Inc.

Walker, B. L.; Cooper, C. D. (1992) Air pollution emission factors for medical waste incinerators. J. Air Waste Manage. Assoc. 42: 784-791.

Warneck, P. (1988) Chemistry of the natural atmosphere. New York, NY: Academic Press, Inc.

Watson, J. G.; Chow, J. C. (1994) Clear sky visibility as a challenge for society. Annu. Rev. Energy Environ. 19: 241-266.

Watson, J. G.; Henry, R. C.; Cooper, J. A.; Macias, E. S. (1981) The state of the art of receptor models relating ambient suspended particulate matter to sources. In: Macias, E. S.; Hopke, P. K., eds. Atmospheric aerosol: source/air quality relationships; based on a symposium jointly sponsored by the Divisions of Nuclear Chemistry and Technology and Environmental Chemistry at the 180th national meeting of the American Chemical Society; August 1980; Las Vegas, NV. Washington, DC: American Chemical Society; pp. 89-106. (Comstock, M. J., ed. ACS symposium series: 167).

Watson, J. G.; Chow, J. C.; Mathai, C. V. (1989) Receptor models in air resources management: a summary of the APCA international specialty conference. JAPCA 39: 419-426.

Watson, J. G.; Chow, J. C.; Pritchett, L. C.; Houck, J. A.; Burns, S.; Ragazzi, R. A. (1990a) Composite source profiles for particulate motor vehicle exhaust source apportionment in Denver, CO. In: Mathai, C. V., ed. Visibility and fine particles: an A&WMA/EPA international specialty conference; October 1989; Estes Park, CO. Pittsburgh, PA: Air & Waste Management Association; pp. 422-436. (A&WMA transactions series no. TR-17).

Watson, J. G.; Chow, J. C.; Pritchett, L. C.; Houck, J. A.; Ragazzi, R. A.; Burns, S. (1990b) Chemical source profiles for particulate motor vehicle exhaust under cold and high altitude operating conditions. Sci. Total Environ. 93: 183-190.

Watson, J. G.; Chow, J. C.; Pace, T. G. (1991) Chemical mass balance. In: Hopke, P. K., ed. Data handling in science and technology: v. 7, receptor modeling for air quality management. New York, NY: Elsevier Press; pp. 83-116.

Watson, J. G.; Chow, J. C.; Lowenthal, L. C.; Pritchett, C. A.; Frazier, C. A.; Neuroth, G. R.; Robbins, R. (1994a) Differences in the carbon compostion of source profiles for diesel- and gasoline-powered vehicles. Atmos. Environ. 28: 2493-2505.

Watson, J. G.; Chow, J. C.; Blumenthal, D. L.; Lurmann, F. W.; Hackney, R. J.; Magliano, K. L.; Pederson, J. R.; Neff, W. D.; Roth, P. M.; Solomon, P. A.; Thuillier, R. H.; Ziman, S. D. (1994b) Planning for data analysis. In: Solomon, P. A.; Silver, T. A., eds. Planning and managing regional air quality modeling and measurement studies: a perspective through the San Joaquin Valley air quality study and AUSPEX. Boca Raton, FL: Lewis Publishers; pp. 335-349.

Went, F. W. (1960) Organic matter in the atmosphere, and its possible relation to petroleum formation. Proc. Natl. Acad. Sci. U. S. A. 46: 212-221.

Wilson, T. R. S. (1975) Salinity and major elements of sea water. In: Riley, J. P.; Skirrow, G., eds. Chemical oceanography. 2nd ed. London, United Kingdom: Academic Press; pp. 365-413.

Wilson, W. E.; Schwartz, W. E.; Kinzer, G. W. (1972) Haze formation—its nature and origin. New York, NY: Coordinating Research Council; report no. CRC-APRAC-CAPA-6-68-3. Available from: NTIS, Springfield, VA; PB-212609.

Wolff, G. T.; Korsog, P. E. (1985) Estimates of the contributions of sources to inhalable particulate concentrations in Detroit. Atmos. Environ. 19: 1399-1409.

Wolff, G. T.; Countess, R. J.; Groblicki, P. J.; Ferman, M. A.; Cadle, S. H.; Muhlbaier, J. L. (1981) Visibility-reducing species in the Denver "brown cloud"—II. sources and temporal patterns. Atmos. Environ. 15: 2485-2502.

Wolff, G. T.; Korsog, P. E.; Kelly, N. A.; Ferman, M. A. (1985a) Relationships between fine particulate species, gaseous pollutants and meteorological parameters in Detroit. Atmos. Environ. 19: 1341-1349.

Wolff, G. T.; Korsog, P. E.; Stroup, D. P.; Ruthkosky, M. S.; Morrissey, M. L. (1985b) The influence of local and regional sources on the concentration of inhalable particulate matter in southeastern Michigan. Atmos. Environ. 19: 305-313.

Wu, J. (1979) Sea spray in the atmospheric surface layer: review and analysis of laboratory and oceanic results. J. Geophys. Res. [Atmos.] 84: 1683-1704.

Xie, Y.; Hopke, P. K.; Casuccio, G.; Henderson, B. (1994a) Use of multiple fractal dimensions to quantify airborne particle shape. Aerosol Sci. Technol. 20: 161-168.

Xie, Y.; Hopke, P. K.; Casuccio, G.; Henderson, B. (1994b) Use of chain code histogram method to quantify airborne particle shapes. Aerosol Sci. Technol. 21: 210-218.

Zeng, Y.; Hopke, P. K. (1989) Three-mode factor analysis: a new multivariate method for analyzing spatial and temporal composition variation. In: Watson, J. G., ed. Receptor models in air resources management: an international specialty conference; February 1988; San Francisco, CA. Pittsburgh, PA: Air & Waste Management Association; pp. 173-189. (APCA transactions series: no. 14).

Zhang, S.-H.; Shaw, M.; Seinfeld, J. H.; Flagan, R. C. (1992) Photochemical aerosol formation from α-pinene and β-pinene. J. Geophys. Res. [Atmos.] 97: 20,717-20,729.

6. ENVIRONMENTAL CONCENTRATIONS

6.1 BACKGROUND, PURPOSE, AND SCOPE

This chapter summarizes the concentrations of particulate matter over the United States, including the spatial, temporal, size and chemical aspects. The information needs for assessing the major aerosol effects of concern are summarized in Table 6-1. The general approach followed in preparing this chapter was to organize, evaluate, and summarize the existing large scale aerosol data sets over the United States. Emphasis was placed on complete national coverage as well as the fusion and reconciliation of multiple data sets.

Space is the main organizing dimension used to structure this chapter. Aerosol concentration data are presented on global, continental, national, regional, and sub-regional/urban scales. Within each spatial domain, the spatial-temporal structure, size, and chemical composition are presented. An overview of the pattern analysis methods is given in the remainder of Section 6.1. The presentation of aerosol patterns begins from the global and continental perspective (Section 6.2). Next, nationwide aerosol patterns (Section 6.3) derived from nonurban and urban PM_{10} and $PM_{2.5}$ monitoring networks are examined. Section 6.3 also includes a discussion of various measures of background $PM_{2.5}$ and PM_{10}. In Section 6.4 the aerosol characteristics over seven subregions of the conterminous United States are examined in more detail. The 10-year trends, seasonal patterns, relationships between $PM_{2.5}$ and PM_{10}, and fine particle chemical composition are examined for each region. Section 6.5 focuses further on the subregional and urban-scale aerosol pattern over representative areas of the United States. Section 6.6 presents more detailed information on the chemical composition of the aerosol from a number of intensive field studies. Section 6.7 deals with measurements of fine particle acidity. Section 6.8 focuses on the concentration of ultrafine particles and Section 6.9 on the chemical composition of ultrafine particles. Section 6.10 examines trends and relationships for $PM_{2.5}$, $PM_{(10-2.5)}$, and PM_{10} in data bases having long term data on both components.

Aerosol concentration data for the United States have been reported by many aerosol researchers over the past decade. This chapter draws heavily on the contribution, of research

groups that have produced data, reports, and analyses of nonurban data. However, their maps, charts, and computations have been re-done for consistency with urban data reports.

6.1.1 Dimensionality and Structuring of the Aerosol Data Space

Aerosol concentration patterns contain endless detail and complexity in space, time, size, and chemical composition. Aerosol samples from the conterminous United States reveal the coexistence of sulfates, hydrogen ions, ammonium, organic carbon (OC), nitrates, elemental carbon (EC [soot]), soil dust, sea salt, and trace metals. This chemically rich aerosol mixture arises from the multiplicity of contributing aerosol sources, each having a unique chemical mixture for the primary aerosol at the time of emission. The primary aerosol chemistry is further enriched by the addition of species during atmospheric chemical processes. Finally, the immensely effective mixing ability of the lower troposphere stirs these primary and secondary particles into a mixed batch with varying degrees of homogeneity, depending on location and time.

A major consideration in structuring the aerosol pattern analysis is that it has to be consistent with the physical and chemical processes that determine the concentrations of the aerosol. The concentration of particulate matter (C), at any given location and time is determined by the combined interaction of emissions (E), dilution (D), and chemical transformation and removal processes (T),expressed as:

$$C = f(D,T,E)$$

Dilution, transformation/removal, and emissions are generic operators and can, in principle, be determined from suitable measurements and models. However, for consideration of aerosol pattern analysis it is sufficient to recognize and separate these three major causal factors influencing the aerosol concentration pattern.

It is convenient to categorize the highly variable aerosol signal along the following major dimensions: space, time, size and chemical composition. The dependence of concentration on space and time is common to all pollutants. However, both the distribution with respect to particle size as well as the chemical distribution within a given size range constitute unique

dimensions of particulate matter that are not present for other pollutants. The concentrations of single-compound gaseous pollutants can be fully characterized by their spatial and temporal pattern. This classification by dimensions is consistent with the size-chemical composition distribution function introduced by Friedlander (1977). It could be said that particulate matter is a composite of hundreds of different substances exhibiting a high degree of spatial and temporal variability.

6.1.2 Spatial Pattern and Scales

The spatial dimension covers the geographic scale and pattern of aerosols. Based on consideration of emissions, meteorology, and political boundaries, the spatial dimension can be broken into global, national, regional-synoptic, meso, urban, and local scales. Some of the characteristics of these spatial scales are illustrated in Table 6-1.

TABLE 6-1. SPATIAL REGIONS AND SCALES

Global	National	Regional	Meso	Urban	Local
Continent	Country	Multi-state	State	County	City center
10,000 - 50,000 km	5,000 - 10,000 km	1,000 - 5,000 km	100 - 1,000 km	10 - 100 km	1 - 10 km

6.1.3 Temporal Pattern and Scales

The time dimension of aerosols extends over at least six different scales (Figure 6-1). A significant, unique feature of the temporal domain is the existence of periodicities. The secular time scale extends over several decades or centuries. Given climatic and chemical stability of the atmosphere the main causes of secular concentration trends are changes in anthropogenic emissions. Emissions, atmospheric dilution, as well as chemical/removal processes, can be influenced by the seasonal cycle. The synoptic scale covers the duration of

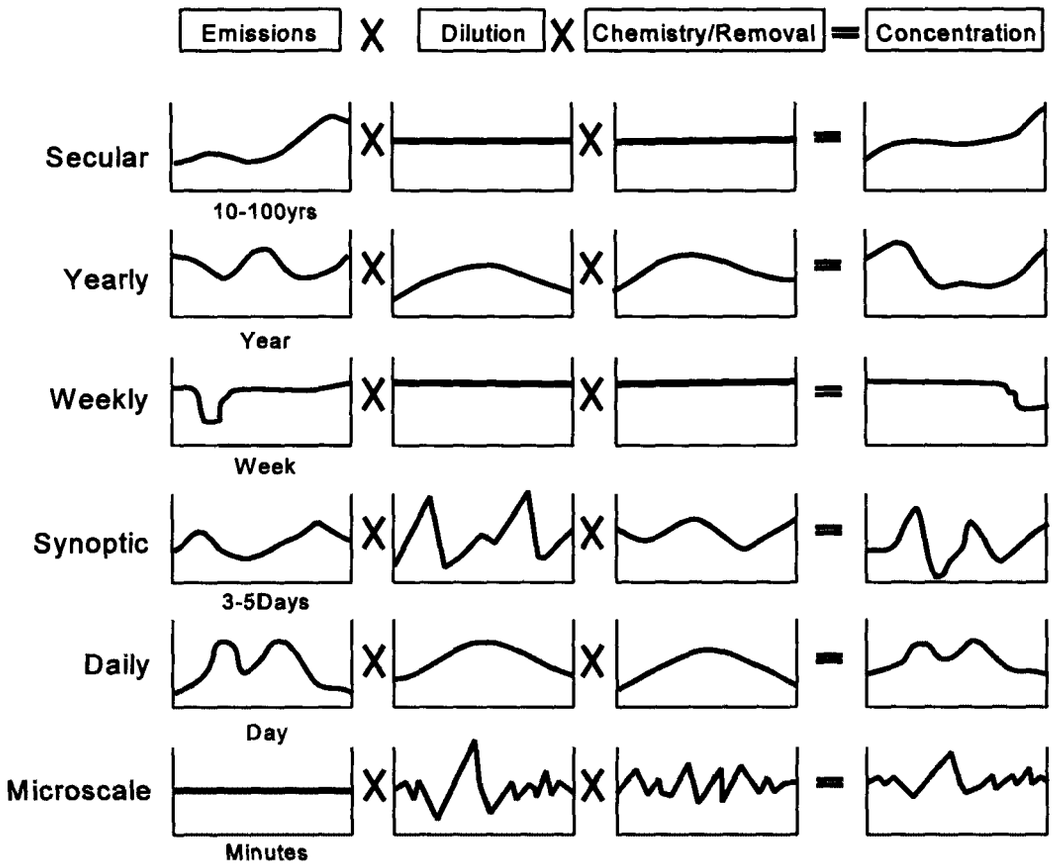

Figure 6-1. Time scales for particle emissions.

synoptic meteorological events (3-5 days). Its role is primarily reflected in dilution and chemical/removal processes. The daily cycle strongly influences the emissions, dilution, and chemical/removal processes. Microscale defines variation of the order of an hour caused by short-term atmospheric phenomena. In the analysis that follows we will emphasize secular trends and yearly cycles, with some consideration of daily aerosol pattern. The microscale patterns will be largely ignored.

6.1.4 Space-Time Relationships

The spatial and time scales of aerosol pattern are linked by the atmospheric residence time of particles. Short residence times restrict the aerosol to a short transport distance from a source, causing strong spatial and temporal gradients. Longer residence times yield more

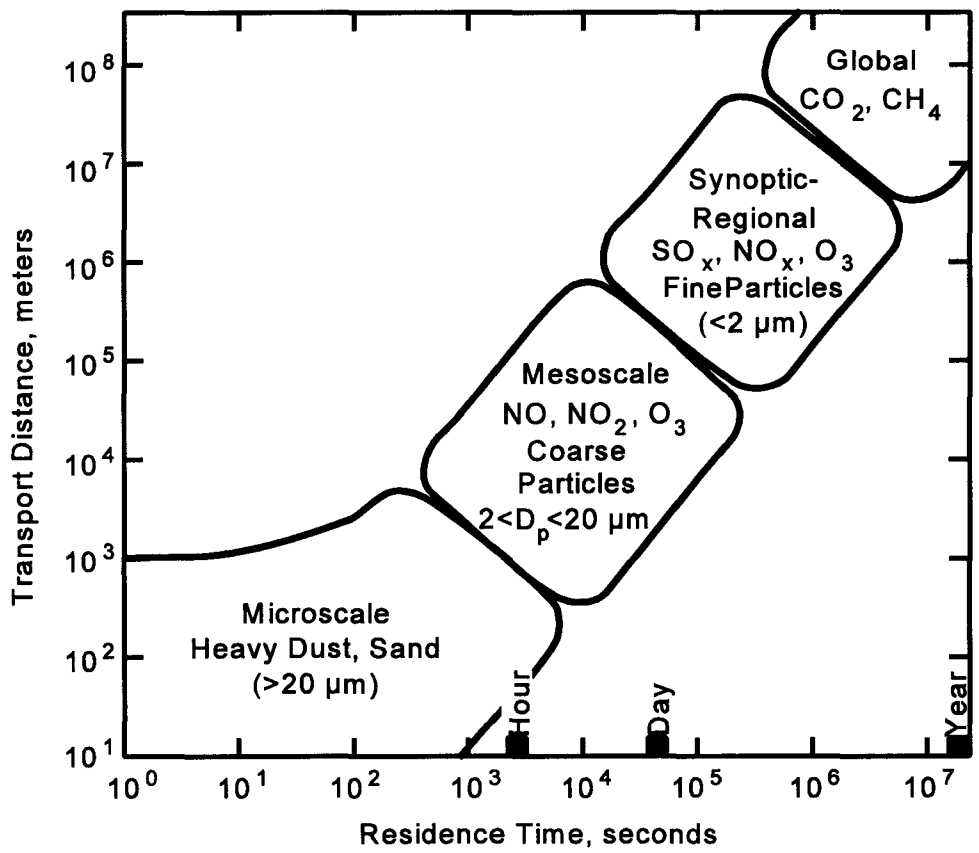

Figure 6-2. Relationship of spatial and temporal scales for coarse and fine particles.

uniform regional patterns caused by long range transport. The relationship between spatial and temporal scales for coarse and fine particles is illustrated in Figure 6-2.

The aerosol residence time itself is determined by the competing rates of chemical transformations and removal. Secondary aerosol formation tends to be associated with multi-day long range transport because of the time delay necessary for the formation. For sulfates, for example, the residence time is 3-5 days. For fine particles, 0.1 μm to several μm, the main removal mechanism involves cloud processing, while coarse particles above 10 μm are deposited by sedimentation. Ultrafine particles, below 0.1 μm, also rapidly coagulate to form particles in the 0.1 to 1.0 μm size range. Another factor which must be considered is local turbulence. As a consequence of low removal rates, aerosols in the 0.1-1.0 μm size range reside in the atmosphere for longer periods than either smaller or larger particles (Figure 6-3).

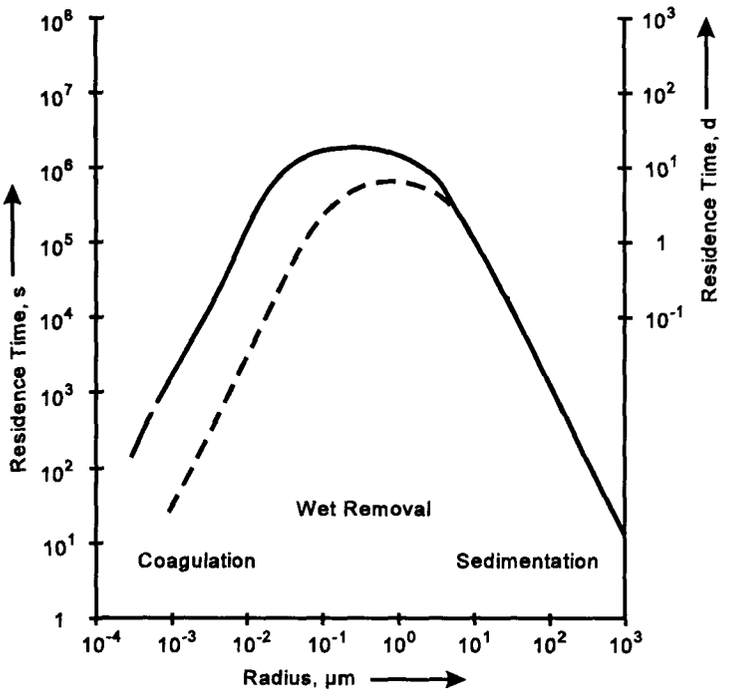

Figure 6-3. Residence time in the lower troposphere for atmospheric particles from 0.1 to 1.0 μm. (— Background aerosol, 300 particles cm^{-3}; --- continental aerosol, 15,000 particles cm^{-3}.)

Source: Jaenicke (1980).

If aerosols are lifted into the mid- or upper-troposphere their residence time will increase to several weeks. Large scale aerosol injections into the stratosphere through volcanoes or deep convection result in atmospheric residences of a month or two months for ash and ≥ 2 years for sulfates formed from SO_2 oxidation.

In the context of the specific analysis that follows, the space-time-concentration relationship in urban and mountainous areas is of particular importance (Figure 6-4). Urban areas have strong spatial emission gradients and also may have corresponding concentration gradients for directly emitted species, particularly in the winter under poor horizontal and vertical transport conditions.

In mountainous regions, the strong concentration gradients are caused by both topography that limits transport as well as the prevalence of emissions in valley floors. Strong

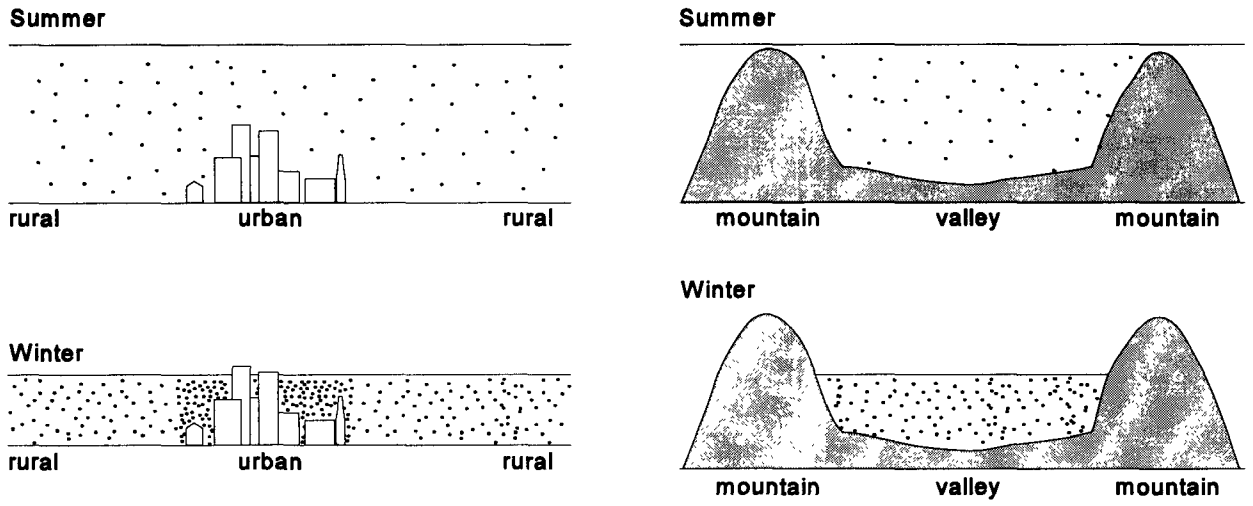

Figure 6-4. Space-time relationship in urban and mountainous areas.

wintertime inversions tend to amplify the valley-mountain top concentration difference. Fog formation also accelerates the formation of aerosols in valleys

6.1.5 Particle Size Distribution

The aerosol size distribution is of importance in quantifying both the formation (generation) as well as the effects of aerosols. Condensation of gaseous substances during combustion in the atmosphere generally produces fine particles below 1 μm in diameter. Resuspension of soil dust and dispersion of sea spray produces coarse particles above 1 μm.

The size distribution of particles also influences both the atmospheric behavior and the effects of aerosols. Atmospheric coagulation, cloud scavenging, and removal by impaction and settling are strongly size dependent (Figure 6-3). The effects on human health depend on size-dependent lung penetration. The effects of light scattering on visibility and climate are also strongly dependent on particle size.

Measurements over the past decades (Whitby et al., 1972; Whitby, 1978) show that atmospheric aerosols may be classified as fine mode particles or coarse mode particles. The size distribution of atmospheric particles is discussed in Section 3.7. The sources, formation mechanisms, and chemical compositions of these two aerosol modes are different. In general,

the two aerosol size modes have independent spatial and temporal patterns as described throughout this chapter. Coarse dust particles tend to be more variable in space and time and can be suspended through natural or human activities. Fine particles during the warmer months of the year are largely of secondary origin and their spatial-temporal pattern is more regional. Notable exceptions are urban-industrial hotspots and mountain valleys where primary submicron size smoke particles can prevail.

6.1.6 Aerosol Chemical Composition

The chemical composition of atmospheric aerosol is believed to influence the effect on human health. While the causal mechanisms are not fully understood, the acidity, carcinogenicity, and other forms of toxicity are chemical properties considered relevant to human health.

The aerosol chemical composition has also become an important property for identifying source types based on chemical "fingerprints" in the ambient aerosol. Since aerosols reside in the atmosphere for days and weeks, there is a substantial amount of mixing that takes place among the contributions of many sources. At any given "receptor" location and time, the aerosol is a mixture of many source contributions each having a chemical signature for possible source type identification.

Fine particles are generally composed of sulfates, hydrogen ions, ammonium, organics, nitrates, elemental carbon (soot), as well as a portion of the trace metals (Section 6.6). Each major chemical form has sub-species such as acidic and neutral sulfates, light and heavy organics, ammonium and sodium nitrates, etc.

The chemical composition of coarse particles is dominated by the elements of the earth's crust, Si, Al, Fe, and other elements commonly found in soil. Near industrial sources, coarse particles may be contaminated by lead and other trace metals. At ocean shores, coarse particles may consist of sea salt arising from breaking of waves. Both resuspended dust and sea salt are primary particles, carrying the chemical signatures of their sources.

6.2 GLOBAL AND CONTINENTAL SCALE AEROSOL PATTERN

There are two data sets which can be used to provide information on fine particle concentration patterns on continental and global scales. Routine visibility distance observations, recorded hourly at many U.S. airports by the U.S. Weather Service, provide an indication of fine particle pollution over the United States. The visibility distance data have been converted to aerosol extinction coefficients and used to access patterns and trends of aerosol pollution over the United States (Husar et al., 1994; Husar and Wilson, 1993). Routine satellite monitoring of backscattered solar radiation over the oceans by the Advanced Very High Resolution Radiometer sensors on polar orbiting meteorological satellites provides a data set which can be used to give an indication of aerosol over the world's oceans. These two data sets have been merged to provide a global and continental perspective. The data analyses presented here were performed for this Criteria Document and have not yet been published elsewhere.

Aerosol detection over the oceans is facilitated by the fact that the ocean reflectance at 0.6 μm is only 0.02. Hence, even small backscattering from aerosols produces a measurable aerosol signal. The backscattering is converted to a vertically integrated equivalent aerosol optical thickness assuming a shape for the aerosol size distribution or phase function. Clouds are eliminated by a cloud mask, so the data are biased toward clear-sky conditions. The oceanic aerosol maps represent a two-year average (July 1989-June 1991) prior to the eruption of Mt. Pinatubo, when the stratosphere was unusually clear of aerosol. Consequently, the images reflect mainly the spatial pattern of tropospheric aerosol.

A continental-scale perspective for North America is shown in Figure 6-5. Seasonal depictions of the oceanic aerosol for the entire globe are shown in Figure 6-6. The average aerosol map of Eastern North America for June, July and August (Figure 6-5) shows areas of high optical depth over the Mid-Atlantic States and over the Atlantic Ocean. The aerosol concentration over the oceans is highest near the coast and declines with distance from the coast. This indicates that the aerosol is of continental origin and represents a plume originating in eastern North America, heading north-east across the Atlantic ocean. This plume can also be seen in the spring and summer season oceanic aerosol patterns shown in Figure 6-6.

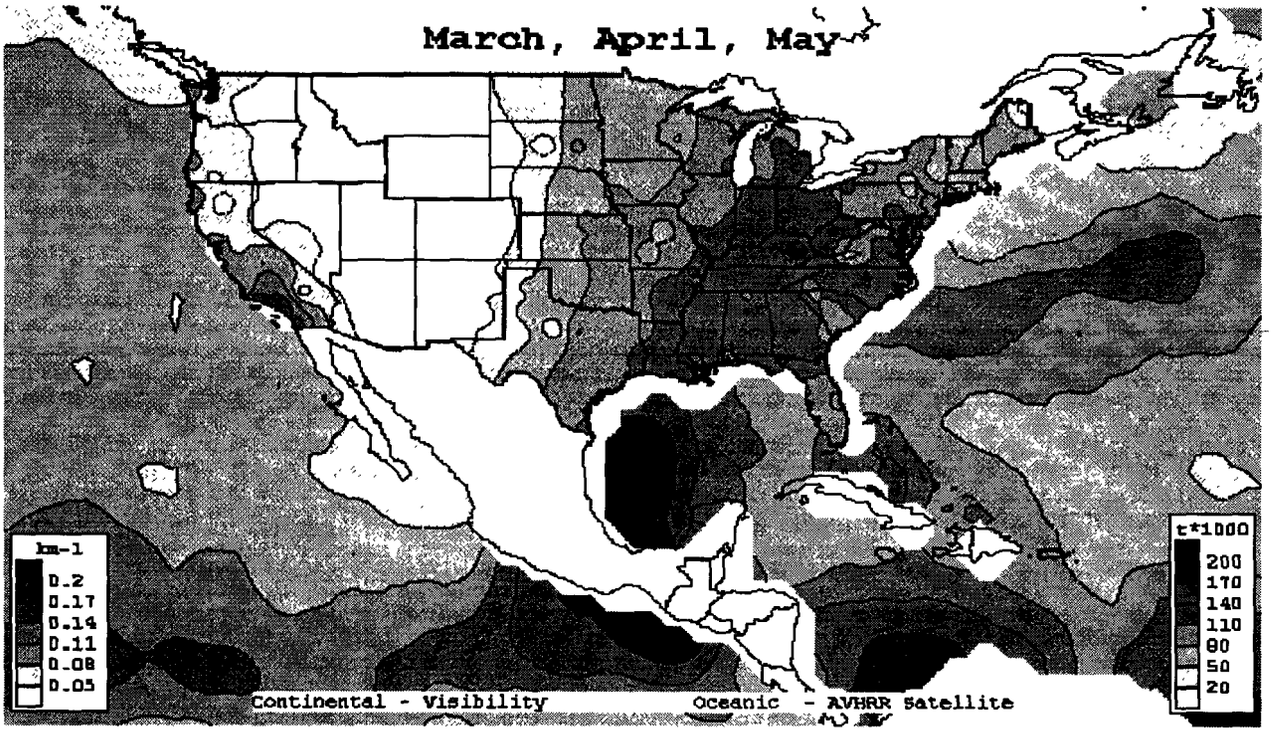

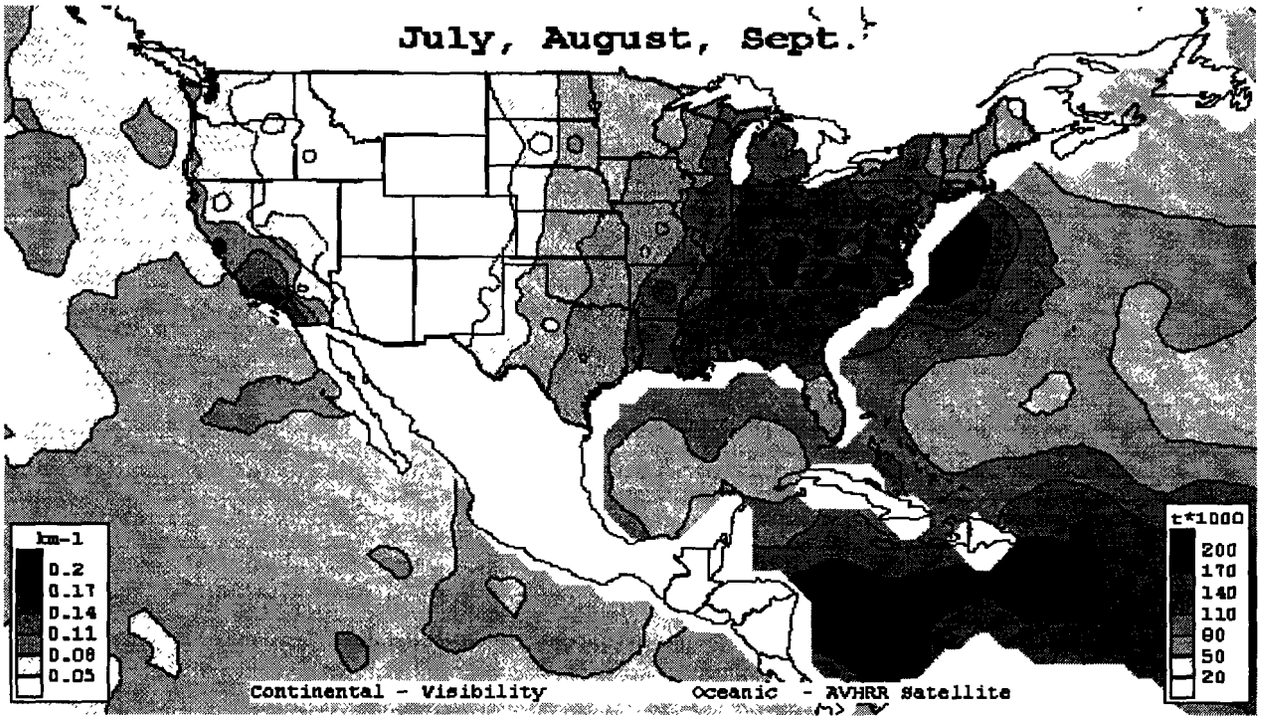

Figure 6-5. Continental scale pattern of aerosols derived from visibility observations over land and satellite monitoring over the oceans: North America.

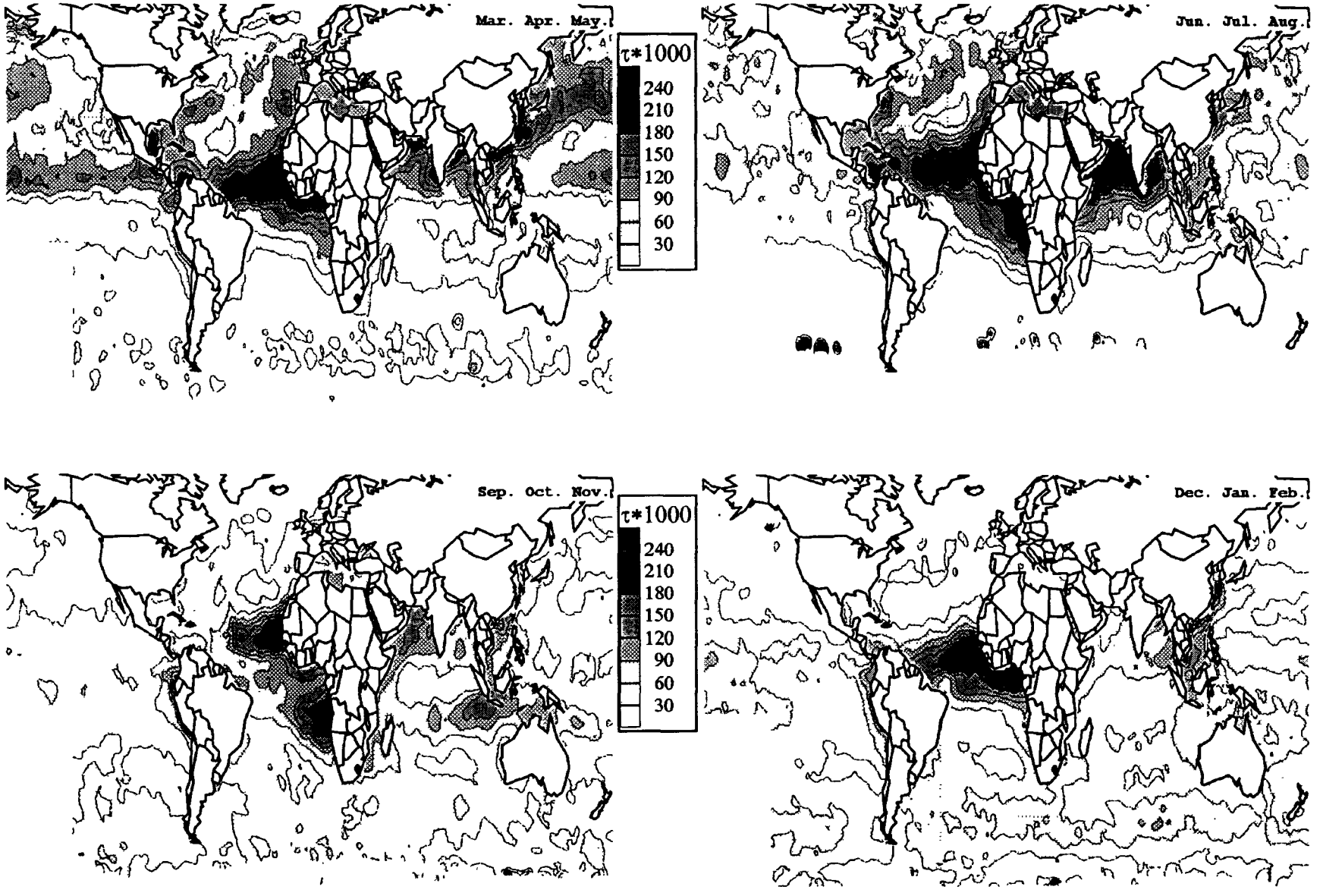

Figure 6-6. Global pattern of oceanic aerosols derived from satellite observations.

The continental aerosol extinction coefficient data for the southwest coast of North America indicate elevated aerosol extinction over southern California. The area includes the hazy South Coast and the San Joaquin Valley air basins. It is interesting to note that somewhat elevated aerosol optical thickness is also recorded over the Pacific near Southern California. However, the low aerosol signal and the semi-quantitative satellite data preclude a clear cause and effect association.

The seasonal aerosol pattern over the oceans reveals that the highest aerosol signal is found near the tropics, where wind-blown dust and biomass burning in Africa and southern Asia produce 5,000 km long aerosol plumes (Figure 6-6). Further aerosol belts which may be of marine origin are observed just north of the Equator and at 30 to 60° latitudes in both hemispheres. The backscattering in the summer hemispheres exceeds the winter values by a factor of 5 to 10. There is a pronounced seasonality in each aerosol region (Figure 6-7); the higher aerosol levels appear in the summer hemisphere although many continental and marine regions show a spring maximum. Thus, the global tropospheric aerosol is a dynamic collection of independent aerosol regions, each having unique sources and temporal patterns.

The seasonal oceanic aerosol maps show two distinctly different spatial patterns: aerosol plumes originating from continents, and oceanic aerosol patches that are detached from the continents. The continental aerosol plumes are characterized by high values near the coastal areas and a decline with distance from the coast. The most prominent aerosol plume is seen over the equatorial Atlantic, originating from West Africa and crossing the tropical Atlantic. It is the well known Sahara dust plume. Additional continental plumes emanate form Southwest Africa, Indonesia, China-Japan, Central America and eastern North America. Aerosols which may be of marine origin dominate large zonal belts (30 to 60° N and S) in the summer hemispheres as well as near the Equator. In summary, the global tropospheric aerosol is a collection of largely independent aerosol regions, each having a bio-geochemically active source and unique spatial temporal pattern.

Based on the above global and continental-scale observations, it can be concluded that the continental plume from eastern North America is not as intense as those from other industrial and non-industrial regions of the world. However, quantitative aerosol comparisons of global regions are not available.

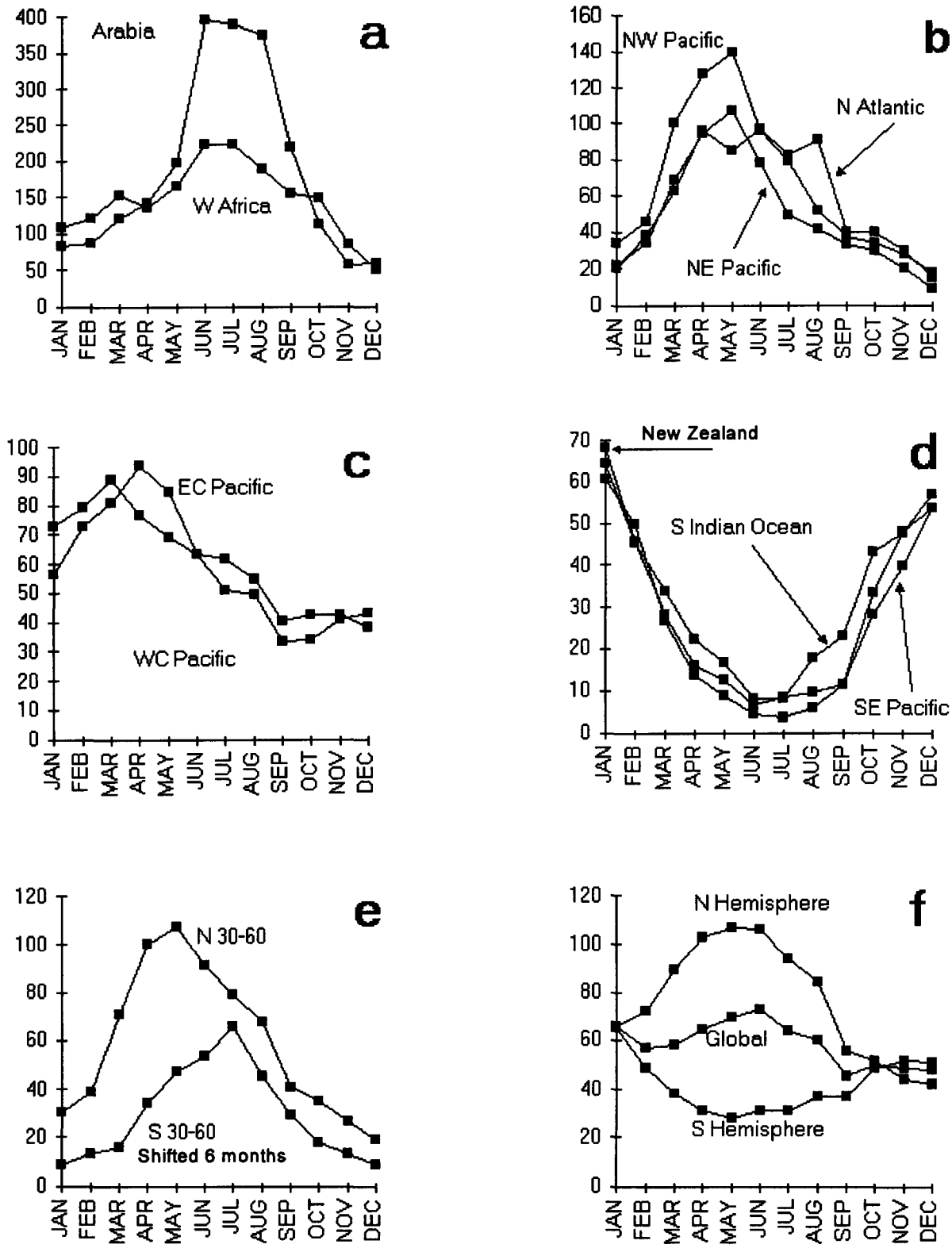

Figure 6-7. Seasonal pattern of oceanic aerosols derived from satellite observations.

6.3 U.S. NATIONAL AEROSOL PATTERN AND TRENDS

Our current understanding of the U.S. national aerosol pattern arises from nonurban, regional background monitoring networks, the Interagency Monitoring of Protected Visual Environments (IMPROVE) (Sisler et al., 1993) and the Northeast States for Coordinated Air Use Management (NESCAUM) (Poirot et al., 1990, 1991), and from a mainly urban network, the Aerometric Information Retrieval System (AIRS) (AIRS, 1995). The nonurban and urban networks yield markedly different national patterns, particularly over the western United States. For this reason the results from the two sets of observations are presented separately and the differences between two networks are evaluated. The data analyses presented here were performed for this Criteria Document and have not yet been published elsewhere.

6.3.1 Nonurban National Aerosol Pattern

Nonurban aerosol concentrations are measured at remote sites, away from urban-industrial activities. Size-segregated aerosol mass and chemical composition data are available for 50 sites, through the IMPROVE (Joseph et al., 1987; Eldred et al., 1987, 1988, 1990; Eldred and Cahill, 1994) and NESCAUM (Poirot et al., 1990, 1991; Flocchini et al., 1990) networks. These are located mostly in national parks and wilderness areas. The PM_{10} and $PM_{2.5}$ mass concentrations are sampled and analyzed on separate filters. The sampling frequency is generally twice a week (Wednesdays and Saturdays) for 24 hours. The $PM_{2.5}$ samples are analyzed for chemical composition which makes the data sets suitable for chemical mass balance computations (e.g., Sisler et al., 1993; Malm et al., 1994b). The IMPROVE/NESCAUM aerosol data are available from 1988 through 1993.

Measurements of PM are available from the IMPROVE/NESCAUM network at a smaller number of sites compared to the number of sites for which measurements are available from the AIRS network. The nonurban sites also have very different geographical distributions from those sites in the urban network. Therefore, the ability to compare PM_{10} concentrations from the nonurban and urban networks is severely limited by these factors.

The monthly distributions of chemical species, the chemical mass balances, obtained from the measurements at nonurban sites are incomplete. Only sulfate, organics, soil, and soot (elemental carbon) are considered. The contributions of hydrogen ion, water, trace

metals and sea salt are not listed. The contribution of nitrate is included on a national basis, but not in the subsequent discussion for regions.

The results of the national spatial and temporal pattern analysis are presented in quarterly contour maps and monthly seasonal time charts. The contours drawn for the eastern United States are derived from only 15 to 20 stations. As a consequence, these contour lines are to be taken as guides to the eye and not as actual patterns. The quarters of the year are calendrical.

6.3.1.1 Nonurban $PM_{2.5}$ Mass Concentrations

Maps of seasonal average nonurban $PM_{2.5}$ concentrations are shown in Figure 6-8. The maps divide the country roughly into eastern and western halves. The eastern United States is covered by large, contiguous $PM_{2.5}$ concentrations that range from 10 $\mu g/m^3$ in Quarter 1, and 17 $\mu g/m^3$ in Quarter 3. During the transition seasons (Quarters 2 and 4) the eastern U.S. nonurban $PM_{2.5}$ concentrations are at about 12 $\mu g/m^3$. Within the eastern U.S., there are subregions such as New England that have lower concentrations ranging between 8 and 12 $\mu g/m^3$. During the third quarter, there is a wider range of geographic distribution of $PM_{2.5}$ concentrations in the eastern United States than in other quarters of the year.

The lowest nonurban $PM_{2.5}$ concentrations are measured over the central mountainous western states. The low winter concentrations are at about 3 $\mu g/m^3$, while the summer values are around 6 $\mu g/m^3$. Somewhat elevated $PM_{2.5}$ concentrations are observed over the southwestern border adjacent to Mexico as well as in California and the Pacific Northwest. The nonurban fine particle mass clearly shows multiple aerosol regions over the conterminous U.S., each exhibiting unique spatial and seasonal characteristics.

6.3.1.2 Nonurban Particulate Matter Coarse Mass Concentrations

In classifying size fractions of PM, PM_{10} refers to PM collected in a sampler with a 50% cutpoint of 10 μm aerodynamic diameter and $PM_{2.5}$ to PM collected in a sampler with a cutpoint of 2.5 μm aerodynamic diameter. PMCoarse or coarse will be used to refer to the PM between the cutpoints of 2.5 and 10 μm, whether determined by subtracting a $PM_{2.5}$ sample mass from a PM_{10} sample mass or determined directly from the coarse particle channel of a dichotomous sampler with a PM_{10} (or PM_{15}) μm diameter upper cutpoint. Fine will also

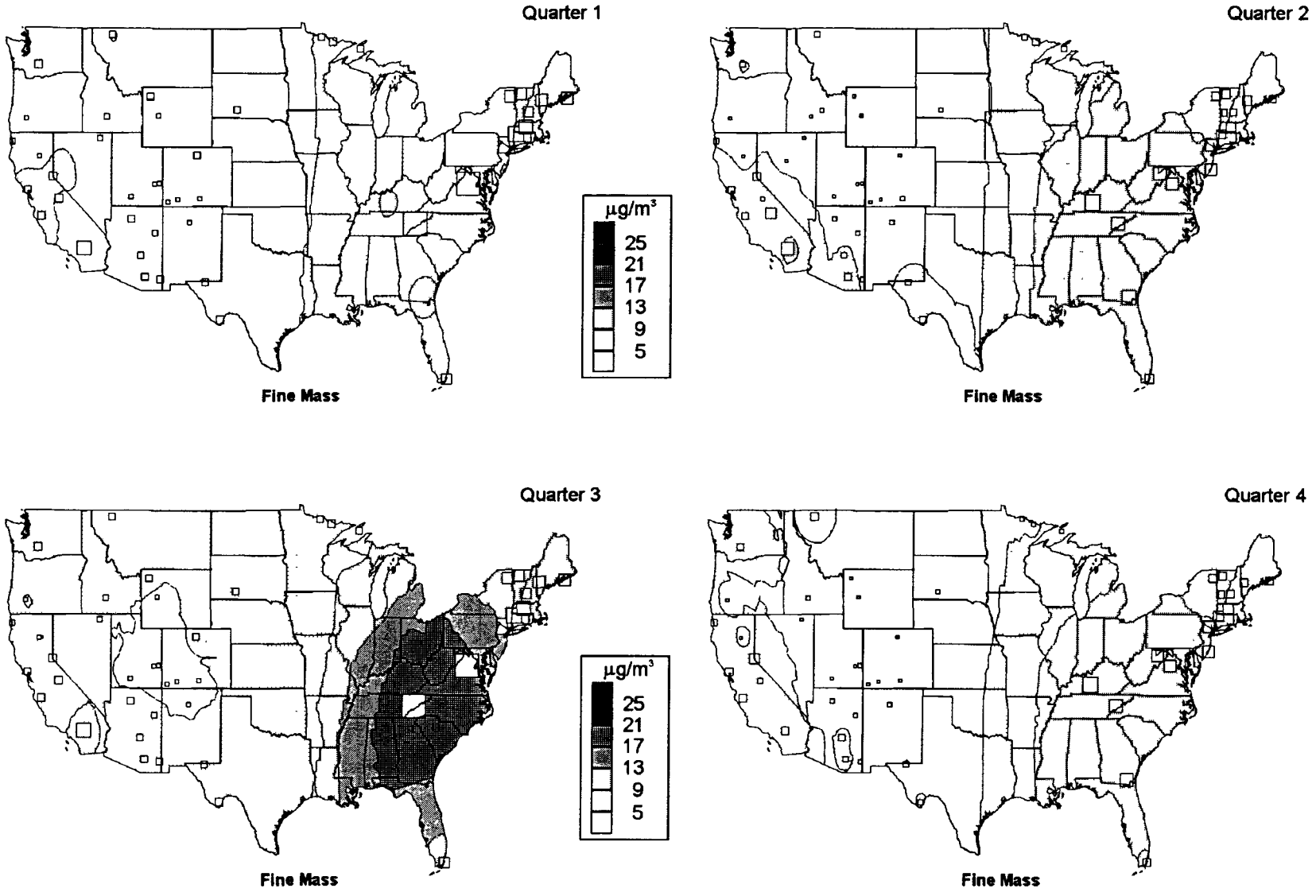

Figure 6-8. Fine mass concentration derived from nonurban IMPROVE/NESCAUM networks.

be used to refer to $PM_{2.5}$. $PM_{2.5}$ is an indicator of the fine mode particle mass but it is not an exact indicator, since $PM_{2.5}$ may contain some coarse mode PM. Likewise, PMCoarse or coarse refers to the inhalable fraction of the coarse mode, not the entire coarse mode. Under high relative humidity conditions PMCoarse may contain some fine mode PM.

The nonurban coarse aerosol mass concentration in the size range 2.5 to 10 μm is given in the seasonal maps in Figure 6-9. It is plotted on the same concentration scale as the nonurban $PM_{2.5}$ and PMCoarse maps to show that the nonurban coarse mass concentration is less than the fine mass concentration over most of the country. The lowest nonurban coarse particle concentration is recorded during the first, second, and fourth calendar quarters when virtually the entire conterminous United States showed values <10 $\mu g/m^3$. The industrialized Midwest, adjacent to the Ohio River, shows low PMCoarse concentration (<10 $\mu g/m^3$) comparable to the relatively clean Rocky Mountains states. The highest nonurban coarse mass concentrations appear during quarters 2 and 3. In quarter 2, the southwestern United States adjacent to the Mexican border shows the highest nonurban coarse mass concentrations. In quarter 3, the monitoring sites in Florida and Southern California exhibit high concentrations (>12 $\mu g/m^3$).

6.3.1.3 Nonurban PM_{10} Mass Concentrations

Maps of seasonal average nonurban PM_{10} concentrations are shown in Figure 6-10. PM_{10} is the sum of the $PM_{2.5}$ and PMCoarse. The spatial pattern from east to west, including the delineation of aerosol regions, is generally similar to the $PM_{2.5}$. However, the PM_{10} concentrations exceed the $PM_{2.5}$ by up to a factor of two depending on region and season. The sparseness of nonurban sites over large areas of the central United States limits the reliability of profiles in these areas.

In the eastern U.S., PM_{10} concentrations range between 12 $\mu g/m^3$ in Quarter 1 and 25 $\mu g/m^3$ in Quarter 3. During the transition seasons (Quarters 2 and 4) the eastern U.S. non-urban PM_{10} concentrations are about 15 $\mu g/m^3$, except in New England. The lowest PM_{10} concentrations are measured over the central mountainous states, 5 $\mu g/m^3$ in Quarter 1, 10 $\mu g/m^3$ in Quarter 3, and 7 $\mu g/m^3$ during the transition seasons. Higher PM_{10} concentrations, between 10 and 20 $\mu g/m^3$, were measured over the southwestern United States

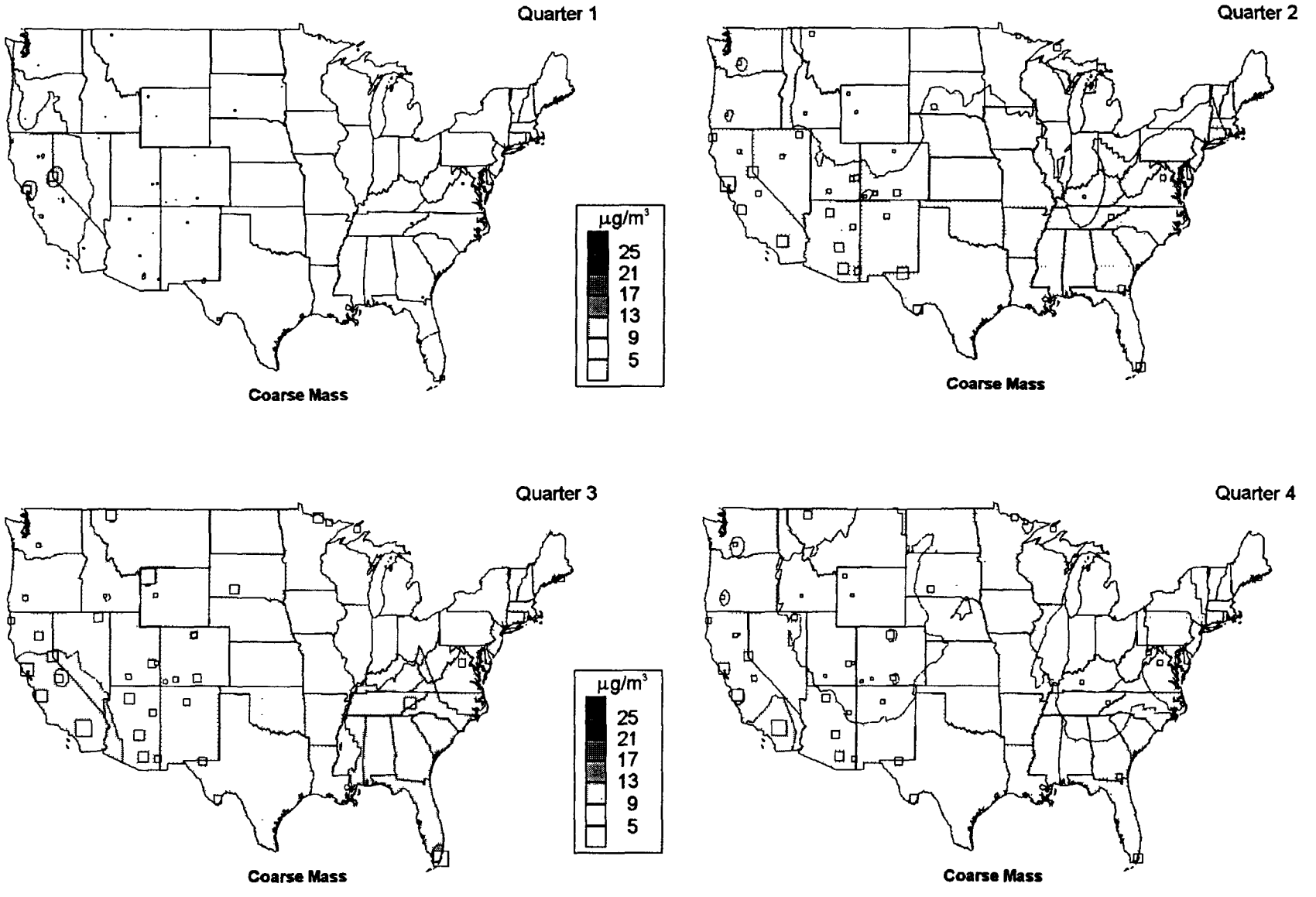

Figure 6-9. Coarse mass concentration derived from nonurban IMPROVE/NESCAUM networks.

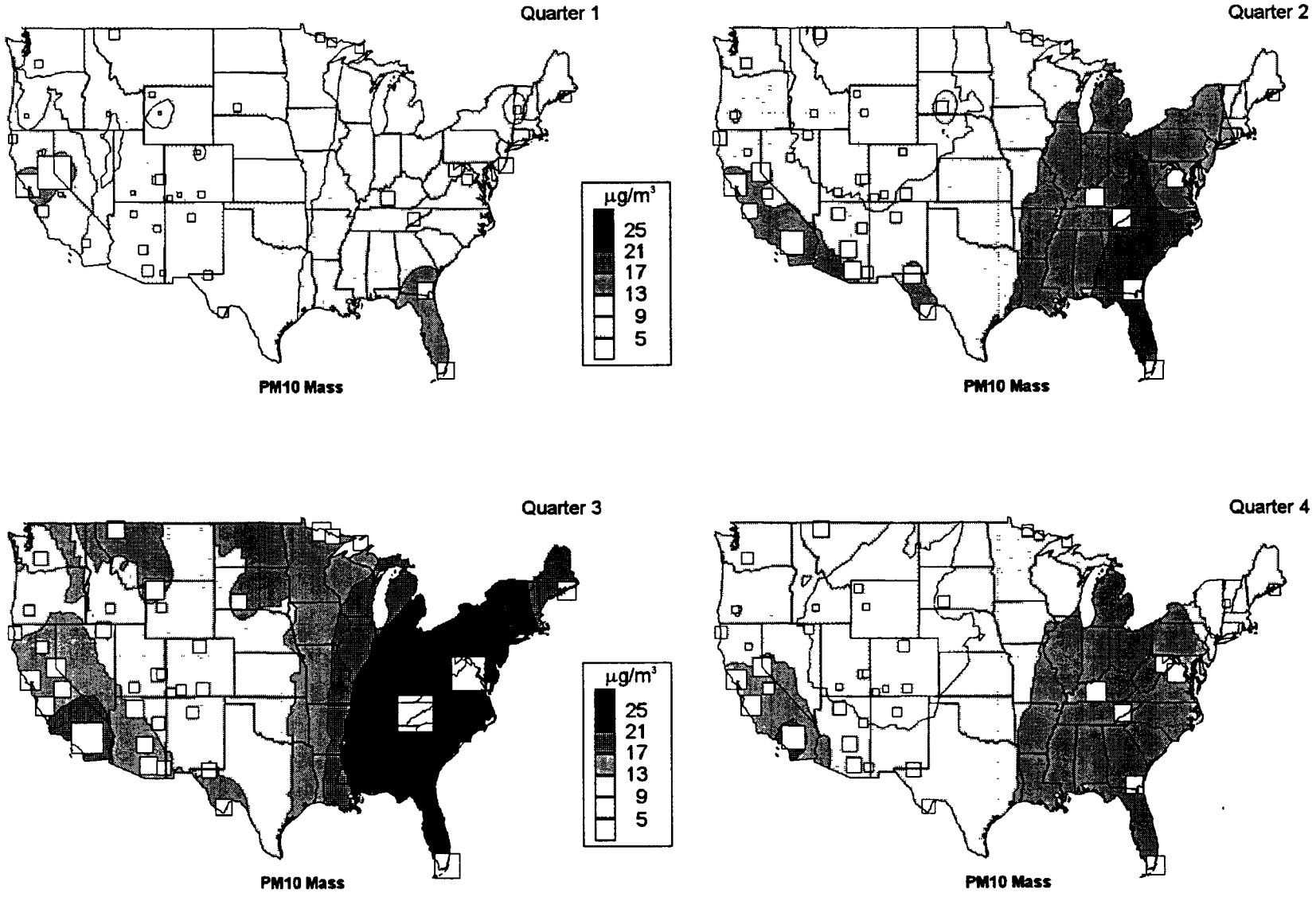

Figure 6-10. PM_{10} mass concentration derived from nonurban IMPROVE/NESCAUM networks.

as well as over the Pacific states from California to the Northwest than over the central mountainous states.

6.3.1.4 $PM_{2.5}/PM_{10}$ Ratio at Nonurban Sites

The PM_{10} aerosol mass is composed of fine mass ($PM_{2.5}$) and coarse mass, below 10μm (Figure 6-10). Both the sources and the effects of fine particles differ markedly from those of coarse particles. For this reason it is beneficial to examine the relative contribution of $PM_{2.5}$ and PM_{10} concentrations. Figure 6-11 shows the seasonal fine mass as a fraction of PM_{10}.

Nationally, the fine fraction at nonurban sites ranges between 0.4 and 0.8. The highest fine fraction is recorded east of the Mississippi River, where 60 to 70% of the PM_{10} mass is in particles <2.5 μm in size. This is also the region that shows the highest PM_{10} concentrations; thus, fine particles dominate the nonurban aerosol concentrations east of the Mississippi River. The fine fraction exceeds the coarse fraction at the nonurban northwestern sites. The fine fraction is the lowest in the southwestern United States ($<$ 50%), particularly in the spring season (Quarter 2).

Spatial and seasonal variation of the fine fraction is a further indication for the existence of different aerosol regions over the conterminous U.S. This is further illuminated in Section 6.4 where the aerosol characteristics over different regions of the United States are discussed.

6.3.1.5 Nonurban Fine Particle Chemistry

The elemental composition of nonurban fine particles over the conterminous United States is now reasonably well understood. The IMPROVE/NESCAUM network provides over five years of aerosol mass and chemical composition data. The data from these networks allows the chemical apportionment of the fine particle mass into aerosol types such as sulfates, organic carbon, elemental carbon, and fine soil (Schichtel and Husar, 1991; Sisler et al., 1993, Sisler and Malm, 1994). The quantification of these aerosol types is relevant to both the determination of aerosol effects and source apportionment of particle mass. It should be emphasized that urban areas, mountain valleys, and remote monitoring sites are likely to have different relative concentrations of the aerosol types. Also, the quantification of semivolatile organic compounds, nitrates, and other unstable species is subject to major uncertainties.

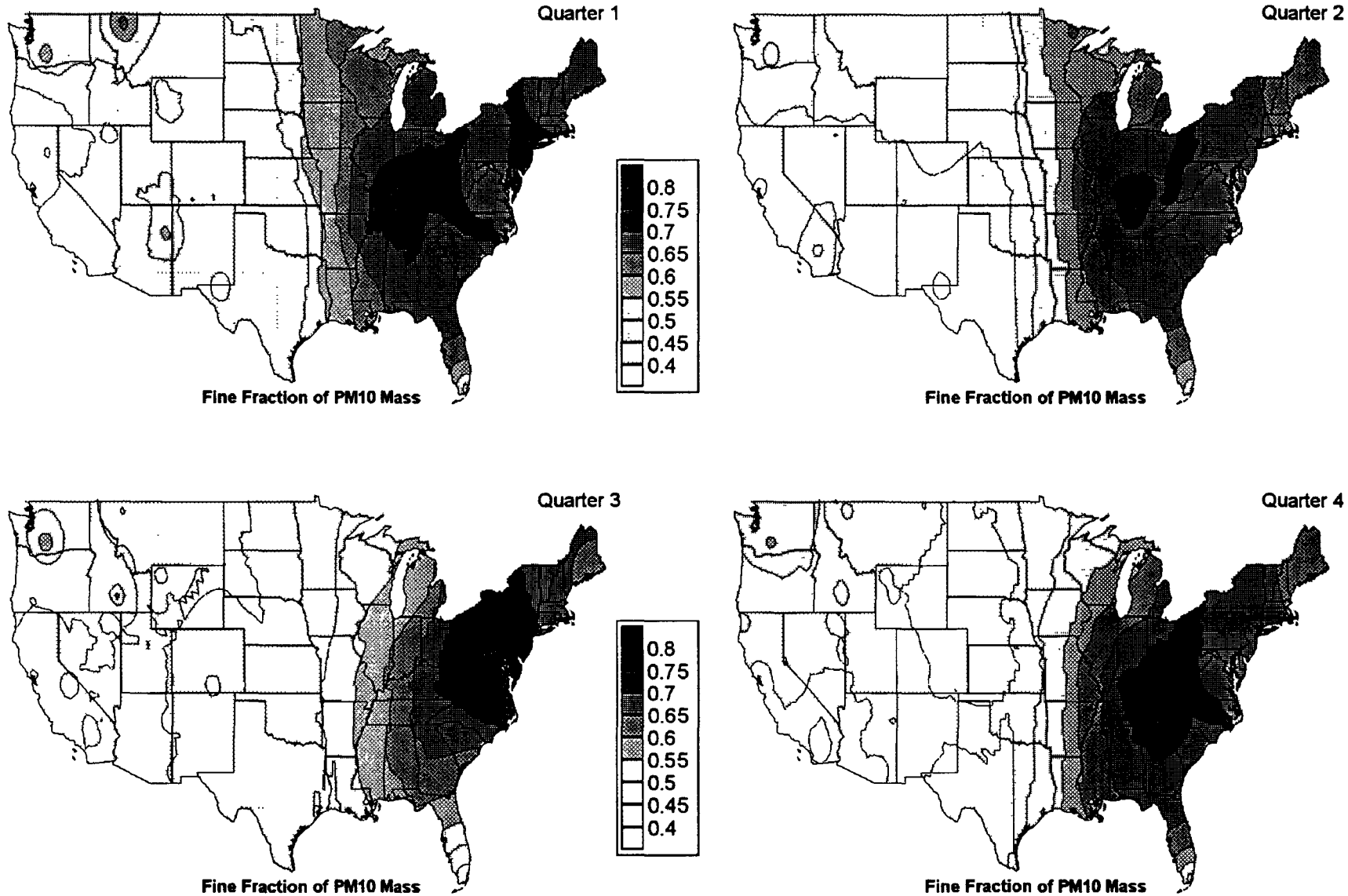

Figure 6-11. Fine fraction of PM_{10} derived from nonurban IMPROVE/NESCAUM networks.

Much work remains in order to define the chemical, as opposed to the elemental, composition, especially for organic compounds.

At nonurban eastern U.S. sites, a large fraction of the fine aerosols are composed of sulfate and related species (ammonium ions, hydrogen ions, and associated water) and organic compounds. In the northeastern and southeastern U.S., organic carbon appear to equal sulfate in the fourth quarter of the year. In the southwestern U.S., wind blown dust is a major component of fine mass while sulfate is less important (Schichtel and Husar, 1991).

Annually averaged fine particle sulfate, as ammonium sulfate; organic carbon; elemental carbon; and nitrate, as ammonium nitrate, concentrations from the IMPROVE network across the U.S. are shown in Figures 6-12 and 6-13 (Sisler et al., 1993; Malm et al., 1994b). The station density is limited, especially in the eastern U.S. The contour lines in the annual average maps are to be used as guides to the eye, rather than precise values. Concentrations of sulfate in the eastern U.S. (Figure 6-12a) exceeds those over the mountainous western states by factor of five or more. Elevated sulfate in excess of 1 $\mu g/m^3$ is also reported over the Pacific coast states. Sulfates typically contribute over 50% of the fine particulate mass in the eastern U.S., while sulfates contribute 30% or below in the West.

Fine particle nitrates (Figure 6-12b) are highest in California, exceeding 4 $\mu g/m^3$ at most sites. Their share of the fine mass at several California sites exceeds 20%. Organic carbon concentrations (Figure 6-13a) are high over California and northwestern sites, as well as at the eastern U.S. sites. Organic carbon contributes over 50% of the fine particle mass in the Northwest, and about 30% throughout the eastern U.S. There is a high degree of uncertainty associated with the measurement of particulate nitrate and organic carbon because of artifacts arising from the adsorption of vapors or the loss of semivolatile materials. The elemental carbon concentrations (Figure 6-13b) are significant over the Northwest and southern California, as well as at the Washington, DC, site. Over most of the country elemental carbon is 5% or less of the fine particle mass.

The chemical composition of PM_{10} and $PM_{2.5}$ aerosols in the IMPROVE network (Eldred et al., 1994b) revealed that the average coarse mass does not differ significantly between the East and West; however, the fine mass is higher in the East. Also about 80% of

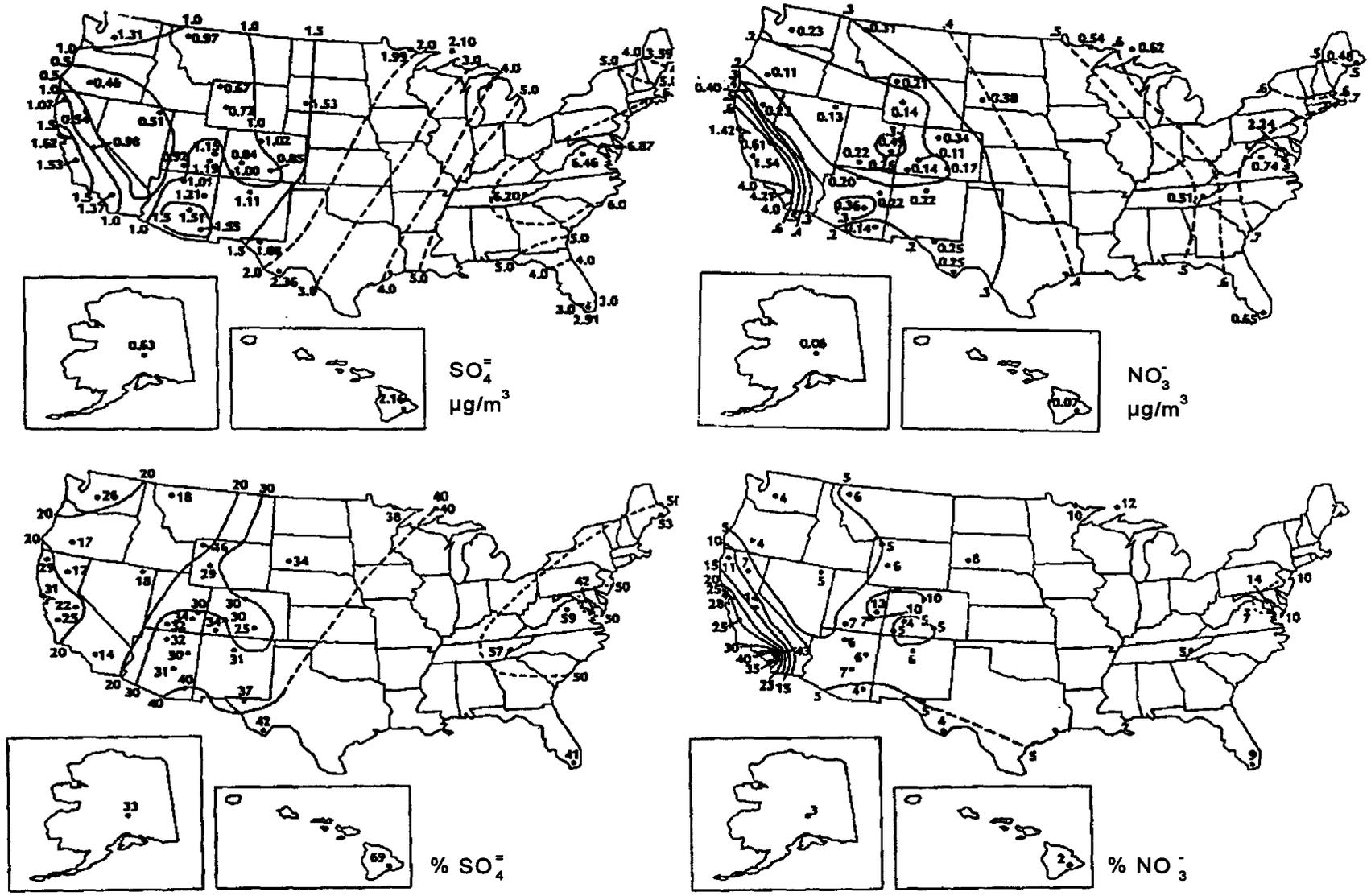

Figure 6-12. Yearly average absolute and relative concentrations for sulfate and nitrate.

Source: Sisler et al. (1993) and Malm et al. (1994b).

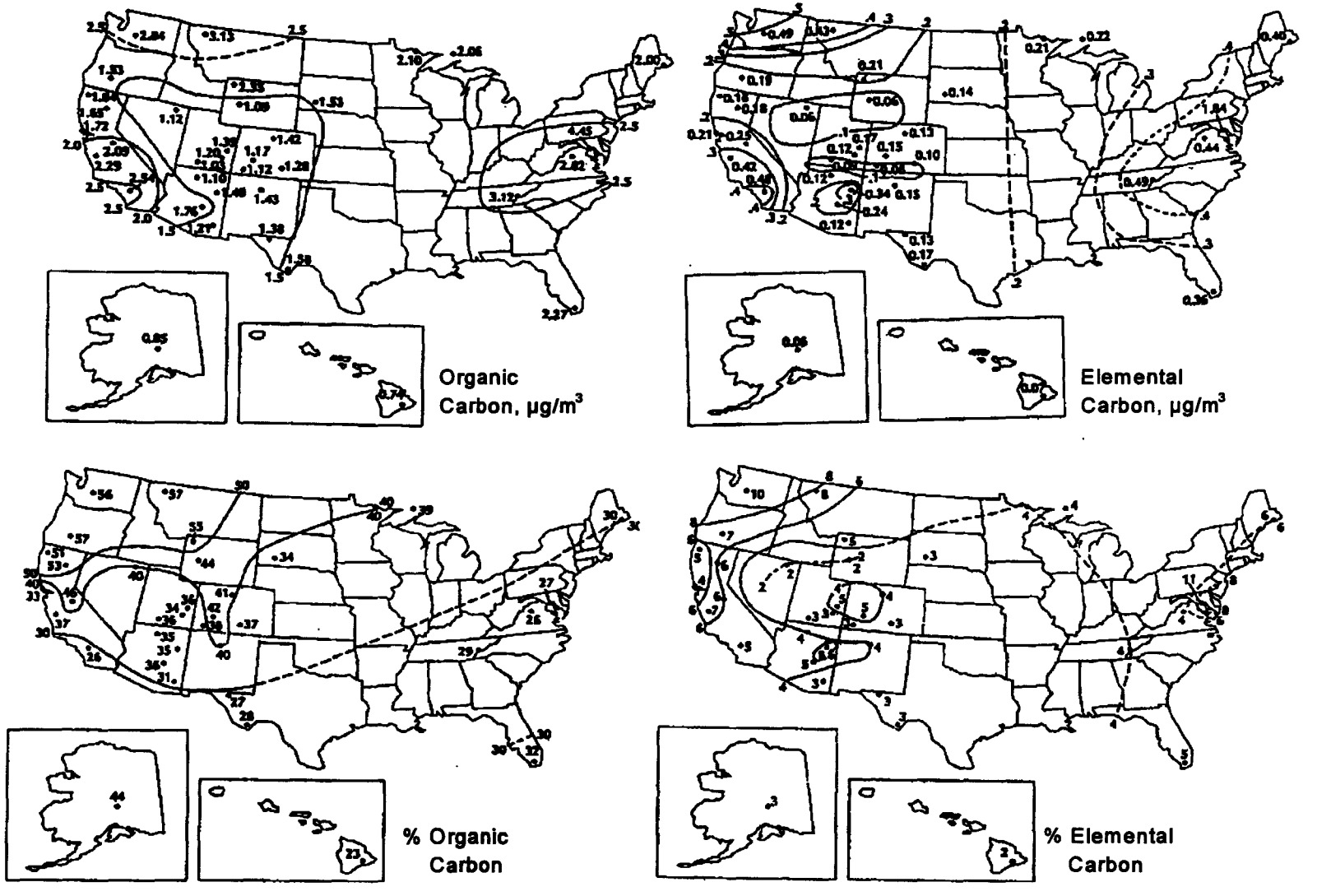

Figure 6-13. Yearly average absolute and relative concentrations for organic carbon and elemental carbon.

Source: Sisler et al. (1993) and Malm et al. (1994b).

soil elements and 20% of sulfur were found in the coarse fraction. Most trace elements were found in the fine fraction, both in the East and in the West. The spatial and seasonal patterns in particle concentrations and their relationships to optical extinction in the United States from the IMPROVE network were summarized by Malm et al. (1994b).

In studying the regional patterns of nonurban trace metals in the IMPROVE network, Eldred et al. (1994a) found a good correlation between selenium and sulfur at all sites in the East. The correlation in the West is lower. Comparison of the S/Se ratios for summer and winter shows that there is approximately twice the sulfur relative to selenium in summer compared to winter. Se is a tracer for S emitted from coal-fired fossil fuel power plants; this shift in S/Se from summer to winter is consistent with a substantial secondary photochemical contribution to $SO_4^{=}$ during the summer. Zinc is highest at the sites in the central East. It does not correlate well with sulfur. Lead and bromine are relatively uniform, with slightly higher mean concentrations in the East. There is poor correlation between lead and bromine. Copper and arsenic are highest in the Arizona copper smelter region. Copper is also higher in the central East.

Trends (1982 to 1992) of nonurban fine particle sulfur, zinc, lead, and soil elements were reported by Eldred et al. (1994a) using the IMPROVE network data. They observe that in the southwest, sulfur trends in spring, summer, and fall decreased, while most of the winter trends increased. The trends in the Northwest increase slightly. The two eastern sites (Shenandoah and Great Smoky Mountains) have increased almost 4% per year in summer, increased 1 to 3% in spring and fall, and decreased 2% in winter. The annual increase was between 2 and 3%. Generally, there were no significant trends in zinc and the soil elements. Lead at all sites decreased sharply through 1986, corresponding to the shift to unleaded gasoline. The ten year trends reported by Eldred et al. (1994b) have not been compared and reconciled with other compatible data.

6.3.1.6 Seasonality of the Nonurban Chemistry

This section discusses the seasonality of size segregated chemical composition at non-urban monitoring sites (IMPROVE/NESCAUM) over the entire U.S. (Figure 6-14).

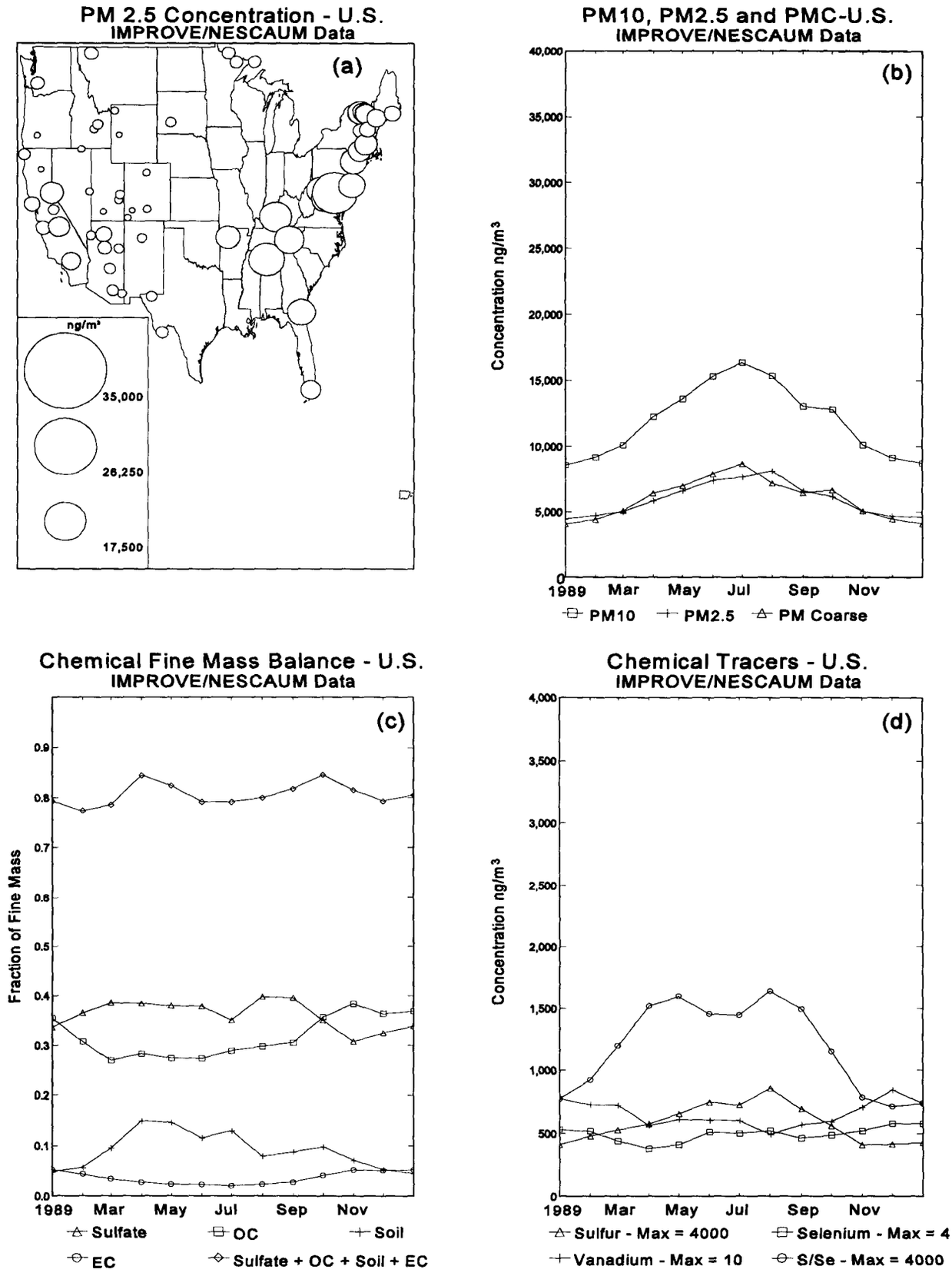

Figure 6-14. Seasonal pattern of nonurban aerosol concentrations for the entire United States: (a) monitoring locations; (b) PM_{10}, $PM_{2.5}$, and PMCoarse (PMC); (c) sulfate, soil, organic carbon (OC), and elemental carbon (EC) fractions; and (d) tracers.

The nationally aggregated average PM_{10}, $PM_{2.5}$ and PMCoarse is shown in Figure 6-14b (See Section 6.3.1.2 for a definition of PMCoarse.). The nonurban PM_{10} concentration ranges from 8 $\mu g/m^3$ in the winter, December through February, to about 15 $\mu g/m^3$ in June to August. On the national scale the PM_{10} seasonality is clearly sinusoidal with a summer peak. Fine particles over the nonurban conterminous United States account for about 50 to 60% of the PM_{10} mass concentration throughout the year. The coarse mass accounts for 40 to 50% throughout the year. Hence, the fine-coarse aerosol ratio does not change dramatically for the average nonurban aerosol.

The relative chemical composition of the aggregated nonurban aerosol pattern is shown in Figure 6-14c, including sulfates, organic carbon, soil, and elemental carbon as a fraction of the fine particle mass concentration. The Figure also shows the sum of these four aerosol species to indicate the fraction of the fine aerosol mass that is not accounted for. Most notable among the missing species is the contribution of nitrates, ammonium ion, and hydrogen ion.

There is mild seasonality in the nationally aggregated sulfate and organic carbon fractions. Throughout the year, sulfate aerosol, including the ammonium cation, accounts for 30 to 40% of the fine mass. Organic carbon also contribute 30 to 40% of the nationally averaged fine particle mass. Thus, sulfates and organic carbon are the two dominant species, contributing about 70% of the fine aerosol mass.

The contribution of soil dust to the fine mass ranges between 4% in the winter months to 12% during April through July. Elemental carbon is about 2% during the summer and 5% during the winter.

The sum of the four measured fine mass components, sulfates, soil, organic carbon, and elemental carbon add up to about 80% of the measured fine mass throughout the year. The remaining, unaccounted fine mass may be contributed by nitrates, trace metals (e.g., Pb, Br, sea salt [NaCl], etc.).

The seasonal pattern of concentration of primary emission tracers, selenium, Se and vanadium, V is shown Figure 6-14d. Se is a known tracer for coal combustion, while V is a trace constituent of fuel oil (Altshuller, 1980; Kleinman et al., 1980; Cass and McRae, 1983; Tuncel et al. 1985). The Figure also shows the monthly average concentration of fine particle sulfur as well as the S/Se ratio.

The national average Se concentration is rather uniform over the seasons, ranging between 400 to 600 pg/m^3. Since Se is a primary pollutant, the seasonal invariance means that the combined effect of emissions and dilution is seasonally invariant over the year.

The concentration of V is between 500 to 700 pg/m^3, with the higher concentrations occurring in the winter season. Evidently, the contributions from V-bearing fuel oil are more pronounced during the cold season. The monthly average sulfur in aerosols exhibits the highest concentrations 1.5 μg/m^3, during June, July, and August, and the lowest values 0.9 μg/m^3, during November, December, and January.

The S/Se mass ratio is about 700 during November to January and climbs to about 1,500 during April through September. The higher S/Se ratio during the warm season is an indication of secondary sulfate production from SO_2 in the plumes of coal fired power plants (Chapter 3).

Eastern United States

The seasonal pattern of the eastern U.S. aerosol chemistry is shown in Figure 6-15. The concentration of PM_{10}, $PM_{2.5}$, PMCoarse (Figure 6-15b) indicates a similar seasonality, highest concentrations in the summer, and lowest in the winter. The PM_{10} levels range between 12 to 24 μg/m^3, the $PM_{2.5}$ ranges between 8 to 12 μg/m^3, while PMCoarse ranges between 4 to 7 μg/m^3 over the year. The size segregated aerosol data for the nonurban East show that the fine mass concentration (8 to 12 μg/m^3) is higher than the national average (4 to 8 μg/m^3), while the coarse mass concentration is comparable to the national average. Eastern U.S. nonurban fine particles contribute 60 to 70% of the fine mass throughout the year.

The apportionment of the fine particle mass into its chemical components (Figure 6-15c) favors sulfates which amount to 40 to 50% of the fine mass throughout the year, compared to about 30% of organic carbon. The contribution of soil dust is about 5% throughout the year, while soot is more important in the winter (6%) than in the summer (3%). The above three aerosol chemical components account for 85 to 90% of the measured fine particle mass, leaving only relatively small contribution to nitrates, hydrogen ions, trace metals, and sea salt.

The coal tracer selenium (Figure 6-15d) exhibits a modest winter peaked seasonality between 600 to 800 ng/m^3. The fuel oil tracer vanadium on the other hand, is factor of two

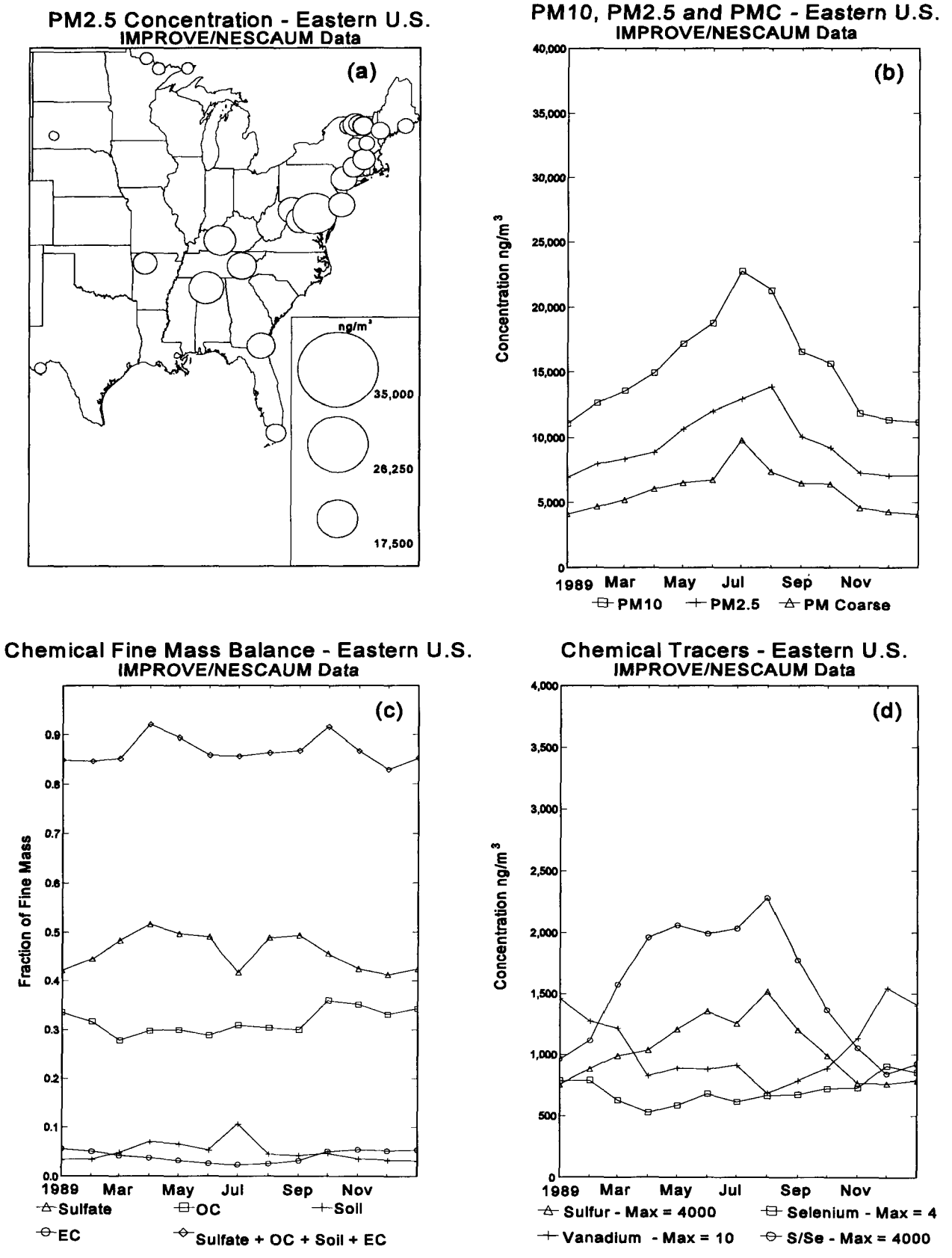

Figure 6-15. Seasonal pattern of nonurban aerosol concentrations for the eastern United States: (a) monitoring locations; (b) PM_{10}, $PM_{2.5}$, and PMCoarse (PMC); (c) sulfate, soil, organic carbon (OC), and elemental carbon (EC) fractions; and (d) tracers.

higher in the winter (1,500 ng/m^3) compared to the summer (750 ng/m^3). Evidently, the primary contribution from fuel oil is winter peaked. The S/Se ratio is about 1,000 in the winter, and it is over 2,000 in the summer months. This suggests the seasonality of secondary sulfate formation during the summer months.

Western United States

The aggregated western U.S. aerosol seasonality is presented in Figure 6-16. The non-urban aerosol concentrations for PM_{10}, $PM_{2.5}$, and PMCoarse are well below the concentrations over the eastern United States (Figure 6-16b). The western United States differs from the eastern United States, having lower fine mass concentrations, which range between 3 to 5 μg/m^3. The coarse mass concentration (4 to 8 μg/m^3) and seasonality is similar over the East and the West. It is worth emphasizing, however, that these measurements are at remote national parks and wilderness areas in both East and West. The examination of monitoring data in urban areas and confined airsheds (Sections 6.4 and 6.5) reveals a highly textured pattern in space and time.

The fine particle chemical mass balance (Figure 6-16c) for the aggregated western United States shows the substantial contribution of organic carbon, which account for 30 to 45% of the fine mass. The higher organic carbon fraction occurs in the November through January season. Sulfates range between 20 to 25% throughout the year. Soil dust plays a prominent role in the western fine mass balance, contributing 20% in April through May, but declining to 5% by January. Elemental carbon ranges between 5% in the winter and 2 % during the summer. About 25% of the fine mass over the western United States is not accounted for by sulfates, soil, organic carbon, and elemental carbon. It is known that nitrates are major contributors to the fine particle mass in the South Coast Basin, as well as other western regions (White and Macias, 1987a; Chow et al., 1992a, 1993a, 1995a).

The concentration of the trace substances (Figure 6-16d) selenium and vanadium shows both low concentrations and weak seasonality. The sulfur concentrations are also less than half of the eastern U.S. values. The S/Se ratio is about 500 in the winter months and 1,000 during the summer. The lower S/Se ratios compared to those in the eastern U.S. are the result

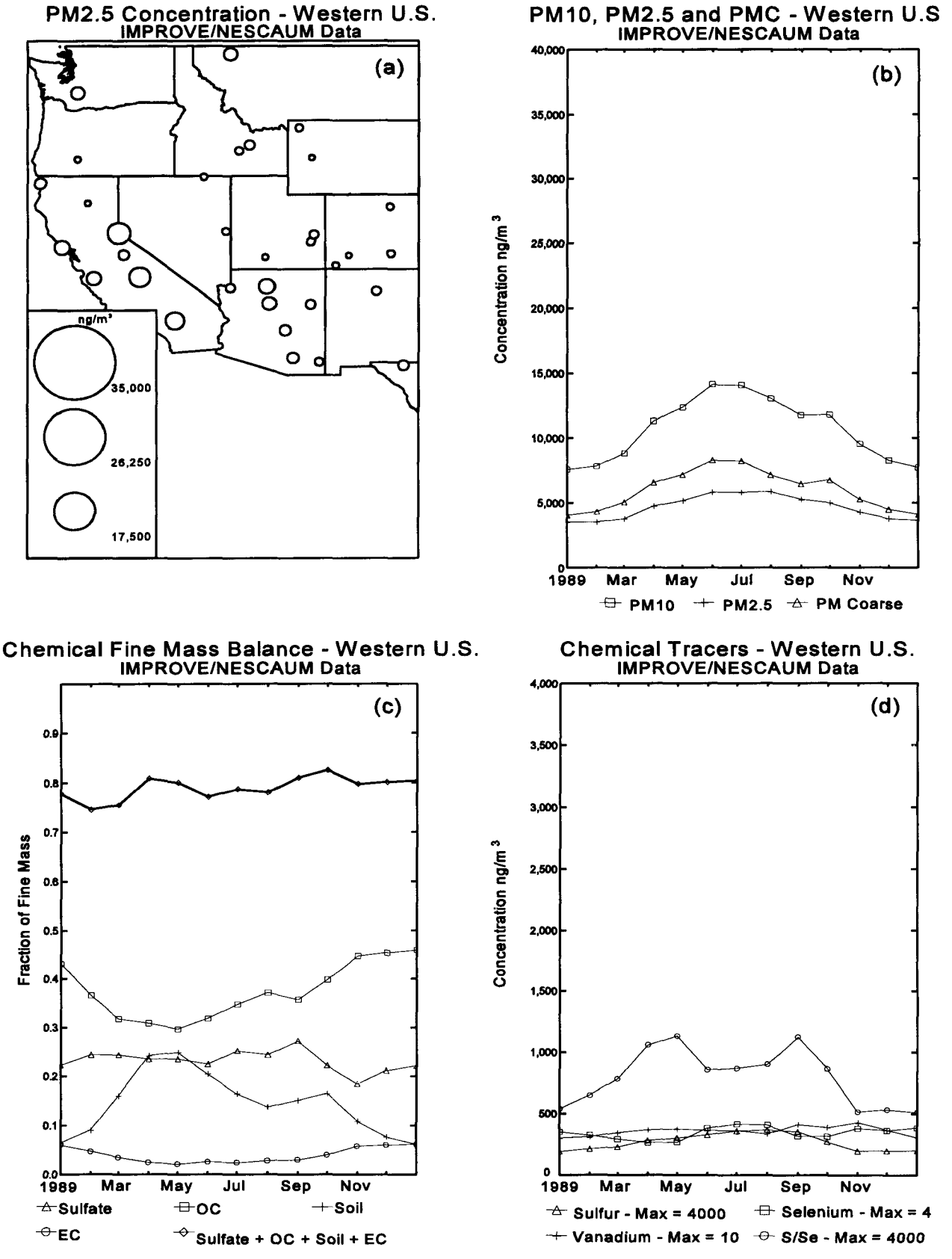

Figure 6-16. Seasonal pattern of nonurban aerosol concentrations for the western United States: (a) monitoring locations; (b) PM_{10}, $PM_{2.5}$, and PMCoarse (PMC); (c) sulfate, soil, organic carbon (OC), and elemental carbon (EC) fractions; and (d) tracers.

of selenium emitting coal-fired power plants not being the only sources of western U.S. sulfur. Smelters make a contribution to S but not Se in the atmosphere.

The above general discussion of national pattern of chemical and size dependence do not provide the more detailed spatial and temporal texture of the U.S. aerosol pattern discussed in the following sections. However, it provides the national scale gross features and serves as a broader context for the more detailed examinations.

6.3.1.7 Background Concentrations of Particle Mass and Chemical Composition

The concentration and chemical composition of background particulate matter can very with geographic location, from monitoring site to monitoring site; with season of the year; and with meteorological conditions which affect the emissions and secondary production of biogenic or geogenic species to the background.

A number of types of background can be considered. These backgrounds include the following: (1) a "natural" background excludes all anthropogenic contributions. This background includes any natural sources contributing to the background for chemical species in North America or globally; (2) a background which excludes all anthropogenic sources within North America, but not from anthropogenic sources contributing to background from outside of North America; (3) a background which excludes the anthropogenic sources inside the United States, but not from elsewhere in North America; (4) a background which excludes anthropogenic sources from other regions into a specified region in the United States; (5) a background which would exclude all sources of particulate matter except those associated with a particular urban area. The two backgrounds directly relevant to the Criteria Document are backgrounds (1) and (2). The problems and limitations in obtaining reasonably accurate annual average and seasonal values for these backgrounds are discussed below. Backgrounds (4) and (5) can be more readily be obtained by measurements. These backgrounds are relevant to subsequent stages in the implementation process. The averaging period over which background levels are defined should also be stated. Annual and seasonal averages may be more appropriate for risk assessments but daily peak values may be more relevant for control strategy implementation.

More specifically, the term non-manmade is meant to encompass sources such as geogenic dust plumes and sea salt as well as biogenic sources. Biogenic sources include (a) combustion products of biomass burning caused by lightning; (b) emissions of volatile sulfur compounds from marshes, swamps or oceans; (c) organic particulate matter formed by the atmospheric reactions of biogenic volatile organic compounds such as terpenes; and (d) particulate nitrates formed by the atmospheric reactions of NO_x emitted from soils. There is an intermediate class of sources associated with agricultural activities. These include biomass burning caused by human intervention and the addition of fertilizers to soils resulting in emissions of NH_3 and NO_x (Section 5.2, 5.3).

Anthropogenic sources include vehicular and stationary sources which emit particles directly or precursors such as sulfur dioxide, nitrogen oxides, or those volatile organic compounds capable of reacting in the atmosphere to form organic particles. Stationary sources of primary particulate matter as well as sulfur oxides and nitrogen oxide precursors include fossil fuel power plants, while smelters are sources of primary particles and sulfur oxides. Vehicles emit primary particulate matter as well as nitrogen oxides and volatile organic compounds. Solvent usage, agricultural coatings, and many other industrial operations also may emit precursors or particulate matter. Wood burning for heating of homes is a source of organic carbon and elemental carbon (Section 5.2, 5.3).

The formation of sulfates from sulfur dioxide emitted by power plant plumes can occur over distances exceeding 300 km and 12 h of transport (Section 3.4.2.1). Nitric acid also can be formed in these plumes and it can be converted to ammonium nitrate, if sufficient ammonia is available to first neutralize the sulfate in plumes. Similar transport can occur in urban plumes. The transport distances in plumes depend on both formation rates of particles and their removal by deposition processes. However, the residence times of fine particles can be long. For example, if the dominant removal process is dry deposition, fine particles transported through a 1000 m deep mixed layer near the surface with deposition velocities of 1 to 0.1 cm/s have atmospheric residence times ranging from 1 to 11 days (Section 3.5.1, 3.5.3). When particles are trapped in a layer well aloft they may survive even longer periods. Therefore, transport distances of several hundred to several thousand kilometers are possible.

Direct evidence of such transport aloft is available from satellite monitoring of back scattered solar radiation. The most prominent plume is that of Sahara dust from West Africa (Section 6.2). This plume has been observed to extend during the spring and summer months to the east coast of the United States, especially over Florida (Figure 6-6). Ground level measurements in Bermuda indicate that southeasterly winds bring high concentrations of soil- and crustal-related aerosols which appear to be from the Sahara desert (Wolff et al., 1986). Other large plumes exist, such as the Asian plume. However, the satellite observations do not indicate that it reaches the west coast of the United States (Figure 6-6).

Field measurements and modeling studies can be used as aids in the derivation of background values for aerosol constituents. Either approach is subject to considerable uncertainty and each has its own advantages and limitations. Field data would be the most logical choice if it could be shown to be completely free of anthropogenic influences originating within North America, i.e., background (2), (following the guidelines set out above for defining background levels unaffected by pollution sources within North America). A number of difficulties arise in interpreting field data for this purpose, namely: (a) there are very few tracers (e.g., ^{14}C) which can be used to distinguish between anthropogenic and biogenic source categories of aerosol constituents; (b) multilayer trajectories should be used to identify source regions since layer-average trajectories may underestimate the geographic area contributing pollutants to the air mass sampled; (c) sampling must also be carried out for long enough periods to obtain statistically representative values over seasonal time scales. Determining the history of air parcels is difficult in locations subject to small scale circulations such as cumulus convection and land-sea or mountain-valley breezes. In addition, all small localized anthropogenic sources of particulate matter must be identified during sampling. Ideally, measurements should be carried out long enough for the measurements to be shown to be generally representative of the time period of interest e.g., seasonal average, annual average.

Alternatively, models which include only natural sources and anthropogenic sources located outside North America could be used. Their utility is limited by inadequacies in model formulation, such as grid spacing and knowledge of the strengths, locations, and variability of various sources. Since a large fraction of particulate matter is secondary, uncertainties in the

chemistry of precursor gases will play a large role in determining the uncertainty of the final results. These uncertainties are especially large for the yield of aerosol produced by the oxidation of biogenic hydrocarbons as pointed out in Chapters 3 and 5. Uncertainties in the chemistry of NO_x and SO_2 are also important in that they affect estimates of the yield of aerosol products versus the deposition of intermediate species.

Trijonis (1982, 1991) has attempted to estimate $PM_{2.5}$ and PM_{10} concentrations corresponding to background (1), the "natural" background. His approach was to obtain concentration values only from those biogenic and geogenic sources which are at or below those possibly associated with preindustrial conditions over North America. Annual average concentrations of the chemical species in particulate matter were estimated for the eastern United States and for mountain/desert regions of the western United States. Seasonal "natural" background concentration values were not estimated. The annual average concentrations of fine particles were estimated separately for sulfates; as NH_4HSO_4, nitrates; as NH_4NO_3; organic carbon; elemental carbon; soil dust and water (Trijonis, 1982, 1991). In the later work, coarse particle concentration values were also estimated (Trijonis, 1991). In addition, in the later work, it was emphasized that the concentration values proposed can have error factors ranging from 1.5 to 3 for individual chemical species in particulate matter.

In the earlier work (Trijonis, 1982), a fine particle "natural" background for the eastern United States is estimated at 5.5 ± 2.5 $\mu g/m^3$. Excluding water, the background value would be 4 ± 2 $\mu g/m^3$ with the largest contribution, 2 $\mu g/m^3$, from organic carbon. In the later estimates (Trijonis, 1991), a fine particle "natural" background for the eastern United States of 3.3 $\mu g/m^3$ is estimated. Excluding water, this background would be 2.3 $\mu g/m^3$ with 1.5 $\mu g/m^3$ associated with organic carbon. A separate estimate is given for the fine particle "natural" background over the mountain/desert regions of the western United States of 1.2 $\mu g/m^3$. Excluding water, this background would be 1 $\mu g/m^3$ with 0.5 $\mu g/m^3$ associated with organic carbon. The coarse particle "natural" background for both the eastern and western United States is estimated at 3 $\mu g/m^3$.

Fernam et al. (1981) also estimated "natural" background concentrations for $PM_{2.5}$ constituents in the eastern United States during summer. They estimated natural contributions

to sulfate of 0.5-1.9 $\mu g/m^3$, to organic carbon of 3.7 $\mu g/m^3$, and to crustal material of 1.7 $\mu g/m^3$.

To obtain these "natural" background estimates, a wide range of approaches are used varying from natural SO_2 and NO_x emissions inventories to $SO_4^=$, NO_3^- and elemental carbon concentration measurements in remote locations in the northern and southern hemispheres. Carbon isotope ratios and organic composition measurements for organic components are used from several sites in the southwestern United States.

Results of three-dimensional models that could be used to estimate each of the five background levels for all the major categories of aerosol composition listed above are not available. Liousse et al. (1996) have performed three-dimensional chemical tracer model simulations of the global distribution of elemental and organic carbon. Background values assuming only natural sources (background 1) were also calculated. Average organic carbon concentrations calculated for the month of July were all less than 1 $\mu g/m^3$ in the United States. These calculations were made assuming a 5% yield of secondary organic carbon from the oxidation of terpenes (cf. Section 5-3).

Another approach is to use results from rural/remote sites in national parks, wilderness areas and national monuments from the IMPROVE monitoring measurements. Results for the period between March 1988 and February 1991 have been published (Malm et al., 1994). The tabulations of results are given on an annual average basis for individual IMPROVE sites and on a seasonal basis by IMPROVE subregion for fine mass; sulfate, as $(NH_4)_2SO_4$; nitrate, as NH_4NO_3; organic and elemental carbon; fine soil and coarse mass. These measurements do not differentiate between anthropogenic and non-anthropogenic contributions and do not stratify measurements values by wind direction or by use of trajectories representing various air masses (Malm et al., 1994). However, a large set of measurements, including seasonal measurements, are provided at a substantial number of rural/remote sites, especially in the western United States.

In stratifying the IMPROVE results a problem arises because the Colorado plateau "subregion" with seven sites straddles the boundary between the southwest and northwest used subsequently (Figure 6-28). Four of the sites are north of the boundary in Utah and Colorado and three of the sites are south of the boundary in Arizona and New Mexico. The authors

place the Colorado plateau in the southwest for purposes of a fine mass composition budget (Malm et al., 1994). Since they assign only one other subregion, Sonora desert, with two sites to the southwest, the method of assigning sites can significantly affect the resulting estimates of regional fine mass concentrations. This problem can be avoided for the annual average values which are shown by individual sites, but not for the seasonal values which are lumped by subregion. This lumping also requires deciding whether a subregion with five sites, central Rocky Mountains, should be given the same or five times the weight of the other subregions in the northwest with only one or two sites each. For the annual average values given in Table 6-2 the sites are assigned consistent with the division between the northwestern and southwestern regions shown in Figure 6-28, excluding three sites in the northern California coastal mountains considered separately. A transitional region between the western mountains and deserts and the eastern United States has been considered consisting of five sites in three subregions from West Texas (2), to South Dakota (1) up to the Boundary Waters subregion (2) near the Canadian border. In addition, the result for particulate matter from the Appalachian subregion (2) are given. Previous measurements of particulate matter at sites in the eastern mountains are available (Stevens et al., 1980); Pierson et al., 1980b; Wolff et al., 1983). The measurements listed in Table 6-2 include $PM_{2.5}$ sulfate, as $(NH_4)_2SO_4$, organic carbon, and $PM_{(10-2.5)}$.

The annual average $PM_{2.5}$ increases substantially from west to east in Table 6-2 from a value of 3.55 $\mu g/m^3$ in the northwestern United States to 10.91 $\mu g/m^3$ in the Appalachian mountains. The annual average $(NH_4)_2SO_4$ concentration increases even more substantially from west to east from a value of 0.88 $\mu g/m^3$ in the northwestern United States to 6.33 $\mu g/m^3$ in the Appalachian Mountains. The lowest annual average organic carbon concentration of 1.38 $\mu g/m^3$ occurs in the southwestern United States and increases to 2.97 $\mu g/m^3$ in the Appalachian Mountains. A smaller range of concentrations occurs for organic carbon from west to east than for $PM_{2.5}$ and $(NH_4)_2SO_4$. The $(NH_4)_2SO_4$, as a percentage of $PM_{2.5}$, increases into the transitional region and the Appalachian Mountains from as low as 25% of the $PM_{2.5}$ at sites in the northwestern United States up to 58% at sites in the Appalachian Mountains. Conversely, organic carbon decrease as a percentage of $PM_{2.5}$ from 46% at sites in northwestern United States down to 27% in the Appalachian Mountains. Within the

TABLE 6-2. ANNUAL AVERAGE CONCENTRATIONS AND CHEMICAL COMPOSITION FROM IMPROVE MONITORING SITES

	No. of	Annual Average Concentrations, $\mu g/m^3$ and Composition				
			$(NH_4)_2SO_4$/	Organics/	PM	
Northwest[a]	15	3.55	0.88/25	1.63/46	4.46	8.0
Southwest[b]	5	3.91	1.28/33	1.38/35	5.62	9.5
California Coastal Mountains[c]	3	4.99	1.41/28	1.95/39	8.85	13.8
Transitional Region[d]	5	5.15	1.97/38	2.01/39	6.54	11.7
Appalachian Mountains[c]	2	10.91	6.33/58	2.97/27	6.24	17.2

[a]Cascades (1), central Rocky Mt. (5), Great Basin (1), N. Rocky Mt. (1), Sierra Nevada (1), Sierra Humboldt (2), and Colorado Plateau (4)
[b]Colorado Plateau (3), Sonora Desert (2)
[c]Same as subregion
[d]Western Texas (2), northern Great Plains (1), Boundary Waters (2).

western United States there are somewhat higher percentages of $(NH_4)_2SO_4$ and lower percentages of organic particles in the southwestern United States than in the northwestern United States. $(NH_4)_2SO_4$ plus organic carbon account for from 67% to 85% of $PM_{2.5}$, with the higher percentages at IMPROVE sites east of the Rocky Mountains (Table 6-2).

Compared to the estimates discussed by Trijonis (1982, 1991) for "natural" background, $PM_{2.5}$ values in the western United States of 1 $\mu g/m^3$, the average measured contractions of $PM_{2.5}$ in the northwestern and southwestern United States of 3.55 $\mu g/m^3$ and 3.91 $\mu g/m^3$ suggest anthropogenic contributions. The IMPROVE measurements are likely to include anthropogenic contributions from sources within North America (background 3). Even the lowest annual average $PM_{2.5}$ value in the contiguous United States of 2.5 $\mu g/m^3$ at Bridger Wilderness Area, WY, is over twice the "natural" background. The Denali NP in Alaska has an average annual $PM_{2.5}$ of 2 $\mu g/m^3$ (Malm et al., 1994). The organic carbon concentrations measured there are somewhat closer to the estimated "natural" background in the western mountains/desert of 0.5 $\mu g/m^3$ (Trijonis, 1991). However, average annual concentrations in the northwestern and southwestern United States are higher with values of 1.63 $\mu g/m^3$ and 1.38 $\mu g/m^3$. The annual average values at several IMPROVE monitoring sites in the Rocky Mountains are near 1 $\mu g/m^3$, while the Denali NP in Alaska has an average annual organic

carbon concentration of 0.85 $\mu g/m^3$. These latter organic carbon concentration values ares at the two fold upper limit of uncertainly in the estimate of "natural" background. On the other hand, the $(NH_4)_2SO_4$ concentrations measured in the west are far above the "natural" background for $(NH_4)_2SO_4$ of 0.1 $\mu g/m^3$ (Trijonis, 1991). The lowest measured annual average $(NH_4)_2SO_4$ at several sites are near 0.5 $\mu g/m^3$. For $PM_{(10-2.5)}$, the annual average concentrations in the northwestern and southwestern United States of 4.46 $\mu g/m^3$ and 5.62 $\mu g/m^3$ are within the two fold upper limit of uncertainty in the estimate of "natural" background. At a number of individual sites, annual average $PM_{(10-2.5)}$ concentrations are 3 $\mu g/m^3$ to 3.5 $\mu g/m^3$, close to the estimated "natural" background. Therefore, the largest deviations from the "natural" background estimates for a major component occur for $(NH_4)_2SO_4$.

Comparisons of the measured concentration values in the "transitional" area of the eastern United States, using sites from west Texas to the Boundary Waters, find that the average annual concentrations for $PM_{2.5}$ of 5.15 $\mu g/m^3$; $(NH_4)_2SO_4$ of 1.97 $\mu g/m^3$; organic carbon of 2.01 $\mu g/m^3$ and $PM_{(10-2.5)}$ of 6.54 $\mu g/m^3$ (Table 6-2) usually are well above the estimates of "natural" background in the eastern United States (Trijonis, 1991) for $PM_{2.5}$ of 2.3 $\mu g/m^3$; $(NH_4)_2SO_4$ of 0.2 $\mu g/m^3$; organics of 1.5 $\mu g/m^3$; and $PM_{(10-2.5)}$ of 3 $\mu g/m^3$. As in the western United States, the measured $(NH_4)_2SO_4$ concentration values are far above the "natural" background value, while the measured concentrations of organics are well within the two fold uncertainty in the "natural" background value.

Another source of lower PM_{10} concentrations are rural/remote AIRS monitoring sites. Based on 1993 measurements, the lowest values of PM_{10} are as follows: Rosebud Co., MT (maximum of 10 $\mu g/m^3$, annual mean of 4.5 $\mu g/m^3$); Campbell Co., WY (maximum of 15 $\mu g/m^3$, annual mean of 7.0 $\mu g/m^3$); and Washington Co., ME (maximum of 23 $\mu g/m^3$, annual mean of 8.8 $\mu g/m^3$). These PM_{10} values agree within a factor of two with the estimated "natural" background PM_{10} in the western United States of 4 $\mu g/m^3$, and in the eastern United States of 5.3 $\mu g/m^3$ (Trijonis, 1991).

Seasonal variations in particulate matter are also important and have been considered. The source used for these seasonal values in particulate matter is the IMPROVE monitoring network (Malm et al., 1994). Because the seasonal values are reported only by IMPROVE

subregions, there is no good approach to averaging values from differing numbers of sites within the varying geographical extent of IMPROVE subregions. Therefore, the values of annual average, summer and winter values for $PM_{2.5}$, $(NH_4)_2SO_4$, organic carbon, and $PM_{(10-2.5)}$ are listed for a number of IMPROVE subregions (Table 6-3).

TABLE 6-3. ANNUAL SUMMER AND WINTER CONCENTRATIONS FROM IMPROVE MONITORING SITES[a]

Subregion	Region of U.S.	No of Sites	Seasons of the Year	$PM_{2.5}$	$(NH_4)_2SO_4$	Organics	PM Coarse
Central Rockies	NW	5	annual	3.3	0.8	1.5	4.8
			summer	4.8	1.0	2.4	7.5
			winter	2.0	0.5	0.9	3.0
Colorado Plateau	NW-SW	7	annual	3.4	1.1	1.2	4.7
			summer	4.1	1.3	1.6	6.4
			winter	2.9	0.9	1.1	3.2
Coastal Mountains	NW	3	annual	5.0	1.4	1.9	8.9
			summer	4.5	1.9	1.4	10.7
			winter	5.6	0.9	2.3	7.7
Sonora Desert	SW	2	annual	4.4	1.5	1.5	6.0
			summer	5.6	2.1	1.8	7.6
			winter	3.2	1.2	1.1	3.3
West Texas	Transitional to east	2	annual	5.4	2.1	1.5	7.5
			summer	6.6	2.5	1.7	7.4
			winter	3.6	1.5	1.1	5.1
Northern Great Plains	Transitional to east	1	annual	4.5	1.5	1.5	6.3
			summer	5.6	1.8	2.2	9.7
			winter	3.4	1.2	1.1	3.9
Boundary Waters	Transitional to east	2	annual	5.3	2.0	2.1	5.7
			summer	6.2	2.2	3.1	8.2
			winter	5.2	2.0	1.4	3.2
Appalachian Mountains	Eastern U.S.	2	annual	10.9	6.3	3.0	6.2
			summer	16.6	10.5	4.4	11.2
			winter	6.5	3.0	2.0	3.1

[a] From Malm et al., 1994.

Annual average concentration almost always are intermediate between the summer and winter concentration of particulate matter listed in Table 6-3. With a few exceptions, the summer concentrations are higher than winter concentrations. The exceptions are the higher winter concentrations for $PM_{2.5}$ and organics in the coastal mountains. Ratios of summer to winter concentrations can equal or exceed two for all listed particulate components in both the central rockies subregion and the Appalachian Mountains. The summer to winter concentration ratios for $PM_{2.5}$ are within the 1.5 to 2.5 range except for the coastal mountains and Boundary Waters subregion. The summer to winter concentration ratios for PM coarse equal or exceeds two except for the coastal mountains. Therefore, in most rural remote sites in IMPROVE subregions summer concentrations of particulate matter substantially exceed winter concentrations. However, it must be emphasized that it is not appropriate to extrapolate these results obtained at IMPROVE sites in 1988 to 1991 to other sites or even to other years of monitoring at IMPROVE sites.

Within the continental United States, there are measurements of particulate mass and chemical composition under conditions identified as "clean" background conditions (Wolff et al., 1983). These are based on 7 days of measurements during the summer of 1978 at a site 40 km northwest of Pierre, South Dakota and 18 days during the summer of 1979 at a site 15 km north of the Gulf Coast, near Abbeville, LA. At the South Dakota site the small variations in anthropogenic pollutants observed was attributed to a lack of any major pollution sources along the trajectories. In contrast, at the Louisiana site the days were stratified into "clean" days when the air had passed over the Gulf of Mexico for several days and much more polluted episode days when the maritime air was modified by air which had undergone transport from the midwestern and northeastern United States.

Fine particle mass on "clean" days averaged 11 to 13 $\mu g/m^3$ and coarse mass between 9 and 19 $\mu g/m^3$ at the two sites. The total mass averaged between 21 and 32 $\mu g/m^3$. Organic carbon at both sites was the most important fine particle species averaging 4 to 8 $\mu g/m^3$ (organic mass multiplied by 1.2 to include H and O), while sulfate averaged 3 $\mu g/m^3$.

At the closest IMPROVE site, the Badlands National Monument, SD in the northern great plains subregion (Table 6-3), for the summers of 1988 and 1989 (Malm et al., 1994) the concentrations were $PM_{2.5}$, 5.6 $\mu g/m^3$; $(NH_4)_2SO_4$, 1.8 $\mu g/m^3$; organic carbon, 2.2 $\mu g/m^3$ and

$PM_{(10-2.5)}$, 9.7 $\mu g/m^3$. These concentration values are substantially lower than those obtained at the site 40 km northwest of Pierre, SD in the summer of 1978 as follows: $PM_{2.5}$, 13 $\mu g/m^3$, $(NH_4)_2SO_4$, 3.2 $\mu g/m^3$; organic carbon 3.8 $\mu g/m^3$ and $PM_{(10-2.5)}$, 19 $\mu g/m^3$.

There are several reasons for the differences between the "clean" values and the IMPROVE values. (a) The measured background varies from year to year and site to site. (b) Precipitation periods were excluded by Kelly et al. (1982) and Wolff et al. (1983), but the IMPROVE monitoring network measurements include all weather conditions. All other conditions being the same, the inclusion of precipitation events in the IMPROVE measurements probably biases the results low because of rain-out of particulate matter. (c) On the other hand, the presence of material from anthropogenic sources probably biases the results high. Wolff et al. (1983) used trajectory analyses to exclude periods with intrusions of polluted air from their analysis. This was not done with the IMPROVE results. However, the layer-averaged trajectories used by Wolff et al. (1983) may have underestimated the mixing of air parcels from surrounding geographical areas leading to an underestimate of the potential for anthropogenic contributions. The exact causes for the differences between these two types of "background" estimates cannot be quantitated from available data.

For sulfate, it is possible to make a limited comparison with measurements at rural sites outside of St. Louis with air flow from the northwest during the third quarters of 1975 and 1976 (Altshuller, 1987), background 5. The average third quarter sulfate concentrations at these sites for these two years was 7 $\mu g/m^3$, a substantially higher sulfate concentration than in South Dakota (Wolff et al., 1983), but lower than measured in other wind directions. These measurements outside of St. Louis also indicate substantially lower sulfate concentrations during the first and fourth quarters of 1975, 1976, and 1977 averaging 3.4 $\mu g/m^3$, comparable to the third quarter sulfate concentrations in South Dakota.

It is important to emphasize that the "background" for particulate matter moving toward cities along the east coast over the Great Smoky Mountains (Stevens et al., 1980); the Allegheny Mountains (Pierson et al., 1980b) and the Blue Ridge Mountains (Wolff et al., 1983), background 4, are much higher than for the "clean" air days in South Dakota and Louisiana. For example, the fine particle matter at the Blue Ridge Mountain site in July and August 1980 with trajectories from the midwest source areas and the Tennessee Valley source

area averaged 27 and 24 $\mu g/m^3$, approximately twice the values under "clean" air conditions in South Dakota and Louisiana (Wolff et al, 1983). The sulfate concentrations for these two trajectory directions averaged 14 and 9 $\mu g/m^3$, with sulfate substantially exceeding organic carbon. This result is a reversal in the chemical composition under the "clean" air conditions in South Dakota and Louisiana, but more consistent with the chemical composition under "episodic" conditions in Louisiana when the sulfate concentration averaged 20 $\mu g/m^3$ and the organic carbon averaged 15 $\mu g/m^3$.

Because of the repeated occurrence of $(NH_4)_2SO_4$ concentrations far above "natural" background even at rural/remote sites, this aspect justifies additional consideration.

A low contribution of natural sources of gaseous sulfur (both terrestrial and marine) occurs in the eastern United States (Trijonis, 1991). However, a more detailed consideration of the contribution of natural sources of gaseous sulfur indicates wide variations over the United States (Placet, 1991). The following estimates for the ratios of total natural gaseous sulfur to total anthropogenic gaseous sulfur by region (Placet, 1991) are as follows: northeast, 0.01; southeast, 0.03; west gulf, 0.03; southwest, 0.12; northwest, 0.19. The corresponding ratios for coastal areas are higher with an estimate of 0.52 for the California coastal areas. If these ratios are converted to ratios of total natural gaseous sulfur to total gaseous sulfur, the ratios would be 0.11 in the southwest and 0.16 in the northwest. If the following assumptions are made (a) both natural and anthropogenic sulfur are converted to $(NH_4)_2SO_4$ to about the same extent; (b) the concentrations of natural $(NH_4)_2SO_4$ can be obtained by multiplying the above ratios by the measured $(NH_4)_2SO_4$ concentrations, the natural sulfur concentrations in the southeast would range from 0.1 to 0.15 $\mu g/m^3$ and in the northwest from 0.08 $\mu g/m^3$ to 0.2 $\mu g/m^3$.

A more detailed consideration of the contribution of natural gaseous sulfur at sites near the Pacific coast is available (Kreidenweis, 1993). In particular, comparisons with measured $(NH_4)_2SO_4$ concentrations were made at the Crater Lake National Park in southwestern Oregon with estimates of natural $(NH_4)_2SO_4$ concentrations. The measured annual average concentration at this site of $(NH_4)_2SO_4$ was 0.5 $\mu g/m^3$ and an average "low" concentration was approximately 0.13 $\mu g/m^3$ (Kreidenweis, 1993). This latter value can be compared with several estimates of natural $(NH_4)_2SO_4$ concentration based on the following approaches (a) a

natural source column burden between 35 to 50° north of 0.05 to 0.15 $\mu g/m^3$; (b) a Pacific natural source column estimate between 35 to 50° N of 0.18 $\mu g/m^3$ and (c) a 3 D model value of 0.14 to 0.28 $\mu g/m^3$. Other approaches gave higher possible values for natural $(NH_4)_2SO_4$ (a) "clean" rainfall sulfate concentrations of 0.1 to 0.5 $\mu g/m^3$ and (b) another 3-D model value of 0.6 $\mu g/m^3$. These comparisons results in a wide range of annual average values of $(NH_4)_2SO_4$ from less than 0.1 $\mu g/m^3$ to less than 0.5 $\mu g/m^3$ (Kreidenweis, 1993).

Even an upper limit value for natural $(NH_4)_4SO_4$ of 0.5 $\mu g/m^3$ would be a third to a half of the measured $(NH_4)_2SO_4$ at IMPROVE sites near the Pacific Coast (Malm et al., 1994). Further inland, at interior western sites, the marine sources of natural sulfur should make an even smaller contribution to the measured concentrations of $(NH_4)_2SO_4$. Comparison of these $(NH_4)_2SO_4$ with the estimates based on regional sulfur inventories (Placet, 1991) of 0.08 to 0.2 $\mu g/m^3$ would indicate a significant anthropogenic contribution even at relatively remote western IMPROVE sites. This result suggests that background 3 may have a substantial contribution from anthropogenic sulfur sources in North America.

As a summary to the discussion in Section 6.3.1.7, the estimated lower limit and upper limit background concentrations for PM_{10} and $PM_{2.5}$ are given on an annual average basis and for winter and summer for the western and eastern United States in Table 6-4.

TABLE 6-4. SUMMARY OF ANNUAL AND SEASONAL AVERAGE RANGES OF BACKGROUND CONCENTRATION LEVELS OF PM_{10} AND $PM_{2.5}$

		Concentrations, $\mu g/m^3$	
PM	Annual or Seasonal	Western United States	Eastern United States
PM_{10}	Annual average	4 - 8	5 - 11
$PM_{2.5}$	Annual average	1 - 4	2 - 5
PM_{10}	Winter	4 - 6	5 - 8
$PM_{2.5}$	Winter	1 - 3	2 - 4
PM_{10}	Summer	4 - 12	5 - 14
$PM_{2.5}$	Summer	1 - 5	2 - 6

The lower limit concentrations are based on the "natural" background midrange concentrations discussed (Trijonis 1991). There are error factors associated with the chemical species used to obtain these concentrations range from 1.5 to 3.

The upper limit concentrations are based on measured concentrations from IMPROVE monitoring sites (Malm et al., 1994). The $PM_{2.5}$ concentrations are the sum of concentrations measured for individual chemical species. As noted earlier in Section 6.3.1.7, these measured concentrations can include some anthropogenic source contributions within North America. Therefore, the upper limit concentrations represent conservative values for the upper end of the background concentration type.

To obtain the upper limit concentrations, the averages were obtained from the concentrations for nine subregions in the western United States giving each region equal weight and also weighing the contribution of each subregion by the number of sites in the subregion. The median values were also obtained. For the eastern United States, the averages were obtained from the concentrations for three subregions in the "transitional" region. For the annual average from 23 individual sites in the western United States and 5 sites in the "transitional" region (Table 6-3). The resulting values for upper limit concentrations were closely clustered usually with a 1 $\mu g/m^3$ range. Within these values, the lower whole value concentration was listed in Table 6-4.

As a supplement to the data collected in the IMPROVE/NESCAUM networks, seasonal and annual average PM_{10} concentrations were also taken from AIRS (1990 - 1995). Four inhabited areas with the lowest annual average PM_{10} concentrations were chosen in areas without nearby IMPROVE/NESCAUM sites. Annual, summer, and winter averages for Penobscot Co., ME (11.1, 13.8, and 10.0 $\mu g/m^3$); Marquette, MI (11.2, 15.5, and 7.0 $\mu g/m^3$); Mercer Co., ND (11.7, 12.9, and 10.6 $\mu g/m^3$); and Lakeport, CA (11.6, 14.3, and 10.0 $\mu g/m^3$) all fall within the upper limits set for PM_{10} shown in Table 6-4. All areas exhibit summertime maxima and wintertime minima. The similarity of these results to the upper limits shown in Table 6-4 suggests an anthropogenic component to those upper limits, since the AIRS values were obtained in inhabited areas.

Again, it should be mentioned that seasonal or annual average "background" values presented above will likely underpredict 24-hour maximum "background" values. Ambient

data could be used to estimate 24-hour maximum values, but their use is subject to considerable uncertainty because of possible anthropogenic inputs.

6.3.2 Urban National Aerosol Pattern—Aerometric Information Retrieval System

The urban monitoring network is operated by state and local agencies as mandated by the Clean Air Act. The data from this network are used to determine exceedences above the particulate matter standards. Federal regulations also require that these monitoring data be submitted to the EPA Aerometric Information and Retrieval System (AIRS). In what follows, AIRS PM_{10} refers to the PM_{10} mass concentration extracted from the AIRS database. The AIRS database is a useful resource for analyzing trends and concentration patterns, and relationships between the fine, coarse, and PM_{10} components of the atmospheric aerosol (Husar and Frank, 1991; Husar and Poirot, 1992).

The national average AIRS concentrations were calculated utilizing all of the available data since the beginning of 1985, when less than 100 monitoring stations were operational (Figure 6-17). Since that time, the number of monitoring stations has risen to more than 1,300 (Figure 6-17). The implications of the changing stations density to the above described national PM_{10} trend is not well studied. The emergence of new stations appeared to be in rough proportion to the final station density shown in Figure 6-17. In other words, in 1985, the national coverage had a pattern similar to 1994, except less dense. Changes in sampling equipment and monitoring protocols are also possible causes of systematic errors in the reported spatial pattern and trends.

The AIRS PM_{10} database reports the concentrations every sixth day for a 24-h sampling period, synchronously over the entire country. The sample duration is one day which, over the long run, provides the concentration distribution function of daily samples. For determination of the effects (human health, visibility, acid deposition) the concentration has to be known at the specific location where the sensitive receptors reside. Also the concentrations have to be known at a short (e.g., daily) time scale, as well as over the long term.

In order to characterize the one day-scale temporal variation over a given region, the entire available data aggregated over the entire region for each monitoring day are plotted as

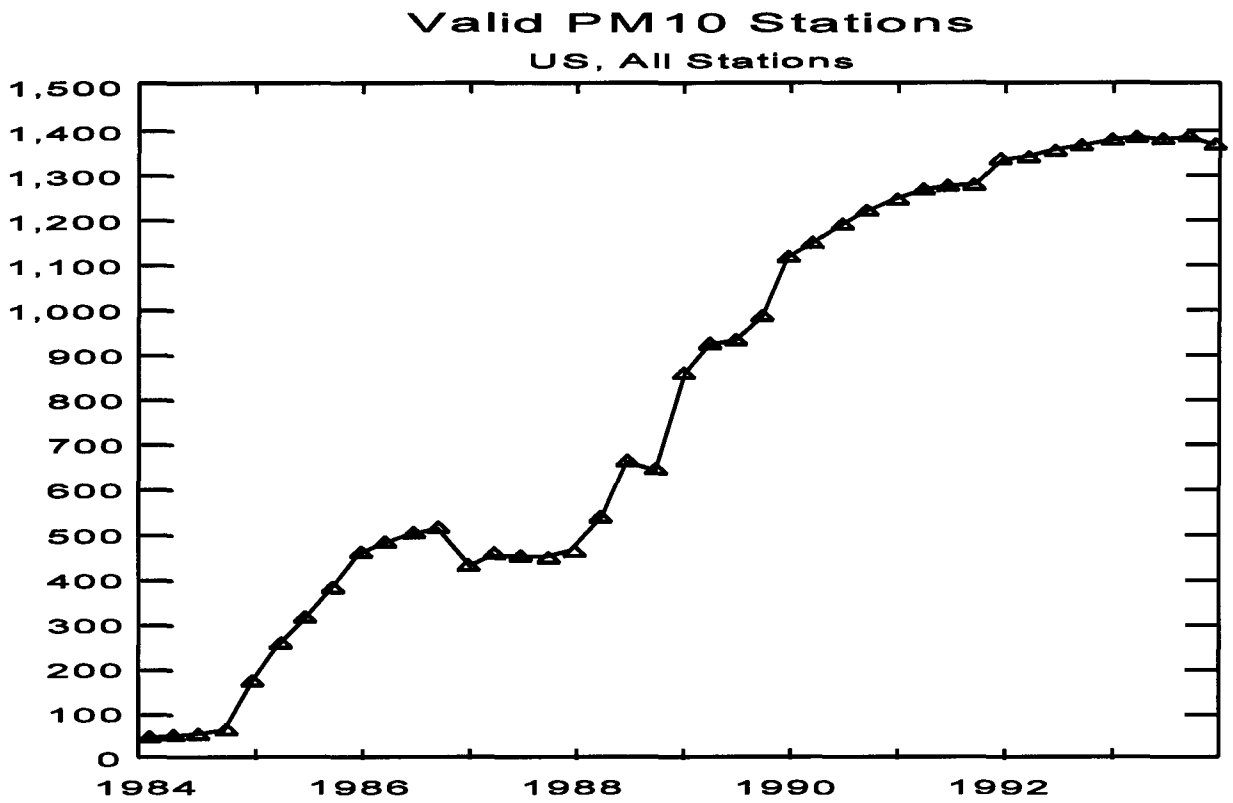

Figure 6-17. Trend of valid PM_{10} monitoring stations in the AIRS database.

time series. It is recognized that during the other five non-monitored days, the concentrations may be different from the reported value. The six day sample increment ensures that both weekday and weekend data are properly taken into account.

The AIRS PM_{10} stations are mostly in urban areas but some suburban and nonurban sites are also reported. The analysis presented in this section is based on PM_{10} and $PM_{2.5}$ data retrieved from AIRS in October 1994.

The results of AIRS PM_{10} aerosol pattern analysis are presented in quarterly contour maps, as well as seasonal time charts. For valid monthly and quarterly aggregation, it was required to have at least two samples a month, and six samples per quarter. For the seasonal maps all the available data between 1985 to 1994 were used.

The seasonal contour maps also show the location of the PM_{10} monitoring sites. The size of the rectangle at each site is proportional to the quarterly average PM_{10} concentration

using all available data between 1985 to 1994. Hence, sampling biases due to station density that changed over time can not be excluded.

The quarterly concentration pattern of PM_{10} is shown in Figure 6-18. The high sampler density allows the resolution of spatial texture on the scale of 100 km, particularly over major metropolitan areas. However, remote regions in the central and western states have poor spatial density. In the absence of rural monitoring data computerized contour plotting of PM_{10} is biased toward extrapolating (spreading) high concentrations over large areas. This bias is particularly evident in the maps for Quarters 1 and 4 in the western states, where the area of high concentration hot spots is exaggerated.

The AIRS PM_{10} concentrations over the eastern United States are lowest during Quarter 1, ranging between 20 to 30 $\mu g/m^3$. The higher concentrations exceeding 30 $\mu g/m^3$ are confined to metropolitan areas.

6.3.2.1 National Pattern and Trend of Aerometric Information Retrieval System PM_{10}

Two trend analysis approaches were used to obtain the 1988 to 1993 trends in PM_{10} shown in Figure 19b are subsequent figures providing AIRS concentration patterns. One of these approaches uses all of the available stations operational each year between 1988 and 1994. The second approach uses only those stations operational from 1988 to 1994, the long term coverage, trend, stations.

During the 1988 to 1994 period there were decreases in the annual average PM_{10} for the continental U.S. from 33 $\mu g/m^3$ to 25 $\mu g/m^3$, for all sites and from 35 $\mu g/m^3$ to 28 $\mu g/m^3$ for trend sites resulting in 24% or 20% reductions in PM_{10}.

The Figure 6-19b also shows the standard deviation among the yearly average PM_{10} concentrations for each year. On the national scale the standard deviation of yearly average concentrations is about 40% of the mean.

The concentrations of $PM_{2.5}$ and PM_{10} are compared in the scatter chart in Figure 6-19c. Each point represents a pair of $PM_{2.5}$-PM_{10} monthly average concentrations. The diagonal line is the 1:1 line and shows the fine particle concentration ranges between 20 and 85% of PM_{10}. The heavy solid line is derived from a linear best fit regression. The detailed correlation statistics is reproduced in the upper-left corner of the scatter charts. The

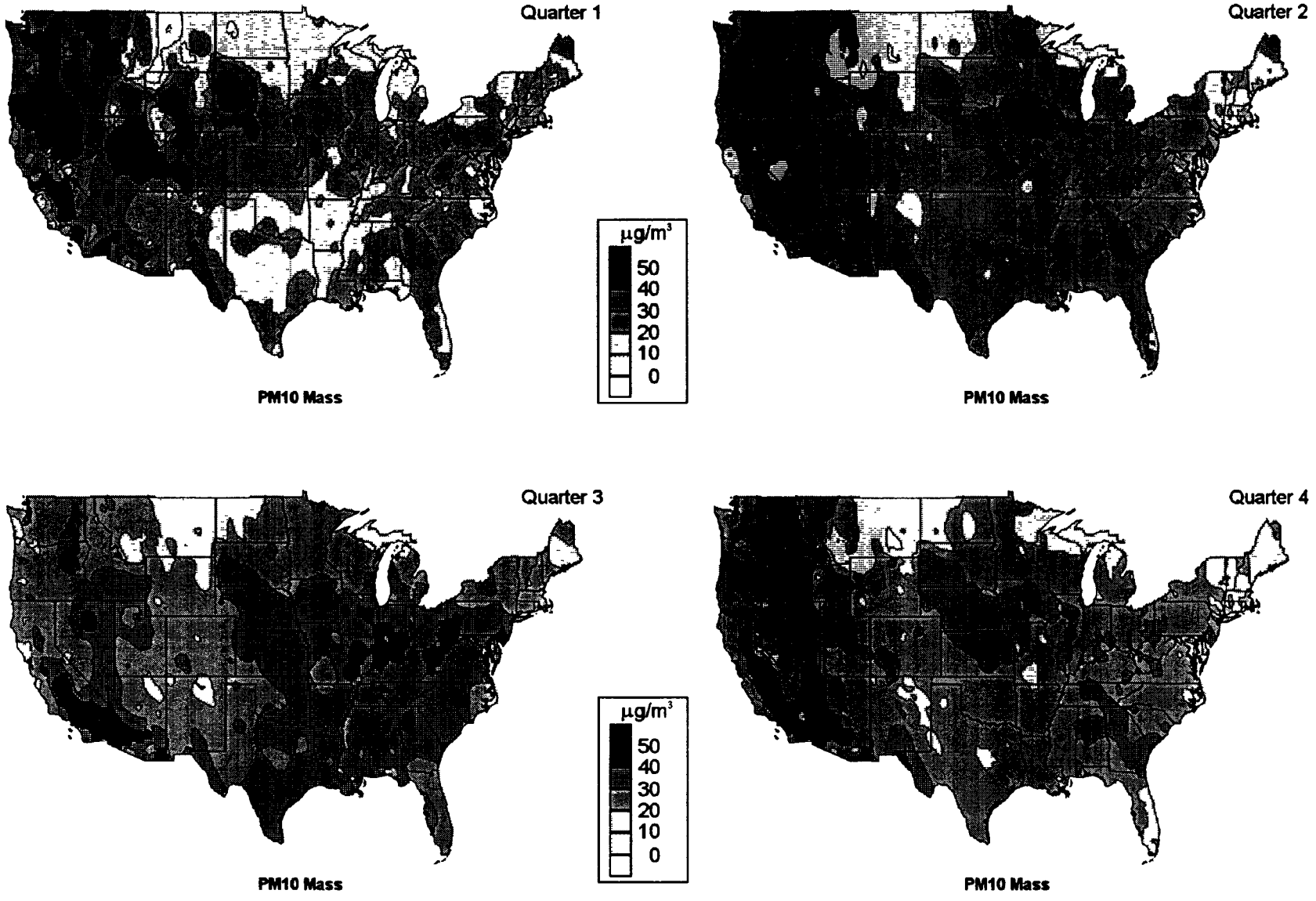

Figure 6-18. AIRS PM_{10} quarterly concentration maps using all available data.

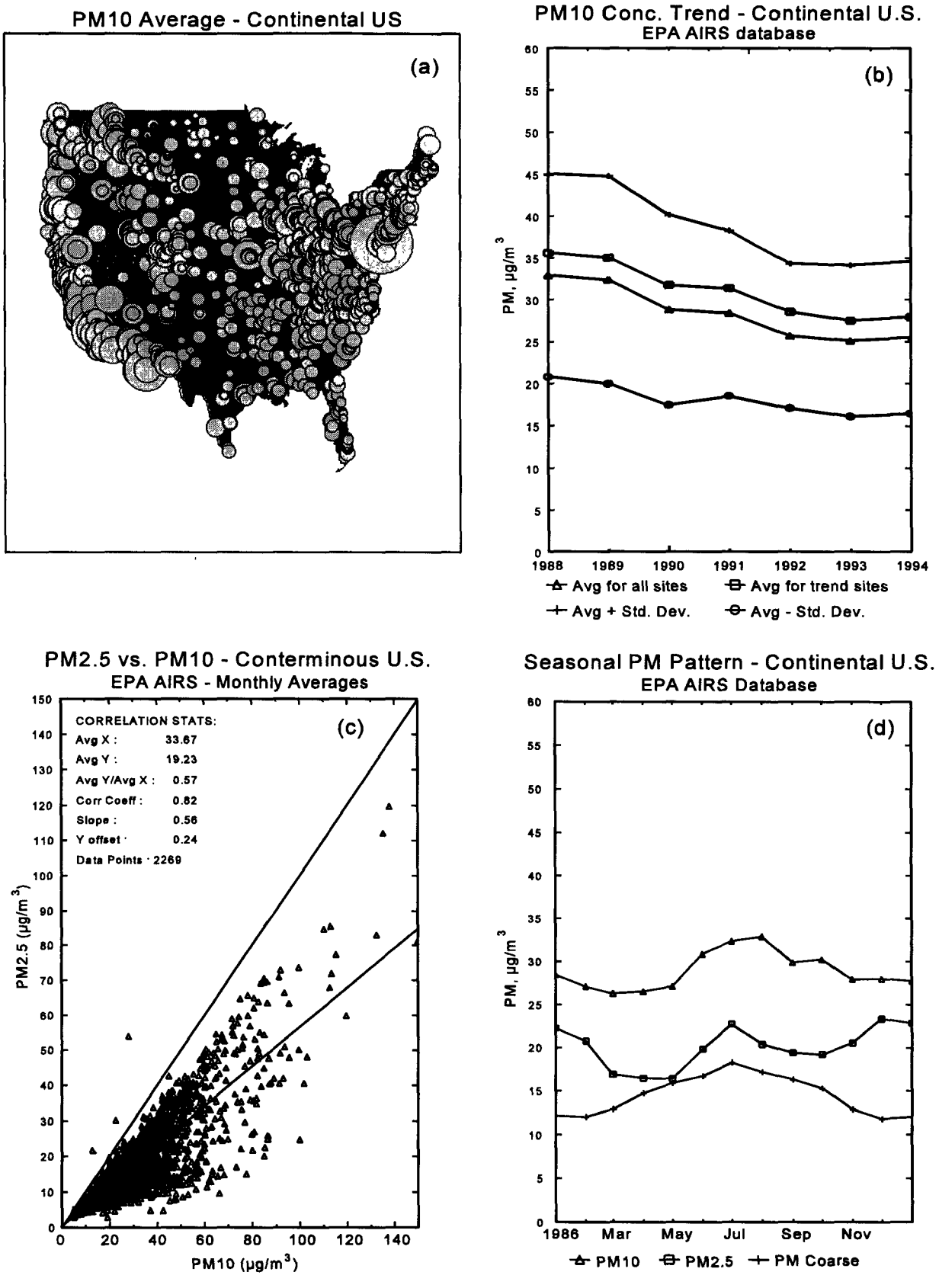

Figure 6-19. AIRS PM_{10} and $PM_{2.5}$ concentration patterns for the conterminous United States.

ratio of overall average $PM_{2.5}$ and overall average PM_{10} is also indicated. For the data when both PM2.5 and PM_{10} data were available, nationally aggregated $PM_{2.5}$ particles accounted for 57% of the PM_{10} mass.

The seasonal pattern of the national PM_{10} concentration is also depicted in Figure 6-19d, utilizing all available data in AIRS. The national average PM_{10} seasonality ranges between 27 $\mu g/m^3$ in March and April, and 33 $\mu g/m^3$ in July and August, yielding a modest 16% seasonal modulation. There is also evidence of slight bimodality with the December through January peak.

The seasonal chart also shows the annual variation of $PM_{2.5}$, and PM_{10}-$PM_{2.5}$ (i.e., coarse particles). The national fine particle concentration shows clear evidence of bimodality with peaks in July and December. It is shown below that the fine particle winter peak arises from western sites, while the summer peak is due to eastern U.S. contributions. The national average coarse particle concentration has a 50 % yearly modulation with a single peak in July.

Stratifying the national PM_{10} concentrations one can obtain results showing that the country has several major aerosol regions, as discussed in more detail below. Each region has a discernible geographic extent as well as seasonal pattern. Over the plains of the eastern United States the spatial texture of PM_{10} is driven by the pattern of the emission fields, while the seasonality of concentrations is likely to be determined by the chemical transformation and removal processes, as well as by the regional dilution. In the mountainous western and Pacific states, pockets of wintertime PM_{10} concentrations exist that well exceed the eastern U.S. values. It is believed that haze and smoke in confined mountain valleys and air basins are strongly influenced by topography which in turn influences the emission pattern, dilution, as well as the chemical transformation and removal rate processes.

Given the regionality of the aerosol concentration pattern much of the discussion that follows will be focused on the characteristics of these aerosol regions. The Rocky Mountains produce a natural division between the eastern and western aerosol regimes which will be discussed next.

6.3.2.2 Eastern U.S. PM_{10} Pattern and Trend

During the 1988 to 1994 period there were decreases in the annual average PM_{10} for the eastern U.S. from 31 $\mu g/m^3$ to 26 $\mu g/m^3$ for all sites and from 34 $\mu g/m^3$ to 28 $\mu g/m^3$ for trend sites resulting in 16% or 18% reductions in PM_{10} (Figure 6-20b). The decline is rather steady over time.

The highest eastern U.S. AIRS PM_{10} concentrations are recorded in Quarter 3 (Figure 6-20d). The peak concentrations are over the Ohio River Valley stretching from Pittsburgh to West Virginia, southern Indiana and St. Louis. In this region, the PM_{10} concentration over the industrialized Midwest during the summer can exceed 40 $\mu g/m^3$. Additional hot-spots with > 40 $\mu g/m^3$ are recorded in Birmingham, AL, Atlanta, GA, Nashville, TN, Philadelphia, PA and Chicago. IL. The summertime PM_{10} concentrations in New England and upstate Michigan are < 20 $\mu g/m^3$.

The transition seasons Quarters 2 and 4 (Figure 6-20d) show PM_{10} concentrations ranging from 25 $\mu g/m^3$ to about 30 $\mu g/m^3$ over much of the eastern U.S., with concentration hot-spots over the industrial Midwest as well as in the Southeast, Atlanta, GA and Birmingham, AL. The PM_{10} concentrations in urban-industrial "hot-spots" exceed their rural surrounding by less than a factor of two.

The spatial variability of PM_{10} occurring over the eastern United States is driven primarily by the varying primary aerosol emission density. This can be deduced from the coincidence of higher concentrations within urban industrial areas. The atmospheric dilution (i.e., horizontal and vertical dispersion) in these areas is not likely to be spatially variable. Also, the chemical aerosol formation and removal processes are likely to have weak spatial gradients when averaged over a calendrical quarter. Hence, the main factor that is believed to be responsible for the spatial variability is the emission field of primary PM_{10} particles and the SO_2, NO_x, and VOC precursors of secondary aerosols.

PM_{10} concentration in excess of 30 $\mu g/m^3$ is recorded over the agricultural states of Iowa, Kansas, Nebraska, and South Dakota. The elevated PM_{10} concentrations over this region tend to persist over all four seasons. The eastern PM_{10} seasonality (Figure 6-20d) is rather pronounced, with winter concentrations (December through March) of 24 $\mu g/m^3$, and

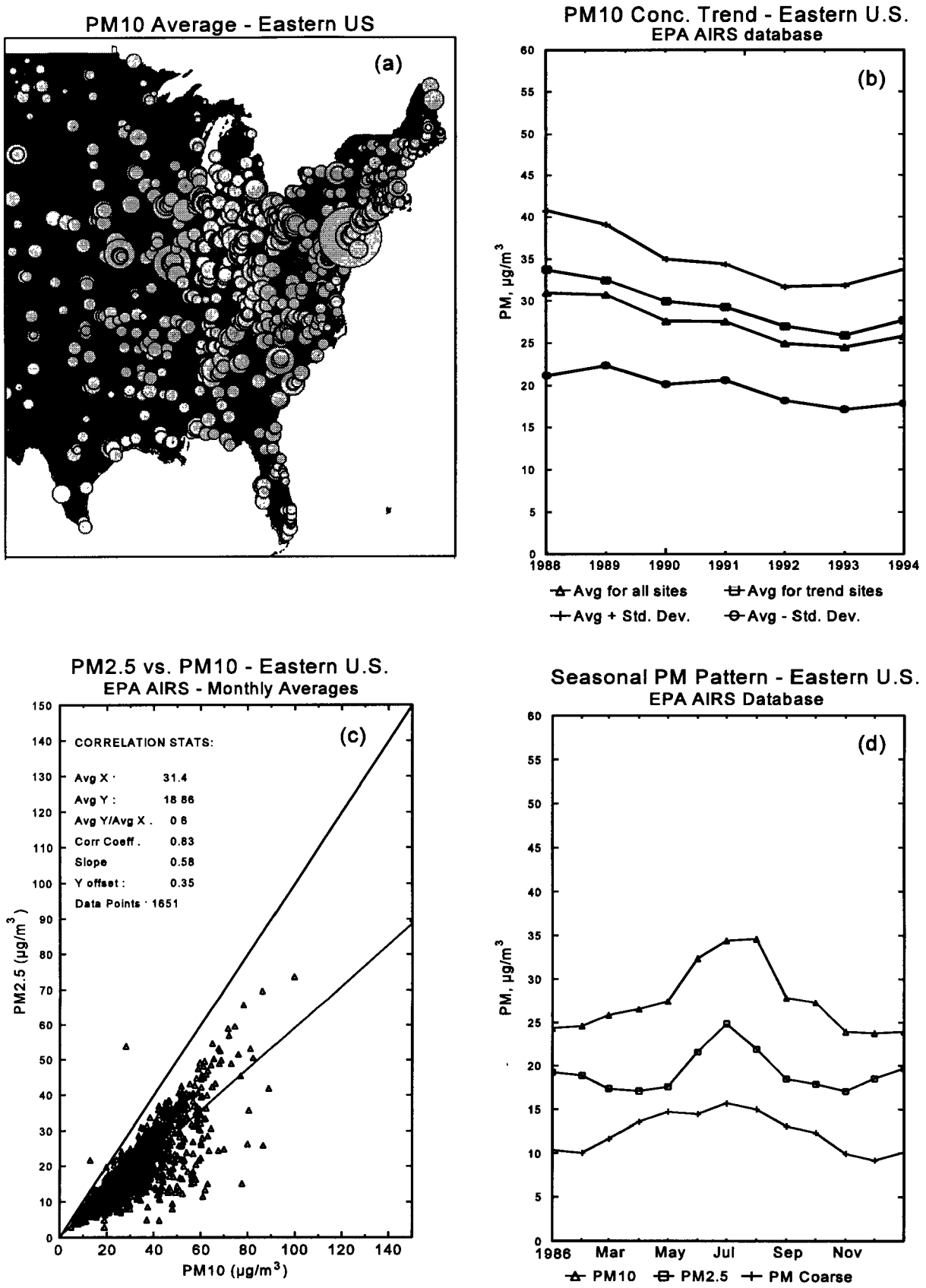

Figure 6-20. AIRS concentration data for east of the Rockies: (a) monitoring locations; (b) PM_{10} concentration trends; (c) PM_{10} and $PM_{2.5}$ relationship; and (d) PM_{10}, $PM_{2.5}$, and PMCoarse seasonal pattern.

July through August peak of 35 $\mu g/m^3$. The amplitude of the PM_{10} seasonal concentrations is about 30%.

The scatter chart of the eastern AIRS $PM_{2.5}$-PM_{10} relationship shows a significant amount of scatter, with a slope of 0.58 (Figure 6-20b). The ratio of the overall average $PM_{2.5}$ and PM_{10} concentration is 0.6 such that 60% of PM_{10} in the sub 2.5 μm size range. The seasonality of the fine AIRS particle concentration over the East is bimodal with a major peak in July and a smaller winter peak in January (Figure 6-20d). As shown in Figure 6-15b, the nonurban IMPROVE/NESCAUM network results for the eastern U.S. for $PM_{2.5}$ show a peak in summer but does not show a winter peak. The coarse particle concentration shows a single broad peak over the warm season, April through October (Figure 6-20d), but with a somwhat different pattern than shown in Figure 6-15b for nonurban cities in the eastern U.S. It is therefore evident that fine and coarse particles (from urban and nonurban measurements) have different seasonal dynamics in the East.

6.3.2.3 Western U.S. PM_{10} Pattern and Trend

The mountainous states, west of the Rockies (Figure 6-21) have higher PM_{10} concentrations in Quarters 1 and 4 than in Quarters 2 and 4 and shown ever higher PM_{10} concentrations (>50 $\mu g/m^3$) at localized hot-spots. These higher concentrations occur over both metropolitan areas such as Salt Lake City, as well as in smaller towns in mountain valleys of states west of the Rockies.

The main geographic feature regions considered in California are the Los Angeles basin and the San Joaquin Valley. Both basins show monthly PM_{10} concentrations sometimes in excess of 50 $\mu g/m^3$. These basins are also confined by surrounding mountains that limit the dilution, facilitate cloud formation, and have emissions that are confined to the basin floor. Accordingly, they represent airsheds with characteristic spatial and temporal pattern. It is likely that the actual local effects on the PM_{10} concentration field in the mountainous western states are greater than depicted in Figure 6-21a.

It appears that the spatial pattern of these high concentration hot spots is driven by emissions as well as by the restricted wintertime ventilation due to mountainous terrain. Over the mountainous western states the atmospheric dilution by horizontal and vertical dispersion is

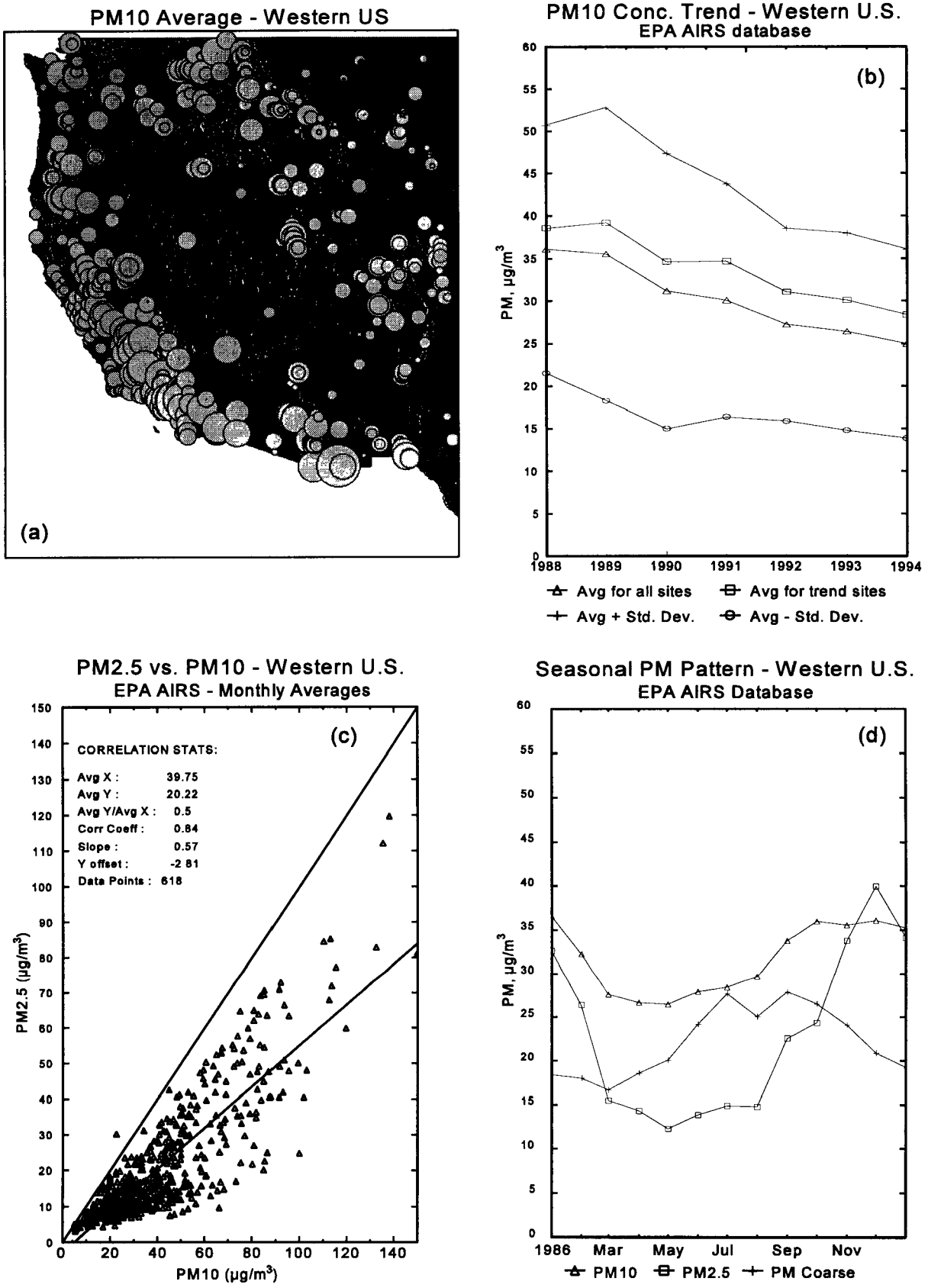

Figure 6-21. AIRS concentration data for west of the Rockies: (a) monitoring trends; (b) PM_{10} concentration trends; PM_{10} and $PM_{2.5}$ relationship; and (d) PM_{10}, $PM_{2.5}$, and PMCoarse seasonal pattern.

severely restricted by mountain barriers and atmospheric stratification due to strong and shallow inversions. Radiative cooling also causes fog formation which enhances the production rate of hydroscopic aerosols in the valleys. As a consequence, mountain tops are generally protruding out of haze layers. Emissions arising from industrial, residential, agricultural, unpaved roadways and other sources are generally confined to mountain valleys. In the wintertime the mountain valleys are frequently filled with fog. All three major factors that determine the ambient concentrations (i.e., emissions, dilution, and chemical rate processes) are strongly influenced by the topography. For this reason, many of the maps depicting the regional pattern use shaded topography as a backdrop.

In the western half of the U.S., west of and including the Rockies, there was a decrease in the PM_{10} concentration of 1988 to 1994 from 36 $\mu g/m^3$ to 25 $\mu g/m^3$ for all sites and from 39 $\mu g/m^3$ to 28 $\mu g/m^3$ for trend sites (Figure 6-21b). The reductions were 31% for all sites and 28% for trend sites. Standard deviation among the western stations of yearly average PM_{10} concentrations is about 40%.

The western AIRS $PM_{2.5}$-PM_{10} relationship (Figure 6-21c) shows that on the average about 50% of the PM_{10} is contributed by fine particles. The scatter of data points (Figure 6-21c) also shows that during high concentration PM_{10} episodes the fine fraction dominates.

The western PM_{10} seasonality (Figure 6-21d) is also rather pronounced, having about 30% amplitude. However, the lowest concentrations (26 $\mu g/m^3$) are reported in the late spring (April through June), while the highest values occur in late fall (October through January).

The seasonality of $PM_{2.5}$ west of the Rockies (Figure 6-21d) is strongly peaked in November through January. In fact, the $PM_{2.5}$ is several times higher than the summertime values. On the other hand, the coarse fraction shows a broad peak during late summer, July through October. It is to be noted that in Figures 6-20 and 6-21, the fine and coarse particle concentrations do not add up to PM 10, because size resolved samples were only available for tens of sites, while the PM_{10} concentrations were obtained from hundreds of monitoring stations.

In summary, there is a 20 to 24% reduction of PM_{10} concentrations for the continental U.S. between 1988 and 1993. On the national average the PM_{10} seasonality is weak.

Desegregation of the national averages into east and west of the Rockies, shows that the downward trend west of the Rockies is more pronounced than over the eastern half of the U.S. The east-west desegregation also shows that the lack of national PM_{10} seasonality arises from two strong seasonal signals that are phase shifted, the eastern United States has a summer peak, the West a fall and winter peak, and the sum of two signals is a weakly modulated seasonal pattern. Nationally, $PM_{2.5}$ mass accounts for about 57% of PM_{10} mass. The East and West show comparable average fine particle fractions (60% in the East and 50% in the West). Fine particles tend to dominate during the fall and winter season in the western U.S., except in the southwest.

It is evident that further examination discussed in the next sections will show that the East-West division itself is rather crude and that dividing the conterminous United States into additional subregions is beneficial in explaining the PM_{10} concentration pattern and trends.

6.3.2.4 Short-Term Variability of PM_{10} Concentrations

The previous aerosol concentration patterns were expressed as quarterly averages. However, for health and other effects, the variance of the concentration, in particular the occurrence of extreme high concentrations is of importance. The PM_{10} concentrations exhibit marked differences in the shape of their distribution functions around the mean values. For example in Figure 6-22, the day to day variations of PM_{10} concentrations in Knoxville, TN are about 40% of the mean value of 35 $\mu g/m^3$. On the other hand, the concentration time series for Missoula, MT shows a coefficient of variation of 60% over the mean of 34 $\mu g/m^3$. During the winter season the coefficient of variation is even higher. It is therefore evident, that for comparable mean concentrations the Missoula, MT site exhibits significantly higher short-term variations. Also note the large variations from a high concentration day to the lower concentrations on the day before and/or the day after (Figure 6-22).

The variability of concentration is examined spatially and seasonally by computing logarithmic standard deviation (ratio of 84/50 concentration percentiles) for each monitoring site. These deviations were then contoured for each season. The results are depicted in the seasonal maps of the logarithmic standard deviation (Figure 6-23). The highest logarithmic standard deviation is recorded over the northern and northwestern states during the cold

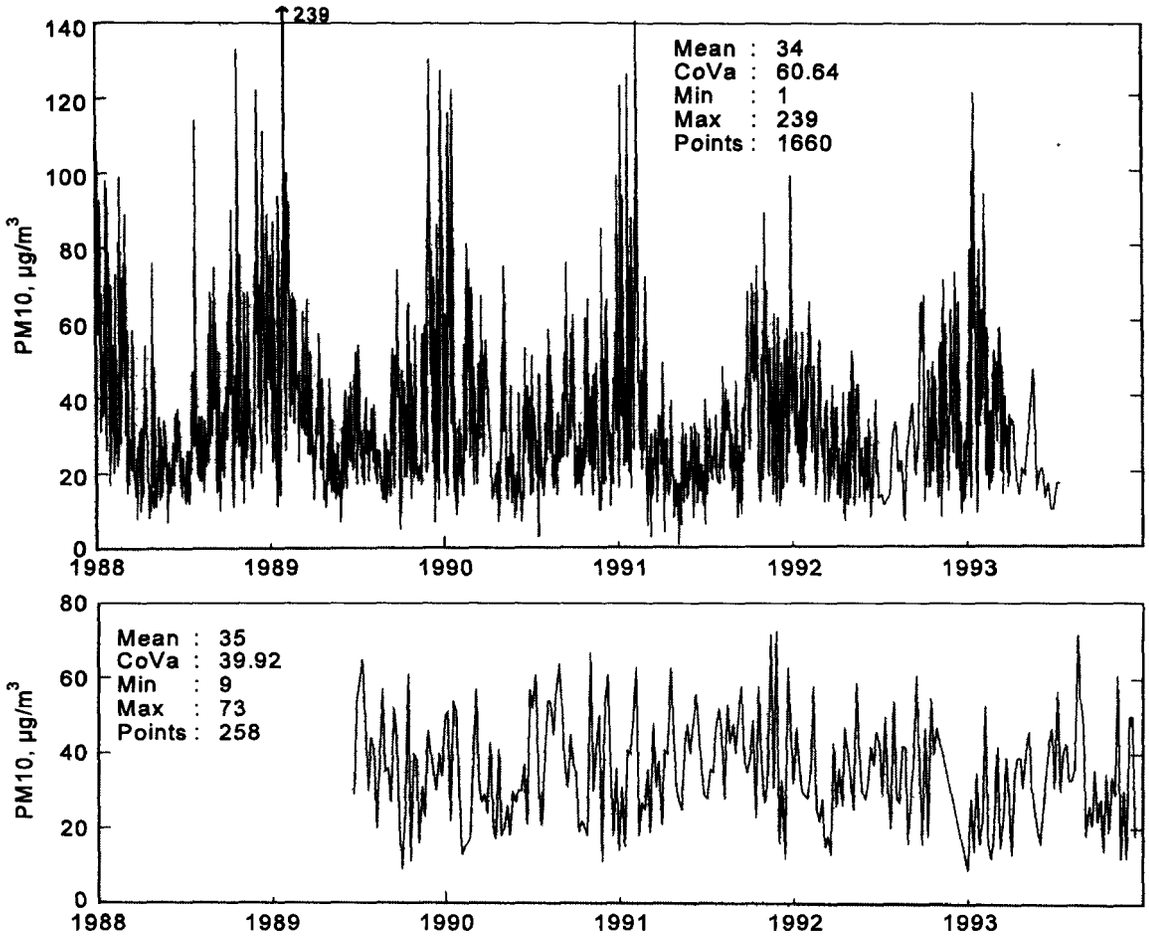

Figure 6-22. Short-term PM_{10} concentration time series for Missoula, MT, and Knoxville, TN.

season, Quarters 1 and 4. Regionally, the logarithmic standard deviation in the north-northwest is about 2.0 with pockets of high winter variability such as Salt Lake City, UT, and Missoula, MT. The lowest variability prevails over the warm season, Quarters 2 and 3, covering the southeastern and southwestern states. Over multistate regions in the southern states the summertime logarithmic standard deviation is below 1.5. This means that these areas are covered more or less uniformly by summertime PM_{10}, while the northern states are more episodic.

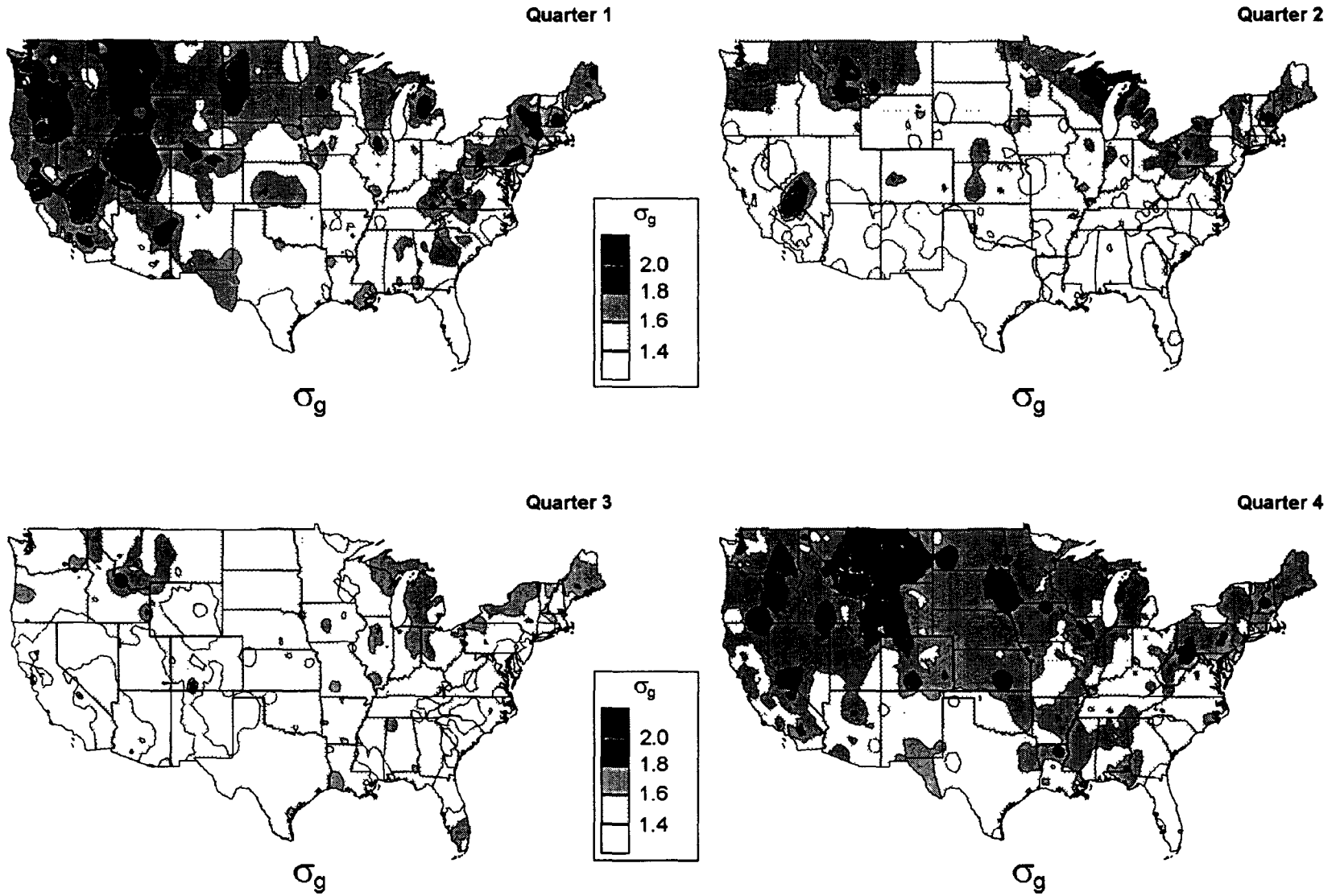

Figure 6-23. Geographic variation of the standard deviation, σ_g, of the lognormal distribution of PM_{10} concentrations from the AIRS.

6.3.2.5 Aerometric Information Retrieval System $PM_{2.5}$ Concentrations

The mass concentration of fine particles in urban areas is not well known. Sampling and analysis of $PM_{2.5}$ is limited by small number of stations (<50), sampling period restricted to few years, and different, non-standard sampling equipment was utilized for $PM_{2.5}$

The yearly average AIRS $PM_{2.5}$ concentrations are shown in Figure 6-24. Figure 6-24 also shows the location and magnitude of $PM_{2.5}$ concentrations from measurements of IMPROVE/NESCAUM monitoring networks. The fine particle data from the IMPROVE/NESCAUM show a pattern of high concentrations (> 15 $\mu g/m^3$) occurring over the eastern United States. This pattern of nonurban fine particle concentrations was discussed in Section 6.3.1.

6.3.2.6 Other National Surveys

A summary of urban PM_{10}, $PM_{2.5}$, PMCoarse at eight urban areas, Birmingham, AL, Buffalo, NY, Houston, TX, Philadelphia, PA, Phoenix, AZ, Pittsburgh, PA, Rubidoux, CA, and Steubenville, OH was reported by Rodes and Evans (1985). The overall ratio of the PM_{10} to Total Suspended Particulate (TSP) was 0.486. The relationships between PM_{10} and the 15 μm fraction (IP) are linear for all sites. With exception of Phoenix, AZ, and Houston, TX, $PM_{2.5}$ exceeded the PMCoarse mass concentration in all six urban areas.

Spengler and Thurston (1983) reported PM concentrations in six U.S. cities: Portage, WI, Topeka, KS, Kingston, TN, Watertown, MA, St. Louis, MO, and Steubenville, OH, using dichotomous virtual impactors in the two size ranges, $PM_{2.5}$, having $d_p < 2.5$ μm, and coarse particle mass with $2.5 < d_p < 15\mu$m. All six cities displayed a seasonal trend of higher summertime and lower wintertime concentrations. Figure 6-25 displays the monthly mean concentrations ($\mu g/m^3$) for PM_{15} (inhalable PM or IP), $PM_{2.5}$ (fine mass), PM_{15}-$PM_{2.5}$ (coarse mass), and sulfate (as ammonium sulfate) for the six cities. The seasonal pattern for $PM_{2.5}$ is pronounced for these cities, especially St. Louis, Portage, and Harriman, where the July monthly mean $PM_{2.5}$ concentration is 60%, 60%, and 40% higher than the January monthly concentration in each city, respectively. Sulfate has been noted to have similar variations in other locations (Altshuller, 1980).

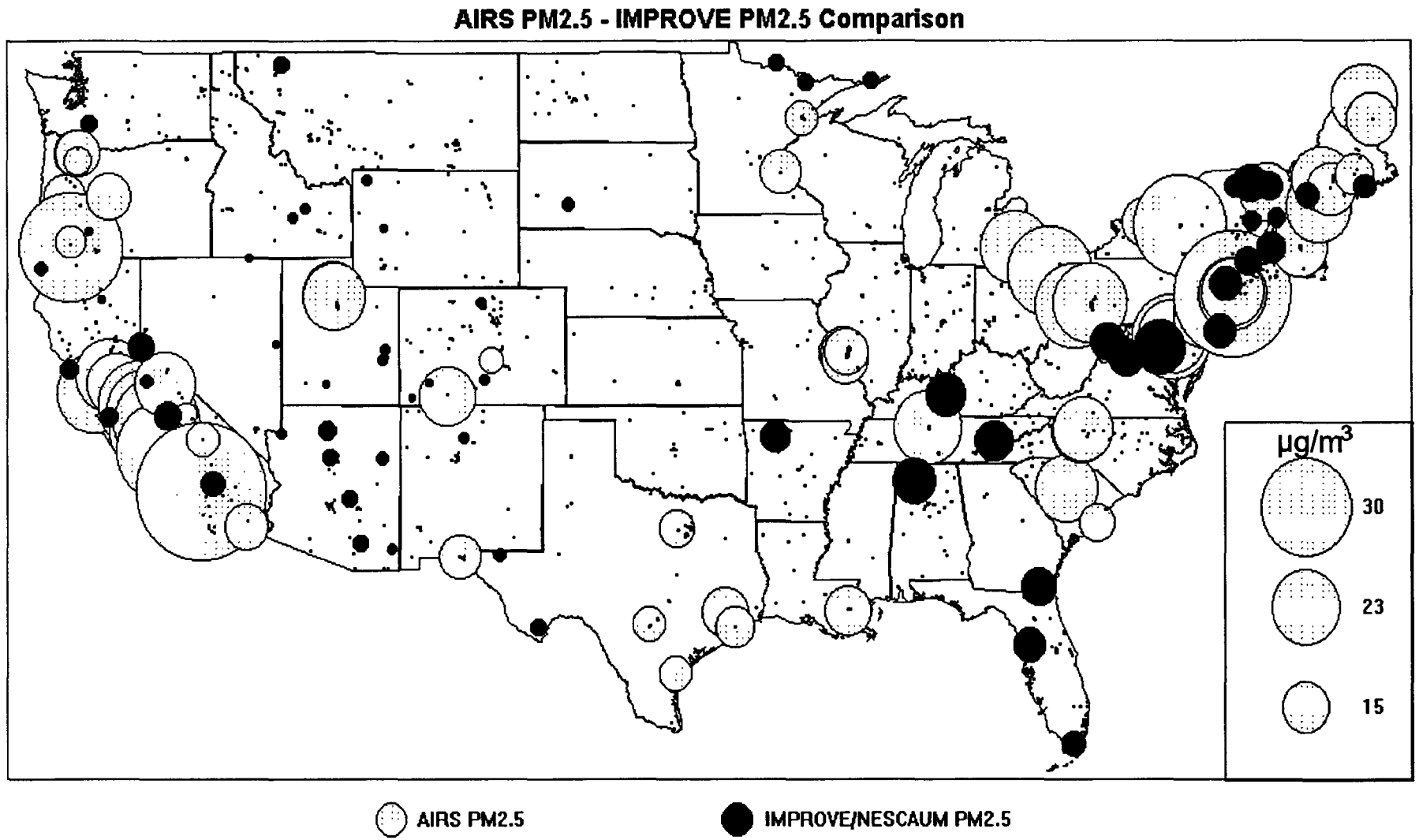

Figure 6-24. Annual $PM_{2.5}$ concentration pattern obtained from IMPROVE/NESCAUM and AIRS networks.

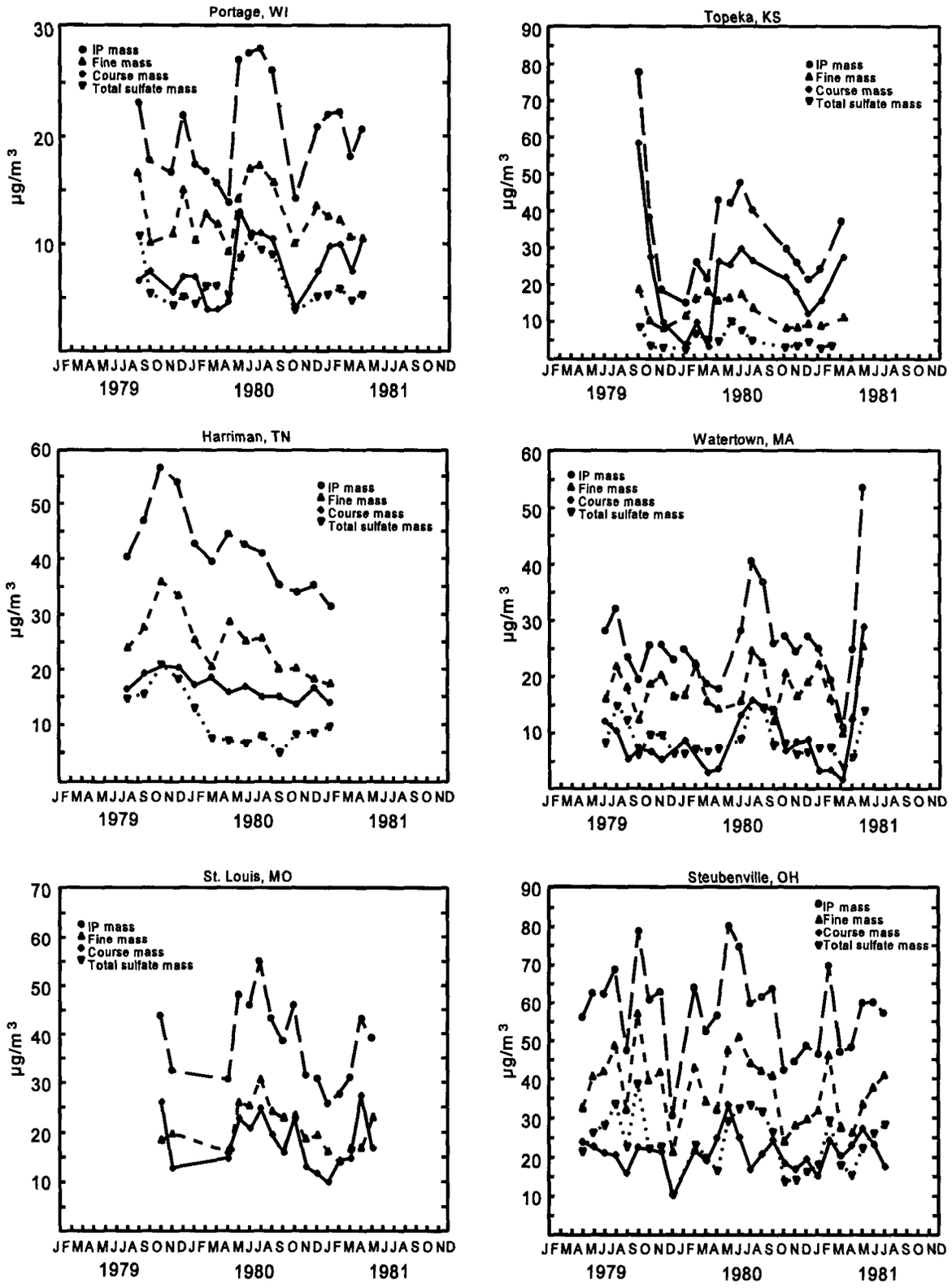

Figure 6-25. Monthly mean concentrations in micrograms per cubic meter of PM_{15} (IP, inhalable mass), $PM_{2.5}$ (fine mass), coarse mass (PM_{15}-$PM_{2.5}$), and total sulfate as $(NH_4)_2SO_4$ in Portage, WI; Topeka, KS; Harriman, TN; Watertown, MA; St. Louis, MO; and Steubenville, OH.

The quartz content and elemental composition of aerosols, collected in dichotomous samplers in selected sites in the EPA Inhalable Particulate network, were reported by Davis et al. (1984). For all network sites, an average of only 4.9 weight per cent of the coarse particle mass and 0.4 weight per cent of the fine mass consisted of quartz. Continental interior sites show the highest average quartz content as well as the greatest variability. The coastal regions and eastern interior sites reveal the lowest quartz concentrations. The complete X-ray spectra from some samples in Portland, OR, show that Si comes primarily from minerals such as feldspars, where the Si in the Buffalo, NY aerosols comes from quartz.

6.3.3 Comparison of Urban and Nonurban Concentrations

Seasonal maps of the AIRS PM_{10}-IMPROVE/NESCAUM PM_{10} spatial concentrations are given in Figure 6-26. In evaluating the subsequent comparisons of the differences between AIRS and IMPROVE/NESCAUM spatial concentrations possible sampling biases and differences in sampling equipment and monitoring protocols may be significant. In addition, the differences in geographical location between the stations for the two networks also can influence the reliability of these comparisons. The AIRS $PM_{2.5}$ concentrations everywhere exceed their adjacent IMPROVE/ NESCAUM concentrations. The highest AIRS $PM_{2.5}$ are reported over the eastern urban industrial centers, such as Philadelphia and Pittsburgh, where the concentrations of 20 to 30 $\mu g/m^3$ exceed the nonurban $PM_{2.5}$ by a factor of 2 to 3. However, the excess urban $PM_{2.5}$ concentrations are evidently confined to the immediate vicinity of urban centers. This indicates that over the eastern United States a regionally homogeneous background of $PM_{2.5}$ concentration exists that has smooth spatial gradients. Superimposed on the smooth regional pattern are local hot-spots with excess concentrations of factor of 2 to 3 that are confined within a few miles of urban industrial centers. The regional homogeneity is an indication that the eastern U.S. $PM_{2.5}$ is composed of a secondary aerosol that is produced several days after the emission of its gaseous precursors. Similar results have been discussed for SO_4^{2-} since the 1970's (Altshuller, 1980). The excess $PM_{2.5}$ concentration in urban centers suggests that primary emissions such as automobile exhaust and heating furnaces are responsible for much the urban $PM_{2.5}$ hot-spots.

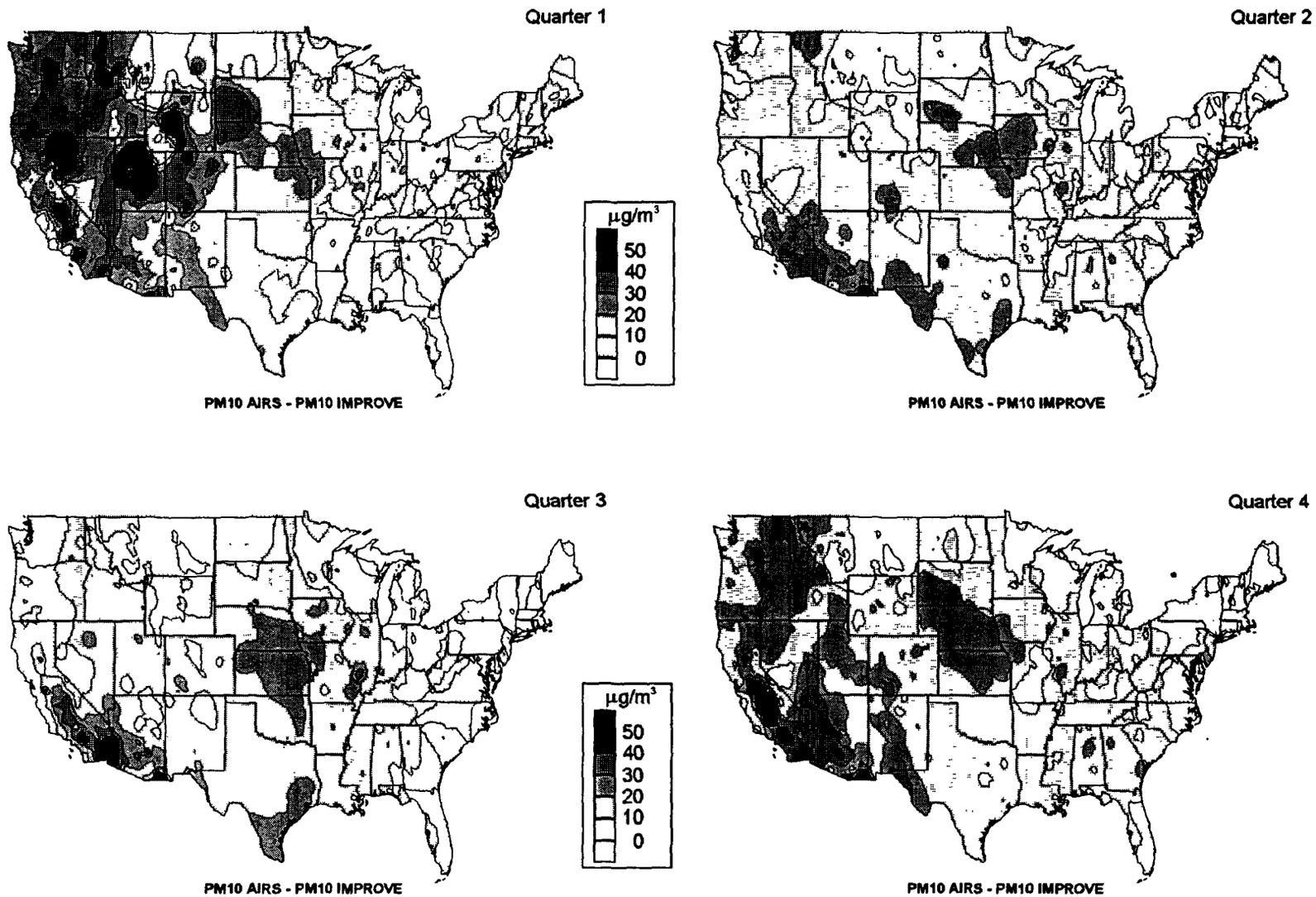

Figure 6-26. Spatial maps of PM_{10} concentration difference between AIRS and IMPROVE/NESCAUM networks.

The reported AIRS $PM_{2.5}$ concentrations over the Pacific states are generally higher and average at 20 to 50 $\mu g/m^3$. This is 5 to 10 times higher than their companion IMPROVE $PM_{2.5}$ concentrations. The dramatic difference is attributable to the pronounced concentration differences between urban-industrial-agricultural centers that exist in mountainous air basins and the concentrations monitored at remote national parks and wilderness areas that are generally at higher elevations. However, it is fair to presume that the AIRS and IMPROVE $PM_{2.5}$ data sets represent the extreme of aerosol concentration ranges that exist over the western U.S. The challenging task of filling in the details (i.e., spatially and temporally extrapolating the aerosol concentrations over the rugged western United States) is discussed in further detail in later regionally and locally focused sections below.

Comparisons have been made of the seasonality of the urban (AIRS) concentrations relative to the nonurban (IMPROVE/NESCAUM) data. In Figure 6-27 the difference in PM_{10}, $PM_{2.5}$, and PMCoarse between AIRS and IMPROVE/NESCAUM sites, using all available data, is used to indicate the urban excess particle concentration compared to the rural concentration. No attempt has been made to evaluate the possible uncertainties in these difference values.

Nationally, the urban excess fine particle concentration ranges between 18 $\mu g/m^3$ in December through February and 10 $\mu g/m^3$ in April through June (Figure 6-27a). The urban excess coarse mass concentration ranges between 10 to 7 $\mu g/m^3$. The sum of the fine and coarse national urban excess mass concentration is about 25 $\mu g/m^3$ in the winter season, and 18 $\mu g/m^3$ during the spring season. Hence, the nationally aggregated urban and nonurban data confirm that urban areas may have excess concentrations on the order of 20 $\mu g/m^3$, and well over half is due to fine particles, particularly in the winter season.

The urban excess (AIRS-IMPROVE/NESCAUM difference) over the eastern United States (Figure 6-27b) shows fine particles excess of 8 to 12 $\mu g/m^3$, with higher value occurring during both winter and summer. The urban excess coarse mass in the eastern United States is only 5 to 8 $\mu g/m^3$, peaking during spring and summer. The sum of fine and coarse urban excess is 15 to 18 $\mu g/m^3$ throughout the year.

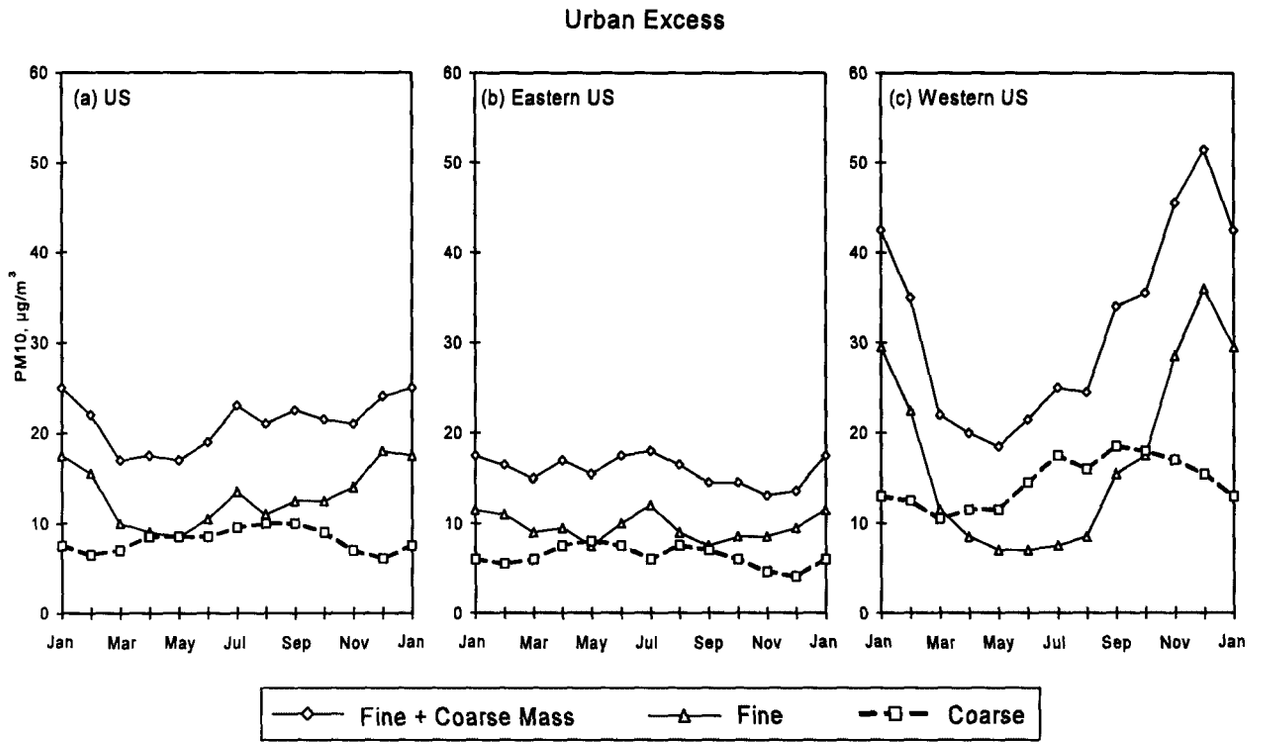

Figure 6-27. Urban excess concentrations (AIRS minus IMPROVE) for (a) the United States, (b) the eastern United States, and (c) the western United States.

The excess urban (AIRS-IMPROVE/NESCAUM) aggregated over the western United States is much more pronounced in magnitude and seasonality. The urban excess fine mass is about 30 $\mu g/m^3$ in November through January and drops to 8 to 10 $\mu g/m^3$ in April through August. The urban excess coarse mass is less in magnitude and seasonality 15 to 18 $\mu g/m^3$ in July through December, and 10 to 12 $\mu g/m^3$ in March through May. The sum of the urban excess fine and coarse mass is 40 to 50 $\mu g/m^3$ in November through January and about 20 $\mu g/m^3$ in the spring March through June. The urban AIRS and nonurban IMPROVE) networks in the western United States monitor aerosols differently because of different goals and mandates. The urban nonurban difference is such that the western nonurban concentrations contribute little to the much higher urban values, particularly in the winter season. On the other hand, the eastern urban sites are greatly influenced by the nonurban, regionally representative concentrations, particularly in the summer season.

6.4 REGIONAL PATTERNS AND TRENDS

This section describes the spatial, temporal, size, and chemical characteristics of seven aerosol regions of the conterminous U.S. The sizes and locations of these regions were chosen mainly on the basis of the characteristics of their aerosol pattern. The main criteria for delineating a region were (1) the region had to possess some uniqueness in aerosol trends, seasonality, size distribution, or chemical composition; (2) each territory of the conterminous United States had to belong to one of the regions; and (3) for reasons of computational convenience the shape of the regions were selected to be rectangular on unprojected latitude longitude maps. The resulting criteria yielded seven rectangular aerosol regions as shown in Figure 6-28. It is recognized that this selection is arbitrary and for future analysis additional regional definition criteria would be desirable. The limitations in the data bases of the two different networks discussed previously also apply to the subsequent discussion.

For sake of consistency and intercomparisons each region is described using maps delineating the spatial pattern and the sampling locations in the subsequent figures (Section a). For the figures showing AIRS monitoring results, Section b shows trends in average PM_{10} concentrations and $\pm \sigma$. As discussed in Section 6.3.2.1 included in (b) are the results of two trend analyses. One of these uses the annual concentrations from all available stations in operation any time in the 1985 to 1994 period. The second approach uses the annual concentrations from only those stations operated continuously from 1985 to 1994, the long term coverage or trend stations. Section c show plots and correlations relating PM_{10} and $PM_{2.5}$. Monthly AIRS concentrations (Section d) for a given region were computed by averaging all the available data for the specific month. In case of nonurban aerosol chemistry some regions only had two to four monitoring stations. The monthly nonurban $PM_{2.5}$, PMCoarse and PM_{10} shown in the subsequent figures (Section b) over regions illustrate the relative seasonality of each aerosol type. The nonurban regional average chemical composition is presented as seasonal charts of chemical aerosol components as a fraction of the fine mass concentration (Section c). The role of some primary sources, such as coal and fuel oil combustion is indicated through seasonal charts of selenium (coal) and vanadium (fuel oil) trace metals (Section d). In addition, for each region figures will be provided showing shorter term variability of PM_{10} concentrations and PM_{10} urban excess concentrations.

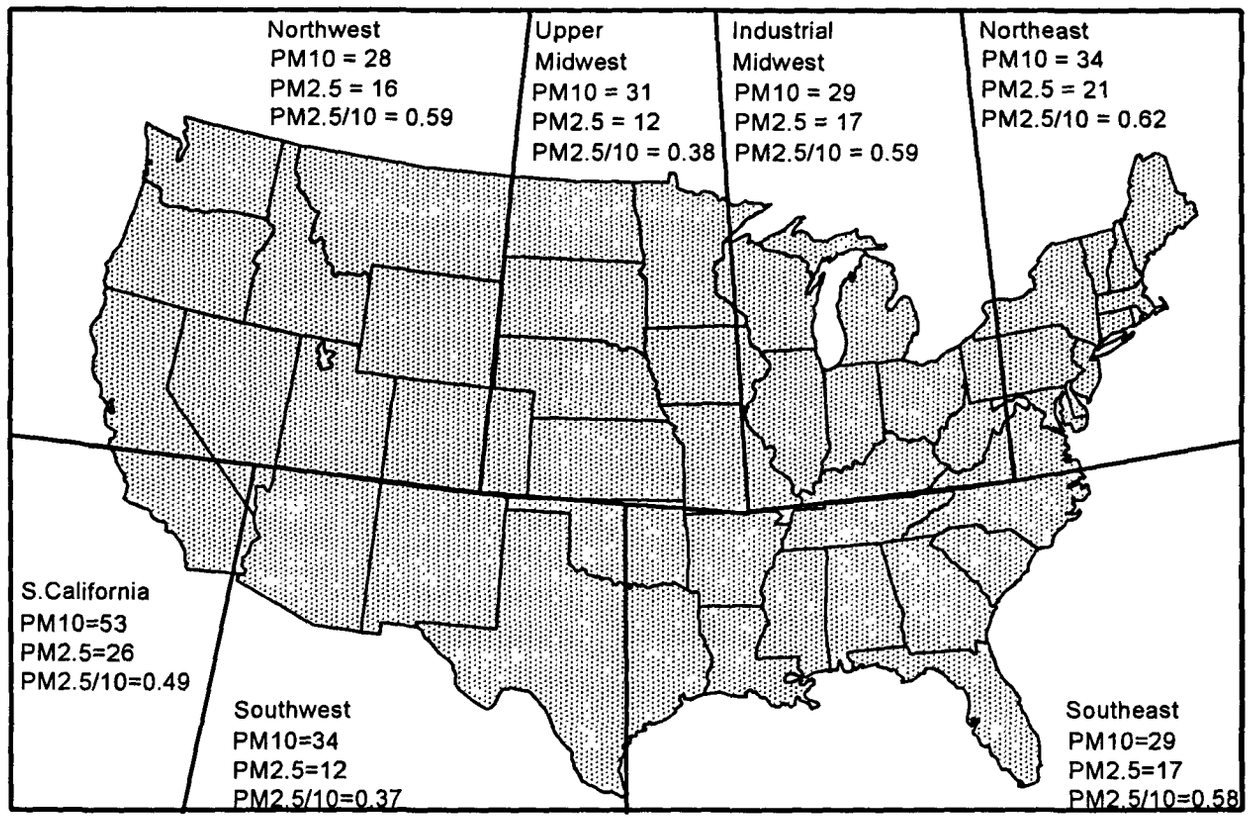

Figure 6-28. Aerosol regions of the conterminous United States.

6.4.1 Regional Aerosol Pattern in Eastern New York, New Jersey, and the Northeast

The Northeast aerosol region covers the New England states, including eastern Pennsylvania and eastern Virginia to the south (Figure 6-29a). In the Northeast, terrain features that significantly influence regional ventilation occur over the mountainous upstate New York, Vermont and New Hampshire. Throughout the year, the Northeast is influenced by Canadian as well as Gulf air masses. The region includes the Boston-New York megalopolis, as well as other urban-industrial centers. It is known that the Northeast is influenced by both local sources, as well as long range transport of fine particles and transformations of precursors to particles from other regions, as well as transport

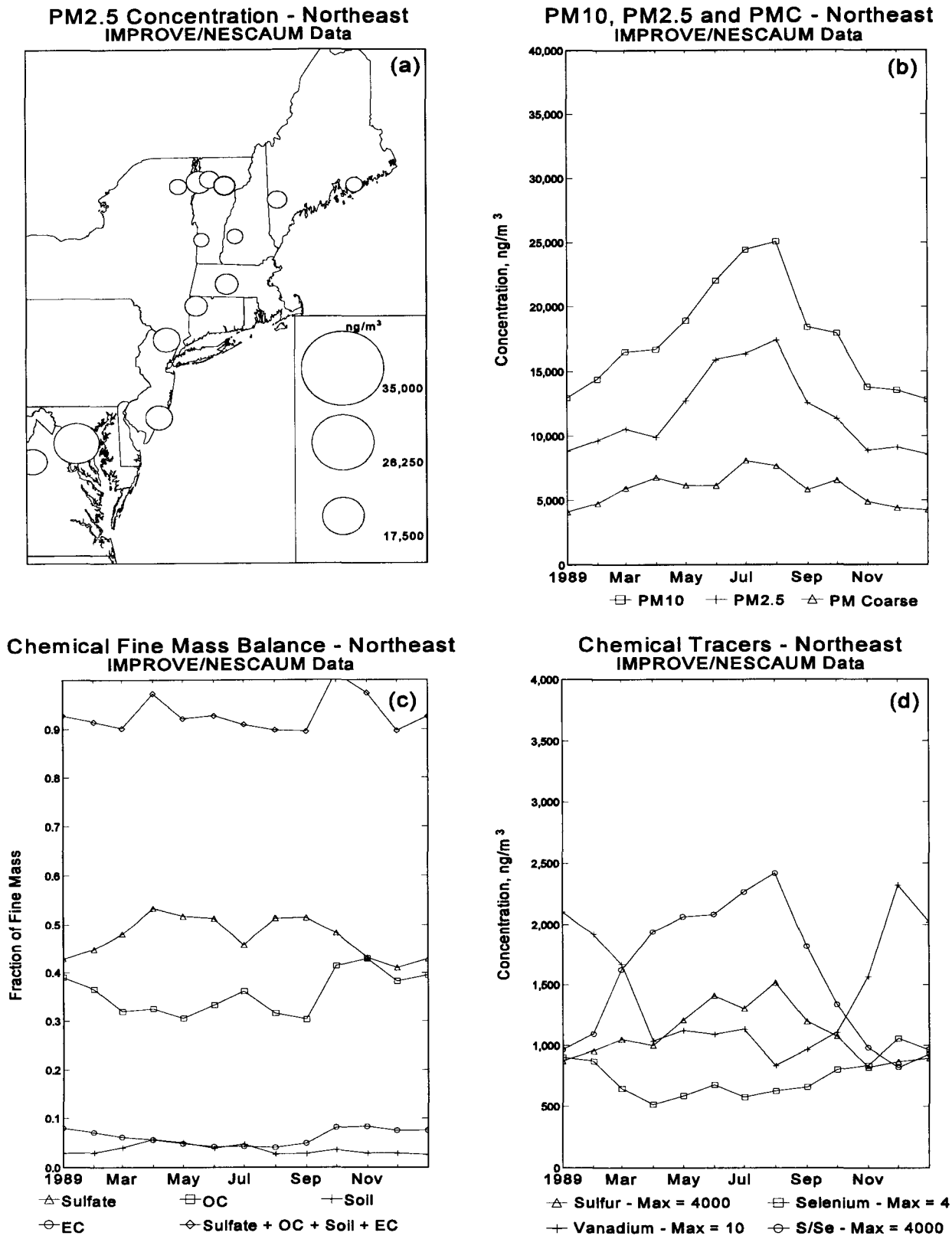

Figure 6-29. IMPROVE/NESCAUM concentration data for the Northeast: (a) monitoring locations; (b) PM_{10}, $PM_{2.5}$, and PMCoarse (PMC); (c) sulfate, soil, organic carbon (OC), and elemental carbon (EC) fractions; and (d) tracers.

and transformation of precursors in single and multiple urban plumes within the region (Chapter 3).

6.4.1.1 Nonurban Size and Chemical Composition in the Northeast

The summary of the nonurban aerosol chemical composition in the Northeast is presented in Figure 6-29c. The region has 14 monitoring sites, 8 of which are part of NESCAUM in upper New England. The geographic locations with respect to nearby urban areas vary from those sites within the northeast corridor to rural sites near the Canadian border.

The PM_{10} concentration exhibits a factor of two seasonal amplitude between 12 $\mu g/m^3$ in the winter, and 25 $\mu g/m^3$ in June and July (Figure 6-29b). About 60% of PM_{10} is contributed by fine particles throughout the year. The $PM_{2.5}$ also contributes to the summer-peaked seasonality.

Data from a two year fine particle network in the Northeast (Bennett et al., 1994) yielded a geometric mean concentration of $PM_{2.5}$ of 12.9 $\mu g/m^3$ and particulate sulfur (1.4 $\mu g/m^3$, equivalent to 4.2 $\mu g/m^3$ of sulfate), which is somewhat lower than other comparable rural data.

Sulfates are the most important contributors of the fine particle mass in the Northeast, particularly in the summer season when they account for half of the fine mass (Figure 6-29c). The regionality of sulfate in the northeastern U.S. has been dicussed for many years (Altshuller, 1980). The organic carbon ranges from 30 to 40%, with the higher percentages occurring in the fall and winter, September through January. In fact, during the late fall the contributions of sulfate and organic carbon are comparable at 40%. Fine particle soil is unimportant throughout the year (<5%). Elemental carbon, on the other hand, is somewhat more significant, particularly during the fall when it contributes about 10% of the fine mass. The sum of the above four nonurban fine particle aerosol components, account for over 90% of the measured fine particle mass throughout the year. These results would appear to indicate ammonium ion, hydrogen ion, nitrates, trace metals and sea salt are of minor importance in the northeastern U.S. fine particle chemical mass balance.

The seasonality of both selenium and vanadium indicates a winter peak (Figure 6-29d). In particular, the vanadium concentration increases by a factor of two for December and January compared to the summer values. Also, the V concentration is higher than over any other region indicating the strongest contribution of fuel oil emissions. The S/Se ratio is strongly seasonal with a winter value of 1,000 and a summer peak of 2,000 to 2,500 consistent with a substantial secondary photochemical contribution of SO_4^{2-} during the summer.

6.4.1.2 Urban Aerosols in the Northeast

In the northeastern U.S. there was a decrease in the annual average PM_{10} concentration between 1988 and 1994 from 28 $\mu g/m^3$ to 23 $\mu g/m^3$ for all sites and from 31 $\mu g/m^3$ to 25 $\mu g/m^3$ for trend sites (Figure 6-30b). The reductions were 18% for all sites and 19% for trend sites. The standard deviation among the monitoring stations for any given year is about 30%. The map of the Northeast shows the magnitude of PM_{10} concentrations in proportion of circle radius. The highest AIRS PM_{10} concentrations tend to occur in larger urban centers (Figure 6-30a).

The seasonality of the urban Northeast PM_{10} concentration (Figure 6-30d) is a modest 20%, ranging from 25 to 31 $\mu g/m^3$, smaller than the seasonality of the nonurban northwest PM_{10} (Figure 6-29b). There is a summer peak in July, and a rather uniform concentration between September and May showing only a slight winter peak. The $PM_{2.5}$-PM_{10} relationship (Figure 6-30c) shows that on the average 62% of PM_{10} is contributed by fine particles.

In general, the regional scale emissions are not expected to vary significantly from one day to another. However, both meteorological transport (i.e., dilution), as well as aerosol formation and removal processes, are important modulators of daily aerosol concentration. The daily concentration of particulate matter exhibits strong fluctuation from one day to another, mainly due to the role of the meteorological transport variability.

The regionally averaged daily concentration is associated with the regional scale meteorological ventilation. High regionally averaged concentrations indicate poor ventilation (i.e., a combination of low wind speeds and low mixing heights and the absence of fast aerosol removal rates, such as cloud scavenging and precipitation). Low regional concentrations, on the other hand, represent strong horizontal transport, deep mixing heights, or high regional

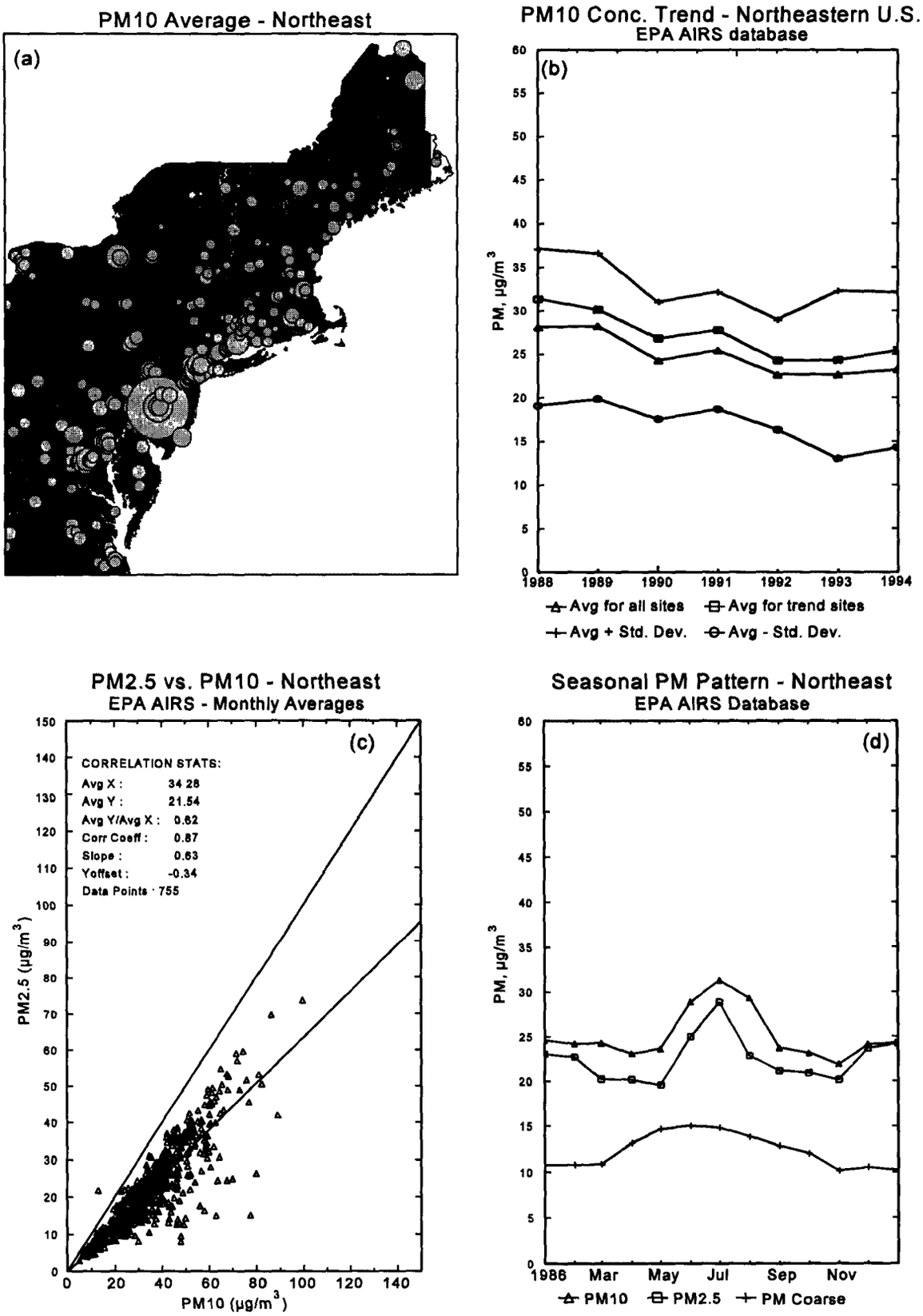

Figure 6-30 AIRS concentration data for the Northeast: (a) monitoring locations; (b) regional PM_{10} concentration trends; (c) PM_{10} and $PM_{2.5}$ relationship; and (d) PM_{10}, $PM_{2.5}$, and PMCoarse seasonal pattern.

removal rates. Advection of high aerosol content air masses from neighboring regions may also be a cause of elevated concentration in a given region.

The daily variation of the regional averaged urban PM_{10} concentration for the Northeast is shown in Figure 6-31. The single day concentration data for every sixth day are connected by a line between the data points, although five in-between days are not monitored. The lowest regionally averaged daily urban PM_{10} is about 10 $\mu g/m^3$, while the highest is about 55 $\mu g/m^3$, with a regional average in the early 1990s of 25 $\mu g/m^3$. The highest concentrations (>40 $\mu g/m^3$) occur primarily in the summer season. The time series also indicate that the high concentration episodes do not persist over consecutive six day periods. This is consistent with the notion that the regional ventilation that is caused by synoptic scale air mass changes, which typically occur every four to seven days over eastern U.S. The daily time series also convey the fact that day to day variation in PM_{10} is higher than the seasonal amplitude. In fact, in Figure 6-31 the concentration seasonality is barely discernible. It can be stated, therefore, that the PM_{10} concentration in the Northeast is highly episodic (i.e., the temporal concentration variation is both substantial and irregular). The excess urban PM_{10} (AIRS-IMPROVE) is shown in Figure 6-32. The excess urban PM_{10} concentration in the Northeast is a relatively small part of the total urban PM_{10} concentration between May and October. The reliability of such estimates of excess regional urban PM_{10} concentrations discussed earlier should be considered (Section 6.3.3).

6.4.2 Regional Aerosol Pattern in the Southeast

The Southeast rectangle stretches from North Carolina to eastern Texas (Figure 6-33). From the point of view of regional ventilation the Southeast terrain is flat, with the exception of the mildly rolling southern Appalachian Mountains. The region is known for increasing population over the past decades, high summertime humidity, and poor regional ventilation due to stagnating high pressure systems.

6.4.2.1 Nonurban Size and Chemical Composition in the Southeast

Only six nonurban stations were available in the Southeast with the absence of monitoring over the southern (Gulf Coast) part of the region, except for Florida. The

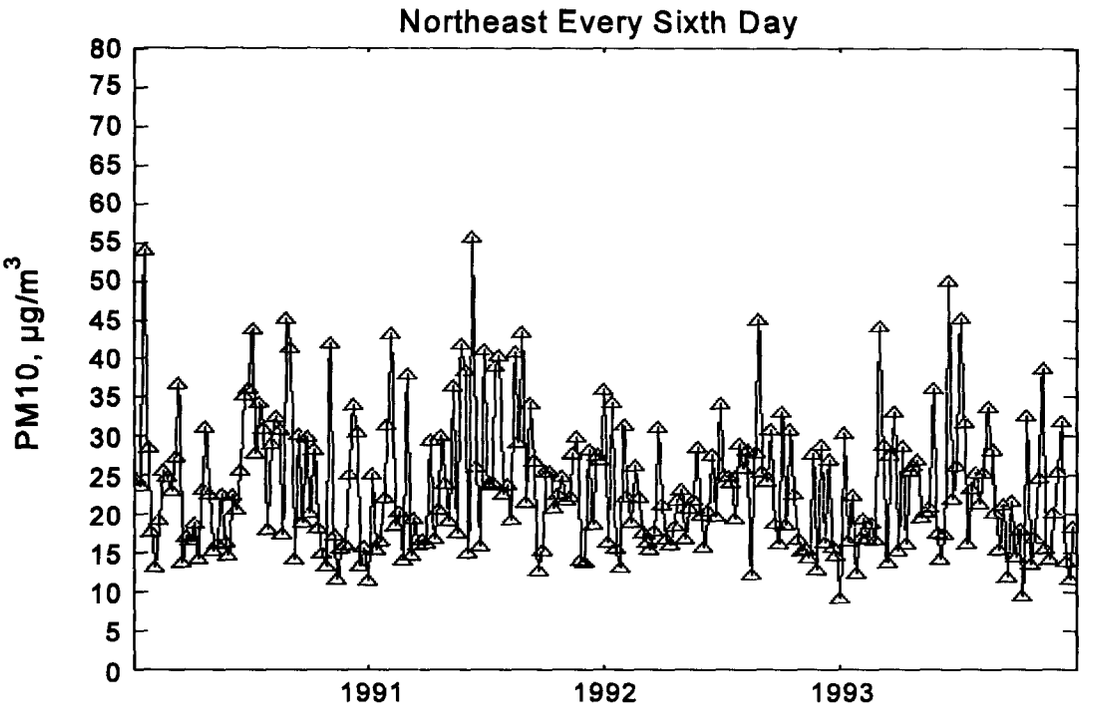

Figure 6-31. Short-term variation of PM_{10} average for the Northeast. Data are reported every sixth day.

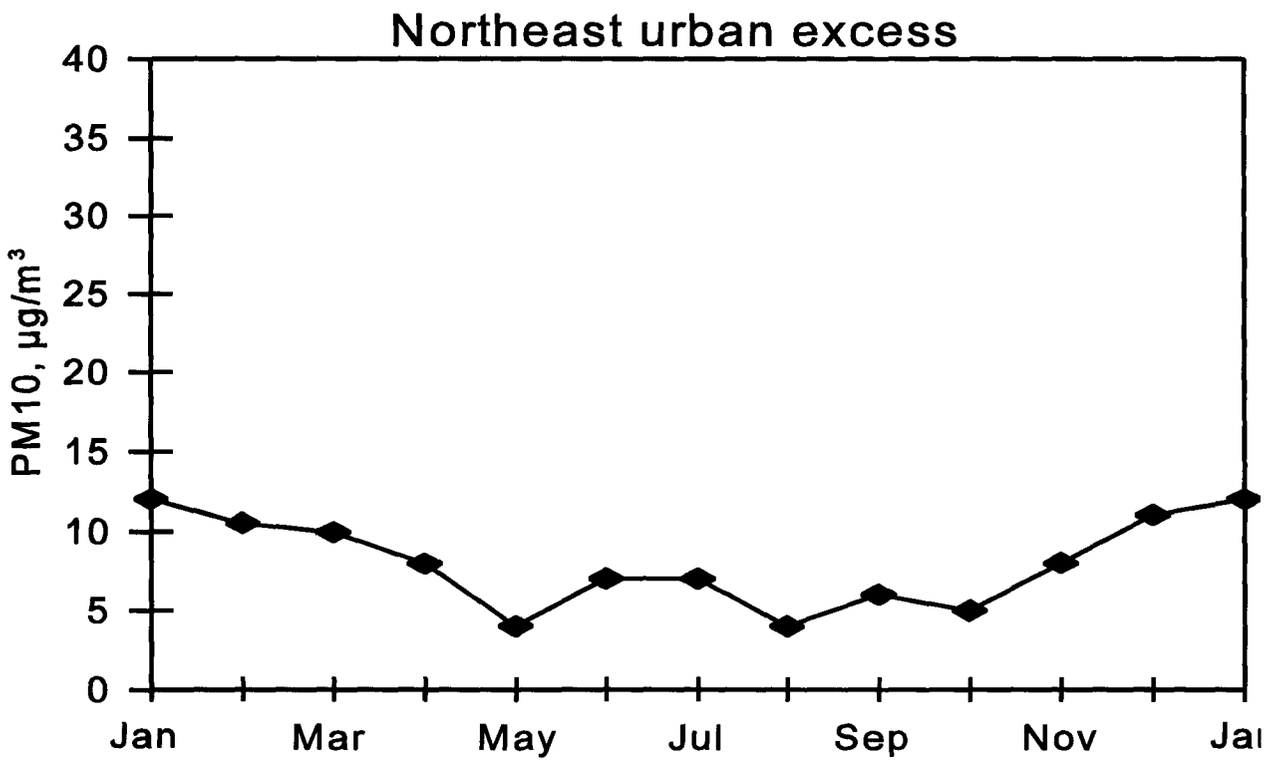

Figure 6-32. Urban excess concentration (AIRS minus IMPROVE) for the Northeast.

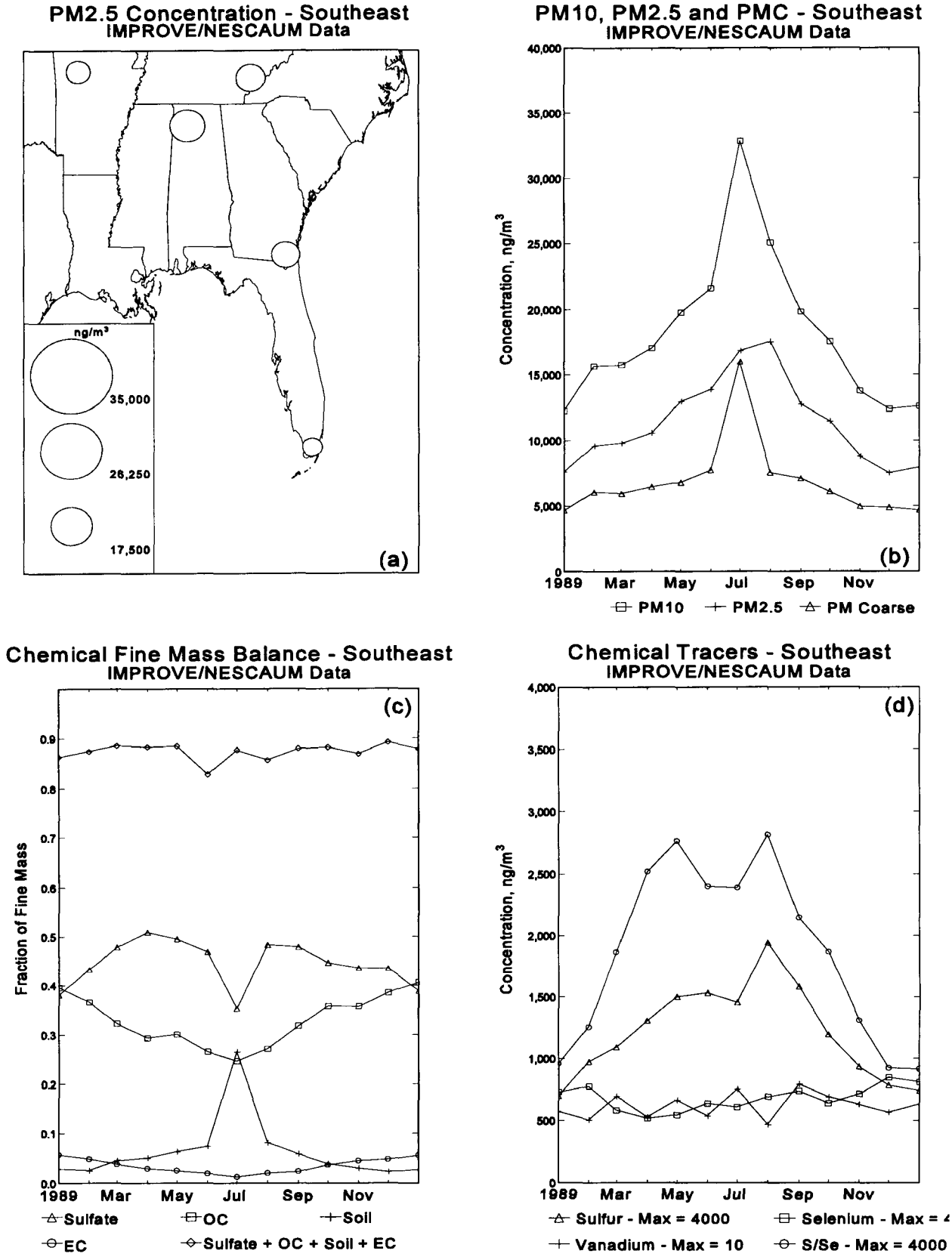

Figure 6-33. IMPROVE/NESCAUM concentration data for the Southeast: (a) monitoring locations; (b) PM_{10}, $PM_{2.5}$, and PMCoarse (PMC); (c) sulfate, soil, organic carbon (OC), and elemental carbon (EC) fractions; and (d) tracers.

nonurban PM_{10} concentration in the Southeast (Figure 6-33b) is roughly comparable to the Northeast, exhibiting about factor of two seasonal concentration amplitude between 12 $\mu g/m^3$ in the winter, and 25 $\mu g/m^3$ in the summer. An anomalous high PM_{10} concentration is shown in July which appears to be contributed by an excess coarse particle concentration of about 10 $\mu g/m^3$. With exception of July, the fine particle mass accounts for about 70% of the nonurban PM_{10}, leaving the coarse mass of 30% or less throughout the year (Figure 6-33b).

The most prominent aerosol species in the Southeast are sulfates contributing 40 to 50% of the fine mass (Figures 6-33c). The anomalously low sulfate fraction (35%) during July coincides with the high (20%) soil contribution during July. For the other months, soil contribution is <5% of the fine mass. The relative role of the organic carbon in the nonurban Southeast is most pronounced during the winter (40%), but declines to 25% during the summer months. The contribution of elemental carbon varies between 2% in the summer to 6% in the winter months.

The trace element concentrations of selenium and vanadium (Figure 6-33d) are constant throughout the year, implying that the combined role of emissions and dilution is seasonally invariant. The concentration of sulfur, on other hand shows a definite summer peak, that is two to three times higher than the winter concentrations. Consequently, the S/Se ratio is strongly seasonal. In fact, the warm season S/Se ratio of 2,500 is higher than over any other region of the country. If Se-bearing coal combustion is the dominant source of sulfur in the Southeast, then the high S/Se ratio implies that the secondary photochemical sulfate production in the summer is several times that in the winter.

6.4.2.2 Urban Aerosols in the Southeast

In the southeastern U.S. there was a decrease in the annual average PM_{10} concentrations between 1988 and 1994 from 33 $\mu g/m^3$ to 27 $\mu g/m^3$ for all sites and from 35 $\mu g/m^3$ to 29 $\mu g/m^3$ for trend sites (Figure 6-34b). The reductions were 18% for all sites and 17% for trend sites. The Southeast PM_{10} concentration trends and the PM_{10} seasonality resemble the industrial Midwest described below. A unique feature of the Southeast is the uniformity of the aerosol concentration among the monitoring stations. In fact the 17% station to station

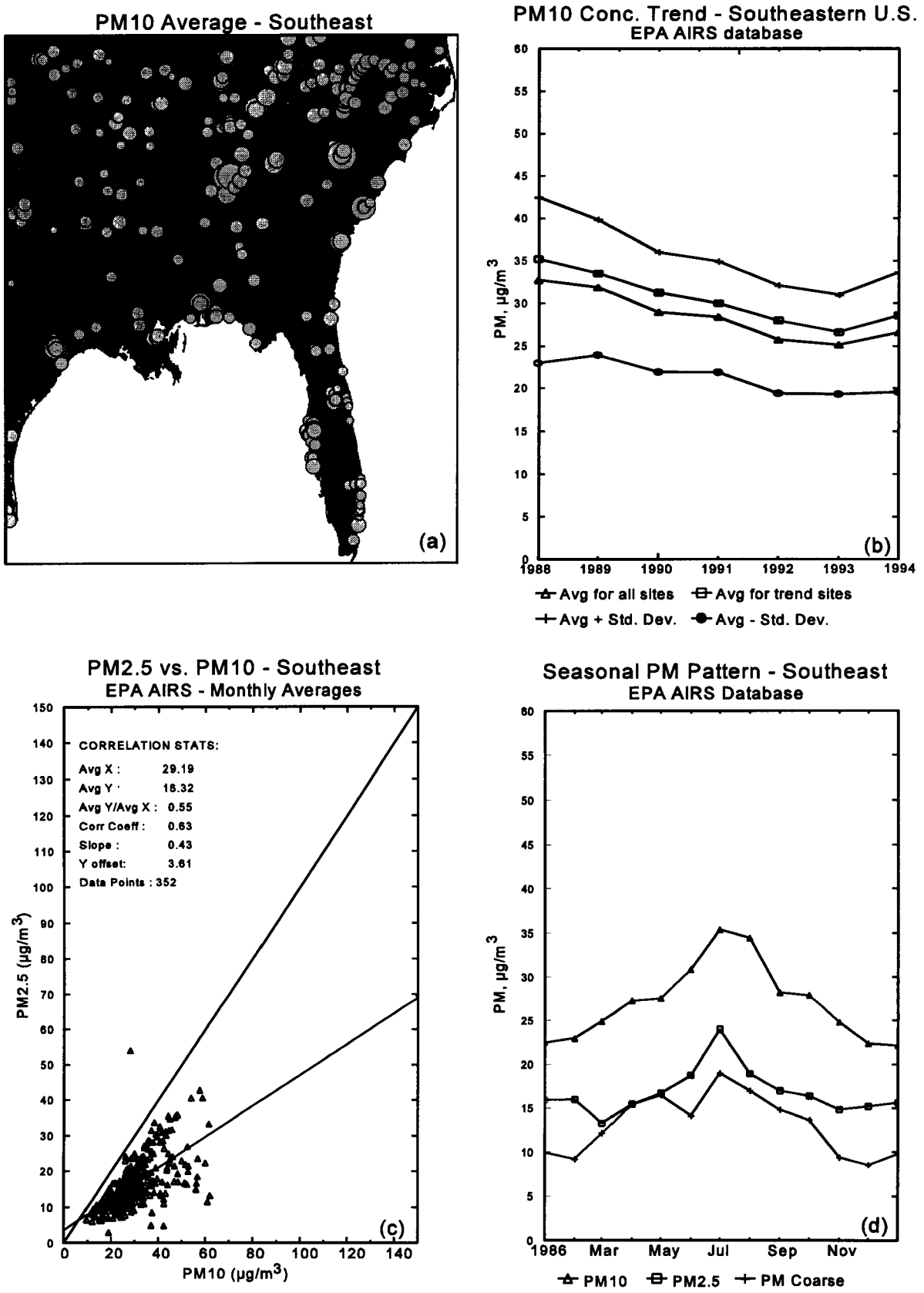

Figure 6-34. AIRS concentration data for the Southeast: (a) monitoring locations; (b) regional PM_{10} concentration trends; (c) PM_{10} and $PM_{2.5}$ relationship; and (d) PM_{10}, $PM_{2.5}$, and PMCoarse seasonal pattern.

standard deviation is by far the lowest among the aerosol regions (Figure 6-34b). This result would appear to be associated with regional meteorological patterns.

The Southeast is also characterized by high seasonal amplitude of 37%, ranging between 22 $\mu g/m^3$ in December through February and 35 $\mu g/m^3$ in July through August (Figure 6-34d). There is no evidence of a winter peak for the southeastern U.S.

The scattergram of $PM_{2.5}$-PM_{10} for the Southeast (Figure 6-34c) shows an average of 58% fine particle contribution, with considerable scatter. It should be noted, however, that size segregated samples were available only briefly and these only for two monitoring sites which may not be representative for the large southeastern region.

The regionally averaged daily PM_{10} concentrations over the Southeast (Figure 6-35) shows a clearly discernible seasonality. The concentrations during the winter months are about factor of two lower than during the summer. Overall, the lowest concentrations are about 12 $\mu g/m^3$, and the highest about 50 $\mu g/m^3$, which is about factor of four. However, seasonality of the temporal signal accounts for about half of the variation. Hence, within a given season the sixth day to sixth day variation is only about 50%. It can be concluded that the PM_{10} concentration over the southeastern United States region is quite uniform during shorter time intervals, although it exhibits a substantial seasonality. The southeastern United States also exhibits the highest spatial homogeneity (i.e., the smallest average deviations of average concentrations between the stations). The PM_{10} urban excess (AIRS-IMPROVE) for the southeast region is given in Figure 6-36. The range of monthly urban excess concentrations in the Southeast is within approximately the same range, 5 $\mu g/m^3$ to 10 $\mu g/m^3$, as for the Northeast. The one distinct feature is the sharp decrease in the urban excess in July which corresponds to the sharp peak attributed to the nonurban coarse soil contribution in July for the Southeast (Figure 6-33).

6.4.3 Regional Aerosol Pattern in the Industrial Midwest

This aerosol region stretches between Illinois and western Pennsylvania, including Kentucky on the south (Figure 6-37a). The industrial Midwest is covered by flat terrain west of the Appalachian Mountains. In the winter the region is under the influence of cold Canadian air masses, while during the summer moist air masses transported from the Gulf

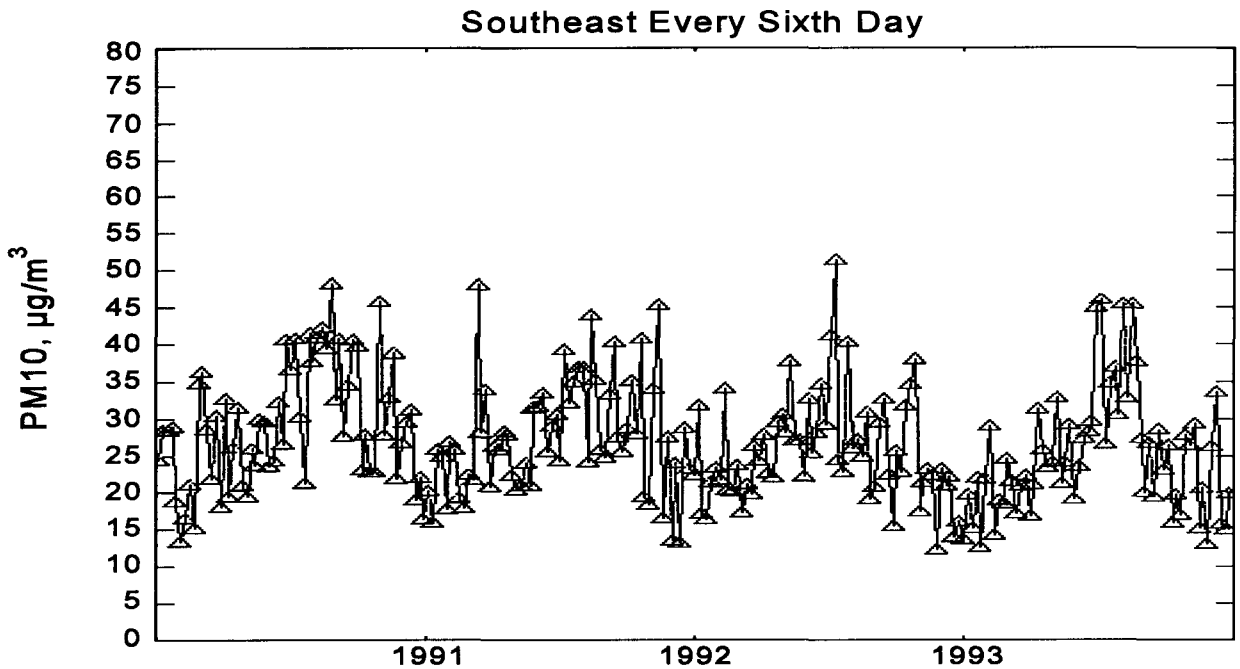

Figure 6-35. Short-term variation of PM_{10} average for the Southeast. Data are reported every sixth day.

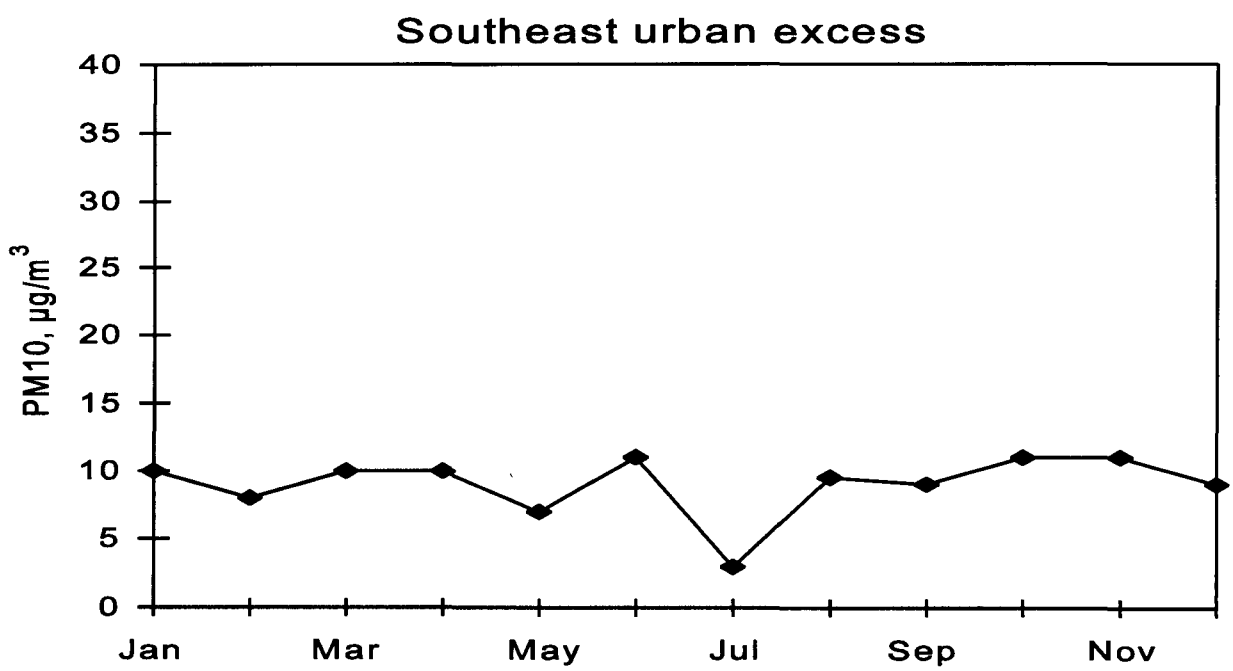

Figure 6-36. Urban excess concentration (AIRS minus IMPROVE) for the Southeast.

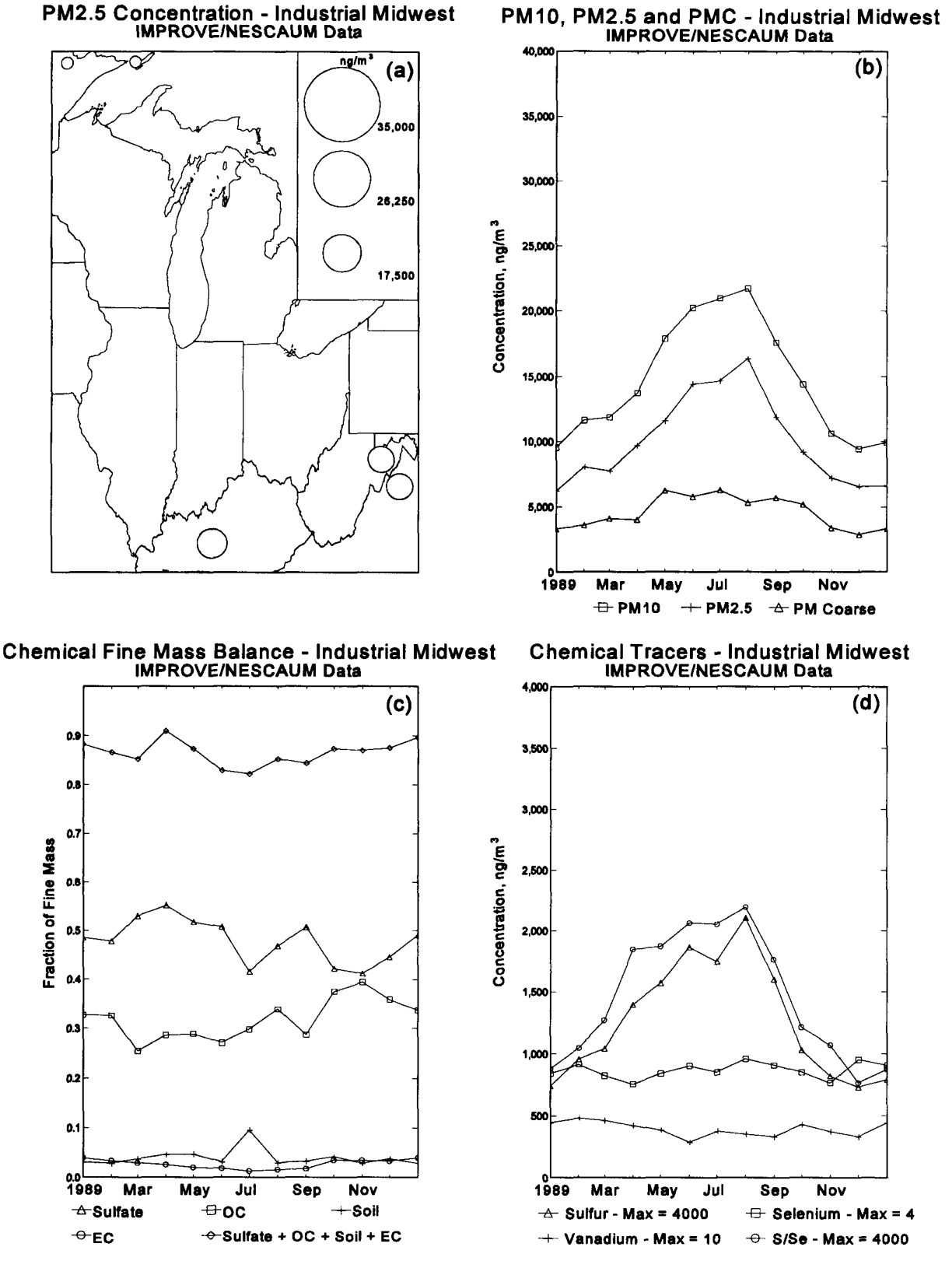

Figure 6-37. IMPROVE/NESCAUM concentration data for the industrial Midwest: (a) monitoring locations; (b) PM_{10}, $PM_{2.5}$, and PMCoarse (PMC); (c) sulfate, soil, organic carbon (OC), and elemental carbon (EC) fractions; and (d) tracers.

Coast prevail. However, the northern most portion of this region in Michigan and Wisconsin is cooler and may be influenced by Canadian air flow at times during the summer. This region includes the Ohio and Mississippi River Valleys that are known for high sulfur emission densities. The region also includes major metropolitan areas.

6.4.3.1 Nonurban Size and Chemical Composition in the Industrial Midwest

The seasonal pattern of the nonurban aerosol in the Industrial Midwest is shown in Figure 6-37b. Only five nonurban monitoring sites are available widely separately geographically between those at the northern most sites and those in the southern portion of the region with no sites over most of the region. Their representativeness is questionable. The PM_{10} concentrations range between 10 and 22 $\mu g/m^3$, comparable to the nonurban levels in other eastern U.S. regions. From 70 to 80% of PM_{10} is contributed by fine particles throughout the year. The coarse particle concentrations are 4 to 5 $\mu g/m^3$, which is lower than over any other region of the U.S. Hence, the contribution of wind blown dust, fly ash, or other man-induced dust entrainment is not a significant factor in the nonurban areas of the Industrial Midwest.

The chemical mass balance (Figure 6-37c) shows that sulfates are 45 to 55% of the fine mass which is higher than the sulfate fractions in other regions. The concentration of vanadium, which is a tracer for oil combustion, is low throughout the year. The concentration of fine particle sulfur Organics exhibit a variable contribution that is high (40%) during the cold season (October through February) and quite low (20%) in July and August. The strong winter peak for the organic fraction differs markedly from the Northeast where the organics are seasonal. Another unusual feature of the chemical mass balance is that the sum of sulfate, organic carbon, soil, and elemental carbon is about 75% during the summer and 95% in the winter. It is not known what is the composition of the missing 25% during the summer time, but the missing fraction could be associated with nitrates, ammonium ion, hydrogen ion, and water.

Chemical tracer data are shown in Figure 6-37d. The chemical tracer for coal combustion, selenium ranges between 1,000 and 1,500 pg/m^3, which is higher than in any other region. There is a sizeable month to month variation in Se concentration (partly due to a

small number of data points) and the seasonality is not appreciable. This means that the combined effects of coal combustion source strength and meteorological dilution are seasonally invariant over the industrial Midwest. exhibits random monthly variation but indicates a summer peak. The S/Se ratio is a rather smooth seasonal curve ranging between 1,000 in the winter and 2,000 during the summer months. Hence, the sulfate yield is about twice as high during the summer as during winter months. For comparison both the Northeast and Southeast exhibit somewhat higher seasonality (factor of 2.5) in S/Se ratio. A possible explanation for this change in S/Se ratio is that over the industrial Midwest the average age of the SO_2 emissions traveling downwind may be less than over the Northeast or Southeast.

6.4.3.2 Urban Aerosols in the Industrial Midwest

In the industrial midwester U.S. there was a decrease in the annual average PM_{10} concentrations between 1988 and 1994 from 33 $\mu g/m^3$ to 29 $\mu g/m^3$ for all sites and from 37 $\mu g/m^3$ to 30 $\mu g/m^3$ for trend sites (Figure 6-38b). The reductions were 12% for all sites and 19% for trend sites. There is also a 28% deviation among the stations within the region. As in the Northeast, the higher concentrations occur within the larger urban-industrial areas (Figure 6-38a). The PM_{10} seasonality (Figure 6-38d) is virtually identical (37% amplitude) to the seasonality of the Southeast: the lowest concentrations (25 $\mu g/m^3$) occur between November and February, while the highest values are recorded in June through August (40 $\mu g/m^3$). The trends and the seasonality of the midwestern PM_{10} aerosols are comparable to those of the Southeast.

Fine particles contribute 60% of the PM_{10} concentration on the average (Figure 6-38c), and high PM_{10} can occur when either fine or coarse particles dominate.

Daily concentration over the industrial Midwest (Figure 6-39) varies between 14 and 75 $\mu g/m^3$. The lowest regional concentrations occur during the winter months, while the highest values (in excess of 40 $\mu g/m^3$) occur during the summer. It is evident that seasonality is an important component of the time series, accounting for about half of the variance. The elevated concentrations occur only one sixth day observation at a time, consistent with the low frequency of prolonged episodes. The industrial Midwest also shows substantial spatial variability. The urban excess PM_{10} (AIRS-IMPROVE) for the industrial midwest is given in

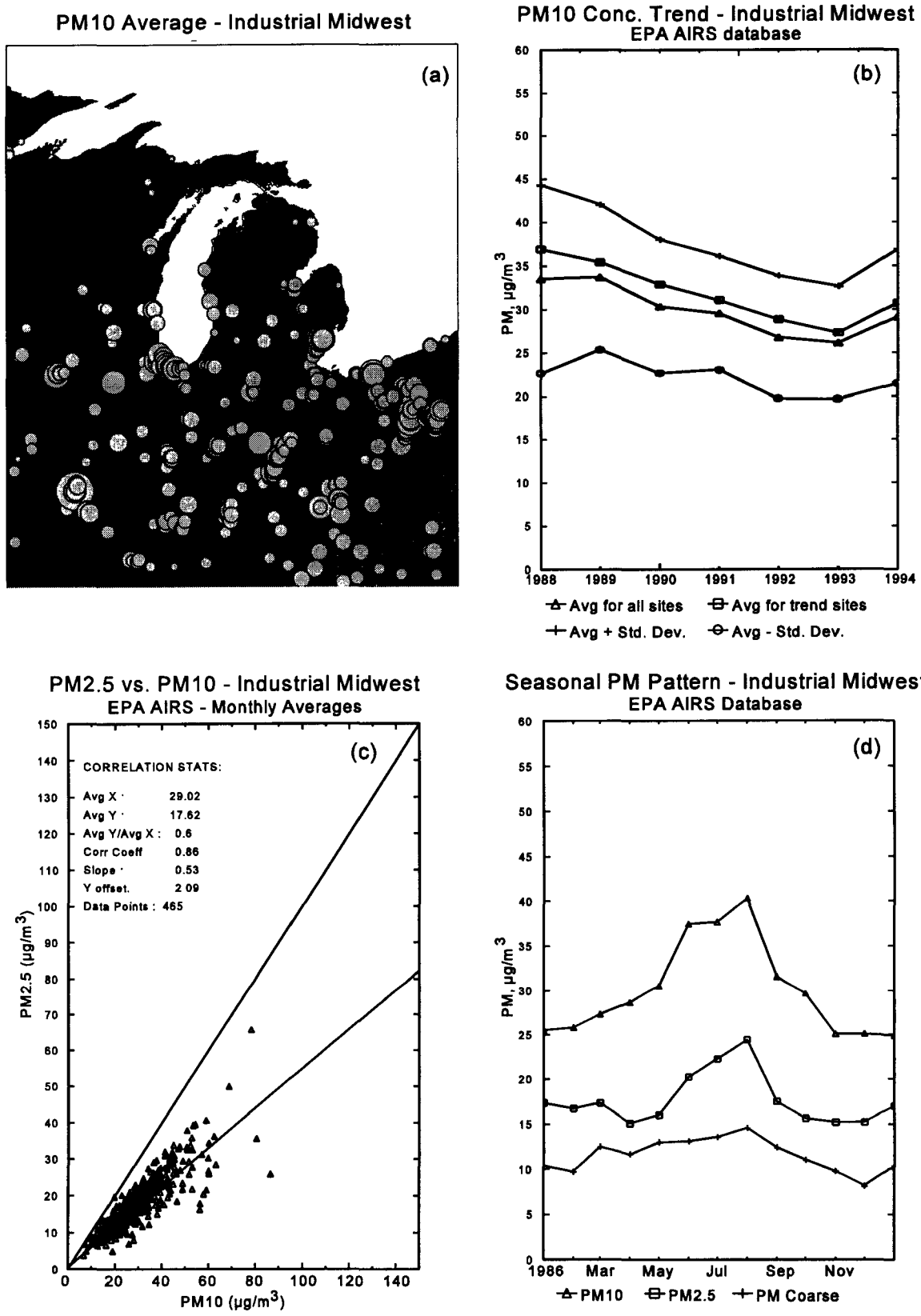

Figure 6-38. AIRS concentration data for the industrial Midwest: (a) monitoring locations; (b) regional PM_{10} concentration trends; (c) PM_{10} and $PM_{2.5}$ relationship; and (d) PM_{10}, $PM_{2.5}$, and PMCoarse seasonal pattern.

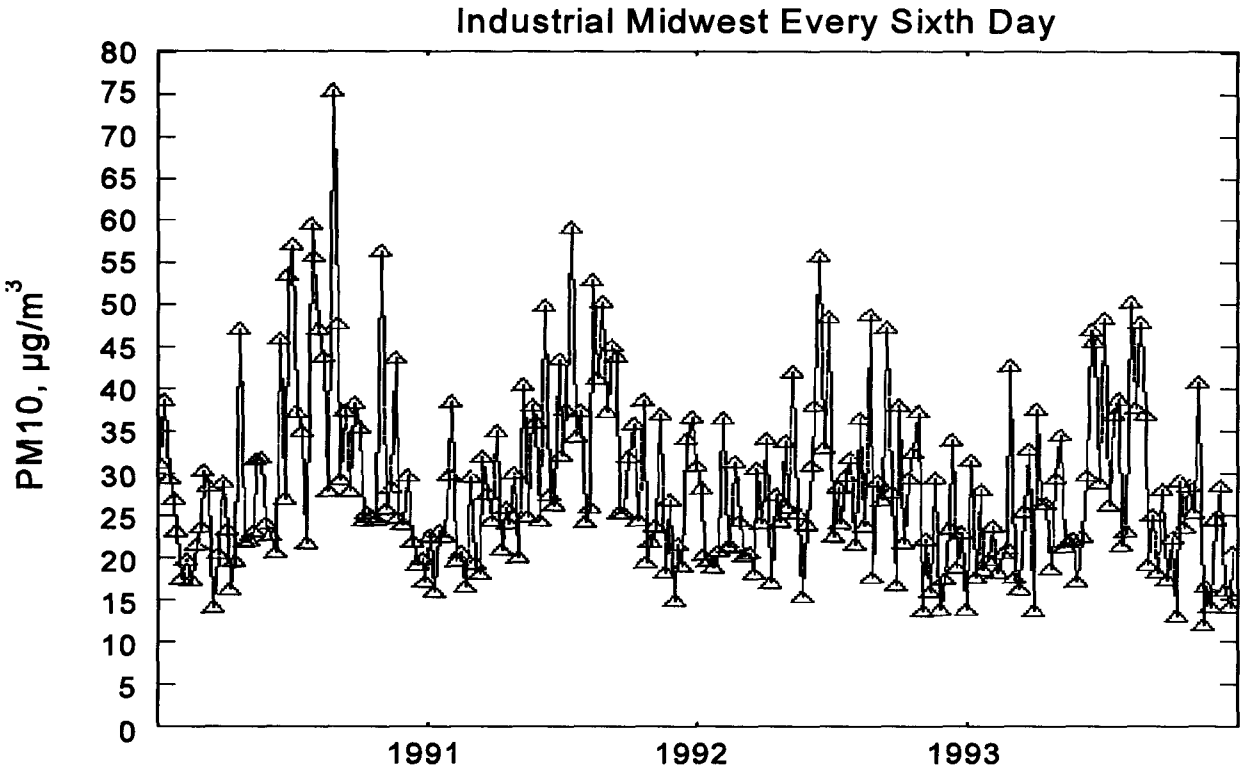

Figure 6-39. Short-term variation of PM_{10} average for the industrial Midwest. Data are reported every sixth day.

Figure 6-40. The pattern for the urban excess PM_{10} differs seasonally from that in the northwest (3-32) or southeast (6-34).

6.4.4 Regional Aerosol Pattern in the Upper Midwest

The upper Midwest covers the agricultural heartland of the country (Figure 6-41). The region is void of any terrain features that would influence the regional ventilation. Industrial emissions and the population density are comparatively low. However, the relatively high PM_{10} concentrations in this region warrant a more detailed examination. In the winter, the region is covered by cold Canadian air masses, while in the summer moist Gulf air alternates and drier Pacific air masses occur.

6.4.4.1 Nonurban Size and Chemical Composition in the Upper Midwest

There is a lack of nonurban monitoring sites in the upper midwest (Figure 6-41a). Compared to the urban sites (Figure 6-42a), these nonurban sites are poorly representative of

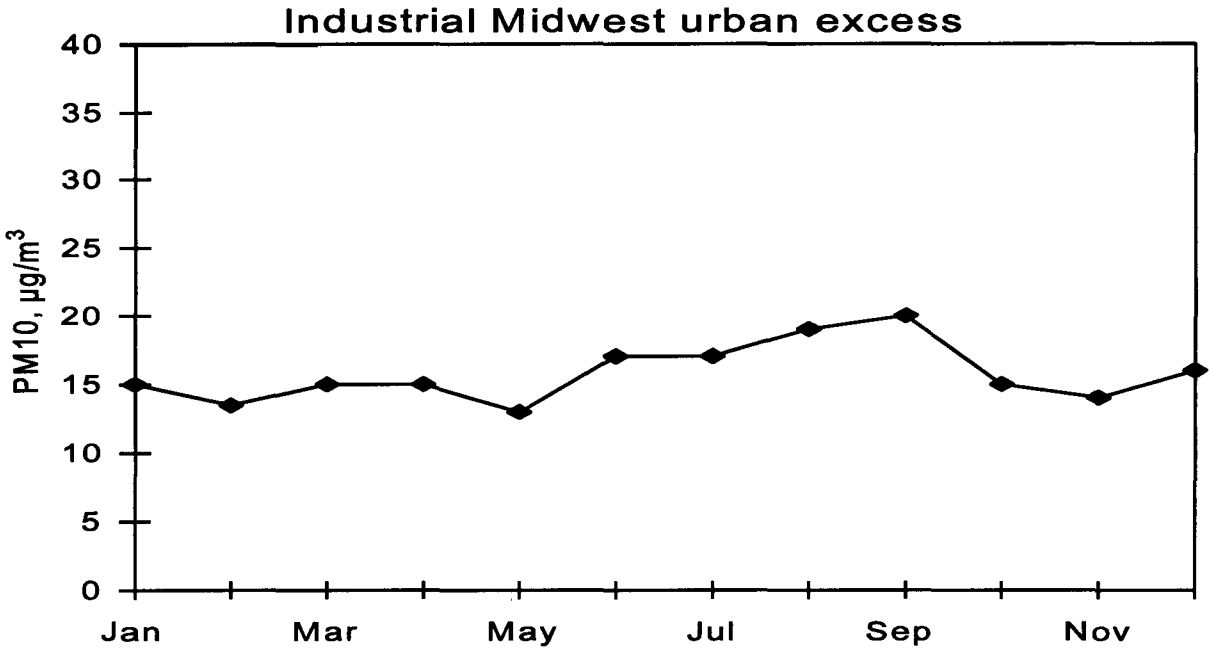

Figure 6-40. Urban excess concentration (AIRS minus IMPROVE) for the industrial Midwest.

the region. Based on these few sites in the upper Midwest, the PM_{10} concentration is about 8 $\mu g/m^3$ during the November through April winter season, and increases to 15 $\mu g/m^3$ during the summer. Fine and coarse particles have a comparable contribution to the PM_{10} mass (Figure 6-41b).

The chemical mass balance (Figure 6-41c) indicates that during the March through May spring season sulfates dominate, but during July through October season organics prevail. This is a rather unusual pattern not observed over any other region. The contribution of fine particle soil exceeds 10% in the spring as well as in the fall season.

Chemical tracers are shown in Figure 6-41d. Selenium concentration is low throughout the year (400 to 600 pg/m^3), with the highest concentrations observed during the summer. This suggests that either the Se sources from coal-fired power plants or the Se transport into the Upper Midwest from other regions is stronger in the summer. The concentration of the fine particle sulfur is <500 ng/m^3 throughout the year, but somewhat higher during March and April. The spring peak of fine particle sulfur has not been observed in any other region. It is also worth noting that S/Se ratio is the highest during the spring and lowest in July

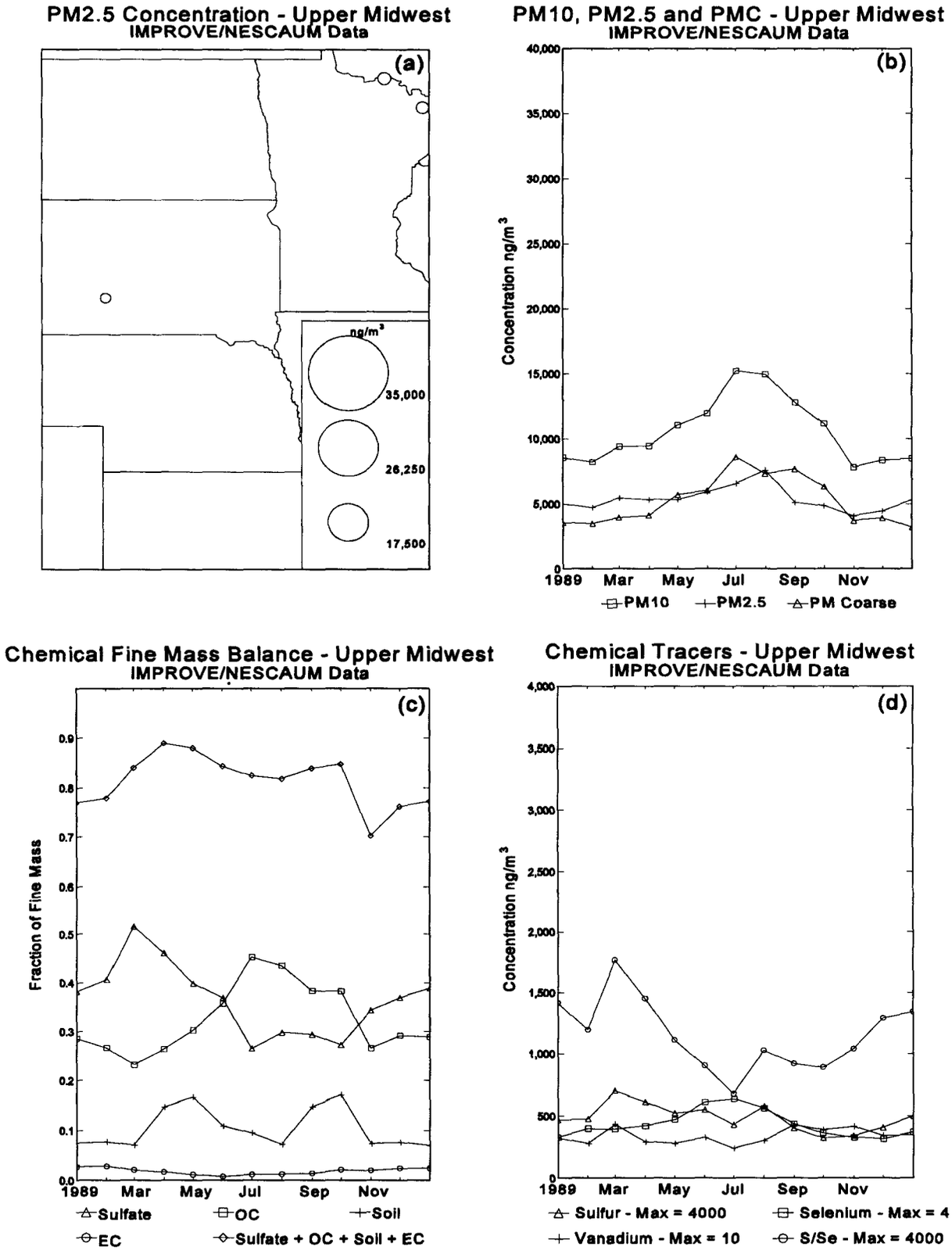

Figure 6-41. IMPROVE/NESCAUM concentration data for the upper Midwest: (a) monitoring locations; (b) PM_{10}, $PM_{2.5}$, and PMCoarse (PMC); (c) sulfate, soil, organic carbon (OC), and elemental carbon (EC) fractions; and (d) tracers.

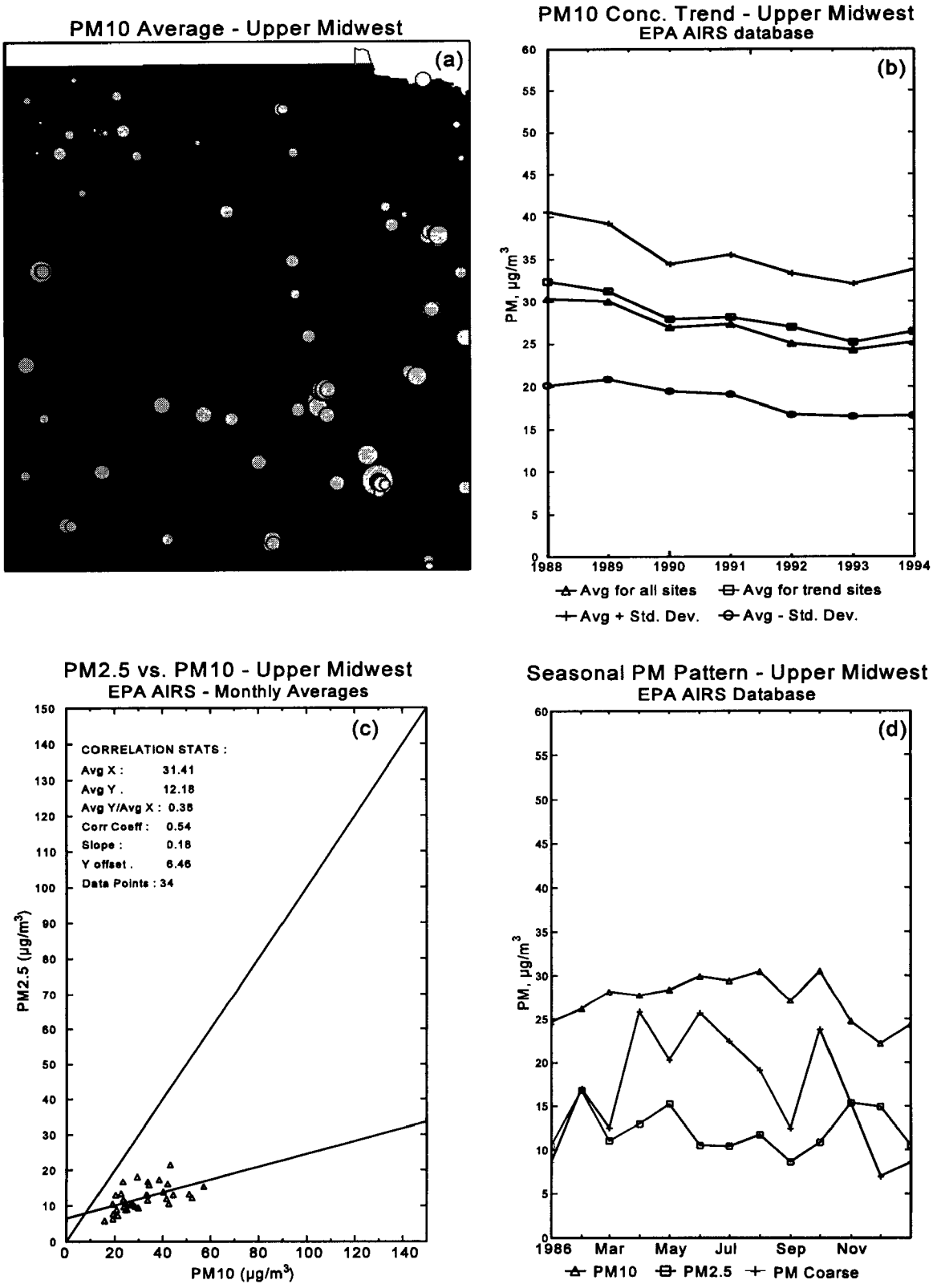

Figure 6-42. Aerometric Information Retrieval System (AIRS) concentration data for the upper Midwest: monitoring locations; regional PM_{10} monitoring trends; PM_{10} and $PM_{2.5}$ relationship; and PM_{10}, $PM_{2.5}$, and PMCoarse seasonal trends.

through September. It needs to be pointed out again that the above chemical patterns are based on only two monitoring stations.

6.4.4.2 Urban Aerosols in the Upper Midwest

The agricultural upper Midwest (Figure 6-42b) shows the smallest decline in PM_{10} concentrations among the regions. In the upper midwestern U.S. there was a decrease in the annual average PM_{10} concentration between 1988 and 1994 from 30 $\mu g/m^3$ to 25 $\mu g/m^3$ for all sites and from 32 $\mu g/m^3$ to 26 $\mu g/m^3$ for trend sites (Figure 6-42b). The reductions were 17% for all sites and 19% for trend sites. As over the eastern U.S., the highest concentrations occur in the vicinity of urban areas. Some of the station-to-station concentration spread arises from low concentrations over western North Dakota. On the average, the deviation among the stations over the region is a moderate 30% (Figure 6-39). The upper Midwest is also unique in that it shows the regionally lowest seasonal amplitude of 19%, with the slightly lower concentrations occurring in December and January. The sparse size segregated data indicate that only 38% of PM_{10} is contributed by fine particles. This is an indication that coarse wind blown dust from natural or man-induced sources prevails. In this sense, the region is similar to the Southwest (see below).

The daily regionally averaged PM_{10} concentrations in the upper Midwest (Figure 6-43) range between 14 and 45 $\mu g/m^3$. The highest values (>40 $\mu g/m^3$) generally occur in the summer season, while the low regional concentrations occur mainly in the cold season, but low values also occur in the summer. It is interesting that the lowest PM_{10} concentrations over the upper Midwest (15 $\mu g/m^3$) are comparable to the Southeast and the industrial Midwest, but differ from these regions by the absence of immediately subsequent high concentration events or episodes. In fact, the PM_{10} "episodes" over the upper Midwest are all in the 40 to 45 $\mu g/m^3$ concentration range, compared to 50 to 75 $\mu g/m^3$ in the Midwest. The seasonality is barely discernible from the time series confirming that the day to day variation exceeds the seasonal modulation. The urban excess PM_{10} (AIRS-IMPROVE) for the upper midwest is given in Figure 6-44, but its reliability may be in question because of the very small number of nonurban sites.

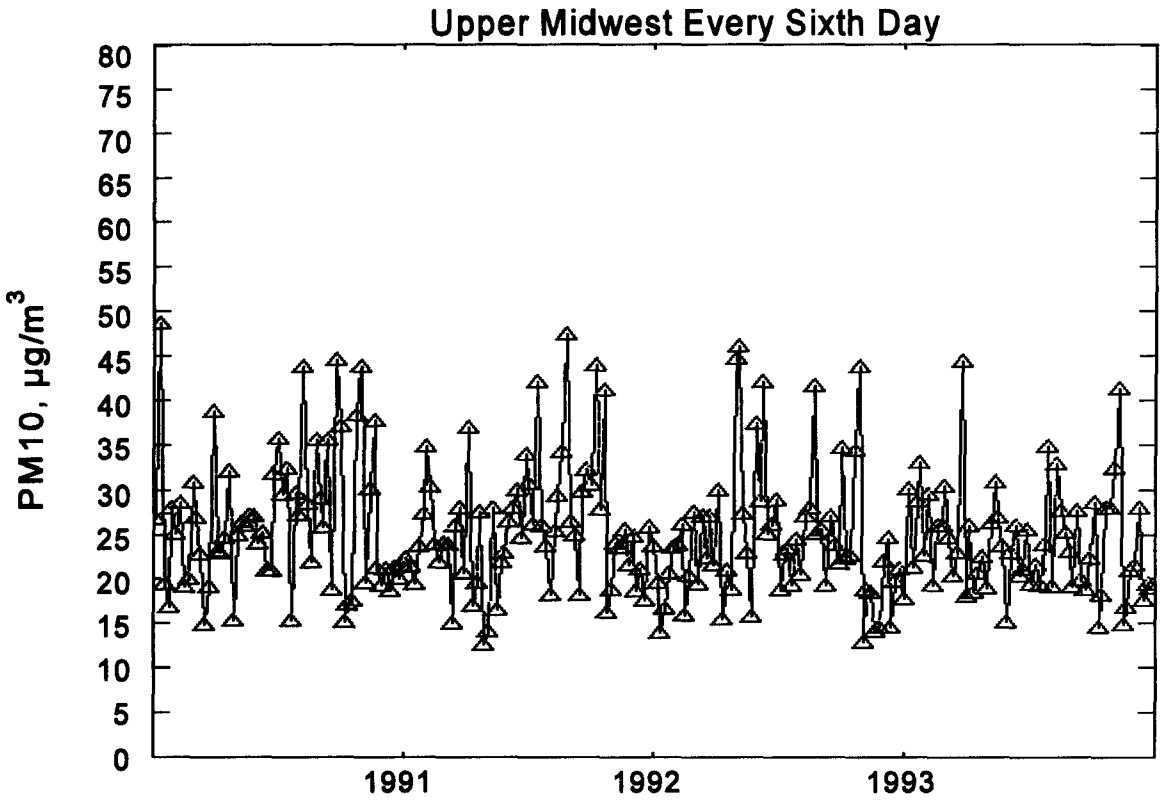

Figure 6-43. Short-term variation of PM_{10} average for the Upper Midwest. Data are reported every sixth day.

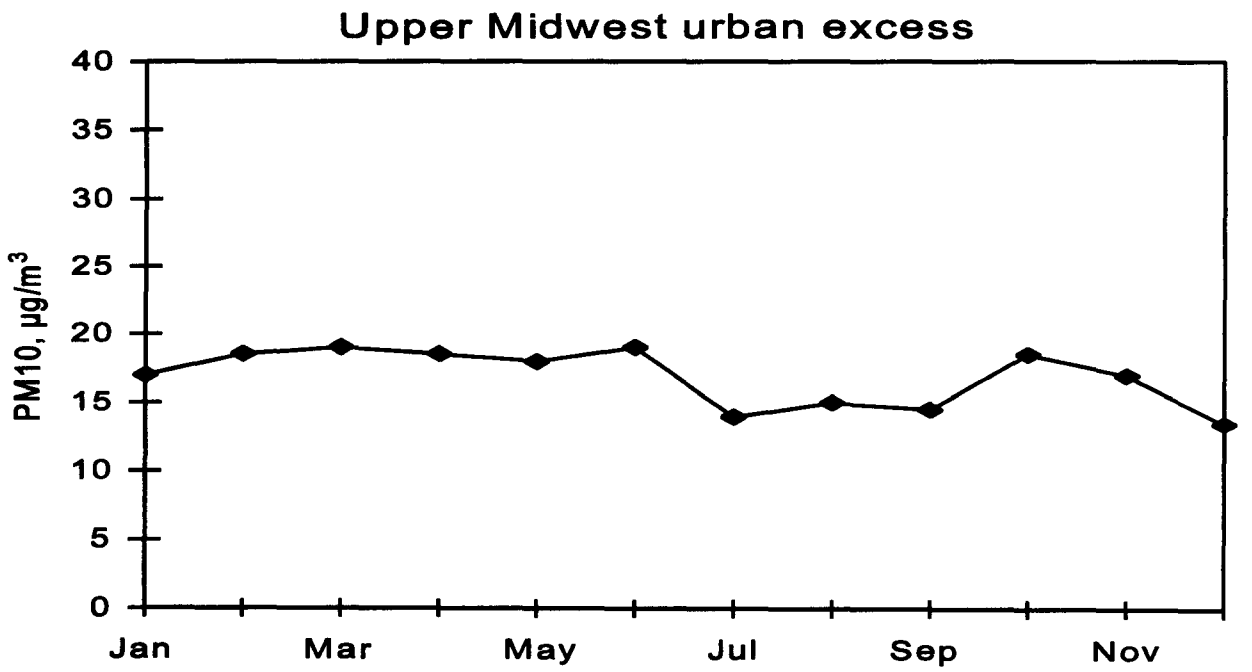

Figure 6-44. Urban excess concentration (AIRS minus IMPROVE) for the Upper Midwest.

6.4.5 Regional Aerosol Pattern in the Southwest

The Southwest covers the arid states from western Texas to Arizona (Figure 6-45a). The Southwest is characterized by mountainous terrain features between the southern Rockies and the Colorado Plateau. The industrial activity and agriculture is minor compared to other regions. Major population centers include El Paso, Phoenix, and Tucson. The meteorology of the region is characterized by low annual precipitation, except during the periods when moist air penetrates from the Gulf of Mexico toward these states, bringing moisture and precipitation.

6.4.5.1 Nonurban Size and Chemical Composition in the Southwest

The PM_{10} concentrations at nonurban southwestern sites show a double peak, one during the late spring (April through July), and another in October. This bimodal seasonality is imposed by the coarse particle mode. The $PM_{2.5}$ mass concentration is unimodal with a summer maximum. Overall, the nonurban PM_{10} concentrations are comparatively low (8 to 15 $\mu g/m^3$) and over 60% contributed by coarse particles (Figure 6-45b).

The chemical mass balance (Figure 6-45c) shows sulfates to be the larger contributor during the winter (December through March) as well as in late summer (July through October). However, sulfate and organic carbon contributions are comparable during March through June as well as during November through December. Fine particle soil plays a prominent role in the spring fine particle chemical mass balance reaching 25%, but the contribution of soil decreases during the summer, and during December through February dwindles to below 10%.

The selenium and vanadium concentrations (Figure 6-45d) are very low and rather invariant throughout the year. The fine particle sulfur concentration is low and exhibiting a weak maximum during August. The S/Se ratio is comparatively low and bimodal, with peaks in April through May as well as August through October.

6.4.5.2 Urban Aerosols in the Southwest

In the southwestern U.S. there was a decrease in PM_{10} concentrations between 1988 and 1994 from 38 $\mu g/m^3$ to 24 $\mu g/m^3$ for all sites and from 43 $\mu g/m^3$ to 29 $\mu g/m^3$ for trend sites (Figure 6-46b). The reductions were 37% for all sites and 33% for trend sites. The

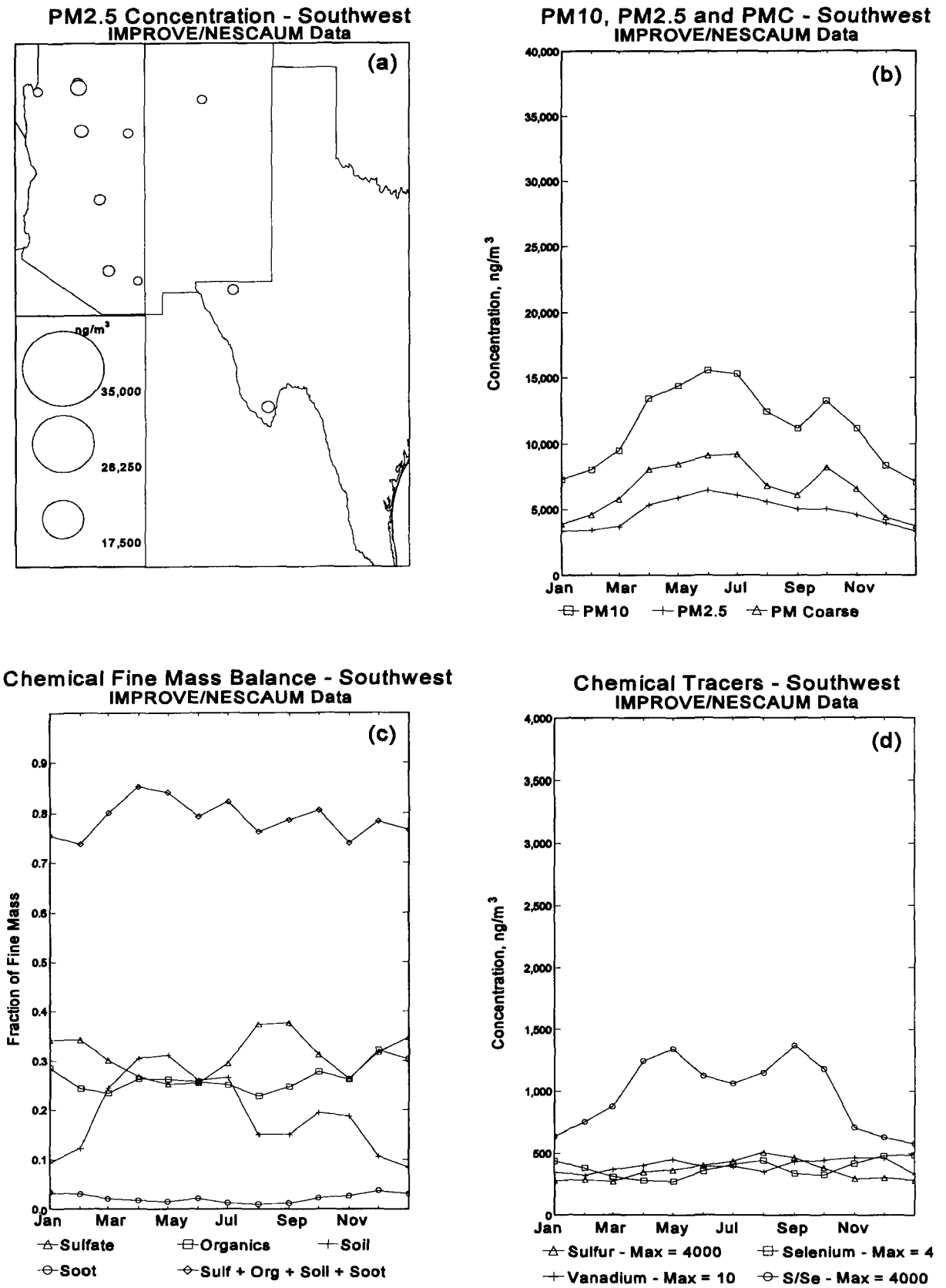

Figure 6-45. IMPROVE/NESCAUM concentration data for the Southwest: (a) monitoring locations; (b) PM_{10}, $PM_{2.5}$, and PMCoarse (PMC); (c) sulfate, soil, organic carbon (OC), and elemental carbon (EC) fractions; and (d) tracers.

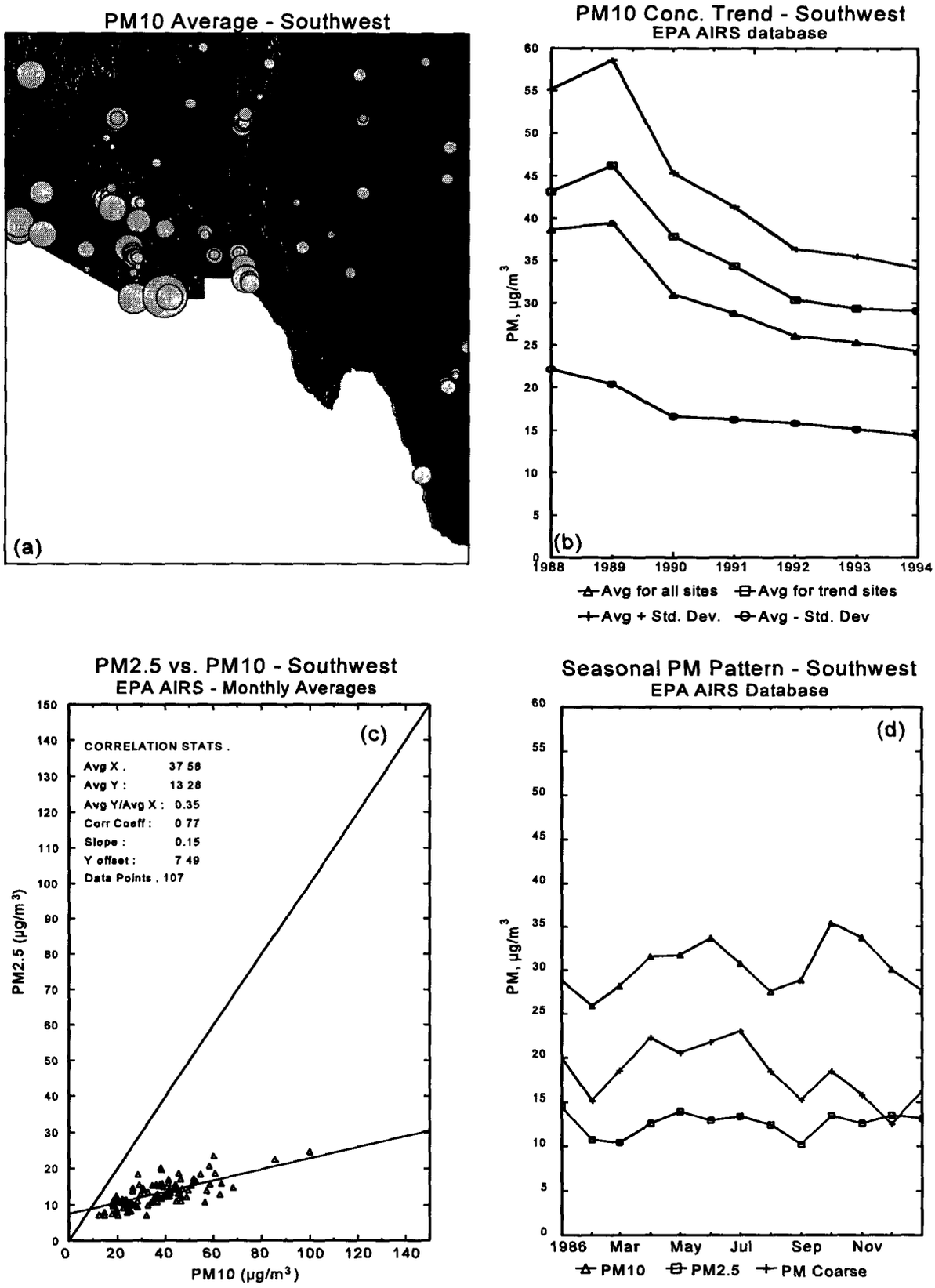

Figure 6-46. AIRS concentration data for the Southwest: (a) monitoring locations; (b) regional PM_{10} monitoring trends; (c) PM_{10} and $PM_{2.5}$ relationship; and (d) PM_{10}, $PM_{2.5}$, and PMCoarse seasonal trends.

downward trends in PM_{10} concentrations were not monotonic. In the Southwest is the large concentration spread of 45% among the monitoring sites (Figure 6-46b). Sites with low concentrations (<20 $\mu g/m^3$) occur adjacent to high concentration sites (>50 $\mu g/m^3$).

Seasonally, the Southwest PM_{10} concentration shows two peaks, one in late spring April through June, and another during the fall October through November. The concentration dip in August and September has not been observed for any other region. The late summer concentration drop coincides with the occurrence of the moist air flows from the Gulf of Mexico.

The size segregated aerosol samples from the Southwest clearly show that coarse particles make the major contribution to the PM_{10} concentration, the fine particles contributing only 37% (Figure 6-46a). The scatter in Figure 6-46c indicates that high PM_{10} concentration months can occur with low concentrations of fine particles. In the Southwest natural and man-induced coarse particle dust is a major contributor to PM_{10} aerosols (Figure 6-45c).

The short term PM_{10} concentration over the Southwest (Figure 6-47) exhibits a highly irregular pattern, that ranges between 11 to 52 $\mu g/m^3$ regional average. Both the lowest (10 to 15 $\mu g/m^3$) as well as the highest values are dispersed throughout the year.

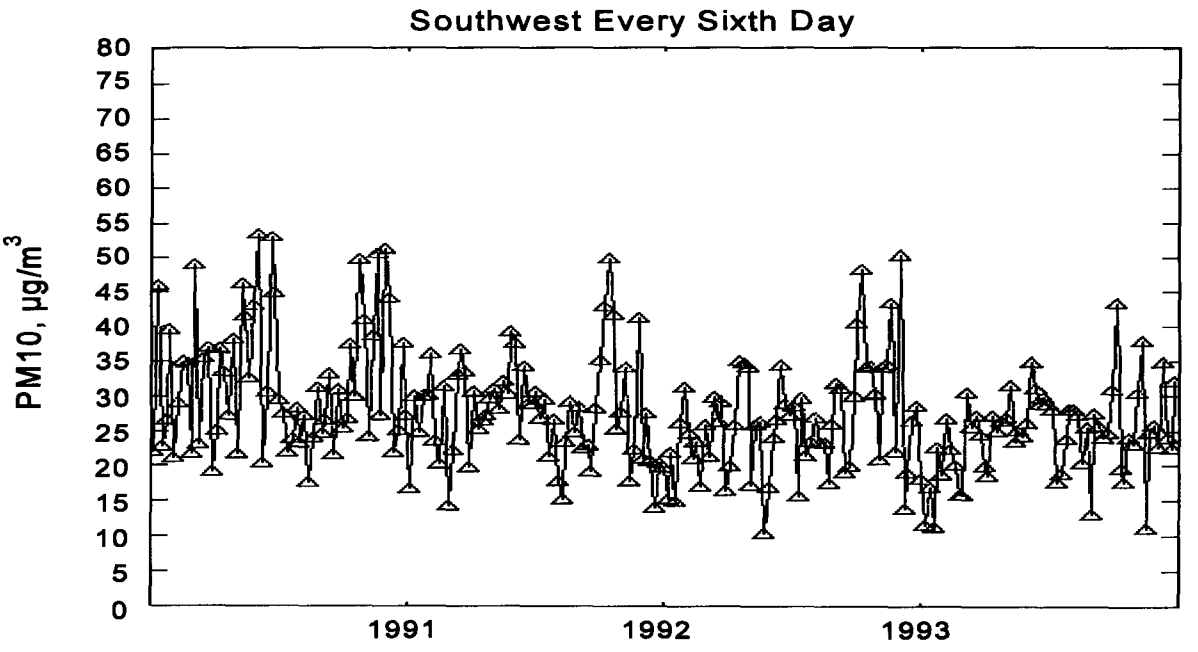

Figure 6-47. Short-term variation of PM_{10} average for the Southwest. Data are reported every sixth day.

The urban excess PM_{10} (AIRS-IMPROVE) for the Southwest is given in Figure 6-48, and the urban excess is substantially larger than in the regions discussed previously.

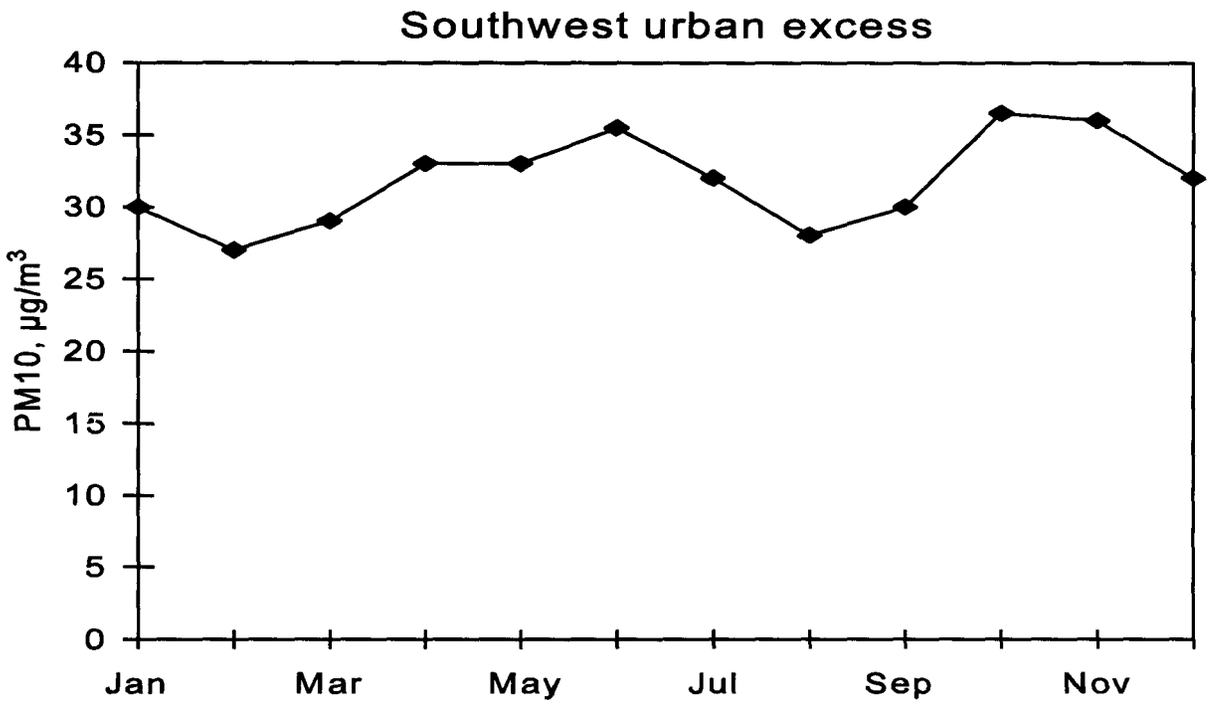

Figure 6-48. Urban excess concentration (AIRS minus IMPROVE) for the Southwest.

6.4.6 Regional Aerosol Pattern in the Northwest

The Northwest is defined to cover the bulk of the western United States north of the Arizona border (Figure 6-49a). It is covered by mountainous terrain of the Rockies, as well as the Sierra-Cascade mountain ranges. The Northwest is actually a collection of many aerosol subregions. The meteorology is highly variable between the Pacific Northwest and the Rocky Mountains with prevailing winds generally from the west. The main feature of the Northwest is pronounced elevation ranges between mountain tops and valleys, and the resulting consequences on emission pattern (confined to the valleys) and limited ventilation. The Northwest has also industrial population centers, such as Seattle, Portland, Salt Lake City and Denver.

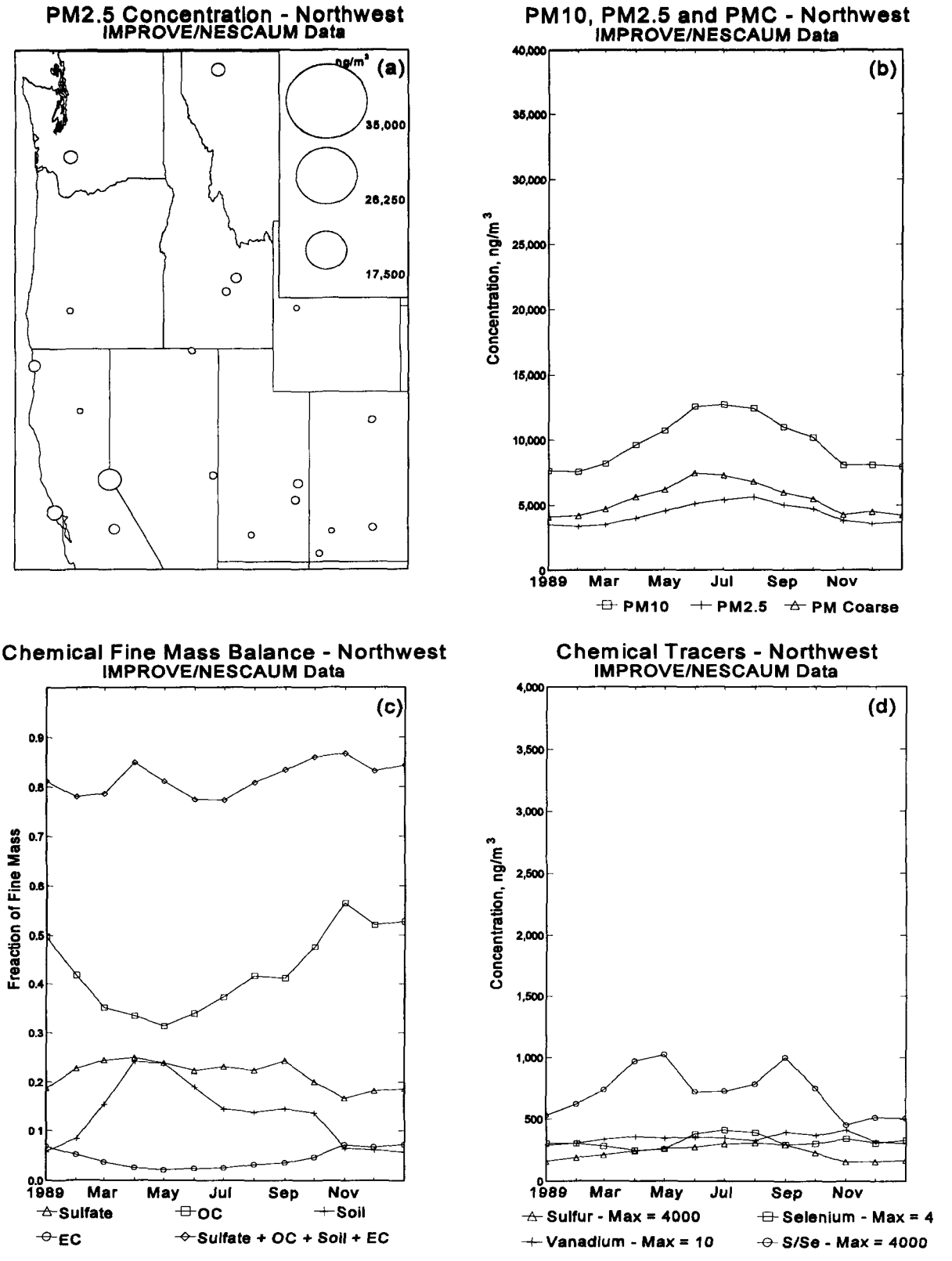

Figure 6-49. IMPROVE/NESCAUM concentration data for the Northwest: (a) monitoring locations; (b) PM_{10}, $PM_{2.5}$, and PMCoarse (PMC); (c) sulfate, soil, organic carbon (OC), and elemental carbon (EC) fractions; and (d) tracers.

6.4.6.1 Nonurban Size and Chemical Composition in the Northwest

The nonurban PM_{10} concentrations show low values ranging between 7 to 14 $\mu g/m^3$ in the northwestern U.S. The seasonality shows a peak in the summer which is contributed by both fine and coarse particles. Coarse particles account for more than half of the PM_{10}, particularly during March through June spring season (Figure 6-49b).

The chemical mass balance (Figure 6-49c) shows roughly comparable contributions from sulfates and organics, but their seasonality is phase shifted. Sulfates prevail during the spring season while organics dominate during late fall (October through January). Fine particle soil dust contributes 20% during April and May, but decline well below 10% during the winter months (November through February). Overall, about 80% of the fine mass is accounted for by the sulfates, organic carbon, soil, and elemental carbon.

Examining the carbonaceous particles and regional haze in the western and northwestern U.S., White and Macias (1989) concluded that in the rural areas the concentrations of particulate carbon are comparable to those of sulfate. Examining particulate nitrate, White and Macias (1987) showed that the particulate nitrate concentration in the northern states (MT, ID, WY) were substantially higher than sulfate concentrations. Aerosol particulate nitrates over rural mountainous West were also episodic (i.e., few samples contributed a large fraction of the fine particle integrated dosage).

Both selenium and vanadium concentrations (Figure 6-49d) are low in the Northwest, but there is an indication of a summer peak of Se. The S/Se ratio is between 500 to 1,000, which is the lowest among the regions. This ratio has both spring peak as well as fall peak, similar to the pattern observed for the southwestern United States.

6.4.6.2 Urban Aerosols in the Northwest

In the northwestern U.S. there was a decrease in the annual average PM_{10} concentration between 1988 and 1994 from 33 $\mu g/m^3$ to 24 $\mu g/m^3$ for all sites and from 35 $\mu g/m^3$ to 27 $\mu g/m^3$ for trend sites (Figure 6-50b). The reductions were 27% for all sites and 23% for trend sites. However, the 1985 to 1994 reductions may be overestimates because of the low station density in the early years. Once again, the average 1993 concentration is 25 $\mu g/m^3$ which is comparable to the 1993 concentrations of the eastern U.S. regions. The spread of

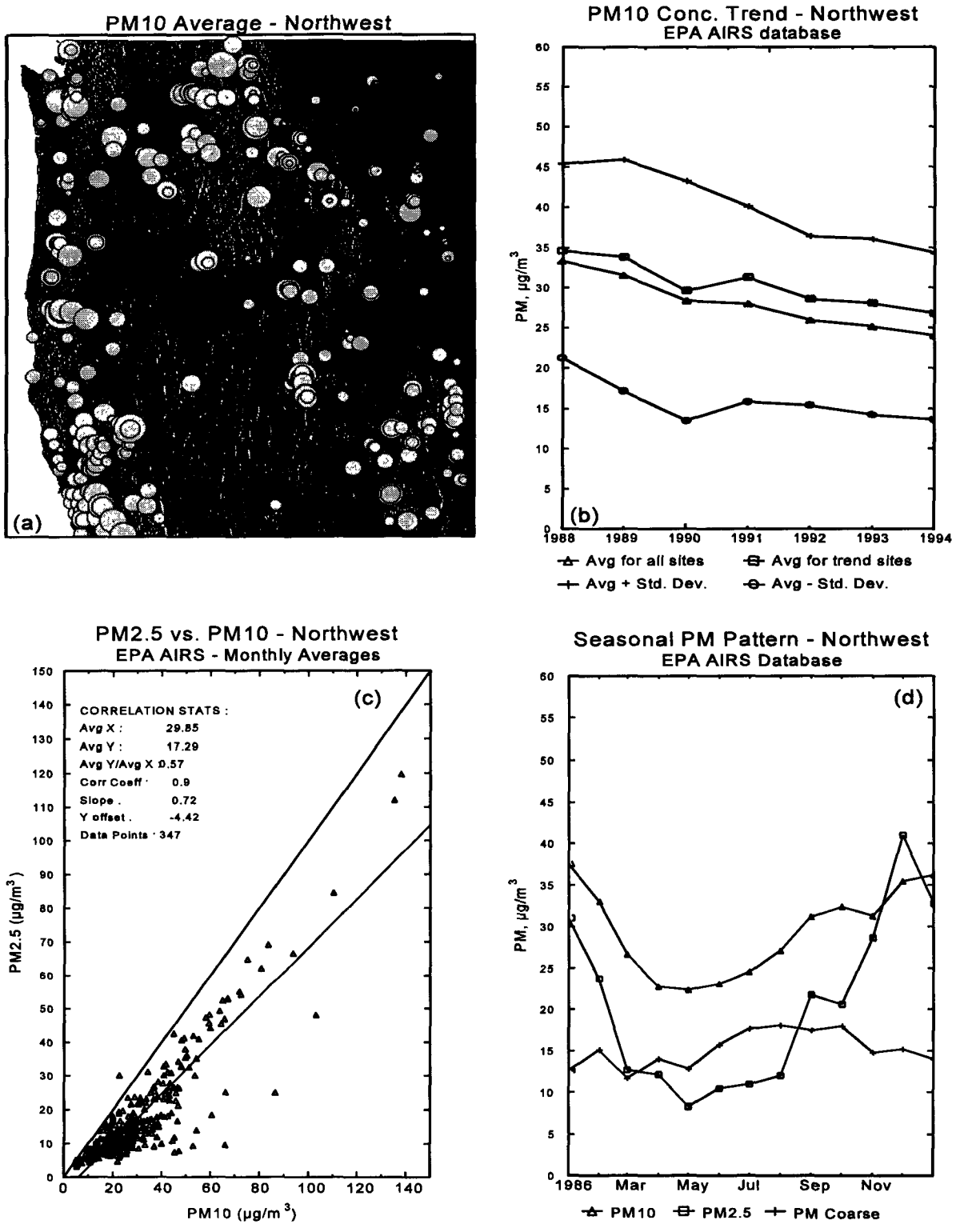

Figure 6-50. AIRS concentration data for the Northwest: (a) monitoring locations; (b) regional PM_{10} monitoring; (c) PM_{10} and $PM_{2.5}$ relationship; and (d) PM_{10}, $PM_{2.5}$, and PMCoarse seasonal trend.

concentration among the Northwest stations is large, with standard deviation of 45% (Figure 6-50b). This spread in the concentration values is also evident from the various circle sizes of the Northwest map (Figure 6-50a). The highest PM_{10} concentrations in the Northwest occur in more remote mountainous valleys, rather than in the center of urban-industrial areas.

The seasonality of the northwestern United States has an amplitude of 36% which is comparable to the strong seasonality of the eastern U.S. The peak PM_{10} concentrations occur in the winter. The lowest PM_{10} concentration occurs during March through May and gradually increases to a peak in December through January, falling sharply between January and March.

The limited $PM_{2.5}$-PM_{10} data for the Northwest indicate that on the average 57% of PM_{10} particles are $PM_{2.5}$. Figure 6-50c also indicates that the extreme PM_{10} concentrations are contributed mainly by fine particles. Furthermore, the extreme PM_{10} concentrations also occur in the winter season.

The daily concentration when averaged over the large and heterogeneous northwestern region exhibits a remarkably small sixth day to sixth day variation (Figure 6-51). Furthermore, there is clear seasonality with a strong winter peak. Within a given season, the regionally averaged concentrations only vary by 20 to 40% from one sixth day to another. Examination of the logarithmic standard deviation (Figure 6-50b) shows that the Northwest is spatially the most heterogeneous and has the highest logarithmic standard deviation among all regions. Evidently, in the Northwest high concentration PM_{10} pockets in topographically confined airsheds result in strong spatial and temporal variations. However, large scale elevated PM_{10} concentrations that cover the entire Northwestern region do not exist because high concentrations are not "synchronized" among the different airsheds. In this sense, the Northwest differs markedly from the eastern U.S., where large regional scale air masses with elevated PM_{10} determine the regionally averaged values. The urban excess PM_{10} (AIRS-IMPROVE) for the Northwest is given in Figure 6-52. The winter urban excesses are almost as large as in the Southwest (Figure 6-48). However, if the region is a collection of aerosol subregions, the small number of nonurban sites may not be representative of this collection of subregions.

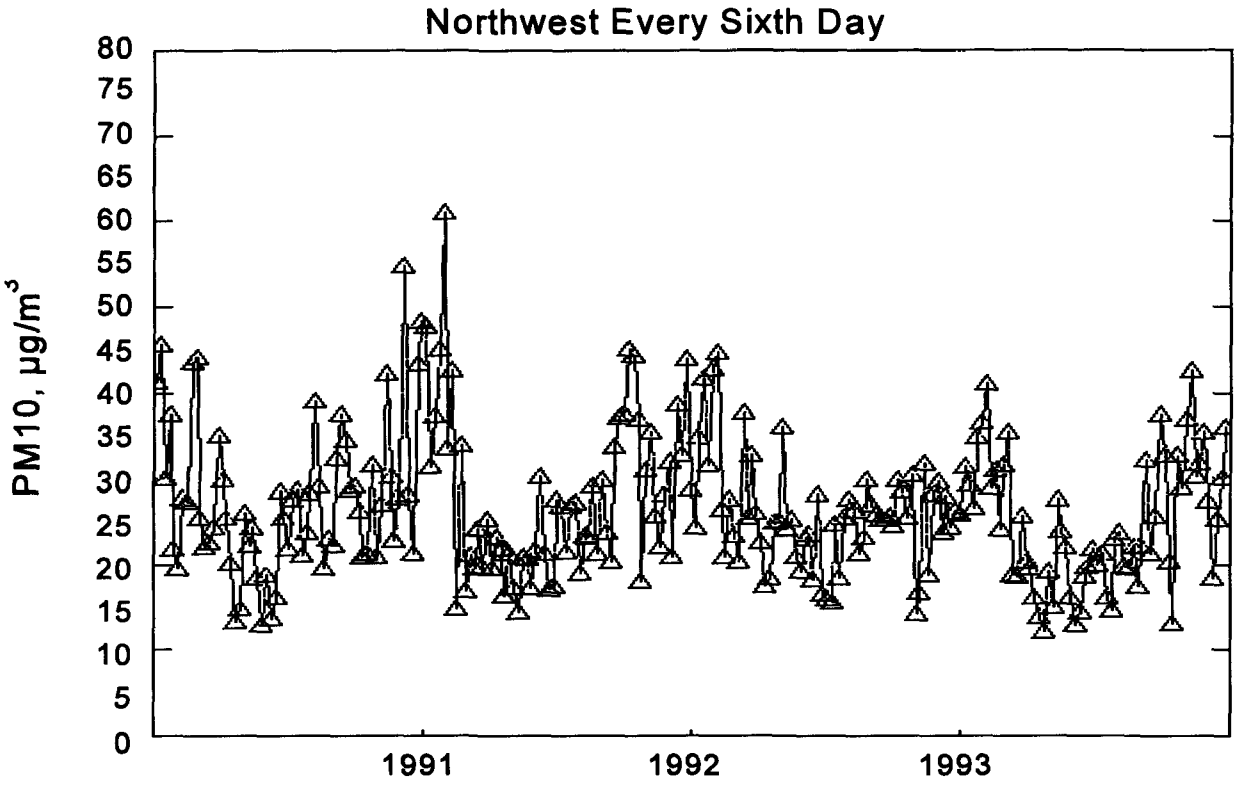

Figure 6-51. Short-term variation of PM_{10} average for the Northwest. Data are reported every sixth day.

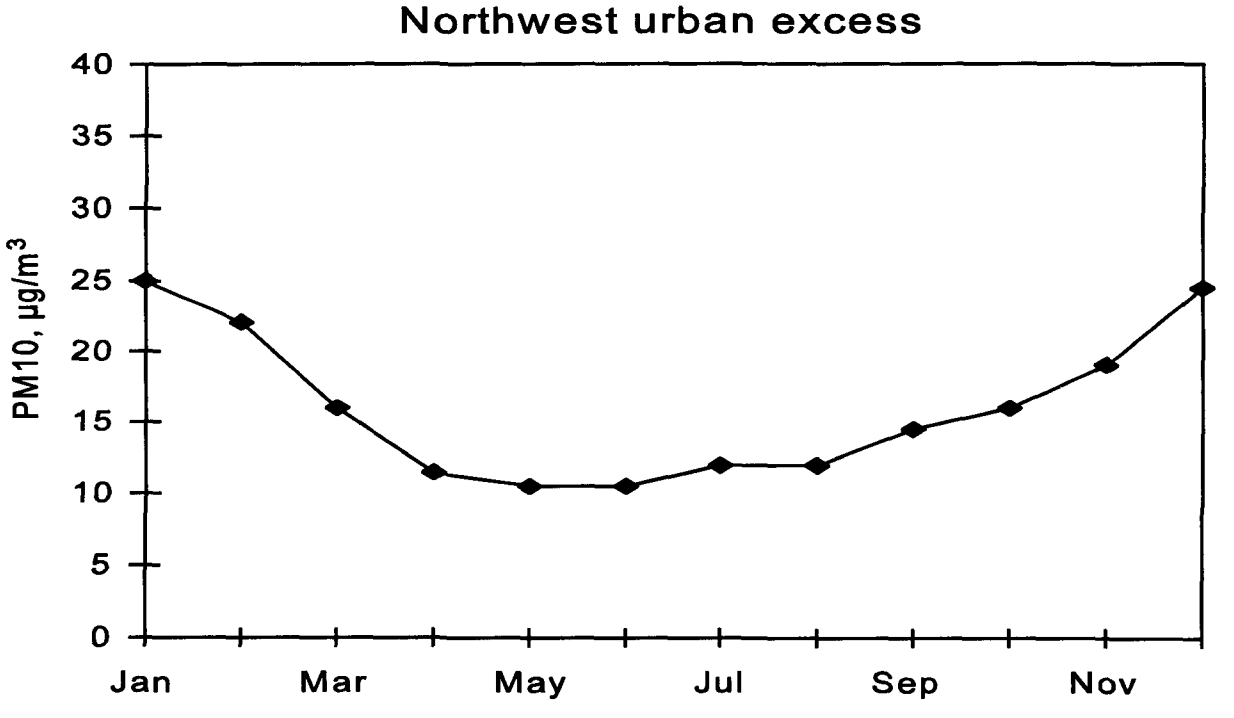

Figure 6-52. Urban excess concentration (AIRS minus IMPROVE) for the Northwest.

6.4.7 Regional Aerosol Pattern in Southern California

The region covers California south of San Francisco Bay (Figure 6-53a). It was considered as a separate region primarily because of the known high aerosol concentrations in the Los Angeles and San Joaquin basins. Meteorologically the region is exposed to the air flows from the Pacific that provide the main regional ventilation toward the south and southeast. The precipitation in the region occurs in the winter season, with the summer being hot and dry. The regional ventilation of the San Joaquin Valley is severely restricted by the Sierra Nevada Mountain range. Also, the San Gabriel Mountains constitute an air flow barrier east of the Los Angeles basin. Both basins have high population, as well as industrial and agricultural activities. Hence, human activities are believed to be the main aerosol sources of the region.

6.4.7.1 Nonurban Size and Chemical Composition in Southern California

The PM_{10} concentration at the few nonurban sites over southern California ranges between 10 $\mu g/m^3$ during December through February, and 20 to 25 $\mu g/m^3$ in April through October. Coarse particles contribute more than 50% of the PM_{10} during the warm season May through October. Both the fine and coarse aerosol fractions are lowest during the winter months (December through March). The summer peak fine particle seasonality at nonurban southern California sites is in marked contrast to the strongly fall peaked urban fine particle concentrations (Figures 6-53b, 6-54d).

The chemical mass balance (Figure 6-53c) of nonurban southern California aerosol has a substantial contribution by organics of 30 to 40% throughout the year. Sulfates account for only 10 to 15% of the fine mass in the winter, and about 20% in the summer months. The sulfate fraction of the nonurban southern California fine mass is the lowest among the regions. Fine particle soil dust is about 10% between April through November and drops to 5% during the winter months. A notable feature of the southern California chemical mass balance is that 45% of the winter, and 35% of the summer fine mass concentration is not accounted by sulfates, soils, organic carbon,and elemental carbon. Nitrates are a major contributor to the southern California aerosols (Solomon et al., 1989).

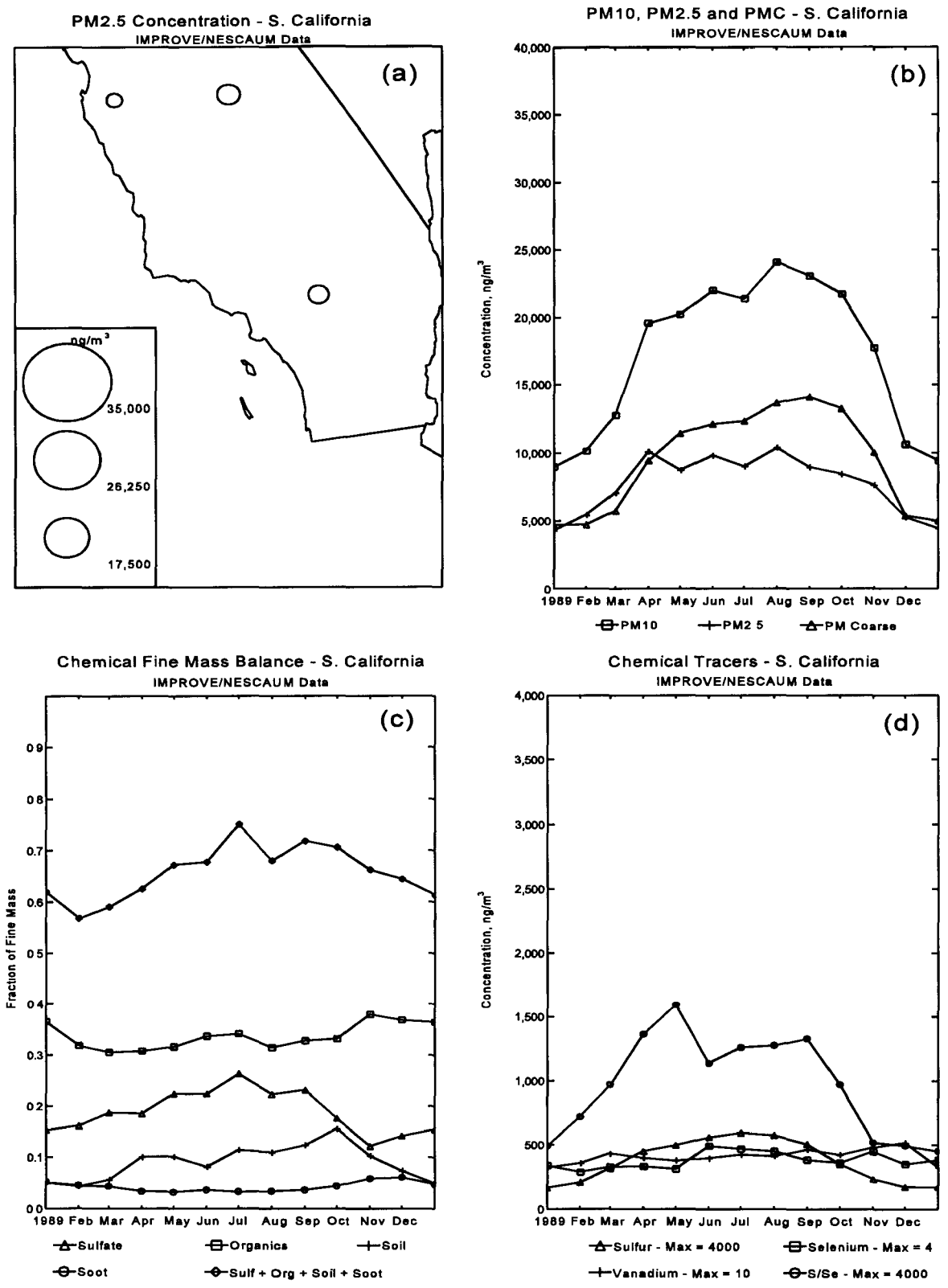

Figure 6-53. IMPROVE/NESCAUM concentration for Southern California: (a) monitoring locations; (b) PM_{10}, $PM_{2.5}$, and PMCoarse (PMC); (c) sulfate, soil, organic carbon (OC), and elemental carbon (EC) fractions; and (d) tracers.

Both selenium and vanadium (Figure 6-53d) show low values throughout the year without significant seasonality. On the other hand the fine particle sulfur concentration shows a definite summer peak at 500 ng/m^3, compared to 200 ng/m^3 during the winter. Consequently, the S/Se ratio increase from 500 in the winter 1,000 to 1,500 in the summer.

6.4.7.2 Urban Aerosols in Southern California

In the southern California region there was a decrease in the annual average PM_{10} concentration between 1988 and 1994 from 41 μg/m^3 to 30 μg/m^3 for all sites and from 42 μg/m^3 to 32 μg/m^3 for trend sites (Figure 6-54b). The reductions were 27% for all sites and 241% for trend sites. There is a sizable concentration spread among the stations (40% standard deviation). Inspection of the circle sizes in the map points (Figure 6-54a) to uniformly high concentrations in the San Joaquin Valley as well as in the Los Angeles basin. The low concentration sites are located either on the Pacific coast outside of the Los Angeles basin or in the Sierra Nevada Mountains. Thus there are clear patterns of basin-wide elevated PM_{10} concentrations with lower values in more remote areas (Figure 6-54a).

The seasonality of the PM_{10} pattern in southern California is significant at 27%. Furthermore, the seasonal pattern is unique that the highest concentrations occur in November and the lowest in March. However, it is a see saw rather than a sinusoidal pattern.

On the average, about half of southern California PM_{10} is contributed by fine particles as shown in the $PM_{2.5}$-PM_{10} scattergram. Most of the high PM_{10} concentration months dominated by fine particles tend to be in the fall.

The sixth day average time series for the southern California region (Figure 6-55) shows remarkably high sixth daily variance, between 10 and 75 μg/m^3. The lowest values tend to occur between January and April, while the highest concentrations (>50 μg/m^3) tend to occur during October through December. Concentration excursions of a factor of two are common between two consecutive six day time periods. However, visual inspection of the sixth daily signal also reveals a substantial seasonality highest in the fall (September through December) and lowest in the spring.

The urban excess PM_{10} (AIRS-IMPROVE) for Southern California is given in Figure 6-56. The urban excesses are larger especially in winter, as are the urban excesses

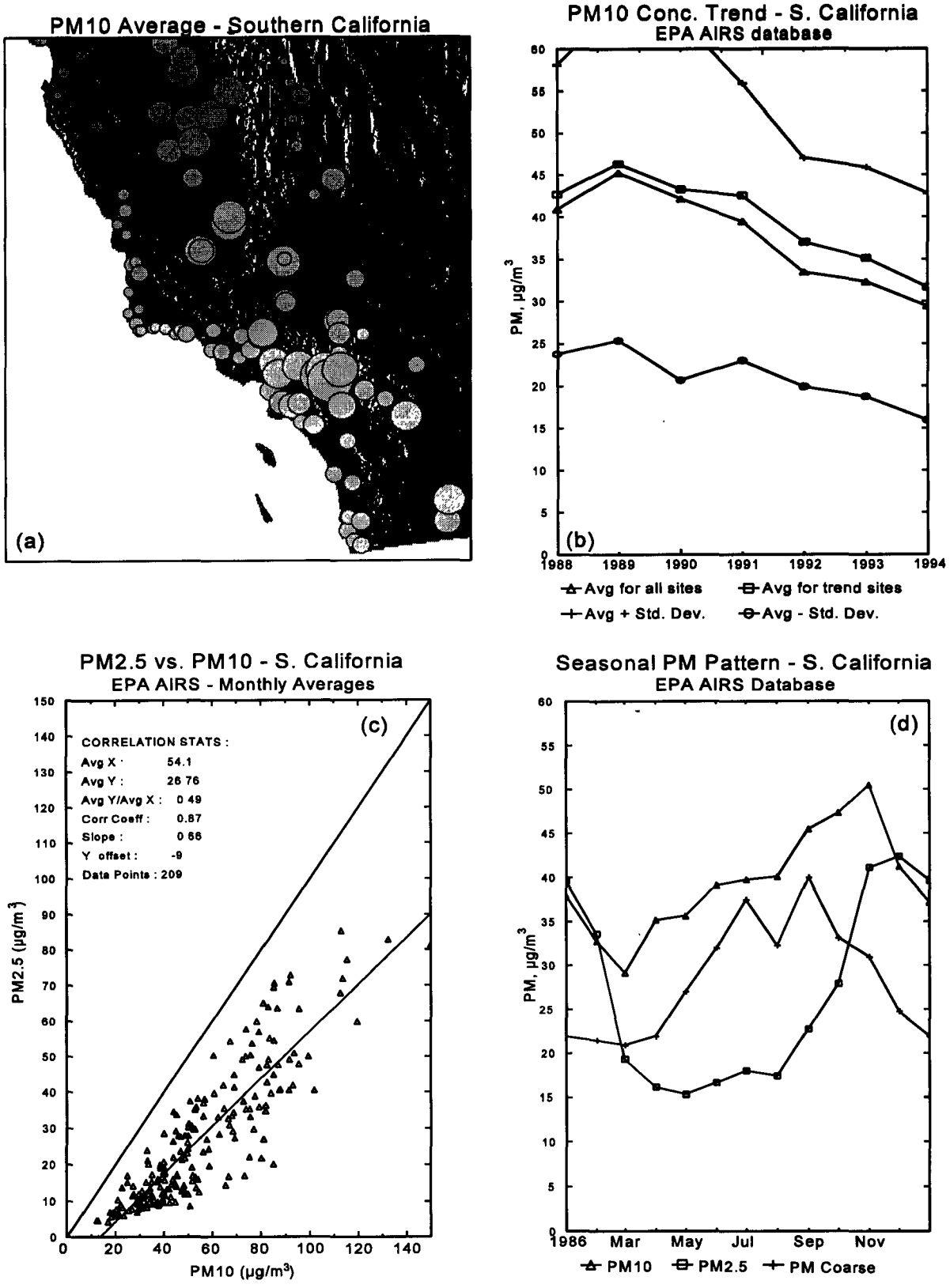

Figure 6-54. AIRS concentrations for Southern California: (a) monitoring locations; (b) regional PM_{10} monitoring trends; (c) PM_{10} and $PM_{2.5}$ relationship; and (d) PM_{10}, $PM_{2.5}$, and PMCoarse seasonal trend.

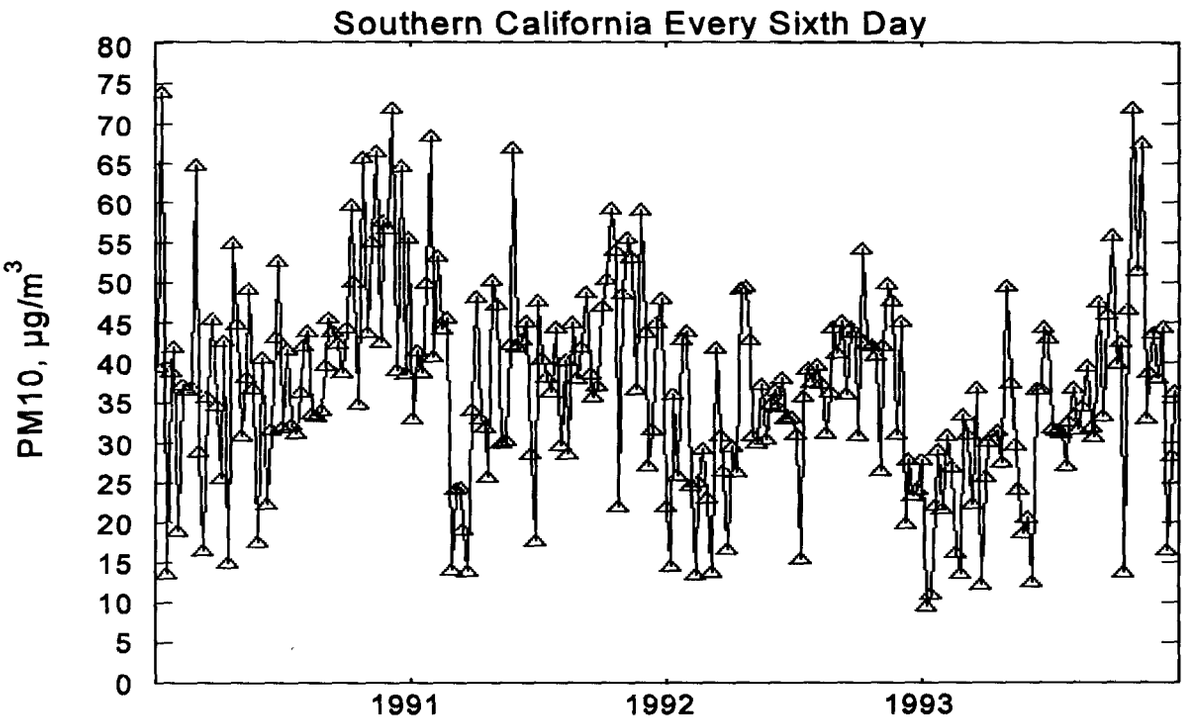

Figure 6-55. Short-term variation of PM_{10} average for Southern California. Data are reported every sixth day.

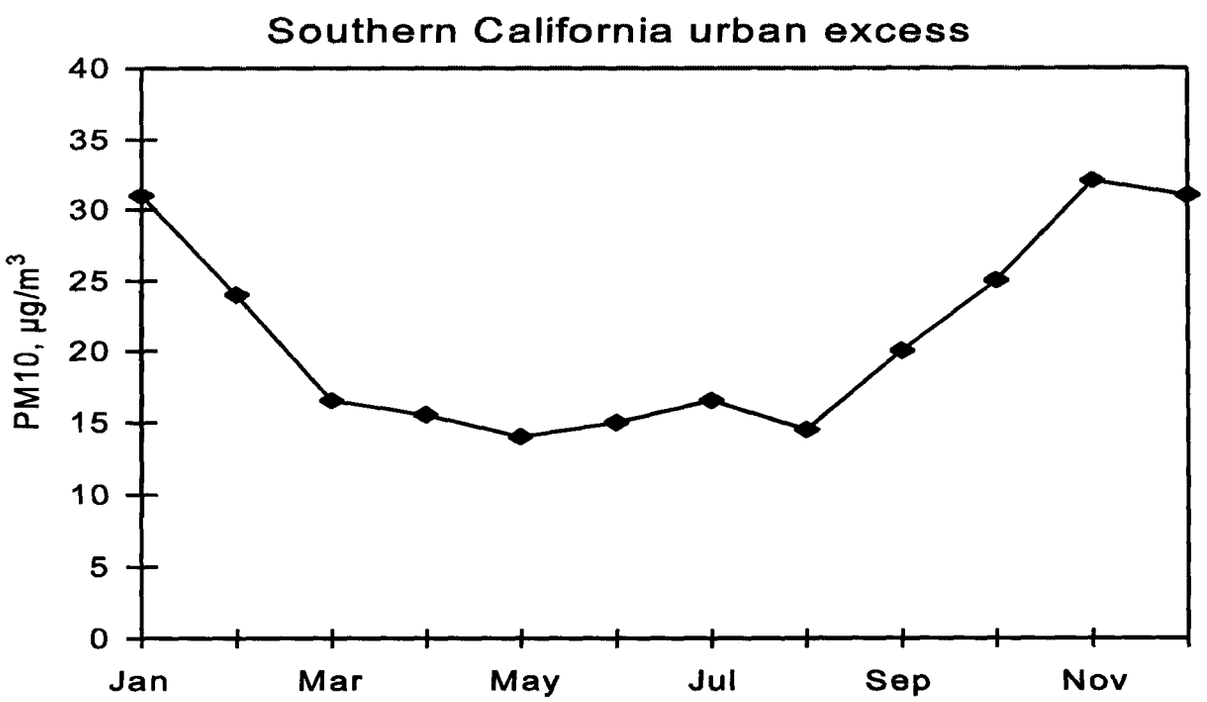

Figure 6-56. Urban excess concentration (AIRS minus IMPROVE) for Southern California.

in the Northwest. Again, these results depend on measurements from a small number of nonurban sites.

6.5 SUBREGIONAL AEROSOL PATTERNS AND TRENDS

The health and other effects of aerosols are imposed on individuals, and the density of population varies greatly in space. Consequently, the evaluation of effects requires the knowledge of aerosol concentrations over specific locations where sensitive receptors reside. The purpose of this section is to characterize the aerosol pattern at specific sites, small airsheds or subregions. The discussions is organized by region and then by monitoring site within a region. Most urban aerosol sampling is confined to PM_{10} or in some instances to $PM_{2.5}$ and PMCoarse . However, detailed chemical composition data are reviewed for several urban areas.

6.5.1 Subregional Aerosol Pattern in the Northeast

In the northeastern region, the Shenandoah National Park and Washington, DC constitute a useful urban-nonurban set of size and chemically resolved aerosol data. New York City and Philadelphia are also major metropolitan areas with substantial aerosol data bases. Whiteface Mountain site distinguishes itself from its background by high elevation.

6.5.1.1 Shenandoah National Park

The PM_{10} concentration at the Shenandoah National Park IMPROVE site (Figure 6-57a) exhibits a pronounced summer peak (27 $\mu g/m^3$), which is a factor of three higher than the winter value of 9 $\mu g/m^3$. The strong seasonality is driven by the seasonal modulation of the fine mass which accounts for 70 to 80% of the PM_{10} mass (Figure 6-57a). The coarse particle concentration ranges between 3 and 6 $\mu g/m^3$, which is small compared to the fine particle mass, particularly in the summer season, when it accounts for $< 25\%$ of the PM_{10}. It is clear that at this nonurban site, in the vicinity of industrial source regions, fine particles determine the magnitude of PM_{10}.

The chemical mass balance for the Shenandoah IMPROVE monitoring site (Figure 6-57b) clearly documents the dominance of sulfate aerosols, which contribute about

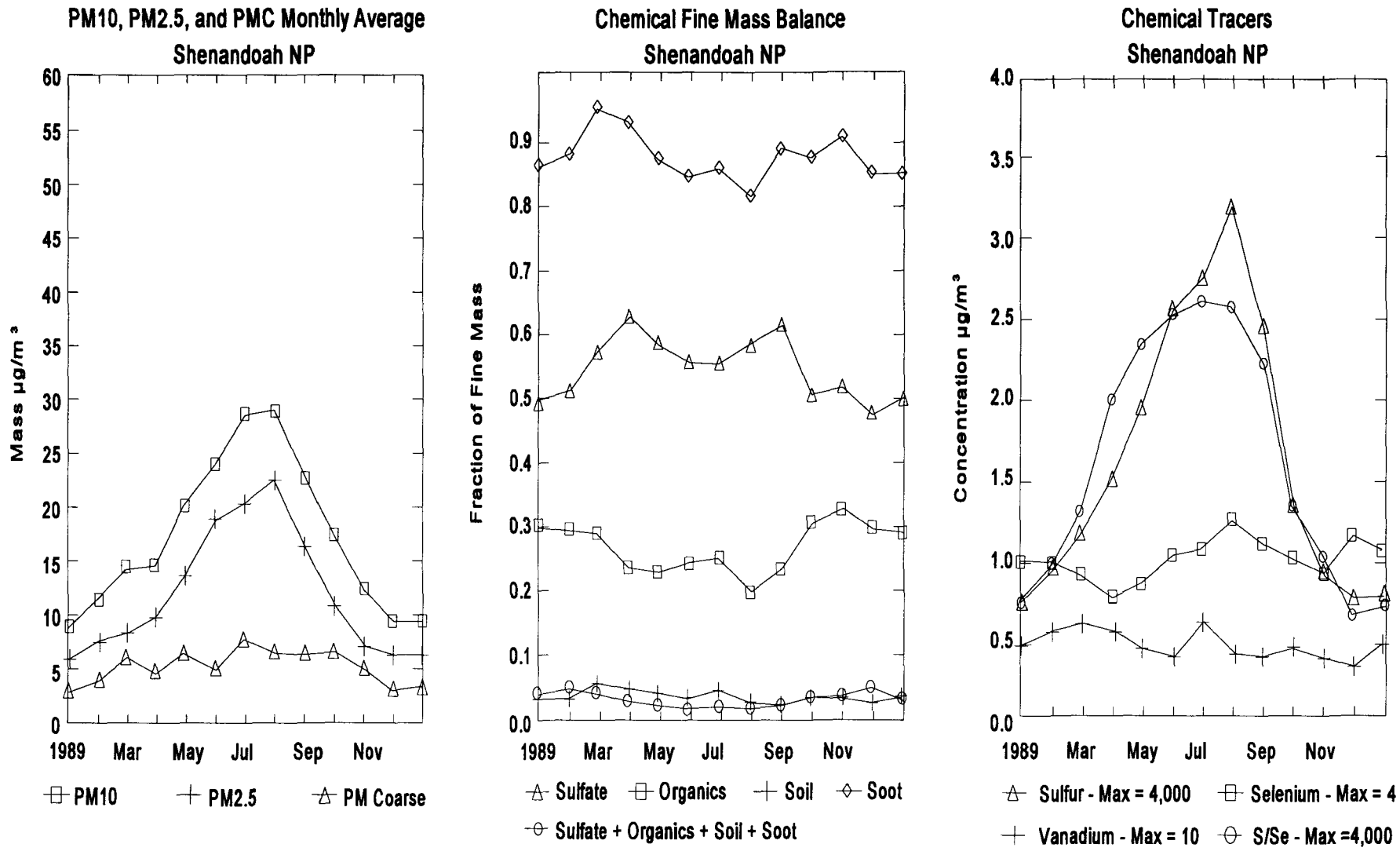

Figure 6-57. IMPROVE/NESCAUM concentration for Shenandoah National Park: (a) PM_{10}, $PM_{2.5}$, and PMCoarse; (b) chemical fraction of sulfate, soil, organic carbon (OC), and elemental carbon (EC); and (c) tracers.

60% of the fine mass during April through September and about 50% during the winter months. Organic carbon, on the other hand, range from 20% in summer to 30% in the winter months. The contribution of fine particle soil and elemental carbon is well below 5%. Throughout the year about 90% of the fine mass is accounted for by these measured substances. At the Shenandoah site, the sulfate aerosols constitute a higher percentage of the chemical mass balance, and lower percentages of organic carbon and elemental carbon than for the averaged nonurban Northeastern sites (Figure 6-29).

Chemical tracer data are shown in Figure 6-57c. The concentration of coal-tracer selenium shows two maximum, one during December through March, and another in June through September. Vanadium is relatively constant throughout the year. The fine particle sulfur concentration is almost a factor of five higher in August (3,300 ng/m^3) than in December (700 ng/m^3). This extreme sulfur seasonality is stronger at the Shenandoah site relative to the averages for sulfur seasonality at all nonurban Northeastern sites (Figure 6-29). The S/Se ratio has a remarkably smooth but highly seasonal variation that varies by about factor of four between the winter (700) and summer (2,600) values. If Se-bearing coal combustion is the exclusive source of sulfur at the Shenandoah National Park , then the sulfate production from the SO_2 associated with coal-fired sources is 3 to 4 times higher in the summer than in the winter.

An examination of the nature and sources of haze in the Shenandoah Valley/Blue Ridge Mountains area (Ferman et al., 1981) showed that sulfate aerosols were the most important visibility reducing species. Averaging 55% of the fine particle mass, sulfates (and associated water) accounted for 78% of the total light extinction. The second most abundant fine particles, accounting for 29% of the fine mass, was organic carbon. The remaining particle mass and extinction were due to crustal materials.

Using an in-situ rapid response measurement of $H_2SO_4/(NH_4)_2SO_4$ aerosol in Shenandoah National Park, VA, Weiss et al. (1982) found that the summer sulfate and ammonium ions average 58% of particle mass smaller than 1 mm. The particle composition in terms of NH_4^+/SO_4^{2-} molar ratio ranged from 0.5 to 2.0 with strong diurnal variation. The particles were most acidic at 1500 EDT and least acidic in the period 0600 to 0900 EDT. The water contained in ambient aerosol particles was more strongly associated with sulfate and ammonium ions than with the remainder of the fine particle mass.

6.5.1.2 Washington, District of Columbia

The PM_{10} concentration at Washington DC (at the top of the National Park Service Headquarters building) is virtually constant over the seasons at 25 to 30 $\mu g/m^3$. Fine particles contribute over 70% of PM_{10} throughout the year (Figure 6-58a). The weak seasonality in the fine particle mass is in sharp contrast to the factor of three seasonal fine mass modulation at the Shenandoah National Park. The coarse particle concentration in Washington, DC is 8 to 10 $\mu g/m^3$ throughout the year, exhibiting virtually no seasonality.

$PM_{2.5}$ at the urban Washington, DC site (figure 6-58b) is dominated by sulfates during the summer months (over 50%), but declines to 30% in January. Organic carbon, on the other hand, is 40% during October through January but only 30% during May through August. Thus, the relative roles of organics and sulfates at the Washington, DC urban site is fully phase shifted by half a year. Elemental carbon is a substantial contributes 9 to 12% during October through December. Fine particle soil contributes a low 2 to 5% to $PM_{2.5}$ at this urban site.

The chemical tracer species are shown in Figure 6-58c. The concentration of the coal tracer selenium ranges between 1.5 to 2.0 pg/m^3 without appreciable seasonality. The urban Se in Washington, DC, is much higher than the Se at the northeastern nonurban sites. Vanadium, the tracer for fuel oil, varies by factor of two between the high winter values (>8 pg/m^3) and low summer values (3 pg/m^3). The pronounced V concentration seasonality is a clear indication of that the emissions from fuel oil and other vanadium sources are seasonal. The fine particle sulfur concentration varies by about factor of two between 1,400 ng/m^3 winter concentration, and about 3,000 ng/m^3 summer peak. The seasonal modulation of sulfur in Washington, DC is only factor of two compared to the factor of four fine sulfur modulation at Shenandoah National Park. The difference is primarily due to the elevated winter sulfur in Washington, DC. The S/Se ratio is about 600 in the winter and about 1500 in the summer. It differs from Shenandoah by the lower summer S/Se ratios. This result may be associated with differences in the air parcels involved in long-range transport and transformation of SO_2 to sulfate at Shenandoah compared to Washington, DC.

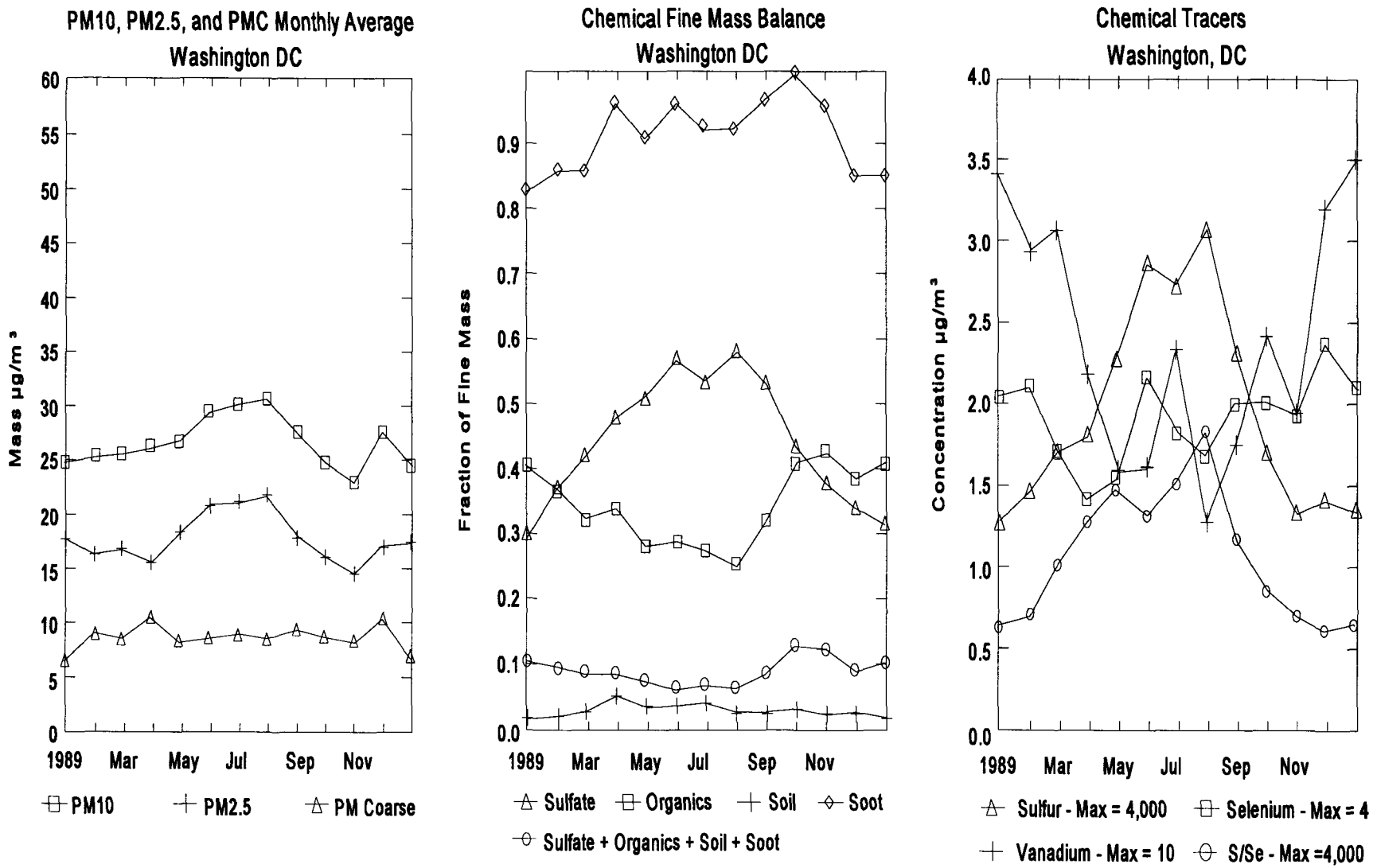

Figure 6-58. IMPROVE/NESCAUM concentration for Washington, DC: (a) PM_{10}, $PM_{2.5}$, and PMCoarse; (b) chemical fraction of sulfate, soil, organic carbon (OC), and elemental carbon (EC); and (c) tracer concentrations.

6.5.1.3 Comparison of Nonurban (Shenandoah) to Urban (Washington, District of Columbia) Aerosols

The Washington, DC, urban site and the companion nonurban Shenandoah monitoring site constitute a rare data pair that allows the quantification of urban-rural differences in fine and coarse particle concentration, and chemical composition. Within Washington, DC, industrial emissions are moderate compared to the industrial midwestern cities. However, both automobile emission density and emissions from winter time heating are expected to be high. In this section the excess aerosol concentrations in Washington, DC, over the Shenandoah site are examined to elucidate the urban influence.

The Washington, DC, excess PM_{10} concentration (Figure 6-59a) ranges between 15-20 $\mu g/m^3$ in the winter, and <3 $\mu g/m^3$ in the summer. Hence, there is almost an order of magnitude higher urban excess during the winter, compared to the summer. The seasonality of the excess PM_{10} is driven by the winter peak excess fine particle concentration of 10-12 $\mu g/m^3$. The modest excess coarse particles is in the 3 to 6 $\mu g/m^3$ range throughout the year. Thus, the urban Washington, DC concentration exceeds its nonurban regional aerosol values during the winter season, and the excess winter time urban aerosol is largely contributed by fine particle mass. This indicates the smaller role of coarse particle fly ash, road dust resuspended by automobiles or construction, road salt and all other sources of urban coarse particles in Washington, DC, in winter.

The chemical composition of the excess fine particle concentration over the Shenandoah nonurban background is also shown in Figure 6-59b. Fine organic carbon dominates the urban excess ranging between 1 $\mu g/m^3$ during the summer, and 5.5 $\mu g/m^3$ during the winter. The seasonality of excess organic carbon also drives the seasonality of excess fine mass. There is an excess sulfate concentration of 1 to 2 $\mu g/m^3$ in Washington, DC, except during July, August, and September. In fact, in August in Washington, DC, sulfate concentration is about 0.3 $\mu g/m^3$ below the Shenandoah values. The urban excess elemental carbon concentration is 1 to 2 $\mu g/m^3$ throughout the year. The soil contribution to the fine particle mass is identical to the values of the Shenandoah National Park, yielding virtually no excess fine soil contribution in the urban area.

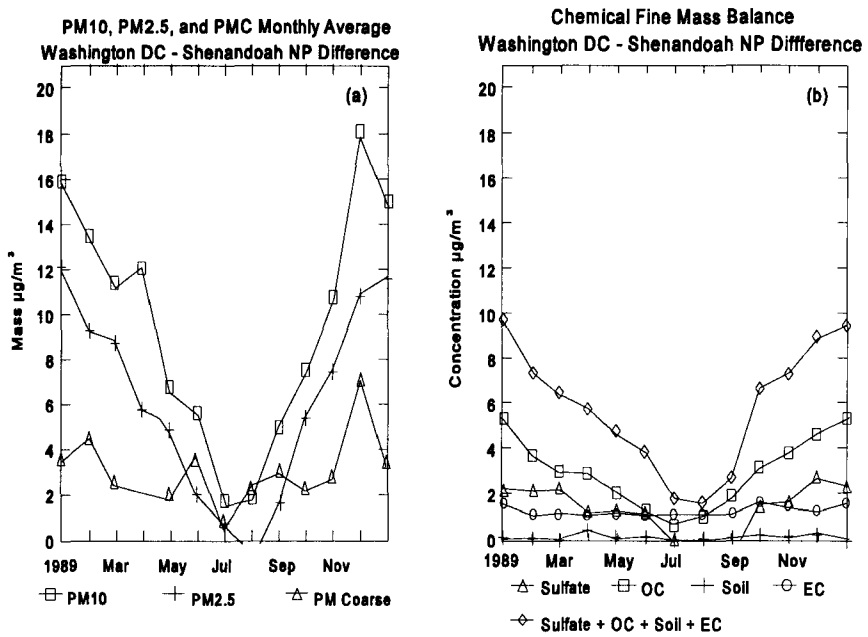

Figure 6-59. Excess aerosol concentration at Washington, DC, compared to Shenandoah National Park: (a) PM_{10}, $PM_{2.5}$, and PMCoarse (PMC); (b) concentration of sulfate, soil, organic carbon (OC), and elemental carbon (EC).

The short-term fine mass concentration at Washington, DC and Shenandoah National Park for the year 1992 is shown in Figure 6-60a. Although the sampling is conducted Wednesdays and Saturdays for 24 h, the data points have been connected. The figure also compares the daily (Wednesdays and Saturdays) fine particle sulfur concentrations at the two monitoring sites. The fine mass concentration time series for Washington, DC, show elevated concentrations (>30 $\mu g/m^3$) that can occur throughout the year. On the other hand, high fine mass levels at Shenandoah are recorded only during the summer season. Particulate sulfur concentrations at the urban and nonurban site are often comparable during the summer (Figure 6-60b). This indicates that particulate sulfur often is a large part of the regional air mass that at any given day influences Washington, DC, and the Shenandoah National Park. Fine particle mass, on the other hand, shows an excess concentration at Washington, DC, particularly during the winter months. The fine mass daily time series clearly indicates that the concentration change from one daily sample to another can be an order of magnitude different. Consequently, most of the concentration variance is due to random synoptic air mass changes, and to a lesser degree due to periodic seasonal variations.

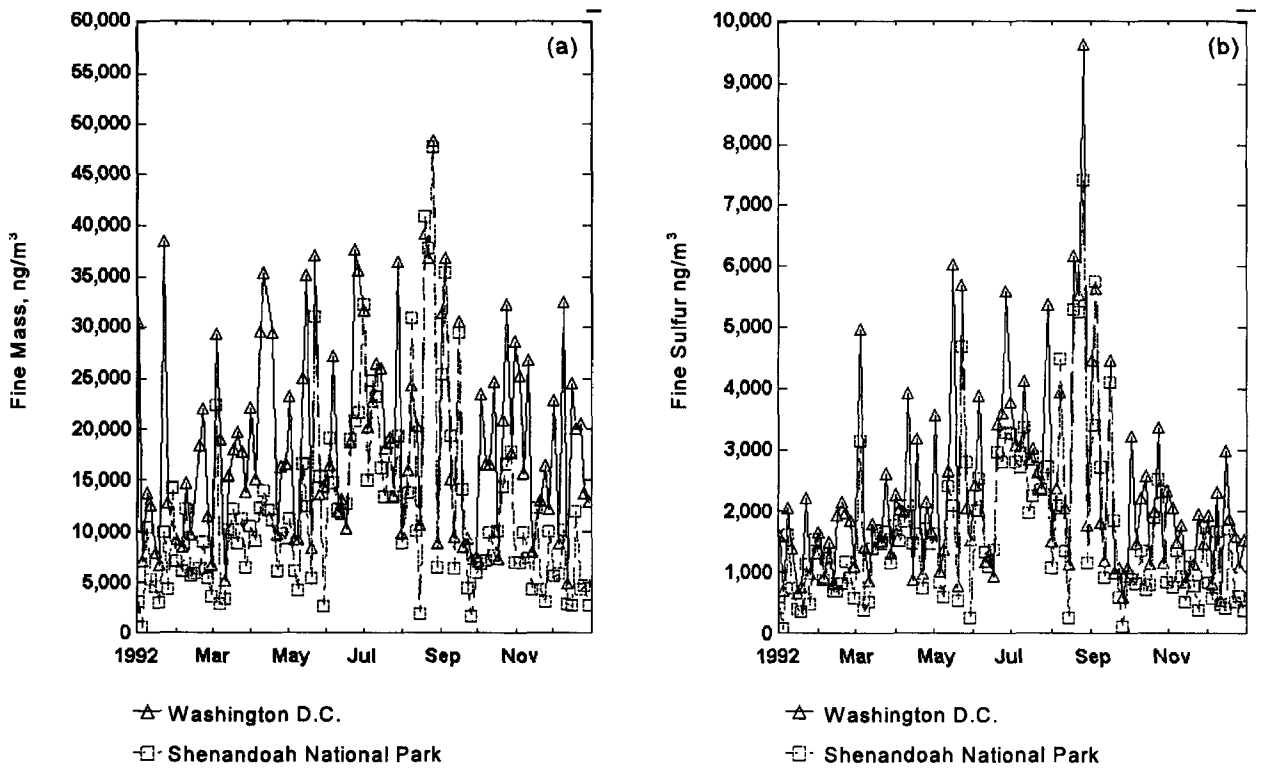

Figure 6-60. Daily concentration of (a) fine mass and (b) fine sulfur at Washington, DC, and Shenandoah National Park.

6.5.1.4 New York City, New York

The New York City metropolitan area is characterized by high population density, moderate industrial activity, and relatively flat terrain. The PM_{10} concentration over the metropolitan area is shown in Figure 6-61a. The circles in the map show the locations of the monitoring sites and the magnitude of each circle is proportional to the average PM_{10} concentration at that site using all available data. The observed average concentrations change by about of factor of two to three from one location to another. Higher average concentrations tend to occur near the center of the metropolitan area.

In the New York City metropolitan area there was a decrease in the annual PM_{10} concentration between 1988 and 1994 from 35 $\mu g/m^3$ to 27 $\mu g/m^3$ for all sites and from 41 $\mu g/m^3$ to 34 $\mu g/m^3$ for trend sites (Figure 6-61b). The reductions were 23% for all sites and 17% for trend sites. There was unusually large difference between the two trends. The average

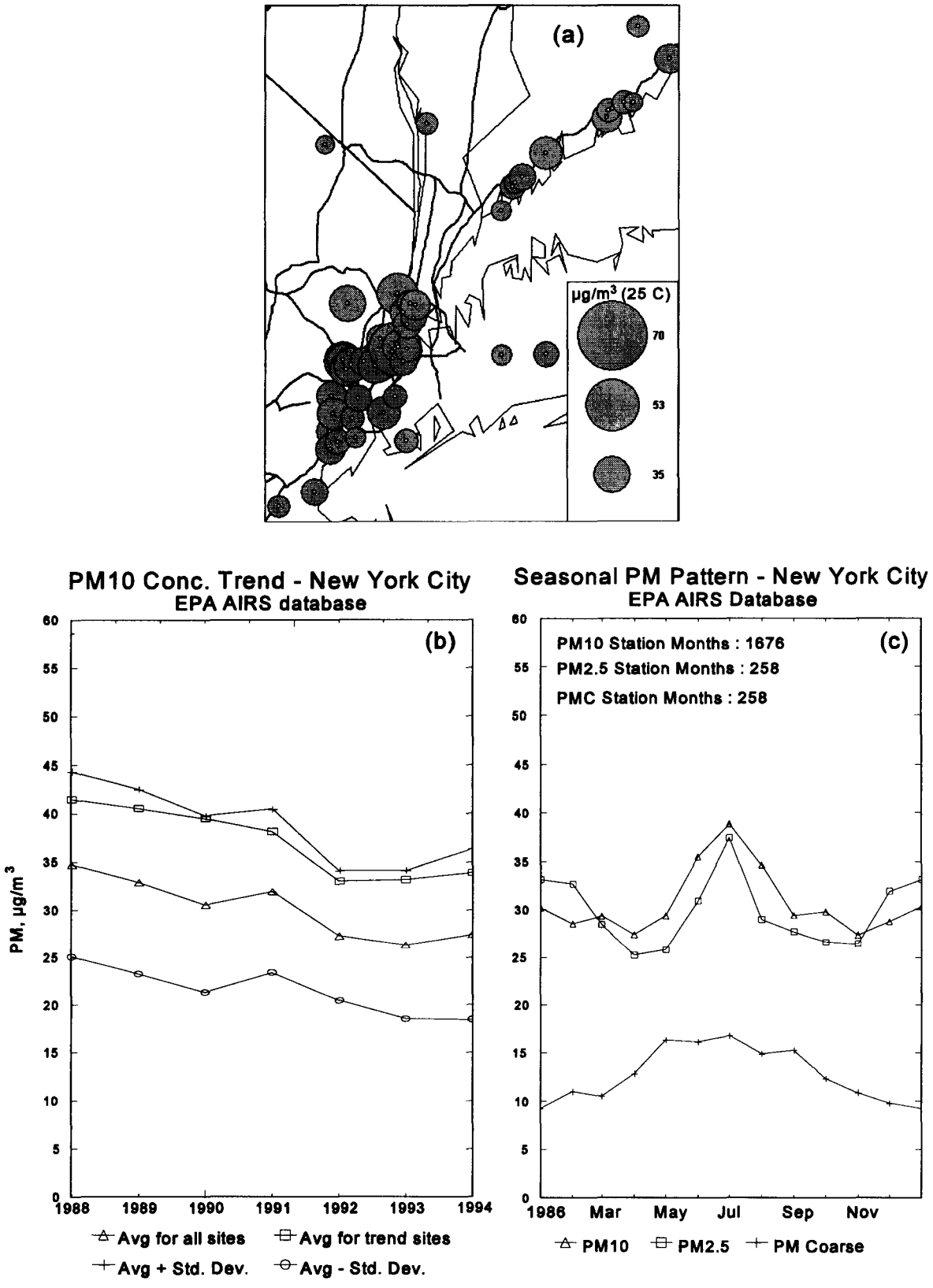

Figure 6-61. New York City region: (a) aerosol concentration map, (b) trend, and (c) seasonal pattern.

seasonal pattern over the subregion (Figure 6-61c) is 25 to 30 $\mu g/m^3$ throughout the year, but rises to about 40 $\mu g/m^3$ in July.

The seasonal pattern at three different individual monitoring sites in the New York City metropolitan area is shown in Figure 6-62a. The three sites all show similar seasonality with a summer peak, but with elevated concentrations closer to the city center.

Size segregated aerosol samples in New York City (Figure 6-62b,c) show that at both sites, PM_{10} concentrations are contributed primarily by fine particles. Based on the discussion of the more extensive Washington, DC (Section 6.5.1.2) measurements, it can be inferred that the summer peak in the fine mass is mainly due to the regional formation of the fine aerosols, while the winter peak is contributed by the local sources, confined to the inner metropolitan area.

As part of the New York Summer Aerosol study (Leaderer et al., 1978) continuous size monitoring confirmed the expected bimodal volume distribution with modes between 0.1 to 1.0 μm and >3.0 μm. A number of interesting patterns were observed when the size distribution was averaged by hour of day. The diurnal average total number concentration showed a pattern which corresponded closely with the normalized diurnal traffic pattern. Particles <0.1 μm showed the most marked diurnal variation, following the total number curve. Moreover, particles in size ranges >0.1 μm showed little variation in the diurnal pattern. Analysis of samples processed by the diffusion battery indicated that approximately 54%±18% of the sulfate measured was in the suboptical range (approximately 0.04 μm to 0.3 μm) with the remainder above 0.3 μm. Little sulfate mass was found in particles in the nuclei range (<0.04 μm). Analysis of impactor samples for sulfates consistently showed that more than 85% of all water soluble sulfates were <2.0 μm in size. Virtually no nitrate was present in the nuclei size range while the suboptical size range accounted for approximately 30% of the total nitrate. 70% of the total nitrate was found in the size range >0.3 μm. Analysis of large stages of Anderson impactor showed that approximately 50% of particulate nitrate was greater than 5.5 μm in size.

Urban and rural particulate sulfur monitoring near New York City in the summer (Leaderer et al., 1982) indicated that sulfate concentration distributions were regionally homogeneous and increased with increasing ozone levels and covariant with several other pollutant and meteorological parameters. Sulfate concentrations correlated strongly with ammonium and strong acid at all sites. Strong acid concentrations were highest at the rural and semi-rural sites,

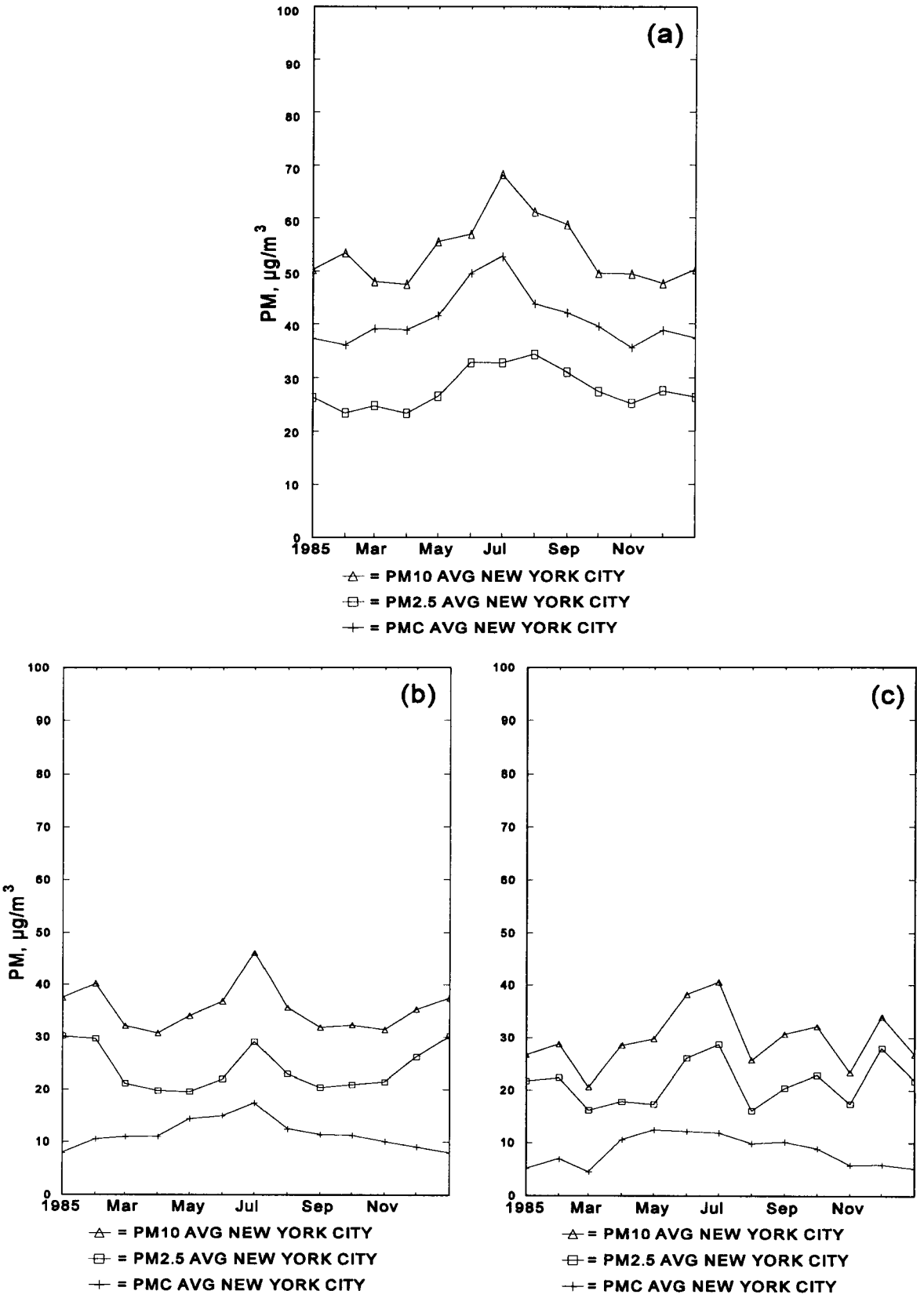

Figure 6-62a,b,c. Fine, coarse, and PM_{10} particle concentrations at three New York City sites.

lowest at the urban sites, increased with increasing ozone levels and exhibited diurnal patterns which matched the ozone diurnal patterns.

Size dependent, mass and composition of New York aerosol for low, medium, and high visibility levels was reported by Patterson and Wagman (1977). At all levels of visibility, bimodal or multimodal particle size distribution were observed for total mass and for individual components. Decreased visibility corresponded to increased particle mass concentrations especially in the fine particle fraction. Increases in the proportion of particulate sulfate and to a lesser extent of nitrate, chloride, ammonium, and carbon were also associated with decreased visibility.

Aerosol pattern analysis of a major wintertime (1983) pollution episode near New York City in northern New Jersey (Lioy et al., 1985) revealed that the intensity of the episode was the greatest in the area of the highest commercial, residential and industrial activities, and that the atmospheric stagnation conditions resulted in the significant accumulation of aerosol mass. The aerosol mass was primarily fine aerosols, and the extractable organic matter comprising about 50% of the particle mass.

6.5.1.5 Philadelphia, Pennsylvania

The metropolitan area of Philadelphia includes urban-industrial emissions over flat terrain. Relatively uniform PM_{10} concentrations throughout the metropolitan area, with the exception of a single site (AIRS #421010149) in the middle of the urban area (Figures 6-63 and 6-64).

The downward trends in PM_{10} concentrations between 1988 and 1994 were largely or completely negated by the upward trends in 1993 and 1994 (Figure 6-63b). The decrease in annual PM_{10} concentrations at trend sites between 1988 and 1994 for all sites was from 39 $\mu g/m^3$ to 32 $\mu g/m^3$, a decrease of 18%. The seasonal concentration of PM_{10} (Figure 6-63c) is about 30 to 35 $\mu g/m^3$ throughout the year, except during the summer months when it rises above 40 $\mu g/m^3$.

The seasonal average PM_{10} concentrations for four sites near the center of Philadelphia is shown in Figure 6-64. The high concentration site noted on the metropolitan map in Figure 6-63a and two nearby sites in the industrial area long the riverfront are shown in Figure 6-64a. The average PM_{10} concentration at that site ranges between 100 to 150 $\mu g/m^3$

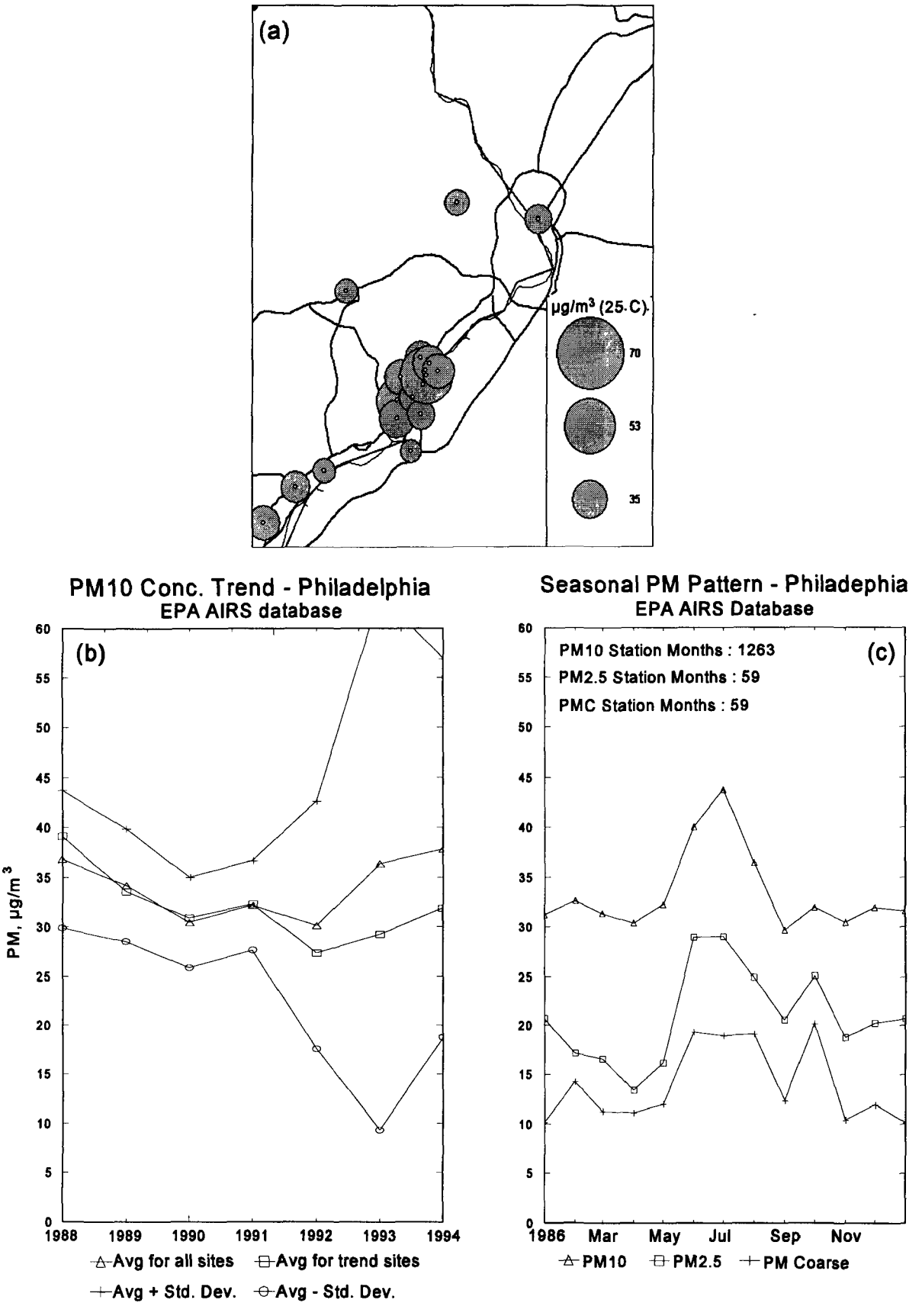

Figure 6-63. Philadelphia region: (a) aerosol concentration map, (b) trend, and (c) seasonal pattern.

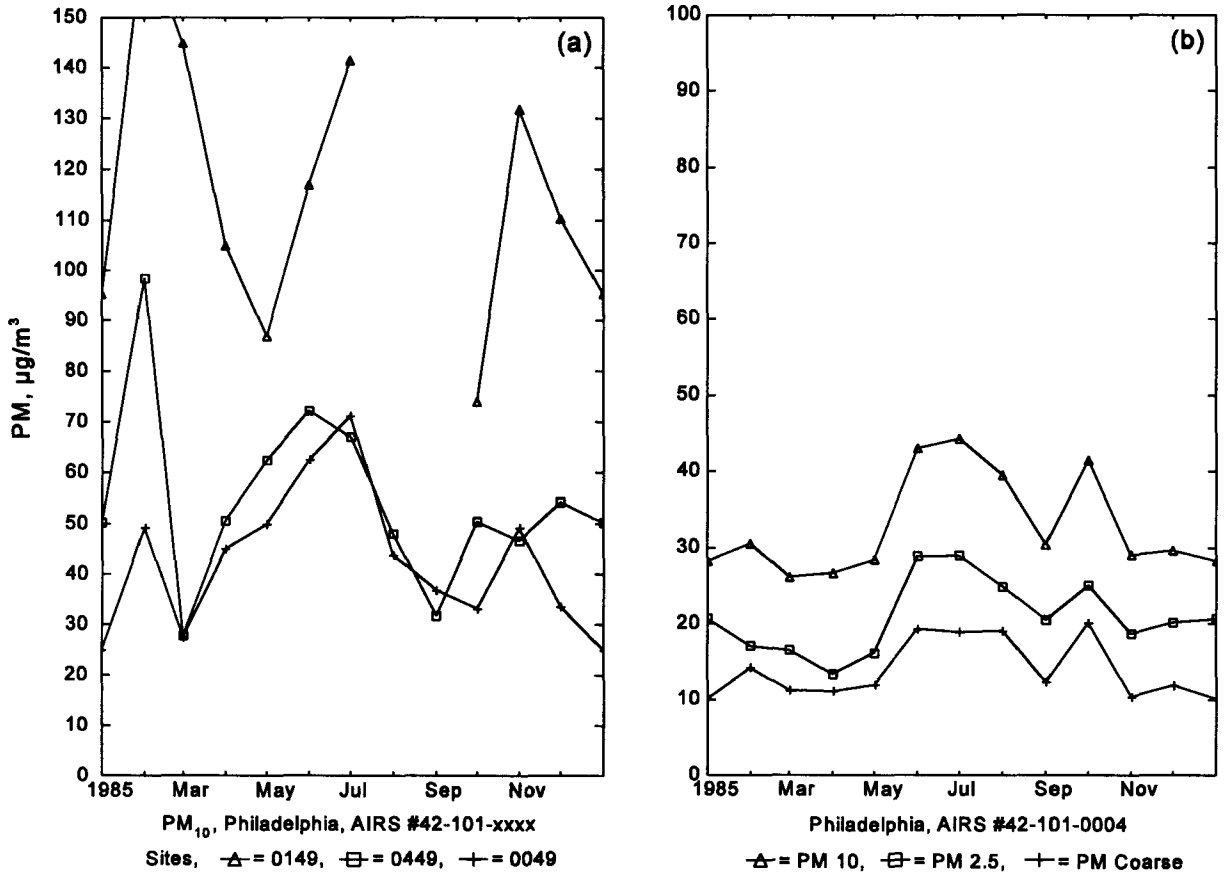

Figure 6-64a,b. Seasonal particle concentrations at four Philadelphia sites. (Note scale for (a) is 150 µg/m³.)

which is a factor of 2 to 3 higher than the concentration at the neighboring sites. The daily concentrations at these source monitoring sites correlate poorly with a nearby site (Figure 6-64b) that is only 4 km away but outside the industrial area. This is an indication that the concentrations at the industrial sites are under the influence of a strong local source of PM_{10}. In contrast, community sites in downtown and suburban Philadelphia that are as much as 30 km apart show a strong correlation of daily measurements, indicating that a spatially uniform regional aerosol influences the daily values in Philadelphia.

Size segregated aerosol samples (Figure 6-64b) show that fine particles contribute more than coarse particles to the PM_{10} at this site. It is possible, however, that at other sampling sites, e.g., the industrial sites (Figure 6-64a), coarse particles may prevail.

Outdoor summertime sulfate ($SO_4^=$) concentrations were found to be uniform within metropolitan Philadelphia (Suh et al., 1995). However, aerosol strong acidity (H^+)

concentrations were found to vary spatially. Also, the wintertime sulfate pattern was likely to be more heterogeneous in space and time. This variation generally was independent of wind direction, but was related to local factors, such as the NH_3 concentration, population density, and distance from the center of the city.

6.5.1.6 Whiteface Mountain, New York

The AIRS sampling location at the Whiteface Mountain in Upstate New York is a high mountain top site elevated from the surrounding terrain. The monitoring site offers the possibility of comparing mountain top concentrations to the surrounding lower elevation sites. The seasonal pattern of PM_{10} concentration for Whiteface Mountain and the surrounding low elevation sites, Saranac Lake and Saratoga Springs, is shown in Figure 6-65. The concentration at the three sites is virtually identical during June through September. However, during the winter the mountain top site at Whiteface has a PM_{10} concentration which is only one third of the low elevation sites. This indicates that during the winter, the Whiteface mountain top is above the surface-based aerosol layer, while during the summer the height of the well mixed aerosol layer rises above the mountain top producing a reasonably uniform concentration at all sites.

6.5.2 Subregional Aerosol Pattern in the Southeast

6.5.2.1 Atlantic Coast States

The average yearly concentration in the southeast Atlantic coast states for all sites and trend sites has decreased from 32 to 24 $\mu g/m^3$ and 25 $\mu g/m^3$ (Figure 6-66a,b). The reductions were 25% and 22%. Seasonal concentrations show a summer peak largely due to $PM_{2.5}$ (Figure 6-66c). Comparison of three AIRS PM_{10} monitoring sites in North Carolina's Piedmont, Winston-Salem, Greensboro, and Raleigh-Durham (Figure 6-66d) shows virtually identical concentrations (within 10%), both in absolute magnitudes and in the seasonality with summer peaks in PM_{10}. This is an indication that these sites in this subregion are exposed to essentially the same air masses throughout the year. It also suggests that the excess PM_{10} concentrations due to local urban sources probably are not signficant.

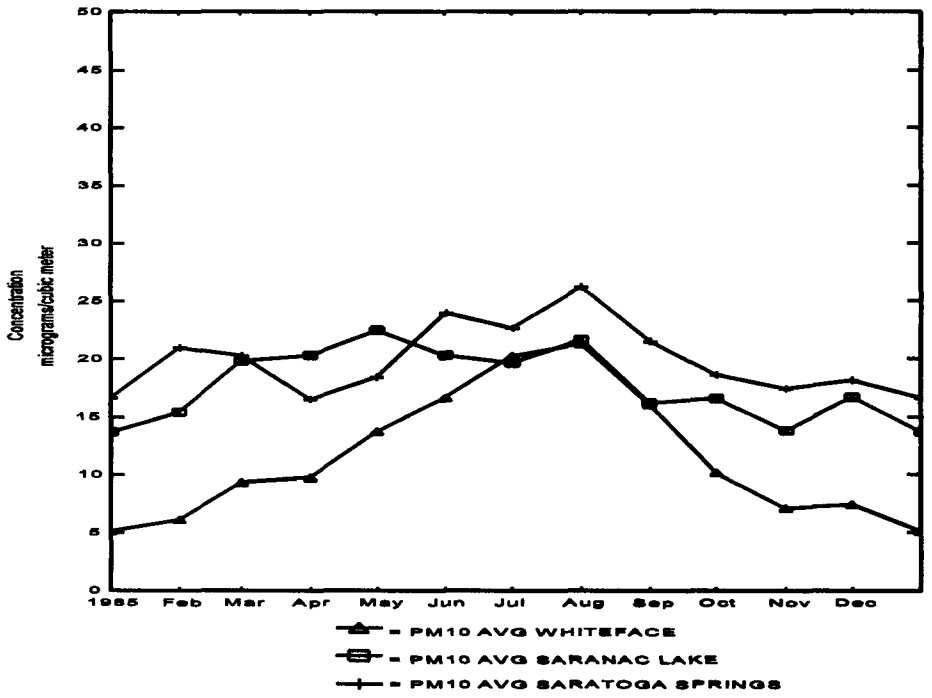

Figure 6-65. PM_{10} concentration seasonality at Whiteface Mountain and neighboring low-elevation sites.

Size segregated monitoring data for Winston-Salem (Figure 6-66f) show that fine particles contribute 70 to 80% of the PM_{10} mass of 25 to 35 $\mu g/m^3$. Coarse particles are seasonally invariant at about 10 $\mu g/m^3$ which is typical for eastern U.S.

The PM_{10} concentration at monitoring sites in Florida (Orlando, Miami, Tampa) show virtually identical concentrations ranging between 25 to 30 $\mu g/m^3$ throughout the year, without appreciable seasonality (Figure 6-66e).

6.5.2.2 Texas and Gulf States

The average yearly concentration between 1988 and 1994 in the Texas-Gulf states has decreased for all sites and tend sites from 28 to 25 $\mu g/m^3$ (Figure 6-67b), a reduction of 11%. Seasonal concentrations show a summer peak largely due to PM2.5 (Figure 6-68c). The seasonal PM_{10} concentration at sites in Odessa, Amarillo, and Lubbock, TX, and in New Orleans, LA, Mobile and Birmingham, AL show uniformity (20 to 40 $\mu g/m^3$) with modest seasonality

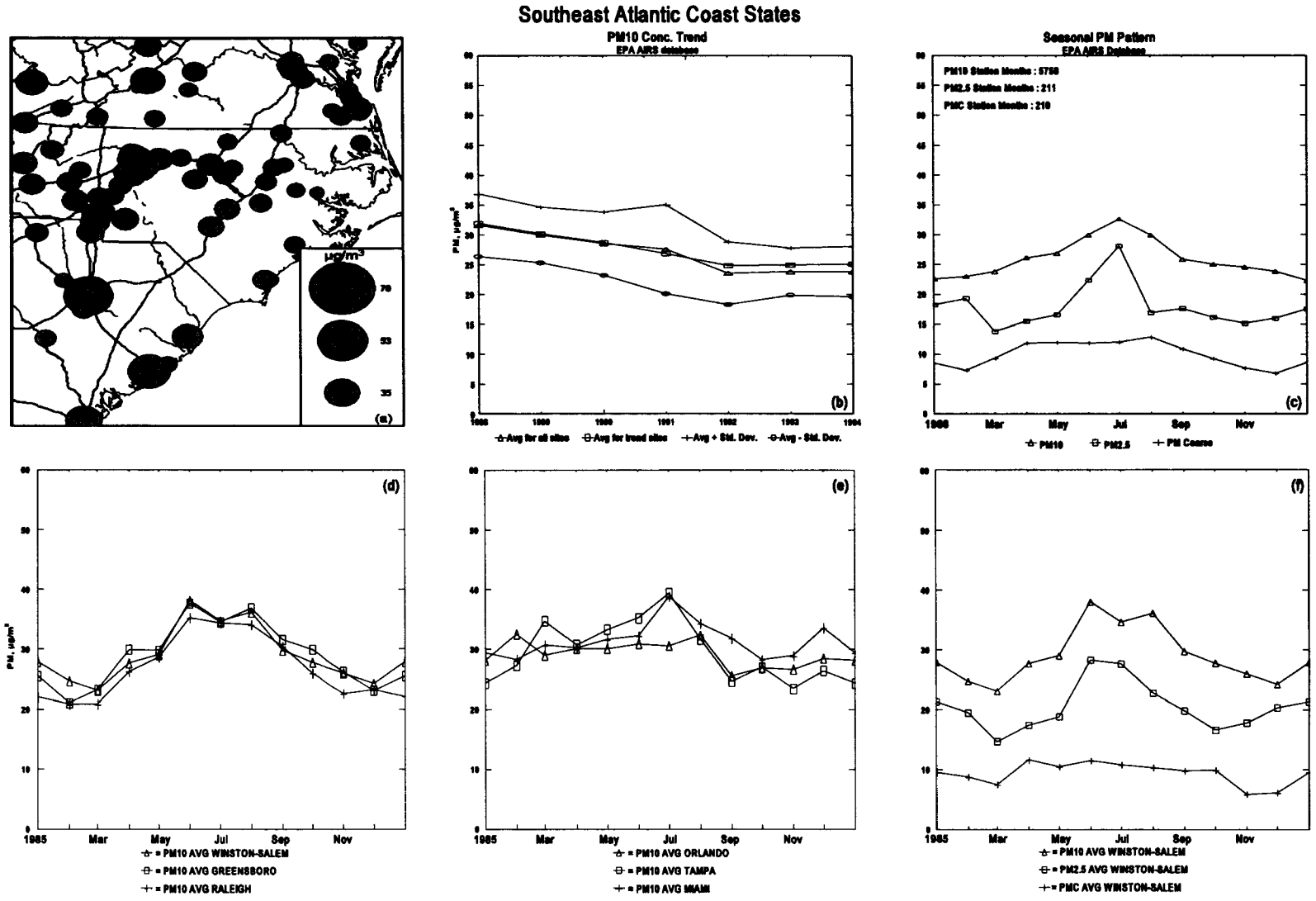

Figure 6-66. Aerosol concentration patterns for the Southeast Atlantic Coast states and sites in North Carolina and Florida: (a) monitoring sites, (b) trends, (c) seasonal pattern, (d) North Carolina sites, (e) Florida sites, and (f) seasonal pattern for Winston-Salem.

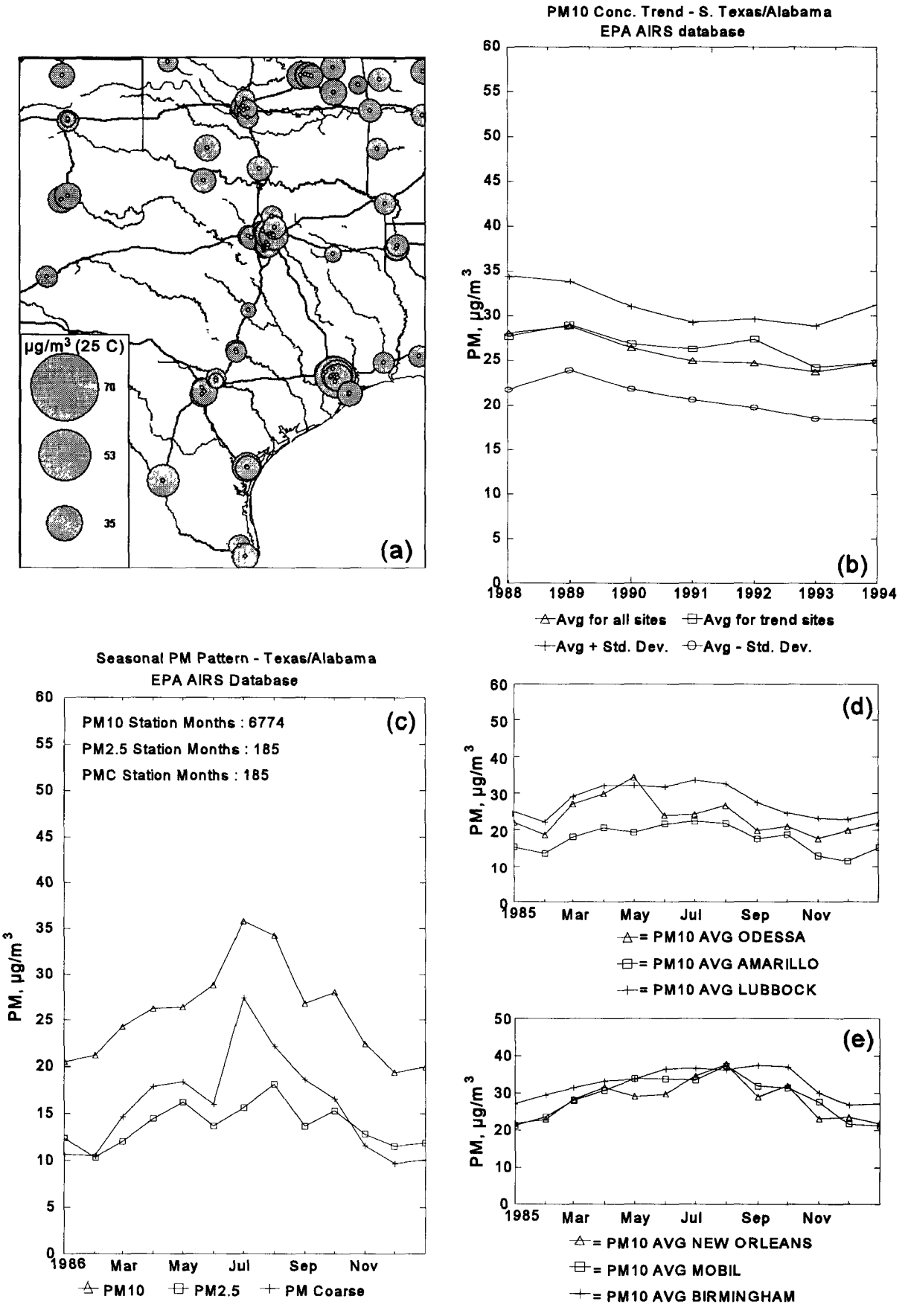

Figure 6-67a,b,c,d,e,f,g,h,i. Aerosol concentration patterns in Texas and Gulf states.

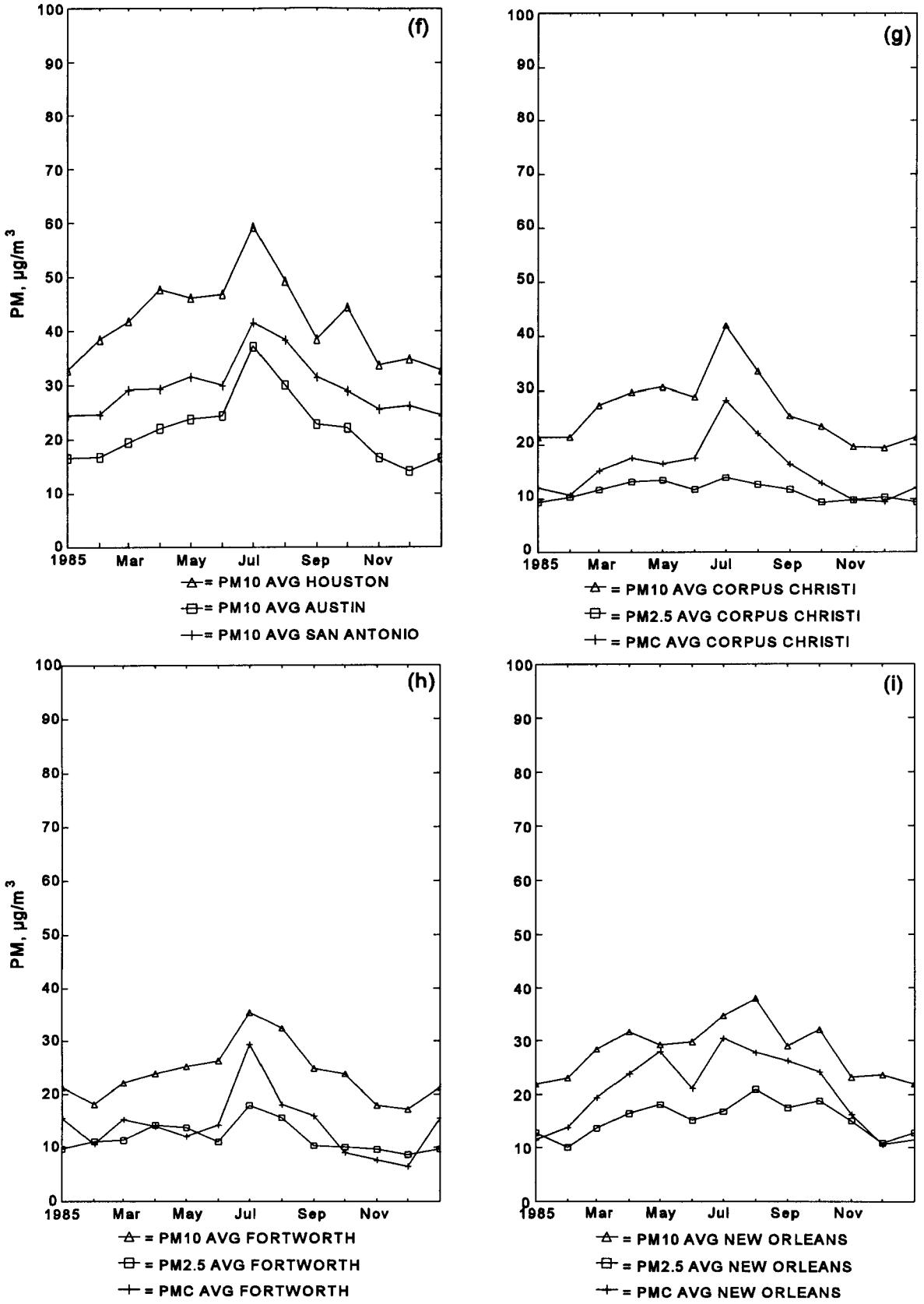

Figure 6-67 (cont'd). Aerosol concentration patterns in Texas and Gulf states.

(Figure 6-67d,e). The sites in Houston, Austin, and San Antonio, TX show a wider range of PM_{10} values with summer peaks (Figure 6-67f).

The size segregated aerosol samples collected in the cities of the Gulf states, Corpus Christi, Forth Worth and New Orleans, LA (Figure 6-67g,h,i) all show fine particle concentrations that are relatively low (10 to 20 $\mu g/m^3$) compared to large eastern cities. Coarse particle concentrations, on the other hand, can account for more than half of the PM_{10} mass. The coarse particle contribution is most pronounced during the summer season.

In Houston, TX, Dzubay et al. (1982) found that in summertime fine particle mass contained 58% sulfate and 18% of carbonaceous material. They also found that the coarse fraction (2.5 to 15 μm) consisted of 69% crustal matter, 12% carbon, and 7% nitrate species.

6.5.2.3 Atlanta

Characterization of the Atlanta area aerosol (Marshall et al., 1986) show that elemental carbon and particulate sulfur represent, respectively 3.1 to 9.9% and 1.9 to 9.4% of the total suspended particulate mass. The concentrations of elemental carbon, sulfur, and TSP exhibit strong seasonal variations, with elemental carbon decreasing from winter to summer, and sulfur and TSP increasing. Elemental carbon appears to be statistically separate from sulfur, indicating that the sources for elemental carbon and particulate sulfur are distinct.

6.5.2.4 Great Smoky Mountains

Size segregated fine and coarse aerosol concentrations were measured at the Great Smoky Mountains National Park in September of 1980 (Stevens et al., 1980). Sulfate and its associated ions contributed to 61% of the fine particle mass, followed by organics (10%) and elemental carbon (5%).

6.5.3 Subregional Aerosol Pattern in the Industrial Midwest

Since the turn of the century, the major cities in the industrial midwestern states had air pollution problems due to smoke and dust. Pittsburgh, St. Louis, Chicago, and Detroit were among the formerly notorious air pollution hot spots. The recently acquired PM_{10} database now

allows the re-examination of these metropolitan areas in the industrial Midwest for their concentration pattern in the 1990s.

6.5.3.1 Pittsburgh, Pennsylvania

The average PM_{10} concentrations for sites in the extended metropolitan area is shown in Figure 6-68. The Pittsburg, PA subregion includes the industrial cities, Steubenville, OH, and Weirton, OH, located on the Ohio River. The average PM_{10} concentration at the 80 sites shown on the map varies only by about 20% from site to site. Outstanding high concentration hot spots are now absent. It is thus evident that during the 1985 to 1993 period, the average PM_{10} concentrations in the Pittsburgh subregion were spatially rather uniform.

In the Pittsburgh, PA metropolitan area there was a decrease in the annual average PM_{10} concentrations between 1988 and 1994 from 37 $\mu g/m^3$ to 32 $\mu g/m^3$ for all sites and from 41 $\mu g/m^3$ to 33 $\mu g/m^3$ for trend sites (Figure 6-68b). The reductions were 14% for all sites and 19% for trend sites. Figure 6-68b also marks the concentration standard deviation among the monitoring sites for each year, which is about 15 to 20% and shrinking over time.

The seasonality of the PM_{10} pattern (Figure 6-68c) is dominated by a summer peak (45 $\mu g/m^3$), which is about 50% higher than the winter concentrations (30 $\mu g/m^3$). The sites in Pittsburgh, PA, Weirton, OH, and Steubenville, OH (Figure 6-69) show comparable seasonality and values that are slightly above the subregional average. Hence, the particles at these formerly highly polluted locations are now virtually identical to their subregional background.

Size segregated aerosol samples in Pittsburgh, PA and Steubenville, OH (Figure 6-69) show that fine particles contribute 70 to 80% of the PM_{10} mass, and also dictate the summer-peak seasonality of the PM_{10} concentrations. As in other urban monitoring sites in the eastern U.S., the coarse particle concentration in Pittsburgh is about 10 $\mu g/m^3$ and seasonally invariant. The size segregated seasonal data for Steubenville, OH, exhibit more random fluctuations as well as a discrepancy between the sum of fine and coarse on one hand, and PM_{10} on the other. The discrepancy is attributed to the small number of size segregated aerosol samples.

Sulfate acidity measurements (Waldman et al., 1991) at Chestnut Ridge, PA (east of Pittsburgh), suggest higher acidity occurred in the overnight period (0000-0800) in the late fall, while sulfate had its highest levels in the morning to afternoon period.

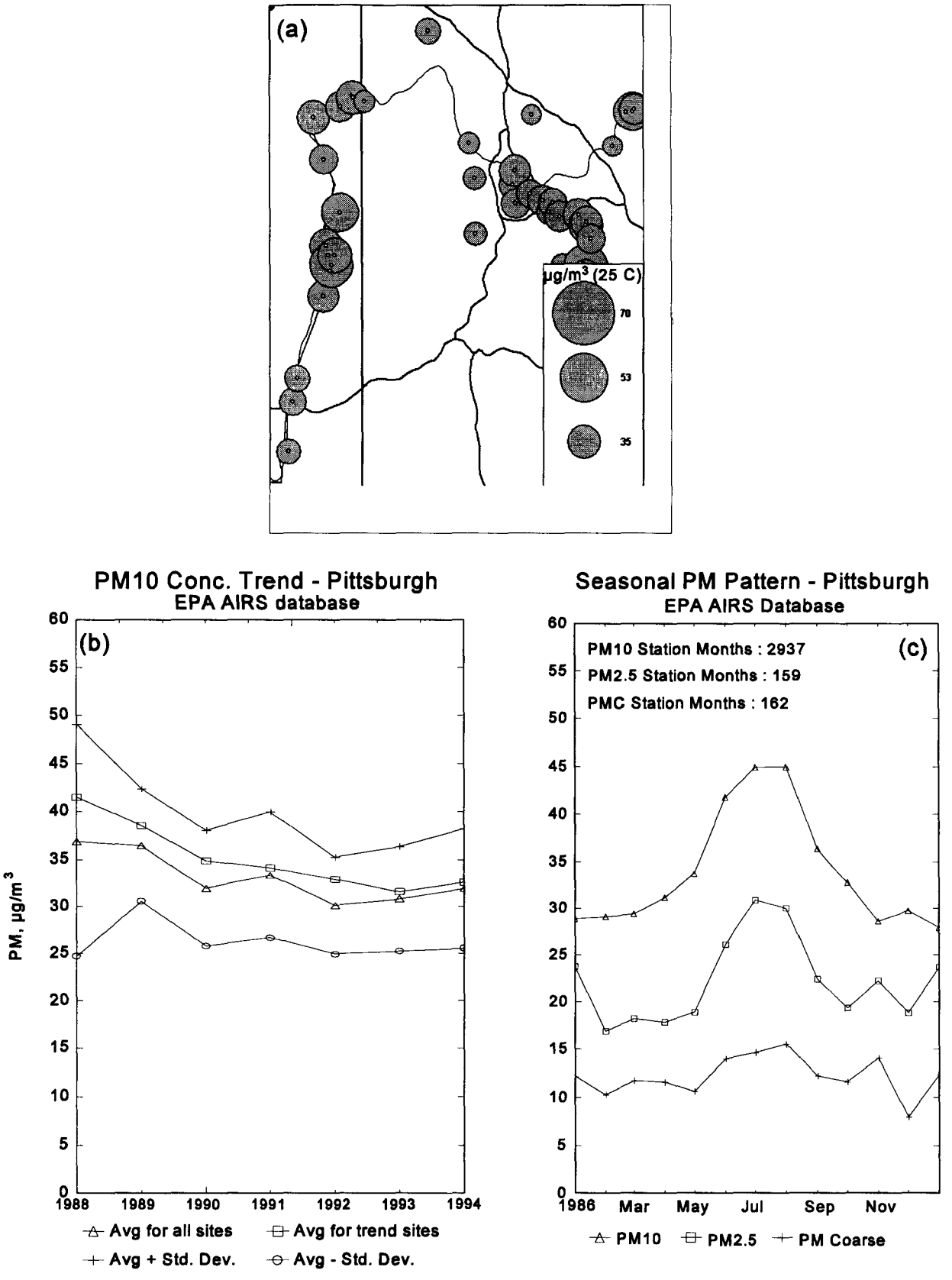

Figure 6-68. Pittsburgh subregion: (a) aerosol concentration map, (b) trends, and (c) seasonal pattern.

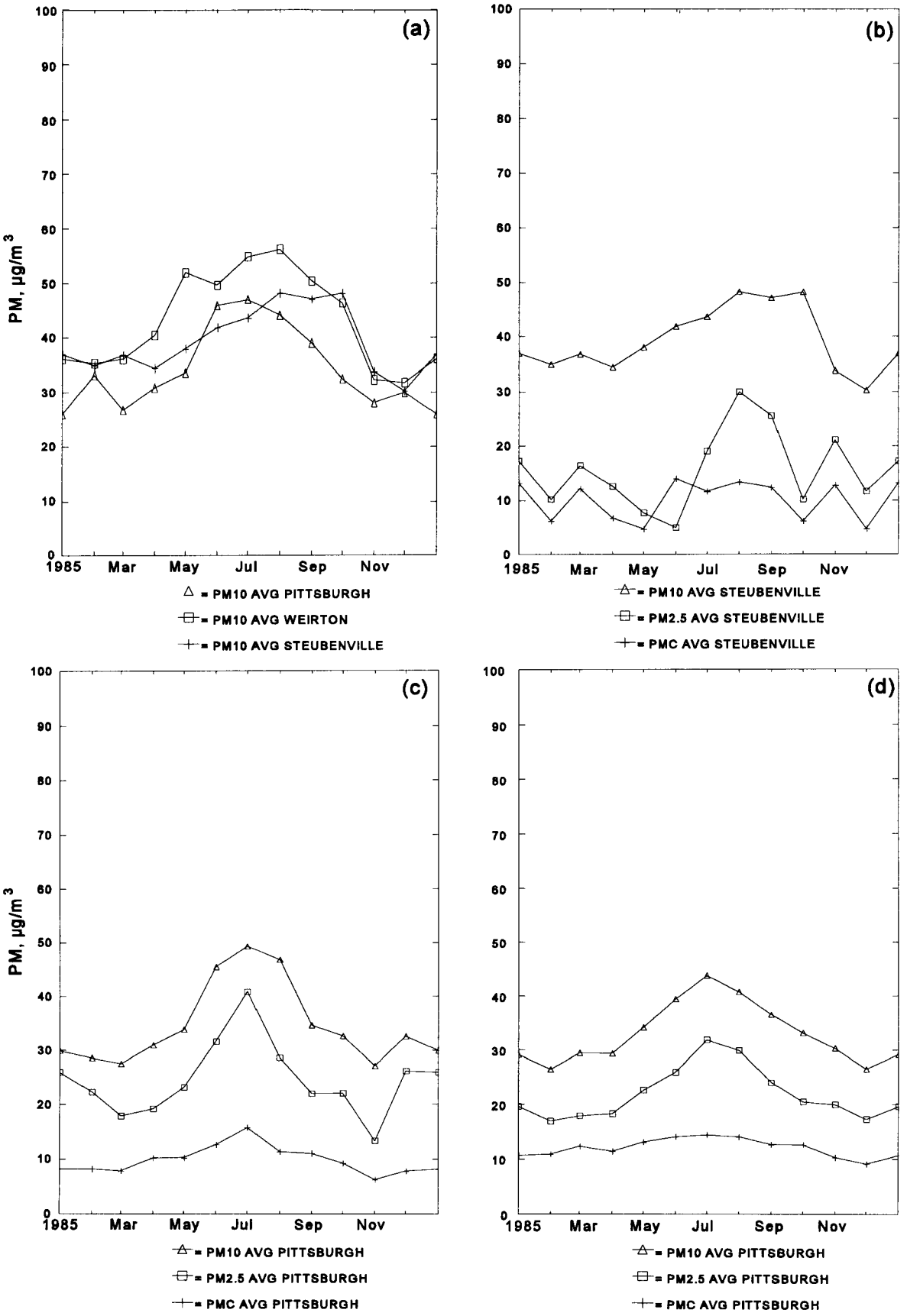

Figure 6-69a,b,c,d. Fine, coarse, and PM_{10} concentration at sites in or near Pittsburgh.

Pierson et al. (1980b, 1989) found no appreciable night/day difference in aerosol H^+ (or NH_4^+ or SO_4^{2-}) - and almost no diurnal variation in O_3 - at two elevated sites (Allegheny Mountain and Laurel Hill, elevations 838 and 850 m) in southwest Pennsylvania. The contrast with behavior at lower sites and particularly with the concurrent measurements at Deep Creek Lake (Vossler et al., 1989) is attributable to isolation from ground-based processes at the elevated sites at night.

The remarkable uniformity of fine particle mass and elemental composition from site to site in the Ohio River Valley was also shown by Shaw and Paur (1983). Sulfur was the predominant element in fine particles. Factor analysis of element concentrations indicated three clusters throughout the year (1) coarse particle crustal elements (2) fine particle sulfur and selenium (3) fine particle manganese, iron and zinc.

The chemical mass balance of Weirton-Steubenville aerosol was examined by Skidmore et al. (1992). Primary aerosols from motor vehicles and secondary ammonium sulfate were dominant contributors to the $PM_{2.5}$ aerosol. Steel emissions were also significant contributors to $PM_{2.5}$. Wood burning and oil combustion were occasionally detected. Geological material was the major contributor to the coarse aerosol fraction. Primary geological material, primary motor vehicle exhaust, and secondary sulfate were the major contributors to PM_{10} at all five monitoring sites.

The composition of size-fractionated summer aerosol in nearby Charleston, West Virginia was reported by Lewis and Macias (1980). Ammonium sulfate was the largest single chemical component (41%) of the fine aerosol mass. Carbon was also a large component of both fine and coarse particle mass constituting 16% and 12% respectively. Factor analysis indicated that four factors were sufficient to satisfactorily represent the variance of 26 measured parameters. The factors were characteristic of crustal material, ammonium sulfate, automotive emissions, and unidentified anthropogenic sources.

6.5.3.2 St. Louis, Missouri

Historically, the St. Louis metropolitan area has been known for high particulate concentrations. The map of the metropolitan area (Figure 6-70a) shows about factor of 2 to 3 concentration differences among the PM_{10} monitoring stations.

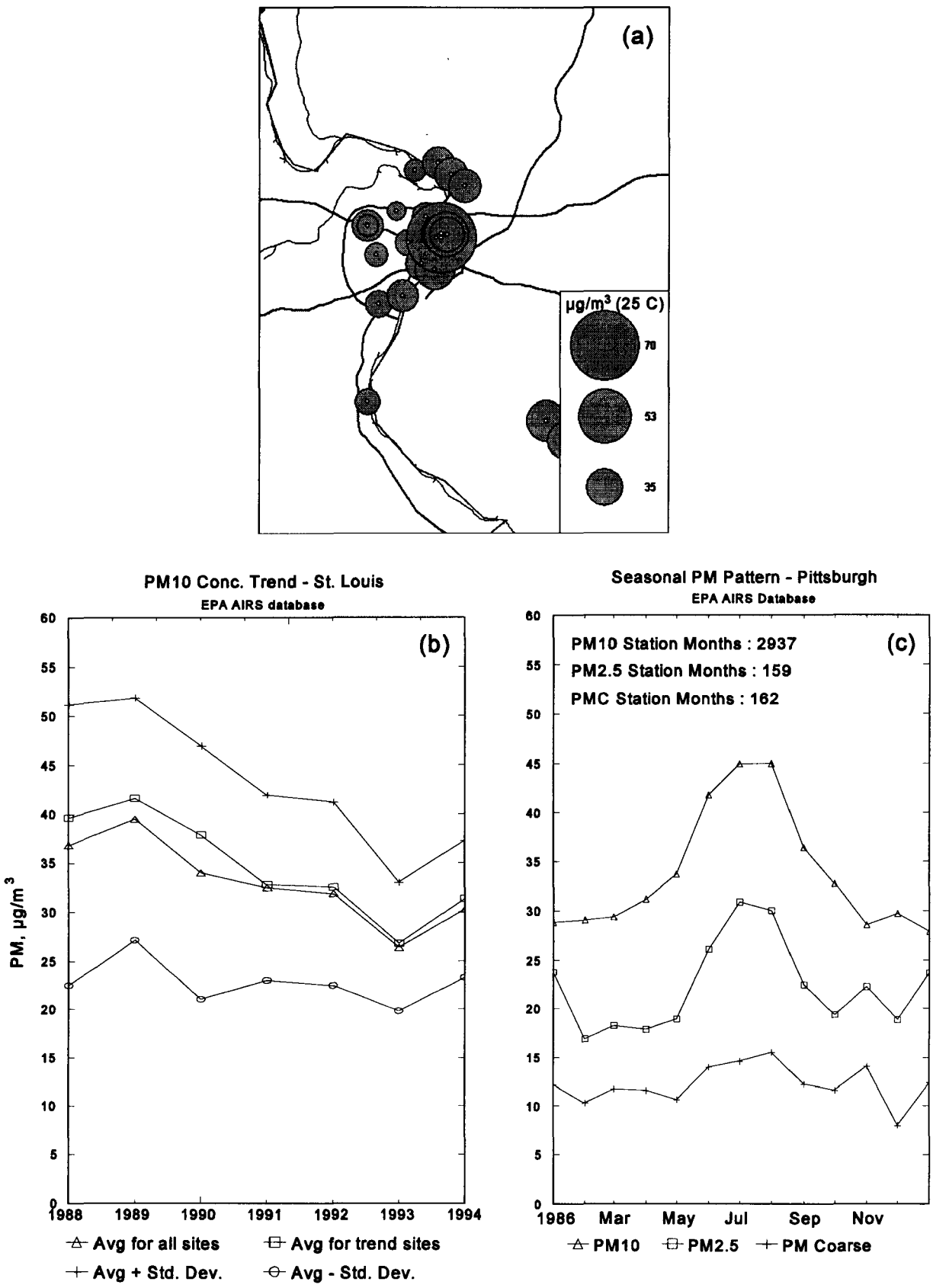

Figure 6-70. St. Louis subregion: (a) aerosol concentration map, (b) trends, and (c) seasonal pattern.

In the St. Louis metropolitan area there was a decrease in the annual average PM_{10} concentration between 1988 and 1994 from 37 $\mu g/m^3$ to 30 $\mu g/m^3$ for all sites and from 40 $\mu g/m^3$ to 31 $\mu g/m^3$ for trend sites (Figure 6-70b). The reductions were 23% for all sites and 22% for trend sites. This decline is comparable to the average reductions over the industrial midwestern region. The seasonality of the sub-regionally averaged concentrations (Figure 6-70c) shows the summer peak with 40 to 50 $\mu g/m^3$ which is about 50% higher than the winter averages.

Seasonal comparison of the individual monitoring sites in the area shows that Granite City, IL and East St. Louis, IL have higher PM_{10} concentrations throughout the year compared to western St. Louis, MO sites.

Size segregated aerosol samples at three sites west of the Mississippi River (Ferguson, MO, Affton, MO, and Clayton, MO) show that fine particles are mostly responsible for PM_{10}, including the seasonality (Figure 6-71). Coarse particles contribute 10 $\mu g/m^3$ or less throughout the year, although corresponding size segregated aerosol data for the more polluted east side of the Mississippi River are not available.

Monitoring the diurnal and seasonal patterns of particulate sulfur and sulfuric acid in St. Louis, Cobourn and Husar (1982) noted an afternoon increase in particulate sulfur concentration of about 20%. For the summertime, particulate sulfur concentration was higher than the annual mean by 40%.

Measurements were made using dichotomous samplers of PM_{10} (expressed as PM_{20}), $PM_{2.5}$ and S at urban, suburban, semi-rural, and rural sites in and around St. Louis, MO, during 1975 to 1976 as part of the Regional Air Pollution Study (RAPS) (Altshuller, 1982). Unlike the nonurban sites compared from the IMPROVE/NESCAUM network with urban sites from AIRS, these rural sites were within 45 km of the center of St. Louis. The comparisons are between three urban sites (103, 105, 106) and three rural sites (118, 112, 124).

The $PM_{2.5}$ constituted 45 to 60% of the PM_{10} with the percentages at rural sites ranging from 0 to 10% higher than at urban sites. The ratios of the concentrations of $PM_{2.5}$ at urban sites to $PM_{2.5}$ at rural sites ranged from 1.4 to 1.5 for the six quarters between the third quarter of 1975 to the fourth quarter of 1976. The ratios of the concentrations of PMCoarse at urban sites to PMCoarse at rural sites ranged from 1.5 to 1.8 for the same six quarters. For fine S, the ratios

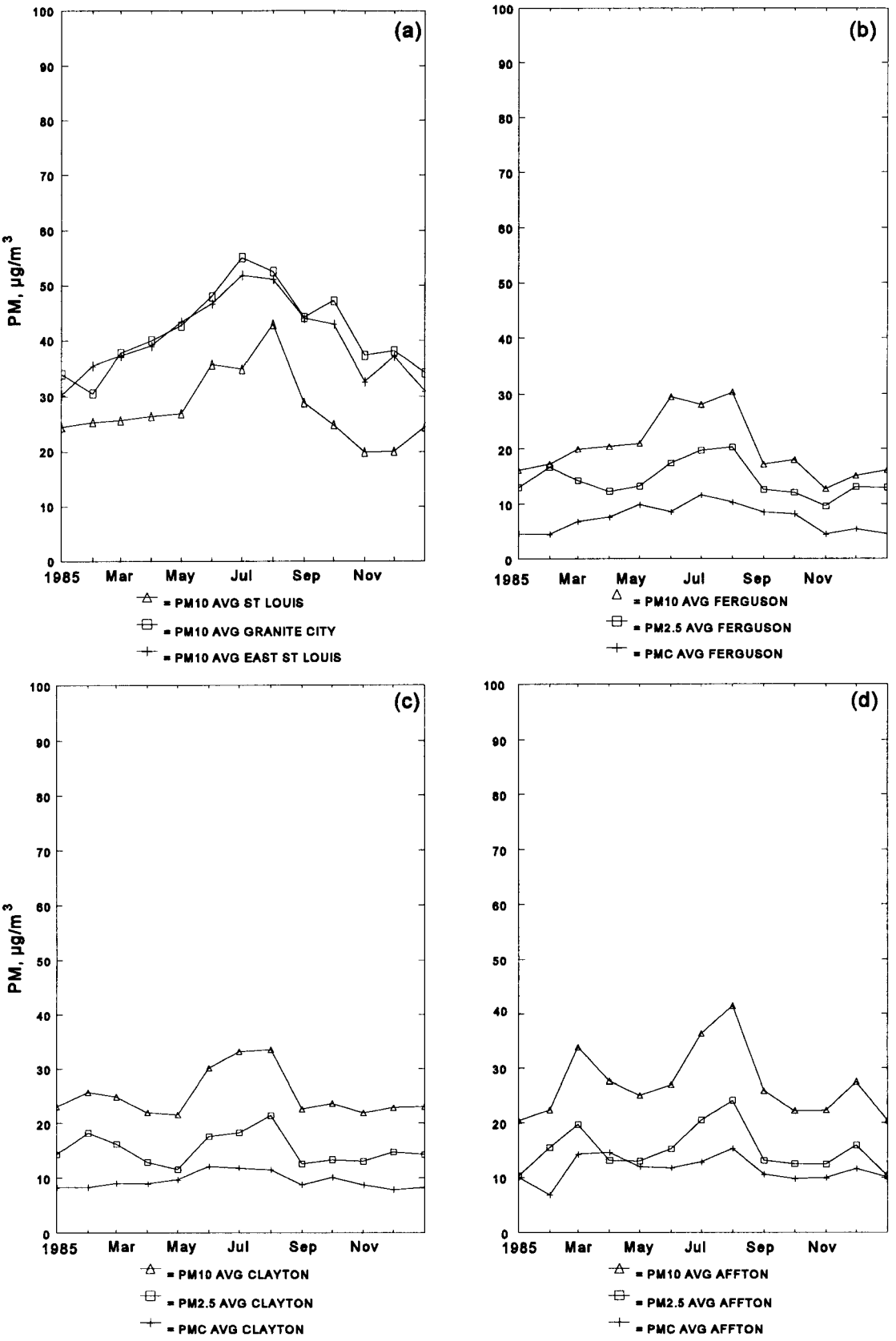

Figure 6-71a,b,c,d. Fine, coarse, and PM_{10} seasonal concentration patterns in or near St. Louis.

between urban and rural sites ranged from 1.1 to 1.2, while for coarse S, the ratios between urban and rural sites ranged from 1.7 to 2.6 for the same six quarters.

These results indicate a very strong regional influence on fine S with a lesser regional influence on $PM_{2.5}$. The ratios of PMCoarse and coarse S indicate stronger local influences on their concentrations than on fine S and $PM_{2.5}$. The percentage of fine S expressed as $(NH_4)_2 SO_4$ to the $PM_{2.5}$ was consistently higher at rural sites than at urban sites in and around St. Louis (Altshuller, 1982). In the third quarters of 1975 and 1976, these percentages averaged 70% at rural sites and 55% at urban sites, while in the fourth quarters of 1975 and 1976, these percentages averaged 45% at rural sites and 35% at urban sites.

As observed near New York City (Leaderer et al., 1982), the fine S in the St. Louis area was regionally homogenous and, during episodic periods, the fine S concentrations followed the variations in O_3 concentrations reasonably closely (Altshuller, 1985). A linear relationship was obtained for fine S and O_3 flows into St. Louis. The fine S with increasing fine S concentration constituted an increasingly large percentage of the $PM_{2.5}$ at an urban site (Altshuller, 1985).

6.5.3.3 Chicago, Illinois

Historically, Chicago has been known for industrial dust, smoke, and haze, as in adjacent East Chicago and Gary, IN. The average PM_{10} concentrations over the Chicago subregion (Figure 6-72a) vary by a factor of two or less throughout the subregion. In the Chicago subregion, there was a decrease in the annual average PM_{10} concentrations between 1988 and 1994 from 32 $\mu g/m^3$ to 29 $\mu g/m^3$ for all sites and from 39 $\mu g/m^3$ to 31 $\mu g/m^3$ for trend sites (Figure 72b). The reductions were 9% for all sites and 20% for trend sites. The seasonality of PM_{10} is also typical with the summer peak of 40 $\mu g/m^3$ and winter values of 20 to 30 $\mu g/m^3$.

Superposition of seasonal PM_{10} data at Chicago, IL, East Chicago, IL, and Gary, IN, demonstrates significant spatial uniformity, as well as indicating in more recent years comparatively low PM_{10} concentrations in this area that has historically been a smoky and dusty industrial subregion.

In the Chicago subregion there was a decrease in the annual average PM_{10} concentration between 1985 and 1994 from 40 $\mu g/m^3$ to 29 $\mu g/m^3$ for all sites and from 40 $\mu g/m^3$ to 31 $\mu g/m^3$ for trend sites (Figure 6-72b). The reductions were 28% for all sites and 23% for trend sites.

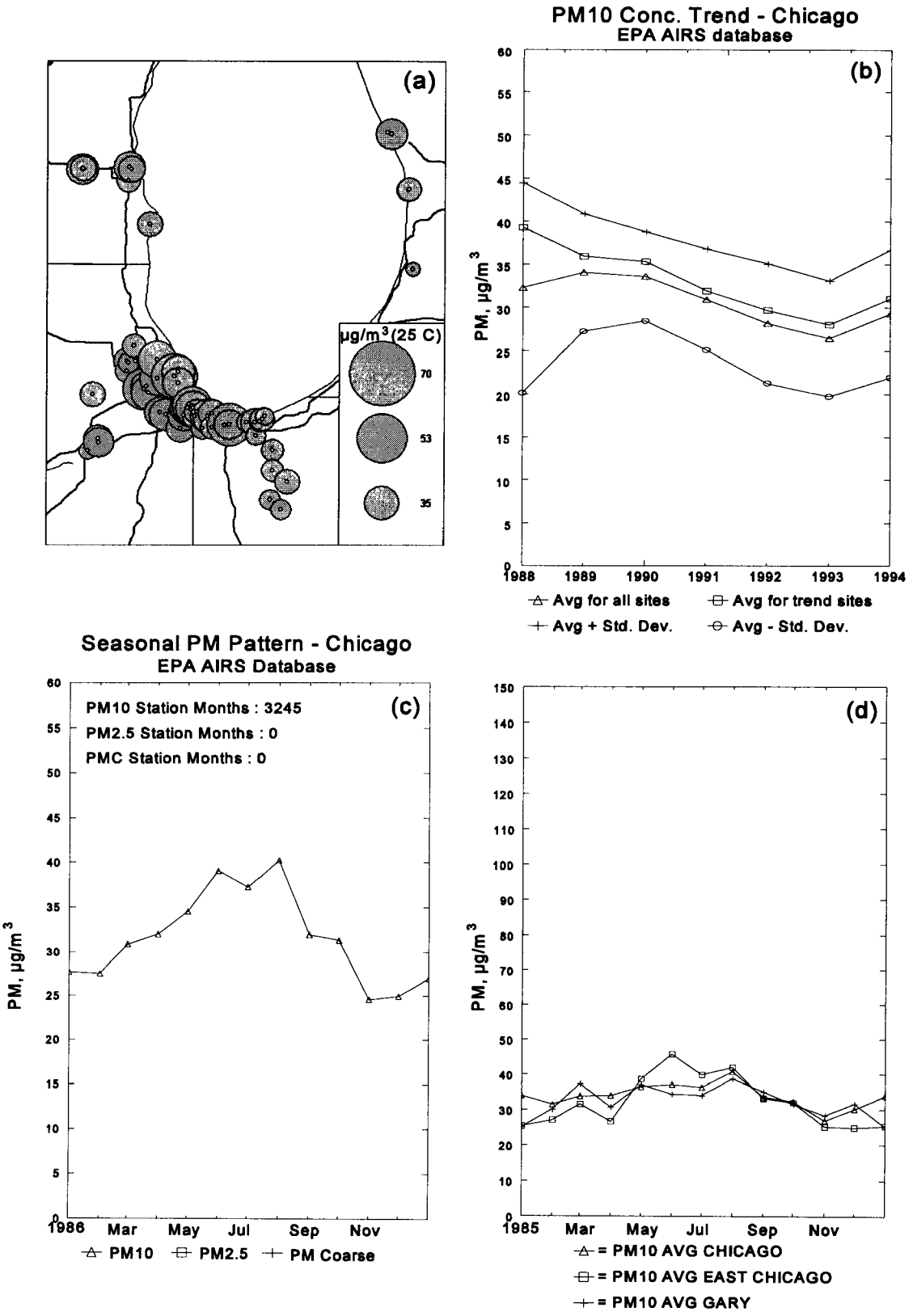

Figure 6-72. Chicago subregion: (a) aerosol concentration map, (b) trends, (c) and (d) seasonal patterns.

Chemical composition measurements in Chicago (Lee et al., 1993) showed that mean concentrations for SO_4^{2-} (5.55 $\mu g/m^3$), NH_4^+ (2.74 $\mu g/m^3$), NH_3 (1.63 $\mu g/m^3$), HNO_3 (0.81 $\mu g/m^3$), HNO_2 (0.99 $\mu g/m^3$), for SO_2 (21.2 $\mu g/m^3$), NO_3^- (4.21 $\mu g/m^3$), and H^+ (7.7 nmol/m^3). The highest values occurred in the summer, except for HNO_2 and NO_3^- which had the highest values in the winter.

Comparison of atmospheric coarse particles at an urban and nonurban site near Chicago, IL, show that the concentration were 50% higher during mid-day than at night. Dry ground samples were 30 % higher than wet ground and 90% higher than frozen ground samples. (Noll et al., 1985).

The analysis of coarse particles in Chicago, IL (Noll et al., 1990) show that the coarse particle mass could be divided into two categories: material that was primarily of crustal origin (Al, Ca, Fe, and Si) and material that was primarily of anthropogenic origin (Cd, Cu, Mn, Ni, Pb, and Zn). The mass of crustal material varied between 14 and 24% of the total coarse mass. The mass of Cd, Cu, Mn, Ni, Pb, and Zn totaled less than 1%.

The composition of atmospheric coarse particles at urban (Chicago, IL) and nonurban (Argonne, IL) were reported by Noll et al. (1987). Limestone and silicates were the main source of material at the non urban site. Anthropogenic sources, represented by flyash and coal, were present in the industrial sector sample and rubber tire was present in the commercial sector sample.

6.5.3.4 Detroit, Michigan

In Detroit, in July, 1981 (Wolff and Korsog, 1985) the average fine mass was found to be 42.4 $\mu g/m^3$. The chemical composition of the fine particles (Wolff et al., 1982) was 52% sulfates, 27% organic carbon, 4% elemental carbon, 8% soil dust. Nitrate was found to be absent from fine mass. Fine particles themselves contributed about 64% of the aerosol mass. The sulfate associated with coal combustion contributed to 50% of the fine particles. The coarse fraction, which averaged as 25.8 $\mu g/m^3$, was dominated by crustal material which accounted for about two-thirds of the coarse material. Significant contributions were also identified from motor vehicles (mostly due to re-entrained road dust) and iron and steel industry emissions.

The seasonal variations in nitric acid, nitrate, strong aerosol acidity, and ammonia in Warren, MI, was examined by Cadle (1985). The greatest variations was for ammonia, which was 8.5 times higher in summer than winter. The least variation was for particulate nitrate which had a summer maximum only 1.8 times higher than in spring minimum. It was noted that ammonium nitrate volatilization from filters and impactors can cause large errors in summertime measurements, but the errors are not significant during the winter.

The influence of local and regional sources on the concentration of particulate matter in urban and rural sites near Detroit, MI was investigated by Wolff et al. (1985). Analysis of spatial variations of the various particulate components revealed: (1) at all four sites the $PM_{2.5}$ was dominated by regional influences rather than local sources. The site in industrial sector had the largest impact of local sources, but even at his site the local influences appears to be smaller than the regional ones. (2) The regional influences were most pronounced on the sulfate levels which accounted for 40 to 50% of the $PM_{2.5}$. (3) Organic carbon compounds were the second most abundant $PM_{2.5}$ species accounting for 20 to 40% of the mass. Organic carbon seems to be controlled by both local and regional organic carbon influences. Vehicular emissions and possibly secondary reactions appear to affect the organic carbon concentrations. (4) Elemental carbon appears to be dominated by local emission. (5) PMCoarse was dominated by local sources, but at the industrial site unknown non-crustal elements were significant components of coarse mass.

6.5.5 Subregional Aerosol Pattern in the Southwest

The arid southwestern U.S. includes metropolitan areas (El Paso, TX, Phoenix-Tucson, AZ) with modest industry and national parks (Grand Canyon) where the prevention of visibility degradation has been stated as a national goal. The southwest is a dusty region and much of the discussion below pertains to coarse particles and soil dust.

6.5.5.1 El Paso, Texas

The PM_{10} concentration in the El Paso, TX, subregion shows that the high and low concentration sites occur near each other (Figure 6-73a). This is an indication that local sources of PM_{10} with limited range of impact are important. In the El Paso, TX, subregion

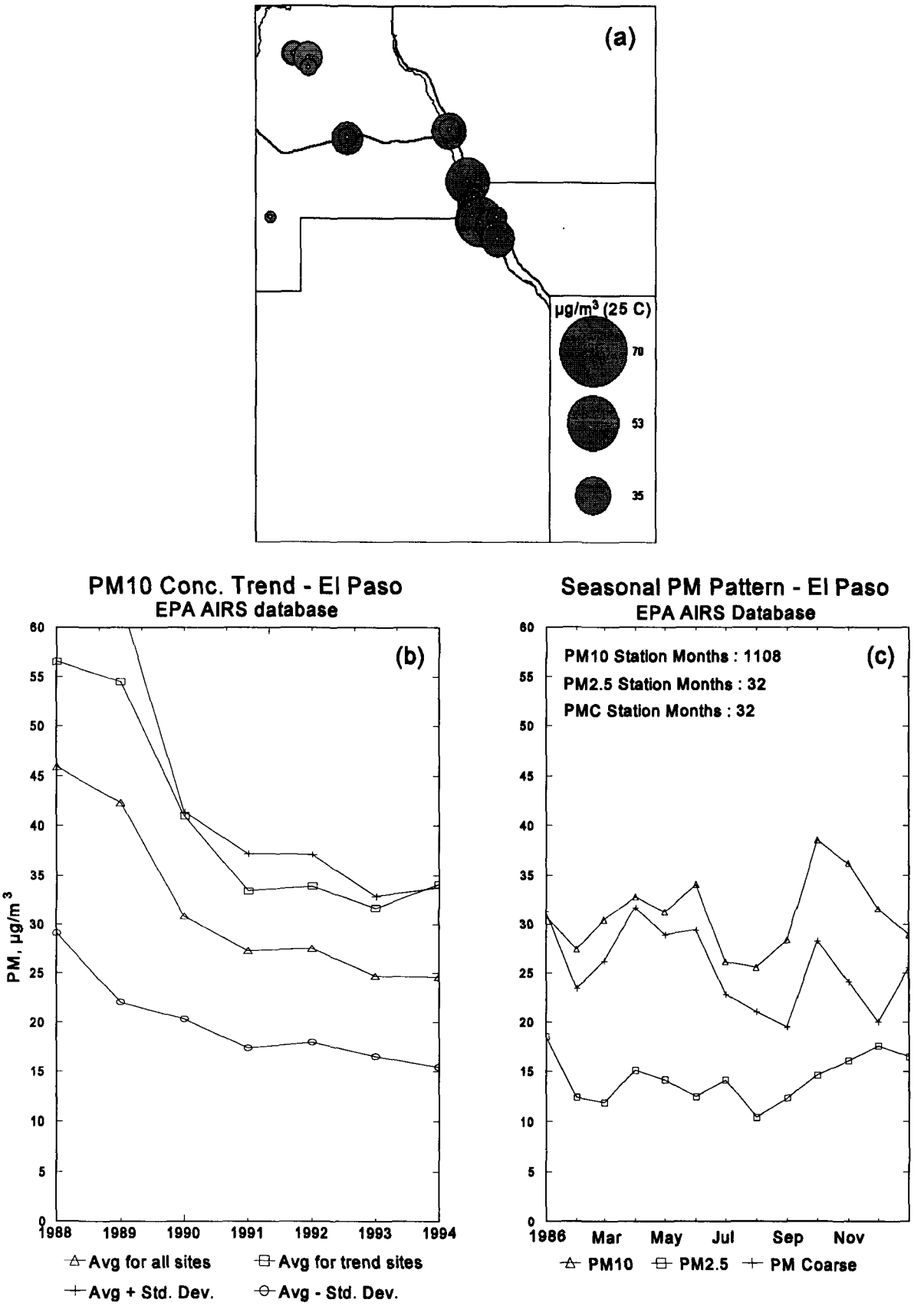

Figure 6-73. El Paso subregion: (a) aerosol concentration map, (b) trends, and (c) seasonal pattern .

there is a decrease in the annual average PM_{10} concentration between 1988 and 1994 from 46 $\mu g/m^3$ to 25 $\mu g/m^3$ for all sites and from 57 $\mu g/m^3$ to 34 $\mu g/m^3$ for trend sites (Figure 6-73b). The reductions were 46% for all sites and 40% for trend sites. This substantial reduction exceeds the PM_{10} decline over the entire southwestern region (Figure 6-46b).

The seasonality of PM_{10} over the El Paso, TX subregion (Figure 6-73c) is bimodal with peaks in the spring time, March through July, as well as another stronger peak, October through November. This double peak seasonality at El Paso, TX, also parallels the seasonality of the entire region. The concentration reduction in August which coincides with the arrival of moist flow from the Gulf of Mexico into states in the southwest (Figure 6-46d).

Size segregated aerosol samples for El Paso, TX (AIRS #481410037) show that coarse particles dominate the PM_{10} concentrations, accounting for about 70% of the PM_{10} mass (Figure 6-74a). This is consistent with the important role of coarse particles over the arid Southwest. In comparison, size segregated data for San Antonio, TX (Figure 6-74b) located closer to the Gulf Coast in Texas, show that fine and coarse mass have comparable contributions, similar to Houston, TX.

6.5.5.2 Phoenix and Tucson, Arizona

The Phoenix-Tucson subregion (Figure 6-75a) shows a substantial PM_{10} concentration range. Samplers within the Phoenix or Tucson area indicate 2 to 3 times higher concentrations than the more remote sites, particularly the ones in the mountains. For the Phoenix-Tucson subregion there was a decrease in the annual average PM_{10} concentration between 1988 and 1993 from 39 $\mu g/m^3$ to 28 $\mu g/m^3$ for all sites and from 49 $\mu g/m^3$ to 32 $\mu g/m^3$ for trend sites (Figure 6-75b). The reductions were 28% for all sites and 35% for trend sites. The decrease in PM concentration were not monotonic. The average PM_{10} seasonality of the Phoenix-Tucson subregion (Figure 6-75c) shows the bimodal spring and fall peak pattern which is characteristic for the entire Southwest region.

During the Phoenix Urban Haze Pilot Study during the winter 1988 to 1989 (Frazier, 1989) a definite diurnal cycle in $PM_{2.5}$ concentrations was observed. The maximum, generally but not

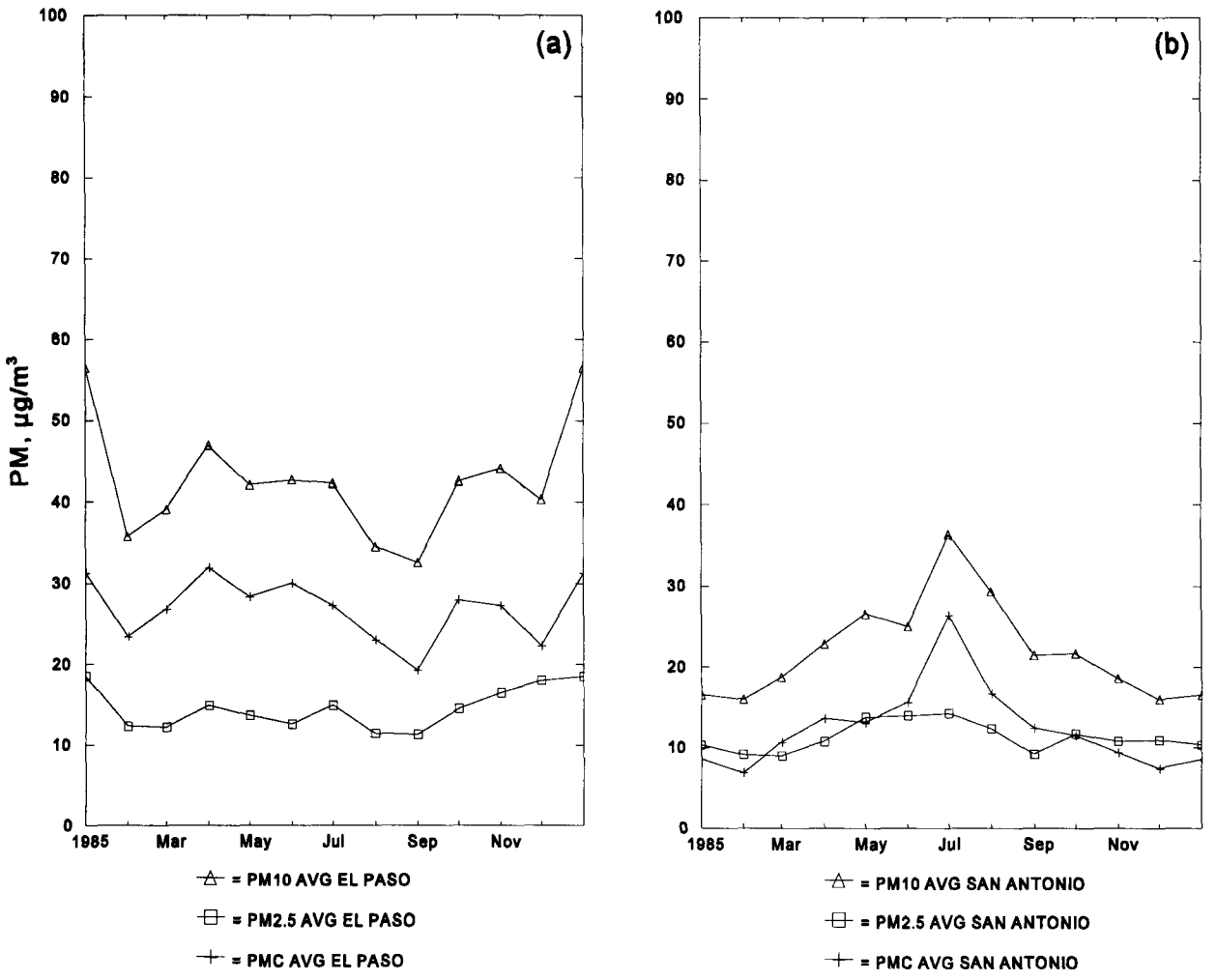

Figure 6-74a,b. Fine, coarse, and PM_{10} concentration patterns in El Paso and San Antonio.

always, occurred at night, which is consistent with the meteorological observations of poor dispersion and dilution.

The wintertime aerosol chemical pattern in Phoenix was reported by Chow et al. (1990) and Solomon and Moyers (1986). These investigators found fine particle crustal species, sulfates, nitrates, and organic and elemental carbon to be at least five times higher in concentration when comparing samples during a period of limited visibility to samples taken during good visibility.

A chemical characterization of wintertime fine particles in Phoenix, AZ (Solomon and Moyers, 1986) showed a dominance of organic carbon and nitrate aerosols. The composition in Phoenix is most like that of Denver, CO, a city which also experiences wintertime inversions

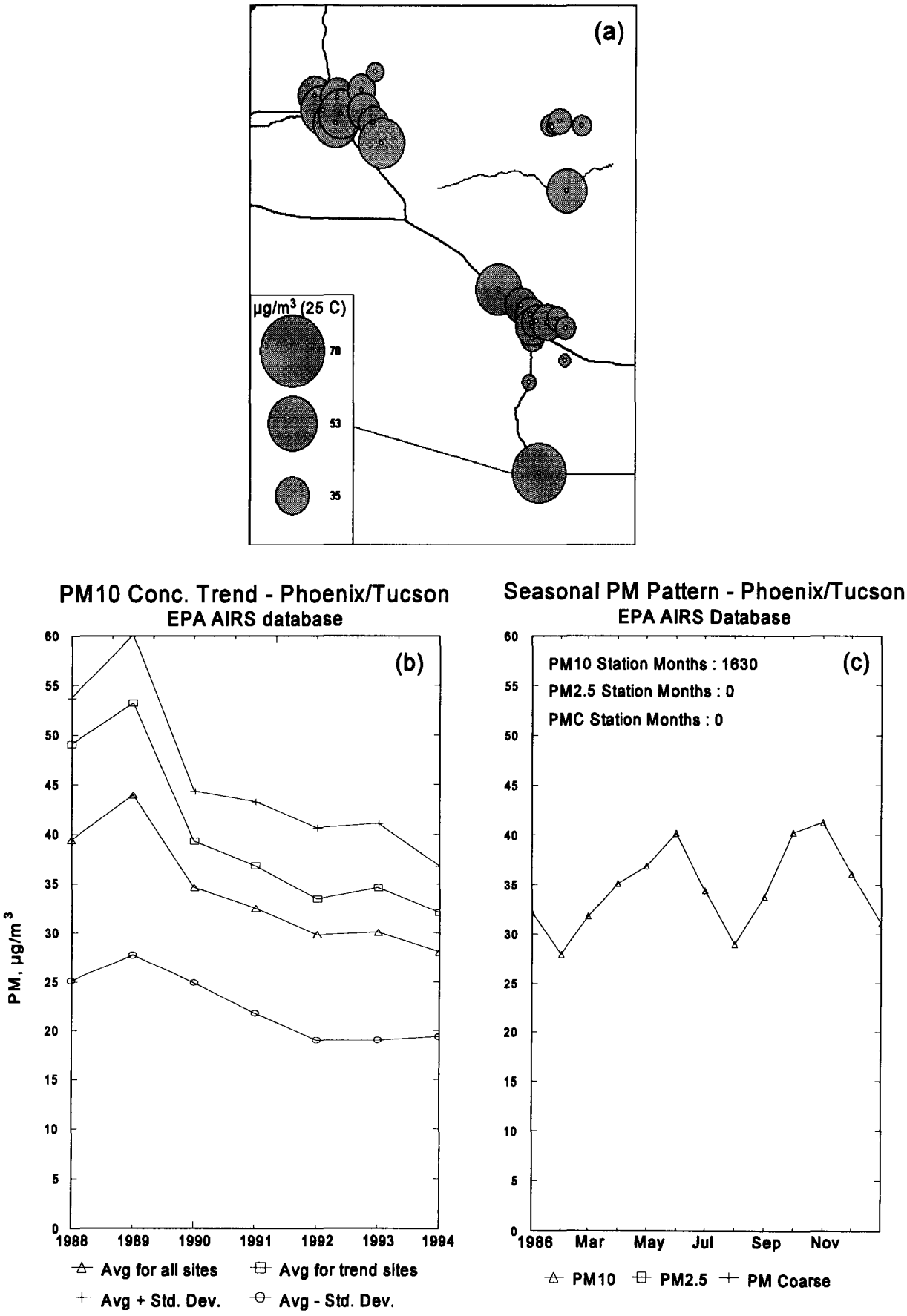

Figure 6-75. Phoenix-Tucson subregion: (a) aerosol concentration map, (b) trends, and (c) seasonal pattern.

(Pierson and Russell, 1979; Countess et al., 1980; Groblicki et al., 1981). In both cities, the average measured NO_3^- concentrations were about 1 to 2 times that of the average $SO_4^=$ concentration. In addition, the average $SO_4^=$ concentration measured in Phoenix was much lower than those observed at other locations throughout the U.S., but similar to the regional values observed in the Southwest (Moyers, 1982).

Wintertime PM_{10} and $PM_{2.5}$ chemical compositions and source contributions in Tucson, AZ (Chow et al., 1992a) show that the major contributors to the highest PM_{10} concentrations were geological material (>50%) and primary motor vehicle exhaust (> 30%) at three urban sampling sites. Secondary ammonium sulfate, secondary ammonium nitrate, and copper smelter aerosols were found to contribute less than 5% to elevated PM_{10} concentrations.

The OC/EC ratio was one to one at Phoenix sites. The average arsenic concentrations in Phoenix was four times higher than observed in other cities, which indicates the potential influence of Arizona smelters located within 100 miles of Phoenix. Average sulfate levels in Phoenix were higher than they were in Denver, which has less local emissions of SO_2.

6.5.5.3 Grand Canyon National Park

McMurry and Zhang (1989) reported the size distribution of ambient organic and elemental carbon near the Grand Canyon and in the Los Angeles basin. Virtually all of the carbon was found in the submicron range, some below 0.1 μm. However, positive sampling artifacts for sub 0.1μm organics were considered significant.

At the Grand Canyon National Park, Zhang et al. (1994) showed that sulfates and carbonaceous particles were the major contributor to $PM_{2.5}$ particle scattering during the three winter months and that their contributions were comparable. Scattering by nitrates and soil dust was typically a factor of five to ten smaller. The low pressure impactor measurements also showed that sulfur size distributions vary considerably (0.07 to 0.66 μm).

6.5.6 Subregional Aerosol Pattern in the Northwest

The mountainous northwestern United States has many aerosol regions with different characteristics. The discussion below will examine South Lake Tahoe, as a case study for

mountain-valley difference, Salt Lake City, UT, Denver, CO, Idaho-Montana sites, and several Washington-Oregon sites.

6.5.6.1 South Lake Tahoe

South Lake Tahoe IMPROVE monitoring site is located in a in a populated area on the south shore of Lake Tahoe. The Bliss State Park IMPROVE monitoring site is to the northwest, elevated (700ft) and removed from the populated areas. The pair of sites illustrates the populated area-remote difference in aerosol pattern. The aerosol and visibility at the two lake Tahoe sites were also examined (Molenar et al., 1994).

The concentration of all aerosol components is substantially higher on the south lake shore compared to the more remote site. The seasonality and chemical composition is also substantially different. The excess PM_{10} concentration at the S. Lake Tahoe site compared to Bliss State Park (Figure 6-76) is about 5 $\mu g/m^3$ during the warm season, May through September, and it climbs to 28 $\mu g/m^3$ excess in January. The factor of five seasonal modulation for valley excess PM_{10} is likely contributed by winter time emission sources, poor dispersion compared to the summer, as well as fog, all of which tend to enhance the aerosol formation. Fine and coarse particles contribute roughly equally to excess PM_{10} mass concentrations. However, fine particles contribute about 60% during the fall season and coarse particles prevail (>60%) during the spring. Both fine and coarse particles show a winter peak concentration.

The chemical composition of the valley excess fine particle mass concentration also shows a strong seasonality for organic carbon and elemental carbon. In fact, the excess organic carbon concentration in the winter (13 $\mu g/m^3$) is almost an order of magnitude higher than the summer values. The seasonal concentration of excess elemental carbon is similar to that of the organic carbon. However, the relative magnitude of organic carbon compared to elemental carbon is higher in the winter (factor of five) than in the summer (factor of two). The concentration of fine particle sulfate is virtually identical for South Lake Tahoe and Bliss State Park. This implies that the South Lake Tahoe aerosol sources do not contain sulfur. It is also worth noting that the excess fine particle soil at South Lake Tahoe is below 1 $\mu g/m^3$, which is a small fraction of the coarse mass. Thus, the crustal component of the South Lake

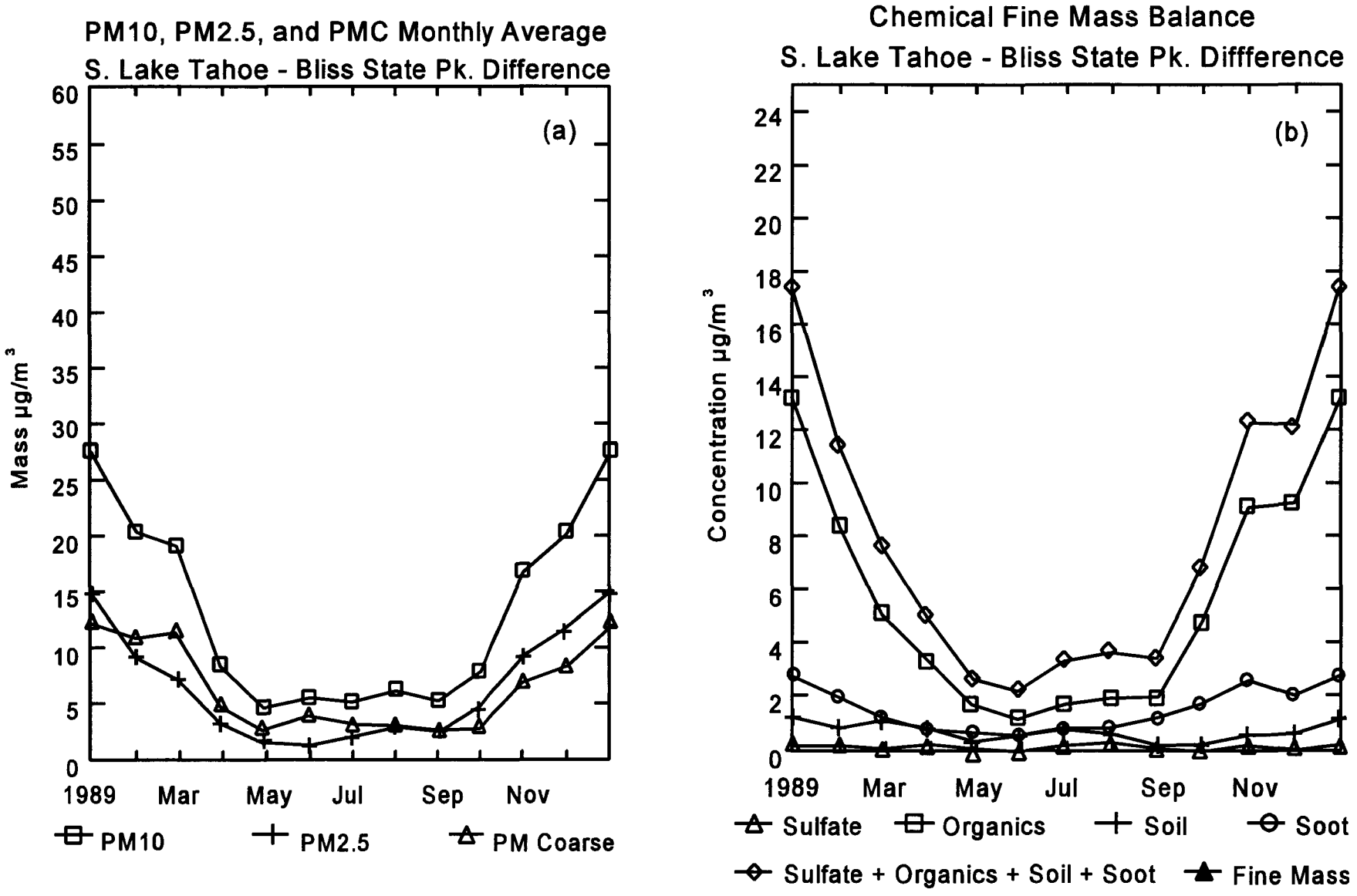

Figure 6-76. Excess aerosol concentration (a) and composition (b) at South Lake Tahoe compared to Bliss State Park.

Tahoe aerosol contributes to the coarse mass but not appreciably to the fine mass concentration.

In summary, there is a significant excess PM_{10} aerosol concentration at S. Lake Tahoe compared to the adjacent Bliss State Park remote site, particularly during the winter season (28 $\mu g/m^3$). The excess mass is about equally distributed between fine and coarse particles. The fine mass is largely composed of organics.

6.5.6.2 Salt Lake City, Utah, Subregion

Salt Lake City, Ogden, and Provo, UT, are part of an airshed that is confined by tall mountains to the East, limiting the dispersion by westerly winds.

The seasonal average PM_{10} concentration at three AIRS sites in Salt Lake City, Ogden, and Provo, UT, is shown in Figure 6-77b. All three sites show virtually identical seasonality, having peak concentrations during December through January. This confirms that the three sites belong to the same airshed with similar source pattern, meteorological dispersion and chemical transformation and removal processes.

During the 1988 to 1994 period there were overall decreases in the annual average PM_{10} for the Salt Lake City, UT subregion from 49 $\mu g/m^3$ to 29 $\mu g/m^3$ for all sites and from 54 $\mu g/m^3$ to 30 $\mu g/m^3$ for trend sites (Figure 6-77b). The reductions were 41% for all sites and 48% for trend sites. The trends were not monotonic, but showed substantial shifts upwards and downwards during the 1988 to 1994 period.

The size segregated fine and coarse concentration data exhibit a dynamic seasonal pattern. Fine particles clearly dominate the high winter concentrations reaching 40 to 50 $\mu g/m^3$, compared to summer concentrations of 10 $\mu g/m^3$. This magnitude of fine mass concentration is among the highest recorded in the AIRS data system. Coarse particles are less seasonal and they are more important during the dry summer season. The formation of sulfate and nitrate during winter inversion fogs near Salt Lake City, UT were studied by Mangelson et al. (1994).

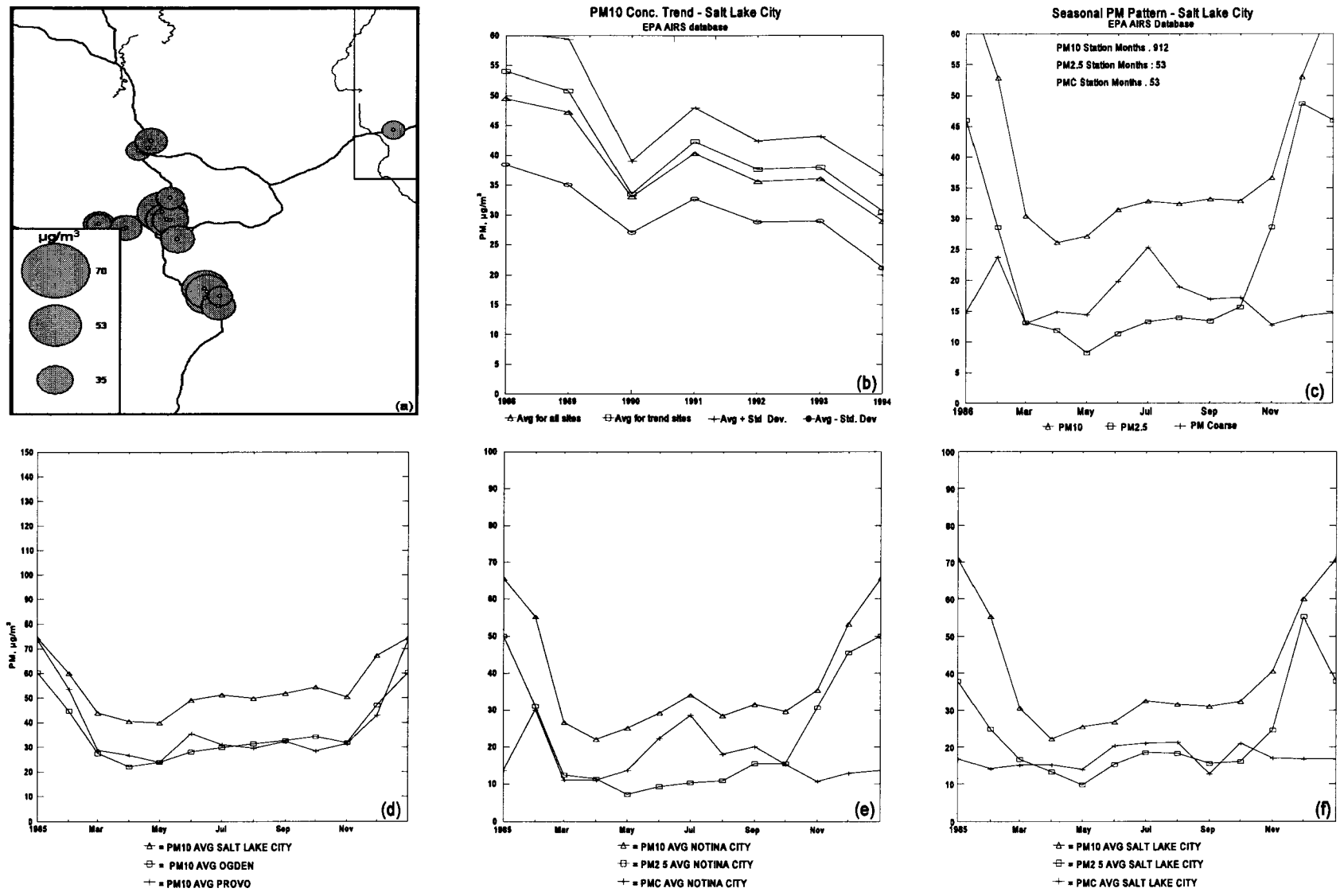

Figure 6-77. Salt Lake City region: (a) aerosol concentration map, (b) trends, (c) seasonal pattern, and (d,e,f) seasonal patterns at sites in or near Salt Lake City.

6.5.6.3 Denver, Colorado

The Denver brown cloud is a manifestation of high wintertime concentration of particles and gases. Several recent studies have focused on the characterization of the Denver brown cloud aerosols.

Size distribution measurements of winter Denver aerosol (Countess et al., 1981) show that on high pollution days that the mass median aerodynamic diameter of the accumulation mode aerosol was about 0.31 μm with $\sigma_g \pm 2.0$. Wolff et al. (1981) found that on the average motor vehicles were responsible for 27% of the elemental carbon while wood burning was responsible for 39% of the elemental carbon.

The chemical composition of wintertime Denver fine aerosol mass (16.4 $\mu g/m^3$) (Sloane et al., 1991) shows the dominance of total carbon consisting of organic carbon (8.1 $\mu g/m^3$) and elemental carbon (2.6 $\mu g/m^3$) over sulfate (1.2 $\mu g/m^3$) and nitrate (3.4 $\mu g/m^3$). The fine particle size distribution of sulfate and nitrates were bimodal.

6.5.6.4 Northern Idaho-Western Montana Subregion

The mountainous northern Idaho and western Montana subregion is characterized by deep valleys and the absence of major industrial sources or large urban-metropolitan areas. Nevertheless, PM_{10} monitoring sites in northern Idaho and western Montana report concentrations that are among the highest in the nation, as illustrated in Figure 6-78a, while neaby sites are among the lowest. The large spatial concentration variability is evidently related to the rugged terrain. Most of the monitoring sites are located in the flat valleys.

In the northern Idaho-western Montana subregion there was a decrease in the annual average PM_{10} concentrations between 1988 and 1993 from 41 $\mu g/m^3$ to 30 $\mu g/m^3$ for all sites and from 40 $\mu g/m^3$ to 31 $\mu g/m^3$ for trend sites. The reductions were 27% for all sites and 23% for trend sites (Figure 6-78b). The average seasonality of the subregion is strongly winter peaked (Figure 6-78c) with a factor of two modulation between 25 and 45 $\mu g/m^3$.

The high spatial variability is illustrated in an example from northern Idaho (Figure 6-79a). Three sites in Missoula, MT, show winter monthly averaged peak concentrations from less than 40 to more than 100 $\mu g/m^3$. This is higher than the monthly average PM_{10} concentration anywhere in the eastern U.S. The site closest to the city center

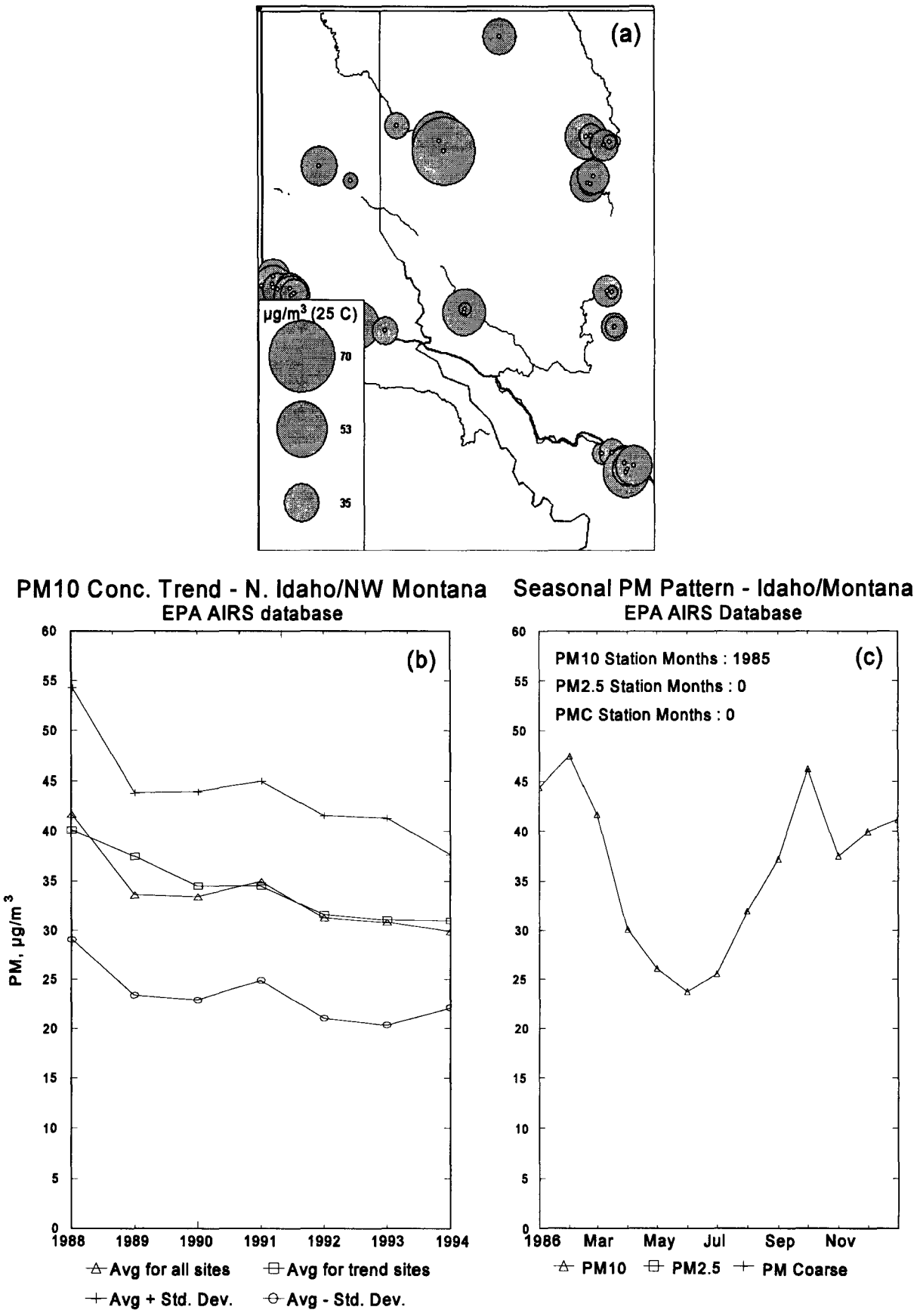

Figure 6-78. Northern Idaho-Northwestern Montana subregion: (a) aerosol concentration map, (b) trends, and (c) seasonal pattern.

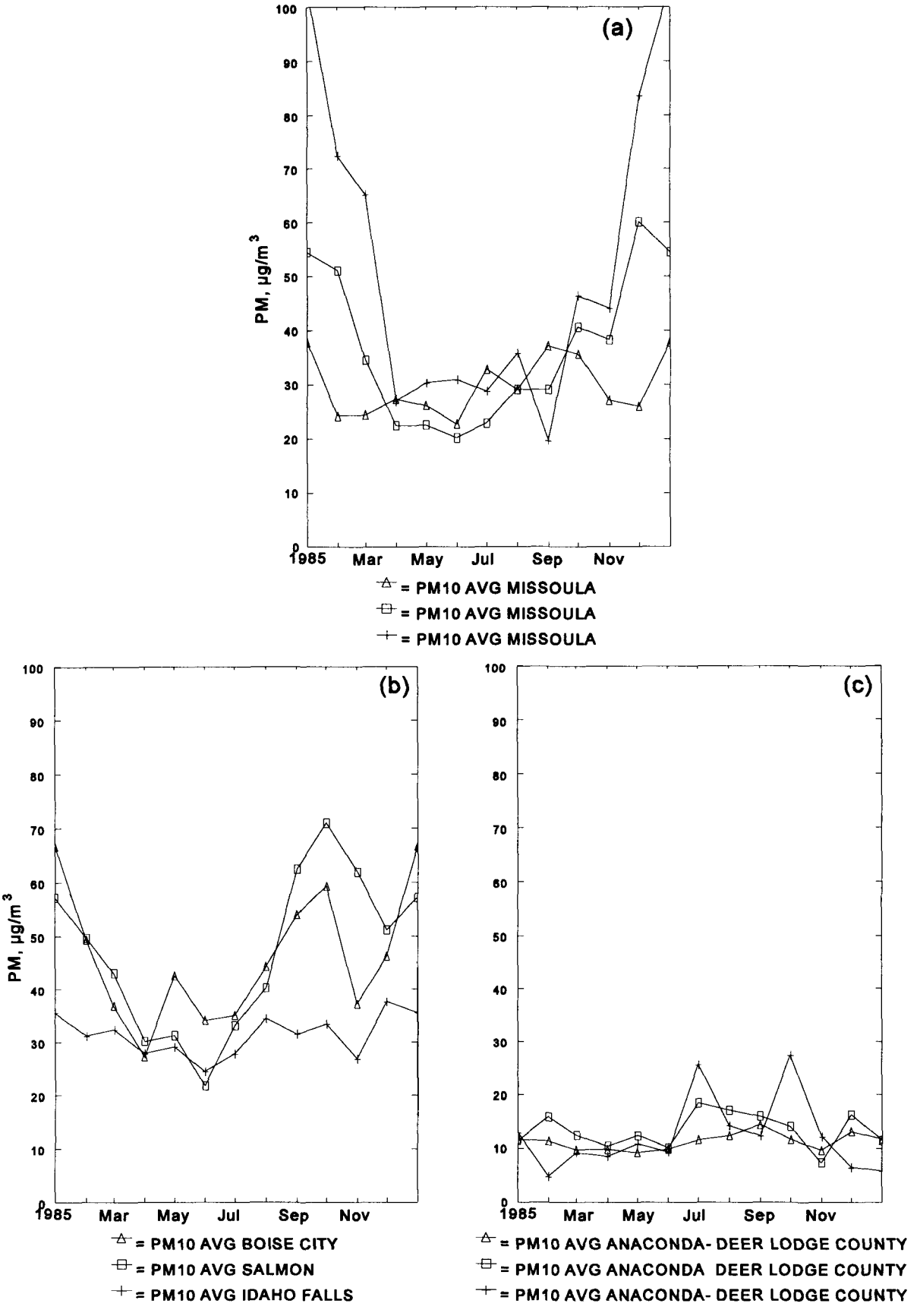

Figure 6-79a,b,c. PM_{10} concentration patterns at sites in the Northern Idaho-Northwestern Montana subregion.

shows the highest winter peak (>100 $\mu g/m^3$), but has summer values that are comparable to the other two sites. It is evident that in Missoula, MT, high concentration gradients exist between the populated areas and remote sites. Boise and Salmon, ID (Figure 6-79b) also show elevated PM_{10} concentrations during the cold season. Idaho Falls, ID, on the other hand, is seasonally uniform at about 30 $\mu g/m^3$, which is comparable to the lowest Missoula, MT, site.

Unusually low PM_{10} concentrations of 10 $\mu g/m^3$ are reported at three PM_{10} monitoring sites near Anaconda-Deer, ID (Figure 6-79c). This result is unexpected because the sites are in a valley. The characteristic winter peak is completely absent. This suggests that pristine, low, PM_{10} sites can exist in the northwestern valleys, and hence the region is not uniformly covered by wintertime haze or smoke.

6.5.6.5 Washington-Oregon Subregion

The Pacific Northwest is also a mountainous subregion that exhibits unique aerosol characteristics. During 1988 to 1994, there were decreases in the annual average PM_{10} concentrations for the Washington-Oregon subregion from 36 $\mu g/m^3$ to 26 $\mu g/m^3$ for all sites and from 39 $\mu g/m^3$ to 28 $\mu g/m^3$ for trend sites. The reductions were 28% for both all sites and trend sites. The subregion shows a strong seasonality with a winter peak due to $PM_{2.5}$ (Figure 6-80b). PM_{10} monitoring sites in Seattle, Bellevue, and Tacoma, WA (Figure 6-80d), show relatively low concentrations and a lower seasonality although higher values occur in the winter. A much more pronounced seasonality of PM_{10} concentrations is recorded in southern Oregon. Medford, Grants Pass, and Klamath Falls, OR (Figure 6-80e) evidently belong to an airshed in which emissions, dispersion, and aerosol formation mechanisms are conducive to the formation of winter time aerosol (60 to 80 $\mu g/m^3$).

Fine and coarse particle data collected over a limited period in 1987 show that the winter peak of PM_{10} is entirely due to the strong winter peak of fine particle mass (50 to 100 $\mu g/m^3$). Coarse mass, on the other hand, is seasonally invariant at about 10 to 20 $\mu g/m^3$. Fine particles clearly are responsible for the winter peak. This is somewhat different from the observations at South Lake Tahoe, where the winter peak was attributed to both fine and coarse particles.

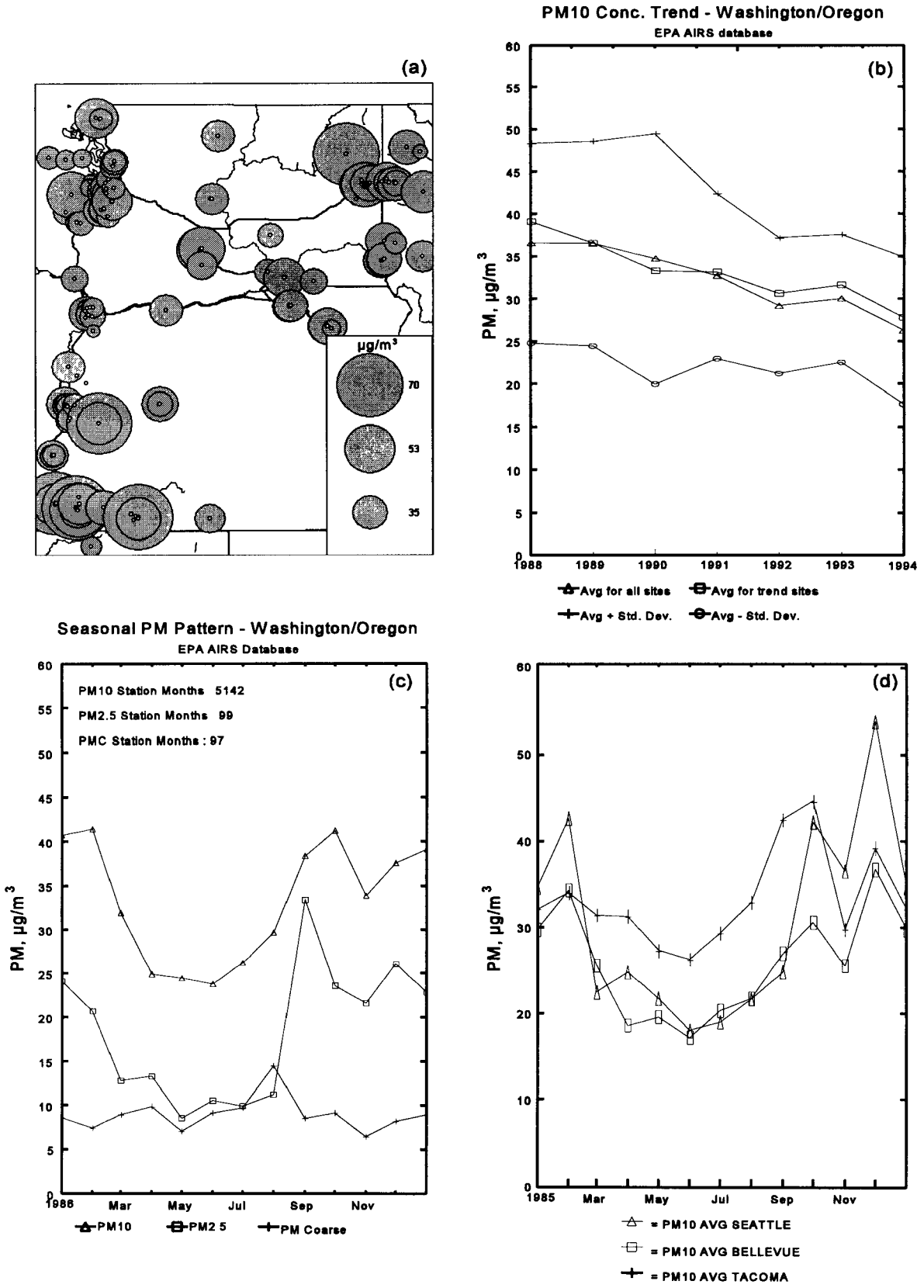

Figure 6-80a,b,c,d,e,f,g,h. Aerosol concentration patterns in Washington State and Oregon.

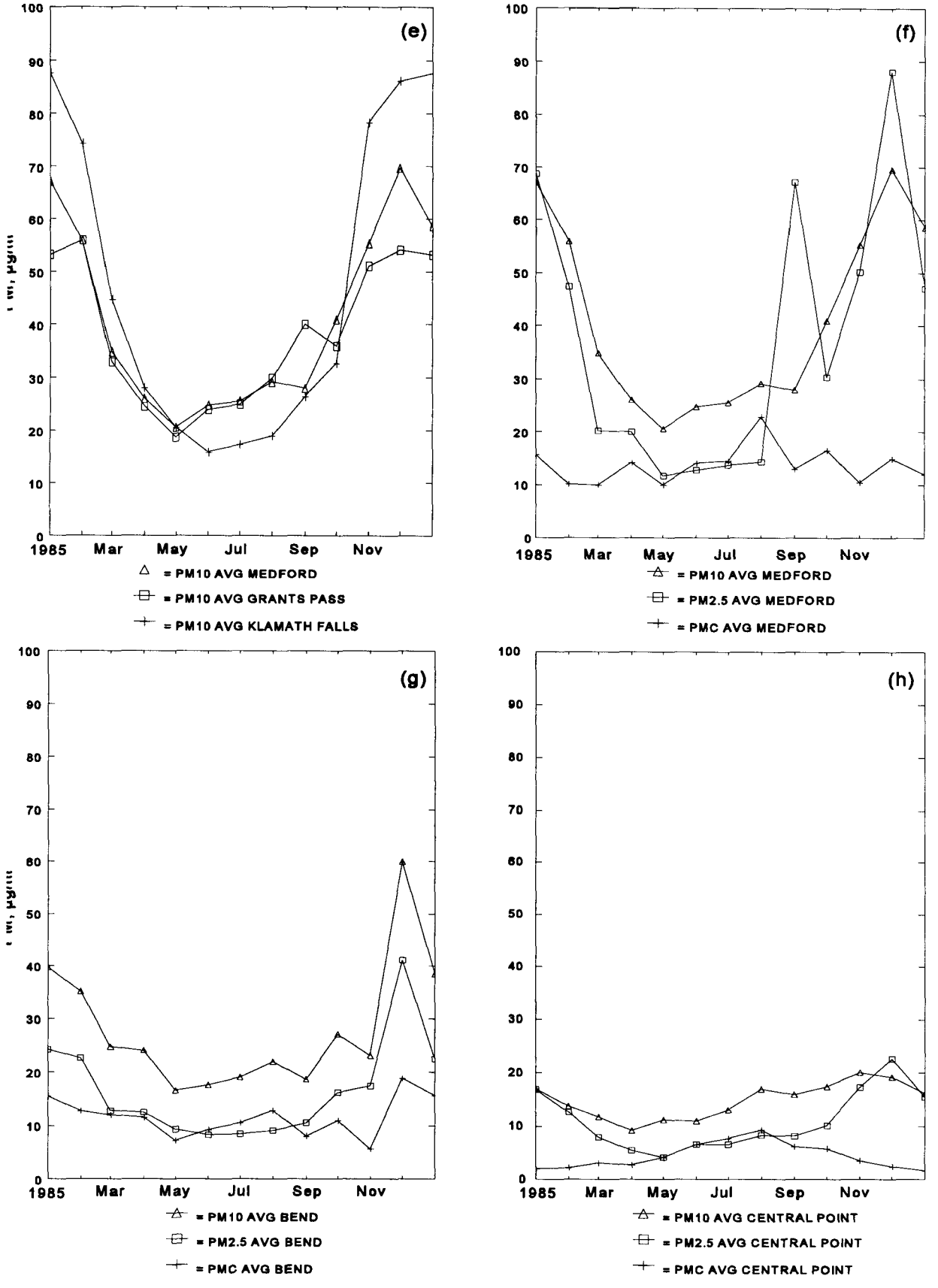

Figure 6-80 (cont'd). Aerosol concentration patterns in Washington State and Oregon.

The size segregated aerosol data for Bend and Central Point, OR (Figure 6-80g,h), show diminishing concentrations compared to Medford (Figure 6-80f), where the reduction of PM_{10} is mainly due to the decrease of the fine particle mass during the winter season.

In Portland, OR, carbonaceous aerosol was found to account for about 50% of fine aerosol mass (Shah et al., 1984).

6.5.6.6 Other Northwestern Locations

Dresser (1988) investigated the winter PM_{10} concentrations in a small ski resort town, Telluride, CO, and found that the street dirt and sand are major contributors, particularly during the dry post snow period. Wintertime source apportionment attributed to 45% of the PM_{10} mass to residential wood combustion in San Jose, CA (Chow et al., 1995a).

6.5.7 Subregional Aerosol Pattern in Southern California

The southern California region has two subregions, the San Joaquin Valley and the Los Angeles-South Coast Air Basin, discussed separately in sections below.

6.5.7.1 San Joaquin Basin

The wide air basin between the coastal mountain ranges of California to the west and the Sierra Nevada Mountains to the east shows reasonably uniform PM_{10} concentrations as indicated on the map (Figure 6-81a). There is evidence of PM_{10} concentration reduction but the trend is not conclusive (Figure 6-81b). The seasonal modulation amplitude over the San Joaquin Valley (Figure 6-81c) is about factor of 2.5 between the low spring concentration 30 to 35 $\mu g/m^3$, and high fall concentration (60 to 70 $\mu g/m^3$). The unique feature of this seasonality is the fall peak which differs from the summer peak in the eastern United States and winter peak over the mountainous northwestern states.

The AIRS database contains valuable size segregated fine and coarse particle concentration data within the San Joaquin Valley, as shown in Figure 6-82 for Fresno, Madera, Visalia, and Bakersfield, CA. These monitoring sites show virtually identical concentration patterns for fine and coarse mass. Both coarse and fine particles are important contributors to the San Joaquin Valley PM_{10} aerosol. However, their respective prevalence is phase shifted. Fine particles are

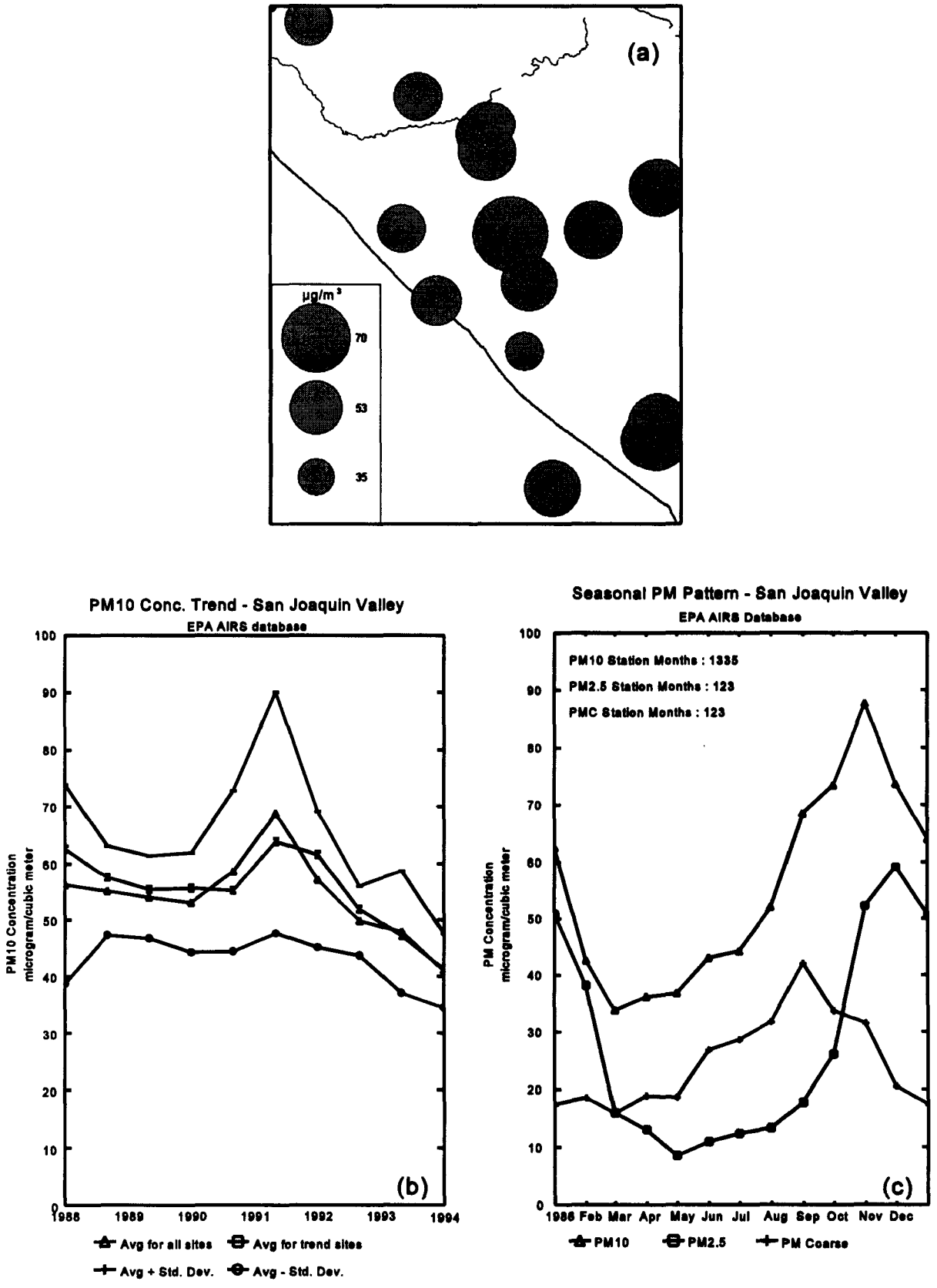

Figure 6-81. San Joaquin Valley: aerosol concentration map, trends, and seasonal pattern.

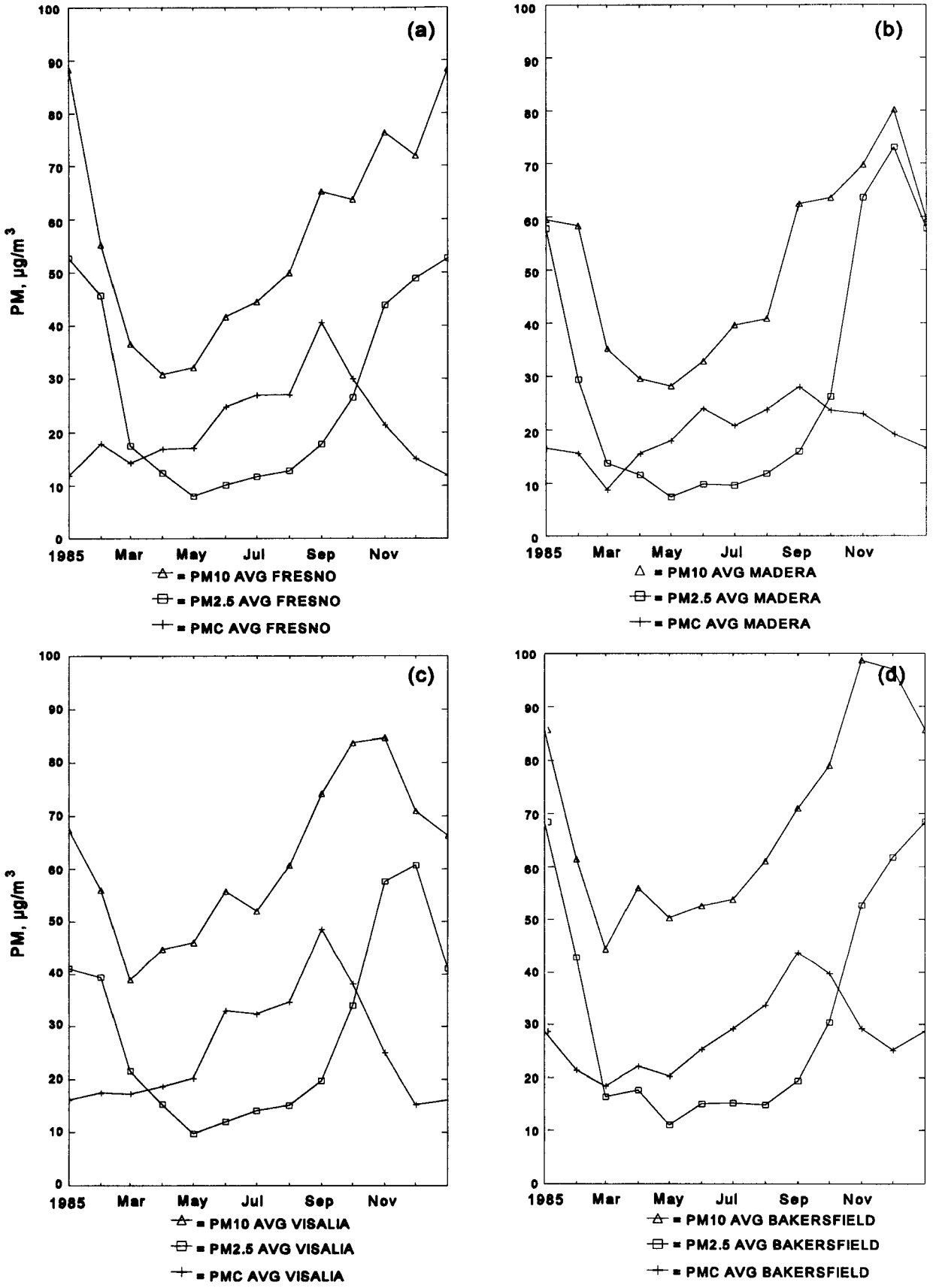

Figure 6-82. Fine, coarse, and PM_{10} seasonal patterns in the San Joaquin Valley.

most important during the November through February winter season, while coarse particles prevail during April through September. In November, both coarse and fine particles contribute to the seasonal peak of PM_{10}. During March through May, neither fine or coarse particles are abundant and the PM_{10} concentration is lowest during the spring season.

The temporal dynamics of the emissions, ventilation and aerosol formation in the San Joaquin Valley has been the subject of detailed aerosol monitoring, and source apportionment studies.

The aerosol composition at nonurban sites (Chow et al., 1995b) provides further characteristics of the central California aerosol pattern (Figure 6-82). A PM_{10} aerosol study was carried out at six sites in California's San Joaquin Valley from 14 June 1988 to 9 June 1989, as part of the 1988 to 1989 Valley Air Quality Study (VAQS). Concentrations of PM_{10} and $PM_{2.5}$ mass, organic and elemental carbon, nitrate, sulfate, ammonium, and elements were determined in 24-h aerosol samples collected at three urban (Stockton, Fresno, Bakersfield) and three non-urban (Crows Landing, Fellows, Kern Wildlife Refuge) locations (Chow et al., 1993a). The VAQS data indicate the federal 24-h PM_{10} standard of 150 $\mu g/m^3$ was exceeded at four out of the six sites and for reasons which differ by season and by spatial region of influence. The annual average source contributions to PM_{10} at Bakersfield, the site with the highest annual average, were 54% from primary geological material, 15% from secondary ammonium nitrate, 10 % from primary motor vehicle exhaust, 8% from primary construction, the remaining 4% is unexplained. The results of the source apportionment at all sites show that geological contributions dominate in summer and fall months, while secondary ammonium nitrate contributions derived from direct emissions of ammonia and oxides of nitrogen from agricultural activities and engine exhaust are largest during winter months. (Chow et al., 1992b).

6.5.7.2 Los Angeles-South Coast Air Basin-Southeastern Desert Air Basin

The Los Angeles basin is confined by the San Gabriel Mountains which limit the ventilation during westerly winds. Intensive emissions from automotive and industrial sources produce the Los Angeles smog with numerous secondary photochemical reaction products from primary emissions. The map of the Los Angeles subregion shows (Figure 6-83a) the

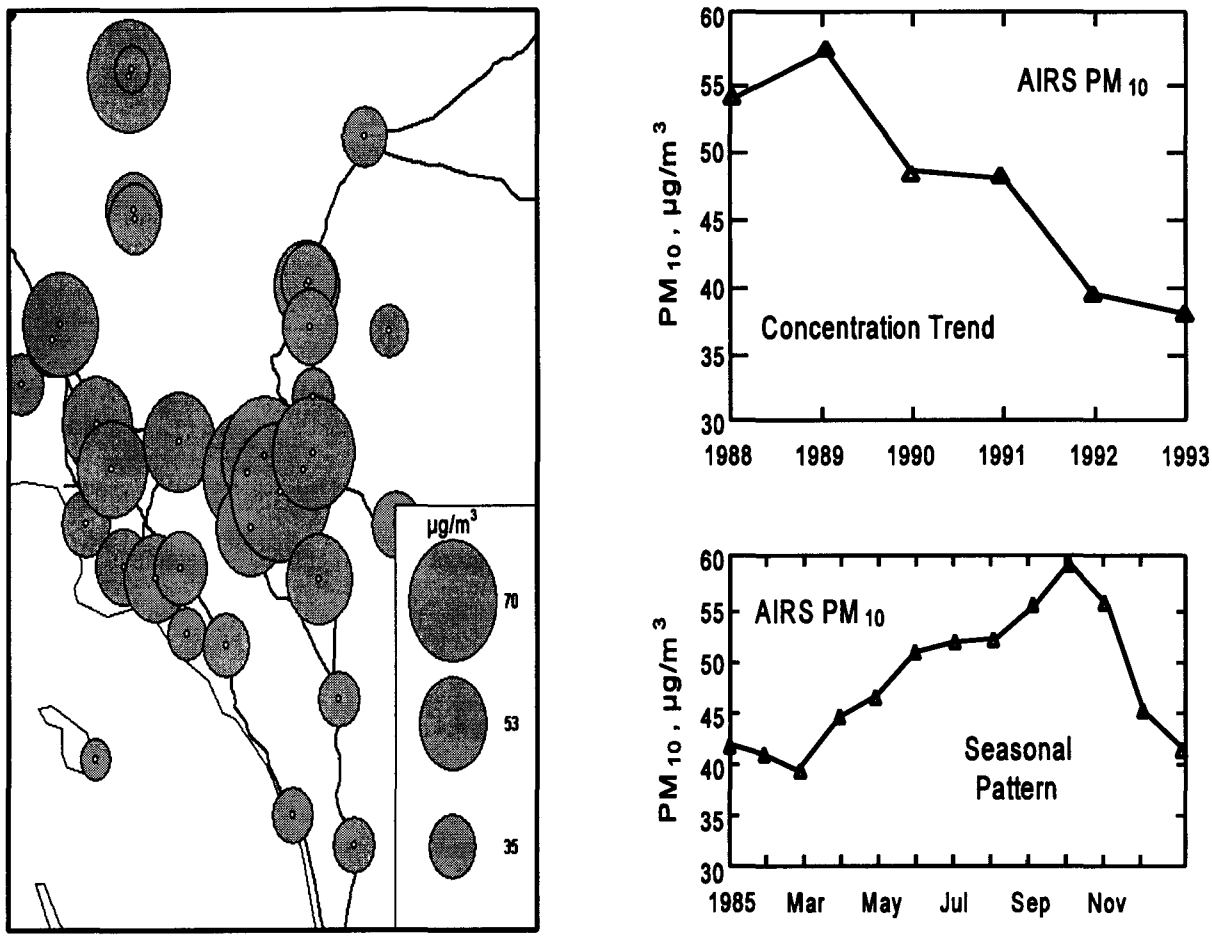

Figure 6-83. Los Angeles: (a) aerosol concentration map, (b) trends, and (c) seasonal pattern.

magnitude of PM_{10} concentrations for individual monitoring stations. Isopleths of PM_{10} concentration for 1992 are consistent with these results showing the highest PM_{10} concentrations are measured in the center of the LA basin with the lower concentration of PM_{10} near the ocean and out in the desert and the mountains (Hoggan et al., 1993).

There has been a substantial reduction of subregion average PM_{10} concentration from 1988 to 1993 from 54 $\mu g/m^3$ down to 38 $\mu g/m^3$ (Figure 6-83b), a reduction of 30%. The seasonality of the basin averaged PM_{10} concentration shows a 50% amplitude, with the peak concentration (60 $\mu g/m^3$) during October and the lowest values (40 $\mu g/m^3$) during January through March (Figure 6-83c). Hence, this fall peaked seasonality is similar to the fall peak over the San Joaquin Valley.

The PM_{10} air quality in the California South Coast Air Basin (CSCAB) and to a limited extent in the Southeastern Desert Air Basin have been analyzed for the 1985 to 1992 period (Hoggan et al., 1993). Although a larger number of monitoring stations exist in more recent years, the analysis involved only the monitoring stations with complete data in Long Beach, Burbank, El Toro, Ontario, Rubidoux, Banning, and Indio. Measurements in downtown Los Angeles also are used in parts of the analysis (Hoggan et al., 1993). The annual average PM_{10} trend line for 1985 to 1992 showed a statistical significant trend downwards with the decrease averaging 3% per year. The sulfate and nitrate also were measured and they accounted for about one-third of the decrease in PM_{10}. The decreases between 1989 and 1993 for this set of stations were smaller than for the larger group of stations (Figure 6-83b). There was a statistically significant decrease (0.05 level of significance) at Burbank, Long Beach, Rubidoux, and Banning. Use of both a decision tree analysis and a multiple linear regression analysis showed that the temperature at 850 mb, a measure of mass stability, was an important variable associated with PM_{10} in the CSCAB. Use of this variable suggests that the observed decreases in annual average PM_{10} concentrations between 1987 and 1992 are not an artifact of meteorology. A more detailed discussion of these analyses as related to various aspects of meteorology is given (Hoggan et al., 1993).

The diurnal patterns of PM_{10} also are discussed (Hoggan et al., 1993). The Rubidoux monitoring station showed peaks in PM_{10} at about the time of peak commuter traffic. The Los Angeles monitoring station showed higher PM_{10} concentrations in the morning and evening than at midday. Azusa and Long Beach monitoring stations showed broad daytime peaks. The Indio monitoring station showed an evening peak.

The weekday to weekend mean PM_{10} concentrations at all monitoring stations showed significantly lower concentrations on weekends (Hoggan et al., 1993). At the two SEDAB stations, Indio and Banning, Saturday PM_{10} concentrations were slightly lower than weekdays, but Sunday PM_{10} concentrations fell within the range of weekday means.

Some seasonal characteristics of the Los Angeles basin are depicted in Figure 6-84. The monitoring sites at different parts of the basin have markedly different seasonal concentration patterns. Hawthorne and Long Beach near the Pacific Coast and Burbank in an inland valley have the higher PM_{10} concentration in late fall and early winter (Figure 6-84b,c). On the

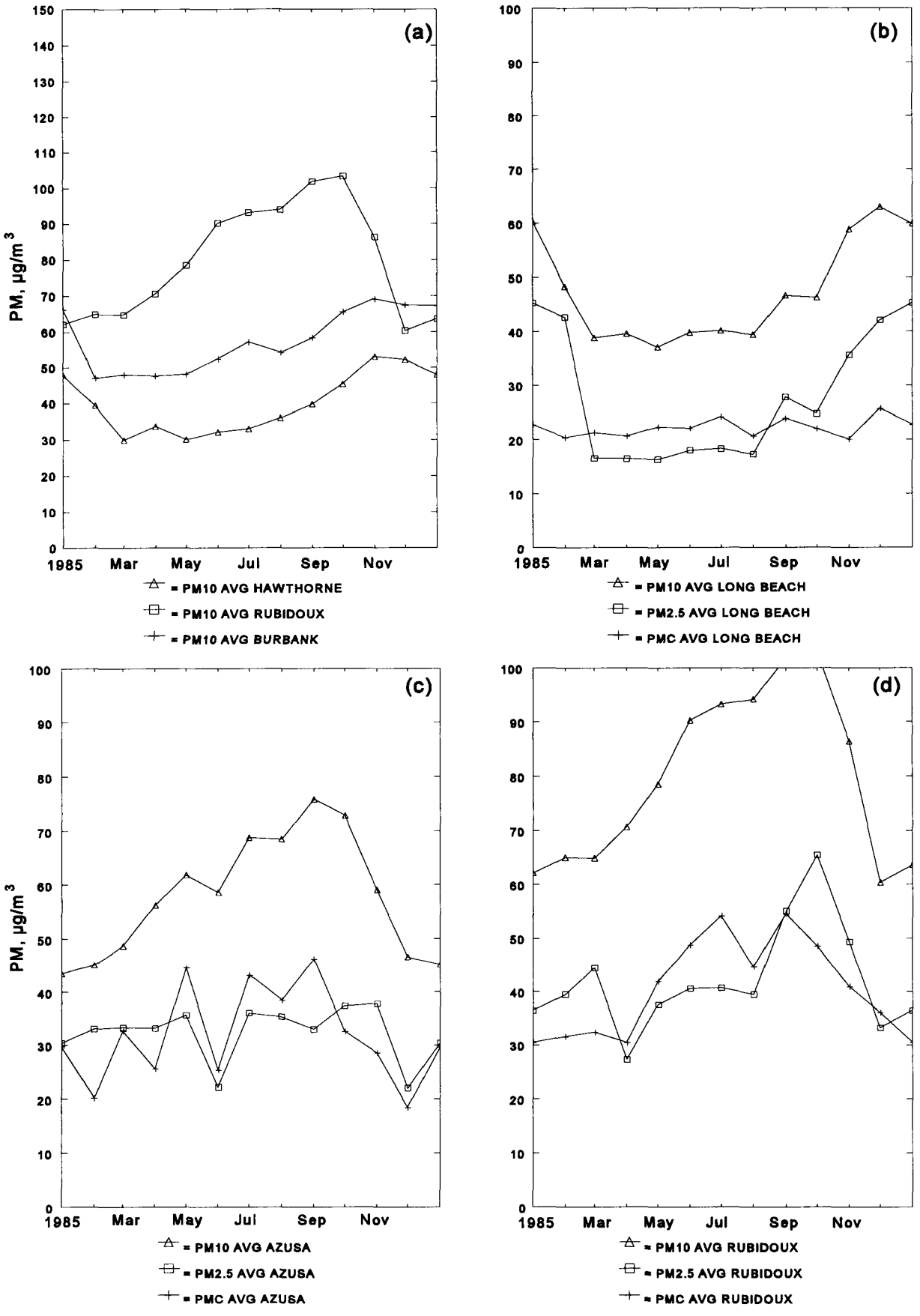

Figure 6-84a,b,c,d. Fine, coarse, and PM_{10} seasonal patterns near Los Angeles. (Note scale for (a) is 150 µg/m³.)

other hand, Azuza and Rubidoux in the eastern part of the basin exhibits the higher PM_{10} concentration during the May to October 'smog season' (Hoggan et al., 1993) (Figure 6-84b,d,e). The main causes of different seasonalities are likely to be associated with seasonally varying meteorological, transport, and chemical transformation patterns. The role of coarse and fine particles in the Los Angeles basin is also illustrated in Figure 6-84. At Long Beach, near the coast (adjacent to Hawthorne), the fine particles dominate the PM_{10} during the November through February winter season (40 to 50 $\mu g/m^3$). Coarse particles at Long Beach are constant throughout the year at about (20 $\mu g/m^3$). At Azuza and Rubidoux fine and coarse particles contribute roughly equally to the high PM_{10} concentrations. Thus, the PM_{10} aerosols over the smoggiest parts of the Los Angeles basin are not dominated by fine secondary aerosols but contributed by both fine and coarse particles.

The Rubidoux site in 1985 to 1988 showed violations of the 24-h PM_{10} standard approximately 12% of the time with a large contribution from ammonium nitrate (Chow et al., 1992c). A large group of dairies and animal husbandry operations in the Chino area approximately 13 km west of the Rubidoux site were identified as major ammonia emitters (Russell and Cass, 1986). To better evaluate the immediate area, measurements were made at the Rubidoux, Riverside-Magnolia, and Riverside sites. The results indicated that the Rubidoux site did represent urban-scale contributions of primary motor vehicle exhaust, secondary sulfate, and secondary nitrate. However, there also were significant neighborhood-scale and urban-scale contributions of primary geological sources and lime/gypsum sources contributing to the PM_{10} concentration (Chow et al., 1992c).

The Los Angeles smog has been the subject of extensive spatial, temporal, size and chemical composition studies since the 1960s (Appel et al., 1976, 1978, 1979; Hidy et al., 1980). A number of individual studies are discussed below.

The chemical characteristics of the PM_{10} aerosols were measured throughout 1986 (Solomon et al., 1989). Five major aerosol components (carbonaceous material, elemental carbon and organic carbon [measured value multiplied by 1.4 to account for O and H associated with C], nitrate, sulfate, ammonium, and soil-related materials, as measured) accounted for over 80% of the 1986 annual average PM_{10} mass. In all, measured chemical components were included from 80 to 94% of the PM_{10} mass was chemically identified. The nitrate and

ammonium concentrations were substantially higher at the Rubidoux and Upland sites than at other sites. Measurements made off the coast at San Nicolas Island suggest that from 28 to 44% of the annual average concentration at individual on-land sites can be associated with a regional background (Solomon et al., 1989).

More recently the LA aerosol characteristics during 11 summer days and 6 fall days in 1987 have been further elucidated by Southern California Air Quality Study (SCAQS) (Lawson, 1990). Several of the SCAQS studies reported are discussed below. The SCAQS study is also discussed in Chapter 3, Section 3.4.2.3.

Nitrate, sulfate, ammonium, and organic and elemental carbon were the most abundant species in the $PM_{2.5}$ fraction during SCAQS (Chow et al., 1994a). The coarse particle fraction was composed largely of soil-related elements (e.g., aluminum, silicon, calcium, iron) at the inland sites and with marine-related elements (e.g., sodium, chloride) at the coastal sites. Average concentrations for most chemical compounds were higher during the fall than during the summer, except for sulfate which was more abundant in summer. The $PM_{2.5}$ constituted one-half to two-thirds of PM_{10} at all sampling sites. $PM_{2.5}$ nitrate and ammonium concentrations were negatively biased for daytime samples compared to nighttime samples, consistent with diurnal changes in temperature and the effect of these changes on the equilibrium between particulate ammonium nitrate and gaseous ammonia and nitric acid. (Chow et al., 1994a; Watson et al., 1994a).

Wolff et al. (1991) measured the smog aerosol pattern during SCAQS at Claremont, CA, and Long Beach, CA, in the eastern and western Los Angles basin, respectively. Claremont's air quality during the summer was characterized by high concentrations of photochemically produced pollutants including ozone, nitric acid, particulate nitrate, and particulate organic carbon (OC). The highest concentrations of these species were experienced during the daytime sampling period (0600 to 1800) and were associated with transport from the western part of the basin. Long Beach's air quality during the fall was characterized by frequent periods of air stagnation that resulted in high concentrations of primary pollutants including PM_{10}, OC and elemental carbon (EC) as well as particulate nitrate. Night -time levels of most constituents exceeded daytime levels due to poorer night-time dispersion conditions. At Claremont, OC and nitrate compounds accounted for 52% of PM_{10} , while at Long Beach they

accounted for 67% of PM_{10}. On the average, there appears to be sufficient particulate ammonium to completely neutralize the nitrate and acidic sulfates.

In situ, time resolved analysis for aerosol organic and elemental carbon in Glendora, CA (Turpin et al., 1990), showed strong diurnal variations with peaks occurring in the daylight hours. Comparison of the diurnal profile of organic carbon with those of elemental carbon provided evidence for the secondary formation of organic aerosol in the atmosphere. Turpin et al. (1991) observed that secondary organic aerosol appears to have contributed roughly half of the organic aerosol in Pasadena during midday summer conditions.

Turpin and Huntzicker (1991) also found that the organic and elemental carbon concentrations exhibit strong diurnal variations. Peak concentrations occur during the daylight hours in the summer and at night in the fall. The maximum concentrations observed in the fall (maximum total carbon, 88 $\mu g/m^3$) were two to three times higher than the summer maxima (maximum total carbon, 36 $\mu g/m^3$). Measurements of elemental and organic carbon have been carried out by Gray et al. (1986). Extensive efforts have been made by Cass and coworkers (e.g. Rogget et al., 1993; Hildemann et al., 1991) to identify the molecular composition of the organic component. While some tracers have been identified, only a fraction of the organic PM has been characterized in terms of its molecular composition.

Gaseous nitric acid and fine particulate nitrate at Claremont, CA (Pierson and Brachaczek, 1988) both showed pronounced ($\sim$10-fold) diurnal variations; however, coarse particles showed little diurnal variation. The average concentrations over the September 11 to 19 study period were for HNO_3, 7.1 $\mu g/m^3$; fine NO_3^-, 7.29 $\mu g/m^3$; and coarse NO_3^-, 7.1 $\mu g/m^3$. Fine NO_3^- may have been underestimated due to volatilization during or after sampling. This problem is discussed in Chapter 4, Section 4.2.10.1.

Careful size distribution measurements in the Los Angeles basin (John et al., 1990) shed light on the size spectrum dynamics for ammonium, sulfate and nitrate. Three modes, two submicron and one coarse, were sufficient to fit all of the size distributions. The smallest mode, at 0.2 ± 0.1 μm aerodynamic diameter, is probably a condensation mode containing gas phase reaction products. A larger mode at 0.7 ± 0.2 μm is defined as a droplet mode. Most of the inorganic particle mass was found in the droplet mode. The observed condensation and droplet modes characterize the overall size distribution in the 0.1 to 1.0 μm range, previously described

by Whitby and coworkers as a single accumulation mode (Whitby et al., 1972; Whitby, 1978). Wall et al. (1988) also found that in September 1985 at Claremont, CA fine particle nitrate was associated with ammonium, while coarse mode nitrate was associated with both ammonium and sodium. Sulfate was primarily in two submicrometer modes.

A clear demonstration of the effect of relative humidity and aerosol loading on atmospheric sulfate size distributions is given by Hering and Friedlander (1982). Days of high relative humidity and aerosol loading correspond to high mass median diameters (0.54±0.07 μm) for the sulfate while low relative humidity and low aerosol loadings correspond to small mass median diameters (0.2±0.02 μm). According to their interpretation, the larger (0.54 μm) sulfate particles resulted from aqueous phase reactions of SO_2. The finer (0.2 μm) sulfate resulted from homogeneous gas phase reactions leading to the nucleation of sulfuric acid particles.

McMurry and Stolzenburg (1989) provide evidence that Los Angeles smog aerosols are externally mixed. Monodisperse ambient aerosols were often found to split into nonhygroscopic (no water uptake) and hygroscopic portions when humidified. An average of 30% of the particles in the 0.2 to 0.5 μm range were nonhygroscopic. However, the proportion of particles that were nonhygroscopic varied considerably from day to day and on occasion was 70 to 80% of the particles. The data show that for the hydrophilic aerosol, the larger particles (0.4 to 0.5 μm) grew more when humidified than did smaller particles (0.05 to 0.2 μm).

Size distributions of aerosol phase aliphatic and carbonyl groups at Claremont, CA (Pickle et al., 1990) showed maxima in the 0.12 to 0.26 μm and the 0.5 to 1.0 μm size functions. From the aliphatic carbon absorbency, the ambient samples generally showed maxima in the 0.076 to 0.12 μm size fraction. The authors attribute the carbonyl absorbance almost entirely attributed to products of atmospheric reactions and the aliphatic absorbencies in particles smaller than 0.12 μm to automotive emissions.

Cahill et al. (1990) found that the sulfate aerosol size at Glendora, CA, is smaller, 0.33 μm (MMD) during clear days compared to 0.5 μm on smoggy days.

The size distributions of organic nitrate groups in ambient Los Angeles aerosol were typically bimodal (Mylonas et al., 1991). During periods of high photochemical activity, the maxima in the mass loadings were in the 0.05 to 0.075 μm and the 0.12 to 0.26 μm size fractions. During periods of low-moderate ozone concentrations, the distributions were shifted to

slightly larger sizes, with maxima appearing in the 0.075 to 012 μm and the 0.5 to 1.0 μm size fractions. A principal component analysis of the organonitrate loadings revealed strong correlations with ozone concentrations and with aerosol phase carbonyl loadings.

The analysis of coarse particles in Claremont, CA (Noll et al., 1990) show that the coarse particle mass could be divided into two categories: material that was primarily of crustal origin (Al, Ca, Fe, and Si) and material that was primarily of anthropogenic origin (Cd, Cu, Mn, Ni, Pb, and Zn). The mass of crustal material varied between 33 and 49% of the total coarse mass, while the mass of anthropogenic elements listed above were <1%.

The daily frequency distribution of the chemical components of the Los Angeles aerosol measured over a 1-year period were approximately lognormal (Kao and Friedlander, 1994). For nonreactive aerosol components, the geometric standard deviation (GSD) is nearly constant at 1.85±0.14 even for components from different source types. An apparent bimodal frequency distribution for sulfates probably corresponds to the two differing reaction pathways by which gas-to-particle conversion occurs. However, the bimodal sulfate distribution function was not found at other Los Angeles sites (Kao and Friedlander, 1995). The authors suspect a relationship between GSD and the level of complexity of the stochastic physical and chemical processes affecting the distributions of the individual species. They also point out that the chemical concentration of the Los Angeles aerosol that corresponded to the peak in the (nearly) lognormal frequency distribution of the total mass is lower than he simple average chemical concentration.

A long term data base for organic and elemental carbon has been constructed (Cass et al., 1984; Gray et al., 1984). The average elemental carbon concentrations at seven monitoring sites in the Los Angeles area, for the 24-year period (1958 to 1982), were estimated to range from 6.4 $\mu g/m^3$ at downtown Los Angeles to 4.5 $\mu g/m^3$ at West Los Angeles. At most monitoring sites studied, elemental carbon concentration were lower in recent years than during the late 1950s and early 1960s.

6.6 CHEMICAL COMPOSITION OF PARTICULATE MATTER AEROSOLS AT URBAN AND NONURBAN SITES

This section summarizes selected data from a number of studies for the composition of atmospheric particles in suburban, urban, and a few rural areas for comparison purposes. Emphasis has been placed on the Harvard six-city study and the inhalable particulate network (1980-1981). Data for fine particle mass and elemental composition were available from these studies. Data for sulfate, nitrate, and elemental and organic carbon content are included from other studies to provide an overview of the chemical composition of the atmospheric aerosol in the United States. Tables presented in Appendix 6A provide relatively detailed representations of the properties of atmospheric particles to which U.S. populations are exposed. Unfortunately, data this complete are generally collected only during intensive studies. The tables are meant to provide examples of the types of information that could be collected as part of future monitoring efforts in support of human exposure investigations.

A summary of all the aerosol sampling studies included in this compilation is given in Tables 6A-1a, 6A-1b, and 6A-1c. Sampling studies have been grouped by geographical region roughly corresponding to the eastern, central, and western United States. Data are tabulated for the $PM_{2.5}$ ($d < 2.5$ μm), the coarse fraction of PM_{10} (2.5 μm $< d <$ 10 μm) and PM-10 ($d < 10$ μm) size fractions of the ambient aerosol in Tables 6A-2a, 6A-2b, and 6A-2c. Compositional data for all size fractions were broken down into the following major components: sulfate, as $SO_4^{=}$; carbon, as organic carbon (OC), which as been multiplied by a factor of 1.4 to account for the presence of oxidized species, and elemental carbon (EC); nitrate as NO_3^-; and remaining trace elements. The NH_4^+, that would be required to neutralize all acidic species in the samples, is shown as $(NH_4^+)^*$. Representing sulfate as ammonium sulfate and using a factor of 1.4 to account for the mass of organic carbon present in oxidized forms allows a firm lower limit to be placed on the fractional mass that is not chemically identified in filter samples. Acidity is given in units of nmoles/M^3 in Tables 6A-2a and 6A-2c. The masses of the trace elements from sodium through lead have been calculated by assuming they are in their most stable forms for conditions at the earth's surface. Reconstructed masses calculated in this way are shown by the entry, Sum, along with measured masses, and the ratio of the two are shown at the bottom of the individual summaries for each size fraction. Not all compositional categories were measured in

the studies for inclusion in the tables. For instance, data for characterizing the carbon or nitrate content of the ambient aerosol are not available for many of the studies listed. Average data are shown in graphical form in Figures 6-85a, 6-85b, and 6-85c for studies in the eastern, central, and western United States.

As can be seen from inspection of Figure 6-85a, sulfate is the major identified component of mass for fine particles (34.1%), followed by elemental and organic carbon (24.8%), minerals (4.3%), and nitrate (1.1%) for studies in the eastern United States. However, this last inference is based on only a few studies in which nitrate was measured. Pierson et al. (1980a,b, 1989) measured nitrate as constituting only 0.8% to 1.4% of aerosol mass at Allegheny Mountain and Laurel Hill in southwest Pennsylvania in the summers of 1977 and 1983. Presumably, the low nitrate in these and other studies in the eastern United States is related to aerosol acidity. Coarse particles are seen to consist mainly of mineral forming elements (51.8%) and sulfate (4.9%). Not enough data were available to determine abundances of carbon species and nitrate in the coarse fraction. A sizable fraction of both the fine (22.8%) and coarse (41.5%) particle mass is shown as unknown. This unknown mass is assumed to be mainly water, either bound as water of hydration or associated with hygroscopic particles. A small fraction of the mass, especially in the coarse fraction, may be present as carbonates. Carbonates are difficult to quantify, in part because of artifact forming reactions with atmospheric CO_2 and acids on filters. Stable carbonates could be identified by SEM in regions where they are known to represent a substantial fraction of soil composition.

Fine particles sampled in the studies shown in Table 6A-1 in the central United States (Figure 6-85b) are seen to consist mainly of sulfate (22.3%), minerals (7.6%), and elemental and organic carbon (53.6%). The reconstructed mass percentages sum to 124.8%. This could be due to an overestimation of the carbon content which was estimated from only a few samples collected during winter in woodsmoke impacted areas. Coarse particles were found to consist mainly of minerals (62.8%), sulfate (3.1%) and an unknown fraction (33.0%). No nitrate or carbon data were available for the coarse fraction from the studies in the central United States.

While gross fine particle composition appears to be broadly similar between the eastern and central United States on the basis of the studies shown in Tables 6A-1a, 6A-1b, and 6A-1c, the fine particle composition is seen to be distinctly different in the western United States

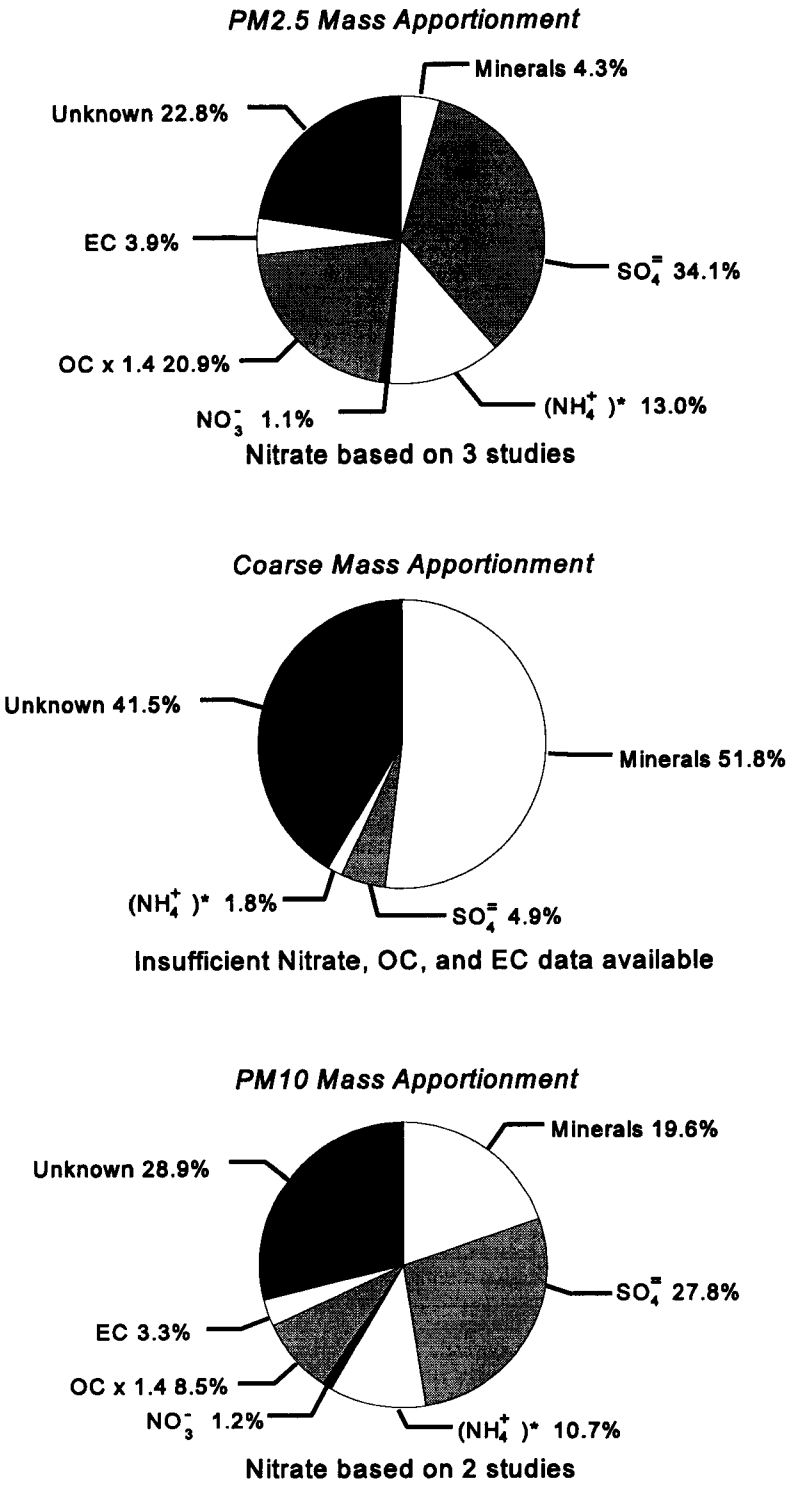

Figure 6-85a. Major constituents of particles measured at sites in the eastern United States, as shown in Tables 6A-2a, 6A-2b, and 6A-2c. $(NH_4^+)^*$ represents the concentration of NH_4^+ that would be required if all $SO_4^=$ were present as $(NH_4)_2SO_4$ and all NO_3^- as NH_4NO_3. Therefore, $(NH_4^+)^*$ represents an upper limit to the true concentration of NH_4^+.

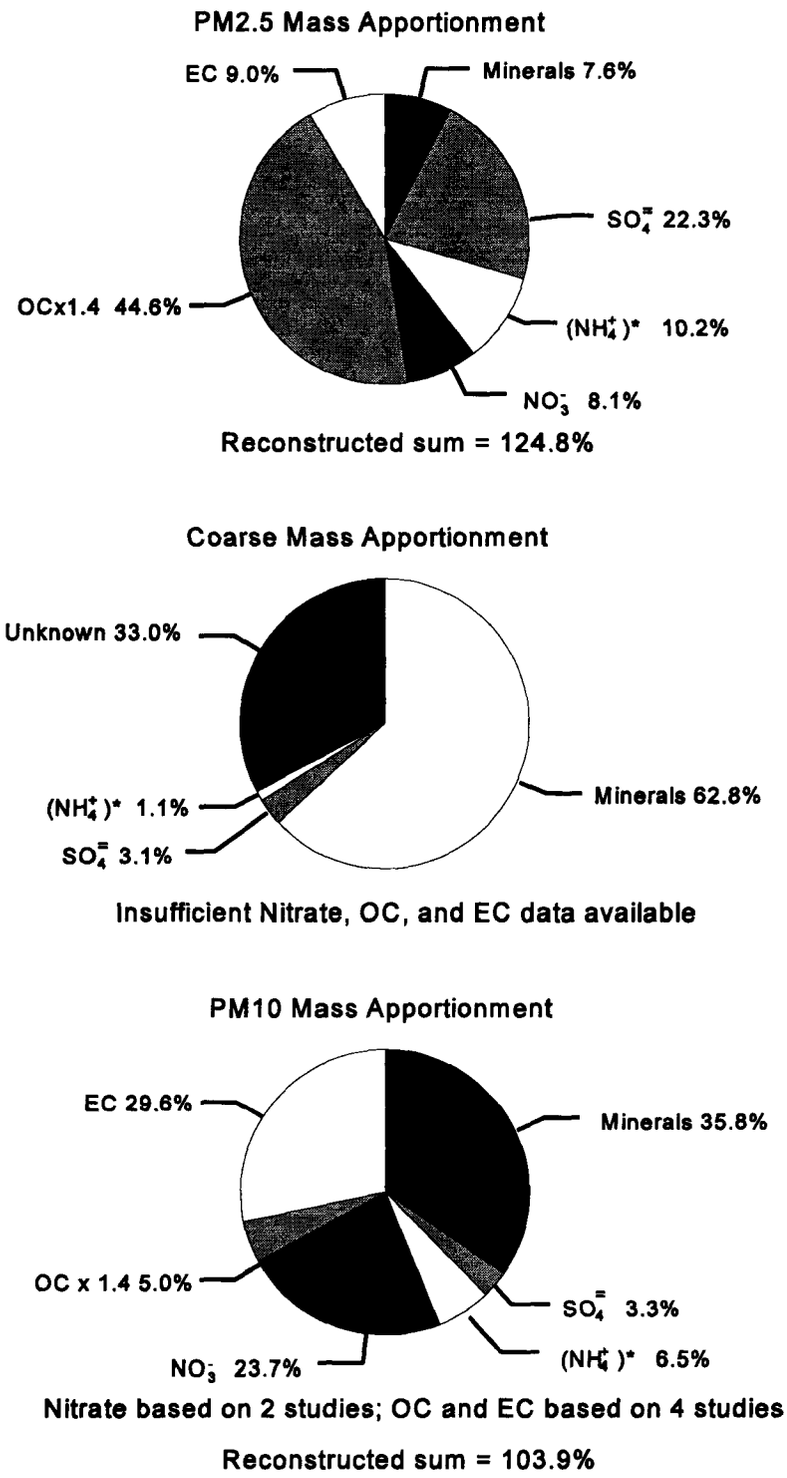

Figure 6-85b. Major constituents of particles measured at sites in the central United States, as shown in Tables 6A-2a, 6A-2b, and 6A-2c. $(NH_4^+)^*$ represents the concentration of NH_4^+ that would be required if all $SO_4^=$ were present as $(NH_4)_2SO_4$ and all NO_3^- as NH_4NO_3. Therefore, $(NH_4^+)^*$ represents an upper limit to the true concentration of NH_4^+.

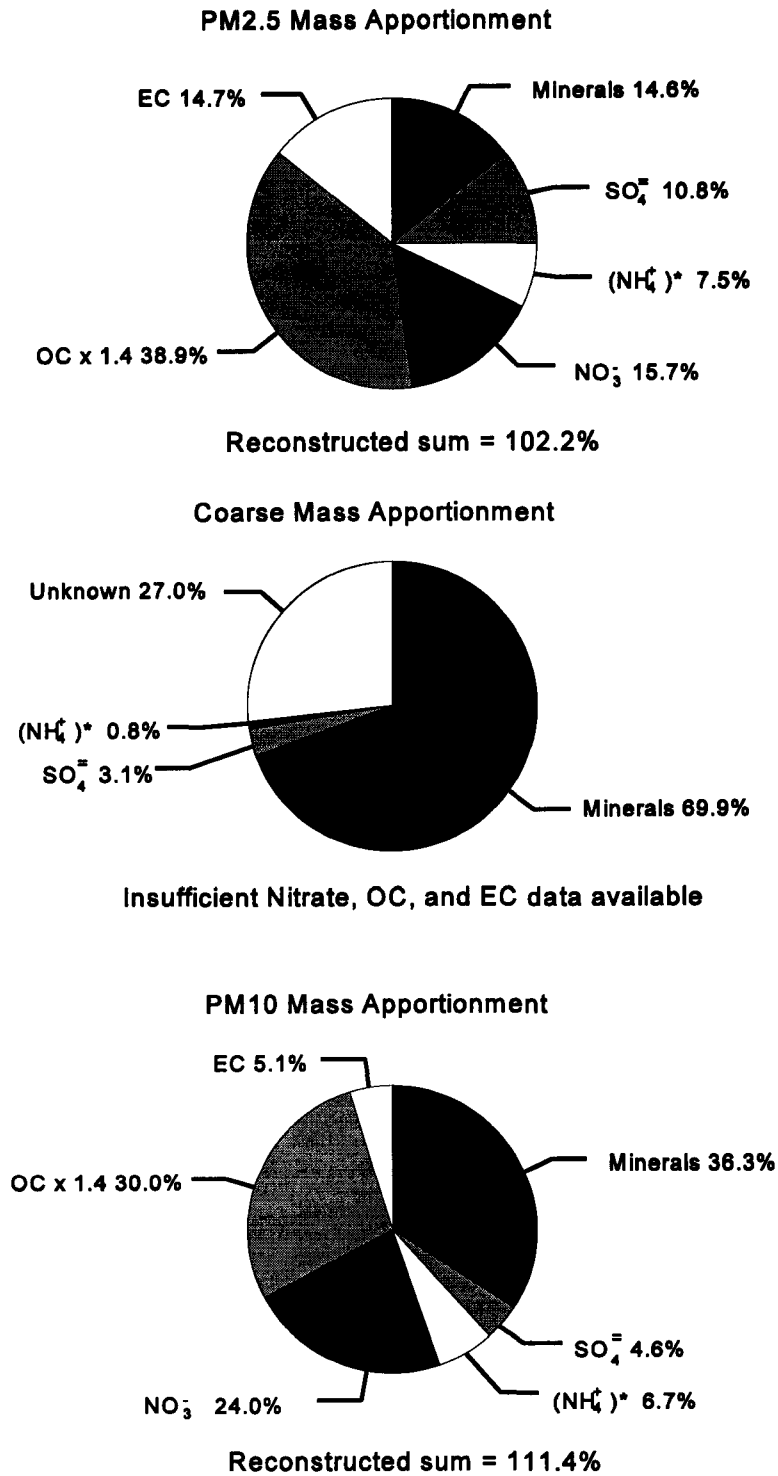

Figure 6-85c. Major constituents of particles measured at sites in the western United States, as shown in Tables 6A-2a, 6A-2b, and 6A-2c. $(NH_4^+)^*$ represents the concentration of NH_4^+ that would be required if all $SO_4^=$ were present as $(NH_4)_2SO_4$ and all NO_3^- as NH_4NO_3. Therefore, $(NH_4^+)^*$ represents an upper limit to the true concentration of NH_4^+.

(Figure 6-85c). Elemental plus organic carbon species (53.6%) are the major identified component of mass, instead of sulfate (10.8%), and minerals and nitrate account for a larger fraction of total mass. While minerals are seen to account for most of the coarse particle mass (69.9%), available data were insufficient to estimate the contributions of elemental and organic carbon species to the coarse mass. Table 6A-3 shows a comparison of selected ratios of mass components for studies conducted in each of the three broad regions of the United States.

Many of the studies listed in Table 6A-3 involved data collected at more than one site within an airshed. Information about the variability of particle mass within an airshed can yield information about the nature of sources of the particles. The variability of mean concentrations measured at multiple sites within a study area is used as a measure of the intersite variability in fine particle composition and is shown in Tables 6A-4a and 6A-4b.

6.7 ACID AEROSOLS

6.7.1 Introduction

Acid aerosols are secondary pollutants formed primarily through oxidation of sulfur dioxide (SO_2), a gas emitted by the combustion of fossil fuels. Oxidation of SO_2 forms sulfate ($SO_4^=$), the major component of acid aerosols. Sulfate is formed to a lesser extent through the oxidation of sulfur species (H_2S and CH_3SCH_3) from natural sources. The oxidation of SO_2 occurs through a series of heterogeneous (gas-particle) or homogeneous (gas or aqueous) phase oxidation reactions that convert SO_2 to sulfuric acid (H_2SO_4) particles. The sulfate species are typically expressed in terms of total $SO_4^=$, with the acidic fraction expressed in terms of titratable H^+ ($[H^+] + [HSO_4^-]$) and referred to as aerosol strong acidity. The chemical aspects of oxidation of SO_2 and formation of aerosol strong acidity are discussed in Chapter 3, Section 3.3.1. H^+ is usually found in the fine particle size fraction (aerodynamic diameter (D_p) < 1.0 μm) (Koutrakis and Kelly, 1993; Pierson et al., 1980a, 1989). However, acidity may be found in larger particles during periods of fog or very high relative humidity. Keeler et al. (1988) and Pierson et al. (1989) report finding acidity in the > 2.5 μm size range when the relative humidity was close to 100%. Although recent research has shown a high correlation between $SO_4^=$ and acidity, data

from summertime sampling have shown that $SO_4^=$ is not always a reliable predictor of H^+ for individual events at a given site (Lipfert and Wyzga, 1993).

A major determinant of the lifetime of H^+ in the atmosphere is the rate of neutralization by ammonia (NH_3). Ammonia reacts with H_2SO_4 to form ammonium sulfate [$(NH_4)_2SO_4$] and ammonium bisulfate (NH_4HSO_4). The major sources of ammonia in the environment are animals and humans (Fekete and Gyenes, 1993). The then current state-of-knowledge regarding acid aerosols was reviewed by EPA in 1989 (U.S. Environmental Protection Agency, 1989) and by Spengler et al., 1990. A more recent summary is given by Waldman et al. (1995).

6.7.2 Geographical Distribution

In North America, ambient concentrations of H^+ tend to be regional in nature with the highest concentrations found in the northeastern United States and southwestern Canada. Spengler et al. (1990) have collected information on maximum values of $SO_4^=$ and H^+ found across the U.S. and southern Canada. This information is shown in Table 6-5.

6.7.3 Spatial Variation (Regional-Scale)

Recent evidence has shown that meteorology and regional transport are extremely important to acid sulfate concentrations. Elevated levels of ambient H^+ were measured simultaneously during a regional episode at multiple sites located from Tennessee to Connecticut (Keeler et al., 1991). Lamborg et al. (1992) measured H^+ concentrations to investigate the behavior of regional and urban plumes advecting across Lake Michigan. Results suggested that aerosol acidity is maintained over long distances (up to 100 km or more) in air masses moving over large bodies of water. Lee et al. (1993) reported that H^+ and $SO_4^=$ concentrations measured in Chicago over a year were similar to levels measured in St. Louis. In an analysis of acid sulfate concentrations measured at Pittsburgh, State College, and Uniontown, PA, Liu et al. (1996) reported high correlations for H^+ between all three locations. The three locations are separated by large distances (approximately 60 to 240 km) and have vastly different population densities. It is commonly believed that the source region for most of the H^+ precursors (primary inorganic pollutant gases —SO_2 and NO_x) is the Ohio River Valley (Lioy et al., 1980). The conversion of the primary gases to secondary pollutants takes place as the prevailing winds carry the precursors

TABLE 6-5. MAXIMUM $SO_4^=$ AND H^+ CONCENTRATIONS MEASURED AT NORTH AMERICAN SITES (H^+ concentrations expressed as sulfuric acid (H_2SO_4)equivalents; "SC" indicates semi-continuous measurements.)

Location	Sample Duration (h)	Maximum Concentration	
		$SO_4^=$ ($\mu g \cdot m^{-3}$)	H_2SO_4 ($\mu g \cdot m^{-3}$)
Lennox, CA	2-8	18	0.1
Smoky Mountains	12	17	10
High Point, NJ	6	37	18
Brookhaven, NY	3	24	10
Tuxedo, NY	1-12	41	9
St. Louis, MO	SC	25	7
St. Louis, MO	SC	43	34
Los Angeles, CA	12	10	3
Harriman, TN	SC	47	18
Watertown, MA	SC	31	14
Fairview Lake, NJ	SC,4	27	12
Warren, MI	24	37	9
Whiteface Mt., NY	24	59	14
Toronto, ON, Canada	8,16	75	19
Allegheny Mt., PA	7,10	45	31
Laurel Hill, PA	7,10	56	42
Harriman, TN	24	28	14
St. Louis, MO	24	40	6
Topeka, KS	24	14	3
Watertown, MA	24	23	9
Steubenville, OH	24	56	18
Portage, WI	24	33	4
Kanawha Valley, WV	24	46	22
Dunville, ON, Canada	24	31	15
Hendersonville, TN	24	23	11
Livermore, CA	24	9	2
Morehead, KY	24	23	14
Monroeville, PA	24	42	18
Pembroke, ON, Canada	24	29	14
Springdale, AR	24	11	2
Newtown, CT	24	26	8
Allegheny Mt., PA	12	33	20
Uniontown, PA	12,24	52	39
State College, PA	12	47	25
Philadelphia, PA	24	39	9
Pittsburgh, PA	6,24	27	15

Source: Spengler et al. (1990).

from the source region, northeastward to the northeastern United States and southwestern Canada. This type of northeasterly wind flow occurs on the backside (western side) of mid-latitude anti-cyclones (high pressure systems).

Pierson et al. (1980a,b, 1989) conducted studies of atmospheric acidity on Allegheny Mountain and Laurel Hill in southwest Pennsylvania, 80 and 100 km southeast of Pittsburgh, in the summers of 1977 and 1983. The aerosol H^+ appeared to represent the net after H_2SO_4 reaction with NH_3(g). The resulting $H^+/SO_4^=$ ratio depended on $SO_4^=$ concentration, approaching that of H_2SO_4 at the highest $SO_4^=$ concentrations. The atmospheric was acidic; the average concentrations of HNO_3 (78 nmole/m_3) and aerosol H^+ (205 nmole/m_3), NH_4^+ (172 nmole/m_3), and $SO_4^=$ (201 nmole/m_3), and the dearth of NH_3 (<15 nmole/m_3), show that the proton acidity of the air exceeded the acid-neutralizing capacity of air by a factor of >2, with one 10-hour period averaging 263 nmole/m_3 for HNO_3 and 844 nmole/m_3 for H^+. SO_2 added another 900 nmole/m_3 (average) of potential H^+ acidity. HNO_3 and aerosol H^+ episodes were concurrent, on 7-8 day cycles, unrelated to SO_2 which existed more in short-lived bursts of apparently more local origin. NO_x was sporadic like SO_2. Laurel and Allegheny, separated by 35.5 km, were essentially identical in aerosol $SO_4^=$, and in aerosol H^+, less so in HNO_3; apparently, chemistry involving HNO_3 and aerosol H^+ or $SO_4^=$ was slow compared to inter-site transport times (1-2 hours). From growth of b_{scat} and decline of SO_2, daytime rate coefficients for SO_2 oxidation and SO_2 dry deposition were inferred to have been, respectively, ~0.05 and ≤0.1 hr^{-1}.

HNO_3 declined at night. Aerosol H^+ and $SO_4^=$ showed no significant diurnal variation, and O_3 showed very little; these observations, together with high PAN/NO_x ratios, indicate that regional transport rather than local chemistry is governing. The O_3 concentration (average 56 ppb or 2178 nmole/m_3) connotes an oxidizing atmosphere conducive to acid formation.

Highest atmospheric acidity was associated with (1) slow westerly winds traversing westward SO_2 source areas, (2) local stagnation, or (3) regional transport around to the back side of a high pressure system. Low acidity was associated with fast-moving air masses and with winds from the northerly directions; upwind precipitation also played a moderating role in air parcel acidity. Much of the SO_2 and NO_x, and ultimately of the HNO_3 and aerosol H^+, appeared to originate from coal-fired power plants. An automotive contribution to the NO_x and HNO_3 could not be discerned.

Size distributions of aerosol H^+ and $SO_4^=$ were alike, with MMED ~0.7 μm, in the optimum range for efficient light scattering and inefficient wet/dry removal. Thus, light scattering and visual range degradation were attributable to the acidic $SO_4^=$ aerosol. With inefficient removal of aerosol H^+, and inefficient nighttime removal of HNO_3, strong acids may be capable of long-distance transport in the lower troposphere. Water associated with the acidic aerosol was shown to account for much of the light scattering.

6.7.4 Spatial Variation (City-Scale)

A study of acid aerosols and ammonia (Suh et al., 1992) found no significant spatial variation of H^+ at Uniontown, Pennsylvania, a suburb of Pittsburgh. Measurements at the central monitoring site accounted for 92% of the variability in outdoor concentrations measured at various homes throughout the town. There was no statistical difference ($p > 0.01$) between concentrations of outdoor H^+ among five sites (a central site and four satellite sites) in Newtown, Connecticut (Thompson et al., 1991). However, there were differences in peak values which were probably related to the proximity of the sampling sites to ammonia sources. These studies suggest that long-term averages should not substantially differ across a suburban community, although peak values may differ significantly.

In small suburban communities outdoor concentrations of H^+ are fairly uniform, suggesting that minor differences in population density do not significantly affect outdoor H^+ or NH_3 concentrations (Suh et al., 1992). In urban areas, however both H^+ and NH_3 exhibit significant spatial variation. Waldman et al. (1990) measured ambient concentrations of H^+, NH_3, and $SO_4^=$ at three locations in metropolitan Toronto. The sites, located up to 33 km apart, had significant differences in outdoor concentrations of H^+. Waldman and co-workers reported that the sites with high NH_3 measured low H^+ concentrations. However, the limited number of sampling sites did not allow for a conclusive determination of the relationship between population density, ammonia concentrations, and concentrations of acid aerosols.

An intensive monitoring study has been conducted during the summers of 1992 and 1993 in Philadelphia (Suh et al., 1995). Twenty-four hour measurements of aerosol acidity (H^+) sulfate and NH_3 were collected simultaneously at 7 sites in metropolitan Philadelphia and at Valley Forge, 30 km northeast of the city center. The researchers reported that $SO_4^=$ was evenly

distributed throughout the measurement area but H^+ concentrations varied spatially within metropolitan Philadelphia. This variation was related to local NH_3 concentrations and the local population density (Figure 6-86). The amount of NH_3 available to neutralize H^+ increased with population density, resulting in lower H^+ concentrations in more densely populated areas. The extent of the spatial variation in H^+ concentrations did not appear to depend on the overall H^+ concentration. It did, however, show a strong inverse association with local NH_3 concentrations.

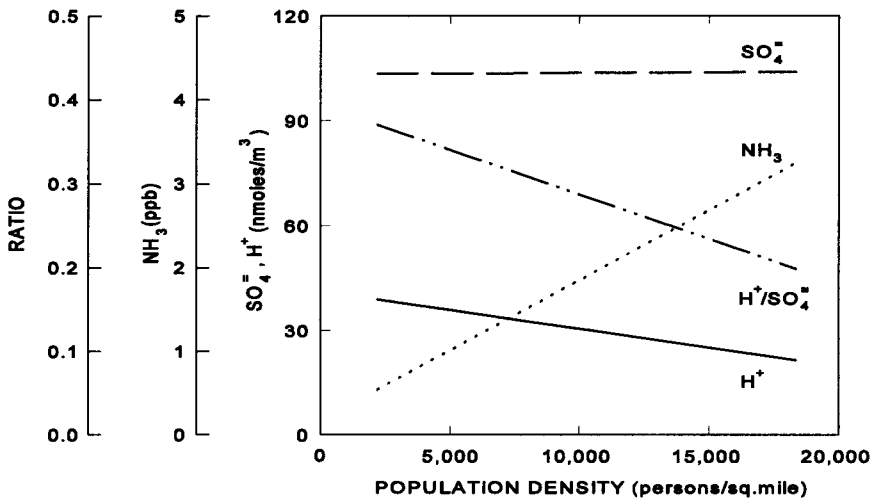

Figure 6-86. Mean air pollutant concentrations for days when winds were from the southerly direction, plotted versus population density. The solid line represents H^+ concentrations; the long dashed line represents SO_4^{2-} concentrations; the dashed and dotted line represents the ratio of H^+ to SO_4^{2-} levels; and the dotted line represents NH_3 concentrations. All data collected in Philadelphia, PA, during the summers of 1992 and 1993.

Source: Adapted from Suh et al. (1995).

6.7.5 Seasonal Variation

An analysis of results from Harvard's 24-City Study (Thompson et al., 1991), which measured acid aerosols concentrations at 8 different small cities across North America each year during a three year period, revealed that the summer H^+ mean concentrations were significantly higher than the annual means at all sites. The results showed that at the sites with high H^+ concentrations, approximately two-thirds of the aerosol acidity occurred from May through

September (Figure 6-87). Little or no seasonal variation was observed at sites with low acidity. These findings were supported by those of Thurston et al. (1992) in which H^+ concentrations measured at Buffalo, Albany, and White Plains, NY, were found to be highest during the summertime. Thurston and co-workers also reported that moderate concentrations of H^+ could occur during non-summer months

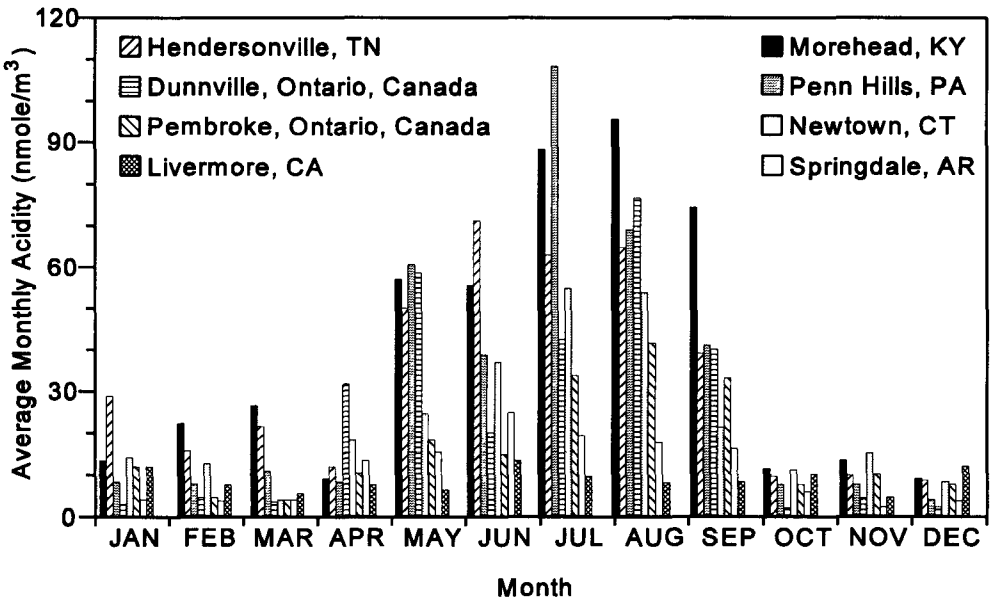

Figure 6-87. Average monthly aerosol strong acidity for Year 1 sites of the Harvard 24-City Study.

Source: Thompson et al. (1991).

6.7.6 Diurnal Variation

Evidence exists of a distinct diurnal pattern in outdoor H^+ concentrations. Wilson et al. (1991) examined concentration data for H^+, NH_3, and $SO_4^=$ from the Harvard 24-City Study for evidence of diurnal variability (Figure 6-88). This investigation found a distinct diurnal pattern for H^+ concentrations and the $H^+/SO_4^=$ ratio, with daytime concentrations being substantially

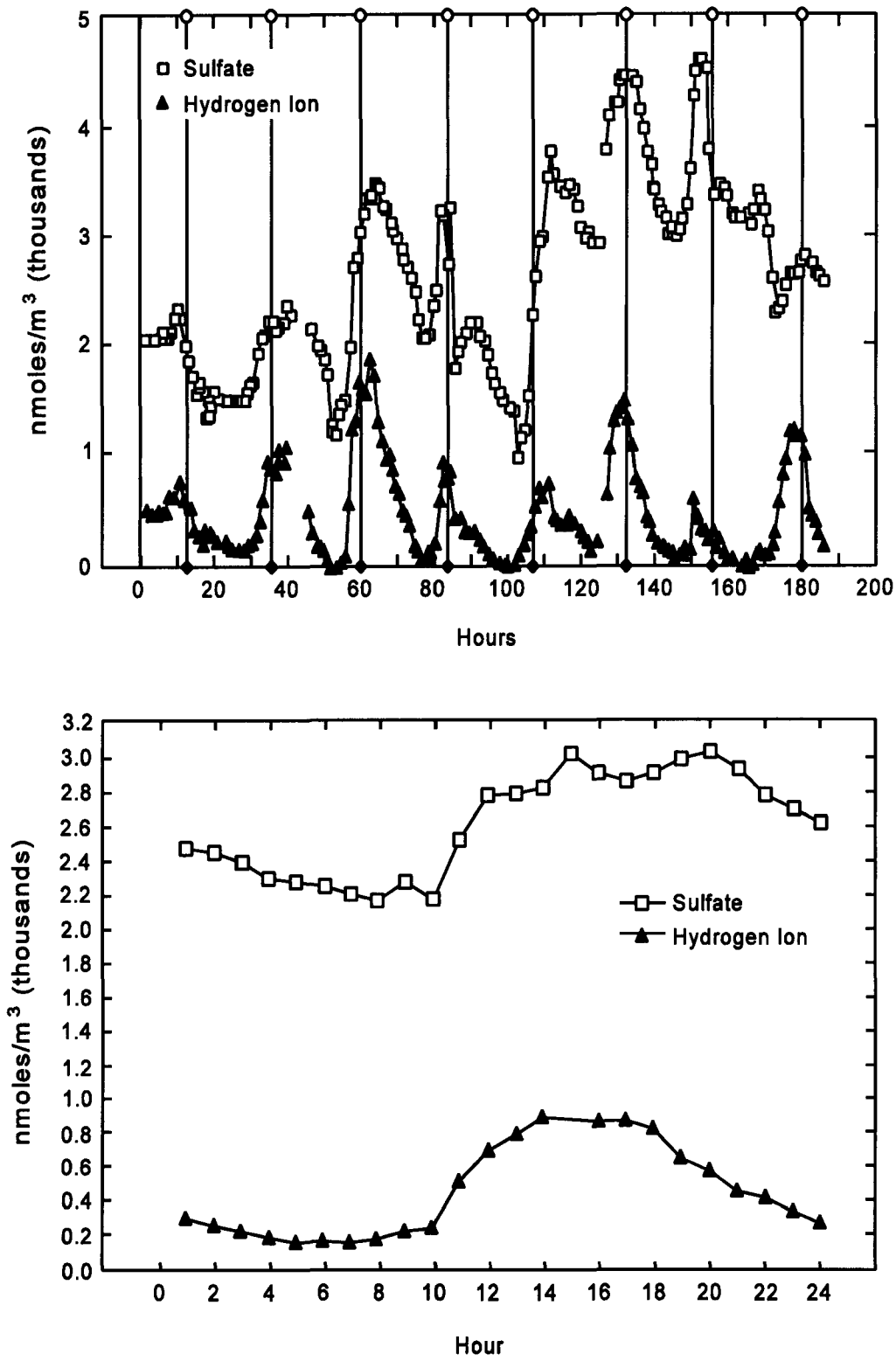

Figure 6-88. Diurnal pattern of sulfate and hydrogen ion at Harriman, TN, weekly pattern and daily average.

Source: Wilson et al. (1991).

higher than nighttime levels. Both H^+ and $SO_4^=$ concentrations peaked between noon and 6:00 pm. No such diurnal variation was found for NH_3. Wilson and co-workers concluded that the diurnal variation in H^+ and $SO_4^=$ was probably due to atmospheric mixing. Air containing high concentrations of H^+ and $SO_4^=$ mixes downward during daylight hours when the atmosphere is unstable and well-mixed. During the night, ammonia emitted from ground-based sources neutralizes the acid in nocturnal boundary layer, the very stable lower part of the atmosphere, but a nocturnal inversion prevents the ammonia from reacting with the acid aerosols aloft. Then in the morning as the nocturnal inversion dissipates, the acid aerosols mix downward again as the process begins anew. Spengler et al. (1986a) also noted diurnal variations in sulfate and sulfuric acid concentrations and suggested atmospheric dynamics as the cause. The diurnal variation in $SO_4^=$ has been observed by other workers and discussed in terms of atmospheric dynamics by Wolff et al. (1979) and Wilson and Stockberger (1990).

This diurnal variation in mixing heights and concentrations does not seem to hold at elevated sites. For example, Pierson et al. (1980a,b, 1989) found no appreciable night/day difference in aerosol H^+ (or NH_4^+ or $SO_4^=$), and almost no diurnal variation in O_3, at two elevated sites (Allegheny Mountain and Laurel Hill, elevations 838 and 850 m) in southwest Pennsylvania. They contrasted this behavior with that at lower sites, and particularly with the concurrent measurements at Deep Creek Lake (Vossler et al., 1989). The differences were attributed to isolation from ground-based processes at the elevated sites at night.

6.7.7 Indoor and Personal Concentrations

Several studies have examined indoor concentrations of acid aerosols and personal monitoring. Brauer et al. (1989) monitored personal exposures to particles (including acidic sulfates) and gases in metropolitan Boston in the summer of 1988, and compared these to measurements collected at a centrally located ambient monitor. They found that personal concentrations of acidic aerosols and gases differed significantly from those measured at the centrally located site. Summer and winter concentrations of acid aerosols and gaseous pollutants also collected in Boston (Brauer et al., 1991) showed indoor/outdoor ratios of H^+ to be 40-50% of the indoor/outdoor $SO_4^=$ ratio indicating neutralization of the acid by the higher indoor NH_3 levels, which were reported.

Indoor, outdoor, and personal acid aerosol monitoring was performed for children living in Uniontown, Pennsylvania, during the summer of 1990 (Suh et al., 1992). The indoor, outdoor, and personal measurements were compared to outdoor measurements collected from a centrally located ambient monitor. Personal concentrations were lower than corresponding outdoor levels but higher than indoor levels. Air conditioning was found to be an important predictor of indoor H^+, while NH_3 was found to influence indoor and personal H^+ concentrations. Similar results were obtained in a study of the relationships between indoor/outdoor concentrations of H^+ and NH_3 conducted in State College, PA, in 1991 (Suh et al., 1994).

In a study characterizing H^+ concentrations at child and elderly care facilities, Liang and Waldman (1992) measured indoor and outdoor acid aerosol concentrations. Results from this study showed that indoor/outdoor H^+ and $SO_4^=$ ratios were comparable to those measured inside residential buildings. Air conditioner use and indoor NH_3 concentrations were again identified as important determinants of indoor H^+ concentrations.

6.8 NUMBER CONCENTRATION OF ULTRAFINE PARTICLES

6.8.1 Introduction

Recent work has suggested that ultrafine particles may be responsible for some of the health effects associated with exposure to particulate matter (Chapter 11, Section 11.4). The hypothesis for explaining a biological effect of ultrafine particles is based on the number, composition and size of particles rather than their mass (Seaton et al., 1995). This has led to an interest in the number concentration of ambient particles. This section examines data on particle number concentration and the relationship between particle number and particle mass or volume.

6.8.2 Ultrafine Particle Number-Size Distribution

In the context of ambient particles, the term ultrafine particles refers to those particles with diameters below 0.1 μm. Ultrafine aerosol size distributions from an urban site at Long Beach, California (Karch et al., 1987), and from a background site in the Rocky Mountains, Colorado (Kreidenwies and Brechtel, 1995) are shown in Figures 6-89 and 6-90. Both of these sets of data were obtained by electrical mobility measurements. For the urban aerosols of Long Beach, the

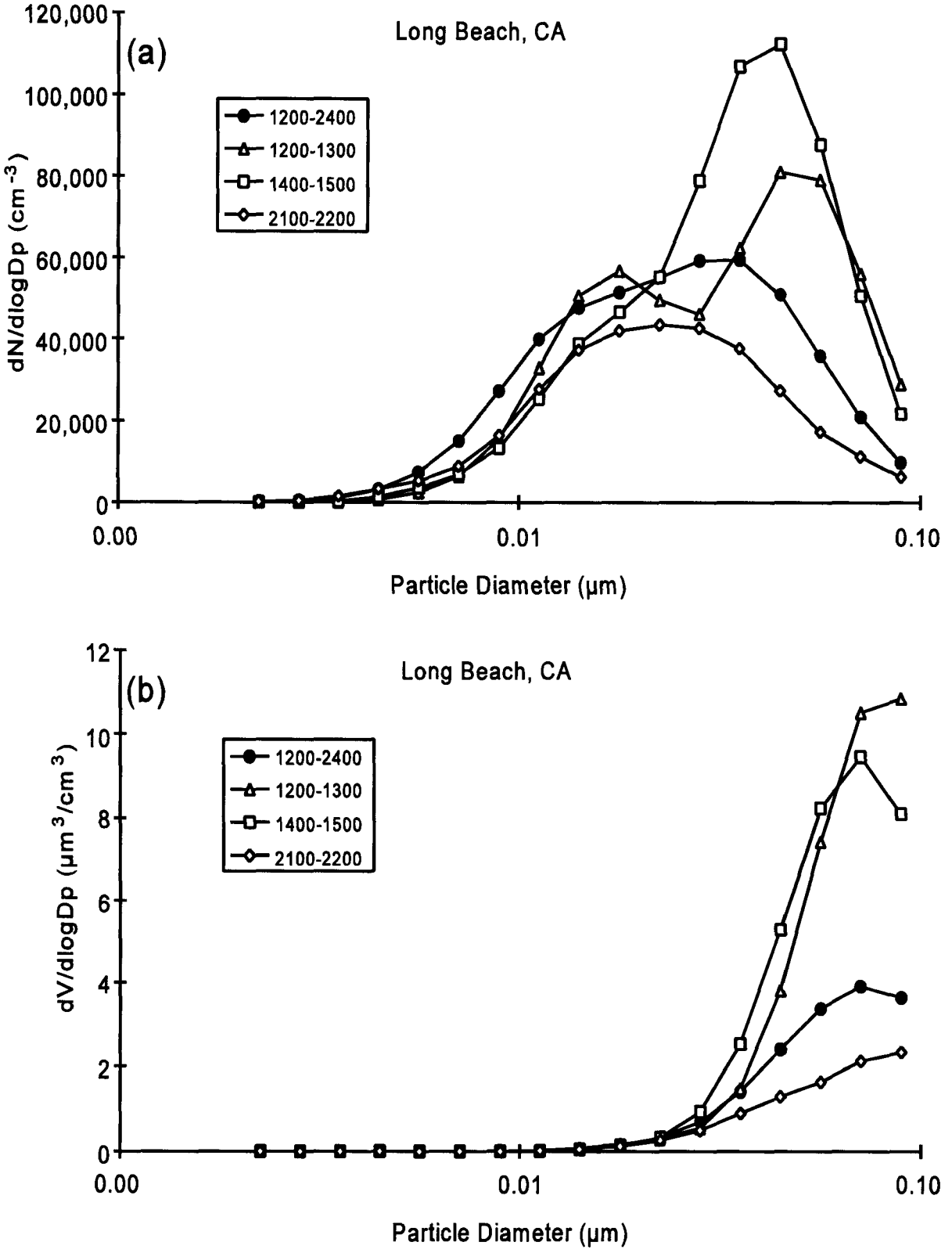

Figure 6-89. Aerosol number (a) and volume (b) size distributions from an urban site at Long Beach, CA.

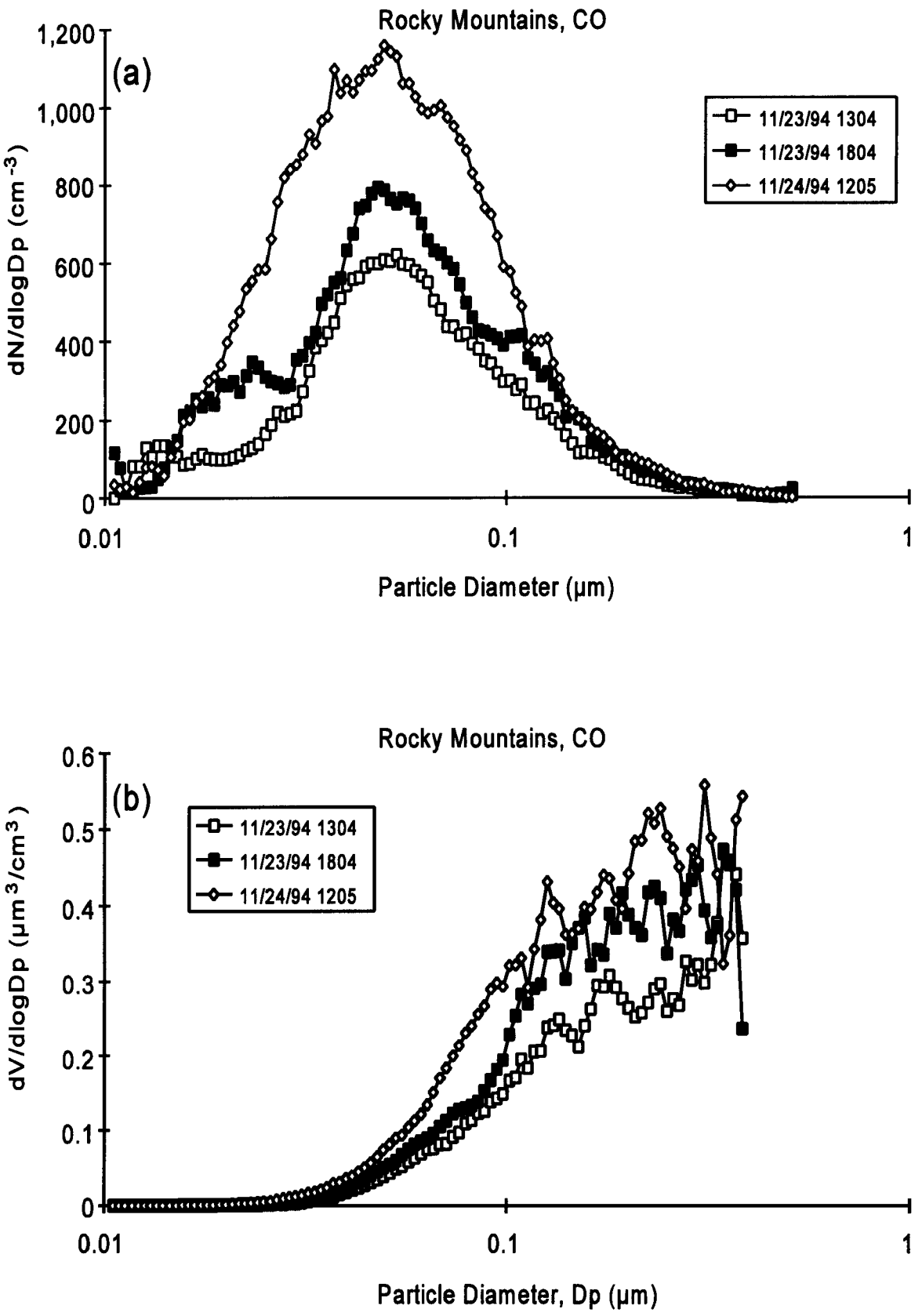

Figure 6-90. Aerosol number (a) and volume (b) size distributions from a background site in the Rocky Mountains, CO.

number geometric mean diameter can vary from 0.012 μm to 0.043 μm. Some of the ultrafine distributions, such as that shown for the 1,200 to 1,300 PST time period, are bimodal. The number concentrations were higher in the early afternoon, 1400-1500 PST, as shown in Figure 6-91. For the background aerosols from Rocky Mountains the number geometric mean diameter of the ultrafine aerosols was somewhat larger than for Long Beach, with geometric mean diameters ranging from 0.047 to 0.075 μm for periods without urban influence. A bimodal character for the ultrafine distribution was also observed for some measurements, as seen in Figure 6-90.

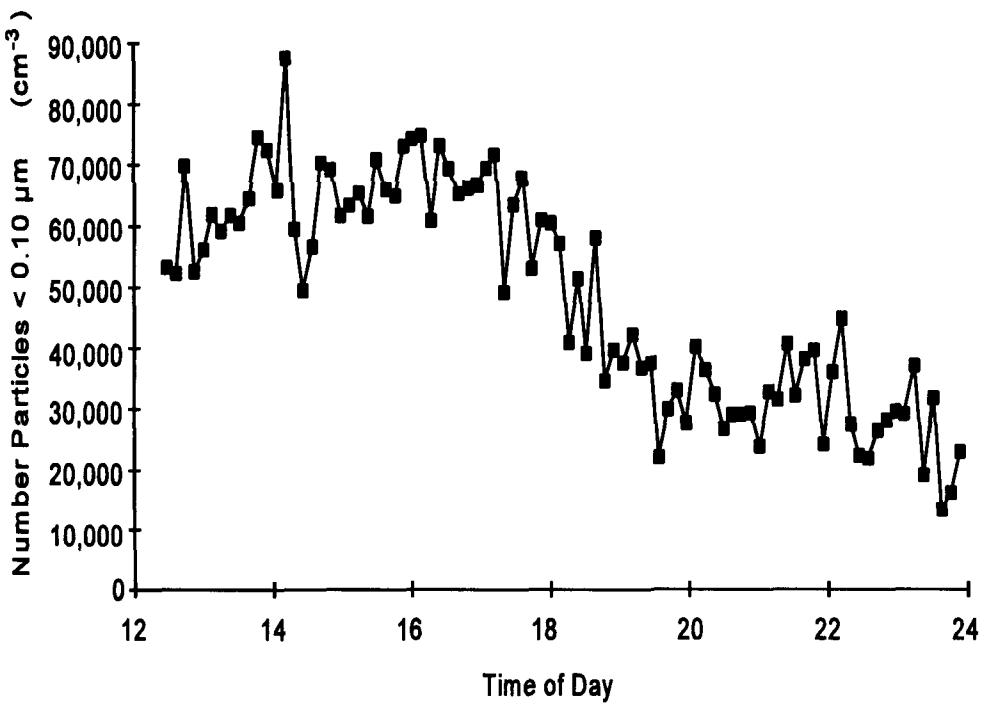

Figure 6-91. Number concentrations as a function of time of day at Long Beach, CA.

The contrast between urban and background ultrafine aerosol size distribtution is demonstrated in Figure 6-92, where a change in the wind direction brought transport from an urban area to the background site at Rocky Mountains. Within a 2-h period, the number

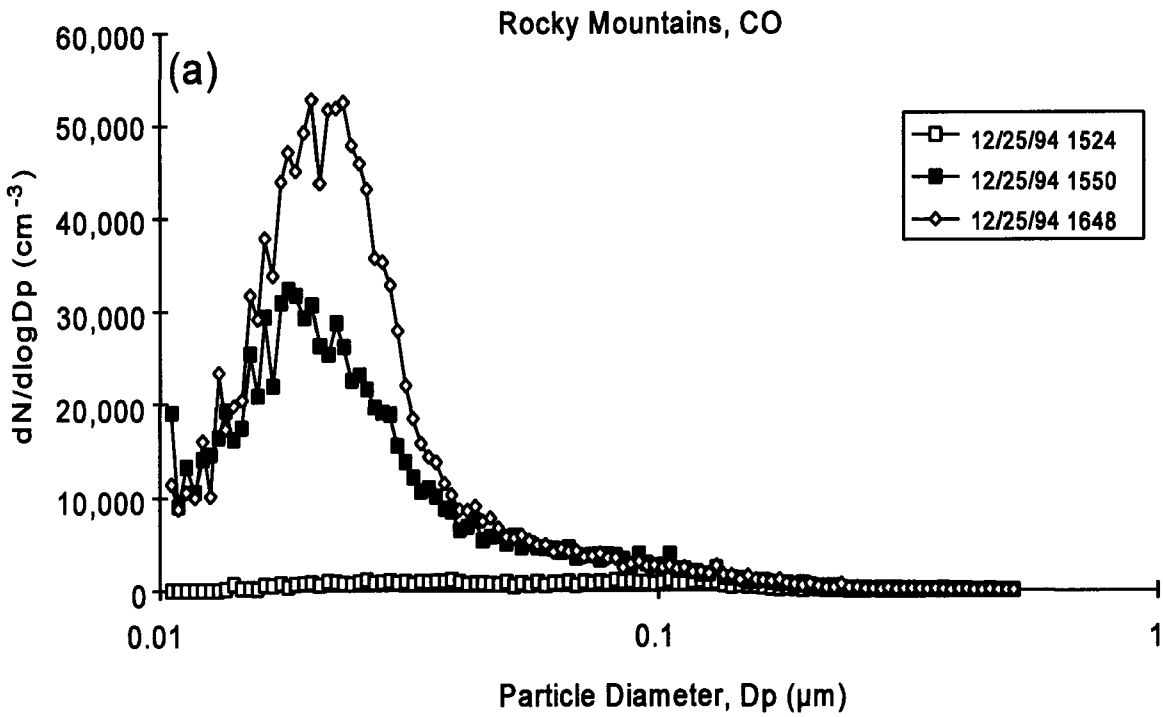

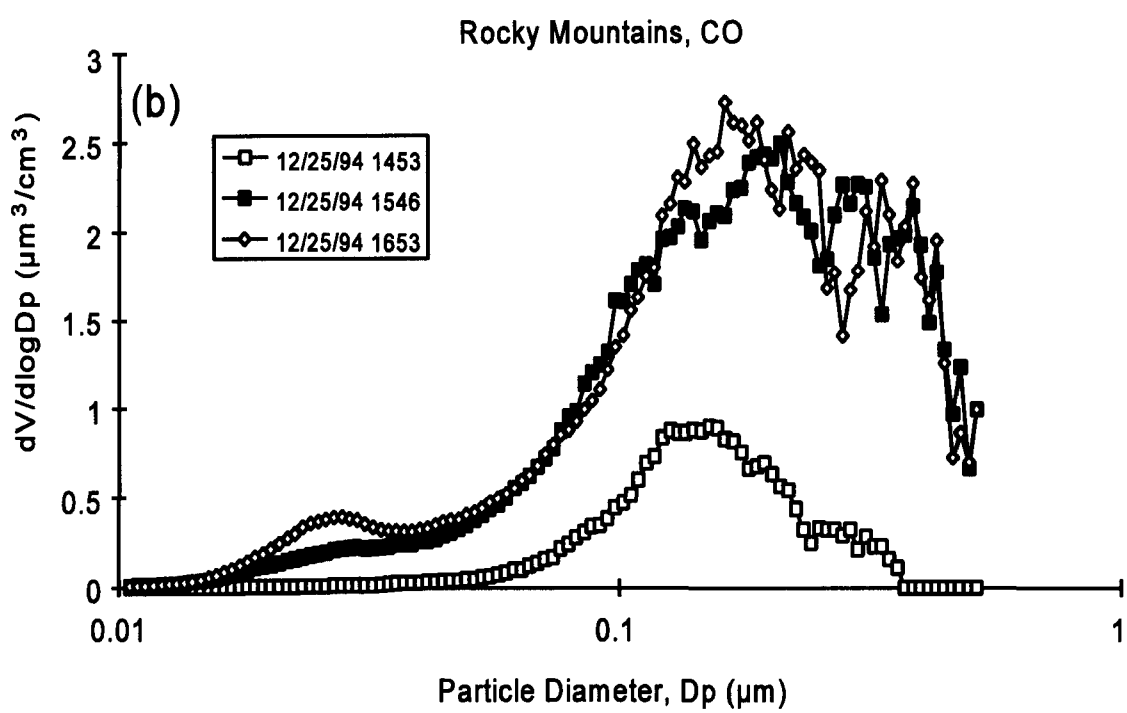

Figure 6-92. Number (a) and volume (b) size distributions at the Rocky Mountain site showing an intrusion of urban air.

concentration increased from 850 cm^{-3} to 19,000 cm^{-3}, an increase of more than a factor of 20. In contrast, the volume distribution increased by less than a factor of 5. The number geometric mean diameter decreased from 0.052 μm for the background aerosol to 0.024 μm for the urban influenced aerosol. For the urban influenced size distributions, over 96% of the particle number was measured in particles below 0.1 μm, while 80% of the particle volume was associated with particles above that size.

6.8.3 Relation of Particle Number to Particle Mass

In general, the majority of airborne particle volume and mass is associated with particles above 0.1 μm, while the highest number concentration of particles is found in particles below 0.1 μm. This was shown for volume in Figures 6-89 to 6-92 and can be seen for mass in the recent data collected in the Los Angeles, CA shown in Figure 6-93. As with the data of Whitby and Sverdrup (1980), the size distributions of Figure 6-93 show data collected by several instruments. Physical size distributions were measured with an electrical aerosol analyzer for particles between 0.01 and 0.4 μm, and with a laser optical particle counter for particles between 0.14 and 3 μm. Additionally, Berner (John et al., 1989, 1990) and MOUDI (Marple et al., 1991) impactors were used to measure the mass size distribution of inorganic ion species and carbonacous species. These data have been combined (Hering et al., 1996) to give a total mass distribution from which the number distribution has been calculated assuming an effective aerosol density of 1.6 g/cm^3 and assuming that the water associated with the aerosol is 15% of the measured dry particle mass (see McMurry and Stolzenburg, 1989). The optical particle counter was calibrated with ambient particles, size classified by a differential mobility analyzer. The ambient aerosol has a lower effective refractive index than the polystyrene latex usually used for calibration (Hering and McMurry, 1991). No fitting was applied to match the different size distributions in the region of overlap.

Figure 6-93 shows the average of distributions collected over six different days in the fall of 1987 in downtown Los Angeles, as part of the Southern California Air Quality Study. Particle number distributions emphasize the ultrafine particles, or "nuclei" mode. Volume distributions place importance on 0.1 to 1 μm particles which are associated with the "accumulation" mode. For this average distribution 88% of the particle number is associated with particles below 0.1

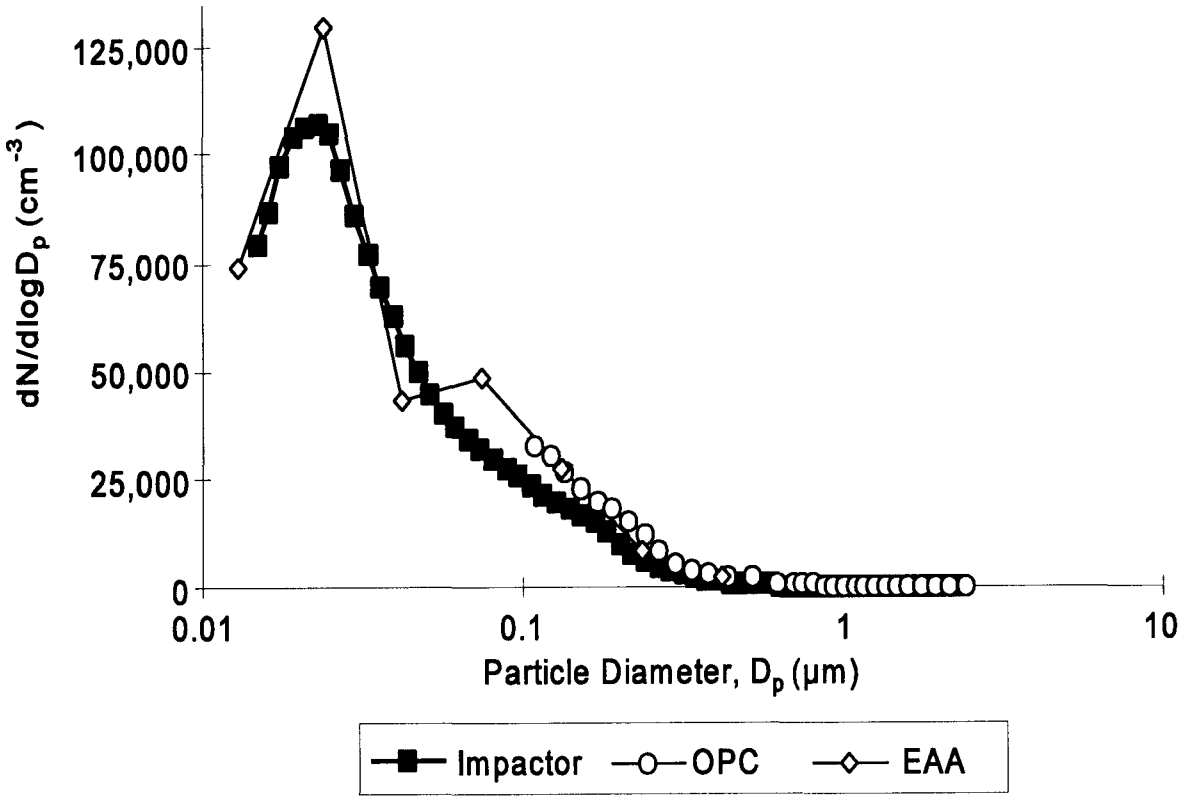

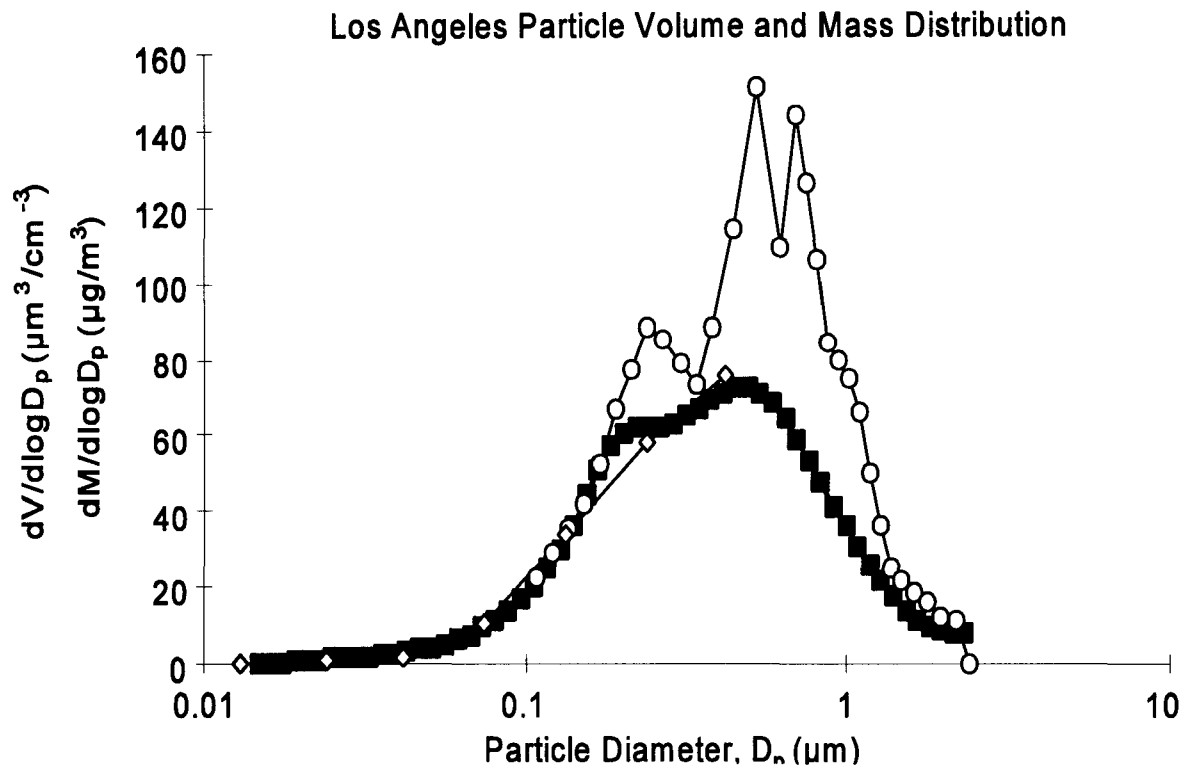

Figure 6-93. Number (a), and volume and mass (b) size distributions from Los Angeles, CA, showing comparison of three measurement techniques.

μm, but 99% of the particle volume is from particles above that size. Both the impactor and optical counter data indicate a weakly bimodal character for the accumulation mode aerosol.

For unimodal, log normal size distributions, the particle volume V is simply related to the particle number N by the relation:

$$V = \frac{\pi}{6} D_{gn}^{3} \exp\left(\frac{9}{2}\ln^2\sigma_g\right) N$$

where D_{gn} is the number geometric mean diameter, and σ_g is the geometric standard deviation. However, because of the multimodal character of ambient aerosol size distributions, one does not expect this simple relationship to hold in the atmosphere. The relationship between particle number and particle volume was examined for data from the Southern California Air Quality Study collected at Riverside, CA over 11 days in the summer of 1987, and at downtown Los Angeles in the fall of 1987 using the methods described above. As shown in Figure 6-94, particle number concentrations are correlated with the volume associated with particles below 0.1 μm, but are not correlated with the total fine particle volume. Similar results are found for the data reported from Rocky Mountains, CO and for the data reported by Whitby and Sverdrup (1980).

6.8.4 Conclusion

The size distribution measurements of aerosols in urban and continental background regions indicate number geometric mean diameters which vary from 0.01 to 0.08, with the larger values found in background regions. Particle number concentrations may vary from less than 1,000/cm^3 at clean, background sites to over 100,000/cm^3 in polluted urban areas. Particle number concentrations are dominated by the ultrafine or nuclei mode aerosols. In contrast, the volume (or mass) of fine particles is associated with particles above 0.1 μm, which are associated with the accumulation mode identified by Whitby and coworkers (Willeke and Whitby, 1975; Whitby and Sverdrup, 1980). Particle number concentrations are correlated with the volume of particles below 0.1 μm. The number concentration of ultrafine particles results from a balance between formation and removal. The rate of removal by coagulation with accumulation mode

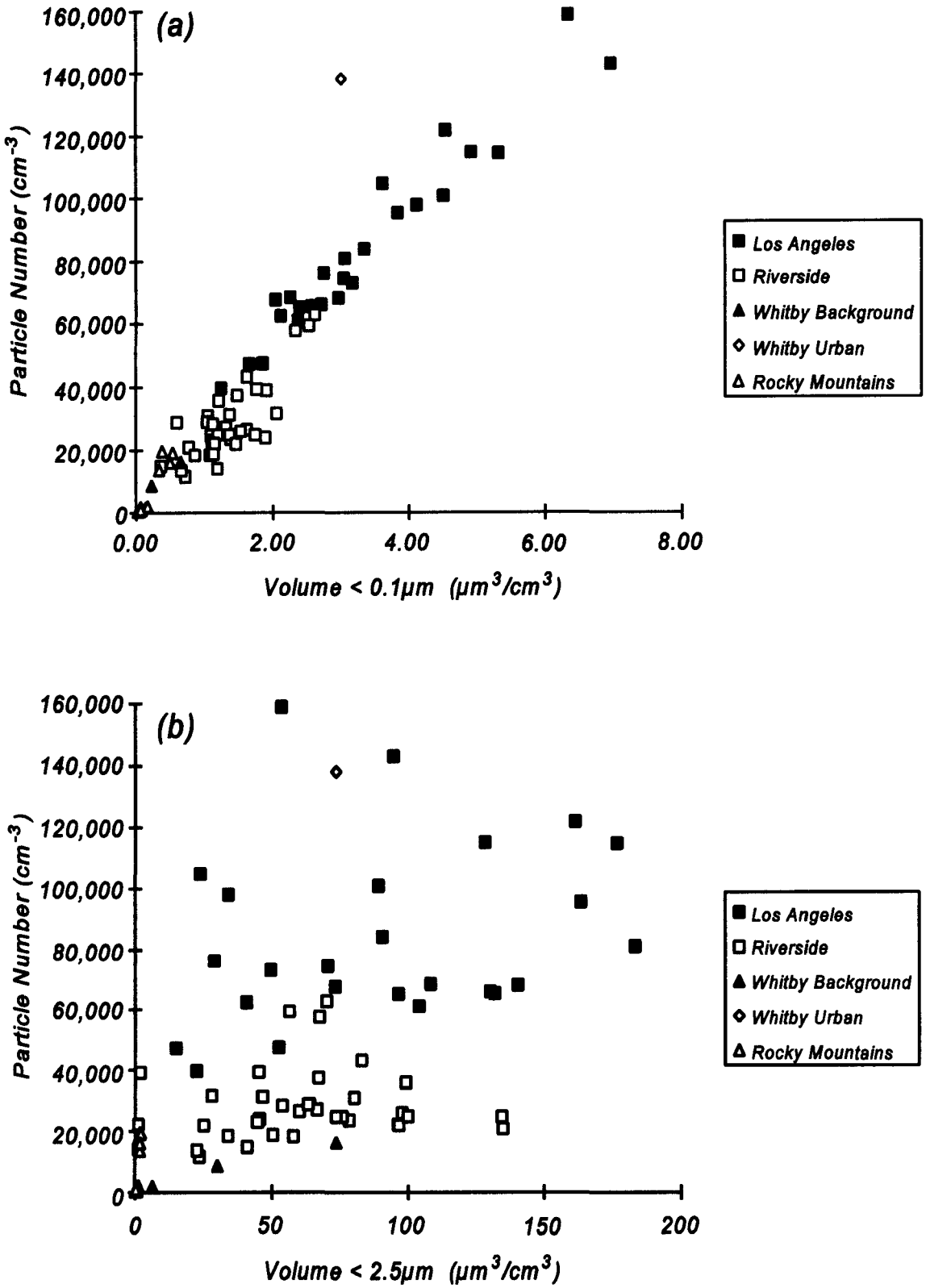

Figure 6-94. Relationship between particle number and particle volume ([a] volume <0.1 and [b] <2.5 μm).

particles will increase as the number (and mass and volume) of accumulation mode particles increases. Therefore, a correlation between number and accumulation mode volume or mass on a short term (e.g., hourly basis), would not be anticipated. However, as suggested by the differences in particle number concentrations from 850 cm^{-3} at a remote site in the Rocky Mountains, to 19,000 cm^{-3} in air transported from an urban area, to in excess of 10^5 cm^{-3} in polluted urban areas, a correlation, between the total number concentration and the total fine article mass or volume, might be expected if comparisons were made over longer periods, e.g. days. However, no such studies have been done.

6.9 AMBIENT CONCENTRATIONS OF ULTRAFINE METALS

6.9.1 Introduction

Nucleation theory (Seinfeld, 1986) indicates that ultrafine particles will consist of materials that have very low vapor pressure but which will, at some time, exist in significant vapor concentrations. This could be the result of rapid formation of a condensible vapor from chemical conversion of a gas or the formation of a vapor at relatively high concentrations during combustion. Very small particles, because of their high curvature, have a higher vapor pressure than larger particles. This is known as the Kelvin effect and becomes increasingly important as the particle size decreases below 0.1 μm in diameter. The critical size, at which a particle will grow instead of evaporating, depends on the saturation ratio, the ratio of the vapor pressure of the particle, p_A, to the vapor pressure over a flat surface, p_A°) ($S = p_A \backslash p_A^\circ$); the surface tension; and the molar volume of the condensed phase. Thus, materials such a elemental carbon, formed in flames, or metal (or metal compound) vapor, formed during combustion, are likely candidates for ultrafine particles. Sulfuric acid can also form ultrafine particles (Weber et al., 1995) but whether it nucleates into ultrafine particles or condenses on existing particles depends on the balance between the formation rate of sulfuric acid and the surface area of preexisting particles (Seinfeld, 1986).

Thus, ultrafine aerosols may be primary, formed from vapor generated during combustion, or secondary, formed from vapor generated by chemical reactions in the atmosphere. Because of their small size, ultrafine particles diffuse rapidly and are lost by deposition to surfaces or by

growth into larger particles by coagulation. Ultrafine particles also serve as nuclei for condensation of vapors. Thus, ultrafine particles grow rapidly by coagulation and condensation, into the accumulation mode. For these reasons, the mass of ultrafine particles in the ambient atmosphere is generally much smaller than that of the accumulation mode, where removal rates of particles reach a minimum in non-cloud conditions. The result is that in ambient conditions, the ultrafine mode is generally indistinct or absent from mass or volume profiles of aerosol particles versus size. However, a distinct ultrafine mode below 0.1 μm diameter has been observed in quasi-ambient samples taken close to combustion sources. In these cases, the distinct ultrafine particle mode is referred to as the nuclei mode (Whitby, 1978).

While there is consensus that ultrafine metal particles are produced and emitted into the atmosphere, there is little information on ambient concentrations of ultrafine metals. The few direct measurements available can be extended with some confidence using indirect methods; i.e., from particle counting techniques that have size information but no chemical information, or from filter collection methods that have limited size information but detailed compositional information. Nevertheless, it is clear that more data on ultrafine metals are urgently needed to gain confidence in the spatial and temporal concentration profiles of this key atmospheric component.

6.9.2 Formation of Ultrafine Particles

Nucleation theory establishes that high temperature processes are generally required to form ultrafine metallic aerosols. Such processes are usually anthropogenic, although natural fires, volcanic eruptions, and other such events can contribute to ultrafine transition and heavy metals in some circumstances. Table 6-6, taken from Seeker (1990), gives the vaporization temperature of EPA-regulated metals (Federal Register, 1986) as a function of temperature, with and without chlorine available in the combustion process.

Note the dramatic shift in temperature for several elements, including lead, for the chlorine-rich combustion scenario. A similar process has been used to prevent lead from coating surfaces in internal combustion engines using leaded gasoline. The process used

TABLE 6-6. REGULATED METALS AND THE VOLATILITY TEMPERATURE

	With No Chlorine		With 10% Chlorine in Waste	
Metal	Volatility Temp. (°F)	Principal Species	Volatility Temp. (°F)	Principal Species
Chromium	2935	CrO_2/CrO_3	2930	CrO_2/CrO_3
Nickel	2210	$Ni(OH)_2$	1280	$NiCl_2$
Beryllium	1930	$Be(OH)_2$	1930	$Be(OH)_2$
Silver	1660	Ag	1160	AgCl
Barium	1560	$Ba(OH)_2$	1660	$BaCl_2$
Thallium	1330	Tl_2O_3	280	TlOH
Antimony	1220	Sb_2O_3	1220	Sb_2O_3
Lead	1160	Pb	5	$PbCl_4$
Selenium	605	SeO_2	605	SeO_2
Cadmium	417	Cd	417	Cd
Osmium	105	OsO_4	105	OsO_4
Arsenic	90	As_2O_3	90	As_2O_3
Mercury	57	Hg	57	Hg

Source: Seeker (1990).

chlorine and bromine-containing additives to form compounds such as PbBrCl which are gaseous at combustion temperatures but form ultrafine particles after leaving the vehicle.

Numerous theoretical and laboratory studies have shown that the typical size of metals derived from combustion is ultrafine (Friedlander, 1977; Senior and Flagan, 1982; Seeker, 1990). Analysis of particles from coal combustion by Natusch and Wallace, 1974 and Natusch et al., 1974 showed an additional aspect. There is a tendency for the condensing metal vapors to form relatively uniform thickness surface coatings on more refractory particles present in the combustion effluent stream. If the particles upon which the metals coat themselves are crustal, as in coal fly ash, this results in a final particle whose enrichment factor compared to crustal averages depends upon the initial size of the refractory particle—minor for large particles, extreme for ultrafine particles (Davison et al., 1974). This result also places the (potentially) toxic metals on the biologically-accessible surface.

Thus, the presence of metals in a combustion process such as incineration of biological and chemical wastes or treatment of contaminated soils poses a problem. Raising the temperature of combustion high enough to completely (> 99.99%) destroy the biological and chemical species will also enhance the volatilization of metallic components in the feed stock, requiring more efficient removal methods for ultrafine and accumulation mode metals. Figure 6-95 shows the enhanced volatilization of metals as the combustion temperature is raised from 1000 °F (540 °C) to 1800 °F (980 °C) (Seeker, 1990).

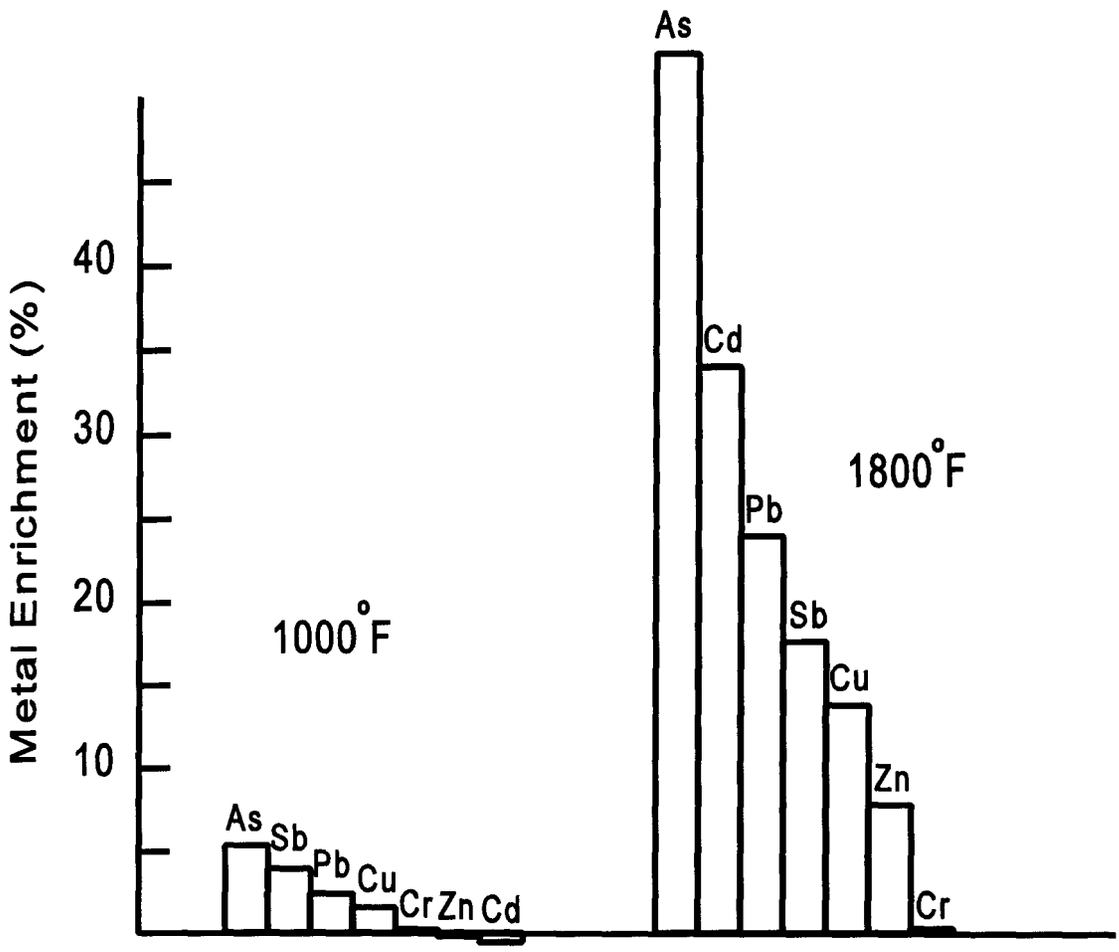

Figure 6-95. Impact of treatment temperature on the enrichment of metals in the fly ash after the thermal treatment of soils from a Superfund site.

Source: Seeker (1990).

The combustion effluent can be partitioned into three components (Seeker, 1990; Barton et al., 1990); emitted (as fly ash), captured (assuming there is an attempt to capture fine particles), and collected in the bottom ash. Assuming no particle removal equipment is in place on the combustion process, emitted particles will include both the "emitted" component and most of the "captured" component. In an uncontrolled incineration facility, 96% of mercury, 88% of cadmium, 58% of lead, and 11% of copper might by emitted into the atmosphere. If control is attempted, the capture efficiency is only 25% for mercury, but is better for most other metals, ranging from 86% for cadmium to 91% for copper (Barton et al., 1990). In addition, the chemical state of the metals in the ultrafine mode can vary from the more toxic phases (for example, arsenite versus arsenate) as a function of combustion conditions (Chesworth et al. 1994). Thus, we must expect that ultrafine metallic components will be emitted from high temperature processes in both toxic and less toxic forms.

6.9.3 Techniques for Collecting and Analyzing Ultrafine Metals

Relatively little information exists on concentrations of ultrafine metal particles in ambient air samples away from combustion sources. There are many reasons. The ultrafine mode falls off rapidly away from the combustion source, due to the rapid migration of some types of ultrafine particles into the accumulation mode, and increased dispersion as one moves away from the source. Many sources of ultrafine metals use tall exhaust stacks, which enhances dispersion. The largest of the ultrafine particles can overlap the smallest particles of the much more abundant accumulation mode, roughly 0.2 to 0.7 μm aerodynamic diameter. Particles must be size-separated using a device with a sharp cut point, ususally a multistage physical impactor, that entails problems in particle collection and analysis. Since ultrafine particles may be hard and dry, adhesive coatings are essential in order to avoid particle bounce in the impactors. Particle bounce typically translates coarser particles onto finer stages, contaminating the ultrafine particles with the enormously more abundant coarser particles. Finally, one can collect only a few monolayers of particles (at most) on the adhesive stages before particle bounce becomes important, assuming the particles themselves are not "sticky". A few monolayers of particles of 0.1 μm diameter amounts to only about 50 $\mu g/cm^2$ of total deposit. If one then desires to perform minor or trace elemental analysis of the deposit, one is

then faced with analytical requirements that reach picogram (10^{-12} gm) sensitivities. This clearly limits analytical options.

For these reasons, much of the data available on ultrafine particles does not depend on compositional analysis. Most information on the presence of ultrafine particles is derived from particle counting techniques such as the Electrical Mobility Analyzer (EMA), in situations in which the source is well known (source-enriched). This was the method pioneered in the 1972 ACHEX studies of Los Angeles (Whitby, 1978). Particle counting devices do not normally result in collection of ultrafine particles in a manner suitable for compositional analysis, although some of the devices ("particle classifiers") could be modified to provide samples for subsequent compositional analysis, if desired. The same can be argued for devices such as diffusion batteries, but to date little has been done along this line in ambient conditions.

Integrated samples of fine particles can be collected on substrates suitable for analysis. While some optical information is available as one approaches the ultrafine size, most optical techniques do not work in the ultrafine size range, which is well below the wavelength of light. A Scanning Electron Microscope (SEM) beam can still resolve ultrafine particles although some details are lost. The ultrafine particle distribution can then be derived by particle counting techniques, either manual or automated, and metal composition can be found by X-ray analysis of the single particles. The enormous gain in signal to noise ratio by selecting individual particles offsets the loss of X-ray sensitivity (typically parts per thousand) caused by use of the electron beams to induce the X rays. SEM and electron microprobe analyses rarely achieve any better than one part per thousand sensitivity. However, for single particles, this is often enough to classify them by source. Proton microprobes are, at present, not quite able to operate in the 0.1 μm diameter region, but can perform Proton Induced X-ray Emission (PIXE) analysis to one part per million by mass on single particles as small as 0.3 μm (Cahill, 1980).

Impactors are designed to separate particles by aerodynamic size in such a way as to allow compositional analysis. Yet here, too, ultrafine particles pose problems. First, most impactors can not operate effectively below 0.1 μm. The Stokes number for separation of a 0.1 μm diameter particle from an air stream requires either extremely high jet velocities,

extremely low pressures in the gas stream, or both. While such performance can be achieved in a physical impactor, most impactors used for ambient particle collection in the 1970's and early 1980's did not possess this capability. For example, the very popular cyclones and virtual impactors are ineffective below about 0.5 μm diameter. The Lundgren-type impactors widely used in California studies (Lundgren,1967; Flocchini et al., 1976; Barone et al. 1978) used 0.5 μm as the lowest cut point. Everything smaller was collected on a filter. The Battelle-type samplers (Mercer, 1964) favored by other groups (Van Grieken et al., 1975) used a lowest cut point of 0.25 μm diameter. Thus, while both these units generated copious information on aerosol composition, they could not separate ultrafine aerosols from accumulation mode aerosols.

In the mid-1980's four new impactors were developed capable of providing information on the composition of particles near 0.1 μm diameter: the Low Pressure Impactor, (LPI) (Hering et al., 1978), the Berner Low Pressure Impactor (BLPI) (Berner and Lürzer, 1980; Wang and John, 1988), the Davis Rotating-drum Unit for Monitoring impactor, (DRUM) (Cahill et al., 1985; Raabe et al., 1988), and the Multiple Orifice Uniform Deposit Impactor (MOUDI) (Marple et al., 1986; Marple et al., 1991). Battelle-type impactors were also modified to add two size cuts below 0.25 μm diameter. However, unlike the other four units, no certification of performance has been published to date on its performance in the ultrafine region. The development of reliable, clean adhesive coatings such as Apiezon™-L grease was also a major advance in the field (Wesolowski et al., 1977; Cahill, 1979), allowing separation of abundant soils from ultrafine size ranges even in dry, dusty conditions. For nominally PM-10 soils, for example, a ratio of coarse to ultrafine soils was measured at 6,600:1 at a temperatures above 30 °C and relative humidity below 20% (Cahill et al., 1985). Performances and specifications of all these units is included in a recent review paper (Cahill and Wakabayashi, 1993)

It is important to mention, however, that the motivation for development of this ultrafine capability was not for extensive studies of ultrafine metals, but rather to get a more complete picture of the accumulation mode behavior of sulfates, nitrates, organics, and other major components of the fine aerosol mix. Thus, compositional analysis was often limited to these species even when suitable samples had been collected. For example, many LPI samples were

collected on stainless steel substrates, ideal for combustion analysis of sulfur, but unsuitable for analysis of transition metals by X-ray techniques.

6.9.4 Observations of Very Fine Metals

Few techniques exist for collecting particles below 0.1 μm diameter for chemical analysis. No compositional data was found for particles below 0.1 μm diameter. However, since ultrafine particles rapidly grow into the accumulation mode, it may be assumed that measurements of the small-size tail of the accumulation mode provide some insight into the composition of the ultrafine particles. Thus, the concentration of metals in the smallest available size-cut will be examined. In order to avoid problems with definitions, particles in the smallest size-cut, which may extend to diameters above 0.1 μm, will be called "very fine" and ultrafine will be reserved for particle distributions with a mass mean diameter below 0.1 μm.

6.9.4.1 Stack and Source-Enriched Aerosols

Observation of very fine metals in source or source-enriched situations lessens problems with dilution of the sample and identification of the source. This eases both particle collection and analysis. Figure 6-96 shows the results of such a study on a coal fired power plant (Maenhaut et al., 1993) using the Berner Low Pressure Impactor (BLPI). The extreme volatilization of selenium is clearly seen, which is also confirmed in aircraft sampling of power plant stacks. Note, however, that the enrichment factor, as a function of particle size, for both sulfur and its chemical analog selenium. More refractory elements, on the other hand, are strongly enhanced in the very fine particles as compared to coarser modes.

The BLPI cuts are as follows: Stage number 1-0.011 μm diameter, 2-0.021, 3-0.032, 4-0.07, 5-0.17, 6-0.30, 7-0.64, 8-1.4, 9-2.6, 10-5.5, 11-10.7 μm. All are for particle density 2.45 g/cm^3 and a temperature 120 °C, the conditions of stack sampling in the coal fired power plant. Both these figures were normalized to Earth crustal averages. Thus, even a two order of magnitude rise in the normalized concentration may not result in a visible "combustion mode" since the mass of soil falls very rapidly as one moves towards very fine particles. This is exactly what is predicted by the results of Natusch et al. (1974). Thus, source testing

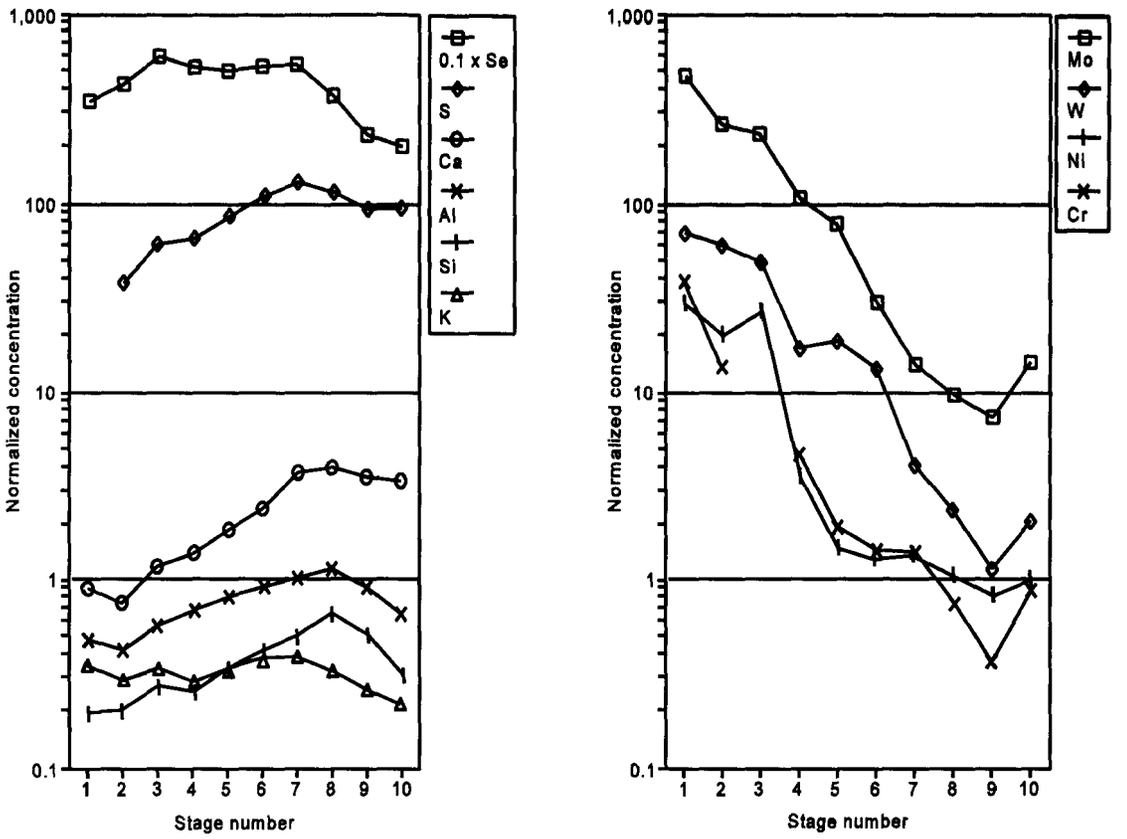

Figure 6-96. Average normalized concentrations as a function of stage number, for selenium (Se), sulfur (S), calcium (Ca), aluminum (Al), silicon (Si), potassium (K), molybdenum (Mo), tungsten (W), nickel (Ni), and chromium (Cr) for five BLPI samples from a coal fired power plant. The smallest size mode is to the left, Stage number 1, 0.011 to Stage number 11, 10.7 μm diameter. Normalization is to average crustal composition.

Source: Maenhaut et al. (1993).

confirms nucleation theory and the laboratory studies and predicts emissions of metals in the very fine particle size range from many types of high temperature combustion sources.

6.9.4.2 Ambient Aerosols

Direct Observations

Because of the difficulties in sampling and analysis, there is relatively little information on the concentrations of very fine metal particles in ambient air. Some quantitative determinations of ambient concentrations have become available in the past 15 years, however,

generally as a result of a number of short but intensive aerosol studies. Examples include the extensive studies near the Grand Canyon National Park (NP) in 1979 (Macias et al., 1981) to the Mohave Studies near the Grand Canyon NP in 1993 and the Southern is California Air Quality Study (SCAQS) in 1985-1987 (Hering et al., 1990; Cahill et al., 1990; Cahill et al., 1992a); studies at Shenandoah NP in 1991 (Cahill and Wakabayashi, 1993) and Mt. Rainier NP in 1992 (Malm et al., 1994a; Cahill and Wakabayashi, 1993), and others. While almost all of these studies used several different types of impactors with ultrafine capabilities, relatively few were analyzed for trace metal content.

An example of very fine particles persisting in ambient air is shown in Figure 6-97 using data collected at Grand Canyon NP 1984 (Cahill et al., 1987). The very fine particles behave independently from the accumulation mode, in fact often showing a net anti-correlation in concentrations of sulfur as well as dramatic differences in metals (Table 6-7). The very fine particles in Table 6-8 can be attributed to non-ferrous metal smelting activities in the region (Eldred et al., 1983; Small et al., 1981), which puts the nearest important sources a hundred miles away from the sampling site. The completely different behaviors of the accumulation and very fine particles in this arid site also show that mis-sizing by particle bounce is not significant.

Table 6-8 presents a summary of more recent data for major EPA-regulated metals (lead, nickel) and other metals, at Long Beach, CA, December in 1987 (Cahill et al., 1992a) and at Shenandoah NP in 1991 (Cahill and Wakabayashi, 1993). The elements span the range from refractory metals like nickel and vanadium to metals with low melting temperatures such as zinc and lead. These data were all taken with the same unit, the Davis Rotating-drum Unit for Monitoring (DRUM) using greased stages and a single orifice impactor (Cahill et al., 1985). The last two stages were modified form the Gand Canyon configuration as a result of theoretical and laboratory studies (Raabe et al., 1988), yielding 0.069 to 0.24 μm for Stage 8, and 0.24 to 0.34 μm diameter for Stage 7.

The DRUM data were used for several reasons: the DRUM's slowly rotating greased stages have a documented ability to handle large amounts of coarse, dry soils without contaminating the very fine stages (Cahill et al., 1985; Cahill and Wakabayashi, 1993), the elemental data are of unprecedented sensitivity for ambient very fine trace metals (PIXE and

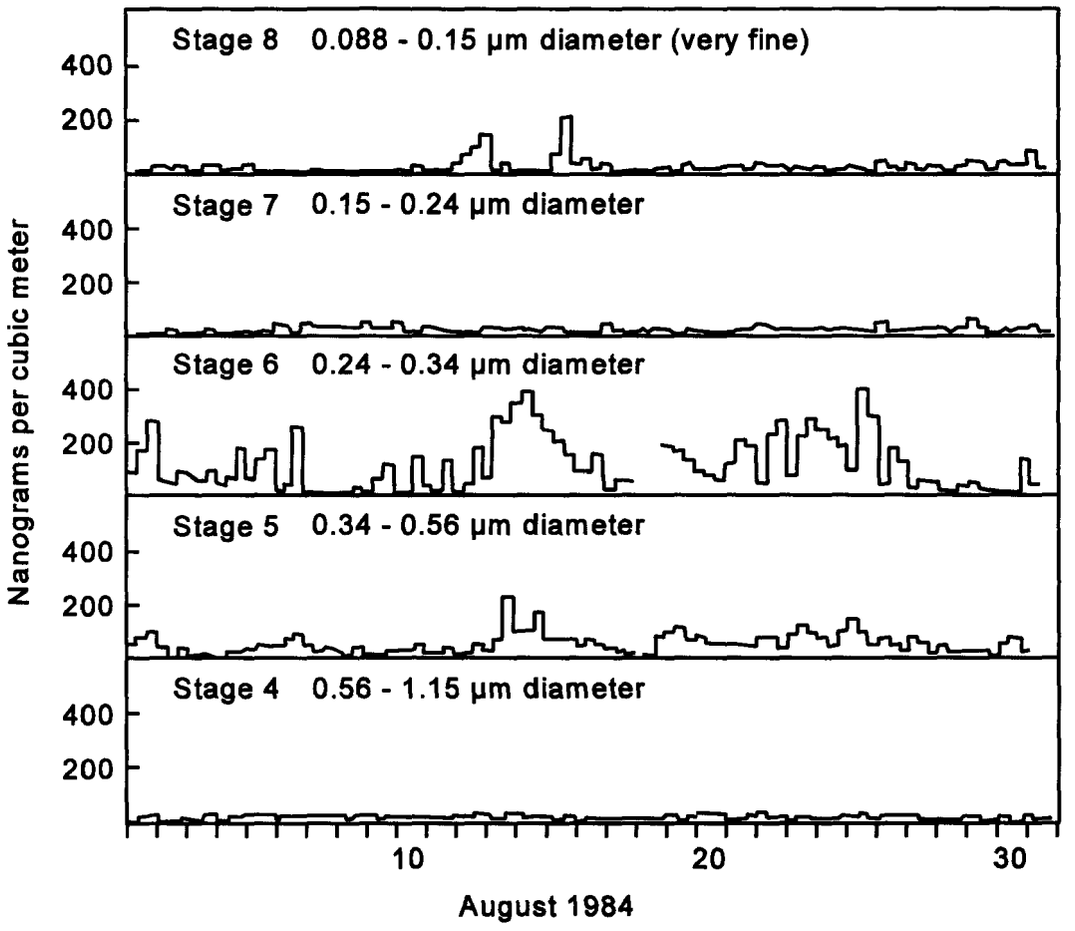

Figure 6-97. Fine and very fine sulfur at Grand Canyon National Park, summer 1984. The sulfur peaks on August 15 and August 16 were used for the compositional analysis in Table 3. The first three cut points are somewhat uncertain due to altitude and flow rate corrections. Final stage configurations are given in Raabe et al. (1988), which were used for all later studies using the DRUM.

Source: Cahill et al. (1987).

synchrotron-XRF), there is a consistency of sampler type and protocols at very different locations, and there are more trace element data from the DRUM than from any other type of unit. These advantages outweigh its disadvantages; the DRUM does not have the very fine sizing detail of either the LPI or BLPI impactor, or the ability to measure mass, ions and organic matter of the MOUDI or BLPI. The analyses were done both by PIXE and by synchrotron-XRF (Cahill et al., 1992a), with most of the trace metal data from the latter

TABLE 6-7. COMPOSITION OF THE AEROSOLS PRESENT AT GRAND CANYON NATIONAL PARK IN THE SUMMER OF 1984 FOR THE SULFATE EPISODES OF AUGUST 15 (ACCUMULATION MODE, STAGE 6) AND AUGUST 16 (VERY FINE PARTICLES, STAGE 8)

Elements	Stage 8, 0.088-0.15 μm (ng/m^3)	Stage 6, 0.24-0.34 μm (ng/m^3)
Sodium	420	10
Silicon and Aluminum	8	6
Sulfur	204	392
Chlorine	208	5
Potassium	59	3
Calcium	150	5
Titanium	2	4
Vanadium	2	3
Iron and Nickel	2	2
Copper	100	1
Zinc	931	2
Arsenic	13	2
Bromine	2	2
Lead	63	4

Source: Cahill et al. (1987).

source. In order to obtain sulfate, multiply sulfur by 3.0. These average values, however, obscure a great deal of structure as a function of time.

The variability as a function of size and time is shown in Figure 6-98 for nickel, selenium, and lead in Long Beach, CA as part of the SCAQS studies of 1987. By 1987, much of the lead was no longer automotive, and there are significant changes in the very fine fraction over periods of four to twelve hours. Note the behavior of very fine metals; almost total absence for selenium, partial absence for nickel, and constant presence for lead. Almost all elements at almost every site show similarly complex behavior. Thus, the summary of Table 6-8 can include only the most basic types of information on fine and very fine metals in the atmosphere.

TABLE 6-8. MEASUREMENTS OF FINE AND VERY FINE METALS

Site Name Duration Frequency Dates	Particle Aerodynamic Diameters	Very Fine Particles					
			Accumulation Mode				
		From To	**From To**	From To	From To	From To	From To
	(D_{ae}, μm)	**0.069 0.24**	**0.069 0.24**	0.24 0.34	0.34 0.56	0.56 1.15	1.15 2.5
	Element	Maximum Values (ng/m^3)	Mean Values (ng/m^3)				
Long Beach, CA							
6 days 6 samples/day (11, 12/87)	Vanadium	**6.6**	**2.5**	6.1	10.5	12.2	8.6
	Nickel	**3.4**	**1.3**	4.4	7.7	4.5	0.5
	Zinc	**51**	**17.6**	46.3	140.4	189.4	39
Mean detectable limit - 0.3 ng/m^3	Selenium	**MDL**	**MDL**	0.32	3.0	1.4	0.65
	Lead	**199**	**71.4**	47.6	59.9	69.9	25.4
	Sulfur[a]		**200**	250	350	500	250
Shenandoah NP							
21 days 6 samples/day (9/91)	Vanadium	**1.2**	**0.24**	0.67	0.52	0.30	0.80
	Nickel	**1.2**	**0.58**	0.48	0.13	0.03	0.01
	Zinc	**3.8**	**1.42**	2.16	2.60	1.92	1.66
Mean detectable limit - 0.15 ng/m^3	Selenium	**2.7**	**0.14**	0.11	0.52	0.35	0.14
	Lead	**50**	**5.38**	5.49	3.01	10.87	16.06
	Sulfur[a]		**334**	929	1235	1727	101

[a]Estimated from graphs.

Source: Cahill et al. (1992a, 1996a).

In addition to the limited US data, comparison data have also become available from foreign sources such as from the Kuwaiti oil fires (Reid et al., 1994) and a study in Santiago, Chile (Cahill et al., 1996). While the former is a unique situation, the Santiago data are

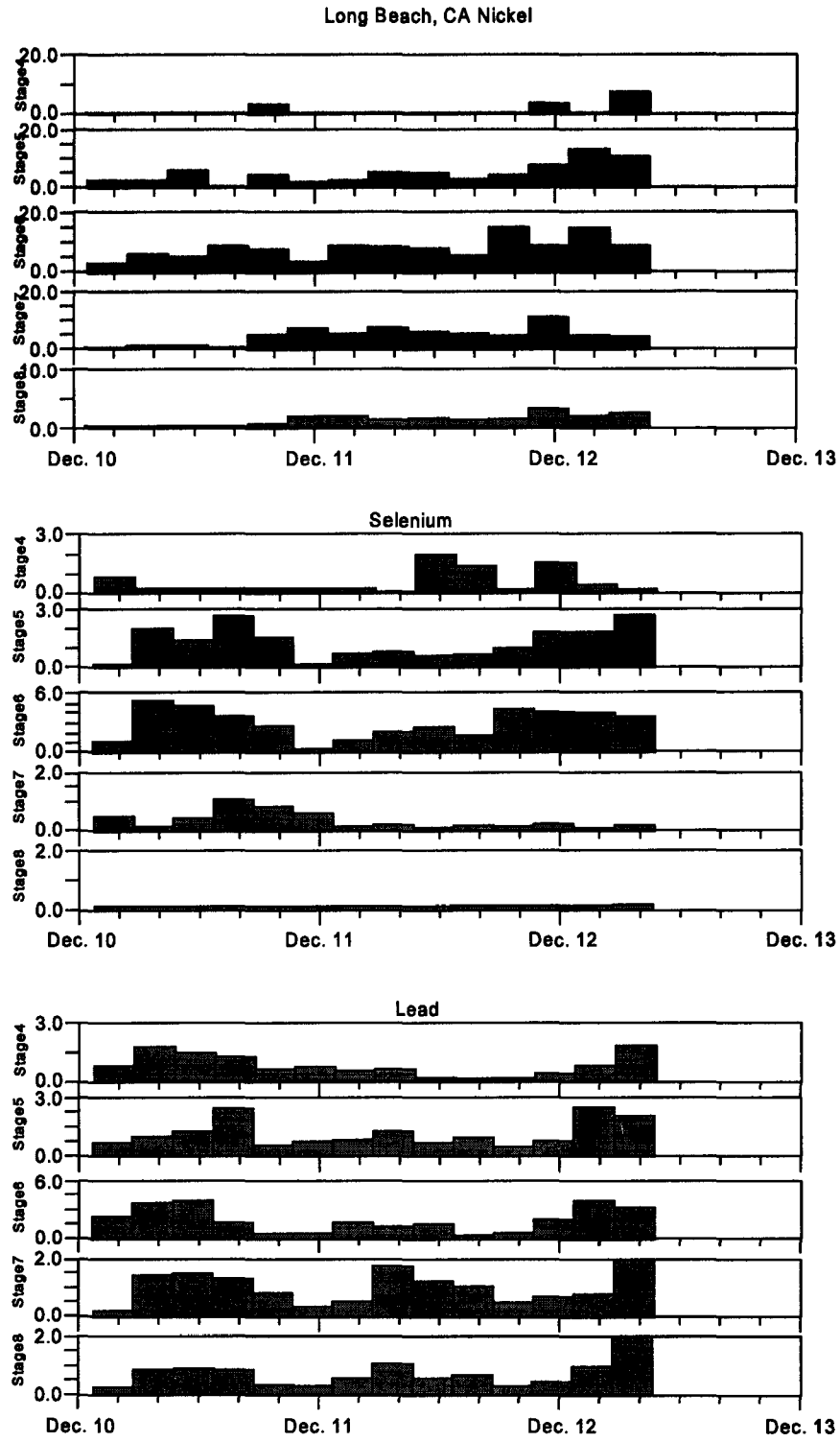

Figure 6-98. Concentration, in micrograms per cubic meter, of fine and very fine metals (nickel, selenium, and lead) in Long Beach, CA, December 10 through 13, 1987, in 4-h increments. Stage 8 is very fine, 0.069-0.24 μm; then 0.34, 0.56, 1.15, 2.5 μm aerodynamic diameter for the upper size-cut.

Source: Cahill et al. (1992a).

especially useful since leaded gasoline is still routinely used in Chile and other countries, generating data impossible to obtain in the United States. Table 6-9 summarizes some of these data for a refractory element, nickel, and a volatile metal, lead. However, the full data set includes 450 samples of four to six hours duration, each analyzed in five fine size fractions, generally with about 20 elements found in each fraction, or approximately 40,000 individual elemental values.

Some general observations can be made from the data; first, there is an enormous variation in the concentration of fine and very fine metals, sometimes spanning 4 or 5 orders of magnitude in a few days. Such behavior can be modeled by plumes of particles that sweep over the site episodically, as opposed to area or regional sources. Second, one often finds a mixture of very fine particle or nuclei mode behavior as well as accumulation mode behavior. However, these modes may be physically separated in time.

Lead in the United States follows a variety of very different patterns. In the rural samples, lead tends to be bimodal, with a coarse component above 1.0 μm diameter and a very fine component below 0.34 μm diameter. This can be modeled by a very fresh fine particle mode and a coarser mode associated with resuspended soil. Urban sites, however, both in the U.S. and in Santiago, show lead in very fine particles as well as in the accumulation mode. Lead in resuspended soil is found in the coarse particle mode.

Other metals at Long Beach, however, lack a distinct concentration of very fine particles all the time (selenium) or part of the time (nickel), merely possessing an accumulation mode that closely mimics sulfates and other secondary species (Cahill et al., 1990). It is well known that nickel and vanadium were derived from high temperature combustion sources, and since each is highly refractory, they will occur primarily as very fine particles near the source. Thus, the similarity between the distributions of these elements and less refractory elements such as zinc can be understood through a rapid condensation and coagulation of the abundant secondary species around these metals, leading to an accumulation mode distribution as the secondary acidic species hydrate. Clearly, such processes are weaker at dry sites such as the arid west in summer (Table 6-8). On the other hand, Shenandoah NP has a mixture of urban and rural behavior, with occasional sharp peaks of very fine metals (nickel) superimposed on an accumulation mode behavior (sulfur, selenium) with some coarse contribution (lead,

TABLE 6-9. MEASUREMENTS OF FINE AND VERY FINE METALS (LEAD AND NICKEL)

Site Duration Frequency Dates	Element	Particle Aerodynamic Diameters	**Very Fine Particles**	Accumulation Mode					
			From To	From To	From To	From To	From To		
		(D_{ae}, μm)	**0.069 0.24**	0.24 0.34	0.34 0.56	0.56 1.15	1.15 2.5		
			ng/m^3	ng/m^3	ng/m^3	ng/m^3	ng/m^3	MDL[a]
Long Beach 6 days 4 samples/ day (11/87)	Lead	Mean	**71.4**	47.6	59.9	69.9	25.4	0.45
		Maximum	**199**	95	129	164	58	
	Nickel	Mean	**1.3**	4.4	7.7	4.5	0.5	0.22
		Maximum	**3.4**	11.4	15.0	13.4	3.7	
Shenandoah NP 21 days 6 samples/ day (9/91)	Lead	Mean	**5.4**	5.5	3.0	10.9	16.1	0.2
		Maximum	**50**	20	16	70	130	
	Nickel	Mean	**0.58**	0.48	0.13	0.03	0.01	0.09
		Maximum	**1.2**	1.6	0.8	1.0	0.14	
Mt. Rainier NP 28 days 6 samples/ day (7, 8/92)	Lead	Mean	**2.3**	6.5	2.0	3.4	6.7	0.5
		Maximum	**6**	15	21	14	29	
	Nickel	Mean	Always less than MDL					0.07
		Maximum	**MDL**	0.4	0.8	0.4	0.7	
Santiago, Chile 14 days 6 samples/ day (9/93)	Lead	Mean	**101**	53	38	108	41	8
		Maximum	**920**	340	320	640	270	
Kuwait 14 days 4 samples/ day(6/91)	Lead	Mean	**429.9**	154.2	84.7	44.7	38.1	0.35
		Maximum	**2580**	580	128	86	70	
	Nickel	Mean	**1.5**	2.5	4.3	3.7	6.0	0.22
		Maximum	**5**	18	11	8	9	

[a]MDL = minimum detectable limit at 95% confidence level, in nanograms per cubic meter

Source: Cahill et al. (1992a,b, 1996a), Malm et al. (1994a), Reid et al. (1994), Cahill and Wakabayashi (1993).

vanadium). Only through a detailed study of meteorology and knowledge of emission sources can such ambient behavior be understood.

Indirect Methods

Lacking a large body of direct data on very fine metallic aerosols, there are indirect ways to increase our knowledge of such aerosols;

1. Combustion studies have established the formation mechanism of very fine metallic aerosols, and,

2. Considerable ambient data exist that, when combined with known combustion processes, yield estimates for the concentration of very fine metallic aerosols by time and locations.

3. In conditions of low ambient concentrations of particles and low humidity, very fine particles have been shown to persist for many hours. (Cahill et al., 1985).

Thus, the numerous observations of fine ($D_p < 2.5\ \mu m$) metallic aerosols in low humidity conditions can yield estimates of the presence of such metals in the very fine particles and set upper limits on their concentrations. The relatively small number of actual measurements can then serve as tests or as confirmation of our level of understanding of these biologically important aerosols. As an example, Figure 6-99 shows concentration profiles of sulfur, selenium, zinc, and arsenic, all of which can occur as very fine particles in the western United States. Arsenic and zinc are annual averages, March, 1993 to February, 1994, while the sulfur (for sulfate, times 3.0) and selenium are for summer, 1993. This was done to exhibit the correlation of these elements, which are chemically akin, during the eastern U.S. sulfate maximum each summer. The regional nature of the elements is very evident, as are certain strong sub-regional sources such as the copper smelter region of Arizona and New Mexico (arsenic).

The non-urban values shown in Figure 6-99, which are derived from the cleanest areas of the United States, are surprisingly relevant to urban areas in the same region for some of the species. Table 6-10 compares major and minor fine elements at Shenandoah NP, where there are detailed measurements of particle size, and Washington, DC, where such size information is lacking. Summer 1993 is the comparison period. Finally, two western sites are compared, both downwind of Los Angeles; San Gorgonio Wilderness, and Grand Canyon NP.

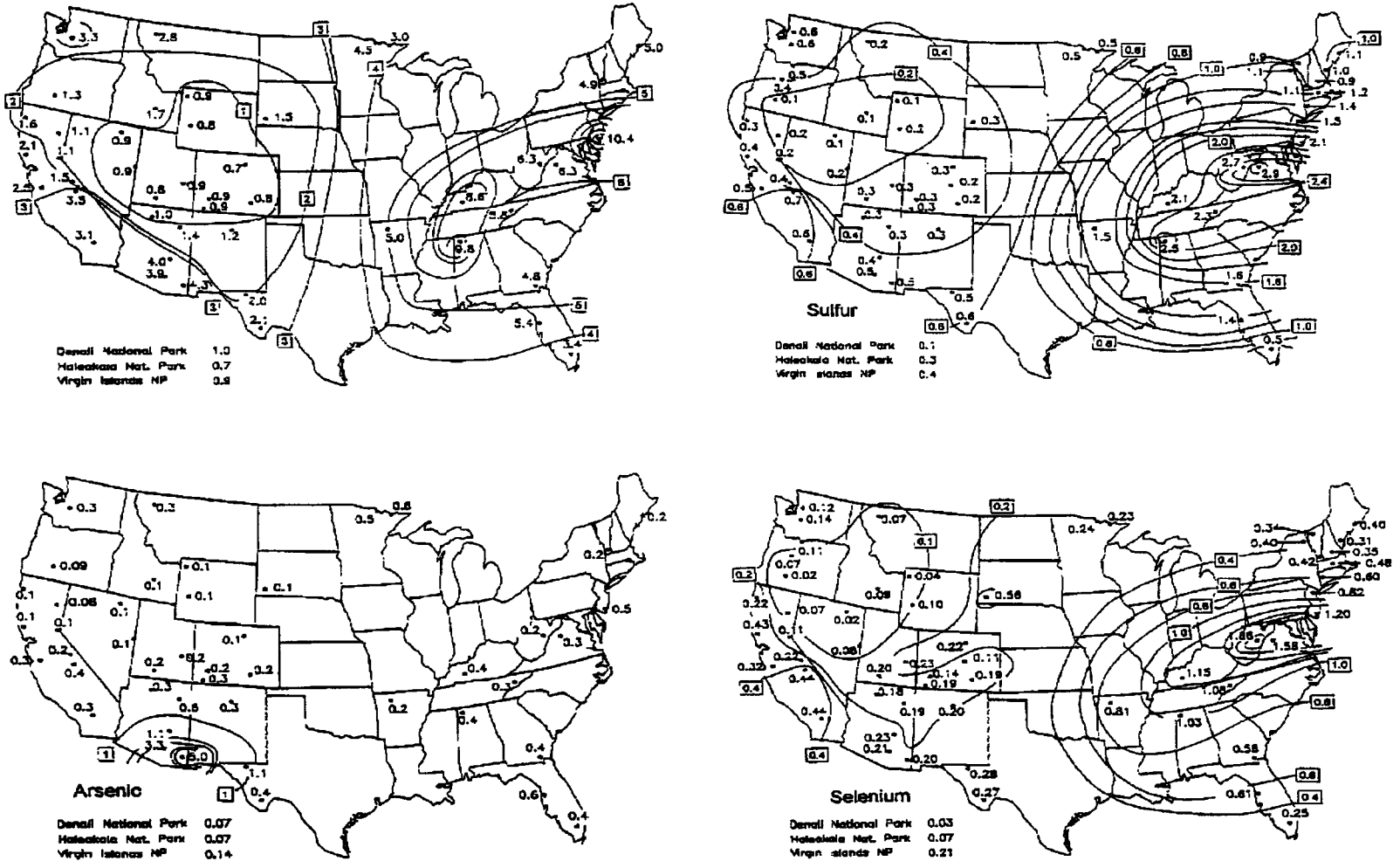

Figure 6-99. Patterns of zinc, arsenic, sulfur, and selenium in the United States.

TABLE 6-10. COMPARISON OF SELECTED SPECIES AT SHENANDOAH NATIONAL PARK; WASHINGTON, DISTRICT OF COLUMBIA; SAN GORGONIO WILDERNESS, CALIFORNIA; AND GRAND CANYON NATIONAL PARK DURING SUMMER 1993

Concentration ($\mu g/m^3$)	Shenandoah National Park	Washington, DC	San Gorgonio Wilderness	Grand Canyon National Park
Mass - PM_{10}	31.00	34.90	21.70	9.37
Mass - $PM_{2.5}$	22.50	26.50	10.30	4.50
Composition - $PM_{2.5}$				
Ammonium sulfate	11.80	14.60	2.55	1.09
Ammonium nitrate	0.40	1.47	4.44	0.25
Organic matter	2.84	5.42	3.88	1.22
Soil	1.41	1.55	0.86	0.63
Trace compositon (ng/m^3)				
Nickel	0.24	0.97	0.18	0.09
Copper	1.06	3.37	0.76	0.30
Zinc	7.93	13.90	3.72	0.63
Arsenic	0.22	0.56	0.16	0.18
Selenium	1.58	2.48	0.44	0.18
Bromine	2.14	4.18	3.67	2.11
Lead	2.17	4.48	1.36	0.51
Bio-smoke tracer (non-soil fine potassium)	8.33	< 2.00	10.00	32.30
Optical Absortion (b(abs), 10^{-6} m^{-1})	19.60	41.90	13.90	5.40

Source: Malm et al. (1994b).

Inhalation of Very Fine Metals

An extensive literature exists on the deposition of fine metals in the human lung, much of which was derived from laboratory studies, some using radioactive tracer isotopes. But an example of one of the few direct measurements of lung capture of ambient very fine metals is found in Desaedeleer et al. (1977) and shown in Figure 6-100. The lower cut point is only 0.25 μm, but even so, the increased capture efficiency of the lung for very fine and very fine particles is clearly shown.

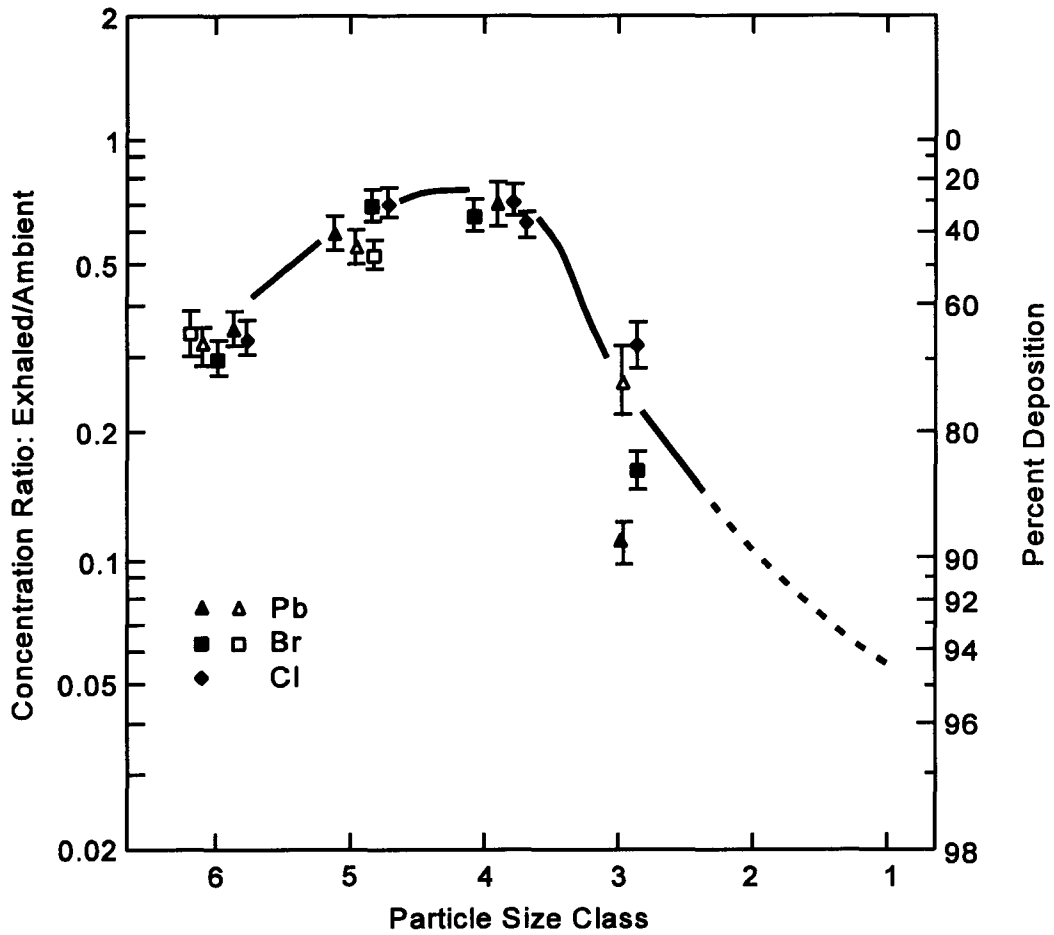

Figure: 6-100. Apparent deposition of automotive lead aerosol in the respiratory tract of one of the authors as determined by cascade impactor and Proton Induced X-ray Emissions (PIXE), as a function of aerodynamic diameter for >4, 4 to 2, 2 to 1, 1 to 0.5, 0.5 to 0.25, and < 0.25 μm particles of size classes 1 through 6, respectively. Extension of the curve to particles of diameter >2 μm (classes 2 and 1) is supported by separateexperiments using chalk dust aerosol.

Source: Desaedeleer et al. (1977).

6.9.5 Conclusions

There are few data on ambient concentrations of ultrafine metals. The few direct measurements can be extended with some confidence using indirect methods; i.e., particle counting techniques that have size information but no chemical information, or filter collection methods that have limited size information but detailed compositional information.

Nevertheless, it is clear that more information is needed on the size and concentration and the spatial and temporal concentration profiles of ultrafine metal particles.

Ultrafine metals are produced by a wide variety of anthropogenic activities and emitted into the ambient air. Ambient concentrations of such metals have been seen not only in urban settings but also at the cleanest sites in the United States. Concentrations are highly variable as a function of site and time. While ultrafine metals have been seen to persist for many hours, or more, in the clean, dry environment of the arid west, they appear to be rapidly transformed into the accumulation mode in polluted urban or humid rural sites.

6.10 FINE AND COARSE PARTICULATE MATTER TRENDS AND PATTERNS

Data for characterizing PM_{10} are available from a number of AIRS sites across the country. However, data for characterizing $PM_{2.5}$ and $PM_{(10-2.5)}$ as well as PM_{10} are not readily available. As discussed in 6.3.1.7, data for $PM_{2.5}$ and $PM_{(10-2.5)}$ have been obtained at sites in the IMPROVE/NESCAUM networks. However, these sites are located in uninhibited areas. Measurements suitable for determining trends and patterns of $PM_{2.5}$ and $PM_{(10-2.5)}$ in populated areas are available from only a few sites.

Most such data have been obtained with dichotomous samplers which measure $PM_{2.5}$ (an indicator of fine mode particles) and $PM_{(10-2.5)}$ (an indicator of the coarse fraction of PM_{10}). These two fractions may be added together to give PM_{10}. $PM_{2.5}$ is sometimes referred to as fine and $PM_{(10-2.5)}$ as coarse although it is understood that $PM_{2.5}$ will contain that fraction of the coarse mode PM below 2.5 μm diameter and neither PM_{10} nor $PM_{(10-2.5)}$ will contain that portion of the coarse mode above 10μm diameter. Sources of $PM_{2.5}$ (fine) and $PM_{(10-2.5)}$ (coarse) data include EPA's Aerometric Information Retrieval System (AIRS) (AIRS, 1995), IMPROVE (Eldred and Cahill, 1994; Cahill, 1996), The California Air Resources Board (CARB) (CARB, 1995), the Harvard Six-Cities Data Base (Spengler et al., 1986b; Neas, 1996), and the Harvard Philadelphia Data Base (Koutrakis, 1995). The Inhalable Particulate Network (IPN) (IPN, 1985; Rodes and Evans, 1982) provides TSP, PM_{15} and $PM_{2.5}$ data with only a small amount of PM_{10} data.

Data suitable for characterizing the daily variability in $PM_{2.5}$ and PM_{10} are available from only one site in southwestern Philadelphia. The National Weather Service provides daily observations of visual range, which when suitably treated, can provide an indication of fine mode particle concentration. The Harvard Six Cities study obtained data for $PM_{2.5}$ and PM_{15} every other day for several years. The California Air Resources Board operates about twenty sites that collect $PM_{2.5}$ and $PM_{(10-2.5)}$ data with a sampling frequency of every sixth day. Every sixth day data for a few sites may be found in AIRS. Because of the small number of data sets for $PM_{2.5}$ and either $PM_{(10-2.5)}$ or PM_{10} levels detailed intercomparisons of the behavior of these aerosol size fractions in different regions of the United States cannot yet be made. Data for characterizing the daily and seasonal variability of $PM_{2.5}$, $PM_{(10-2.5)}$, and PM_{10} will be discussed in 6.10.1, the longer term variability (i.e., trends) of $PM_{2.5}$, $PM_{10-2.5}$, and PM_{10} will be discussed in 6.10.2, and the interrelations and correlations among the various PM components and parameters will be discussed in 6.10.3.

The results presented in this section were derived from data bases available to the public. Except for the visibility and National Park trend data, the results presented in this section were prepared for this Criteria Document and have not yet been published elsewhere.

6.10.1 Daily and Seasonal Variability in $PM_{2.5}$ and PM_{10}

In addition to considering patterns of seasonal variations over broad geographical areas, a great deal of information, useful for relating ambient concentrations to health effects, can be obtained by analyzing long time series of concentration data at a single site. Collocated 24-hour $PM_{2.5}$ and PM_{10} filter samples were collected at a site in southwestern Philadelphia from May 1992 through April 1995 (Koutrakis, 1995). This unique data set was collected on a nearly daily basis, thereby allowing an assessment of day-to-day variability in aerosol properties.

The data are presented as box plots showing the lowest, lowest tenth percentile, lowest quartile, median, highest quartile, highest tenth percentile, and highest $PM_{2.5}$ values in Figure 6-101. The four three-month averaging periods shown (March-May, June-August, September-November, December-February) correspond to the so-called climatological or meteorological seasons. Highest median (20.8 $\mu g/m^3$) and extreme (72.6 $\mu g/m^3$)

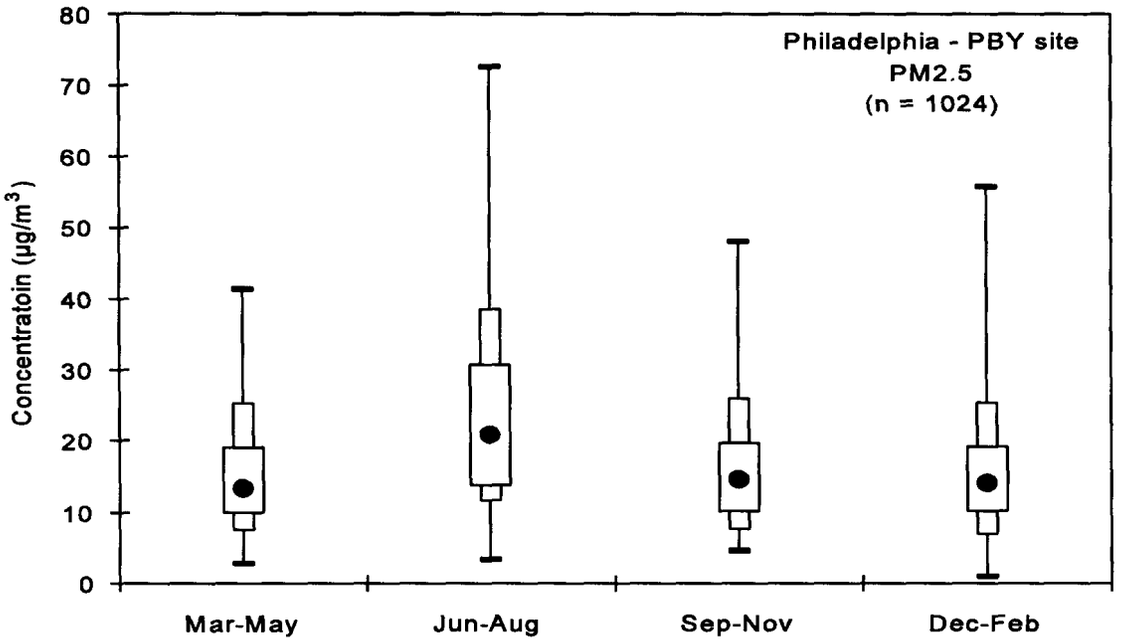

Figure 6-101. Concentrations of $PM_{2.5}$ measured at the PBY site in southwestern Philadelphia. The data show the lowest, lowest tenth percentile, lowest quartile, median (black circles), highest quartile, highest tenth percentile, and highest $PM_{2.5}$ values.

$PM_{2.5}$ concentrations were found during summer, with a difference of 50 $\mu g/m^3$ between them. Median $PM_{2.5}$ concentrations are 14.6, 14.2, and 13.4 $\mu g/m^3$ for the three quarterly periods from September through May, while maximum concentrations ranged from 41 to 55 $\mu g/m^3$. Corresponding PM_{10} data are shown in Figure 6-102. PM_{10} concentrations exhibit strong maxima during both the summer (82.4 $\mu g/m^3$) and winter (77.5 $\mu g/m^3$). Maximum PM_{10} concentrations during spring and fall are 54.7 and 58.5 $\mu g/m^3$. The difference between median and maximum values was 54.4 $\mu g/m^3$ during summer and 58.3 $\mu g/m^3$ during winter. The median PM_{10} concentration was 28.0 $\mu g/m^3$ in summer, and ranged between 19.2 and 20.9 $\mu g/m^3$ during the other seasons.

$PM_{2.5}$ and PM_{10} concentrations were highly correlated ($r=0.92$). PM_{10} and $PM_{(10-2.5)}$ concentrations were less highly correlated ($r=0.63$) and $PM_{2.5}$ and $PM_{(10-2.5)}$ concentrations were even less well correlated ($r=0.30$). The day-to-day difference in $PM_{2.5}$ concentrations was 6.8 $\pm$ 6.5 $\mu g/m^3$ and the maximum difference was 54.7 $\mu g/m^3$, while the day-to-day

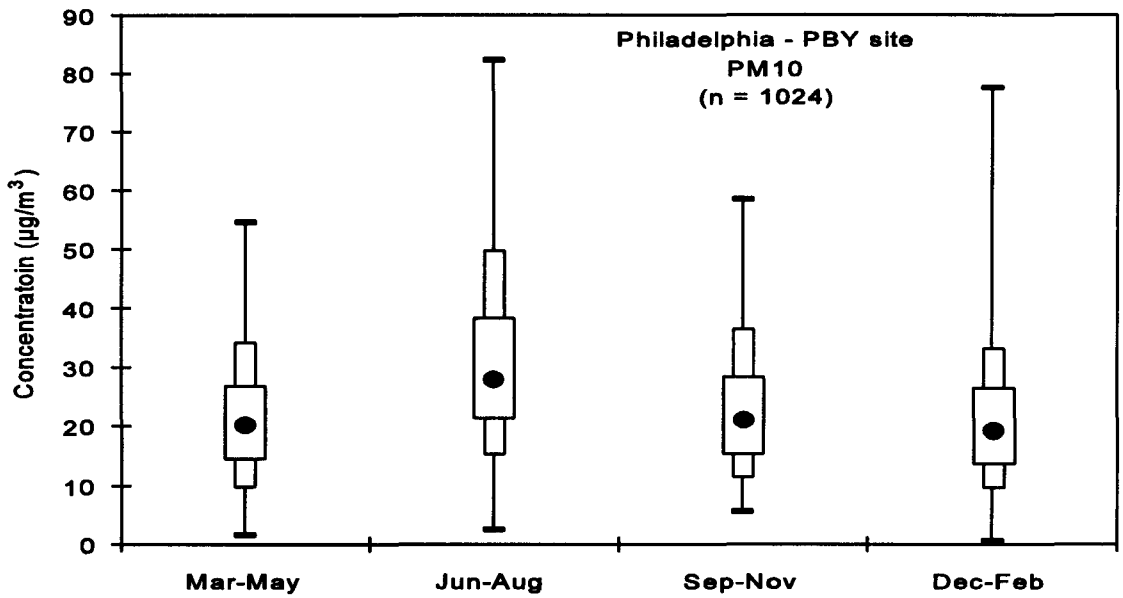

Figure 6-102. Concentrations of PM_{10} measured at the PBY site in southwestern Philadelphia. The data show the lowest, lowest tenth percentile, lowest quartile, median (black circles), highest quartile, highest tenth percentile, and highest $PM_{2.5}$ values.

difference in PM_{10} concentrations was 8.6 ± 7.5 $\mu g/m^3$ with a maximum difference of 50.4 $\mu g/m^3$. The day-to-day difference in $PM_{(10-2.5)}$ concentrations was 3.7 ± 3.5 $\mu g/m^3$ with a maximum difference of 35.1 $\mu g/m^3$. The ratio of $PM_{2.5}$ to PM_{10} throughout the measurement period was 0.71 ± 0.13. The high correlation coefficient between $PM_{2.5}$ and PM_{10} along with the high ratio of $PM_{2.5}$ to PM_{10} suggests that variability in $PM_{2.5}$ was driving the variability in PM_{10} levels.

Frequency distributions for the entire three-year $PM_{2.5}$, $PM_{(10-2.5)}$, and PM_{10} data sets are shown in Figures 6-103, 6-104, and 6-105, respectively. Concentrations predicted from the log-normal distribution, using mean values and geometric standard deviation derived from the data, are also shown. The small number of apparently negative $PM_{(10-2.5)}$ values reflects measurement error at low concentration levels. Frequency distributions of aerosol concentrations at several sites in the South Coast Air Basin (Kao and Friedlander, 1995) have also been shown to be reasonably approximated by log-normal distributions.

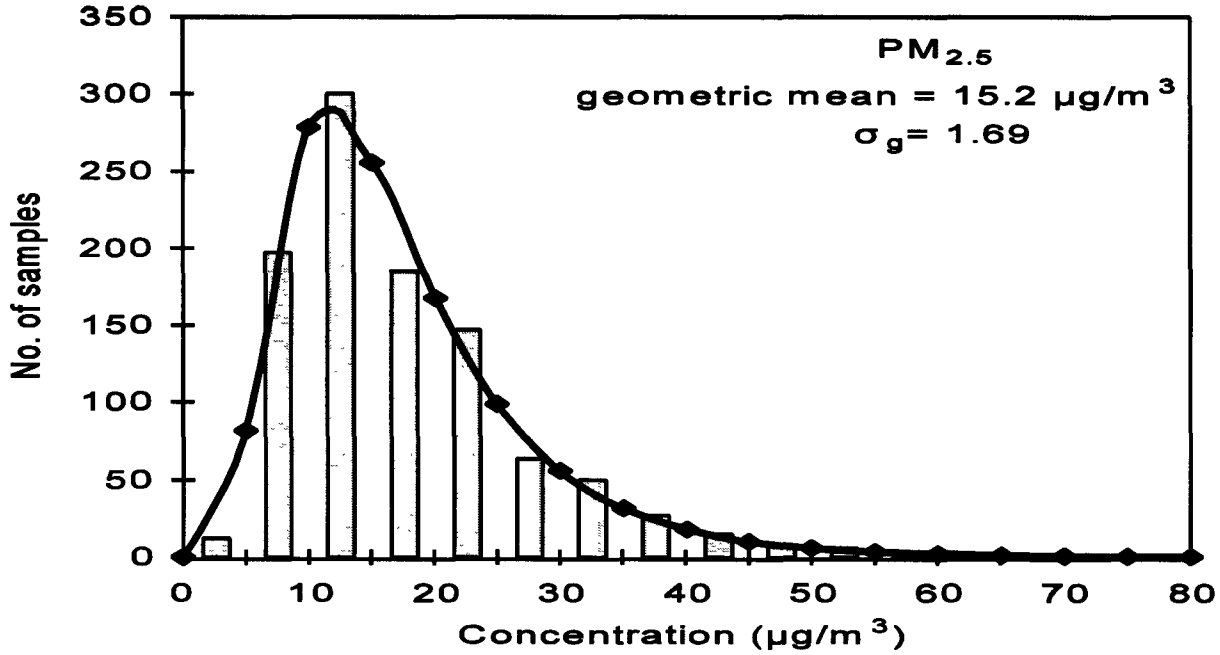

Figure 6-103. Frequency distribution of $PM_{2.5}$ concentrations measured at the PBY site in southwestern Philadelphia. Log-normal distribution fit to the data shown as solid line.

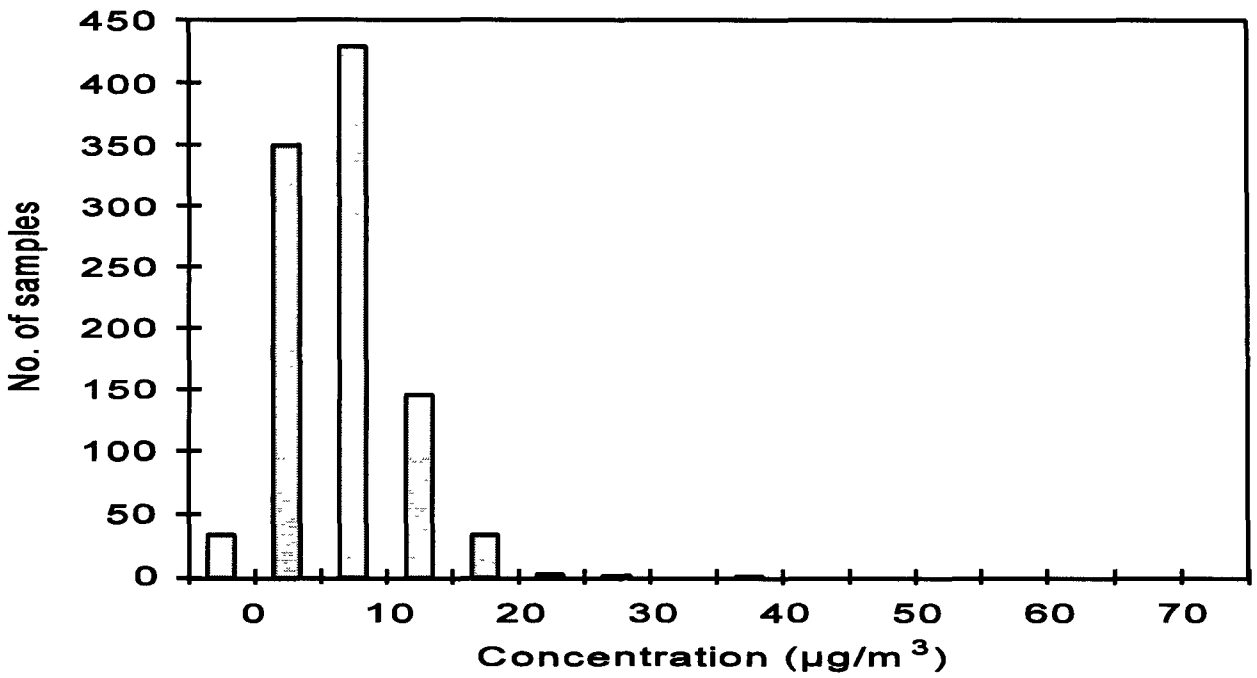

Figure 6-104. Frequency distribution of coarse mode mass derived by difference between PM_{10} and $PM_{2.5}$. Log-normal distribution not shown because of derivative nature of entries.

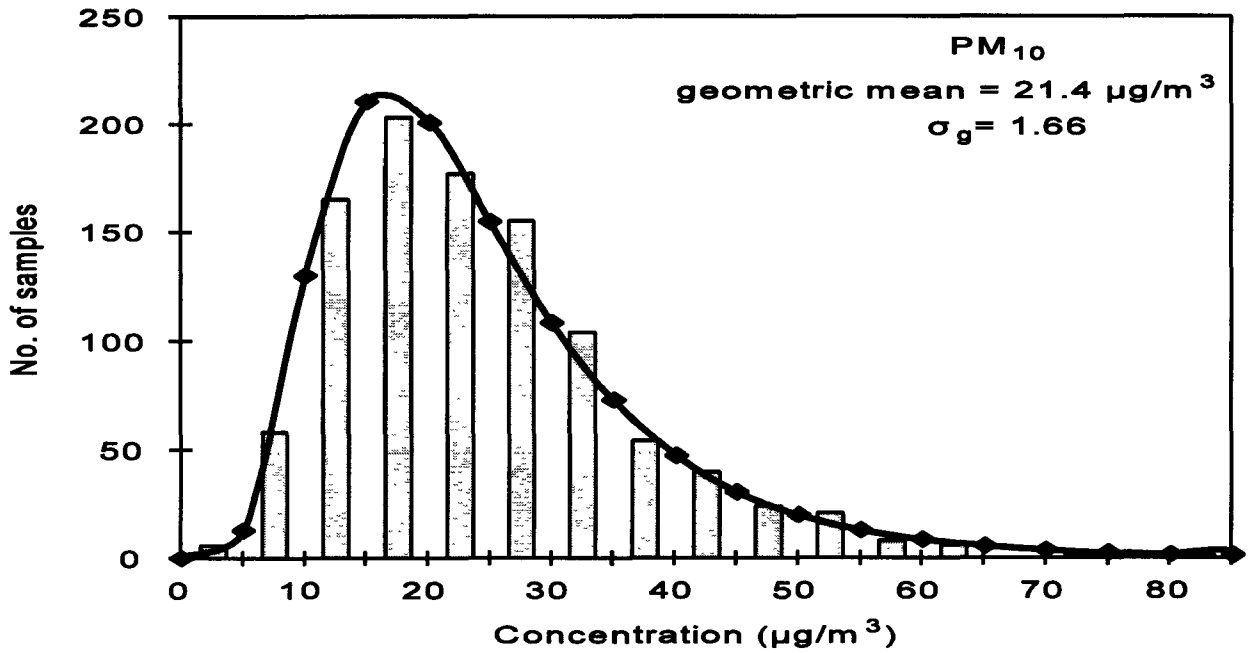

Figure 6-105. Frequency distribution of PM_{10} concentrations measured at the PBY site in southwestern Philadelphia. Log-normal distribution fit to the data shown as solid line.

In general, the highest $PM_{2.5}$ values are observed when winds are from the southwest during sunny but hazy high presure conditions. In contrast, the lowest values are found after significant rainstorms during all seasons of the year. The highest $PM_{2.5}$ values were observed during episodes driven by high sulfate abundances and are due, at least partly, to higher sulfate concentrations. Correlation coefficients between $SO_4^=$ and $PM_{2.5}$ were 0.97 during the summer of 1993. Similar correlations between $SO_4^=$ and $PM_{2.5}$ were found at a site in northeastern Philadelphia (24 km distant from the site under discussion) during the summer of 1993. In addition, $PM_{2.5}$ was found to be stongly correlated ($r > 0.9$) between seven urban sites and one background site (Valley Forge, PA) during the summer of 1993 (Suh et al., 1995). The same relations were also found during the summer of 1994 at four monitoring sites as part of a separate study (Pinto et al., 1995). The results from these studies strongly suggest that $PM_{2.5}$ and $SO_4^=$ concentrations are spatially uniform throughout the Philadelphia area, and that variablility in PM_{10} levels is caused largely by variability in $PM_{2.5}$ (Wilson and

Suh, 1996). However, not enough data are available from regional sites to define the total areal extent of the spatial homogeneity observed in the urban concentrations.

Different conclusions could be drawn about data collected elsewhere in the United States. $PM_{2.5}$ and $PM_{(10-2.5)}$ data were obtained at a number of sites in California on a sampling schedule of every six days with dichotomous samplers (California Air Resources Board, 1995). As an example, frequency distributions of $PM_{2.5}$, $PM_{(10-2.5)}$, and PM_{10} concentrations (calculated as the sum of $PM_{2.5}$ and $PM_{(10-2.5)}$) obtained at Riverside-Rubidoux from 1989 to 1994 are shown in Figures 6-106, 6-107, and 6-108, respectively. It can be seen that the data cannot be satisfactorily fit by a single function, mainly as the result of the complexity of the concentration distribution of the coarse size mode shown in Figure 6-107.

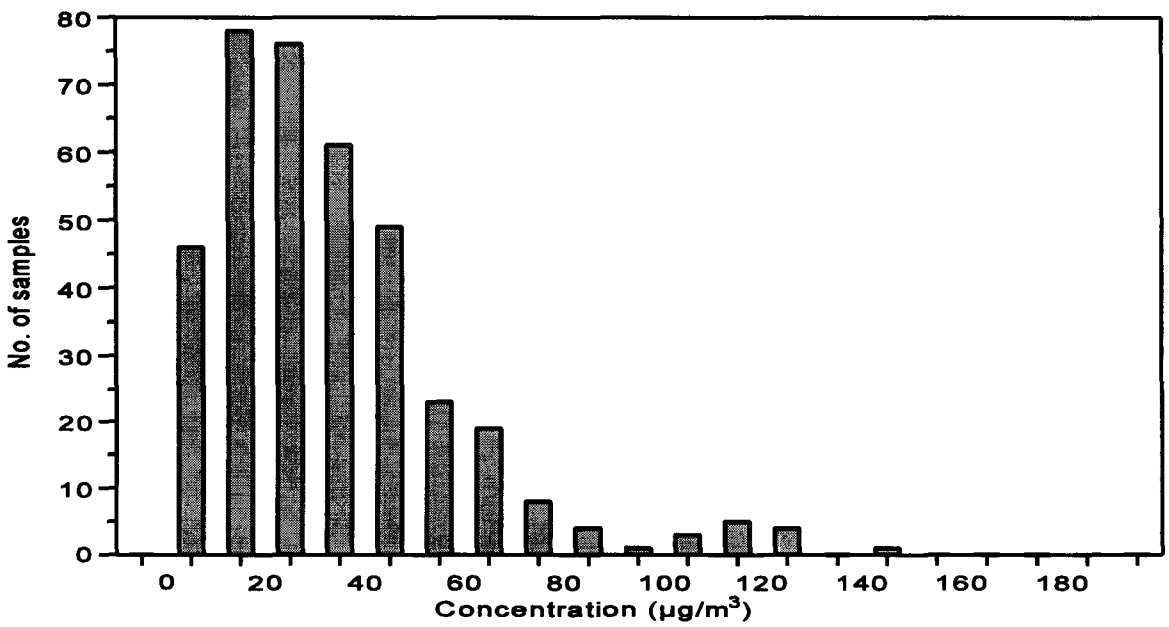

Figure 6-106. Frequency distribution of $PM_{2.5}$ concentrations measured at the Riverside-Rubidoux site.

The data are also presented as box plots showing the lowest, lowest tenth percentile, lowest quartile, median, highest quartile, highest tenth percentile, and highest $PM_{2.5}$ values in Figure 6-109 for four three-month averaging periods (January-March, April-June,

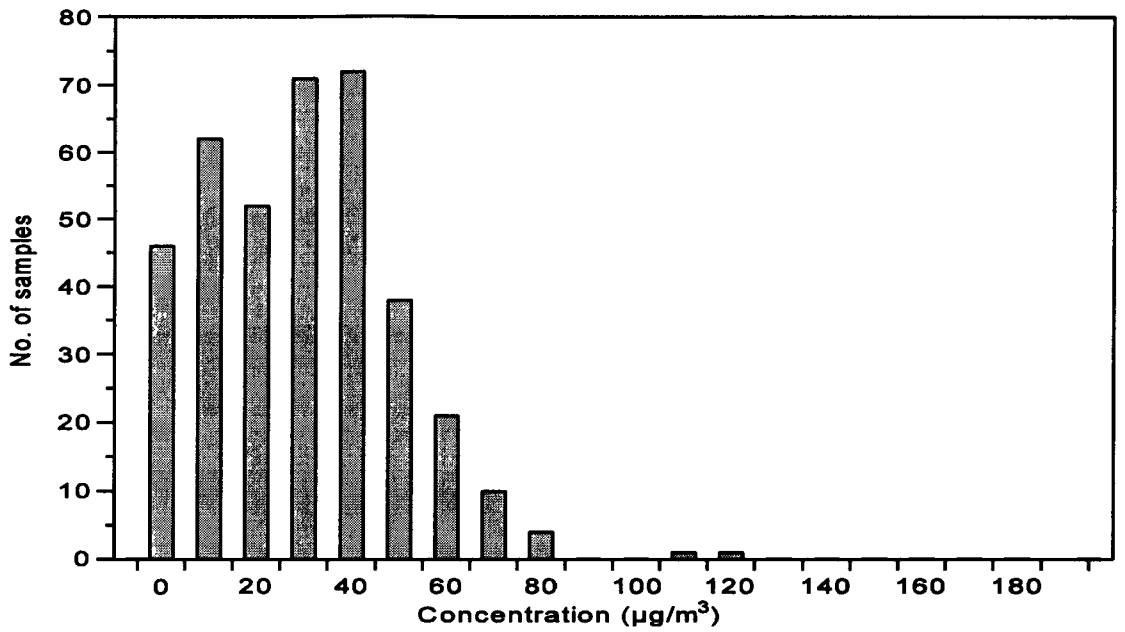

Figure 6-107. Frequency distribution of $PM_{(10-2.5)}$ concentrations measured at the Riverside-Rubidoux site.

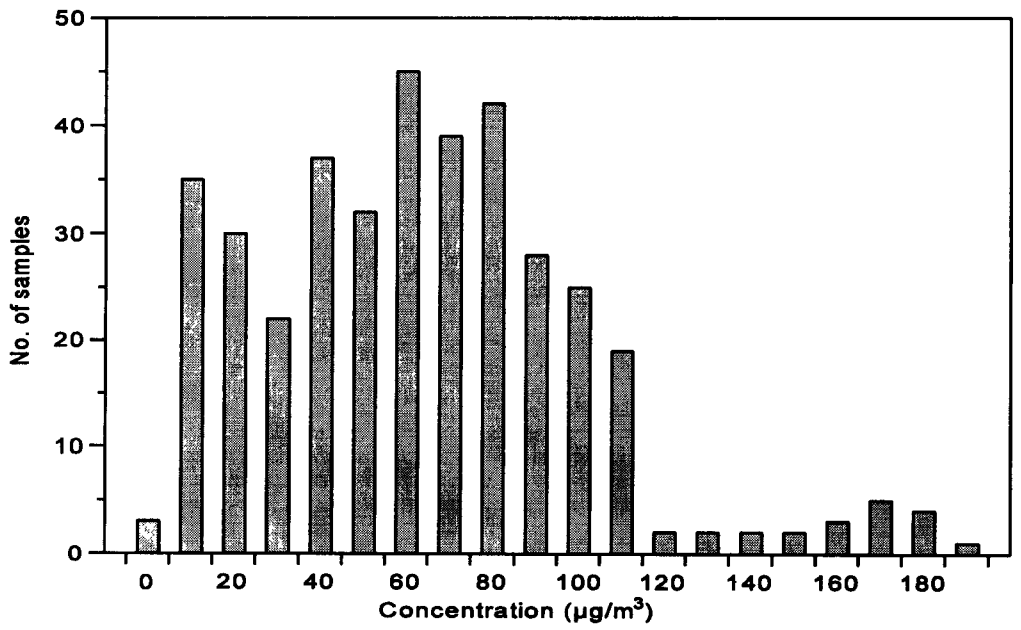

Figure 108. Frequency distribution of PM_{10} concentrations calculated as the sum of $PM_{2.5}$ and $PM_{(10-2.5)}$ masses measured at the Riverside-Rubidoux site.

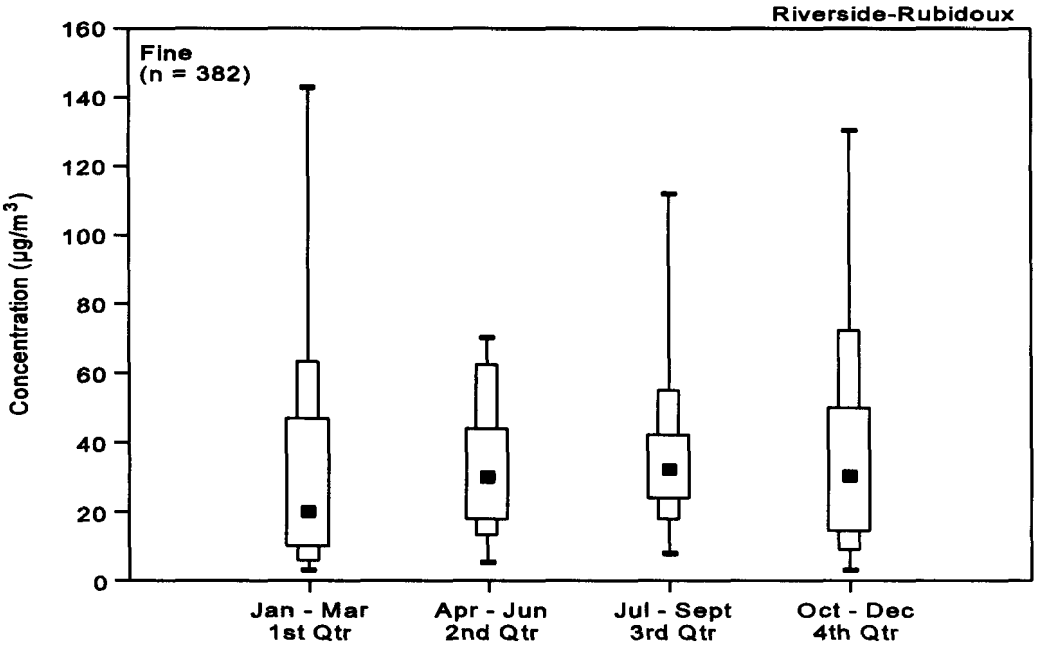

Figure 6-109. Concentrations of $PM_{2.5}$ measured at the Riverside-Rubidoux site. The data show the lowest, lowest tenth percentile, lowest quartile, median (black squares), highest quartile, highest tenth percentile, and highest $PM_{2.5}$ values.

July-September, October-December). Data for $PM_{(10-2.5)}$ and reconstructed PM_{10} are similarly plotted in Figures 6-110 and 6-111. As can seen from these figures, variability in concentrations within an averaging period is high. Differences between median and maximum $PM_{2.5}$ levels range from 40 $\mu g/m^3$ during the spring to 123 $\mu g/m^3$ during the winter, while differences between median and maximum $PM_{(10-2.5)}$ levels range from 23 $\mu g/m^3$ during winter to 83 $\mu g/m^3$ during summer. Variations in both size fractions combine to yield differences between median and maximum PM_{10} levels ranging between 83 $\mu g/m^3$ and 136 $\mu g/m^3$. Median $PM_{2.5}$ levels do not show a clear seasonal cycle. However, $PM_{(10-2.5)}$ concentrations show a maximum during the summer which causes a weak maximum in PM_{10} levels. In fact, median $PM_{2.5}$ (30 $\mu g/m^3$) and $PM_{(10-2.5)}$ (34 $\mu g/m^3$) levels are identical during the spring and fall quarters. The ratio of $PM_{2.5}$ to PM_{10} mass throughout the measurement period was 0.48 $\pm$ 0.13 and $PM_{2.5}$ and PM_{10} levels were moderately correlated ($r = 0.47$).

An examination of the data from Philadelphia, PA and Riverside, CA indicates that substantial differences exist in aerosol properties between widely separated geographic

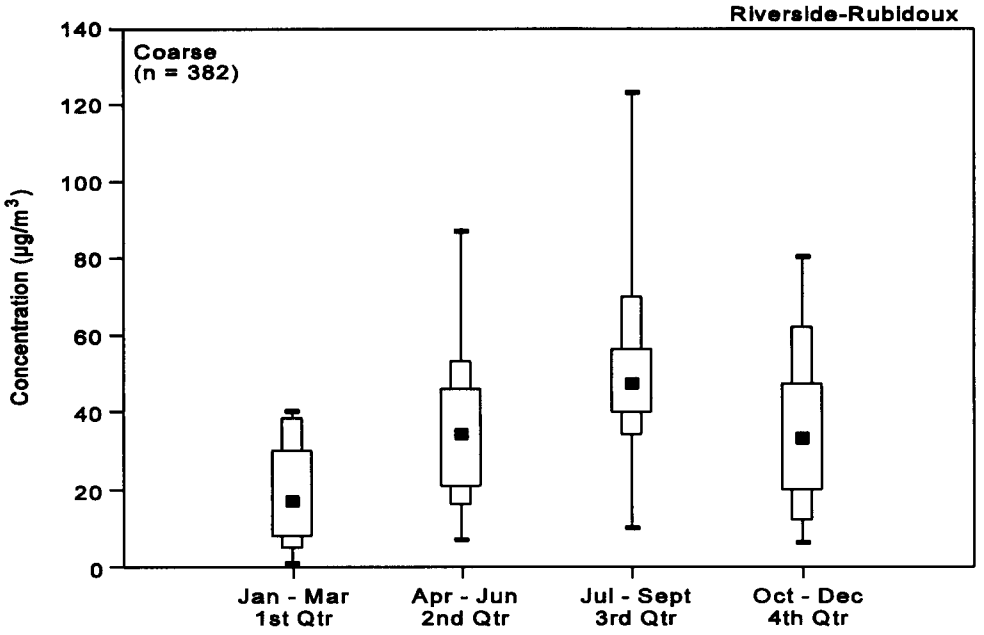

Figure 6-110. Concentrations of $PM_{(10-2.5)}$ measured at the Riverside-Rubidoux site. The data show the lowest, lowest tenth percentile, lowest quartile, median (black squares), highest quartile, highest tenth percentile, and highest PM_{coarse} values.

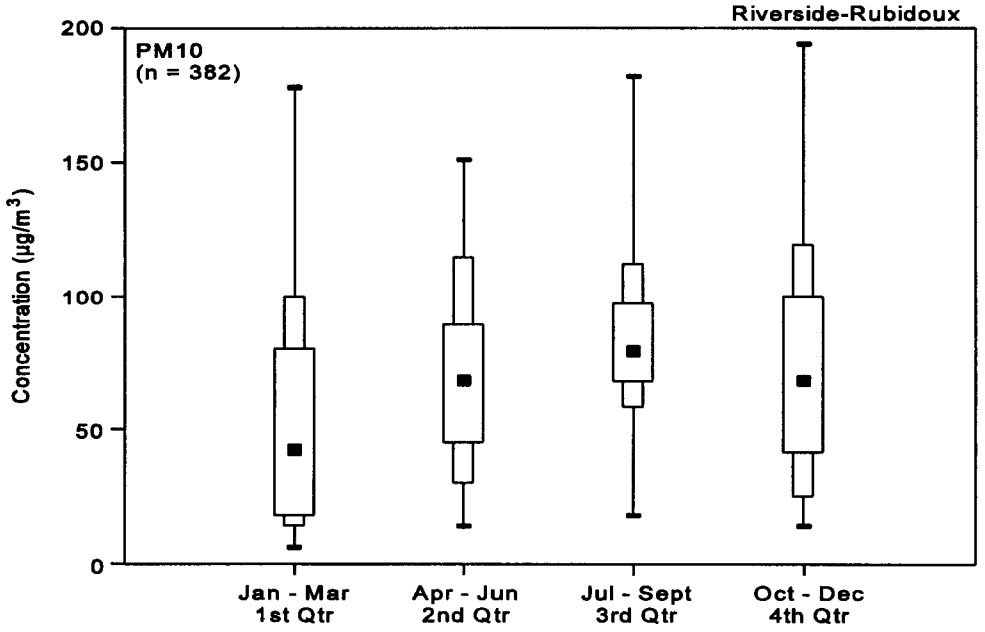

Figure 6-111. Concentrations of PM_{10} measured at the Riverside-Rubidoux site. The data show the lowest, lowest tenth percentile, lowest quartile, median (black squares), highest quartile, highest tenth percentile, and highest PM_{10} values.

regions. Fine mode particles make up most of the PM_{10} mass observed in Philadelphia and appear to drive the daily and seasonal variability in PM_{10} concentrations there. Coarse mode particles are a larger fraction of PM_{10} mass in Riverside and drive the seasonal variability in PM_{10} seen there. The range in the seasonal variation of the ratio of $PM_{2.5}$ to PM_{10} mass is much smaller in Philadelphia (0.70 to 0.75) than in Riverside (0.41 to 0.57) for the four averaging periods used. Differences between median and maximum concentrations in any size fraction are much larger at the Riverside site than at the Philadelphia site. Many of these differences could reflect the more sporadic nature of dust suspension at Riverside. These considerations demonstrate the hazards in extrapolating conclusions about the nature of variability in aerosol characteristics inferred at one location to another.

6.10.2 Fine and Coarse Particulate Matter Trends and Relationships

6.10.2.1 Visual Range/Haziness

Observations of visual range, obtained by the National Weather Service and available through the National Climatic Data Center of the National Oceanic and Atmospheric Administration, provide one of the few truly long-term, daily records of any parameter related to air pollution. After some manipulation, the visual range data may be used as an indicator of fine mode particle pollution. The data reduction process and analyses of resulting trends have been reported by Husar et al. (1994), Husar and Wilson (1993), and Husar et al. (1981).

Visual range i.e., the maximum distance at which an observer can discern the outline of an object, is an understandable and for many purposes an apporpriate measure of the optical environment. It has the disadvantage, however, of being inversely related to aerosol concentration. It is usual, therefore, to convert visual range to a direct indicator of fine mode. particle concentration. The quantitative measure of haziness is the extinction coefficient, B_{ext}, defined as B_{ext}=K/visual range, where K is the Koschmieder constant. The value of K is determined both by the threshold sensitivity of the human eye and the initial contrast of the visible object against the horizon sky. Husar et at. (1994) use K=1.9 in accordance with the data by Griffing (1980). The extinction coefficient is in units of km^{-1} and is proportional to the concentration of light scattering and absorbing aerosols and gases. The radiative transfer

characteristics which determine the visual range depend on time of day. Only local noon observations are used.

Haze Trend Summary

The U.S. haze patterns and trends since 1960 are presented in 16 haze maps that represent four time periods and four seasons (Figure 6-112). The selected time periods are 5 year averages centered at 1960, 1970, 1980, and 1990. The quarters are calendrical, i.e., winter is January, February, and March. View horizonally for secular trends by quarter. View vertically for seasonal variation by decade.

The overall national view shows two large contiguous haze regions, one over the eastern U.S. and another over the western Pacific states. The two haze regions are divided by a low-haze territory between the Rocky Mountains and the Sierra-Cascade mountain ranges. This general pattern is preserved over the past 30-year period. However, notable trends have occurred over both the western and eastern haze regions.

The haziness in the western Pacific states covers all of the coastal states, with California having the highest values. In the 1960s a large fraction of western California was very hazy, particularly during Quarters 1 and 4. By the 1990s the magnitude of the Pacific Coast haziness has declined markedly for all seasons.

The eastern haze region extends from the East Coast to the Rocky Mountains. The western boundary of the eastern haze region has been markedly constant over both the seasons and the years. In fact, haze in the mid-section of the U.S., extending from the Rocky Mountains to the Mississippi River, has changed little over the 30-year history.

The most dynamic pattern can be observed over the eastern U.S., extending from the Mississippi River to the East Coast. The eastern U.S. shows a significant seasonal variation. There is also a significant trend over the past 30 years. Furthermore, these seasonal and secular (long-term) trends are different for sub-regions within the eastern U.S., such as the Northeast, Mid-Atlantic and Gulf States regions.

In the 1960s, the highest extinction values were recorded for the cold season (Q1, Q4), with significantly lower values for the warm quarters (Q2, Q3). The remarkable reduction in haziness during the cold season and the strong increase during the warm season has shifted the

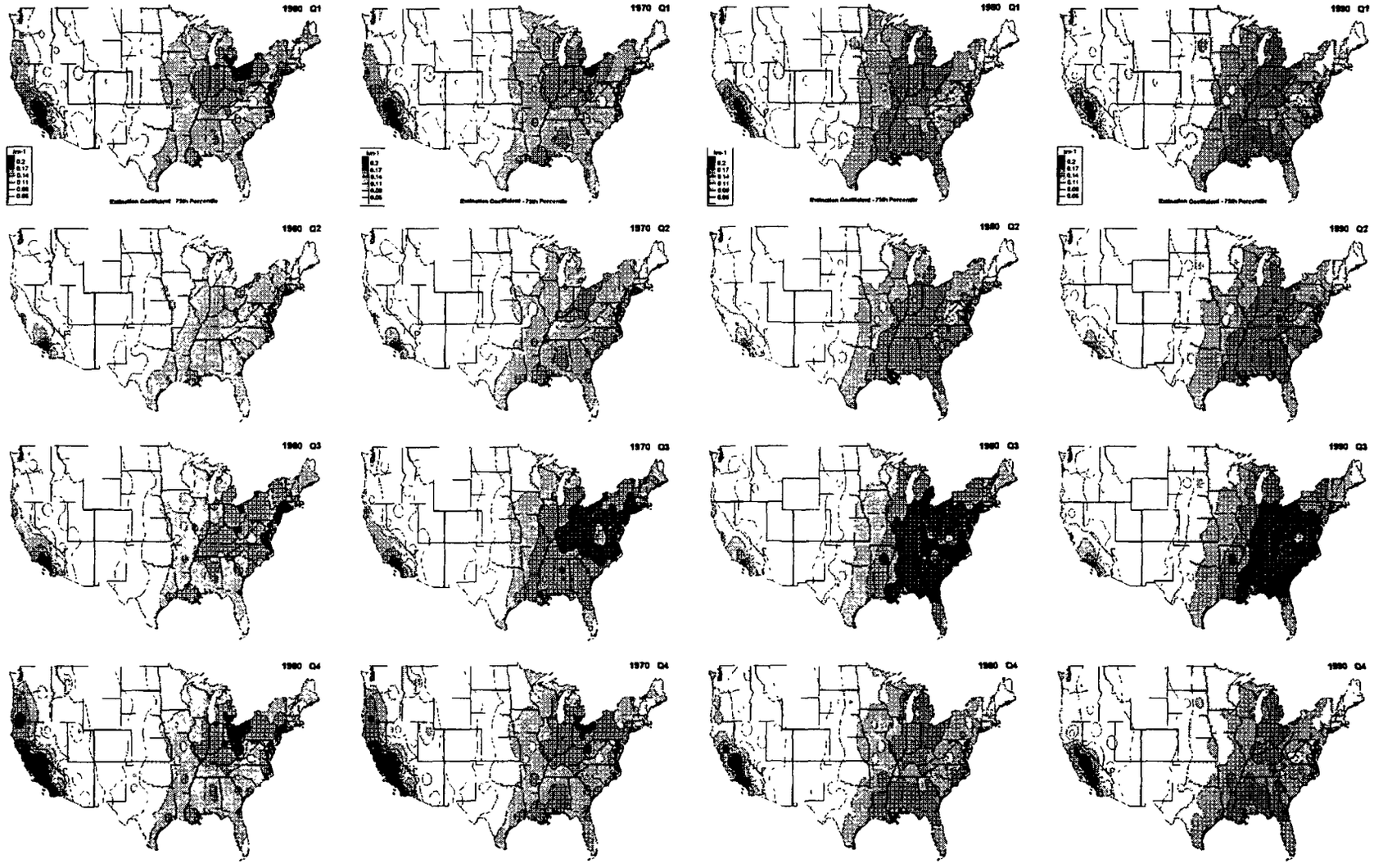

Figure 6-112. United States trend maps for the 75th percentile extinction coefficient, B_{ext} for winter (Q1), spring (Q2), summer (Q3), and fall (Q4). Bext [km^{-1}] is derived from visual range, VR, data by B_{ext}=1.9/VR. Data obtained during natural obstructions to vision (i.e., rain, snow, fog) were eliminated.

haze peak from winter to summer. This seasonal change has been accompanied by a regional shift in highest haze pattern. In the 1960s, the worst haziness occurred around Lake Erie and the New York-Washington megalopolis, during the cold season. By the 1990s the area with the worst haze had shifted southward toward Tennessee and Carolinas and occurred in the summer season.

The decade of the 1980s shows less change than the earlier decades. However, there has been a continued haze reduction in the Northeast, north of the Ohio and east of the Mississippi Rivers. The southeastern U.S. as well as the Pacific states remained virtually unchanged in the 1980s.

Regional Pattern

Trends for specific regions in the eastern U.S., and the number and location of visual range reporting stations for each region, are shown in Figure 6-113. The trend graphs represent the 75th percentile of B_{ext} for the stations located within the designated region. The trends are presented for Quarters 1 (winter) and 3 (summer) separately. The northwestern U.S. exhibits an increase of Quarter 3 haze between 1960 and 1970, and a steady decline between 1973 (0.22) and 1992 (0.12). In the winter quarter the haziness has steadily declined from 0.15 to 0.10 in the 30-year period. The Mid-Atlantic region that includes the Virginias and Carolinas shows a strong summer increase between 1960 and 1973, followed by a decline. The winter haze was virtually unchanged over the 30-year period. The haziness over the Gulf states increased between 1960 and 1970, and remained virtually unchanged since then. The central Midwest including Missouri and Arkansas exhibit virtually no change during the winter season and a slight increased in the summer (1960-1970). The upper Midwest (Figure 14) shows an opposing trend for summer and winter. While summer haze has increased, mostly 1960-1973, the winter haze has declined.

6.10.2.2 IMPROVE

The National Park Service-EPA monitoring network for Class I areas is designed to monitor visibility in national parks and other designated areas. Most of these are remote. However, data from two southeastern sites, Shenandoah National Park and the Great Smoky

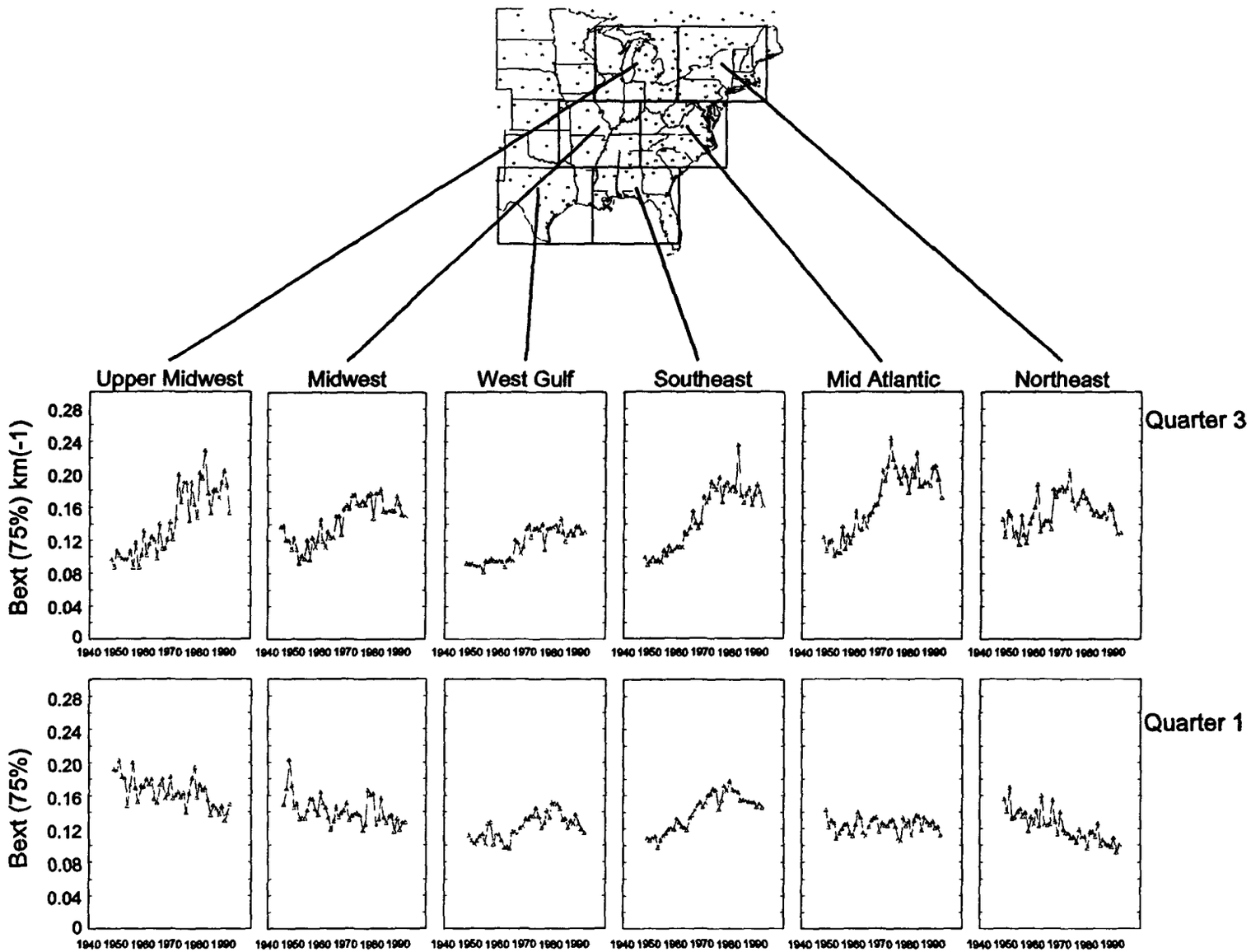

Figure 6-113. Secular haze trends (1960 to 1992) for six eastern U.S. regions, summer (Q1) and winter (Q3)

Mountains National Park, provide useful information on the regional background of sulfate (Eldred and Cahill, 1994; Cahill et al., 1996b). As shown in Figure 6-114, there is a distinct increase in sulfate. This increase can be correlated with increases in SO_2 emissions in the summer from power plants in the Tennessee Valley (Cahill et al., 1996b). The increased emissions may be related to an increase in demand for power for air conditioning. The increase in regional background will impact urban centers along the eastern U.S. Visibility measurements over the northeastern U.S. show an increase in haze from 1960 to 1970 in both winter and summer. Between 1970 and 1983, there was a decrease in haze in the winter but little change during the summer (Husar and Wilson, 1993; Husar et al., 1994). Concern has been expressed that the indicated trends may have been impacted, or even produced, by changes in monitoring protocols (White, 1996a,b). However, these issues have been addressed by Cahill et al. (1996b).

6.10.2.3 Philadelphia

Philadelphia is of special interest because of the extensive monitoring conducted there and the use of Philadelphia data in epidemiological studies. Extensive measurements of TSP have been conducted in Philadelphia. Several data sets have been combined to give an indication of long-term trends in Philadelphia (Figure 6-115). The TSP data set was construed from the AIRS data base (Wyzga and Lipfert , 1996; Li and Roth, 1995). There was a steady decrease in TSP from 1973 to 1983 with variable but slightly increasing TSP levels between 1983 and 1990.

Fine PM was estimated from the Inhalable Particle Network (Rodes and Evans, 1985) from 1980 to 1983, from AIRS (AIRS, 1995), from 1987 to 1990, and from the Harvard Data Base (Koutrakis, 1996) for 1993 and 1994. During the period 3/79 to 12/83, the Inhalable Particulate Network conducted measurements in Philadelphia with dichotomous samplers. These used 15 μm upper cut points except for a period at the end of the study (3/82 to 12/83) when two co-located PM_{10} samplers were run at one site. The IPN data set allows construction of four annual averages for 1980 through 1983 by averaging $PM_{2.5}$ data from $PM_{15}/PM_{2.5}$ dichotomous samplers from the several IPN sites across Philadelphia. These are shown in Figure 6-115, along with the one year of $PM_{2.5}$ data from $PM_{10}/PM_{2.5}$ dichotomous samplers at the South Broad St. site.

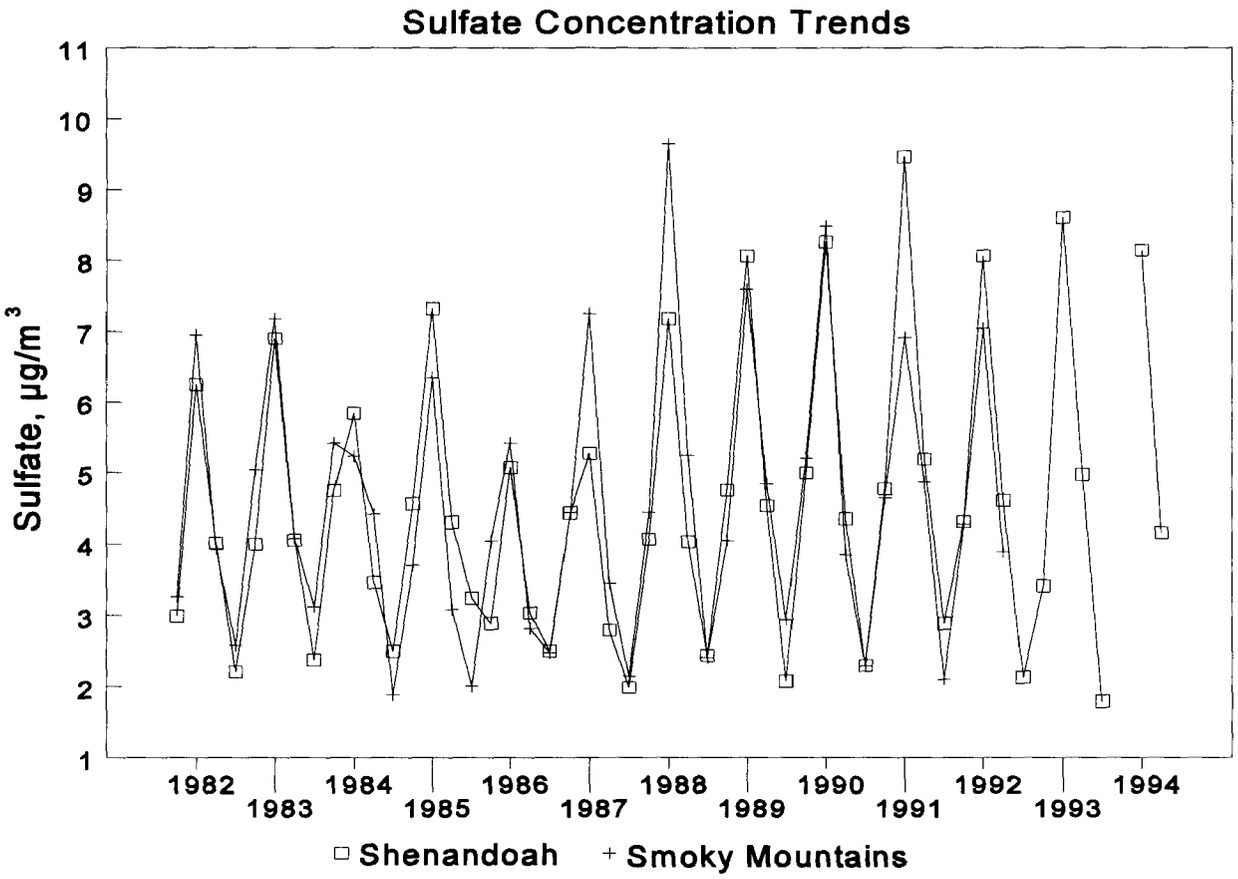

Figure 6-114. Eastern U. S. regional background trend of sulfate indicated by seasonal trend data from Shenadoah and Great Smoky Mountains National Parks.

A $PM_{10}/PM_{2.5}$ dichotomous sampler, run in the Philadelphia area from 1987 through 1990 allows annual averages of $PM_{2.5}$ for those years to be added to Figure 6-115. Harvard University measured PM_{10} and $PM_{2.5}$ at the Presbyterian Home site from 5/92 to 5/92 allowing annual averages for 93 and 94 to be added to the graph. Since $PM_{2.5}$ is expected to be relatively uniform across Philadelphia (Wilson and Suh, 1996), this data can be used to estimate a $PM_{2.5}$ trend from 1979 to 1994. A downward trend is indicated.

The samplers were not at the same sites during the different time periods. Since $PM_{(10-2.5)}$ does not seem to be uniform across Philadelphia (Wilson and Suh, 1996), no PM_{10} or $PM_{(10-2.5)}$ trend could be constructed. Comparisons of PM_{10} and $PM_{(10-2.5)}$ and $PM_{2.5}/PM_{10}$ (Figure 6-116) for 1983 and 1993 are shown. Differences in $PM_{(10-2.5)}$ and the ratio of

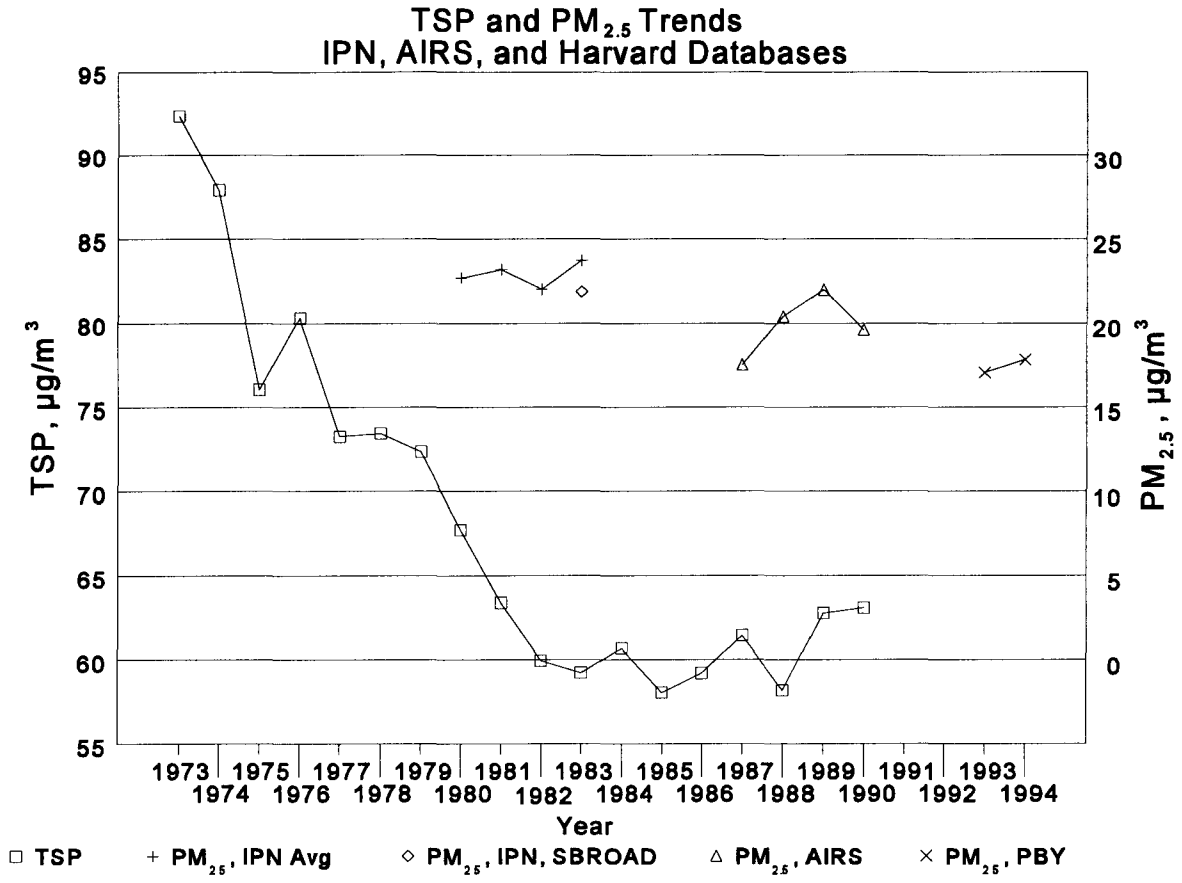

Figure 6-115. TSP and $PM^{2.5}$ trend data for the city of Philadlphia from AIRS, IPN, and Harvard database.

$PM_{2.5}/PM_{10}$ may represent geographical differences in the coarse fraction of PM_{10} as well as relative changes in $PM_{2.5}$ and $PM_{(10-2.5)}$.

6.10.2.4 Harvard Six-Cities Study

During 1979 to 1986, the Harvard School of Public Health measured particulate matter in 6 cities in eastern and central United States (Spengler et al., 1986b; Neas, 1996). Means and 90th percentiles for fine, coarse, PM_{15}, and TSP are shown in Figures 6-117 to 6-119. (Measurements were made with dichotomous samplers with a 15 μm diameter cut point from 1979 to 1984 and with a 10μm diameter cut point from 1984 to 1986. The coarse fractions of PM_{10} and PM_{15} were not significantly different during the overlapping year.) In the dirtier cities, Steubenville, St. Louis, and Harrison, there were decreases in all PM indicators, especially in the earlier years.

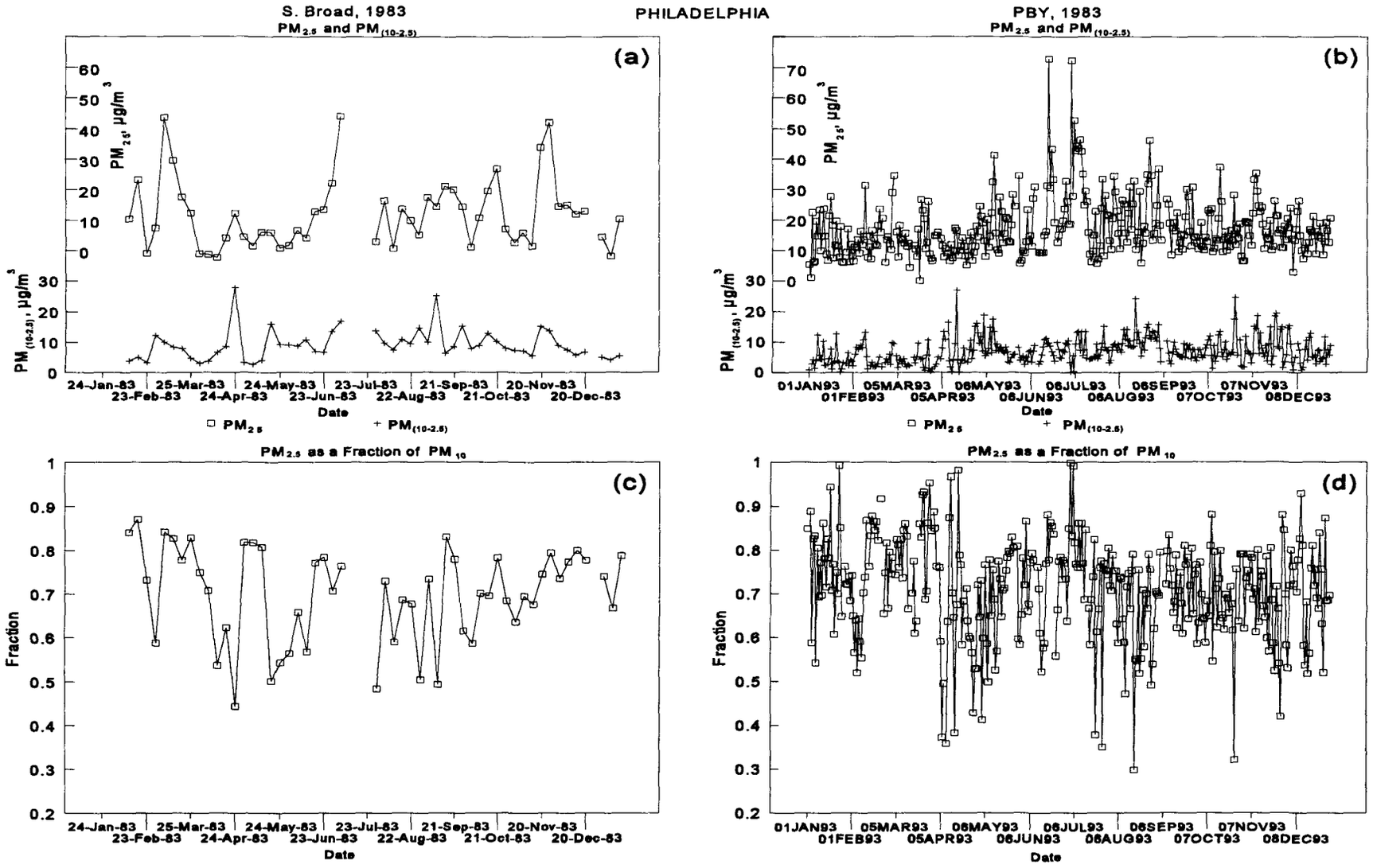

Figure 6-116. Comparison of fine and coarse particle parameters in Philadelphia in 1983 and 1993: (a) $PM_{2.5}$ and $PM_{(10-2.5)}$ at South Broad St. site, 1983; (b) $PM_{2.5}/PM_{10}$ at South Broad St. site, 1983; (c) $PM_{2.5}$ and $PM_{(10-2.5)}$ at Presbyterian Home site, 1993; (d) $PM_{2.5}/PM_{10}$ at Presbyterian Home Site, 1993.

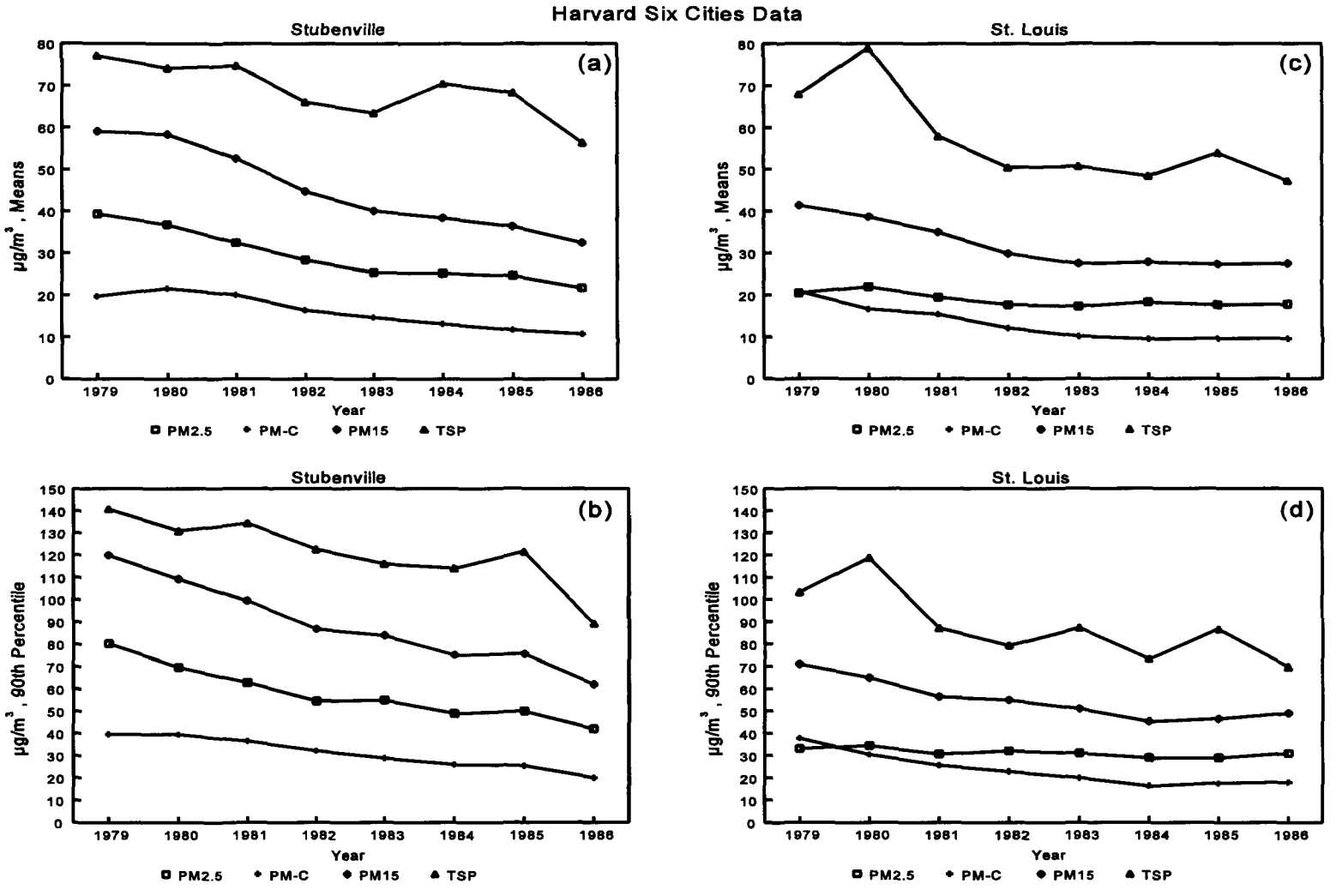

Figure 6-117. Trend data from the Harvard Six-Cities Study: (a) Steubenville, fine, coarse, PM_{15}, and TSP means; (b) Steubenville, fine, coarse, PM_{15}, and TSP 90th percentiles; (c) St. Louis, fine, coarse, PM_{15}, and TSP means; (d) St. Louis, fine, coarse, PM_{10}, and TSP 90th percentiles.

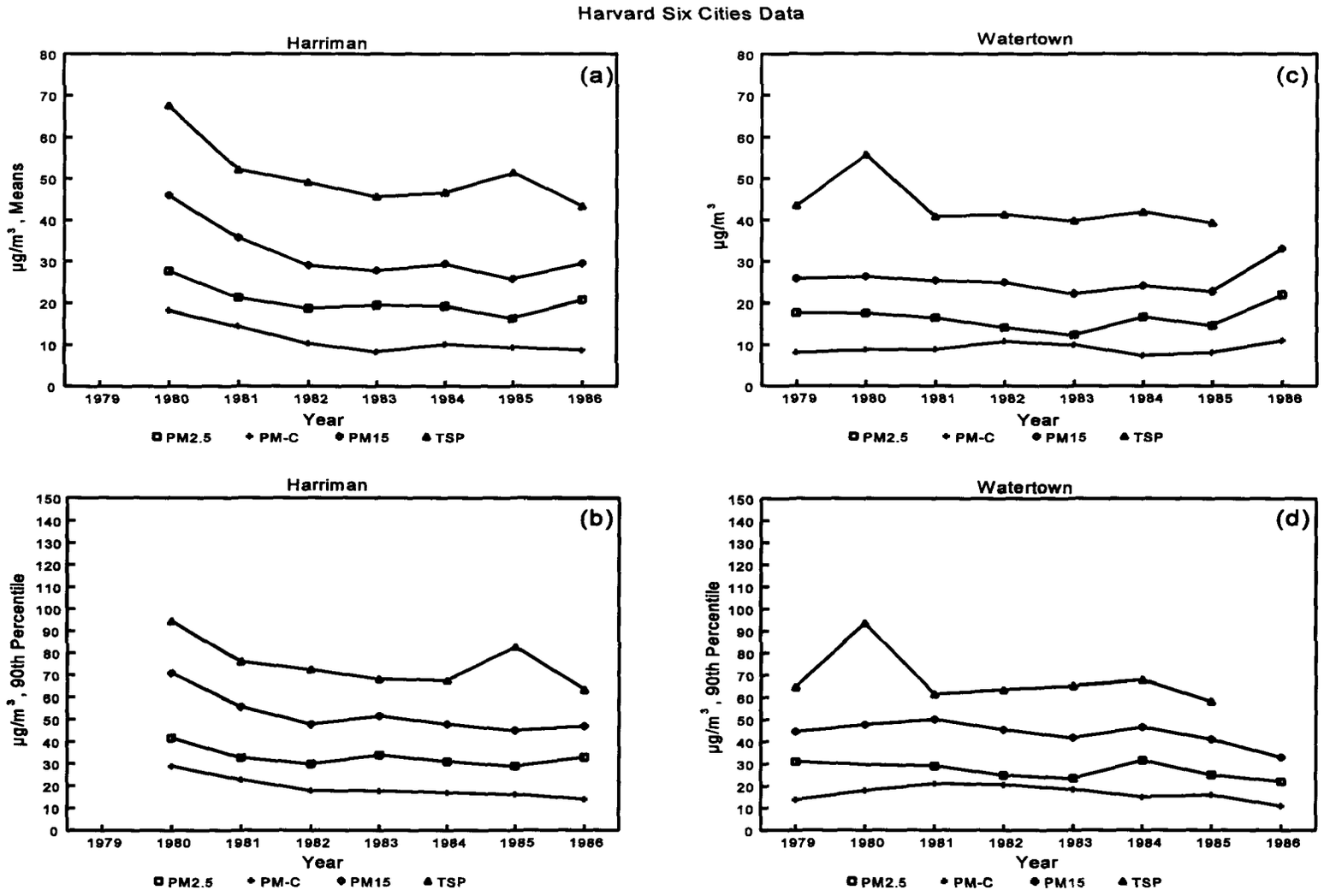

Figure 6-118. Trend data from the Harvard Six-Cities Study: (a) Harriman, fine, coarse, PM_{15}, and TSP means; (b) Harriman, fine, coarse, PM_{15}, and TSP 90th percentiles; (c) Watertown, fine, coarse, PM_{15}, and TSP means; (d) Watertown, fine, coarse, PM_{15}, and TSP 90th percentiles.

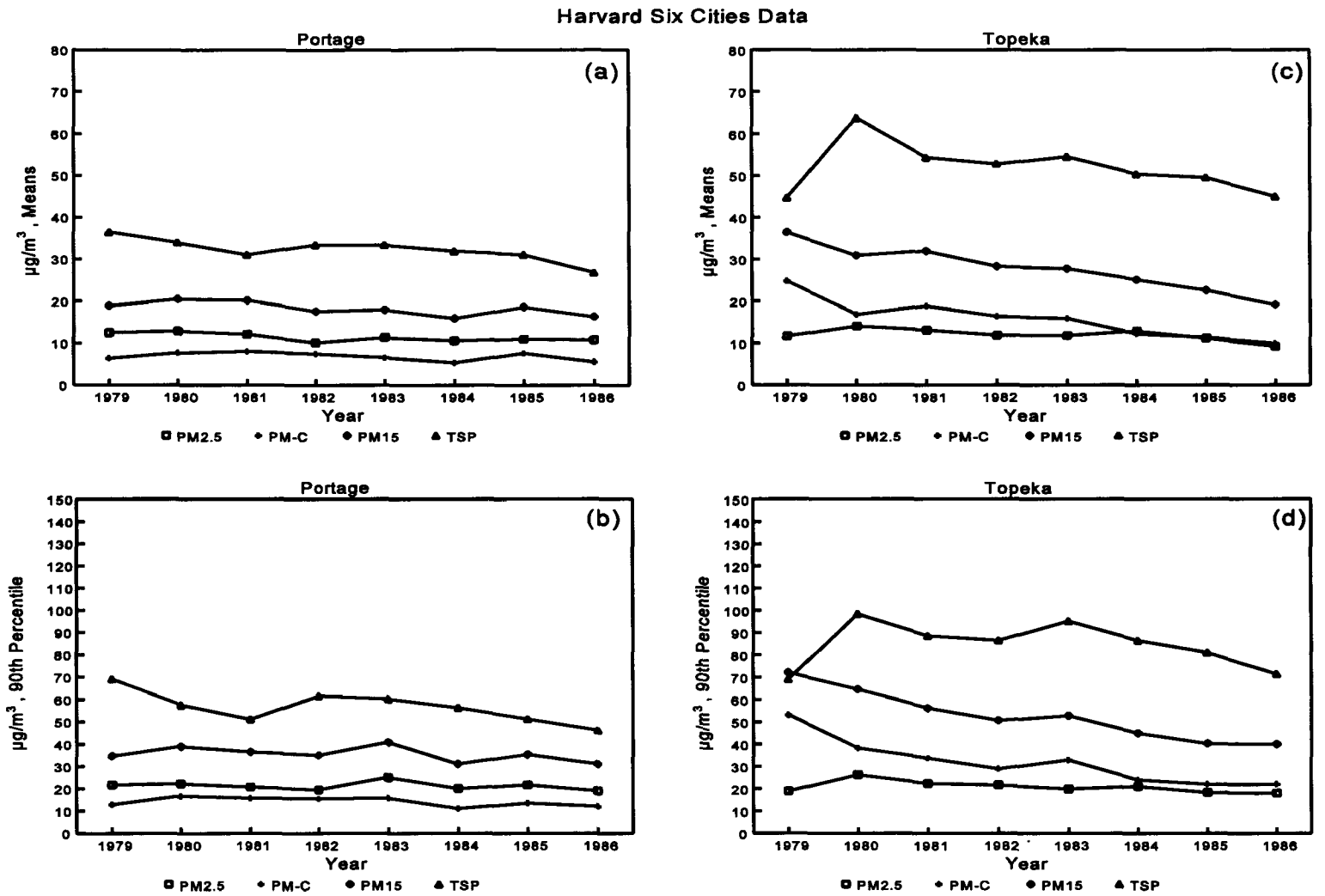

Figure 6-119. Trend data from the Harvard Six-City Study: (a) Portage, fine, coarse, PM_{15}, and TSP means; (b) Portage, fine, coarse, PM_{15}, and total TSP 90th percentiles; (c) Topeka, fine, coarse, PM_{15}, and TSP means; (d) Topeka, fine, coarse, PM_{15}, and TSP 90th percentiles.

There was also an apparent decrease in Topeka, one of the cleaner cities. No trend can be discerned in Watertown or Portage. It is difficult to determine whether there was a greater trend in fine or coarse particles.

6.10.2.5 AIRS

The AIRS data base was searched for sites with 4 or more years of fine and coarse data (AIRS, 1995). Five such sites were found. Values for the mean and the 90th percentile are shown in Figures 6-120 to 6-123. No significant trends are evident in $PM_{2.5}$ or $PM_{(10-2.5)}$ either in the means or the 90th percentile values. PM_{10} and $PM_{(10-2.5)}$ at the dirtier site in New York City do appear to have decreased from 1988 to 1992 but to have increased between 1992 and 1994.

6.10.2.6 California Sites

The California Air Resources Board conducted dichotomous sample measurements, every sixth day, beginning in 1989 at a number of California sites (CARB, 1995). Some results from 8 sites are shown in Figures 6-124 to 6-130. The means (Panel a) and 90th percentile values (Panel b) are given for $PM_{2.5}$, $PM_{(10-2.5)}$, and PM_{10}. Most of the sites show slight downward trends for PM_{10} and both $PM_{2.5}$ and $PM_{(10-2.5)}$.

The California sites are of special interest because of the substantial seasonal and daily variability. The individual every-sixth-day values are plotted for 1991 (plus 1 day in the preceeding and following years)(Panel c). Strong seasonal and daily variation are evident. Based on the every-sixth-day measurements, it would appear that the day-to-day variability at the California sites is higher than in Philadelphia. Also shown is the $PM_{2.5}$ fraction of PM_{10} (Panel d). These ratios are also show a strong seasonal variation.

6.10.3 Interrelations and Correlations

The availability of data on four PM size fractions at several sites for a number of years makes it possible to examine relationships and correlations among $PM_{2.5}$, $PM_{(10-2.5)}$, PM_{10}, and TSP. It is also possible to examine the distribution of values in the upper range and the relationship of the fine fraction to other PM parameters. Sufficient data for these purposes are

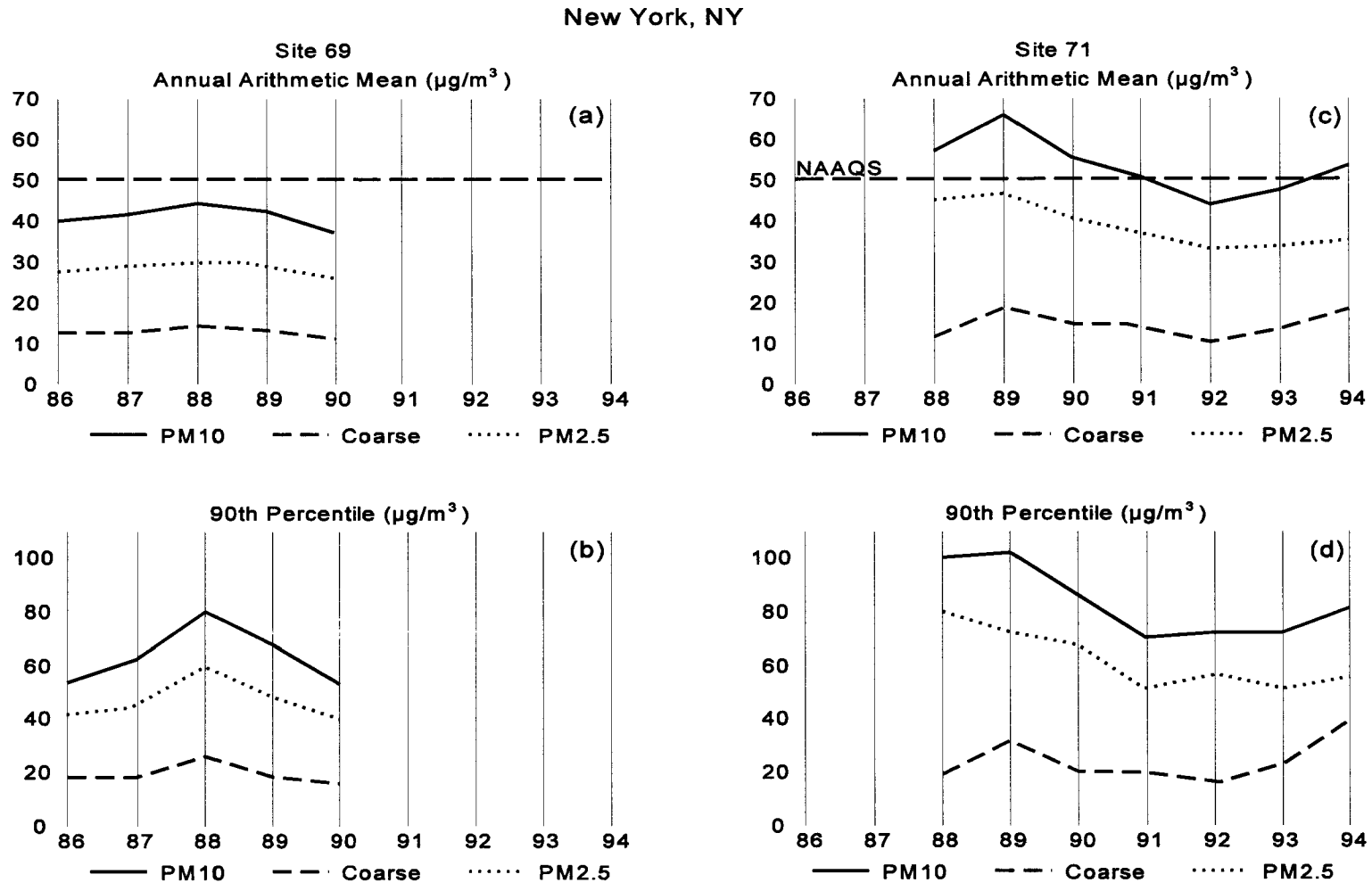

Figure 6-120. Trend data from AIRS: (a) New York City, Site 69, fine, coarse, and PM_{10} means; (b) New York City, Site 69, fine, coarse, and PM_{10} 90th percentiles; (c) New York City, Site 71, fine, coarse, and PM_{10} means; (d) New York City, Site 71, fine, coarse, and PM_{10} 90th percentiles.

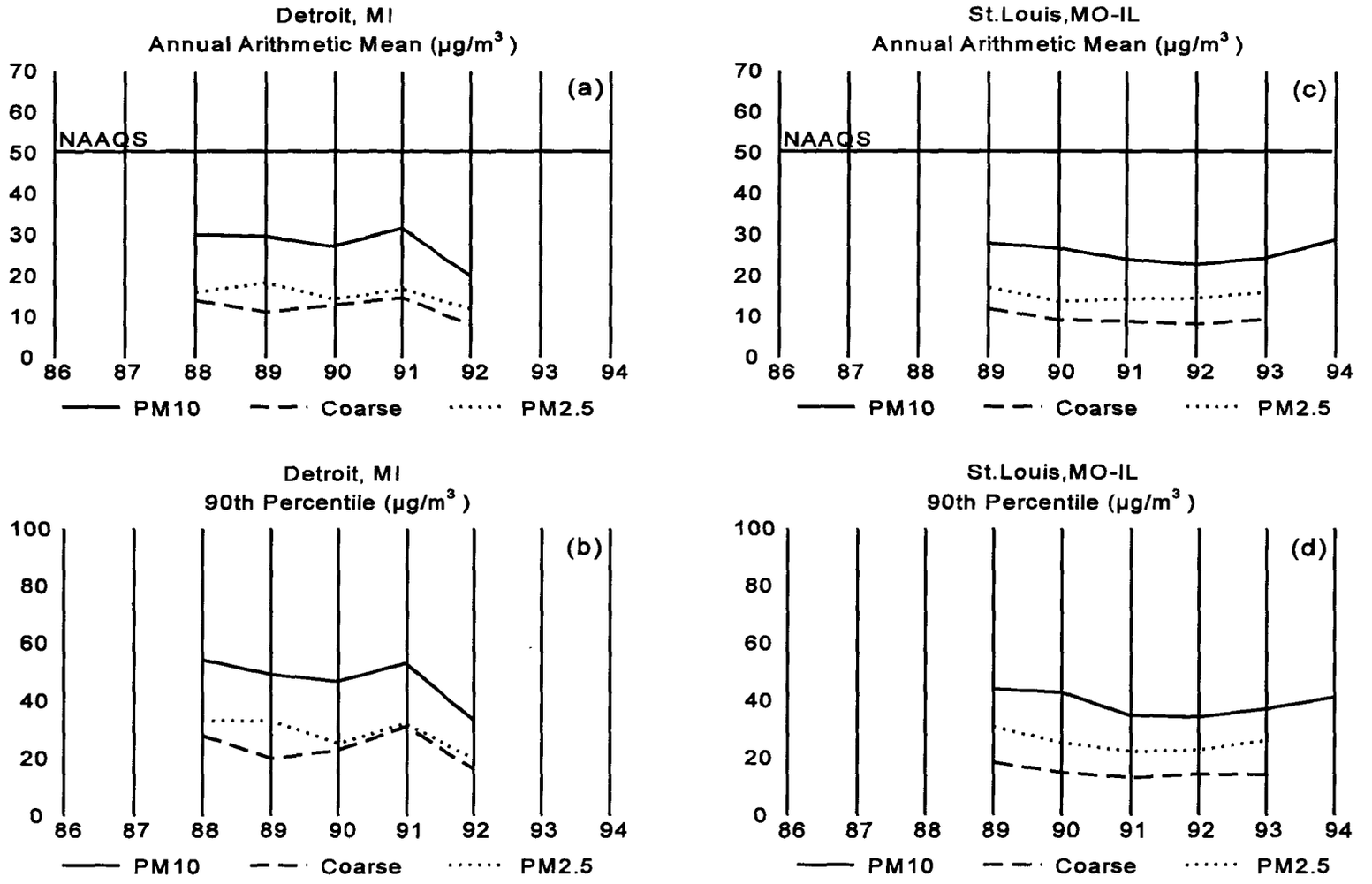

Figure 6-121. Trend data from AIRS: (a) Detroit, fine, coarse, and PM_{10} means; (b) Detroit, fine, coarse, and PM_{10} 90th percentiles; (c) St. Louis, fine, coarse, and PM_{10} means; (d) St. Louis, fine, coarse, and PM_{10} 90th percentiles.

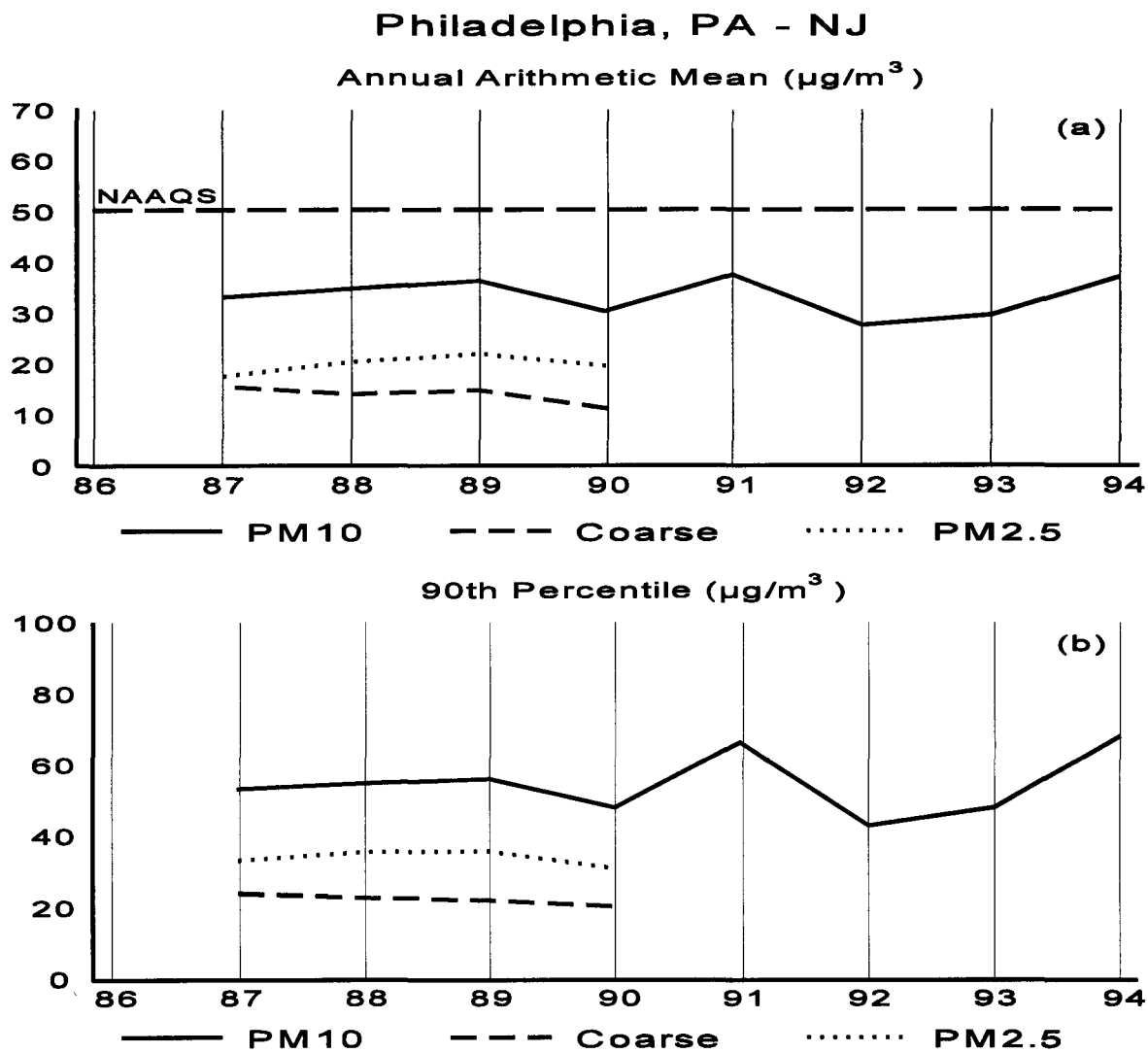

Figure 6-122. Trend data from AIRS: (a) Philadelphia, fine, coarse, and PM_{10} means; (b) Philadelphia, fine, coarse, and PM_{10} 90th percentiles.

available from several sites in California (CARB, 1995) and from Philadelphia (IPN, 1985; AIRS, 1995; Harvard 1995). However, only the Philadelphia data allows examination of the relationship of $PM_{2.5}$ and PM_{10} with TSP.

6.10.3.1 Upper Range of Concentration for Various PM Size Fractions

Some information on the upper range of concentrations and relationships among the four PM size fractions are shown in Tables 6-11 and 6-12. The maximum value; the 2nd, 3rd, 4th,

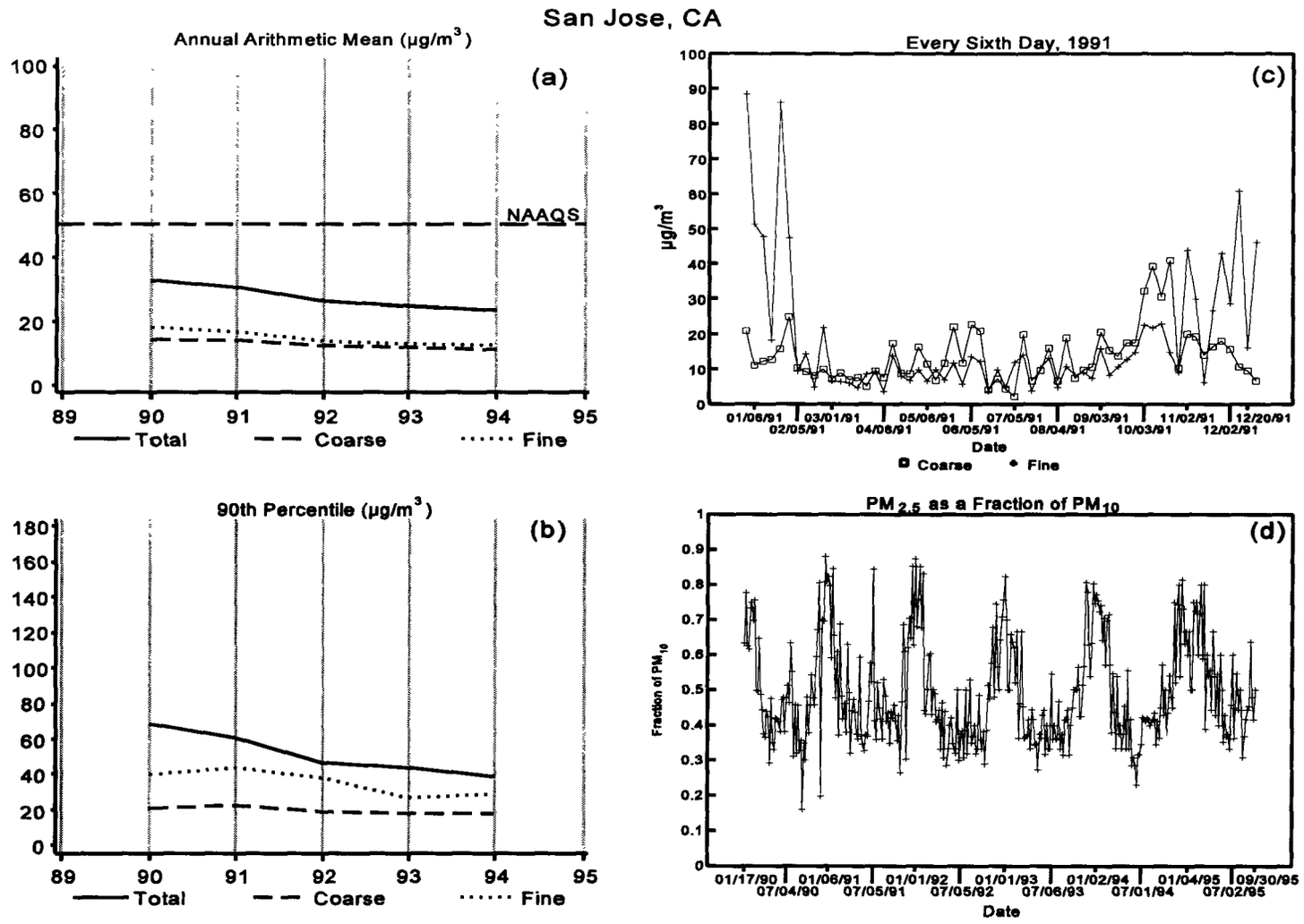

Figure 6-123. Trend data from San Jose from CARB: (a) Fine, coarse and total means; (b) Fine, coarse and total 90th percentiles; (c) Every sixth day fine and coarse mass for 1991; (d) Fine and coarse mass as a fraction of PM_{10}.

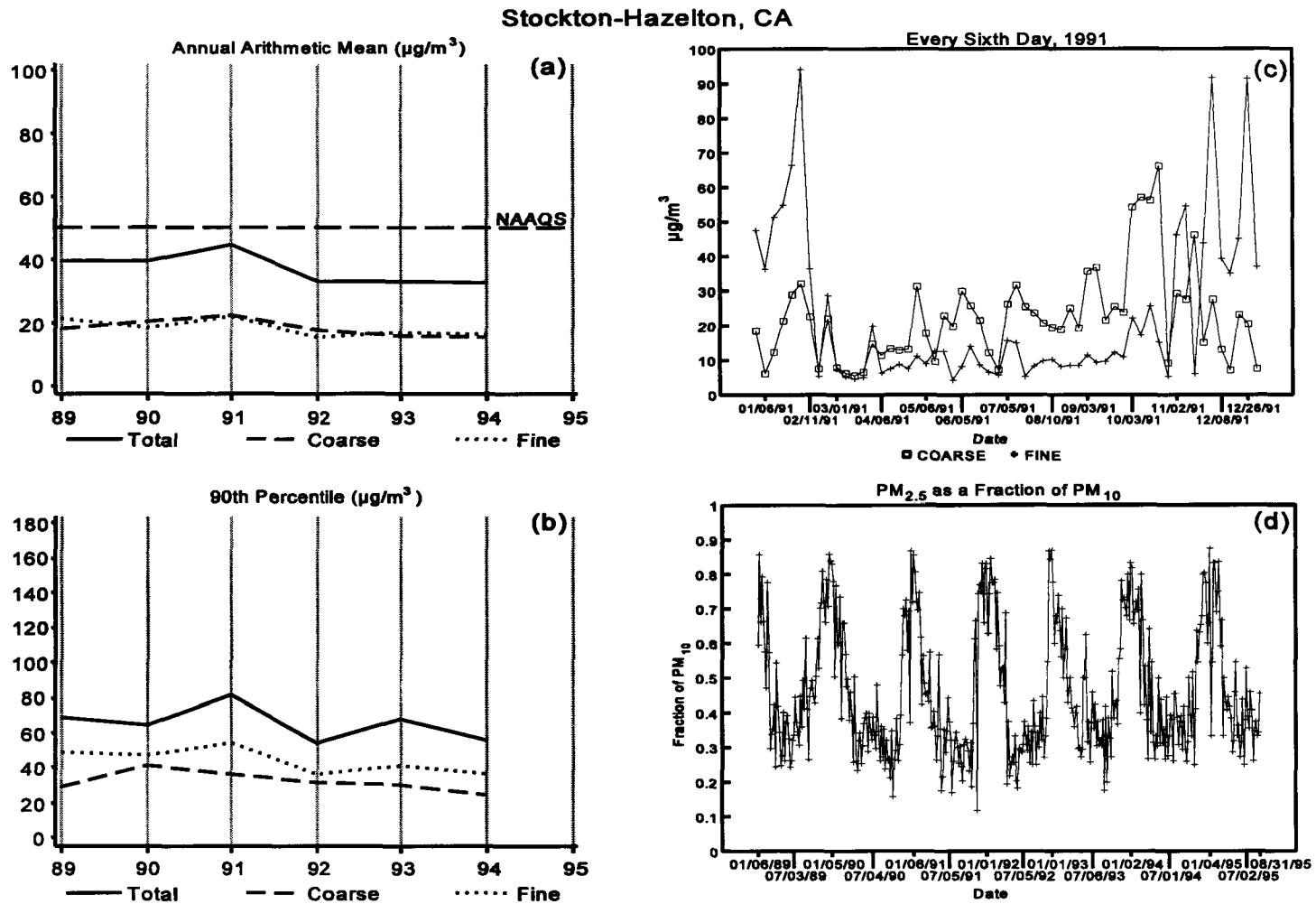

Figure 6-124. Trend data from Stockton-Hazelton from CARB: (a) Fine, coarse and total means; (b) Fine, coarse and total 90th percentiles; (c) Every sixth day fine and coarse mass for 1991; (d) Fine and coarse mass as a fraction of PM_{10}.

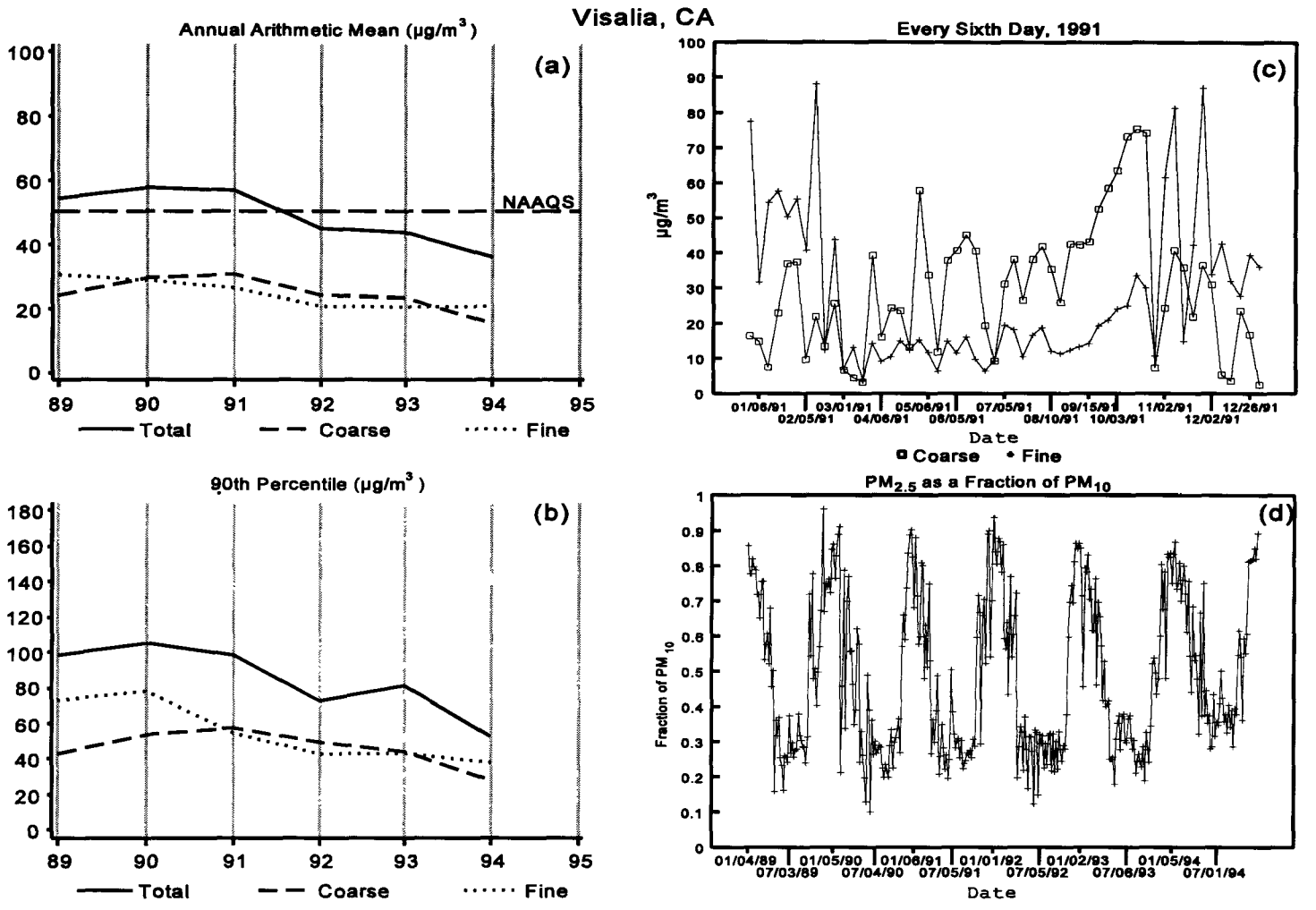

Figure 6-125. Trend data from Visalia from CARB: (a) Fine, coarse and total means; (b) Fine, coarse and total 90th percentiles; (c) Every sixth day fine and coarse mass for 1991; (d) Fine and coarse mass as a fraction of PM_{10}.

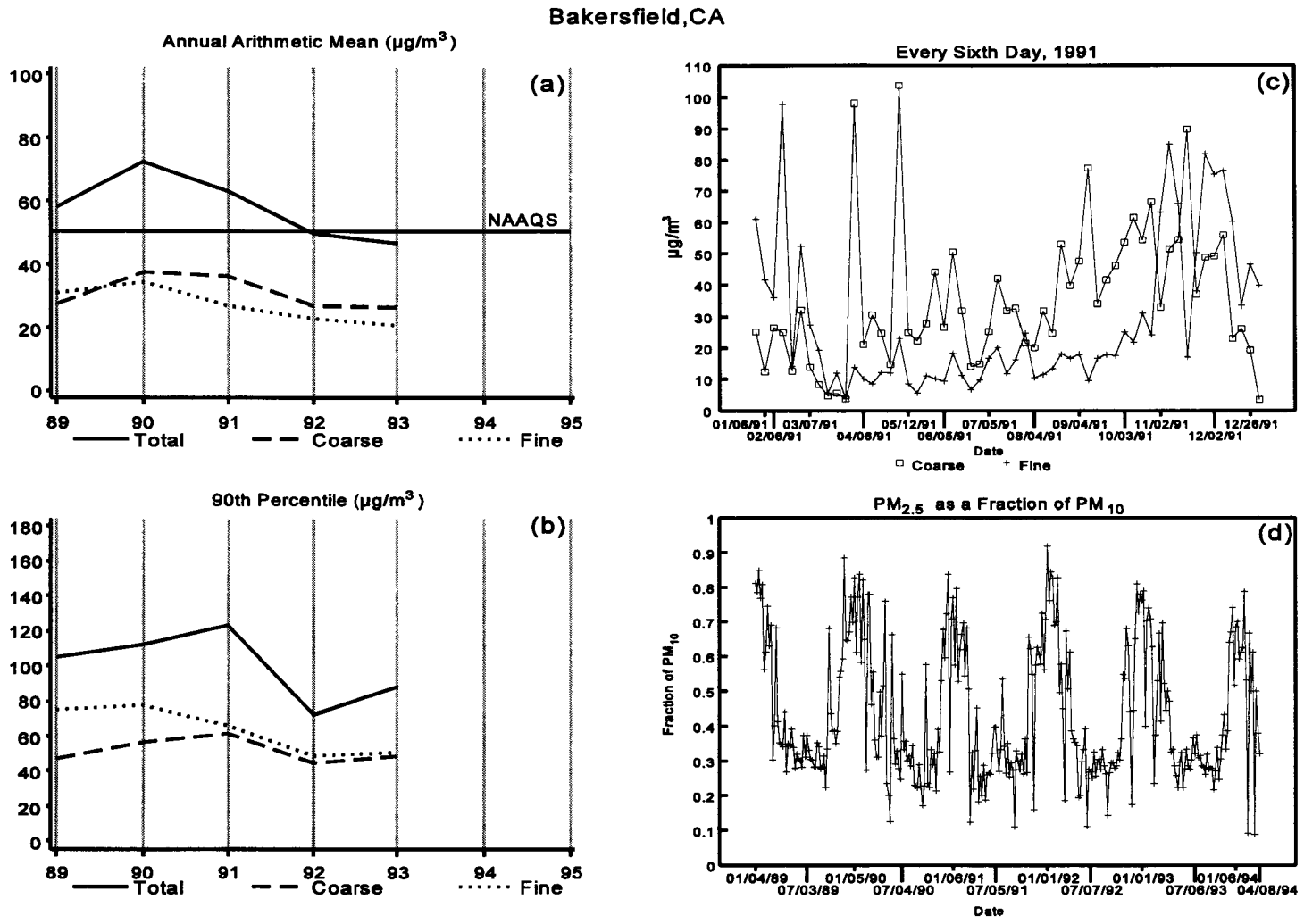

Figure 6-126. Trend data from Bakersfield from CARB: (a) Fine, coarse and total means; (b) Fine, coarse and total 90th percentiles; (c) Every sixth day fine and coarse mass for 1991; (d) Fine and coarse mass as a fraction of PM_{10}.

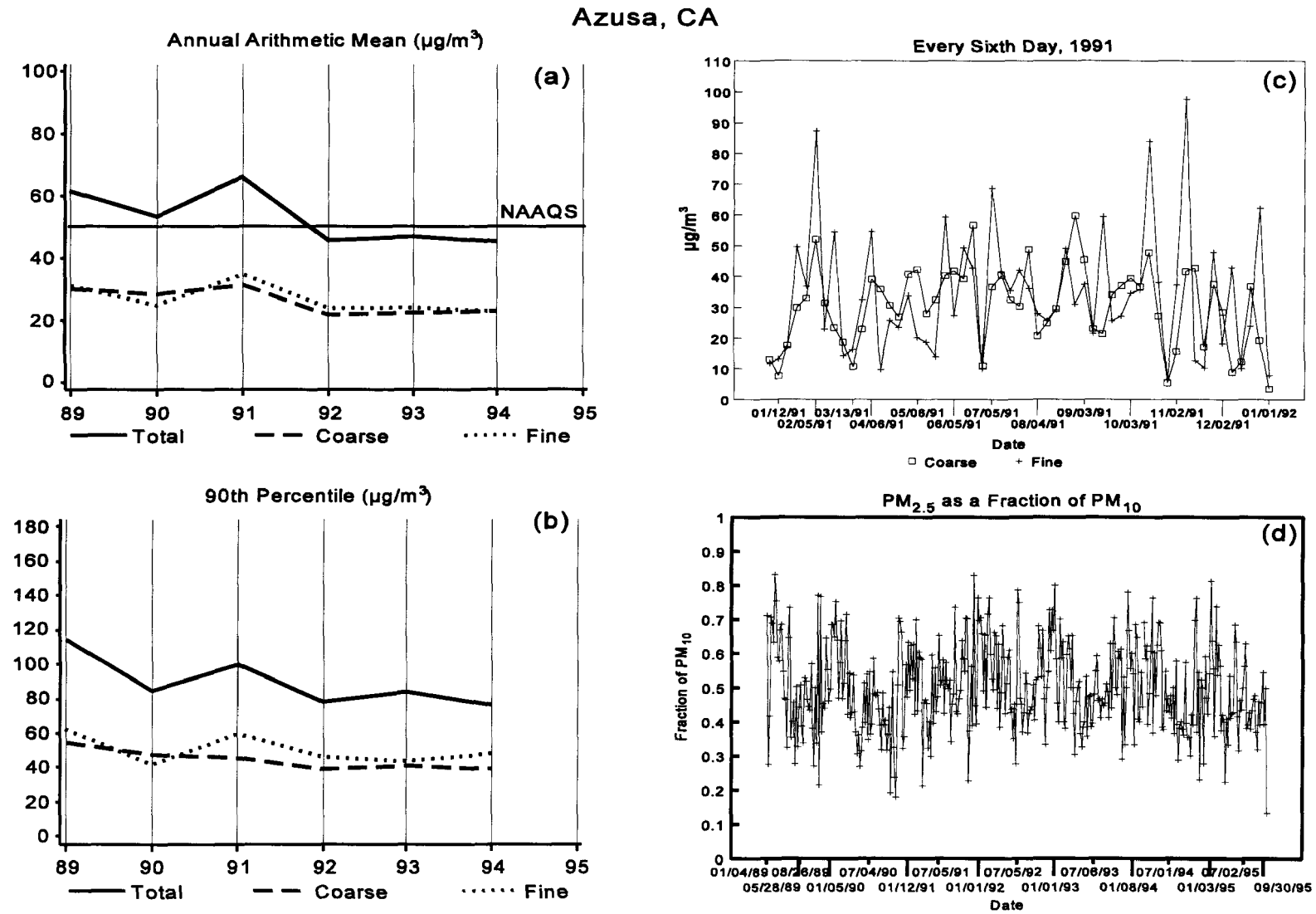

Figure 6-127. Trend data from Azusa from CARB: (a) Fine, coarse and total means; (b) Fine, coarse and total 90th percentiles; (c) Every sixth day fine and coarse mass for 1991; (d) Fine and coarse mass as a fraction of PM_{10}.

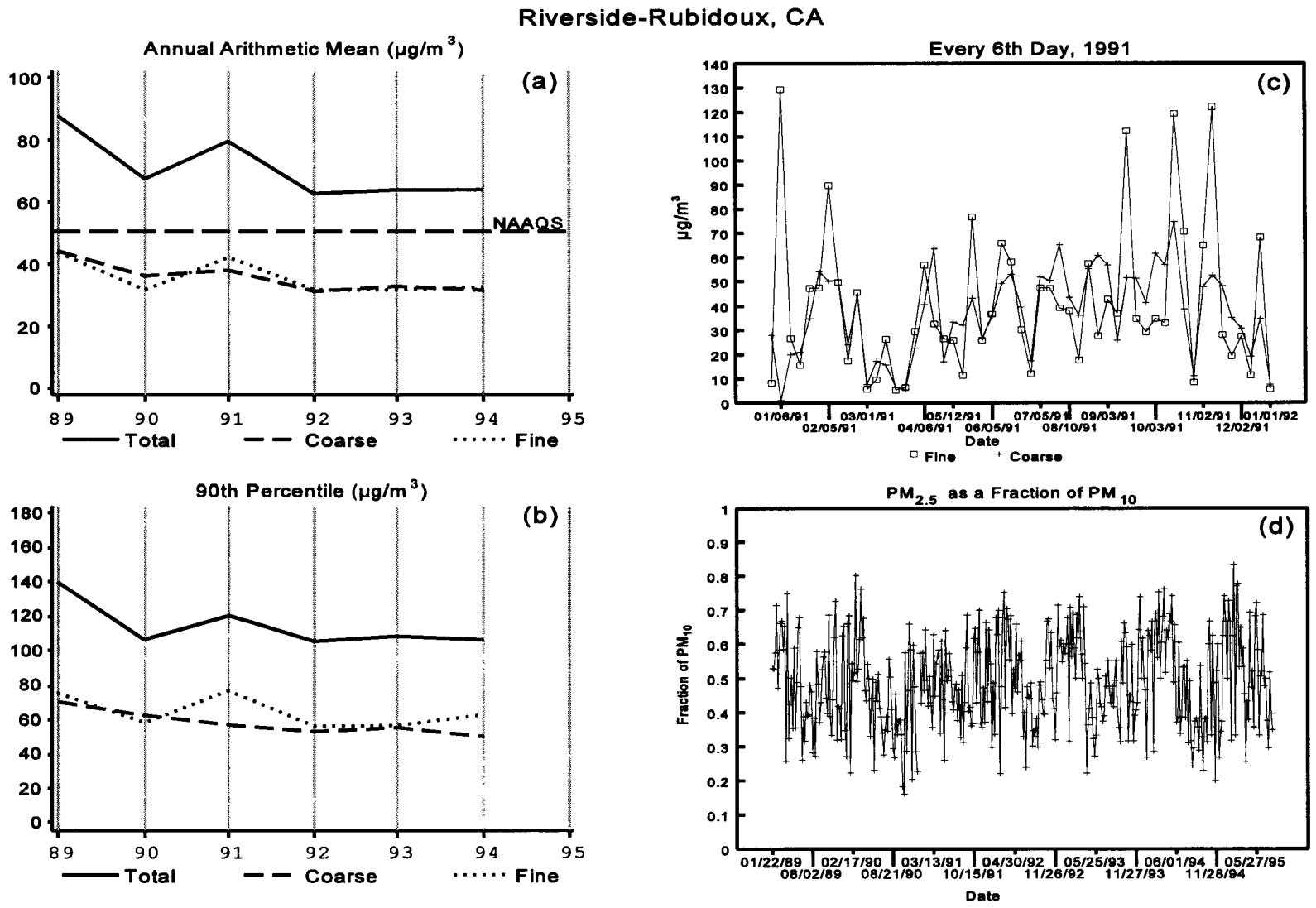

Figure 6-128. Trend data from Riverside-Rubidoux from CARB: (a) Fine, coarse and total means; (b) Fine, coarse and total 90th percentiles; (c) Every sixth day fine and coarse mass for 1991; (d) Fine and coarse mass as a fraction of PM_{10}.

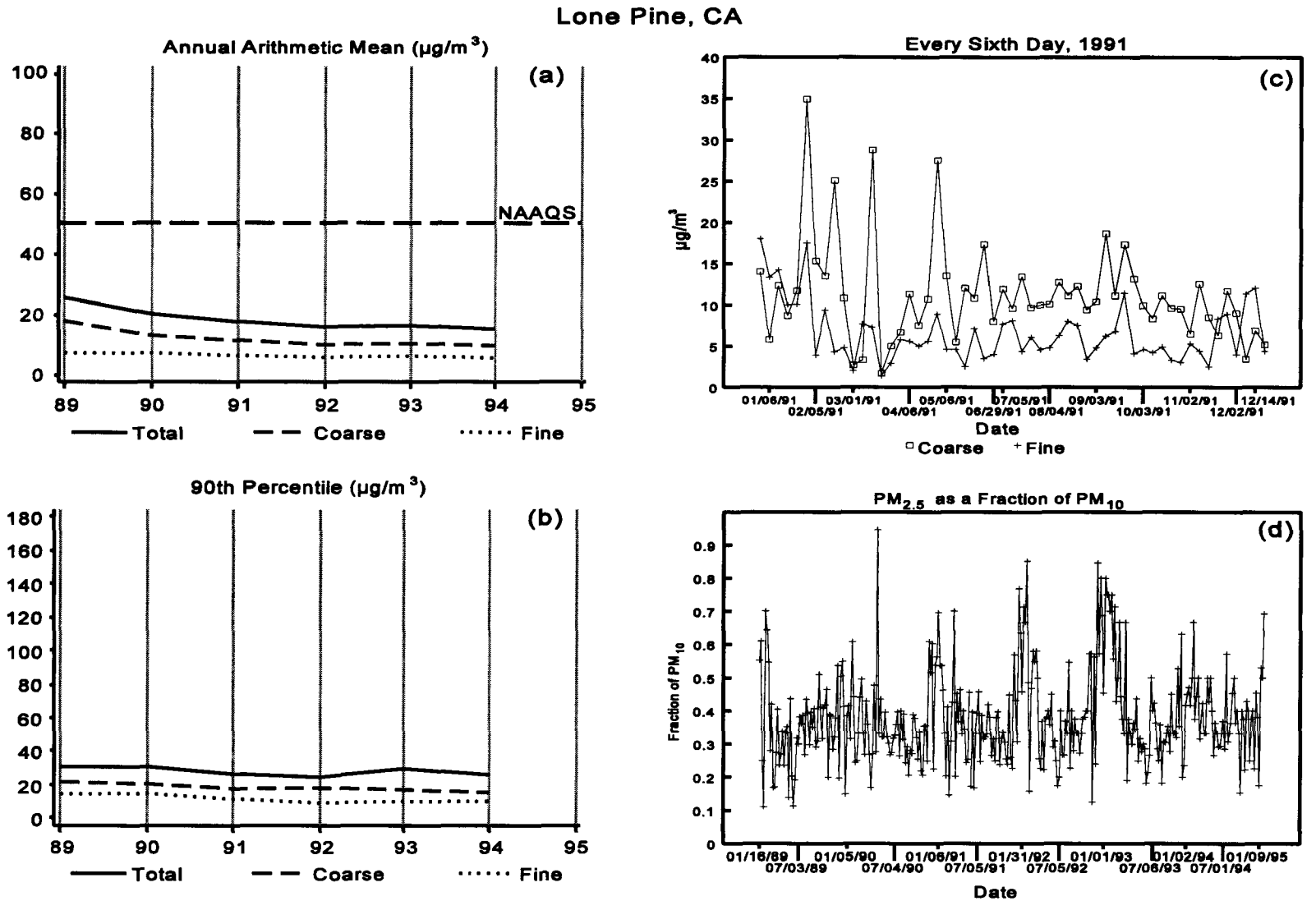

Figure 6-129. Trend data from Lone Pine from CARB: (a) Fine, coarse and total means; (b) Fine, coarse and total 90th percentiles; (c) Every sixth day fine and coarse mass for 1991; (d) Fine and coarse mass as a fraction of PM_{10}.

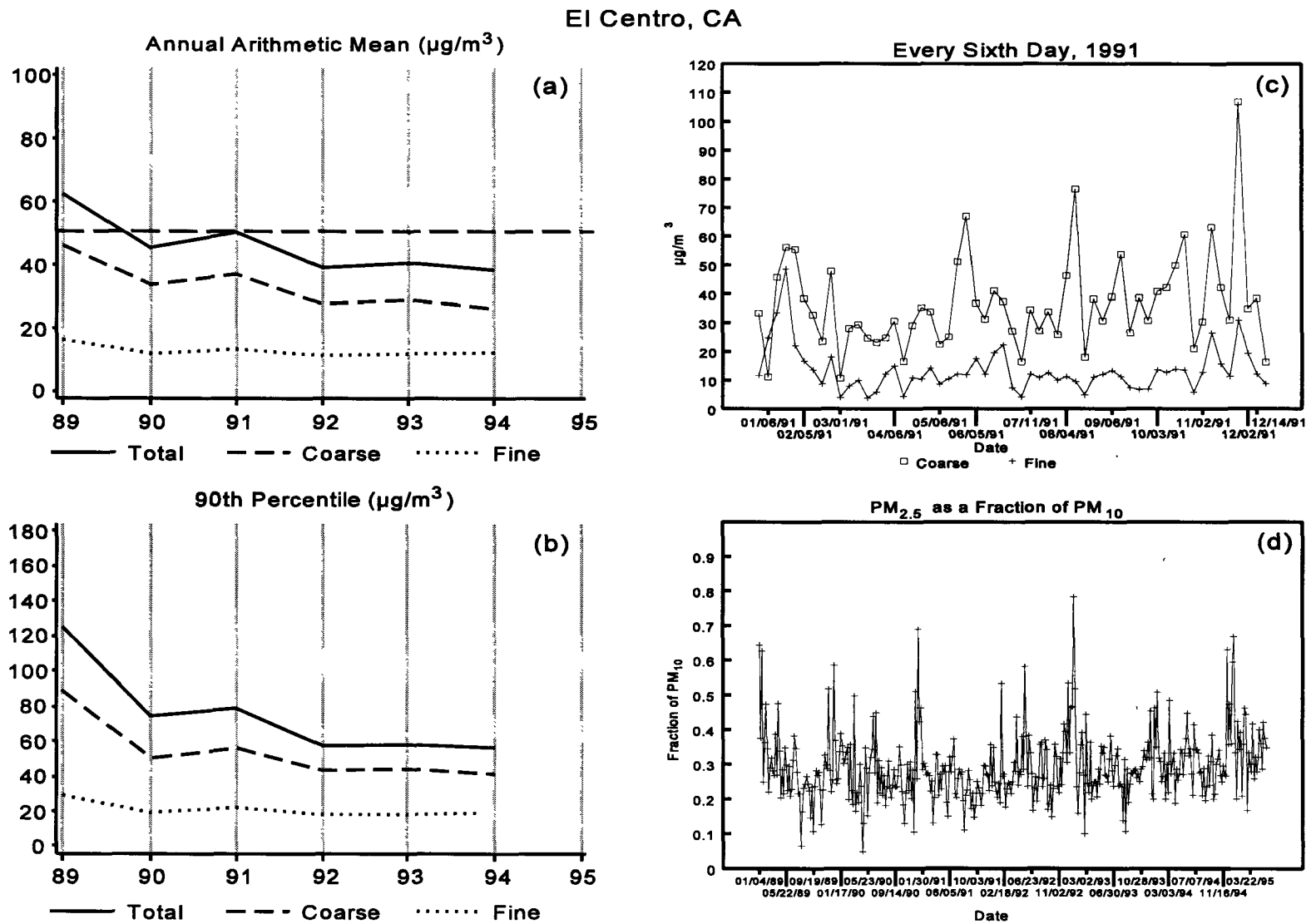

Figure 6-130. Trend data from El Centro from CARB: (a) Fine, coarse and total means; (b) Fine, coarse and total 90th percentiles; (c) Every sixth day fine and coarse mass for 1991; (d) Fine and coarse mass as a fraction of PM_{10}.

TABLE 6-11. MAXIMUM VALUE; 2ND, 3RD, 4TH, AND 5TH HIGHEST VALUES; 98TH AND 95TH PERCENTILE VALUES; 50TH PERCENTILE VALUE (MEDIAN); Δ, THE DIFFERENCE BETWEEN THE MEDIAN AND THE MAXIMUM VALUES AND #, THE NUMBER OF MEASUREMENTS AVAILABLE FROM EIGHT CALIFORNIA AIR RESOURCES BOARD SITES: (a) $PM_{2.5}$, (b) $PM_{(10-2.5)}$, and (c) PM_{10}

SITE	Max	2nd	3rd	4th	5th	98%	95%	50%	Δ	#
					$PM_{2.5}$					
Riverside	142	130	129	122	121	114	77	29	113	368
Azusa	98	95	88	88	87	84	60	23	75	371
Bakersfield	447	147	119	100	98	93	77	16	431	296
Visalia	140	121	105	91	91	82	69	15	125	389
Stockton	94	92	91	75	75	70	55	11	83	381
San Jose	105	88	86	69	66	59	44	9	96	341
El Centro	73	62	52	49	47	39	26	11	62	392
Lone Pine	29	23	22	19	18	17	13	6	23	322
					$PM_{(10-2.5)}$					
Riverside	123	114	87	86	86	76	68	34	89	368
Azusa	108	98	71	62	61	57	50	24	84	371
Bakersfield	320	104	99	98	90	76	61	27	293	296
Visalia	86	75	74	73	70	64	51	21	65	389
Stockton	66	57	57	56	56	54	41	16	50	381
San Jose	55	45	41	39	32	64	51	11	44	341
El Centro	324	176	160	150	132	108	63	27	297	392
Lone Pine	107	105	84	71	67	42	26	10	97	322
					PM_{10}					
Riverside	194	189	189	182	182	178	130	68	126	368
Azusa	203	152	139	139	135	127	99	50	153	371
Bakersfield	766	218	183	163	144	135	120	48	718	296
Visalia	187	164	138	137	130	109	98	43	144	389
Stockton	126	119	112	110	102	98	82	30	96	381
San Jose	151	109	102	87	85	76	61	22	129	341
El Centro	347	228	222	167	158	130	90	39	308	392
Lone Pine	122	120	101	93	76	54	36	16	106	322

TABLE 6-12. MAXIMUM VALUE; 2ND, 3RD, 4TH, AND 5TH HIGHEST VALUES; 98TH AND 95TH PERCENTILE VALUES; 50TH PERCENTILE VALUE (MEDIAN); Δ, THE DIFFERENCE BETWEEN THE MEDIAN AND THE MAXIMUM VALUES AND #, THE NUMBER OF MEASUREMENTS AVAILABLE FOR STIES IN PHILADELPHIA FROM 1979 TO 1995: (a) $PM_{2.5}$, (b) $PM_{(10-2.5)}$, and (c) PM_{10},AND (d) TSP

Philadelphia											
					$PM_{2.5}$						
Site	Dates	Max	2nd	3rd	4th	5th	98%	95%	50%	Δ	#
IPN Average	3/79 12/83	98	94	74	65	65	61	50	21	74	366
IPN S. Broad	3/82 12/83	54	54	52	50	50	53	50	22	32	91
AIRS	1/87 12/90	55	55	47	46	45	46	43	18	37	219
Harvard PBY	5/92 5/59	73	72	56	53	53	43	36	15	58	1014
					$PM_{(10-2.5)}$						
IPN Average	3/79 12/83	NA	NA	NA	NA	NA	NA	NA	NA	NA	0
IPN S. Broad	3/82 12/83	28	25	20	19	17	25	18	9	19	91
AIRS	1/87 12/90	39	39	38	37	30	37	25	12	27	219
Harvard PBY	5/92 5/59	40	28	27	25	24	18	15	6	34	970
					PM_{10}						
IPN Average	3/79 12/83	NA	NA	NA	NA	NA	NA	NA	NA	NA	0
IPN S. Broad	3/82 12/83	71	66	66	65	64	67	64	30	41	91
AIRS	1/87 12/90	86	83	82	79	73	79	60	31	55	219
Harvard PBY	5/92 5/59	82	78	72	64	64	54	48	22	60	1025
					TSP						
IPN Average	3/79 12/83	196	150	148	140	138	129	114	64	132	366
IPN S. Broad	3/82 12/83	116	107	105	101	99	109	100	61	55	91
AIRS	1/87 12/90	131	124	116	116	112	116	104	56	75	219
Harvard PBY	5/92 5/59	NA	NA	NA	NA	NA	NA	NA	NA	NA	0

and 5th highest values; the 98th and 95th percentile values; the 50th percentile (median value) and the difference between the median and the maximum value are given for the measurement period available at each site. The maximum $PM_{2.5}$, $PM_{(10-2.5)}$, and PM_{10} levels were substantially higher at all the California sites, including the site at Lone Pine (estimated 1980 population, 1800), than at the Philadelphia sites. Differences between maximum and median levels are also larger at the California sites. The causes for the extremely high values observed at the Bakersfield site are not known. Data on the upper ranges of TSP are shown for Philadelphia sites as available.

6.10.3.2 Relationships Between $PM_{2.5}$; $PM_{(10-2.5)}$, PM_{10}, and TSP in Philadelphia

Epidemiologists have made extensive use of a long-term TSP data set from Philadelphia (Chapter 12; Wyzga and Lipfert, 1996; Li and Roth, 1995) to investigate the statistical relationships between TSP and mortality. It is possible, however, that $PM_{2.5}$ or PM_{10}, instead of TSP, may be the causal agent and that TSP may serve as an indicator for $PM_{2.5}$ or PM_{10}. PM indicators for Philadelphia, other than TSP, have not been available until recently. Therefore, an examination of relationships between TSP, $PM_{2.5}$, and PM_{10} in the Philadelphia area may provide data that will be useful in interpreting the epidemiological results obtained in Philadelphia with TSP. Such relationships are displayed in a series of Figures (6-131 to 6-135) that show: (Panel a) TSP plotted versus PM_x (where PM_x is either $PM_{2.5}$ or PM_{10}) (Panel b) the distribution of values of PM_x/TSP, (Panel c) PM_x/TSP plotted versus PM_x, and (Panel d) PM_x/TSP plotted versus TSP.

It would appear from Figures 6-131 to 6-135 that there is some relationship between PM_x and TSP and that the relationship improves at higher values of TSP. The PM_x/TSP ratio does not appear to vary significantly with PM_x. However, the ratio does appear to increase with TSP until a certain level of TSP is reached and then levels off. These visual observations are quantified by comparison of the PM_x/TSP ratios at various levels and statistical regressions of PM_x with various TSP fractions shown in Table 6-13.

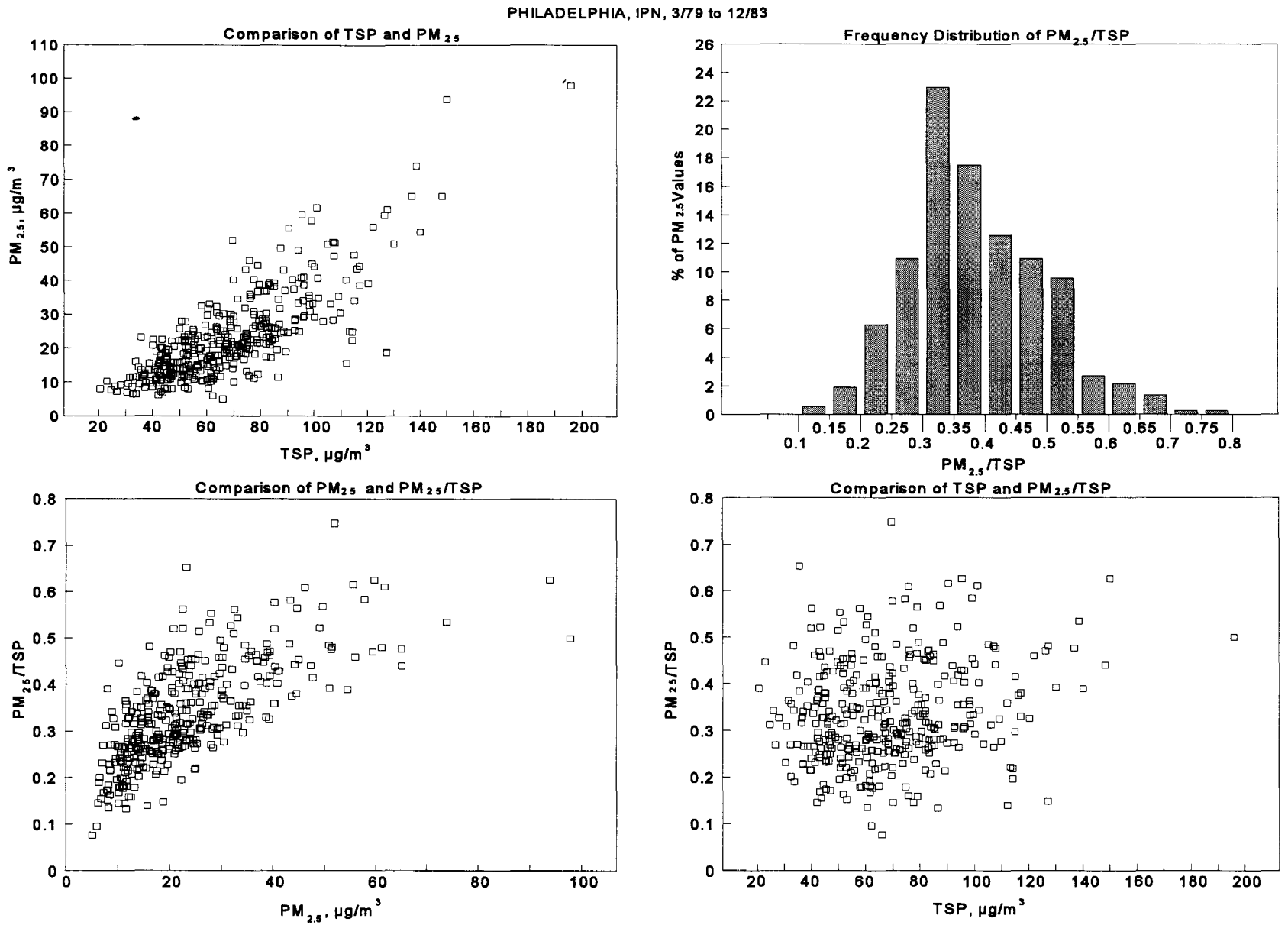

Figure 6-131. $PM_{2.5}$ and TSP Relationships in Philadelphia, IPN Average, 3/79 to 12/83: (a) comparison of $PM_{2.5}$ with TSP, (b) frequency distribution of $PM_{2.5}$/TSP, (c) comparison of $PM_{2.5}$ /TSP with $PM_{2.5}$, (d) comparison of $PM_{2.5}$/TSP with TSP.

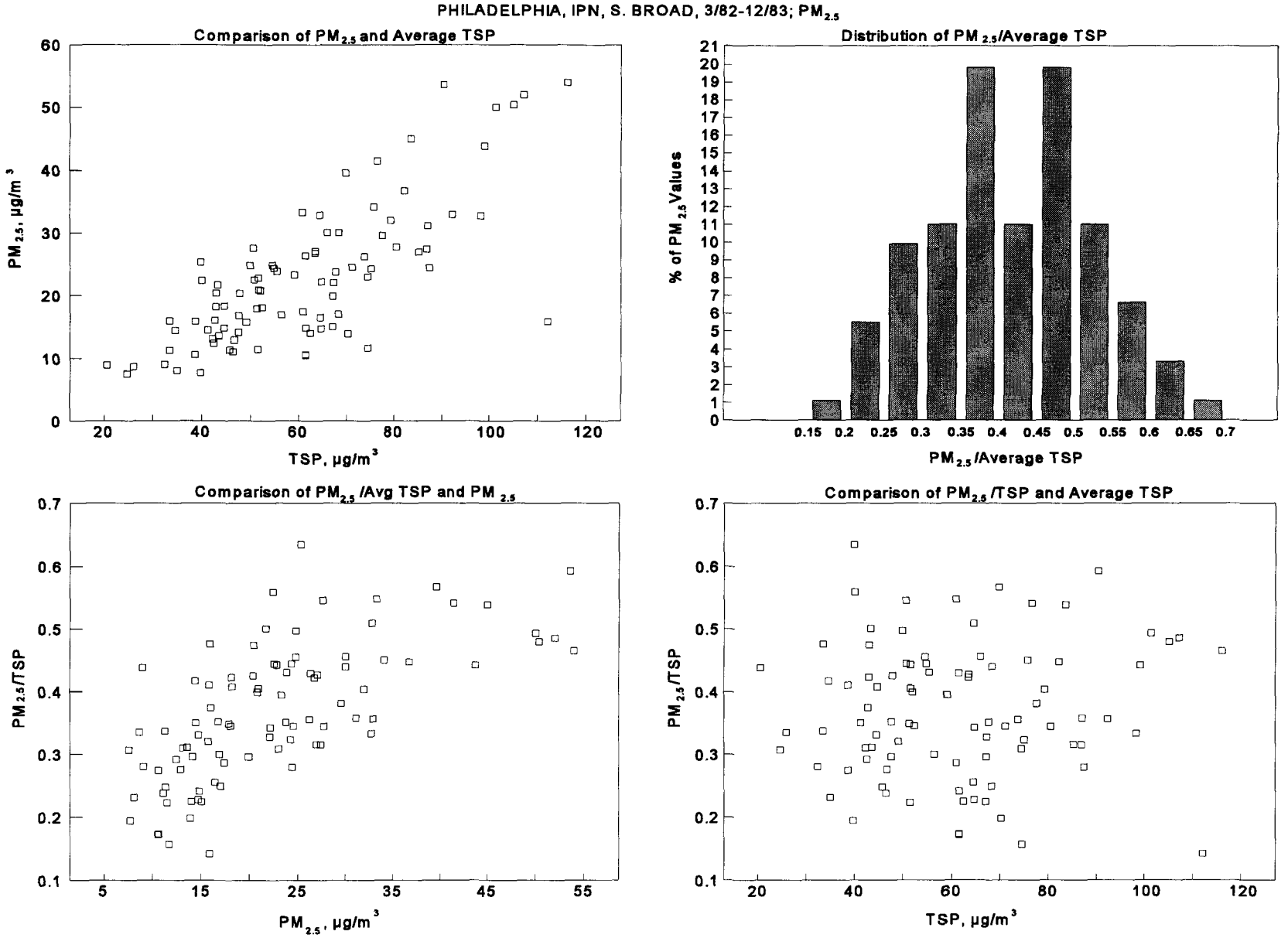

Figure 6-132. $PM_{2.5}$ and TSP Relationships in Philadelphia, IPN, South Broad Site, 3/82 to 12/83: (a) comparison of $PM_{2.5}$ with TSP, (b) frequency distribution of $PM_{2.5}$/TSP, (c) comparison of $PM_{2.5}$/TSP with $PM_{2.5}$, (d) comparison of $PM_{2.5}$/TSP with TSP.

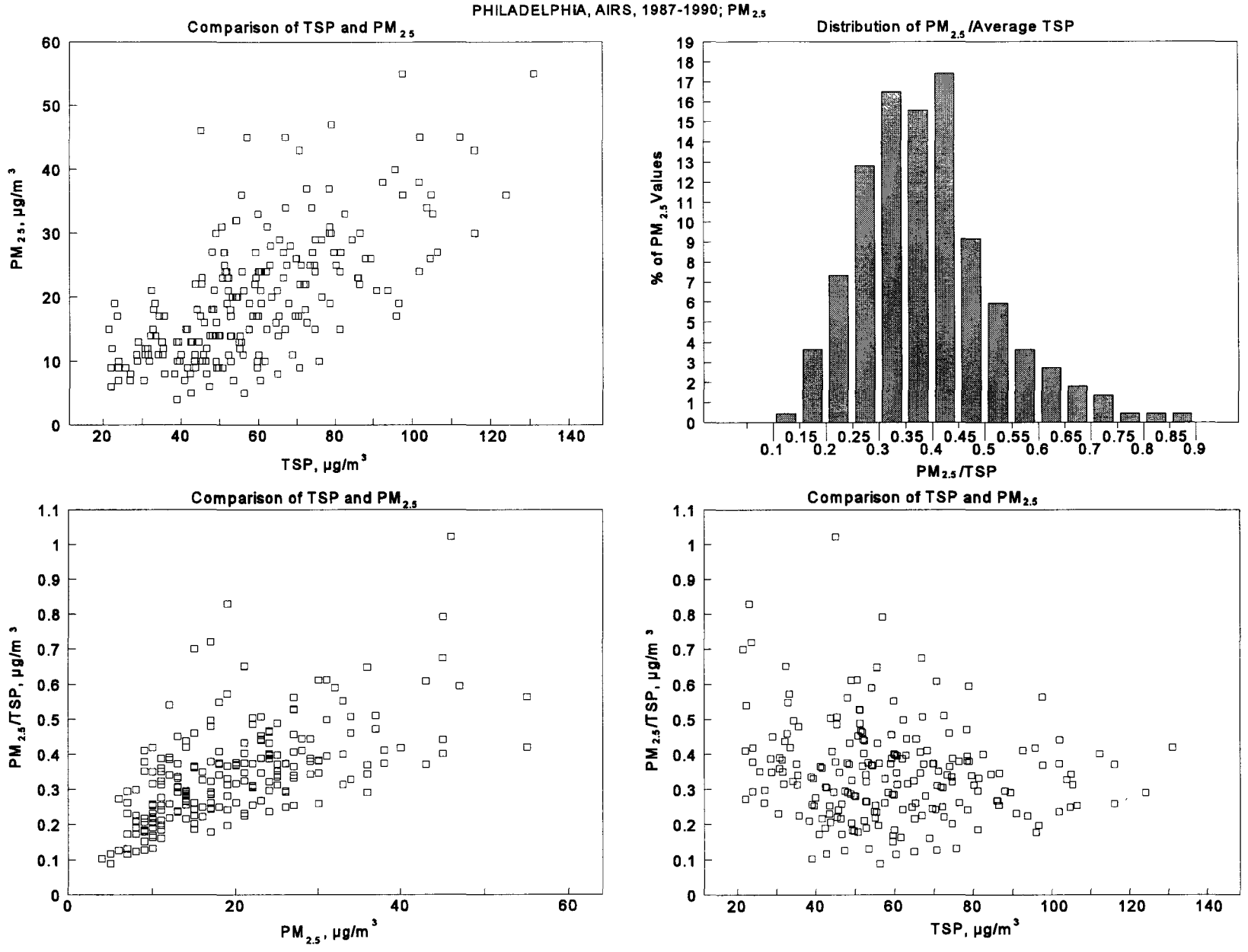

Figure 6-133. $PM_{2.5}$ and TSP Relationships in Philadelphia, AIRS, 1987 to 1990: (a) comparison of $PM_{2.5}$ with TSP, (b) frequency distribution of $PM_{2.5}$/TSP, (c) comparison of $PM_{2.5}$ /TSP with $PM_{2.5}$, (d) comparison of $PM_{2.5}$//TSP with TSP.

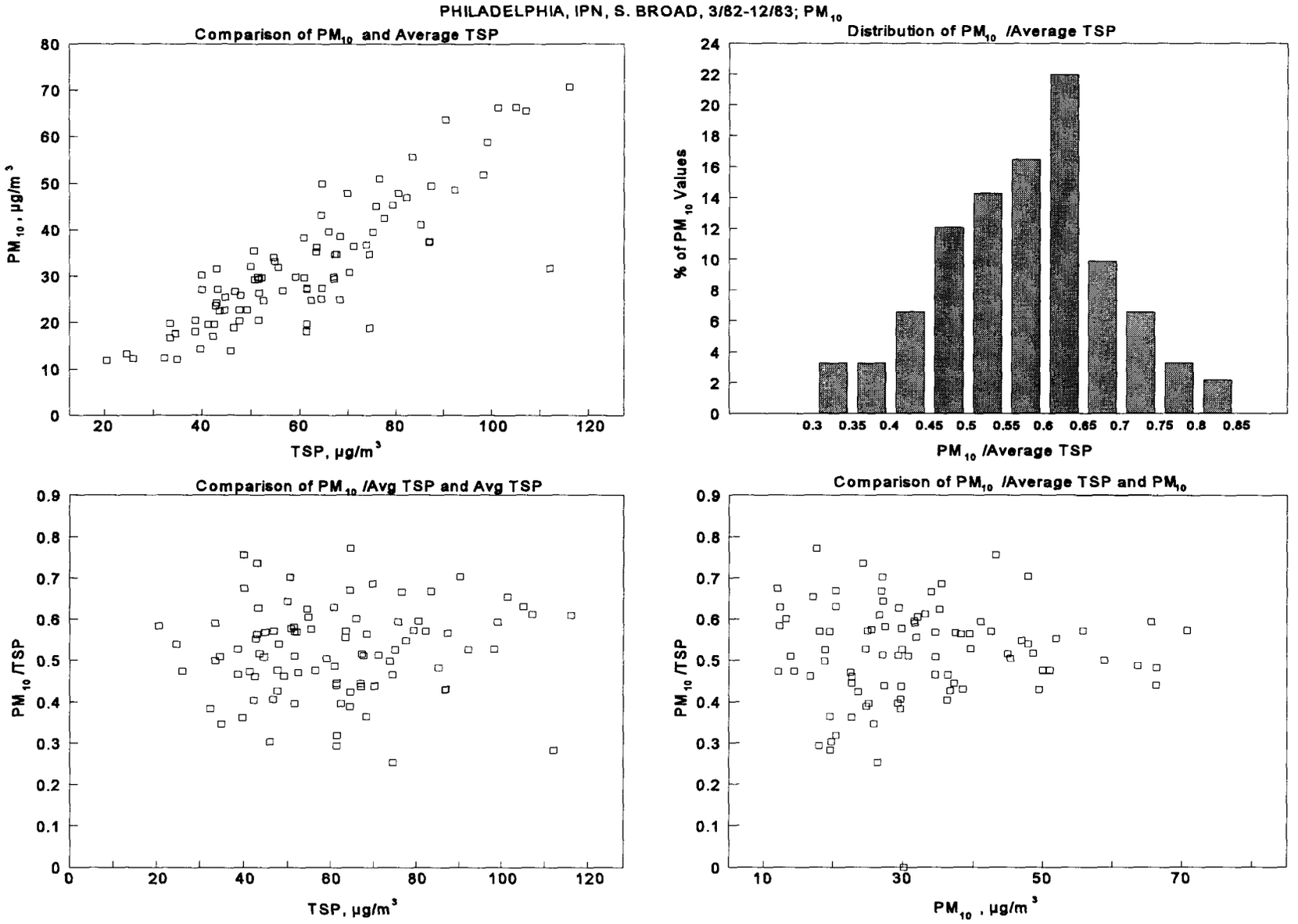

Figure 6-134. PM_{10} and TSP Relationships in Philadelphia, IPN, South Broad Site, 3/82 to 12/83: (a) comparison of PM_{10} with TSP, (b) frequency distribution of PM_{10}/TSP, (c) comparison of PM_{10}/TSP with PM_{10}, (d) comparison of PM_{10}/TSP with TSP.

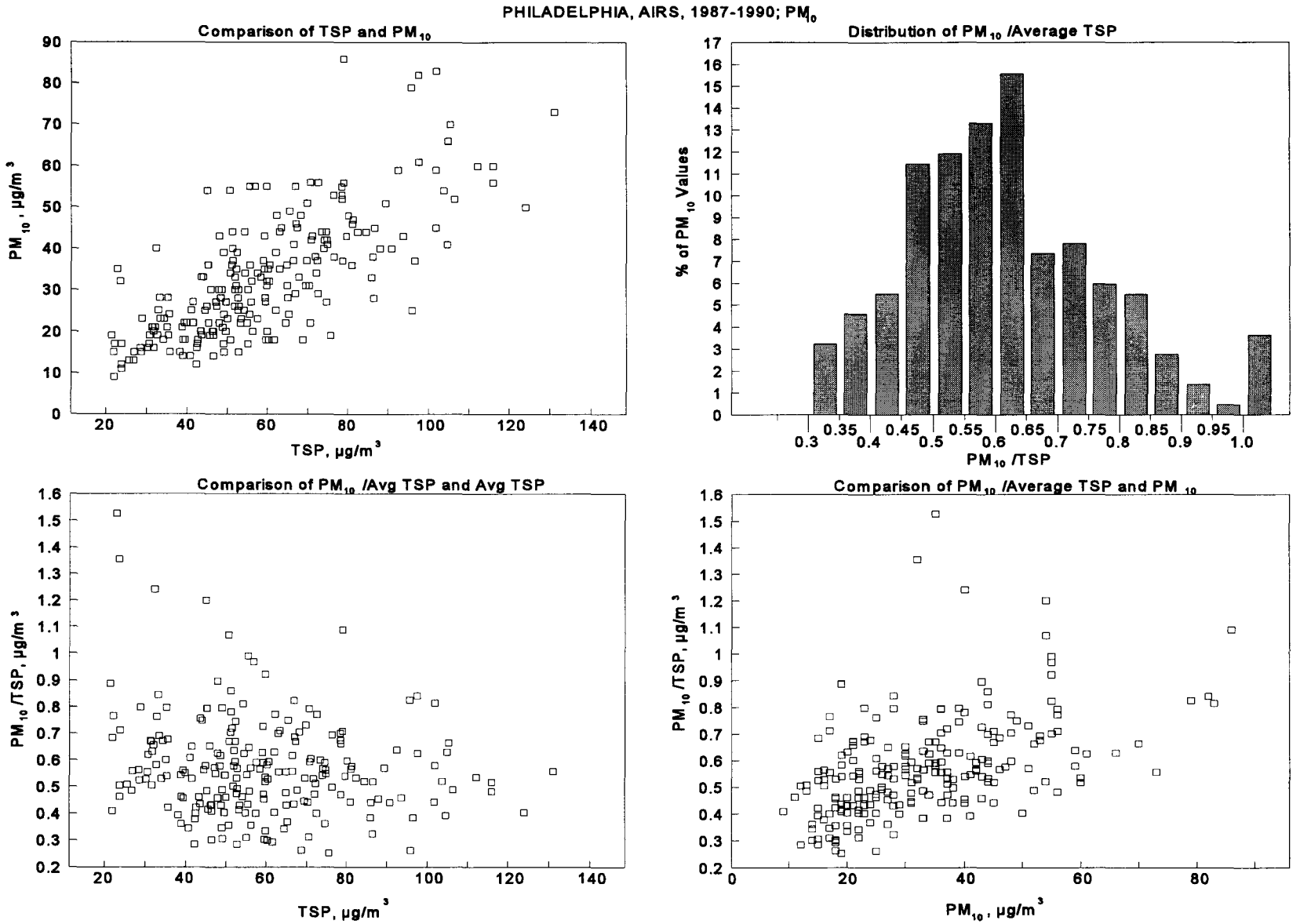

Figure 6-135. PM_{10} and TSP Relationships in Philadelphia, AIRS, 1987 to 1990: (a) comparison of PM_{10} with TSP, (b) frequency distribution of PM_{10}/TSP, (c) comparison of PM_{10}/TSP with PM_{10}, (d) comparison of PM_{10}/TSP with TSP.

TABLE 6-13. RELATIONSHIPS BETWEEN PM_X ($PM_{2.5}$ OR PM_{10}) AND TSP AS A FUNCTION OF TSP CONCENTRATION LEVELS FOR SEVERAL SITES IN PHILADELPHIA: (a) RATIO OF PM_x TO TSP, (b) COEFFICIENT OF DETERMINATION (R_2)

		(a) Ratio of PM_x/TSP					
		$PM_{2.5}$/TSP			PM_{10}/TSP		
Philadelphia		TSP	TSP	TSP	TSP	TSP	TSP
Site	Dates	All	<80	>80	All	<80	>80
IPN Average	3/79 12/83	0.335 ± 0.108	0.325 ± 0.107	0.363 ± 0.107	NA	NA	NA
IPN S. Board	3/82 12/83	0.371 ± 0.105	0.361 ± 0.106	0.416 ± 0.090	0.525 ± 0.105	0.516 ± 0.107	0.573 ± 0.079
AIRS	1/87 12/90	0.345 ± 0.137	0.350 ± 0.114	0.317 ± 0.083	0.573 ± 0.187	0.581 ± 0.194	0.528 ± 0.131

		(b) Coefficients of Determination, R^2					
		$PM_{2.5}$ with			PM_{10} with		
Philadelphia		TSP	TSP	TSP	TSP	TSP	TSP
Site	Dates	All	<80	>80	All	<80	>80
IPN Average	3/79 12/83	0.64	0.36	0.50	NA	NA	NA
IPN S. Board	3/82 12/83	0.57	0.38	0.48	0.78	0.57	0.61
AIRS	1/87 12/90	0.45	0.29	0.34	0.55	0.42	0.24

6.10.3.3 Correlations Between $PM_{2.5}$, $PM_{(10-2.5)}$, and PM_{10}

The analysis of epidemiological results suggest that the smaller size fraction of particulate matter may have a stronger association with health outcomes than fractions that contain larger size particles (Chapter 12). It is of interest, therefore, to examine the correlations between $PM_{2.5}$, $PM_{(10-2.5)}$, and PM_{10}. The means of these fractions and the coefficient of determinination, R^2, for their relationships are shown in Table 6-14 for eight sites in California (CARB, 1995) and in Table 6-15 for several sites and times for Philadelphia (IPN, 1985; AIRS, 1995; Harvard, 1995).

If correlation between $PM_{2.5}$ and PM_{10} is high but the correlation of $PM_{(10-2.5)}$ with both $PM_{2.5}$ and PM_{10} is low, it is possible that PM_{10} is serving as an indicator of $PM_{2.5}$ and that any health effects of $PM_{(10-2.5)}$ would be masked by the larger $PM_{2.5}$ (Wilson and Suh, 1996). This may be the case in Philadelphia since $PM_{2.5}$ to PM_{10}. In general, $PM_{(10-2.5)}$ is a larger fraction of PM_{10} at the California sites than at the Philadelphia site. However, there is still substantial variability (~40% from minimum to maximum) in this ratio in the data sets from California. Correlations between $PM_{2.5}$ and $PM_{(10-2.5)}$ are highly variable at the sites in California and encompass the Philadelphia value. The large correlations seen between $PM_{2.5}$ and $PM_{(10-2.5)}$ at several California sites suggest a significant contribution from crustal material to $PM_{2.5}$. In contrast, at the Philadelphia site, only $PM_{2.5}$ and not $PM_{(10-2.5)}$ was highly correlated with PM_{10}. These data support the desirability of having independent data on fine mode particles and coarse mode particles for epidemiological investigations.

6.10.3.4 Fine Fraction

The fine fractions of PM_{10} ($PM_{2.5}/PM_{10}$) were shown for Philadelphia in Figure 6-116 (Panels c and d) and for California sites in Figures 6-123 to 6-130. A strong seasonal variation is evident at the California sites but not in Philadelphia. Numerical values of the $PM_{2.5}$ fractional contribution to PM_{10} are given for Philadelphia and for several California sites in Table 6-16. These variations in $PM2.5/PM_{10}$ demonstrate the difficulty of inferring $PM_{2.5}$ from PM_{10} measurements unless some information is available on $PM_{2.5}/PM_{10}$ on a seasonal and geographic basis.

TABLE 6-14. MEANS AND STANDARD DEVIATIONS FOR $PM_{2.5}$, $PM_{(10-2.5)}$, AND PM_{10} AND COEFFICIENTS OF DETERMINATION (R^2) BETWEEN PAIRS FOR EIGHT CALIFORNIA AIR RESOURCES BOARD SITES DURING THE PERIOD 1989 TO 1990

	Mean ± Standard Deviation		
Site	$PM_{2.5}$	$PM_{(10-2.5)}$	PM_{10}
Riverside	34.1 ± 24.3	34.5 ± 19.5	68.6 ± 37.6
Azusa	25.9 ± 17.2	25.5 ± 14.5	51.3 ± 27.7
Bakersfield	24.2 ± 24.2	33.7 ± 33.6	57.0 ± 27.7
Visalia	23.0 ± 20.5	23.3 ± 15.9	46.3 ± 26.7
Stockton	17.4 ± 16.7	17.8 ± 10.8	35.6 ± 21.8
San Jose	13.9 ± 14.1	11.9 ± 6.7	25.8 ± 17.9
El Centro	12.3 ± 8.2	31.5 ± 25.4	43.8 ± 30.5
Lone Pine	6.5 ± 3.7	12.1 ± 11.7	18.6 ± 13.8
	Coefficient of Determination, R^2		
Site	$PM_{2.5}$ to $PM_{(10-2.5)}$	$PM_{2.5}$ to PM_{10}	$PM_{(10-2.5)}$ to PM_{10}
Riverside	0.21	0.79	0.67
Azusa	0.27	0.79	0.71
Bakersfield	0.36	0.86	0.74
Visalia	0.36	0.66	0.41
Stockton	0.05	0.77	0.44
San Jose	0.16	0.88	0.48
El Centro	0.27	0.50	0.94
Lone Pine	0.19	0.42	0.94

TABLE 6-15. MEANS AND STANDARD DEVIATIONS FOR $PM_{2.5}$, $PM_{(10-2.5)}$, PM_{10}, and TSP AND COEFFICIENTS OF DETERMINATION (R^2) BETWEEN PAIRS FOR SEVERAL SITES IN PHILADELPHIA DURING PERIODS FROM 1979 TO 1995

Philadephia		Mean ± Standard Deviation			
Site	Dates	$PM_{2.5}$	$PM_{(10-2.5)}$	PM_{10}	TSP
IPN Average	3/79 12/83	23.3 ± 13.3	NA	NA	68.2 ± 24.7
IPN S. Board	3/82 12/83	22.6 ± 11.0	9.7 ± 4.7	32.1 ± 13.5	61.1 ± 20.5
AIRS	1/87 12/90	19.9 ± 10.0	13.1 ± 6.7	33.0 ± 14.9	58.4 ± 21.9
Harvard PBY	5/92 5/95	17.4 ± 9.4	7.0 ± 4.3	24.3 ± 11.5	NA
		Coefficient of Determination, R^2			
Site	Dates	$PM_{2.5}$ with $PM_{(10-2.5)}$	$PM_{2.5}$ with PM_{10}	$PM_{(10-2.5)}$ with PM_{10}	$PM_{2.5}$ with TSP
IPN Average	3/79 12/83	NA	NA	NA	0.64
IPN S. Board	3/82 12/83	0.14	0.90	0.42	0.57
AIRS	1/87 12/90	0.32	0.86	0.69	0.45
Harvard PBY	5/92 5/95	0.11	0.88	0.41	NA

6.11 SUMMARY AND CONCLUSIONS

This chapter presents ambient concentration measurements of particulate mass, PM_{10}, $PM_{2.5}$, and $PM_{(10-2.5)}$, and of the chemical composition of particulate matter. For PM_{10} measurements the number of urban monitoring stations in the AIRS network increased rapidly in the years immediately after 1985, but the increase slowed substantially in the early 1990s. The measurements of PM_{10} at most of these stations were made every 6th day. Measurements

TABLE 6-16. $PM_{2.5}/PM_{10}$ (FRACTION OF PM_{10} CONTRIBUTED BY $PM_{2.5}$)

	Mean	Standard Deviation	Coefficient of Variation (%)	Range
Philadelphia	0.71	0.13	18	
Mar-May	0.73	0.14	19	0.09-1.09
Jun-Aug	0.73	0.16	22	0.30-1.56
Sept-Nov	0.72	0.17	24	0.17-1.81
Dec-Feb	0.75	0.15	20	0.03-1.55
Azusa	0.50	0.13	26	
Visalia	0.49	0.22	45	
San Jose	0.49	0.15	31	
Riverside	0.49	0.14	29	
Stockton	0.46	0.18	39	
Bakersfield	0.44	0.19	43	
Lone Pine	0.38	0.14	37	
El Centro	0.29	0.10	34	
Riverside				
Winter	0.57	0.14	25	0.22-0.99
Spring	0.48	0.13	27	0.22-0.76
Summer	0.41	0.09	22	0.23-0.69
Fall	0.48	0.15	15	0.16-0.74

of chemical species in urban areas usually are obtained in special studies of limited duration. Data for chemical species in urban areas are discussed as appropriate in the text.

The mass concentration measurements in urban areas have been used to obtain (a) annual trends in PM_{10}, (b) ratios and correlations of $PM_{2.5}$ to $PM_{(10-2.5)}$ and PM_{10} and (c) seasonal variations in PM_{10}, $PM_{2.5}$, and $PM_{(10-2.5)}$.

The measurements at non-urban sites were collected at a much smaller number of locations relative to the number of urban stations by region. The geographical location of the sites in the IMPROVE/NESCAUM networks were not selected to optimize their locations relative to AIRS stations in the same region. As a result, not only are there small numbers of

non-urban sites by region, but most of these sites are geographically well displaced from urban areas.

The non-urban concentration measurements include both mass and chemical composition so they were used to obtain (a) the variations in PM_{10}, $PM_{2.5}$, and $PM_{(10-2.5)}$ with month of the year, (b) the chemical balances for sulfates, organic carbon, elemental carbon, and soil with month of the year and (c) the variations in the concentrations of S, Se, and V and the S to Se ratio with month of the year.

From the urban and non-urban PM_{10} concentration measurements, an "urban excess" was obtained from the monthly differences in AIRS and IMPROVE/NESCAUM PM_{10} values. Because of the limitations mentioned above and the lack of tests of statistical significance, these "urban excess" values should be viewed as preliminary and used very cautiously with respect to quantitative results.

Additional sections of Chapter 6 include the following discussions: (1) the mass apportionment of chemical species obtained from a group of selected research studies of the chemical composition at locations in the eastern, central and western U.S.; (2) acid sulfate study results by (a) their geographical distribution in the U.S. and southern Canada, (b) spatial variations on a city and urban scale, (c) seasonal variations, (d) diurnal variations, and (e) indoor and personal monitoring relative to outdoor hydrogen ion concentration measurements; (3) particle number concentrations with emphasis on ultrafine particles; (4) some information on metals potentially present in ultrafine particles; and (5) information on fine and coarse PM trends and patterns for sites where both fine and coarse PM measurements were available.

Based on these various concentration measurements a considerable number of conclusions may be obtained. Many of these conclusions are limited by (a) the number of monitoring sites available, (b) their geographical location, (c) the frequency of measurement and (d) differences in methodology used between networks or stations as well as between individual studies of chemical composition.

Trends in PM_{10} mass concentration, averaged over regions or by city, usually indicate a substantial decrease in PM_{10} concentrations by year from 1988 to 1994. There are exceptions to this significant downward trend in Philadelphia and at some locations within the Southern

California Basin. The trend plots shown in Chapter 6 have not been tested for statistical significance. The trend plots can also be influenced by the approach taken in the selection of stations. Since the number of stations increased rapidly between 1985 and 1990, the trends that might be obtained using early data could be biased by the added stations being influenced by location towards higher or lower PM_{10} concentration measurements. For this document, the set of stations in operation from 1988 to 1994 was used to obtain PM_{10} concentration trends during this period. It should also be noted that meteorological influences which are known to be important for deducing trends of O_3 concentrations also may affect PM_{10} concentrations on a year-to-year basis.

Keeping the limitations mentioned above in mind, urban trend analyses for PM_{10} are presented using all stations in operation in a given year and the smaller set of trend stations in operation over the entire 1988 to 1994 time period. The range for the averaged decrease in PM_{10} between 1988 and 1994 at urban stations was: for the contiguous U.S., all sites, 24%, trend sites, 20%; for the eastern U.S., all sites, 16%, trend sites, 18%; and for the western U.S., all sites, 31%, trend sites 28%. There were appreciable differences between regions in the range of averaged decreases in PM_{10} between 1988 and 1994 with the decrease for urban stations in the northeast ranging from 18% (all) to 19% (trend) while in the industrial midwest the decreases ranged from 12% (all) to 19% (trend). The ranges of averaged decreases for the three western regions were from 27% to 37% (all) and 23% to 33% (trend). These decreases in PM_{10} concentrations resulted in 1994 annual average regional AIRS concentrations in the range of 25 $\mu g/m^3$ to 32 $\mu g/m^3$.

For individual cities, both between and within cities, the decreases in PM_{10} for individual stations could show substantial variability. In the Los Angeles Basin, 3 of 6 stations showed statistically significant downward trends in PM_{10} while other stations showed no significant trends. In the western U.S. several large cities showed larger downward trends in PM_{10} than the regional averages. PM2.5 and PM(10-2.5) or PM10 data, suitable for determining trends of both fine and coarse components of PM10, are available from only a few sites in the eastern United States and a few sites in California. While a general decrease is evident in both fine and coarse components of PM10 at most sites where data is available, it is not possible to ascertain differential trends in the two components.

A few attempts to infer various types of background levels of $PM_{2.5}$ and PM_{10} have been made. The backgrounds most relevant to the Criteria Document include a "natural" background which excludes all anthropogenic sources anywhere in the world, and a background which excludes anthropogenic sources in North America, but not elsewhere. Annual average natural background levels of PM_{10} have been estimated to range from 4 to 8 $\mu g/m^3$ in the western United States and 5 to 11 $\mu g/m^3$ in the eastern United States. Corresponding $PM_{2.5}$ levels have been estimated to range from 1 to 4 $\mu g/m^3$ in the western United States and 2 to 5 $\mu g/m^3$ in the eastern United States. Twenty-four hour average concentrations may be substantially higher than the annual or seasonal average background concentrations presented in Chapter 6. The 24-hour averages are usually considered for control strategies while the annual and seasonal averages are suitable for risk analyses.

Based either on the correlation of individual values or on the average $PM_{2.5}$ to PM_{10} values, the annual ratios of $PM_{2.5}$ to PM_{10} from urban stations fell within a relatively narrow range of 0.55 to 0.6, for both the entire eastern and western U.S. However, for two regions, the upper midwest and southwest, the correlations yielded ratios of less than 0.2 while the average $PM_{2.5}$ to PM_{10} values yielded ratios between 0.3 and 0.4.

Ratios of $PM_{2.5}$ to $PM_{(10-2.5)}$ from urban stations can vary with season as well as between regions. In the northeast, southeast, and industrial midwest regions, there is appreciable uniformity with $PM_{2.5}$ exceeding $PM_{(10-2.5)}$ during all seasons of the year. In contrast, in the southwest, the $PM_{2.5}$ is less than the PM coarse during all seasons of the year. In the northwest and in southern California, $PM_{2.5}$ exceeds PM_{10} in the fall and winter with the reverse occurring in the spring and summer.

Measurements of the day to day variability in $PM_{2.5}$ and PM_{10} are available from only one site located in Philadelphia, PA. The data show day to day variations of 8.6 ± 7.5 $\mu g/m^3$ for PM_{10}, 6.8 ± 6.5 $\mu g/m^3$ for $PM_{2.5}$, and 3.7 ± 3.4 $\mu g/m^3$ for $PM_{10-2.5}$ from May 1992 to April 1995. Maximum day to day differences were 50 $\mu g/m^3$ for PM_{10}, 55 $\mu g/m^3$ for $PM_{2.5}$, and 35 $\mu g/m^3$ for $PM_{(10-2.5)}$. The ratio of $PM_{2.5}$ to PM_{10} was 0.72 ± 0.16 over the measurement period and the correlation between $PM_{2.5}$ and PM_{10} was 0.86 (R^2) suggesting that variability in $PM_{2.5}$ was forcing the variability in PM_{10}. Data collected by dichotomous samplers at several sites in California showed that $PM_{(10-2.5)}$ accounted for roughly half of

PM_{10} and that both $PM_{2.5}$ and $PM_{(10-2.5)}$ were highly correlated with PM_{10}. Differences among the Philadelphia data set and the California data sets illustrate the dangers in extrapolating relations among different size fractions from one region of the country to other regions.

Comparisons of seasonal profiles of PM_{10} show summer peaks for both urban and nonurban sites in the northeast, southeast, and industrial midwest. These summer peaks usually, but not exclusively, are associated with the summer peaks in $PM_{2.5}$. The $PM_{2.5}$ concentrations at non-urban sites in the northeast, southeast, and industrial midwest exceed the $PM_{(10-2.5)}$ concentrations in all seasons of the year, as is the case for urban stations. The northwest urban PM_{10} and $PM_{2.5}$ concentrations show a spring and early summer minimum with the highest values in fall and winter, while the non-urban PM_{10} and $PM_{2.5}$ concentrations show a summer peak similar to the seasonal profiles in the eastern U.S. In southern California, the urban PM_{10} and $PM_{2.5}$ seasonal profiles show fall peaks, while the non-urban seasonal profiles have a relatively flat maximum from spring into early fall. Again it must be emphasized that with so few nonurban sites in most regions any conclusions drawn from the comparisons above are very tentative for most regions of the U.S.

The every-sixth-day urban PM_{10} averaged concentrations for most regions of the United States ranged during 1990 to 1994 from 10 to 15 $\mu g/m^3$ up to 40 to 60 $\mu g/m^3$. The southern California region had PM_{10} values averaging up to 70 to 75 $\mu g/m^3$. Day-to-day variations in PM_{10} concentrations in Knoxville, TN, ranged from 10 to 20 $\mu g/m^3$, while in Missoula, MT, PM_{10} concentrations ranged from <10 to 120 to 140 $\mu g/m^3$ with one value over 200 $\mu g/m^3$.

A quantity termed an urban excess has been discussed extensively in the text of Chapter 6. In view of the distinctions discussed above between the number and geographical distribution of urban and non-urban sites, the quantitative results probably should be interpreted with considerable caution. While it is reasonable that additional sources within cities should increase PM_{10} concentrations significantly above those at non-urban sites, the quantitative differences can be sensitive to the location of the non-urban sites with respect to individual cities. The most striking feature of the urban excess is its large increase in the fall and winter in the western United States compared to the eastern United States.

The chemical compositions at the nonurban IMPROVE/NESCAUM sites are discussed within the earlier sections of Chapter 6. Later in Chapter 6 an independent evaluation of chemical composition is given based on a mixture of intensive studies at both urban and nonurban sites. The results from both approaches appear reasonably consistent in showing geographical variations in chemical composition.

Both approaches indicate that sulfate, presumably present either as $(NH_4)HSO_4$ or as $(NH_4)_2SO_4$, is the largest contributor to the chemical species measured in the eastern United States. Other results indicate that a large regional background of sulfate is superimposed on a smaller urban contribution. Results also indicate that sulfate is relatively uniform in concentration throughout much of the eastern United States. These results are less pronounced in the late fall and winter months. The contribution of sulfate to PM_{10} is somewhat smaller than sulfate is to $PM_{2.5}$. Comparisons of the eastern United States with the central United States and western United States show a decreasing contribution of sulfate to the chemical composition. Conversely, the soil and/or mineral concentrations become an increasingly important contributor to PM_{10} and $PM_{2.5}$ going from the eastern to the western United States. The nitrates, as NH_4NO_3, also appear to be a much more important contributor to the composition in areas of the western United States than in the eastern United States. Organic compounds also appear to increase in importance relative to sulfate going from the eastern to the western United States. For $PM_{(10-2.5)}$, sulfates are relatively unimportant. Soil or mineral components dominate the $PM_{(10-2.5)}$, but there is a substantial unknown fraction of $PM_{(10-2.5)}$.

Particle strong acidity, defined as H_2SO_4 plus HSO_4^-, is a regional pollutant fairly evenly distributed across large areas of the central portion of the eastern United States. It is relatively evenly distributed across small cities, but in the one large urban area from which results have been reported, the higher concentrations of ammonia in the central city apparently neutralize a significant portion of the acidity. Thus, higher concentrations of acidity are found in rural areas, small towns, and suburban areas than in the centers of larger urban areas. The concentration of acidity is higher in the summer and peaks during the early afternoon in urban areas. Indoor, outdoor, and personal monitoring indicates that indoor and personal concentrations of acidity are lower than outdoor concentrations, presumably due to

neutralization by indoor ammonia. Particle strong acidity is normally found exclusively in the fine particle mode. Coarse particles tend to be basic. Exceptions may occur during periods of fog or very high relative humidity.

The number concentration of particles is generally dominated by particles below 0.1 μm or 100 nm in diameter, termed ultrafine particles. When a distinct mode is present, it is called the nuclei mode. Number geometric mean diameter ranged from 12 to 43 nm in Long Beach, CA and 47 to 75 nm in clean air in the Rocky Mountains. Particle number concentrations varied from less than 1,000/cm^3 at clean background sites to over 100,000/cm^3 in polluted urban areas and were correlated with the volume of particles below 0.1 μm. Particle number concentrations were not found to be correlated with accumulation mode volume on an hourly basis. Correlations of particle number and accumulation mode volume might be expected if compared over longer time intervals (e.g., days), but such studies have not yet been done.

An examination of the size distribution of metals suggests that metals that may be volatilized during combustion may appear as ultrafine particles. Such metals include copper, zinc, and lead and possibly nickel and vanadium, as well as nonmetals selenium and sulfur. Ultrafine particles appear to exist longer under conditions of low concentrations and high relative humidity.

REFERENCES

AIRS, Aerometric Information Retrieval System [database]. (1995) [PM_{10} and $PM_{2.5}$ data]. Research Triangle Park, NC: U.S. Environmental Protection Agency, Office of Air Quality Planning and Standards.

Altshuller, A. P. (1980) Seasonal and episodic trends in sulfate concentrations (1963-1978) in the eastern United States. Environ. Sci. Technol. 14: 1337-1349.

Altshuller, A. P. (1982) Relationships involving particle mass and sulfur content at sites in and around St. Louis, Missouri. Atmos. Environ. 16: 837-843.

Altshuller, A. P. (1985) Relationships involving fine particle mass, fine particle sulfur and ozone during episodic periods at sites in and around St. Louis, MO. Atmos. Environ. 19: 265-276.

Altshuller, A. P. (1987) Relationships between direction of wind flow and fine particle sulfur concentrations within and upwind of St. Louis, MO. Atmos. Environ. 21: 1023-1032.

Appel, B. R.; Colodny, P.; Wesolowski, J. J. (1976) Analysis of carbonaceous materials in southern California atmospheric aerosols. Environ. Sci. Technol. 10: 359-363.

Appel, B. R.; Kothny, E. L.; Hoffer, E. M.; Hidy, G. M.; Wesolowski, J. J. (1978) Sulfate and nitrate data from the California Aerosol Characterization Experiment (ACHEX). Environ. Sci. Technol. 12: 418-425.

Appel, B. R.; Hoffer, E. M.; Kothny, E. L.; Wall, S. M.; Haik, M.; Knights, R. L. (1979) Analysis of carbonaceous material in southern California atmospheric aerosols. 2. Environ. Sci. Technol. 13: 98-104.

Ashbaugh, L. L.; Watson, J. G.; Chow, J. (1989) Estimating fluxes from California's dry deposition monitoring data. Presented at: 82nd annual meeting of the Air & Waste Management Association; June; Anaheim, CA. Pittsburgh, PA: Air & Waste Management Association; paper no. 89-65.3.

Barone, J. B.; Cahill, T. A.; Eldred, R. A.; Flocchini, R. G.; Shadoan, D. J.; Dietz, T. M. (1978) A multivariate statistical analysis of visibility degradation at four California cities. Atmos. Environ. 12: 2213-2221.

Barton, R. G.; Clark, W. D.; Seeker, W. R. (1990) In: Proceedings of the 1st international conference on toxic combustion byproducts.

Bennett, R. L.; Stockburger, L.; Barnes, H. M. (1994) Comparison of sulfur measurements from a regional fine particle network with concurrent acid modes network results. Atmos. Environ. 28: 409-419.

Berner, A.; Lürzer, C. (1980) Mass size distributions of traffic aerosols at Vienna. J. Phys. Chem. 84: 2079-2083.

Brauer, M.; Koutrakis, P.; Spengler, J. D. (1989) Personal exposures to acidic aerosols and gases. Environ. Sci. Technol. 23: 1408-1412.

Brauer, M.; Koutrakis, P.; Keeler, G. J.; Spengler, J. D. (1991) Indoor and outdoor concentrations of inorganic acidic aerosols and gases. J. Air Waste Manage. Assoc. 41: 171-181.

Burton, R. M.; Liu, L. J. S.; Wilson, W. E.; Koutrakis, P. (1995) Comparison of aerosol acidity in urban and semi-rural environments. Atmos. Environ.: submitted.

Cadle, S. H. (1985) Seasonal variations in nitric acid, nitrate, strong aerosol acidity, and ammonia in an urban area. Atmos. Environ. 19: 181-188.

Cahill, T. A. (1979) Comments on surface coating for Lundgren-type impactors. In: Lundgren, D. A.; Lippmann, M.; Harris, F. S., Jr.; Clark, W. E.; Marlow, W. H.; Durham, M. D., eds. Aerosol measurement: [papers from a workshop]; March 1976; Gainesville, FL. Gainesville, FL: University Presses of Florida; pp. 131-134.

Cahill, T. A. (1980) Proton microprobes and particle-induced X-ray analytical systems. Annu. Rev. Nucl. Part. Sci. 30: 211-252.

Cahill, T. A. (1996) [Data from IMPROVE data base.] Research Triangle Park, NC: U.S. Environmental Protection Agency, Office of Air Quality Planning and Standards.

Cahill, T. A.; Wakabayashi, P. (1993) Compositional analysis of size-segregated aerosol samples. In: Newman, L., ed. Measurement challenges in atmospheric chemistry. Washington, DC: American Chemical Society; pp. 211-228. (Advances in chemistry series no. 232).

Cahill, T. A.; Goodart, C.; Nelson, J. W.; Eldred, R. A.; Nasstrom, J. S.; Feeney, P. J. (1985) Design and evaluation of the drum impactor. In: Ariman, T.; Veziroglu, T. N., eds. Proceedings of the international symposium on particulate and multi-phase processes. Washington, DC: Hemisphere Publishing Corporation; pp. 319-325.

Cahill, T. A.; Feeney, P. J.; Eldred, R. A. (1987) Size-time composition profile of aerosols using the drum sampler. In: Proceedings of the 4th international PIXE conference; June 1986; Tallahassee, FL. Nucl. Instrum. Methods Phys. Res. B22: 344-348.

Cahill, T. A.; Surovik, M.; Wittmeyer, I. (1990) Visibility and aerosols during the 1986 Carbonaceous Species Methods Comparison Study. Aerosol Sci. Technol. 12: 149-160.

Cahill, T. A.; Wakabayashi, P.; Raabe, O.; Teague, S. (1992a) A new inertial impactor for visibility-reducing aerosols. Presented at: 85th annual meeting and exhibition of the Air & Waste Management Association; June; Kansas City, MO. Pittsburgh, PA: Air & Waste Management Association; paper no. 92-60.08.

Cahill, T. A.; Wilkinson, K.; Schnell, R. (1992b) Composition analyses of size-resolved aerosol samples taken from aircraft downwind of Kuwait, spring 1991. J. Geophys. Res. [Atmos.] 97: 14,513-14,520.

Cahill, T. A.; Morales, R.; Miranda, J. (1996a) Comparative aerosol studies of Pacific rim cities—Santiago, Chile (1987); Mexico City, Mexico (1987-1990); and Los Angeles, U.S.A. (1973 and 1987). Atmos. Environ. 30: 747-749.

Cahill, T. A.; Eldred, R. A.; Wakabayashi, P. H. (1996b) Trends in fine particle concentrations at Great Smoky Mountains National Park. For presentation at: Annual meeting of the Air & Waste Management Association; June; Nashville, TN. Pittsburgh, PA: Air & Waste Management Association; submitted paper no. 96-MP1A.05.

California Air Resources Board. (1995) [Data base provided by John R. Holmes, Chief, Research Division.] Sacramento, CA: California Air Resources Board.

Cass, G. R.; McRae, G. J. (1983) Source-receptor reconciliation of routine air monitoring data for trace metals: an emission inventory assisted approach. Environ. Sci. Technol. 17: 129-139.

Cass, G. R.; Conklin, M. H.; Shah, J. J.; Huntzicker, J. J.; Macias, E. S. (1984) Elemental carbon concentrations: estimation of an historical data base. Atmos. Environ. 18: 153-162.

Chesworth, S.; Yang, G.; Chang, D. P. Y.; Jones, A. D.; Kelly, P. B.; Kennedy, I. M. (1994) The fate of arsenic in a laminar diffusion flame. Combust. Flame 98: 259-266.

Chow, J. C.; Watson, J. G.; Frazier, C. A.; Egami, R. T.; Goodrich, A.; Ralph, C. (1988) Spatial and temporal source contributions to PM_{10} and $PM_{2.5}$ in Reno, NV. In: Mathai, C. V.; Stonefield, D. H., eds. PM-10: implementation of standards, an APCA/EPA international specialty conference; February; San Francisco, CA. Pittsburgh, PA: Air Pollution Control Association; pp. 438-457. (APCA transactions series TR-13).

Chow, J. C.; Watson, J. G.; Pritchett, L.; Lowenthal, D.; Frazier, C.; Neuroth, G.; Evans, K.; Moon, D. (1990) Wintertime visibility in Phoenix, Arizona. Presented at: the 83rd annual meeting & exhibition; June; Pittsburgh, PA. Pittsburgh, PA: Air & Waste Management Association; paper no. 90-66.6.

Chow, J. C.; Watson, J. G.; Lowenthal, D. H.; Frazier, C. A.; Hinsvark, B. A.; Prichett, L. C.; Neuroth, G. R. (1992a) Wintertime PM_{10} and $PM_{2.5}$ chemical compositions and source contributions in Tucson, Arizona. In: Chow, J. C.; Ono, D. M., eds. PM_{10} standards and nontraditional particulate source controls, an A&WMA/EPA international specialty conference, v. I; January; Scottsdale, AZ. Pittsburgh, PA: Air & Waste Management Association; pp. 231-243. (A&WMA transactions series no. 22).

Chow, J. C.; Watson, J. G.; Lowenthal, D. H.; Solomon, P. A.; Magliano, K. L.; Ziman, S. D.; Richards, L. W. (1992b) PM10 source apportionment in California's San Joaquin Valley. Atmos. Environ. Part A 26: 3335-3354.

Chow, J. C.; Liu, C. S.; Cassmassi, J.; Watson, J. G.; Lu, Z.; Pritchett, L. C. (1992c) A neighborhood-scale study of PM_{10} source contributions in Rubidoux, California. Atmos. Environ. Part A 26: 693-706.

Chow, J. C.; Watson, J. G.; Lowenthal, D. H.; Solomon, P. A.; Magliano, K. L.; Ziman, S. D.; Richards, L. W. (1993a) PM_{10} and $PM_{2.5}$ compositions in California's San Joaquin Valley. Aerosol Sci. Technol. 18: 105-128.

Chow, J. C.; Watson, J. G.; Ono, D. M.; Mathai, C. V. (1993b) PM_{10} standards and nontraditional particulate source controls: a summary of the A&WMA/EPA international specialty conference. J. Air Waste Manage. Assoc. 43: 74-84.

Chow, J. C.; Watson, J. G.; Fujita, E. M.; Lu, Z.; Lawson, D. R.; Ashbaugh, L. L. (1994a) Temporal and spatial variations of $PM_{2.5}$ and PM_{10} aerosol in the Southern California Air Quality Study. Atmos. Environ. 28: 2061-2080.

Chow, J. C.; Watson, J. G.; Solomon, P. A.; Thuillier, R. H.; Magliano, K. L.; Ziman, S. D.; Blumenthal, D. L.; Richards, L. W. (1994b) Planning for SJVAQS/AUSPEX particulate matter and visibility sampling and analysis. In: Solomon, P. A.; Silver, T. A., eds. Planning and managing regional air quality: modeling and measurement studies: a perspective through the San Joaquin Valley air quality study and AUSPEX. Boca Raton, FL: Lewis Publishers; pp. 171-216.

Chow, J. C.; Fairley, D.; Watson, J. G.; DeMandel, R.; Fujita, E. M.; Lowenthal, D. H.; Lu, Z.; Frazier, C. A.; Long, G.; Cordova, J. (1995a) Source apportionment of wintertime PM_{10} at San Jose, Calif. J. Environ. Eng. (NY) 121: 378-387.

Chow, J. C.; Watson, J. G.; Lu, Z.; Lowenthal, D. H.; Frazier, C. A.; Solomon, P. A.; Thuiller, R. H.; Magliano, K. (1995b) Descriptive analysis of $PM_{2.5}$ and PM_{10} regionally representative locations during SJVAQS/AUSPEX. Atmos. Environ.: in press.

Cobourn, W. G.; Husar, R. B. (1982) Diurnal and seasonal patterns of particulate sulfur and sulfuric acid in St. Louis, July 1977-June 1978. Atmos. Environ. 16: 1441-1450.

Conner, T. L.; Miller, J. L.; Willis, R. D.; Kellogg, R. B.; Dann, T. F. (1993) Source apportionment of fine and coarse particles in southern Ontario, Canada. Presented at: 86th annual meeting & exhibition of the Air & Waste Management Association; June; Denver, CO. Pittsburgh, PA: Air & Waste Management Association; paper no. 93-TP-58.05.

Countess, R. J.; Wolff, G. T.; Cadle, S. H. (1980) The Denver winter aerosol: a comprehensive chemical characterization. J. Air Pollut. Control Assoc. 30: 1194-1200.

Countess, R. J.; Cadle, S. H.; Groblicki, P. J.; Wolff, G. T. (1981) Chemical analysis of size-segregated samples of Denver's ambient particulate. J. Air Pollut. Control Assoc. 31: 247-252.

Davis, B. L.; Johnson, L. R.; Stevens, R. K.; Courtney, W. J.; Safriet, D. W. (1984) The quartz content and elemental composition of aerosols from selected sites of the EPA inhalable particulate network. Atmos. Environ. 18: 771-782.

Davison, R. L.; Natusch, D. F. S.; Wallace, J. R.; Evans, C. A., Jr. (1974) Trace elements in fly ash: dependence of concentration on particle size. Environ. Sci. Technol. 8: 1107-1113.

Desaedeleer, G. G.; Winchester, J. W.; Akselsson, K. R. (1977) Monitoring aerosol elemental composition in particle size fractions for predicting human respiratory uptake. Nucl. Instrum. Methods 142: 97-99.

Desert Research Institute. (1995) [Unpublished data]. Reno, NV: Energy and Environmental Engineering Center.

Dockery, D. W.; Schwartz, J.; Spengler, J. D. (1992) Air pollution and daily mortality: associations with particulates and acid aerosols. Environ. Res. 59: 362-373.

Dockery, D. W.; Pope, C. A., III; Xu, X.; Spengler, J. D.; Ware, J. H.; Fay, M. E.; Ferris, B. G., Jr.; Speizer, F. E. (1993) An association between air pollution and mortality in six U.S. cities. N. Engl. J. Med. 329: 1753-1759.

Dresser, A. L. (1988) A dispersion and receptor model analysis of a western community's PM-10 problem. JAPCA 38: 1419-1421.

Dzubay, T. G. (1980) Chemical element balance method applied to dichotomous sampler data. Ann. N. Y. Acad. Sci. 338: 126-144.

Dzubay, T. G.; Stevens, R. K.; Lewis, C. W.; Hern, D. H.; Courtney, W. J.; Tesch, J. W.; Mason, M. A. (1982) Visibility and aerosol composition in Houston, Texas. Environ. Sci. Technol. 16: 514-525.

Dzubay, T. G.; Stevens, R. K.; Gordon, G. E.; Olmez, I.; Sheffield, A. E.; Courtney, W. J. (1988) A composite receptor method applied to Philadelphia aerosol. Environ. Sci. Technol. 22: 46-52.

Eldering, A.; Cass, G. R. (1994) A source-oriented model for air pollutant effects on visibility. J. Geophys. Res. [Atmos.]: submitted.

Eldred, R. A.; Cahill, T. A. (1994) Trends in elemental concentrations of fine particles at remote sites in the United States of America. Atmos. Environ. 28: 1009-1019.

Eldred, R. A.; Ashbaugh, L. L.; Cahill, T. A.; Flocchini, R. G.; Pitchford, M. L. (1983) Sulfate levels in the southwest during the 1980 copper smelter strike. J. Air Pollut. Control Assoc. 33: 110-113.

Eldred, R. A.; Cahill, T. A.; Feeney, P. J.; Malm, W. C. (1987) Regional patterns in particulate matter from the National Park Service network, June 1982 to May 1986. In: Bhardwaja, P. S., ed. Visibility protection: research and policy aspects, an APCA international specialty conference; September 1986; Grand Teton National Park, WY. Pittsburgh, PA: Air Pollution Control Association; pp. 386-396. (APCA transactions series no. TR-10).

Eldred, R. A.; Cahill, T. A.; Pitchford, M.; Malm, W. C. (1988) IMPROVE--a new remote area particulate monitoring system for visibility studies. Presented at: 81st annual meeting of the Air Pollution Control Association; June; Dallas, TX. Pittsburgh, PA: Air Pollution Control Association; paper no. 88-54.3.

Eldred, R. A.; Cahill, T. A.; Wilkinson, L. K.; Feeney, P. J.; Chow, J. C.; Malm, W. C. (1990) Measurement of fine particles and their chemical components in the IMPROVE/NPS networks. In: Mathai, C. V., ed. Visibility and fine particles: an A&WMA/EPA international specialty conference; October 1989; Estes Park, CO. Pittsburgh, PA: Air & Waste Management Association; pp. 187-196. (A&WMA transactions series no. TR-17).

Eldred, R. A.; Cahill, T. A.; Feeney, P. J. (1994a) Regional patterns of selenium and other trace elements in the IMPROVE network. In: Proceedings of the international specialty conference on aerosol and atmospheric optics: radiative balance and visual air quality, volume A. Pittsburgh, PA: Air and Waste Management Association.

Eldred, R. A.; Cahill, T. A.; Flocchini, R. G. (1994b) Comparison of PM_{10} and $PM_{2.5}$ aerosols in the IMPROVE network. In: Proceedings of an international specialty conference on aerosol and atmospheric optics: radiative balance and visual air quality, volume A. Pittsburgh, PA: Air and Waste Management Association. Air Waste: submitted.

Ellenson, W. D.; Schwab, M.; Egler, K. A.; Shadwick, D.; Willis, R. D. (1994) Draft technical report for the pilot project of lower Rio Grande valley environmental study. ManTech Environmental Technology. Submitted to U.S. EPA.

Fairley, D. (1990) The relationship of daily mortality to suspended particulates in Santa Clara county, 1980-86. Environ. Health Perspect. 89: 159-168.

Federal Register. (1986) Hazardous waste management system; land disposal restrictions. F. R. (November 7) 51: 40572-40654.

Fekete, K. E.; Gyenes, L. (1993) Regional scale transport model for ammonia and ammonium. Atmos. Environ. Part A 27: 1099-1104.

Ferman, M. A.; Wolff, G. T.; Kelly, N. A. (1981) The nature and sources of haze in the Shenandoah Valley/Blue Ridge Mountains area. J. Air Pollut. Control Assoc. 31: 1074-1082.

Flocchini, R. G.; Cahill, T. A.; Shadoan, D. J.; Lange, S. J.; Eldred, R. A.; Feeney, P. J.; Wolfe, G. W.; Simmeroth, D. C.; Suder, J. K. (1976) Monitoring California's aerosols by size and elemental composition. Environ. Sci. Technol. 10: 76-82.

Flocchini, R. G.; Cahill, T. A.; Eldred, R. A.; Feeney, P. J. (1990) Particulate sampling in the northeast: a description of the Northeast States for Coordinated Air Use Management (NESCAUM) network. In: Mathai, C. V., ed. Visibility and fine particles: an A&WMA/EPA international specialty conference; October 1989; Estes Park, CO. Pittsburgh, PA: Air & Waste Management Association; pp. 197-206. (A&WMA transactions series no. TR-17).

Frazier, C. A. (1989) Letter [report on mass and chemical concentrations and b_{abs} measurements for Phoenix pilot study samples]. Reno, NV: Desert Research Institute, Energy and Environmental Engineering Center.

Friedlander, S. K. (1977) Smoke, dust and haze: fundamentals of aerosol behavior. New York, NY: John Wiley & Sons.

Gray, H. A.; Cass, G. R.; Huntzicker, J. J.; Heyerdahl, E. K.; Rau, J. A. (1984) Elemental and organic carbon particle concentrations: a long-term perspective. Sci. Total Environ. 36: 17-25.

Gray, H. A.; Cass, G. R.; Huntzicker, J. J.; Heyerdahl, E. K.; Rau, J. A. (1986) Characteristics of atmospheric organic and elemental carbon particle concentrations in Los Angeles. Environ. Sci. Technol. 20: 580-589.

Griffing, G. W. (1980) Relations between the prevailing visibility, nephelometer scattering coefficient and sunphotometer turbidity coefficient. Atmos. Environ. 14: 577-584.

Groblicki, P. J.; Wolff, G. T.; Countess, R. J. (1981) Visibility-reducing species in the Denver "brown cloud" - I. relationships between extinction and chemical composition. In: White, W. H.; Moore, D. J.; Lodge, J. P., Jr., eds. Plumes and visibility: measurements and model components, proceedings of the symposium; November 1980; Grand Canyon National Park, AZ. Atmos. Environ. 15: 2473-2484.

Hasan, H.; Dzubay, T. G. (1987) Size distributions of species in fine particles in Denver using a microorifice impactor. Aerosol Sci. Technol. 6: 29-39.

Hering, S. V.; Friedlander, S. K. (1982) Origins of aerosol sulfur size distributions in the Los Angeles basin. Atmos. Environ. 16: 2647-2656.

Hering, S. V.; McMurry, P. H. (1991) Optical counter response to monodisperse atmospheric aerosols. Atmos. Environ. Part A 25: 463-468.

Hering, S. V.; Flagan, R. C.; Friedlander, S. K. (1978) Design and evaluation of new low-pressure impactor. I. Environ. Sci. Technol. 12: 667-673.

Hering, S. V.; Appel, B. R.; Cheng, W.; Salaymeh, F.; Cadle, S. H.; Mulawa, P. A.; Cahill, T. A.; Eldred, R. A.; Surovik, M.; Fitz, D.; Howes, J. E.; Knapp, K. T.; Stockburger, L.; Turpin, B. J.; Huntzicker, J. J.; Zhang, X.-Q.; McMurry, P. H. (1990) Comparison of sampling methods for carbonaceous aerosols in ambient air. Aerosol Sci. Technol. 12: 200-213.

Hering, S.; Eldering, A.; Seinfeld, J. H. (1996) Bimodal character of accumulation mode aerosols in southern California. Atmos. Environ.: submitted.

Hidy, G. M.; Mueller, P. K.; Grosjean, D.; Appel, B. R.; Wesolowski, J. J., eds. (1980) The character and origins of smog aerosols: a digest of results from the California Aerosol Characterization Experiment (ACHEX). New York, NY: John Wiley & Sons.

Hildemann, L. M.; Markowski, G. R.; Cass, G. R. (1991) Chemical composition of emissions from urban sources of fine organic aerosol. Environ. Sci. Technol. 25: 744-759.

Hoggan, M. C.; Banayan, S. C.; Sin, R. W.; Davidson, A. (1993) An analysis of PM_{10} air quality in California's South Coast Air Basin, 1985-1992. In: Criteria air pollutants: volume 3B, papers from the 86th annual meeting & exhibition of the Air & Waste Management Association; June ; Denver, CO. Pittsburgh, PA: Air & Waste Management Association; paper no. 93-WA-75.04. (A&WMA publication no. AM93-3).

Houck, J. E.; Rau, J. A.; Body, S.; Chow, J. C. (1992) Source apportionment: Pocatello, Idaho PM_{10} nonattainment area. In: Chow, J. C.; Ono, D. M., eds. PM_{10} standards and nontraditional particulate source controls, an A&WMA/EPA international specialty conference, v. I; January; Scottsdale, AZ. Pittsburgh, PA: Air & Waste Management Association; pp. 219-230. (A&WMA transactions series no. 22).

Husar, R. B.; Frank, N. H. (1991) Interactive exploration and analysis of EPA's Aerometric Information and Retrieval System (AIRS) data sets. Presented at: 84th annual meeting and exhibition of the Air & Waste Management Association; June; Vancouver, BC, Canada. Pittsburgh, PA: Air & Waste Management Association; paper no. 91-119.4.

Husar, R. B.; Poirot, R. (1992) Exploration of the AIRS database: weekly cycle of ozone and PM 10 aerosols. Presented at: 85th annual meeting of the Air & Waste Management Association; June; Kansas City, MO. Pittsburgh, PA: Air & Waste Management Association; paper no. 92-77.06.

Husar, R. B.; Wilson, W. E. (1993) Haze and sulfur emission trends in the eastern United States. Environ. Sci. Technol. 27: 12-16.

Husar, R. B.; Holloway, J. M.; Patterson, D. E.; Wilson, W. E. (1981) Spatial and temporal pattern of eastern U.S. haziness: a summary. Atmos. Environ. 15: 1919-1928.

Husar, R. B.; Elkins, J. B.; Wilson, W. E. (1994) U.S. visibility trends, 1960-1992, regional and national. Presented at: 87th annual meeting of the Air & Waste Management Association; June; Cincinnati, OH. Pittsburgh, PA: Air & Waste Management Association; paper no. 94-MP3.05.

IPN. (1985) [Inhalable Particulate Network Database.] Research Triangle Park, NC: U.S. Environmental Protection Agency, National Exposure Research Laboratory; Jose M. Sune, contact.

Jaenicke, R. (1980) Natural aerosols. In: Kneip, T. J.; Lioy, P. J., eds. Aerosols: anthropogenic and natural, sources and transport. Ann. N. Y. Acad. Sci. 338: 317-329.

Japar, S. M.; Brachaczek, W. W.; Gorse, R. A., Jr.; Norbeck, J. M.; Pierson, W. R. (1986) The contribution of elemental carbon to the optical properties of rural atmospheric aerosols. Atmos. Environ. 20: 1281-1289.

John, W.; Wall, S. M.; Ondo, J. L.; Winklmayr, W. (1989) Acidic aerosol size distributions during SCAQS. Sacramento, CA: California Air Resources Board; report no. CA/DOH/AIHL/SP-51.

John, W.; Wall, S. M.; Ondo, J. L.; Winklmayr, W. (1990) Modes in the size distributions of atmospheric inorganic aerosol. Atmos. Environ. Part A 24: 2349-2359.

Johnson, R. L.; Shah, J. J.; Cary, R. A.; Huntzicker, J. J. (1981) An automated thermal-optical method for the analysis of carbonaceous aerosol. In: Macias, E. S.; Hopke, P. K., eds. Atmospheric aerosol: source/air quality relationships; based on a symposium jointly sponsored by the Divisions of Nuclear Chemistry and Technology at the 180th national meeting of the American Chemical Society; August 1980; Las Vegas, NV. Washington, DC: American Chemical Society; pp. 223-233. (Comstock, M. J., ed. ACS symposium series: 167).

Johnson, D. L.; Davis, B. L.; Dzubay, T. G.; Hasan, H.; Crutcher, E. R.; Courtney W. J.; Jaklevic, J. M.; Thompson, A. C.; Hopke, P. K. (1984) Chemical and physical analyses of Houston aerosol for interlaboratory comparison of source apportionment procedures. Atmos. Environ. 18: 1539-1553.

Joseph, D. B.; Metsa, J.; Malm, W. C.; Pitchford, M. (1987) Plans for IMPROVE: a federal program to monitor visibility in class I areas. In: Bhardwaja, P. S., ed. Visibility protection: research and policy aspects, an APCA international specialty conference; September 1986; Grand Teton National Park, WY. Pittsburgh, PA: Air Pollution Control Association; pp. 113-125. (APCA transactions series no. TR-10).

Kao, A. S.; Friedlander, S. K. (1994) Chemical signatures of the Los Angeles aerosol ($d_p < 3.5$ μm). Aerosol Sci. Technol. 21: 283-293.

Kao, A. S.; Friedlander, S. K. (1995) Frequency distributions of PM_{10} chemical components and their sources. Environ. Sci. Technol. 29: 19-28.

Karch, R.; Kruisz, C.; Reischl, G. P.; Winklmayr, W. (1987) Continuous measurement of ultrafine particle size distributions in the range from 2 to 200 nm from the southern California air quality study, June-July 1987 [preliminary report]. Vienna, Austria: Institut fur Experimentalphysik der Universitat Wien.

Keeler, G. J.; Brachaczek, W. W.; Gorse, R. A., Jr.; Japar, S. M.; Pierson, W. R. (1988) Effect of ambient humidity on dichotomous sampler coarse/fine ratios. Atmos. Environ. 22: 1715-1720.

Keeler, G. J.; Japar, S. M.; Brachaczek, W. W.; Gorse, R. A., Jr.; Norbeck, J. M.; Pierson, W. R. (1990) The sources of aerosol elemental carbon at Allegheny Mountain. Atmos. Environ. Part A 24: 2795-2805.

Keeler, G. J.; Spengler, J. D.; Castillo, R. A. (1991) Acid aerosol measurements at a suburban Connecticut site. Atmos. Environ. Part A 25: 681-690.

Kelly, N. A.; Wolff, G. T.; Ferman, M. A. (1982) Background pollutant measurements in air masses affecting the eastern half of the United States - 1. air masses arriving from the northwest. Atmos. Environ. 16: 1077-1088.

Kim, B. M.; Zeldin, M. D.; Liu, C. S. (1992) Source apportionment study for state implementation plan development in the Coachella Valley. In: Chow, J. C.; Ono, D. M., eds. PM10 standards and nontraditional particulate source controls, an A&WMA/EPA international specialty conference, v. II; January; Scottsdale, AZ. Pittsburgh, PA: Air & Waste Management Association; pp. 979-991. (A&WMA transactions series no. 22).

Kleinman, M. T.; Pasternack, B. S.; Eisenbud, M.; Kneip, T. J. (1980) Identifying and estimating the relative importance of sources of airborne particulates. Environ. Sci. Technol. 14: 62-65.

Koutrakis, P. (1995) [$PM_{2.5}$ and PM_{10} data for Philadelphia, 1992-1995]. Boston, MA: Harvard School of Public Health.

Koutrakis, P.; Kelly, B. P. (1993) Equilibrium size of atmospheric aerosol sulfates as a function of particle acidity and ambient relative humidity. J. Geophys. Res. [Atmos.] 98: 7141-7147.

Koutrakis, P.; Spengler, J. D. (1987) Source apportionment of ambient particles in Steubenville, OH using specific rotation factor analysis. Atmos. Environ. 21: 1511-1519.

Kreidenweis, S. M. (1993) Towards development of a northern hemisphere natural sulfate aerosol budget. Presented at: 86th annual meeting of the Air & Waste Management Association; June; Denver, CO. Pittsburgh, PA: Air & Waste Management Association; paper no. 93-MP-4.08.

Kreidenweis, S.; Brechtel, F. (1995) [Particle number and size-distribution database]. Fort Collins, CO: Colorado State University, Foothill Campus, Atmospheric Sciences Department.

Lamborg, C.; Keeler, G. J.; Evans, G. (1992) Atmospheric acidity measurements during the Lake Michigan Urban Air Toxics Study. Research Triangle Park, NC: U.S. Environmental Protection Agency, Atmospheric Research and Exposure Assessment Laboratory; EPA report no. EPA/600/A-92/250. Available from: NTIS, Springfield, VA; PB93-121069.

Lawson, D. R. (1990) The Southern California Air Quality Study. J. Air Waste Manage. Assoc. 40: 156-165.

Leaderer, B. P.; Bernstein, D. M.; Daisey, J. M.; Kleinman, M. T.; Kneip, T. J.; Knutson, E. O.; Lippmann, M.; Lioy, P. J.; Rahn, K. A.; Sinclair, D.; Tanner, R. L.; Wolff, G. T. (1978) Summary of the New York summer aerosol study (NYSAS). J. Air Pollut. Control Assoc. 28: 321-327.

Leaderer, B. P.; Tanner, R. L.; Holford, T. R. (1982) Diurnal variations, chemical composition and relation to meteorological variables of the summer aerosol in the New York subregion. Atmos. Environ. 16: 2075-2087.

Lee, H. S.; Wadden, R. A.; Scheff, P. A. (1993) Measurement and evaluation of acid air pollutants in Chicago using an annular denuder system. Atmos. Environ. Part A 27: 543-553.

Lewis, C. W.; Dzubay, T. G. (1986) Measurement of light absorption extinction in Denver. Aerosol Sci. Technol. 5: 325-336.

Lewis, C. W.; Macias, E. S. (1980) Composition of size-fractionated aerosol in Charleston, West Virginia. Atmos. Environ. 14: 185-194.

Lewis, C. W.; Baumgardner, R. E.; Stevens, R. K.; Russwurm, G. M. (1986) Receptor modeling study of Denver winter haze. Environ. Sci. Technol. 20: 1126-1136.

Li, Y.; Roth, H. D. (1995) Daily mortality analysis by using different regression models in Philadelphia County, 1973-1990. In: Phalen, R. F.; Bates, D. V., eds. Proceedings of the colloquium on particulate air pollution and human mortality and morbidity; January 1994; Irvine, CA. Inhalation Toxicol. 7: 45-58.

Liang, C. S. K.; Waldman, J. M. (1992) Indoor exposures to acidic aerosols at child and elderly care facilities. Indoor Air 2: 196-207.

Liousse, C.; Penner, J. E.; Chuang, C.; Walton, J. J.; Eddleman, H.; Cachier, H. (1996) A global three-dimensional model study of carbonaceous aerosols. J. Geophys. Res. [Atmos.] 101: in press.

Lioy, P. J.; Samson, P. J.; Tanner, R. L.; Leaderer, B. P.; Minnich, T.; Lyons, W. (1980) The distribution and transport of sulfate "species" in the New York metropolitan area during the 1977 summer aerosol study. Atmos. Environ. 14: 1391-1407.

Lioy, P. J.; Daisey, J. M.; Greenberg, A.; Harkov, R. (1985) A major wintertime (1983) pollution episode in northern New Jersey: analyses of the accumulation and spatial distribution of inhalable particulate matter, extractable organic matter and other species. Atmos. Environ. 19: 429-436.

Lipfert, F. W.; Wyzga, R. E. (1993) On the spatial and temporal variability of aerosol acidity and sulfate concentration. Air Waste 43: 489-491.

Liu, L.-J. S.; Burton, R.; Wilson, W. E.; Koutrakis, P. (1996) Comparison of aerosol acidity in urban and semi-rural environments. Atmos. Environ. 30: 1237-1245.

Lundgren, D. A. (1967) An aerosol sampler for determination of particle concentration as a function of size and time. J. Air Pollut. Control Assoc. 17: 225-229.

Macias, E. S.; Zwicker, J. O.; Ouimette, J. R.; Hering, S. V.; Friedlander, S. K.; Cahill, T. A.; Kuhlmey, G. A.; Richards, L. W. (1981) Regional haze case studies in the southwestern U.S. - I. aerosol chemical composition. In: White, W. H.; Moore, D. J.; Lodge, J. P., Jr., eds. Plumes and visibility: measurements and model components, proceedings of the symposium; November 1980; Grand Canyon National Park, AZ. Atmos. Environ. 15: 1971-1986.

Maenhaut, W.; Royset, O.; Vadset, M.; Kauppinen, E. I.; Lind, T. M. (1993) Analysis of size-fractionated coal combustion aerosols by PIXE and other analytical techniques. Nucl. Instrum. Methods Phys. Res. Sect. B 75: 266-272.

Malm, W. C.; Gebhart, K. A.; Molenar, J.; Cahill, T.; Eldred, R.; Huffman, D. (1994a) Examining the relationship between atmospheric aerosols and light extinction at Mount Rainier and North Cascades National Parks. Atmos. Environ. 28: 347-360.

Malm, W. C.; Sisler, J. F.; Huffman, D.; Eldred, R. A.; Cahill, T. A. (1994b) Spatial and seasonal trends in particle concentration and optical extinction in the United States. J. Geophys. Res. [Atmos.] 99: 1347-1370.

Mangelson, N. F.; Rees, L. B.; Lewis, L.; Joseph, J. M.; Cui, W.; Machir, J.; Eatough, D. J.; Wilkerson, T. D.; Jensen, D. T. (1994) The formation of sulfate and nitrate during winter inversion fogs in Cache Valley, Utah. In: Proceedings of an international specialty conference on aerosol and atmospheric optics: radiative balance and visual air quality, volume A. Pittsburgh, PA: Air and Waste Management Association.

Marple, V.; Rubow, K.; Ananth, G.; Fissan, H. J. (1986) Micro-orifice uniform deposit impactor. J. Aerosol Sci. 17: 489-494.

Marple, V. A.; Rubow, K. L.; Behm, S. M. (1991) A microorifice uniform deposit impactor (MOUDI): description, calibration, and use. Aerosol Sci. Technol. 14: 434-446.

Marshall, B. T.; Patterson, E. M.; Grams, G. W. (1986) Characterization of the Atlanta area aerosol, elemental composition and possible sources. Atmos. Environ. 20: 1291-1300.

McMurry, P. H.; Stolzenburg, M. R. (1989) On the sensitivity of particle size to relative humidity for Los Angeles aerosols. Atmos. Environ. 23: 497-507.

McMurry, P. H.; Zhang, X. Q. (1989) Size distributions of ambient organic and elemental carbon. Aerosol Sci. Technol. 10: 430-437.

Mercer, T. T. (1964) The stage constants of cascade impactors. Ann. Occup. Hyg. 7: 115-124.

Molenar, J. V.; Dietrich, D. L.; Cismoski, D. S.; Cahill, T. A.; Wakabayashi, P. H. (1994) In: Proceedings of an international specialty conference on aerosol and atmospheric optics: radiative balance and visual air quality, volume A. Pittsburgh, PA: Air & Waste Management Association.

Moyers, J. L. (1982) 1981-1982 aerosol studies for nine southwest national parks and monuments. Washington, DC: U.S. Department of the Interior, National Park Service, Southwest Region.

Mukerjee, S.; Fox, D. L.; Stevens, R. K.; Shy, C. M.; Vescio, N.; Lumpkin, T. A.; Kellogg, R. B. (1993) A methodology to apportion ambient air measurements to investigate potential effects on air quality near waste incinerators. Research Triangle Park, NC: U.S. Environmental Protection Agency, Atmospheric Research and Exposure Assessment Laboratory; report no. EPA/600/A-93/104. Available from: NTIS, Springfield, VA; PB93-191393.

Mylonas, D. T.; Allen, D. T.; Ehrman, S. H.; Pratsinis, S. E. (1991) The sources and size distributions of organonitrates in Los Angeles aerosol. Atmos. Environ. Part A 25: 2855-2861.

Natusch, D. F. S.; Wallace, J. R. (1974) Urban aerosol toxicity: the influence of particle size. Particle size, adsorption, and respiratory deposition profiles combine to determine aerosol toxicity. Science (Washington, DC) 186: 695-699.

Natusch, D. F. S.; Wallace, J. R.; Evans, C. A., Jr. (1974) Toxic trace elements: preferential concentration in respirable particles. Science (Washington, DC) 183: 202-204.

Neas, L. M. (1996) [Data provided for 1986 from Harvard six cities data base.] Boston, MA: Harvard School of Public Health.

Noll, K. E.; Pontius, A.; Frey, R.; Gould, M. (1985) Comparison of atmospheric coarse particles at an urban and non-urban site. Atmos. Environ. 19: 1931-1943.

Noll, K. E.; Draftz, R.; Fang, K. Y. P. (1987) The composition of atmospheric coarse particles at an urban and non-urban site. Atmos. Environ. 21: 2717-2721.

Noll, K. E.; Yuen, P.-F.; Fang, K. Y.-P. (1990) Atmospheric coarse particulate concentrations and dry deposition fluxes for ten metals in two urban environments. Atmos. Environ. Part A 24: 903-908.

Patterson, R. K.; Wagman, J. (1977) Mass and composition of an urban aerosol as a function of particle size for several visibility levels. J. Aerosol Sci. 8: 269-279.

Pickle, T.; Allen, D. T.; Pratsinis, S. E. (1990) The sources and size distributions of aliphatic and carbonyl carbon in Los Angeles aerosol. Atmos. Environ. Part A 24: 2221-2228.

Pierson, W. R.; Brachaczek, W. W. (1988) Coarse- and fine-particle atmospheric nitrate and $HNO_3(g)$ in Claremont, California, during the 1985 Nitrogen Species Methods Comparison Study. Atmos. Environ. 22: 1665-1668.

Pierson, W. R.; Russell, P. A. (1979) Aerosol carbon in the Denver area in November 1973. Atmos. Environ. 13: 1623-1628.

Pierson, W. R.; Brachaczek, W. W.; Korniski, T. J.; Truex, T. J.; Butler, J. W. (1980a) Artifact formation of sulfate, nitrate, and hydrogen ion on backup filters: Allegheny Mountain experiment. J. Air Pollut. Control Assoc. 30: 30-34.

Pierson, W. R.; Brachaczek, W. W.; Truex, T. J.; Butler, J. W.; Korniski, T. J. (1980b) Ambient sulfate measurements on Allegheny Mountain and the question of atmospheric sulfate in the northeastern United States. Ann. N. Y. Acad. Sci. 338: 145-173.

Pierson, W. R.; Brachaczek, W. W.; Gorse, R. A., Jr.; Japar, S. M.; Norbeck, J. M. (1986) On the acidity of dew. J. Geophys. Res. [Atmos]. 91: 4083-4096.

Pierson, W. R.; Brachaczek, W. W.; Gorse, R. A., Jr.; Japar, S. M.; Norbeck, J. M.; Keeler, G. J. (1987) Acid rain and atmospheric chemistry at Allegheny Mountain. Environ. Sci. Technol. 21: 679-691.

Pierson, W. R.; Brachaczek, W. W.; Gorse, R. A., Jr.; Japar, S. M.; Norbeck, J. M.; Keeler, G. J. (1989) Atmospheric acidity measurements on Allegheny Mountain and the origins of ambient acidity in the northeastern United States. Atmos. Environ. 23: 431-459.

Pinto, J. P.; Pleasant, M.; Kellogg, R.; Torok, Sz.; Stiles, D.; Willis, R. D.; Koutrakis, P.; Allen, G. A. (1995) Chemical characterization of the ambient aerosol in Philadelphia. Presented at: Particulate matter: health and regulatory issues: an A&WMA international specialty conference; April; Pittsburgh, PA. Pittsburgh, PA: Air & Waste Management Association; submitted abstract.

Placet, M.; Battye, R. E.; Fehsenfeld, F. C.; Bassett, G. W. (1991) Emissions involved in acidic deposition processes. In: Irving, P. M., ed. Acidic deposition: state of science and technology, volume 1: emissions, atmospheric processes, and deposition. Washington, DC: The U.S. National Acid Precipitation Assessment Program. (State of science and technology report no. 1).

Poirot, R. L.; Flocchini, R. G.; Husar, R. B. (1990) Winter fine particle composition in the northeast: preliminary results from the NESCAUM monitoring network. Presented at: 83rd annual meeting of the Air & Waste Management Association; June; Pittsburgh, PA. Pittsburgh, PA: Air & Waste Management Association; paper no. 90-84.5.

Poirot, R. L.; Galvin, P. J.; Gordon, N.; Quan, S.; Van Arsdale, A.; Flocchini, R. G. (1991) Annual and seasonal fine particle composition in the northeast: second year results from the NESCAUM monitoring network. Presented at: 84th annual meeting and exhibition of the Air & Waste Management Association; June; Vancouver, BC, Canada. Pittsburgh, PA: Air & Waste Management Association; paper no. 91-49.1.

Pope, C. A., III; Schwartz, J.; Ransom, M. R. (1992) Daily mortality and PM_{10} pollution in Utah valley. Arch. Environ. Health 47: 211-217.

Raabe, O. G.; Braaten, D. A.; Axelbaum, R. L.; Teague, S. V.; Cahill, T. A. (1988) Calibration studies of the drum impactor. J. Aerosol Sci. 19: 183-195.

Reid, J. S.; Cahill, T. A.; Wakabayashi, P. H.; Dunlap, M. R. (1994) Geometric/aerodynamic equivalent diameter ratios of ash aggregate aerosols collected in burning Kuwaiti well fields. Atmos. Environ. 28: 2227-2234.

Rodes, C. E.; Evans, E. G. (1985) Preliminary assessment of 10 μm particulate sampling at eight locations in the United States. Atmos. Environ. 19: 293-303.

Rogge, W. F.; Mazurek, M. A.; Hildemann, L. M.; Cass, G. R.; Simoneit, B. R. T. (1993) Quantification of urban organic aerosols at a molecular level: identification, abundance and seasonal variation. Atmos. Environ. Part A 27: 1309-1330.

Russell, A. G.; Cass, G. R. (1986) Verification of a mathematical model for aerosol nitrate and nitric acid formation and its use for control measure evaluation. Atmos. Environ. 20: 2011-2025.

Schichtel, B. A.; Husar, R. B. (1991) Apportionment of light extinction by aerosol types over the U.S. Hawscom Air Force Base, MA: Air Force Systems Command, Phillips Laboratory; scientific report no. 4.

Schwartz, J. (1994) Air pollution and hospital admissions for the elderly in Birmingham, Alabama. Am. J. Epidemiol. 139: 589-598.

Schwartz, J.; Dockery, D. W. (1992) Increased mortality in Philadelphia associated with daily air pollution concentrations. Am. Rev. Respir. Dis. 145: 600-604.

Seaton, A.; MacNee, W.; Donaldson, K.; Godden, D. (1995) Particulate air pollution and acute health effects. Lancet (8943): 176-178.

Seeker, W. R. (1990) Waste combustion. In: Proceedings of the 23rd international symposium on combustion; pp. 867-885.

Seinfeld, J. H. (1986) Atmospheric chemistry and physics of air pollution. New York, NY: John Wiley and Sons.

Senior, C. L.; Flagan, R. C. (1982) Ash vaporization and condensation during combustion of a suspended coal particle. Aerosol Sci. Technol. 1: 371-383.

Shah, J. J.; Watson, J. G., Jr.; Cooper, J. A.; Huntzicker, J. J. (1984) Aerosol chemical composition and light scattering in Portland, Oregon: the role of carbon. Atmos. Environ. 18: 235-240.

Shaw, R. W., Jr.; Paur, R. J. (1983) Composition of aerosol particles collected at rural sites in the Ohio River Valley. Atmos. Environ. 17: 2031-2044.

Sisler, J. F.; Malm, W. C. (1994) The relative importance of soluble aerosols to spatial and seasonal trends of impaired visibility in the United States. Atmos. Environ. 28: 851-862.

Sisler, J. F.; Huffman, D.; Lattimer, D. A.; Malm, W. C.; Pitchford, M. L. (1993) Spatial and temporal patterns and the chemical composition of the haze in the United States: an anlysis of data from the IMPROVE network, 1988-1991. Fort Collins, CO: Colorado State University, Cooperative Institute for Research in the Atmosphere (CIRA).

Skidmore, L. W.; Chow, J. C.; Tucker, T. T. (1992) PM10 air quality assessment for the Jefferson County, Ohio air quality control region. In: Chow, J. C.; Ono, D. M., eds. PM_{10} standards and nontraditional particulate source controls, an A&WMA/EPA international specialty conference, v. II; January; Scottsdale, AZ. Pittsburgh, PA: Air and Waste Management Association; pp. 1016-1031. (A&WMA transactions series no. 22).

Sloane, C. S.; Watson, J.; Chow, J.; Pritchett, L.; Richards, L. W. (1991) Size-segregated fine particle measurements by chemical species and their impact on visibility impairment in Denver. Atmos. Environ. Part A 25: 1013-1024.

Small, M.; Germani, M. S.; Small, A. M.; Zoller, W. H.; Moyers, J. L. (1981) Airborne plume study of emissions from the processing of copper ores in southeastern Arizona. Environ. Sci. Technol. 15: 293-299.

Solomon, P. A.; Moyers, J. L. (1986) A chemical characterization of wintertime haze in Phoenix, Arizona. Atmos. Environ. 20: 207-213.

Solomon, P. A.; Fall, T.; Salmon, L.; Cass, G. R.; Gray, H. A.; Davidson, A. (1989) Chemical characteristics of PM_{10} aerosols collected in the Los Angeles area. JAPCA 39: 154-163.

Spengler, J. D.; Thurston, G. D. (1983) Mass and elemental composition of fine and coarse particles in six U.S. cities. J. Air Pollut. Control Assoc. 33: 1162-1171.

Spengler, J. D.; Allen, G. A.; Foster, S.; Severance, P.; Ferris, B., Jr. (1986a) Sulfuric acid and sulfate aerosol events in two U. S. cities. In: Lee, S. D.; Schneider, T.; Grant, L. D.; Verkerk, P. J., eds. Aerosols: research, risk assessment and control strategies - proceedings of the second U.S.-Dutch international symposium; May 1985; Williamsburg, VA. Chelsea, MI: Lewis Publishers, Inc.; pp. 107-120.

Spengler, J. D.; Briggs, S. L. K.; Özkaynak, H. (1986b) Relationship between TSP measurements and size-fractionated particle mass measurements in six cities participating in the Harvard Air Pollution Health Study. Research Triangle Park, NC: U.S. Environmental Protection Agency, Office of Air Quality Planning and Standards; EPA cooperative agreement no. CR-812667-01-0; December 5.

Spengler, J. D.; Brauer, M.; Koutrakis, P. (1990) Acid air and health. Environ. Sci. Technol. 24: 946-956.

Stevens, R. K. (1985) Sampling and analysis methods for use in source apportionment studies to determine impact of wood burning on fine particle mass. Environ. Int. 11: 271-283.

Stevens, R. K. (1995) [Unpublished data].

Stevens, R. K.; Dzubay, T. G.; Shaw, R. W., Jr.; McClenny, W. A.; Lewis, C. W.; Wilson, W. E. (1980) Characterization of the aerosol in the Great Smoky Mountains. Environ. Sci. Technol. 14: 1491-1498.

Stevens, R. K.; Dzubay, T. G.; Lewis, C. W.; Shaw, R. W., Jr. (1984) Source apportionment methods applied to the determination of the origin of ambient aerosols that affect visibility in forested areas. Atmos. Environ. 18: 261-272.

Stevens, R. K.; Hoffman, A. J.; Baugh, J. D.; Lewis, C. W.; Zweidinger, R. B.; Cupitt, L. T.; Kellogg, R. B.; Simonson, J. H. (1993) A comparison of air quality measurements in Roanoke, VA, and other integrated air cancer project monitoring locations. In: Measurement of toxic and related air pollutants: proceedings of the 1993 U.S. EPA/A&WMA international symposium; May; Durham, NC. Pittsburgh, PA: Air & Waste Management Association; pp. 185-189. (A&WMA specialty conference VIP-34).

Suh, H. H.; Spengler, J. D.; Koutrakis, P. (1992) Personal exposures to acid aerosols and ammonia. Environ. Sci. Technol. 26: 2507-2517.

Suh, H. H.; Koutrakis, P.; Spengler, J. D. (1993) Validation of personal exposure models for sulfate and aerosol strong acidity. J. Air Waste Manage. Assoc. 43: 845-850.

Suh, H. H.; Koutrakis, P.; Spengler, J. D. (1994) The relationship between airborne acidity and ammonia in indoor environments. J. Exposure Anal. Environ. Epidemiol. 4: 1-23.

Suh, H. H.; Allen, G. A.; Koutrakis, P.; Burton, R. M. (1995) Spatial variation in acidic sulfate and ammonia concentrations within metropolitan Philadelphia. J. Air Waste Manage. Assoc. 45: 442-452.

Thanukos, L. C.; Miller, T.; Mathai, C. V.; Reinholt, D.; Bennett, J. (1992) Intercomparison of PM_{10} samplers and source apportionment of ambient PM_{10} concentrations at Rillito, Arizona. In: Chow, J. C.; Ono, D. M., eds. PM_{10} standards and nontraditional particulate source controls, an A&WMA/EPA international specialty conference, v. I; January; Scottsdale, AZ. Pittsburgh, PA: Air & Waste Management Association; pp. 244-261. (A&WMA transactions series no. 22).

Thompson, K. M.; Koutrakis, P.; Brauer, M.; Spengler, J. D.; Wilson, W. E.; Burton, R. M. (1991) Measurements of aerosol acidity: sampling frequency, seasonal variability, and spatial variation. Presented at: 84th annual meeting and exhibition of the Air & Waste Management Association; June; Vancouver, BC, Canada. Pittsburgh, PA: Air & Waste Management Association; paper no. 91-89.5.

Thurston, G. D.; Gorczynski, J. E., Jr.; Jaques, P.; Currie, J.; He, D. (1992) An automated sequential sampling system for particulate acid aerosols: description, characterization, and field sampling results. J. Exposure Anal. Environ. Epidemiol. 2: 415-428.

Trijonis, J. (1982) Existing and natural background levels of visibility and fine particles in the rural East. Atmos. Environ. 16: 2431-2445.

Trijonis, J. C. (1991) Visibility: existing and historical conditions--causes and effects. Appendix A: characterization of natural background aerosol concentrations. In: Irving, P. M., ed. Acidic deposition: state of science and technology, volume III: terrestrial, materials, health and visibility effects. Washington, DC: The U.S. National Acid Precipitation Assessment Program; pp. 24-A1 - 24-A7. (State of science and technology report no. 24).

Trijonis, J.; McGown, M.; Pitchford, M.; Blumenthal, D.; Roberts, P.; White, W.; Macias, E.; Weiss, R.; Waggoner, A.; Watson, J.; Chow, J.; Flocchini, R. (1988) Visibility conditions and causes of visibility degradation in the Mojave Desert of California: executive summary, RESOLVE project final report. China Lake, CA: Department of the Navy, Naval Weapons Center; document no. NWC TP 6869. Available from: NTIS, Springfield, VA; AD-A206 322.

Tuncel, S. G.; Olmez, I.; Parrington, J. R.; Gordon, G. E.; Stevens, R. K. (1985) Composition of fine particle regional sulfate component in Shenandoah Valley. Environ. Sci. Technol. 19: 529-537.

Turpin, B. J.; Huntzicker, J. J. (1991) Secondary formation of organic aerosol in the Los Angeles basin: a descriptive analysis of organic and elemental carbon concentrations. Atmos. Environ. Part A 25: 207-215.

Turpin, B. J.; Cary, R. A.; Huntzicker, J. J. (1990) An in situ, time-resolved analyzer for aerosol organic and elemental carbon. Aerosol Sci. Technol. 12: 161-171.

Turpin, B. J.; Huntzicker, J. J.; Larson, S. M.; Cass, G. R. (1991) Los Angeles summer midday particulate carbon: primary and secondary aerosol. Environ. Sci. Technol. 25: 1788-1793.

U.S. Environmental Protection Agency. (1989) An acid aerosols issue paper: health effects and aerometrics. Research Triangle Park, NC: Office of Health and Environmental Assessment, Environmental Criteria and Assessment Office; EPA report no. EPA-600/8-88-005F. Available from: NTIS, Springfield, VA; PB91-125864.

Van Grieken, R. E.; Johansson, T. B.; Winchester, J. W.; Odom, L. A. (1975) Micro-determination of zirconium-hafnium ratios in zircons by proton induced X-ray emission. Z. Anal. Chem. 275: 343-348.

Vermette, S. J.; Williams, A. L.; Landsberger, S. (1992) PM_{10} source apportionment using local surface dust profiles: examples from Chicago. In: Chow, J. C.; Ono, D. M., eds. PM_{10} standards and nontraditional particulate source controls, an A&WMA/EPA international specialty conference, v. I; January; Scottsdale, AZ. Pittsburgh, PA: Air & Waste Management Association; pp. 262-278. (A&WMA transactions series no. 22).

Vossler, T. L.; Lewis, C. W.; Stevens, R. K.; Dzubay, T. G.; Gordon, G. E.; Tuncel, S. G.; Russwurm, G. M.; Keeler, G. J. (1989) Composition and origin of summertime air pollutants at Deep Creek Lake, Maryland. Atmos. Environ. 23: 1535-1547.

Waldman, J. M.; Lioy, P. J.; Thurston, G. D.; Lippmann, M. (1990) Spatial and temporal patterns in summertime sulfate aerosol acidity and neutralization within a metropolitan area. Atmos. Environ. Part B 24: 115-126.

Waldman, J. M.; Liang, S.-K. C.; Lioy, P. J.; Thurston, G. D.; Lippmann, M. (1991) Measurements of sulfate aerosol and its acidity in the SO_2 source region of Chestnut Ridge, PA. Atmos. Environ. Part A 25: 1327-1333.

Waldman, J. M.; Koutrakis, P.; Allen, G. A.; Thurston, G. D.; Burton, R. M.; Wilson, W. E. (1995) Human exposures to particle strong acidity. In: Phalen, R. F.; Bates, D. V., eds. Proceedings of the colloquium on particulate air pollution and human mortality and morbidity, part II; January 1994; Irvine, CA. Inhalation Toxicol. 7: 657-669.

Wall, S. M.; John, W.; Ondo, J. L. (1988) Measurement of aerosol size distributions for nitrate and major ionic species. Atmos. Environ. 22: 1649-1656.

Wang, H.-C.; John, W. (1988) Characteristics of the Berner impactor for sampling inorganic ions. Aerosol Sci. Technol. 8: 157-172.

Watson, J. G.; Chow, J. C.; Richards, L. W.; Neff, W. D.; Andersen, S. R.; Dietrich, D. L.; Houck, J. E.; Olnez, I. (1988) The 1987-88 metro Denver brown cloud study: v. I, II, III. Reno, NV: Desert Research Institute; final report no. 8810.1F(1-3).

Watson, J. G.; Chow, J. C.; Lu, Z.; Fujita, E. M.; Lowenthal, D. H.; Lawson, D. R.; Ashbaugh, L. L. (1994a) Chemical mass balance source apportionment of PM_{10} during the Southern California Air Quality Study. Aerosol Sci. Technol. 21: 1-36.

Watson, J. G.; Roth, P. M.; Blumenthal, D. L.; Ranzieri, A. J.; Solomon, P. A.; Thuillier, R. H. (1994b) Recommendations on planning a large-scale combined monitoring and modeling effort based on the SJVAQS/AUSPEX air quality study. In: Solomon, P. A.; Silver, T. A., eds. Planning and managing regional air quality modeling and measurement studies: a perspective through the San Joaquin Valley air quality study and AUSPEX. Boca Raton, FL: Lewis Publishers; pp. 369-382.

Weber, R. J.; McMurry, P. H.; Eisele, F. L.; Tanner, D. J. (1995) Measurement of expected nucleation precursor species and 5 to 500 nm diameter particles at Mauna Loa, Hawaii. J. Atmos. Sci. 52: 2242-2257.

Weiss, R. E.; Larson, T. V.; Waggoner, A. P. (1982) In situ rapid-response measurement of $H_2SO_4/(NH_4)_2SO_4$ aerosols in rural Virginia. Environ. Sci. Technol. 16: 525-532.

Wesolowski, J. J.; John, W.; Devor, W.; Cahill, T. A.; Feeney, P. J.; Wolfe, G.; Flocchini, R. (1977) Collection surfaces of cascade impactors. In: Dzubay, T. G., ed. X-ray fluorescence analysis of environmental samples. Ann Arbor, MI: Ann Arbor Science Publishers, Inc.; pp. 121-131.

Whitby, K. T. (1978) The physical characteristics of sulfur aerosols. Atmos. Environ. 12: 135-159.

Whitby, K. T.; Sverdrup, G. M. (1980) California aerosols: their physical and chemical characteristics. In: Hidy, G. M.; Mueller, P. K.; Grosjean, D.; Appel, B. R.; Wesolowski, J. J., eds. The character and origins of smog aerosols: a digest of results from the California Aerosol Characterization Experiment (ACHEX). New York, NY: John Wiley & Sons, Inc.; pp. 477-517. (Advances in environmental science and technology: v. 9).

Whitby, K. T.; Husar, R. B.; Liu, B. Y. H. (1972) The aerosol size distribution of Los Angeles smog. J. Colloid Interface Sci. 39: 177-204.

White, W. H. (1996a) Alternative perspectives on a trend in eastern fine-particle sulfur concentrations. Environ. Manager: in press.

White, W. H. (1996b) Deteriorating air or improving measurements?—on interpreting concatenate time series. J. Geophys. Res. [Atmos.]: submitted.

White, W. H.; Macias, E. S. (1987) Particulate nitrate measurements in rural areas of the western United States. Atmos. Environ. 21: 2563-2571.

White, W. H.; Macias, E. S. (1989) Carbonaceous particles and regional haze in the western United States. Aerosol Sci. Technol. 10: 111-117.

Willeke, K.; Whitby, K. T. (1975) Atmosperic aerosols: size distribution interpretation. J. Air Pollut. Control Assoc. 25: 529-534.

Wilson, W. E.; Stockburger, L. (1990) Diurnal variations in aerosol composition and concentration. In: Masuda, S.; Takahashi, K., eds. Aerosols: science, industry, health and environment: proceedings of the third international aerosol conference, v. 2; September; Kyoto, Japan. Oxford, United Kingdom: Pergamon Press plc; pp. 962-965.

Wilson, W. E.; Suh, H. H. (1996) Fine and coarse particles: concentration relationships relevant to epidemiological studies. J. Air Waste Manage. Assoc.: accepted.

Wilson, W. E.; Koutrakis, P.; Spengler, J. D. (1991) Diurnal variations of aerosol acidity, sulfate, and ammonia in the atmosphere. Presented at: 84th annual meeting and exhibition of the Air & Waste Management Association; June; Vancouver, BC, Canada. Pittsburgh, PA: Air & Waste Management Association; paper no. 91-89.9.

Wolff, G. T.; Korsog, P. E. (1985) Estimates of the contributions of sources to inhalable particulate concentrations in Detroit. Atmos. Environ. 19: 1399-1409.

Wolff, G. T.; Monson, P. R.; Ferman, M. A. (1979) On the nature of the diurnal variation of sulfates at rural sites in the Eastern United States. Environ. Sci. Technol. 13: 1271-1276.

Wolff, G. T.; Countess, R. J.; Groblicki, P. J.; Ferman, M. A.; Cadle, S. H.; Muhlbaier, J. L. (1981) Visibility-reducing species in the Denver "brown cloud"--II. sources and temporal patterns. Atmos. Environ. 15: 2485-2502.

Wolff, G. T.; Ferman, M. A.; Kelly, N. A.; Stroup, D. P.; Ruthkosky, M. S. (1982) The relationships between the chemical composition of fine particles and visibility in the Detroit metropolitan area. J. Air Pollut. Control Assoc. 32: 1216-1220.

Wolff, G. T.; Kelly, N. A.; Ferman, M. A.; Morrissey, M. L. (1983) Rural measurements of the chemical composition of airborne particles in the eastern United States. J. Geophys. Res. C: Oceans Atmos. 88: 10,769-10,775.

Wolff, G. T.; Korsog, P. E.; Stroup, D. P.; Ruthkosky, M. S.; Morrissey, M. L. (1985) The influence of local and regional sources on the concentration of inhalable particulate matter in southeastern Michigan. Atmos. Environ. 19: 305-313.

Wolff, G. T.; Ruthkosky, M. S.; Stroup, D. P.; Korsog, P. E.; Ferman, M. A.; Wendel, G. J.; Stedman, D. H. (1986) Measurements of SO_x, NO_x and aerosol species on Bermuda. Atmos. Environ. 20: 1229-1239.

Wolff, G. T.; Ruthkosky, M. S.; Stroup, D. P.; Korsog, P. E. (1991) A characterization of the principal PM-10 species in Claremont (summer) and Long Beach (fall) during SCAQS. Atmos. Environ. Part A 25: 2173-2186.

Wyzga, R. E.; Lipfert, F. W. (1996) [Philadelphia TSP data.] Palo Alto, CA: Electric Power Research Institute.

Zhang, X.; Turpin, B. J.; McMurry, P. J.; Herring, S. V.; Stolzenburg, M. R. (1994) Mie theory evaluation of species contributions to the 1990 wintertime visibility reduction in the Grand Canyon. J. Air Waste Manage. Assoc. 44: 153-162.

APPENDIX 6A:

TABLES OF CHEMICAL COMPOSITION OF PARTICULATE MATTER

TABLE 6A-1a. SUMMARY OF $PM_{2.5}$ STUDIES

EAST	REF	NOTE	WEST	REF	NOTE	CENTRAL	REF	NOTE
Smoky Mtn.	1		Boise	5	d	Albuquerque	5	d
Shenandoah	1		Tarrant CA	8	a	St. Louis	6,7	
Camden	2	b	Five Points CA	8	a	Steubenville	6,7	
Philadelphia	3		Riverside CA	8	a	Harriman	6,7	
Deep Creek	4	c	San Jose	8	a	Portage	6,7	
Roanoke	5	d	Honolulu	8	a	Topeka	6,7	
Raleigh	5	d	Winnemucca NV	8	a	Inglenook AL	8	a
Watertown	6,7		Portland	8	a	Braidwood IL	8	a
Hartford	8	a	Seattle	8	a	Kansas City KS	8	a
Boston	8	a	Southern California	9,31	g,h	Minneapolis	8	a
Res.Tr. Pk.	8	a	San Joaquin Valley	10	i	St. Louis	8	a
Charlotte	20	e	Phoenix	11	j	Kansas City MO	8	a
Allegheny Mtn.	44		Nevada	12	f	Akron	8	a
Allegheny Mtn.	45-50					Cincinnati	8	a
Laurel Hill	45-50					Buffalo	8	a
						Dallas	8	a
						El Paso	8	a
						Denver	13	
						Urban Denver	14	m
						Non-urban Denver	14	aa
						Chicago	15	
						Houston	16	
						St.Louis	17	
						Harriman	17	
						St. Louis	18	k
						Steubenville	21	
						Brownsville	24	n
						Ontario	37	l

TABLE 6A-1b. SUMARY OF COARSE FRACTION STUDIES

EAST	REF	NOTE	WEST	REF	NOTE	CENTRAL	REF	NOTE
Smoky Mtn.	1	o	Tarrant CA	8	a,o	St. Louis	6,7	o,p
Shenandoah	1	o	Five Points CA	8	a,o	Steubenville	6,7	o,p
Camden	2	b	Riverside CA	8	a,o	Harriman	6,7	o,p
Philadelphia	3	ab	San Jose	8	a,o	Portage	6,7	o,p
Watertown	6,7	o,p	Honolulu	8	a,o	Topeka	6,7	o,p
Hartford	8	a,o	Winnemucca NV	8	a,o	Inglenook AL	8	a,o
Boston	8	a,o	Portland	8	a,o	Braidwood IL	8	a,o
Res.Tr. Pk.	8	a,o	Seattle	8	a,o	Kansas City KS	8	a,o
Allegheny Mtn.	44		Southern California	9,31	g	Akron	8	a,o
Allegheny Mtn.	45-50		San Joaquin Valley	10	i	Cincinnati	8	a,o
Laurel Hill	45-50		Phoenix	11	j	Buffalo	8	a,o
						Dallas	8	a,o
						El Paso	8	a,o
						Denver	13	o
						Chicago	15	s
						Houston	16	o
						St. Louis	17	
						Harriman	17	
						St. Louis	18	k,r
						Brownsville	24	n
						Ontario	37	l

TABLE 6A-1c. SUMMARY OF PM_{10} STUDIES

EAST	REF	NOTE	WEST	REF	NOTE	CENTRAL	REF	NOTE
Smoky Mtn.	1	o,q	Tarrant CA	8	a,q	St. Louis	6,7	p,q
Shenandoah	1	o,q	Five Points CA	8	a,q	Harriman	6,7	p,q
Camden	2	b	Riverside CA	8	a,q	Steubenville	6,7	p,q
Philadelphia	3	ab	San Jose CA	8	a,q	Portage	6,7	p,q
Kingston	6,7	p,q	Honolulu HI	8	a,q	Topeka	6,7	p,q
Watertown	6,7	p,q	Winnemucca NV	8	a,q	Inglenook AL	8	a,q
Hartford	8	a,q	Portland OR	8	a,q	Braidwood IL	8	a,q
Boston	8	a,q	Seattle	8	a,q	Kansas City KS	8	a,q
Res.Tr. Pk.	8	a,q	Southern California	9,31	g,h	Minneapolis	8	a,q
Allegheny Mtn.	44		San Joaquin Valley	10	i	St. Louis	8	a,q
Allegheny Mtn.	45-50		Phoenix	11	j	Kansas City MO	8	a,q
Laurel Hill	45-50		San Fran. Bay	29	v	Akron	8	a,q
			San Jose	29	w	Cincinnati	8	a,q
			Palm Springs	38	t	Buffalo	8	a,q
			Pocatello, ID	39		Dallas	8	a,q
			Tuscon	40	u	El Paso	8	a,q
			Rillito, AZ	42		Denver	13	q
						Chicago	15	s
						Houston	16	q
						St.Louis	17	
						Harriman	17	
						St. Louis	18	x
						Brownsville	24	
						Utah Valley	26	
						Ontario	37	l
						SE Chicago, IL	41	
						Ohio	43	y

FOOTNOTES FOR TABLES 6A-1a THROUGH 6A-2c

a. Inhalable Particle Network (IPN) Data. Only represents days of elevated concentrations—dichot filter loadings >50 $\mu g/cm^2$.

b. Data from Site 28 only.

c. Average of all 6-h samples.

d. Avg over all day/nite samples.

e. Average of all 12-h samples at 2 incin. sites and 2 background sites. Only XRF values which exceeded associated uncertainties more than half the time at all four sites were included.

f. Average from Sparks site and Reno site.

g. Sampling only during intensive episodes.

h. Averages based on 12-h day/nite samples. There were 59 sampling days at Claremont and 23 sampling days at Long Beach.

i. Avg over all sites: Stockton, Crow's Landing, Fresno, Kern, Fellows, and Bakersfield.

j. Average of Central Phoenix, West Phoenix, and Scottsdale sites.

k. Avg of RAPS site 106.

l. Average from Walpole, Windsor 1, and Windsor 2 sites.

m. Avg of 3 urban sites: Auraria, Federal, and Welby.

n. Median VAPS values from Central site.

o. 2.5-15 μm.

p. Coarse concentrations may be 30% or more underestimated due to losses from handling filters.

q. PM_{15}.

r. 2.4-20 μm.

s. No upper size cutoff on VAPS inlet.

t. Average of Palm Springs and Indio, CA.

u. Avg. of Downtown Tuscon, Orange Grove, Craycroft, and Corona de Tuscon sites.

v. Mean of annual avgs (1988-1992) from ~9 sites in Alameda, San Francisco, and Santa Clara counties.

w. 24-h average of day/nite concentrations at two sites in San Jose.

x. PM_{20}. Average from RAPS site 106.

y. Avg. of Follansbee, Mingo, Sewage Plant, Steubenville, and WTOV Tower sites in Ohio.

z. Average of urban sites: Fresno, Bakersfield and Stockton.

aa. Average of nonurban sites: Brighton and Tower.

ab. Castor Avenue site only.

APPENDIX FOR TABLES 6A-1a THROUGH 6A-2c. BIBLIOGRAPHY FOR PM STUDIES

Ref No.	Sites	Dates	Types of Samples	Data	Comments
1	1) Smoky Mtn. 2) Shenandoah Valley 3) Abastumani Mtn.	1) Sept 1978 2) Jul-Aug 1980 3) Mar 24-Jul 1979	F+C(2.5-15), EC, OC, $SO_4^=$, Nitrate. 12-h samples.	1) Comparison of avg F&C composition for 3 sites.	
2	Philadelphia - 3 sites	Jul 14-Aug 13 1982	F+C(2.5-10), EC, OC, $SO_4^=$, NO_3^-. 12-h (0600-1800) and (1800-0600).	1) F+C composition at site 28. 2) 9-source CMB source app. for site 28. 3) Mass Balance for 3 sites.	
3	Philadelphia	Jul 25-Aug 14 1994	Fine mass, elements, OC, EC, SD, uncert., from 4 sites	1) Measured $PM_{2.5}$ mass, OC, EC, elements, SD, unc. at each site.	
4	Deep Creek Lake	August, 1983	Day/nite sampling (1000-2200, 2200-1000). Dichots. FM, CM, OC, EC, Gases, FP nitrate	1) Mean FP mass, OC, EC, nitrate, elements stratified by day/nite/all.	
5	1) Albuquerque 2) Raleigh 3) Boise 4) Roanoke	1) Dec 1984-Mar 1985 2) Jan 1985-Mar 1985 3) Dec 1986-Mar 1987 4) Oct 1988-Feb 1989	F & C (2.5-10) + Carbon, EOM, VOCs. 12-h samples, Day/night: 0700-1900,1900-0700.	1) Mean comp. of F mass, EC, OC EOM, at 4 sites. 2) daytime/ nightime/24-havgs for key species at 4 sites.	No CP data presented; Sampling only in winter; focus on woodstove impact
6	Portage, Topeka,Harriman, Kingston, St. Louis, Steubenville, Watertown	1979-1981 Multi-season	FP & IP(2.5-15). 24-h (midnite-midnite), every other day. No Carbon data.	1) Mean+-SE by city for F+C mass, metals. 2) Box-line plots by city showing means and percentiles for F+C mass, sulfate, Cl. 3) Time-series plots of F+C mass & tot Sulfate. 4) Data summaries only--no raw data.	Source of info on geographical and temporal PM composition variability.

APPENDIX FOR TABLES 6A-1a THROUGH 6A-2c (cont'd). BIBLIOGRAPHY FOR PM STUDIES

Ref No.	Sites	Dates	Types of Samples	Data	Comments
7	Harvard 6-cities	1) 1977-1985 TSP 2) 1979-1985 PM_{10} & $PM_{2.5}$ 3) 1979-1984 Sulfate		1) Table of Mean Air pollution values for 6 cities: TSP, Inhalable, Fine, Sulfate. No comp.	
8	IPN study ~25 sites.	Throughout 1980.	F+C(2.5-15), 24-h sample every 6th day. Only moderately or highly-loaded samples were included. No Carbon.	1) F+C mass for ~25 sites. 2) F+C mass, composition for 22 sites (No carbon)	
9	Los Angeles (SCAQS) 40 locations *Aerosol composition*	Summer (11 episode days) and fall (7 episode days) 1987	Sequential 4-, 5-, and 7-h $PM_{2.5}$ and PM_{10} on summer episode days, and 4- and 6-h samples in fall. Mass, elements, ions, sulfate, nitrate, Carbon, ammonium.	1) Avg & Max PM_{10} and $PM_{2.5}$ mass, ions, comp, Cv, Ce stratified into summer and fall. 2) Plots of temp and spatial variations of $PM_{2.5}$ and PM_{10}, $PM_{2.5}$ nitrate. 3) C_{tot}/EC for some sites	Temp and spatial variations of $PM_{2.5}$ and PM_{10}
10	San Joaquin Valley 6 sites *Aerosol Composition*	Jun 1988-Jun 1989	24-h PM_{10} & $PM_{2.5}$ every 6 days. Mass, elements, ions (K^+, $SO_4^=$, NH_4^+,Na^+), EC, OC	1) Summary of annual geometric avg, arith. avg, max 24-h PM_{10} and $PM_{2.5}$ mass by site. 2) Ann. Avg Mass and comp. for PM_{10} and $PM_{2.5}$ by site.	PM_{10} highest in winter and dominated by F mass; C >50% of PM_{10} in summer and fall. Data show spatial and temporal variations of PM_{10} and $PM_{2.5}$

APPENDIX FOR TABLES 6A-1a THROUGH 6A-2c (cont'd). BIBLIOGRAPHY FOR PM STUDIES

Ref No.	Sites	Dates	Types of Samples	Data	Comments
11	Phoenix PM Study	Oct. 1989 - Jan. 1990	F&C mass, elements, uncertainties from 6 sites		
12	Phoenix 4 sites Also comparison aerosol data from Denver, Reno, and Sparks	Sept. 1989 - Jan. 1990	6-h samples, 2x/day, (0600-1200, 1300-1900) PM_{10} & $PM_{2.5}$: mass, elements, HNO_3, SO_2, NH_3, FP NO_3^- and $SO_4^=$, ionic species, OC, EC.	1) temporal variation of $PM_{2.5}$ mass at 4 sites. 2) Mean, SD, & Max: $PM_{2.5}$, EC, OC, NO_3^-, $SO_4^=$, NH_4^+ and elements for 3 Phoenix sites 3) Same for Denver (11/87-1/88) 4) Same for Reno (11/86-1/87) 5) Same for Sparks (11/86-1-87)	Moudi size-resolved (0-5.6 μm in 9 bins) mass, NO_3^-, $SO_4^=$, OC, EC.
13	Denver	Jan. 11-30, 1982	Dichotomous sampler, OC, EC, nitrate, sulfate	1) Measured $PM_{2.5}$ and Coarse, elements, OC, EC, nitrate, day/night samples; light extinction.	Source apportionment for F&C particles and extinction.
14	Denver (SCENIC)	Nov. 1987-Jan. 1988	2x daily (0900-1600, 1600-0900). $PM_{2.5}$ mass, comp, sulfate, nitrate, OC, EC, ionic species, gases	1) Avg, SD, Min, Max $PM_{2.5}$ mass for 6 sites. 2) Avg, SD, Min, Max, for $PM_{2.5}$ mass, ionic species, EC, OC, elements for 3 sites. 3) Source profiles 4) SCE for 4 sites by day and night	Source Apportionment study
15	Chicago	July, 1994	VAPS & Dichot. FM, CM, OC, EC, elements, SO_2, HONO, HNO_3.	1) Avg VAPS mass, SD, uncert. for F & C, OC, EC.	
16	Houston	Sept. 10-19, 1980	Dichotomous sampler: 0.1-2.5, 2.5-15. 4 sites. Consecutive 12 h samples.	1) Average F&C mass, elements, Carbon, NH_4^+, NO_3^-, Sulfate	Source apportionment.
17	St. Louis & Harriman	Sept. 1985 - Aug. 1986	Daily F & C (2.5-10μm). Also SO_2, NO_2, and O_3.	1) Mean, SD, range for PM_{10}, $PM_{2.5}$, $SO_4^=$, H^+, SO_2, NO_2, O_3 for both sites.	

APPENDIX FOR TABLES 6A-1a THROUGH 6A-2c (cont'd). BIBLIOGRAPHY FOR PM STUDIES

Ref No.	Sites	Dates	Types of Samples	Data	Comments
18	St. Louis	Jul 1976-Aug 1976 (St.Louis) RAPS data for St. Louis exist for May 1975-Mar 1977 but were not in this article	F(<2.4) & C (2.4-20) 6-12 hr. No Carbon.	1) 2-mo avg of F+C mass, metals, sulfate, for one site. 2) F+C composition of selected samples (different sites) during events. 3) CMB apportionment of F+C fractions to 6 components (crustal shale, crustal limestone, ammonium sulfate, motor vehicles, steel, paint). 4) Plots ofintercity variations in source component concentrations	1) Crude CMB source apportionment of FP with 6 sources.
19	1) Albuquerque 2) Denver	1) Jan 3-4, 1983 2) Jan 19-20, 1982	F & C (2.5-10) + Carbon, Nitrate & Sulfate (IC) 12-h samples, Day/Night: 0700-1900,1900-0700.	1) Mean daytime and nightime comp. of F&C, EC, OC, nitrate, sulfate, for each site. 2) Source app. of Denver winter FP composition.	More complete source app results in Lewis & Enfield paper.
20	Charlotte (2 incin sites and 2 control sites).	Apr 30-Jun 4, 1992 & Sept 21-28, 1992.	VAPS F&C + Acid gases. no carbon. 12-h samples	1) Mean ambient FP conc. + XRF unc. at 4 sites 2) CMB results for FP.	
21	Steubenville	Jan-Dec 1984	24-h, F+C. No Carbon	1) avg F mass + comp. 2) avg source contributions by SRFA 3) SRFA-derived source profiles	
22	Review of PM_{10} studies	1984-1990	PM_{10}	1) SCE's for PM_{10} mass for ~15 studies	ambient PM_{10} data sources are cited but no data is presented
23	Phoenix	Jan 5-27, 1983	F(<2.8)+C(>2.8). 1800-0800 12 h samples.	1)avg F+C nightime comp, mass, Cv,Ce, gases. 2) CMB of FP	
24	Brownsville -- residential and central sites.	Spring+Summer 1993	1)FP MES indoor/outdoor 2) VAPS central site 3) Dichot central site	1) min, med, max for fine MES comp+mass 2) min, med, max F+C comp, mass for VAPS and dichot at central site	No avg values, only median.

APPENDIX FOR TABLES 6A-1a THROUGH 6A-2c (cont'd). BIBLIOGRAPHY FOR PM STUDIES

Ref No.	Sites	Dates	Types of Samples	Data	Comments
25	Sparks, Reno, Verdi, NV (SNAPS)	Apr 1986-Mar 1987	1) $PM_{2.5}$ & PM_{10} every 6th day. 24-h samples. Also diurnal sampling.	1) Seasonal avg SCE for PM_{10} at 3 sites. (geological, motor veh, construction, vegetative, sulfate, nitrate, OC, EC)	No raw data
26	Utah Valley (Linden site)	Apr 1985-Dec 1989	1) PM_{10} for 1736 days. Also, SO_2, NO_2, O_3, acidity data.	1)avg PM_{10} = 47 $\mu g/m^3$. sd=38, (min,max)=(1,365 $\mu g/m^3$). 2) freq distribution of PM10 mass.	no comp. data. Highest pm10 during winter.
27	Santa Clara County	1980-1986: only Nov, Dec, Jan data used.	"COH" --coefficient of haze. [COH/PM10=1.87 or 1.64 (1985 and 1986)].	1) Plots of COH vs daily mortality for 2-yr periods.	Examines relation between mortality and COH
28	San Joaquin Valley 6 sites *Source apportionment*	Jun 1988-Jun 1989	24-h PM_{10} & $PM_{2.5}$ every 6 days. Mass, elements, ionic species, Carbon,	1) Table of ann. avg. SCE to PM10 and PM2.5 for data above, by site	For PM10 Mass, Sulfate, and Nitrate data, see ref 27.
29	SF Bay Area 2 sites	Dec 16, 1991-Feb 24, 1992	12-h daily day & nite (0600-1800, 1800-0600) PM_{10} samples. Mass, elements, ions (K^+,Cl, $SO_4^=$, NH_4^+ , Na^+) Carbon, ammonium.	1)Table of ann. avg. PM_{10} mass, sulfate, nitrate statistics at 3 sites for 1988-1992 2) Avg. & Max day & nite PM_{10} mass, ions, comp, EC, OC, for both sites 3) Source profiles 4) SCE pie charts for each site.	1. Highest PM_{10} mass during Nov, Dec, Jan. 2. Wood combust. contributes ~45% of PM_{10}.
30	Los Angeles (SCAQS) 40 locations *CMB Source Apport.*	Summer (11 episode days) and fall (7 episode days) 1987	Sequential 4-, 5-, and 7-h $PM_{2.5}$ and PM_{10} on summer episode days, and 4- and 6-h samples in fall. Mass, elements, ions, sulfate, nitrate, Carbon, ammonium.	1) Source profiles 2) PM_{10} SCE for summer and fall. 3) Diurnal SCE to PM_{10} at each site.	Data show diurnal changes in SCE for PM_{10} mass.

APPENDIX FOR TABLES 6A-1a THROUGH 6A-2c (cont'd). BIBLIOGRAPHY FOR PM STUDIES

Ref No.	Sites	Dates	Types of Samples	Data	Comments
31	1) Claremont (SCAQS) 2) Long Beach (SCAQS)	1) Summer 1987 (59d) 2) Fall 1987 (23d)	Continuous 12-h PM_{10} and $PM_{2.5}$. Mass, elements, ionic species, EC, OC	1) Mean, SD, & Max: PM_{10}, FPM, CPM, EC, OC, NO_3^-, $SO_4^=$, NH_4^+. 2) Mean values of above species during intensive and non-intensive periods. 3) Day/nite values of above 4) PM_{10} and $PM_{2.5}$ mass balances 5) Summary of EC, OC data.	
32	CADMP -- 8 sites: Gasquet, Fremont, Bakersfield, Yosemite, Sequoia, Long Beach, Los Angeles, Azusa	Summer 1988	2 samples every 6th day. 0600-01800, 1800-0600. $PM_{2.5}$, PM_{10}. Mass, ionic species,	1) Graph of avg PM_{10} & $PM_{2.5}$ mass and ratio at 8 sites 2) Graphs of PM_{10} & $PM_{2.5}$ ionic concentrations.	Ask Chow/Watson for raw data.
33	Central California -53 sites in SF Bay area, Sacramento Valley, San Joaquin Valley, North and South Central Coast, Mountain Counties	1) 1989 2) July & August, 1988	PM_{10} every 6th day. Sulfate and nitrate measured on a subset of these samples.	1) 1989 Max and Avg PM_{10} mass, Sulfate, and Nitrate for ~53 sites. 2) Summertime 1988 Avg, SD, and Max PM_{10} and $PM_{2.5}$ Mass, comp, OC,EC, Ionic species, for 3 SJVAQS sites. [Annual data summary is in ref 20].	
34	Birmingham	1986-1989	Daily 24-h PM_{10} mass. Also Ozone data. No composition data.	1) Table of percentile points of the distribution of PM_{10}, O_3, T, DewPoint, Pneumonia, Chronic obstructive pulmonary disease. 2) Avg PM_{10} and O_3 by season	Aside: Indoor/Outdoor ratios of 0.63 for PM_{10} were reported in Tuscon.
35	Philadelphia	1973-1980	24-h (midnite-midnite) TSP. No composition data.	1) Table of percentile points of the distribution of TSP, SO_2, T, DewPoint, Mortality.	
36	State College, PA	summer 1990	Indoor, outdoor, personal $SO_4^=$, H^+, and NH_3		Validation of personal exposure models

APPENDIX FOR TABLES 6A-1a THROUGH 6A-2c (cont'd). BIBLIOGRAPHY FOR PM STUDIES

Ref No.	Sites	Dates	Types of Samples	Data	Comments
37	Southern Ontario 3 sites	Jan.-Nov., 1991	24-h, midnite-midnite, every 6th day. PM_{10} dichot sampler.	1)Avg mass, elements, for F&C fractions, for 3 sites. No OC, EC.	
38-43	Miscellaneous sites 14 sites	1984-1990	PM_{10} concentrations.	1) Measured PM_{10} mass and avg source contributions (up to 10 source categories).	Primary reference is Ref 10.
44	Allegheny Mtn. SW PA elev. 838 m	July 24-Aug. 10 1977	Filters, impactors, gas samplers, day/night	Aerosol mass, elements, H^+, NH_4^+, $SO_4^=$, NO_3^-, total C, size distributions, b_{scat}, L_v, gases	Strong aerosol H^+ found, associated with $SO_4^=$
45-50	Allegheny Mtn. and Laurel Hill, SW PA separation 35.5 km	Aug. 5-Aug. 28, 1983	Filters, dichotomous samplers, impactors, denuders, gas analyzers, day/night	Fine, coarse, and PM_{10} mass, elements, EC, H^+, NH_4^+, $SO_4^=$, NO_3^-, size distributions, CN counts, b_{scat}, b_{abs}, L_v, HNO_3 and other gases, rain, dew, 2-site correlation	Coordinated with Deep Creek Lake experiment, Ref. 4, ≈60 km to SSW

References:

1. Stevens et al. (1984)
2. Dzubay et al. (1988)
3. Pinto et al. (1995)
4. Vossler et al. (1989)
5. Stevens et al. (1993)
6. Spengler and Thurston (1983)
7. Dockery et al. (1993)
8. Davis et al. (1984)
9. Chow et al. (1994a)
10. Chow et al. (1993a)
11. Desert Research Institute (1995)
12. Chow et al (1990)
13. Lewis et al. (1986); Lewis and Dzubay (1986)
14. Watson et al. (1988)
15. Stevens, R. K. (1995) [Unpublished data].
16. Johnson et al. (1984)
17. Dockery et al. (1992)
18. Dzubay (1980)
19. Stevens (1985)
20. Mukerjee et al. (1993)
21. Koutrakis and Spengler (1987)
22. Chow et al. (1993b)
23. Solomon and Moyers (1986)
24. Ellenson et al. (1994)
25. Chow et al. (1988)
26. Pope et al. (1992)
27. Fairley (1990)
28. Chow et al. (1992b)
29. Chow et al. (1995a)
30. Watson et al. (1994a)
31. Wolff et al. (1991)
32. Ashbaugh et al. (1989)
33. Chow et al. (1994b); Watson et al. (1994b)
34. Schwartz (1994)
35. Schwartz and Dockery (1992)
36. Suh et al. (1993)
37. Conner et al. (1993)
38. Kim et al. (1992)
39. Houck et al. (1992)
40. Chow et al. (1992a)
41. Vermette et al. (1992)
42. Thanukos et al. (1992)
43. Skidmore et al. (1992)
44. Pierson et al. (1980b)
45. Pierson et al. (1986)
46. Japar et al. (1986)
47. Pierson et al. (1987)
48. Keeler et al. (1988)
49. Pierson et al. (1989)
50. Keeler et al. (1990)

TABLE 6A-2a. $PM_{2.5}$ COMPOSITION FOR THE EASTERN UNITED STATES ($\mu g/m^3$)

Ref	1	1	2(b)	3	4(c)	46, 49, 50	46, 49, 50	5(d)	5(d)	6,7	8(a)	8(a)	8(a)
Site	Smoky Mtn.	Shenandoah	Camden	Philadelphia	Deep Creek	Allegheny Mtn.	Laurel Hill	Raleigh	Roanoke	Watertown	Hartford	Boston	Res.Tr.Pk
Dates	9/20-26/78	7/23-5/08/80	7/14-8/13, 1982	7/25-8/14/94	8/83	8/5-28/83	8/6-27/83	1/85-3/85	10/88-2/89	5/79-6/81	1980	1980	1980
Time	0-12-24	0-12-24	6-18-6	9-9	4x daily	day/night	day/night	7-19-7	7-19-7	00-24	NR	NR	NR
Duration (h)	12	12	12	24	6	~10	~10	12	12	24	24	24	24
Number	12	28	50	21	98	44	39	NR	NR	354	2	1	3
Mass	24.00	27.00	28.70	32.18	40.00	49	46	30.30	19.90	14.90	26.75	34.80	28.77
OC	2.22	0.44	2.05	4.51	1.45	2	2	10.00	7.30				
EC	1.10	1.12	1.87	0.76	0.18	1.2	1.4	0.50	1.50				
Nitrate	0.30		<0.48		0.57	0.5	0.6						
Sulfate	12.00	13.60	11.20			17	18			5.85			
Acidity[$]						9	10			20.300			
Al	<0.054	<0.105	0.053	0.114		0.058	0.048	0.009	0.176		0.035		0.073
As	<0.003	<0.003	0.001		0.001	0.0005	0.0006	0.001	0.002			0.002	0.002
Ba						0.0048	0.0033						
Br	0.018	0.008	0.029	0.009	0.005	0.004	0.004	0.028	0.005	0.088	0.036	0.020	0.007
Ca	0.016	0.035	0.040	0.058	0.048	0.027	0.023	0.018	0.047	0.041	0.070	0.070	0.035
Cd			0.002			0.0004	0.0004						
Cl	<0.010	0.010	0.003	0.026		0.061	0.038	0.007	0.053	0.084			
Cr			0.002			0.0016	0.0011		0.001		0.003	0.004	
Cu	0.003	0.005		0.007		0.0012	0.0020	0.020	0.007		0.043	0.035	0.016
Fe	0.028	0.054	0.091	0.127	0.058	0.046	0.062	0.044	0.114	0.074	0.125	0.121	0.120
K	0.040	0.061	0.101	0.060	0.044	0.041	0.040	0.159	0.177		0.171	0.096	0.148
Mg				0.023		0.011	0.009						
Mn			0.006	0.003	0.003	0.0032	0.0038	0.003	0.012	0.004	0.007	0.001	0.003
Mo			0.001			0.0037	0.0031	0.001	0.001				
Na			0.146	0.070	0.034	0.036	0.034						
Ni			0.011	0.007		0.0009	0.0011			0.009	0.010	0.012	0.001

TABLE 6A-2a (cont'd). $PM_{2.5}$ COMPOSITION FOR THE EASTERN UNITED STATES ($\mu g/m^3$)

Ref	1	1	2(b)	3	4(c)	44, 45-50	45-50	5(d)	5(d)	6,7	8(a)	8(a)	8(a)
Site	Smoky Mtn.	Shenandoah	Camden	Philadelphia	Deep Creek	Allegheny Mtn.	Laurel Hill	Raleigh	Roanoke	Watertown	Hartford	Boston	Res.Tr.Pk
Dates	9/20-26/78	7/23-5/08/80	7/14-8/13 '82	7/25-8/14/94	8/83	8/5-28/83	8/6-27/83	1/85-3/85	10/88-2/89	5/79-6/81	1980	1980	1980
Time	00-12-24	00-12-24	6-18-6	9-9	4x daily	day/night	day/night	7-19-7	7-19-7	00-24	NR	NR	NR
Duration (h)	12	12	12	24	6	~10	~10	12	12	24	24	24	24
Number	12	28	50	21	98	44	39	NR	NR	354	2	1	3
P				0.015		0.013	0.019					0.009	0.042
Pb	0.097	0.052	0.249	0.019	0.048	0.035	0.039	0.096	0.027	0.329	0.510	0.285	0.106
Rb						0.0005	0.0002						
S	3.744	4.539	4.200	3.251	6.700	5.9	5.5	1.729	1.177	1.800	2.219	3.869	2.835
Sb			0.079		0.001	0.0006	0.0006						
Se	0.001	0.001	0.002	<0.002	0.003	0.0018	0.0020	0.002	0.002	0.001	0.001	0.001	0.002
Si	0.038	0.116	0.103	0.165	0.150	0.23	0.21	0.076	0.077	0.100	0.177	0.144	0.350
Sn			<0.012										
Sr			<0.002			0.0026	0.0027						
Ti	<0.006	<0.010	<0.027	<0.042		0.0041	0.0047				0.002		
V	<0.004	<0.010	0.013	<0.013	0.001	0.0019	0.0017	0.003	0.004	0.022	0.017	0.020	
Zn	0.009	0.011	0.082	0.041	0.013	0.010	0.012	0.015	0.083		0.079	0.046	0.018

References are listed in Table 1 Appendix. Associated notes are explained in Table 1.
*Values for this size fraction are calculated from the average measured values reported for the other two size fractions.
$Units for acidity are nmoles/m^3.
NR = not reported.

TABLE 6A-2a (cont'd). $PM_{2.5}$ COMPOSITION FOR THE WESTERN UNITED STATES ($\mu g/m^3$)

Ref	9(g)	9(g)	10(i)	11(j)	5(d)	12(f)	8(a)	8(a)	8(a)	8(a)	8(a)	8(a)	8(a)	8(a)
Site	Los Angeles	Los Angeles	San Joaquin Valley	Phoenix	Boise	Nevada	Tarrant CA	Five Points CA	Riverside CA	San Jose CA	Honolulu	Winnemucca	Portland	Seattle
Dates	Summer 1987	Fall 1987	6/88-6/89	10/13/89-1/17/90	12/86-3/87	11/86-1/87	1980	1980	1980	1980	1980	1980	1980	1980
Time	NR	NR	NR	NR	7-19-7	00-24	NR	NR	NR	NR	NR	NR	NR	NR
Duration (h)	4,5 and 7	4 and 6	24	6 h, 2x/day	12	24	24	24	24	24	24	24	24	24
Number	11 days	6 days	~35	~100 days	NR	24	6	3	4	6	1	5	4	1
Mass	41.10	90.20	29.89	29.37	35.70	56.92	57.05	31.80	35.18	36.28	21.10	9.68	37.18	10.70
OC	8.27	18.46	4.87	10.10	12.70	19.97								
EC	2.37	7.28	3.24	7.47	1.70	15.17								
Nitrate	4.34	22.64	8.17	3.60		2.43								
Sulfate	9.41	4.38	3.00	1.33		1.67								
Acidity[$]														
Al	0.035	0.250	0.152	0.130	0.102	0.275	0.177	0.239	0.036	0.123	1.127	0.361	0.581	0.002
As	0.022	0.015		<0.020	0.002	0.001				0.001			0.012	0.006
Ba	0.015	0.043	0.012	<0.106		0.013								
Br	0.013	0.065	0.010	0.011	0.014	0.033	0.102	0.015	0.037	0.188	0.017	0.006	0.093	0.019
Ca	0.022	0.335	0.096	0.170	0.026	0.215	0.455	0.150	0.301	0.089	1.024	0.243	0.154	0.037
Cd			<0.007	<0.018										
Cl	0.093	0.453	0.094	0.365	0.122	0.145		0.004	0.009	0.050	0.518		0.021	
Cr	0.022	0.025	0.003	0.003	0.001	0.002	0.002	0.001		0.003	0.004		0.009	0.002
Cu	0.063	0.273	0.096	0.015	0.011	0.010	0.047	0.024	0.040	0.043	0.018	0.026	0.072	0.024
Fe	0.099	0.557	0.180	0.216	0.022	0.310	0.316	0.216	0.127	0.148	0.726	0.231	0.270	0.098
K	0.041	0.217	0.188	0.207	0.145	0.280	0.186	0.244	0.120	0.248	0.371	0.149	0.218	0.080
Mg	0.024	0.075												
Mn	0.016	0.043	0.006	0.023	0.002	0.015	0.032	0.005	0.007	0.006	0.020	0.003	0.052	0.004
Mo				<0.006	0.002									
Na	0.202	0.466												
Ni	0.005	0.007	0.016	0.003		0.006	0.003	0.025	0.007	0.006	0.002	0.001	0.027	0.006

TABLE 6A-2a (cont'd). $PM_{2.5}$ COMPOSITION FOR THE WESTERN UNITED STATES ($\mu g/m^3$)

Ref	9(g)	9(g)	10(i)	11(j)	5(d)	12(f)	8(a)	8(a)	8(a)	8(a)	8(a)	8(a)	8(a)	8(a)
Site	Los Angeles	Los Angeles	San Joaquin Valley	Phoenix	Boise	Nevada	Tarrant CA	Five Points CA	Riverside CA	San Jose CA	Honolulu	Winnemucca	Portland	Seattle
Dates	Summer 1987	Fall 1987	06/88-06/89	10/13/89-1/17/90	12/86-3/87	11/86-1/87	1980	1980	1980	1980	1980	1980	1980	1980
Time	NR	NR	NR	NR	7-19-7	00-24	NR	NR	NR	NR	NR	NR	NR	NR
Duration (h)	4, 5 and 7	4 and 6	24	6 h, 2x/day	12	24	24	24	24	24	24	24	24	24
Number	11 days	6 days	~35	~100 days	NR	24	6	3	4	6	1	5	4	1
P	0.060	0.046	0.007	<0.051		0.041		0.007		0.013	0.002		0.017	0.006
Pb	0.038	0.185	0.029	0.039	0.045	0.115	0.619	0.087	0.376	0.891	0.071	0.042	0.422	0.215
Rb			0.001	<0.0025		0.001								
S	2.832	1.998	1.242	0.437	0.603	0.765	2.578	1.129	1.653	0.852	0.313	0.358	1.944	0.831
Sb			<0.002	<0.033										
Se	0.013	0.011	0.001	<0.002	0.001			0.001	0.001				0.001	0.001
Si	0.052	0.520	0.460	0.430	0.069	0.860	0.583	0.656	0.234	0.292	2.363	0.914	0.377	0.092
Sn			<0.015	<0.028										
Sr	0.019	0.028	0.002			0.004								
Ti	0.005	0.060	0.017	<0.030		0.043	0.010	0.005			0.063	0.009	0.005	
V	0.006	0.007	0.015	<0.016	0.001	0.009		0.006	0.003	0.002	0.001		0.014	
Zn	0.090	0.298	0.078	0.056	0.019	0.033	0.095	0.016	0.029	0.061	0.011	0.011	0.081	0.059

References are listed in Table 1 Appendix. Associated notes are explained in Table 1.
*Values for this size fraction are calculated from the average measured values reported for the other two size fractions.
$Units for acidity are nmoles/m^3.
NR = not reported.

TABLE 6A-2a (cont'd). $PM_{2.5}$ COMPOSITION FOR THE CENTRAL UNITED STATES ($\mu g/m^3$)

Ref	5(d)	13	14(m)	14(aa)	15	16	6,7	17	6,7	6,7	6,7	8(a)	8(a)
Site	Albuquerque	Denver	Urban Denver	Non-urban Denver	Chicago	Houston	Harriman	Harriman	Kingston	Portage	Topeka	El Paso	Inglenook
Dates	12/84-3/85	1/11-30/82	11/87-1/88	11/87-1/88	7/94	9/10-19/80	5/80-5/81	9/85-8/86	5/80-6/81	3/79-5/81	8/79-5/81	1980	1980
Time	7-19-7	6-18-6	9-16-9	9-16-9	8-8	NR	00-24	NR	00-24	00-24	00-24	NR	NR
Duration (h)	12	12	7&17	7&17	24	12	24	24	24	24	24	24	24
Number	NR	~26	~136	~150	16	20	256	330	169	271	286	10	8
Mass	20.60	20.73	19.67	10.35	13.57	38.60	20.80	21.00	24.60	11.00	12.50	27.16	32.03
OC	13.20	7.11	7.25		5.39	5.68							
EC	2.10	2.15	4.41		1.31	1.42							
Nitrate		2.22	3.96			0.59							
Sulfate		2.06	1.55			14.61	8.10	8.70		4.95	4.40		
Acidity$							36.1	36.1		10.5	11.6		
Al	0.077	0.394	0.037		0.046	0.123						0.155	0.082
As		<0.002			<0.003	<0.005						0.025	0.001
Ba		0.031			<0.091	0.048							
Br	0.085	0.103	0.018		0.004	0.055	0.038		0.044	0.011	0.045	0.070	0.040
Ca	0.059	0.047	0.058		0.045	0.155	0.150		0.120	0.045	0.250	0.332	0.326
Cd		0.006	0.005		<0.029	<0.003							
Cl	0.036	0.052	0.141		0.011	0.032	0.021		BQL	0.027	0.031		0.003
Cr		<0.009	0.003		<0.005	<0.005						0.001	0.002
Cu		0.010	0.017		0.011	0.028						0.036	0.032
Fe	0.045	0.079	0.111		0.089	0.162	0.120		0.097	0.049	0.090	0.134	0.281
K	0.074	0.079	0.077		0.061	0.119						0.127	0.408
Mg					0.012								
Mn		0.011	0.012		0.005	0.014	0.017		0.010	0.003	0.004	0.004	0.037
Mo					<0.002								
Na					0.022	<0.38							
Ni		0.003	0.002		<0.001	0.004	BQL		BQL	BQL	BQL	0.001	0.001

TABLE 6A-2a (cont'd). $PM_{2.5}$ COMPOSITION FOR THE CENTRAL UNITED STATES ($\mu g/m^3$)

Ref	5(d)	13	14(m)	14(aa)	15	16	6,7	17	6,7	6,7	6,7	8(a)	8(a)
Site	Albuquerque	Denver	Urban Denver	Non-urban Denver	Chicago	Houston	Harriman	Harriman	Kingston	Portage	Topeka	El Paso	Inglenook
Dates	12/84-3/85	1/11-30/82	11/87-1/88	11/87-1/88	7/94	9/10-19/80	5/80-5/81	9/85-8/86	5/80-6/81	3/79-5/81	8/79-5/81	1980	1980
Time	7-19-7	6-18-6	9-16-9	9-16-9	8-8	NR	00-24	NR	00-24	00-24	00-24	NR	NR
Duration (h)	12	12	7&17	7&17	24	12	24	24	24	24	24	24	24
Number	NR	~26	~136	~150	16	20	256	330	169	271	286	10	8
P		0.043			0.008	0.028							0.008
Pb	0.237	0.326	0.075		0.027	0.465	0.180		0.194	0.061	0.163	0.481	0.309
Rb		<0.003				<0.002							
S	0.507	0.709	0.642		1.321	4.834	2.500		2.400	1.400	1.100	0.823	2.655
Sb			0.004		<0.042	0.006							
Se			0.001		<0.001	<0.002	0.002		0.002	0.001		0.002	0.001
Si	0.076	0.277	0.272		0.074	0.210	0.120		0.200	0.075	0.190	0.436	0.685
Sn			0.006		<0.049	<0.005							
Sr		<0.003	0.001			<0.002							
Ti		<0.027	0.009		<0.029	<0.014						0.003	
V					<0.009	<0.008	BQL		BQL	BQL	BQL		
Zn	0.007	0.046	0.031		0.052	0.084						0.055	0.133

TABLE 6A-2a (cont'd). $PM_{2.5}$ COMPOSITION FOR THE CENTRAL UNITED STATES ($\mu g/m^3$)

Ref	8(a)	8(a)	8(a)	8(a)	8(a)	8(a)	8(a)	8(a)	8(a)	18(k)	6,7	17	6,7
Site	Braidwood	Kansas City KS	Minneapolis	Kansas City MO	Akron	Cincinnati	Buffalo	Dallas	St. Louis	St. Louis	St. Louis	St. Louis	Steubenville
Dates	1980	1980	1980	1980	1980	1980	1980	1980	1980	8-9/76	9/79-6/81	9/85-8/86	4/79-4/81
Time	NR	NR	NR	NR	NR	NR	NR	NR	NR	NR	00-24	NR	00-24
Duration (h)	24	24	24	24	24	24	24	24	24	6-12	24	24	24
Number	1	8	6	3	7	2	14	4	5	NR	306	311	499
Mass	28.20	25.66	15.50	16.77	36.09	29.80	38.75	28.93	23.06	34.00	19.00	17.70	29.60
OC													
EC													
Nitrate													
Sulfate											7.40	8.00	10.94
Acidity[$]											10.3	9.7	25.2
Al	0.089	0.091			0.046	0.062	0.192	0.111	0.119	0.203			
As		0.003	0.004	0.007	0.012	0.013	0.009	0.033	0.003	0.002			
Ba										0.020			
Br	0.003	0.027	0.047	0.064	0.039	0.024	0.003	0.223	0.025	0.132	0.078		0.042
Ca	0.084	0.519	0.103	0.213	0.110	0.062	0.218	0.691	0.090	0.132	0.101		0.097
Cd										0.004			
Cl										0.087	0.052		0.092
Cr		0.004	0.001	0.002	0.010	0.003	0.002	0.005		0.006			
Cu	0.024	0.032	0.035	0.021	0.037	0.024	0.026	0.043	0.018	0.029			
Fe	0.071	0.189	0.087	0.140	0.609	0.174	0.671	0.248	0.076	0.275	0.190		0.590
K	0.052	0.311	0.092	0.142	0.268	0.136	0.310	0.125	0.126	0.261			
Mg													
Mn	0.001	0.006	0.005	0.006	0.085	0.011	0.033	0.015	0.002	0.036	0.021		0.029
Mo													
Na													
Ni	0.001	0.002	0.001	0.001	0.006	0.004	0.008	0.002	0.002	0.004	0.003		0.005

TABLE 6A-2a (cont'd). $PM_{2.5}$ COMPOSITION FOR THE CENTRAL UNITED STATES ($\mu g/m^3$)

Ref	8(a)	8(a)	8(a)	8(a)	8(a)	8(a)	8(a)	8(a)	8(a)	18(k)	6,7	17	6,7
Site	Braidwood	Kansas City KS	Minneapolis	Kansas City MO	Akron	Cincinnati	Buffalo	Dallas	St. Louis	St. Louis	St. Louis	St. Louis	Steubenville
Dates	1980	1980	1980	1980	1980	1980	1980	1980	1980	8-9/76	9/79-6/81	9/85-8/86	4/79-4/81
Time	NR	NR	NR	NR	NR	NR	NR	NR	NR	NR	00-24	NR	00-24
Duration (h)	24	24	24	24	24	24	24	24	24	6-12	24	24	24
Number	1	8	6	3	7	2	14	4	5	NR	306	311	499
P		0.013			0.059	0.043	0.060	0.018	0.020	0.001			
Pb	0.041	0.180	0.308	0.369	0.412	0.343	0.359	1.066	0.277	0.688	0.327		0.216
Rb													
S	2.060	1.816	0.907	0.763	3.419	2.876	3.706	1.514	2.333	4.655	2.100		4.700
Sb										0.006			
Se	0.001	0.001	0.001		0.008	0.005	0.005		0.002	0.004	0.002		0.005
Si	0.220	0.434	0.169	0.177	0.522	0.328	0.241	0.442	0.170	0.458	0.160		0.290
Sn										0.009			
Sr										0.002			
Ti		0.004			0.009	0.003		0.007		0.112			
V							0.001	0.002		0.002	BQL		0.011
Zn	0.011	0.034	0.045	0.046	0.150	0.053	0.078	0.054	0.023	0.101			

References are listed in Table 1 Appendix. Associated notes are explained in Table 1.
*Values for this size fraction are calculated from the average measured values reported for the other two size fractions.
$Units for acidity are nmoles/m^3.
NR = not reported.

TABLE 6A-2b. COARSE PARTICLE COMPOSITION FOR THE EASTERN UNITED STATES ($\mu g/m^3$)

Ref	1(o)	1(o)	2(b)	3(ab)	4(c)	46,49,50	46,49,50	5(d)	5(d)	6,7(o,p)*	8(a,o)	8(a,o)	8(a,o)
Site	Smoky Mtn.	Shenandoah	Camden	Philadelphia	Deep Creek	Allegheny Mtn.	Laurel Hill	Raleigh	Roanoke	Watertown	Hartford	Boston	Res.Tr.Pk
Dates	9/20-26/78	7/23-5/08/80	7/14-8/13 '82	7/25-8/14/94	8/83	8/5-28/83	8/6-27/83	1/85-3/85	10/88-2/89	5/79-6/81	1980	1980	1980
Time	NR	NR	6-18-6	NR	4x daily	day/night	day/night	7-19-7	7-19-7	00-24	NR	NR	NR
Duration (h)	12	12	12	24	6	~10	~10	12	12	24	24	24	24
Number	12	28	50	21	98	44	39	NR	NR	354	2	1	3
Mass	5.60	7.40	11.40	8.42		15	13			9.30	27.85	105.60	8.17
OC			<3.00										
EC			0.42										
Nitrate			0.57										
Sulfate		0.78	<0.90							0.65			
Acidity$													
Al	<0.300	0.311	0.550	0.325		0.39	0.39				1.875	3.458	0.606
As	<0.001	<0.002				0.0002	0.0002					0.001	
Ba						0.007	0.006						
Br	0.005	0.003	0.015	0.003		0.0011	0.0011			0.022	0.046	0.025	0.003
Ca	0.322	0.304	0.360	0.421		0.27	0.28			0.209	0.864	1.069	0.086
Cd			<0.006			0.0004	0.0003						
Cl	<0.012	0.179	0.069	0.047		0.044	0.039			0.305	0.302	0.301	
Cr			<0.009			0.0014	0.0015				0.008	0.004	0.002
Cu	<0.005	0.006		0.014		0.0016	0.0025				0.026	0.023	0.010
Fe	0.118	0.158	0.490	0.352		0.24	0.24			0.276	1.070	1.612	0.182
K	0.108	0.129	0.151	0.100		0.11	0.10				0.310	0.533	0.068
Mg				0.104		0.060	0.061						
Mn		<0.006	0.011	0.006		0.0063	0.0068			0.006	0.021	0.029	0.003
Mo						0.0026	0.0021						
Na				0.136		0.054	0.044						
Ni	<0.002	<0.003	0.004	0.002		0.0008	0.0009				0.005	0.022	

TABLE 6A-2b (cont'd). COARSE PARTICLE COMPOSITION FOR THE EASTERN UNITED STATES ($\mu g/m^3$)

Ref	1(o)	1(o)	2(b)	3(ab)	4(c)	46,49,50	46,49,50	5(d)	5(d)	6,7(o,p)*	8(a,o)	8(a,o)	8(a,o)
Site	Smoky Mtn.	Shenandoah	Camden	Philadelphia	Deep Creek	Allegheny Mtn.	Laurel Hill	Raleigh	Roanoke	Watertown	Hartford	Boston	Res.Tr.Pk
Dates	9/20-26/78	7/23-5/08/80	7/14-8/13 '82	7/25-8/14/94	8/83	8/5-28/83	8/6-27/83	1/85-3/85	10/88-2/89	5/79-6/81	1980	1980	1980
Time	NR	NR	6-18-6	NR	4x daily	day/night	day/night	7-19-7	7-19-7	00-24	NR	NR	NR
Duration (h)	12	12	12	24	6	~10	~10	12	12	24	24	24	24
Number	12	28	50	21	98	44	39	NR	NR	354	2	1	3
P				0.027		0.006	0.007				0.033	0.016	
Pb	0.014	0.009	0.054	0.013		0.007	0.007			0.076	0.171	0.177	0.013
Rb						0.0004	0.0005						
S	<0.560	<0.711	0.230	BQL		0.59	0.56			0.200	0.428	0.502	0.223
Sb			0.181			0.0002	0.0002						
Se	<0.0006	<0.001	<0.0015	BQL		0.0003	0.0003						
Si	0.580	0.813	1.610	0.933		1.48	1.41			1.000	4.517	6.760	1.387
Sn			<0.009										
Sr			0.002			0.0029	0.0025						
Ti	0.018	0.017	0.065	0.030		0.029	0.027				0.094	0.154	0.021
V			0.007	BQL		0.0011	0.0010				0.008	0.008	
Zn	<0.004	0.006	0.030	0.052		0.010	0.011				0.054	0.054	0.007

References are listed in Table 1 Appendix. Associated notes are explained in Table 1.
*Values for this size fraction are calculated from the average measured values reported for the other two size fractions.
$Units for acidity are nmoles/m_3.
NR = not reported.

TABLE 6A-2b (cont'd). COARSE PARTICLE COMPOSITION FOR THE WESTERN UNITED STATES ($\mu g/m^3$)

Ref	9(g)*	9(g)*	10(i)*	11(j)	5(d)	12(f)	8(a,o)	8(a,o)	8(a,o)	8(a,o)	8(a,o)	8(a,o)	8(a,o)	8(a,o)
Site	Los Angeles	Los Angeles	San Joaquin Valley	Phoenix	Boise	Nevada	Tarrant CA	Five Points CA	Riverside CA	San Jose CA	Honolulu	Winnemucca	Portland	Seattle
Dates	Summer 1987	Fall 1987	6/88-6/89	10/13/89-1/17/90	12/86-3/87	11/86-1/87	1980	1980	1980	1980	1980	1980	1980	1980
Time	NR	NR	NR	NR	7-19-7	00-24	NR	NR	NR	NR	NR	NR	NR	NR
Duration (h)	4,5 and 7	4 and 6	24	6 h, 2x/day	12	24	24	24	24	24	24	24	24	24
Number	11 days	6 days	~35	~100 days	NR	24	6	3	4	6	1	5	4	1
Mass	26.30	8.50	44.17	33.09			43.85	92.57	71.03	30.40	25.80	55.74	80.38	25.30
OC	3.34	4.89	5.71	4.46										
EC	0.82	1.21	2.38	0.84										
Nitrate	5.13	4.86	2.38	0.86										
Sulfate	1.87	1.01	0.62	0.37										
Acidity$														
Al	0.723	0.597	3.418	2.539			2.230	7.078	3.513	1.930	1.865	6.564	6.351	2.294
As	BQL	0.004		<0.002									0.002	0.002
Ba	0.055	0.084	0.040	<0.077										
Br	0.003	0.006	0.006	0.002			0.047	0.004	0.028	0.062	0.006	0.004	0.028	0.014
Ca	0.563	0.854	0.961	1.929			4.088	1.636	4.781	0.682	0.957	1.934	1.305	0.548
Cd				<0.016										
Cl	1.026	0.426	0.393	0.194				0.022	0.164	0.430	0.938	0.176	0.176	0.228
Cr	0.002	0.017	0.007	0.008			0.005	0.006	0.005	0.006	0.005	0.006	0.010	0.003
Cu	BQL	BQL	BQL	0.021			0.030	0.013	0.021	0.028	0.007	0.017	0.037	0.017
Fe	0.737	1.635	1.453	1.259			0.941	3.059	1.888	1.066	0.658	1.764	1.789	0.903
K	0.196	0.243	0.632	0.669			0.255	1.193	0.961	0.260	0.294	1.051	0.587	0.151
Mg	0.311	0.212												
Mn	0.017	0.021	0.031	0.032			0.035	0.050	0.042	0.021	0.014	0.041	0.056	0.018
Mo				<0.005										
Na	1.431	0.052												
Ni	BQL	BQL	BQL	0.003			0.003	0.012	0.006	0.008	0.003	0.002	0.009	0.001

TABLE 6A-2b (cont'd). COARSE PARTICLE COMPOSITION FOR THE WESTERN UNITED STATES ($\mu g/m^3$)

Ref	9(g)*	9(g)*	10(i)*	11(j)	5(d)	12(f)	8(a,o)	8(a,o)	8(a,o)	8(a,o)	8(a,o)	8(a,o)	8(a,o)	8(a,o)
Site	Los Angeles	Los Angeles	San Joaquin Valley	Phoenix	Boise	Nevada	Tarrant CA	Five Points CA	Riverside CA	San Jose CA	Honolulu	Winnemucca	Portland	Seattle
Dates	Summer 1987	Fall 1987	6/88-6/89	10/13/89-1/17/90	12/86-3/87	11/86-1/87	1980	1980	1980	1980	1980	1980	1980	1980
Time	NR	NR	NR	NR	7-19-7	00-24	NR	NR	NR	NR	NR	NR	NR	NR
Duration (h)	4,5 and 7	4 and 6	24	6 h, 2x/day	12	24	24	24	24	24	24	24	24	24
Number	11 days	6 days	~35	~100 days	NR	24	6	3	4	6	1	5	4	1
P	0.127	0.053	0.052	0.038			0.002	0.148	0.144	0.032			0.011	
Pb	0.046	0.066	0.032	0.022			0.167	0.018	0.113	0.228	0.022	0.021	0.115	0.077
Rb				0.003										
S	0.520	0.264	0.222	0.178			0.310	0.293	0.720	0.257	0.258	0.215	0.427	0.121
Sb				<0.030										
Se	BQL	BQL		<0.002										
Si	1.988	1.642	7.577	7.013			5.208	16.001	7.544	5.214	3.766	11.903	12.128	4.332
Sn				<0.026										
Sr	BQL	BQL	0.012	0.014										
Ti	0.072	0.106	0.130	0.121			0.083	0.272	0.182	0.086	0.067	0.164	0.186	0.091
V	BQL	0.003	BQL	<0.014				0.007					0.004	
Zn	0.024	BQL	0.016	0.034			0.052	0.016	0.030	0.044	0.008	0.015	0.038	0.034

References are listed in Table 1 Appendix. Associated notes are explained in Table 1.
*Values for this size fraction are calculated from the average measured values reported for the other two size fractions.
$Units for acidity are nmoles/m^3.
NR = not reported.

TABLE 6A-2b (cont'd). COARSE PARTICLE COMPOSITION FOR THE CENTRAL UNITED STATES ($\mu g/m^3$)

Ref	5(d)	13(o)	14(m)	14(ab)	15(s)	16(o)	6,7(o,p)*	17	6,7(o,p)*	6,7(o,p)*	6,7(o,p)*	8(a,o)	8(a,o)
Site	Albuquerque	Denver	Urban Denver	Non-urban Denver	Chicago	Houston	Harriman	Harriman	Kingston	Portage	Topeka	El Paso	Inglenook
Dates	12/84-3/85	1/11-30/82	11/87-1/88	11/87-1/88	7/94	9/10-19/80	5/80-5/81	9/85-8/86	5/80-6/81	3/79-5/81	8/79-5/81	1980	1980
Time	7-19-7	6-18-6	9-16-9	9-16-9	8-8	NR	00-24	NR	00-24	00-24	00-24	NR	NR
Duration (h)	12	12	7 & 17	7 & 17	24	12	24	24	24	24	24	24	24
Number	NR	~26	~136	~150	16	20	256	330	169	271	286	10	8
Mass		35.73			14.97	24.80	11.70	9.00	10.80	7.20	13.90	49.05	40.43
OC						3.10							
EC													
Nitrate						1.63							
Sulfate		0.39				0.91				0.35	0.40		
Acidity$													
Al		2.900			0.223	1.093						2.748	2.426
As					<0.0013	<0.006						0.012	
Ba		0.058			<0.038	0.091							
Br		0.024			0.007	0.036	0.014		0.012	0.003	0.010	0.033	0.021
Ca		0.658			0.716	2.780	1.650		0.840	0.335	2.150	3.632	2.598
Cd		0.012			<0.012	<0.006							
Cl		1.235			0.036	0.366	0.029		0.018	0.056		0.043	
Cr		<0.009			<0.0024	0.007						0.003	0.004
Cu		0.008			0.006	0.018						0.047	0.027
Fe		0.954			0.344	0.604	0.570		0.263	0.181	0.490	0.812	1.193
K		0.648			0.101	0.170						0.496	0.309
Mg					0.106								
Mn		0.021			0.008	0.021	0.021		0.018	0.006	0.016	0.023	0.041
Mo					<0.0017								
Na					<0.017	<0.74							
Ni		0.005			<0.0007	0.004	0.001		BQL	0.001	0.001	0.001	0.002

TABLE 6A-2b (cont'd). COARSE PARTICLE COMPOSITION FOR THE CENTRAL UNITED STATES ($\mu g/m^3$)

Ref	5(d)	13(o)	14(m)	14(ab)	15(s)	16(o)	6,7(o,p)*	17	6,7(o,p)*	6,7(o,p)*	6,7(o,p)*	8(a,o)	8(a,o)
Site	Albuquerque	Denver	Urban Denver	Non-urban Denver	Chicago	Houston	Harriman	Harriman	Kingston	Portage	Topeka	El Paso	Inglenook
Dates	12/84-3/85	1/11-30/82	11/87-1/88	11/87-1/88	7/94	9/10-19/80	5/80-5/81	9/85-8/86	5/80-6/81	3/79-5/81	8/79-5/81	1980	1980
Time	7-19-7	6-18-6	9-16-9	9-16-9	8-8	NR	00-24	NR	00-24	00-24	00-24	NR	NR
Duration (h)	12	12	7 & 17	7 & 17	24	12	24	24	24	24	24	24	24
Number	NR	~26	~136	~150	16	20	256	330	169	271	286	10	8
P		0.113			0.027	<0.1							0.022
Pb		0.099			0.005	0.124	0.057		0.040	0.013	0.040	0.191	0.079
Rb		0.005				<0.003							
S		<0.48			0.043	<1.29	BQL		BQL	BQL	BQL	0.249	0.314
Sb					<0.017	<0.009							
Se					<0.0006							0.001	
Si		7.460			0.739	2.990	1.880		1.700	0.905	2.310	5.377	6.312
Sn					<0.021	<0.009							
Sr		0.009				<0.008							
Ti		0.090			0.019	0.036						0.077	0.116
V					<0.004	<0.03							
Zn		0.039			0.038	0.058						0.057	0.055

TABLE 6A-2b (cont'd). COARSE PARTICLE COMPOSITION FOR THE CENTRAL UNITED STATES ($\mu g/m^3$)

Ref	8(a,o)	8(a,o)	8(a,o)	8(a,o)	8(a,o)	8(a,o)	8(a,o)	8(a,o)	8(a,o)	18(k,r)	6,7(o,p)*	17	6,7(o,p)*
Site	Braidwood	Kansas City KS	Minneapolis	Kansas City MO	Akron	Cincinnati	Buffalo	Dallas	St. Louis	St. Louis	St. Louis	St. Louis	Steubenville
Dates	1980	1980	1980	1980	1980	1980	1980	1980	1980	8-9/76	9/79-6/81	9/85-8/86	4/79-4/81
Time	NR	NR	NR	NR	NR	NR	NR	NR	NR	NR	00-24	NR	00-24
Duration (h)	24	24	24	24	24	24	24	24	24	6-12	24	24	24
Number	1	8	6	3	7	2	14	4	5		306	311	499
Mass	28.70	41.67	30.85	41.67	34.81	33.15	44.57	32.63	33.76	28.00	12.40	9.90	16.90
OC													
EC													
Nitrate													
Sulfate											0.70		1.86
Acidity[$]													
Al	1.931	2.284	2.191	2.284	2.509	2.910	2.808	1.294	3.837	1.209			
As	0.002	0.003	0.001	0.003	0.003			0.006	0.001	0.001			
Ba										0.034			
Br	0.003	0.029	0.022	0.029	0.025	0.017	0.012	0.051	0.021	0.047	0.021		0.010
Ca	1.406	3.754	1.571	3.754	1.431	1.312	2.550	3.436	1.784	2.817	1.499		1.023
Cd										0.001			
Cl		0.530	0.293	0.530	0.572	0.103	0.728	0.029	0.053	0.257	0.093		0.211
Cr	0.002	0.004	0.002	0.004	0.014	0.002	0.015	0.005	0.001	0.009			
Cu	0.020	0.015	0.022	0.015	0.018	0.014	0.022	0.023	0.014	0.014			
Fe	0.656	0.979	0.744	0.979	1.640	0.883	2.040	0.720	0.587	1.218	0.580		1.610
K	0.303	0.361	0.310	0.361	0.324	0.363	0.206	0.210	0.291	0.392			
Mg													
Mn	0.017	0.025	0.026	0.025	0.044	0.021	0.078	0.020	0.017	0.035	0.019		0.039
Mo													
Na													
Ni	0.001	0.002	0.001	0.002	0.005	0.003	0.009	0.002	0.002	0.005	0.002		0.004

TABLE 6A-2b (cont'd). COARSE PARTICLE COMPOSITION FOR THE CENTRAL UNITED STATES ($\mu g/m^3$)

Ref	8(a,o)	8(a,o)	8(a,o)	8(a,o)	8(a,o)	8(a,o)	8(a,o)	8(a,o)	8(a,o)	18(k,r)	6,7(o,p)*	17	6,7(o,p)*
Site	Braidwood	Kansas City KS	Minneapolis	Kansas City MO	Akron	Cincinnati	Buffalo	Dallas	St. Louis	St. Louis	St. Louis	St. Louis	Steubenville
Dates	1980	1980	1980	1980	1980	1980	1980	1980	1980	8-9/76	9/79-6/81	9/85-8/86	4/79-4/81
Time	NR	NR	NR	NR	NR	NR	NR	NR	NR	NR	00-24	NR	00-24
Duration (h)	24	24	24	24	24	24	24	24	24	6-12	24	24	24
Number	1	8	6	3	7	2	14	4	5		306	311	499
P	0.014					0.037				0.098			
Pb	0.013	0.109	0.098	0.109	0.097	0.099	0.108	0.252	0.095	0.189	0.088		0.043
Rb										0.002			
S	0.572	0.280	0.224	0.280	0.451	0.389	0.765	0.240	0.279	0.533	0.200		0.800
Sb										0.001			
Se	0.001									0.001			
Si	5.767	4.809	4.679	4.809	5.009	6.633	2.675	3.210	4.468	4.470	1.940		2.010
Sn										0.001			
Sr										0.007			
Ti	0.083	0.074	0.062	0.074	0.107	0.096	0.051	0.051	0.058	0.475			
V										0.004	BQL		0.002
Zn	0.012	0.040	0.027	0.040	0.069	0.148	0.043	0.030	0.021	0.074			

References are listed in Table 1 Appendix. Associated notes are explained in Table 1.
*Values for this size fraction are calculated from the average measured values reported for the other two size fractions.
$Units for acidity are nmoles/m^3.
NR = not reported.

TABLE 6A-2c. PM_{10} COMPOSITION FOR THE EASTERN UNITED STATES ($\mu g/m^3$)

Ref	1(o,q)*	1(o,q)*	2(b)*	3(ab)*	4(c)	5(d)	5(d)	6,7(p,q)	8(a,q)*	8(a,q)*	8(a,q)*
Site	Smoky Mtn.	Shenandoah	Camden	Philadelphia	Deep Creek	Raleigh	Roanoke	Watertown	Hartford	Boston	Res.Tr.Pk
Dates	9/20-26/78	7/23-5/08/80	7/14-8/13 '82	7/25-8/14/94	8/83	1/85-3/85	10/88-2/89	5/79-6/81	1980	1980	1980
Time	NR	NR	6-18-6	NR	4x daily	7-19-7	7-19-7	00-24	NR	NR	NR
Duration (h)	12	12	12	24	6	12	12	24	24	24	24
Number	12	28	50	21	98	NR	NR	354	2	1	3
Mass	29.60	34.40	40.10	40.60				24.20	54.60	140.40	36.93
OC	2.22	0.44	2.05	4.51							
EC	1.10	1.12	2.29	0.76							
Nitrate	0.30		0.57								
Sulfate	12.00	14.38	11.20					6.50			
Acidity$											
Al	BQL	0.311	0.603	0.439					1.910	3.458	0.679
As	BQL		0.001							0.003	0.002
Ba											
Br	0.023	0.011	0.044	0.012				0.110	0.082	0.045	0.010
Ca	0.338	0.339	0.400	0.479				0.250	0.934	1.139	0.121
Cd			0.002								
Cl	BQL	0.189	0.072	0.073				0.389	0.302	0.301	
Cr			0.002						0.011	0.008	0.002
Cu	0.003	0.011		0.021					0.069	0.058	0.026
Fe	0.146	0.212	0.581	0.479				0.350	1.195	1.733	0.302
K	0.148	0.190	0.252	0.160					0.481	0.629	0.216
Mg				0.126							
Mn		BQL	0.017	0.010				0.009	0.028	0.030	0.006
Mo			0.001								
Na			0.146	0.206							
Ni	BQL	BQL	0.015	0.009				0.011	0.015	0.034	0.001

TABLE 6A-2c (cont'd). PM_{10} COMPOSITION FOR THE EASTERN UNITED STATES ($\mu g/m^3$)

Ref	1(o,q)*	1(o,q)*	2(b)*	3(ab)*	4(c)	5(d)	5(d)	6,7(p,q)	8(a,q)*	(a,q)*	8(a,q)*
Site	Smoky Mtn.	Shenandoah	Camden	Philadelphia	Deep Creek	Raleigh	Roanoke	Watertown	Hartford	Boston	Res.Tr.Pk
Dates	9/20-26/78	7/23-5/08/80	7/14-8/13/82	7/25-8/14/94	8/83	1/85-3/85	10/88-2/89	5/79-6/81	1980	1980	1980
Time	NR	NR	6-18-6	NR	4x daily	7-19-7	7-19-7	00-24	NR	NR	NR
Duration (h)	12	12	12	24	6	12	12	24	24	24	24
Number	12	28	50	21	98	NR	NR	354	2	1	3
P				0.042					0.033	0.025	0.042
Pb	0.111	0.061	0.303	0.032				0.405	0.681	0.462	0.119
Rb											
S	3.744	4.539	4.430	3.251				2.000	2.647	4.371	3.058
Sb			0.260								
Se	0.001	0.001	0.002					0.001	0.001	0.001	0.002
Si	0.618	0.929	1.713	1.098				1.100	4.694	6.904	1.737
Sn			BQL								
Sr			0.002								
Ti	0.018	0.017	0.065	0.030					0.096	0.154	0.021
V	BQL	BQL	0.020					0.022	0.025	0.028	
Zn	0.009	0.017	0.112	0.092					0.133	0.100	0.025

References are listed in Table 1 Appendix. Associated notes are explained in Table 1.
*Values for this size fraction are calculated from the average measured values reported for the other two size fractions.
$Units for acidity are nmoles/m^3.
NR = not reported.

TABLE 6A-2c (cont'd). PM_{10} COMPOSITION FOR THE WESTERN UNITED STATES ($\mu g/m^3$)

Ref	9(g)	9(g)	10(i)	11(j)	5(d)*	12(f)	8(a,q)*	8(a,q)*	8(a,q)*	8(a,q)*	8(a,q)*	8(a,q)*	8(a,q)*	8(a,q)*
Site	Los Angeles	Los Angeles	San Joaquin Valley	Phoenix	Boise	Nevada	Tarrant CA	Five Points CA	Riverside CA	San Jose CA	Honolulu	Winnemucca	Portland	Seattle
Dates	Summer 1987	Fall 1987	Jun. 1998- Jun. 1989	10/13/89-1/17/90	12/86-3/87	11/86-1/87	1980	1980	1980	1980	1980	1980	1980	1980
Time	NR	NR	NR	NR	7-19-7	00-24	NR	NR	NR	NR	NR	NR	NR	NR
Duration (h)	4,5 and 7	4 and 6	24	6 h, 2x/day	12	24	24	24	24	24	24	24	24	24
Number	11 days	6 days	~35	~100 days	NR	24	6	3	4	6	1	5	4	1
Mass	67.40	98.70	74.05	62.45			100.90	124.37	106.20	66.68	46.90	65.42	117.55	36.00
OC	11.61	23.35	10.59	14.56										
EC	3.19	8.49	5.62	8.30										
Nitrate	9.47	27.50	10.55	4.46										
Sulfate	11.28	5.39	3.62	2.34										
Acidity$														
Al	0.758	0.847	3.570	2.669			2.407	7.317	3.549	2.053	2.992	6.925	6.932	2.296
As	0.007	0.019		BQL						0.001			0.014	0.008
Ba	0.070	0.127	0.051	0.013										
Br	0.016	0.072	0.015	0.014			0.149	0.019	0.065	0.250	0.023	0.010	0.121	0.033
Ca	0.585	1.190	1.057	2.099			4.543	1.786	5.082	0.771	1.981	2.177	1.459	0.585
Cd				BQL										
Cl	1.119	0.880	0.487	0.559				0.026	0.173	0.480	1.456	0.176	0.197	0.228
Cr	0.023	0.042	0.010	0.011			0.007	0.007	0.005	0.009	0.009	0.006	0.019	0.005
Cu	0.022	0.178	0.087	0.036			0.077	0.037	0.061	0.071	0.025	0.043	0.109	0.041
Fe	0.836	2.192	1.633	1.475			1.257	3.275	2.015	1.214	1.384	1.995	2.059	1.001
K	0.237	0.460	0.820	0.876			0.441	1.437	1.081	0.508	0.665	1.200	0.805	0.231
Mg	0.335	0.287		BQL										
Mn	0.033	0.063	0.037	0.054			0.067	0.055	0.049	0.027	0.034	0.044	0.108	0.022
Mo				BQL										
Na	1.632	0.518		BQL										
Ni	0.005	0.005	0.010	0.006			0.006	0.037	0.013	0.014	0.005	0.003	0.036	0.007

TABLE 6A-2c (cont'd). PM_{10} COMPOSITION FOR THE WESTERN UNITED STATES ($\mu g/m^3$)

Ref	9(g)	9(g)	10(i)	11(j)	5(d)*	12(f)	8(a,q)*	8(a,q)*	8(a,q)*	8(a,q)*	8(a,q)*	8(a,q)*	8(a,q)*	8(a,q)*
Site	Los Angeles	Los Angeles	San Joaquin Valley	Phoenix	Boise	Nevada	Tarrant CA	Five Points CA	Riverside CA	San Jose CA	Honolulu	Winnemucca	Portland	Seattle
Dates	Summer 1987	Fall 1987	Jun. 1988 -Jun. 1989	10/13/89-1/17/90	12/86-3/87	11/86-1/87	1980	1980	1980	1980	1980	1980	1980	1980
Time	NR	NR	NR	NR	7-19-7	00-24	NR	NR	NR	NR	NR	NR	NR	NR
Duration (h)	4,5 and 7	4 and 6	24	6 h, 2x/day	12	24	24	24	24	24	24	24	24	24
Number	11 days	6 days	~35	~100 days	NR	24	6	3	4	6	1	5	4	1
P	0.187	0.099	0.059	0.054			0.002	0.155	0.144	0.045	0.002		0.028	0.006
Pb	0.084	0.251	0.061	0.062			0.786	0.105	0.489	1.119	0.093	0.063	0.537	0.292
Rb			0.004	BQL										
S	3.353	2.262	1.463	0.615			2.888	1.422	2.373	1.109	0.571	0.573	2.371	0.952
Sb				BQL										
Se	0.008	0.010	0.001	BQL				0.001	0.001				0.001	0.001
Si	2.040	2.162	8.037	7.443			5.791	16.657	7.778	5.506	6.129	12.817	12.505	4.424
Sn				BQL										
Sr	0.018	0.024	0.014	0.014										
Ti	0.077	0.165	0.147	0.136			0.093	0.277	0.182	0.086	0.130	0.173	0.191	0.091
V	0.005	0.009	0.014	BQL				0.013	0.003	0.002	0.001		0.018	
Zn	0.114	0.293	0.094	0.090			0.147	0.032	0.059	0.105	0.019	0.026	0.119	0.093

References are listed in Table 1 Appendix. Associated notes are explained in Table 1.
*Values for this size fraction are calculated from the average measured values reported for the other two size fractions.
$Units for acidity are nmoles/m^3.
NR = not reported.

TABLE 6A-2c (cont'd). PM_{10} COMPOSITION FOR THE CENTRAL UNITED STATES ($\mu g/m^3$)

Ref	8(a,q)*	13(q)*	14(m)	14(aa)	15(s)*	16(q)*	6,7(p,q)	17*	6,7(p,q)	6,7(p,q)	6,7(p,q)	8(a,q)*	8(a,q)*
Site	Albuquerque	Denver	Urban Denver	Non-urban Denver	Chicago	Houston	Harriman	Harriman	Kingston	Portage	Topeka	El Paso	Inglenook
Dates	12/84-3/85	1/11-30/82	11/87-1/88	11/87-1/88	7/94	9/10-19/80	5/80-5/81	9/85-8/86	5/80-6/81	3/79-5/81	8/79-5/81	1980	1980
Time	7-19-7	6-18-6	9-16-9	9-16-9	8-8	NR	00-24	NR	00-24	00-24	00-24	NR	NR
Duration (h)	12	12	7 & 17	7 & 17	24	12	24	24	24	24	24	24	24
Number	NR	~26	~136	~150	16	20	256	330	169	271	286	10	8
Mass		56.46			28.54	63.40	32.50	30.00	35.40	18.20	26.40	76.21	72.45
OC		7.11			5.39	8.78							
EC		2.15			1.31	1.42							
Nitrate		2.22				2.22							
Sulfate		2.45			5.46	15.52	8.10	8.70		5.30	4.80		
Acidity$								36.1					
Al		3.294			0.269	1.216						2.903	2.508
As		<0.004			<0.0043	<0.015						0.037	0.001
Ba		0.089			<0.130	0.139							
Br		0.127			0.011	0.091	0.052		0.056	0.014	0.055	0.103	0.061
Ca		0.705			0.761	2.935	1.800		0.960	0.380	2.400	3.964	2.924
Cd		0.018			<0.041	<0.012							
Cl		1.287			0.047	0.398	0.050		0.018	0.083	0.031	0.043	0.003
Cr		<0.018			<0.0073	0.007						0.004	0.006
Cu		0.018			0.017	0.046						0.083	0.059
Fe		1.033			0.432	0.766	0.690		0.360	0.230	0.580	0.946	1.474
K		0.727			0.161	0.289						0.623	0.717
Mg					0.118								
Mn		0.031			0.013	0.035	0.038		0.027	0.009	0.020	0.027	0.078
Mo					<0.0041								
Na					0.022	<1.49							
Ni		0.008			<0.0018	0.008	0.001		ND	0.001	0.001	0.002	0.003
P		0.155			0.035	0.128							0.030
Pb		0.424			0.032	0.589	0.237		0.234	0.074	0.203	0.672	0.388

TABLE 6A-2c (cont'd). PM_{10} COMPOSITION FOR THE CENTRAL UNITED STATES ($\mu g/m^3$)

Ref	8(a,q)*	13(q)*	14(m)	14(aa)	15(s)*	16(q)*	6,7(p,q)	17*	6,7(p,q)	6,7(p,q)	6,7(p,q)	8(a,q)*	8(a,q)*
Site	Albuquerque	Denver	Urban Denver	Non-urban Denver	Chicago	Houston	Harriman	Harriman	Kingston	Portage	Topeka	El Paso	Inglenook
Dates	12/84-3/85	1/11-30/82	11/87-1/88	11/87-1/88	7/94	9/10-19/80	5/80-5/81	9/85-8/86	5/80-6/81	3/79-5/81	8/79-5/81	1980	1980
Time	7-19-7	6-18-6	9-16-9	9-16-9	8-8	NR	00-24	NR	00-24	00-24	00-24	NR	NR
Duration (h)	12	12	7 & 17	7 & 17	24	12	24	24	24	24	24	24	24
Number	NR	~26	~136	~150	16	20	256	330	169	271	286	10	8
Rb		0.005				<0.006							
S		0.709			1.363	4.83	2.500		2.400	1.500	1.200	1.072	2.969
Sb		<0.004			<0.059	0.006							
Se		<0.004			<0.0017	<0.003	0.002		0.002	0.001		0.003	0.001
Si		7.737			0.813	3.200	2.000		1.900	0.980	2.500	5.813	6.997
Sn		<0.004			<0.070								
Sr		0.009											
Ti		0.09			0.019	0.036						0.080	0.116
V		<0.004			<0.013	<0.045	ND	ND	ERR	ND	ND		
Zn		0.085			0.090	0.142						0.112	0.188

TABLE 6A-2c (cont'd). PM_{10} COMPOSITION FOR THE CENTRAL UNITED STATES ($\mu g/m^3$)

Ref	8(a,q)*	8(a,q)*	8(a,q)*	8(a,q)*	8(a,q)*	8(a,q)*	8(a,q)*	8(a,q)*	8(a,q)*	18(x)*	6,7(p,q)	17*	6,7(p,q)
Site	Braidwood	Kansas City KS	Minneapolis	Kansas City MO	Akron	Cincinnati	Buffalo	Dallas	St. Louis	St. Louis	St. Louis	St. Louis	Steubenville
Dates	1980	1980	1980	1980	1980	1980	1980	1980	1980	8-9/76	9/79-6/81	9/85-8/86	4/79-4/81
Time	NR	NR	NR	NR	NR	NR	NR	NR	NR	NR	00-24	NR	00-24
Duration (h)	24	24	24	24	24	24	24	24	24	6-12	24	24	24
Number	1	8	6	3	7	2	14	4	5		306	311	499
Mass	56.90	70.33	46.35	58.43	70.90	62.95	83.32	61.55	56.82	62.00	31.40	27.60	46.50
OC													
EC													
Nitrate													
Sulfate											8.10	8.00	12.80
Acidity$												9.7	
Al	2.020	2.144	2.191	2.284	2.555	2.972	3.000	1.405	3.956	1.412			
As	0.002	0.003	0.005	0.010	0.015	0.013	0.009	0.039	0.004	0.003			
Ba										0.054			
Br	0.006	0.036	0.069	0.093	0.064	0.041	0.015	0.274	0.046	0.179	0.099		0.052
Ca	1.490	4.371	1.674	3.967	1.541	1.374	2.768	4.127	1.874	2.949	1.600		1.120
Cd										0.005			
Cl			0.293	0.530	0.572	0.103	0.728	0.029	0.053	0.344	0.145		0.303
Cr	0.002	0.010	0.003	0.006	0.024	0.005	0.017	0.010	0.001	0.015			
Cu	0.044	0.048	0.057	0.036	0.055	0.038	0.048	0.066	0.032	0.043			
Fe	0.727	0.989	0.831	1.119	2.249	1.057	2.711	0.968	0.663	1.493	0.770		2.200
K	0.355	0.660	0.402	0.503	0.592	0.499	0.516	0.335	0.417	0.653			
Mg													
Mn	0.018	0.026	0.031	0.031	0.129	0.032	0.111	0.035	0.019	0.071	0.040		0.068
Mo													
Na													
Ni	0.002	0.005	0.002	0.003	0.011	0.007	0.017	0.004	0.004	0.009	0.005		0.008

TABLE 6A-2c (cont'd). PM_{10} COMPOSITION FOR THE CENTRAL UNITED STATES ($\mu g/m^3$)

Ref	8(a,q)*	8(a,q)*	8(a,q)*	8(a,q)*	8(a,q)*	8(a,q)*	8(a,q)*	8(a,q)*	8(a,q)*	18(x)*	6,7(p,q)	17*	6,7(p,q)
Site	Braidwood	Kansas City KS	Minneapolis	Kansas City MO	Akron	Cincinnati	Buffalo	Dallas	St. Louis	St. Louis	St. Louis	St. Louis	Steubenville
Dates	1980	1980	1980	1980	1980	1980	1980	1980	1980	8-9/76	9/79-6/81	9/85-8/86	4/79-4/81
Time	NR	NR	NR	NR	NR	NR	NR	NR	NR	NR	00-24	NR	00-24
Duration (h)	24	24	24	24	24	24	24	24	24	6-12	24	24	24
Number	1	8	6	3	7	2	14	4	5		306	311	499
P	0.014	0.013			0.059	0.080	0.060	0.018	0.020	0.099			
Pb	0.054	0.237	0.406	0.478	0.509	0.442	0.467	1.318	0.372	0.877	0.415		0.259
Rb										0.002			
S	2.632	2.031	1.131	1.043	3.870	3.265	4.471	1.754	2.612	5.188	2.300		5.500
Sb										0.007			
Se	0.002	0.001	0.001		0.008	0.005	0.005		0.002	0.005	0.002		0.005
Si	5.987	4.976	4.848	4.986	5.531	6.961	2.916	3.652	4.638	4.928	2.100		2.300
Sn										0.010			
Sr										0.009			
Ti	0.083	0.076	0.062	0.074	0.116	0.099	0.051	0.058	0.058	0.587			
V							0.001	0.002		0.006	ND		0.013
Zn	0.023	0.060	0.072	0.086	0.219	0.201	0.121	0.084	0.044	0.175			

References are listed in Table 1 Appendix. Associated notes are explained in Table 1.
*Values for this size fraction are calculated from the average measured values reported for the other two size fractions.
$Units for acidity are nmoles/m^3.
NR = not reported.

TABLE 6A-3. SELECTED RATIOS OF PM COMPOSITION BY GEOGRAPHIC REGION

	EAST		WEST		CENTRAL	
	Mean	N	Mean	N	Mean	N
FM/CM	2.59	8	0.89	11	1.06	25
FM/PM_{10}	0.65	8	0.41	11	0.51	25
Tot Carbon/FM	0.25	7	0.54	5	0.64	5
$SO_4^{=}$ /FM	0.34	12	0.11	13	0.28	28

N = number of studies contributing to the calculated ratios.
FM, CM, PM_{10} = Mass concentrations of $PM_{2.5}$, Coarse fraction, and PM_{10} respectively.
Total Carbon = (OC x 1.4 + EC).

TABLE 6A-4a. SITE-TO-SITE VARIABILITY OF $PM_{2.5}$ CONCENTRATIONS

Study Area	Denver Metropolitan		Phoenix		Philadelphia		San Joaquin Valley	
No. of Sites	3,a		3,b		4,c		6,d	
Study Dates	11/2/87 - 1/31/88		10/13/89 - 1/17/90		7/25/94 - 8/14/94		6/14/88 - 6/9/89	
Reference	14		11		3		10	
	Mean	Spread	Mean	Spread	Mean	Spread	Mean	Spread
Fine Mass	19.672	2.889	29.379	3.493	32.183	2.172	29.888	10.020
OC	7.245	0.789	10.089	2.690	4.164	0.935	4.873	2.695
EC	4.409	0.780	7.490	1.710	0.685	0.215	3.242	2.580
Nitrate	3.956	0.931	3.597	0.370			8.165	2.270
Sulfate	1.547	0.162	1.329	0.240	13.426	0.333	3.003	1.325
Al	0.037	0.006	0.131	0.015	0.114	0.009	0.152	0.055
Br	0.018	0.006	0.011	0.003	0.009	0.005	0.010	0.006
Ca	0.058	0.001	0.167	0.034	0.058	0.014	0.096	0.050
Cl	0.141	0.013	0.366	0.356	0.026	0.007	0.094	0.070
Cr	0.003	0.002	0.003	0.001			0.003	0.002
Cu	0.017	0.008	0.015	0.003	0.007	0.001	0.096	0.036
Fe	0.111	0.023	0.216	0.035	0.127	0.037	0.180	0.060
K	0.077	0.009	0.209	0.020	0.060	0.008	0.188	0.080
Mn	0.012	0.003	0.023	0.010	0.003	0.000	0.006	0.003
Ni	0.002	0.002	0.003	0.001	0.007	0.002	0.016	0.030
Pb	0.075	0.017	0.039	0.009	0.019	0.010	0.029	0.021
S	0.642	0.077	0.436	0.038	3.251	0.081	1.242	0.565
Si	0.272	0.009	0.430	0.066	0.165	0.022	0.460	0.245
Ti	0.009	0.001					0.017	0.004
V					0.019	0.003	0.015	0.028
Zn	0.031	0.008	0.056	0.030	0.041	0.018	0.078	0.027

Mean = Mean over all sites of the average concentrations determined at each site for the sampling period.
Spread = ABS ({Highest Mean Conc. - Lowest Mean Conc.}/2) for all the sites.
a. Federal, Auraria, and Welby sites in urban Denver.
b. Central Phoenix, Scottsdale, and Western Phoenix sites.
c. Broad Street, Castor Avenue, Roxboro, and Northeast Airport sites.
d. Stockton, Crow's Landing, Fresno, Kern, Fellows, and Bakersfield sites.

TABLE 6A-4b. SITE-TO-SITE VARIABILITY OF PM_{10} CONCENTRATIONS

Study Area	San Jose		Phoenix		San Joaquin Valley	
No. of Sites	2,a		3,b		6,c	
Study Dates	12/16/91 - 2/24/92		10/13/89 - 1/17/90		6/14/88 - 6/9/89	
Reference	29		11		10	
	Mean	Spread	Mean	Spread	Mean	Spread
Fine Mass	64.950	1.650	62.465	7.064	62.920	17.280
OC	19.390	0.150	14.549	3.481	7.870	4.150
EC	9.015	0.415	8.327	1.777	3.505	2.760
Nitrate	10.900	0.600	4.459	0.452	9.437	3.015
Sulfate	2.240	0.090	1.704	0.287	3.565	1.460
Al	0.845	0.035	2.670	0.273	2.993	1.570
Br	0.012	0.001	0.014	0.003	0.012	0.005
Ca	0.670	0.049	2.096	0.317	0.950	0.390
Cl	0.728	0.032	0.559	0.349	0.388	0.225
Cr	0.003	0.001	0.011	0.002	0.009	0.003
Cu	0.029	0.002	0.036	0.009	0.084	0.046
Fe	0.834	0.027	1.475	0.170	1.413	0.445
K	0.823	0.021	0.878	0.083	0.720	0.220
Mn	0.014	0.001	0.054	0.014	0.030	0.011
Ni	0.003	0.000	0.006	0.002	0.019	0.032
Pb	0.035	0.004	0.062	0.013	0.039	0.027
S	1.147	0.091	0.615	0.041	1.472	0.605
Si	2.905	0.045	7.442	0.862	7.517	1.765
Ti	0.088	0.024	0.121	0.024	0.128	0.033
V	0.007	0.003			0.022	0.031
Zn	0.065	0.005	0.090	0.034	0.085	0.029

Mean = Mean over all sites of the average concentrations determined at each site for the sampling period.
Spread = ABS ({Highest Mean Conc. - Lowest Mean Conc.}/2) for all the sites.
a. San Carlos St. and Fourth St. sites.
b. Central Phoenix, Scottsdale, and Western Phoenix Sites.
c. Stockton, Crow's Landing, Fresno, Kern, Fellows, and Bakersfield sites.

7. HUMAN EXPOSURE TO PARTICULATE MATTER: RELATIONS TO AMBIENT AND INDOOR CONCENTRATIONS

7.1 INTRODUCTION

The 1982 Air Quality Criteria Document for Particulate Matter and Sulfur Oxides (U.S. Environmental Protection Agency, 1982) thoroughly reviewed the PM exposure literature through 1981. The later "Second Addendum to Air Quality Criteria for Particulate Matter and Sulfur Oxides (1982)" (U.S. Environmental Protection Agency, 1986a) added coverage of newly available health effects information up to 1986. This chapter first summarizes key points from the 1982 Criteria Document, and then thoroughly reviews the PM exposure literature from 1982 through 1995 and includes some literature published and in press through February, 1996.

The U.S. Environmental Protection Agency (U.S. EPA) regulatory authority for PM only extends to the ambient air, defined in 40 CFR 50.1(e) as that portion of the atmosphere, external to buildings, to which the general public has access (Code of Federal Regulations, 1994). By the operative definition of ambient air, polluted air inside a building, or on private property owned or controlled by the source of pollution, is not regulated by the National Ambient Air Quality Standards (Costle, 1980; Bennett, 1983). However, it is necessary to consider total personal exposure to PM, both from the regulated ambient air and non-regulated indoor air. This is because ambient (outdoor) particles penetrate into non-ambient environments (indoors) where people spend approximately 85% of their time (U.S. Environmental Protection Agency, 1989). Therefore, when people are indoors, they are exposed to a mixture of ambient PM and particles generated indoors from non-regulated sources, such as PM from cigarette smoke and personal activities.

Personal exposure to total PM is important in itself, because the body may react differently to ambient and non-ambient particles of identical size but different chemical composition. Comparison of personal exposures to indoor and outdoor concentrations may provide clues as to whether or not these two types of PM have similar toxicity on a unit size and mass basis. Personal exposure may also act as a confounder in epidemiological studies

which use an inferred community exposure to ambient PM as a parameter to correlate with community health parameters, and an individual's personal exposure to total PM is a critical parameter for analysis if that person is a member of a cohort whose health outcomes are being tracked individually. Therefore, this chapter examines not only indoor air quality in regard to PM, but also community and individual exposures to PM, which include that portion of ambient PM which penetrates into indoor microenvironments (μEs). This is to aid in interpretation of acute and chronic epidemiology studies assessed in Chapter 12, in which ambient PM concentrations are assumed to be an indicator or a surrogate for mean community exposure to ambient PM or an individual exposure to ambient PM. Thus, this chapter has three objectives: (a) to provide a review of pertinent studies of indoor and personal exposures to PM; (b) to evaluate linkages between monitored personal exposures and exposures estimated from a fixed-site monitor located at some central monitoring site; and (c) to quantify the contribution of ambient air to personal PM exposure.

In this chapter, Sections 7.1.1 - 7.1.3 discuss the concept of ambient PM as a surrogate for a personal exposure and the relationship of a measured personal PM exposure to the ambient and nonambient concentrations of PM that may influence it.

Section 7.2 next reviews PM concentrations found indoors where people spend about 85% of their time (U.S. Environmental Protection Agency, 1989). This subject is discussed in detail because of the importance of indoor conditions for understanding total exposure to PM. Indoor air particles from indoor sources may be an important factor in the analysis and interpretation of epidemiology studies, because they may influence both the personal PM exposure and personal health of the exposed people.

Section 7.2.5 reviews the literature covering biological aerosols, which may produce direct health effects or act as a source of antigens capable of sensitizing people to the effects of other PM exposures.

Section 7.3 reviews the fundamental principles of personal PM monitoring and factors that influence the personal PM measurement.

Section 7.4 covers the literature on direct measurements of personal exposures to PM and PM constituents such as sulfates.

Section 7.5 reviews the literature on indirect exposure estimation procedures that predict exposures from time-weighted averages of concentrations measured indoors and outdoors.

Section 7.6 discusses the relationship of individual PM exposures to ambient PM concentrations and establishes a linkage between average personal PM exposures in a community to the ambient PM concentrations.

Section 7.7 discusses implications of PM exposure relationships for mortality and morbidity analyses.

Section 7.8 provides a Summary of Conclusions for Chapter 7.

7.1.1 Ambient Particulate Matter Concentration as a Surrogate for Particulate Matter Dosage

The health effects of PM experienced by an individual depend upon the mass, size and composition of those particles deposited within various regions of the respiratory tract during the time interval of interest. The amount of this potential dose will depend on the concentration inhaled (e.g., the instantaneous personal exposure); the ventilation rate (a function of physical activity and basal metabolism); and the fractional deposition, which is a function of ventilation rate, mode of breathing (e.g., oral or nasal), and any alterations due to lung dysfunction. If all people had identical ventilation rates and deposition patterns, then the potential-dosage distribution could be linearly scaled to the personal exposure distribution which would serve as a suitable primary surrogate. The usage of ambient PM concentration in health studies as a surrogate for personal PM exposure, and thereby a secondary surrogate for the PM dosage, would be suitable if ambient concentration was also linearly related to the personal exposure (Mage, 1983).

Adult ventilation rates are lowest (mean $\approx$ 6 L/min) during the night while asleep, at a maximum (mean $\approx$ 12 L/min; peak $\approx$ 60 L/min) during the day while awake (Adams, 1993), and in phase with PM exposure, which is also lower at night than during the day (Clayton et al., 1993). Consequently, the product of the 24-h average PM exposure, the 24-h average ventilation rate, and the average deposition parameter for the average ventilation would seriously under-predict the amount of PM deposited in the respiratory tract (Mage, 1980).

In practice, when relating human health to PM pollution variables (as in Chapter 12) one is forced to use time-weighted-average (TWA) ambient PM concentration as a surrogate for PM exposure and PM dosage because only fragmentary data are typically available on personal exposures to PM in populations. Data are also limited on ventilation rates as a function of basal metabolism and physical activities (Adams, 1993), as are data on pulmonary deposition rates of particles people are inhaling, since the size distribution is unknown and deposition is affected by unmeasured individual physiological parameters. According to Hodges and Moore (1977), "even when an explanatory variable (ambient PM concentration) can be measured with negligible error it may often be standing as a proxy for some other variable (dosage) which cannot be measured directly, and so it (dosage) is subject to measurement error". Pickles (1982) shows "that (such) uncertainties in air pollution levels lead to two kinds of error in the air pollution/mortality regression coefficient - a systematic underestimate and a random scatter". In addition, measurement error can also bias a threshold in the dose-response function towards zero (Yoshimura, 1990).

In the sections that follow, the relationships between ambient PM concentration, indoor PM concentrations and personal exposures to PM are discussed in detail. The following five caveats should be kept in mind while reading this chapter:

1. Ambient PM concentrations are often measured as a 24-h time-weighted-average (TWA) expressed as $\mu g/m^3$. This quantity, by necessity, is assumed to be a surrogate for the mass of ambient PM deposited in people's respiratory tracts per unit body weight, expressed as μg/kg-day.

2. This daily quantity of ambient PM deposited per unit body weight is in turn a surrogate for the amount of the true (but unknown) species and/or size fraction of the total PM that is the specific etiologic toxic agent(s) that act by a presently unknown mechanism. This latter quantity should be the independent variable for delineating underlying relationships between ambient PM TWA concentrations to the health indices used as the dependent variables.

3. Virtually all analyses and discussions of exposure presented here are based on personal exposure to PM of non-smokers. Only Dockery and Spengler (1981b) included 6 smokers out of 37 subjects. Smokers are often excluded from these studies because a personal exposure monitor (PEM) on a smoker will not capture the main-stream tobacco smoke that is directly inhaled. In Section 7.2 on indoor air pollution, it is shown that side-stream environmental tobacco smoke (ETS) is the largest identifiable indoor source of PM where smoking occurs. For the average smoker, the amount of direct inhalation (several milligrams of PM per cigarette) can be two-to-three orders of magnitude greater than the microgram amounts of ETS

which the PEM captures (Federal Trade Commission, 1994). The relationships presented below, of ambient PM concentration to individual total PM exposure, therefore only apply to non-smokers.

4. A total TWA personal exposure to PM (ambient PM plus indoor PM) will be a poor surrogate for the personal exposure to PM of ambient origin for those people whose personal exposures are dominated by indoor (residential and occupational) sources, such as ETS.

5. All studies of indoor concentrations and personal exposures described below evaluated subjects recruited either in a nonrandom manner or in a scientific probability sampling scheme. In the former case, the results cannot be extrapolated with confidence beyond the subjects themselves. In the latter case, the results can be extrapolated with a known confidence to the target population from which the sample was drawn. However, in both cases, there is a cohort of people who are nonresponders. If the reason for their refusal to participate in the survey is directly or indirectly related to their PM exposure, then the study results represent a sample with a bias of unknown sign and magnitude.

7.1.2 General Concepts for Understanding Particulate Matter Exposure and Microenvironments

Particulate matter represents a generic class of pollutants which requires a different interpretation of exposure in contrast to that for the other specific criteria gaseous pollutants, such as CO (Mage, 1985). Whereas a molecule of CO emitted from a motor vehicle is indistinguishable from a molecule of CO emitted from a fireplace, a 1-μm aerodynamic diameter (AD) particle emitted from a motor vehicle and a 1-μm particle emitted from a fireplace can have a different shape, mass, chemical composition, and/or toxicity. Thus, a "particle" can be a single entity, or an agglomeration of smaller particles, such as a small Pb particle bound to a larger crustal particle. Furthermore, indoor sources of particles produce a wide variety of particles of varying size and composition that people are exposed to, as shown in Figure 7-1 (Owen et al., 1992). Given that the health effects of inhalation of any particle can depend upon its mass and chemical composition, it would be of use to measure PM exposure in terms of mass and chemical composition as a function of size distribution (Mage, 1985).

The total PM exposure of an individual during a period of time is composed of exposure to many different particles from various sources in different microenvironments (μE). A μE was defined by Duan (1982) as "a chunk of air space with homogeneous

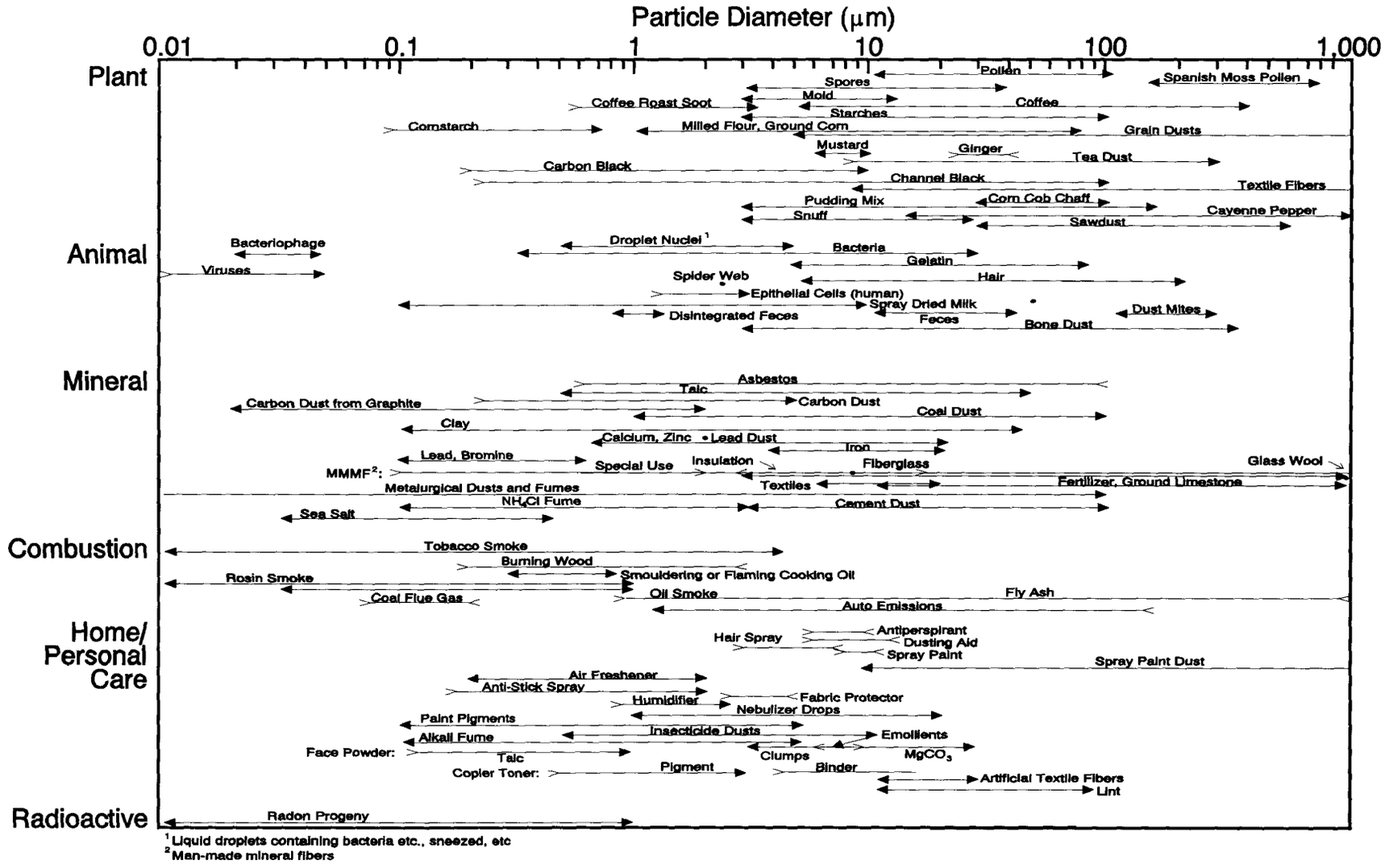

Figure 7-1. Sizes of various types of indoor particles.

Source: Owen et al. (1992).

pollutant concentration"; it has also been defined (Mage, 1985) as a volume in space, during a specific time interval, during which the variance of concentration within the volume is significantly less than the variance between that μE and its surrounding μEs. For example, a kitchen with a wood stove can constitute a single μE for total PM when the stove is off, and all people in the kitchen would have similar PM exposures. When the stove is in operation, the kitchen could have a significant vertical PM concentration gradient and a child on the floor in a far corner and an adult standing at the stove could be exposed to significantly different PM concentrations.

In a given μE, such as one in the kitchen example, the particles may come from a wide variety of sources. PM may be generated from within (e.g. the stove, deep frying, burning toast), from without (ambient PM entering through an open window), from another indoor μE (cigarette smoke from the living room), or from a personal activity that generates a heterogeneous mix of PM (sweeping the kitchen floor and resuspending a mixture of PM from indoor and outdoor sources that had settled out).

In general, as people move through space and time, they pass through a series of μEs and their average total exposure (X $\mu g/m^3$) to PM for the day can be expressed by the following equation,

$$X = \Sigma X_i t_i / \Sigma t_i \qquad (7\text{-}1)$$

where X_i is the total exposure to PM in the ith μE, visited in sequence by the person for a time interval t_i (Mage, 1985).

With appropriate averaging over sets of 4 classes of μEs (e.g., indoors, ambient-outdoors, occupational, and in-traffic) Equation 7-1 can be simplified as follows (Mage, 1985):

$$X = (X_{in}\, t_{in} + X_{out}\, t_{out} + X_{occ}\, t_{occ} + X_{tra}\, t_{tra}) / T \qquad (7\text{-}2)$$

where each value of X is the mean value of total PM concentration in the μE class *while the subject is in it*, time (t) is the total time the subject is in that μE during the day, and T is equal to the sum of all times (usually one day). Similar equations may be written for personal exposures to particles from specific sources (e.g., diesel soot), for specific chemicals (e.g., Pb), or for specific size intervals (PM $\leq$ 2.5 μm AD).

Many excellent studies have reported data on air quality concentrations in μE settings that do not meet a rigorous definition of an exposure, which requires actual occupancy by a person (Ott, 1982). Section 7.2, on Indoor Concentrations and Sources of PM, cites Thatcher and Layton (1995) who report that "merely walking into a room increased the particle concentration by 100%". Consequently, an integrated measurement of air quality in an enclosed space that includes time when it is unoccupied may not be a valid measure that can be used to estimate an exposure while occupied. If this measure includes periods of time when the space is unoccupied, it will tend to be biased low as a measure of the exposure within it during periods of occupancy. For example, it is incorrect to associate an average PM exposure to a person while cooking at a stove in a kitchen with a kitchen concentration measurement that is influenced by periods when the stove was off (Smith et al., 1994).

The literature on 24-h average PM concentrations in indoor μEs, such as residential settings, is treated separately in Section 7.2, as is done for 24-h average ambient PM concentrations in Chapter 6. In the exposure portion of this chapter, specific reference is made to some studies where simultaneous personal PM exposures and indoor PM measurements have been made, so that the relationship between indoor concentration and personal exposure can be examined.

In practice, a cascade sampler can collect ambient PM samples by size fractionation for separate chemical analyses, but such a complete definition of personal exposure to PM by chemistry and size is difficult to obtain. Although some personal monitors can be equipped with a cyclone or impactor separator and several filters to capture several PM sizes (e.g., <2.0 μm, 2.0 to 10 μm, and >10 μm; Tamura et al., 1996), most published studies of PM exposure used a PEM with a single integrated measurement of particle mass collected (e.g., <2.5 μm or <10 μm). Consequently, health studies on individuals are usually only able to develop associations between their observed health effects and their observed exposure expressed as an integral mass of PM collected and its average chemical composition.

Health studies on populations can make multiple measurements of ambient and indoor PM concentrations simultaneously (e.g., $PM_{2.5}$, PM_{10}, TSP) along with components of PM, such as polycyclic aromatic hydrocarbons (PAHs), to help understand the size distribution and chemistry of the particles in the ambient and indoor atmospheres.

7.1.3 Summary of State-of-Knowledge in the 1982 Criteria Document

In 1982 it was known, from personal monitoring and indoor monitoring, that SO_2 is almost always lower indoors than outdoors because of the virtual absence of indoor sources and the presence of sinks for SO_2 in indoor settings (exceptions can occur if high sulfur coal or kerosene are used as fuel in a poorly vented stove or space heater). However, this relationship does not hold for PM, as the indoor and personal monitoring data show both higher- and lower-than ambient PM concentrations in indoor settings as a function of particle size and human activity patterns.

The largest coarse mode particles (>10 μm), which are generally of nonanthropogenic origin (wind blown dust, etc.), require turbulence to provide vertical velocity components greater than their settling velocity to allow them to remain suspended in the air (Figure 7-1). Outdoor particles enter into an indoor setting either by bulk flow, as through an open window, in which all particles can enter at the inlet condition, or by pressure driven drafts and diffusional flows through cracks and fissures in the barriers of the building envelope when all windows are closed. In the latter mode of entry, velocities are relatively lower, thereby settling out the largest coarse particles (>25 μm AD) in the passage through the barriers (Thatcher and Layton, 1995).

Indoor settings are usually quiescent (Matthews et al., 1989), and ambient particles that enter indoors quickly settle out by gravity or electrostatic forces, leading to familiar dust layers on horizontal surfaces and vertical TV screens that require constant cleaning (Raunemaa et al., 1989). However, human activity in indoor settings, such as smoking, dusting, vacuuming and cooking, does generate fine particles (<2.5 μm) and coarser particles (>2.5 μm) and resuspends coarse particles (>10 μm) that previously had settled out (Thatcher and Layton, 1995; Litzistorf et al., 1985).

Only three studies of personal PM exposures, compared to ambient PM concentrations, were referenced in the 1982 Criteria Document (U.S. Environmental Protection Agency, 1982). Binder et al. (1976) reported that "outdoor air measurements do not accurately reflect the air pollution load experienced by individuals who live in the area of sampling", in a study in Ansonia, CT, where personal exposures to PM_5 were double the outdoor PM concentrations measured as TSP (115 versus 58 $\mu g/m^3$). Spengler et al. (1980) was cited as reporting that "there was no correlation [R^2 = 0.04] between the outdoor level [of respirable

particles] and the personal exposure of individuals" in a study in Topeka, KS. Figure 7-2, from Repace et al. (1980), was cited as an example of the variability of PM exposures which show very little influence of ambient concentration. Thus, at the time of the 1982 Criteria Document, two major factors were known to influence ambient PM relationships to indoor PM air quality: (1) the variability of indoor levels of PM compared to outdoor concentrations as a function of particle size (e.g., fine indoor $\geq$ fine outdoor, and coarse indoor $<$ coarse outdoor); and (2) the variation of exposures of individuals related to different activities involved in local generation of particles in their immediate surroundings (smoking, traffic, dusting and vacuuming at home, etc.). This understanding was summarized on pg. 5-136 of the 1982 Criteria Document, as follows:

- long term personal exposures to fine fraction PM (<2.5 μm) of outdoor origin, may be estimated by ambient measurements of the <2.5 μm PM fraction.
- Personal activities and indoor concentrations cause personal exposures to PM to vary substantially. Ambient measurements appear to be a poor predictor of personal exposure to PM.
- Tobacco smoke is an important contributor to indoor concentrations and personal exposures where smoking takes place (U.S. Environmental Protection Agency, 1982).

7.2 INDOOR CONCENTRATIONS AND SOURCES OF PARTICULATE MATTER

7.2.1 Introduction

Although EPA regulates particles in ambient air, which excludes the air internal to buildings, it is still important to consider indoor air. Most people spend most of their time indoors. A U.S. Environmental Protection Agency (1989) report indicates that U.S. residents spend 85.2% of their time indoors, 7.4% in or near a vehicle, and only 7.4% outdoors. Also, it is important to understand how outdoor particles are affected as they cross building envelopes. For a home with no indoor sources, how much protection is offered against particles of various size ranges? How do parameters such as volume of the house, air exchange rate, cleaning frequency and methods, and materials in the home affect

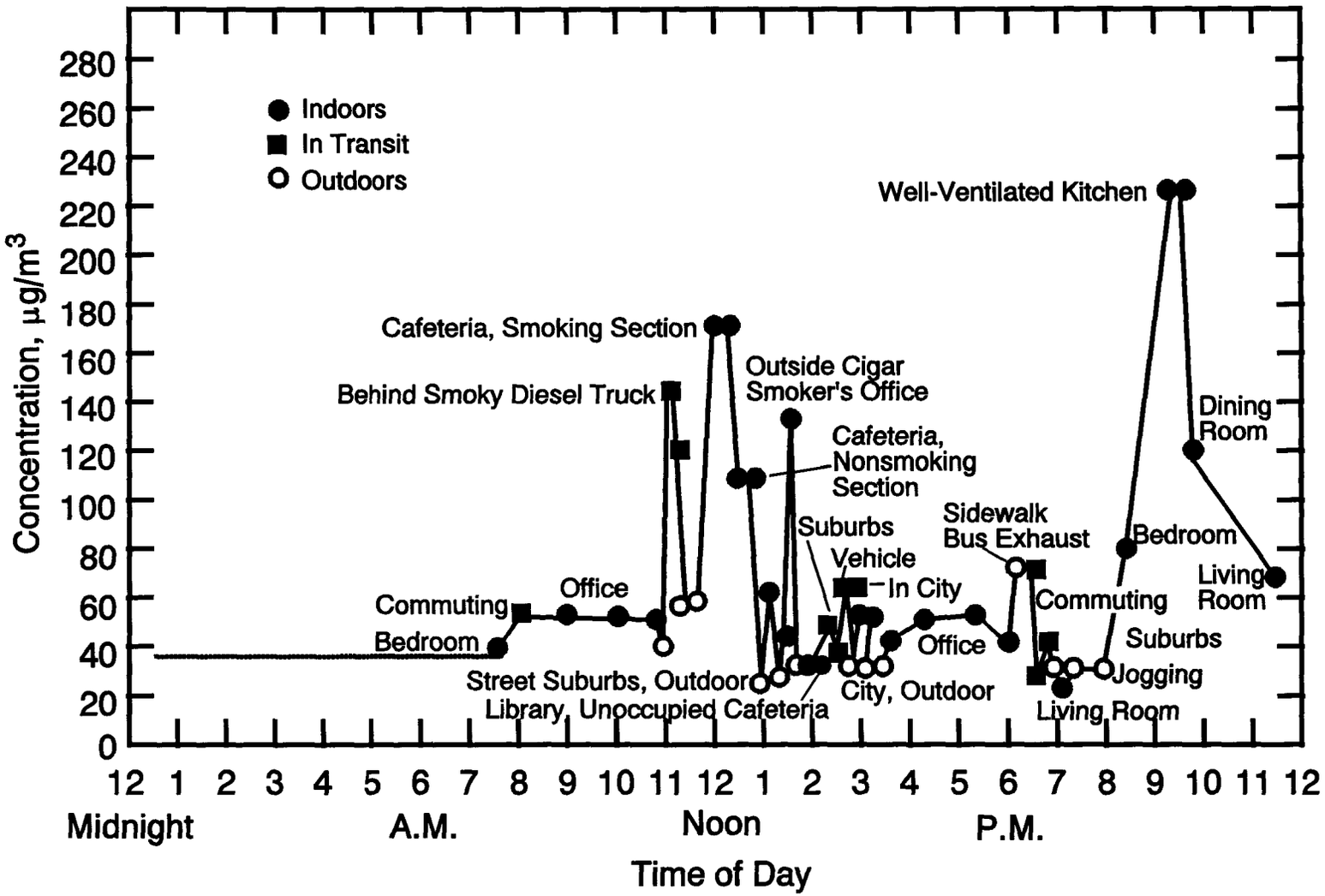

Figure 7-2. An example of personal exposure to respirable particles.

Source: Repace et al. (1980).

concentrations of particles of outdoor origin? This section has several parts that address these questions.

The first part (7.2.2; 7.2.3; and 7.2.4) deals with field studies of particles indoors and outdoors, focussing mainly on large-scale surveys of many homes and buildings. Besides presenting observed indoor and outdoor particle concentrations, information on important parameters such as air exchange rates, source emission rates, and deposition rates is also reported. This section also discusses a few studies dealing with inorganic and organic constituents of particles, as well as other considerations such as the role of house dust in exposure to metals. Section 7.2.3 provides a brief introduction to indoor air quality models. Finally, Section 7.2.4 summarizes the main findings.

The second part (7.2.5) is a discussion of bioaerosols from plants, molds, insects, etc. Although these sources of PM are uncontrolled by EPA, they affect measured PM indoors and can potentiate the effects of PM from other sources through allergenic properties.

In keeping with EPA's regulatory responsibilities, the many studies in industrial workplaces and the "dusty trades" are omitted, as are studies of lead (Pb) in indoor locations, since lead is a separate criteria pollutant and such studies are reviewed in a separate lead criteria document (U.S. Environmental Protection Agency, 1986b).

7.2.2 Concentrations of Particles in Homes and Buildings

At least seven major reviews of field studies of indoor particles have been published since 1980 (Sterling et al., 1982; National Research Council, 1986; Repace, 1987; Guerin et al., 1992; U.S. Environmental Protection Agency, 1992; Holcomb, 1993; Wallace, 1996). The last of these reviews reports on several recently completed important studies, including EPA's major probability-based PTEAM Study. Since the two microenvironments where people spend the most time are (a) home and (b) work or school, studies of these environments are summarized in turn, with emphasis on the former.

7.2.2.1 Particle Concentrations in Homes: Large-Scale Studies in the United States

There have been three large-scale studies (greater than 150 homes) of airborne particles inside U.S. homes. In chronological order, these are:

1. The Harvard Six-City study, carried out by the Harvard School of Public Health from 1979 through 1988, with measurements taken in 1,273 homes;

2. The New York State ERDA study, carried out by Research Triangle Institute (RTI) in 433 homes in two New York State counties during 1986;

3. The EPA Particle TEAM (PTEAM) study, carried out by RTI and Harvard School of Public Health in 178 homes in Riverside, CA in 1990.

The findings of each are discussed in detail, since these studies present the most complete investigations to date of indoor and outdoor concentrations of particles.

7.2.2.1.1 The Harvard Six-City Study

The Harvard Six-City Study is a prospective epidemiological study of health effects of particles and sulfur oxides. Focused mainly on children, it has included pulmonary function measurements on more than 20,000 persons in the six cities, chosen to represent low (Portage, WI and Topeka, KS), medium (Watertown, MA and Kingston-Harriman, TN), and high (St. Louis, MO and Steubenville, OH) outdoor particle and sulfate concentrations.

The study took place in two measurement phases. The first involved monitoring of about 10 homes in each city for respirable particles ($PM_{3.5}$), with measurements made every sixth day (24-h samples) for one to two years. In the second phase, a larger sample of 200 to 300 homes was selected from each city, with week-long $PM_{2.5}$ samples collected both indoors and outdoors during two weeks of sampling in summer and winter. Ultimately, more than 1,200 homes were monitored in this way.

Spengler et al. (1981) described the first five years of the study. During the Phase I period, pulmonary function measurements were made for 9,000 adults, and 11,000 children in grades 1 through 6. In each home, a 24-h sample (beginning at midnight) was collected every sixth day, using a cyclone sampler with a cut point of ≈ 3.5 μm at a flow rate of 1.7 Lpm. About 10 sites in each city were kept in operation for two years. The annual mean indoor and outdoor $PM_{3.5}$ concentrations are shown in Figure 7-3. The indoor concentrations exceeded the outdoor levels in all cities except Steubenville, OH, where the outdoor levels of about 46 $\mu g/m^3$ slightly exceeded the indoor mean of about 43 $\mu g/m^3$. The authors noted that the major source of indoor particles was cigarette smoke, and categorized their data by number of smokers in the home (Table 7-1).

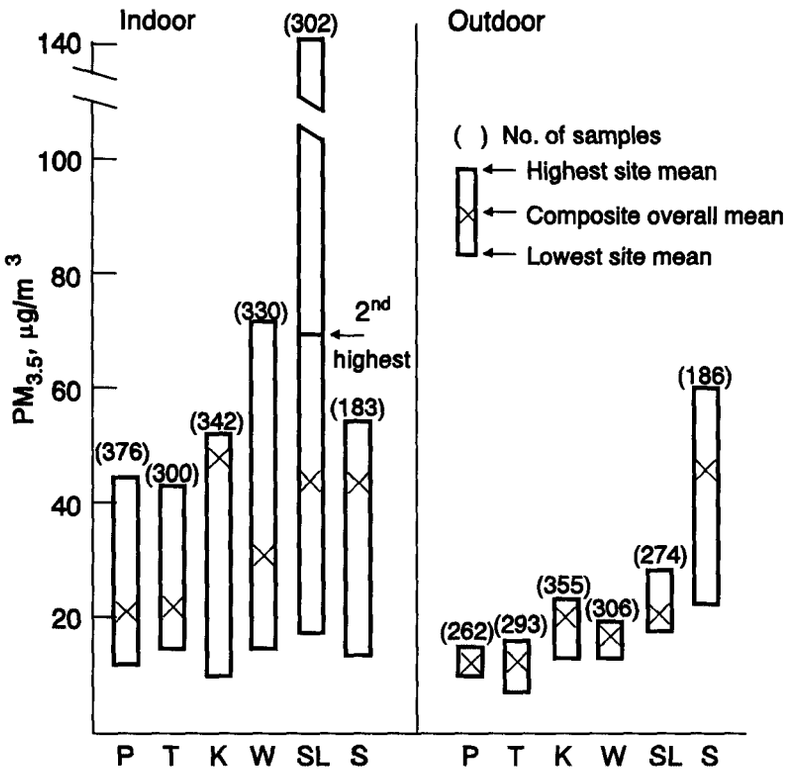

Figure 7-3. The annual mean concentration of respirable particles ($PM_{3.5}$) for the highest and lowest site from the network of indoor and outdoor monitors in each city (P-Portage, T-Topeka, K-Kingston/Harriman, W-Watertown, SL-St. Louis, S-Steubenville) in the Harvard Six-City study. Overall composite mean and the number of samples are also shown.

Source: Spengler et al. (1981).

TABLE 7-1. CONCENTRATIONS OF PARTICLES ($PM_{3.5}$) IN HOMES OF CHILDREN PARTICIPATING IN THE HARVARD SIX-CITY STUDY

Location	No. of Homes	No. of Samples	Mean (SD) ($\mu g/m^3$)
Indoors			
No smokers	35	1,186	24.4 (11.6)
One smoker	15	494	36.5 (14.5)
Two or more smokers	5	153	70.4 (42.9)
Outdoors	55	1,676	21.1 (11.9)

Source: Spengler et al. (1981).

Dockery and Spengler (1981a) provided additional data analyses drawn from the same study but including data from 68 homes compared to the 55 reported on in Spengler et al. (1981). Annual (every sixth day) mean indoor $PM_{3.5}$ concentrations (in $\mu g/m^3$) were 20 and 23 in the two "clean" locations (Portage and Topeka); 31 and 36 in the two "medium" locations (Watertown and Kingston-Harriman); and 39 and 47 in the two "dirty" locations (Steubenville and St. Louis). Outdoor $PM_{2.5}$ concentrations measured by dichotomous samplers every other day ranged from 13 $\mu g/m^3$ in Portage and Topeka to 20 $\mu g/m^3$ in St. Louis, 24 $\mu g/m^3$ in Kingston-Harriman, and 36 $\mu g/m^3$ in Steubenville (Spengler and Thurston, 1983). A mass balance model allowed estimation of the impact of cigarette smoking on indoor particles. Long-term mean infiltration of outdoor $PM_{3.5}$ was estimated to be 70% for homes without air conditioners, but only 30% for homes with air conditioners. A contribution of 0.88 $\mu g/m^3$ per cigarette (24-h average) was estimated for homes without air conditioning; for homes with air conditioning, it increased to 1.23 $\mu g/m^3$ per cigarette. A residual amount of 15 $\mu g/m^3$ not explained by the model was attributed to indoor sources such as cooking, vacuuming and dusting.

From the one to two years of indoor-outdoor data on 57 homes in the six cities, Letz et al. (1984) developed an equation relating indoor to outdoor particle concentrations:

$$C_{in} = 0.385\ C_{out} + 29.4\ (\text{Smoking}) + 13.8.$$

Thus, homes with smokers had a $PM_{3.5}$ ETS component of 29.4 $\mu g/m^3$. The residual of 13.8 $\mu g/m^3$ was assumed to be due to other household activities.

Neas et al. (1994) presented summary results for the entire Phase 2 of the Six-City Study (1983 to 1988). In Phase 2, for 1,237 homes containing white, never-smoking children, 7 to 11 years old at enrollment, three questionnaires were completed and two weeks of summer and winter monitoring indoors and outdoors for $PM_{2.5}$ was done, using the Harvard $PM_{2.5}$ impactor. At the start of the indoor monitoring study, 55% of the children were exposed to ETS in the home, and 32% were exposed to two or more smokers. Household smoking status changed for 173 children, (13% of smoking households ceased to smoke, and 15% of the nonsmoking households became smoking ones). The annual (winter and summer) household $PM_{2.5}$ mean concentration for the 580 children living in consistently smoking households was 48.5 $\pm$ 1.4 (SE) $\mu g/m^3$ compared to 17.3 $\pm$ 0.5 $\mu g/m^3$ for the

470 children in consistently nonsmoking households. Among the 614 exposed children for whom complete information on smoking consumption was available, 36% were exposed to < 1/2 pack daily, 40% to 1/2 to 1 pack daily, and 25% to >1 pack daily. The distribution of household concentrations for children in these smoking categories is shown in Figure 7-4.

Spengler et al. (1985) reported on the Kingston-Harriman, TN data from the Six-City Study. Of 101 participants, 28 had cigarette smoke exposure at home, and each had an indoor and personal monitor (cutpoints of 3.5 μm). Each town had a centrally located outdoor dichotomous sampler providing two size fractions (2.5 μm and 15 μm). Both towns had similar outdoor $PM_{2.5}$ concentrations of 18 $\mu g/m^3$, so the values were pooled for subsequent analyses. Indoor concentrations averaged 42 $\pm$ 2.6 (SE) $\mu g/m^3$. Indoor values in homes with smoking averaged 74 $\pm$ 6.6 $\mu g/m^3$, compared to 28 $\pm$ 1.1 $\mu g/m^3$ in homes without smoking ($p < 0.0001$). No significant correlations between indoor and outdoor concentrations were observed.

Lebret et al. (1987) reported on the Watertown, MA portion of the Six-City Study where 265 homes were monitored for two one-week periods. Homes with smoking averaged 54 $\mu g/m^3$ (N = 147 and 152 during weeks 1 and 2), while homes without smoking averaged 21.6 $\mu g/m^3$ (N = 70 and 74). The effect of smoking one cigarette/day was estimated at 0.8 $\mu g/m^3$ of $PM_{2.5}$.

Spengler et al. (1987) reported on a new round of measurements in three Six-City Study communities: Watertown, MA; St. Louis, MO; and Kingston-Harriman, TN. In each community, about 300 children were selected to take part in a year-long diary and indoor air quality study. $PM_{2.5}$ measurements were taken indoors at home for two consecutive weeks in winter and in summer, using the automated Harvard sampler which collected an integrated sample for the week except for 8 a.m. to 4 p.m. weekday periods when the child was at school. During this 40-h period, samples were taken in one classroom in each of the elementary schools involved. Results were presented for smoking and non-smoking homes in each city by season (Figure 7-5); the authors noted that mean concentrations in homes with smokers were about 30 $\mu g/m^3$ greater than homes without smokers, the difference being greater in winter than in summer for all cities.

Santanam et al. (1990) reported on a more recent and larger-scale monitoring effort in Steubenville and Portage as part of the Six-City Study; 140 homes in each city, equally

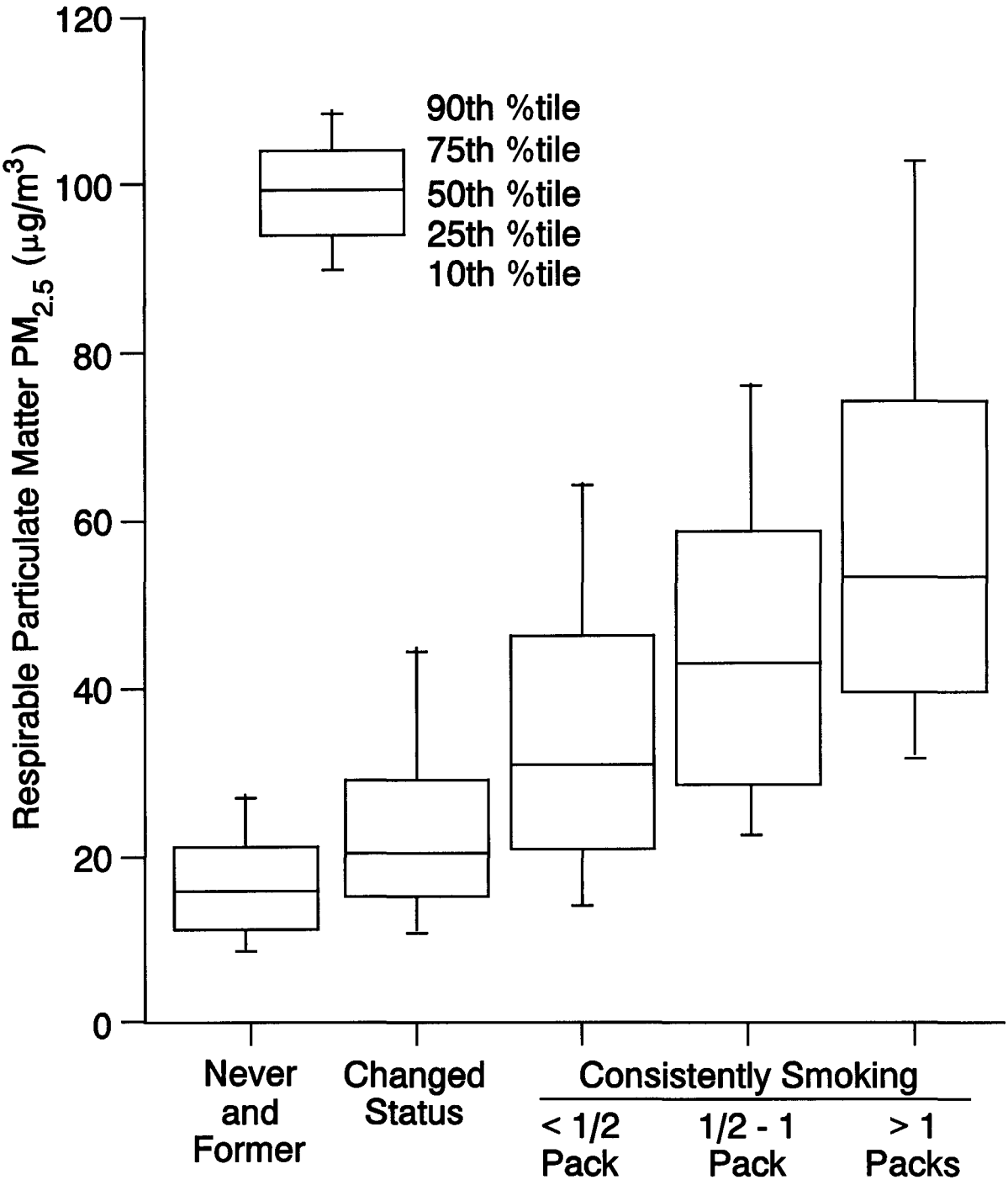

Figure 7-4. Distribution percentiles for annual average concentrations of indoor respirable particulate matter ($PM_{2.5}$) by household smoking status and estimated number of cigarette packs smoked in the home during Phase 2 Harvard Six-City study.

Source: Neas et al. (1994).

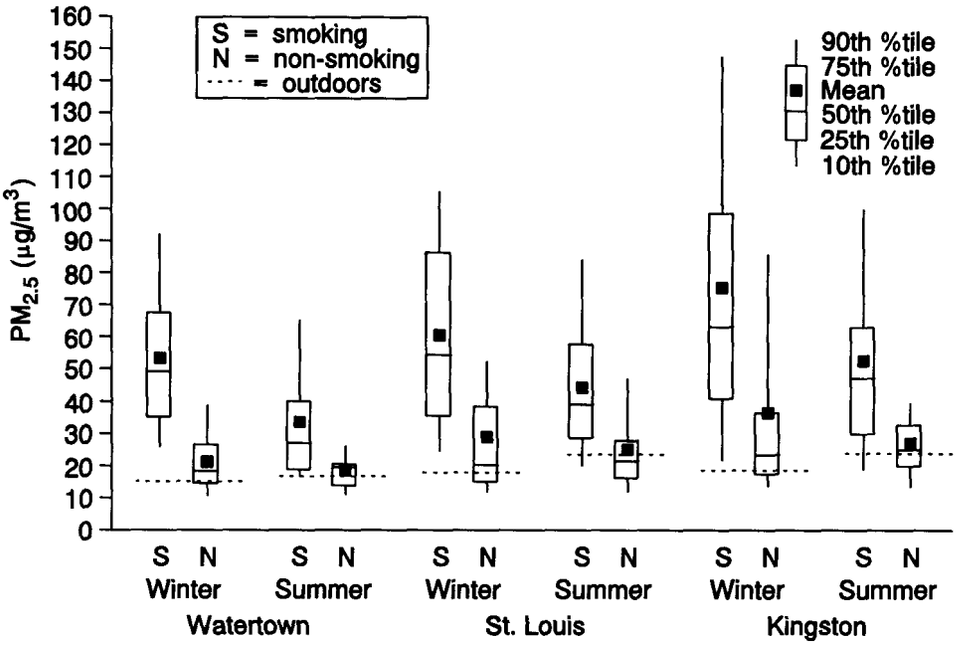

Figure 7-5. $PM_{2.5}$ ($\mu g/m^3$) in smoking (S) and nonsmoking (N) homes in three of the Harvard Six-City Study sites.

Source: Spengler et al. (1987).

distributed among households with and without smoking were monitored for one week in summer and in winter. The Harvard impactor sampler was used to collect $PM_{2.5}$ samples between 4 p.m. and 8 a.m. on weekdays and all day on weekends, corresponding to likely times of occupancy for school-age children. Outdoor samples were collected from one site in each city. Target elements were determined by XRF. A source apportionment using principal components analysis (PCA) and linear regressions on the elemental data were carried out (Table 7-2a,b). Cigarette smoking was the single largest source in smokers' homes, accounting for 20 to 27 $\mu g/m^3$ indoor $PM_{2.5}$ in Steubenville (Table 7-2a) and 10 to 25 $\mu g/m^3$ in Portage (Table 7-2b). Wood smoke was estimated to account for about 4 $\mu g/m^3$ indoors and outdoors in Steubenville in winter, but only for about 1 $\mu g/m^3$ indoors and outdoors in Portage. Sulfur-related sources accounted for 8 to 9 $\mu g/m^3$ indoors and 16 $\mu g/m^3$ outdoors in Steubenville in the summer, but were apparently not important in winter. Auto-related sources accounted for 2 to 5 $\mu g/m^3$ in the two cities. Soil sources

TABLE 7-2a. RECONSTRUCTED SOURCE CONTRIBUTIONS TO INDOOR $PM_{2.5}$ MASS FOR STEUBENVILLE, OH[1]

	WINTER			SUMMER		
Source	Smokers' Homes	Non-Smokers' Homes	Outdoor Site	Smokers' Homes	Non-Smokers' Homes	Outdoor Site
Soil	7.9 (3.45)	17.6 (3.45)	9.6 (1.79)	NS	NS	NS
Wood smoke	9.5 (4.15)	21.2 (4.15)	23.0 (4.31)	NS	NS	NS
O.C.-I	10.3 (4.47)	22.9 (4.47)	24.8 (4.65)	NS	NS	NS
Tobacco Smoke	45.6 (19.9)	NA	NA	53.7 (26.8)	NA	NA
Sulfur-related	NS	NS	NS	17.8 (8.90)	33.3 (8.23)	52.5 (15.5)
Auto-related	NS	NS	NS	7.3 (3.65)	14.8 (3.65)	5.3 (1.55)
O.C.-II	NS	NS	NS	8.8 (4.40)	16.5 (4.07)	26.0 (7.67)
Indoor dust	NS	NS	NA	7.4 (3.70)	15.0 (3.70)	NA
Unexplained	26.7 (11.6)	38.3 (7.47)	42.6 (7.95)	5.0 (2.4)	20.4 (5.05)	16.2 (4.78)
Total	100 (43.57)	100 (19.54)	100 (18.7)	100 (49.85)	100 (24.7)	100 (29.5)

[1]All entries in % ($\mu g/m^3$)
NS = not significant.
NA = not applicable.
O.C.-I: Iron and steel, and auto-related sources.
O.C.-II: Iron and steel, and soil sources.

Source: Santanam et al. (1990).

TABLE 7-2b. RECONSTRUCTED SOURCE CONTRIBUTIONS TO INDOOR $PM_{2.5}$ MASS FOR PORTAGE, WI[1]

	WINTER			SUMMER		
Source	Smokers' Homes	Non-Smokers' Homes	Outdoor Site	Smokers' Homes	Non-Smokers' Homes	Outdoor Site
Sulfur-related	13.2 (4.56)	30.7 (4.56)	39.2 (4.04)	23.3 (5.80)	38.1 (5.30)	45.8 (6.23)
Auto-related	5.1 (1.78)	12.0 (1.78)	17.3 (1.78)	18.1 (4.50)	29.6 (4.12)	35.6 (4.84)
Soil	3.8 (1.31)	8.8 (1.31)	13.4 (1.38)	7.5 (1.86)	13.4 (1.86)	16.5 (2.25)
Tobacco Smoke	71.0 (24.6)	NA	NA	40.1 (9.99)	NA	NA
Wood smoke	2.7 (0.94)	6.3 (0.94)	13.0 (1.34)	NA	NA	NA
Unexplained	4.2 (1.38)	42.2 (6.23)	17.1 (1.80)	11.0 (2.75)	18.9 (2.62)	2.10 (0.28)
Total	100 (34.6)	100 (14.8)	100 (10.3)	100 (24.9)	100 (13.9)	100 (13.6)

[1]All entries in % ($\mu g/m^3$)
NA = not applicable.

Source: Santanam et al. (1990).

accounted for only about 1 to 3 $\mu g/m^3$ of indoor and outdoor $PM_{2.5}$ concentrations. Nonsmoking homes in both cities had indoor mean $PM_{2.5}$ concentrations very close to the outdoor mean concentrations. Quite large percentages of particle concentrations were due to unexplained sources.

7.2.2.1.2 The New York State ERDA Study

Sheldon et al. (1989) studied $PM_{2.5}$ and other pollutants in 433 homes in two New York State counties. One goal of the study was to determine the effect of kerosene heaters, gas stoves, wood stoves or fireplaces, and cigarette smoking on indoor concentrations of combustion products. A stratified design included all 16 combinations of the four combustion sources and required about 22,000 telephone calls to fill all cells. The sampler was a portable dual-nozzle impactor developed at Harvard University. Two oiled impactor plates in series were used to reduce the probability that some particles larger than 2.5 μm would reach the filter. Samples were collected in the main living area and in one other room (containing a combustion source if possible) using a solenoid switch to collect alternate 15-min samples over a 7-day period. Outdoor samples were collected at a subset of 57 homes. All samples were collected during the winter (January to April) of 1986.

$PM_{2.5}$ mean concentrations indoors for all homes, with and without any combustion sources, were approximately double those outdoors in both counties (Table 7-3). However, in homes without combustion sources, $PM_{2.5}$ concentrations were approximately equal (Leaderer et al., 1990). Of the four combustion sources, only smoking created significantly higher indoor $PM_{2.5}$ concentrations in both counties (Table 7-4). Use of kerosene heaters was associated with significantly higher concentrations in Suffolk (N = 22) but not in Onondaga (N = 13). Use of wood stoves/fireplaces and gas stoves did not significantly elevate indoor concentrations in either county.

Leaderer et al. (1990) extended the analysis of these data by collapsing the gas stove category, reducing the number of categories from 16 to 8 (Table 7-5). By inspection of Table 7-5, it is clear that smoking was the single strongest source of indoor fine particles, with geometric means of indoor PM ranging from 28.5 to 61.4 $\mu g/m^3$, whereas the four nonsmoking categories ranged from 14.1 to 22.0 $\mu g/m^3$.

TABLE 7-3. WEIGHTED SUMMARY STATISTICS BY NEW YORK COUNTY FOR RESPIRABLE SUSPENDED PARTICULATE ($PM_{2.5}$) CONCENTRATIONS ($\mu g/m^3$)

	Main Living Area		Outdoors	
	Onondaga	Suffolk	Onondaga	Suffolk
Percent Detected	98.9	99.6	100	100
Sample Size	224	209	37	20
Population Estimate	94,654	286,580		
Arithmetic Mean ($\mu g/m^3$)	36.7[a]	46.4	16.8	21.8
Arithmetic Standard Error ($\mu g/m^3$)	2.14	2.77	1.00	4.54
Geometric Mean ($\mu g/m^3$)	25.7[a]	35.9	15.8	18.6
Geometric Standard Error	1.07	1.06	1.06	1.11
Minimum ($\mu g/m^3$)	0.72	2.18	6.32	12.0
Maximum ($\mu g/m^3$)	172	284	28.4	106
Percentiles				
10th	9.93	13.8		
16th	11.2	16.8		
25th	13.5	18.9	12.8	13.6
50th (median)	23.9	33.6	15.1	16.7
75th	48.4	62.8	20.5	22.3
84th	68.0	76.6		
90th	85.2	89.4		
95th	112	112		
99th	136	155		

[a] Significantly different between counties at 0.05 level.

Source: Sheldon et al. (1989).

Leaderer and Hammond (1991) continued analysis of the New York State data by selecting a subset of 96 homes for which both nicotine and $PM_{2.5}$ data were obtained. In the 47 homes where nicotine was detected (detection limit = 0.1 $\mu g/m^3$), the mean concentration of RSP was 44.1 ($\pm$ 25.9 SD) $\mu g/m^3$ compared to 15.2 ($\pm$ 7.4) $\mu g/m^3$ in the 49 homes without detected nicotine. Thus, homes with smoking had an increased weekly mean $PM_{2.5}$ concentration of about 29 $\mu g/m^3$. Imperfect agreement with reported smoking was observed, with nicotine being measured in 13% of the residences that reported no smoking, while nicotine was not detected in 28% of the residences that reported smoking. A regression on

TABLE 7-4. WEIGHTED ANALYSIS OF VARIANCE OF RESPIRABLE SUSPENDED PARTICULATE ($PM_{2.5}$) CONCENTRATIONS ($\mu g/m^3$) IN THE MAIN LIVING AREA OF HOMES VERSUS SOURCE CLASSIFICATION

	F Value	Probability	Coefficient
Onondaga (R^2 = 0.17)			
Model	20.5	0.00	
Independent variables:			
Intercept			20.3
Gas stove	1.87	0.17	5.25
Kerosene heater	1.06	0.30	5.05
Tobacco smoking	81.6	0.00	45.1
Wood stove/fireplace	2.42	0.12	7.81
Suffolk (R^2 = 0.21)			
Model	36.9	0.00	
Independent variables:			
Intercept			26.1
Gas stove	0.13	0.72	−1.52
Kerosene heater	12.0	0.00	30.1
Tobacco smoking	114	0.00	46.8
Wood stove/fireplace	0.71	0.40	9.88

Source: Sheldon et al. (1989).

TABLE 7-5. RESPIRABLE SUSPENDED PARTICULATE ($PM_{2.5}$) CONCENTRATION ($\mu g/m^3$) IN HOMES BY SOURCE CATEGORY

	Suffolk			Onondaga		
Source	N	Mean	Standard	N	Mean	Standard
None	30	17.3	1.7	45	14.1	1.7
W	15	18.1	1.6	16	19.1	1.7
K	7	22.0	1.6	4	21.2	1.0
S	61	49.3	1.8	80	36.5	2.4
KW				4	19.7	1.5
SW	29	38.0	1.8	31	33.9	2.2
SK	23	61.4	2.0	4	35.3	1.5
SKW	6	30.3	1.4	4	28.5	1.6
Outdoor	19	16.9	1.3	36	15.8	1.5

Abbreviations: W = woodstove; K = kerosene heater; S = tobacco smoking.

Source: Leaderer et al. (1990).

all (smoking and nonsmoking) homes of $PM_{2.5}$ on total number of cigarettes smoked during the week (T) gave the result:

$$PM_{2.5} = 17.7 + 0.322T \ (N = 96; R^2 = 0.55).$$

For the subset of 47 homes with measured nicotine, the regression gave the result:

$$PM_{2.5} = 24.8 + 0.272T \ (N = 47; R^2 = 0.40).$$

Thus each cigarette produces about a 0.3 ($\pm$0.03) $\mu g/m^3$ increase in the weekly mean $PM_{2.5}$ concentration, equivalent to a 2.1 ($\pm$0.2) $\mu g/m^3$ increase in the daily concentration.

Koutrakis et al. (1992) also analyzed the New York State data, using a mass-balance model to estimate $PM_{2.5}$ and elemental source strengths for cigarettes, wood burning stoves, and kerosene heaters. Homes with cigar or pipe smoking and fireplace use were eliminated, resulting in 178 indoor air samples. $PM_{2.5}$ source strength for smoking was estimated at 12.7 $\pm$ 0.8 (SE) mg/cigarette; but $PM_{2.5}$ source strengths could not be estimated for wood burning or kerosene heater usage (only seven homes in each category were available for analysis). For a residual category of all other indoor sources, a source strength of 1.16 mg/h was calculated. For nonsource homes (N = 49), the authors estimated that 60% (9 $\mu g/m^3$) of the total $PM_{2.5}$ mass was from outdoor sources and 40% (6 $\mu g/m^3$) from unidentified indoor sources. However, indoor concentrations were not significantly correlated with outdoor levels. For smoking homes, they estimated that 54% (26 $\mu g/m^3$) of the $PM_{2.5}$ mass was from smoking, 30% (15 $\mu g/m^3$) from outdoor sources, and 16% (8 $\mu g/m^3$) from unidentified sources. The elemental emissions profile for cigarettes included potassium (160 μg/cig), chlorine (69 μg/cig), and sulfur (65 μg/cig), as well as smaller amounts of bromine, cadmium, vanadium, and zinc. The woodburning profile included three elements: potassium (92 μg/h), silicon (44 μg/h) and calcium (38 μg/h). The kerosene heater profile included a major contribution from sulfur (1500 μg/h) and fairly large inputs of silicon (195 μg/h) and potassium (164 μg/h). A drawback of the mass-balance model was an inability to separately estimate the value of the penetration coefficient *P* and the decay rate

k for particles and elements; Koutrakis et al. (1992) assumed a constant rate of 0.36 h^{-1} for k, and then solved for P.

7.2.2.1.3 The U.S. Environmental Protection Agency Particle Total Exposure Assessment Methodology Study

EPA designed a study of exposure to particles and associated elements in the late 1980s. Personal exposure and indoor and outdoor $PM_{2.5}$ and PM_{10} concentrations were measured. The personal exposure portion of the study is discussed in 7.4.1.1.1. The study was carried out under the Total Exposure Assessment Methodology (TEAM) program, and is known as the Particle TEAM, or PTEAM Study.

A pilot study was undertaken in nine homes in Azusa, CA in March of 1989 to test the sampling equipment. The first five households were monitored concurrently for seven days (March 6-13, 1989; Wiener, 1988, 1989; Wiener et al., 1990; Spengler et al., 1989); the last four households were then monitored for four consecutive days (March 16-20, 1989). Indoor and outdoor particle concentrations were monitored using impactors with a 10 Lpm pump (Marple et al., 1987). Indoor monitors, capable of sampling both fine and inhalable particles simultaneously, were placed in different rooms in each house to determine the magnitude of room-to-room variation.

Room-to-room variation of 12-h integrated particle levels was generally less than 10%. Therefore the several indoor values in a particular house were averaged to provide a single mean indoor value to compare to the corresponding outdoor value. The mean (SE) 24-h indoor PM_{10} concentration was 58.7 (3.4) $\mu g/m^3$ compared to the outdoor mean of 62.6 (3.5) $\mu g/m^3$. Corresponding $PM_{2.5}$ concentrations were 36.3 (2.6) $\mu g/m^3$ indoors and 42.6 (3.0) $\mu g/m^3$ outdoors.

Regressions of indoor on outdoor concentrations (N = 26 for each size fraction and time period) resulted in the following equations for PM_{10}:

$$C_{in}\ (\text{day}) = 36\ (11) + 0.44\ (0.14)\ C_{out} \qquad (R^2 = 0.17)$$
$$C_{in}\ (\text{night}) = 44\ (11) + 0.14\ (0.19)\ C_{out} \qquad (R^2 = 0.01)$$

and for $PM_{2.5}$:

$$C_{in}\ (\text{day}) = 18\ (5) + 0.47\ (0.10)\ C_{out} \qquad (R^2 = 0.30)$$

$$C_{in}\ (\text{night}) = 24\ (6) + 0.23\ (0.15)\ C_{out} \qquad (R^2 = 0.05)$$

where the values in parentheses are the standard errors of the parameter estimates. (In most epidemiology studies, PM exposures are related to PM concentrations at a community ambient monitoring station, rather than to these PM concentrations measured outside indivdual homes).

The R^2 values improved considerably when the regressions for individual homes were calculated (Wallace, 1996; see also Table 7-6). For the five homes with seven days of monitoring (14 12-h periods) all slopes were significant, and R^2 values ranged from 0.34 to 0.79 for PM_{10} and from 0.49 to 0.85 for $PM_{2.5}$. For the four homes having only four days of monitoring, only home 8 had significant slopes and R^2 values above 0.5.

TABLE 7-6. REGRESSIONS OF INDOOR ON OUTDOOR PM_{10} AND $PM_{2.5}$ CONCENTRATIONS ($\mu g/m^3$): PARTICLE TOTAL EXPOSURE ASSESSMENT METHODOLOGY PREPILOT STUDY

				PM_{10} ($\mu g/m^3$)				
House	N	Intercept	SE	p	Slope	SE	p	R^2
1	13	23	9	0.026	0.27	0.12	0.038	0.34
2	13	−25	17	NS	1.14	0.23	0.0003	0.7
3	14	13	7	NS	0.64	0.1	0.00002	0.79
4	13	16	9	NS	0.52	0.14	0.004	0.54
5	14	14	13	NS	0.67	0.16	0.001	0.59
6	8	175	38	0.004	−1.52	0.78	NS	0.39
7	8	30	34	NS	0.34	0.62	NS	0.05
8	8	−2.7	23	NS	1.38	0.5	0.03	0.56
9	7	48	42	NS	0.94	0.87	NS	0.19
				$PM_{2.5}$ ($\mu g/m^3$)				
House	N	Intercept	SE	p	Slope	SE	p	R^2
1	14	14	3.4	0.001	0.19	0.06	0.005	0.49
2	14	−12	9	NS	0.96	0.16	0.00007	0.74
3	14	7.3	4.5	NS	0.72	0.09	0.00001	0.85
4	13	6	5	NS	0.52	0.13	0.002	0.6
5	14	11	6	NS	0.58	0.1	0.0001	0.72
6	8	65	26	0.046	−0.32	1.01	NS	0.02
7	8	10	8	NS	0.35	0.22	NS	0.3
8	8	−0.34	13	NS	0.99	0.39	0.045	0.51
9	8	37	47	NS	0.78	1.3	NS	0.05

Source: Data from PTEAM Prepilot Study upon which R^2 values were generated as reported by Wallace (1996).

After the pilot study in Azusa, CA, the EPA sponsored a study of personal, indoor, and outdoor concentrations of PM_{10}, and indoor and outdoor concentrations of $PM_{2.5}$ in Riverside, CA (Pellizzari et al., 1992, 1993; Perritt et al., 1991; Sheldon et al., 1992; Clayton et al., 1993; Thomas et al., 1993; Özkaynak et al., 1993a,b, 1996). Personal exposure results of this study are discussed in Section 7.4.1.1.2. The main goal was to estimate the frequency distribution of exposures to PM_{10} for all nonsmoking Riverside residents aged 10 and above; and 178 households were selected, using probability sampling to represent about 61,000 households throughout most of the city of Riverside. Homes were sampled between September 22 and November 9, 1990, and each home had two 12-h samples for both size fractions. A central site operated throughout the 48 days of the study, producing 96 12-h samples collected by side-by-side reference samplers (dichotomous samplers and modified hi-volume samplers) along with the low-flow (4 Lpm) impactors with nominal cutpoints at 2.5 and 10 μm designed for this study. (Laboratory tests [Thomas et al., 1993] revealed that the actual cutpoints were 2.5 μm and 11.0 μm, but this section shall refer to PM_{10} in keeping with the investigators [Clayton et al., 1993] who reported their data as PM_{10}). A subset of the homes was monitored for PAHs (Sheldon et al., 1992); 125 were monitored indoors and 65 of those were monitored outdoors for two consecutive 12-h periods.

The precision of the three types of particle samplers at the central site was excellent, with median RSDs of about 4 to 5% (Wallace, et al., 1991a). The low-flow sampler produced estimates about 12% greater than the dichotomous sampler, which was about 7% greater than the modified hi-vol sampler (Wallace, et al., 1991b). Part of the difference may be due to the different cutpoints (estimated to be 11 μm for the new sampler, 9.5 for the dichot, and 9.0 for the modified hi-vol), and part due to particle bounce (large particles bouncing off the impactor and being re-entrained in the flow to the filter), such that the $PM_{2.5}$ and PM_{10} fractions in the low-flow sampler may be contaminated with a small number of larger-size particles. However, particle bounce was found in laboratory tests to account for less than 7% of the total mass.

The population-weighted distributions of personal (PEM), indoor (SIM), and outdoor (SAM) particle concentrations are provided in Table 7-7. PM_{10} mean concentrations (150 $\mu g/m^3$) were more than 50% higher than either indoor or outdoor levels (95 $\mu g/m^3$).

TABLE 7-7. WEIGHTED DISTRIBUTIONS OF PERSONAL, INDOOR, AND OUTDOOR[a] PARTICLE CONCENTRATIONS ($\mu g/m^3$)

	DAYTIME					NIGHTTIME				
	$PM_{2.5}$		PM_{10}			$PM_{2.5}$		PM_{10}		
	SAM	SIM	SAM	SIM	PEM	SAM	SIM	SAM	SIM	PEM
Sample size	167	173	165	169	171	161	166	162	163	168
Minimum	7.4	2.8	16.2	16.6	35.1	3.4	2.9	13.6	14.1	19.1
Maximum	187.8	238.3	506.6	512.8	454.8	164.2	133.3	222.9	180.3	278.3
Mean	48.9	48.2	94.9	94.7	149.8	50.5	36.2	86.3	62.7	76.8
(Std. error)	(3.5)	(4.1)	(5.5)	(5.7)	(9.2)	(3.7)	(2.2)	(4.4)	(3.2)	(3.5)
Geometric Mean	37.7	35.0	82.7	78.2	128.7	37.2	26.7	74.5	53.1	67.9
(Std. error)	(2.5)	(3.3)	(4.1)	(5.0)	(8.5)	(3.1)	(1.9)	(4.0)	(3.1)	(3.1)
Std. deviation	37.6	41.2	57.2	61.4	84.3	40.3	29.5	47.7	37.4	39.7
Geometric std. deviation[b]	2.07	2.25	1.68	1.88	1.75	2.23	2.21	1.74	1.78	1.64
Percentiles										
10th	14.9	11.5	42.8	30.9	59.9	14.5	10.0	39.3	25.2	36.6
25th	23.4	19.3	56.9	49.5	86.1	23.0	14.8	53.6	33.5	48.1
50th (median)	35.5	33.5	84.1	81.7	129.7	35.0	25.9	74.1	51.6	66.2
75th	60.1	61.5	110.8	127.2	189.1	64.9	48.9	103.7	84.8	98.8
90th	102.2	101.0	157.2	180.7	263.1	120.7	82.7	167.8	116.9	135.0
Std. errors of percentiles										
10th	1.6	3.4	2.3	3.4	4.0	2.1	0.9	7.4	1.5	1.5
25th	2.1	1.4	4.5	4.3	9.4	2.7	1.3	3.4	2.4	3.1
50th	4.0	4.5	4.7	8.3	7.5	2.4	2.4	4.8	3.5	4.3
75th	3.9	3.3	4.0	9.4	10.8	4.6	5.3	5.1	4.7	8.2
90th	4.6	6.7	7.2	11.0	12.0	5.8	5.8	4.3	5.3	10.1

[a]Statistics other than the sample size, minimum, and maximum are calculated using weighted data; they provide estimates for the target population of person-days (PEM) or of household-days (SIM, SAM).
[b]In contrast to the other statistics, the gsd is a unitless quantity.

Source: Pellizzari et al. (1992).

Overnight mean personal PM_{10} concentrations (77 $\mu g/m^3$) were similar to the indoor (63 $\mu g/m^3$) and outdoor (86 $\mu g/m^3$) levels. The reason for the higher daytime personal exposures (PEM) than daytime SIM or SAM is not completely understood: it may be due to persons often being close to sources of particles (e.g., cooking, dusting, or vacuuming) or to re-entrainment of household dust (Thatcher and Layton, 1995). It appears not to be due to skin flakes or clothing fibers; many skin flakes were found on filters but their mass does not account for more than 10% of the excess personal exposure (Mamane, 1992).

Mean $PM_{2.5}$ daytime concentrations were similar indoors (48 $\mu g/m^3$) and outdoors (49 $\mu g/m^3$), but indoor concentrations fell off during the sleeping period (36 $\mu g/m^3$) compared to 50 $\mu g/m^3$ outdoors. Thus the fine particle contribution to PM_{10} concentrations averaged about 51% during the day and 58% at night, both indoors and outdoors. The distributions of these ratios are provided in Table 7-8.

TABLE 7-8. WEIGHTED DISTRIBUTIONS[a] OF $PM_{2.5}/PM_{10}$ CONCENTRATION RATIO

	Daytime		Nighttime	
	Outdoor	Indoor	Outdoor	Indoor
Sample Size	160	167	154	160
Mean	0.470	0.492	0.522	0.550
(Std. error)	(0.016)	(0.021)	(0.017)	(0.014)
Geometric Mean	0.444	0.455	0.497	0.517
(Std. error)	(0.017)	(0.022)	(0.019)	(0.016)
Percentiles				
10th	0.274	0.250	0.308	0.301
25th	0.371	0.347	0.406	0.440
50th (median)	0.469	0.498	0.515	0.556
75th	0.571	0.607	0.646	0.694
90th	0.671	0.735	0.731	0.771
Std. errors of percentiles				
10th	0.018	0.030	0.023	0.023
25th	0.018	0.046	0.028	0.017
50th	0.015	0.020	0.022	0.015
75th	0.019	0.024	0.027	0.023
90th	0.012	0.028	0.016	0.012

[a]Statistics other than sample size are calculated using weighted data; they provide estimates for the target population of household-days.

Source: Pellizzari et al. (1992).

Unweighted distributions are displayed in Figures 7-6 and 7-7 for 24-h average PM_{10} and $PM_{2.5}$ personal, indoor, and outdoor concentrations. For 24-h data, the indoor PM is less than the outdoor PM at all percentiles. Most of the distributions were not significantly different from log-normal distributions, as determined by a chi-square test. About 25% of the nonsmoking population of Riverside was estimated to have 24-h personal PM_{10} exposures exceeding the 150 $\mu g/m^3$ 24-h NAAQS for ambient air. Since participants were monitored for only one day, the percentage of persons with exposures exceeding the outdoor 24-h standard more than once per year would be greater than 25%.

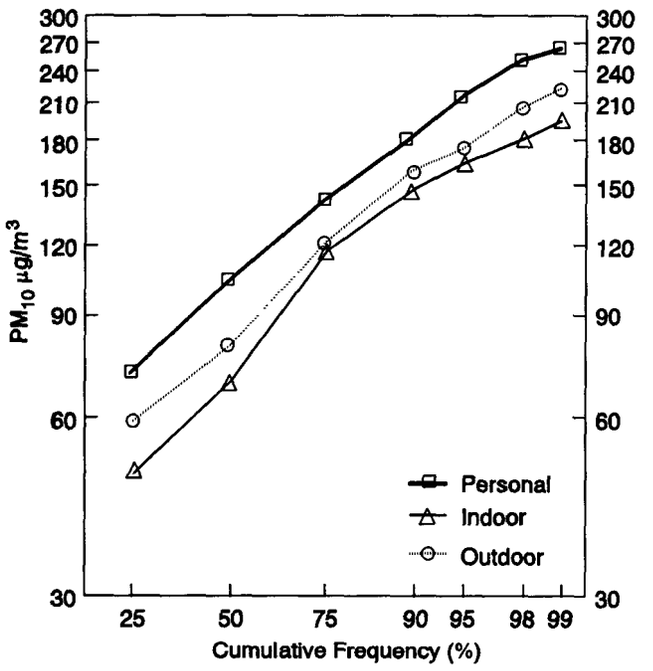

Figure 7-6. Cumulative frequency distribution of 24-h personal, indoor, and outdoor PM_{10} concentrations in Riverside, CA.

Source: Adapted from PTEAM study data (Pellizzari et al., 1992).

The 48-day sequence of outdoor PM_{10} and $PM_{2.5}$ concentrations is shown in Figure 7-8 (Wallace et al., 1991a). At least two extended episodes of high fine-particle concentrations occurred, and four days of high Santa Ana winds, with correspondingly high coarse-particle concentrations from desert sand, were observed.

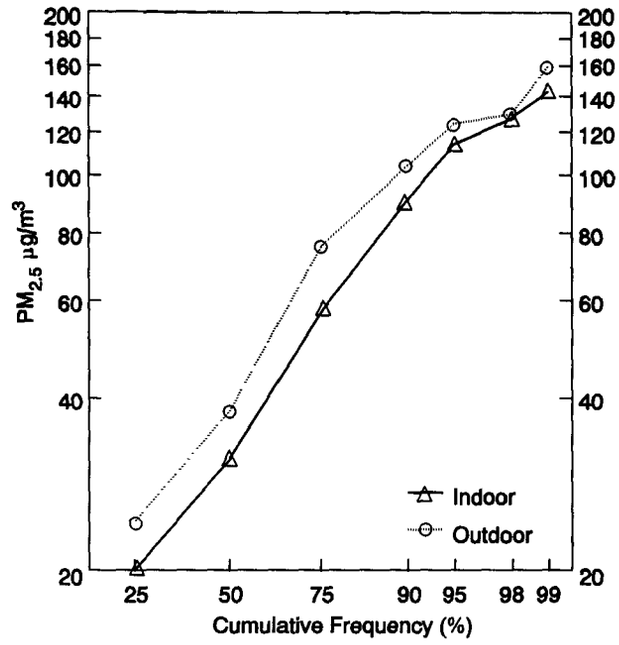

Figure 7-7. Cumulative frequency distribution of 24-h indoor and outdoor $PM_{2.5}$ concentrations in Riverside, CA.

Source: Adapted from PTEAM study data (Pellizzari et al., 1992).

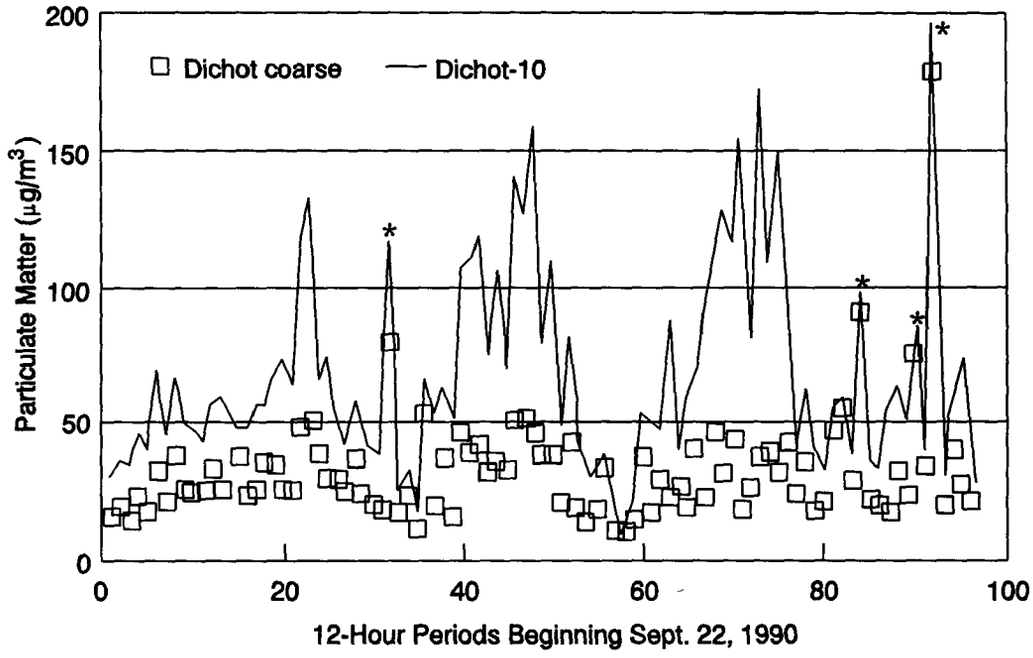

Figure 7-8. Forty-eight day sequence of PM_{10} and coarse PM (PM_{10} − $PM_{2.5}$) in Riverside, CA, PTEAM study. Santa Ana wind conditions are noted by an asterisk.

Source: Wallace et al. (1991a).

Central-site $PM_{2.5}$ and PM_{10} concentrations agreed well with back yard concentrations. Pearson correlations of the log-transformed data were 0.96 and 0.92 for overnight and daytime $PM_{2.5}$ and 0.93 for overnight PM_{10} values (Özkaynak et al., 1993a), but dropped to 0.64 for daytime PM_{10} values. However, two homes in one Riverside area showed very high outdoor concentrations of 380 and 500 $\mu g/m^3$ on one day, while two homes in another Riverside area and the central-site monitor showed more typical concentrations. A local event likely produced the higher concentrations at the former two homes. If they are removed from the data set, the correlation improves from 0.64 to 0.90, suggesting that a single central-site monitor can represent well $PM_{2.5}$ and PM_{10} concentrations throughout a wider area such as a town or small city (at least in the Riverside area) except for unusual local conditions.

Daytime indoor PM_{10} and $PM_{2.5}$ concentrations showed low-to-moderate Pearson correlations of 0.46 and 0.55, respectively, with outdoor concentrations (N = 158 to 173). At night, the correlations improved somewhat to 0.65 and 0.61, respectively (N = 50 to 168). Outdoor PM_{10} concentrations explained about 27% of the variance of indoor levels (Figure 7-9) with the two outliers included.

Simple regressions of indoor on outdoor PM_{10} and $PM_{2.5}$ resulted in the following equations (standard errors in parentheses):

$$\text{Indoor } PM_{10} = 48\ (9) + 0.51\ (0.08) \times \text{Outdoor } PM_{10} \text{ (day)} \quad N=159 \quad R^2 = 0.22$$
$$\text{Indoor } PM_{10} = 20\ (5) + 0.52\ (0.05) \times \text{Outdoor } PM_{10} \text{ (night)} \quad N=151 \quad R^2 = 0.42$$
$$\text{Indoor } PM_{2.5} = 14\ (4) + 0.70\ (0.07) \times \text{Outdoor } PM_{2.5} \text{ (day)} \quad N=162 \quad R^2 = 0.42$$
$$\text{Indoor } PM_{2.5} = 9\ (3) + 0.56\ (0.04) \times \text{Outdoor } PM_{2.5} \text{ (night)} \quad N=153 \quad R^2 = 0.54$$

Simple regressions of personal PM_{10} on outdoor and indoor PM_{10} resulted in the following equations:

$$\text{Personal } PM_{10} = 71\ (9) + 0.78\ (0.08) \times \text{Indoor } PM_{10} \text{ (day)} \quad N=163 \quad R^2 = 0.40$$
$$\text{Personal } PM_{10} = 21\ (4) + 0.90\ (0.05) \times \text{Indoor } PM_{10} \text{ (night)} \quad N=158 \quad R^2 = 0.65$$
$$\text{Personal } PM_{10} = 100\ (12) + 0.48\ (0.10) \times \text{Outdoor } PM_{10} \text{ (day)} \quad N=158 \quad R^2 = 0.12$$
$$\text{Personal } PM_{10} = 31\ (6) + 0.53\ (0.06) \times \text{Outdoor } PM_{10} \text{ (night)} \quad N=155 \quad R^2 = 0.38$$

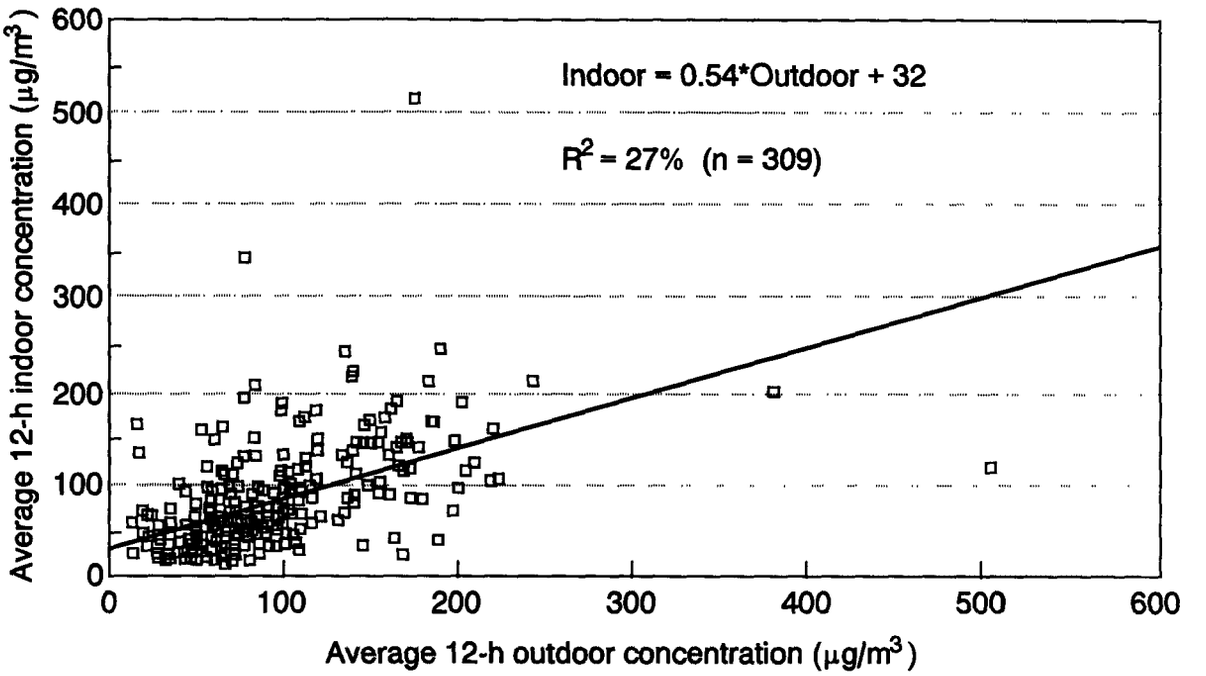

Figure 7-9. Average indoor and outdoor 12-h concentrations of PM_{10} during the PTEAM study in Riverside, CA.

Source: Özkaynak et al. (1993b).

Correlation analyses and regressions relating personal to indoor, indoor to outdoor, and personal to outdoor concentrations of the 14 prevalent elements were carried out for the appropriate size fractions and both 12-h monitoring periods. For most of the elements, as with particle mass, moderate correlations were noted for personal-indoor and indoor-outdoor concentrations but low correlations for personal-outdoor concentrations. One element was a strong exception to this rule: sulfur. Unlike any of the other elements, sulfur was not elevated in the PEM relative to the SIM, and, thus, personal concentrations were much more closely related to indoor concentrations (r_s = 0.91 during the day and 0.95 at night). Moreover, because few sources of sulfur are found indoors, the indoor-outdoor correlations were high (r_s varied between 0.90 and 0.95 for both size fractions), and even the personal-outdoor correlations showed little degradation (the Spearman correlation r_s = 0.85 during the day and 0.92 at night).

Regressions of outdoor sulfur on indoor levels gave the following results for PM_{10} sulfur ($\mu g/m^3$):

S_{in} (day) = 0.26 (0.06 SE) + 0.80 (0.02) S_{out} N = 164 R^2 = 0.88

S_{in} (night) = 0.20 (0.06) + 0.71 (0.03) S_{out} N = 155 R^2 = 0.84

and for fine ($PM_{2.5}$) sulfur:

S_{in} (day) = 0.046 (0.04 SE) + 0.85 (0.02) S_{out} N = 164 R^2 = 0.92

S_{in} (night) = 0.061 (0.04) + 0.80 (0.02) S_{out} N = 154 R^2 = 0.89

Stepwise regressions resulted in smoking, cooking, and either air exchange rates or house volumes being added to outdoor concentrations as significant variables (Table 7-9). Homes with smoking added about 27 to 32 $\mu g/m^3$ to the total $PM_{2.5}$ concentrations and about 29 to 37 $\mu g/m^3$ to the PM_{10} values. Cooking added 12 to 26 $\mu g/m^3$ to the daytime PM_{10} concentration and about 13 $\mu g/m^3$ to the daytime $PM_{2.5}$ concentration, but was not significant during the overnight period.

A model developed by Koutrakis et al. (1992) was solved using nonlinear least squares to estimate penetration factors, decay rates, and source strengths for particles and elements from both size fractions in the PTEAM study. In this model, which assumes perfect instantaneous mixing and steady-state conditions throughout each 12-h monitoring period, the indoor concentration of particles or elements is given by

$$C_{in} = \frac{PaC_{out} + Q_{is}/V}{a + k} \tag{7-3}$$

where

C_{in} = indoor concentration (ng/m^3 for elements, $\mu g/m^3$ for particles)
P = penetration coefficient
a = air exchange rate (h^{-1})
C_{out} = outdoor concentration (ng/m^3 or $\mu g/m^3$)
Q_{is} = mass flux generated by indoor sources (ng/h or $\mu g/h$)
V = volume of room or house (m^3)
k = decay rate due to diffusion or sedimentation (h^{-1})

From initial multivariate analyses, the most important indoor sources appeared to be smoking and cooking. Therefore the indoor source term Q_{is} was replaced by the following expression:

TABLE 7-9. STEPWISE REGRESSION RESULTS FOR INDOOR AIR CONCENTRATIONS OF PM_{10} AND $PM_{2.5}$ ($\mu g/m^3$) COEFFICIENTS (STANDARD ERRORS OF ESTIMATES)

	PM_{10}			$PM_{2.5}$		
Variable	All	Day	Night	All	Day	Night
N	310	158	147	324	156	149
R^2	41%	39%	58%	55%	53%	71%
Intercept		57			21	
		(21)			(7.8)	
Outdoor air	0.52	0.66	0.45	0.64	0.71	0.53
	(0.05)	(0.09)	(0.05)	(0.04)	(0.07)	(0.04)
Smoking[a]	37	29	38	28	27	32
	(6)	(8)	(11)	(3.5)	(7)	(10)
No. cigarettes[b]	3.2	3.0	3.9	2.5	2.4	4.0
	(0.7)	(1.0)	(0.9)	(0.4)	(0.6)	(0.6)
Cooking[c]	20	26	12	9.4	13	
	(5)	(9)	(5)	(2.9)	(5)	
Air exchange	5.2		12			4.5
	(2.0)		(5)			(2)
House volume[d]	−0.08	−2.7			−2.0	
	(0.02)	(1)			(0.6)	

All listed coefficients significantly different from zero at $p < 0.05$.
[a]Binary variable: 1 = at least one cigarette smoked in home during monitoring period.
[b]This variable was interchanged with the smoking variable in alternate regressions to avoid colinearity problems.
[c]Binary variable: 1 = cooking reported for at least one min in home during monitoring period.
[d]Volume in thousands of cubic feet.

Source: Özkaynak et al. (1996).

$$Q_{is} = (N_{cig}S_{cig} + T_{cook}S_{cook})/T + Q_{other} \tag{7-4}$$

where

T = duration of the monitoring period (h)
N_{cig} = number of cigarettes smoked during monitoring period
S_{cig} = mass of elements or particles generated per cigarette smoked (ng/cig or μg/cig)
T_{cook} = time spent cooking (min) during monitoring period
S_{cook} = mass of elements or particles generated per min of cooking (ng/min or μg/min)
Q_{other} = mass flux of elements or particles from all other indoor sources (ng/h or μg/h)

With these changes, the equation for the indoor concentration due to these indoor sources becomes

$$C_{in} = \frac{PaC_{out}}{a+k} + \frac{N_{cig}S_{cig} + T_{cook}S_{cook}}{(a + k)V\,T} + \frac{Q_{other}}{(a + k)V} \tag{7-5}$$

The indoor and outdoor concentrations, number of cigarettes smoked, monitoring duration, time spent cooking, house volumes, and air exchange rates were all measured or recorded. The penetration factor, decay rates, and source strengths for smoking, cooking, and all other indoor sources (Q_{other}) were estimated using a nonlinear model (NLIN in SAS software). The Gauss-Newton approximation technique was used to regress the residuals onto the partial derivatives of the model with respect to the unknown parameters until the estimates converge. On the first run, the penetration coefficients were allowed to "float" (no requirement was made that they be ≤ 1). Since nearly all coefficients came out close to 1, a second run was made bounding them from above by 1. The NLIN program provides statistical uncertainties (upper and lower 95% confidence intervals) for all parameter estimates. However, it should be noted that these uncertainties assume perfect measurements and are therefore underestimates of the true uncertainties.

Results are presented in Table 7-10 for the combined day and night samples. The penetration factors were very close to unity for nearly all particles and elements. The calculated average decay rate (lower and upper 95% confidence levels) for $PM_{2.5}$ was 0.39 (0.22; 0.55) h^{-1}, and for PM_{10} was 0.65 (0.36; 0.93) h^{-1}. Since PM_{10} contains the $PM_{2.5}$ fraction, a separate calculation was made for the coarse particles ($PM_{10} - PM_{2.5}$) with a resulting decay rate of 1.01 (0.6; 1.4) h^{-1}. Each cigarette emitted 22 (14; 30) mg of PM_{10} on average, about two-thirds of which 14 (10; 17) mg is in the fine fraction. Cooking emitted 4.1 (2.6; 5.7) mg/min of inhalable particles, of which about 40% or 1.7 (1.0; 2.3) mg/min, was in the fine fraction. All target elements emitted by cooking were limited almost completely to the coarse fraction. Sources other than cooking and smoking emitted about 5.6 (2.6; 8.7) mg/h of PM_{10}, of which only about 1.1 mg/h (0.0; 2.1) (20%) was in the fine fraction.

Decay rates for elements associated with the fine fraction were generally lower than for elements associated with the coarse fraction, as would be expected. For example, sulfur,

TABLE 7-10. PENETRATION FACTORS, DECAY RATES, AND SOURCE STRENGTHS: NONLINEAR ESTIMATES

	Penetration			Decay Rate (1/h)			S_cook (μg/min)			S_smoke (μg/cig)			Other Sources (μg/h)		
VAR	Mean	l95	u95	Mean	l95[b]	u95	Mean	l95[b]	u95	Mean	l95[b]	u95	Mean	l95[b]	u95
$PM_{2.5}$[a]	1.00	0.89	1.11	0.39	0.22	0.55	1.7	1.0	2.3	13.8	10.2	17.3	1.1	0.0	2.1
Al	1.00	0.95	1.05	0.03	−0.03	0.09	0.9	−1.4	3.1	9.0	−2.5	20.5	3.0	−3.7	9.8
Mn	0.87	0.78	0.95	0.23	0.07	0.38	0.1	−0.1	0.2	0.2	−0.4	0.8	0.5	0.2	0.9
Br	0.90	0.81	0.99	0.28	0.15	0.41	0.1	0.0	0.2	1.9	1.3	2.5	0.6	0.3	0.9
Pb			Fail to converge												
Ti			Fail to converge												
Cu	1.00	0.56	1.44	1.63	0.38	2.88	0.6	0.0	1.2	3.7	0.2	7.2	3.8	1.4	6.3
Sr	0.97	0.93	1.01	0.07	0.01	0.12	0.0	0.0	0.0	0.1	−0.1	0.2	0.1	0.0	0.2
Si	0.98	0.75	1.20	0.54	0.04	1.05	6.1	−8.6	20.9	14.4	−58.3	87.2	57.3	12.5	102.0
Ca	1.00	0.65	1.35	0.61	−0.02	1.25	11.9	−0.6	24.4	165.6	72.0	259.1	34.1	3.4	64.8
Fe	1.00	0.76	1.24	0.70	0.11	1.29	4.5	−3.3	12.3	23.8	−16.3	63.9	23.8	1.8	45.7
K	1.00	0.81	1.19	0.16	−0.04	0.37	0.0	−4.4	4.4	121.3	85.7	156.9	8.9	−0.5	18.3
S	1.00	0.97	1.03	0.16	0.12	0.19	1.0	−3.9	5.9	27.1	2.4	51.7	4.0	−3.7	11.7
Zn	0.71	0.57	0.86	0.78	0.31	1.25	0.4	−0.5	1.2	2.9	−1.5	7.4	7.5	4.2	10.9
Cl	0.50	0.28	0.72	0.64	0.05	1.24	5.9	0.1	11.6	102.6	54.0	151.2	20.6	7.2	34.0
PM_{10}[a]	1.00	0.85	1.15	0.65	0.36	0.93	4.1	2.6	5.7	21.9	13.6	30.2	5.6	2.6	8.7
Al	1.00	0.80	1.20	0.80	0.38	1.21	69.5	16.6	122.4	97.6	−159.0	354.2	154.5	52.0	257.0
Mn	1.00	0.80	1.20	0.69	0.30	1.07	0.9	0.1	1.7	1.1	−2.7	4.9	1.2	−0.2	2.6
Br	1.00	0.90	1.10	0.21	0.11	0.32	0.1	0.0	0.3	1.8	1.2	2.5	0.4	0.1	0.6
Pb	1.00	0.89	1.11	0.14	0.01	0.26	0.0	−0.3	0.3	2.1	0.4	3.9	0.0	−0.6	0.6
Ti	1.00	0.80	1.20	0.60	0.22	0.98	4.0	0.3	7.8	10.0	−8.4	28.4	10.3	2.6	18.1
Cu	0.83	0.62	1.05	0.77	0.18	1.36	0.5	0.0	1.1	3.5	0.4	6.5	3.2	1.3	5.1
Sr	1.00	0.83	1.16	0.62	0.28	0.97	0.3	0.0	0.5	2.6	1.2	3.9	0.9	0.3	1.5
Si	1.00	0.81	1.19	0.62	0.26	0.97	149.3	26.9	271.8	296.4	−293.9	886.6	237.8	16.1	459.6
Ca	1.00	0.68	1.32	0.63	0.06	1.20	118.7	37.3	200.1	800.0	329.0	1271.0	107.6	−27.0	242.3
Fe	1.00	0.80	1.20	0.66	0.26	1.06	46.7	8.5	84.8	73.0	−109.8	255.9	51.5	−15.5	118.5
K	1.00	0.83	1.17	0.46	0.17	0.75	17.6	0.1	35.2	215.7	116.9	314.5	43.6	8.6	78.5
S	1.00	0.96	1.04	0.21	0.17	0.26	6.8	−0.7	14.3	68.0	29.3	106.7	22.7	10.4	34.9
Zn	1.00	0.81	1.19	0.37	0.10	0.64	1.2	−0.2	2.5	4.0	−3.0	11.0	7.4	3.4	11.4
Cl	0.94	0.44	1.43	2.36	0.48	4.24	45.7	17.6	73.9	320.2	107.0	533.4	148.4	49.4	247.4

[a]Mass units in mg for $PM_{2.5}$ and PM_{10} only.
[b]A negative lower confidence interval implies a nonzero mean is not statistically significant.

Source: Özkaynak et al. (1993a).

which has the lowest mass median diameter of all the elements, had calculated decay rates of 0.16 (0.12; 0.19) h^{-1} and 0.21 (0.17; 0.26) h^{-1} for $PM_{2.5}$ and PM_{10} fractions, respectively. The crustal elements (Ca, Al, Mn, Fe) had decay rates ranging from 0.6 to 0.8 h^{-1}.

Based on the mass-balance model, outdoor air was the major source of indoor particles, providing about 3/4 of fine particles and 2/3 of thoracic particles in the average home. It was also the major source for most of the target elements, providing 70 to 100% of the observed indoor concentrations for 12 of the 15 elements. It should be noted that these conclusions are applicable only to Riverside, CA. In five of the six cities studied by Harvard and in both New York counties, outdoor air could not have provided as much as half of the indoor air particle mass for the average home, because the observed indoor-outdoor ratios of the mean concentrations were ≥ 2. However, for homes without smoking or combustion sources (Santanam et al., 1990; Leaderer et al., 1990; Table 7-5), indoor-outdoor ratios were ≈ 1. In general, homes in areas with colder winters (such as New York) would be expected to have tighter construction than homes in warmer areas (such as Riverside) and, therefore, more protection against outdoor air particles.

Unidentified indoor sources accounted for most of the remaining particle and elemental mass collected on the indoor monitors. The nature of these sources is not yet completely understood (Thatcher and Layton, 1995). They apparently do not include smoking, other combustion sources, cooking, dusting, vacuuming, spraying, or cleaning, since all these sources together account for less than the unidentified sources. For example, the unidentified sources accounted for 26% of the average indoor PM_{10} particles, whereas smoking accounted for 4% and cooking for 5% (Figure 7-10).

Of the identified indoor sources, the two most important were smoking and cooking (Figures 7-11 and 7-12). Smoking was estimated to increase 12-h average indoor concentrations of PM_{10} and $PM_{2.5}$ by 3.2 and 2.5 $\mu g/m^3$ per cigarette, respectively. Homes with smokers averaged about 30 $\mu g/m^3$ higher levels of PM_{10} than homes without smokers, most of this increase being in the fine fraction. Cooking increased indoor concentrations of PM_{10} by about 0.6 $\mu g/m^3$ per minute of cooking, most of the increase being in coarse particles.

Emission profiles for target elements were obtained for smoking and for cooking. Major elements emitted by cigarettes were K, Cl, and Ca; those from cooking included Al,

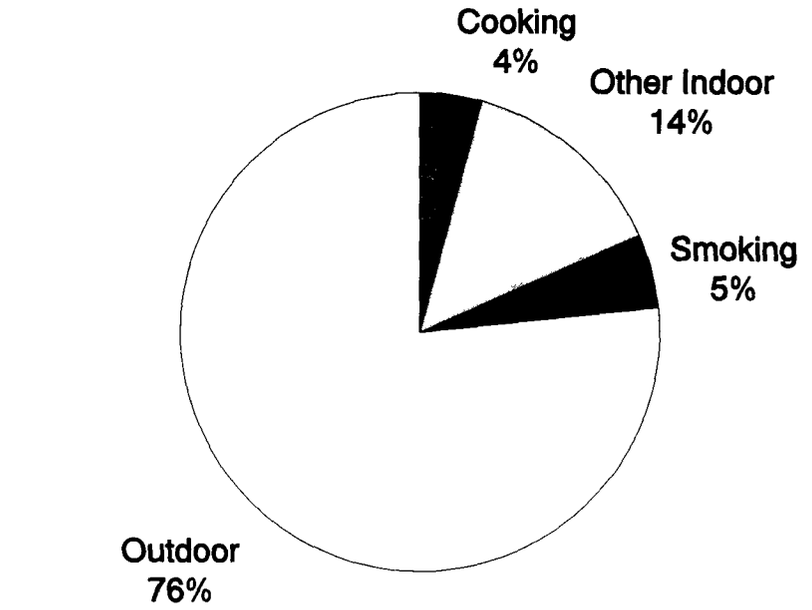

N = 352 Samples from 178 homes

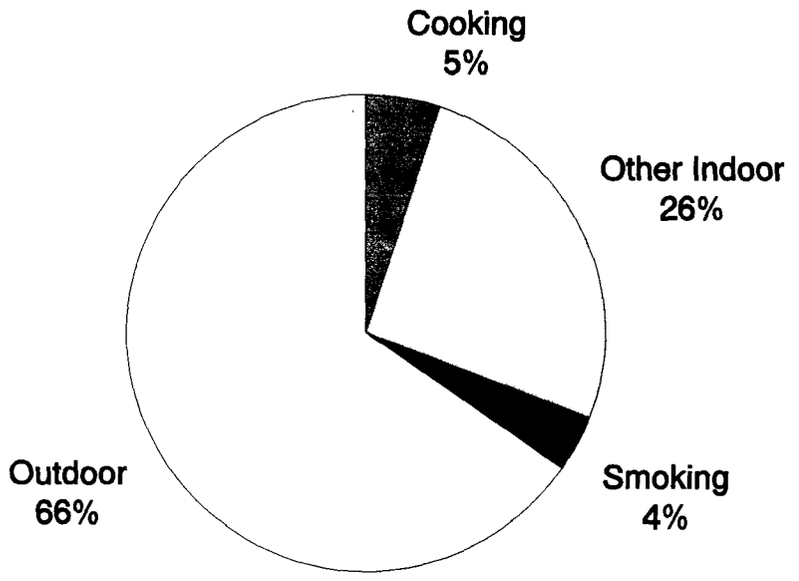

N = 350 Samples from 178 homes

Figure 7-10. Sources of fine particles ($PM_{2.5}$) (top) and thoracic particles (PM_{10}) (bottom) in all homes (Riverside, CA).

Source: Özkaynak et al. (1993a).

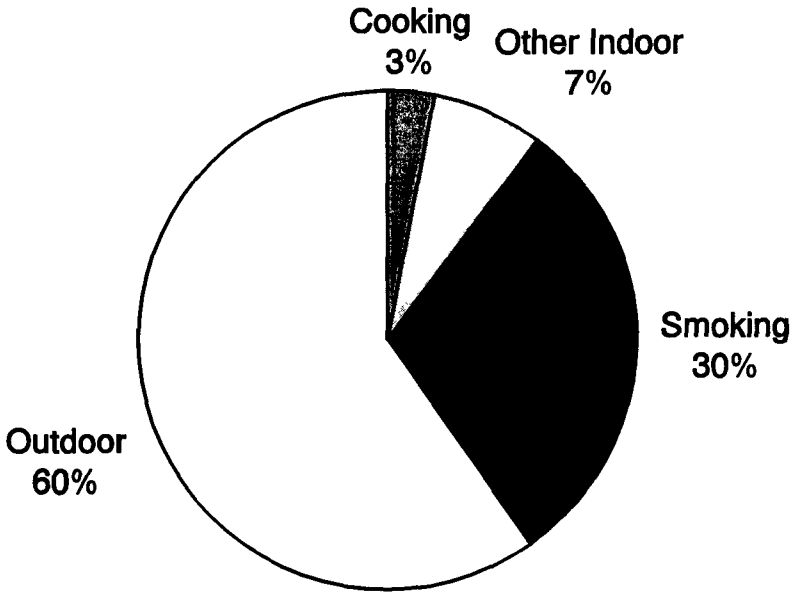

N = 61 Samples from 31 homes

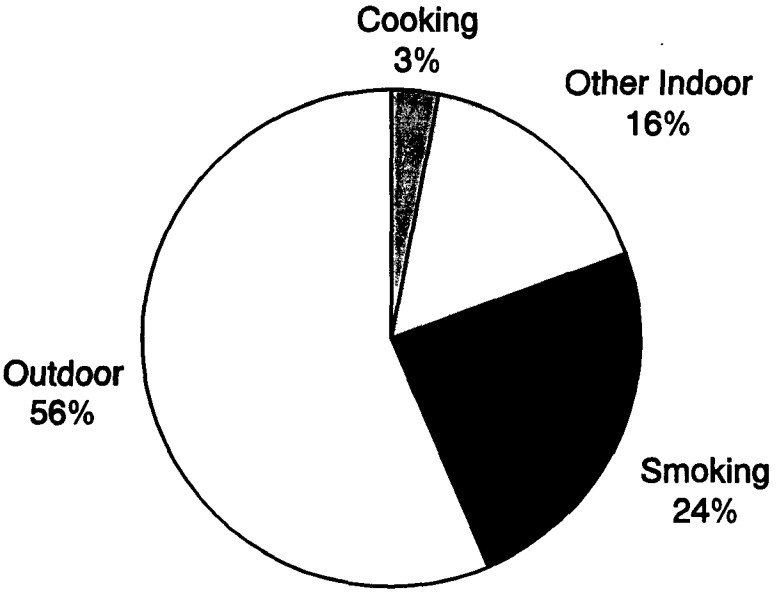

N = 61 Samples from 31 homes

Figure 7-11. Sources of fine particles ($PM_{2.5}$) (top) and thoracic particles (PM_{10}) (bottom) in homes with smokers (Riverside, CA).

Source: Özkaynak et al. (1993a).

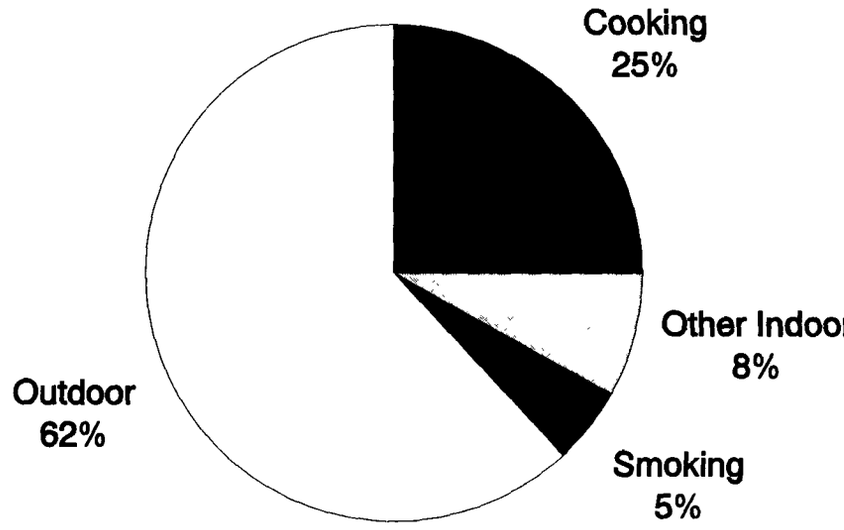

N = 62 Samples from 33 homes

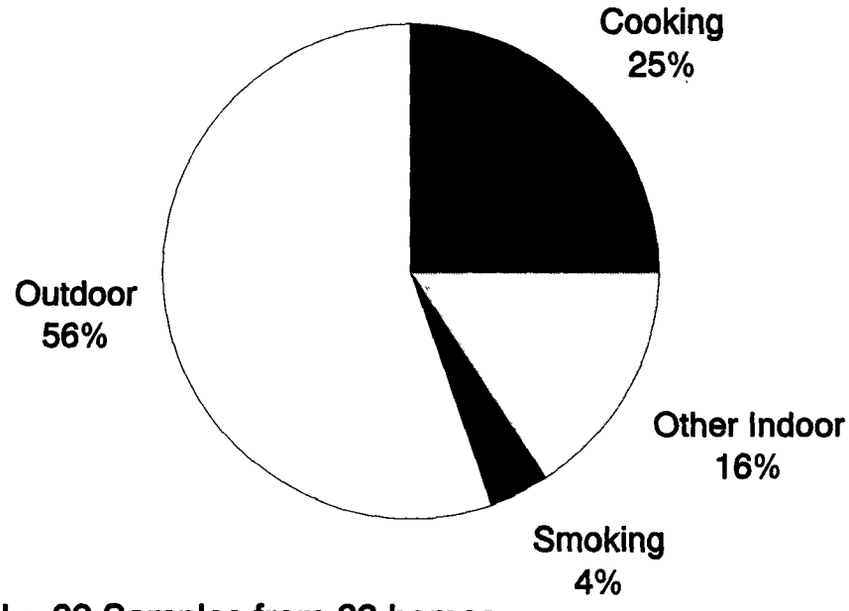

N = 62 Samples from 33 homes

Figure 7-12. Sources of fine particles ($PM_{2.5}$) and thoracic particles (PM_{10}), top and bottom panels, respectively, for homes with cooking during data collection (Riverside, CA).

Source: Özykaynak et al. (1993a).

Fe, Ca, and Cl. Other household activities such as vacuuming and dusting appeared to make smaller contributions to indoor particle levels. Commuting and working outside the home resulted in lower particle exposures than for persons staying at home. As with the particle mass, daytime personal exposures to 14 of 15 elements were consistently higher than either indoor or outdoor concentrations. At night, levels of the elements were similar in all three types of samples.

7.2.2.1.4 Comparison of the Three Large-Scale Studies

The three studies had somewhat different aims and therefore different study designs. The Harvard Six-City study selected homes based on various criteria, especially a requirement that a school-age child be in the home, but did not employ a probability-based sample. Therefore the results strictly apply only to the homes in the sample and not to a wider population; however, the very large number of homes suggests that the results should be broadly applicable to homes with school-age children in the six cities. The New York State study used a probability-based sample, but stratified on the basis of combustion sources. Hence, there are likely to be a higher fraction of homes with kerosene heaters, wood stoves, and fireplaces in the sample than in the general population. The PTEAM study used a fully probability-based procedure, and its results are likely the most broadly applicable to the entire population of Riverside households. However, the participants were limited to nonsmokers, so homes with only smokers were excluded; as a consequence, maximum indoor concentrations were likely underestimated. Also, the three studies used different monitors, with different cutpoints precluding exact comparisons. However, large differences between the $PM_{3.5}$ and $PM_{2.5}$ cutpoints and the PM_{11} and PM_{10} cutpoints are not likely (Willeke and Baron, 1993); thus, these results can be more readily compared. In what follows, the term "fine particles" refers to the $PM_{3.5}$ and $PM_{2.5}$ size fractions collected in the three studies.

Indoor-Outdoor Relationships. Outdoor concentrations of fine particles in five of the Harvard six cities and the two New York counties were relatively low, typically in the range of 10 to 20 $\mu g/m^3$ (Table 7-11). Only Steubenville, with an annual mean of 45 $\mu g/m^3$ (but a range among the outdoor sites of 20 to 60 $\mu g/m^3$) approached the mean outdoor level of 50 $\mu g/m^3$ observed in Riverside. It is interesting to note that average indoor concentrations

TABLE 7-11. INDOOR-OUTDOOR MEAN CONCENTRATIONS ($\mu g/m^3$) OF FINE PARTICLES IN THREE LARGE-SCALE STUDIES

Study Name	Homes	Out	In	In/Out
Harvard Six-City Study				
Portage, WI	11	10	20	2.0
Topeka, KS	10	10	22	2.2
Kingston-Harriman, TN	8	18	44	2.4
Watertown, MA	8	15	29	1.9
St. Louis, MO	10	18	42	2.3
Steubenville, OH	8	45	42	0.9
New York State ERDA Study				
Onondaga County	224	17	37	2.2
Suffolk County	209	22	46	2.1
EPA Particle TEAM Study				
Riverside, CA	178	50	43	0.9

Harvard: $PM_{3.5}$ measured using cyclone sampler. Samples collected every sixth day for one year (May 1986 to April 1987).

NYS: $PM_{2.5}$ measured using impactor developed at Harvard. Samples collected for one week at each household between January and April 1986.

PTEAM: $PM_{2.5}$ measured using Marple-Harvard-EPA sampler. Samples collected for two 12-h periods at each home between September and November 1990.

Source: Harvard data—Spengler et al. (1981); NYS data—Sheldon et al. (1989); PTEAM data—Pellizzari et al. (1992).

exceeded outdoor concentrations in the seven sites with low outdoor levels, (indoor/outdoor ratios were contained in a small range between 1.9 and 2.4), but were slightly less than outdoor concentrations in the two sites with high outdoor levels (ratios of 0.9).

Effect of Smoking. All three studies found cigarette smoking to be a major source of indoor fine particles. Multivariate calculations in all three studies result in rather similar estimates of the effect of smoking on fine particle concentrations. Spengler et al. (1981) estimated an increase of about 20 $\mu g/m^3$ per smoker based on 55 homes from all six cities. Since the 20 homes with at least one smoker averaged at least 1.25 smokers per home, this corresponds to about 25 $\mu g/m^3$ per smoking home. Spengler et al. (1985) found a smoking effect of about 32 $\mu g/m^3$ for smoking homes in multivariate models based on the Kingston-Harriman data. Santanam et al. (1990) found a smoking-related increase of 20-27 $\mu g/m^3$ in Steubenville and Portage (winter only) but only 10 $\mu g/m^3$ in Portage in summer. Sheldon et al. (1989) found an increase of 45 (Onondaga) and 47 (Suffolk) $\mu g/m^3$ per smoking home in a multivariate model of the New York State data. Özkaynak et al. (1993b) found an

increase of about 27 to 32 $\mu g/m^3$ in homes with smokers in a multivariate regression model of the PTEAM $PM_{2.5}$ data. Thus, the effect of a home with smokers on indoor fine particle concentrations was estimated to be about 20 to 30 $\mu g/m^3$ in the Six-City and PTEAM studies, but about 45 $\mu g/m^3$ in the New York State study.

Dockery and Spengler (1981a) found an effect of 0.88 $\mu g/m^3$ per cigarette for homes without air conditioning, and 1.23 $\mu g/m^3$ per cigarette for homes with air conditioning, based on 68 homes from all six cities. Lebret et al. (1987) found an effect of 0.8 $\mu g/m^3$ per cigarette for homes in the Watertown, MA, area. Leaderer and Hammond (1991) found an effect ranging between 1.9 and 2.3 $\mu g/m^3$ per cigarette contribution to a 24-h average. In a series of stepwise regressions on the PTEAM data, Özkaynak et al. (1993b) found an effect ranging between 1.2 and 2.4 $\mu g/m^3$ per cigarette smoked during a 24-h period. Taking the midpoint of these ranges leads to estimates for the Harvard Six-City, New York State and PTEAM studies of about 1.1, 2.1, and 1.8 $\mu g/m^3$ increases in fine particle concentrations per cigarette smoked in the home over a 24-h period.

Both the New York State study and the PTEAM study were able to estimate source strengths for different variables using a mass-balance model. The estimates for $PM_{2.5}$ emissions from cigarettes were very comparable, with Koutrakis et al. (1992) estimating 12.7 mg/cig compared to the PTEAM estimate of 13.8 mg/cig (Özkaynak et al., 1993a). Both studies also found similar elemental profiles for smoking, with potassium and chlorine being emitted in substantial amounts.

Effect of Other Variables. In the PTEAM Study, the second most powerful indoor source of PM_{10}, and possibly $PM_{2.5}$ particles, was cooking. Quite large emission strengths of several mg/minute of cooking were determined from the mass-balance model, while multiple regressions indicated that cooking could contribute between 10 and 20 $\mu g/m^3$ PM_{10}, and somewhat smaller amounts of $PM_{2.5}$, to the 12-h concentration.

Both the New York State and PTEAM studies also measured air exchange in every home, and both studies found that air exchange significantly affected indoor particle concentrations. In the PTEAM study, increased air exchange led to increased indoor air concentrations for both $PM_{2.5}$ and PM_{10} at night only, perhaps because outdoor concentrations were larger than indoor levels at night. In the New York State study, increased air exchange led to decreased RSP concentrations in Onondaga ($p < 0.02$) but no

effect was noted in Suffolk ($p < 0.90$). In both of these counties, indoor levels generally exceeded outdoor levels, so increased air exchange would generally reduce indoor concentrations.

7.2.2.2 Other Studies of PM Indoors

Several other large-scale studies of indoor PM in homes have taken place in other countries, and a number of smaller U.S. studies have been conducted. These are discussed below in order of the number of homes included in the study.

Lebret et al. (1990) carried out week-long RSP measurements (cutpoint not described) in 260 homes in Ede and Rotterdam, The Netherlands, during the winters of 1981 to 1982 and 1982 to 1983, respectively; 60% of the Ede homes and 66% of the Rotterdam homes included smokers. Diary information collected during the measurement period indicated that, on average, one to two cigarettes were smoked during the week, presumably by guests, even in the nonsmoking homes. Homes with one smoker averaged seven cigarettes smoked per day at home in Ede (N = 53) and 11 per day in Rotterdam (N = 35). Homes with two smokers averaged 21 cigarettes per day in Ede (N = 23) and 25 per day in Rotterdam (N = 15).

Geometric means for the combined smoking and nonsmoking homes were similar in the two cities (61 and 56 $\mu g/m^3$, respectively), with maxima of 560 and 362 $\mu g/m^3$. Outdoor concentrations averaged about 45 $\mu g/m^3$ (N not given). Indoor concentrations in the homes with smokers averaged about 70 $\mu g/m^3$ (calculated from data in the paper), compared to levels in the nonsmoking homes of about 30 $\mu g/m^3$. Multiple regression analysis indicated that the number of smoking occupants explained about 40% of the variation in the log-transformed RSP concentrations—family size, frequency of vacuuming, volume of the living room, type of space heating, and city (Ede versus Rotterdam) had no significant effect on RSP concentrations. In a second regression, the number of smoking occupants was replaced by the number of cigarettes and cigars smoked during the week. The regression equation was

$$\log(RSP) = 1.4 + 0.37 \log(\#\text{ cigarettes}) + 0.53 \log(\#\text{ cigars}) + 0.03 \log(\text{family size})$$

$$R^2 = 0.49;\ \text{d.f.} = 250 \quad F = 83.7 \quad p < 0.0001$$

From this equation, the authors estimated that one cigarette smoked per day would increase weekly average indoor RSP concentrations by 2 to 5 $\mu g/m^3$, whereas one cigar smoked per day would increase indoor levels by 10 $\mu g/m^3$. Instantaneous RSP concentrations were measured using a TSI Piezobalance on the day the technicians were setting up the equipment. Table 7-12 shows the influence of smoking on these measurements.

TABLE 7-12. INFLUENCE OF RECENT CIGARETTE SMOKING ON INDOOR CONCENTRATIONS OF PARTICULATE MATTER[1]

Time Since Smoking	N	RSP (geom. mean) ($\mu g/m^3$)
No smoking	98	41
More than 1 h ago	18	52
Between 1/2 and 1 h ago	7	76
Less than 1/2 an hour ago	27	141
During the measurements	54	191

[1]Size cuts for measured particles not specified.

Source: Lebret et al. (1990).

Heavner et al. (1995) studied $PM_{3.5}$ at home and at work for 104 New Jersey and Pennsylvania females. The personal sampler used consisted of a cyclone sampling head attached to a 37-mm Fluoropore filter, connected by Tygon tubing to a 1.7 Lpm pump. The sampling head was worn on a lapel, collar, or pocket in the breathing zone of the participant until she went to bed, when the sampler was placed on the bedside table. The "home" pumps were turned on at 6 p.m. and sampled until about 8 a.m. the next morning (an average of 14 h); the "work" pumps were turned on at work and sampled for an average of 7 h. Participants were selected to include those with exposure to smoking at home or at work or both or neither. The 14-h evening and overnight concentrations in the homes averaged 86.7 $\pm$ 145.4 (SD) $\mu g/m^3$ for 30 homes with smokers and 27.6 $\pm$ 19.9 $\mu g/m^3$ for 58 homes without smokers. Corresponding values for workplaces were 67.0 $\pm$ 44.3 $\mu g/m^3$ for those 28 allowing smoking and 30.3 $\pm$ 17.6 $\mu g/m^3$ for the 52 without smoking, the differences being significant at $p < 0.0001$ (Wilcoxon rank sum) for both comparisons.

Diemel et al. (1981) measured particles in 101 residences in an epidemiological study related to a lead smelter in Arnhem, the Netherlands. The indoor sampler collected samples at a flowrate of 1 to 1.5 Lpm. The authors stated that particles $\leq$ 3 to 4 μm diameter should have been sampled efficiently, but presented no data on measured cutpoint size. The outdoor samplers (number not given) were high-volume samplers. The 28-day average levels indoors ranged from 20 to 570 $\mu g/m^3$, with an arithmetic mean of 140 $\mu g/m^3$ (SD not presented) and a geometric mean of 120 $\mu g/m^3$; corresponding outdoor concentrations (2-mo averages of 24-h daily samples) ranged from 53.7 to 73.3 $\mu g/m^3$ (N not given), with nearly identical arithmetic and geometric means of 64 $\mu g/m^3$.

Kulmala et al. (1987) measured indoor and outdoor air in approximately 100 dwellings (including some office buildings) in Helsinki, Finland between 1983 and 1986. Samples were collected on Nuclepore filters using a stacked foil technique. The geometric mean for the combined fine particle (<1 μm) samples indoors was 16 $\mu g/m^3$, with a 95% range of 4 to 67 $\mu g/m^3$. The corresponding value for the indoor coarser particles (>1 μm) was 13 $\mu g/m^3$ with a range of 3 to 63 $\mu g/m^3$. Outdoors, the fine particles had a geometric mean of 20 $\mu g/m^3$ with a 95% range of 5 to 82 $\mu g/m^3$, and the coarser particles had a geometric mean of 16 $\mu g/m^3$ with a range of 3 to 91 $\mu g/m^3$.

Quackenboss et al. (1989) reported PM_{10} and $PM_{2.5}$ results from 98 homes in the Tucson, AZ area selected as part of a nested design for an epidemiological study. The Harvard-designed dual-nozzle indoor air sampler (Marple et al., 1987) was used for indoor air measurements. Outdoor air was measured within each geographic cluster by the same instrument; supplementary data were obtained from the Pima County Air Quality Control District, but these data did not include $PM_{2.5}$ measurements and some data were apparently PM_{15}. Homes were classified by (a) tobacco smoking and (b) use of evaporative ("swamp") coolers, which apparently act as a removal mechanism for particles (Table 7-13). Homes without smoking averaged about 15 $\mu g/m^3$ $PM_{2.5}$, compared to 27 $\mu g/m^3$ for homes reporting one or less pack a day, and 61 $\mu g/m^3$ for homes reporting more than one pack a day. $PM_{2.5}$ particles accounted for about half of the PM_{10} fraction in nonsmoking homes, increasing with the amount of smoking to about 80% in those homes with heavy smoking. Outdoor PM_{10} particles were not strongly correlated with indoor levels ($R^2 = 0.18$; $N \approx 90$).

TABLE 7-13. INDOOR AVERAGE $PM_{2.5}$ AND PM_{10} ($\mu g/m^3$) BY REPORTED SMOKING IN THE HOME AND EVAPORATIVE COOLER USE DURING SAMPLING WEEK FOR TUCSON, AZ STUDY

Smoking Cigarettes/Day	Evaporative Cooler	$PM_{2.5}$ Mean	$PM_{2.5}$ S.D.	$PM_{2.5}$ Homes	PM_{10} Mean	PM_{10} S.D.	PM_{10} Homes
None	Yes	8.8	5.0	(20)	21.0	9.7	(20)
	No	20.3	19.0	(25)	38.4	22.9	(23)
	Total	15.2	15.5	(45)	30.3	19.9	(43)
1-20	Yes	19.3	8.8	(10)	33.9	12.0	(10)
	No	32.3	28.5	(16)	53.4	33.9	(17)
	Total	27.3	23.6	(26)	46.2	29.1	(27)
>20	Yes	36.2	32.9	(8)	47.4	39.6	(9)
	No	82.7	55.4	(9)	102.5	60.6	(9)
	Total	60.8	50.8	(17)	75.0	57.2	(18)

$PM_{2.5}$: Significant ($p < 0.01$) main effects for smoking and evaporative cooler use; two-way interaction nearly significant ($p = 0.06$).
PM_{10}: Significant ($p < 0.01$) main effects for evaporative cooler and smoking.

Source: Quackenboss et al. (1989).

Quackenboss et al. (1991) extended the analysis of the Tucson homes over three seasons. Median indoor $PM_{2.5}$ levels in homes with smokers were about 20 $\mu g/m^3$ in the summer and spring/fall seasons compared to about 10 $\mu g/m^3$ in homes without smokers in those seasons. In winter, however, the difference was considerably increased, with the median level in 24 homes with smokers at about 36 $\mu g/m^3$ compared to 13 $\mu g/m^3$ in 26 homes without smokers.

Sexton et al. (1984) reported on a study in Waterbury, VT. This study included 24 homes, 19 with wood-burning appliances, and none with smokers. 24-h samples were collected in each home every other day for two weeks, providing 163 valid indoor samples. Indoor RSP levels ranged from 6 to 69 $\mu g/m^3$ with a mean value of 25 $\mu g/m^3$. Outdoor levels ranged from 6 to 30 $\mu g/m^3$ with a mean value of 19 $\mu g/m^3$. Indoor concentrations were not significantly correlated with outdoor concentrations ($r = 0.11$, $p > 0.16$.)

Kim and Stock (1986) reported results for 11 homes in the Houston, TX area. (Year and the season not reported in the paper.) For most homes, two 12-h $PM_{2.5}$ samples (day and night) were collected for approximately one week. Sampling methods were not fully discussed, but apparently they involved samples collected using a mobile van near each home. The mean weekly concentrations in the five smoking homes averaged 33.0 ± 4.7 (SD) $\mu g/m^3$, versus mean outdoor concentrations averaging 24.7 ± 7.4 $\mu g/m^3$

(calculated from data presented in paper). Indoor concentrations in the six nonsmoking homes averaged 10.8 ± 4.9 $\mu g/m^3$ compared to outdoor levels of 12.0 ± 5.9 $\mu g/m^3$.

Morandi et al. (1986) reported on 13 Houston, TX, homes monitored during 1981 as part of a larger personal monitoring study of 30 nonsmoking participants. The TSI Piezobalance (cutpoint at about $PM_{3.5}$) was employed for personal monitoring, with technicians "shadowing" the participants and taking consecutive 5-min readings. At the homes, dichotomous samplers (cutpoints at $PM_{2.5}$ and PM_{10}) were used for two 12-h daytime samples (7 a.m. to 7 p.m.) both inside and outside the homes for seven consecutive days. Little difference was noted in the indoor concentrations at homes (25 ± 30 (SD) $\mu g/m^3$) and at work or school (29 ± 25 $\mu g/m^3$). The highest overall respirable suspended particle (RSP) concentrations occurred in the presence of active smoking (89 $\mu g/m^3$), significantly different from mean RSP values measured in the absence of smokers (19 $\mu g/m^3$; $p < 0.0001$). Among homes with smokers, those homes with central air conditioning were significantly ($p<0.0001$) higher (114 versus 52 $\mu g/m^3$) than those with no air conditioning. Cooking was associated with significantly higher RSP concentrations (27 $\mu g/m^3$ compared to 20 $\mu g/m^3$, $p < 0.01$). The single highest RSP concentration (202 $\mu g/m^3$) was found in a home with no smokers and no air conditioning but with active cooking. The authors concluded that cooking was a more important source of indoor RSP than smoking, at least in the few homes they studied.

Coultas et al. (1990) measured $PM_{2.5}$ in 10 homes containing at least one smoker, using the Harvard aerosol impactor. Samples were collected for 24 h every other day for 10 days and then for 24 h every other week for 10 weeks, resulting in 10 samples per household. The mean concentrations of $PM_{2.5}$ ranged from 32.4 ± 13.1 (SD) to 76.9 ± 32.9 $\mu g/m^3$. Outdoor particle concentrations were not reported; thus it is difficult to calculate the portion of the observed $PM_{2.5}$ that might be due to ETS.

Kamens et al. (1991) measured indoor particles in three homes without smokers in North Carolina in November and December 1987 (no measurements of outdoor particles were taken). Two dichotomous samplers ($PM_{2.5}$ and PM_{10}), several prototype personal samplers (also $PM_{2.5}$ and PM_{10}), three particle sizing instruments including a TSI electrical aerosol mobility analyzer (EAA) with 10 size intervals between 0.01 and 1.0 μm, and two optical scattering devices covering the range of 0.09 to 3.0 and 2.6 to 19.4 μm were

employed. Air exchange measurements were made using SF_6 decay over the course of the seven 8-h (daytime) sampling periods. There were also three 13-h (evening and overnight) sampling periods. For the entire study, 37% of the estimated total mass collected was in the fine fraction, and another 37% was > 10 μm. The remainder (26%) was in the inhalable coarse ($PM_{10} - PM_{2.5}$) fraction. However, considerable variation was noted in these size distributions. For example, on one day with extensive vacuuming, cooking, and vigorous exercising of household pets, 52% of the total mass appeared in the fraction >10 μm, but only 18% in the fine fraction. The peak in particle mass on that day coincided with vacuuming and sweeping of carpets and floors. On another day, cooking of stir-fried vegetables and rice produced a large number of small particles, with those <0.1 μm accounting for 30% of the total EAA particle volume, much more than the normal amount. The cooking contribution of that one meal to total 8-h daytime particle volume exposure was calculated to be in the range of 5 to 18%. The authors concluded that the most significant indoor source of small particles (<2.5 μm) in all three of these nonsmoking homes was cooking, while the most significant source of large particles (>10 μm) was vacuum sweeping. Inhalable coarse particles ($PM_{10} - PM_{2.5}$) appeared to be of largely biological (human dander and insect parts) and mineral (clay, salt, chalk, etc.) origin.

In a test of a new sampling device (a portable nephelometer), Anuszewski et al. (1992) reported results from indoor and outdoor sampling at nine Seattle, WA, homes sampled for an average of 18 days each during the winter of 1991 to 1992. The nephelometer is a light-scattering device with rapid (1-min) response to various household activities such as sweeping, cigarette smoking, frying, barbecuing, and operating a fireplace. Homes with fewer activities showed high correlations of indoor and outdoor light-scattering coefficients, both between hourly averages and 12-h averages. However, homes with electrostatic precipitators, with weather-stripped windows or doors, and with gas cooking or heating devices showed weak 12-h indoor-outdoor correlations.

Chan et al. (1995) studied particles and nicotine in seven homes with one smoker each in Taiwan. Sampling was carried out in summer and winter of 1991. Each home had one indoor PM_5 sampler in the living room and another in the yard. In the winter study, two homes had PM_{10} samplers added inside and outside and at two central sites. Indoor mean

PM_5 concentrations averaged 44 ± 32 (SD) $\mu g/m^3$ in summer compared to outdoor levels of 27 ± 15 $\mu g/m^3$. Corresponding winter values were 107 ± 44 $\mu g/m^3$ and 92 ± 40 $\mu g/m^3$.

Daisey et al. (1987) measured RSP, PAH, and extractable organic matter (EOM) in seven Wisconsin homes with wood stoves; one 48h (1,000 m^3) sample was collected during woodburning and a second sample was collected when no woodburning occurred. Five of seven homes had somewhat higher RSP levels during woodburning, but the mean difference was not significant.

Highsmith et al. (1991) reported on two 20-home studies in Boise, ID and Roanoke, VA. The Boise study assessed the effects of wood burning on ambient and indoor concentrations in the area. Ten homes with wood burning stoves were matched with 10 homes without such stoves. One matched pair of homes was monitored from Saturday through Tuesday for eight consecutive 12-h periods. Ambient $PM_{2.5}$ levels increased by about 50% at night, suggesting an influence of woodburning. Indoor $PM_{2.5}$ concentrations also were increased (by about 45%) in the homes with the wood burning stoves compared to those without (26.3 versus 18.2 $\mu g/m^3$), although coarse particles showed no increase (10.2 versus 9.7 $\mu g/m^3$). The Roanoke study, designed to assess the effects of residential oil heating, showed no effects on indoor levels of fine or coarse particles.

Löfroth et al. (1991) measured particle emissions from cigarettes, incense sticks, "mosquito coils," and frying of various foods. Emissions were 27 and 37 mg/g for two brands of Swedish cigarettes, 51 and 52 mg/g for incense sticks and cones, and 61 mg/g for the mosquito coil. Emissions from frying pork, hamburgers, herring, pudding, and Swedish pancakes ranged from 0.07 to 3.5 mg/g.

Mumford et al. (1991) measured PM_{10}, PAH, and mutagenicity in eight mobile homes with kerosene heaters. Each home was monitored for 2.6 to 9.5 h/day (mean of 6.5 h) for three days a week for two weeks with the kerosene heaters off and for two weeks with them on (average on-time of 4.5 h). Mean PM_{10} levels were not significantly increased when the heaters were on (73.7 ± 7.3 (SE) $\mu g/m^3$ versus 56.1 ± 5.7 $\mu g/m^3$), but in two homes levels increased to 112 and 113 $\mu g/m^3$ when the heaters were on. Outdoor concentrations averaged 18.0 ± 2.1 $\mu g/m^3$.

Colome et al. (1990) measured particles using PM_{10} and PM_5 (cyclone) samplers inside and outside homes of 10 nonsmokers, including eight asthmatics, living in Orange County,

CA. Indoor PM_{10} samples were well below outdoor levels for all homes (mean of 42.5 ± 3.7 (SE) $\mu g/m^3$ indoors versus 60.8 ± 4.7 $\mu g/m^3$ outdoors). No pets, wood stoves, fireplaces, or kerosene heaters were present in any of these homes.

Lioy et al. (1990) measured PM_{10} at eight homes (no smokers) for 14 days in the winter of 1988 in Phillipsburg, NJ, which has a major point source consisting of a grey-iron pipe manufacturing company. The Harvard impactor was used indoors to collect 14 24-h samples beginning at 4:30 p.m. each day; Wedding hi-vol PM_{10} samples were deployed at three outdoor sites. A fourth outdoor site was located on a porch of one of the homes, directly across the street from the pipe manufacturer. The first three sites showed little difference from one another, whereas on day 4 and day 6 of the study, the outdoor sampler on the porch had readings that were considerably (about 40 $\mu g/m^3$) higher than the other outdoor samplers, suggesting an influence of the nearby point source. The geometric mean outdoor PM_{10} concentration was 48 $\mu g/m^3$ (GSD not provided) compared to 42 $\mu g/m^3$ indoors. A simple regression equation for all homes (N = 101 samples) explained 45% of the cross-sectional variance in indoor PM_{10}:

$$\text{Indoor } PM_{10} = 0.496 \text{ Outdoor } PM_{10} + 21.5 \qquad (R^2 = 0.45)$$

However, individual regressions by home showed much better R^2 values in most cases, ranging from 0.36 to 0.96 (Table 7-14). All slopes were significant.

Thatcher and Layton (1995) measured optical particle size distributions inside and outside a residence in the summer. Measured deposition velocities for particles between 1 and 5 μm closely matched the calculated gravitational settling velocities; however, for particles >5 μm, the deposition velocity was less than the calculated settling velocity, perhaps due to the non-spherical nature of these particles. The deposition velocities determined by the authors corresponded to a particle deposition rate k of 0.46 h^{-1} for particles of size range 1 to 5 μm and 1.36 h^{-1} for particles of size range 5 to 10 μm. These values are very comparable with the values of 0.39 h^{-1} for particles less than 2.5 μm and 1.01 h^{-1} for particles between 2.5 and 10 μm found by the PTEAM Study. The authors measured the penetration factor P by the following method: They first carried out vigorous house cleaning activities to raise the level of resuspended dust well above outdoor levels.

TABLE 7-14. REGRESSION OF INDOOR ON OUTDOOR PM_{10} CONCENTRATIONS: THEES STUDY, PHILLIPSBURG, NJ ($\mu g/m^3$)

House	N	Intercept	SE	p	Slope	SE	p	R^2
1	14	19	9	NS	0.44	0.06	S	0.79
2	14	16	14	NS	0.40	0.08	S	0.68
3	9	9	5	NS	0.55	0.04	S	0.96
4	14	20	21	NS	0.73	0.15	S	0.66
5	13	6	10	NS	0.43	0.07	S	0.75
6	13	−1	18	NS	0.89	0.13	S	0.81
7	12	24	25	NS	0.70	0.29	S	0.36
8	14	27	8	S	0.54	0.05	S	0.91

S = Significant
NS = Non-significant

Source: Data from THEES Study (Lioy et al., 1990).

They then left the house, while automated instruments measured the deposition rate k for the different particle sizes and the air exchange rate a for SF_6 tracer gas. With these values of a and k in hand, they solved the equation for P, using the steady-state values for C_{in} and C_{out} observed long after the dust had settled:

$$P = \frac{C_{in}\ (a+k)}{C_{out}\ a} \tag{7-6}$$

For all size ranges tested, including the largest (10 to 25 μm), the experimentally determined value for P was not significantly different from 1 (Figure 7-13). This result is in agreement with the PTEAM conclusion that P is 1 for both fine and coarse particles, although the latter conclusion was derived from a nonlinear (statistical) approach whereas the present result was experimentally obtained.

The resuspension results of Thatcher and Layton (1995) (Figure 7-14) show the effect of a vigorous housecleaning activity. The authors concluded "Although particles larger than 5 μm show significant resuspension in these experiments, particles smaller than 5 μm are not readily resuspended, and particles less than 1 μm show almost no resuspension even with vigorous activity." Figure 7-15 shows that just one person walking in and out of a carpeted

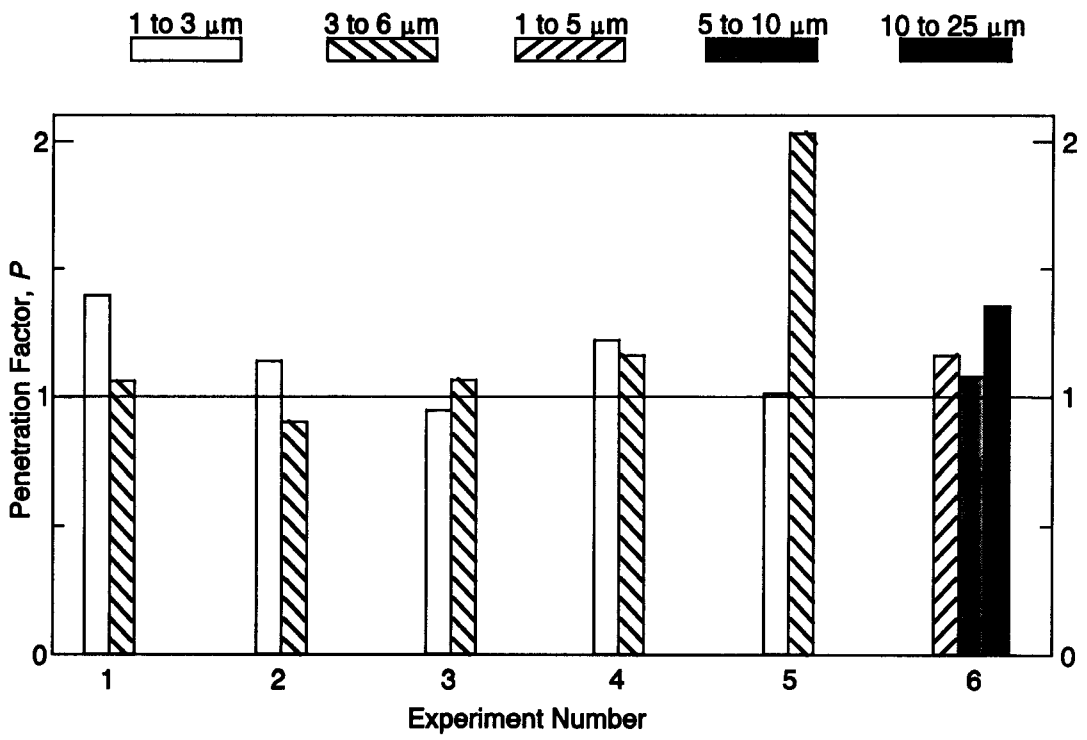

Figure 7-13. Results of six penetration experiments in a test home.

Source: Thatcher and Layton (1995).

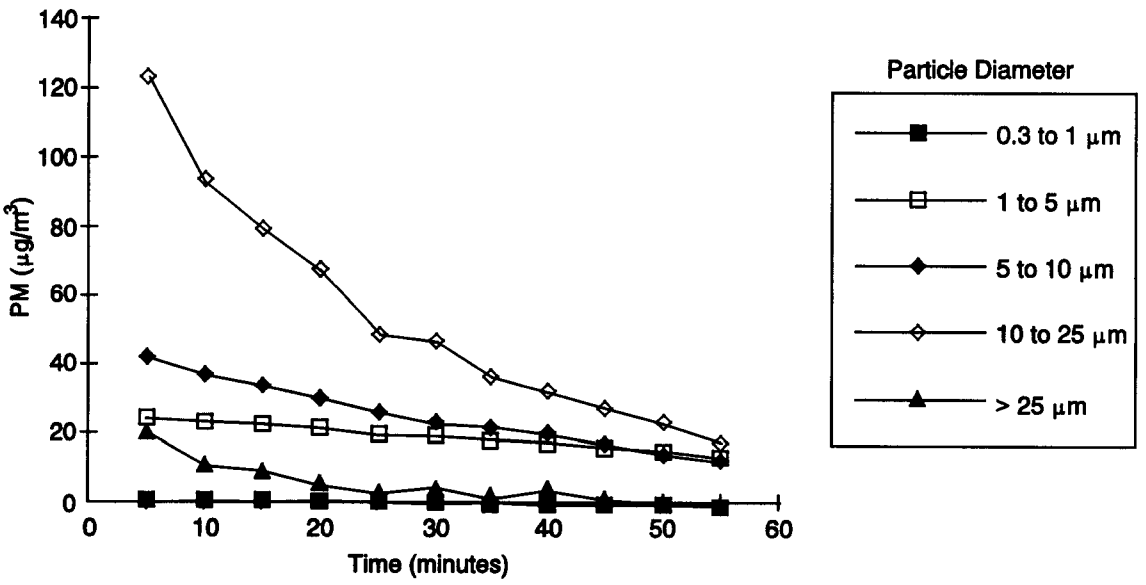

Figure 7-14. The change in suspended particle mass concentration versus time, as measured by optical particle counter, assuming spherical particles of unit density. All resuspension activities are stopped at t = 0.

Source: Thatcher and Layton (1995).

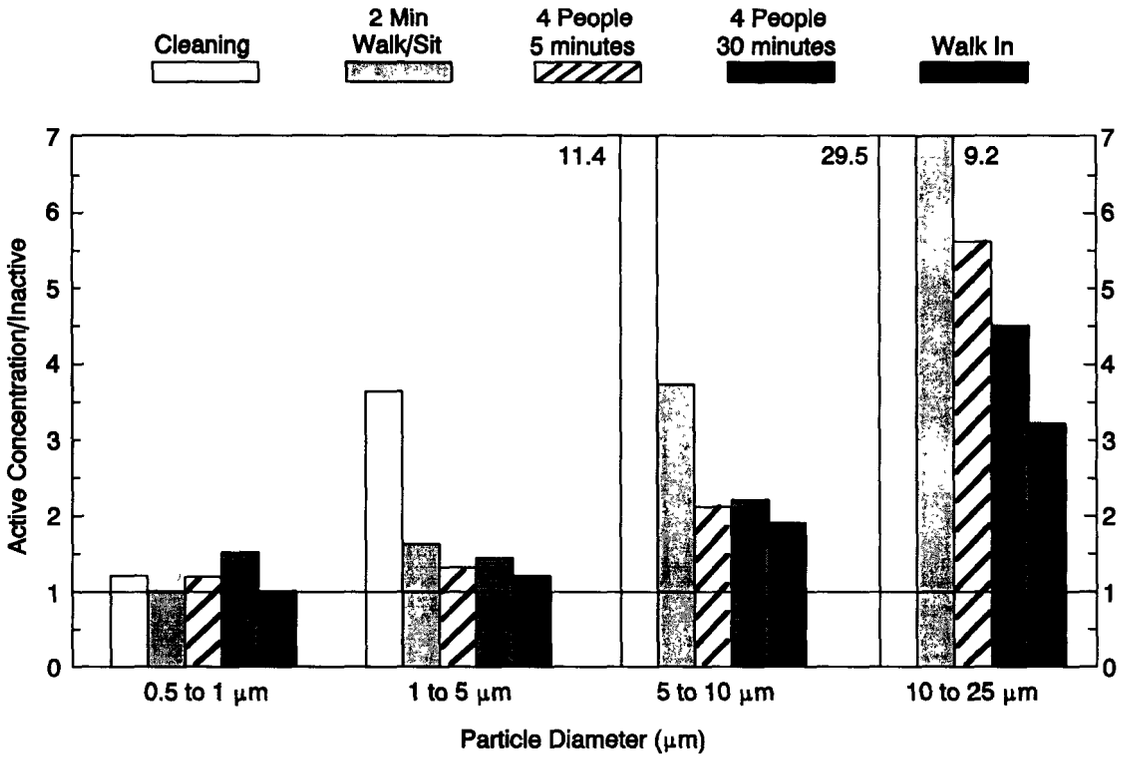

Figure 7-15. The ratio of the suspended particle concentration after a resuspension activity to the indoor concentration before that activity, by particle size. The activities tested are (1) vigorous vacuuming and housecleaning, (2) 2 min of continuous walking and sitting in the living area by one person, (3) 5 min of normal activity by four people, (4) 30 min of normal activity and (5) one person walking into and out of the living area.

Source: Thatcher and Layton (1995).

living area can increase indoor particle concentrations in the ranges 5 to 10 μm by 100% and 10 to 25 μm by 200%. The absolute increase in indoor concentrations by this activity is a function of the surface dust loading in those size ranges. Surface dust loadings ($\mu g/m^2$) increase with the time since last cleaning (Raunemaa et al., 1989; Wilmoth et al., 1991).

Because fluffy house dust can be resuspended, it will contribute to total airborne exposure to particles and constituents such as metals and pesticides. Roberts et al. (1990) studied 42 homes in Washington State. Geometric mean lead concentration in 6 homes where shoes were removed on entry was 240 $\mu g/m^2$ on carpets, compared to 2,900 $\mu g/m^2$ on carpets in 36 homes where shoes were kept on. In Japan, where shoes are removed on entry and straw mats (tatami) are usually used instead of carpets, Tamura et al. (1996) found

evidence of negligible PM_{10} resuspension. These findings suggest that most of the carpet dust in a home enters via track-in on shoes rather than by infiltration of ambient air.

7.2.2.3 Personal Exposures to Environmental Tobacco Smoke.

Jenkins et al. (1995a) reported on the first 12 cities of a 16-city sampling survey comparing ETS exposures at home and at work. About 100 nonsmoking persons in each city were recruited to wear a personal monitor at work and another personal monitor away from work. The monitors collected $PM_{3.5}$ particles, which were then analyzed for tobacco smoke markers (UVPM, FPM and solanesol). Nicotine and other gas-phase markers were also collected. Subjects provided saliva samples, which were used to screen out smokers reporting themselves as nonsmokers. (Using different cutoff points of 10, 30, or 100 μg/L, between 1.82 and 5.2% of the 1073 subjects would have been misclassified as nonsmokers). Four cells were defined: persons exposed to smoke at home and at work (N = 119); persons exposed at home but not at work (110); persons exposed at work but not at home (163); and persons exposed neither at home nor at work (504). All four particle markers agreed in ranking the four cells for total ETS exposure in the order listed—that is, nonwork (including home) ETS exposures were greater than work exposures as shown in Table 7-15. The authors identified several problems with the selection of the sample. First, the sample was 68% female. Secondly, the socioeconomic level was biased high, with about twice as many persons having some college or being college graduates as the population as a whole. It is well known that smoking rates decrease as education and income rise, and this study confirmed that observation--when broken out by income, ETS markers decreased by factors of 2 to 5 as annual income rose from $10,000 to $100,000. The authors compared ETS levels in offices with no smoking (N = 629), restricted smoking (N = 297) and unrestricted smoking (N = 113). Median (mean) levels of RSP increased from 13 (18) to 16 (28) to 33 (58) $\mu g/m^3$ in the three categories, with corresponding nicotine medians (means) of 0.025 (0.11), 0.09 (0.87), and 0.44 (2.7) $\mu g/m^3$.

Jenkins et al. (1995b) updated the results to the full 16 cities. The final number of participants in the four cells were 157, 234, 281, and 808, respectively. The median RSP ($PM_{3.5}$) values changed only slightly, increasing to 33.6 from 32 $\mu g/m^3$ in Cell 1 and decreasing to 23.3 $\mu g/m^3$ in Cell 2, with no changes in the remaining two cells.

TABLE 7-15. MEDIAN VALUES ($\mu g/m^3$) FOR ENVIRONMENTAL TOBACCO SMOKE MARKERS

Cell (N)	Nonwork	Work	RSP	UVPM	FPM	Solanesol	Nicotine
1 (119)	S	S	32	12	7.7	0.113	1.46
2 (110)	S	NS	24	7.6	5.9	0.058	0.56
3 (163)	NS	S	20	2.3	1.2	0.003	0.11
4 (504)	NS	NS	15	1.1	0.6	ND	0.02

S = smoker; NS = nonsmoker; ND = not detectable.

Source: Jenkins et al. (1995a).

ETS Exposures in Restaurants and Buildings. Oldaker et al. (1993) reported results of analyzing ETS markers in four office buildings. Median RSP levels were 30 and 34 $\mu g/m^3$ in two buildings allowing smoking, compared to 5 and 7 $\mu g/m^3$ in two buildings without smoking. Crouse et al. (1989) reported on measurements of RSP ($PM_{3.5}$) in 42 North Carolina restaurants. Geometric mean (arithmetic mean) values were 5.3 (8.6), 26.1 (34.1) and 62.0 (80.8) $\mu g/m^3$, respectively. Oldaker et al. (1990) measured $PM_{3.5}$ in 33 restaurants in the Winston-Salem, NC, area during the summer of 1986 and the winter of 1988 to 1989; in the winter, the cutpoint was changed to $PM_{2.5}$. A wide range of particle concentrations was noted, from 18 to 1,374 $\mu g/m^3$ in the summer, and <25 to 281 $\mu g/m^3$ in winter.

7.2.2.4 The Fraction of Outdoor Air Particles Penetrating Indoors

Having reviewed the literature on particles in homes, it is useful to return to one of the questions we asked at the outset: For a home with no indoor sources or resuspension of settled dust of ambient origin, how much protection is offered against outdoor particles of various size ranges?

The governing equation in this case is

$$\frac{C_{in}}{C_{out}} = \frac{Pa}{a+k} \tag{7-6}$$

Thus, there are three parameters affecting the fraction of outdoor air particles to be found indoors: the penetration factor P, the air exchange rate a, and the particle deposition rate k.

Penetration Factor P. The penetration factor P is a measure of the ability of a gas or particle to penetrate the building envelope; $0 \leq P \leq 1$. For a nonreactive gas, such as CO, the factor is expected to be 1. For large particles, the factor would be expected to go to zero with increasing particle size and decreasing air exchange rate. The question is at what combinations of size range and air exchange rate does the factor P begin to decrease significantly from unity for PM?

Two recent studies have attempted to determine the value of P for different particle size ranges. The PTEAM study (Özkaynak et al., 1996) found a value of $P \approx 1$ for both $PM_{2.5}$ and PM_{10} particles. The value was determined statistically by a nonlinear solution of Equation 7-5 (including all indoor sources) for 178 homes. Thatcher and Layton (1995) also found a value of $P \approx 1$ for all size ranges tested, including the ranges 1 to 3 μm, 3 to 6 μm, 1 to 5 μm, 5 to 10 μm, and 10 to 25 μm. The authors determined their values experimentally by direct measurement on one instrumented house. The results for the first two size ranges were obtained in five replicate experiments; for the last three size ranges, in only one experiment (Figure 7-13). Thus the two studies used different methods but arrived at the same conclusion: *particles less than 10 μm in aerodynamic diameter penetrate building envelopes with an efficiency approaching that of nonreactive gases.* Clearly, more work needs to be done to test this finding at lower air exchange rates.

Air Exchange Rate a. Air exchange rates in residences depend on three major factors: building construction, ambient conditions, and resident activities.

The building construction determines the lower bound of the air exchange rate. That is, rates cannot be reduced below the rate allowed by diffusion through the building cracks, holes, and other uncontrolled means of particle ingress in the absence of wind and buoyancy differences. Tests by building pressurization (e.g., using "blower doors") are able to determine a parameter ("crack length") that quantifies this lower bound. Buildings that are extremely tightly constructed for energy efficiency are able to reduce the lower bound of the air exchange rate to the order of 0.1 air change per hour (ach, or h^{-1}).

Ambient conditions, particularly temperature and wind velocity, can also drive air exchange rates. Strictly speaking, it is the *difference* between indoor and outdoor temperatures that creates either a pressure difference (closed windows) or a convective behavior (open windows) leading to higher air exchange rates as the temperature difference increases. As wind velocity rises, pressure differences also increase and therefore the air exchange rate rises. Besides these immediate ambient conditions we also have climatic conditions. A region that can expect a daily sea breeze is more likely to use open windows than air conditioning for ventilation. Northern areas are more likely to have tightly constructed buildings than southern areas in the USA.

In most cases, by far the most important factor affecting air exchange rates is the behavior of the resident(s). This includes such considerations as the number of residents, the number and age of children, the number of pets that spend time outdoors, whether or not air conditioning is used, and how much time doors and windows are open. Since residents are more active during the day, and doors are opened and closed more often, air exchange rates during the day typically exceed those at night, both in winter and in summer. In the PTEAM Study, the median daytime air exchange rate was 1.02 h^{-1} compared to an overnight median of 0.80 h^{-1} (Wallace et al., 1993). In the Parkville community of Baltimore, MD, in the spring, the daytime median was 0.40 h^{-1} and the overnight median was 0.28 h^{-1}. In Los Angeles coastal communities in the summer, the daytime median was 2.2 h^{-1} and the overnight median was 1.2 h^{-1}. (All values derived from U.S. Environmental Protection Agency, 1995)

Fortunately, a large number of surveys have been carried out in which air exchange rates of homes have been measured. These include the three major particle studies already mentioned, and some studies of other pollutants. A paper collecting results from many surveys found a geometric mean for 2844 U.S. residences of 0.53 h^{-1} with a geometric standard deviation of 2.3 (Murray and Burmaster, 1995). The mean value for all 2844 homes was 0.76 h^{-1}, which corresponded to the 70th percentile. However, the geometric means varied by season (a low of 0.31 h^{-1} in fall and a high of 1.00 h^{-1} in summer) and by region (a low of 0.31 h^{-1} in the North and a high of 0.69 h^{-1} in the South—mainly southern California). The geometric standard deviations for individual seasons and regions were generally very close to 2, ranging from 1.9 to 2.5. (It should be

noted here that the homes were not selected to represent the nation, and that there are very great disparities in the number of homes sampled in any one region.)

A second paper (Koontz and Rector, 1995) used a nearly identical data set, but weighted the 2889 measured homes by the state populations to estimate more closely the national distribution. Their estimates are similar to those of Murray and Burmaster (1995) with an arithmetic mean of 0.63 h^{-1}, a geometric mean of 0.46 h^{-1} and a GSD of 2.25.

However, certain smaller areas with pronounced climatic conditions could have very much higher air exchange rates. In a region such as the South Bay of Los Angeles, Wallace et al. (1991c) found that 49 of 50 homes had no air conditioning and depended on the daily land-sea breeze for ventilation. In this area, winter air exchange rates had a geometric mean of 0.75 h^{-1} and summer air exchange rates were much higher, with a geometric mean of 2.16 h^{-1}. Both these ranges are much higher than the typical values reported above. Thus, it is important to consider the individual geographic region of study and its local climatic characteristics before selecting a range of air exchange rates to characterize the region.

With that caveat, the empirical distribution for a large number of U.S. homes across all seasons, but with disparate representation among the various regions of the country, appears to have a median value of about 0.5 h^{-1}, with a one geometric standard deviation ($\pm\ \sigma$) range of 0.2 to 1.1 h^{-1}, and a $\pm 2\sigma$ range of 0.1 to 2.2 h^{-1} (Murray and Burmaster, 1995; Koontz and Rector, 1995).

Deposition Rate k. In a residence, the deposition rate k depends on many factors, such as scale of turbulence, and the size, shape, electrostatic charge, and density of the particle. For larger particles, the deposition rate is determined largely by gravitational settling; for smaller particles, deposition on vertical surfaces by diffusion may also be important (Nazaroff et al., 1993). Unfortunately, fine particle deposition rates are not well characterized. Typically, one must measure over very long periods of time (weeks to months) to collect enough particles for analysis by sophisticated techniques. A series of studies in nearly unoccupied buildings containing telephone-switching electrical equipment resulted in average values for the deposition velocity of sulfate particles ranging from 0.003 to 0.005 cm/s (Sinclair et al., 1988, 1990, 1992; Weschler et al., 1989); these values correspond to values of k (using a surface to volume ratio of 3 m^{-1}) of 0.3 to 0.5 h^{-1}.

However, another series of studies in museums resulted in values an order of magnitude smaller (Ligocki et al., 1990; Nazaroff et al., 1990a,b). Results for the sulfur ($PM_{2.5}$) deposition rate in the PTEAM studies were 0.16 h^{-1}, lying between the values found by these two groups. Nazaroff et al. (1993) concluded that deposition rates could vary as a result of different surfaces or near-surface air flows, amount of thermal isolation of the surfaces from building walls, turbulence, and many other factors. Thus it is not likely that theoretical calculations of deposition rates will provide trustworthy estimates. Nor is it likely that chamber studies, with their limited ability to reproduce the variety of floor coverings and air flows found in residences, can provide much information relevant to real-world residences.

In the absence of precise theory or widely applicable chamber study estimates, the largest study of residences including a calculation of empirical deposition rates is the PTEAM study. The estimate for $PM_{2.5}$ was 0.39 h^{-1}, for PM_{10} it was 0.65 h^{-1}, while for the coarse fraction (the difference between PM_{10} and $PM_{2.5}$) it was 1.01 h^{-1}.

What Is the Fraction of Outdoor Air Particles Found Indoors at Equilibrium?

Based on the values of P, a, and k discussed above, an answer can be provided to this question. Figure 7-16 shows the fraction of outdoor fine and coarse particles found in homes under equilibrium conditions for a range of air exchange rates. This fraction is calculated using the value of $P = 1$ determined in the PTEAM and the Thatcher and Layton (1995) studies, and the values of k for fine and coarse particles calculated in the PTEAM study. The fractions are displayed over the 95% range of observed air exchange rates (0.1 to 2.2 h^{-1}) in studies reported on by Murray and Burmaster (1995). It can be seen that at the mean air exchange rate of 0.76 h^{-1} reported in Murray and Burmaster (1995), the fractions of outdoor fine (<2.5 μm) and coarse particles (>2.5 and <10 μm) that will be found indoors under equilibrium conditions are 66% and 43%, respectively. The fraction of PM_{10} found indoors will lie between these two curves, with the exact placement dependent on the relative proportions of fine and coarse particles constituting the PM_{10}.

The actual distribution of values of $a/(a+k)$ observed in the PTEAM Study is provided in Table 7-16 for PM_{10} and for its fine and coarse fractions. As can be seen, the average values across day and night were about 67% for fine particles and 47% for coarse particles, with PM_{10} exactly between the two size fractions at 57%.

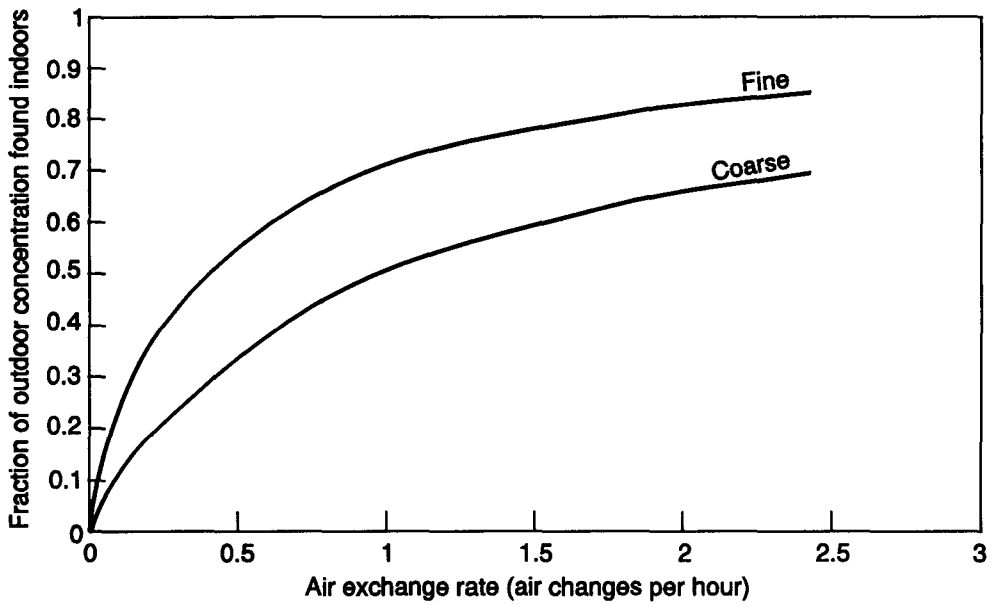

Deposition rate = 0.39/h for fine particles, 1.01/h for coarse

Figure 7-16. Fraction of indoor particulate matter (PM) from outdoor airborne PM, under equilibrium conditions, as a function of air-exchange rate, for two different size fractions.

Source: Calculated from PTEAM database (Özkaynak et al., 1993a; Wallace, 1996).

These results suggest that if persons at risk of health effects from outdoor particle pollution are able to significantly decrease the air exchange rates in their homes (by weatherization, installation of air conditioning to reduce use of windows, etc.) they could decrease the fraction of outdoor air particle concentration in their homes. A decrease in the air exchange rate from the mean level of 0.76 h^{-1} reported above to an achievable (16th percentile) value of 0.25 h^{-1} would decrease the indoor air level of outdoor-generated fine $PM_{2.5}$ particles from 66% to 39% of the outdoor level, and of PM_{10} from 54% to 28%.

7.2.2.5 Studies of PM in Buildings

The single largest study of particles in buildings was carried out by the Lawrence Berkeley Laboratory (LBL) for the Bonneville Power Administration (BPA) (Turk et al., 1987, 1989). Thirty-eight buildings were chosen from two climatic regions in the Pacific Northwest: Portland-Salem, OR (representing mild coastal conditions), and Spokane-Cheney,

TABLE 7-16. FRACTION OF CONCENTRATION OF OUTDOOR PARTICLES ESTIMATED TO BE FOUND INDOORS AT EQUILIBRIUM: RESULTS FROM THE PARTICULATE TOTAL EXPOSURE ASSESSMENT METHODOLOGY STUDY

	Daytime (N=174)			Overnight (N=175)		
Statistic	Fine	PM_{10}	Coarse	Fine	PM_{10}	Coarse
Mean	0.68	0.58	0.49	0.66	0.55	0.46
Standard deviation	0.17	0.19	0.20	0.15	0.17	0.17
Standard error	0.013	0.015	0.015	0.012	0.013	0.013
Geometric mean	0.66	0.55	0.45	0.64	0.53	0.42
Minimum	0.28	0.19	0.13	0.28	0.19	0.13
25th percentile	0.55	0.42	0.32	0.55	0.43	0.32
Median	0.70	0.58	0.47	0.66	0.54	0.43
75th percentile	0.83	0.75	0.65	0.79	0.69	0.59
Maximum	0.95	0.93	0.89	0.94	0.90	0.85

Fractions calculated from the formula $Pa/(a+k)$, where
$P = 1$;
$k = 0.39\ h^{-1}$ for fine particles, $PM_{2.5}$;
$k = 0.65\ h^{-1}$ for PM_{10}; and
$k = 1.01\ h^{-1}$ for coarse particles 2.5 μm < AD < 10 μm.
Values for a measured in 175 homes during the PTEAM Study.

Source of data: Values calculated from PTEAM database (Wallace, 1996).

WA (representing extreme inland conditions). The buildings were studied for a variety of pollutants to determine how ventilation rates affect indoor air quality. Buildings were measured in winter (21 buildings in both regions), spring (10 buildings in both regions) and summer (nine buildings in the inland region only). All but four buildings were government or public properties, and therefore the 38 buildings cannot be considered to represent the full mix of building types.

Each building was monitored for 10 working days over a two-week period. From four to eight particle sampling sites were chosen in each building according to size. The sampler was an LBL-developed flow controlled device with a 3 μm cutpoint. The pumps sampled only during hours the building was occupied. If filters had to be changed due to excessive loading, the combined weight of all filters from one site was determined—thus all values are

approximately 10 working-day (80-h) averages. Buildings had varied types of smoking policies, from relatively unrestricted to very tightly controlled, as in one elementary school. In most buildings, an attempt was made to site at least one monitor in an area where smoking was allowed. Data were obtained from smoking areas in about 30 of the 38 buildings.

Results comparing smoking and non-smoking areas are provided in Table 7-17 and Figure 7-17. Mean RSP concentrations in the smoking areas were more than three times higher than in the non-smoking areas (70 versus 19 $\mu g/m^3$). Since these arithmetic means showed evidence of being driven by one or two high values, the geometric mean (averaged across all sites in a building) may be a better comparison. Here the ratio is very close to 3 to 1 (44 versus 15 $\mu g/m^3$). Outdoor results at 30 sites had the identical arithmetic mean as the indoor non-smoking sites: 18.9 $\mu g/m^3$.

Repace and Lowrey (1980) sampled 19 establishments allowing smoking (seven restaurants, three bars, church bingo games, etc.) and 14 where no smoking occurred (including five residences and four restaurants) between March and early May of 1978. Sampling occurred for short periods of time (2 to 50 min) using a TSI Piezobalance to measure $PM_{3.5}$. Indoor concentrations ranged from 24 to 55 $\mu g/m^3$ in the areas without smoking, and from 86 to 697 $\mu g/m^3$ in places with active smoking.

Miesner et al. (1989) sampled particles and nicotine in 57 locations within 21 indoor sites in Metropolitan Boston, MA, between July 1987 and February 1988. $PM_{2.5}$ was sampled using Harvard aerosol impactors. Sampling times ranged from about 3 h in a bus station to 16 h in a library, depending partly on how "clean" the environment was perceived to be. $PM_{2.5}$ concentrations ranged from 6 $\mu g/m^3$ (in the library) to 521 $\mu g/m^3$ in a smoking room in an office building. For 42 measurements in non-smoking areas, the mean $PM_{2.5}$ concentration was 25 $\pm$ 30 (SD) $\mu g/m^3$. Six of these measurements included a classroom with visible levels of chalk dust on the impactor, four measurements in subways, and the bus station. The remaining 36 nonsmoking areas had a mean $PM_{2.5}$ concentration of 15 $\pm$ 7 $\mu g/m^3$. The 15 smoking areas ranged from 20 to 520 $\mu g/m^3$ with a mean of 110 $\pm$ 120 $\mu g/m^3$.

Sheldon et al. (1988a,b) reported on the EPA 10-building study of hospitals, homes for the elderly, schools, and office buildings. Particle measurements were taken in six buildings using a National Bureau of Standards portable particle sampler (McKenzie et al., 1982) to

TABLE 7-17. SMOKING, NONSMOKING, AND OUTDOOR RSP CONCENTRATIONS AND RATIOS

Building No.	Outdoor ($\mu g/m^3$)	Indoor ($\mu g/m^3$) Arithmetic Mean (Range)			Ratios		
		Nonsmoking	Smoking[c]	Mean[d]	Indoor Nonsmoking ÷ Outdoor	Indoor Smoking ÷ Outdoor	Indoor Mean ÷ Outdoor
1	ND	25(19-36)	ND	25(19-36)	NA	NA	NA
2	ND	19(18-21)	ND	19(18-21)	NA	NA	NA
3	ND	ND	20(16-25)	20(16-25)	NA	NA	NA
4	8	7(6-8)	ND	7(6-8)	0.9	NA	0.9
5	BD	13(13)	14(14)	13(13-14)	NA	NA	NA
6	35	12(11-13)	35(23-59)	28(11-59)	0.3	1.0	0.8
7	35	38(32-44)	39(39)	38(32-44)	1.1	1.1	1.1
8	8	7(7-8)	ND	7(7-8)	0.9	NA	0.9
9	8	11(11)	16(13-20)	15(11-20)	1.3	2.0	1.9
10	9	65(53-74)	95(67-127)	86(53-127)	7.0	11.0	9.6
11[a]	8	23(9-49)	209(209)	63(9-209)	2.9	26.1	7.9
12	ND	10(10)	63(63)	36(10-63)	NA	NA	NA
13	10	5(5-6)	ND	5(5-6)	0.5	NA	0.5
14	6	ND	30(26-34)	30(26-34)	NA	5.0	5.0
15	BD	11(7-14)	12(12)	11(7-14)	NA	NA	NA
16	10	9(8-11)	73(73)	31(8-73)	0.9	7.3	3.1
17[b]	7	11(10-13)	105(105)	40(10-105)	1.6	15.0	6.1
18	7	ND	19(19)	19(19)	NA	2.7	2.7
19	7	ND	20(11-29)	20(11-29)	NA	2.9	2.9
20	18	11(10-11)	ND	11(10-11)	0.6	NA	0.6
21	17	11(9-12)	ND	11(9-12)	0.7	NA	0.7
22	20	18(18)	57(22-165)	50(18-165)	0.9	2.9	2.5
23	11	9(BD-20)	ND	9(BD-20)	0.8	NA	0.8
24	11	44(10-77)	24(24)	37(10-77)	4.0	2.2	3.4
25	68	35(32-38)	109(109)	60(32-109)	0.5	1.6	0.9
26	32	45(20-70)	82(55-123)	67(20-123)	1.4	2.6	2.1
27	52	36(33-38)	61(33-89)	48(33-89)	0.7	1.2	0.9
28	65	36(29-43)	BD	24(BD-43)	0.6	NA	0.4
29	29	10(8-12)	144(144)	32(8-144)	0.3	5.0	1.1
30[b]	33	24(20-30)	113(113	37(20-113)	0.7	3.4	1.1
31	13	12(8-18)	268(268)	64(8-268)	0.9	20.6	4.9
32	ND	13(10-17)	36(21-52)	21(10-52)	NA	NA	NA
33	ND	ND	29(12-74)	29(12-74)	NA	NA	NA
34	16	13(10-16)	54(13-117)	28(10-117)	0.8	3.4	1.8
35	18	20(6-35)	50(50)	23(6-50)	1.1	2.8	1.3
36[a]	20	14(9-18)	72(17-127)	28(9-127)	0.7	3.6	1.4
37	19	21(12-32)	27(11-62)	25(11-62)	1.1	1.4	1.3
38	14	7(BD-9)	308(308)	46(BD-308)	0.5	22.0	3.3
39	11	8(8-9)	13(11-14)	11(8-14)	0.7	1.3	1.0
40	11	10(8-12)	26(11-40)	15(8-40)	0.9	2.4	1.4
AM	19	19	70	30	1.2	6.0	2.3
ASD	16	14	73	19	1.3	7.2	2.2
GM	14	15	44	24	0.9	3.6	1.7
GSD	2.2	1.9	2.7	2.0	2.0	2.6	2.3

[a]Repeated test of building #11.
[b]Repeated test of building #17.
[c]Smoking within 10 m radius of site.
[d]Arithmetic average of all sites in building.

NA = Not applicable.
ND = No data collected.
BD = Below detection limit.

Source: Turk et al. (1987).

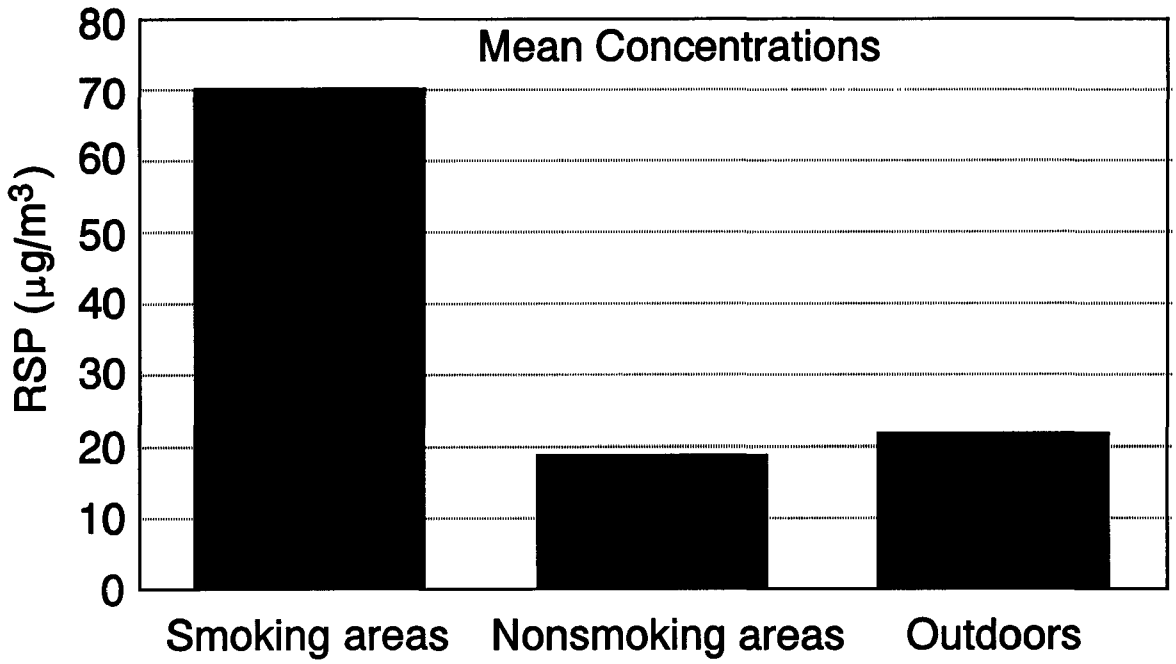

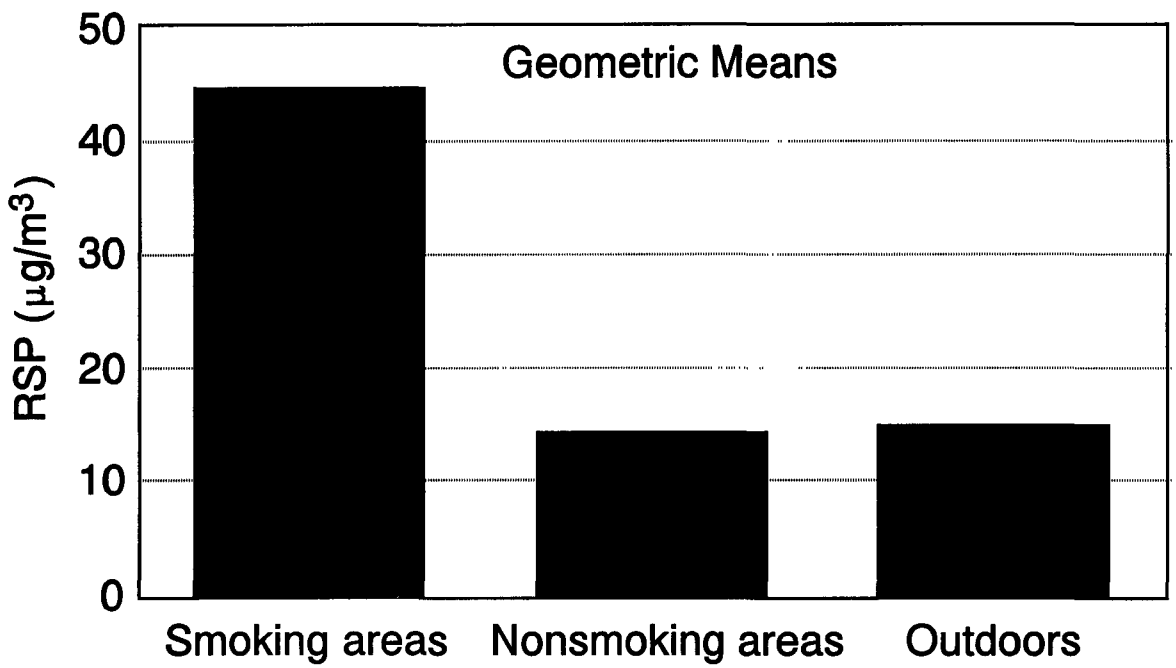

Figure 7-17. Comparison of respirable particles in smoking and nonsmoking areas of 38 buildings in the Pacific Northwest.

Source: Turk et al. (1987).

collect two size fractions: PM_3 and a coarse fraction between PM_3 and PM_{15}. The sampler employed two filters in series: an 8.0 μm Nuclepore filter for PM_{15} and a 3 μm Ghia Zefluor Teflon filter for fine particles. The flow rate was 6 Lpm for a 24-h sample. Three consecutive 24-h samples were collected at each building. Additional particle monitoring was provided at certain locations (e.g., smoking lounge, cafeteria) using a Piezobalance ($PM_{3.5}$) and a dichotomous sampler ($PM_{2.5}$ and PM_{10}).

In areas without smoking, indoor concentrations of both size fractions were generally lower than outdoor levels; for example, the coarse fraction ranged from 0.2 to 0.66 of the outdoor level (13 to 17 $\mu g/m^3$) in the three buildings with no smoking. The fine fraction was present at higher indoor-outdoor ratios, ranging from 0.56 to 0.99 in the same three buildings (outdoor fine fraction ranged from 16 to 33 $\mu g/m^3$). The fine fraction was elevated in the regions of smoking (range of 14 to 56 $\mu g/m^3$). Piezobalance results for several buildings showed uniformly low (7 to 29 $\mu g/m^3$) for 800 min of monitoring in nonsmoking areas.

Concentrations in the areas allowing smoking were more often in the 40 to 60 $\mu g/m^3$ range, with short-term peaks as high as 345 $\mu g/m^3$. It was possible to use the observed declines in $PM_{3.5}$ following cessation of smoking to calculate an effective air exchange rate and thus a source strength for $PM_{3.5}$ emissions from cigarettes. Four estimates gave an average value of about 6 mg/cigarette, somewhat below the chamber study estimates of 10 to 15 mg/cig. An estimate due to Repace and Lowrey (1980) of concentrations of respirable particulates due to smoking was also tested, with good agreement. The Repace and Lowrey equation is

$$C\ \mu g/m^3 = 27.6\ P_a/a \qquad (7\text{-}7)$$

where P_a is smoking occupancy in persons per 100 square meters and a is the air exchange rate h^{-1}. Equation 7-7 was developed assuming one of every three occupants are smokers who smoke two cigarettes per hour. Assuming a background concentration of 15 $\mu g/m^3$, the measured values for the smoking lounge for zero, three, and nine smokers were 10, 78, and 284 $\mu g/m^3$, respectively. Equation 7-7 predicts 0, 99, and 296 $\mu g/m^3$, respectively. In two of the homes for the elderly, apartments with smokers and nonsmokers were measured for

three consecutive days using the NBS samplers. In one building, the smoker's apartment had a 2-day PM_3 average of 39 $\mu g/m^3$, compared to 9.4 $\mu g/m^3$ in the nonsmoker's apartment; in the other home for the elderly, where two smokers shared one apartment, the average 2-day PM_3 concentration was 88 $\mu g/m^3$ compared to 8.6 $\mu g/m^3$ in the nonsmoking apartment. The simultaneous ambient values were not measured at Home 1. At Home 2, the ambient value was 11 $\mu g/m^3$.

Owen et al. (1990) studied particle size distributions in an office under varying conditions of ventilation and occupancy. The unoccupied office using minimum outdoor air had concentrations at least as low as the occupied office using maximum outdoor air. $PM_{3.5}$ concentrations (measured using the TSI Piezobalance) were about twice as high (75 versus 39 $\mu g/m^3$) in the occupied office when the dampers were closed as when they were open. The main source of particle generation appeared to be the hallway, suggesting that resuspension of tracked-in dust was an important indoor source of particles as reported by Roberts et al. (1990) for residences.

7.2.3 Indoor Air Quality Models and Supporting Experiments

Indoor concentrations of particles are a function of penetration of outdoor particles and generation of particles indoors. The concentrations are modified by air exchange rates and deposition rates of the particles onto indoor surfaces.

7.2.3.1 Mass Balance Models

Mass balance models have been used for more than a century in various branches of science. All such models depend on the law of the conservation of mass. They simply state that the change in mass of a substance in a given volume is equal to the amount of mass entering that volume minus the amount leaving the volume. Usually they are written in the form of first-order linear differential equations. That is, consider a volume V filled with a gas of mass m. The change in mass Δm over a small time Δt will simply be the difference between the mass entering the volume (m_{in}) and the mass leaving the volume (m_{out}):

$$\frac{\Delta m}{\Delta t} = \frac{(m_{in} - m_{out})}{\Delta t} \tag{7-8}$$

Taking the limit as Δt approaches zero, we have the differential equation for the rate of change of the mass:

$$\frac{dm}{dt} = \frac{d}{dt}(m_{in} - m_{out}) \tag{7-9}$$

If we require that the mass be uniformly distributed throughout the volume at all times, we have a condition that the physical chemists call "well-mixed". We assume that any mass gained or lost in the volume V is instantaneously distributed evenly throughout the volume. We may then replace the mass term (m) by the concentration $C = m/V$, so that $dm/dt = V\,dC/dt$.

The above equations are the basis for all such mass-balance models. Equation 7-9 takes on many forms depending on the type of processes involved in transporting mass into or out of the volume being considered. A large class of models assume that the volume V is a single perfectly mixed compartment. More complex models assume multiple compartments to allow for incomplete mixing in the total volume V (Mage and Ott, 1996). A detailed mass-balance model that includes changes in particle size, chemical composition, and turbulence is described in Nazaroff and Cass (1989).

7.2.4 Summary of Indoor Particulate Matter Studies

At low outdoor levels of fine ($PM_{3.5}$ or $PM_{2.5}$) particles (as in most of the cities in the Harvard Six-City and New York State studies), mean indoor concentrations have been found to be twice as high as outdoor levels. However, for homes without smokers or combustion sources, indoor levels are often roughly equal to outdoor levels (Santanam et al., 1990; Leaderer et al., 1994; Neas et al., 1994). At high outdoor levels, mean indoor concentrations have been about 10% lower than the mean outdoor concentrations in the two areas studied (Steubenville, OH, and Riverside, CA). Indoor concentrations are considerably higher during the day, when people are active, than at night. Based on a mass-balance model, outdoor air was the major source of indoor particles in the PTEAM study, providing

about 3/4 of fine particles ($PM_{2.5}$) and 2/3 of inhalable particles (PM_{10}) in the average home. However, outdoor air contributed less than half of the indoor particle concentrations at seven out of eight other sites with extensive indoor-outdoor measurements. Indoor concentrations are much higher during the day, when people are active, than at night.

In the PTEAM study (with very high outdoor particle concentrations), indoor levels were significantly influenced by outdoor levels, but with relatively low R^2 values ranging between 0.22 and 0.54. In the other two major studies, no significant indoor-outdoor relation was observed. Regressions of indoor on outdoor particles seldom explained more than half the variance of any study ($R^2 < 50\%$). However, in those studies with repeated measures on the same house, (e.g., the PTEAM prepilot [Table 7-6], the Phillipsburg, NJ, study [Table 7-15] and Tamura et al. [1996] in Section 7.4.2.1), longitudinal regressions of indoor on outdoor particles often had much higher R^2 values of 0.6 to 0.9 for each individual house. Since the epidemiological studies of health effects of particles have been studies of variation over time, the longitudinal regressions by individual home are expected to be more relevant to the epidemiology studies than cross-sectional regressions across all homes in the study. The better relationship showed by these regressions suggests that whatever structural or behavioral characteristics affect indoor particle concentrations in the home tend to persist or be repeated over time. This gives better support to the epidemiological findings than would be inferred from the typically low R^2 values reported for the cross-sectional regressions performed in most studies.

Deposition rates k ranged from 0.16 h^{-1} for sulfur to 0.4 h^{-1} for fine ($PM_{2.5}$) particles to 1 h^{-1} for coarse particles ($PM_{10} - PM_{2.5}$), with an intermediate estimate of 0.65 h^{-1} for PM_{10}. The penetration factor P for both fine and coarse fractions was estimated to be unity. For a home with no indoor sources whatever and a typical air exchange rate of about 0.75 h^{-1}, these values for k and P would imply that sulfur indoors would be about $0.75/(0.16 + 0.75) = 82\%$ of the outdoor value at equilibrium, fine particles indoors would be about $0.75/(0.4+0.75) = 65\%$ of the outdoor value at equilibrium, indoor PM_{10} would be about 54% of outdoor levels, and indoor coarse particles would be about 43% of outdoor levels. Since very few homes were observed to have concentrations this low, it can be inferred that very few homes are free of important indoor sources of particles.

A crucial question is the impact of outdoor particles on indoor particle concentrations. It was found that the governing equation is a function of only two parameters: air exchange rate a and particle deposition rate k: $a/(a+k)$. Air exchange rates measured in the United States appear to follow a roughly log-normal distribution with a geometric mean of 0.5 and a geometric standard deviation about 2. With the values for the deposition rates provided above, one can calculate the impact of outdoor particles on indoor concentrations for any given value of the air exchange rate. At a low air exchange rate of, say, 0.4 h^{-1}, sulfates indoors will be 71% of their outdoor values, fine particles indoors will be 50% of their outdoor values, while coarse particles will be 0.4/1.4 or 28% of their outdoor values. At a higher air exchange rate of 1 h^{-1}, sulfates will be 86% of their outdoor concentration, fine particles will be 1/1.4 or 71% of their outdoor concentration, whereas coarse particles will be 50% the outdoor concentration. The difference in both cases between the two size fractions is about 0.2; that is, for the entire range of realistic air exchange rates (from 0.2 h^{-1} to 2 h^{-1}), if the fraction of outdoor coarse ($PM_{10} - PM_{2.5}$) particles found indoors is f, then the fraction of fine particles found indoors will be approximately $f + 0.2$. It can be seen that a reduction in air exchange rate would reduce the impact of outdoor air on indoor air particle concentrations.

7.2.5 Bioaerosols

Biologically-derived particles are frequently ignored components of both ambient and indoor aerosols. This lack of attention is, in part, due to the fact that the bioaerosols are considered "natural" and not amenable to control. Methods for their analysis are, in many cases, highly variable, and very little exposure or exposure/response information is available. Measurement methods for bioaerosols are discussed in Chapter 4 (Section 4.4). Various health effects associated with bioaerosols are discussed in Chapter 11. A few reference works that focus on bioaerosols include Gregory (1973), Edmonds (1979), Cox (1987), Lighthart and Mohr (1994), and Cox and Wathes (1995).

For bioaerosols, there is considerable confusion among the terms reservoir, source, particle, and agent. For the purposes of this chapter, the following definitions apply:

- Reservoir: the environmental niche in which source organisms are living
- Source: the organism that produced the particle

- Particle: the particle shed from the organism
- Agent: the part(s) of the particle that actually mediate the disease process.

Examples of bioaerosol sources, particles and agents are presented in Table 7-18.

TABLE 7-18. AN OVERVIEW OF ORGANISMS, AEROSOLS, AND DISEASE AGENTS

Sources	Aerosol Particles	Disease Agents
Plants	Pollen and pollen fragments, fragments of other plant parts, spores (ferns, mosses), algal cells	Glycoprotein allergens
Animals	Skin scales, secretions (saliva, skin secretions), excreta, body parts (arthropods)	Glycoprotein allergens
Fungi	Spores, hyphae, yeast cells, metabolites (toxins, digested substrate material)	Glycoprotein allergens, infectious units, glucans, mycotoxins
Bacteria	Cells, fragments, metabolites (toxins, digested substrate material)	Infectious units, allergens, endotoxin, exotoxins
Viruses	Viral particles	Infectious units

7.2.5.1 Plant Aerosols

Pollen

Pollen is produced by vascular flowering plants: trees (pines, cedars, birch, elm, maple, oak, hickory, walnut, etc.), grasses, and weeds (ragweed, sage, Russian thistle, lambs quarters, etc.). Within these large groupings, specific types are regionally common. For example, ragweed is most common in the eastern United States. Birch pollen dominants the spring pollen season in New England, while mountain cedar pollen is abundant early in the year in the southwest (Lewis et al., 1983).

Pollen levels outdoors are controlled by the number of plants available for pollen release, the amount of pollen produced by each plant, factors that control pollen release and dispersion from the plant, and factors that directly affect the aerosols (Edmonds, 1979). The number of plants available depends on the many environmental factors that control plant

prevalence, some of which are human factors. As an example, the abundance of the ragweed plant in a particular year depends on the number of plants that produced seed in the previous year, disturbed ground available for seed germination and growth, and meteorological factors during the growing season. Once a crop of ragweed has been produced, pollen production depends on temperature, rainfall, and day length.

Pollen grains are relatively large complex particles that consist of cellular material surrounded by a cell membrane and a complex wall. Pollen grain structure has been well studied. Pollen shed is controlled by temperature, humidity, wind, and rain. Pollen levels in air depend on all of these factors as well as wind and rain conditions after release, and on surfaces available for impaction. Figure 7-18 represents day to day ragweed pollen prevalence in Kalamazoo, MI, for 1994.

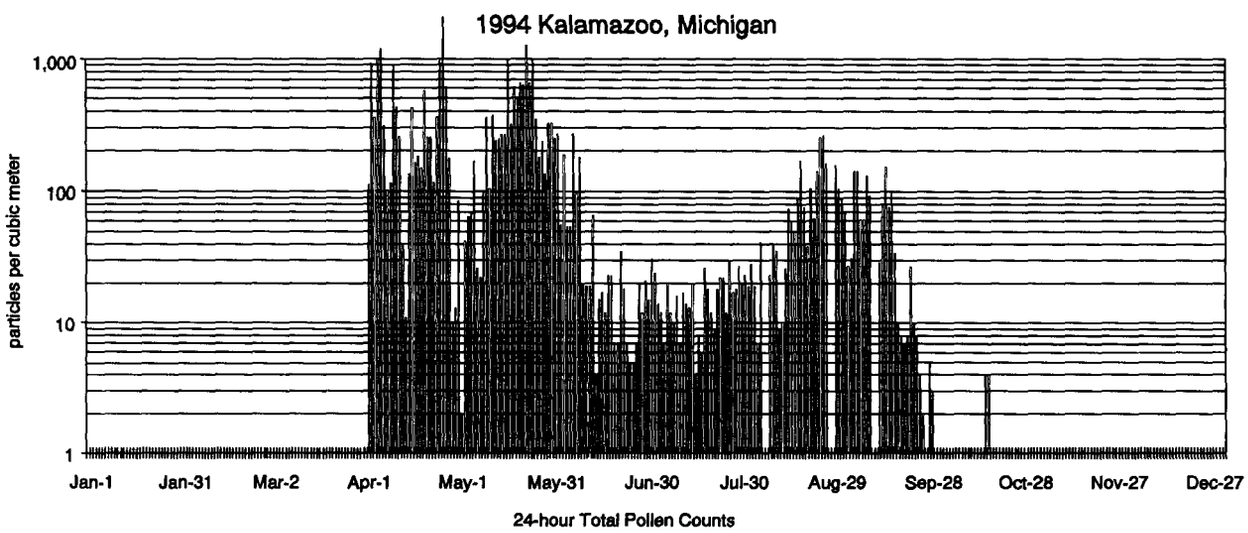

Figure 7-18. Chart of ragwood pollen prevalence. Sampling was not conducted before April and during the first few days of October.

Source:

Pollen allergens are (apparently) water-soluble glycoproteins that rapidly diffuse from the grain when it contacts a wet surface. The glycoproteins are (generally) specific to the type of pollen, although large groups may be represented by a single allergen. For example,

many different kinds of grasses carry similar allergens in their pollen grains. A number of pollen allergens have been characterized: Amb a I (ragweed), Bet p I (birch), Par j I (parietaria), etc.

Other Natural Plant Aerosols

Other plant-derived particles that are a natural part of outdoor air include algal cells; spores of mosses, liverworts, club mosses, and ferns; and fragments of all kinds of plants. Very little has been reported about the prevalence or human impact of any of these aerosol particles, although they are presumed to carry allergens.

Man-Made Plant Aerosols (Soy, Latex, Occupational)

Man-made accumulations of plant material that are subsequently handled inevitably produce bioaerosols. The most common practices that involve such accumulations are storage, handling, and transport of farm products (hay, straw, grain), composting, and manufacturing processes that involve the use of plant material. In addition, the use of some plant products can result in disease-causing aerosols (Alberts and Brooks, 1992). The aerosols produced from most of these processes are complex, and few have been accurately characterized.

Grain Dust. It is well-recognized that grain dusts include respirable-size particles ($< 10\ \mu m$) although the exact nature of the particles and the agents of disease remain speculative. Soybean dust aerosols released from freighters unloading the beans in port have been blamed for epidemics of asthma.

Wood Dust. Wood trimmer's disease (from particles released from wood during high-speed cutting). Sewage composting involves the use of wood chips that can release allergenic aerosols.

Latex. Latex-containing powder aerosols are produced when surgical gloves are used. Latex particles also may be released from automobile tires.

7.2.5.2 Animal Aerosols

Mammalian Aerosols

All mammals produce aerosols, from humans to the smallest mouse. Human aerosols (skin scales, respiratory secretions) do not cause disease except, of course, for agents of infection (see below). Other mammals release aerosols that cause hypersensitivity diseases. The most common of these are cats, dogs, farm animals, laboratory animals, and house mice, although all animals release aerosols that could be sensitizing under appropriate conditions (Burge, 1995). Mammals only cause human disease when appropriate exposure conditions occur. For cats, simply having a cat in a house will create such conditions, as will handling any animal regardless of the environment. Cat allergens apparently become aerosolized on very small particles (< 1 μm) shed from skin and saliva. There is some indication that dog, mouse, and other rodent allergens are borne on dried urine particles, and particle sizes are similar to those of cat allergen. Little is known about other mammalian aerosols. Cat and dog allergens have been characterized (Fel d I, Can f I) and other mammalian allergens are under active study.

Avian Aerosols

Wild and domesticated birds associated with disease-causing aerosols include for example: starlings (histoplasmosis); pigeons (histoplasmosis, pigeon-breeders disease); parrots (psittacosis); poultry (poultry-handlers disease); etc. Of these diseases, only the hypersensitivity diseases (pigeon breeders and poultry handlers disease) are caused by "bird" aerosols. The others are infections caused by agents inhabiting the birds (see below). The birds that release antigens that have caused human disease are those that are confined or congregate close to people. The avian aerosol-hypersensitivity diseases are almost exclusively confined to sites where birds are bred and handled extensively, especially in indoor environments. Relatively little is known about avian aerosols. Probably skin scales, feather particles, and fecal material are all released as antigen-containing aerosols. The antigens (allergens) responsible for avian-related diseases have not been characterized.

Insect Aerosols

Dust Mites. Dust mites are arthropods belonging to the family Pyrogliphidae. There are two common species in temperate climates: *Dermatophagoides farinae* (which proliferates under relatively dry conditions) and *D. pteronyssinus* which dominates populations in more humid environments (Arlian, 1989). Dust mites thrive in environments where relative humidity consistently exceeds 60 % and where skin scales and fungal spores are available as a food source. Primary reservoirs for exposure are bedding and carpet dust. The mite itself is about 100 μm long, but it excretes 20 μm membrane-bound fecal particles that contain the allergens. Exposure to dust mite allergens apparently occurs only when reservoirs are disturbed. Dust mites produce allergens that are a major cause of sensitization in children. The allergens are digestive enzymes that gradually diffuse from fecal particles after deposition on mucous membranes. Several dust mite allergens have been characterized and monoclonal antibodies against each have been raised and cloned. These include Der f I and II, and Der p I and II (Platts-Mills and Chapman, 1987).

Cockroaches. Cockroaches are insects belonging to the Orthoptera (Mathews, 1989). The most common cockroach infesting temperate climate buildings is *Blatella germanica*, the German cockroach. Cockroaches are nocturnal, and inhabit dark environments where food and water are available. Common food sources include stored animal or human food, and discarded food (garbage). Cockroaches are extremely prolific, given appropriate environmental conditions. Population pressure will eventually drive the roaches into the daylight in search of food. Cockroaches shed body parts, egg cases, and fecal particles, all of which probably carry allergens. Little is known about the particles that actually carry the allergens. Two German cockroach allergens have been characterized: Bla g I, and Bla g II. The function within the cockroach of these allergens is unknown. Cockroach allergens are probably a major cause of asthma for some populations of children.

Other Insects. Fragments of gypsy moths and other insects that undergo massive migrations can become abundant in ambient air. Sizes, nature, and allergen content of such particles have not been studied. Cases of occupational asthma from exposure to insects (e.g., sewer flies) have been reported.

Other Animal Allergens

It is likely that proteinaceous particles shed from any animal could cause sensitization if exposure conditions are appropriate. For example, exposure to proteins aerosolized during seafood processing have caused epidemics of asthma.

7.2.5.3 Fungal Aerosols

Fungi are primarily filamentous microorganisms that reproduce and colonize new environments by means of airborne spores. Most use complex non-living organic material for food, require oxygen, and have temperature optima within the human comfort range. The major structural component of the cell wall is acetyl-glucosamine polymers (chitin). Cell walls also may contain B-glucans, waxes, mucopolysaccharides, and a wide variety of other substances. In the process of degrading organic material, the fungi produce CO_2, ethanol, many other volatile organic compounds, water, organic acids, ergosterol, and a broad spectrum of secondary metabolites including many antibiotics and mycotoxins.

The fungi colonize dead organic materials in both outdoor and indoor environments. Some fungi are able to invade living plant tissue and cause many important plant diseases. A few fungi will invade living animal hosts, including people. Fungi are also universally present in indoor environments unless specific efforts are made for their exclusion (i.e., as in clean rooms). The kinds of fungi that are able to colonize indoor materials are generally those with broad nutritional requirements (e.g., *Cladosporium sphaerospermum*), those that are able to colonize very dry environments (e.g., members of the *Aspergillus glaucus* group), or organisms that readily degrade the cellulose and lignin present in many indoor materials (e.g., *Chaetomium globosum*, *Stachybotrys atra*, *Merulius lacrymans*). Yeasts (which are unicellular fungi) and other hydrophilic taxa (e.g., Fusarium, Phialophora) are able to colonize air/water interfaces. Water, in fact, is the most important factor controlling indoor fungal growth, since food sources are ubiquitous (Kendrick, 1992).

Particles that become airborne from fungal growth include spores (the unit of most fungal exposure), fragments of the filamentous body of the fungus, and fragments of decomposed substrate material. Fungal spores range from about 1.5 μm to >100 μm in size and come in many different shapes. The simplest are smooth spheres; the most complex are large multicellular branching structures. Most fungal spores are near unit density or less.

Some include large air-filled vacuoles. Fungal spores form the largest and most consistently present component of the outdoor bioaerosols. Levels vary seasonally, with lowest levels occurring during periods of snow. While rain may initially wash large dry spores from the air, these are immediately replaced by wet (hydrophilic) spores that are released in response to the rain.

Some kinds of spores are cosmopolitan in outdoor air (e.g., *Cladosporium herbarum*, *Alternaria tenuissima*). Others produced by fungi with more fastidious nutritional requirements are only locally abundant. A typical indoor fungal aerosol is composed of particles penetrating from outdoors, particles released from active growth on indoor substrates, and reaerosolized particles that have settled into dust reservoirs. Indoor fungal aerosols are produced by active forcible discharge of spores, by mechanisms intrinsic to the fungus that "shake" spores from the growth surface, and (most commonly) by mechanical disturbance (e.g., air movement, vibration).

Allergic rhinitis and asthma are the only commonly reported diseases resulting from fungal exposures outdoors, and which also commonly occur indoors. The allergens of fungi are probably digestive enzymes that are released as the spore germinates. Other spore components (of unknown function) may also be allergenic. Only very few fungal allergens (out of possibly hundreds of thousands) have been characterized: (e.g., *Alt a* I, *Cla h* I, and *Asp f* I).

Allergic fungal sinusitis and allergic bronchopulmonary mycoses occur when fungi colonize thick mucous in the sinuses or lungs of allergic people. The patterns of incidence of allergic fungal sinusitis may be explained in part by geographic variability in ambient fungal exposures. Figure 7-19 shows total fungal spore counts in Kalamazoo, MI, for 1994. This disease is most commonly caused by Bispora, Curvularia, and other dark-spored fungi. Exposure patterns required for allergic bronchopulmonary mycoses are unknown. This disease is usually caused by *Aspergillus fumigatus*. Histoplasmosis and Coccidioidomycoses are fungal infectious diseases that result from outdoor exposures to *Histoplasma capsulatum* (a fungus that contaminates damp soil enriched with bird droppings) and *Coccidioides inmitis* (a fungus that growth in desert soils. Indoor aerosol-acquired fungal infections are rare, and restricted to immunocompromised people (Rippon, 1988).

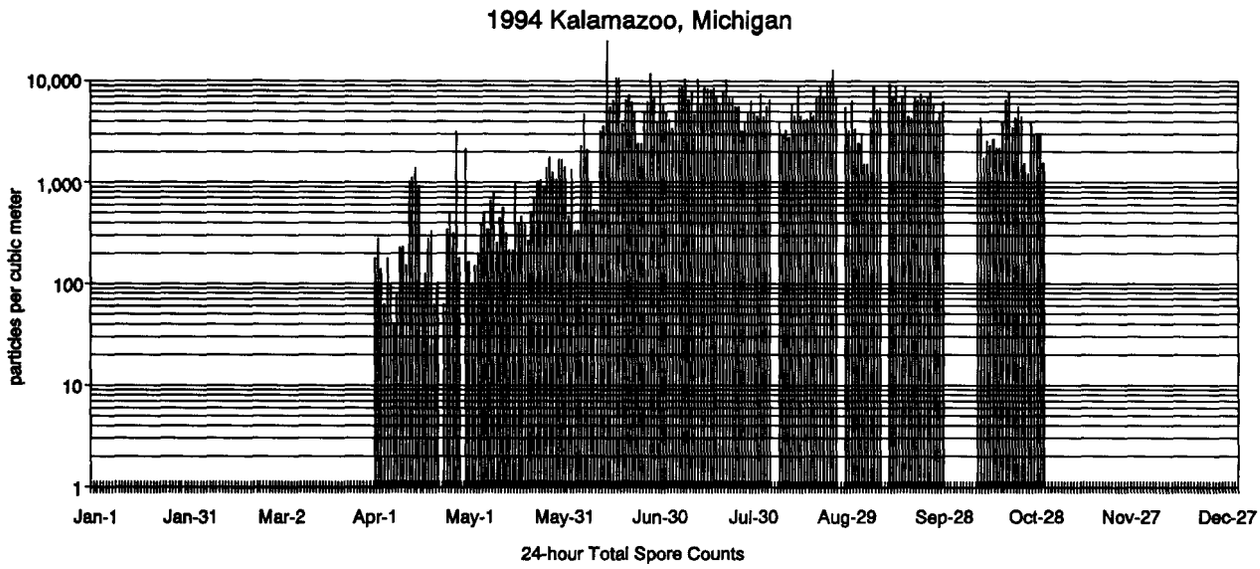

Figure 7-19. Chart of fungal spore prevalence in Kalamazoo, MI, for 1994.

Source:

Toxic agents produced by fungi include antibiotics, mycotoxins, and some cell-wall components that have toxic or irritant properties. The antibiotics and mycotoxins are secondary metabolites that are produced during fungal digestion of substrate materials, and their presence depends, in part, on the nature of the substrate. The locations of the toxins in spores or other mycelial fragments are unknown, as are the dynamics of release in the respiratory tract. Aerosol exposure to fungal antibiotics in levels sufficient to cause disease is unlikely. Mycotoxicoses have been reported as case studies from exposure to spores of *Stachybotrys atra* (Croft et al., 1986), and epidemiologically for *Aspergillus flavus* (Baxter et al., 1981).

7.2.5.4 Bacterial Aerosols

Bacteria, in contrast to plants, animals and fungi, contain neither nuclei or mitochondria. Most are unicellular, although some form "pseudo" filaments when cells remain attached following cell division. The actinomycetes are bacteria that do form filaments and (in some cases) dry spores designed for aerosol dispersal. The bacteria can be broadly categorized into two groups based on a response to the Gram stain procedure. The cell walls of Gram positive bacteria are able to absorb a purple stain; the walls of Gram

negative bacteria resist staining. The Gram negative cell wall contains endotoxin (see above).

Most infectious agents are maintained in diseased hosts. A few, including *Legionella pneumophila*, reside in water-filled environmental reservoirs such as water delivery systems, cooling towers, air conditioners, and (outdoors) oceans, lakes, streams, etc.

Infectious agents are often released from hosts in droplets released from the respiratory tract. Each droplet contains one or more of the infectious agent, probably one or more other organisms, and respiratory secretions. Most droplets are very large and fall quickly. Smaller droplets dry quick to droplet nuclei, which range in size from the size of the individual organism (<1 μm for the smallest bacteria) to clumps of larger organisms (>10 μm for larger bacteria). Environmental-source aerosols are produced by mechanical disturbances that include wind, rain splash, wave action, and by mechanical disturbance such as occurs in recirculation and sprays of washes and coolants, and in humidifiers. Particle sizes from all of these activity cover a wide range from well below 1 μm to >50 μm. The thermophilic actinomycetes produce dry aerial spores that require only slight air movements to stimulate release. Each spore is about 1 μm in diameter.

Whole living bacteria are agents of infectious disease (e.g., Tuberculosis, Legionnaires' disease). For tuberculosis, a single virulent bacterial cell deposited in the appropriate part of the lung is likely to cause disease in a host without specific immunity. For Legionnaires' disease, the number of organisms required to make disease development likely depends on how well the host's general protective immune system is operating. Some bacteria release antigens that cause hypersensitivity pneumonitis. The antigens may be enzymes (e.g., *Bacillus subtilis* enzymes used in the detergent industry) or may be cell wall components as in the thermophilic actinomycetes. Bacteria also produce toxins of which endotoxin is the most important from an aerosol exposure point of view.

7.2.5.5 Viral Aerosols

The viruses are units of either RNA or DNA surrounded by a protein coat. They have no intrinsic mechanism for reproduction, and require living cells whose enzyme systems they utilize to make new particles. They can be crystallized and remain able to reproduce, and are often considered intermediates between non-life and life. Because viruses require living

cells to reproduce, reservoirs for them are almost exclusively living organisms. Rarely, viruses survive (but do not reproduce) in environmental reservoirs from which they are re-aerosolized to cause disease. The Hanta virus that causes severe respiratory disease in people exposed to intense aerosols of infected mouse urine is an example of this phenomenon. Viral aerosols are produced when the infected organism coughs, sneezes, or otherwise forces respiratory or other secretions into the air. The viral particles are coated with secretions from the host, and, as for the bacteria, there may be one to many in a single droplet. The size of a single viral particle is very small (a small fraction of a μm). However, infectious droplets are probably within a much larger size range (1 to 10 μm). Each kind of virus produces a specific disease, although some of the diseases present with similar symptoms. Thus, the measles virus produces measles, the chicken pox viruses produces chicken pox and shingles. Influenza and common colds are produced by a range of viruses all of which produce symptoms that are similar (but not necessarily identical).

7.2.5.6 Ambient and Indoor Air Concentrations of Bioaerosols

A general rough estimate of the contribution of bioaerosols to collected PM mass can be made as follows: for an "average" 3 μm spherical spore of 0.9 density, each spore would weigh $\approx 13 \times 10^{-6}$ μg; for a clean indoor environment with $\approx 10^3$ spores/m^3 the mass would be on the order of 0.01 μg/m^3; for a typical outdoor condition, with $\approx$ 50 x 10^3 spores/m^3, the contribution would be on the order of 0.5 μg/m^3. In contaminated indoor environments, where spore levels above 10^6 spores/m^3 are possible, the spore weight could be on the order of 10 μg/m^3 or more.

In summary, the minor mass concentrations of bioaerosols in ambient and indoor air are independent of the concentrations of the non-bioaerosol constituents in ambient and indoor air. However, the deposition of bioaerosols at the same respiratory tract loci as the other PM can cause irritation and infection foci that may make the affected host more susceptible to the effects of other deposited PM.

7.3 DIRECT METHODS OF MEASUREMENT OF HUMAN PM EXPOSURE BY PERSONAL MONITORING

7.3.1 Personal Monitoring Artifacts

Human exposure to air pollution can be measured by placing a personal exposure monitor (PEM) close to the breathing zone of an individual. However, the very act of studying the subjects can alter their behavior, which influences the measured values of their exposures and creates an erroneous reading. This influence, known as the "Hawthorne Effect" (Mayo, 1960; Last, 1988), arises because the subjects are aware of the study objectives, and the presence of the PEM on their body is a constant reminder.

The physical location of the monitor inlet, as worn by the subject, can also influence the subject's PM exposure and the recorded PM (Cohen et al., 1982, 1984). The movements of the subject's body and the PEM sampling flow rate can alter the air currents in the subject's breathing zone. "The presence of the body and its movement affect what a personal sampler collects" (Ogden et al., 1993). When in close proximity to a source actively emitting PM (within a meter) a small change in PEM position (e.g. from left side to right side) can vary the PM measurement. The vertical position of the personal monitor sampling inlet (e.g., at the waist or at the lapel near the breathing zone), can influence the captured amount of PM that is generated from the floor and stuffed furniture (Aso et al., 1993).

In performance of a personal monitoring study, people often refuse to participate. The refusal rate increases with the burden on the respondents due to the time required to complete questionnaires, diaries and the need to carry the personal monitor with them throughout the study. If the cohort of people who refuse to participate have significantly different personal PM exposures than the participants, then the study will produce a biased estimate of the exposures of the total population.

Two other important errors that influence the personal exposure measurements are: (1) "the monitor effect", by which the monitor reduces PM concentration in the breathing zone by "self dilution" (Cohen et al., 1984), the alteration of stream lines in the area of the nose and mouth, or by electrostatic charge on a plastic cassette filter holder collecting charged particles (Cohen et al., 1982); and (2) "the subject effect", by which the subject

contaminates the data set by a purposeful action, such as blowing smoke into the inlet, or forgetting to wear the monitor and not admitting that error in the log of daily activity.

These unquantifiable "errors" in a PM PEM measurement study may be greater than the filter weighing errors and flow rate measurement errors that can be quality controlled through calibration procedures. This may be important for interpretation of published PM PEM data because these errors likely inflate the variance of the measurements.

7.3.2 Characterization of Particulate Matter Collected by Personal Monitors

The amount of PM collected by different types of personal monitors with the identical nominal cut-point can be variable. The difference between two PM measurements, made by two nominally identical monitors of different design, can be a function of the wind speed and the size distribution of the PM in the air mass being sampled. A recent field comparison by Groves et al. (1994) of different types of respirable dust samplers used in occupational settings where coarse mode PM predominates shows that there is considerable difference between the mass collected by sets of paired cyclones and paired impactors sampling in a concentration range of 500 to 6600 $\mu g/m^3$. The cyclones collected from 53 to 165% of the mass collected by the impactors. This type of comparison study has not been done for personal monitors used in nonoccupational studies at ambient and indoor respirable PM concentrations on the order of 10 to 100 $\mu g/m^3$, where the fine mode can be more important.

7.3.3 Microscale Variation and the Personal Cloud Effect

The study of Thatcher and Layton (1995) described in Section 7.2.2.2 reports the increase of indoor PM of various size ranges from household activities, such as walking into and out of a room. The tendency for such human activity in the home or at work to generate a "personal activity cloud" of particles from clothing and other items (stuffed furniture, carpet, etc.), that will be intense in the breathing zone and diluted near an area monitor located several meters away, has also been cited as a contributing factor to the discrepancy between personal measures of exposure and time-weighted-average (TWA) exposures using microenvironmental measurements (Martinelli et al., 1983; Cohen et al., 1984; Rodes et al., 1991). Fletcher and Johnson (1988) also measured metal concentrations (measurement

method and size unspecified) in an occupational exposure situation (metal spraying of spindles on a lathe) and found 50% higher concentrations measured from the left lapel compared to the right lapel, which reflected the orientation of the operator to the lathe.

7.4 NEW LITERATURE ON PARTICLE EXPOSURES SINCE 1981

The following sections review studies that measured PEM PM in the general non-smoking population. In these studies, the subjects spent time at home and in other indoor environments that include time at work. In the USA, recent data indicate that on a daily basis, an average US resident spends approximately 21 h indoors (85.6%), 100 minutes in (or near) a vehicle (7.2%), and 100 minutes outdoors (7.2%) (U.S. Environmental Protection Agency, 1989).

Almost all the studies of PM exposure in the general public have been conducted on urban and suburban residents. These subjects are often working in occupations that do not require PM monitoring to assure that occupational standards are being met (e.g. in an office). However, PM monitoring in an industrial workplace by a subject - independently of an official corporate industrial hygiene program - can have legal or security implications for an employer. A further complication arises from the fact that industrial exposures tend to be dominated by a specific type of particle. Coal miners are exposed to coal dust, textile workers are exposed to cotton dust, etc.

7.4.1 Personal Exposures in U.S. Studies

Dockery and Spengler (1981b) compared personal $PM_{3.5}$ exposures and ambient $PM_{3.5}$ concentrations in Watertown, MA, and in Steubenville, OH. In Watertown, 24-h personal samples were collected on a 1-in 6-day schedule, and in Steubenville, 12-h personal samples (8 a.m. to 8 p.m.) were collected on a Monday-Wednesday-Friday schedule. A correlation coefficient of 0.692 between the mean personal and the mean ambient concentration for 37 subjects, 18 in Watertown and 19 in Steubenville, was reported for the pooled data. However, this appears to be an artifact of two separate clusters formed by these data, each with considerably lower correlation. When these data are analyzed separately, the regression

coefficient between personal and ambient for Watertown is $R^2 = 0.00$ and for Steubenville it is $R^2 = 0.18$.

Sexton et al. (1984) studied personal exposures to respirable particles ($PM_{3.5}$) for 48 nonsmokers during a winter period in Waterbury, VT, where firewood was either the primary or secondary heating source for the subject. Their results showed that personal exposures were 45% higher than indoor averages (36 $\mu g/m^3$ versus 25 $\mu g/m^3$) and indoor averages were 45% higher than outdoor averages (25 $\mu g/m^3$ versus 17 $\mu g/m^3$). Ambient air pollution, measured by an identical stationary ambient monitor (SAM) outside each residence (a pump contained in a heated box was connected to an external cyclone and filter), had no correlation with the residents' personal exposures ($R^2 = 0.00$) and 95% of the subjects had personal exposures *greater* than the median outdoor concentration.

Spengler et al. (1985) reported a study of $PM_{3.5}$ exposures in the non-industrial cities of Kingston and Harriman, TN, during the winter months of February through March, 1981. In this study, two Harvard/EPRI $PM_{3.5}$ monitors were used for each person. One stationary indoor monitor (SIM) remained indoors in the home, and the second monitor (PEM) was carried for 24-h to obtain the personal exposure. In each community, identical Harvard/EPRI samplers (SAM) were placed at a central site to represent ambient $PM_{3.5}$ concentrations. The results of the study are shown in Table 7-19. In both communities, 95% of the subjects had personal exposures to $PM_{3.5}$ *greater* than the average ambient concentrations. The mean personal exposure and indoor concentrations (44 ± 3 $\mu g/m^3$ and 42 ± 3 $\mu g/m^3$) were more than 100% greater than the mean ambient average of 18 ± 2 $\mu g/m^3$ sampled on the same days.

For the complete cohort, the correlation between PM PEM and PM SAM was $r = 0.07$ ($p = 0.30$), and between PM PEM and PM SIM was $r = 0.70$ ($p = 0.0001$). The correlation between simultaneous PM PEM and PM SAM was $r = 0.15$ for 162 nonsmoke exposed individual observations ($p = 0.06$). For 63 observations on smoke exposed individuals, the correlation $r = 0.16$ was not significant ($p = 0.16$) between PM PEM and PM SAM. An important finding was that in nonsmoking households, the PM PEM is always higher than SIM and SAM. "This implies that individuals encounter elevated concentrations away from home and/or that home concentrations are elevated while they are at home and reduced while they are away". This observation is supported by the findings of Thatcher and

TABLE 7-19. QUANTILE DESCRIPTION OF PERSONAL, INDOOR, AND OUTDOOR $PM_{3.5}$ CONCENTRATIONS ($\mu g/m^3$), BY LOCATION IN TWO TENNESSEE COMMUNITIES

City	Group	N	95%	75%	50%	25%	5%	Mean	S.E.
Kingston	Personal	133	99	47	34	26	19	42	2.5
	Indoor	138	110	47	31	20	10	42	3.5
	Outdoor	40	28	22	16	12	6	17	2.7
Harriman	Personal	93	122	54	35	24	15	47	4.8
	Indoor	106	129	45	27	18	10	42	4.1
	Outdoor	21	34	23	15	13	9	18	4.0
Total[a]	Personal	249	113	48	34	26	17	44	2.8
	Indoor	266	119	46	29	20	10	42	2.6
	Outdoor	71	33	23	17	13	7	18	2.1

[a]Includes samples from 13 subjects living outside Kingston and Harriman town limits and from four field personnel residing in these communities.
N = number of samples.
S.E. = Standard error.

Source: Spengler et al. (1985).

Layton (1995), reported in Section 7.2.2.2: merely walking into a room can raise the concentrations of PM by 100%. This study is relevant to the analyses by Dockery et al. (1992) of PM mortality in St. Louis, MO, and in Eastern Tennessee counties surrounding Kingston and Harriman as discussed in Chapter 12. Although the Spengler et al. (1985) and Dockery et al. (1992) studies are not directly comparable, because different years of data were used (1981 versus 1985/1986), the authors' assumption in Dockery et al. (1992) that the Harriman, TN, data represent exposures to PM in all of eastern Tennessee is called into question.

Morandi et al. (1988) investigated the relationship between personal exposures to PM and indoor and outdoor PM concentrations, using a TSI Model 3500 piezobalance that measures respirable particles in the range <3.5 μm. For the group of 30 asthmatics in Houston, TX, that were studied, outdoor concentrations averaged 22 $\mu g/m^3$, indoor concentrations averaged 22% higher than outdoor (27 $\mu g/m^3$) and, in motor vehicles, the average concentration of particles was 60% higher than the average outdoors (35$\mu g/m^3$).

Personal 12-h (7 a.m. to 7 p.m.) daytime exposures to PM were not predicted as well by fixed site dichotomous sampler ambient monitors (R^2 = 0.34) as by the indoor exposures (R^2 = 0.57). However, for 1-h exposures, they found no correlation (R^2 = 0.00) between the personal exposures to PM_5 and the indoor exposures measured with a TSI model 5000 stationary continuous piezobalance located in the "den" area of the home. The authors noted that use of home air conditioning and recirculation tended to increase the PM exposures.

Lioy et al. (1990) reported a study done during the winter (January 1988) in the industrial community of Phillipsburg, NJ, where personal PM_{10} was monitored along with indoor and outdoor PM_{10}. They collected PM_{10} (fine plus coarse particles on a single filter). In this study of eight residences of 14 nonsmoking individuals not smoke exposed at home, geometric mean 24-h concentrations were 68, 48 and 42 $\mu g/m^3$ for personal, outdoor and indoor sites, respectively. The arithmetic mean personal PM exposure of 86 $\mu g/m^3$ was 45% higher than the mean ambient concentration of 60 $\mu g/m^3$. The higher ambient than indoor concentrations in this study, a reversal of the relationships found in the Sexton et al. (1984), Spengler et al. (1985) and Morandi et al. (1988) studies, may be caused by the local industrial source of coarse particles in that community and the absence of cigarette smokers in the residences sampled. This difference also may be partially explained by the 10 μm particle sizes sampled in the NJ study and the 3.5 μm particle sizes in the other studies. The regression coefficient between personal and ambient PM_{10} for all 14 people on the 14 days of the study (n = 191 valid personal values) was 0.19 (R^2 = 0.037, p = 0.008). With three personal exposure extreme values removed (n = 188 personal values) and without correction for missing data, the coefficient was 0.50 (R^2 = 0.25, p = 0.007).

Lioy et al. (1990) report individual regression equations of PEM and SAM for the six of 14 subjects with significant relationships ($p < 0.01$). These data are shown in Table 7-20. For individuals with constant daily activities in the same microenvironments, the increment of PM exposure due to nonambient sources is repeatable with lower variability than that of the ambient PM. Therefore their variation of personal exposure from day-to-day is highly driven by the variation of the ambient PM. For subjects with intermittent exposures to nonambient PM, through non-repetitive activity patterns or intermittent source operation, the regression of PEM on SAM can become non-significant. This improvement in

TABLE 7-20. REGRESSION EQUATION OF THOSE INDIVIDUALS HAVING STATISTICALLY SIGNIFICANT RELATIONSHIPS OF EXPOSURE (PEM) WITH OUTDOOR AIR CONCENTRATIONS (SAM)

Participant	Equation	R^2	N	p
01	y = 0.62 (0.12) X + 26.5 (17.3)	0.66	14	< 0.01
31	y = 0.55 (0.07) X + 7.3 (9.9)	0.83	14	< 0.01
52	y = 0.63 (0.11) X + 15.3 (14.7)	0.74	14	< 0.01
62	y = 1.29 (0.27) X + 33.0 (37.1)	0.67	13	< 0.01
81	y = 1.07 (0.24) X + 39.0 (32.6)	0.63	14	< 0.01
91	y = 0.59 (0.12) X + 42.0 (19.9)	0.63	13	< 0.01

y = Personal air PM-10.
X = Outdoor air PM-10.
( ) = Confidence interval.

Source: Lioy et al. (1990).

correlation was also shown for their indoor versus outdoor relationships, between cross-sectional and individual comparisons, as described in Section 7.4.2.3.

In all these studies, the personal PM was measured to be higher than either the indoor or the outdoor PM measurements. This relationship of PEM > SIM and PEM > SAM has also been found in the PTEAM study (Clayton et al., 1993) described in detail in Section 7.2.2.1.3 and later in Section 7.4.1.1. For the PTEAM study during the day (7 a.m. to 7 p.m.) average personal PM_{10} exposure data (150 $\mu g/m^3$) were 57% higher than the average indoor and outdoor concentrations, which were virtually equal (95 $\mu g/m^3$). Consequently, a time-weighted-average (TWA) of the daytime indoor and outdoor PM concentrations appears to always underestimate the personal exposures to PM because the daytime PEM data are higher than either the SIM or SAM data. At night (7 p.m. to 7 a.m.) average PM_{10} personal exposures (77 $\mu g/m^3$) were higher than the average indoor concentrations (63 $\mu g/m^3$) but lower than the average outdoor concentration (86 $\mu g/m^3$).

It has been proposed (World Health Organization, 1982a; Spengler et al., 1985; Mage, 1985) that such a discrepancy between the TWA and the personal monitoring measurements may be caused by two factors described as follows: (1) human exposure to PM at work and in traffic are only partially accounted for in a TWA of indoor and outdoor ambient PM

values; and (2) indoor and outdoor averages reflect periods of low concentration during which the subject is not present. The PM pollution generating activities in a home usually occur only when a person is at home, as discussed in Section 7.1.2 concerning Equation 7-2. Therefore, the PM in a home will be higher when a person is present than when the home is unoccupied. A 24-h average of the indoor concentration thereby underestimates the average exposure of a person while in that home.

Ambient PM is also higher during the day (when industry and traffic are active, and wind speeds are high) than at night when PM generating activities are at a minimum and the air is still (Miller and Thompson, 1970). Consequently, a 24-h average ambient PM value generally underpredicts the concentrations during the daylight hours and the exposures of people going outdoors during that period.

7.4.1.1 The Particle Total Exposure Assessment Methodology Study

In 1986, the U. S. Congress mandated that EPA's Office of Research and Development "carry out a TEAM Study of human exposure to particles." The main goal of the study was to estimate the frequency distribution of exposures to particles for nonsmoking Riverside, CA, residents. Another goal was to determine particle concentrations in the participants' homes and immediately outside the homes. The detailed analyses of the indoor PM and outdoor PM data were described in Section 7.2.2.1.3.

7.4.1.1.1 Pilot Study

Study Design

A prepilot study, described in Section 7.2.2.1.3, was undertaken in nine homes in Azusa, CA in March of 1989 to test the sampling equipment (Özkaynak et al., 1990). Newly-designed personal exposure monitors (PEMs) were equipped with thoracic (PM_{10}) and fine ($PM_{2.5}$) particle inlets. The PEMs were impactors with 4-Lpm Casella pumps (Wiener, 1988). Two persons in each household wore the PEMs for two consecutive 12-h periods (night and day). Each day they alternated inlet nozzles. A central site with a PEM, a microenvironmental monitor (MEM), and two EPA reference methods (dichotomous and high-volume samplers) with a 10 μm size-selective inlet was also operated throughout the 11 days (22 12-h periods) of the study.

Results

The personal exposure levels were about twice as great as the indoor or outdoor concentrations for both PM_{10} (Table 7-21a) and $PM_{2.5}$ (Table 7-21b). Considerable effort was expended to demonstrate that this was not a sampling artifact, due for example to the constant motion of the sampler; however, no evidence could be found for an artifactual effect. Nonetheless, to reduce chances for an artifactual finding in the main study, it was decided to use identical PEMs for both the personal and fixed (indoor and outdoor) samples in the main study. Cross-sectional personal exposures were essentially uncorrelated (slightly negatively) with outdoor concentrations (R^2 = 0 to 2%) (Özkaynak et al., 1993a). However, a serial correlation analysis of these pilot PTEAM data were performed for the six or eight 12-h averages that comprised the three or four 24-h averages reported for the residents of the first five homes in Table 7-21a,b. The residents of four homes only carried the PEM for two days, so the four 12-h individual measurements were too few for development of a meaningful serial relationship. The results for the ten people in homes 1 to 5 are shown in Table 7-22. The medians of R^2 equal 0.12 for PEM $PM_{2.5}$ vs SAM $PM_{2.5}$ and 0.07 for PEM PM_{10} vs SAM PM_{10}, neither of which is significant. More importantly, the serial slopes were positive for 15 of the 20 cases which is the expected behavior, as opposed to the counter-intuitive negative correlation found for the pooled PEM vs SAM data for all residents of the nine homes.

In Azusa, the excess $PM_{2.5}$ and PM_{10} generated by personal activities increased the personal exposures by approximately 100% above the average of the indoor and outdoor values. These results are in marked contrast to the data of Tamura and Ando (1994) and Tamura et al. (1996) in which seven Japanese elderly housewives and male retirees had PM_{10} PEM exposures less than the time weighted average of SIM and SAM PM_{10} concentrations.

7.4.1.1.2 Main Study

Study Design

Ultimately 178 residents of Riverside, CA took part in the study in the fall of 1990. Respondents represented 139,000 ± 16,000 (S.E.) nonsmoking Riverside residents aged 10 and above. Their homes represented about 60,000 Riverside homes. Each participant wore the PEM for two consecutive 12-h periods. Concurrent PM_{10} and $PM_{2.5}$ samples were

TABLE 7-21a. PARTICLE TOTAL EXPOSURE ASSESSMENT METHODOLOGY PREPILOT STUDY: 24-HOUR PM_{10} CONCENTRATIONS ($\mu g/m^3$)

House	Day	Person 1	Person 2	Indoors	Outdoors
1	1	102	86	54	132
1	3	142	125	38	49
1	5	158	150	49	70
1	7	92	127	34	49
2	1	109	158	122	112
2	3	99	140	37	48
2	5	131	87	41	70
2	7	62	56	32	46
3	1	98	107	86	115
3	3	100	141	39	45
3	5	143	132	71	79
3	7	76	103	36	44
4	2	109	92	77	102
4	4	90	77	34	47
4	6	99	122	36	37
5	2	80	104	76	99
5	4	70	77	62	65
5	6	80	78	54	50
6	8	130	152	114	39
6	10	150	102	106	51
7	9	209	126	46	72
7	11	80	71	29	39
8	9	135	178	73	59
8	11	97	151	38	28
9	8	136	102	63	43
9	10	273	91	121	48
Mean		117.2	112.9	60.3	63.0
SD		44.9	30.8	28.5	27.1
SE		8.8	6.0	5.6	5.3

Source: Data from PTEAM Prepilot Study used to calculate R^2 values as shown in Table 7-22 and published by Wallace (1996).

TABLE 7-21b. PARTICLE TOTAL EXPOSURE ASSESSMENT METHODOLOGY PREPILOT STUDY: 24-H $PM_{2.5}$ CONCENTRATIONS ($\mu g/m^3$)

House	Day	Person 1	Person 2	Indoors	Outdoors
1	2	44	96	22	67
1	4	55	88	25	39
1	6	55	382	21	33
2	2	58	53	31	52
2	4	46	100	27	43
2	6	51	50	28	40
3	2	53	66	48	58
3	4	62	94	30	35
3	6	109	88	39	39
4	1	75	61	33	71
4	3	46	43	19	29
4	5	118	94	31	46
4	7	40	40	17	26
5	1	65	69	62	96
5	3	59	70	35	38
5	5	40	56	42	55
5	7	34	53	25	28
6	9	71	81	56	33
6	11	77	75	53	18
7	8	64	135	17	27
7	10	111	67	32	35
8	8	53	100	27	27
8	10	110	1453*	35	35
9	9	178	48	70	40
9	11	105	58	42	28
Mean		71.2	140.8*	34.7	41.6
SD		32.7	275.5	13.7	16.8
SE		6.5	55.1	2.7	3.4

* Horseback riding at an indoor ring. If this point is deleted, mean = 86.1.

Source: Data from PTEAM Prepilot Study used to calculate R^2 values as shown in Table 7-22 and published by Wallace (1996).

TABLE 7-22. REGRESSIONS OF PERSONAL EXPOSURE ON INDOOR AND OUTDOOR PM_{10} AND $PM_{2.5}$ CONCENTRATIONS: PARTICULE TOTAL EXPOSURE ASSESSMENT METHODOLOGY PREPILOT STUDY

House	Person	N	Intercept	SE	p	Slope	SE	p	R^2
PM_{10}: Personal vs. Outdoor									
1	1	8	124	42	0.03	−0.0004	0.51	NS	0
	2	8	134	60	NS	−0.16	0.73	NS	0.01
2	1	8	47	44	NS	0.77	0.58	NS	0.23
	2	8	26	52	NS	1.22	0.68	NS	0.35
3	1	8	83	47	NS	0.3	0.61	NS	0.04
	2	8	116	54	NS	0.07	0.7	NS	0.002
4	1	6	87	20	0.01	0.2	0.29	NS	0.1
	2	6	106	28	0.02	−0.15	0.4	NS	0.03
5	1	6	47	31	NS	0.42	0.41	NS	0.2
	2	6	22	26	NS	0.9	0.35	NS	0.63
$PM_{2.5}$: Personal vs. Outdoor									
1	1	6	41	20	NS	0.22	0.4	NS	0.07
	2	6	274	266	NS	−1.8	5.3	NS	0.03
2	1	6	8.8	20	NS	0.96	0.41	NS	0.58
	2	6	47	34	NS	0.47	0.7	NS	0.1
3	1	6	87	58	NS	−0.29	1.25	NS	0.01
	2	6	40	54	NS	0.97	1.2	NS	0.15
4	1	8	40	24	NS	0.7	0.48	NS	0.26
	2	8	45	22	NS	0.34	0.45	NS	0.09
5	1	8	27	15	NS	0.42	0.24	NS	0.34
	2	8	46	16	0.03	0.3	0.27	NS	0.17

NS = not significant ($p > 0.05$).
N = Number of 12-h observations.

Source: Wallace (1996).

collected by the stationary indoor monitor (SIM) and stationary ambient monitor (SAM) at each home. A total of ten particle samples were collected for each household (day and night samples from the PEM_{10}, SIM_{10}, $SIM_{2.5}$, SAM_{10}, and $SAM_{2.5}$). Air exchange rates were also determined for each 12-h period. Participants were asked to note activities that might involve exposures to increased particle levels. Following each of the two 12-h monitoring

periods, they answered an interviewer-administered questionnaire concerning their activities and locations during that time. A central outdoor site was maintained over the entire period (September 22, 1990 through November 9, 1990). The site had two high-volume samplers (Wedding & Assoc.) with 10-μm inlets (actual cutpoint about 9.0 μm), two dichotomous PM_{10} and $PM_{2.5}$ samplers (Sierra-Andersen) (actual cutpoint about 9.5 μm), one PEM, one PM_{10} SAM, and one $PM_{2.5}$ SAM.

Results

Of 632 permanent residences contacted, 443 (70%) completed the screening interview. Of these, 257 were asked to participate and 178 (69%) agreed.

Quality of the Data

More than 2,750 particle samples were collected, about 96% of those attempted. All filters were analyzed by X-ray fluorescence (XRF) for a suite of 40 metals. More than 1,000 12-h average air exchange rate measurements were made. A complete discussion of the quality of the data is found in Pellizzari et al. (1993) and in Thomas et al. (1993).

Concentrations

Concentrations of particles and target elements have been reported (Clayton et al., 1993; Özkaynak et al., 1993a; Pellizzari et al., 1993; Wallace et al., 1993). Population-weighted daytime personal PM_{10} concentrations averaged about 150 $\mu g/m^3$, compared to concurrent indoor and outdoor mean concentrations of about 95 $\mu g/m^3$ (Table 7-23). The overnight personal PM_{10} mean was much lower (77 $\mu g/m^3$) and more similar to the indoor (63 $\mu g/m^3$) and outdoor (86 $\mu g/m^3$) means. About 25% of the population was estimated to have exceeded the 24-h National Ambient Air Quality Standard for PM_{10} of 150 $\mu g/m^3$. Over 90% of the population exceeded the 24-h California Ambient Air Quality Standard of 50 $\mu g/m^3$.

Correlations

The central site appeared to be a moderately good estimator of outdoor particle concentrations throughout the city. Spearman correlations of the central-site concentrations

TABLE 7-23. POPULATION-WEIGHTED[a] CONCENTRATIONS AND STANDARD ERRORS ($\mu g/m^3$) PTEAM STUDY

Sample type	N	Geom. Mean	GSD	Arith. Mean ± SE	Percentile 90% ± SE	Percentile 98%
Daytime PM_{10}						
Personal	171	129	1.75	150 ± 9	260 ± 12	380
Indoor	169	78	1.88	95 ± 6	180 ± 11	240
Outdoor	165	83	1.68	94 ± 6	160 ± 7	240
Overnight PM_{10}						
Personal	168	68	1.64	77 ± 4	140 ± 10	190
Indoor	163	53	1.78	63 ± 3	120 ± 5	160
Outdoor	162	74	1.74	87 ± 4	170 ± 5	210
Daytime $PM_{2.5}$						
Indoor	173	35	2.25	48 ± 4	100 ± 7	170
Outdoor	167	38	2.07	49 ± 3	100 ± 6	170
Overnight $PM_{2.5}$						
Indoor	166	27	2.21	36 ± 2	83 ± 6	120
Outdoor	161	37	2.23	51 ± 4	120 ± 5	160

[a]Personal samples weighted to represent nonsmoking population of 139,000 Riverside residents aged 10 or above. Indoor-outdoor samples weighted to represent 61,500 homes with at least one nonsmoker aged 10 or above.

Source: Pellizzari et al. (1993).

measured by all three methods (PEM-SAM, dichot, Wedding) with outdoor near-home concentrations as measured by the SAMs ranged from 0.8 to 0.85 ($p<0.00001$). Linear regressions indicated that the central-site 12-h readings could explain 57% of the variance observed in the near-home 12-h outdoor concentrations (Figure 7-20).

Outdoor 12-h concentrations of PM_{10} could explain about 25 to 30% of the variance observed in indoor concentrations of PM_{10}, but only about 16% of the variance in 12-h personal exposures to PM_{10} (Figure 7-21). This is understandable in view of the importance of indoor activities such as smoking, cooking, dusting, and vacuuming on exposures to

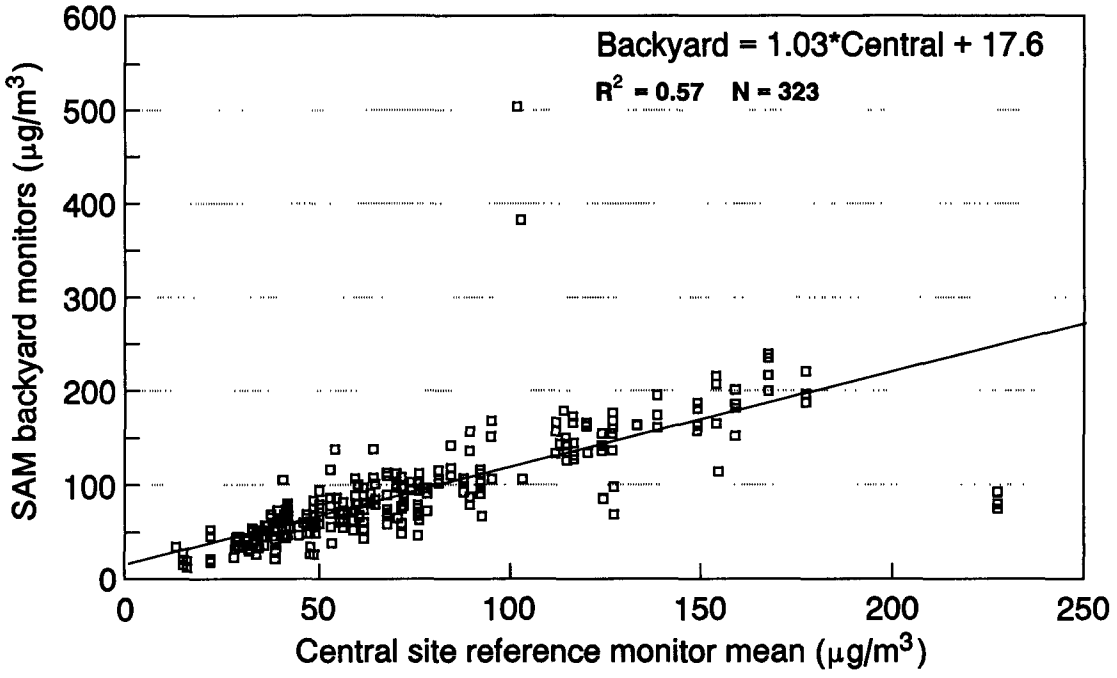

Figure 7-20. Residential outdoor monitors versus central-site mean of two dichotomous samplers in Riverside, CA. R^2 = 57%.

Source of Data: Pellizzari et al. (1993).

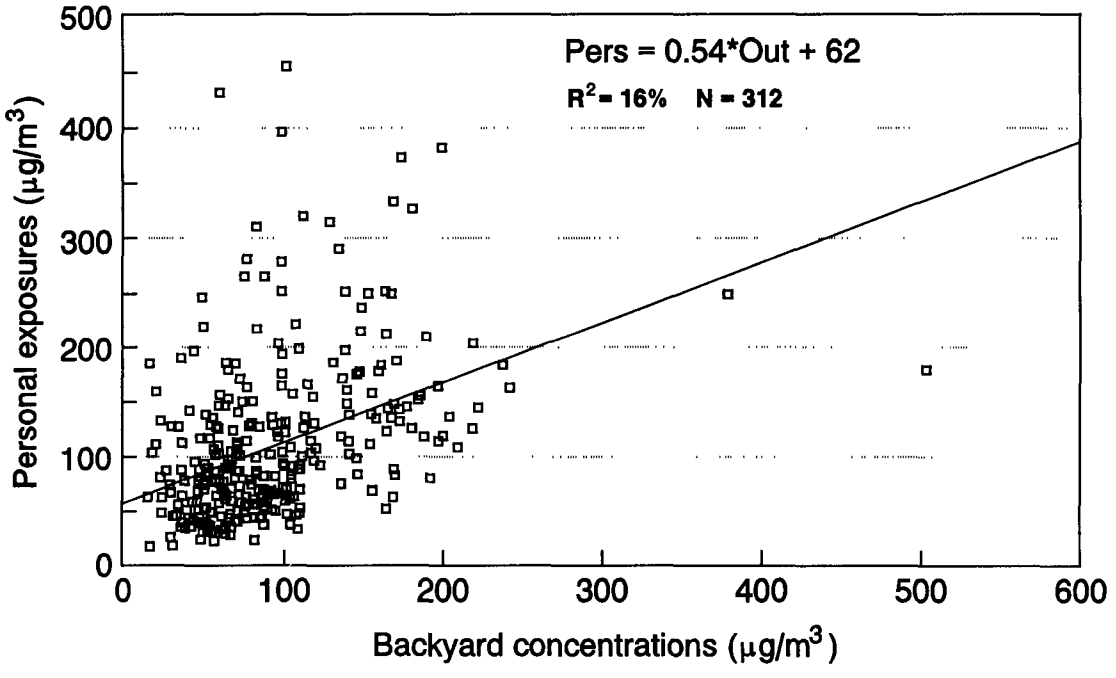

Figure 7-21. Personal exposures versus residential (back yard) outdoor PM_{10} concentrations in Riverside, CA. R^2 = 16%.

Source of Data: Pellizzari et al. (1993).

particles. The higher daytime exposures were even less well represented by the outdoor concentrations.

Indoor concentrations accounted for about half of the variance in personal exposures. However, neither the indoor concentrations alone, nor the outdoor concentrations alone, nor time-weighted averages of indoor and outdoor concentrations could do more than explain about two-thirds of the observed variance in personal exposures. The remaining portion of personal exposure is assumed to arise from personal activities or unmeasured microenvironments that are not well represented by fixed indoor or outdoor monitors.

Discussion

The more than 50% increase in daytime personal exposures compared to concurrent indoor or outdoor concentrations suggested that personal activities were important determinants of exposure. However, the nature of this "personal cloud" of particles has not yet been determined. An approach to the composition of the personal cloud is elemental analysis, using X-ray fluorescence. Analysis of all personal and indoor filters showed that 14 of 15 elements were elevated by values of 50 to 100% in the personal filters compared to the indoor filters (Figure 7-22). This observation suggests that a component of the personal cloud is an aerosol of the same general composition as the indoor aerosol. This could be particles created by activities (e.g., cooking) or re-entrained household dust from motion (walking across carpets or sitting on upholstered furniture; Thatcher and Layton, 1995). House dust is a mixture of airborne outdoor PM (primarily coarse mode), tracked-in soil and road dust, and PM produced by indoor sources. As such, it should contain crustal elements from soil, lead and bromine from automobiles, and other elements from combustion sources. This would be consistent with the observation that nearly all elements were elevated in personal samples. The lack of elevated values for sulfur may be due to the fact that submicron particles are not resuspended by human activity (Thatcher and Layton, 1995). The personal overnight samples that showed smaller mass increases than the personal daytime samples are also consistent with the fact that the participants were sleeping for much of the 12-h overnight monitoring period and were thus not engaging in these particle-generating or reentraining activities.

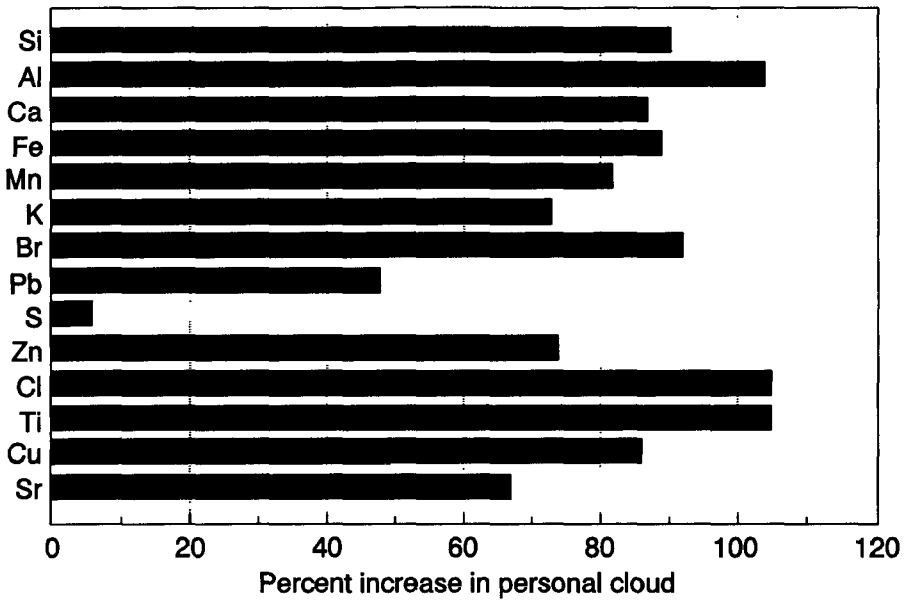

Figure 7-22. Increased concentrations of elements in the personal versus the indoor samples.

Source: Özkaynak et al. (1996).

A source apportionment of the personal PM_{10} mass during the daytime period is shown on Figure 7-23 (Özkaynak et al., 1996). This chart is derived by subtracting the average SIM and SAM (95 $\mu g/m^3$) from the mean PEM (150 $\mu g/m^3$) given on Table 7-23. The 55 $\mu g/m^3$ difference is shown as the 37% fraction of the total of 150 $\mu g/m^3$ labelled Personal 37%. The source of this "personal cloud" is indeterminable from the SIM, SAM and PEM data. As discussed previously, it is likely to consist primarily of resuspended dust that would have a composition of a mixture of all the other sources. The 15% other-indoor PM represents the indoor mass that could not be assigned to ETS, cooking or ambient PM. It is likely that the 52% of other-indoor plus personal-cloud categories contains an appreciable amount of ambient PM that came indoors over a long period of time and is resuspended by activity. If so, then the PEM would be about 50% of ambient origin.

7.4.2 Personal Exposures in International Studies

As part of World Health Organization/United Nations Environment Programme (WHO/UNEP) Global Environment Monitoring System (GEMS) activities, four pilot studies

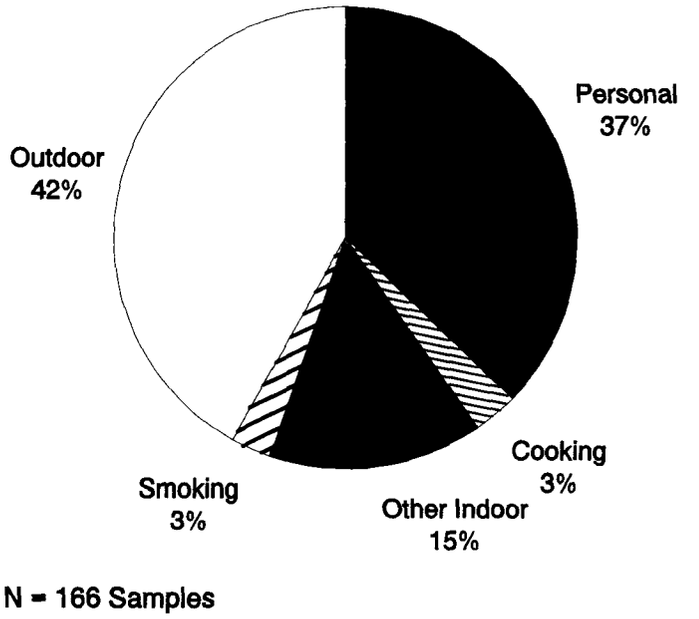

Figure 7-23. Source apportionment of PTEAM PM_{10} Personal Monitoring (PEM) Data. "Other Indoor" represents PM found by the indoor monitor (SIM), for which the source is unknown. "Personal" represents the excess PM captured by the PEM that cannot be attributed to either indoor (SIM) or outdoor (SAM).

Source: Clayton et al. (1993).

of personal exposure to PM were conducted in: Zagreb (World Health Organization, 1982a); Toronto (World Health Organization, 1982b); Bombay (World Health Organization, 1984); and Beijing (World Health Organization, 1985). In these studies, people who worked in the participating scientific institutes were recruited to carry a PM sampler, and their exposures were matched to the ambient concentrations measured outside their home or at a central station in their communities. The results of these studies, expressed as mean personal exposure (PEM) and mean ambient (SAM) concentration, and the cross-sectional regression R^2 between them are presented in Table 7-24.

The net result of these four international studies is that they appear to confirm the lack of a consistent cross-sectional relationship between individual personal PM exposures and ambient concentrations as found in the U.S. studies described in Section 7.4.1.

TABLE 7-24. SUMMARY OF WHO/UNEP GLOBAL ENVIRONMENT MONITORING SYSTEM/PERSONAL EXPOSURE PILOT STUDY RESULTS

Location Season	PM Size Cut (μm)	N	m	Time	PEM Mean ± SE	SAM Mean ± SE	R^2 PEM vs. SAM	p
Toronto	25*	13		8-h				
Winter			72		122±9	68±9	0.15	NS
Summer			78		124±4	78±4	0.10	NS
Zagreb	5	12		1-wk				
Summer			12		114±?	55±?	0.00	NS
Winter			12		187±?	193±?	0.50	NR
Bombay	3.5	15		24-h				
Winter			105		127±6	117±5	0.26	NR
Summer			102		67±3	65±3	0.20	NR
monsoon			101		58±3	51±2	0.02	NS
Beijing	3.5	20						
Winter			71	24-h	177±?	421±?	0.07	NS
Summer			40	1-wk	66±?	192±?	0.03	NS

N = number of subjects carrying personal exposure monitor (PEM).
m = total number of observations.
PEM = mean ± SD of PM concentrations (in $\mu g/m^3$) from personal exposure monitors.
SAM = mean ± SD of PM concentrations (in $\mu g/m^3$) from stationary ambient monitors.
NR = Not Reported, but listed as significant.
NS = Not significantly different from 0.
? = Not Reported.
*25 μm AD computed from flow rate and open filter design.

Source: World Health Organization (1982a,b, 1984, 1985).

7.4.2.1 Personal Exposures in Tokyo (Itabashi Ward), Japan

Tamura and Ando (1994), National Institute for Environmental Studies (1994) and Tamura et al. (1996) report results of a PM personal monitoring study conducted during 1992 in Tokyo. Seven elderly non-smoke exposed individuals who lived in traditional Japanese homes with "tatami" reed mat or carpeting on tatami or wooden flooring, and cooked with city gas, carried a PEM cascade impactor with cut-points of 2 μm and 10 μm (Sibata Science Technology, Ltd.). The seven individuals lived near the Itabashi monitoring station close to a main road. Indoor PM (SIM) and outdoor PM (SAM) were measured simultaneously for 11 48-h periods distributed in all four seasons of the year. The dataset was screened to remove observations that included indoor combustion source exposures, such as ETS from visitors, and burning of incense or mosquito coils. The reported findings were as follows:

1. The cross sectional correlation coefficient of SIM vs SAM was "relatively high" ($r^2 = 0.72$), but the individual coefficients for each house were higher as shown in Figure 7-24.

2. The cross sectional correlation coefficient of PEM vs SAM (measured under the eaves of the subject's house) was "relatively high" ($r^2 = 0.70$), but the individual coefficients for most of the subjects were higher as shown in Table 7-25.

3. The cross sectional correlation coefficient of PEM vs PM measured at the Itabashi monitoring station was slightly lower than that for the outside air ($r^2 = 0.68$), as shown in Figure 7-25, and the individual coefficients for most of the subjects were higher as shown in Table 7-25.

4. The individual SAM values were all linearly related with the central monitor at the Itabashi station with the coefficient of regression (R^2) in the range between 0.70 and 0.94.

5. The individual PEM values varied from 30% to 50% of the SAM values. These {PEM < SAM} data are quite different from the US data sets, such as PTEAM, where {PEM > SAM}, because they were designed to measure the influence of the outdoors on personal exposures. The difference may be due to the exclusion of ETS exposure and incense/mosquito coil burning and the Japanese customs of using reed mat (tatami) flooring and taking shoes off when entering a home. These factors would all tend to reduce the generation and resuspension of PM in the home. Tamura and Ando (1994) and Tamura et al. (1996) confirm the findings of Thatcher and Layton (1995) that PM < 5 μm AD has negligible resuspension in homes. Their SIM PM_2 and SIM ($PM_{10} - PM_2$) were highly correlated with the SAM of identical size ($r = 0.879$ and 0.839 respectively) but there was a negative correlation between the SIM and SAM (TSP $- PM_{10}$) fraction ($r = -0.036$).

The importance of this study is that it demonstrates that there are very strong correlations between PEM and SAM ($0.747 < r < 0.964$) when the masking influences of indoor combustion sources are removed and resuspension of PM is minimized. This provides strong support to the use of an ambient monitoring station to represent the exposure of people in the community to PM of *ambient* origin.

7.4.2.2 Personal Exposures in the Netherlands

Janssen et al. (1995) preliminarily reported in an abstract results of personal PM monitoring conducted during 1994 in Amsterdam and Wageningen, NL as part of a doctoral study. Participants were 13 non-smoking adults (age 50 to 70) in Amsterdam (urban) with

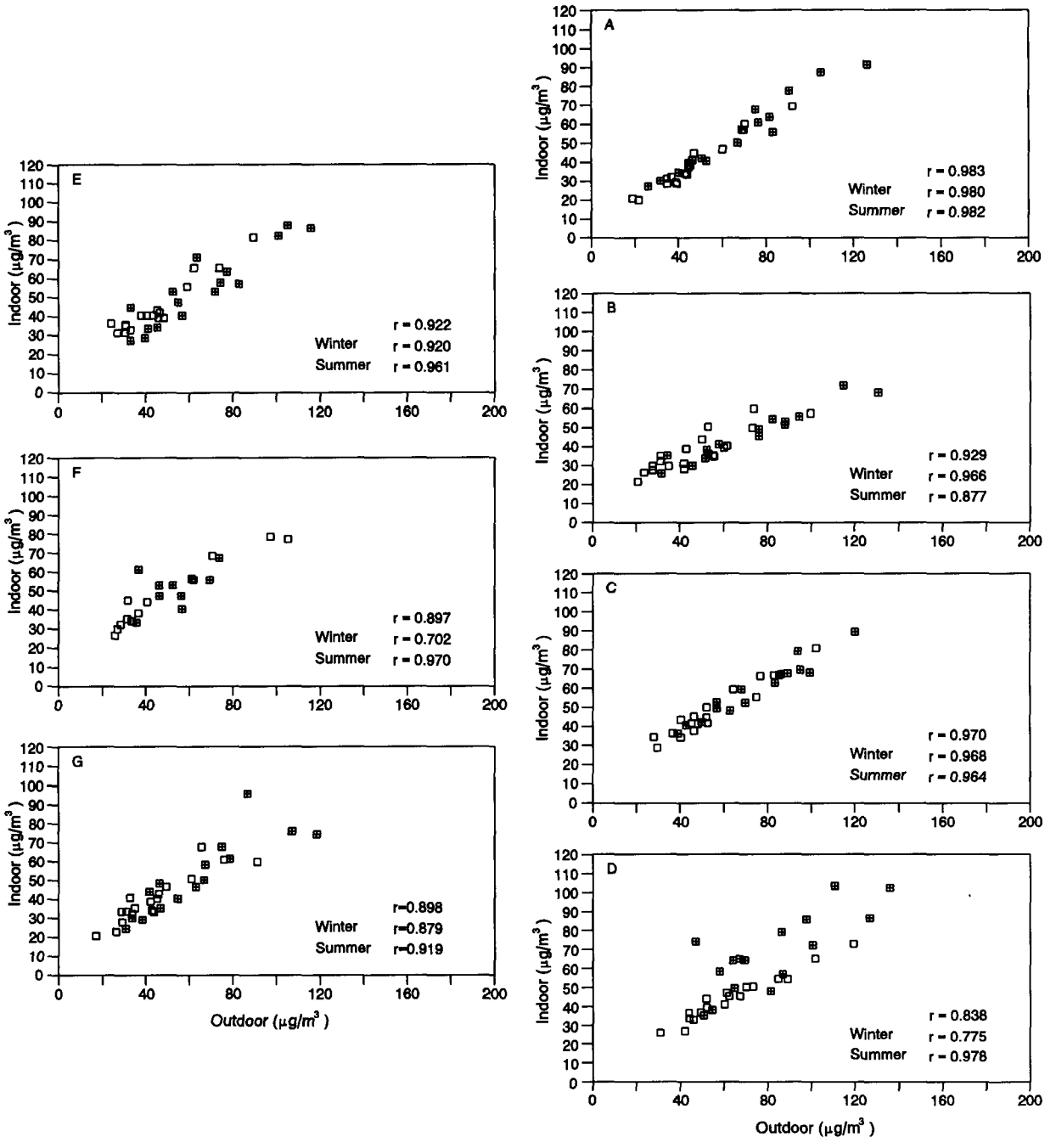

Figure 7-24. The relationship between PM_{10} in outdoor air and indoor air at each house in the study. A, B, C, D, E, F, and G, refer to the individuals identified later in Tables 7-29 and 7-30.

Source: Tamura and Ando (1994); Tamura et al., (1996).

TABLE 7-25. SUMMARY OF CORRELATIONS BETWEEN PM_{10} PERSONAL EXPOSURES OF 7 TOKYO RESIDENTS AND THE PM_{10} MEASURED OUTDOORS UNDER THE EAVES OF THEIR HOMES, AND THE PM MEASURED AT THE ITABASHI MONITORING STATION

Subject ID	Number of Samples 48-h PM_{10}	Correlation between Personal and Outdoor at home (r)	Correlation between Personal and Itabashi Station (r)
A	9	0.958	0.876
B	9	0.874	0.747
C	11	0.846	0.848
D	9	0.922	0.964
E	10	0.960	0.925
F	7	0.776	0.801
G	9	0.961	0.952
A - G	64	0.834	0.830

Source: Tamura et al. (1996).

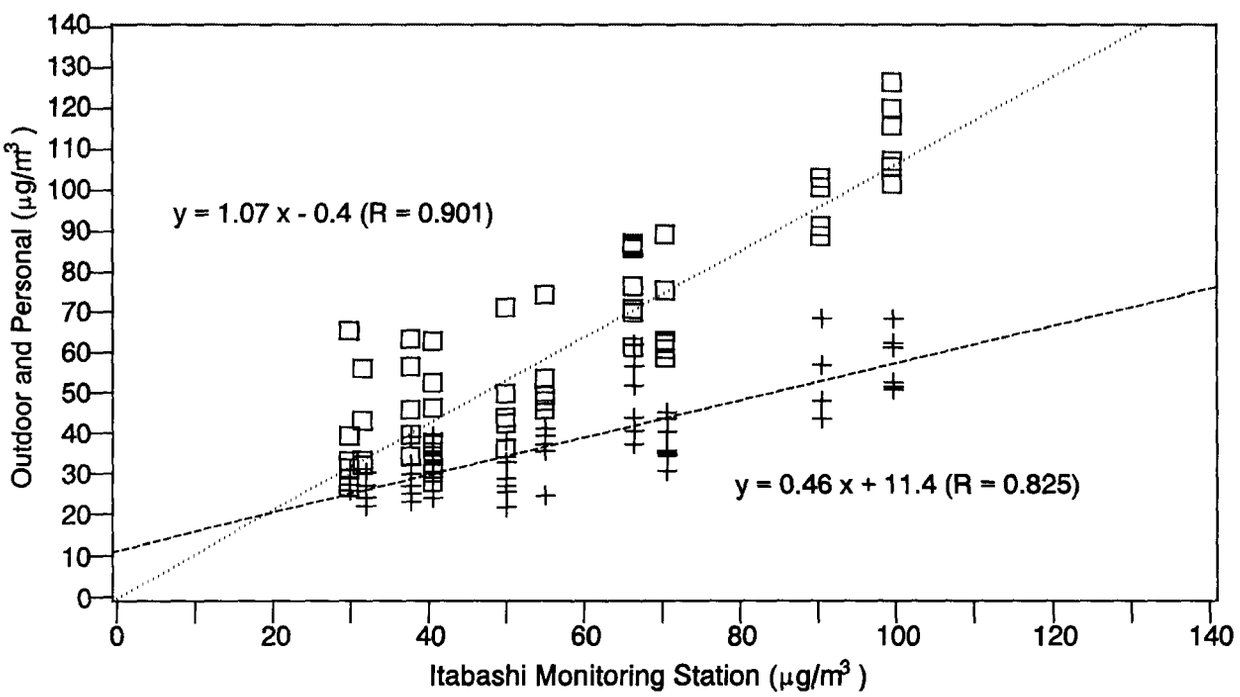

Figure 7-25. Correlations between PM_{10} at the Itabashi monitoring station and PM_{10} in outdoor and personal exposure (□ = outdoor; + = personal).

Source: Tamura and Ando (1994); Tamura et al. (1996).

no occupational exposure to PM, and 15 children (age 10 to 12) in Wageningen (rural) who are presumably non-smokers. Four to eight measurements were obtained for each subject which allowed for correlating PEM and SAM within individuals (longitudinally). Only the median individual regressions were reported, as follows: adults, PEM = 26 + 0.70 SAM, R = 0.57, R^2 = 0.32; and children, PEM = 78 + 0.43 SAM, R = 0.67, R^2 = 0.44. For the children, parental smoking explained 35% of the variance between PEM and SAM. For the adults, "living near a busy road", time spent in traffic, and exposure to ETS explained 75% of the variance between PEM and SAM. The authors interpreted their preliminary results to "suggest a reasonably high correlation between personal and ambient PM_{10} within individuals". Janssen et al. (1995) also note that the low correlations observed in most of the other studies reported in the literature were cross-sectional (calculated on a group level), and were therefore mostly determined by the variation *between* subjects (e.g., ETS exposed and non-ETS exposed subjects combined in the same regression).

7.4.2.3 Reanalysis of Phillipsburg, NJ Data

With insight from the Jansen work, Wallace (1996) reanalyzed the complete Lioy et al. (1990) data from Phillipsburg, NJ, as shown partially in Table 7-20 (see also Table 7-37). Wallace (1996) compared the cross-sectional regressions of PEM on SAM for all the 14 subjects on each of the 14 days sampled, to the longitudinal regressions of each of the 14 subjects on all 14 days sampled. He found that the median R^2 (range) of the 14 individual (longitudinal) regressions was 0.46 (0.02 to 0.82); and that for the 14 daily (cross-sectional) regressions was 0.06 (0.00 to 0.39). The difference appears to indicate that, although one household may have a smoker and another not, the relationship of the indoor air in each home to the outdoor air may be the same from day to day (i.e., consistently higher than ambient in the first case, but may be consistently similar in the second). Because it provides a linkage between PEM and SAM, it bears reiteration to make certain that it is clearly understood. This PEM vs SAM relationship can be visually demonstrated with the following hypothetical example as shown on Figure 7-26a,b.

- Let two people live next door to each other at a location where the ambient PM for 5 consecutive days has a sequence {1, 2, 3, 4, 5}.

- Let person A live without ETS exposure and have a corresponding PEM series {1, 2, 3, 4, 5}, (R^2 = 1).

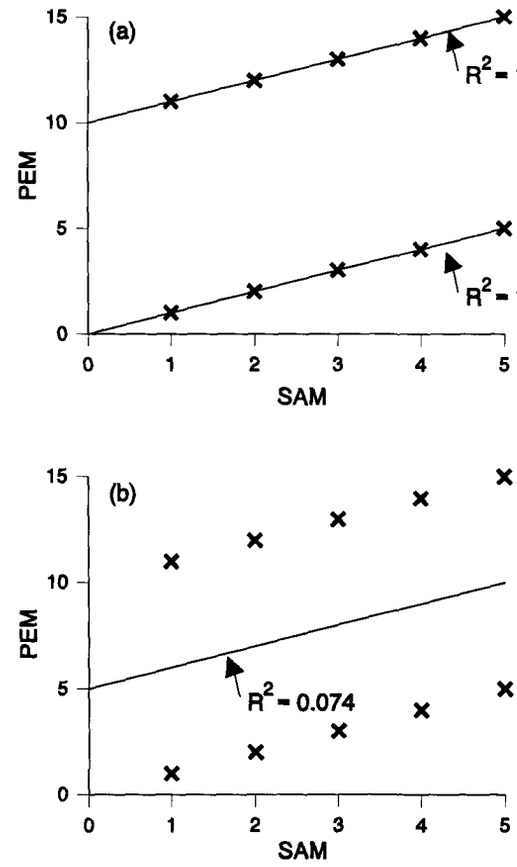

Figure 7-26. Example of difference between serial correlation (a) and cross-sectional correlation (b) of PEM and SAM, showing how pooling of individuals together can mask an underlying relationship of PEM and SAM.

- Let neighbor B live with ETS exposure and have a corresponding PEM series {11, 12, 13, 14, 15}, (R^2 = 1).

- When their PEM values are pooled so that they are analyzed together (cross-sectionally) {(1,11), (2,12), (3,13), (4,14), (5,15)} vs the SAM set {1, 2, 3, 4, 5}, then R^2 = 0.074.

- However, had the two PEM series been averaged each day, the sequence of averages {6, 7, 8, 9, 10} would have a correlation of R^2 = 1 with the same SAM sequence. This averaging process is described later in more detail in Section 7.6.2.

The explanation by Janssen et al. (1995) for the low cross-sectional correlations of PM PEM with PM SAM found in the literature and the new analyses reported by Tamura et al. (1996), Jansen et al. (1995), and Wallace (1996) represent a major advance in our understanding of contributions of ambient PM to personal exposures.

7.4.2.4 Overview of Comparison of Personal Exposure to Ambient PM Concentrations

The PTEAM Study and the other key PEM studies discussed in this chapter so far are summarized in Table 7-26. This table shows that many of the early studies reported no statistically significant correlation between PEM and SAM. However, these early studies were all characterized by a non-probability sample and a relatively small sample size. The PTEAM study in Riverside which was a probability sample (Clayton et al., 1993) and the Lioy et al. (1990) study in Phillipsburg, which was not a probability sample, have large sample sizes and achieved significance. The other studies, such as World Health Organization (1982a,b) or Morandi et al. (1988) are equivocal. In the following sections, PEM/SAM comparisons for some PM constituents and two means of visualizing the complex relationships of PM measured by a SAM and a PEM are developed.

7.4.3 Personal Exposures to Constituents of Particulate Matter

Suh et al. (1993) measured personal exposures to sulfate ($SO_4^=$) and acidity (H^+), and ambient and indoor concentrations in State College, PA, summer 1991. The correlations between personal and ambient values of sulfate and acidity were $R^2 = 0.92$ and 0.38 respectively, which is in marked contrast to the $R^2 \approx 0$ between earlier reported ambient PM and personal PM studies (Table 7-26). This relationship is supported by Figure 7-22, indicating that personal activities in the PTEAM study do not generate or resuspend sulfates less than 10 μm.

Figure 7-27 shows the consistent relation between ambient and personal sulfate measurements (slope = 0.78 $\pm$ 0.02), and Figure 7-28 shows the improvement in prediction by using the TWA with a correction factor (estimated personal sulfate = 0.885*TWA, $R^2 = 0.95$ with slope = 0.96 $\pm$ 0.02). Personal acidity was also computed by the same equation with a correction for personal ammonia (NH_3) exposure that gave an $R^2 = 0.63$. As opposed to PM which has both indoor and outdoor sources, the sulfate and acidity are virtually all of outdoor origin. Consequently, only the characteristics of the indoor environment, such as air conditioning and ammonia sources, modify the personal exposures indoors.

TABLE 7-26. COMPARISON OF PERSONAL EXPOSURE MONITOR (PEM) EXPOSURE OF INDIVIDUALS TO THE SIMULTANEOUS AMBIENT PARTICULATE MATTER (SAM) CONCENTRATION IN SEVERAL U.S. AND FOREIGN CITIES ($\mu g/m^3$)

Reference	Year[a]	Location	PM μm	N	Time	Mean PEM	Mean SAM	R^2 PEM vs SAM	p
Binder et al.	1976	Ansonia	5	20	24-h	115	59	NS	NS
Dockery and Spengler	1981b	Watertown	3.5	18	24-h	35	17	0.00	NS
Dockery and Spengler	1981b	Steubenville	3.5	19	12-h	57	64	0.19	NR
Spengler et al.	1980	Topeka	3.5	46	12-h	30	13	0.04	NS
World Health	1982a	Toronto	25						
Organization	Winter	Non-asthmatic		13	8-h	122	68	0.15	NS
	Summer	Non-asthmatic		13	8-h	124	78	0.10	NS
	Winter	Asthmatic		13	8-h	91	54	0.00	NS
	Summer	Asthmatic		13	8-h	124	80	0.07	NS
Spengler et al.	1985	Kingston/ Harriman	3.5	97	24-h	44	18	0.00	NS
World Health	1982b	Zagreb	5	12	1-wk				
Organization	Summer					114	55	0.00	NS
	Winter					187	193	0.50	NR
Sexton et al.	1984	Waterbury	3.5	48	24-h	36	17	0.00	NS
World Health	1984	Bombay	3.5	15	24-h				
Organization	Winter					127	117	0.26	NR
	Summer					67	65	0.20	NR
	Monsoon					58	51	0.02	NS
World Health	1985	Beijing	3.5	20					
Organization	Winter				24-h	177	421	0.07	0.09
	Summer				1-wk	66	192	0.03	NS
Morandi et al.	1988	Houston	3.5	30	12-h	27	16	0.34	<0.05
Lioy et al.	1990	Phillipsburg	10	14[b]	24-h	86	60	0.04	0.008
				14[c]	24-h	76	60	0.25	0.001
Perritt et al.	1991	Azusa	2.5	9	24-h	79	43	0.01	NS
			10	9	24-h	115	62	0.01	NS
Clayton et al.	1993	Riverside	10	141	24-h	113	84	0.23	NR
Tamura et al.	1996	Tokyo	10	7	48-h	37	56	0.68	0.000

N = Number of individuals carrying personal monitors.
NS = Not statistically significant from 0.
NR = p Value not reported, but mentioned as significant.
[a] = Year of publication.
[b] = 14 Subjects carried PEMS for 14 days for 191 valid measurements.
[c] = Three outliers are removed and regression is for 188 measurements.

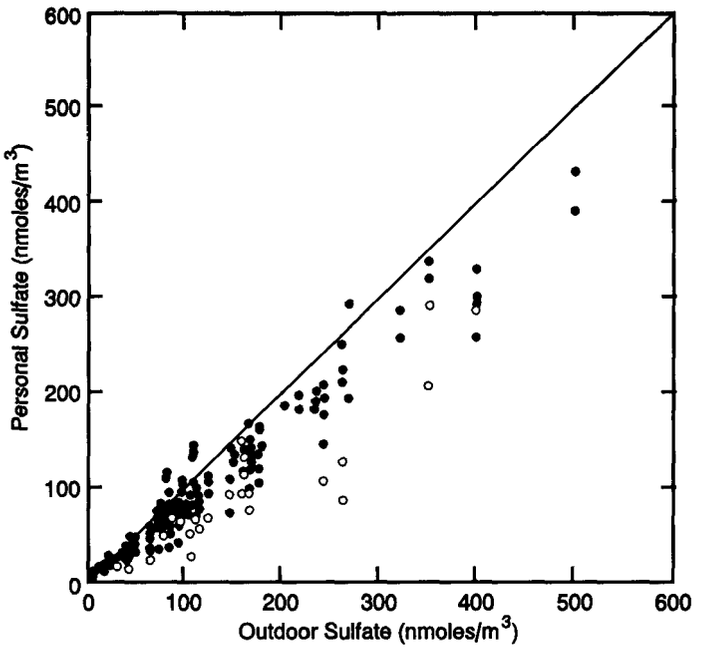

Figure 7-27. Personal versus outdoor $SO_4^{=}$. Open circles represent children living in air conditioned homes; the solid line is the 1:1 line.

Source: Suh et al. (1993).

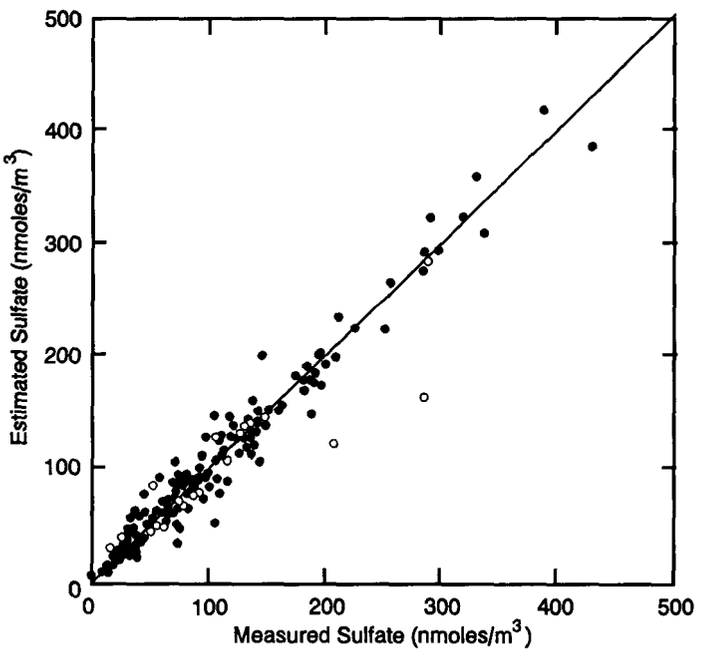

Figure 7-28. Estimated ("best fit" model) versus measured personal $SO_4^{=}$. Model includes indoor and outdoor concentration and activity data. Open circles are air conditioned homes; the solid line is the 1:1 line.

Source: Suh et al. (1993).

Similar high correlations for total sulfur were found by Özkaynak et al. (1996) in the PTEAM study. Regressions of personal exposures in the PM_{10} fraction on outdoor sulfur gave the following results ($\mu g/m^3$):

S_{pers} (day) = 0.62 (0.07 SE) + 0.69 (0.03) S_{out} N = 168 R^2 = 0.78

S_{pers} (night) = 0.27 (0.06) + 0.68 (0.03) S_{out} N = 162 R^2 = 0.81

Another important consideration in evaluating personal exposures, from the indoor and outdoor environmental measurements, is that the chemical composition of the excess in personal exposure compared to the TWA exposure calculation may be significantly different than that predicted from the indoor and ambient data alone.

In addition to the two factors cited just above, a microscale "personal cloud" can be generated by the person's activities which complicates the exposure measurement process. This effect is most important in occupational settings where personal exposures are not readily comparable to weighted area sampling measurements. For example, Lehmann et al. (1990) measured workers exposure to diesel engine exhaust by personal monitoring of PM_{10} with a range of 0.13 to 1.2 mg/m^3, compared to an area estimate range of 0.02 to 0.80 mg/m^3. The U.S. Centers for Disease Control (1988) reports the exposures of nurses and respiratory therapists to the aerosols of ribavirin during treatment of patients by ribavirin aerosols administered inside an oxygen tent. Bedside area monitors averaged 317 $\mu g/m^3$ while personal exposures ranged from 69 to 316 $\mu g/m^3$ with an average of 161 $\mu g/m^3$.

Environmental Tobacco Smoke (ETS) is a category of PM found in many indoor settings where smoking is taking place or recently occurred. As stated in Section 7.2, ETS is the major indoor source of PM where smoking occurs. Because of the depth of discussion of ETS in Section 7.2.2.2, no further discussion is made here other than to note that ETS adds on the order of 25 to 30 $\mu g/m^3$ to 24-h average personal exposures and residential indoor environments where smoking takes place (Holcomb, 1993; Spengler et al., 1985).

The random ETS increment will tend to reduce the correlation between PEM and SAM. If one were able to subtract out the ETS from the PEM PM data, the correlation of SAM with the non-ETS PEM PM might be improved (Dockery and Spengler, 1981b). As stated as a *caveat* in the introductory section 7.1, the inhalation of main-stream tobacco smoke will be a major additive exposure to PM for the smokers, which dwarfs the nonsmoker's PEM PM. Therefore the results presented so far apply only to nonsmokers, and a major

proportion of the US population (e.g., smokers) has a total exposure to PM that is at least one order of magnitude greater than that of the nonsmokers.

7.5 INDIRECT MEASURES OF EXPOSURE

7.5.1 Time-Weighted Averages of Exposure

The early air pollution literature related health to ambient particulate matter (TSP) concentrations as a surrogate for personal exposures to PM. Although this relationship has been shown to be highly questionable for specific individuals, it still is used in studies such as Pengelly et al. (1987) who estimated TSP exposures of school children in Hamilton, Ontario, by interpolation of ambient TSP concentrations to the school locations.

The first usage of a time-weighted-average (TWA) of environmental exposures to estimate total human personal exposure to an air pollutant (Pb) was by Fugaš et al. (1973). In theory, a human exposure to PM could be estimated by use of Equation 7-2 and knowledge of the average PM concentration while in each microenvironment (μE) that a person experiences and the duration of the exposure in each such μE (Duan, 1982; Mage, 1985). For a room with no source in operation, the whole room could be treated as a single μE. However, when a PM source is in operation and gradients exist, that very same room may need to be described by multiple μEs. These μEs could have dimensions of an order of a few centimeters close to the source and of several meters farther from the source.

Ogden et al. (1993) compared exposures from personal sampling and static area sampling data for cotton dust exposures. The British cotton dust standard specifies static sampling, because the 1960 dose-response study used to set the standard used static sampling data to compute worker exposure and dosage. Ogden et al. (1993) found median personal exposures of 2.2 mg/m^3 corresponding to a mean static background concentration of 0.5 mg/m^3. They concluded that "The presence of the body and its movement affect what a personal sampler collects, so static comparisons cannot be used to infer anything about the relationship of the (static) method with personal sampling." Ingham and Yan (1994) confirmed this finding by modelling the human body as a cylinder and showing that unless the personal monitor length/diameter ratio was greater than four, the aspiration efficiency

(the fraction of particles sampled that would be sampled in the absence of the body) could be greatly affected.

Rodes et al. (1991) compared the literature relationships of personal exposure monitoring (PEM) to μE area monitoring (MEM) for PM, as shown in Figure 7-29, to which Ogden et al. (1993) is added as a single point. The authors found that PEM/MEM ratios ranged from 3 to 10 in occupational settings, and from 1.2 to 3.3 in residential settings. These combined data show that approximately 50% of all measured PEM PM values are more than 100% greater than the estimated simultaneous MEM values using the TWA approach. Their explanation points to this excess PM as due to the spatial gradient about indoor sources of PM which are usually well away from area monitors which thus fail to capture the high exposures individuals may get when in close proximity to a source. They suggest that clothing lint and skin dander could only add, at most, a few percent to the total PM mass collected by a personal exposure monitor.

The Tokyo PM_{10} data of Tamura et al. (1996), added on Figure 7-29, show that for their cohort of five elderly housewives and two male retirees that there is no evidence of a large personal cloud effect as seen in the other studies listed. Japanese people customarily take shoes off before entering a home and do not use wall-to-wall carpets, which would reduce track-in of soil and eliminate a major reservoir for resuspension of dust. However, this same cohort does display a "personal cloud" effect for the PM greater than PM_{10}, with a maximum PEM/MEM value of 3.3 for PEM = 55 $\mu g/m^3$ vs MEM 17 $\mu g/m^3$. This is consistent with the findings of Thatcher and Layton (1995) showing, on Figure 7-15, an indoor increase due to human activity, primarily for the PM greater than 10 μm in size, and Sheldon et al. (1988a,b) showing two U.S. homes for the elderly with less than 10 $\mu g/m^3$ PM_3 over a 72-h period in a nonsmoker's room.

7.5.2 Personal Exposure Models Using Time-Weighted Averages of Indoor and Outdoor Concentrations of Particulate Matter

Several studies have used the relationship of Equation 7-2 to compute the time-weighted-average (TWA) PM exposure of subjects. The procedure calls for a time-activity diary to be kept so that the time at-home, outdoors, at-work, in-traffic, etc., can be defined. By use of μE monitoring data from the study itself (or literature values of PM concentrations

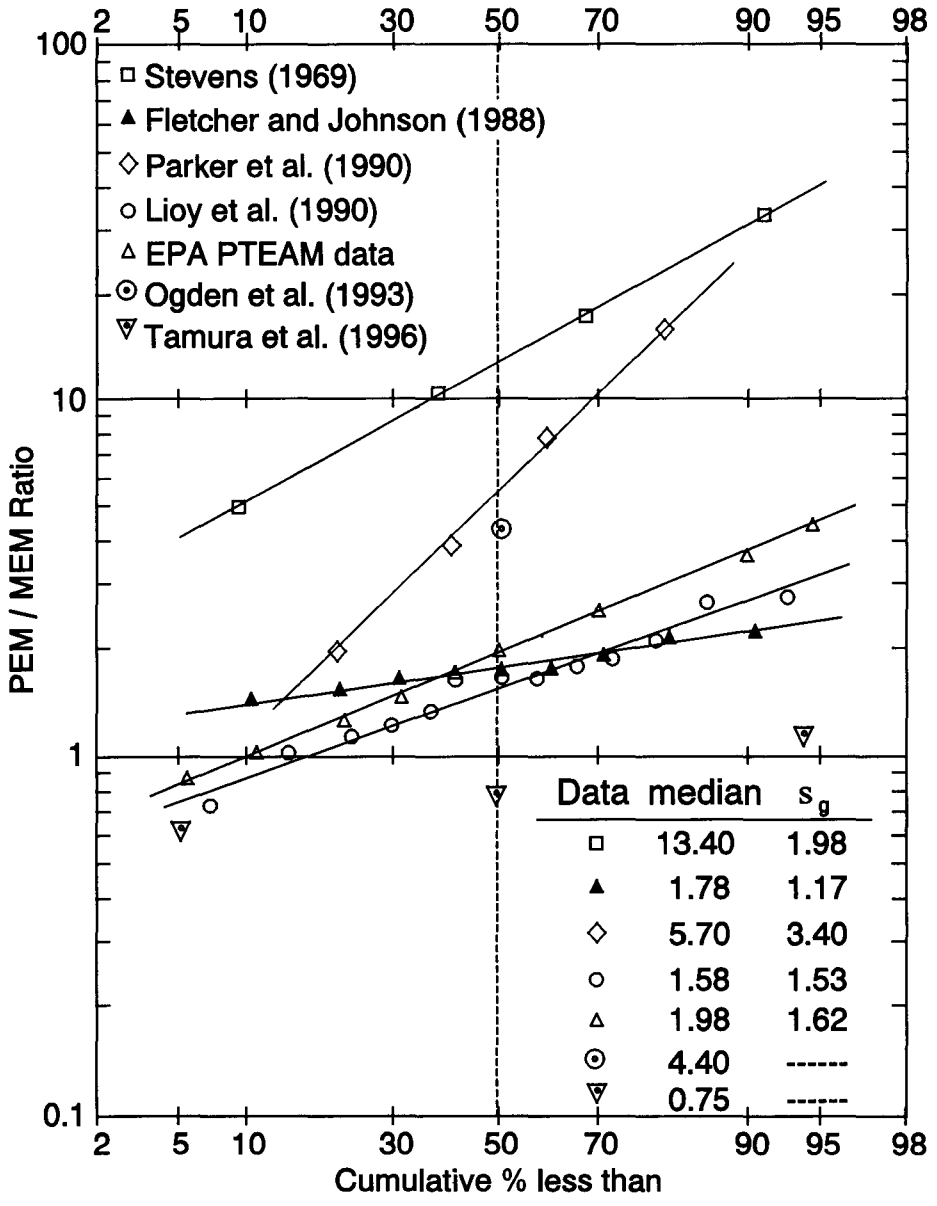

Figure 7-29. Personal activity cloud (PEM) and time-weighted average exposure (MEM).

Source: Rodes et al. (1991), Ogden et al. (1993), Tamura et al. (1996).

in similar μEs) and concurrent ambient monitoring, one can predict the concentration that would be measured if the subject had carried a PEM.

Because people in the United States spend, on average, 21 h indoors each day (U.S. Environmental Protection Agency, 1989), the concentration in indoor μEs is a most

important quantity for usage within a TWA PM model. The important articles on indoor air quality for PM have been reviewed extensively by Wallace (1996) and are covered in Section 7.2. The articles that are discussed here predict PM exposures of non-smokers that include ETS, and most provide PEM data for comparison. As opposed to the gaseous pollutants for which continuous hour-to-hour time series of SAM data are available, PM SAM monitoring data have been often only available as a time series of 24-h SAM measurements. Consequently, in much of the early PM TWA literature, the modelers assumed, by necessity, the same ambient PM in the morning and evening, which might not be accurate (Dockery and Spengler, 1981b).

Spengler et al. (1980) in a study of PEM, SAM and SIM in Topeka, Kansas, found the averages of PEM = 30 $\mu g/m^3$, SIM = 24 $\mu g/m^3$ and SAM = 13 $\mu g/m^3$. They note "It suggests that somewhere in an individual's daily activities, they are being exposed to PM at concentrations higher than what is measured either indoors or outdoors". This relationship has been found in almost all other studies, such as PTEAM (Clayton et al., 1993) where daytime PEM averaged 150 $\mu g/m^3$ and SIM and SAM averaged just under 100 $\mu g/m^3$. Spengler et al. (1985) measured 24-h PEM, SIM and SAM. The resulting relationship based on Equation 7-1 was: PEM = 17.7 $\mu g/m^3$ + 0.9 TWA. The authors noted, in addition to the previous suggestion, that the excess of PEM over TWA may be due to an incorrect assumption that the indoor and outdoor are constant during the 24-h sampling period.

Koutrakis et al. (1992), in a study discussed in Section 7.2 on Indoor Air, report that their source-apportionment mass-balance model predicts penetration from outdoors to indoors on the order of 85-90% for Pb and sulfur compounds. The authors claim that:

> "We can satisfactorily predict indoor fine aerosol mass and elemental concentrations using the respective outdoor concentrations, source type and usage, house volume and air exchange rate."

The authors further note that this may be a cost-effective approach to estimating peoples' exposure while indoors, since the necessary ambient data may be available and the housing profile may be collected with a simple interview.

Colome et al. (1992) measured indoor and outdoor PM-10 at homes of asthmatics in California. Their personal monitoring data, limited to three individuals, confirmed the relation in Figure 7-16 that "some protection from higher outdoor concentration is afforded by shelter if smokers and other particulate sources are not present". This observation may

be important for estimating the exposure of elderly and infirm people who are assumed to be the susceptible cohort (Sheldon et al., 1988a,b).

Klepeis et al. (1994) present an up-to-date TWA PM Model that uses, as an input, real-time hourly PM SAM data and a mass balance equation to predict exposures of nonsmokers in various indoor settings based on ambient PM data, presence of PM sources such as smokers, and other variables relating to air exchange rates. The inclusion of the additive terms that allow for sources, such as cooking and presence of smokers adds to the TWA of Equation 7-2, which in effect is a correction for the underprediction of the μE concentration.

In summary, as described by several authors, the PM PEM exposure of individuals who are not smoke exposed has been shown to be higher than their corresponding TWA of SIM and SAM in U.S. studies. The exact reason for this excess in PM, sometimes called a "personal cloud", is not known (Rodes et al., 1991). It has been thought to reflect the fact that the person's presence itself can stir up loosely settled-dust by induced air motion and vibration (Ogden et al., 1993; Aso et al., 1993). Thatcher and Layton (1995) gave an example where merely walking into and out of a room raised the total suspended dust (PM_{10}) by 100%. A study by Litzistorf et al. (1985) of asbestos type fibers in a classroom showed how fibers (f) were stirred up when it was occupied. The levels rose from below the detectable level of 10000 f/m^3 to 80000 f/m^3 when occupied, and they returned to below detectable levels within 1 h after the end of the class. Millette and Hays (1994) present a detailed discussion of the general topic of resuspended dust in their text on settled asbestos dust.

It may not be a proper procedure to use a 24-h average concentration in a physical setting, such as a kitchen, to estimate a person's exposure while in the kitchen. As described previously in the discussion of the definition of a microenvironment in Section 7.1.2, the same kitchen can constitute one or more μEs depending on the source operation pattern. In many studies, such as Spengler et al. (1985), the SIM sampled the indoor residential setting for 24-h in phase with the PEM. The resulting average SIM will often underestimate the person's exposure while they are at home and may contribute to the difference between a TWA exposure and the PEM.

In a similar manner, a person's workplace exposure may be more or less than that in their home. In the PTEAM study (Clayton et al., 1993), there was a general decrease in

exposure for those employed outside their home. However, employment in a "dusty trade", such as welding, may increase their PM PEM. Lioy et al. (1990) give an example of a subject with a hobby involving welding having a 24-h PEM reading of 971 $\mu g/m^3$.

Indirect estimation of a person's time-weighted-average (TWA) PM exposure may be a cost-effective alternative to direct PEM PM measurement. Mage (1991) compared the advantages and disadvantages of the TWA indirect method compared to the direct PEM method. The primary advantages of the indirect method are the lower cost and lower burden on the subject, because it uses only a time-activity diary and no PM PEM is required; the disadvantage is the lower accuracy. The primary advantage of the PEM PM method is that it is a higher accuracy direct measurement; the main disadvantages are the higher cost and higher burden on the subject (see Section 7.3.1). Mage (1991) proposed a combined study design in which direct measurements on a subset of subjects can be used to calibrate the TWA estimates of other subjects. Duan and Mage (1996) present an expression for the optimum fraction of subjects to carry the PEM as a function of the relative cost of the PM PEM to the TWA PM estimate and the correlation coefficient between the PM PEM data and the PM TWA estimates.

7.6 DISCUSSION

7.6.1 Relation of Individual Exposures to Ambient Concentration

The previous sections discussed the individual PM PEM vs PM SAM relationships of the studies listed in Table 7-26. In many of the cross-sectional PM studies, no statistically significant linear relationship was found between PEM and SAM, but in some other studies the relationship is positive and statistically significant. However, as shown by Lioy et al. (1990), Janssen et al. (1995), and Tamura et al. (1996), the serial correlations between PEM and SAM within an individual's time series are often highly positive and significant. This section discusses these data in terms of understanding the complex relationship between the SAM concentrations and the *individual* PEM exposures. In the following section, the relationship of the SAM to the *mean* PEM in the community surrounding the SAM will be presented.

The principle of superposition is offered as a basis for visualization of the process involved in creating a total exposure. A linear system will exist for respirable-PM PEM exposures if the expected PEM response to a source emitting 2 mg/min of PM is exactly twice the PEM response to that identical source emitting 1 mg/min of identical PM. If superposition applies, then we can construct the total exposure by adding all the increments of exposures from the various source classes and activities that a subject performs on a given day.

Let the SAM be representative of the macroscale ambient PM concentration in the community as shown on Figure 7-30a. This is the exposure that would be measured for a person if they spent 24-h per day outdoors near the SAM site. Neglecting local microscale variation (e.g. backyard barbecue or leaf burning), while people are outdoors they are exposed to 100% of the SAM value (Figure 7-30b). Assume that this exposure is also the baseline PM for a location in traffic which occurs outdoors. The increment produced by the local traffic is considered later.

While people are indoors, they are exposed to a variable fraction of time-lagged SAM PM. This constitutes an amount of (1) the fresh PM which depends on recent SAM and the air exchange rate between indoors and outdoors, and the PM deposition sinks (filtration of recirculated air, surfaces, etc.), and (2) PM from outdoor sources that had been deposited in the past but is resuspended due to human activity and air currents. PTEAM (Özkaynak et al., 1996), as cited in Section 7.2, found that outdoor air was the major source of indoor particles, accounting for 75% of the fine fraction (<2.5 μm AD) and 67% of the thoracic fraction (< 10 μm AD) in indoor air. It is noted that these average fractions will be lower in communities with lower average SAM values. Lewis (1991) reported an apportionment of indoor air PM in 10 homes within a wood burning community in Boise, ID. The results showed that 50% of the fine PM was of outdoor origin (SAM), and in 9 of 10 homes, 90% of the sulfur was from outdoors (one home had an anomalous sulfate injection from a humidifier using tap water). This is consistent with indoor sources varying independently of the SAM in a stationary manner (constant mean and variance), so that the relative contribution of indoor sources to indoor exposures decreases as SAM increases. Figure 7-30c represents the increment to PEM from outdoor sources of SAM while the

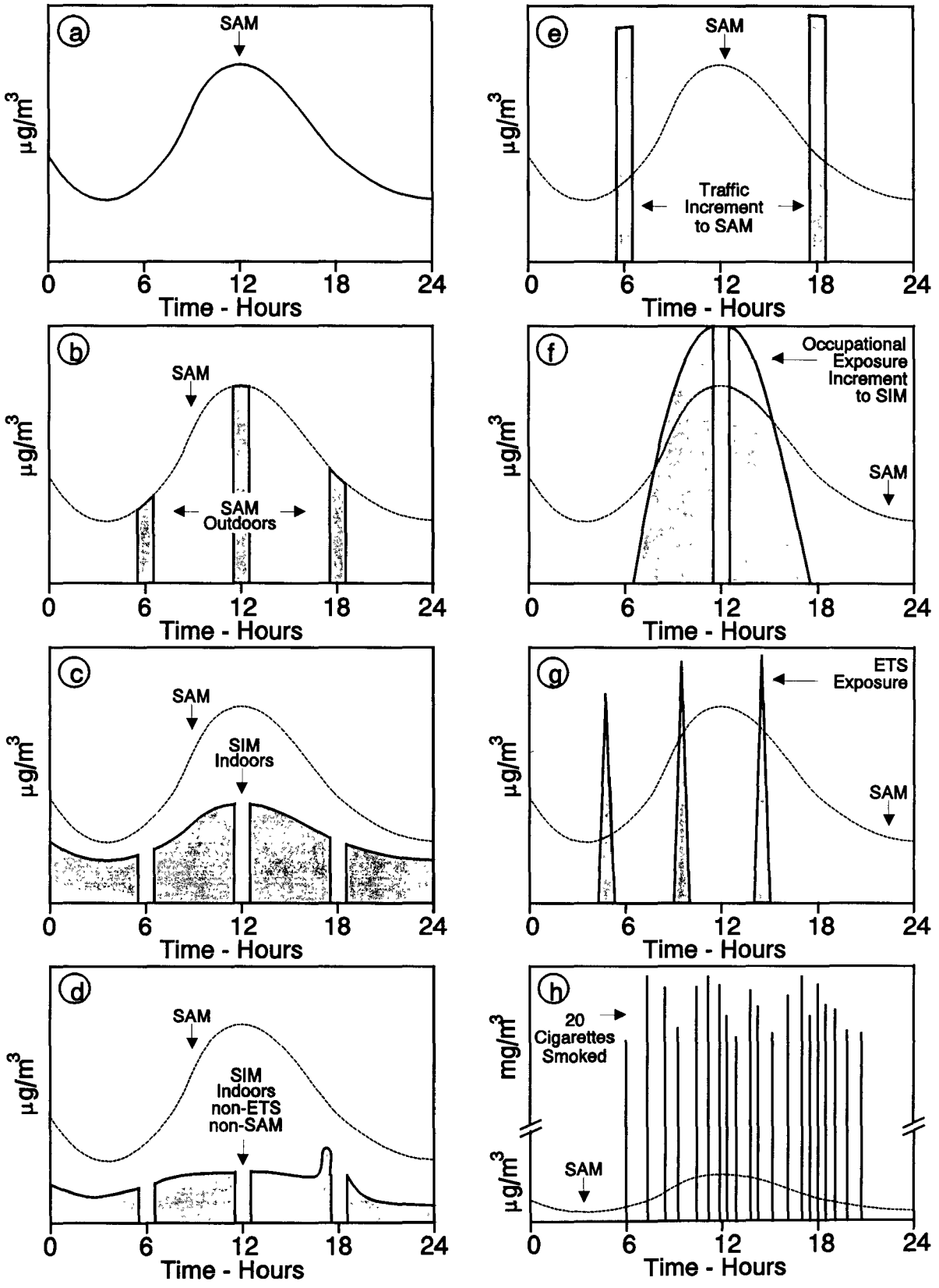

Figure 7-30. Components of personal exposure.

subjects are indoors at home and at work. The SAM value is shown as the dotted line for reference in this and all the following Figures 7-30c to 7-30h.

While people are indoors, at home, and at work, they also are exposed to PM emitted by indoor sources - *other than* ETS from passive smoking and specific occupational sources. These sources, such as cooking, lint from clothing and furnishings, mold, insects, etc., create PM that agglomerates and deposits as visible dust that can be continuously resuspended, which constitutes an additional PEM increment. Figure 7-30d shows the additive effect of this source. In traffic, or near vehicles in a parking garage or parking lot, people are exposed to an increment of PM over and above the SAM value for that location. Figure 7-30e shows the additive PM for this setting that would be added to Figure 7-30b for the local vehicular emissions.

At work in a "dusty trade" (e.g., welder, mechanic, or miner) there is an increment of exposure associated with these occupational activities that generate PM. Figure 7-30f represents the additive PM for these activities which are assumed to take place "indoors".

In an indoor setting, in the presence of a smoker or the wake of a smoker, a PEM will record an increment of ETS associated with the act of smoking. Figure 7-30g shows the added PM increment for this source.

Last, but not least, is the physical act of smoking itself. As described previously, the main stream smoke from a cigarette, cigar, or pipe is inhaled directly without being sampled by a PEM. The mass of PM directly inhaled from smoking one-pack-per-day of cigarettes rated as delivering "1 mg 'tar' per cigarette by FTC method" is 20 mg per day (Federal Trade Commission, 1994). If this were distributed into a nominal 20 m^3 of air inhaled per day, it would be an additive increment on the order of 1 mg/m^3 to a 24-h PEM reading. Tar emissions as rated by the Federal Trade Commission (1994) range from <0.5 mg/cigarette to 27 mg/cigarette. Therefore one-pack-per-day smokers can have a PM exposure standard deviation that is much larger than the mean exposure to PM of non-smokers, simply from choice of brand. Figure 7-30h represents the impact of the act of smoking as creating exposures represented by the vertical spikes with an integral area $\geq$ 1 $mg\text{-}day/m^3$ per day.

For all subjects, by the principle of superposition, the sum of the areas shown in Figures 7-30b and 7-30c represents the exposure of an individual to the PM constituents that are characterized by a SAM PM concentration. The additional exposure categories that are

independent of the SAM concentration (Figures 7-30d through 7-30g) and are appropriate for that subject would represent the portion of 24-h PEM PM that is not associated with SAM. Variance of SAM should explain much of the variance in the SAM related PEM fraction as defined by Figures 7-30b and 7-30c. The summation over a full day for all categories 7-30b to 7-30g would be the PEM for any subject, such as is shown in Figure 7-2 (Repace and Lowery, 1980).

Although there are no data for PEM PM exposures of individuals living in homes without any indoor sources of PM, there are data for PEM sulfate as discussed previously in Section 7.4.3. Given that there are negligible sources of sulfur (S) that originate in the home (matches, low-grade kerosene, humidifiers using tap water), the high correlation of PEM sulfate and SAM sulfate ($R^2 = 0.92$) of Figure 7-27 reported by Suh et al. (1993), where no appreciable sources of S were present, is an indication that the same relationship should hold for all SAM PM of that size range. The data of Anuszewski et al. (1992) show that light scattering particles measured by nephelometry had a very high correlation between indoor and outdoor concentrations ($R^2 > 0.9$) for one home, but were lower for others. Lewis (1991) and Cupitt et al. (1994) report that PM_{10} appears to penetrate with an average factor of 0.5 in Boise homes without woodburning. The factor goes up to 0.7 with woodburning, and the authors assume that the factor would go up to 0.9 in the summer when homes are less tightly sealed. However, the authors did not consider the deposition rate k. This is in contrast to the data of Thatcher and Layton (1995), who measured k and found penetration factors of 1.0 for all PM sizes $< 10\ \mu m$.

If the variance of the PEM PM portion which is uncorrelated to SAM (Figure 7-30d to 7-30g) is very large, the percentage of the variance of the PEM PM that can be explained by the variance of SAM PM will be very small. It may be possible that the different populations sampled, cited in the studies of Table 7-26, have widely different home characteristics, occupations, mode of commuting, and smoking exposures that contribute to the different PEM vs SAM relationships. In some of the cleaner communities (such as Watertown, MA; Topeka, KS; Waterbury, VT; and Kingston and Harriman, TN) SAM averaged less than 20 $\mu g/m^3$. The non-SAM increments to PEM exposure in these locales were greater than the SAM and may have been so variable between people (eg. ETS and non-ETS exposures pooled together) that the PEM PM became insignificantly correlated with

the SAM PM data. The exception is Houston, TX, with a SAM = 16 $\mu g/m^3$ and a significant $R^2 = 0.34$ ($0.005 < p < 0.05$). However, Morandi et al. (1988) note that deletion of two outlier observations would reduce R^2 and make it nonsignificantly different from 0 ($p > 0.2$). This is in contrast to the three studies in communities with high SAM levels (Tamura et al., 1996; Clayton et al., 1993; Lioy et al., 1990), where the relations between PEM and SAM were significant.

All discussions above relate to nonsmokers. As for the smoker, the exposure from Figure 7-30h would outweigh the sum of all the other exposures, 7-30b through 7-30g. This smoking increment may have an important implication for interpretation of epidemiology studies that relate ambient PM, as a surrogate of exposure, to mortality or morbidity.

Because the daily amount of individual smoking and other exposures from indoor sources (cooking, ETS, resuspension of settled dust by walking into carpeted rooms, hobbies) is independent of the daily SAM value, the variance of the PM SAM value is a surrogate for the variance component of total personal exposures to PM associated with PM SAM. For nonsmokers ambient PM reflects about 50 to 70% of their PM_{10} exposure that by definition does not contain directly inhaled smoke exposure (Tamura et al., 1996; Özkaynak et al., 1996). This relationship would also hold for the total PM exposure of smokers minus the effective increment they receive from their direct smoking which is independent of PM SAM. Therefore, a relationship between ambient PM (SAM) and human exposure to PM (PEM) that makes sense, is that the SAM value is a surrogate for personal exposure to PM (PEM) from PM originating in the ambient air. This relationship would apply to everyone, smokers and nonsmokers alike. However, treating SAM as a surrogate for total personal exposure to PM from all sources, including those major sources of PM that vary independently of SAM (active smoking and occupational exposures), would be wrong.

7.6.2 Relation of Community Particulate Matter Exposure to Ambient Particulate Matter Concentration

For the morbidity/mortality studies described in Chapter 12 that use SAM as the independent variable, that SAM can be interpreted to stand as a surrogate for the average community exposure to PM from sources that influence the SAM data. These sources of ambient PM do not include indoor sources such as the "personal cloud" of skin flakes and

lint, ETS, cooking fumes, and resuspended PM from walking on a dirty carpet. Thus, if we could subtract off from each PEM measurement the contribution to the total exposure from the indoor sources, such as smoking, cooking, carpets, and personal clouds, the residual PM from ambient sources would probably improve the correlation with SAM, as described by the data of Tamura et al. (1996) for nonsmoking-noncarpeted homes occupied by elderly people. Mage and Buckley (1995) tested the relationship of the mean PEM to SAM as a means to minimize the affect of variations of these indoor sources of PM on the relation of PEM to SAM, and their results, with modifications, are presented in the following section.

There are several different models for these analyses and although most describe the same linear relationship, the models differ greatly in their assumptions about the error terms. The discussion of the various models is followed by U.S. EPA reanalyses of five different PEM-SAM data sets described previously in Section 7.4.

7.6.2.1 Methodology

Methods for Missing Data

One common difficulty in the use of aerometric data is the presence of missing data elements. For example, consider the following PEM data from the study of Tamura et al. (1996). The authors measured the 48-h personal exposure to PM_{10} for seven individuals living near a main road for 11 periods in four seasons distributed over a complete year. This example has a great deal of missing data, and for purposes of computation, the data were split into a group living close to the road (persons A, B, C, and D), and a group living farther from the road (persons E, F, and G). Their indoor and outdoor data were shown previously on Figure 7-24. The PEM data for the first group are shown in Table 7-27.

Unless pairwise correlations are computed, the standard solution to the problem is to delete all observations for which any of the variables are missing. This approach, known as a complete-case analysis, is standard in the majority of the statistical packages. For this example, we would be left with only 5 of the original 11 periods of observation. This section will describe a model which will allow for the inclusion of all available data.

The reason for the missingness of the data is extremely important because it determines our ability to obtain maximum likelihood estimates (MLE). The following definitions are paraphrased from Little and Rubin (1987): If the probability of being missing is independent

TABLE 7-27. 48-HOUR PERSONAL EXPOSURE TO PM_{10} ($\mu g/m^3$)
(Data Taken by Subjects Living Along a Main Road in Tokyo)

Period	Person A	Person B	Person C	Person D
1	43.7	40.4	37.5	52.3
2	27.4	31.5	29.8	26.0
3	30.2	39.2	32.7	M
4	22.4	29.2	25.9	38.2
5	57.4	43.2	43.3	M
6	M	26.1	27.9	39.9
7	M	37.9	35.8	34.6
8	24.6	M	41.4	39.8
9	31.0	34.5	36.0	45.6
10	22.9	M	24.3	30.6
11	68.7	51.8	52.6	68.1

M = Missing observation.

Source: Tamura et al. (1996).

of both the variables missing and the variables present, then the data are said to be missing completely at random (MCAR). If the probability of being missing depends on the variables present, but not on the variables missing, then the data are said to be missing at random (MAR). If neither situation holds, then there are no general solutions to the problem. This would happen if the value of the missing variable (which is not known to us) is directly related to its probability of being missing. Laird (1988) discusses models used for maximum likelihood estimation with missing data, as well as a detailed discussion of the non-response mechanism.

One solution is to assume that the measurements are distributed as a multivariate normal distribution (or to assume that some transformation of the data give a multivariate normal distribution). The estimation of the parameters of a multivariate normal model with missing data is a problem which has been discussed for many years (see Afifi and Elashoff, 1966). The first general solution to the problem of estimating a mean vector and covariance matrix from a multivariate normal distribution with data missing at random was given by Woodbury and Hasselblad (1970). The solution, referred to as the "Missing Information

Principle", was generalized to other missing data problems by Orchard and Woodbury (1972). Proof that the method always improved the likelihood was given by Dempster et al. (1977), and the generalized solution method was named the E-M algorithm.

To describe the problem, the following notation will be used. Let $\mathbf{x} = x_1, x_2, \ldots, x_k$ be a k-dimensional random vector from a multivariate normal distribution

$$f(x|\mu,\Sigma = (2\pi)^{-k/2}|\Sigma|^{-1/2}e^{-(x-\mu)\Sigma^{-1}(x-\mu)/2} \tag{7-10}$$

where Σ is a symmetric positive definite matrix and μ is a vector. The mean of the vector $\mathbf{x}$ is μ and its covariance is Σ. Assume that we have n observations from this distribution, $\mathbf{X}_1, \mathbf{X}_2, \ldots, \mathbf{X}_n$.

The E-M algorithm can be used to estimate the parameters of a multivariate normal distribution. The method starts with any reasonable first estimate of the parameters. Assume that we have initial estimates of the parameters μ and Σ, which can be obtained by filling in the missing data with the column means and then estimating the parameters in the usual manner. The E step consists of estimating the sufficient statistics. For this model, the sufficient statistics are the sums and sums of squares of cross products.

Assume that at one particular point, $\mathbf{X}_i$, some of the observations are missing and some of the observations are present. Without loss of generality, we will drop the subscript, i, and rearrange the subscripts so that the vector $\mathbf{X}$ is $[\mathbf{X}_1, \mathbf{X}_2]$ where all of the observations, $\mathbf{X}_1$, are missing and all the observations $\mathbf{X}_2$ are present. Partition the mean vector μ and the covariance matrix Σ in a similar fashion

$$\boldsymbol{\mu} = \begin{bmatrix} \boldsymbol{\mu}_1 \\ \boldsymbol{\mu}_2 \end{bmatrix} \text{ and } \boldsymbol{\Sigma} = \begin{bmatrix} \boldsymbol{\Sigma}_{11} & \boldsymbol{\Sigma}_{12} \\ \boldsymbol{\Sigma}_{21} & \boldsymbol{\Sigma}_{22} \end{bmatrix}. \tag{7-11}$$

Compute the regression of the missing observations on the observations present

$$\boldsymbol{\beta} = \Sigma_{12}\Sigma_{22}^{-1}. \tag{7-12}$$

Estimate the missing values, $\mathbf{X}_1$, by their expected values

$$E(X_1) = \mu_1 + \beta(X_2 - \mu_2). \tag{7-13}$$

Compute the correction to the expected sums of squares

$$\Sigma_{11|2} = \Sigma_{11} - \Sigma_{12}\Sigma_{22}^{-1}\Sigma_{21}. \tag{7-14}$$

Now add the vector **X** to the sums and **XX'** to the sums of squares and cross products using their expected values for the missing values; remember to add $\Sigma_{11|2}$ to the cross products corresponding to $\mathbf{X}_1$.

The M step consists of recomputing the estimates of μ and Σ from the completed sums and sums of squares and cross products. This procedure will converge, typically taking five to 20 iterations for a moderately sized problem. Using the methods just described, the estimates of both the missing values and the parameters for the data of Tamura et al. (1996), based on U.S. EPA reanalyses, are shown in Table 7-28.

This method was also used to fill in the missing values for persons E, F, and G (shown in Table 7-29). Once the missing data were estimated, the average across all seven persons was computed and compared with the ambient measurement monitor as shown in Table 7-30. These data will be used as examples for the next section.

Linear Regression Models

The various linear regression models are illustrated next using the average personal exposure values from the Tamura et al. (1996) data set which were described in the previous section. For these examples, the average personal exposure will be considered the dependent variable and the ambient concentration at the Itabashi site will be the independent variable.

The first model is often referred to as the fixed independent variable model (see Dunn and Clark, 1974, p. 225). The model assumes that the dependent variable is a linear function of the independent variable with random error which is normally distributed (this is a bad assumption but this is the most commonly used model). This can be written as

TABLE 7-28. PARAMETER ESTIMATES FOR 48-HOUR PM_{10} PERSONAL EXPOSURE MONITOR DATA TAKEN BY SUBJECTS LIVING NEAR A MAIN ROAD IN TOKYO ($\mu g/m^3$)
(Estimated Missing Values Shown in Parentheses)

Day	Person A	Person B	Person C	Person D
1	43.7	40.4	37.5	52.3
2	27.4	31.5	29.8	26.0
3	30.2	39.2	32.7	(37.4)
4	22.4	29.2	25.9	38.2
5	57.4	43.2	43.3	(58.4)
6	(29.3)	26.1	27.9	39.9
7	(28.9)	37.9	35.8	34.6
8	24.6	(43.3)	41.4	39.8
9	31.0	34.5	36.0	45.6
10	22.9	(26.7)	24.3	30.6
11	68.7	51.8	52.6	68.1
Means	35.1	36.7	35.2	42.8
	Covariance/Correlation Matrix (Correlation below diagonal)			
Person A	215.8	83.9	96.4	157.4
Person B	0.745	58.9	58.4	67.6
Person C	0.819	0.949	64.3	79.0
Person D	0.888	0.731	0.816	145.6

Source: Parameter estimates, including the calculation of estimated missing values, and covariance/correlation matrix results from reanalyses by U.S. EPA of data from Tamura et al. (1996).

$$Y_i = \beta_0 + \beta_1 X_i + \varepsilon_i, \text{ where} \tag{7-15}$$

$i = 1,2,...,n$, n is the number of observations, and ϵ_i is normal with mean 0 and variance σ^2. No assumption is made about the distribution of the independent variable since it is considered to be fixed.

Using the previous example, the estimated coefficients are given in Table 7-31, and the results are shown graphically in Figure 7-31.

The second model is often referred to as the bivariate normal model (see Dunn and Clark, 1974, p. 239). This model assumes that the dependent variable and the independent variable are both normally distributed. Actually, the assumption is stronger—it assumes that

TABLE 7-29. PARAMETER ESTIMATES FOR 48-H PM_{10} PERSONAL EXPOSURE MONITOR DATA TAKEN BY SUBJECTS LIVING FARTHER FROM THE SAME TOKYO MAIN ROAD DESCRIBED IN TABLE 7-28 (in $\mu g/m^3$)
(Estimated Missing Values Shown in Parentheses)

Period	Person E	Person F	Person G
1	57.1	62.2	(37.1)
2	(30.9)	26.5	(29.0)
3	26.8	23.1	25.3
4	32.9	(30.6)	27.2
5	68.6	(69.2)	48.0
6	31.2	26.6	24.4
7	26.5	24.0	29.7
8	35.8	(28.7)	37.7
9	40.7	(36.9)	35.4
10	29.8	27.5	22.4
11	62.5	51.2	61.0

Source: Parameter estimates, including the calculation of estimated missing values, based on reanalyses by U.S. EPA of data from Tamura et al. (1996).

the joint distribution of the two variables is bivariate normal. The bivariate normal distribution is a special case of the multivariate normal distribution described earlier. The intercept, β_0, and regression coefficient, β_1, are estimated by the same formulas as were used in the first model even though the assumption is not the same. The R-squared term is also the same, but the ANOVA Table no longer makes any sense.

The third linear model is the same as the first except that a lognormal error term is used. This kind of model requires the use of a general linear model fitting routine. The model gives less weight to large deviations about the predicted line where the predicted values are already large. The model still assumes that the independent variable is fixed and measured without error. The fit to the previous example is shown in Table 7-32. There is no measure comparable to R^2, but the log-likelihoods can be compared directly. Note that

TABLE 7-30. AVERAGE PERSONAL EXPOSURE DATA COMPARED WITH ITABASHI SITE MONITOR (PM_{10}; $\mu g/m^3$)

Period	Itabashi Site	Average Personal
1	66.5	47.2
2	30.1	28.7
3	37.9	30.7
4	50.3	29.5
5	90.5	55.4
6	40.7	29.3
7	40.5	31.1
8	55.1	35.9
9	70.6	37.2
10	31.9	26.3
11	99.5	59.4

Source: Data from Tamura et al. (1996).

TABLE 7-31. RESULTS OF LINEAR REGRESSION ANALYSIS, ASSUMING A NORMAL ERROR USING THE EXPOSURE DATA FROM JAPAN

Linear regression
Y = intercept + slope X

Variable	Beta	Std. Err. Beta
Intercept	11.32	3.025
Slope	0.466	0.050

ANOVA Table

Source	Sum of Squares	Mean Square Error	D.F.	F-value
Regression	1194.3	597.2	2	42.9
Error	125.3	13.9	9	
TOTAL	1319.6	120.0	11	

R-squared = 0.905
Log-likelihood = −28.99

Source: U.S. EPA reanalyses of data from Tamura et al. (1996).

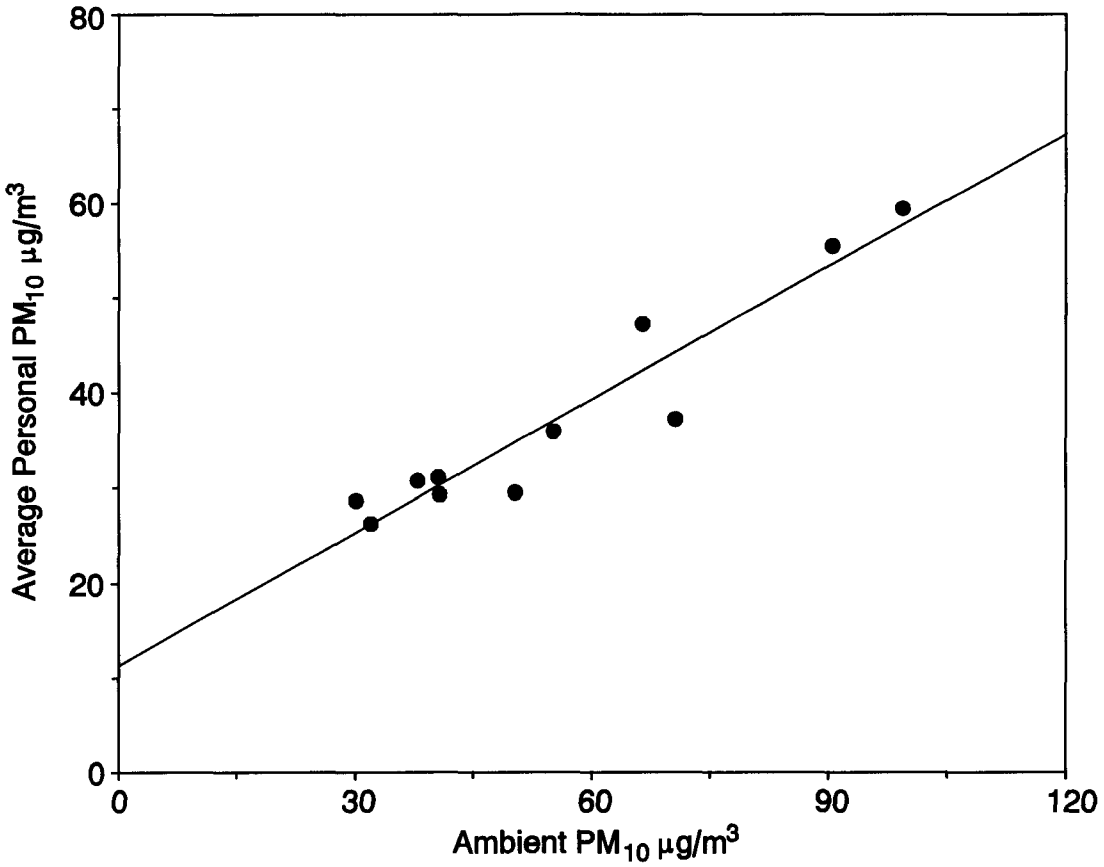

Figure 7-31. Plot of 48-h average personal PM_{10} exposure and ambient PM_{10} data from Japan—linear regression.

Source: U.S. EPA reanalyses of data from Tamura et al. (1996).

TABLE 7-32. RESULTS OF LINEAR REGRESSION ANALYSIS, ASSUMING A LOGNORMAL ERROR USING THE EXPOSURE DATA FROM JAPAN

Multiple log-linear regression analysis

Variable	Mean	Beta	Std.Err.Beta
Ambient	55.78	0.43	0.06
Mean	1	13.07	3.26

Sum of squares for error = 0.089

Mean square error = 0.010, d.f. = 9

Log-likelihood = −28.50

Source: U.S. EPA reanalyses of data from Tamura et al. (1996).

the linear model with a lognormal error fits slightly better than the normal error model, although the difference of 0.49 in the log-likelihood is not statistically significant.

Orthogonal Regression Models

Orthogonal regression is also known as principle components regression. There is no real assumption about the model. The purpose of the analysis is to pass a line through the data such that as much of the variation is explained as possible. Variation is measured as the squared distance from the points to the fitted line. Because no distributional assumptions are made, no confidence limits can be placed on the estimated line. The measure of the total variation is

$$\text{Total variation} = \sigma_{11}\sigma_{22} - \sigma_{12}^2. \tag{7-16}$$

The fraction of the variation explained is derived from the eigenvalues of the covariance matrix, and the regression line corresponds to the first eigenvector. That is, the eigenvalues are the solution of

$$\left| \begin{pmatrix} \sigma_{11} & \sigma_{12} \\ \sigma_{12} & \sigma_{22} \end{pmatrix} - \lambda \begin{pmatrix} 1 & 0 \\ 0 & 1 \end{pmatrix} \right| = 0. \tag{7-17}$$

The values of λ which satisfy equation (7-17) are

$$\lambda = \frac{\sigma_{11} + \sigma_{22} \pm \sqrt{(\sigma_{11} - \sigma_{22})^2 + 4\sigma_{12}^2}}{2}. \tag{7-18}$$

The slope of the line corresponding to the largest eigenvalue, λ_1, is

$$\beta = \frac{-\sigma_{22} - \lambda_1}{\sigma_{12}}. \tag{7-19}$$

The intercept, β_0, is easily calculated because the line must pass through the mean of the data.

The measure, percent of variation explained, is a generalization of the multiple R^2 measure from a single dependent variable, but its behavior is somewhat different. For a two variable problem it can be calculated as $\lambda_1/(\lambda_1 + \lambda_2)$. In general, for correlations near 1, it will be about twice as good (.975 to .98 instead of .95), but for correlations near 0, the behavior is not as simple. As a result, it can only be used to compare one orthogonal regression with another. Because the standard correlation coefficient is a non-parametric measure of association, it can be used for orthogonal regression as well. The results of fitting by U.S. EPA of an orthogonal regression model to the previous example are in Table 7-33. The slope and intercept are almost identical to the normal error model values shown in Table 7-31.

TABLE 7-33. RESULTS OF AN ORTHOGONAL REGRESSION ANALYSIS OF THE EXPOSURE DATA FROM JAPAN

Y = intercept + slope X	
Variable	Beta
Intercept	10.83
Slope	0.475
Total variation	5686.9
Percent explained	98.5

Source of data: U.S. EPA reanalyses of data from Tamura et al. (1996).

Measurement Error Models

In general, most linear regression analyses assume the independent variable has no measurement error. When this error exists and no correction is made for it, the estimated regression coefficients tend to be biased towards zero. Because we often have multiple monitors we can often attempt to estimate these components of variation, and therefore correct our estimated regression coefficients. The solution usually requires some additional assumptions—in particular the assumption of multivariate normality is necessary for most of the solutions. Additionally, some information must be available about the error variance. Either the error variance of the independent variable or the dependent variable, or the ratio

of the error variance to the variance of the dependent variable must be known exactly. In some cases, these values are known with sufficient accuracy from other experiments so that the values can be treated as known.

Much of the material on measurement error in continuous variables comes from the work of Kendall and Stuart (1961) and Fuller (1987). Both authors make the same distinction that was made in the earlier section regarding the fixed or random nature of the independent variable. We will consider the more interesting case of measurement error in an independent random variable.

This subsection assumes a model with a continuous dependent variable and a continuous independent variable whose values are considered to be random and measured with error. For example, Hasabelnaby et al. (1989) described an analysis of pulmonary function data using measurements of NO_2 exposure as a covariate. The true NO_2 exposure was assumed to be a random variable which was estimated by sampling NO_2 levels in the home for two weeks out of the year. The other terms in the model were height and gender of the individual, and these were measured with little or no error.

The single random independent variable model assumes a single independent variable whose values, x_i, are random values. The model is

$$y_i = \beta_0 + \beta_1 x_i, \tag{7-20}$$

and we wish to estimate β_0 and β_1. Assume that the expected value of x is μ_x, the expected value of y is μ_y, and that the variance of x is σ_{xx}. We do not observe y_i and x_i, but rather Y_i and X_i, where

$$Y_i = y_i + \gamma_i \quad \text{and} \tag{7-21}$$

$$X_i = x_i + \delta_i, \tag{7-22}$$

and where γ_i is normal with mean 0 and variance σ_{yy} and δ_i is normal with mean 0 and variance σ_{xx}. The covariances between x_i, δ_i, and γ_i are assumed to be zero. This

assumption implies that the vector (Y,X) is distributed as a bivariate normal vector with mean

$$E(Y,X) = (\mu_y, \mu_x) = \beta_0 + \beta_1 \mu_x, \mu_x \tag{7-23}$$

and covariance

$$\begin{bmatrix} \sigma_{YY} & \sigma_{XY} \\ \sigma_{XY} & \sigma_{XX} \end{bmatrix} = \begin{bmatrix} \beta_1^2 \sigma_{xx} + \sigma_{xx} & \beta_1 \sigma_{xx} \\ \beta_1 \sigma_{xx} & \sigma_{xx} + \sigma_{yy} \end{bmatrix}. \tag{7-24}$$

Let $\hat{\beta}_1$ be the standard regression estimate based on the observed data, (Y_i,X_i),

$$\hat{\beta}_1 = \left[\sum_{i=1}^{n} (X_i - \bar{X})^2\right]^{-1} \sum_{i=1}^{n} (X_i - \bar{X})(Y_i - \bar{Y}). \tag{7-25}$$

The expected value of $\hat{\beta}_1$ is

$$E(\hat{\beta}_1) = \sigma_{XX}^{-1} \sigma_{XY} = \beta_1 (\sigma_{xx} + \sigma_{yy})^{-1} \sigma_{xx}. \tag{7-26}$$

Thus, for the bivariate normal model, the least squares regression coefficient is biased towards zero. The ratio, $\sigma_{XX}^{-1}\sigma_{xx}$ is known by several names including the attenuation, the reliability ratio, and in genetics as the heritability (Fuller, 1987).

Maximum likelihood equations can be set up for the bivariate normal model with measurement error. The first and second moments, which are sufficient to determine the distribution, will give five equations in the six unknown parameters, μ_x, σ_{XX}, σ_{xx}, σ_{yy}, β_0, and β_1. Clearly, some additional information is needed to make the problem identifiable. The three possibilities for additional information are σ_{xx}, σ_{yy}, or the ratio $\sigma_{xx}^{-1}\sigma_{yy}$, which lead to three different solutions. Two of these solutions are discussed in the following subsections.

If the measurement error in X, σ_{xx}, is known, then the solution is straightforward. For example, assume we know the variation between the ambient monitors because we have multiple monitors. Let S_{XX} be the maximum likelihood estimate of σ_{XX}, S_{YY} be the

maximum likelihood estimate of σ_{YY}, and S_{XY} be the maximum likelihood estimate of σ_{XY}. The maximum likelihood estimate of β_1 becomes

$$\hat{\beta}_1 = S_{XY} / (S_{XX} - \sigma_{xx}). \tag{7-27}$$

Note that this estimator reduces to equation (7-25) when the measurement error in x, σ_{xx}, is 0.

If the measurement error in Y, σ_{yy}, is known, then there is a comparable solution. Let S_{XX}, S_{YY}, and S_{XY} be defined as before. The maximum likelihood estimate of β_1 becomes

$$\hat{\beta}_1 = (S_{YY} - \sigma_{yy}) / S_{XY}. \tag{7-28}$$

All of this was based on the assumption that there was a true relationship between x and y that had no error. If, in fact, there was some error so that

$$y_i = \beta_0 + \beta_1 x_i + \varepsilon_i, \tag{7-20}$$

where ϵ_i is normal with mean 0 and variance σ_{ee}^2, then the estimate of β_1 would still come from equation (7-25), but the correlation would be estimated as

$$\hat{\rho} = \frac{\hat{\sigma}_{xy}}{\sqrt{\sigma_{xx}\,\sigma_{yy}}} = \frac{\hat{\sigma}_{xy}}{\sqrt{(S_{XX} - \hat{\sigma}_{xx})(S_{YY} - \hat{\sigma}_{yy})}}. \tag{7-30}$$

In order to estimate σ_{xx} and σ_{yy}, we can use an analysis as described in the following section. This correlation represents the upper bound to the observed correlation. That is, it is the correlation of the personal and ambient monitors if we had an infinite number of both. Under the assumption of equation (7-20), the value of this correlation is 1.

Components of Variance Models

If we have measurements from several individuals over time or several ambient monitors over time, then these measurements can be used in an analysis of variance (ANOVA) model. The purpose of the model is to estimate the variation between individuals and/or the variation between monitors. This information can then be used to adjust our slope estimates as described earlier, as well as letting us estimate the correlation between ambient and personal monitors assuming we had an infinite sample of both.

The logical analysis for this kind of data is a repeated measures design (see Winer, 1962, pp. 105-124). For most examples, the necessary components can be obtained from the results of a standard two-way ANOVA table. For example, consider the data of Tamura et al. (1996) after the missing values have been estimated (Tables 7-28, 7-29). There are 7 individuals measured over 11 48-h periods, resulting in the following ANOVA Table 7-34.

TABLE 7-34. RESULTS OF AN ANOVA ANALYSIS OF THE EXPOSURE DATA FROM JAPAN

Source of Variation	D.F.	S.S.	M.S.
date	10	9235.41	923.54
person	6	634.53	105.76
date × person	60	2248.66	37.48
Total	76	12118.60	

Source of data: U.S. EPA reanalyses of data from Tamura et al. (1996).

These results indicate that the mean square error for person is 105.76. This represents an estimate of 7 σ_{yy} + σ_{ee} (mean squared error). The value, 37.48, represents an estimate of σ_{ee}, so that σ_{yy} can be estimated by (105.76 - 37.48) / 7 = 9.75. Because we will actually use the mean of 7 persons to estimate the average, the variance component we need for equation (7-28) is estimated by 9.75/7 = 1.39.

For example, consider the data of Tamura et al. (1996). From the above analysis, we have an estimate of the person variation, σ_{yy}, of 1.39 (for the mean of 7 individuals). Thus using equation (7-28), we can estimate β_1 as (119.97 - 1.39) / 232.83 = 0.509.

7.6.3 U.S. EPA Analysis of Data Sets

7.6.3.1 Tokyo, Japan Data Set

The data set of Tamura and Ando (1994) and Tamura et al. (1996) presents an interesting problem. Shown in Table 7-35 is the correlation matrix for average personal exposure with the two nearby ambient sites as well as their average. The Yamato site is located near a highway intersection 0.7 km from the central Itabashi site.

TABLE 7-35. COVARIANCE AND CORRELATION MATRIX FOR AVERAGE PERSONAL EXPOSURE AND AMBIENT EXPOSURES FROM JAPAN

Covariance/Correlation Matrix (Correlation below diagonal)

	Average Personal	Itabashi Site	Yamato Site	Average Site
Average person	119.97	232.83	308.81	270.82
Itabashi site	(0.951)	499.30	748.50	623.90
Yamato site	(0.736)	(0.874)	1467.62	1108.06
Average site	(0.840)	(0.949)	(0.983)	865.98

Source of data: U.S. EPA reanalyses of data from Tamura et al. (1996).

Note that the correlation of the average personal exposure is much higher with the Itabashi site than with the Yamato Site or the Average of the two sites. The estimated components of variance can give strange results when there are only two sites and one is much more highly correlated. For this reason, only the Itabashi site is used in the following analyses. If there had been additional sites it would have been possible to make all of the analyses in Table 7-36, but only those single site analyses are included at this time.

7.6.3.2 Phillipsburg, New Jersey Data Set

The personal exposure data (Lioy et al., 1990) contained some missing values and three outlier values, and they all were estimated as described earlier. The results of U.S. EPA reanalyses are shown in Table 7-37. In order to estimate the error variances, these data were used in an analysis of variance as described earlier. The results are shown in Table 7-38.

TABLE 7-36. SUMMARY OF RESULTS OF THE ANALYSIS OF THE EXPOSURE DATA FROM JAPAN

Regression Model	β_1	β_0
Linear, normal error	0.466	11.3
Linear, lognormal error	0.431	13.1
Orthogonal	0.475	10.8
Linear adjusted for person error	0.509	8.9
Linear adjusted for ambient error	(Not available)	
Measures of Association		**Value**
Correlation of personal averages with Itabashi site		0.951
Correlation adjusted for measurement error		(Not available)
Average correlation of ambient with mean person		(Not available)
Average correlation of person with mean ambient		0.872
Fraction of variation explained by orthogonal regression		0.985

Source: U.S. EPA reanalyses of data from Tamura et al. (1996).

The site monitoring data contained some missing values, and they were estimated by U.S. EPA as described in Section 7.6.2.1. The means, covariances and correlations were also estimated. The results are in Table 7-39. In order to estimate the error variances, the same data were used in an analysis of variance as described earlier. The results of the EPA analyses are shown in Table 7-40. The individual exposure values were averaged as well as the site exposure values. These means are shown in Table 7-41.

The same regression analyses described earlier were performed by U.S. EPA. A plot of the linear regression is shown in Figure 7-32. The orthogonal regression gives virtually an identical plot and is not shown. The results of the analyses are in Table 7-42.

Note that all estimated regression equations are quite similar. The interesting value is the correlation adjusted for measurement error. This represents an estimate of the correlation between the mean of an infinite number of personal samplers and the mean of an infinite number of fixed site samplers. This value is relatively close to one, but we do not have good estimates of its variance to tell if the value is really different from one.

TABLE 7-37. PERSONAL EXPOSURE SUSPENDED PARTICULATE MATTER DATA FROM PHILLIPSBURG, NEW JERSEY. MISSING VALUES ESTIMATED ( ); OUTLIER VALUES RECOMPUTED [ ].

	Person Identifier ($\mu g/m^3$)													
Day	01	02	11	31	41	42	51	52	61	62	81	82	91	92
1	59	85	54	39	(53.2)	36	41	28	123	67	96	79	50	32
2	52	58	85	17	(76.7)	45	50	53	104	56	50	49	66	63
3	74	69	94	56	86	77	90	93	200	134	166	81	77	187
4	115	88	136	104	65	116	112	120	125	272	193	98	164	172
5	65	37	139	38	77	64	56	52	184	190	79	49	(95.7)	89
6	45	16	56	22	34	27	28	21	60	58	57	12	54	99
7	75	77	65	35	36	80	27	34	92	(110.2)	124	77	107	184
8	104	81	79	67	83	32	69	61	112	91	144	69	96	198
9	84	29	48	56	85	122	30	36	57	96	156	123	91	[100.6]
10	55	29	70	35	59	81	25	39	199	77	63	41	66	135
11	10	60	65	25	36	[48.1	49.4]	43	93	84	99	32	78	122
12	39	59	80	23	127	57	32	35	121	95	31	45	63	72
13	26	44	65	35	31	47	114	67	47	95	71	18	31	109
14	45	44	89	17	105	117	(24.8)	24	117	63	44	14	57	108

Source: Data from Lioy et al. (1990). Missing values estimates and recomputed outlier values calculated by U.S. EPA.

TABLE 7-38. RESULTS OF AN ANOVA ANALYSIS OF THE PERSONAL EXPOSURE DATA OF PHILLIPSBURG, NEW JERSEY

Source of Variation	d.f.	s.s.	m.s.
Date	13	119,600	9202
Person	13	103,300	7942
Date × Person	169	149,900	887
Total	195	372,800	

Source: U.S. EPA reanalyses of data from Lioy et al. (1990).

TABLE 7-39. SAM SITE CONCENTRATIONS, PM_{10} DATA ($\mu g/m^3$) FROM PHILLIPSBURG, NEW JERSEY [Missing Values Estimated ( )].

Day	Site 101	Site 102	Site 103	Site 020
01	26	41	28	24
02	51	(55.6)	55	46
03	94	(101.8)	112	98
04	148	155	165	209
05	76	81	76	85
06	15	17	13	50
07	44	47	49	51
08	101	105	119	99
09	59	67	68	66
10	46	52	50	57
11	37	36	35	34
12	28	33	28	28
13	27	27	27	25
14	21	23	19	38
Means	55.2	60.1	60.3	65.0
Covariance/Correlation Matrix (Correlation below diagonal)				
Site 101	1313.9	1346.5	1538.9	1596.6
Site 102	0.995	1393.8	1581.4	1630.9
Site 103	0.996	0.994	1816.2	1850.1
Site 020	0.943	0.935	0.929	2183.4

Source: U.S. EPA reanalyses of data from Lioy et al. (1990).

TABLE 7-40. RESULTS OF AN ANOVA ANALYSIS OF THE SITE EXPOSURE DATA OF PHILLIPSBURG, NEW JERSEY

Source of Variation	d.f.	s.s.	m.s.
Site	3	671	223.6
Day	13	90286	6945.1
Site × Day	39	3615	92.7
Total	55	94572	

Source: U.S. EPA reanalyses of data from Lioy et al. (1990).

TABLE 7-41. AVERAGE PERSONAL PM_{10} EXPOSURE DATA COMPARED WITH THE SITE EXPOSURE DATA FOR PHILLIPSBURG, NEW JERSEY

Day	Ambient Average ($\mu g/m^3$)	Average Personal ($\mu g/m^3$)
1	29.75	60.15
2	51.55	58.91
3	101.45	106
4	169.25	134.29
5	79.5	86.76
6	23.75	42.07
7	47.75	80.23
8	106	91.86
9	65	79.19
10	51.25	69.57
11	35.5	60.74
12	29.25	62.79
13	26.5	57.14
14	25.25	62.04

Source: U.S. EPA reanalyses of data from Lioy et al. (1990).

7.6.3.3 Beijing, China Data Set

The Beijing, China data set reported by the World Health Organization (1985) is listed in Table 7-43. From these data, daily mean values of the ambient and personal exposure values were computed. An U.S. EPA reanalysis of these data is shown in Table 7-44 and in Figure 7-33. The results of the analysis indicate that there is not a significant linear relationship between the personal and ambient monitoring data. For this reason, it does not

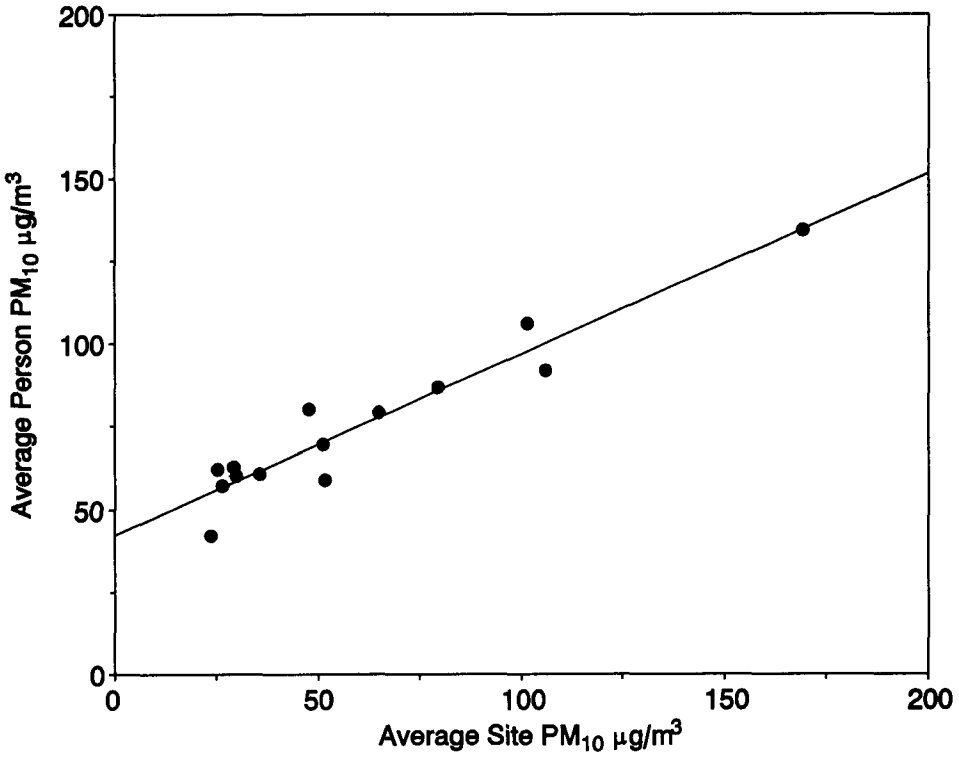

Figure 7-32. Plot of relationship between average personal PM_{10} exposure versus ambient PM_{10} monitoring data from Phillipsburg, NJ and regression line calculated by U.S. EPA.

Source: Lioy et al. (1990).

make any sense to adjust the coefficient for measurement error. The subjects all worked at the same institute so their daytime personal exposures may not have been independent of each other.

7.6.3.4 Riverside, California Data Set

Both the personal exposure and the monitoring data used in analyses by Clayton et al. (1993) contained some missing values, and they were estimated by U.S. EPA as described earlier. The estimated correlation/covariance matrix results of U.S. EPA reanalyses of these data are shown in Table 7-45.

Because the individual monitors were placed on different individuals each period, we can't really estimate the variation between individuals. Based on previous analyses, we know that most of the residual is variation between individuals, and so we will use this as a

TABLE 7-42. RESULTS OF THE ANALYSIS OF THE EXPOSURE DATA FROM PHILLIPSBURG, NEW JERSEY

Regression Model	β_1	β_0
Linear, normal error	0.546	42.3
Linear, lognormal error	0.560	41.4
Orthogonal	0.556	41.9
Linear adjusted for person error	0.556	41.9
Linear adjusted for ambient error	0.587	40.1
Measures of Association		**Value**
Correlation of averages		0.955
Correlation adjusted for measurement error		0.974
Average correlation of ambient with mean person		0.944
Average correlation of person with mean site		0.633
Fraction of variation explained by orthogonal regr.		0.984

Source: U.S. EPA reanalyses of data from Lioy et al. (1990).

surrogate. On average there were 3.5 persons per period and this number of individuals was used in the analysis of variance shown in Table 7-46. The dichot monitoring data contained little missing data, and so it was analyzed against the personal monitoring data for those days with data. The results of the linear regression are in Table 7-47 and are shown graphically in Figure 7-34. The individual exposure values were averaged so that they could be compared with the site exposure values. These means are shown in Table 7-48. Note that the orthogonal regression slope is larger than either of the linear regression slopes. Note also that the linear regression slope adjusted for measurement error is larger than any of the other slopes.

7.6.3.5 Azusa, CA Data Set

The Azusa, CA data set for PM_{10} reported on by Wiener et al. (1990) was described earlier in Section 7.4.1.1.1 and presented in Table 7-21a. The same regression analyses described earlier in this section were performed on the 24-h cross-sectional data and the results are shown in Table 7-49. A plot of the linear regression analysis, resulting in a

TABLE 7-43. PERSONAL AND AMBIENT EXPOSURE DATA FOR BEIJING, CHINA (mg/m^3)

Day	Personal	Ambient	Day	Personal	Ambient
1	0.13	0.19	6	0.15	0.42
2	0.15	0.25	6	0.17	0.42
2	0.10	0.25	6	0.13	0.42
2	0.12	0.25	6	0.16	0.42
2	0.23	0.25	6	0.21	0.42
2	0.14	0.25	6	0.08	0.42
3	0.11	0.31	7	0.35	0.44
3	0.09	0.31	7	0.24	0.44
3	0.09	0.31	7	0.20	0.44
4	0.31	0.33	8	0.15	0.53
4	0.12	0.33	9	0.23	0.55
4	0.13	0.33	9	0.18	0.55
4	0.35*	0.33	9	0.10	0.55
4	0.12	0.33	9	0.38	0.55
4	0.25	0.33	10	0.11	0.59
5	0.10	0.36	11	0.23	0.69
5	0.22	0.36	11	0.32	0.69
5	0.32	0.36	11	0.11	0.69
5	0.12	0.36	11	0.21	0.69
5	0.08	0.36	11	0.11	0.69
5	0.13	0.36	11	0.20	0.69
5	0.07	0.36	11	0.29	0.69

*The only personal value higher than the ambient value.

Source: World Health Organization (1985).

TABLE 7-44. RESULTS OF LINEAR REGRESSION ANALYSIS FOR THE BEIJING, CHINA EXPOSURE DATA

Linear regression analysis of average personal exposure versus ambient exposure

Y = intercept + slope X

Variable	Beta	Std. Error Beta
Intercept	0.116	0.040
Slope	0.142	0.088

ANOVA Table

Source	Sum of Squares	Mean Square Error	D.F.	F-Value
Regression	0.0179	0.00893	2	1.2911
Error	0.2835	0.00692	41	
TOTAL	0.3014	0.00701	43	

R-squared = 0.05925, r = 0.2434

Log-likelihood = −46.95

Source: U.S. EPA reanalyses of data from World Health Organization (1985).

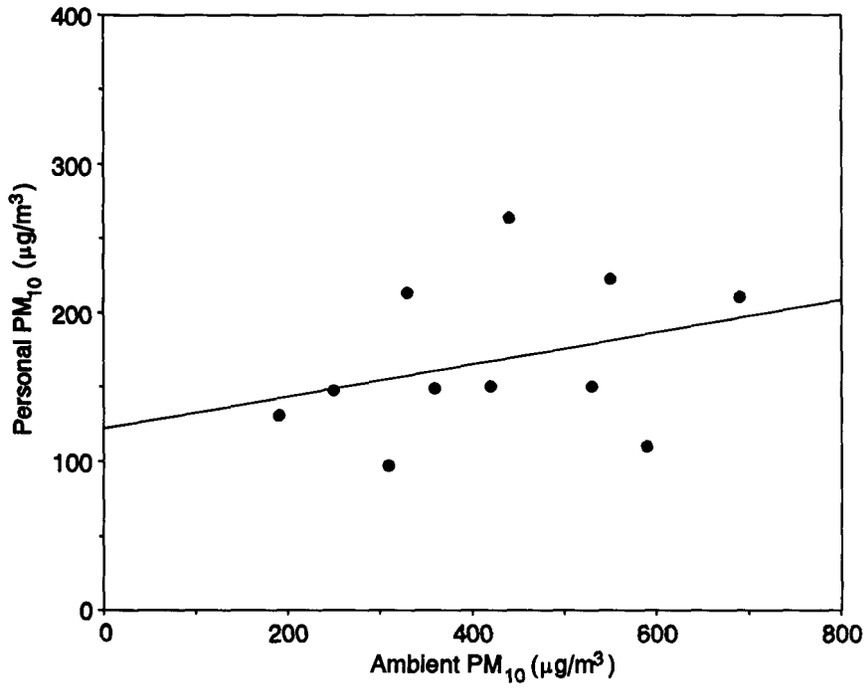

Figure 7-33. Plot of means of personal exposures and ambient PM_{10} from Beijing, China and regression line calculated by U.S. EPA.

Source: U.S. EPA reanalyses of data from World Health Organization (1985).

TABLE 7-45. ESTIMATED MEAN VECTOR, COVARIANCE MATRIX, AND CORRELATION MATRIX OF PERSONAL EXPOSURE PM_{10} DATA FROM RIVERSIDE, CALIFORNIA (24-h, $\mu g/m^3$)

	Monitor					
	Personal	Indoor	Backyard	Dichot	Wedding	PEM-SAM
Means	109.9	79.9	91.7	71.2	68.4	80.4
Covariance/Correlation Matrix (Correlation below diagonal)						
Personal	1055.0	917.4	1024.7	749.0	838.9	913.7
Indoor	(0.849)	1107.6	1017.9	832.7	897.0	987.4
Backyard	(0.725)	(0.703)	1893.2	1165.6	1296.9	1427.4
Dichot	(0.707)	(0.767)	(0.821)	1063.4	1116.6	1232.9
Wedding	(0.721)	(0.753)	(0.832)	(0.956)	1282.8	1337.1
PEM-SAM	(0.736)	(0.776)	(0.858)	(0.989)	(0.976)	1462.3

Source: U.S. EPA reanalyses of data reported on by Pellizzari et al. (1992).

TABLE 7-46. RESULTS OF AN ANOVA ANALYSIS OF THE PERSONAL EXPOSURE DATA OF RIVERSIDE, CALIFORNIA

Source of Variation	D.F.	S.S.	M.S.
period	46	167,400	3640
residual	114	275,000	2412
Total	160	442,400	

Source: U.S. EPA reanalyses of data reported on by Pellizzari et al. (1992).

TABLE 7-47. RESULTS OF THE ANALYSIS OF THE EXPOSURE DATA FROM RIVERSIDE, CALIFORNIA

Regression Model	β_1	β_0
Linear, normal error	0.6174	59.7
Linear, lognormal error	0.6185	57.1
Orthogonal	0.8071	44.2
Linear adjusted for person error	0.9675	31.0
Linear adjusted for ambient error	(Not applicable)	
Measures of Association		**Value**
Correlation of averages		0.721
Correlation adjusted for measurement error		(Not applicable)
Fraction of variation explained by orthogonal regr.		0.864

Source: U.S. EPA reanalyses of data reported on by Pellizzari et al. (1992).

negative slope, is shown in Figure 7-35. There clearly is no relationship between the pooled PEM and SAM variables for this data set. The statistical explanation for the negative correlation and slope (PEM decreases with increasing SAM) is that one of the observations (PEM = 273 $\mu g/m^3$, SAM = 48 $\mu g/m^3$, for House 9, Day 10, person 1, as shown in Table 7-21a) is an outlier (273 $\mu g/m^3$ > mean + 3*SD). Removal of this single datum point changes both the correlation and the slope to slightly positive values of similar magnitude. Because of the insignificance of the slope and correlation, further adjustments for measurement error do not make sense.

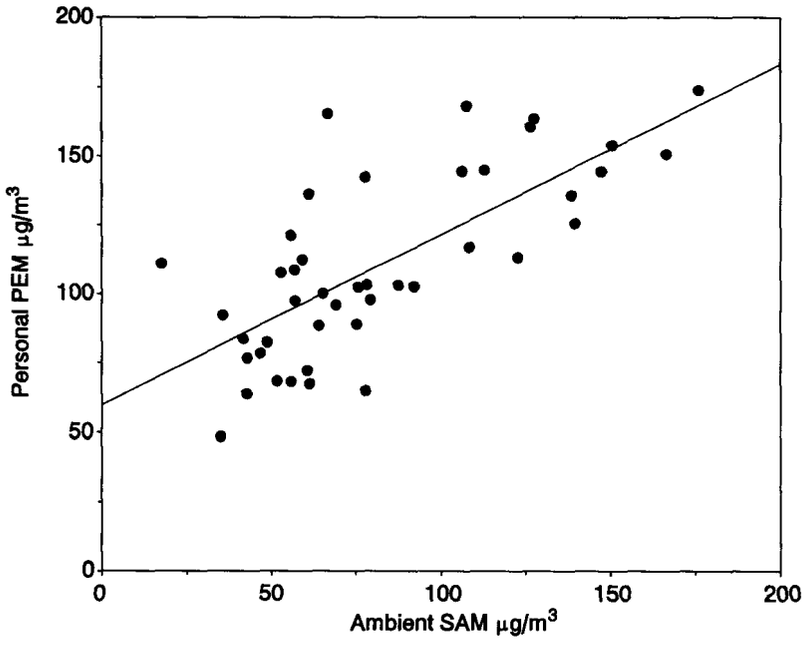

Figure 7-34. PTEAM mean 24-h PM_{10} data compared for personal PEM and SAM.

Source: U.S. EPA reanalyses of data reported on by Pellizzari et al. (1992).

7.6.4 Discussion of Statistical Analyses: Mean PEM Versus Mean SAM

The Beijing study had an insignificant positive slope and the Azusa study gave an estimated slope less than zero that becomes insignificant positive with the removal of one outlier. Possible explanations for the low slope of the Beijing study may be related to the unusually low ratio of PEM to SAM of order 0.4. Either the SAM $PM_{3.5}$ monitor that was used may have been influenced by a local PM source, and thereby was not representative of the Beijing locality where the subjects worked and lived, or the air exchange between indoors and outdoors during the winter period was greatly minimized for personal comfort.

In the Beijing dataset of 44 pairs of simultaneous SIM and SAM (Table 7-43) only one $PM_{3.5}$ PEM value was greater than SAM, as opposed to Azusa where in the 50 pairs of simultaneous SIM and SAM (Table 7-21b) only six $PM_{2.5}$ PEM values were less than SAM. On a day where SAM $PM_{3.5}$ reached 690 $\mu g/m^3$ in Beijing, seven simultaneous PEM values all ranged between 110 $\mu g/m^3$ and 320 $\mu g/m^3$. In relation to Figure 7-16, these PEM/SAM ratios between 0.16 and 0.45 correspond to low air exchange rates of order 0.1 to 0.3 air changes per hour. In the tightly-sealed poorly-heated building where all the subjects worked

TABLE 7-48. AVERAGE 24-HOUR PM_{10} PERSONAL EXPOSURE DATA COMPARED WITH THE PEM-SAM SITE EXPOSURE DATA FOR RIVERSIDE, CALIFORNIA ($\mu g/m^3$)

Period	Average Personal	PEM-SAM Site
1	48.3	35.1
3	83.6	41.7
5	108.6	56.9
7	88.3	64.1
9	68.3	51.7
11	121.0	55.8
15	68.2	56.0
17	95.8	69.1
19	102.5	92.0
21	116.8	108.2
23	160.5	126.4
25	97.7	79.4
27	72.2	60.7
29	107.6	52.9
31	103.0	87.4
37	165.3	66.8
39	144.4	106.2
41	135.6	138.5
43	168.2	107.5
47	173.8	175.9
49	144.9	112.9
51	65.0	77.9
53	76.7	42.8
57	110.9	17.6
59	78.4	46.7
61	136.1	61.1
63	103.1	78.4
65	142.4	77.9
67	163.6	127.6
69	153.7	150.4
71	144.2	147.4
73	150.6	166.4
75	125.4	139.6
77	112.1	59.2
79	63.7	42.7
81	67.5	61.4
83	102.2	75.8
85	92.0	35.7
87	100.0	65.3
89	88.9	75.3
91	113.0	122.7
93	82.4	48.8
95	97.3	57.1

Source: U.S. EPA-calculated 24-h averages, based on 12-h data reported on by Pellizzari et al. (1992).

TABLE 7-49. RESULTS OF THE LINEAR REGRESSION ANALYSIS OF THE EXPOSURE DATA FROM AZUSA, CALIFORNIA

Variable	Beta	Std. Error Beta
Intercept	119.1	13.77
Slope	−0.054	0.201

Covariance Matrix of Parameter Estimates	Intercept	Slope
Intercept	189.7	−2.543
Slope	−2.543	0.040

Log-likelihood = −263.4

ANOVA Table

Source	Sum of Squares	Mean Square Error	D.F.	F-Value
Regression	111.2	55.6	2	0.0363
Error	76590	1531.8	50	
TOTAL	76700	1475.1	52	

R-squared = 0.0015

Source: U.S. EPA reanalyses of data reported on by Wiener et al. (1990).

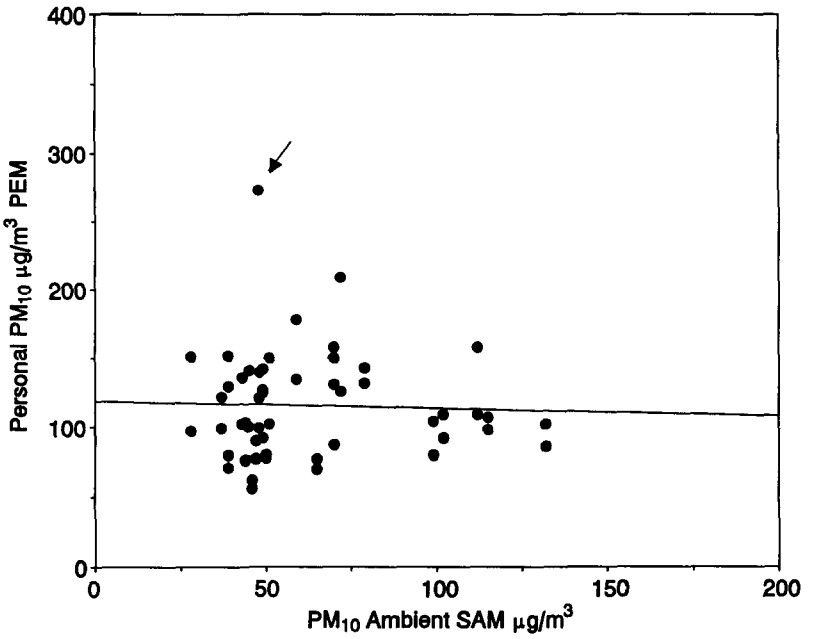

Figure 7-35. Plot of ambient and personal monitoring PM_{10} data from Azusa, CA and calculated (slightly negative slope) regression line, which becomes positive if single outlier value (↙) is deleted.

Source: U.S. EPA reanalyses of data reported on by Wiener et al. (1990).

during the Beijing winter, a small variation in air exchange could result in a relatively large difference in the indoor PM, which would result in PEM that appears to be uncorrelated with SAM. If a contribution of PM generated by personal activity and ETS is subtracted from the PEM values then the estimated air exchange rates would be even lower. The remaining discussion will be based on the other three studies, realizing that the discussion is not supported by these two studies.

The major conclusions which can be reached from the remaining three studies are as follows.

(1) The average of several ambient monitors correlates better with mean personal exposure than does an individual site (as would be predicted by the Central Limit Theorem).

(2) The average of several personal monitors correlates better with mean ambient exposure than does the ensemble of individual monitors.

(3) There is no evidence of the existence of a maximum (ceiling) correlation between personal and ambient measurements. The only study with fixed multiple ($n > 2$) ambient SAM locations and multiple personal monitors is the Phillipsburg, NJ, study. The estimated correlation adjusted for measurement error was 0.97. The true (unknown) correlation between an infinite average of personal monitors with an infinite average of fixed site monitors may be different (smaller) in other locations, but we do not have the data to evaluate that.

(4) The correlation coefficient is probably the best measure of association between personal and ambient measurements. It can be used independent of the regression technique or model and does not assume a distributional form. The "percent of variation explained" as derived from orthogonal regression is not comparable to any measure used for other models.

(5) The choice of a model (linear, linear with lognormal error, orthogonal) makes less difference than the adjustment for measurement error.

(6) Based on the results of the Phillipsburg, NJ, analysis, one or more fixed site monitors can do an excellent job of predicting the average of all personal exposures (if they could be measured) even though the prediction for most individual exposures is quite poor. This is also supported by the Tokyo, Japan, data set (Tamura et al., 1996). The other data sets did not provide adequate information to either confirm or deny this conclusion.

The value of the improvement of the mean PEM relationship to SAM is that it provides a better visualization that helps in understanding how mean PEM varies with SAM. It thus provides a measure of the validity of the use of a daily PM SAM as a surrogate for the mean

PM PEM in the community for nonsmokers. It is clear that the uncertainty in predicting mean personal exposure PM is much smaller than the uncertainty in predicting the personal exposure PM for a nonsmoking individual when we note that the means have a much smaller variability about the line as shown in Figures 7-31, 7-32, and 7-34.

There appears to be two distinct categories of cross-sectional exposure studies that were examined: In the first type of study, such as Lioy et al. (1990), Clayton et al. (1993), and Tamura et al. (1996), there is a significant R^2 between individual PM PEM and PM SAM. In this category, there is an appreciable improvement in correlation between the mean PEM and SAM. It has been suggested that these cases with higher correlation of PEM PM with SAM PM may arise where the fine portion of the ambient PM ($PM_{2.5}$) is highly variable from day-to-day, and the ambient coarse fraction is relatively constant (Wilson and Suh, 1995). In an urban area, the fine particle composition and the fine particle concentration are often highly correlated from site-to-site on any given day. This is due, in part, to the gas phase reactions of SO_x and NO_x, associated with regional sources, to produce sulfates and nitrates in the submicron range. Because of the long residence times of these species due to their negligible deposition velocities, they are well mixed throughout the air mass (Suh et al., 1995; Burton et al., 1996).

On the other hand, ambient coarse particles are generated locally, and they have higher deposition velocities than the fine particles. Their impact may then be limited by fallout to a locality downwind of their emission point, as they are not readily transported across an urban area. Therefore, during an air pollution episode, people living in an urban area may be exposed to fine PM of similar chemical composition and concentrations, whereas they will be exposed to coarse PM of ambient origin with a chemical composition that can depend on the location of the exposure. Because ambient PM penetrates readily into a nonambient setting, the correlation between the mean $PM_{2.5}$ PEM and $PM_{2.5}$ SAM would be high because all the people would have similar exposure to the ambient fine PM - plus exposure to indoor generated $PM_{2.5}$ which may have less fluctuation in the absence of smoking.

In the second type of study, such as Sexton et al. (1984), Spengler et al. (1985), and Wiener et al. (1990), there is negligible correlation between individual PEM PM and SAM PM, and consequently there will be little correlation between their mean PEM and the SAM. In these cases, if the fine fraction is not an appreciable portion of the ambient PM, or there

are significant indoor sources, then the correlations between mean PM PEM and PM SAM will be lower and possibly not significantly different from zero.

7.7 IMPLICATIONS FOR PARTICULATE MATTER AND MORTALITY MODELING

PM related mortality may be specific to the most highly susceptible portion of the population. Such a cohort may be the elderly people with the most serious chronic obstructive pulmonary disease (COPD) and cardiac insufficiency. Smithard (1954) relates the findings of Dr. Arthur Davies (Lewisham coroner) who autopsied 44 people who died suddenly during the 1952 London Fog:

> "The great majority of deaths occurred in people who had pre-existing heart and lung trouble, that is to say they were chronic bronchitic and emphysematous people with consequent commencing myocardial damage. The suddenness of the deaths, Dr. Davies thought, was due to a combination of anoxia and myocardial degeneration resulting in acute right ventricular dilatation."

Mage and Buckley (1995) hypothesized that these people with compromised cardio-pulmonary systems may be relatively inactive, while selecting to live in homes or institutional settings without sources of indoor pollution. When their time is spent in clean settings (e.g. where smoking is prohibited), they would have little exposure to PM other than from the ambient pollution that intrudes into their living quarters (Sheldon et al., 1988a,b). The exposure to PM of this cohort, would be highly correlated with PM SAM, and so would be their mortality, if this ambient PM was reactive in their pulmonary tracts as described by West (1982). However, there have been no results reported of an exposure study done on people with COPD who correspond to the Lewisham mortality cohort. The cohort of five elderly housewives and two male retirees in Tokyo (Tamura et al., 1996) may come close to this susceptible cohort. Individual PM PEM of people outside these cohorts, who could be relatively insensitive to ambient PM, might not be significantly correlated with PM SAM, as reported in most of the other studies of nonsmokers cited in Table 7-26. This suggests a model to relate PM and mortality as follows. Let any person (j) on a given day have a probability of mortality, $p(m) = k_j X_j$, where k_j is the unit probability of mortality per $\mu g/m^3$ of PM per day, X_j is the daily average exposure to PM, $\mu g/m^3$, independent of k_j. Let us

assume that each individual (j) has their own personal value of k_j that can vary from day-to-day with changes in their respiratory health, such as a transient pulmonary infection (West, 1982).

The expectation of total mortality (M) in a community of size N can be shown to be the summation of k X over all individuals (j = 1 to N) as follows:

$$M = \Sigma k_j X_j \tag{7-31}$$

If k_j is independent of X_j, then we can define K as (1/N) Σk_j, and the mean community exposure $\bar{X}$ as (1/N) ΣX_j, and it follows

$$M = NK\bar{X} \tag{7-32}$$

This implies that, given a linear relationship of mortality with PM PEM exposure (X) as assumed in most studies discussed in Chapter 12, the expected mortality is proportional to the mean community personal exposure to PM. The individual in the community, on any given day, with the highest probability of dying from a PM exposure related condition is that individual with the highest product $k_j X_j$, not necessarily the highest exposed individual with the maximum value of X_j (West, 1982).

The Phillipsburg, NJ, data set is a case in point. In this study, three subjects had excessively high PEM PM. These values were caused by a hobby involving welding in a detached garage (971 $\mu g/m^3$), a home remodeling activity (809 $\mu g/m^3$) and usage of an unvented kerosene heater (453 $\mu g/m^3$). Excessive PM generating activities are not expected of elderly people who may have compromised pulmonary systems. In fact, the elderly and infirm husband of the remodeler had a personal exposure of 45 $\mu g/m^3$ on the day of the remodeling activity. The indoor monitors in the homes of the welder and remodeler only recorded 55 $\mu g/m^3$ and 19 $\mu g/m^3$, respectively, during those events, indicating the specificity of the high exposure to only the individual involved. These three outliers were removed from the analysis and were replaced by the procedure for missing data of section 7.6.2.1, which estimates their exposures as if they had not done those specific activities responsible for their noncharacteristic exposures (see Table 7-37). This procedure is reasonable, since it

is unlikely that these activities would be performed by individuals with pulmonary conditions similar to those of the Lewisham mortality cohort (Smithard, 1954). As shown on Table 7-42 and Figure 7-32, the regression improves markedly to a value of $R^2 = 0.914$.

It is this relation of the average PM PEM exposure to PM SAM concentration, as shown in Figure 7-32 that may be a better representation of the true situation underlying the PM vs mortality relationships because of the "healthy worker" effect. Chronically ill people who are sensitive to PM might change their behavior to minimize their exposure to irritants. Consequently, healthy people with high PEM PM measures in occupations and indoor settings can cause the regression R^2 between PEM and SAM for nonsmokers to be low, but they may not be the individuals at highest risk of the acute effects of PM exposure.

7.7.1 Relative Toxicity of Ambient Particulate Matter and Indoor Particulate Matter

In the previous sections the SAM PM was evaluated as a predictor of PEM PM of nonsmokers on the implied basis that the health effects of PM were only mass dependent, and independent of chemical composition. It was shown in Table 7-26 that many early PM studies of PEM had a low correlation between PEM and SAM on a cross-sectional basis that was often not significantly different from zero. But, in the later studies (Tamura et al., 1996; Lioy et al., 1990), a significant relationship was observed between PEM and SAM on an individual basis. Further analysis showed that on a daily basis, SAM would appear to be a good predictor of mean community exposure to ambient PM_{10} of nonsmoke exposed people from the results of the Tokyo, Japan; Riverside, CA; and Phillipsburg, NJ; studies. However, there can be a large difference in toxicity of PM per unit mass which is related to the chemical composition, solubility and size of the particles. For example, mercury (Hg) and arsenic (As) have significantly different toxicities in their inorganic and organic forms. Hexavalent chromium (Cr) is more toxic than trivalent Cr. Anthropogenic PM, from combustion of fossil fuels, is much more toxic than PM of natural origin (Beck and Brain, 1982; Mage et al., 1996). Fine urban particulate matter generated by coal smoke during the 1952 London Fog at concentrations of order 2,000 $\mu g/m^3$ caused thousands to die (Holland et al., 1979; United Kingdom Ministry of Health, 1954) but 2,000 $\mu g/m^3$ of soil dust from dust storms (Hansen et al., 1993) would not have been as deadly.

Soil constituents that are tracked-in to a home on shoes, and are subsequently resuspended, contribute to the personal cloud (Roberts et al., 1990; Thatcher and Layton, 1995). "Even if this crustal PM is relatively inert, its presence in the lung potentiates the toxicity of the anthropogenic particles because it increases the residence time of the more toxic PM (WHO, 1995)" (Mage et al., 1996). This increase in soil constituents was also shown in the PTEAM study (Özkaynak et al., 1996) on Figure 7-22 "by observation that nearly all [soil] elements were elevated in personal samples" but sulfur, which is in the ambient fine mode, was not a personal cloud constituent. This is consistent with the observations of Wilmoth et al. (1991) that "extremely small particles (below two micrometers) require local airflow (sampling) velocities near 100 miles per hour [45 m/s] to overcome surface attraction forces and dislodge [them] for sampling".

Figure 7-36 shows an example of resuspension of Pb in a Denver, CO, home (Moschandreas et al., 1979). During the one-week sample, a wind shift brought a clean air mass to below 0.01 $\mu g/m^3$. In this time period, the average indoor Pb dropped from 0.085 to 0.048 $\mu g/m^3$. The residual 0.048 $\mu g/m^3$ represents the effect of resuspension by human activity. When the wind shifted again, and ambient Pb rose to 0.360 $\mu g/m^3$ the indoor Pb rose to 0.180 $\mu g/m^3$. Note the peaks in the indoor concentration of Pb up to and above 0.10 $\mu g/m^3$ during the clean air period which are indicative of variations in resuspension by human activities.

There is also some indication in laboratory animal studies, using transpleural catheterization and intratracheal instillation, that products of fossil fuel combustion are more acutely toxic to animals than wood smoke and soil constituents (U.S. Environmental Protection Agency, 1982, Table 12-6; Beck and Brain, 1982). Although these laboratory animal studies may have no direct relation to toxicity in humans, they provide an indication of their relative toxicity in animals when administered by those two routes.

In summary, there is evidence that not all PM constituents have the same toxicity per unit mass. These differences are due to differences in aerodynamic diameter and chemical composition. As shown on a Venn diagram (Figure 7-37, Mage [1985]), the focusing of the description of a PM_{10} exposure increases the ability to estimate the potential toxicity of the exposure. In the sequential description given below, the uncertainty in the toxicity of the mixture is decreased as more information is provided.

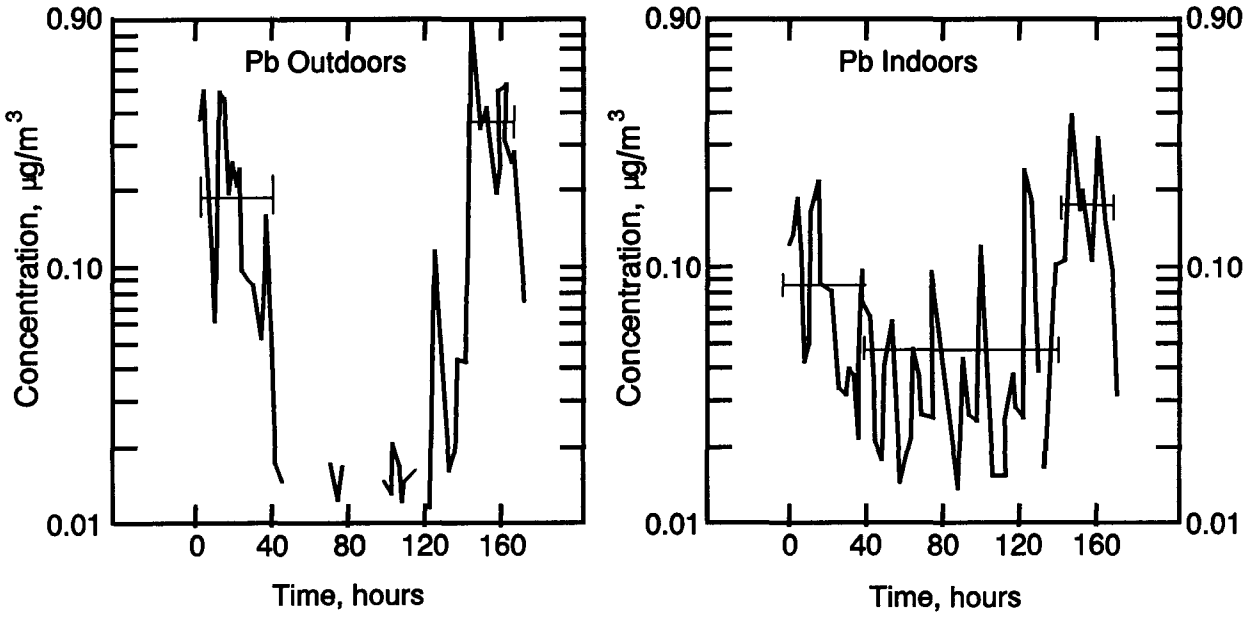

Figure 7-36. Comparison of indoor and outdoor concentrations of lead in a home in Denver, October 1976, for 1 week, starting at 1600 h. Mean values are given by horizontal bars.

Source: Moschandreas et al. (1979).

1. 2 $\mu g/m^3$ of PM_{10}.

2. 2 $\mu g/m^3$ of PM_{10} in the size interval 2 to 2.5 μm.

3. 2 $\mu g/m^3$ of PM_{10} in the size interval 2 to 2.5 μm, 50% of automotive origin and 50% of indoor source origin.

4. 2 $\mu g/m^3$ of PM_{10} in the size interval 2 to 2.5 μm, 50% of automotive origin and 50% of indoor source origin, 0.5 $\mu g/m^3$ of Pb, 0.5 $\mu g/m^3$ of BaP and 1 $\mu g/m^3$ of unspecified inorganic material.

As applied to human exposure to PM, this concept of differential toxicity suggests that data collections might benefit by providing data that would allow the toxicity of a PM exposure to be evaluated in terms of chemical information, in addition to the mass collected per unit volume.

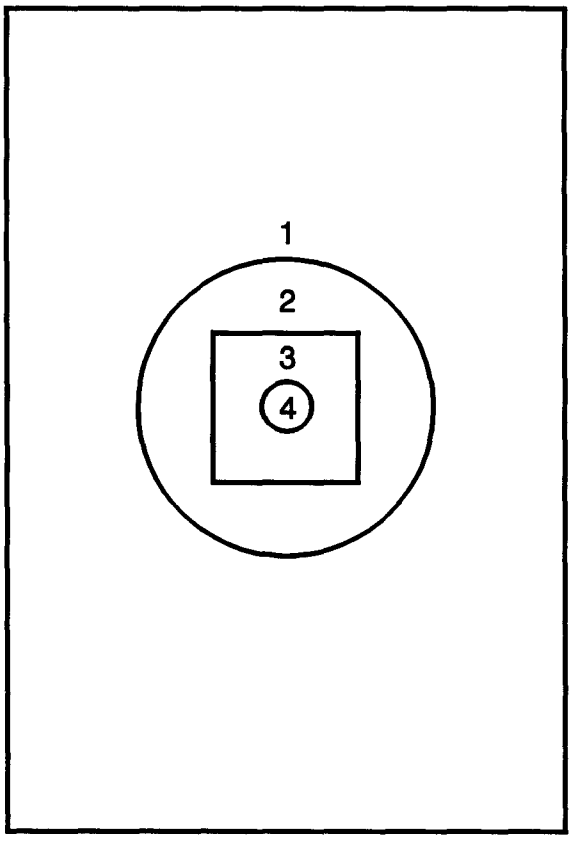

Figure 7-37. Venn diagram (Mage, 1985) showing focusing of information to more completely specify toxicity of a given PM mixture: (1) universe of all possible mixtures of PM with concentration of 2 $\mu g/m^3$; (2) subuniverse of all combinations of PM with concentration of 2 $\mu g/m^3$ in size interval 2.0 to 2.5 μm; (3) subuniverse of all combinations of PM with concentration of 2 $\mu g/m^3$ in size interval 2.0 to 2.5 μm AD with 50% of automotive origin and 50% from indoor sources; and (4) subuniverse of all combinations of PM with concentration of 2 $\mu g/m^3$ in size interval 2.0 to 2.5 μm AD with 50% of automotive origin and 50% from indoor sources; 25% Pb, 25% BaP and 50% unspecified inorganic materials.

7.7.2 Summary: Linkage of Ambient Concentrations of Particulate Matter to Personal Exposures to Particulate Matter

As described by Wilson and Suh (1995), total exposure to ambient PM (X_{ae}) of any given size range is equal to the summation of exposures to ambient PM over both ambient (X_a) and nonambient (X_{na}) microenvironmental conditions. Total exposure to PM is equal to X_{ae} plus exposure to nonambient PM concentrations generated independently of personal activities (X_{nai}) and nonambient PM concentrations generated dependently on personal

activities (X_{nap}) which may correspond to smoking and the personal cloud effect. For a period (T) of constant ambient PM a subject spends time T_a outdoors and time ($T - T_a$) in *n* different nonambient microenvironments. The total exposure to ambient PM can be expressed as:

$$X_{ae} = \frac{[T_a X_a + (T - T_a) X_{na}]}{T} \tag{7-33}$$

For a nonambient microenvironment, the equilibrium concentration of ambient particles in it will be equal to

$$X_{na} = \frac{X_a P a}{(a + k)} \tag{7-6}$$

where P = penetration fraction of PM in the ambient air entering the nonambient microenvironment,

a = air exchange rate, h^{-1}

k = deposition rate (a function of AD), h^{-1}.

As discussed in section 7.2, the penetration factor P is virtually equal to 1 for all particles less than 10 μm (Thatcher and Layton, 1995) and the fraction of X_{na}/X_a is as shown on Figure 7-16. Combining equations 7-33 and 7-6, we obtain

$$X_{ae} = \frac{X_a[T_a + \Sigma t_j a_j/(a_j + k)]}{T} \tag{7-34}$$

where $T - T_a = \Sigma t_j$, total time spent indoors,

j = 1 to n, index of indoor microenvironment visited.

Defining z as the overall ratio of exposure to ambient PM (X_{ae}) to the ambient concentration (X_a), so that $X_{ae} = z X_a$, letting $y = T_a/T$, the fraction of time the subject is outdoors, we obtain the average relation,

$$z = y + (1 - y) \overline{\left[\frac{a}{a + k}\right]}, \tag{7-35}$$

where $\overline{\left(\frac{a}{a + k}\right)}$ is a time weighted average.

As shown on Figure 7-38, on a daily basis, z can vary by an appreciable amount by spending a fraction (y) of time outdoors. For $y = 1/3$ (8 h), exposures to fine ambient $PM_{2.5}$ increase by 100% for people living in homes with an air exchange rate $a = 0.1\ h^{-1}$.

The total exposure (X) can now be written as,

$$X = z\, X_a + \frac{\Sigma\ [(X_{nai})_j + (X_{nap})_j]\ t_j}{T}, \tag{7-36}$$

where $\Sigma\ [(X_{nai})_j + (X_{nap})_j]\ t_j / T = \beta$, the personal exposure increment produced by sources that do not influence the ambient concentration as measured by a stationary ambient monitor (SAM). Simplifying, we can rewrite Equation 7-36 as,

$$X = z\, X_a + \beta \tag{7-37}$$

which gives a physical significance to the slope and intercepts of the regressions of PEM (X) versus SAM (X_a) as discussed in Section 7.6.

The values of z, which depend on y, a, k and P can be determined from their independent measurements described previously. $P = 1$ for all PM $\leq 10\ \mu m$ A.D. (Thatcher and Layton, 1995) and $y = 0.074$ [U.S. mean fraction of time spent outdoors per day; U.S. Environmental Protection Agency (1989)]. From PTEAM (Wallace et al., 1993), $a = 0.9\ h^{-1}$ as a median value for night and day. Özkaynak et al. (1993a,b) have determined values for k as follows:

For sulfate $k = 0.16\ h^{-1}$

For $PM_{2.5}$ $k = 0.39\ h^{-1}$

For PM_{10} $k = 1.01\ h^{-1}$

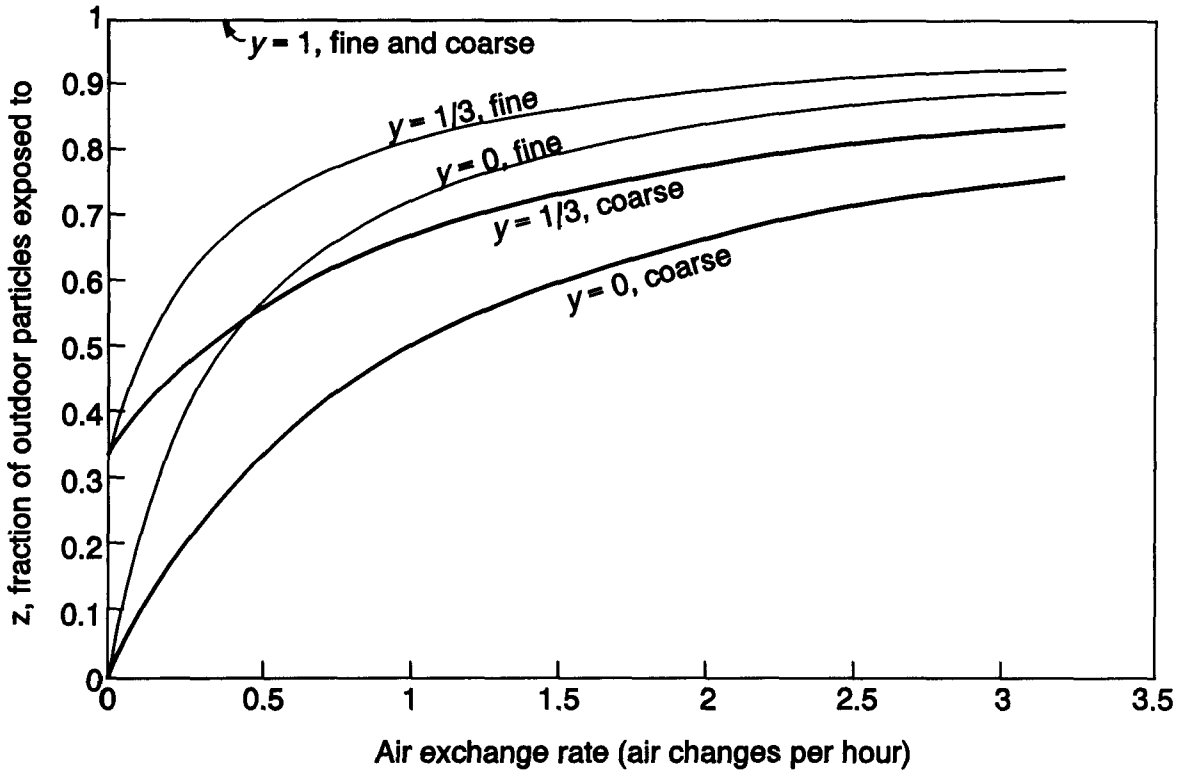

Figure 7-38. Fraction of ambient PM to which people are exposed (*z*) as a function of fraction of time outdoors (*y*) and air exchange rate for fine ($PM_{2.5}$) and coarse (PM_{10} − $PM_{2.5}$) particles.

From the equation $z = y + (1 - y)\, P\, \overline{a/(a + k)}$

for sulfate, $z = 0.074 + 0.926\ (0.9)/(0.9 + 0.16) = 0.859$

for $PM_{2.5}$ it is $z = 0.074 + 0.926\ (0.9)/(0.9 + 0.39) = 0.720$

for PM_{10} it is $z = 0.074 + 0.926\ (0.9)/(0.9 + 1.01) = 0.512$

These predicted values match closely to the reported values of z cited in this Chapter 7 as follows:

Suh et al. (1993) report $z = 0.87 \pm 0.02$ ($r^2 = 0.92$) for $SO_4^=$

Tamura et al. (1996) [Table 7-32] report $z = 0.466$ ($r^2 = 0.905$) for PM_{10},

Lioy et al.(1990) [Table 7-44] report $z = 0.546$ ($r^2 = 0.91$) for PM_{10}

It is not known what the average values of y and a were for the State College, PA, and Phillipsburg, NJ, cohorts of Suh et al. (1995) and Lioy et al. (1990), or the Tokyo, Japan,

cohort of Tamura et al. (1996). Therefore these results can only be considered as tentative at this time.

The parameter ß in Equation 7-37 represents the contribution to personal exposures (PEM) from nonambient sources both independent of and dependent on personal activities. In general the composition of the PM emitted by indoor sources (or resuspended by human activity) that influence ß will be different from the PM emitted into the ambient atmosphere from sources controlled by State Implementation Plans (SIP)s. The nonambient μE emissions are from the activities of the subject (cooking, heating, smoking, resuspension of housedust, hobbies, etc.) or independent activities of others in the same μE that are independent of the ambient concentration (Xa).

For the situation in Tokyo (Tamura and Ando, 1994; Tamura et al., 1996) the PM_{10} PEM vs PM_{10} SAM correlation is good for all subjects individually, as well as their average PEM, because the data were collected in a manner to minimize ß. These data for the seven nonsmoke exposed elderly subjects were culled to remove observations which were influenced by overt particle generating activities such as visitors' smoking, burning of incense, and burning of antimosquito coils. The custom of taking off shoes on entry into Japanese residences and use of "tatami" mat flooring minimized resuspension of PM less than 10 μm AD, although indoor activity did raise dust above 10 μm AD (Tamura et al., 1996).

For the U.S. cities of Phillipsburg, NJ, and Riverside, CA, with large numbers of observations, the correlations of PEM vs SAM for PM_{10} were significantly positive but less than for Tokyo, Japan, possibly due to the passive smoking and house dust generation in the Riverside, CA, and Phillipsburg, NJ, studies. Even so, in Riverside, CA, ambient sources provided about 67% of PM_{10} mass measured indoors (Özkaynak et al., 1996). Finally, the results of the studies in Beijing, China, and Azusa, CA, gave positive correlations of PEM and SAM that were not significantly different from zero (If one outlier is included in the Azusa analysis, the PEM vs SAM correlation is negative). These low correlations may be due to low air exchange rates in Beijing during the winter as evidenced by the low PEM/SAM ratios, and the presence of indoor sources in Azusa, as evidenced by the PEM almost double the SIM or SAM. These latter studies are typical of the results in other U.S. cities such as Kingston and Harriman, TN (Spengler et al., 1985), where ambient pollution is relatively low, so that the personal cloud and indoor source effects predominate.

In summary, it appears that the first exposure conclusion of the previous PM criteria document (U.S. Environmental Protection Agency, 1982), quoted in section 7.1.3, has been generally supported by recent studies. If the relation of equation 7-35 which appears to predict the observed relations in several studies cited in this document is a reasonable model of the personal exposure to ambient PM, then that conclusion can be adjusted more specifically as follows:

1. Long-term personal exposures to fine PM sulfates of outdoor origin may be estimated by approximately 85% of the sulfate in the fine fraction of ambient PM.

2. Long-term personal exposures to PM < 2.5 μm A.D. of outdoor origin may be estimated by approximately 70% of the PM < 2.5 μm A.D. in the ambient PM.

3. Long-term personal exposures to PM < 10 μm A.D. of outdoor origin may be estimated by approximately 50% of the PM < 10 μm A.D. in the ambient PM.

These relationships still need to be validated in populations other than those from which they were derived. Variations will exist for cohorts with different fractions of time spent outdoors (y) and air exchange rates (a) than the values chosen for representing the national averages.

Ambient concentrations of PM_{10} measured at properly sited monitoring stations are highly uniform in urban areas (Burton et al., 1996, Suh et al., 1995), have no losses in penetration into μEs (Thatcher and Layton, 1995), and may be highly correlated with personal exposures to PM_{10} (Tamura et al., 1996) where indoor sources of PM_{10} are minimal. Even where indoor sources of PM_{10} exist, they tend to produce different chemical species than those found in the $PM_{2.5}$ fraction, as shown by the sulfates which do not appear in the personal cloud (Özkaynak et al., 1996; Suh et al., 1993).

It is therefore concluded that the presence of variable indoor sources of PM_{10} tends to lower the observed correlations between PEM PM_{10} (derived from both ambient and nonambient sources) and SAM PM_{10} (derived only from ambient sources) and even achieve values nonsignificantly different from zero. Consequently, the use of an ambient concentration of $PM_{2.5}$ or PM_{10} in relation to daily changes of mortality and morbidity may be a reasonable surrogate for the average personal exposure of people in the community to the $PM_{2.5}$ or PM_{10} generated by ambient sources. "The consistently higher R^2 values observed in the longitudinal regressions support the epidemiological findings more strongly

than the poor correlations noted in the standard cross-sectional regressions" (Wallace, 1996), as per the U.S. EPA reanalyses shown in Tables 7-36 and 7-42.

7.8 SUMMARY AND CONCLUSIONS

For PM, the total exposure of an individual consists of the summation of the individual's exposure to PM in a variety of microenvironments. This typically includes exposures while (a) outdoors and (b) indoors (at-home or in microenvironments such as shops and public buildings; at-work in an office or factory; and in a vehicle). The principle of superposition is a useful mechanism to visualize the summation process. A simplification of this summation process for an arbitrary individual, described in detail by Figure 7-30, is illustrated in Figure 7-39. In each sub-figure (a to d) of Figure 7-39, the shaded area represents PM exposure (in μg-h/m^3) of ambient origin appropriately indexed by a central (community) monitoring station. The clear area represents that PM exposure (in μg-h/m^3) the individual is exposed to which is not characterized by the PM measured at the central monitoring station.

Figure 7-39a shows that while outdoors, the subject can be exposed to (a) widely dispersed ambient PM that is represented by the community monitoring station and, independently, also to (b) proximal PM that does not markedly influence the monitoring station reading (from tobacco smoking, standing over a grill at a backyard barbecue, "personal cloud", etc.). For example, in the PTEAM Study, backyard concentrations of $PM_{2.5}$ and PM_{10} had a correlation on the order of 0.9 with a central monitoring station. Also, in Tokyo (Figure 7-25), outdoor concentrations immediate to the homes of subjects studied by Tamura et al. (1996) had a correlation of 0.9 with the local ambient monitoring station.

Figure 7-39b shows that, while indoors (not at work), the subject can be exposed not only to (a) ambient PM (represented by the monitoring station) that infiltrates indoors but also to (b) PM of indoor origin that does not influence the ambient monitoring station reading (from smoking, cooking, vacuuming, "personal cloud", etc.). Obviously, the proportion of exposure to PM of ambient origin versus that of indoor origin can vary widely, depending on: outdoor concentrations of the ambient PM; the air exchange rate of indoor spaces; the

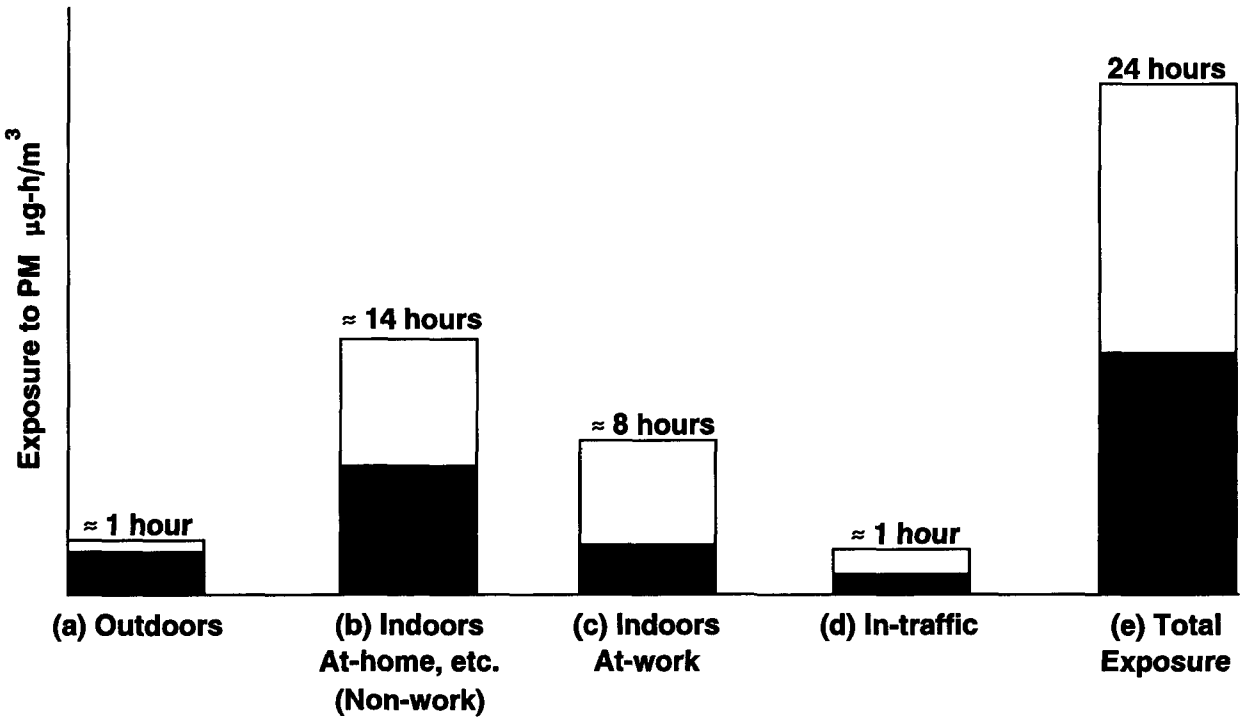

Figure 7-39. **Conceptual representation of potential contributions of PM of ambient origin and PM generated indoors to total human exposure of a hypothetical individual. The total personal exposure (e) of that individual will consist of the sum of exposures to widely dispersed PM of ambient origin (shaded areas) characterized by measurements at a centrally-located community monitoring site and all other exposures (non-shaded areas) to proximally generated particles either outdoors or indoors in situations designated for (a), (b), (c), and (d). Times of exposure in the various situations reflect typical time-action patterns for U.S. adults. Depicted exposures to PM of non-ambient origin may vary greatly from those shown there for qualitative impression only, depending on various factors described in the text.**

presence or absence of indoor PM sources; and the removal efficiency of indoor sinks for specific constituents of the respective PM of ambient or indoor origin. In the absence of major indoor PM sources (e.g., smoking), the percentage of total exposure contributed by PM of ambient origin can be substantial. For example, as shown in Table 7-2, between 60% and 80% of indoor air PM was estimated by source apportionment methods to be of ambient origin in non-smokers' homes in two U.S. cities (Steubenville, OH; Portage, WI) included in the Harvard Six-City Study. Even in smokers' homes, it was estimated that 60% of the non-smoking related PM was of ambient origin in the same two cities. The New York State

ERDA Study (see page 7-23) also showed that, in homes without combustion sources, 60% of the total indoor $PM_{2.5}$ was from outdoor sources. For homes with smokers in the same study, about 66% of the non-tobacco smoke indoor particles were found to be of ambient origin. Similarly, based on the Tamura et al. (1996) data shown in Figure 7-24, it can be estimated that as much as 80% of the measured indoor PM_{10} in Japanese homes without combustion sources was of ambient origin.

Figure 7-39c shows that while indoors at work the subject can also be exposed to (a) ambient PM (represented by the community monitoring station) which infiltrates indoors, and (b) PM of indoor origin that does not influence the monitoring station reading (from smoking, welding, machining, "personal cloud", etc.). It can be expected that, for office-type work, similar relationships as described above for the other indoor conditions (e.g., smokers' or non-smokers' homes) would apply. However, for work conditions involving particle generation (e.g., wood working, welding, mining, etc.), the personal exposure of "dusty-trade" workers to indoor-generated particles can be several orders of magnitude greater than their exposure to indoor particles of ambient origin.

Figure 7-39d shows that while in traffic, the subject can be exposed to (a) ambient PM that is represented by the monitoring station (via ambient air infiltration into the vehicle), and (b) PM of on-board or proximal vehicle origin that does not directly influence the community monitoring station reading (from smoking, exhaust penetration from nearby vehicles, etc.). For example, in one study, Morandi et al. (1988) found that the average concentration of $PM_{3.5}$ in motor vehicles in traffic (55 $\mu g/m^3$) was 60% higher than the average outdoor $PM_{3.5}$ level (35 $\mu g/m^3$).

Figure 7-39e is a simple rearrangement of the shaded and non-shaded areas to show that an individual's total daily exposure ($\mu g\text{-}h/m^3$) can be thought of as the sum of two quantities: (a) exposure to PM characterized by the local community monitoring station, and (b) exposure to PM of immediately proximal origin that varies independently of the PM measured at the monitoring station. Conceptually, everyone in the community will be exposed to the mix of PM represented by the shaded area that is characterized by the local monitoring station, due to their time outdoors and the penetration of PM into indoor microenvironments and vehicles. However, not everyone in the community will be exposed to the identical mix of PM represented by the clear area, because this exposure and its

chemical composition is idiosyncratically related to their individual habits and practices (smoking, home cleanliness, hobbies, "personal cloud", etc.), their occupation (home maker, student, office worker, welder, miner, etc.) and their mode and usage of transportation (car, bus, train, etc.).

Evaluation of information useful in determining relative contributions of ambient (outdoor) and non-ambient (indoor) particles to total human exposures leads to the following key conclusions:

(1) For PM, the ambient environment can be a major source of indoor pollution due to air exchange and infiltration. Whether the ambient is the dominant source of indoor PM depends on the relative magnitude of indoor sources of PM.

(2) For PM of size fractions that include coarse particles, some studies have identified statistically significant relationships between personal exposures and ambient concentrations, while other studies have not, probably due to overwhelming effects of indoor sources, "personal clouds" and other individual activities.

(3) Cross-sectional regressions of personal exposure on outdoor $PM_{2.5}$ and PM_{10} concentrations generally explain less than 25% of the variance ($R^2 < 0.25$). However, longitudinal regressions for each person in the study (in those cases where the person was measured repeatedly) often show much better relationships between personal exposure and outdoor air concentrations.

(4) Personal exposures to outdoor-generated PM of any size fraction $\leq PM_{10}$ can be estimated from the fraction of time spent indoors and an estimate of the air exchange rate and deposition rate associated with that size fraction.

(5) The relationship between ambient concentration and personal exposure is better for finer size fractions of ambient PM, than for coarser PM. Higher correlations between ambient concentration and personal exposures have been found for fine PM constituents (such as sulfates) without indoor sources.

(6) For a study population of nonsmokers in which there is a significant positive correlation between personal exposures and ambient concentrations, the ambient concentration can predict the mean personal exposure with much less uncertainty than it can predict the personal exposure of any given individual.

(7) For Riverside, CA, where 25% of the nonsmoking population was estimated to have personal exposures on the day they were monitored that exceeded the 24-h National Ambient Air Quality Standard for PM_{10} of 150 $\mu g/m^3$, approximately 50% of this mass was found to be of ambient origin.

(8) The personal exposure to PM of smokers is dominated by the milligram quantities of PM inhaled with each cigar, pipe, or cigarette smoked.

(9) For the U.S. studies, almost all personal exposures to PM are greater than the ambient concentrations.

(10) The penetration factor from outdoors to indoors for both $PM_{2.5}$ and PM_{10} was found to be unity in the PTEAM and Thatcher and Layton (1995) studies.

(11) Deposition rates in indoor microenvironments for PM_{10} and its fine and coarse fractions were determined in the PTEAM Study. Similar deposition rates were found by Thatcher and Layton (1995). Deposition reduces exposure to ambient PM; coarse mode PM is removed more rapidly than $PM_{2.5}$, which is removed more rapidly than sulfate.

(12) Under equilibrium conditions, residential indoor concentrations of outdoor-generated PM of any size fraction $\leq PM_{10}$ can be estimated for any given air exchange rate, by employing the deposition rate associated with that size fraction.

(13) For PM, studies have detected a "personal cloud" related to the activities of an individual who may generate significant levels of airborne PM in his/her vicinity which may not be picked up by an indoor PM monitor at a distance.

(14) There is some evidence that nonsmoke-exposed elderly people have lower residential indoor PM concentrations than the simultaneous ambient PM concentrations, as opposed to the general population who have indoor PM concentrations comparable to or greater than ambient PM concentrations.

(15) Measured indoor air concentrations of $PM_{2.5}$ and PM_{10} generally exceed outdoor air concentrations (often by a factor of two) except in areas where outdoor concentrations are high (e.g., Steubenville, OH and Riverside, CA).

(16) Indoor concentrations are higher during the day than at night.

(17) Correlations between indoor and outdoor particle mass concentrations were not significant in two of the three major studies reviewed. In the third (PTEAM) study, they ranged between 0.22 and 0.54.

(18) Regressions of indoor on outdoor $PM_{2.5}$ and PM_{10} concentrations generally explain less than half of the variance ($R^2 < 50\%$) if the regressions are carried out simultaneously on all homes in the study. However, regressions for a single home (in those cases where homes were measured repeatedly) often have much better indoor-outdoor relationships (R^2 up to 90%). Since most epidemiological studies deal with repeated measurements over time, "longitudinal" regressions by individual home may be more relevant to these studies than "cross-sectional" regressions across all homes.

(19) The largest identified indoor source of particles in both homes and buildings is cigarette smoking. Homes with smokers have an ETS-related $PM_{2.5}$ concentration increment ranging between 25 and 45 $\mu g/m^3$.

(20) The second largest identified indoor source of particles is cooking. Homes with cooking had increased levels of PM_{10} on the order of 10 to 20 $\mu g/m^3$.

(21) Unknown indoor sources accounted for a substantial fraction (25%) of indoor concentrations of both $PM_{2.5}$ and PM_{10} in the PTEAM Study. These sources appear to be due to personal activities, including resuspension of house dust.

(22) Variations in personal exposure due to fluctuations produced by indoor sources of PM are independent of the variations in personal exposure produced by ambient sources.

REFERENCES

Adams, W. C. (1993) Measurement of breathing rate and volume in routinely performed daily activities [final report]. Davis, CA: University of California, Physical Education Department, Human Performance Laboratory; contract no. A033-205.

Afifi, A. A.; Elashoff, R. M. (1966) Missing observations in multivariate statistics: I. review of the literature. J. Am. Stat. Assoc. 61: 595-604.

Alberts, W. M.; Brooks, S. M. (1992) Advances in occupational asthma. Clin. Chest Med. 13: 281-302.

American Academy of Allery & Immunology. (1994) Aeroallergen Monitoring Network 1994 pollen and spore report. Milwaukee, WI: American Academy of Allery & Immunology.

Anuszewski, J.; Larson, T. V.; Koenig, J. Q. (1992) Simultaneous indoor and outdoor particle light-scattering measurements at nine homes using a portable nephelometer. Presented at: 11th annual meeting of the American Association for Aerosol Research; October; San Francisco, CA. Cincinnati, OH: American Association for Aerosol Research; paper no. 3A.5.

Arlian, L. G. (1989) Biology and ecology of house dust mites, *Dermatophagoides* spp. and *Euroglyphus* spp. Immunol. Allergy Clin. North Am. 9: 339-356.

Aso, N.; Yoshizawa, S.; Tang, H. (1993) Behavior of particles generated from floor. In: Kalliokosi, P.; Jantunen, M.; Seppänen, O., eds. Indoor air '93: proceedings of the 6th international conference on indoor air quality and climate, v. 4, particles, microbes, radon; July; Helsinki, Finland. Helsinki, Finland: Indoor Air '93; pp. 43-48.

Baxter, C. S.; Wey, H. E.; Burg, W. R. (1981) A prospective analysis of the potential risk associated with inhalation of aflatoxin-contaminated grain dusts. Food Cosmet. Toxicol. 19: 765-769.

Beck, B. D.; Brain, J. D. (1982) Prediction of the pulmonary toxicity of respirable combustion products from residential wood and coal stoves. In: Proceedings: residential wood & coal combustion specialty conference; March; Louisville, KY. Pittsburgh, PA: Air Pollution Control Association; pp. 264-280.

Bennett, K. M. (1983) [Letter to H. H. Hovey, Jr., New York State Department of Environmental Conservation, regarding the national ambient air quality standards]. Washington, DC: U.S. Environmental Protection Agency, Assistant Administrator for Air, Noise, and Radiation; March 18.

Binder, R. E.; Mitchell, C. A.; Hosein, H. R.; Bouhuys, A. (1976) Importance of the indoor environment in air pollution exposure. Arch. Environ. Health 31: 277-279.

Burge, H. A. (1995) Bioaerosols in the residential environment. In: Cox, C. S.; Wathes, C. M., eds. Bioaerosols handbook. Boca Raton, FL: CRC Press, Inc.; pp. 579-597.

Burton, R. M.; Suh, H. H.; Koutrakis, P. (1996) Spatial variation in particulate concentrations within metropolitan Philadelphia. Environ. Sci. Technol. 30: 400-407.

Chan, C.-C.; Huang, S.-K.; Chen, Y.-C.; Wang, J.-D. (1995) Personal, indoor, and outdoor concentrations of respirable suspended particulates (RSP) and nicotine in seven smoker's families in Taiwan. Atmos. Environ.: submitted.

Clayton, C. A.; Perritt, R. L.; Pellizzari, E. D.; Thomas, K. W.; Whitmore, R. W.; Wallace, L. A.; Özkaynak, H.; Spengler, J. D. (1993) Particle total exposure assessment methodology (PTEAM) study: distributions of aerosol and elemental concentrations in personal, indoor, and outdoor air samples in a southern California community. J. Exposure Anal. Environ. Epidemiol. 3: 227-250.

Code of Federal Regulations. (1994) National primary and secondary ambient air quality standards; definitions. C. F. R. 40: part 50, §50.1.

Cohen, B. S.; Chang, A. E.; Harley, N. H.; Lippmann, M. (1982) Exposure estimates from personal lapel monitors. Am. Ind. Hyg. Assoc. J. 43: 239-243.

Cohen, B. S.; Harley, N. H.; Lippmann, M. (1984) Bias in air sampling techniques used to measure inhalation exposure. Am. Ind. Hyg. Assoc. J. 45: 187-192.

Colome, S. D.; Kado, N. Y.; Jacques, P.; Kleinman, M. (1990) Indoor-outdoor relationships of particles less than 10 μm in aerodynamic diameter (PM10) in homes of asthmatics. In: Indoor air '90: precedings of the 5th international conference on indoor air quality and climate, volume 2, characteristics of indoor air; July-August; Toronto, ON, Canada. Ottawa, ON, Canada: International Conference on Indoor Air Quality and Climate, Inc.; pp. 275-280.

Colome, S. D.; Kado, N. Y.; Jaques, P.; Kleinman, M. (1992) Indoor-outdoor air pollution relations: particulate matter less than 10 μm in aerodynamic diameter (PM10) in homes of asthmatics. Atmos. Environ. Part A 26: 2173-2178.

Costle, D. M. (1980) [Letter to J. Randolph, U.S. Senate, regarding EPA's definition of "ambient"]. Washington, DC: U.S. Environmental Protection Agency, Administrator; December 19.

Coultas, D. B.; Samet, J. M.; McCarthy, J. F.; Spengler, J. D. (1990) Variability of measures of exposure to environmental tobacco smoke in the home. Am. Rev. Respir. Dis. 142: 602-606.

Cox, C. S. (1987) The aerobiological pathway of microorganisms. New York, NY: John Wiley & Sons.

Cox, C. S.; Wathes, C. M., eds. (1995) Bioaerosols handbook. Boca Raton, FL: CRC Press, Inc.

Croft, W. A.; Jarvis, B. B.; Yatawara, C. S. (1986) Airborne outbreak of trichothecene toxicosis. Atmos. Environ. 20: 549-552.

Crouse, W. E.; Ireland, M. S.; Johnson, J. M.; Striegel, R. M., Jr.; Williard, C. S.; DePinto, R. M.; Oldaker, G. B., III; McBride, R. L. (1989) Results from a survey of environmental tobacco smoke (ETS) in restaurants. In: Harper, J. P., ed. Combustion processes and the quality of the indoor environment: transactions of an international specialty conference; September 1988; Niagara Falls, NY. Pittsburgh, PA: Air & Waste Management Association; pp. 214-222. (A&WMA transactions series: TR-15).

Cupitt, L. T.; Glen, W. G.; Lewtas, J. (1994) Exposure and risk from ambient particle-bound pollution in an airshed dominated by residential wood combustion and mobile sources. In: Symposium of risk assessment of urban air: emissions, exposure, risk identification, and risk quantitation; May-June 1992; Stockholm, Sweden. Environ. Health Perspect. 102(suppl. 4):75-84.

aisey, J. M.; Spengler, J. D.; Kaarakka, P. (1987) A comparison of the organic chemical composition of indoor aerosols during woodburning and non-woodburning periods. In: Seifert, B.; Esdorn, H.; Fischer, M.; Rüden, H.; Wegner, J., eds. Indoor air '87: proceedings of the 4th international conference on indoor air quality and climate: v. 1, volatile organic compounds, combustion gases, particles and fibres, microbiological agents; August; Berlin, Federal Republic of Germany. Berlin, Federal Republic of Germany: Institute for Water, Soil and Air Hygiene; pp. 215-219.

Dempster, A. P.; Laird, N. M.; Rubin, D. B. (1977) Maximum likelihood from incomplete data via the *EM* algorithm. J. R. Stat. Soc. Ser. B 39: 1-38.

Diemel, J. A. L.; Brunekreef, B.; Boleij, J. S. M.; Biersteker, K.; Veenstra, S. J. (1981) The Arnhem lead study: II. indoor pollution, and indoor/outdoor relationships. Environ. Res. 25: 449-456.

Dockery, D. W.; Spengler, J. D. (1981a) Indoor-outdoor relationships of respirable sulfates and particles. Atmos. Environ. 15: 335-343.

Dockery, D. W.; Spengler, J. D. (1981b) Personal exposure to respirable particulates and sulfates. J. Air Pollut. Control Assoc. 31: 153-159.

Dockery, D. W.; Schwartz, J.; Spengler, J. D. (1992) Air pollution and daily mortality: associations with particulates and acid aerosols. Environ. Res. 59: 362-373.

Duan, N. (1982) Models for human exposure to air pollution. Environ. Int. 8: 305-309.

Duan, N.; Mage, D. T. (1996) Combination of direct and indirect approaches for exposure assessment. J. Exposure Anal. Environ. Epidemiol.: accepted.

Dunn, O. J.; Clark, V. A. (1974) Applied statistics: analysis of variance and regression. New York, NY: John Wiley & Sons; pp. 221-251. (Wiley series in probability and mathematical statistics).

Edmonds, R. L., ed. (1979) Aerobiology: the ecological systems approach. Stroudsburg, PA: Dowden, Hutchinson & Ross, Inc. (US/IBP synthesis series 10).

Federal Trade Commission. (1994) Tar, nicotine, and carbon monoxide of the smoke of 933 varieties of domestic cigarettes. Washington, DC: Federal Trade Commission.

Fletcher, B.; Johnson, A. E. (1988) Comparison of personal and area concentration measurements and the use of a manikin in sampling. In: Vincent, J. H., ed. Ventilation '88. New York, NY: Pergamon Press; pp. 161-165.

Fugaš, M.; Wilder, B.; Pauković, R.; Hršak, J.; Steiner-Škreb, D. (1973) Concentration levels and particulate size distribution of lead in the air of an urban and an industrial area as a basis for the calculation of population exposure. In: Barth, D.; Berlin, A.; Engel, R.; Recht, P.; Smeets, J., eds. Environmental health aspects of lead: proceedings [of an] international symposium; October 1972; Amsterdam, The Netherlands. Luxembourg: Commission of the European Communities; pp. 961-968; report no. EUR 5004 d-e-f.

Fuller, W. A. (1987) Measurement error models. New York, NY: John Wiley & Sons.

Gregory, P. H. (1973) The microbiology of the atmosphere. 2nd ed. New York, NY: John Wiley & Sons.

Groves, W. A.; Hahne, R. M. A.; Levine, S. P.; Schork, M. A. (1994) A field comparison of respirable dust samplers. Am. Ind. Hyg. Assoc. J. 55: 748-755.

Guerin, M. R.; Jenkins, R. A.; Tomkins, B. A. (1992) The chemistry of environmental tobacco smoke: composition and measurement. Chelsea, MI: Lewis Publishers.

Hansen, A. D. A.; Kapustin, V. N.; Kopeikin, V. M.; Gillette, D. A.; Bodhaine, B. A. (1993) Optical absorption by aerosol black carbon and dust in a desert region of central Asia. Atmos. Environ. Part A 27: 2527-2531.

Hasabelnaby, N. A.; Ware, J. H.; Fuller, W. A. (1989) Indoor air pollution and pulmonary performance: investigating errors in exposure assessment. Stat. Med. 8: 1109-1126.

Heavner, D. L.; Morgan, W. T.; Ogden, M. W. (1995) Determination of volatile organic compounds and ETS apportionment in 49 homes. Environ. Int. 21: 3-21.

Highsmith, V. R.; Hoffman, A. J.; Zweidinger, R. B.; Cupitt, L. T.; Walsh, D. (1991) The IACP: overview of the Boise, Idaho, and the Roanoke, Virginia, field studies. Presented at: 84th annual meeting and exhibition of the Air & Waste Management Association; June; Vancouver, BC, Canada. Pittsburgh, PA: Air & Waste Management Association; paper no. 91-131.1.

Hodges, S. D.; Moore, P. G. (1977) Data uncertainties and least squares regression. Appl. Stat. 44: 185-195.

Holcomb, L. C. (1993) Indoor air quality and environmental tobacco smoke: concentration and exposure. Environ. Int. 19: 9-40.

Holland, W. W.; Bennett, A. E.; Cameron, I. R.; Florey, C. du V.; Leeder, S. R.; Schilling, R. S. F.; Swan, A. V.; Waller, R. E. (1979) Health effects of particulate pollution: reappraising the evidence. Am. J. Epidemiol. 110: 525-659.

Ingham, D. B.; Yan, B. (1994) The effect of a cylindrical backing body on the sampling efficiency of a cylindrical sampler. J. Aerosol Sci. 25: 535-541.

Janssen, N. A. H.; Hoek, G.; Harssema, H.; Brunekreef, B. (1995) A relation between personal and ambient PM10. Epidemiology 6(suppl.): S45.

Jenkins, R. A.; Palausky, M. A.; Counts, R. W.; Guerin, M. R.; Dindal, A. B.; Bayne, C. K. (1995a) Determination of personal exposure of nonsmokers to environmental tobacco smoke in the United States. Lung Cancer: submitted

Jenkins, R. A.; Palausky, M. A.; Guerin, M. R.; Dindal, A. B.; Counts, R. W.; Bayne, C. K. (1995b) Personal exposure to environmental tobacco smoke in workplace and away-from work settings: a 16 city case study. In: Measurement of toxic and related air pollutants, 1995 abstracts book of an EPA/A&WMA international symposium; May; Research Triangle Park, NC. Pittsburgh, PA: Air & Waste Management Association; pp. 40-41.

Kamens, R.; Lee, C.-T.; Wiener, R.; Leith, D. (1991) A study to characterize indoor particles in three non-smoking homes. Atmos. Environ. Part A 25: 929-948.

Kendall, M. G.; Stuart, A. (1961) The advanced theory of statistics, v. 2: inference and relationship. London, United Kingdom: Charles Griffin & Co., Ltd.; pp. 378-415.

Kendrick, B. (1992) The fifth kingdom. 2nd ed. Newburyport, MA: Focus Information Group.

Kim, Y. S.; Stock, T. H. (1986) House-specific characterization of indoor and outdoor aerosols. Environ. Int. 12: 75-92.

ıepeis, N. E.; Ott, W. R.; Switzer, P. (1994) A Total Human Exposure Model (THEM) for Respirable Suspended Particles (RSP). Presented at: 87th annual meeting & exhibition of the Air & Waste Management Association; June; Cincinnati, OH. Pittsburgh, PA: Air & Waste Management Association; paper no. 94-WA75A.03.

Koontz, M. D.; Rector, H. E. (1995) Estimation of distributions for residential air exchange rates: final report. Washington, DC: U.S. Environmental Protection Agency, Office of Pollution Prevention and Toxics; contract nos. 68-D9-0166 and 68-D3-0013.

Koutrakis, P.; Briggs, S. L. K.; Leaderer, B. P. (1992) Source apportionment of indoor aerosols in Suffolk and Onondaga Counties, New York. Environ. Sci. Technol. 26: 521-527.

Kulmala, M.; Saari, H.; Raunemaa, T.; Olin, M. (1987) Indoor air aerosols: outdoor air influence on indoor air. In: Seifert, B.; Esdorn, H.; Fischer, M.; Rüden, H.; Wegner, J., eds. Indoor air '87: proceedings of the 4th international conference on indoor air quality and climate, v. 1, volatile organic compounds, combustion gases, particles and fibres, microbiological agents; August; Berlin, Federal Republic of Germany. Berlin, Federal Republic of Germany: Institute for Water, Soil and Air Hygiene; pp. 564-568.

Laird, N. M. (1988) Missing data in longitudinal studies. Stat. Med. 7: 305-315.

Last, J. M., ed. (1988) A dictionary of epidemiology. 2nd ed. New York, NY: Oxford University Press; p. 56.

Leaderer, B. P.; Hammond, S. K. (1991) Evaluation of vapor-phase nicotine and respirable suspended particle mass as markers for environmental tobacco smoke. Environ. Sci. Technol. 25: 770-777.

Leaderer, B.; Koutrakis, P.; Briggs, S.; Rizzuto, J. (1990) Impact of indoor sources on residential aerosol concentrations. In: Indoor air '90: precedings of the 5th international conference on indoor air quality and climate, volume 2, characteristics of indoor air; July-August; Toronto, ON, Canada. Ottawa, ON, Canada: International Conference on Indoor Air Quality and Climate, Inc.; pp. 269-274.

Leaderer, B. P.; Koutrakis, P.; Briggs, S. L. K.; Rizzuto, J. (1994) The mass concentration and elemental composition of indoor aerosols in Suffolk and Onondaga Counties, New York. Indoor Air 4: 23-34.

Lebret, E.; McCarthy, J.; Spengler, J.; Chang, B.-H. (1987) Elemental composition of indoor fine particles. In: Seifert, B.; Esdorn, H.; Fischer, M.; Rüden, H.; Wegner, J., eds. Indoor air '87: proceedings of the 4th international conference on indoor air quality and climate: v. 1, volatile organic compounds, combustion gases, particles and fibres, microbiological agents; August; Berlin, Federal Republic of Germany. Berlin, Federal Republic of Germany: Institute for Water, Soil and Air Hygiene; pp. 569-574.

Lebret, E.; Boleij, J.; Brunekreef, B. (1990) Environmental tobacco smoke in Dutch homes. In: Indoor air '90: precedings of the 5th international conference on indoor air quality and climate, volume 2, characteristics of indoor air; July-August; Toronto, ON, Canada. Ottawa, ON, Canada: International Conference on Indoor Air Quality and Climate, Inc.; pp. 263-268.

Lehmann, E.; Rentel, K.-H.; Allescher, W.; Hohmann, R. (1990) Messung von Dieselabgas am Arbeitsplatz [Measurement of diesel exhaust at the workplace]. Zentralbl. Arbeitsmed. Arbeitsschutz Prophyl. Ergon. 40: 2-11.

Letz, R.; Ryan, P. B.; Spengler, J. D. (1984) Estimated distributions of personal exposure to respirable particles. Environ. Monit. Assess. 4: 351-359.

Lewis, C. W. (1991) Sources of air pollutants indoors: VOC and fine particulate species. J. Exposure Anal. Environ. Epidemiol. 1: 31-44.

Lewis, W. H.; Vinay, P.; Zenger, V. E. (1983) Airborne and allergenic pollen of North America. Baltimore, MD: The Johns Hopkins University Press.

Lighthart, B.; Mohr, A. J. (1994) Atmospheric microbial aerosols: theory and applications. New York, NY: Chapman & Hall.

Ligocki, M. P.; Liu, H. I. H.; Cass, G. R.; John, W. (1990) Measurements of particle deposition rates inside Southern California museums. Aerosol Sci. Technol. 13: 85-101.

Lioy, P. J.; Waldman, J. M.; Buckley, T.; Butler, J.; Pietarinen, C. (1990) The personal, indoor and outdoor concentrations of PM-10 measured in an industrial community during the winter. Atmos. Environ. Part B 24: 57-66.

Little, R. J. A.; Rubin, D. B. (1987) Statistical analysis with missing data. New York NY: John Wiley & Sons.

Litzistorf, G.; Guillemin, M. P.; Buffat, P.; Iselin, F. (1985) Influence of human activity on the airborne fiber level in paraoccupational environments. J. Air Pollut. Control Assoc. 35: 836-837.

Löfroth, G.; Stensman, C.; Brandhorst-Satzkorn, M. (1991) Indoor sources of mutagenic aerosol particulate matter: smoking, cooking and incense burning. Mutat. Res. 261: 21-28.

Mage, D. T. (1980) The statistical form for the ambient particulate standard annual arithmetic mean vs annual geometric mean. J. Air Pollut. Control Assoc. 30: 706-708.

Mage, D. T. (1983) Public health aspects of air quality surveillance. Public Health Rev. 11: 5-54.

Mage, D. T. (1985) Concepts of human exposure assessment for airborne particulate matter. Environ. Int. 11: 407-412.

Mage, D. T. (1991) A comparison of the direct and indirect methods of human exposure. In: Gledhill, B. L.; Mauro, F., eds. New horizons in biological dosimetry: proceedings of the international symposium on trends in biological dosimetry; October 1990; Lerici, Italy. New York, NY: Wiley-Liss, Inc.; pp. 443-454. (Progress in clinical and biological research: v. 372).

Mage, D. T.; Buckley, T. J. (1995) The relationship between personal exposures and ambient concentrations of particulate matter. Presented at: 88th annual meeting of the Air & Waste Management Association; June; San Antonio, TX. Pittsburgh, PA: Air & Waste Management Association; paper no. 95-MP18.01.

Mage, D. T.; Ott, W. R. (1996) Accounting for nonuniform mixing and human exposure in indoor environments. In: Tichenor, B. A., ed. Characterizing sources of indoor air pollution and related sink effects. Philadelphia, PA: American Society for Testing and Materials; pp. 263-278.

Mage, D.; Ozolins, G.; Peterson, P.; Webster, A.; Orthofer, R.; Vandeweerd, V.; Gwynne, M. (1996) Urban air pollution in megacities of the world. Atmos. Environ. 30: 681-686.

Mamane, Y. (1992) Characterization of PTEAM indoor aerosol samples (electron microscopy analysis). Research Triangle Park, NC: U.S. Environmental Protection Agency, Atmospheric Research and Exposure Assessment Laboratory.

Marple, V. A.; Rubow, K. L.; Turner, W.; Spengler, J. D. (1987) Low flow rate sharp cut impactors for indoor air sampling: design and calibration. JAPCA 37: 1303-1307.

Martinelli, C. A.; Harley, N. H.; Lippmann, M.; Cohen, B. S. (1983) Monitoring real-time aerosol distribution in the breathing zone. Am. Ind. Hyg. Assoc. J. 44: 280-285.

ews, K. P. (1989) Inhalant insect-derived allergens. Immunol. Allergy Clin. North Am. 9: 321-338.

ıtthews, T. G.; Thompson, C. V.; Wilson, D. L.; Hawthorne, A. R.; Mage, D. T. (1989) Air velocities inside domestic environments: an important parameter in the study of indoor air quality and climate. Environ. Int. 15: 545-550.

Mayo, E. (1960) Hawthorne and the Western Electric Company. In: Merrill, H. F., ed. Classics in management. New York, NY: American Management Association; pp. 417-436.

McKenzie, R. L.; Bright, D. S.; Fletcher, R. A.; Hodgeson, J. A. (1982) Development of a personal exposure monitor for two sizes of inhalable particulates. Environ. Int. 8: 229-233.

Miesner, E. A.; Rudnick, S. N.; Hu, F.-C.; Spengler, J. D.; Özkaynak, H.; Preller, L.; Nelson, W. (1989) Particulate and nicotine sampling in public facilities and offices. JAPCA 39: 1577-1582.

Miller, A.; Thompson, J. M. (1970) Elements of meteorology. Columbus, OH: Charles E. Merrill Publishing Co.; p. 50.

Millette, J. R.; Hays, S. M. (1994) Resuspension of settled dust. In: Settled asbestos dust sampling and analysis. Boca Raton, FL: CRC Press, Inc.; pp. 59-65.

Morandi, M. T.; Stock, T. H.; Contant, C. F. (1986) Characterization of indoor microenvironmental exposures to respirable particulate matter. Presented at: 79th annual meeting of the Air Pollution Control Association; June; Minneapolis, MN. Pittsburgh, PA: Air Pollution Control Association; paper no. 86-67.2.

Morandi, M. T.; Stock, T. H.; Contant, C. F. (1988) A comparative study of respirable particulate microenvironmental concentrations and personal exposures. Environ. Monit. Assess. 10: 105-122.

Moschandreas, D. J.; Winchester, J. W.; Nelson, J. W.; Burton, R. M. (1979) Fine particle residential indoor air pollution. Atmos. Environ. 13: 1413-1418.

Mumford, J. L.; Williams, R. W.; Walsh, D. B.; Burton, R. M.; Svendsgaard, D. J.; Chuang, J. C.; Houk, V. S.; Lewtas, J. (1991) Indoor air pollutants from unvented kerosene heater emissions in mobile homes: studies on particles, semivolatile organics, carbon monoxide, and mutagenicity. Environ. Sci. Technol. 25: 1732-1738.

Murray, D. M.; Burmaster, D. E. (1995) Residential air exchange rates in the United States: empirical and estimated parametric distributions by season and climatic region. Risk Anal. 15: 459-465.

National Institute for Environmental Studies. (1994) Experimental studies on the health effects of air pollutants containing diesel exhaust particles [FY 1988 ~ 1992]. Kokuritsu Kogai Kenkyusho Tokubetsu Kenkyu Hokoku (SR-14-'94): 26-32.

National Research Council. (1986) Environmental tobacco smoke: measuring exposures and assessing health effects. Washington, DC: National Academy Press.

Nazaroff, W. W.; Cass, G. R. (1989) Mathematical modeling of indoor aerosol dynamics. Environ. Sci. Technol. 23: 157-166.

Nazaroff, W. W.; Salmon, L. G.; Cass, G. R. (1990a) Concentration and fate of airborne particles in museums. Environ. Sci. Technol. 24: 66-77.

Nazaroff, W. W.; Ligocki, M. P.; Ma, T.; Cass, G. R. (1990b) Particle deposition in museums: comparison of modeling and measurement results. Aerosol Sci. Technol. 13: 332-348.

Nazaroff, W. W.; Gadgil, A. J.; Weschler, C. J. (1993) Critique of the use of deposition velocity in modeling indoor air quality. In: Nagda, N. L., ed. Modeling of indoor air quality and exposure. Philadelphia, PA: American Society for Testing and Materials; pp. 81-104. (ASTM special technical publication no. 1205).

Neas, L. M.; Dockery, D. W.; Ware, J. H.; Spengler, J. D.; Ferris, B. G., Jr.; Speizer, F. E. (1994) Concentration of indoor particulate matter as a determinant of respiratory health in children. Am. J. Epidemiol. 139: 1088-1099.

Ogden, T. L.; Bartlett, I. W.; Purnell, C. J.; Wells, C. J.; Armitage, F.; Wolfson, H. (1993) Dust for cotton manufacture: changing from static to personal sampling. Ann. Occup. Hyg. 37: 271-285.

Oldaker, G. B., III; Ogden, M. W.; Maiolo, K. C.; Conner, J. M.; Conrad, F. W., Jr.; DeLuca, P. O. (1990) Results from surveys of environmental tobacco smoke in restaurants in Winston-Salem, North Carolina. In: Indoor air '90: precedings of the 5th international conference on indoor air quality and climate, volume 2, characteristics of indoor air; July-August; Toronto, ON, Canada. Ottawa, ON, Canada: International Conference on Indoor Air Quality and Climate, Inc.; pp. 281-285.

Oldaker, G. B., III; Taylor, W. D.; Parrish, K. B. (1993) Investigations of ventilation, smoking activity, and indoor air quality at four large office buildings. In: Proceedings of IAQ '92. American Society of Heating, Refrigerating and Air-Conditioning Engineers, Inc.; pp. 365-374.

Orchard, T.; Woodbury, M. A. (1972) A missing information principle: theory and applications. In: LeCam, L.; Newman, J.; Scott, E., eds. Proceedings of the 6th Berkeley symposium on mathematical statistics and probability, v. 1. Berkeley, CA: University of California Press; pp. 697-715.

Ott, W. R. (1982) Concepts of human exposure to air pollution. Environ. Int. 7: 179-196.

Owen, M. K.; Ensor, D. S.; Hovis, L. S.; Tucker, W. G.; Sparks, L. E. (1990) Particle size distributions for an office aerosol. Aerosol Sci. Technol. 13: 486-492.

Owen, M. K.; Ensor, D. S.; Sparks, L. E. (1992) Airborne particle sizes and sources found in indoor air. Atmos. Environ. Part A 26: 2149-2162.

Özkaynak, H.; Spengler, J. D.; Ludwig, J. F.; Butler, D. A.; Clayton, C. A.; Pellizzari, E.; Wiener, R. W. (1990) Personal exposure to particulate matter: findings from the Particle Total Exposure Assessment Methodology (PTEAM) prepilot study. In: Indoor air '90: precedings of the 5th international conference on indoor air quality and climate, volume 2, characteristics of indoor air; July-August; Toronto, ON, Canada. Ottawa, ON, Canada: International Conference on Indoor Air Quality and Climate, Inc.; pp. 571-576.

Özkaynak, H.; Xue, J.; Weker, R.; Butler, D.; Spengler, J. (1993a) The particle TEAM (PTEAM) study: analysis of the data, volume III [draft final report]. Research Triangle Park, NC: U.S. Environmental Protection Agency; EPA contract no. 68-02-4544.

Özkaynak, H.; Spengler, J. D.; Xue, J.; Koutrakis, P.; Pellizzari, E. D.; Wallace, L. (1993b) Sources and factors influencing personal and indoor exposures to particles, elements and nicotine: findings from the particle TEAM pilot study. In: Jantunen, M.; Kalliokoski, P.; Kukkonen, E.; Saarela, K.; Seppänen, O.; Vuorelma, H., eds. Indoor air '93: proceedings of the 6th international conference on indoor air quality and climate, v. 3, combustion products, risk assessment, policies; July; Helsinki, Finland. Helsinki, Finland: Indoor Air '93; pp. 457-462.

Özkaynak, H.; Xue, J.; Spengler, J. D.; Wallace, L. A.; Pellizzari, E. D.; Jenkins, P. (1996) Personal exposures to airborne particles and metals: results from the particle TEAM study in Riverside, California. In: Lippmann, M., ed. Papers from the ISEA-ISEE annual meeting; September 1994; Research Triangle Park, NC. J. Exp. Anal. Environ. Epidemiol.: in press.

Pellizzari, E. D.; Thomas, K. W.; Clayton, C. A.; Whitmore, R. W.; Shores, R. C.; Zelon, H. S.; Perritt, R. L. (1992) Particle total exposure assessment methodology (PTEAM): Riverside, California pilot study, volume I [final report]. Research Triangle Park, NC: U.S. Environmental Protection Agency, Atmospheric Research and Exposure Assessment Laboratory; EPA report no. EPA/600/R-93/050. Available from: NTIS, Springfield, VA; PB93-166957/XAB.

Pellizzari, E. D.; Thomas, K. W.; Clayton, C. A.; Whitmore, R. C.; Shores, H.; Zelon, S.; Peritt, R. L. (1993) Particle total exposure assessment methodology (PTEAM): Riverside, California pilot study - volume I [project summary]. Research Triangle Park, NC: U.S. Environmental Protection Agency, Atmospheric Research and Exposure Assessment Laboratory; EPA report no. EPA/600/SR-93/050.

Pengelly, L. D.; Goldsmith, C. H.; Kerigan, A. T.; Furlong, W.; Toplack, S. (1987) The Hamilton study: estimating exposure to ambient suspended particles. JAPCA 37: 1421-1428.

Perritt, R. L.; Clayton, C. A.; Pellizzari, E. D.; Thomas, K. W.; Wallace, L. A.; Spengler, J. D.; Özkaynak, H. (1991) Particle Total Exposure Assessment Methodology (PTEAM) Pilot Study: personal, indoor, and outdoor particulate concentration distributions for southern California fall 1990 - preliminary results. In: Measurement of toxic and related air pollutants: proceedings of the 1991 U.S. EPA/A&WMA international symposium, v. 2; May; Durham, NC. Pittsburgh, PA: Air & Waste Management Association; pp. 665-671. (A&WMA publication VIP-21).

Pickles, J. H. (1982) Air pollution estimation error and what it does to epidemiological analysis. Atmos. Environ. 16: 2241-2245.

Platts-Mills, T. A. E.; Chapman, M. D. (1987) Dust mites: immunology, allergic disease, and environmental control. J. Allergy Clin. Immunol. 80: 755-775.

Pope, C. A., III; Thun, M. J.; Namboodiri, M. M.; Dockery, D. W.; Evans, J. S.; Speizer, F. E.; Heath, C. W., Jr. (1995) Particulate air pollution as a predictor of mortality in a prospective study of U.S. adults. Am. J. Respir. Crit. Care Med. 151: 669-674.

Quackenboss, J. J.; Lebowitz, M. D.; Crutchfield, C. D. (1989) Indoor-outdoor relationships for particulate matter: exposure classifications and health effects. Environ. Int. 15: 353-360.

Quackenboss, J. J.; Krzyzanowski, M.; Lebowitz, M. D. (1991) Exposure assessment approaches to evaluate respiratory health effects of particulate matter and nitrogen dioxide. J. Exposure Anal. Environ. Epidemiol. 1: 83-107.

Raunemaa, T.; Kulmala, M.; Saari, H.; Olin, M.; Kulmala, M. H. (1989) Indoor air aerosol model: transport indoors and deposition of fine and coarse particles. Aerosol Sci. Technol. 11: 11-25.

Repace, J. L. (1987) Indoor concentrations of environmental tobacco smoke: field surveys. In: O'Neill, I. K.; Brunnemann, K. D.; Dodet, B.; Hoffmann, D., eds. Environmental carcinogens: methods of analysis and exposure measurement, volume 9 - passive smoking. Lyon, France: World Health Organization; pp. 141-162. (IARC scientific publications: no. 81).

Repace, J. L.; Lowrey, A. H. (1980) Indoor air pollution, tobacco smoke, and public health. Science (Washington, DC) 208: 464-472.

Repace, J. L.; Ott, W. R.; Wallace, L. A. (1980) Total human exposure to air pollution. Presented at: 73rd annual meeting of the Air Pollution Control Association; June; Montreal, PQ, Canada. Pittsburgh, PA: Air Pollution Control Association; paper no. 80-61.6.

Rippon, J. W. (1988) Medical mycology: the pathogenic fungi and the pathogenic actinomycetes. 3rd ed. Philadelphia, PA: W. B. Saunders Company.

Roberts, J. W.; Camann, D. E.; Spittler, T. M. (1990) Monitoring and controlling lead in house dust in older homes. In: Indoor air '90: precedings of the 5th international conference on indoor air quality and climate, volume 2, characteristics of indoor air; July-August; Toronto, ON, Canada. Ottawa, ON, Canada: International Conference on Indoor Air Quality and Climate, Inc.; pp. 435-440.

Rodes, C. E.; Kamens, R. M.; Wiener, R. W. (1991) The significance and characteristics of the personal activity cloud on exposure assessment measurements for indoor contaminants. Indoor Air 2: 123-145.

Santanam, S.; Spengler, J. D.; Ryan, P. B. (1990) Particulate matter exposures estimated from an indoor-outdoor source apportionment study. In: Indoor air '90: precedings of the 5th international conference on indoor air quality and climate, volume 2, characteristics of indoor air; July-August; Toronto, ON, Canada. Ottawa, ON, Canada: International Conference on Indoor Air Quality and Climate, Inc.; pp. 583-588.

Sexton, K.; Spengler, J. D.; Treitman, R. D. (1984) Personal exposure to respirable particles: a case study in Waterbury, Vermont. Atmos. Environ. 18: 1385-1398.

Sheldon, L. S.; Handy, R. W.; Hartwell, T. D.; Whitmore, R. W.; Zelon, H. S.; Pellizzari, E. D. (1988a) Indoor air quality in public buildings: v. I. Washington, DC: U.S. Environmental Protection Agency, Office of Acid Deposition, Environmental Monitoring, and Quality Assurance; report no. EPA 600/6-88/009a. Available from: NTIS, Springfield, VA; PB89-102503.

Sheldon, L.; Zelon, H.; Sickles, J.; Eaton, C.; Hartwell, T. (1988b) Indoor air quality in public buildings: volume II. Research Triangle Park, NC: U.S. Environmental Protection Agency, Environmental Monitoring Systems Laboratory; report no. EPA 600/6-88/009b. Available from: NTIS, Springfield, VA; PB89-102511.

Sheldon, L. S.; Hartwell, T. D.; Cox, B. G.; Sickles, J. E., II; Pellizzari, E. D.; Smith, M. L.; Perritt, R. L.; Jones, S. M. (1989) An investigation of infiltration and indoor air quality: final report. Albany, NY: New York State Energy Research and Development Authority; New York State ERDA contract no. 736-CON-BCS-85.

Sheldon, L.; Clayton, A.; Keever, J. Perritt, R.; Whitaker, D. (1992) PTEAM: monitoring of phthalates and PAHs in indoor and outdoor air samples in Riverside, California, volume II [final report]. Sacramento, CA: California Environmental Protection Agency, State Air Resources Board, Research Division; contract no. A933-144. Available from: NTIS, Springfield, VA; PB93-205649/XAB.

Sinclair, J. D.; Psota-Kelty, L. A.; Weschler, C. J. (1988) Indoor/outdoor ratios and indoor surface accumulations of ionic substances at Newark, New Jersey. Atmos. Environ. 22: 461-469.

Sinclair, J. D.; Psota-Kelty, L. A.; Weschler, C. J.; Shields, H. C. (1990) Measurement and modeling of airborne concentrations and indoor surface accumulation rates of ionic substances at Neenah, Wisconsin. Atmos. Environ. Part A 24: 627-638.

Sinclair, J. D.; Psota-Kelly, L. A.; Peins, G. A.; Ibidunni, A. O. (1992) Indoor/outdoor relationships of airborne ionic substances: comparison of electronic equipment room and factory environments. Atmos. Environ. Part A 26: 871-882.

ı, K. R.; Apte, M. G.; Ma, Y.; Wongsekiarttirat, W.; Kulkarni, A. (1994) Air pollution and the energy ladder in Asian cities. In: Tyler, S.; Sathaye, J.; Goldman, N., eds. Energy use in Asian Cities. Energy (Oxford) 19: 587-600.

Smithard, E. H. R. (1954) The 1952 fog in a metropolitan borough. Mon. Bull. Minist. Health Public Health Lab. Serv. (G. B.) 13: 26-35.

Spengler, J. D.; Thurston, G. D. (1983) Mass and elemental composition of fine and coarse particles in six U.S. cities. J. Air Pollut. Control Assoc. 33: 1162-1171.

Spengler, J. D.; Dockery, D. W.; Reed, M. P.; Tosteson, T.; Quinlan, P. (1980) Personal exposures to respirable particles. Presented at: 73rd annual meeting of the Air Pollution Control Association; June; Montreal, PQ, Canada. Pittsburgh, PA: Air Pollution Control Association; paper no. 80-61.5b.

Spengler, J. D.; Dockery, D. W.; Turner, W. A.; Wolfson, J. M.; Ferris, B. G., Jr. (1981) Long-term measurements of respirable sulfates and particles inside and outside homes. Atmos. Environ. 15: 23-30.

Spengler, J. D.; Treitman, R. D.; Tosteson, T. D.; Mage, D. T.; Soczek, M. L. (1985) Personal exposures to respirable particulates and implications for air pollution epidemiology. Environ. Sci. Technol. 19: 700-707.

Spengler, J. D.; Ware, J.; Speizer, F.; Ferris, B.; Dockery, D.; Lebret, E.; Brunnekreef, B. (1987) Harvard's indoor air quality respiratory health study. In: Seifert, B.; Esdorn, H.; Fischer, M.; Rüden, H.; Wegner, J., eds. Indoor air '87: proceedings of the 4th international conference on indoor air quality and climate: v. 2, environmental tobacco smoke, multicomponent studies, radon, sick buildings, odours and irritants, hyperreactivities and allergies; August; Berlin, Federal Republic of Germany. Berlin, Federal Republic of Germany: Institute for Water, Soil and Air Hygiene; pp. 218-223.

Spengler, J. D.; Özkaynak, H.; Ludwig, J.; Allen, G.; Pellizzari, E. D.; Wiener, R. (1989) Personal exposures to particulate matter: instruments and methodologies P-TEAM. In: Measurement of toxic and related air pollutants: proceedings of the 1989 U.S. EPA/A&WMA international symposium; May; Raleigh, NC. Pittsburgh, PA: Air & Waste Management Association; pp. 449-463. (A&WMA publication VIP-13).

Sterling, T. D.; Dimich, H.; Kobayashi, D. (1982) Indoor byproduct levels of tobacco smoke: a critical review of the literature. J. Air Pollut. Control Assoc. 32: 250-259.

Suh, H. H.; Koutrakis, P.; Spengler, J. D. (1993) Validation of personal exposure models for sulfate and aerosol strong acidity. J. Air Waste Manage. Assoc. 43: 845-850.

Suh, H. H.; Allen, G. A.; Koutrakis, P.; Burton, R. M. (1995) Spatial variation in acidic sulfate and ammonia concentrations within metropolitan Philadelphia. J. Air Waste Manage. Assoc. 45: 442-452.

Tamura, K.; Ando, M. (1994) Suspended particulate matter in indoor and outdoor air along a main road and personal exposure assessment. Presented at: Sixth conference of the International Society for Environmental Epidemiology/fourth conference of the International Society for Exposure Analysis joint conference; September; Research Triangle Park, NC. Chapel Hill, NC: University of North Carolina, School of Public Health; abstract no. 116.

Tamura, K.; Ando, M.; Sagai, M.; Matsumoto, Y. (1996) Estimation of levels of personal exposure to suspended particulate matter and nitrogen dioxide in Tokyo. Environ. Sci. (Tokyo) 6: accepted.

Thatcher, T. L.; Layton, D. W. (1995) Deposition, resuspension, and penetration of particles within a residence. Atmos. Environ. 29: 1487-1497.

Thomas, K. W.; Pellizzari, E. D.; Clayton, C. A.; Whitaker, D. A.; Shores, R. C.; Spengler, J.; Özkaynak, H.; Froehlich, S. E.; Wallace, L. A. (1993) Particle total exposure assessment methodology (PTEAM) 1990 study: method performance and data quality for personal, indoor, and outdoor monitoring. J. Exposure Anal. Environ. Epidemiol. 3: 203-226.

Turk, B. H.; Brown, J. T.; Geisling-Sobotka, K.; Froehlich, D. A.; Grimsrud, D. T.; Harrison, J.; Koonce, J. F.; Prill, R. J.; Revzan, K. L. (1987) Indoor air quality and ventilation measurements in 38 Pacific Northwest commercial buildings: final report to the Bonneville Power Administration, volume I: measurement results and interpretation [final report]. Berkeley, CA: U.S. Department of Energy, Lawrence Berkeley Laboratory, Indoor Environment Program; report no. LBL-22315-1/2. Available from: DE88014064/XAB.

Turk, B. H.; Grimsrud, D. T.; Brown, J. T.; Geisling-Sobotka, K. L.; Harrison, J.; Prill, R. J. (1989) Commercial building ventilation rates and particle concentrations. ASHRAE Trans. 95(part 1): 422-433.

U.S. Centers for Disease Control. (1988) Assessing exposures of health-care personnel to aerosols of ribavirin—California. Morb. Mortal. Wkly. Rep. 37: 560-563.

U.S. Environmental Protection Agency. (1982) Air quality criteria for particulate matter and sulfur oxides. Research Triangle Park, NC: Office of Health and Environmental Assessment, Environmental Criteria and Assessment Office; EPA report no. EPA-600/8-82-029aF-cF. 3v. Available from: NTIS, Springfield, VA; PB84-156777.

U.S. Environmental Protection Agency. (1986a) Second addendum to air quality criteria for particulate matter and sulfur oxides (1982): assessment of newly available health effects information. Research Triangle Park, NC: Office of Health and Environmental Assessment, Environmental Criteria and Assessment Office; EPA report no. EPA-600/8-86-020F. Available from: NTIS, Springfield, VA; PB87-176574.

U.S. Environmental Protection Agency. (1986b) Air quality criteria for lead. Research Triangle Park, NC: Office of Health and Environmental Assessment, Environmental Criteria and Assessment Office; EPA report no. EPA-600/8-83/028aF-dF. 4v. Available from: NTIS, Springfield, VA; PB87-142378.

U.S. Environmental Protection Agency. (1989) Exposure factors handbook. Washington, DC: Office of Health and Environmental Assessment; EPA report no. EPA/600/8-89/043. Available from: NTIS, Springfield, VA; PB90-106774.

U.S. Environmental Protection Agency. (1992) Respiratory health effects of passive smoking: lung cancer and other disorders. Washington, DC: Office of Research and Development, Office of Health and Environmental Assessment; EPA report no. EPA/600/6-90/006F. Available from: NTIS, Springfield, VA; PB93-134419/XAB.

U.S. Environmental Protection Agency. (1995) PFT database for residential air flow measurements: database documentation, final report. Washington, DC: Office of Toxic Substances; contract no. 68-D3-0013, task 3-18.

United Kingdom Ministry of Health. (1954) Mortality and morbidity during the London fog of December 1952. London, United Kingdom: Her Majesty's Stationery Office. (Reports on public health and medical subjects no. 95).

Wallace, L. (1996) Indoor particles: a review. J. Air Waste Manage. Assoc. 46: 98-126.

.ce, L.; Clayton, A.; Whitmore, R.; Shores, R.; Thomas, K.; Whitaker, D.; Reading, P.; Pellizzari, E.; Spengler, J.; Özkaynak, H.; Froehlich, S.; Jenkins, P.; Ota, L.; Westerdahl, D. (1991a) Initial results from the PTEAM study: survey design, population response rates, monitor performance and quality control. In: Measurement of toxic and related air pollutants: proceedings of the 1991 U.S. EPA/A&WMA international symposium, v. 2; May; Durham, NC. Pittsburgh, PA: Air & Waste Management Association; pp. 659-664. (A&WMA publication VIP-21).

Wallace, L. A.; Pellizzari, E.; Sheldon, L.; Whitmore, R.; Zelon, H.; Clayton, A.; Shores, R.; Thomas, K.; Whitaker, D.; Reading, P.; Spengler, J.; Özkaynak, H.; Froehlich, S.; Jenkins, P.; Ota, L.; Westerdahl, D. (1991b) The TEAM study of inhalable particles (PM_{10}): study design, sampler performance, and preliminary results. Presented at: 84th annual meeting of the Air & Waste Management Association; June; Vancouver, British Columbia, Canada. Pittsburgh, PA: Air & Waste Management Association; paper no. 91-171.3.

Wallace, L.; Nelson, W.; Ziegenfus, R.; Pellizzari, E.; Michael, L.; Whitmore, R.; Zelon, H.; Hartwell, T.; Perritt, R.; Westerdahl, D. (1991c) The Los Angeles TEAM study: personal exposures, indoor-outdoor air concentrations, and breath concentrations of 25 volatile organic compounds. J. Exposure Anal. Environ. Epidemiol. 1: 157-192.

Wallace, L. A.; Özkaynak, H.; Spengler, J. D.; Pellizzari, E. D.; Jenkins, P. (1993) Indoor, outdoor, and personal air exposures to particles, elements, and nicotine for 178 southern California residents. In: Jantunen, M.; Kalliokoski, P.; Kukkonen, E.; Saarela, K.; Seppänen, O.; Vuorelma, H., eds. Indoor air '93: proceedings of the 6th international conference on indoor air quality and climate, v. 3, combustion products, risk assessment, policies; July; Helsinki, Finland. Helsinki, Finland: Indoor Air '93; pp. 445-450.

Weschler, C. J.; Shields, H. C.; Kelty, S. P.; Psota-Kelly, L. A.; Sinclair, J. D. (1989) Comparison of effects of ventilation, filtration and outdoor air at telephone office buildings. In: Nagda, N. L.; Harper, J. P., eds. Design and protocol for monitoring indoor air quality. Philadelphia, PA: American Society for Testing and Materials; pp. 9-34. (ASTM special technical publication 1002).

West, J. B. (1982) Pulmonary pathophysiology—the essentials. 2nd ed. Baltimore, MD: Williams & Wilkins; p. 168.

Wiener, R. W. (1988) Measurement and evaluation of personal exposure to aerosols. In: Measurement of toxic and related air pollutants: proceedings of the 1988 EPA/APCA international symposium; May; Research Triangle Park, NC. Pittsburgh, PA: Air Pollution Control Association; pp. 84-88. (APCA publication no. VIP-10).

Wiener, R. W. (1989) Particle total exposure assessment methodology—an overivew of planning and accomplishments. In: Measurement of toxic and related air pollutants: proceedings of the 1989 U.S. EPA/A&WMA international symposium; May; Raleigh, NC. Pittsburgh, PA: Air & Waste Management Association; pp. 442-448. (A&WMA publication VIP-13).

Wiener, R. W.; Wallace, L.; Pahl, D.; Pellizzari, E.; Whittaker, D.; Spengler, J.; Özkaynak, H. (1990) Review of the particle TEAM 9 home field study. In: Measurement of toxic and related air pollutants: proceedings of the 1990 EPA/A&WMA international symposium, v. 2; May; Raleigh, NC. Pittsburgh, PA: Air & Waste Management Association; pp. 452-460. (A&WMA publication VIP-17).

Willeke, K.; Baron, P. A., eds. (1993) Aerosol measurement: principles, techniques and applications. New York, NY: Van Nostrand Reinhold Publishers.

Wilmoth, R. C.; Powers, T. J.; Millette, J. R. (1991) Observations on studies useful to asbestos O&M activities. Microscope 39: 299-312.

Wilson, W. E.; Suh, H. H. (1995) Differentiating fine and coarse particles: definitions and exposure relationships relevant to epidemiological studies. In: Schmidt-Ott, A., ed. Trends in aerosol research IV: new approaches in aerosol science and technology, proceedings of the seminar; January; Gerhard Mercator University, Duisburg, Germany. Duisburg, Germany: Gerhard Mercator University of Duisburg; pp. 57-71.

Winer, B. J. (1962) Statistical principles in experimental design. New York, NY: McGraw-Hill Book Co., Inc.; pp. 105-124.

Woodbury, M.; Hasselblad, V. (1970) Maximum likelihood estimates of the variance covariance matrix from the multivariate normal. In: Proceedings of SHARE XXXIV, v. 3; pp. 1550-1561.

World Health Organization. (1982a) Human exposure to carbon monoxide and suspended particulate matter in Zagreb, Yugoslavia. Geneva, Switzerland: World Health Organization; GEMS (Global Environmental Monitoring System) report no. EFP/82.33.

World Health Organization. (1982b) Human exposure to SO_2, NO_2 and suspended particulate matter in Toronto, Canada. Geneva, Switzerland: World Health Organization; GEMS (Global Environmental Monitoring System) report no. EFP/82.38.

World Health Organization. (1984) Human exposure to suspended particulate matter and sulfate in Bombay, India. Geneva, Switzerland: World Health Organization; GEMS (Global Environment Monitoring System) report no. EFP/84.86.

World Health Organization. (1985) Human exposure to carbon monoxide and suspended particulate matter in Beijing, People's Republic of China. Geneva, Switzerland: World Health Organization; GEMS (Global Environmental Monitoring System) report no. PEP/85.11.

World Health Organization. (1995) Interpretation of WHO air quality guidelines: report of an expert working group. Geneva, Switzerland: World Health Organization; report no. WHO/EOS/95; in press.

Yoshimura, I. (1990) The effect of measurement error on the dose-response curve. Environ. Health Perspect. 87: 173-178.

*U.S. GOVERNMENT PRINTING OFFICE: 1996-752-126/49039